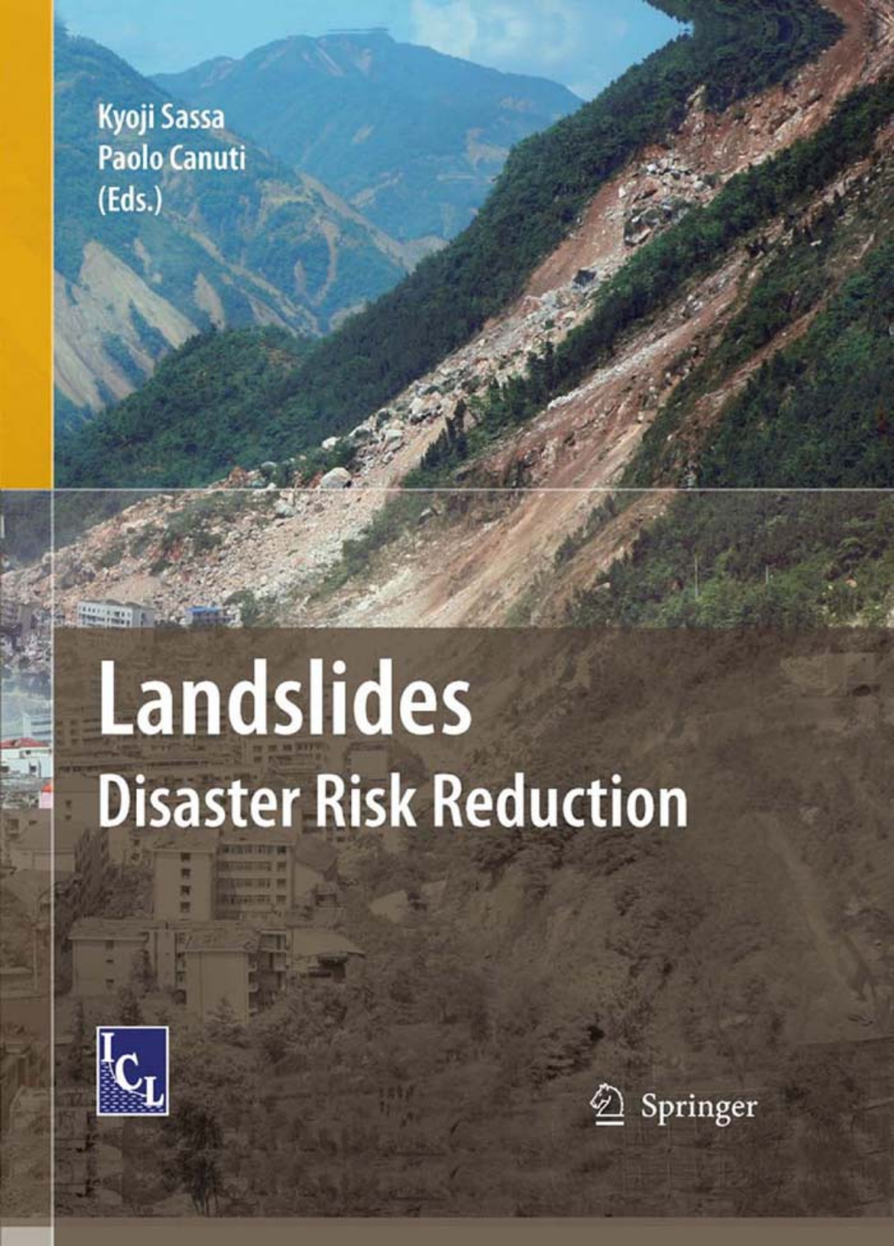

Kyoji Sassa
Paolo Canuti
(Eds.)

Landslides

Disaster Risk Reduction

ICL

Springer

Landslides – Disaster Risk Reduction

Kyoji Sassa · Paolo Canuti
(Eds.)

Landslides – Disaster Risk Reduction

Springer

Editors

Prof. Dr. Kyoji Sassa
UNITWIN Headquarter Building
Kyoto University Uji Campus
Uji, Kyoto 611-0011, Japan
sassa@iclhq.org

Prof. Dr. Paolo Canuti
Università di Firenze
Dipto. Scienze della Terra
via G. La Pira, 4
50121 Firenze
Italy
canuti@geo.unifi.it

Associate Editors

Nicola casagli
University of Florence, Department
of Earth Sciences
Via G. La Pira n.4, I – 50121 FIRENZE, Italy
nicola.casagli@unifi.it

Lynn Highland
U.S. Geological Survey, National
Landslide Information Center,
MS 966, Box 25046, Denver,
CO 80225, USA
highland@usgs.gov

Satoshi Tsuchiya
Shizuoka University, Faculty of Agriculture,
836 Ohya, Suruga-ku Shizuoka-shi 422-8529,
Japan
afstuti@agr.shizuoka.ac.jp

Fawu Wang
Kyoto University, Research Centre
on Landslides, Disaster Prevention
Research Institute,
Uji, Kyoto 611- 0011, Japan
wangfw@landslide.dpri.kyoto-u.ac.jp

ISBN: 978-3-540-69966-8 e-ISBN: 978-3-540-69970-5

Library of Congress Control Number: 2008935360

© Springer-Verlag Berlin Heidelberg 2009

This work is subject to copyright. All rights are reserved, whether the whole or part of the material is concerned, specifically the rights of translation, reprinting, reuse of illustrations, recitation, broadcasting, reproduction on microfilm or in any other way, and storage in data banks. Duplication of this publication or parts thereof is permitted only under the provisions of the German Copyright Law of September 9, 1965, in its current version, and permission for use must always be obtained from Springer. Violations are liable to prosecution under the German Copyright Law.

The use of general descriptive names, registered names, trademarks, etc. in this publication does not imply, even in the absence of a specific statement, that such names are exempt from the relevant protective laws and regulations and therefore free for general use.

Cover design: deblik, Berlin

Cover photo: Beichuan Landslide, Sichuan, China (Courtesy of Yueping Yin, China Geological Survey)

Printed on acid-free paper

9 8 7 6 5 4 3 2 1

springer.com

Foreword

A series of extremely high-profile disasters – the Indian Ocean tsunami of December in 2004, Hurricane Katrina, South Asian earthquake and the East African drought in 2005, floods in Asia in 2007, Myanmar Cyclone and Sichuan Earthquake in 2008, among other, underscored the importance of how better cooperation between Government authorities and the international community including scientific community would have played a critical role in helping people make life changing decisions about where and how they live before the disaster strikes, in particular high-risk urban areas.

Landslide, floods, drought, wildfire, storms, tsunami, earthquakes and other types of natural hazards are increasingly affecting the world. In the decade 1976–1985, close to billion people were affected by disasters. But by the most recent decade, 1996–2005, the decade total had more than doubled, to nearly two and a half billion people. In the last decade alone, disasters affected 3 billion people, killed over 750,000 people and cost around US$600 billion.[1]

We cannot let this trend continue. Disaster risk concerns every person, every community, and every nation; indeed, disaster impacts are slowing down development, and their impact and actions in one region can have an impact on risks in another, and vice versa. Without taking into consideration the urgent need to reduce risk and vulnerability, the world simply cannot hope to move forward in its quest for sustainable development and reduction of poverty.

The *Hyogo Framework for Action 2005–2015: Building the Resilience of Nations and Communities to Disasters*, adopted at the World Conference on Disaster Reduction (WCDR, Kobe, Hyogo, Japan, in January 2005), represents the most comprehensive action-oriented policy guidance in universal understanding of disasters induced by vulnerability to natural hazards and reflects a solid commitment to implementation of an effective disaster reduction agenda. In order to ensure effective implementation of the Hyogo Framework at all levels, tangible and coordinated activities must be carried out. For the last three years, we have seen many activities and initiatives developed to implement

[1] Data derived from the EM-DAT: The OFDA/CRED International Disaster Database, www.en-dat.net, Universite Catholiqué de Louvain – Brussels – Belgium

the Hyogo Framework in various areas. As a concrete activity in the area of landslide risk reduction, the International Programme on Landslides has maintained the momentum created at the WCDR and has been moving forward, led by the International Consortium on Landslides.

In January 2006, the Tokyo Action Plan on the International Programme on Landslides (IPL) was adopted by IPL partners. The Tokyo Action Plan proposed the creation of World Centers of Excellence on Landslide Risk Reduction (WCoE), global cooperating Network of the IPL, and established the IPL Global Promotion Committee and the IPL World Center as its secretariat to coordinate and support implementation of the International Programme on Landslides. The establishment of WCoE was decided at the first session of IPL Global promotion committee in January 2007, and further examined and endorsed in the second session of the IPL Global Promotion Committee held in Tokyo, at the United Nations University on 21 January 2008. The World Centres of Excellence on Landslide Risk Reduction should also further improve the global recognition of landslide risk reduction and its social-economic relevance and entities contribution to this field.

As the Action Plan proposed, the first World Landslide Forum will be held this year in order to bring together academics, practitioners, politicians and other stakeholders to a global, multidisciplinary, problem-focused platform. The objectives of the First World Landslides Forum are:

1. Promotion of research and exchange of experience through open Forums, Symposia and Thematic Sessions
2. Sharing of advances and achievements of the International Programme on Landslides
3. Designation of World Centers of Excellence on Landslide Risk Reduction

It is my great pleasure to see this valuable development. I expect the First World Landslide Forum to make a substantive contribution in the area of landslide risk reduction by the promotion of exchange of experience and achievements in science and facilitating discussion on sustainable disaster risk management.

Sálvano Briceño
Director of United Nations Secretariat of the International Strategy for Disaster Reduction

Preface – Aims of This Volume

The United Nations World Conference on Disaster Reduction (WCDR) was held in Kobe, Hyogo, Japan on 18–22 January 2005. People from United Nations organizations, governments, non-governmental organizations and individuals who were willing to contribute to disaster reduction joined this Global Cooperation Conference. This Conference was organized soon after the Indian Ocean Tsunami disaster on 26 December 2004 which killed about 230,000 people. It is apparent that this tragedy would have been reduced by understanding of mechanism, preparedness, early warning, and evacuation. Landslide disaster can be reduced by understanding of mechanism, prediction, hazard assessment, early warning and risk management. In addition, landslides can be prevented from occurring by various measures to remove landslide causes and to stabilize slopes, while it is not possible to prevent most other hazards such as earthquakes, volcanic eruptions, tsunamis, and typhoons. Thus, landslide disaster reduction is the function where human efforts and financial investment are most effective.

The International Consortium on Landslides (ICL), which was founded on 21 January 2002, sent 51 delegates to the WCDR. The number of delegates was one of the biggest within participating entities. The ICL organized a thematic session on the International Programme on Landslides (IPL) and the International Flood Initiative (IFI) together with the flood group and UNESCO and other global stakeholders. This session resulted in a Letter of Intent (LoI) concerning strengthening cooperation in research and learning on earth system risk analysis and sustainable disaster management within the United Nations International Strategy for Disaster Reduction (UN-ISDR). The LoI was approved by seven global stakeholders: the United Nations Educational, Scientific and Cultural Organization (UNESCO), the World Meteorological Organization (WMO), the Food and Agriculture Organization of the United Nations (FAO), the United Nations International Strategy for Disaster Risk Reduction (UN-ISDR), the United Nations University (UNU), the International Council for Science (lCSU), and the World Federation of Engineering Organizations (WFEO) within the year 2005.

Based on this Letter of Intent, the Tokyo Round Table Discussion "Strengthening Research and Learning on Earth System Risk Analysis and Sustainable Disaster Management within he UN-ISDR as Regards Landslides"- towards a dynamic global network of the International Programme on Landslides (IPL) was held at the United Nations University, Tokyo, from 18 to 20 January, 2006. The 2006 Tokyo Action Plan of the International Programme on Landslides (IPL) was adopted by the participants in this Tokyo Round Table Discussion. The Action Plan proposed the global cooperating network of the IPL, and established the IPL Global Promotion Committee and the IPL World Centre as its secretariat to coordinate and support implementation of the International Programme on Landslides. The Plan also proposed organization of a World Landslide Forum in order to bring together academics, practitioners, politicians, and other stakeholders to a global, multidisciplinary, problem-focused platform. The first IPL Global Promotion Committee was held in January 2007 at the UNU, Tokyo, where it was decided to organize the First World Landslide Forum at the UNU on 18–21 November 2008. This decision led to a very short preparation time. The ICL is expected by its Statutes to organize its General Assembly every 3 years in order to disseminate its activities and to provide a forum for open discussion and new initiatives from all participants. The First General Assembly was organized at the Keck Center of the National Academy of Sciences, Washington, D.C., U.S.A. on 12–14 October 2005. Aims of the General Assembly are well represented by the World Landslide Forum. Thus, the First World Landslide Forum was planned for 2008, including the aim of the General Assembly of ICL. The First World Landslide Forum is jointly organized by the following global stakeholders together with the ICL:

Organizers: The International Consortium on Landslides (ICL), United Nations Educational, Scientific and Cultural Organization (UNESCO), World Meteorological Organization (WMO), Food and Agriculture Organization of the United Nations (FAO), United Nations International Strategy for Disaster Risk Reduction (UN-ISDR), United Nations University (UNU), United Nations Environment Programme (UNEP), World Bank (IBRD), United Nations Development Programme (UNDP), International Council for Science (ICSU), World Federation of Engineering Organizations (WFEO), Kyoto University (KU), and the Japan Landslide Society (JLS).

Honorary Chairpersons: Salvano BRICENO (Director of UNIISDR), Jacques DIOUF (Director-General of FAO), Konrad OSTERWALDER (Rector of UNU), Michel JARRAUD (Secretary-General of WMO), Koichiro MATSUURA (Director-General of UNESCO), Goverdhan MEHTA (President of ICSU), Shuzo NISHIMURA (Executive Vice President of Kyoto University)

Chairperson: Kyoji SASSA (President of ICL, IPL World Centre), **Co-Chairpersons**: Paolo CANUTI (European Centre of ICL, University of Florence), Srikantha HERATH (Senior Academic Programme Officer of UNU), Kazuhiro ISHIHARA (Director of Disaster Prevention Research Institute of Kyoto University), Howard MOORE (Senior Advisor of ICSU), Badaoui ROUHBAN (Chief, Section for Disaster Reduction of UNESCO), Peter Lytlle (U.S. Geological Survey)

The Forum will organize an Open Forum "Progress of IPL Activities"; a Plenary Symposium "Global Landslide Risk Reduction"; Keynote lectures; Thematic Parallel Sessions; Public forum "Protection of Society and Cultural and Natural Heritage from Landslides", including a session titled "Landslides for Children", which will invite 50 children from landslide disaster areas of the Philippines, Shikoku Island and Niigata Prefecture, Japan; and the monthly exhibition "Landslides and Risk Mitigation of the World". This volume presents

(1) Progress of IPL Activities, (2) eight keynote lectures, (3) three examples of IPL Projects from research, capacity building and the protection of cultural heritage, (4) Major contents of 16 thematic parallel sessions which are classified by four global cooperation fields proposed by the Tokyo Action Plan as follows:

Global Cooperation Field (l): Technological Development

1. A look from space, 2. Mapping: Inventories, susceptibility, hazard and risk, 3. Monitoring, prediction and early warning

Global Cooperation Field (2): Targeted Landslides: Mechanism and Impacts

1. Catastrophic slides and avalanches, 2. Cultural Heritage and Landslides: research for risk prevention and conservation, 3. Landslides and multi-hazards, 4. Rainfall, debris flows and wildfires

Global Cooperation Field (3): Capacity Building

1. Case studies and national experiences, 2. Education, capacity building and public awareness for disaster reduction, 3. International cooperation initiatives, 4. Policy and institutional framework for disaster reduction

Global Cooperation Field (4): Mitigation, Preparedness and Recovery

1. Climate change and slope instability, 2. Economic and social impact of landslides, 3. Environmental impact of landslides, 4. Engineering measures for landslide disaster mitigation, 5. Watershed and forest management for risk reduction

Acknowledgements

I express my gratitude for all organizers of the First World Landslide Forum and all members of the Organizing Committee for the organization of this First Forum. Thanks also go to conveners of 16 thematic parallel sessions and 8 keynote lectures as well as all programme participants to this forum from many countries around the world by understanding the significance of this forum in spite of a very short in-advance announcement.

It is acknowledged that the organization of this forum and publication of this book is financially supported by a Grant-in-Aid for Publication of Scientific Research Results of the Ministry of Education, Culture, Sports, Science and Technology, Japan (MEXT), and the Commemorative Organization for the Japan World Exposition ('70). The Ministry of Foreign Affairs of Japan (MOFA) provided funds for the planning of the First World Landslide Forum in 2007 and supported the organization in 2008 in cooperation with the United Nations Secretariat of the International Strategy for Disaster Reduction.

Kyoji Sassa
President of the International Consortium on Landslides

Contents

Part I Progress of IPL Activities

1 **Progress of the International Programme on Landslides (IPL) – Objectives of the IPL and the World Landslide Forum** 3
Kyoji Sassa

2 **Projects of International Programme on Landslides** 15
Nicola Casagli, Giacomo Falorni and Veronica Tofani

Part II Keynote Lectures

3 **Landslide Risk Assessment and Mitigation Strategy** 31
Suzanne Lacasse and Farrokh Nadim

4 **Understanding to Predict** 63
Luciano Picarelli

5 **Mechanics-Based Approach Toward the Mitigation of Debris Flow Disasters** 89
Tamotsu Takahashi

6 **Submarine Mass Movements and Their Consequences: An Overview** 115
Jacques Locat and Homa Lee

7 **Satellite Remote Sensing Applications for Landslide Detection and Monitoring** 143
Vern Singhroy

8 **Huge Landslides Caused by Massive Earthquakes and Long-Lasting Geotechnical Risks** 159
Konagai Kazuo, Johansson Jorgen, Takatsu Shigeki and Ikeda Takaaki

9 **The Increasing Wildfire and Post-Fire Debris-Flow Threat in Western USA, and Implications for Consequences of Climate Change** 177
Susan H. Cannon and Jerry DeGraff

10 **Recovery of the Buddha's Niches and Cliff in Bamiyan (Central Afghanistan) after the Taliban Destruction of 2001** 191
Claudio Margottini

Part III Achievements of IPL Projects

11 **Assessment of Global High-Risk Landslide Disaster Hotspots** 213
Farrokh Nadim and Oddvar Kjekstad

12 **International Summer School on Rockslides and Related Phenomena in the Kokomeren River Valley, Tien Shan, Kyrgyzstan** 223
Alexander L. Strom and Kanatbek E. Abdrakhmatov

13 **Landslide Investigation and Capacity Building in the Machu Picchu – Aguas Calientes Area (IPL C101-1)** 229
Kyoji Sassa, Hiroshi Fukuoka and Raul Carreno

14 **Monitoring, Geomorphological Evolution and Slope Stability of Inca Citadel of Machu Picchu: Results from Italian INTERFRASI project** 249
P. Canuti, Claudio Margottini, N. Casagli, G. Delmonaco, L. Falconi, R. Fanti, A. Ferretti, G. Lollino, C. Puglisi, D. Spizzichino and D. Tarchi

15 **Dilatometric and Extensometric Monitoring of Rock Blocks Displacements Within Machu Picchu Archaeological Site, Peru** 259
Vít Vilímek, Jan Klimeš, Jiří Zvelebil and Fernando V. Astete

16 **Geophysical Surveys at Machu Picchu, Peru: Results for Landslide Hazard Investigations** 265
Melvyn Best, Peter Bobrowsky, Marten Douma, Victor Carlotto and Walter Pari

17 **Integration of VHR Satellite Images with Field Data for the Analysis of Debris Sheet Instability in the Machu Picchu Area** 275
Nicola Casagli, Riccardo Fanti and Gaia Righini

Part IV Parallel Sessions

Global Cooperation Field (1): Technological Development

18 **A Look from Space** 287
Nicola Casagli, Veronica Tofani and Robert F. Adler

19 **Mapping: Inventories, Susceptibility, Hazard and Risk** 321
Javier Hervás and Peter Bobrowsky

20 **Monitoring, Prediction and Early Warning** 351
Kyoji Sassa, Luciano Picarelli and Yin Yueping

Global Cooperation Field (2): Targeted Landslides: Mechanism and Impacts

21 **Catastrophic Slides and Avalanches** 379
Alexander L. Strom

22 Cultural Heritage and Landslides: Research for Risk Prevention and Conservation 401
Paolo Canuti, Claudio Margottini, Riccardo Fanti and Edward N. Bromhead

23 Landslides and Multi-Hazards 435
Hideaki Marui and Farrokh Nadim

24 Rainfall, Debris Flows and Wildfires 451
Jerome V. DeGraff and Hirotaka Ochiai

Global Cooperation Field (3): Capacity Building

25 Case Studies and National Experiences 475
Srikantha Herath and Yi Wang

26 Education, Capacity Building and Public Awareness for Disaster Reduction 499
Rajib Shaw, Yukiko Takeuchi and Badaoui Rouhban

27 International Cooperation Initiatives 517
Wolfgang Eder, Kaoru Takara and Fawu Wang

28 Policy and Institutional Framework for Landslide Mitigation and Risk Reduction 531
Gue See-Sew, Karnawati Dwikorita and Wong Shiao-Yun

Global Cooperation Field (4): Mitigation, Preparedness and Recovery

29 Climate Change and Slope Instability 557
John J. Clague

30 Economic and Social Impacts of Landslides 573
Oddvar Kjekstad and Lynn Highland

31 Environmental Impact of Landslides 589
Marten Geertsema, Lynn Highland and Laura Vaugeouis

32 Engineering Measures for Landslide Disaster Mitigation 609
Mihail E. Popescu and Katsuo Sasahara

33 Watershed and Forest Management for Landslide Risk Reduction 633
Nicolas Dolidon, Thomas Hofer, Libor Jansky and Roy Sidle

Contributors

Abdrakhmatov E. Kanatbek Institute of Seismology, National Academy of Science, Kyrgyzstan

Adler F. Robert NASA/Goddard Space Flight Center, Laboratory for Atmospheres, Greenbelt, U.S.A

Astete V. Fernando Instituto National de Cultura, Cusco, Peru

Best Melvyn BEMEX Consulting International, 3701 Wild Berry Bend, Victoria, B.C., Canada, best@islandnet.com

Bobrowsky Peter Geological Survey of Canada, Ottawa, Canada

Bromhead N. Edward Kingston University, UK

Cannon H. Susan U.S. Geological Survey, Box 25046 DFC MS 966, Denver, CO 80225, cannon@usgs.gov

Canuti Paolo University of Firenze, Earth Sciences Department, Via G. La Pira, 4, I-50121, Firenze, Italy, paolo.canuti@unifi.it

Carlotto Victor Instituto Geologico Minero y Metalurgico de Peru, Lima, Perú

Carreno Raul Grudec Ayal, Cusco

Casagli Nicola Univerzity of Firenze, Earth Sciences Department, Via G. La Pira, 4, I-50121, Firenze, Italy, nicola.casagli@unifi.it

Clague J. John Centre for Natural Hazard Research, Simon Fraser University, 8888 University Drive, Burnaby, BC V5A 1S6 Canada, jclague@sfu.ca

DeGraff Jerry U.S.D.A. Forest Service, Sierra National Forest, 1600 Tollhouse Road, Clovis, CA 93611, jdegraff@fs.fed.us

G. Delmonaco ENEA, Via Anguillarese, 301 – 00060 S. Maria di Galeria (Rome) Italy; ISPRA – Italian Institute for Environment Protection and Research – Via Curtatone 3, 00185, Rome, Italy

Dolidon Nicolas ndolidon@gmail.com

Douma Marten Geological Survey of Canada, Ottawa, Canada

Eder Wolfgang Dept. Earth and Environmental Sciences, Geology, University Munich, Luisenstrasse 37, 80333 Muenchen, Germany, w.eder-geo@hotmail.de; w.eder-geo@iaag.geo.uni-muenchen.de

L. Falconi Consorzio Civita, Via del Corso 300, 00186 Rome (Italy); ENEA, Via Anguillarese, 301 – 00060 S. Maria di Galeria (Rome) Italy

Falorni Giacomo Department of Earth Sciences, University of Firenze, Italy

R. Fanti University of Firenze, Department of Earth Sciences Via Giorgio La Pira, 4, 50121, Firenze, Italy

Fanti Riccardo Department of Earth Sciences, University of Firenze, Italy

A. Ferretti Tele-Rilevamento Europa, T.R.E., Via Vittoria Colonna 7, 20149 Milano (Italy)

Fukuoka Hiroshi Kyoto University, Kyoto, Japan, sassa@iclq.org

Geertsema Marten Northern Interior Forest Region, BC Forest Service, 1011 4th Ave, Prince George, BC V2L 3H9 Canada, Marten.Geertsema@gov.bc.ca

Gue See-Sew G&P PROFESSIONALS SDN BHD, 39-5 Jalan 3/146, Bandar Tasik Selatan, 57000 Kuala Lumpur, Malaysia, ssgue@pc.jaring.my

Herath Srikantha United Nations University, 5-53-70, Jingumae, shibuya-ku, Tokyo 150-8925, Japan, herath@hq.unu.edu

Hervás Javier Land Management and Natural Hazards Unit, Institute for Environment and Sustainability, Joint Research Centre (JRC) - European Commission, 21027 Ispra (VA), Italy, javier.hervas@jrc.it

Highland Lynn U.S. Geological Survey, Mail Stop 966, Box 25046, Denver Federal Center, Denver, CO 80225 USA

Hofer Thomas Forestry Department, Food and Agriculture Organization of the United Nations, Via delle Terme di Caracalla, 00100 Roma, Italy, thomas.hofer@fao.org

Jansky Libor United Nations University, Bonn, Germany

Jorgen Johansson Institute of Industrial Science, University of Tokyo, Japan

Karnawati Dwikorita University Gadjah Mada, Indonesia

Kazuo Konagai Institute of Industrial Science, University of Tokyo, 4-6-1 Komaba, Meguro-ku, Tokyo 153-8505, Japan, konagai@iis.u-tokyo.ac.jp

Kjekstad Oddvar Norwegian Geotechnical Institute, P.O. Box 3930 Ullevaal Stadion, NO-0806, Oslo, NORWAY, oddvar.kjekstad@ngi.no

Klimeš Jan Academy of Sciences, Prague, Czech Republic

Lacasse Suzanne Norwegian Geotechnical Institute(NGI), P.O. Box 3930 Ullevaal Stadion, 0806 Oslo NORWAY, Suzanne.Lacasse@ngi.no

Laura Vaugeouis Washington State Department of Natural Resources, 1111 Washington St SE, PO Box 47012 Olympia, WA 98504-7012, USA

Lee Homa United States Geological Survey, Menlo Park, USA

Locat Jacques Department of Geology and Geological Engineering, Laval University, Québec, Qc, Canada, G1K 7P4, Jacques.Locat@ggl.ulaval.ca

G. Lollino CNR-IRPI Torino, Strada delle Cacce 73, 10135 Torino Italy

Claudio Margottini Agency for Environmental Protection and Technical Services (APAT) - Geological Survey of Italy, Via Vitaliano Brancati, 48-00144-Roma, Italy

Marui Hideaki Research Center for Natural Hazards and Disaster Recovery, Niigata University, 8050 Ikarashi-Ninocho, nishi-ku, Niigata 950-2181 JAPAN, maruihi@cc.niigata-u.ac.jp

Nadim Farrokh International Centre for Geohazards, c/o NGI, P.O. Box 3930 Ullevaal Stadion, NO-0806 Oslo, NORWAY, Farrokh.Nadim@ngi.no

Ochiai Hirotaka Foresty and Forest Product Research Institute, Japan

Pari Walter Instituto Geologico Minero y Metalurgico de Peru

Picarelli Luciano Second Napoli University, Italy, via Roma 29 - 81031 Aversa (CE) ITALY, luciano.picarelli@unina2.it

Popescu E. Mihail Illinois Institute of Technology, 6117 River Bend Drive, Lisle, Illinois 60532, USA, mepopescu@usa.com

C. Puglisi ENEA, Via Anguillarese, 301 – 00060 S. Maria di Galeria, Rome, Italy

Righini Gaia Department of Earth Sciences, University of Firenze, Italy

Rouhban Badaoui UNESCO, France

Sasahara Katsuo Kochi University, Japan

Sassa Kyoji International Consortium on Landslides, UNITWIN H.Q. Building, Uji Campus, Kyoto University, Gakasho, Uji 611-0011, Japan, sassa@iclq.org

Shaw Rajib Graduate School of Global Environmental Studies, Kyoto University, Yoshida Honmachi, Sakyo-ku, Kyoto 606-8501, JAPAN, shaw@global.mbox.media.kyoto-u.ac.jp

Shiao-Yun Wong G&P Geotechnics, Malaysia

Shigeki Takatsu CTI Engineering Co. Ltd., Tokyo, Japan

Sidle Roy Kyoto University, Kyoto, Japan

Singhroy Vern Canada Centre for Remote Sensing, 588 Booth St, Ottawa, KIA0Y7, Canada, vern.singhroy@ccrs.nrcan.gc.ca

D. Spizzichino Consorzio Civita, Via del Corso 300, 00186 Rome, Italy; ISPRA – Italian Institute for Environment Protection and Research – Via Curtatone 3, 00185, Rome, Italy

Strom L. Alexander Institute of Geospheres Dynamics, RAS, Leninskiy Avenue, 38, Building 1, 119334, Moscow, Russia, a.strom@g23.relcom.ru

Takaaki Ikeda Research Institute of Technology, Tobishima Corporation, Chiba, Japan

Takahashi Tamotsu Assoc. for Disaster Prevention Research, Japan, Tanaka-Asukaicho 138-1, Sakyo-ku, Kyoto 606-8226, Japan, ta-taka@iris.eonet.ne.jp

Takara Kaoru Kyoto University, Kyoto, Japan

Takeuchi Yukiko Kyoto University, Kyoto, Japan

D. Tarchi European Commission, Joint Research Centre, SERAC Unit, Via E. Fermi, 1 - TP 723, 21020 Ispra (VA) – Italy

Tofani Veronica Department of Earth Sciences, University of Firenze, Italy

Vilímek Vít Department of Physical Geography and Geoecology, Faculty of Science, Charles University, Albertov 6, 128 43 Prague 2, Czech Republic, vilimek@natur.cuni.cz

Wang Fawu Kyoto University, Kyoto, Japan

Wang Yi Environment and Sustainable Development Program, United Nations University, Tokyo

Yin Yueping China Geological Survey, China

Zvelebil Jiří Geological Survey of Czech Republic

Part I

Progress of IPL Activities

Progress of the International Programme on Landslides (IPL) – Objectives of the IPL and the World Landslide Forum

1

Kyoji Sassa

Abstract The First World Landslide Forum is organized on 18–21 November 2008 at the United Nations University, Tokyo, Japan. Landslides are known to cause significant disasters every year over many parts of the world. The risk reduction of disastrous landslides is essential for the Hyogo Framework for Action 2005–2015 "Building the Resilience of Nations and Communities to Disasters" which was adopted during the United Nations World Conference on Disaster Reduction (WCDR) held in Kobe, Japan in 2005.

The International Consortium on Landslides (ICL), United Nations Organizations, Governments and Non-government organizations collaborated to organize a global cross-cutting and cooperative platform for the 2006 Tokyo Action Plan. As a basis of joint discussion for the development of the International Programme on Landslides (IPL) during and after the 2008 World Landslide Forum, the process from the 2002 establishment of ICL to the organization of 2008 WLF and their concepts are presented herein.

Keywords Landslides • Disaster risk reduction • International Consortium on Landslides (ICL) • International Programme on Landslides (IPL) • World Conference on Disaster Reduction (WCDR)

1.1 Establishment of ICL and IPL

Landslide researchers and representatives from United Nations Organizations related to landslides attended the UNESCO-Kyoto University Joint symposium "Landslide risk mitigation and cultural and natural heritage" held in January 2002 in Kyoto, Japan. The symposium was supported by the Ministry of Foreign Affairs of Japan and the Japanese National Commission for UNESCO. Participants included Mr. Michel Jarraud, Secretary-General of World Meteorological Agency, Badaoui Rouhban (Section Chief for Disaster Reduction of UNESCO), Andras Szollosi-Nagy (Director of Water Science, UNESCO), Pedro Basabe (Technical Advisor of UN/ISDR) in the present affiliation, as well as Robert Schuster (the First Varnes Medal recipient), Paolo Canuti (University of Florence) and many other landslide experts. Participants from the scientific community, United Nations Organizations and Governments examined the need to establish an organization promoting research and learning to reduce the impact of landslide disasters. Consequently, they agreed to establish an International Consortium on Landslides (ICL) by adopting the 2002 Kyoto Declaration,

K. Sassa (✉)
President of International Consortium on Landslide,
Director of IPL World Centre

K. Sassa, P. Canuti (eds.), *Landslides – Disaster Risk Reduction*,
© Springer-Verlag Berlin Heidelberg 2009

the Statutes of ICL, and the nomination K. Sassa as the first President.

2002 Kyoto Declaration "Establishment of an International Consortium on Landslides

We, international experts in the fields of landslide research, disaster reduction, in particular landslide risk mitigation and protection of cultural and natural heritage, who are gathering in the ICL Foundation Meeting held in the International Symposium on Landslide Risk Mitigation and Protection of Cultural and Natural Heritage organized in January 2002 in Kyoto, discussed the foundation of an international non-governmental and non-profit making scientific organization named as an International Consortium on Landslides (ICL) to promote and coordinate landslide research for the benefit of society and the environment in the global scale, and agreed on the following principal objectives of ICL:

(1) To promote landslide research and capacity building including education for the benefit of society and the environment;
(2) To integrate geosciences and technology within the appropriate cultural and social contexts with an aim to evaluate landslide risk in urban, rural and developing areas and cultural and natural heritage sites, as well as to contribute to the protection of the natural environment and sites of high societal value;
(3) To combine and coordinate international expertise in landslide risk assessment and mitigation studies, thereby resulting in a renowned international organization, which will act as a partner in various international and national projects; and
(4) To promote a global multidisciplinary Programme on landslides.

Members of ICL shall include, inter alia, (a) Intergovernmental entities, (b) Non-governmental Organizations, (c) Governmental agencies and departments, universities, research institutes and other public institutions and (d) Other organizations that support the objectives of ICL intellectually, practically and financially. The United Nations system Organizations, entities and Programmes will be invited to provide special support.

Accordingly, we have unanimously agreed and declared to found the International Consortium on Landslides under the Statutes attached.

Date: 21 January 2002
Place: Kyoto, Japan

Fig. 1.1 presents a group photo of participants of this founding meeting of ICL.

Following the ICL foundation meeting, two Interim Steering Committee meetings of ICL were organized in Prague and UNESCO. A new global multidisciplinary Programme on landslides originally proposed in the 2002 Kyoto Declaration was developed and named the International Programme on Landslides (IPL). Basic principles regarding the ICL and IPL management and the bylaws were established. Members of ICL were called. The initial 33 ICL members gathered at the First Session of the Board of Representatives held at UNESCO Headquarters in Paris, France. The International Programme on Landslides was then formally initiated. The publication of the New International Journal "Landslides" was the primary and life-time project of the International Programme on Landslides. The publication started in April 2004. The journal was the first full color scientific journal without additional color contribution fee. The common information for various specific fields of landslide scientists and engineers is photos of landslides. Full color publication of photos, geological maps and cross sections, and other information are vitally important for the cross-disciplinary field of landslide science.

1.2 Motivation for IPL and ICL

Most of the initial members of ICL were members of the UNESCO and IUGS (International Union of

Fig. 1.1 Establishment of the international consortium on landslides on 21 January 2002

Geological Sciences) joint programme called as IGCP (International Geological Correlation Programme, later changed to International Geoscience Programme), No. 425 entitled "Landslide hazard assessment and mitigation for Cultural heritage sites and other locations of high societal value". The project started in 1998 and terminated 2004 during which time it supported 31 subprojects from various countries. The budget allocated from the IGCP was approximately 4000 USD/year. As with most IGCP projects, this funding was shared amongst participants to the meeting of IGCP-425. It was a few hundred USD per each subproject. However, this "seed" funding and the authorization as a sub-project of the international programme was very effective for obtaining evaluation and raising funds in each country. Subsequently, participants wished to create a New International Programme focusing on Landslides by themselves as an evolution of IGCP-425. It was clear that no existing organization was able to create such a "consortium" because "landslides" are a marginal issue for most other existing organizations. The founding members aimed to launch an international organization (ICL) focusing on Landslides to host a new International Programme for Landslide research and capacity building (IPL). Therefore, ICL itself was not the main purpose of the members, but rather it was to create an organization to host the IPL.

1.3 Development of IPL from WCDR to Tokyo Action Plan

The United Nations World Conference on Disaster Reduction (WCDR) was organized in Kobe, Japan in 18–22 January 2005. Many UN organizations, government organizations, and Non-governmental organizations joined this conference to contribute towards an International Strategy for Disaster Reduction (ISDR). ICL organized a thematic session 3.8 "New International Initiative for Research and Risk Mitigation of Floods (IFI) and Landslides (IPL) together with UNESCO, WMO, FAO, UNU, IAHS, Kyoto University, Public Works Research Institute, etc. Originally the flood group and landslide group planned to organize events independently, but were advised to combine by the UN/ISDR office. As a result, it was quite successful. Within the session, ICL proposed a

> Letter of Intent concerning strengthening cooperation in research and learning on earth system risk analysis and sustainable disaster management within ISDR.

It was agreed and approved by seven global stakeholders of UNESCO, WMO, FAO, UN/ISDR,

Fig. 1.2 Round table discussion based on the letter of intent to promote the international programme on landslides

UNU, ICSU (International Council for Science) and WFEO (World Federation of Engineering Organizations). The electronically combined Letter of Intent is attached at the end of this article. This Letter of Intent by 7 global stakeholders is one of several milestones for the development of the International Programme on Landslides.

To implement an activity related to this Letter of Intent, ICL, UNESCO, WMO, FAO, UN/ISDR, UNEP, UNU and Kyoto University jointly organized the Round Table Discussion on Strengthening Research and Learning on Earth System Risk Analysis and Sustainable Disaster Management within UN-ISDR as regards "Landslides", toward a dynamic global network of International Progrmme on Landslides (IPL) on 18–20 January 2006 at the United Nations University, Tokyo, Japan.

Figure 1.2 shows the participants of the 3 days long round table discussion, where participants agreed and approved the 2006 Tokyo Action Plan for the activities in the field of landslides until the next milestone of WCDR in 2015. The Tokyo Action Plan is the most important achievement of ICL and ICL supporting organizations to contribute to the landslide disaster reduction. It is attached in the end of this chapter.

1.4 Objectives of IPL

The International Program on Landslides (IPL) is an international initiative of the IPL Global Promotion Committee which consists of members of the International Consortium on Landslides and ICL supporting organizations.

IPL aims to conduct international cooperative research and capacity building on landslide risk mitigation, notably in developing countries. Protection of cultural and natural heritage will be addressed for the benefit of society and the environment. The activities of IPL will contribute to the International Strategy for Disaster Reduction (ISDR).

The IPL projects will comprise 3 types as shown in Fig. 1.3:

1) Core project: Landslide Journal (C100) for the life time of IPL

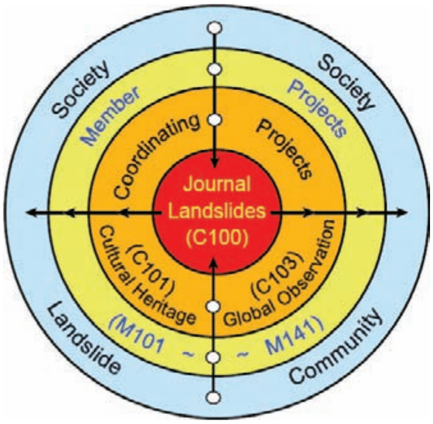

Fig. 1.3 Types of international programme on landslides

2) Coordinating Projects which are proposed and approved by IPL Global Promotion Committee for the long term (more than 5 years)
3) Member projects which are proposed by one or more ICL members and approved by IPL Global Promotion Committee (2–5 years)

The policy and basic principle of IPL adopted in the first IPL Global Promotion Committee in 2007 is;

1) IPL member projects will be proposed to the IPL Global Promotion Committee from ICL members. When it will be approved by the IPL Global Promotion Committee, it is identified to be an on-going IPL member project.
2) IPL Coordinating projects may be suggested by anybody in the IPL Global Promotion Committee. When it will be approved after examination by the Committee, it is identified to be an on-going IPL coordinating project.
3) ICL supporting members which exchange MoU with ICL or provide Subvention to IPL and all ICL members have voting rights in the decision on IPL project and its management in the IPL Global Promotion Committee. One member organization has one voting right.
4) Global Stakeholders and Government agencies which are willing to support IPL are invited to the IPL Global Promotion Committee as supporting members.
5) IPL projects shall be applied to the IPL Global Promotion Committee using the following Proposal Form.

1.5 Objectives of WLF

The First World Landslide Forum aims to create a global cross-cutting information and cooperative platform for all types of organizations from academia, United Nations, governments, private sectors, and individuals that are contributing to landslide research and learning, and also willing to strengthen landslide and other related earth system risk reduction. The objectives of WLF are;

1.5.1 Promotion of Research and Exchange of Experience

Various types of meetings are proposed and organized including open forums, symposia, thematic sessions, panel discussion, dialogues on country landslide issues, consultation of specific landslide and monthly exhibition. Research and exchange of experience are promoted through these activities.

1.5.2 Advances and Achievements of IPL

Proposals and reports on IPL projects will be presented for the planned global cooperating fields, which are listed hereafter.

1.5.3 Nomination of the World Centres of Excellence on Landslide Risk Reduction

The IPL Global Promotion Committee is now calling for application from candidates of the World Centre of Excellence. The explanation of WCoE is as follows:

The 2006 Tokyo Action Plan proposed the creation of World Centres of Excellence on Landslide Risk Reduction as follows: "The Global Promotion Committee (GPC) of the International Programme on Landslides (IPL) will identify and promote World Centres of Excellence (WCoEs) every 3 years within eligible organizations, such as universities, institutes, NGOs, government ministries and local governments, contributing to "Risk Reduction for Landslides and Related Earth System Disasters". Linkages to WCoEs at the national level will be used to promote cooperation with the ICL and dissemination of knowledge and information. An independent Panel of Experts, set up by the Global Promotion Committee of International Programme on Landslides (IPL-GPC), may be appointed to endorse the WCoEs. The establishment of WCoE was decided at the first session of the IPL Global Promotion committee in January 2007, and further examined and endorsed during the second session of the IPL Global Promotion Committee held at UNU on 21 January 2008.

Objectives of WCoE:

To strengthen the International Programme on Landslides (IPL) and IPL Global Promotion Committee;

To create "A Global Network of entities contributing to landslide risk reduction"; and

To improve the global recognition of "Landslide Risk Reduction" and its social-economic relevance, and entities contributing to this field.

Criteria for WCoE Candidates:

Governmental and non-governmental entities such as universities, agencies, and other institutions, and their subsidiary entities (faculties, departments, centres, divisions or others) which meet the following two conditions:

- Contributing to "Risk Reduction for Landslides and Related Earth System Disasters"; and
- Willing to support IPL intellectually, practically and financially by either joining ICL or contributing to IPL-GPC and promote "landslide research and risk reduction" on a regional and/or global scale in a mutually beneficial manner.

Acknowledgement We wish to develop an effective global cooperation network for research and leaning on landslide risk mitigation through the Forum and the follow-up activities, and our landslide community can contribute to the Hyogo Framework for Action 2005–2015 "Building the Resilience of Nations and Communities to Disasters". Finally we appreciate the encouragement and continued support we obtain from United Nations Organizations, Governments, NGOs as well as individual landslide experts since the foundation of ICL in January 2002.

LETTER OF INTENT

"United Nations World Conference on Disaster Reduction (WCDR)", Kobe, Japan, 18-22 January 2005

This 'Letter of intent' aims to provide a platform for a holistic approach in research and learning on 'Integrated Earth system risk analysis and sustainable disaster management'.

Rationale

- Understanding that any discussion about global sustainable development without addressing the issue of Disaster Risk Reduction is incomplete;
- Acknowledging that risk-prevention policies including warning systems related to Natural Hazards must be improved or established;
- Underlining that disasters affect poor people and developing countries disproportionately;
- Stressing that after years of under-investment in preventive scientific, technical and communicational infrastructure activities it is time to change course and develop all activities needed to better understand natural hazards and to reduce the vulnerability notably of developing countries to natural hazards, and
- Acknowledging that a harmful deficiency in coordination and communication measurements related to Disaster Risk Reduction exists.

Proposal

Representatives of United Nations Organisations, as well as the Scientific (ICSU) and Engineering (WFEO) Communities propose to promote further joint global activities in disaster reduction and risk prevention through

Strengthening research and learning on 'Earth System Risk Analysis and Sustainable Disaster Management' within the framework of the 'United Nations International Strategy for Disaster Risk Reduction' (ISDR).

More specifically it is proposed,

based on the existing structural framework of the ISDR and plan of action of the UN-WCDR, as well as other relevant networks and institutional and international expertise,

to establish specific, goal-oriented 'Memoranda of Understanding' (MoUs) between international stakeholders targeting Disaster Risk Reduction, for example focusing on landslide risk reduction, and other natural hazards.

Invitation

Global, regional and national competent institutions are invited to support this initiative by joining any of the specific MoUs following this letter through participation in clearly defined projects related to the issues and objectives of any of the MoUs.

Signatories:

Mr. Koïchiro Matsuura
Director-General
United Nations Educational, Scientific and Cultural Organization
4 MAR 2005
Date

Mr. Michel Jarraud
Secretary-General
World Meteorological Organization
22. 3. 2005
Date

Mr. Jacques Diouf
Director-General
Food and Agriculture Organization of the United Nations
21. VI. 2005
Date

Mr. Sálvano Briceño
Director
UN International Strategy for Disaster Risk Reduction
19.01.05
Date

Mr. Hans van Ginkel
Rector
United Nations University
19.01.05.
Date

Ms. Jane Lubchenco
President
International Council for Science
21. 04. 05
Date

Ms Françoise Come
Executive Director
World Federation of Engineering Organizations
24/ 2/ 2005
Date

The International Consortium on Landslides (ICL) proposed the "Letter of Intent" at the thematic session 3.8 "New International Initiatives for Research and Risk Mitigation of Floods (IFI) and Landslides (IPL)" of the United Nations World Conference on Disaster Reduction held on 19 January 2005 in Kobe, Japan. This is the Letter of Intent, which was electronically combined based on the original Letters of Intent, formally approved and signed by all parties. All of the original Letters of Intent with signatures are deposited in the secretariat of the International Consortium on Landslides which is located in the Research Centre on Landslides of the Disaster Prevention Research Institute, Kyoto University.

ICL

International Consortium on Landslides

Secretariat : Research Centre on Landslides, Disaster Prevention Research Institute, Kyoto University, Kyoto, Japan
Web: http://ICL.dpri.kyoto-u.ac.jp, E-mail: jimu@landslide.dpri.kyoto-u.ac.jp, Tel: +81-774-38-4110, Fax: +81-774-32-5597

The 2006 Tokyo Action Plan

Strengthening Research and Learning on Landslides and Related Earth System Disasters for Global Risk Preparedness

Adopted in the Round Table Discussion on 20 January 2006 in Elizabeth Rose Hall of the United Nations University, Tokyo

The 2006 Tokyo Round Table Discussion "Strengthening Research and Learning on Earth System Risk Analysis and Sustainable Disaster Management within UN-ISDR as Regards Landslides" -towards a dynamic global network of the International Programme on Landslides (IPL) was held at the United Nations University, Tokyo, from 18th to 20th January, 2006 to formulate a framework for cooperation and to identify focus areas to reduce landslide risk worldwide. The following action plan was adopted as a summary of the meeting, to be implemented within the scope of the Hyogo Framework for Action 2005–2015, "Building the Resilience of Nations and Communities to Disasters", declared at the United Nations World Conference on Disaster Reduction held in Kobe, Japan in 2005.

Preamble

Large and small landslides occur almost every year in nearly all regions of the world. Fig. 1 shows the example for casualties in Japan for 1967–2004. Landslide disasters in Japan have occurred every year; the total number of deaths due to landslides is about one half of those caused by earthquakes, including the catastrophic 1995 Kobe earthquake.

"Landslides" are a complex-disaster phenomenon that can be caused by earthquakes, volcanic eruptions, heavy rainfall (typhoons, hurricanes), sustained rainfall, heavy snowmelt, unregulated anthropogenic developments, mining, and others (Fig. 2a). Large-scale coastal or marine landslides are known to cause tsunami waves that kill many people; an example was the 1792 UNZEN-Mayuyama landslide, which caused a devastating tsunami that resulted in 16,000 fatalities from the landslides and the tsunami in Japan. Also large-scale landslides on volcanoes can dislocate the mountain tops and trigger volcanic eruptions; such was the case for the 1980 eruption of Mount St. Helens in the USA and presumably for Mt. Bandai in Japan. Landslides also may occur without earthquakes, heavy rains, volcanic eruptions, or

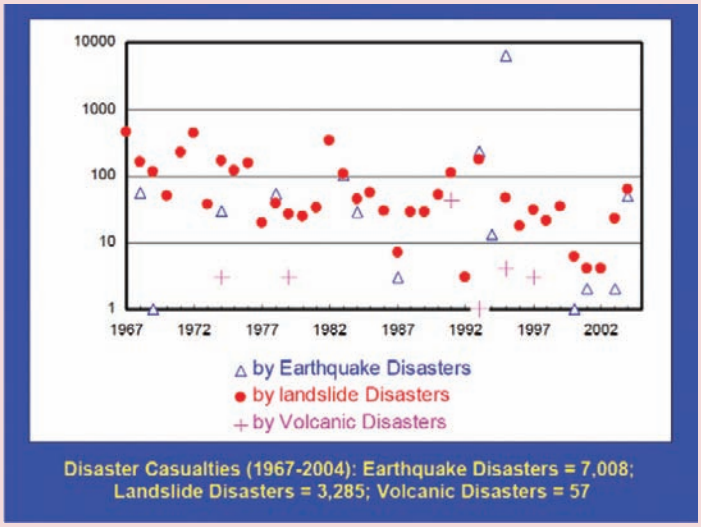

Fig. 1 Comparison of the numbers of victims in Japan from 1967–2004 due to landslide disasters, earthquake disasters including deaths by earthquake-induced-landslides, and volcanic disasters including deaths due to volcanic gas (The statistics of victims by landslide disasters since 1967 was published by the Sabo Technical Center)

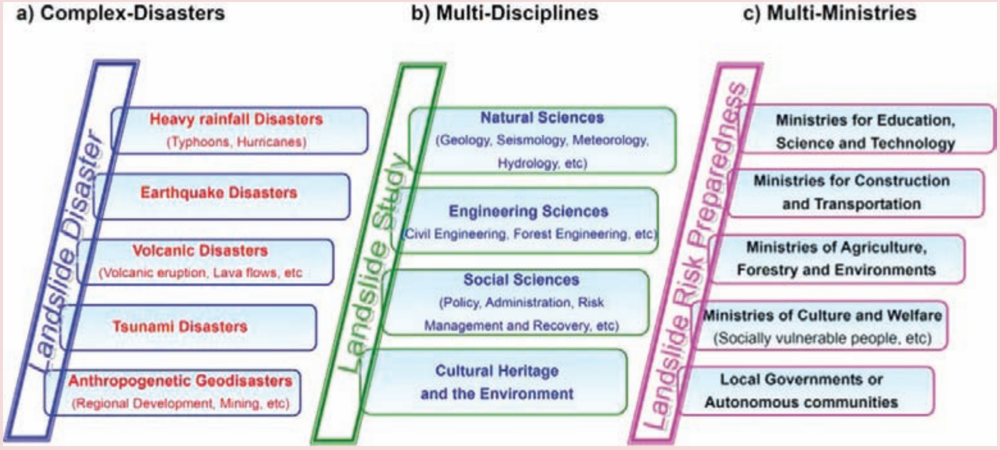

Fig. 2 Characteristics of landslide disasters

human activities due to progress of natural weathering; therefore, they occur almost everywhere in the world. Landslides most commonly impact residents living on and around slopes.

Landslides are a natural phenomenon which can only be effectively studied in an integrated, multi-disciplinary fashion, including contribution from different natural and engineering sciences (earth and water sciences), and different social sciences. This is also the case because landslides are strongly related to cultural heritage and the environment (Fig. 2b). Landslides should be jointly managed by cooperation of different ministries and departments of government including some representing education, science and technology, construction and transportation, agriculture, forestry, and the environment, culture and vulnerable groups (the poor, aged, handicapped, or children). As landslides are highly localized phenomena it is crucial to seek the contribution of local governments or autonomous communities (Fig. 2c).

The disasters caused by landslides are of very complex nature wherever they occur around the world. Research on landslides should be integrated into a new multi-disciplinary science field of landslide study. Landslide risk preparedness is to be managed by multi-ministries.

Action Plan

Global cooperation in landslide-risk reduction research and learning will be carried out encompassing related disasters affecting the earth-system, such as heavy rainfall, earthquakes, volcanic eruptions, tsunamis, and disasters of anthropogenic origin. Establishment of a 'Dynamic Global Network of the International Programme on Landslides" and its operation will effectively function for landslide and related risk reduction through the implementation of the following Action Items adopting a multi-hazard, multi-sectoral approach;

Actions

1. Establishment of the IPL Framework

(1) Establishment of the IPL Global Promotion Committee

The IPL Global Promotion Committee shall be established by ICL members and ICL supporting organizations, as illustrated in Fig. 3. The committee will meet annually, on the occasion of ICL Board of Representative meetings, or possibly at other occasions and locations. The committee will conceive a strategy to promote the 2006 Tokyo Action Plan, and will discuss the management of IPL global cooperation fields, and their possible modification, selection, and termination.

Fig. 3 Structure of the IPL global-cooperation framework

(2) Establishment of IPL World Centre

The IPL World Centre will be established to coordinate and support implementation of the global cooperating fields of the International Programme on Landslides (IPL), which works as the secretariat of the IPL Global Promotion Committee and the International Programme on Landslides (IPL). The Centre will be hosted by the Headquarter of the UNESCO-KU-ICL UNITWIN Cooperation Programme "Landslide Risk Mitigation for Society and the Environment" in the Research Centre on Landslides, Disaster Prevention Research Institute, Kyoto University, Kyoto, Japan, where the secretariat of the International Programme on Landslides has been located since its foundation in 2002.

2. Promotion of the Global Cooperating Fields of the International Programme on Landslides (IPL)

The global cooperating fields of IPL are identified as follows for the initial phase:

(1) Technology Development

A. Monitoring and Early Warning

- Use of various on-site, in-situ technologies, as well as satellite observations in monitoring landslide effects and contributing factors for early-warning purposes
- Development of automated monitoring methods covering large spatial extent and real-time data communication, as well as low-cost monitoring devices
- Development of early-warning methodologies, in particular for rain-induced landslides
- Applications linking meteorological, hydrological and landslide models

B. Hazard Mapping, Vulnerability and Risk Assessment

- Hazard Mapping at local and global scales
- Vulnerability assessment, considering human life, land resources, structures, infrastructure, and cultural heritage
- Risk assessment and communicating risk in an easily understood manner

(2) Targeted Landslides: Mechanisms and Impacts

A. Catastrophic Landslides
- Catastrophic landslides induced by natural and anthropogenic factors such as rainfall, earthquakes, volcanic activity, river erosion, and human activities, and their combinations
- Landslides threatening human lives and high societal values
- Gigantic coastal landslides and marine landslides causing tsunamis

B. Landslides Threatening Heritage Sites
- Studies for protection of cultural heritage, cultural landscape, and the natural heritage from landslides using non-invasive technologies and appropriate mitigation strategies (e.g. Machu Picchu, Bamiyan, Lishan, Cordillera Blanca)

(3) Capacity Building

A. Enhancing Human and Institutional Capacities
- Building human capacities and expertise in landslide management
- Institution building at national and local levels through Centers of Excellence
- Enhancing implementation and action at local level

B. Collating and Disseminating Information/Knowledge
- Developing a culture of awareness on landslide risks
- Developing model policy frameworks, standards, guidelines/checklists, and training modules.

(4) Mitigation, Preparedness and Recovery

A. Preparedness
- Strengthening disaster preparedness of all stakeholders
- Strengthening capacities of communities and local institutions to cope with landslide hazards
- Forecasting and providing early warning of adverse conditions likely to lead to landslide activity
- Preparing contingency recovery plans, including pre-positioning of technical and material resources for likely landslide events

B. Mitigation
- Development of innovative, low-cost, and ecologically appropriate landslide mitigation techniques
- Mountain conservation methods, including soil conservation, forest and watershed management, and appropriate land-use techniques
- Appropriate civil engineering works, including construction and urban and coastal development;
- Restricting inappropriate development in landslide prone areas
- Development of appropriate policy and planning mechanisms, such as land-use management (including zoning)
- Promotion and strengthening of monitoring and warning systems

C. Recovery
- Post-landslide recovery and rebuilding efforts should integrate landslide mitigation measures
- Prevention of secondary risks of landslides resulting from inappropriate re-building efforts in response to any disaster (for example, earthquakes, volcanic eruptions, extreme weather events, etc.)
- Implementation of landslide recovery efforts and programmes (including psycho-social and health aspects) with the participation of affected communities and local authorities
- Providing long-term support to ensure sustainable recovery

3. **Promotional Activities**

(a) **World Landslides Forum**

Capitalizing on the competence, international experience and established organizational network of ICL-IPL, it is proposed to create a global information platform for future joint activities of the world-wide landslide community, named the 'World Landslide Forum' that shall be convened every 3 years.

The first World Landslides Forum – organized by the ICL – can be planned to take place in January 2009, bringing together academics, practitioners, politicians, et al. to a global, multi-disciplinary, problem-focused platform. This forum will provide an opportunity for the first identification of a WCoE. Linkages to ISDR activities, as well as other global events, including the World Water Forum, the International Year of Planet Earth, etc., will be established.

(b) **Identificaion and Promotion of Workd Centres of Excellence on Landslide Risk Reduction**

The IPL Global Promotion Committee will identify and promote World Centres of Excellence (WCoE) every 3 years within eligible organizations, such as universities, institutes, NGOs, government ministries and local governments, contributing to "Risk Reduction for Landslides and Related Earth System Disasters". Linkages to CoE at the national level will be used to promote cooperation with the ICL and dissemination of knowledge and information. An independent Panel of Experts, set up by the Global Promotion Committee of IPL, may be appointed to endorse the CoEs.

(c) **Contributions to Global Landslide Issues**

The IPL will mobilize global cooperation for strengthening research and learning on risk reduction for landslides and related earth system disasters at sites identified as of great concern to the global community, such as Macchu-Picchu, the Kashmir, Central Asia high mountainous area, and Bamiyan.

(d) **Partnerships**

Mutually beneficial partnerships with other global initiatives, such as the International Hydrological Program (IHP), the International Geoscience Program (IGCP), and The Mountain Partnership will be developed.

2 Projects of International Programme on Landslides

Nicola Casagli, Giacomo Falorni and Veronica Tofani

2.1 Background

The International Program on Landslides (IPL) was launched in 2002 as an initiative of the International Consortium on Landslides (ICL). The main goal of the program is to conduct cooperative research and capacity building on landslide risk mitigation, with particular emphasis on developing countries. Within this framework the different projects carried out under the IPL umbrella aim to contribute to the International Strategy for Disaster Reduction (ISDR).

The IPL Global Promotion Committee was established within the 2006 Tokyo Action Plan. The Committee consists of ICL members and ICL supporting organizations and convenes annually during the ICL Board of Representatives meetings, and occasionally during other international events. The main objectives of the committee are to conceive the strategies for promoting the 2006 Tokyo Action Plan, and to manage the IPL global cooperation fields, the topics that are considered by IPL as the most relevant for promoting international research, cooperation and capacity building on landslide risk mitigation. Since its establishment IPL has supported over 60 projects worldwide (Fig. 2.1).

Nicola Casagli (✉)
Department of Earth Sciences, University of Firenze,
Via Giorgio La Pira 4, 50121 Firenze, Italy

Giacomo Falorni
Department of Earth Sciences, University of Firenze, Italy

Veronica Tofani
Department of Earth Sciences, University of Firenze, Italy

2.2 The Global Cooperation Fields

In the initial stages of the IPL several global cooperation fields (GCFs) have been identified as priorities. These can be modified in the future, following new technological developments or changing global scenarios. The global cooperation fields were indentified in the 2006 Tokyo Action Plan which is attached in the end of Chapter 1 "Progress of the International Programme on Landslides – Objectives of IPL and WLF and the World Landslide Forum-" of this book.

2.3 Overview of IPL Projects

In total, over 60 projects have been carried out within the IPL community. Each year new projects are proposed, ongoing projects are sustained and completed projects are brought to a close. A comprehensive overview of the status of all IPL projects is listed in Annex 2.1. Projects have regarded many different areas of landslide research and engineering, creating opportunities of communication and collaborative work between scientists and researchers from five continents (Fig. 2.2).

The geographic distribution of projects can also be analyzed based on the countries involved (Fig. 2.3). At least 23 nations have participated in IPL projects. In cases of special interest, such as the Machu Picchu Citadel in Peru, many international consortiums have teamed up to analyze all aspects of

© Springer-Verlag Berlin Heidelberg 2009

Fig. 2.1 Worldwide distribution of IPL projects. Yellow stars mark countries with at least one project

landslide risk, leading to a concentration of projects in these areas of particular societal value.

The IPL Promotion committee will continue working on encouraging scientists and researchers all around the world to apply for landslide-related projects, and continue its scientific and financial support of these initiatives.

The IPL Promotion committee will also work towards the definition of global strategies for landslide research with an aim to help bringing different actors together for the benefit of landslide research, engineering, and best practices.

Brief descriptions of the Coordinating projects and of some Member projects follow.

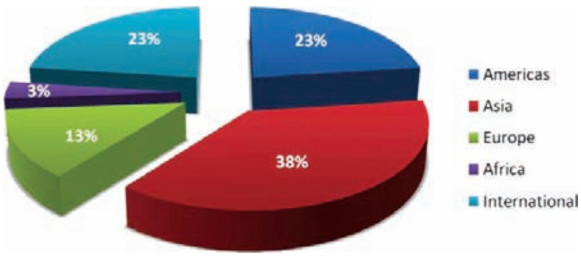

Fig. 2.2 Distribution of IPL projects. International projects are those with a global outreach

Some projects were terminated as IPL projects in 2007 and restarted as New IPL projects managed by the IPL Global Promotion Committee in 2008. Those are presented as 2002/2008.

Coordinating projects

Project no: C100
Project title: Landslides: Journal of the International Consortium on Landslides
Leader: Kyoji Sassa
Period: 2002/2008–
Status: In progress
Main Project field: (3) Capacity Building (B. Collating and Disseminating Information/Knowledge)
Description: The aim of the journal Landslides is to be the common platform for the publication of integrated research on landslide processes, hazards, risk analysis, mitigation, and the protection of our cultural heritage and the environment. Landslides are gravitational mass movements of rock, debris or earth. They may occur in conjunction with other major natural disasters such as floods, earthquakes and volcanic eruptions. Expanding urbanization and changing land-use practices have increased the incidence of landslide disasters. Landslides as catastrophic events include human injury, loss of

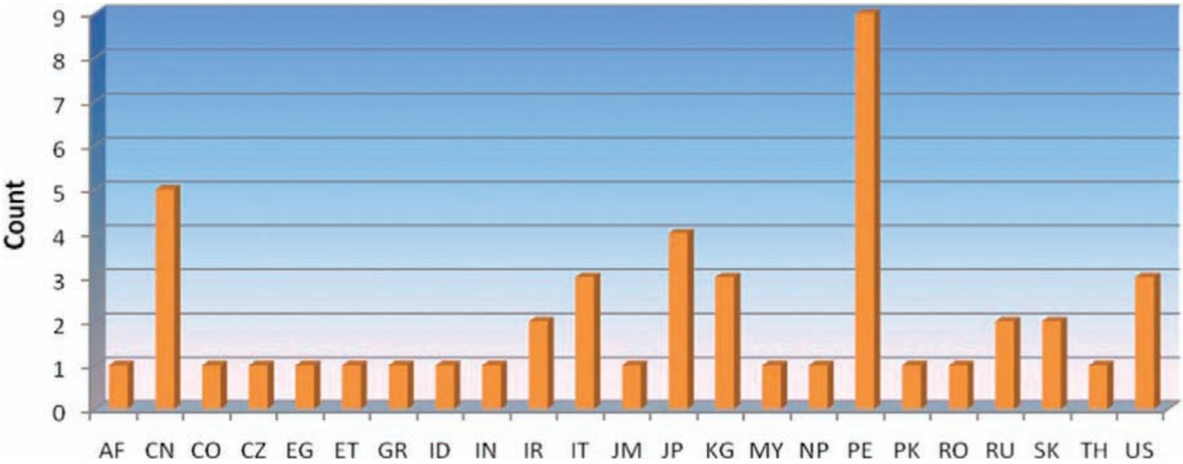

Fig. 2.3 Number of IPL projects per country. The horizontal axis contains the country codes

life and economic devastation and are studied as part of the fields of earth, water and engineering sciences. The journal publishes research papers, news of recent landslide events and information on the activities of the International Consortium on Landslides. The main topics are:

- Landslide dynamics, mechanisms and processes
- Landslide risk evaluation: hazard assessment, hazard mapping, and vulnerability assessment
- Geological, Geotechnical, Hydrological and Geophysical modeling
- Effects of meteorological, hydrological and global climatic change factors
- Monitoring including remote sensing and other non-invasive systems
- New technology, expert and intelligent systems
- Application of GIS techniques
- Rock slides, rock falls, debris flows, earth flows, and lateral spreads
- Large-scale landslides, lahars and pyroclastic flows in volcanic zones
- Marine and reservoir related landslides
- Landslide related tsunamis and seiches
- Landslide disasters in urban areas and along critical infrastructure
- Landslides and natural resources
- Land development and land-use practices
- Landslide remedial measures/prevention works
- Temporal and spatial prediction of landslides
- Early warning and evacuation
- Global landslide database

Project no: C101-1
Project title: Landslide investigation and capacity building in Machu Picchu – Aguas Calientes area.
Leader: Kyoji Sassa
Period: 2002/2008–
Status: In progress
Main Project field: (2) Targeted landslides: mechanism and impacts (B. Landslide threatening heritage sites)
Description: The objectives of the project are to assess the landslide risk in the in Machu Picchu – Aguas Calientes area and to build human capacities and expertise in landslide risk management in order to educate people to protect themselves and to reduce the landslide risk using landslide monitoring and early warning system.

The area of Machu Picchu – Aguas Calientes is very dangerous, being often affected by landslides, debris flows and rock falls. Many of poor people are working in the Machu Picchu areas because of recent rapid development of tourism. They do not have enough knowledge and experience on landslides and their risk reduction measures.

The Project will be carried out through the installation of landslide monitoring system at the toe of Machu Picchu slope and of debris flow detectors in two debris flow torrents in Aguas Calientes area.

Furthermore education of residents and officers of the Municipality of Machu Picchu will be done. A workshop in the Peruvian Embassy in Tokyo will be organized in order to disseminate theachieved results to wider public.

Project no: C101-1-1
Project title: Low environmental impact technologies for slope monitoring by radar interferometry: application to Machu Picchu site
Leader: Claudio Margottini
Period: 2002–2006
Status: Completed
Main Project field: (2) Targeted landslides: mechanism and impacts (B. Landslide threatening heritage sites)
Description: The project proposes the application of an integrated package of advanced technologies for remote slope monitoring. Synthetic aperture radar interferometry (SAR), implemented from satellite and ground-based installations, is the core of this integrated package, which also comprehends GPS, optical/satellite image interpretation, field surveys and geological/geomorphological investigations. The proposed techniques are particularly suitable for archaeological sites due to their remote sensing nature, their low environmental impact, and the possibility of investigating surface movements over large areas without direct access to the unstable sites.

All the activities which have been carried out during the project are:

- collection and survey of basic data (geology, geomorphology, etc.) on the large Inca Park area (32 km^2);
- development of remote sensing monitoring by means of satellite radar interferometry; calibration with GPS network;
- geomorphological hazard map of the large Inca Park area:
- application of ground based radar at a specific site, selected on the base of task 3 and local specific needs; calibration with GPS network;
- geomorphological hazard and risk map for local site (Machupicchu hill);
- definition of low environmental impact mitigation strategies.

Project no: C101-1-2
Project title: Expressions of risky geomorphologic processes in deformations of rock structures at Machu Picchu
Leader: Vit Vilimek and Jiri Zvelebil
Period: 2002–2007
Status: Completed
Main Project field: (2) Targeted landslides: mechanism and impacts (B. Landslide threatening heritage sites)
Description: The objectives are:

- Evaluation of recent geomorphologic processes as well as paleogeographical evolution of the area of Mach Picchu Sanctuary. Multihazard analysis.
- Dilatometric monitoring of displacements of rock outcrops;
- extenzometric monitoring across main Plaza.
- Hydrogeological investigations (reveal the role of water in destruction of some structures in the archaeological area)
- Weathering analysis and relative dating.
- General field research of debris flows in the surrounded area of the archaeological site.

Project no: C101-1-3
Project title: Shallow geophysics and terrain stability mapping techniques applied to the Urubamba Valley, Peru: Landslide hazard evaluation
Leader: Romulo Mucho and Peter Bobrowsky
Period: 2002–2006
Status: Completed
Main Project field: (2) Targeted landslides: mechanism and impacts (B. Landslide threatening heritage sites)
Description: The objective of this project is to apply a suite of shallow geophysical techniques at Machu Picchu in order to evaluate the nature and character of overburden and bedrock at this World Heritage Site. The methods are all nondestructive and non-invasive and provide a good three-dimensional expression of the subsurface which can then be used by archaeologists, geologists and engineers for slope stability analysis and mitigation.

The aim of this collaborative work is to establish the presence or absence of shear planes, failure planes and/or significant faults at the site and determine their importance in potentially triggering landslides. This work is important because the nature of this site limits the possibility of using subsurface drilling methods for confirmation of models. The shallow geophysical results will be the only evidence available for assessing the subsurface and proving/disproving the landslide potential theory.

Project no: C101-2
Project title: Landslides monitoring and slope instability at selected historic sites in Slovakia
Leader: Jan Vlcko
Period: 2002–
Status: In progress
Main Project field: (1) Technological development (A. Monitoring and early warning)
Description: The objectives are to clarify deep seated deformations mechanism including preparatory factors on selected historic sites with the help of advanced monitoring techniques, including monitoring of thermomechanical rock behavior and methods reliable to predict the slope movement behavior.

The studies carried out in project proved that volume change of the rock is irreversible and brings permanent thermal deformation to the rock or rock mass. In order to better understand these processes the project will focus our attention to the study of thermo-mechanical behavior of rocks or rock mass which form the subgrade of several historic sites in Slovakia. The combination of in situ monitoring techniques and laboratory tests will provide quantitative data which will serve as input for modeling of the slope failure mechanism and thus to create the prediction models of slope failure development in space and time and should serve as a practical tool for the recommendation of effective remedial measures.

Project no: C101-3
Project title: The geomorphological instability of the Buddha niches and surrounding cliff in Bamiyan valley (Central Afghanistan)
Leader: Claudio Margottini
Period: 2002/2008–
Status: In progress
Main Project field: (2) Targeted landslides: mechanism and impacts (B. Landslide threatening heritage sites)
Description: The project it is aimed at (i) investigating major processes occurring on the niches and cliff, natural and consequence of explosion, (ii) defining a feasibility project for the complete restoration of the cultural heritage site, (iii) defining some practical emergency intervention, considered as part of the general master plan, (iv) concluding the complete restoration of the site.

The Bamiyan valley is located in central Afghanistan, in a mountainous region, in a dry part of the world, which experiences extremes of climate and weather. The explosion of March 2001, apart the collapse of statues, produced a deterioration of the stability conditions, mainly in the shallower part of the niches.

In the small Buddha niche, apart the collapse of statue, three minor rock falls occurred in the top of it. In the mean time the blasting produced a degradation of the upper-right part of the niche, where a stair-cave is located inside the cliff and the sect between the stairs and the niche is quite thin (about 30–50 cm). This part is presently the most critical for future stability. The left side, as consequence of the existing buttress, did not suffered substantially. Only in the upper part a rock fall occurred and some instabilities are now evident.

In the great Buddha major effect were the collapse of statue and the consequent instability of the back side of the niche. A small rock fall occurred on the top of the niche, left side. Probably, the large thickness of sect between the stairs going up into the cliff and the niche (about 1 m), did not allow a large propagation of the effects of blasting and than a severe damage.

A feasibility project (master plan) for the entire consolidation of the niches and cliff was prepared. This include mainly control of water circulation on the top of the cliff, nails, anchors and grouting, exhibiting low environmental impact on the site.

Project no: C101-4
Project title: Stability assessment and prevention measurement of Lishan Landslide, Xian, China Valley
Leader: Qing Jin Yang
Period: 2002–2007
Status: Completed
Main Project field: (2) Targeted landslides: mechanism and impacts (B. Landslide threatening heritage sites)
Description: Lishan's landslide is located in Lishan National Forest Park, in the south of Huaqing pool. The landslide directly threatens Lishan National Forest Park and Huaqing pool. It is important for protecting Huaqing pool and Lishan, the venerable cultural remains and the famous beauty spots to monitor the landslide for a long time, knowing the distortion of it, and the taking the corresponding defence.

The landslide has widely been monitored. The main methods include: measured the inclined change in vertical holes, measured the level change by GTS, measured the ground stretch, and measured the 3D form change in level bores. After analyzed the results of measure, we found there were obvious distortions in II area of the landslide.

Project no: C101-5
Project title: Environment protection and disaster mitigation of rock avalanches landslides and debris flow in Tianchi Lake region and natural preservation area of Changbai Mountains, Northeast China
Leader: Binglan Cao
Period: 2002–2007
Status: Completed
Main Project field: (2) Targeted landslides: mechanism and impacts (B. Landslide threatening heritage sites)
Description: The objectives of the project are:

- To study the properties and formation conditions of avalanche, landslide and debris flow.
- To analyze the activities and the formation mechanism and activity regularity of avalanche, landslide and debris flow.
- Stability analysis of some special slope, as well as to predict the hazard of rock avalanche and landslide.
- To study the types and distribution of debris flow, as well as to evaluate the risk degree of debris flow.
- To put forward the measurement and strategy of the reserved area.

During the project various kinds of tests, including normal regular tests and ring- shear tests, have been conducted on weak volcanic rocks and have been investigated types and formation conditions of rock avalanches, landslides and to evaluate and to simulate the key mount slope, meanwhile to analyze the stability of slope by calculating debris flows. Furthermore suggestions for disaster risk mitigation have been suggested.

Project no: C102
Project title: Assessment of global high-risk landslide disaster hotspots
Leader: Farrokh Nadim
Period: 2002–2004
Status: Completed
Main Project field: (1) Technological development (B. Hazard mapping, Vulnerability and Risk Assessment)
Description: The objective of this project is to develop global hazard and risk maps for landslides and avalanches in order to identify the most exposed countries. Allocating resources for natural hazard risk management has high priority in development banks and international agencies working in developing countries. Based on the global datasets of climate, lithology, earthquake activity, and topography, areas with the highest hazard, or "hotspots", were identied. The applied model was based on classed values of all input data. The model output is a landslide and avalanche hazard index, which is globally scaled into nine levels. The model results were calibrated and validated in selected areas where good data on slide events exist. The results from the landslide and avalanche hazard model together with global population data were then used as input for the risk assessment. Regions with the highest risk can be found in Colombia, Tajikistan, India, and Nepal where the estimated number of people killed per year per 100 km2 was found to be greater than one. The model made a reasonable prediction of the landslide hazard in 240 of 249 countries. More and better input data could improve the model further. Future work will focus on selected areas to study the applicability of the model on national and regional scales.

Project no: C103
Project title: Global Landslides Observation Strategy
Leader: Kaoru Takara and Nicola Casagli
Period: 2004/2008–
Status: In progress
Main Project field: (1) Technological development (A. Monitoring and early warning)
Description: This project seeks better methodologies for monitoring and forecasting landslides in many hazardous areas in the world by using earth observation systems including satellite, airborne and ground-based remote sensing techniques, and facilitate focused pilot studies by providing new in situ instrumental and mapping support.

The project will:

(1) Advocate integration of InSAR technology into landslide disaster warning and prediction systems. The ERS (European Remote Sensing) and Envisat missions of the European Space Agency

(ESA) have pioneered these applications and shall be continued for global, long-term applications. As part of this effort, facilitate efficient exploitation of data from Japan's upcoming Advanced Land Observation Satellite (ALOS) with PALSAR, an L-band SAR sensor (spatial resolution of 10 m).

(2) Utilize other high-resolution optical sensors relevant to landslide monitoring and detection, such as QUICKBIRD and IKONOS (1 m), ALOS's PRISM (2.5 m) and AVNIR-2 (10 m), and terra/ASTER (15 m). A passive-microwave capability would help in determining soil moisture repeatedly over broad areas.

(3) Facilitate the development and sharing of critical airborne sensors and capabilities, such as hyper-spectral sensors, high-resolution infrared sensors, synthetic aperture radar (SAR) and LiDAR.

(4) Facilitate the development and sharing of remote sensors using ground-based platforms such as SAR, infrared cameras, laser scanners and hyper-spectral sensors.

(5) Advocate systematic expansion of landslide zonation maps, Geographic GIS and GPS as critical tools for managing spatial information for disaster management, including precision topography, mapping support, and deformation monitoring, as well as geolocation for search and rescue operations.

(6) Facilitate ongoing capacity building activities, with a focus on transferring technologies and best practices: dissemination of real-time information and early warnings to end users and the public, in concert with efforts by UNESCO and WMO to expand and improve sediment- and flood-related initiatives.

Project no: C104
Project title: World landslide database
Leader: Hiroshi Fukuoka and Nicola Casagli
Period: 2006/2008–
Status: In progress
Main Project field: (3) Capacity Building (B. Collating and Disseminating Information/Knowledge)
Description: The objectives are: (i) to create a global landslide database of major events considering only those which have caused fatalities; (ii) to register them in a standard data-format on-line; (iii) to represent them on a global map service on the web.

To date a global landslide database does not exist. In the 90's two major projects were carried out: the World Area Slope Stability Server (WASSS) and the World Landslide Inventory (WLI) but in both cases they failed to obtain a complete worldwide coverage. Several national databases exist which, in most cases, are very accurate but often they are not homogenous at a national level and their criteria are not comparable across nations. Today, new technologies on on-line information management, satellite imagery, geolocalization and mapping services could allow us to organize a trans-national database with the continuous inbuilt updating system.

The world landslide database will be carried through the preparation of a standard and simple data collection and the selection of relevant information sources. Furthermore a continuous and automatic collection of information using web-syndication systems will be set up together with a web distributed database. An appropriate mapping service platform will be selected and implemented.

Project no: C105
Project title: Early Warning of Landslides
Leader: Kyoji Sassa
Period: 2007–
Status: In progress
Main Project field: (1) Technology Development B. Monitoring and Early Warning
Description: The objectives is to develop early warning system which are suitable for Asian countries and to implement capacity building through international cooperation within participating institutions.

The project will develop a feasible and effective monitoring system suitable for landslides in Asian countries. Using satellite data and landslide susceptibility map will be made and time prediction of landslide initiation will be developed based on rainfall data, meteorological forecast, and landslide monitoring using extensometers and others.

Spatial prediction based on ring shear test and computer simulation will be carried out, and the methodology will be improved.

Furthermore disaster risk mitigation policy and governmental administration will be examined including the population shifts and vulnerability change due to urban development.

Project no: C106-1
Project title: Landslide museum in Civita di Bagnoregio
Leader: Claudio Margottini
Period: 2006/2008–
Status: In progress
Main Project field: (3) Capacity Building B. Collating and Disseminating Information/Knowledge
Description: The objectives is to increase awareness in the field of landslides, through the spectacularisation of recent and historic mass movements, as well as to show methodologies and tools for managing landslides hazards.

Civita di Bagnoregio lies in a hilly area surrounded by steep valleys intensively eroded by two torrents presenting an E-W direction. Due to the particular geological and geomorphological features, large and frequent slope instability phenomena occur: in the clayey formation landslides are represented by mudflows, debris-flows and rotational slides, while in the upper portion of the volcanic cliff, due to a retrogressive mechanism of erosion, rock-falls, toppling and block-slides are the common landslide typologies.

In the last decade many landslides have affected the northern border of the cliff of Civita largely increasing the risk conditions of that area of the town. ENEA and other partners, starting from two decades of monitoring results, have presented an innovative project of consolidation that takes into account properly the geological dynamics acting on the town as well as the particular historical and environmental context of the area.

The present museum will be an exhibition for landslide phenomena but also the main portal to the real museum that is outside, on the cliff and valleys. The visitors will find in the museum many scenic spot that are presented from a "Landslide" point of view but, in the mean time, they will be encouraged to visit the real site and to touch by hand the reality.

Project no: C106-2
Project title: International Summer School on Rockslides and Related Phenomena in the Kokomeren River Valley, Tien Shan, Kyrgyzstan
Leader: Alexander Strom
Period: 2008–2010
Status: In progress
Main Project fields: (3) Capacity Building B. Collating and Disseminating Information/Knowledge
Description: The aim of the International Field Summer School is to demonstrate to students and young landslide researchers various types of bedrock landslides and basic methods of their identification and study directly at the rockslide sites. Analysis of the relationships between rockslides, active tectonics manifestations, evidences of river valley inundation and outburst flooding will promote better understanding of bedrock slopes failure causes and of rockslide hazard assessment.

Numerous rockslides and rock avalanches of various types ranging from few millions to more than 1 billion cubic meters in volume are concentrated in the Kokomeren River valley (Central Tien Shan) within a limited area of about 40×40 km at a one-day trip distance from Bishkek city – capital of Kyrgyzstan. Most of them are located near a road along the Kokomeren River connecting villages in the Suusamyr and Djumgal depressions. Sites in tributary valleys without motorways require only a few hours of hiking to reach them.

Besides rockslides and landslides, the study area is extremely rich in the expressive manifestations of Neotectonics and Quaternary tectonics such as active faults, one of which had been ruptured by 1992 M7.3 Suusamyr earthquake, and numerous examples of tilted and folded pre-Neogene planation surface.

The annual ICL International Summer School has been organized since 2006. It was attended by participants from Czech Republic, Italy, USA and Kyrgyzstan. In 2008 it is planned to organize similar ICL training course focused basically on the geological and geomorphic features typical of large rockslides in rugged terrain. It will be supplemented with the training course organized within the frames of the EU Specific Support Action "International Working Group on Natural Hazards in the Tien Shan" (NATASHA) that will be focused more on the geophysical and geotechnical methods of rockslide field studies.

Member projects

Project no: M101
Project title: Areal Prediction of Earthquake and Rain Induced Rapid and Long-Traveling Flow Phenomena (APERITIF)

Leader: Hiroshi Fukuoka
Period: 2002/2008–
Status: In progress
Main Project fields: (1) Technology Development B. Hazard Mapping, Vulnerability and Risk Assessment
Description: The objective is to develop a practical method for site prediction and movement assessment of rapid and long run-out landslides. Among various landslide types, the rapid, and long run-out landslides, especially those that occur in urbanizing areas often cause catastrophic damage to the community.

APERITIF project consists of following 3 subprojects.

1. Mechanism of rapid long-runout landslides triggered by earthquakes and heavy rainfall:

   This sub-project uses the new ring shear apparatus with a special sample box visible from outside for research on the mechanisms of generation of sliding-surface liquefaction, funded and developed by the 2001-2003 APERIF project. Undrained torque-controlled/speed-controlled ring shear tests, triaxial tests, and flume tests will be conducted for the study of fluidization mechanism. Portable ring shear apparatus and vane-type apparatus for in-situ measurement of grain-crushing susceptibility will be developed and a new index for sliding-surface liquefaction will be proposed.
2. Research on process and areal prediction of flowslides:

   This sub-project uses a large flume for real-scale flowslides in a large-scale rainfall simulator, and middle size flume in Tsukuba to conduct tests on heavy rainfall induced flowslides. The study will focus on processes and mechanisms of landslide mass fluidization. Development of a new and sophisticated flowslide movement simulation program is being developed for the purpose of practical areal prediction of landslide runout. Ball and rectangle element DEM simulation approach for fluidization mechanism is conducted.
3. Integrated study for prediction of landslide hazards in urbanized areas:

   Applying new techniques developed by the previously noted two sub-projects, with all researchers cooperating on establishing the methodology for producing practical landslide hazard maps for the three sites in the urbanized residential areas of urbanizing area of big cities.

Project no: M103
Project title: Capacity building on the management of risks caused by landslides in Central America countries.
Leader: Farrokh Nadim
Period: 2002–2007
Status: Completed
Main Project fields: (3) Capacity building A. Enhancing Human and Institutional Capacities
Description: The objectives of the project are (i) to improve the knowledge and skills of professionals from a selection of relevant organizations in the region who are dealing with landslide hazards, (ii) to create a forum and network where representatives from the Central America countries can exchange experience, derive common methodologies and assist each other on practical issues when needed, and (iii) to create mechanisms that secure dissemination of knowledge and methodologies generated in the capacity building program to a larger audience.

One week training program with 18 participating middle managers from Costa Rica, Panama, Nicaragua, Honduras, El Salvador and Guatemala was executed in April 2005 at University of Costa Rica with NGI/ICG as facilitator. The training program included 24 technical presentations, 3 sessions with group discussions and one day with field work studying possible landslide mitigation measures and use of early warning system for a debris flow threatened community outside the capital city.

Project no: M106
Project title: A best practices handbook for landslide hazard mitigation
Leader: Lynn Highland and Peter Bobrowsky
Period: 2002–2007
Status: Completed
Main Project fields: (3) Capacity Building B. Collating and Disseminating Information/Knowledge
Description: This handbook will be distributed worldwide, and will be published in English, French, Spanish, Chinese, and other languages as needed, and as funds become available. It is a small, "pocketbook" size, with a spiral binding for durability, and

can be easily understood in simplified language with many graphics, illustrations, and photos.

Project no: M110
Project title: Capacity Building in Landslide Hazard Management and Control for Mountainous Developing Countries in Asia
Leader: Hideaki Marui
Period: 2002–2007
Status: Completed
Main Project fields: (3) Capacity building A. Enhancing Human and Institutional Capacities
Description: The objective is to improve the knowledge and skills of professionals and officials of the academic institutions as well as implementing organizations in South and Central Asian Countries in Landslide Hazard Management and Control through the enhancement of capacities of those institutions/individuals by the organization of training courses and seminars on the proposed field.

The Project M110 has played a certain role according to the direction of the capacity building activity proposed in the Tokyo Action Plan in 2006. Annual meetings in the framework of the M110 project were organized every year since 2003 in Niigata and Kathmandu. Major agenda discussed throughout the annual meetings are as follows:

- Present education on Landslide hazard management and control in Southern and Central Asian Countries
- Existing data base of landslides in those countries
- Primary areas to be focused for the training courses and seminars in those countries
- Responsible institutions for the landslide management and control in those countries
- Possible cooperation from various national and international organizations

Through the discussions necessary contents and curriculum for training courses are clarified. Although practical training courses were not realized until now because of financial problem, basic framework for implementation of training courses is formed.

Project no: M111
Project title: Detail study of the internal structure of large rockslide dams in the Tien Shan and the International field mission “Internal structure of the dissected rockslide dams in Kyrgyzstan”
Leader: Alexander Strom
Period: 2002–2006
Status: Completed
Main Project fields: (2) Targeted Landslides: Mechanisms and Impacts B. Catastrophic landslides
Description: The objective of the project was to focus on comprehensive study of rockslides that had been completely dissected by subsequent erosion. They are considered as analogues of existing rockslide dams. Such investigations allow studying internal structure and geotechnical parameters of rockslide deposits in such detail that is practically inaccessible at most of the present-day (and future) natural dams. Thus, results for these investigations can be used for natural dams hazard assessment and for blast-fill dams design. Another goal of the Project was to acquaint International community of landslide researchers with very interesting case studies from the Tien Shan Region.

An important part of the Project was to collect reliable data on grain-size composition of rockslide debris, especially from those parts of rockslide bodies that were strongly comminuted. To be able to deal with debris containing fragments up to first decimetres in size we collected several large samples from 40 to more than 100 kg. Large verity of rockslides and rock avalanches that are located in the Kokomeren River valley, which was the key region for this Project makes it an excellent place for students’ training in various methods of rockslide identification, mapping, dating and detail study.

Project no: M122
Project title: Inka Cultural Heritage And Landslides: Detailed Studies In Cusco And Sacred Valleys, Peru
Leader: Raul Carreno
Period: 2004–2007
Status: Completed
Main Project fields: (2) Targeted Landslides: Mechanisms and Impacts B. Landslides Threatening Heritage Sites
Description: The objectives of the project are:

- To contribute to the preservation and rational exploitation of the Inka cultural heritage.
- To identify and to evaluate the instability phenomena threatening or destroying inka cultural heritage.
- To propose monitoring programs and appropriate remediation projects for the critical cases.

The project point to identify, understand and evaluate the instability processes that are menacing the cultural heritage. Neither geological nor geodynamic detailed studies of the archaeological heritage exist. The conservation-restoration programs carried-out by the entities in charge of this task don't consider the geological risks, so they become very relative to protect this heritage. Excluding Machupicchu, the IPL M-122 is the first systematic project in this field carried out in Cusco region.

The results of the project must be useful to improve the conservation activities and to plan a sustainable exploitation of this cultural-tourist resource, the main (almost the only) development possibility for the Cusco region.

The project includes detailed geological and geomorphologic studies, the active and potential instability phenomena characterization and evaluation, the evaluation of conjugated dangers, and the geotechnical analysis of the critical cases. Starting from this information different monitoring systems and remediation programs have been proposed for each case.

Annex 2.1 Status of IPL Projects

Project Code	Project Name	Coordinator	Period	Status
C100	Landslides: Journal of the International Consortium on Landslides	Kyoji Sassa	2002/2008–	In progress
C101	Landslide risk evaluation and mitigation in cultural and natural heritage sites	Kyoji Sassa and Paolo Canuti	2002/2008–	In progress
C101-1	Landslide investigation and capacity buildng in Machu Pichu- Aguas Calientes area	Kyoji Sassa	2002/2008–	In progress
C101-1-1	Low environmental impact technologies for slope monitoring by radar interferometry: application to Machu Picchu site	Claudio Margottini	2002–2006	Completed
C101-1-2	Expressions of risky geomorphologic processes as well as paleogeographical evolution of the area of Machu Picchu	Vit Vilimek, Jiri Zvelebil	2002–2007	Completed
C101-1-3	Shallow geophysics and terrain stability mapping techniques applied to the Urubamba Valley, Peru: Landslide hazard evaluation	Romulo Mucho, Peter Bobrowsky	2004–2006	Completed
C101-1-4	A proposal for an integrated geophysical study of the Cuzco region	Daniel Nieto Yabar	2004–2006	Completed
C101-1-5	UNESCO-Italian-ESA Satellite monitoring of Machu Picchu	Paolo Canuti, Claudio Margottini, Fabio Rocca	2004–2006	Completed
C101-2	Landslides monitoring and slope stability at selected historic sites in Slovakia	Jan Vlcko	2002/2008–	In progress
C101-3	The geomorphological instability of the Buddha niches and surrounding cliff in Bamiyan valley (Central Afghanistan)	Claudio Margottini	2002/2008–	In progress
C101-4	Stability assessment and prevention measurement of Lishan Landslide, Xian, China	Qing Jin Yang	2002–2007	Completed
C101-5	Environment protection and disaster mitigation of rock avalanches landslides and debris flow in Tianchi Lake region and natural preservation area of Changbai Mountains, Northeast China	Binglan Cao	2002–2007	Completed

Annex 2.1 (continued)

Project Code	Project Name	Coordinator	Period	Status
C101-6	Conservation of Masouleh Town	S. H. Tabatabaei	2002–2007	Completed
C101-7	Cultural and natural heritage threatened by landslides in the region of Iassy, Romania	Nicolae Botu	2005–2007	Completed
C102	Assessment of global high-risk landslide disaster hotspots	Farrokh Nadim	2002–2004	Completed
C103	Global landslide observation strategy	Kaoru Takara, Nicola Casagli	2004/2008–	In progress
C104	World Landslide Database	Hiroshi Fukuoka, Nicola Casagli	2006/2008–	In progress
C105	Early Warning of Landslides	Kyoji Sassa	2007–	In progress
C106	Capacity building and outreach	Claudio Margottini, Alexander Strom	2008–	In progress
C106-1	Landslide museum in Civita di Bagnoregio	Claudio Margottini	2006/2008–	In progress
C106-2	International Summer School on Rockslides and Related Phenomena in the Kokomeren River Valley, Tien Shan, Kyrgyzstan	Alexander Strom	2008–2010	In progress
M101	Areal prediction of earthquake and rain induced rapid and long-travelling flow phenomena (APERITIF)	Hiroshi Fukuoka	2002/2008–	In progress
M102	Disaster evaluation and mitigation of the giant Jinnosuke-dani Landslide in the Tedori water reservoir area, Japan	Tatsunori Matsumoto	2002–2004	Completed
M103	Capacity building on management of risks caused by landslides in Central American countries	Farrokh Nadim	2002–2007	Completed
M104	A global literature study on the use of critical rainfall intensity for warning against landslide disasters	Haakon Heyerdal	2002–2004	Completed
M105	Hurricane-flood-landslide continuum: a forecast system	Randall Updike	2002–2006	Completed
M106	A best practices handbook for landslide hazard mitigation	Lynn Highland, Peter Bobrowsky	2002–2007	Completed
M107	Landslide risk assessment in landslide prone regions of Slovakia – modelling of climatic changes impact	Rudolf Hozer	2002–2006	Completed
M108	Disaster evaluation and mitigation of landslides in the Three-Gorge water reservoir area, China	Renjie Ding	2002–2005	Completed
M109	Recognition, mitigation and control of landslides of flow type in Greater Kingston and adjoining parishes in Eastern Jamaica, including public education on landslide hazard	Rafi Ahmad	2002–2006	Completed
M110	Capacity Building in Landslide Hazard Management and Control for Mountainous Developing Countries in Asia	Hideaki Marui	2002–2007	Completed

Annex 2.1 (continued)

Project Code	Project Name	Coordinator	Period	Status
M111	Detail study of the internal structure of large rockslide dams in the Tien Shan and international field mission	Alexander Strom	2002–2006	Completed
M112	Landslide mapping and risk mitigation planning in Thailand	Saowanee Prachansri	2002/2008–	In progress
M113	Zone risk map: Towards harmonized, intercomparable landslide risk assessment and risk maps	Yasser Elshayeb	2002–2005	Completed
M114	Landslide hazard assessment along Tehran-Caspian seaside corridors	Zieaoddin Shoaei	2002–2007	Completed
M115	Establishment of a regional network for disaster mitigation, disaster education, and disaster database system in Asia	Ryuichi Yatabe	2003–2007	Completed
M116	Standardization of terminology, integration of information and the development of decision support software in the area of landslide hazards	Catherine Hickson	2003–2006	Completed
M117	Geomorphic Hazards from landslide dams	Oliver Korup	2003–2006	Completed
M118	Development of an expert DSS for assessing landscape impact mitigation works for cultural heritage at risk	Giuseppe Delmonaco	2003–2007	Completed
M119	Slope instability phenomena in Korinthos county	Nikos Nikolaou	2002–2005	Completed
M120	Landslide hazard zonation in Garwal using GIS and geological attributes	Ashok Kumar Pachauri	2003–2004	Completed
M121	Integrated system of a new generation for monitoring of dynamics of unstable rock slopes and rock fall early warning	Jiri Zvelebil, Vit Vilimek	2003–2007	Completed
M122	Inka cultural heritage and landslides: detailed studies in Cusco and Sacred Valleys, Peru	Raul Carreno	2004–2007	Completed
M123	Cusco regional landslide hazard mapping and preliminary assessment	Raul Carreno	2004–2007	Completed
M124	The influence of clay mineralogy and ground water chemistry on the mechanism of landslides	Viktor Osipov	2004–2007	Completed
M125	Landslide mechanisms on volcanic soils	Carlos Edusrdo Rodriguez	2004–2007	Completed
M126	Compliation of landslide / rockslide inventory of the Tien Shan mountain system	Alexander Strom	2004–2007	Completed
M127	Development of low-cost detector of slope instability for individual use	Ikuo Towhata	2004–2007	Completed
M128	Development of sounding methodology for a root-reinforced landslide mass	Kazuo Konagai	2004–2007	Completed
M129	Evaluation of natural hazards associated with rapid glacial retreat in Cordillera Blanca (Peru)	Vit Vilimek	2005–2007	Completed
M131	Technology development for landslide monitoring in China	Yueping Yin and Peter Bobrowsky	2006–2007	Completed

Annex 2.1 (continued)

Project Code	Project Name	Coordinator	Period	Status
M132	Research on vegetation protection system for highway soil slope in seasonal frozen regions	Wei Shan, Fawu Wang	2006/2008–	In progress
M133	Establishment of rainfall-soil chart for erosion induced landslide prediction	Roslan Abidin	2006–2007	Completed
M134	Large-scale rockslides in coarse-bedded carbonate rocks in the Apennines (Italy), Caucasus (Russia) and Zagros (Iran): evaluation of possible triggers and hazard assessment	Alexander Strom	2007–	In progress
M135	Landslide hazard assessment in Changunarayan hill of Kathmandu, Nepal - Geotechnical investigation and preventive plan-	Ryuichi Yatabe	2008–	In progress
M136	Shear behaviour and mechanics of Megaslides and their nearby faults in Hittian Balla, Pakistan and Shaolin, Taiwan	Kazuo Konagai, Kyoji Sassa	2008–	In progress
M137	Italian Landslide Inventory (IFFI Project)	Alessandro Triglia	2008–	In progress
M138	Long run out and Catastrophic Landslides study: Yigong Landslide, Tibet China.	Yin Yueping	2008–	In progress
M139	Development of low-cost early warning system of slope instability for civilian use	Ikuo Towhata, Taro Uchimura	2008–	In progress
M140	Landslide and multi geohazards mapping for community empowerment in Indonesia	Dwikorita Karnawati	2008–	In progress
M141	Geo-Risks Management for Third World Countries - Mapping and Assessment of Risky Geo-factors for Land Use (e.g. in Ethiopia)	Jiří Zvelebil	2008–	In progress

Note: All projects as IPL by ICL were completed in 2007. New projects by IPL Global Promotion Committee started either in 2007 or in 2008. Some projects restarted under the same or a slightly revised title in the same project number.

Part II

Keynote Lectures

3 Landslide Risk Assessment and Mitigation Strategy

Suzanne Lacasse and Farrokh Nadim

Abstract Each year, natural disasters cause countless deaths and formidable damage to infrastructure and the environment. In 2004–2005, more than 200 000 people lost their lives in natural disasters. Material damage was estimated at USD 300 billion. Many lives could have been saved if more had been known about forecasting and mitigation. The need to improve the ability to deal with the hazards and risks was accentuated by increased sliding and flooding in many regions around the world in recent years, concern for their disastrous consequences on mankind, infrastructure and material property and the catastrophic Indian Ocean tsunami in December 2004.

One of the most common natural disasters is landslides caused by heavy precipitation, floods, earthquakes and erosion, and by anthropogenic actions. Many of the casualties reported after rainstorms, large floods and earthquakes are actually caused by the landslides triggered by these events. Studies show that developing countries are greatly affected by landslides. Of the total number of persons who died due to natural disasters, highly developed countries count only 5% of the casualties. Material damage in Industrialized countries is however greatest. International collaboration is needed to reduce losses in countries where the landslide risk is high. The measures for effective mitigation require solutions encompassing the technological and the societal perspectives, which demonstrate the importance and challenge of a multi-disciplinary approach, where scientists and engineers need to interact and communicate freely with partners with entirely different backgrounds. The paper presents recent work on the assessment, mitigation and management of landslide risk, including several examples. Societal aspects risk, are considered. Early warning systems have gained strong interest in recent years. The paper goes into the principles and elements of early warning systems, the key factors for success and some of the available technology. Society and technologists need to invest into the mitigation of landslide hazard and risk to improve the reliability and efficiency of the results obtained.

Keywords Hazard • Vulnerability • Risk • Landslide

Suzanne Lacasse (✉)
ICG/NGI (International Centre for Geohazards/Norwegian Geotechnical Institute), Norway
e-mail: suzanne.lacasse@ngi.no

Farrokh Nadim
ICG/NGI (International Centre for Geohazards/Norwegian Geotechnical Institute), Norway
e-mail: farraokh.nadim@ngi.no

3.1 Introduction

“Geohazards”, i.e. natural hazards that are driven by geological features and processes, pose severe threats to humans, property and the natural and built environment. During 2005, geohazards

K. Sassa, P. Canuti (eds.), *Landslides – Disaster Risk Reduction*,
© Springer-Verlag Berlin Heidelberg 2009

accounted for about 100,000 deaths worldwide, of which 84% were due to October's South Asia earthquake. In that year, natural disasters affected 161 million people and cost around US$ 160 billion – over double the decade's annual average. Hurricane Katrina accounted for three quarters of this cost. During the period 1996 to 2005, natural disasters caused nearly one million lives lost, or double the figure for the previous decade, affecting 2.5 billion people across the globe (World Disaster Report 2006). When the trend of fatalities due to natural hazards is studied over the last 100 years, it appears that the increase in the known number of deaths is due to the increase in the exposed population in this time scale and the increased dissemination of the information, and not to an increase in the frequency and/or severity of natural hazards.

3.2 Threat Due to Landslides

Landslides represent a major threat to human life, property and constructed facilities, infrastructure and natural environment in most mountainous and hilly regions of the world (Nadim et al. 2006). Statistics from The Centre for Research on the Epidemiology of Disasters (CRED) show that landslides are responsible for at least 17% of all fatalities from natural hazards worldwide. The socio-economic impact of landslides is underestimated because landslides are usually not separated from other natural hazard triggers, such as extreme precipitation, earthquakes or floods. This underestimation contributes to reducing the awareness and concern of both authorities and general public about landslide risk.

In the last century, Europe has experienced the second highest number of fatalities and the highest economic losses caused by landslides compared to other continents (Fig. 3.1): 16,000 people have lost their lives because of landslides and the material losses amounted to over USD 1700 M in Europe during the 20th century. Within Europe, Italy has been the country that has suffered the greatest human and economic losses due to landslides. The actual casualty figures in Fig. 3.1 are likely to be greatly underestimated in the EM-DAT because events with less than 10 persons killed are not reported. Furthermore, the number of people affected by landslides is much larger than reported: in Italy, while about 500 people have been killed by landslides over the past 25 years, the total number of persons impacted is 50 times that number.

As a consequence of climate change and increase in exposure in many parts of the world, the risk associated with landslides is growing. In areas with high demographic density, protection works often cannot be built because of economic or environmental constraints, and is it not always possible to evacuate people because of societal reasons. One needs to forecast the occurrence of landslide and the hazard and risk associated with them. Climate change, increased susceptibility of surface soil to instability, anthropogenic activities, growing urbanisation, uncontrolled land-use and increased vulnerability of population and infrastructure as a result, contribute to the growing landslide risk. According to the European Union Strategy for Soil Protection (COM232/2006), landslides are one of the main eight threats to European soils.

Water has a major role in triggering of landslides. Fig. 3.2 shows the relative contribution of various

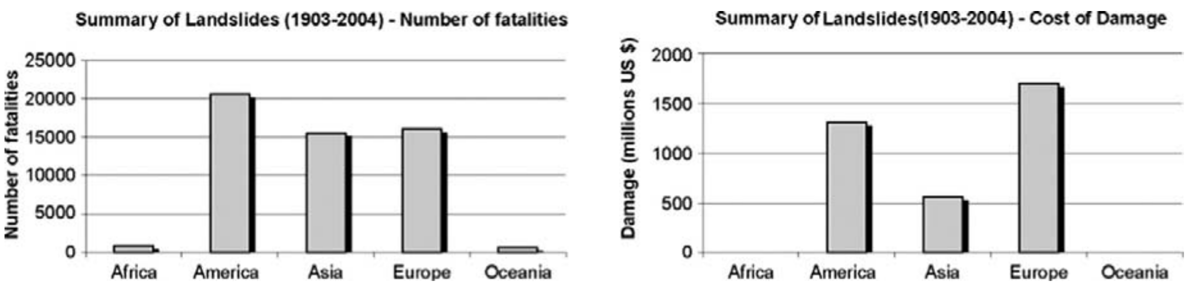

Fig. 3.1 Fatalities and cost of damage caused by landslides 1903 to 2004 (EM-DAT, OFDA/CRED International Disaster database)

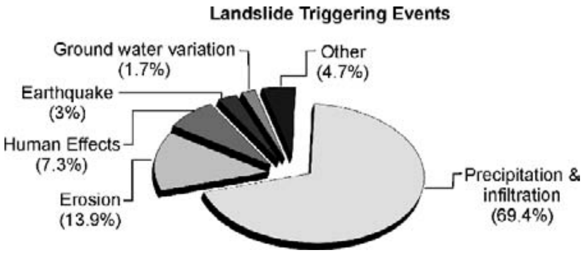

Fig. 3.2 Landslide triggers in Italy (CNR-GNDCI AVI Database of areas affected by landslides and floods in Italy)

landslide triggering events factor in Italy. Heavy rainfall is the main trigger for mudflows, the deadliest and most destructive of all landslides.

Many coastal regions have cliffs that are susceptible to failure from sea erosion (by undercutting at the toe) and their geometry (slope angle), resulting in loss of agricultural land and property. This can have a devastating effect on small communities. For instance, parts of the north-east coast cliffs of England are eroding at rates of 1 m/yr.

As a consequence of climatic changes and potential global warming, an increase of landslide activity is expected in the future, due to increased rainfalls, changes of hydrological cycles, more extreme weather, concentrated rain within shorter periods of time, meteorological events followed by sea storms causing coastal erosion and melting of snow and of frozen soils in the Alpine regions.

The growing hazard and risk, the need to protect people and property, the expected climate change and the reality for society to live with hazard and risk and the need to manage risk to set the agenda for the profession to assessing and mitigating landslide risk.

3.3 Examples of Slide Hazard

The main natural hazards in Norway are landslides, snow avalanches, floods and, to a lesser extent, earthquakes (Solheim et al. 2005a). Statistically, 10 large slides can be expected in the next 50–100 years, each with possibly 20–100 associated deaths. The number of lives lost due to all types of slides over the past 150 years exceeds 2000 in Norway.

3.3.1 Rock Slides

As the last glaciers receded, about 11,000 years ago, large portions of east and mid-Norway were left covered with clay deposits, while in other areas (western and northern Norway) high mountains rose and deep valleys were eroded. Many of the mountain sides and leached clay deposits were unstable, and, based on the landslide scars and moraine residues observed today, a large number of slides took place. The sliding activity also took place offshore in the North Sea and Norwegian Sea. Today, the profession knows that a number of large rock slides and clay slides occurred between 5,000 and 10,000 years ago. The sliding activity in Norway has continued since the last ice period, but less frequently than immediately after the retreat of the glaciers (Lied 2008). The sliding activity is expected to continue in the future.

Rockfalls and rockslides are among the most critical geohazards in Norway, mainly because of their tsunamigenic potential. The largest known rock slide in Norway is Tjelleskredet in Langfjorden in Romsdal in 1756. The 15 million m^3 slide triggered a tsunami with a height up to 50 m, causing 32 fatalities (Jørstad 1956).

The natural disasters causing the largest number of deaths in Norway in the 20th century involved large rock slides into fjords (narrow bodies of water) having generated a tsunami: Loen in 1905 (350,000 m^3, 40 m tsunami, 61 fatalities), 1936 (1,000,000 m^3, 74 m tsunami, 73 fatalities) and Tafjord in 1934 shown in Fig. 3.3 (1,500,000 m^3, 62 m tsunami, 41 fatalities) (Helland 1905; 1911; Helland and Steen 1895; Holmsen 1936; Grimstad 2005). In Loen, a rockslide of 1,000,000 m^3 also occurred in 1950, but caused no fatalities.

3.3.2 Quick Clay Landslides

About 5000 km^2 of Norway is covered by soft marine clay deposits. Nearly 20% of this area consists of highly sensitive or quick clay. Landslides in quick clay represent a common and important threat, especially in Norway and Sweden (and parts of Canada). Landslides in quick clay are frequently triggered without warning and turn into a flowing

Fig. 3.3 Municipality of Fjøra in Tafjord, Norway, before and after the tsunami triggered by a massive rockslide (April 1934)

Fig. 3.4 Quick clay slides in Norway: the Rissa slide, 1978 (*left*) and the Trøgstad slide, 1967 -1 million m^3, 4 fatalities- (*right*)

liquid in a matter of minutes, and they can progressively involve very large volumes of soil. Statistically, at intervals of about 4 years, large quick clay slides with moving clay masses of several million cubic metres occur in Norway (Aas 1979, 1981).The largest quick clay slide in Norway in the 20th century occurred at Rissa near Trondheim in 1978 (Fig. 3.3, left, Gregersen 1981), covering an area of 330,000 m^2. Near 6 million m^3 of clay moved out at high velocity. The largest historical quick clay slide in Norway occurred on 20 May 1893 in Verdal, north of Trondheim, where 55 million m^3 of clay ran out, and 116 fatalities were recorded. This is the largest known natural catastrophe in Norway in historical times.

A typical quick clay slide consists of a minor initial slide followed by a progressive failure process developing very rapidly in all directions from the first slide. The Rissa quick clay slide started with the failure of a small fill by a lakeside. The initial slide involved only 200 m^3 of sediments. It grew to 6 million m^3 in a few hours through retrogressive sliding.

3.3.3 Underwater Slides

The exploitation of offshore petroleum resources, development of oil and gas pipeline corridors, fishing habitat protection, and protection of coastal communities, have contributed to a growing interest in Norway for underwater slides, in particular seafloor mass movements and their consequences. The development of the Ormen Lange field, which is the second largest gas field on the Norwegian

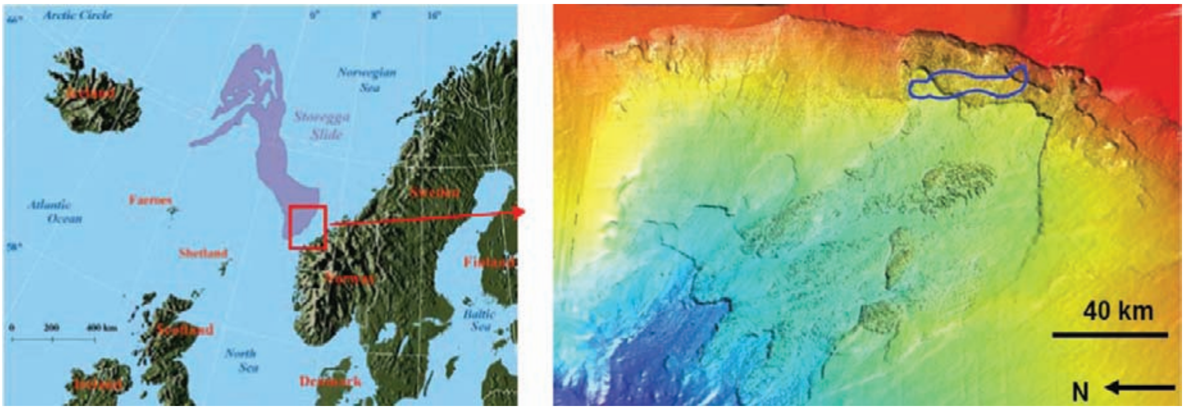

Fig. 3.5 Map of Storegga slide (*left*) and deepest part of Storegga slide scar, with outline of Ormen Lange gas field in blue (*right*)

Continental Shelf, contributed greatly to the understanding of underwater slides. The field is in the Norwegian Sea in water depths 800–1,100 m, approximately 120 km from the coastline, and within the scar of the prehistoric Storegga slide (Fig. 3.5). The Storegga slide, which took place 8,200 years ago, is one of the world's largest known submarine slides with an estimated slide volume in excess of 3,000 km^3 and run-out of 300 km (e.g. Solheim et al. 2005a,b). Evidence of a major tsunami generated by the Storegga slide has been found along the coasts of Norway, Scotland and the Faeroe Islands. Considering the enormity of the Storegga slide and the potentially catastrophic consequences of a similar event today, it was essential to clarify and quantify the risks associated with submarine slides in the area to obtain approval for field development from the authorities (Nadim et al. 2005; Bryn et al. 2005). The numerous studies carried out in the Ormen Lange offshore geohazards study were summarised in a special volume of Marine and Petroleum Geology journal in 2005.

3.3.4 Hazard Zonation

Many countries have experienced increased vulnerability to landslides and increased awareness of the need for mapping, due to industrial and recreational development over the entire country, infrastructure development, the consequences of interruption in the communication arteries and increase in population. A few major disasters in the past 30 years also helped "convince" the authorities to take preventive measures.

To increase safety and reduce hazard and risk, and to assist with emergency preparedness, a priority mapping is needed for landslides in clays, rock slides and snow avalanches. Susceptibility mapping has been done continuously in Norway since the late 1970 s. The hazard and risk maps are especially useful for prevention and the planning of new dwellings, schools, recreation areas, etc. The entire network of communication corridors and military and humanitarian (Red Cross) exercises have need for such maps (Karlsrud et al. 1984; Gregersen 1989).

3.4 Hazard and Risk Management

Risk management integrates the recognition and assessment of risk with the development of appropriate strategies for its mitigation. Landslide risk management typically (but not solely) involves decisions at the local level, and a lack of information about landslide risk and how this risk is changing on account of climate, land-use and other factors, appears to be a major constraint to providing improved mitigation in many areas. Beyond risk communication and awareness, pro-active mitigation and prevention options can broadly be categorised as (1) structural slope-stabilization measures to reduce the frequency and severity of the hazard, (2) non-structural measures, such as land-use planning and early warning systems, to reduce the hazard consequences, and measures to pool and transfer the risks. The selection of appropriate mitigation strategies should be based on a future-oriented quantitative probabilistic risk assessment, coupled with useful knowledge on the technical feasibility, as well as costs and benefits, of risk-reduction measures.

Figure 3.6 illustrates in a "bow-tie" diagram the components of hazard and risk mitigation. Risk is the measure of the probability and severity of an adverse event to life, health, property or the environment. Quantitatively, risk is the probability of an adverse event times the consequences if the event occurs, where the consequences are obtained from the elements at risk and their vulnerability. Mitigation of risk can be done by reducing the frequency (probability) of the adverse event or by reducing the vulnerability and/or exposure of the elements at risk, or even reducing both hazard and consequence.

Experts acting alone cannot choose the "appropriate" set of mitigation and prevention measures in many risk contexts. The complexities and technical details of managing landslide risk can easily conceal that any strategy is embedded in a social/political system and entails value judgments about who bears the risks and benefits, and who decides. Policy-makers and affected parties engaged in solving risk problems are increasingly recognizing that traditional expert-based decision-making processes are insufficient, especially in controversial risk contexts. Often shaped by scientific analysis and judgment (e.g. acceptable risk), traditional policy approaches are vulnerable to two major critiques: (1) because they de-emphasise the consideration of affected interests in favour of "objective" analyses, they suffer from a lack of popular acceptance; (2) because they rely on systematic observation, they often slight the local and anecdotal knowledge of the people most

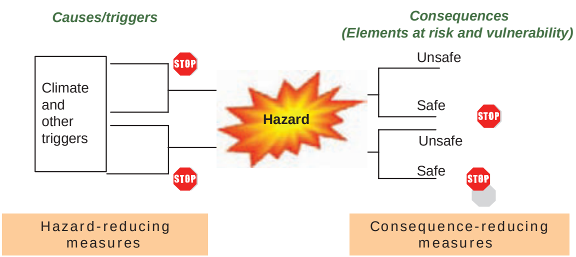

Fig. 3.6 Illustration of hazard and risk

familiar with the problem, and risk producing outcomes that are incomplete. Conflicting values and interests, as well as conflicting and uncertain expert evidence, characterise many landslide risk decision processes. These characteristics become more complex with long time horizons and uncertain information on climate and other global changes.

Risk communication and stakeholder involvement has been widely acknowledged for supporting decisions on uncertain and controversial environmental risks, with the added bonus that participation enables the addition of local and anecdotal knowledge of the people most familiar with the problem. Precisely which citizens, authorities, NGOs, industry groups, etc., should be involved in which way, however, has been the subject of much experimentation and theorising. The decision is ultimately made by political representatives, but stakeholder involvement, combined with good risk-communication strategies, can often bring new options to light and delineate the terrain for agreement.

3.4.1 Example – Hazard Assessment

The Building and Planning Act in Norway has been under development since 1924 and the act was put into force for the whole country in 1966. The last revision was done in 1987. The Building Act is used when a detailed hazard plan is made with corresponding detailed maps. The on-going hazard mapping on survey maps at 1:50,000 scale has been operative since 1979. The building council of the counties has to follow the rules stated in the Act. The assessment of hazard for natural events is subject to the Norwegian Planning and Building Law. According to the technical regulations in the law, three classes of avalanche and slide frequencies should be taken into account (Table 3.1). There is also a fourth class, where the consequences are so important that the buildings can not be placed in a "hazard zone". How one determines a "no-hazard" zone is however not defined. The building regulation states that rebuilding after fires or other kinds of reparation may be done for Class 2, when the nominal yearly frequency is less than 3 × 10–3, i.e. a return period of 333 years or more. By using the word "nominal" as opposed to "real", one admits

Table 3.1 Safety class in technical regulations in the norwegian planning and building law

Safety class	Maximum nominal frequency (per yr)	Return period (yrs)	Type of construction
1	10^{-2}	100	Garages, smaller storage rooms of one floor, boat houses
2	10^{-3}	1000	Dwelling houses up to two floors, operational buildings in agriculture
3	$<10^{-3}$	>1000	Hospital, schools, public halls, etc.

that the exact calculation of avalanche run-out distance for the given frequencies is not possible, and that the use of subjective judgment is necessary. The rules were first established for the mapping of snow avalanche hazard.

In Norway, ROS-analyses (vulnerability and risk analyses) are run before regulation plans and building requests can be approved. The ROS-process includes: (1) assembly of all relevant data from national or local databases, and new site investigations; (2) mapping of hazard and consequence; (3) presentation of proposed project to the county authority; (4) implementation in the existing regulation plan in the area; (5) if needed, requirement of further detailed analyses and iteration from start; (6) reply to building request.

At the county level, the project proponent needs to establish whether the area is susceptible or not to landslides, and document the process and conclusions drawn. Figure 3.7 gives an example for landslides in quick clays.

As part of the assessment, the process in Fig. 3.8 is followed, where the proponent needs to determine if there is a hazard and the potential consequences. Later, in the building plans, the proponent needs to document safety or prepare mitigation measures.

The Norwegian standard NS 5814 (1991) considers risk analysis, including the necessary steps for planning and execution of risk analysis and guidelines for presentation of results and conclusions. NS 5814 can be used for all types of risks including multi-hazard situations. The planning of the risk analysis includes: Initiation, description of problems and objectives, establishment of working groups and establishment of areas of responsibility. The working group shall be familiar with methods for risk analysis and the type of problems at hand. The verification of the work shall be ensured by a competent person not actively involved in the analysis. The execution part of NS 5814 includes: Description of subject for analysis (include limitations and circumstances that are important for safety); Selection of

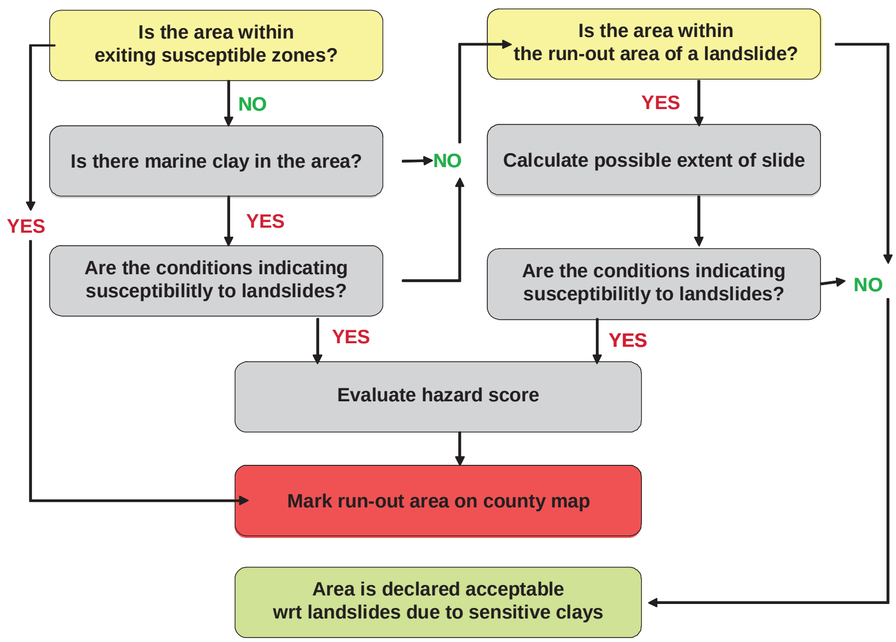

Fig. 3.7 Landslide hazard assessment at planning stage

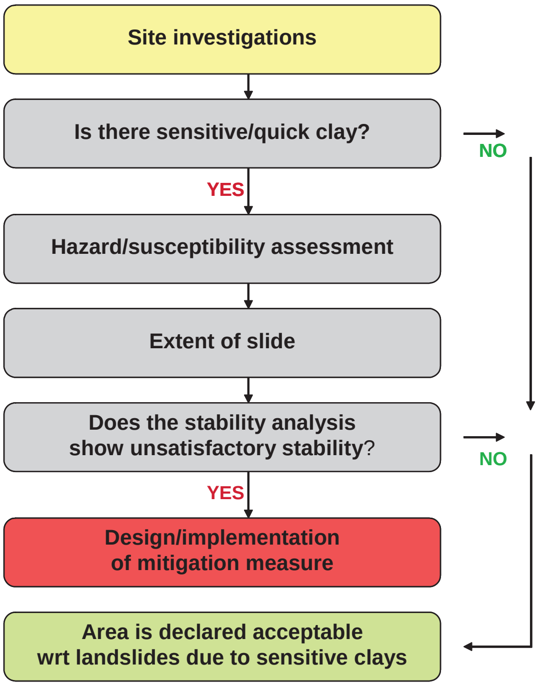

Fig. 3.8 Implementation of hazard assessment

procedures and methods (include uncertainties); Selection of data sources; Identification of undesired events; Causal analysis (based on the selected undesired events, considering measures to eliminate the causes, and if quantitative, including quantification of the probability of undesired events); Consequence analysis (including long and short term consequences and mitigation measures to reduce the consequences; the consequence analysis can be qualitative or quantitative; a quantitative consequence analysis shall contain i) calculation of the extent of damage caused by the undesired events and ii) quantification of the probability of the consequences given the occurrence of the undesired events); Description of risk (based on both the causal analysis and the consequence analysis) and Presentation of results. The NS framework does not include an evaluation of the risk as a function of acceptance criteria and gives no quantitative acceptance criteria. (The standard is presently under review.)

In the petroleum sector, the NORSOK Z-013 standard considers risk analysis. The NORSOK Z-013 framework has four levels (Fig. 3.9):

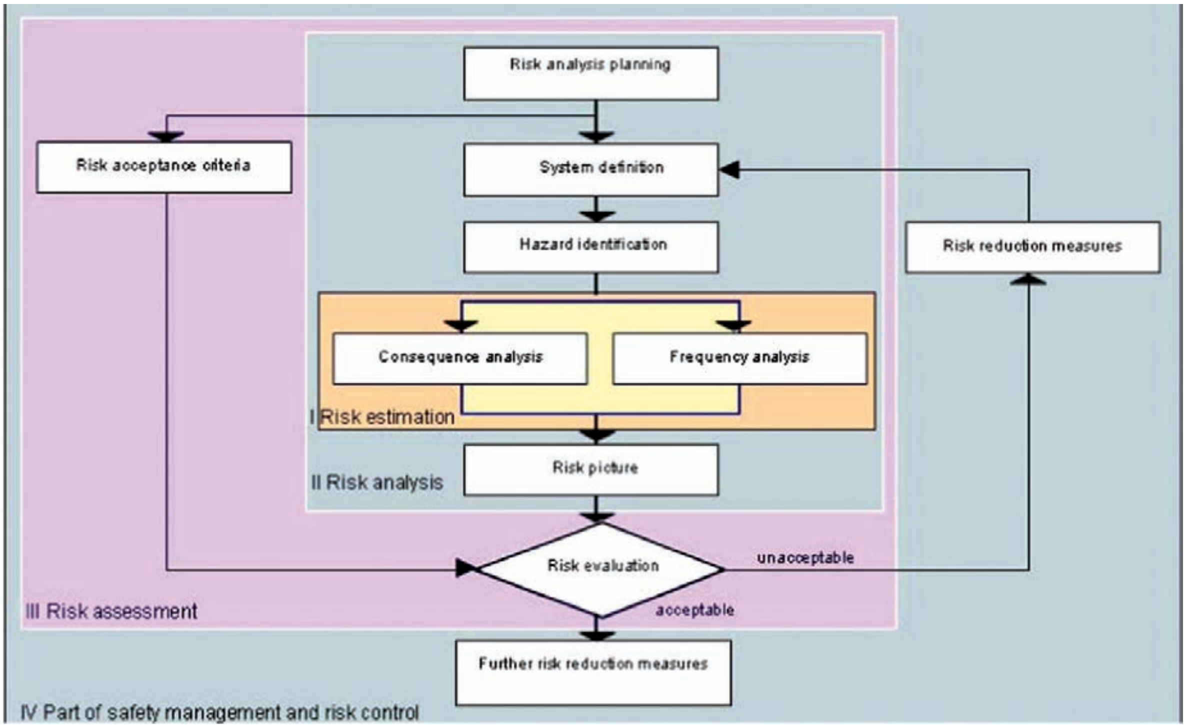

Fig. 3.9 Risk analysis framework (NORSOK Standard Z-013, 2001)

Level I: Risk estimation (inner level)
Level II: Risk analysis
Level III: Risk assessment
Level IV: Safety management and risk control (outer level)

The NORSOK Z-013 standard is more comprehensive than the NS 5814 standard. However, NORSOK does not provide quantitative acceptance criteria for hazard or risk.

3.4.2 Example- Risk Zonation for Quick Clay

As part of work for The Norwegian Water Resources and Energy Directorate (NVE), Gregersen (2001) developed a simple method to classify and map the risk posed by potential quick clay slides. Potential slide areas are given "engineering scores" based on an evaluation of the geotechnical parameters, local conditions, persons or properties exposed and engineering judgement. Hazard classes are described as low, medium and high. Consequence classes are discussed as not severe, severe and highly severe. The resultant risk, based on engineering evaluation and experience, is divided in five risk classes (Lacasse et al. 2004).

3.4.2.1 Hazard Classes

The hazard level depends on topography, geological and geotechnical conditions, and changes at the site. The evaluation of the hazard is done with the help of Table 3.2. The weight given to each hazard in Table 3.2 (or later, to consequence in Table 3.3) describes its importance relative to the stability of the slope. The hazard classes are:

Low: Favourable topography and soil conditions; extensive site investigations; no erosion; no earlier sliding; no planned changes, or changes will improve stability.

Medium: Less favourable topography and soil conditions; limited site investigations; active erosion; important earlier sliding in area; planned changes give little or no improvement of stability.

Table 3.2 Evaluation of hazard for slides in quick clay in Norway

Hazard	Weight	Score for hazard			
		3	2	1	0
TOPOGRAPHY					
Earlier Sliding	1	Frequent	Some	Few	None
Height of slope, H [(i)]	2	>30 m	20–30 m	15–20 m	<15 m
GEOTECHNICAL CHARACTERISTICS					
Overconsolidation ratio (OCR)	2	1.0–1.2	1.2–1.5	1.5–2.0	>2.0
Pore pressures [(ii)]	3	> + 30	10–30	0–10	Hydrostatic
– In excess (kPa)	−3	> − 50	−(20-50)	−(20-0)	Hydrostatic
– Under pressure (kPa)					
Thickness of quick clay layer [(iii)]	2	>H/2	H/2-H/4	<H/4	Thin layer
Sensitivity, S_t	1	>100	30-100	20–30	<20
NEW CONDITIONS					
Erosion [(iv)]	3	Active/sliding	Some	Little	None
Human activity	3	Important	Some	Little	None
– Worsening effect	–3	Important	Some	Little	None
– Improving effect					
TOTAL SCORE					
Maximum weighted score		51	34	16	0
% of max. weighted score		100%	67%	33%	0%

(i) For the quick clays in the study, inclination was identical for all slopes (1:3), and slope inclination was not included as a variable. In a general study, slope inclination should be added in the list of hazards.
(ii) Relative to hydrostatic pore pressure
(iii) In general, the extent and location of the quick clay are also important.
(iv) Erosion at the bottom of a slope reduces stability.

Table 3.3 Evaluation of consequence for slides in quick clay in Norway

Possible damage	Weight	Score for consequence			
		3	2	1	0
HUMAN LIFE AND HEALTH					
Number of dwellings[(i)]	4	> 5 Closely spaced	> 5 Widely spaced	≤ 5 Widely spaced	0
Persons, industry building	3	> 50	10–50	< 10	0
INFRASTRUCTURE					
Roads (traffic density)	2	High	Medium	Low	None
Railways (importance)	2	Main	Required	Level	None
Power lines	1	Main	Regional	Distrib. network	Local
PROPERTY					
Buildings, value[(ii)]	1	High	Significant	Limited	0
Consequence of flooding[(iii)]	2	Critical	Medium	Small	None
TOTAL SCORE					
Maximum weighted score		45	30	15	None
% of max. weighted score		100%	67%	33%	0%

[(i)] Permanent residents, in both sliding area and within run-out distance.
[(ii)] Normally no one on premises, but building(s) have historical or cultural value
[(iii)] Slides may cause water blockage or even dam overflow, flooding may cause new slides; there should be time for evacuation; damage depends on a complex interaction of several factors.

High: Unfavourable topography and soil characteristics; limited site investigations; active erosion; extensive earlier sliding in area; planned changes will reduce stability.

The zones with weighted score between 0 and 17 (up to 33% of maximum score) are mapped as "low hazard" and have low probability of failure by sliding. The zones with weighted score between 18 and 25 (up to 50% of maximum score) are mapped as "medium hazard" and have a higher, though not critical, probability of failure. The zones with weighted score between 26 and 51 are mapped as "high hazard" and have a relatively high probability of failure.

3.4.2.2 Consequence Classes

Consequences are commonly evaluated in terms of human life safety, environmental, financial and social effects. The evaluation of the consequences is done with the help of Table 3.3, with consequence classes:

Not severe: No or small danger for loss of human life, costly damage or consequences.
Severe: Danger for loss of life or property or important economical or social loss
Highly severe: High exposure of human life loss or large economical or social loss.

The zones with weighted score between 0 and 6 (13% of maximum score) are mapped as "not severe". In these zones, there would be very few or no permanent residents. The zones with weighted score between 7 and 22 (up to 50% of maximum score) are mapped as "severe". The zones with weighted score between 23 and 45 are mapped as "highly severe"; they would hold a large number of persons, either as residents or as persons on the premises temporarily.

3.4.2.3 Risk Classes

The risk score to classify the mapped zones into a risk class is obtained from:

$$\text{Risk} = \text{Hazard} \times \text{Consequence}$$
$$\text{R}_{\text{WS}} = \text{H}_{\text{WS}(\%)} \times \text{C}_{\text{WS}(\%)}$$

where

$$R_{WS} = \text{Weighted score for risk mapping}$$
$$H_{WS}(\%) = \text{Hazard weighted score in \%}$$
$$C_{WS}(\%) = \text{Consequence weighted score in \%}$$

Table 3.4 gives the risk scores for the five risk classes used for quick clay slides in Norway. Figure 3.10 shows a risk mapping of the area Modum in Norway.

Table 3.4 Risk classes for slides in quick clay in Norway

Risk Class	1 (lowest)	2	3	4	5 (highest)
Risk Weighted Score (RWS)	0–160	167–600	628–1900	1906–3200	3200–10,000
RWS (% of max RWS)	0–1.6%	1.6–6%	6.3–19%	19–32%	32–100%

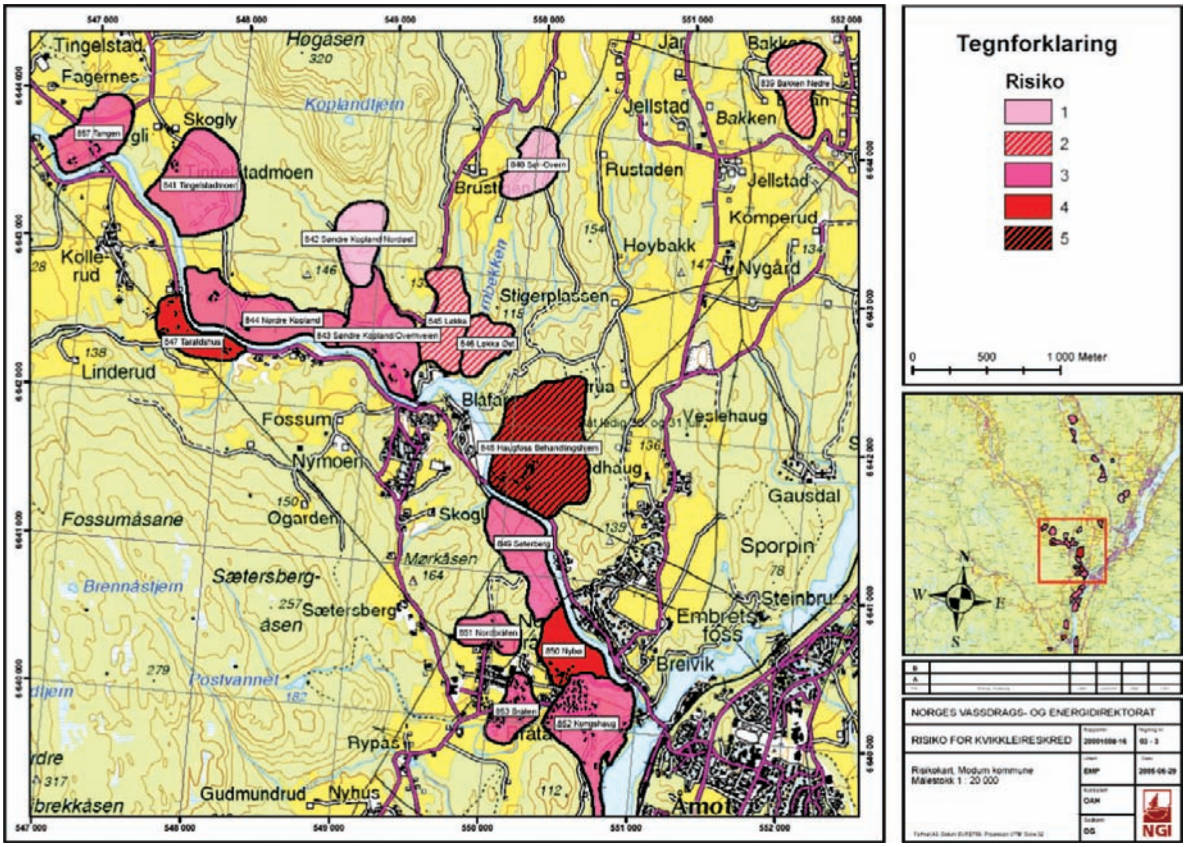

Fig. 3.10 Quick clay risk map for Modum, Norway

3.4.2.4 Decision-Making on Remedial Measures

To make decisions on the need for additional soil investigations, stability analyses or other remedial actions, Table 3.5 gives recommendations for quick clay areas in Norway.

The volume of the sliding material is probably the most important factor for the extent of the run-out zone. If several millions of cubic metre is involved, the run-out cannot be evaluated by simple dynamic or topographic models. This is especially important if large rivers are blocked and huge amounts of water are dammed with the possibility of generation of catastrophic flood waves downstream.

3.5 Digital Technology

3.5.1 Landslide Prediction

Landslide evaluation and prediction has several stages, including: (i) detection of movement through monitoring, (ii) temporal evaluation

Table 3.5 Activity matrix as a function of risk class

Activity	Risk class			
	1–2	3	4	5
Soil investigations	None	Consider additional *in situ* tests and pore pressure measurements	Require additional *in situ* tests and pore pressure measurements	Require additional *in situ* tests, pore pressure measurements and laboratory tests
Stability analyses	None	None	Consider doing	Require
Remediation[(i)]	None	None	Consider doing	Require

[(i)] e.g. erosion protection, stabilizing berm, unloading, soil stabilization, moving of residents

through analysis of data and numerical simulation, and (iii) definition of thresholds identifying critical instability. For site-specific slopes with monitoring by instruments, the slope displacement represents one of the key indicators of actual slope performance. The monitoring may include: in-situ, remote, and surface/subsurface methods. It is important to consider the issues of "what to measure" and "where to measure", system uncertainty and reliability etc, in order to avoid misleading results.

Instrumentation systems to monitor landslide behaviour are employed in many different locations, often in conjunction with surface mapping and sub-surface investigations, for a diverse range of landslide types in many different geological settings and landscapes. To determine where protective measures are necessary, landslide inventories and risk assessment maps over large areas are needed. Scientists are today increasingly relying on global satellite data to produce landslide inventories and risk assessment maps over wide areas; remote sensing data from optical and radar sensors (Synthetic Aperture Radar, SAR) are applicable to landslide mapping due to multispectral and textural information, high repetition cycles and global coverage. The integration of SAR and optical images, along with SAR interferometric techniques, are currently used for characterising landslides. New techniques such as DInSAR and high resolution image processing are increasingly exploited for risk assessment studies. DInSAR is a powerful technique to measure from satellite displacements and has been successfully applied to detect subsidence and landslides, earthquakes or volcanic activity. The ground-based radar device such as LISA (Linear SAR) is capable of assessing the deformation field of an unstable slope in the areas characterised by a high radar reflectivity.

Near surface geophysical methodologies (seismic, gravimetric, magnetic, electric and electromagnetic) are often applied to monitor hydrogeological phenomena. New electric and electromagnetic survey techniques have been applied to areas with complex geology (seismic, geothermal, volcanic and landslide areas, etc.).

In many landslide risk areas, it may be too costly to stabilise a landslide area. Mitigation work may too intrusive in sites of cultural heritage, of outstanding beauty, or for other reasons. Early warning systems allow the adoption of strategies for the mitigation of landslide risk not involving the construction of expensive and environmentally damaging protective measures. On an operational basis, hazard/susceptibility maps, movements identification and monitoring need to be coupled with "real time" continuous measurement and with observations on possible "triggering" events. The output should call for action at different levels, involving local, regional, national and even international authorities.

3.5.1.1 Monitoring and Remote Sensing

The objectives of the monitoring of the movement include (1) monitoring for public safety and risk management, (2) health or performance monitoring, (3) regional warning (e.g. landslide), (4) construction quality control and (5) the understanding of the behaviour observed (technical development). Different purposes will have different monitoring and follow-up requirements. One needs to consider the likely modes of failure in data interpretation and the setting of threshold values (e.g. brittle versus ductile failure controlled, among others, by material and mass properties).

The detection of movement is a more direct measure of the potential instability than the other measurements. If only pore pressures are monitored, it may be difficult to foretell how imminently the instability may occur. It is however best to relate the movement monitored to other monitoring data (e.g. pore pressure, rainfall, etc.) to have a more complete appreciation of the slope behaviour.

Remote sensing tools, such as LiDAR, InSAR or other imagery, are practical and for many of them, affordable tools in landslide hazard assessment programs. Table 3.6 presents the consensus reached at the Landslide Risk Management Forum Hong Kong in 2007 (Lacasse 2008) on the strengths and limitations of most of the techniques in use today. Issues of “where”, “when”, “why” and “costs” influence the selection of technique(s) in practice. In plenum, the session participants agreed with the table presented and the evaluations made.

3.5.1.2 Interpretation of Movement Data

The interpretation of movement data needs a suitable model for projection of behaviour, e.g. the observational approach, which is typically done empirically or based on common sense instead of theoretical/numerical analyses.

Numerical simulation can be used to set-up a framework to interpret ground movement; with the observed data used to calibrate the model predicting the slope behaviour up to failure. It is best to do the calibration against a slope that has gone to failure. The code will differ from conventional limit equilibrium stability calculations, but will be more complex, and require more input parameters and hence have more uncertainty.

Thresholds need to relate to anticipated mode of failure and time for response. In the case of a brittle failure with little warning signs before collapse with fast-moving debris, the movement monitoring could give result to a false sense of security! One also needs to consider whether there are potential mechanisms under which ductile failures could become brittle failures. Where a slope failure is brittle, an observation of no movement could give a false sense of security.

3.5.2 Digital Mapping

Mapping should be available to enable landslide risk management to be effective. The mapping can consist of (1) susceptibility maps for general land-use planning; (2) hazard maps, which give more information and allow for finer tuning of risk management; (3) risk maps, forming the basis for disaster preparedness and early warning; and (4) risk maps for risk-based design of remedial measures.

Susceptibility mapping is possible and useful, both in terms of source area and run-out area. Establishing hazard maps is difficult, establishing risk is even more difficult. Landslide inventory is essential, and vulnerability information is usually where there is most information missing. It is important to be aware that vulnerability is much more than just the physical vulnerability.

The mapping scale depends on the objectives of the mapping: scale of study, available data, techniques and models used and whether the mapping is static or dynamic (dynamic meaning that the data change with time). At the site investigation level, the mapping seems less useful and can be replaced by engineering design.

The scale of a susceptibility map is dictated by the constraints of the terrain and quality of data. For instance, if the quality of data is not too reliable, only small-scale maps can be prepared. Depending on the scale wanted, one has to choose the adequate data needed.

There are many uncertainties in susceptibility, hazard and risk mapping that need to be dealt with, including landslide inventory, input data (geology, geomorphology, terrain, slope inclination, soil layer thickness, properties of soils), models and methods used and temporal changes for the elements at risk. Vulnerability and hazard change continuously.

In considering the vulnerability of a facility, other types of hazard should also be considered in addition to the landslide hazard. Multi-hazard risk is important.

Table 3.6 Remote sensing technologies: strength and limitations (Hutchinson, J. 2008 Personal communication; Lacasse 2008)

System		Applications	Resolution	Limitations	Strengths-DEM from all	Future
Photogrammetry	Terrestrial	joint survey, scrap and change detection	cm to m, depending on scale	field of view, image resolution, requirement for surveyed positions, vegetation obscurance	rapid, cheap, long term record, stereoscopic-build DEMs and see terrain conditions	digital imagery, use of high resolution scanners and video
	Airborne	landslide inventory and time series analysis				
LiDAR	Ground based-static	landslide monitoring, landslide mapping, topography extraction HR, joint surveys, moisture detection	mm to cm	hunidity, distance limitations, angular limitations, reflectivity, vegetation obscurance, too much data?, field of view	multi-return LiDAR allows bare earth model, very high accuracy, high rate of acquisition, perspective views possible	costs will decrease, signal analysis will improve, automated feature extraction?
	Ground based-mobile					
	Airborne-fixed wing					
	Airborne-helicopter					
InSAR	Standard	movement detection and monitoring, time series displacement, HR movement detection (ground based)	mm	visibility and shadowing, need reflectance, doesn't penetrate vegetation, limited to slow movements	large area survey, long term monitoring, return frequency affects use, comparison or combination of ascending and descending paths, movement measurement, rapid mapping of targeted	more frequent passes of satellite, monitoring of faster landslides
	PS			as above, plus only works with stable reflectors, very expensive	as above, plus mm accuracy movement detection	
	Ground based			as above, but can monitor faster movements, but semi-permanent installation and view point is required	as above, plus can pick up larger movements	

Optical satellite images		landslide inventory and time series analysis	10's cm to D11 10's m	expensive, image quality can be poor due to cloud cover	landslide surveys, large area coverage, historical record since 1990's, change detection, rapid mapping of targeted areas	higher resolution satellites to be deployed, more satellites will increase coverage and frequency
Weather Radar		precipitation intensity, early warning from rainfall intensity and accumulation	depending on calibration, km	calibration is required	helps map spatial distribution of weather	enhanced mapping of weather systems, cheaper systems
Others	Thermal, IR			low resolution	vegetation classification, water content, change detection	

3.6 Monitoring and Early Warning Systems for Landslides

Faced with natural hazards, especially landslides, society's only recourse is to learn to live with them. It is therefore important to understand and predict landslide behaviour. One can live with a threat, provided the risk associated with it is acceptable or provisions are made to reduce the risk to an acceptable level. The role of landslide monitoring and warning is to gather information useable for avoiding or reducing the impact of landslide activity. After the recent natural catastrophes around the world, landslide monitoring and especially early warning, have gain enormous interest. The ever increasing need to locate new land areas for urban expansion also requires development in areas with unstable slopes. On the other hand, technological advances in measurement technology as well as data acquisition, transmission and analysis procedures have made monitoring and early warning systems easier to implement.

3.6.1 Requirements for an Early Warning System

As opposed to a monitoring programme, a reliable early warning system needs:

– Understanding of the sliding process
– Historical knowledge of triggers (e.g. rainfall)
– Effective monitoring programme
– Interpretation of data
– Decision-making, including possibility for human intervention
– Public tolerance of false alarms
– Communication system
– Pre-established action plans for implementation
– Feedback loop and adaptability of system and to "new" knowledge

If a landslide occurs or is on the verge of occurring, time is needed for detection through the EWS, notification (authorities -police, city council-required action (closure of roads, evacuation, . . .). Societal needs and controls are also a factor. But utmost, communication is the most critical need.

Sharing information on the monitoring system is an absolute requirement for an effective early warning system. The expectations from the general public and the regulator differ. Efficient sharing of information is a challenge. There is generally very little time for the regulator to disseminate monitoring information is a challenge. Communication also depends on public tolerance, method used to share the information and the measurements themselves and the perception of their reliability.

3.6.2 Landslide Monitoring

Monitoring is the key to slope instability assessment, management and mitigation. The objective of a landslide monitoring program is to collect, record and analyse in a systematic and purposeful manner qualitative and quantitative information required to evaluate specific problems associated with the slope or landslide being studied. The information may comprise maps, photographs, boring logs, topographical data, weather data and visual observations. In most cases, monitoring will also include installation of instruments and taking physical measurements. Landslide monitoring programs are implemented for a number of reasons, including providing input for early warning systems.

Monitoring programs vary considerably depending on the risk a potential unstable slope poses. Programs can range from only visual inspections to extensive programs comprising observations from orbiting satellites and arrays of sophisticated instruments installed at the site.

3.6.3 Designing and Carrying Out a Monitoring Program

A successful monitoring program depends on (1) ensuring that the monitoring is necessary, (2) knowing what to monitor and (3) knowing how to do it. Monitoring programs will differ in methodology and scope because landslides also differ, both in size, velocities and type of movement associated with them. For the following types of mass movements, rock falls, topples, rotational, sagging, spread and flows, the approach to monitoring the displacements will be quite different. The most important step in the design of a successful landslide monitoring program is to identify and understand the objective of the program. Designing a monitoring program for landslides include the following steps:

- Gather as much site information as possible, including maps, geological and topographical data, geotechnical data, records of previous slides and extent of potential sliding mass.
- Perform a stability analysis and hazard assessment to gain an improved understanding of the hazard
- Define the objective of the monitoring program and select the type of measurements to be included in the program, assigning a priority to the measurements.
- On the basis of cost, availability and reliability information, decide on the measurement methods to be used and select the appropriate instruments
- Determine the optimum number of instruments and locations; if available, use theoretical or empirical models to optimise the number and placement of instruments.
- Decide on the preferred method of data acquisition, e.g. manual or automatic recordings.
- Arrange for proper installation, protection and marking of instruments and reference points in the field
- Plan for data flow, data management and analysis. Insure that there are sufficient funds to properly analyse the measurement data.
- Plan for adequate maintenance of the monitoring system.

As a general rule of thumb, one should use the simplest monitoring methods and equipment possible. Monitoring implies observations and physical measurements. A landslide monitoring program will normally comprise one or more of the following: visual observations to look for evidence of instability and to determine the areal extent of a slide; remote sensing for classification and detection of movement over large surface areas; surface measurements for site characterization and monitoring displacements; subsurface measurements for site characterization, monitoring displacements and pore water pressure, and environmental data, particularly magnitude and intensity of rainfall. Landslide monitoring techniques range from simple and inexpensive manual and visual observations to costly and sophisticated surveillance via satellites and automatic systems. DiBiagio and Kjekstad (2007) describe the approaches in detail.

3.6.4 Early Warning Systems for Landslides

Early warning systems (EWS) mitigate risk by reducing the consequences. The system issues alerts or warnings early enough to give sufficient lead time to implement actions to protect persons and/or property. Early warning systems for landslides are monitoring systems specifically designed to detect events that precede a landslide in time to issue an imminent hazard warning and initiate mitigation measures. The key to a successful early warning system is to be able to identify and measure small but significant indicators that precede a landslide.

The relevant precursor depends on the type of landslide. Typical examples of precursors are intense rainfall, ground vibrations and earthquakes, blasting, acceleration or high rate of movement in the slope, rapid increases in pore water pressure or stream flow at the toe of a slope. Typical instruments in an early warning system are rain gauges, geophones, seismographs, piezometers, inclinometers, extensometers and devices for measuring the movement of slopes.

The reliability of measurements is paramount in any monitoring system, but particularly so in an early warning system. A false alarm generated by an automatic early warning system may pose more of a hazard than the landslide itself. Thus, redundancy and alternate measurement methods should be considered to avoid false alarms. The consequences of false alarms in a warning system are so serious that every possible action must be taken to eliminate them. One important step in this process is to include data quality control measures in data acquisition and processing to insure that erroneous data is not used in analysis and forecasting of

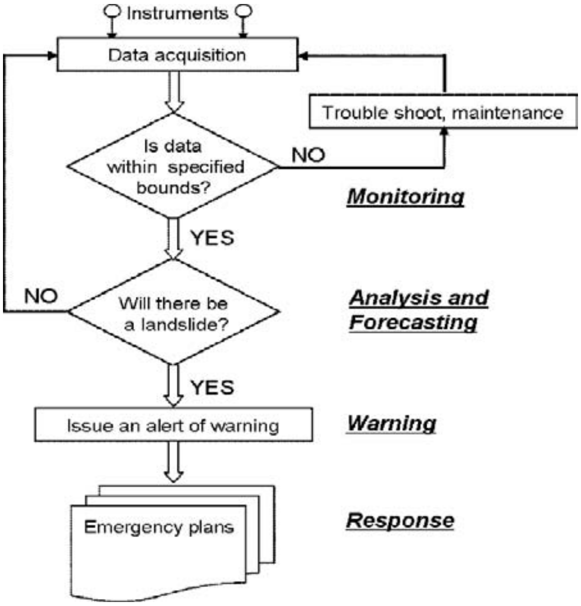

Fig. 3.11 Block diagram of a typical early warning system (DiBiagio and Kjekstad 2007)

landslide activity. Another step is to make maximum use of human intelligence and "engineering judgment" in decision-making – a process that, unfortunately, does have practical limitations in a fully automatic warning system.

The components of an early warning system are the sensors and measuring devices, a real-time data acquisition unit with communication link and software to process and analyse the measurements. The system issues warnings via the communication link automatically when predefined alarm threshold values are exceeded. An early warning system comprises four main activities: monitoring, analysis of data and forecasting, warning and response. Figure 3.11 presents a block diagram of a typical early warning system.

The major problem in designing an early warning system is to be able to specify reliable and effective threshold values. This generally involves some form of forecasting based on past trends in the measurements. Engineering judgment is an important element in the process of forecasting and setting thresholds. The system must also be so flexible that the threshold parameters can be changed as more information becomes available on the performance of the monitoring system and the behaviour of the slope being monitored.

There is the need for more than one alert or action level, related to the assessed/judged probability of failure and the time to develop failure. It is difficult to come up with absolute limits on tolerable slope movement because of the lack of experience. The rate of change of movement is usually of the essential and central focus of the measurements and warning. One must allow sufficient time for response. Risk communication is also essential if monitoring is to be used for risk management decisions.

The issues of false alarms and loss of credibility remain an issue. Based on past experience in Hong Kong, the use of movement monitoring results may be more effective than measurements of groundwater pressure. There are more frequent false alarms when threshold groundwater pressure values are reached because of conservative pore pressure assumptions made in the slope stability analyses.

Early warning systems also benefit greatly from lessons learned. The Val Pola landslide monitoring system developed in 1987 for protecting personnel working in a landslide is such an example. Some of the lessons learned then include (Bruzzi 1989):

- Standard instrumentation provides data of sufficient quality for the evaluation of landslides.
- The reliability of instruments is in general more important than accuracy and resolution because a small decrease in instrument performance is negligible compared to the uncertainties in the models used to evaluate the data.
- Great care must be taken to insure adequate protection of instruments against environmental and mechanical damage, electrical damage from thunderstorms and vandalism if relevant.
- A microseismic network is a powerful tool for qualitative global monitoring of landslides, but considerable experience and long-term observations are necessary for a quantitative analysis of the data.
- Radio telemetry is well suited for data transmission under adverse operating conditions. When distances are large, radio telemetry may be significantly less expensive than communication over cables.

The technology exists today, both the instruments, systems and models. The profession needs to make all this knowledge work together. It is not the State-of-the-Art that is the problem, it is the application of the State-of-the-Art that needs to be improved (Lacasse 2008).

Future directions are expected to move towards: (1) making simple visual observation in the field, improving accessibility and enhancing rapid communication; (2) education and awareness; (3) training of public, including having then input information; and (4) improving interpolating solutions.

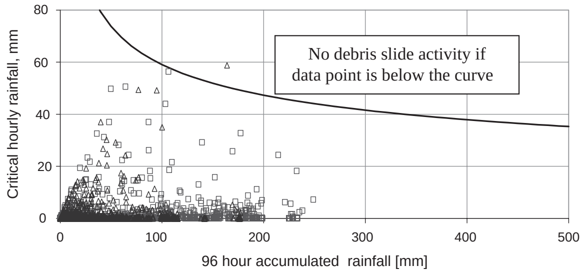

Fig. 3.12 Threshold trigger for debris flows in Nicaragua for critical hourly rainfall vs. 96-h accumulated rainfall (Heyerdahl et al. 2003)

3.6.5 Early Warning for Debris flows

Debris flows strike quickly and move rapidly with little warning. Debris flows are fast moving relatively fluid masses of soil and water that can flow for long distances even on slopes of only a few degrees. They destroy or bury objects in their paths and are particularly dangerous to life and property because they can strike with little warning.

Studies of historical records of debris flows show that it is the maximum intensity of rainfall within a short period of time that determines whether a slide will occur or not. Thus, rainfall, duration and intensity, is a critical factor in predicting debris slides. It follows, therefore, that rainfall is the best and perhaps the only realistic input to an early warning system for debris flows. The most reliable method to predict critical rainfall intensities that can trigger debris flows is to correlate rainfall records to observe debris flows within one geographical area.

To develop an early warning system for debris flows or rainfall-induced landslides, one needs to set the critical duration-intensity threshold values. Figure 3.12 illustrates an example of such a threshold used in Nicaragua.

If there is no landslide inventory available for a correlation study, the best approach is to search the literature for the critical rainfall intensity studies for similar geographic and climatic areas. These start values can be modified as more information becomes available form the monitoring. Statistical methods are also used to determine critical rainfall intensities. Statistical data from Norway indicates that debris slides can be expected if the accumulated rainfall in one day is greater than 8% of the annual rainfall. It has been possible to greatly simplify critical rainfall threshold values in Hong Kong using the large database of rainfall and landslide statistics accumulated over many years of observations. Early warnings are now issued in Hong Kong on the basis of two simple triggering conditions namely: when rainfall exceeds 70 mm in one hour or when rainfall exceeds 100 mm in 24 h.

3.7 Example – EWS in Remote Location

Lake Sarez is located in the Pamir Mountain Range in eastern Tajikistan. The lake was created in 1911 when an earthquake triggered a massive rock slide (volume: $\sim$2 km^3) that blocked the Murgab river valley. A natural dam, Usoi Dam, was formed by the rockslide which retains the lake. The dam is at an altitude of 3200 m. With a height of over 550 m, it is by far the largest dam, natural or man-made, in the world.

Lake Sarez, impounded by this natural dam, is now about 60 km long and has a maximum depth of approximately 550 m and a volume of 17 km^3. The lake has never overtopped the dam but the current freeboard between the lake surface and the lowest point of the dam crest is only about 50 m. The lake level is currently increasing about 30 cm per year. If this natural dam were to fail, a worst-case scenario would be a catastrophic outburst flood endangering thousands of people in the Bartang, Panj, and Amu Darya valleys downstream.

There is another natural hazard at Lake Sarez, namely, a large active landslide on the right bank (Fig. 3.13). If this unstable slope should fail and slide into the lake, it would generate a surface wave large enough to overtop the dam and cause a severe

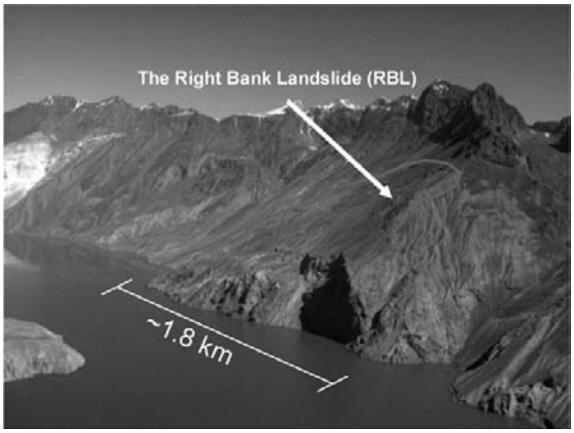

Fig. 3.13 Active landslide on the right bank of Lake Sarez (Photo SECO, State Secr. for Economic Affairs, Switzerland)

flooding downstream. Experts who have studied the hazards agree that the most probable scenario at Lake Sarez is failure of the right bank slope and overtopping of the dam (DiBiagio and Kjekstad 2007).

In 2000, an international "Lake Sarez Risk Mitigation Project (LSRMP)" was launched under the auspices of the World Bank to deal with the risk elements posed by Usoi dam and Lake Sarez. The two main objectives of the project were to find long-term measures to minimize the hazard and to install an early warning system to alert the most vulnerable communities downstream. The early warning system for Lake Sarez has been in operation since 2005. The system has 9 remote monitoring units linked to a central data acquisition system at a local control centre near the dam. Data is transmitted via satellite to the main control centre in Dushanbe, Tajikistan's capital. Alerts and warning messages are sent from Dushanbe to 22 communities connected to the system. The local control centre is manned 24 h per day, every day. The measurements included in the monitoring program are listed in Table 3.7.

At present, the warning system comprises three alarm levels. Each level is based on monitored data and/or visual observations. Threshold values for triggering alarms include both maximum measured values and rate of change with time. These are listed in Table 3.8. Alarm states and emergency warning plans are summarized in Table 3.9.

At the start, some initial operational and maintenance were encountered, but these have been resolved underway. The principal problem has been insufficient power in some of the remote villages. The system satisfied the specified one-year error-free test program and has been formally turned over to the Ministry of Defence who now has responsibility for operation of the system. The plan is to keep the early warning system in operation until 2020 which is the target date for completion of the mitigation works. The least expensive mitigation measure to reduce the risk is to permanently lower the lake level by about 120 m using a diversion tunnel around the landslide.

3.8 Example – EWS for Rock Slide-Triggered Tsunami

Rock falls and rockslides are among the most dangerous natural hazards in Norway, mainly because of their tsunamigenic potential. The three most dramatic natural disasters in Norway in the 20th century were tsunamis triggered by massive rockslides into fjords or lakes (Loen in 1905 and 1936 and Tafjord in 1934), causing more than 170 fatalities (Bjerrum and Jørstad 1968; Anda and Blikra 1998; Blikra et al. 2002). As public attention on natural hazards increases, the potential rockslides in the Storfjord region in western Norway have earned renewed focus. A massive rockslide at Åknes could

Table 3.7 Early warning system measurements at Lake Sarez (Stucky 2007)

Measurement	Methodology
Lake elevation	Pressure transducer in the lake
Detection of large surface wave	Pressure transducer in the lake
Seismic event	Strong motion accelerometers
Surface displacements	GPS
Flow in Murgab river downstream	Radar type level sensor
Turbidity in the outflow water	Turbidity meter
Flood conditions down stream	Level switches
Meteorological data	Complete weather station

Table 3.8 Threshold values for Level 1 and Level 3 alarm states (Stucky 2007)

Level	Source	Threshold value
1	Seismic acceleration	$a > 0.05$ g
	Lake level elevation	$H > 3270$ m above sea level
	Rate of change of lake level	$dH/dt > 25$ cm/day
	River flow downstream	$Q > 300\ m^3/s$ or $Q < 10\ m^3/s$
	Manual alarm input	Unusual visual observation
3	Height of wave on lake	Wave height > 50 m
	Flood sensor	$Q > 400\ m^3/s$
	River flow down stream	$Q > 400\ m^3/s$ or $Q < 5\ m^3/s$
	Rate of change of river flow	$dQ/dt > 15\ m^3/s/h$
	Manual alarm	Major event observed

be catastrophic as the rock slide-triggered tsunami is a threat to all the communities around the fjord. The Åknes/Tafjord project was initiated in 2005 by the municipalities, with funding from the Norwegian government, to investigate rockslides, establish monitoring systems and implement a warning system and evacuation plan to prevent fatalities, should a massive rockslide take place.

Åknes is a rock slope over a fjord arm on the west coast of Norway. The area is characterised by frequent rockslides, usually with volumes between 0.5 and 5 millions m^3. Massive slides have occurred in the region, e.g. the Loen and Tafjord disasters (Fig. 3.1). Bathymetric surveys of the fjord bottom deposits show that numerous and gigantic rockslides have occurred many thousands of years ago. The Åknes/Tafjord project (www.aknes-tafjord.no) includes site investigations, monitoring, and an early warning system for the potentially unstable rock slopes at Åknes in Stranda County and at Hegguraksla in Norddal County. The project also includes a regional susceptibility and hazard analysis for the inner Storfjord region, which includes Tafjord, Norddalsfjord, Sunnylvsfjord and Geirangerfjord. The potential disaster associated with a rockslide and tsunami involves many parties, with differing opinions and perceptions.

As part of the on-going hazard and risk assessment and validation of the early warning system, event trees were prepared by pooling the opinion of engineers, scientists and stakeholders. The objective was to reach consensus on the hazard and risk associated with a massive rockslide at Åknes (Lacasse et al. 2008).

Table 3.9 Alarm states and emergency warning plan (DiBiagio and Kjekstad 2007)

Level 0 –Normal state		Level 1 – Abnormal state but not critical	
Definition	All systems operating properlyNo abnormal conditions detected	Definition	Abnormal situation due to a natural phenomenon or technical problem
Origin of warning	Early Warning System Local operating personnel	Origin of warning	Early warning system Local operating personnel
Destination of warning	Local control centre and Dushanbe	Destination of warning	Local control centre and Dushanbe
Action	Daily operation and maintenance	Action	Inspection, checking, repair and observation
Level 3 –Escape Signal		**Level 4 –Back to normal signal**	
Definition	Abnormal condition detected based on several sources	Definition	Normal conditions confirmed after a Level 3 alarm
Origin of warning	Early Warning System Local control centre or Dushanbe	Origin of warning	Dushanbe
Destination of warning	Local control centre and all villages downstream	Destination of warning	Local control centre and all villages
Action	People in villages evacuate to predefined safe areas	Action	Back to Level 0

3.8.1 Observed Displacements

Experience from Norway and abroad shows that rockslide events are often preceded by warning signs such as increased displacement rate, micro-tremors and local sliding. Accelerating rate of displacement several weeks and even months before a major rockslide event is typical. Slope movements have been detected at Åknes down to 60 m depth (Fig. 3.14). New borehole data suggest movements down to 100 m. Important uncertainties lie in the most likely failure depth and location, and whether the slide will occur as one large 30–60 millions m^3 sliding event or a succession of several “small” slide events. Figure 3.14 presents the Åknes slope and two slide scenarios. Figure 3.15 shows some of the displacements observed at the upper crack. Water seeps (“springs”) are seen emerging on the down-stream slope (Kveldsvik et al. 2008). The displacements in Fig. 11 appear to move linearly with time. The total annual displacements vary from less than 2 cm up to about 10 cm.

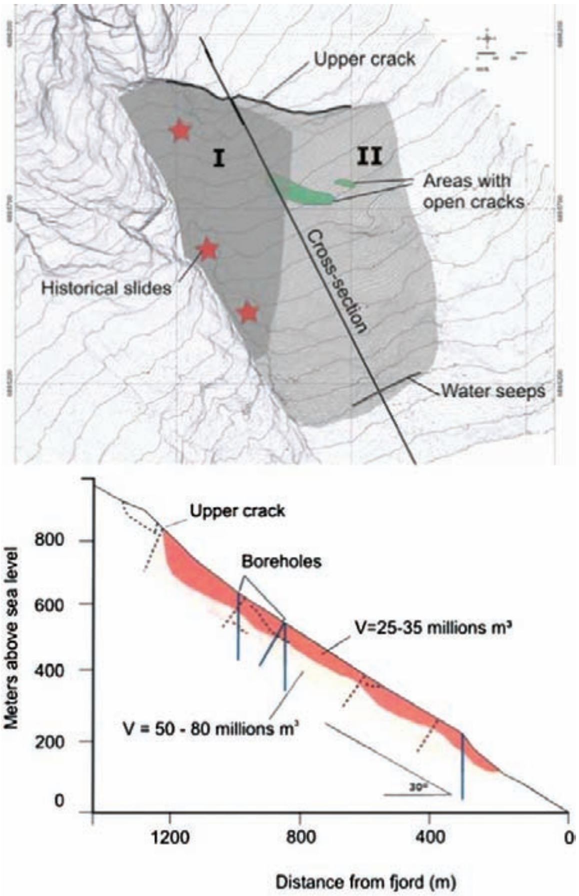

Fig. 3.14 Sliding volume scenarios. Surficial area (*left*) and cross-section (*right*) (modified from Blikra et al. 2007)
Area I: Slide volume 10–15 millions m^3, displacement = 6–10 cm/yr
Area II: Slide volume 25–80 millions m^3, displacement = 2–4 cm/yr

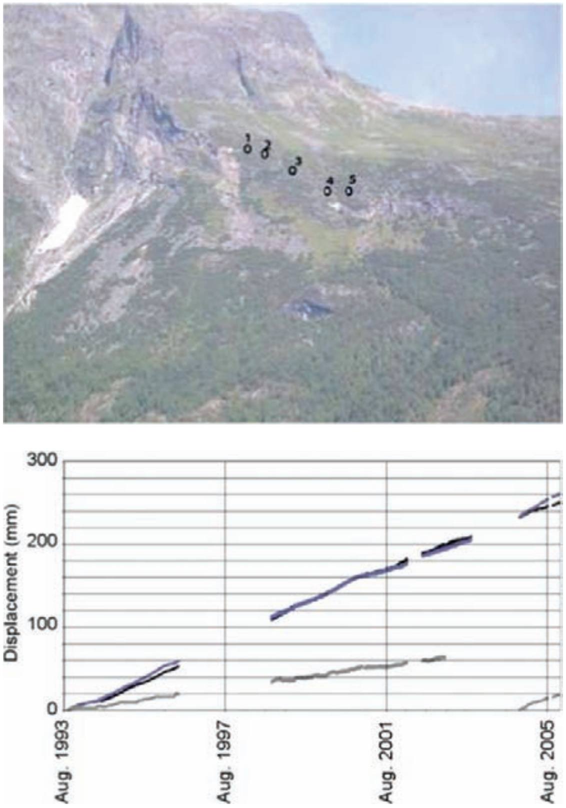

Fig. 3.15 Location of extensometers and displacements from extensometer 1, 2, 3, 4 and 5 at the top scarp at Åknes (Kveldsvik et al. 2006)

3.8.2 Instrumentation and Monitoring

The large variations in weather and atmospheric conditions in the fjord and mountain areas pose unusual challenges to the instrumentation. For example, the hazard due to snow avalanche and rock bursts is high in most of the area to be monitored. Solar panels do not provide sufficient electricity, and energy has to be obtained from several sources to ensure a stable and reliable supply. Significant effort is underway to deploy robust instruments and improve data communication during periods of adverse weather. An Emergency Preparedness Centre is located in Stranda. The monitoring data will be integrated into a database that will form the basis for future analyses. Based on the experience with similar projects and the specific needs in Storfjord, the overall monitoring system was equipped with:

Surface monitoring
- GPS-network with 8 antennas
- total station with 30 prisms
- ground-based radar with 10 reflectors
- 5 extensometers measuring crack opening
- 2 lasers measuring opening of the 2 largest cracks
- geophones that measure vibrations

Monitoring in borehole
- inclinometers measuring displacements
- piezometers measuring pore pressure
- temperature
- electrical resistivity of water

Meteorological station
- temperature
- precipitation and snow depth
- wind speed
- ground temperature
- radiation

Light Detection and Ranging (LiDAR) mapping and radar measurements were also done. Several independent systems were installed to ensure continuous operation at all times, and different communication systems were implemented to ensure continuous contact with the Emergency Preparedness Centre in Stranda.

3.8.3 Modelling of Tsunami Following Rock Slide

The tsunami wave propagation due to an Åknes rock slide was modelled numerically for two rock slide scenarios: slide volume of 8 million m^3 and 35 million m^3. Run-up values were estimated for 15 locations in the Storfjord region (Eidsvig and Harbitz 2005; Glimsdal and Harbitz 2006; Eidsvig et al. 2008). The results of the simulation for three locations are shown in Table 3.10. Preliminary results of tsunami modelling suggest an inundation height of up to 35 m at Hellesylt for rockslide volume of 35 million m^3 at Åknes. The modelling of the tsunami caused by the rockslide includes several uncertainties. To reduce the uncertainties, physical modelling is presently underway in university laboratories in Oslo and Trondheim (University of Oslo and the Norwegian University of Science and Technology (NTNU) in Trondheim. The model tests are run to improve the understanding of the initial wave pattern generated by the sliding rock masses. A rock slide as large as 30 million m^3 will pose a serious threat to coastal areas of several communities in the Storfjord region, and may have also serious consequences further out along the fjord.

Table 3.10 Estimated run-up heights in the Storfjord region

Location	Run-up heights 8 millions m^3	Run-up heights 35 millions m^3
Hellesylt	8–10 m	25–35 m
Geiranger	8–15 m	20–40 m
Stranda	1–3 m	3–6 m
Fjøra	1–2 m	5–7 m
Tafjord	3–5 m	12–18 m

3.8.4 Event Tree Analysis (ETA)

An event tree is a graphical construction that describes the sequence of the occurrence of events in a logical system. The tree identifies the possible outcomes and contains estimates of their probability of occurrence. As the number of events increases, the construction fans out like the branches of a tree. Each path in the event tree represents a specific sequence of events, resulting in a particular consequence. The events are defined such that they are mutually exclusive. ETA is a valuable analysis tool because it is simple and graphic, it provides qualitative insight into a system, and it can be used to assess a system's reliability in a quantitative manner (Hartford and Baecher 2004; Høeg 1996).

3.8.4.1 Achieving Consensus

In a multi-disciplinary process such as the analysis of hazard and risk associated with natural hazards, a number of "experts", specialists and stakeholders are assembled and need to agree on the numbers set on the branches of the event tree. One needs then to achieve "consensus". Consensus derives from Latin, "cum" meaning "together with " and "sentire" meaning to "think" or "feel". Etymologically, "consensus" therefore means to think or feel together'. In a decision-making process, consensus aims to be:

- inclusive: as many stakeholders as possible should be involved in the consensus decision-making process.
- participatory: the process should actively solicit the input and participation of all decision-makers
- cooperative: participants should strive to reach the best possible decision for the group and all of its members, rather than opt to pursue a majority opinion, potentially to the detriment of a minority.
- egalitarian: all members of a consensus decision-making body should be allowed, as much as possible, equal input into the process; all members have the opportunity to table, amend, veto or "block" proposals.
- solution-oriented: the decision-making body strives to emphasise common agreement rather than differences and use compromise and other techniques to reach decisions and resolve mutually-exclusive positions.

3.8.4.2 Example of ETA Results for Åknes

The event trees were constructed by pooling the opinion of engineers, scientists and stakeholders. The objective was to reach consensus on the hazard, vulnerability and risk associated with a rockslide at Åknes and quantify the hazard (probability of a rockslide and tsunami occurring) and the potential losses (human life and material and environmental damage). Different triggers for the rockslide were analysed.

The ETA was carried out over three days, where scientists and stakeholders with relevant competence to grasp the situation as a whole were assembled. The objectives of the analysis were also to examine the required parameters for an effective early warning system and suggest possible mitigation measures, e.g. drainage wells and drainage galleries. The paper describes the event trees used for estimating risk. Progress is underway on the analysis and the results are only preliminary. The other topics will be the object of future papers.

The participant list for the results shown below included the following representatives:

- manager for Åknes/Tafjord project
- mayor of community
- social scientist from community
- city planner from community
- policeman working on emergency plans and evacuation
- local politician
- representative from community office
- directorate for safety and emergency preparedness
- journalist/media
- officer from ministry of highways
- meteorologist
- physical geographer
- social geographer
- geologist
- engineering geologist
- rock mechanics specialist
- geotechnical engineer
- tsunami specialist
- instrumentation specialist
- earthquake engineer
- seismologist
- mathematician
- statistician
- risk analysis specialist

The following event trees were constructed during the three-day meeting:

- event tree, rockslide due to seismic trigger
- event tree, rockslide due to high pore pressure trigger
- event tree, rockslide due to weathering and creep trigger
- event tree, tsunami wave against Hellesylt
- event tree, consequences of tsunami
- event tree, optimum observations for early warning

Table 3.11 Estimated probability of run-up heights at Hellesylt, given that a rock slide of larger volume has occurred

Run-up height $\leq$ 5 m	Run-up height > 5m; $\leq$ 20 m	Run-up height > 20 m
$P = 3 \times 10^{-4}$/yr	$P = 5 \times 10^{-4}$/yr	$P = 1 \times 10^{-4}$/yr

Event trees were constructed for three triggers of rock slope instability: earthquake, high pore pressure and weathering creep and weakening of sliding plane. The event trees represent the judgment for the "today" (October 2007) situation. The trees set numbers for the probability of a slide within the next year, but the probability changes with time. The event trees should therefore be updated as new information becomes available.

Figure 3.16 (Lacasse et al. 2008) presents an example of the event tree for tsunami propagation, given that the rockslide has occurred. The numbers are given to illustrate the process, and are not to be used as estimates for the rock slope at Åknes. The steps for the tsunami event tree included: (1) rockslide is triggered; (2) slide is in one massive volume or in pieces; (3) volume of rockslide ($V < 5$ millions m^3 to $V > 35$ millions m^3); (4) resulting run-up height on land ($R \leq 5$ m to $R > 20$ m). The failure probability is the summation of the failure probabilities, P_f, in all the branches of the tree (Table 3.11).

As part of the evaluation of the consequences of a rockslide and tsunami, the magnitude of the consequences (loss of life and material property and environmental damage) depends on: warning time before the rockslide or tsunami hazard occurs, reliability of emergency preparedness plan, run-up height, local water level, local water flow velocity, availability of escape routes and distance to safe havens, time of the day, time of the year, training of professionals and public, unforeseen concurrent

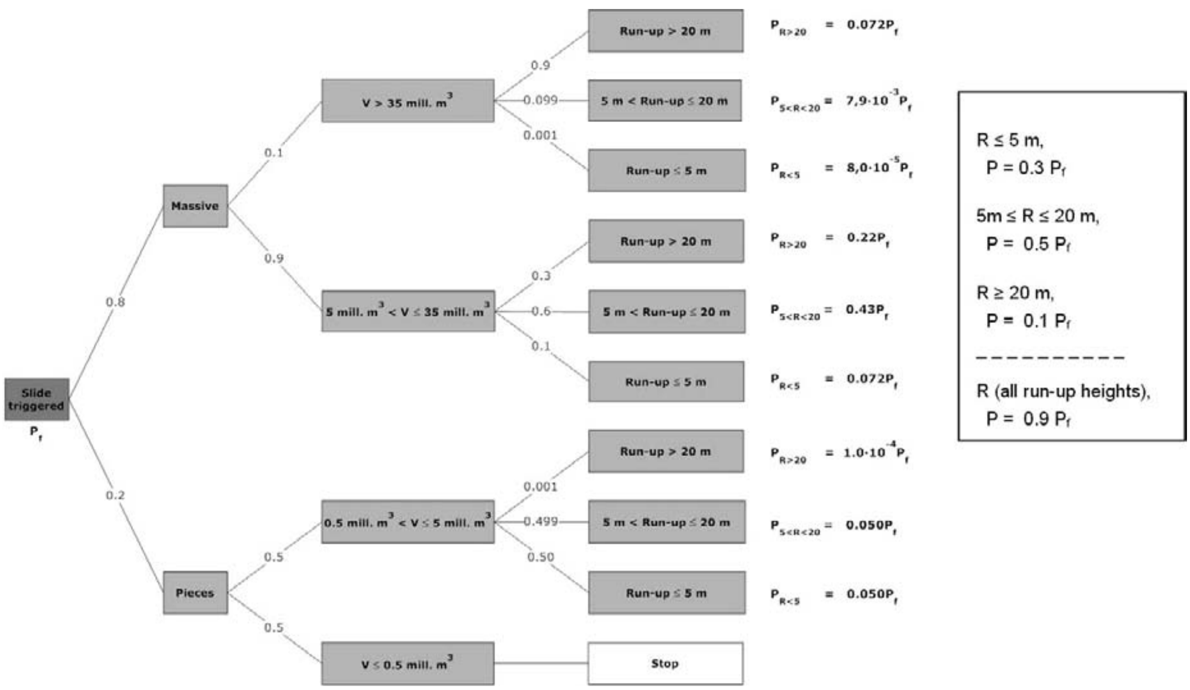

Fig. 3.16 Event tree for tsunami propagation, given that rock slide has occurred (V = rockslide volume, R = run-up height)

event etc. These factors will form the steps of the event tree on consequences.

3.8.5 Early Warning and Emergency Preparedness

The Åknes/Tafjord early warning and emergency preparedness system was implemented early 2008. As part of this system, the Emergency Preparedness Centre in Stranda is in operation continuously (24 h, 7 days). Alarm levels and responses are under development. The aim is to establish guidelines for monitoring and alert levels as a function of observed displacement rates on the extensometers, in the case of impending failure. Figure 3.17 and Table 3.12 present an example of the alarm and response system. The system is in constant evolution. The evaluation of the alarm status is done on the basis of an integrated interpretation of all measurements available, and their evolution over time (Blikra et al. 2007; Blikra 2008).

The Åknes/Tafjord early warning and emergency preparedness system was implemented early 2008. As part of this system, the Emergency Preparedness Centre Stranda is in operation continuously (24 h, 7 days). Alarm levels and responses are under development. The aim is to establish guidelines for monitoring and alert levels in the case of impending failure. Figure 3.9 and Table 3.3 present an example of the alarm and response system.

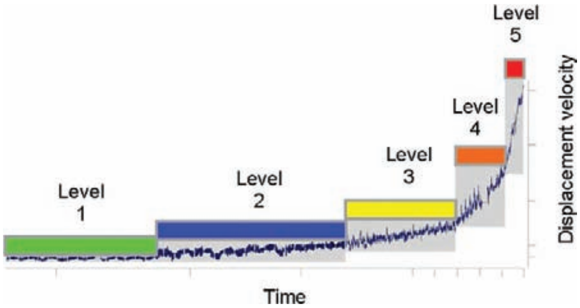

Fig. 3.17 Illustration of the alarm levels as function of displacement velocities (*vertical axis*: displacement rate in mm/day; *horizontal axis*: relative time before failure)

The event tree for the Åknes early warning system involved, among others, the following steps: (1) time needed for warning (t in weeks, days or hours, some triggers give more time than other); (2) technology (working, yes or no); (3) are signals picked up? (yes or no); (4) are signals correctly interpreted? (human element, time available, delegation of authority, etc); (5) warning parameter(s) to follow up before and during warning; (6) choice of threshold values. A number of factors were seen as important to consider:

– 4–5 wks/yr are the most critical because of climatic factors; at that time, one should define an increased alarm level

Table 3.12 Sketch of alarm levels and response indicated in Fig. 3.14

Alarm level	Activities and alarms	Response
Level 1 Normal situation	Minor seasonal variations No alarm	EPC staff only Technical maintenance
Level 2 Awareness	Important seasonal fluctuations for individual and multiple sensors Values<excess thresholds for Level 2	Increase frequency of data review, compare different sensors Call in geotechnical/geological/monitoring expert
Level 3 Increase awareness	Increased displacement velocity, seen on from several individual sensors Values<excess thresholds for Level 3	Do continuous review, do field survey, geo-expert team at EPC full time Inform police and emergency/preparedness teams in municipalities
Level 4 High hazard	Accelerating displacement velocity observed on multiple sensors Values<excess thresholds for Level 4	Increase preparedness, continuous data analysis Alert municipalities to stand prepared for evacuation
Level 5 Critical situation	Continuous displacement acceleration Values>excess thresholds for Level 4	Evacuation

EPC = Emergency Preparedness Centre in Stranda

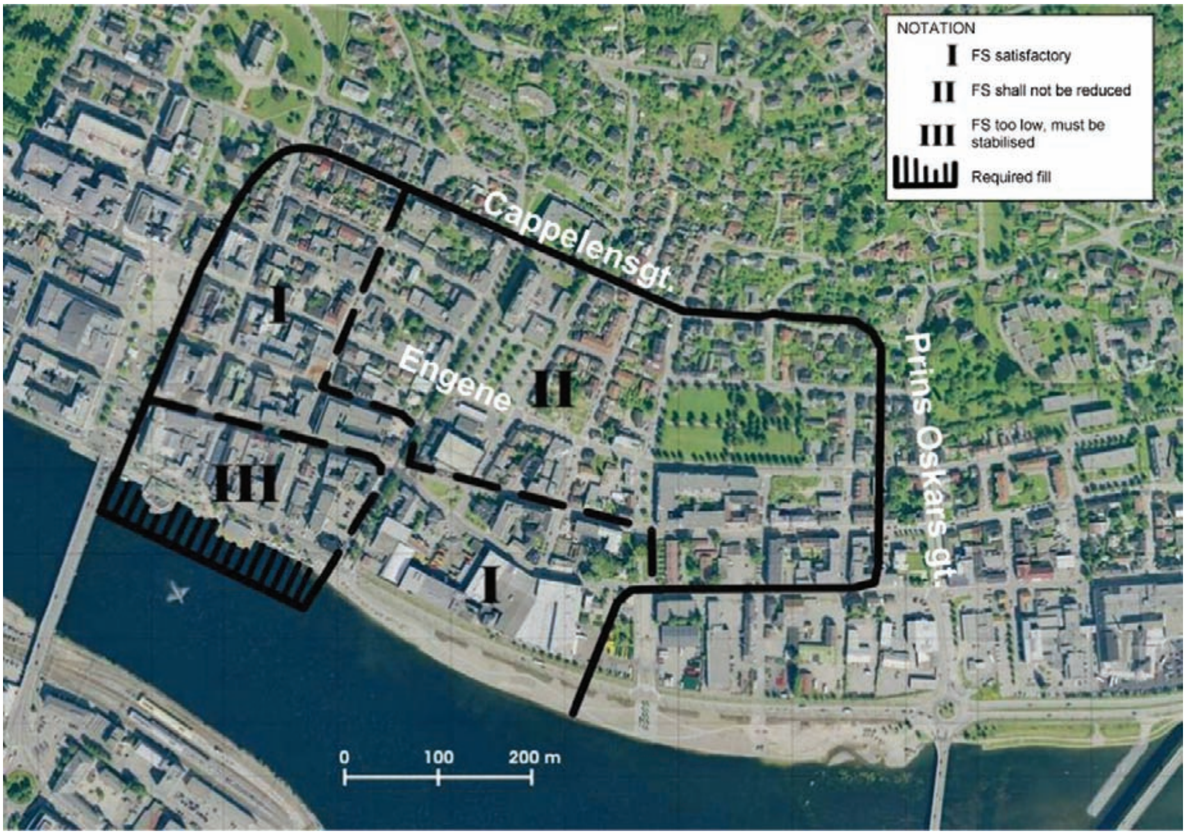

Fig. 3.18 Classification in hazard zones (Karlsrud 2008; Gregersen 2008)(SF = Safety Factor)

– life and range of operation of sensors (e.g. extensometers) should be checked continuously
– any presence of large amount of water should be monitored
– careful thought should be given to what is/are the most representative measurements for early warning
– monitoring should be spread out, as failure may occur in other locations than crack; consider additional boreholes and other measurements
– when making decision, look at snow avalanche warning
– statistical evaluation of measured data should be built in system; consider Bayesian updating
– adapt warning curve (Fig. 3.17) as more knowledge is acquired
– consider whether police and other authorities should be on standby earlier than suggested in Table 3.12 (police needs 72 h to evacuate entire Storfjord area)
– establish threshold values to decide on when to move back after false alarm, but bake in the possibility of slide developing with time
– be prepared with a new monitoring system to be set in operation quickly after a first slide that has probably destroyed the instrumentation in place

3.9 Mitigation Measures

Landslide mitigation measures can be classified as structural and non-structural. Structural measures include, but are not limited to: slope stabilisation, drainage, erosion protection, channelling, vegetation and ground improvement, barriers such as earth ramparts, walls, artificial elevated land, anchoring systems and retaining structures; buildings designed (and placed) in locations to withstand the impact forces of landslides and to provide safe dwellings for people, and escape routes. Non-structural measures include land-use planning and other consequence-reducing measures. Consequence-reducing measures include, but are not limited to: retreat from hazard, land-use planning, early warning, public preparedness, (escape routes, etc.) and emergency management. The risks may also be pooled through insurance mechanisms.

It is important, when evaluating mitigation measures, to weigh benefits of the measures to be implemented and the possible negative effects these measures may have. Decision-making will rest in finding an optimal solution.

3.9.1 Example – Hazard and Risk Mitigation in Drammen

The city of Drammen, along the Drammensfjord and the Drammen River, is built on a deposit of soft clay. Stability analyses were done in an area close to the centre of the city, and indicated that some areas did not have satisfactory safety against a slope failure. Based on the results of the stability analyses and the factors of safety (FS) obtained, the area under study was divided into three zones (Gregersen 2005):

– Zone I FS satisfactory
– Zone II FS shall not be reduced
– Zone III FS too low, area must be stabilised

Figure 3.19 illustrates the mitigation done in Zone III: a counter fill was immediately placed in the river to support the river bank, and the factor of safety checked again. The counter fill provided adequate stability (Gregersen 2008).

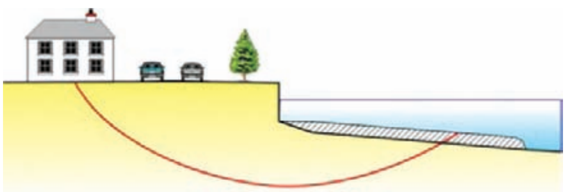

Fig. 3.19 Mitigation in Zone III in Drammen

In Zone II, no immediate geo-action was taken, but a ban was placed on any new structurel and foundation work without first ensuring increased stability. Figure 3.20 illustrates four cases (Gregersen 2008; Karlsrud 2008): (1) if an excavation is planned, it will have to be stabilised with anchored sheetpiling or with soil stabilisation, e.g. with chalk-cement piles; (2) new construction or new

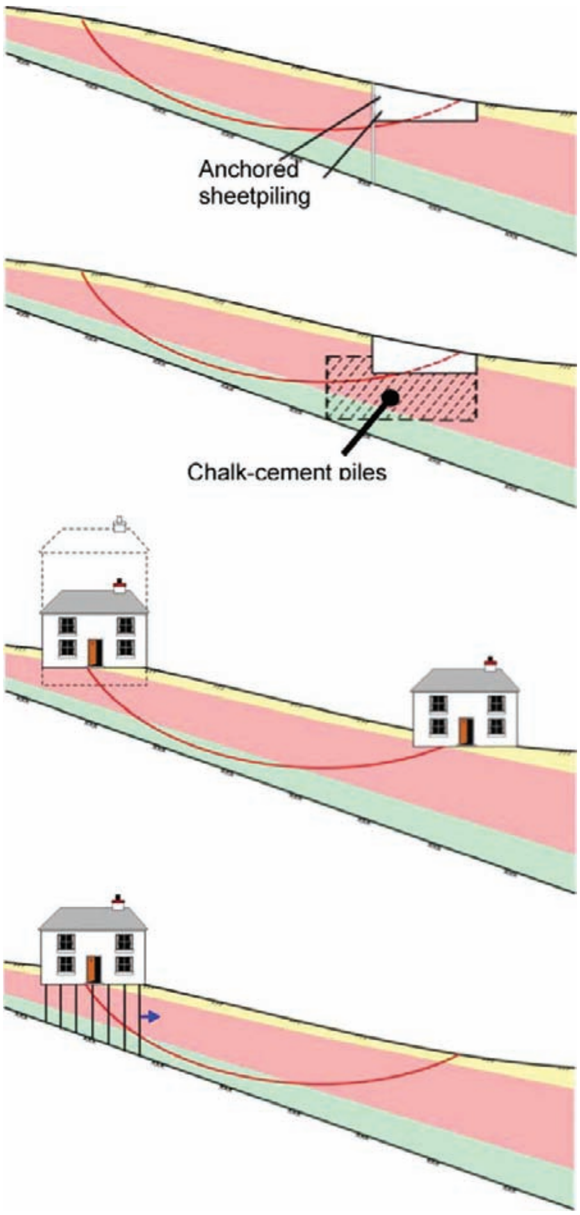

Fig. 3.20 Hazard, mitigation and preventive measures in Zone II in Drammen

foundations cannot be done without first checking their effect on the stability down slope; for example, adding a floor to a dwelling may cause failure because of the added driving forces due to the additional loading, and new piling up slope will cause a driving force on the soil down slope.

3.10 Summary and Conclusions

As a consequence of climate change and increase in exposure in many parts of the world, the risk associated with landslides is growing. The profession needs to forecast the occurrence of landslide and the hazard and risk associated with them.

Climate change, increased susceptibility of surface soil to instability, anthropogenic activities, growing urbanization, uncontrolled land-use and increased vulnerability of population and infrastructure as a result, contribute to the growing landslide risk. In areas with high demographic density, protection works often cannot be built because of economic or environmental constraints, and is it not always possible to evacuate people, because of societal, geographical, seasonal, warning time or other reasons.

People living in cities are less exposed to the risk posed by landslides than people living in rural areas. The exception is the poorest segment of the population who live in slums that develop at a pace that no urban planner can control.

The mitigation and prevention of the risk posed by natural hazards have not attracted widespread and effective public support in cities during recent decades. If geohazards risk reduction is to be successful in the future, geoscientists and engineers need to develop new solutions that are appropriate for dealing with the global changing due to climate, demography and policies.

This will involve refocusing attention on the little-explored interface between technical and natural sciences on one hand, and social and political sciences on the other (Nadim and Lacasse 2008). Such a stance will bring the different professions face to face with the problem of fostering risk reduction measures that have broad appeal to stakeholders as well as victims, researchers and risk management professionals. Geoscientists and engineers can contribute to an improved understanding of risk assessment, mitigation and management.

A proactive approach to risk management is instrumental for reducing significantly loss of lives and material damage associated natural hazards. The major natural disasters that have taken place over the last 5–10 years and received wide media attention, have clearly changed people's mind in terms of acknowledging risk management as an alternative to emergency management.

One can observe a positive trend internationally where preventive measures are increasingly recognized, both on the government level and among international donors. There is, however, a great need for intensified efforts, because the risk associated with natural disasters clearly increases far more rapidly than the efforts made to reduce this risk.

Kjekstad (2007) suggested an approach based on three pillars for landslide risk management for developing countries:

Pillar 1: Hazard and Risk Assessment

Hazard and risk assessment are the central pillar in the management of geohazards risk. Without knowledge and characteristics of hazard and risk, it would not be meaningful to plan and implement mitigation measures.

Pillar 2: Landslide Mitigation Measures

Mitigation means implementing activities that prevent or reduce the adverse effects of extreme natural events. Mitigation includes structural and non-structural measures and political, legal and administrative measures. Mitigation also includes efforts to influence the lifestyle and behaviour of endangered population in order to reduce the risk. Many factors within human control that can help minimize number of casualties, such as knowledgeable population, effective early warning system and constructions built with disasters in mind.

Pillar 3: International Cooperation and Support

Most of the developing countries lack the resources, capacity and technical skills to proceed with geohazards risk reduction measures at a pace that is desired and needed. International cooperation and support are therefore highly desirable. The development agencies of the United States (USAID), Canada (CIDA), Japan (JICA), Germany (GTZ/BGR), Switzerland (CONSUDE and

SDC), Sweden (SIDA), Norway (NORAD/Ministry of Foreign Affairs), UK (DIFID), the Netherlands (SNV), Austria (ADA), and Australia (AusAid), as well as many NGOs, support projects related to the mitigation of risk due to natural hazards in developing countries.

A key challenge for the donor countries is to secure that they are need-based, sustainable and well anchored in the countries' own development plans. Another challenge is coordination which often has proven to be difficult because the agencies generally have different policies and the implementation period often differ in time. There is also the need to secure ownership of the project in the country receiving assistance.

A milestone in international collaboration for natural disaster risk reduction was the approval of the "Hyogo Framework for Action 2005–2015: Building the Resilience of Nations and Communities to Disasters" (ISDR 2005). This document, which was approved by 165 UN countries during the World Conference on Disaster Reduction in Kobe, January 2005, clarifies international working modes, responsibilities and priority actions for the coming 10 years.

The Hyogo Framework of Action has increased the awareness and importance of preventive and mitigation measures. It will also contribute to a much better practice for the implementation of risk reduction projects for two reasons: (a) by the fact that governments will be in the driving seat, which means that coordination is likely to be improved, and (b) the fact that ISDR is given the responsibility for the follow-up of the plan will put pressure for action from countries that are most exposed.

Reducing the impact of landslide with mitigation measures, is both an economical and social necessity. Loss statistics show that number of fatalities is much higher in developing countries than in developed countries. The frequency of landslide disasters is increasing due to more extreme weather than before, increased population and increased vulnerability. The situation calls for intensified focus on and action to provide preventive measures.

Acknowledgment The authors wish to thank the following who provided the case studies or shared generously their competence for completing the case studies: Mr. Kjell Jogerud, Dr. L.H. Blikra and all participants to the Event Tree Analysis for the Åknes rock slope held at NGI in late 2007, Dr. Elmo DiBiagio for his documentation on the Lake Sarez case study and Mssrs. Odd Gregersen and Kjell Karlsrud for the Drammen case study. The authors also thank the participants at the Hong Kong Landslide Risk Management Forum for their input in the session on digital technology.

References

Aas, G. (1979). "Skredfare og arealplanlegging. Vurdering av faregrad og sikringstiltak". Ullensvang Hotell, Lofthus i Hardanger, NIF-kurs.

Aas, G. (1981). "Stability of natural slopes in quick clays." Proc., 10th International Conference on Soil Mechanics and Foundation Engineering, Stockholm, Sweden. V 3, pp. 333–338.

Anda, E. and Blikra, L. (1998). "Rock-avalanche hazard in Møre og Romsdal, Western Norway. 25 Years of Snow Avalanche Research." Norwegian Geotechnical Institute, Publikasjon nr. 203.

Bjerrum, L. and Jørstad F. (1968). "Stability of Rock Slopes in Norway." NGI publication No. 79.

Blikra, L.H. 2008. "The Åknes rockslide; monitoring, threshold values and early-warning" 10th International Symposium on Landslides and Engineered Slopes, Xi'an, June 2008. China.

Blikra, L.H., Longva, O., Braathen, A. and Anda, E. (2002). "Rock-slope failures in Norwegian fjord areas: Examples, spatial distribution and temporal pattern". NATO Advanced Research Workshop. Italy.

Blikra, L.H., Jogerud, K., Hole, J. and Bergeng, T. (2007). "Åknes/Tafjord prosjektet – Status og framdrift for overvåking og beredskap". Report 01-2007. www.aknes-tafjord.no, 30p.

Bruzzi, D. (1989). "Control of landslides and instrumentation." Discussion session 21. Proc. 12th International Conference on Soil Mechanics and Foundation Engineering, Rio de Janeiro, Vol. 5, pp. 3075–3080.

Bryn, P., Berg, K., Forsberg, C.F., Solheim, A. and Kvalstad, T.J. (2005). "Explaining the Storegga Slide. Ormen Lange – An integrated study for safe field development in the Storegga submarine slide area". In Solheim, A. et al. Ormen Lange – An Integrated Study for Safe Field Development in the Storegga Submarine Slide Area. Elsevier. pp. 11–20.

DiBiagio, E. and Kjekstad, O. (2007). "Early Warning, Instrumentation and Monitoring Landslides". 2nd Regional Training Course, RECLAIM II, 29th January–3rd February 2007.

Eidsvig, U. and Harbitz, C. 2005. "Innledende numerisk analyser som følge av mulige skred fra Åkneset" ("Preliminary numerical analyses of tsunamis generated by a slide at Åknes"). NGI Report 20031100-2. Oslo, Norway. 100p.

Eidsvig, U.K., Lacasse, S., Nadim, F. and Høeg, K. (2008). "Event tree analysis of hazard and risk associated with the Åknes rockslide". ICG/NGI Rpt 20071653-1. Oslo, Norway.

Glimsdal, S. and Harbitz, C. 2006. "Preliminary results using an improved tsunami model". NGI Rpt 20051018-1. Oslo, Norway. 70p.

Gregersen, O. (1981). "The quick clay landslide in Rissa, Norway." Int. conf. on oil Mechanics and Foundation Engineering, 10. Stokholm 1981. Vol. 3. pp. 421–426.

Gregersen, O. (1989). "Landomfattende kartlegging av kvikkleireavsetninger, Fjellsprengningsteknikk." Bergmekanikk/Geoteknikk konferanse. Oslo, Norway.

Gregersen, O. (2001). "Metode for klassifisering av faresoer, kvikkleire". 20001008-1, Norwegian Geotechnical Institute, Oslo, Norway, 24 January 2000.

Gregersen, O. (2005). "Program for økt sikkerhet mot leirskred. Risiko for kvikkleireskred Bragernes, Drammen". Report 2004 1343-1. Norwegain Gotechncial institute, 26 January 2005.

Gregersen, O. (2008). "Kartlegging av skredfarlige kvikkleireområder". Paper for NGM-2008 (Northern Geotechnical Conference 3-5 September 2008). Sandefjord, Norway. 9p. pp. 178–186.

Grimstad, E. (2005). "The Loen Rock Slide – An Analysis of the Stability". International Conference and Field trip on Landslides. Norway.

Hartford, D.N.D. and Baecher, G.B. (2004). "Risk and uncertainty in dam safety". Thomas Telford. London, UK. 391p.

Helland, A. (1905). "Raset på Ravnefjell i Loen". Naturen 29, 6/7.

Helland, A. and Steen, H. (1895). "Lerfaldet i Guldalen i 1345". Archiv for Mathematik og Naturvideskaberne, Bind 17, Nr. 6, Christiania 1895.

Helland, A. (1911). Norges land og folk, XV, 1. del, Kristiania.

Heyerdahl, H., Harbitz, C.B., Domaas, U., Sandersen, F., Tronstad, K., Nowaki, F., Engen, A., Kjekstad, O., Devoli, G., Buezo, S.G., Diaz, M.R. and Hernandez, W. (2003). "Rainfall induced lahars in volcanic debris in Nicaragua and El Salvador." Practical mitigation. International Conference on Fast Slope Movements, FSM 2003. Naples/Sorrento, May 2003. Proceedings, Vol. 1. 9p.

Høeg, K. (1996). "Performance evaluation, safety assessment and risk analysis of dams". Hydropower and Dams. 6, 3, November 1996. 8p.

Holmsen, G. (1936). "De siste bergskred i Tafjord og Loen, Norge". Svensk geografisk årsbok. Lunds universitet. Geografiska institutionen. Meddelande 124.

ISDR (International Strategy for Disaster Reduction) (2005). Hyogo Framework for Action 2005–2015, 21 pp.

Jørstad, F. (1956). "Fjellskredet ved Tjelle. Et 200-årsminne". Naturen 80, 6.

Karlsrud, K., Aas, G. and Gregersen, O. (1984). "Can we predict landslide hazards in soft sensitive clays? Summary of Norwegian practice and experiences". International Symposium on Landslides, 4. Toronto 1984. Proceedings, Vol. 1, pp. 107–130.

Karlsrud, K. (2008). "Hazard and Risk Mapping for Landslides". Paper for 33rd IGC (International Geology Congress). (6–14 August 2009). Oslo. (CD only).

Kjekstad, O. (2007). "The challenges of landslide hazard mitigation in developing countries." Keynote lecture, First North American Landslide Conference, Vail, Colorado, 3–8 June.

Kveldsvik, V., Eiken, T, Ganerød G. V., Grøneng, G. and Ragvin, N. (2006). "Evaluation of movement data and ground conditions for the Åknes rock slide"; South African Institute of Mining and Metallurgy, International Symposium on Stability of Rock Slopes in Open Pit Mining and Civil Engineering. pp. 279. 299.

Kveldsvik, V., Einstein, H.H., Nilsen, B. and Blikra, L.H. (2008): "Numerical stability models of the 650,000 m^2 Åknes rock slope based on measured displacements and geotechnical data". Rock Mechanics Rock Engineering DOI 10.1007/s00603-008-0005-1.

Lacasse, S. (2008). "Landslide Risk Management Country Report For Norway". Hong Kong Landslide Risk Management Forum (in press).

Lacasse, S., Eidsvik, U., Nadim, F., Høeg, K. and Blikra, L. H. (2008). "Event Tree analysis of Åknes rock slide hazard". IV Geohazards Québec, 4th Canadian Conf. on Geohazards. pp. 551–557.

Lacasse, S., Nadim, F., Høeg, K. and Gregersen, O. (2004). "Risk Assessment in Geotechnical Engineering: The Importance of Engineering Judgement". The Skempton Conference, Proc. London UK. Vol. 2, pp. 856–867.

Lied, K. (2008). Skred. (Book in press).

Nadim, F. and Lacasse, S. (2008). "Effects of Global Change on Risk associated with Geohazards in Megacities". Proc Development of Urban Areas and Geotechnical Engineering Conf. 16–19 June 2008. St Petersburg. Russia. Vol 1. pp. 109–118.

Nadim, F., Kjekstad, O., Peduzzi, P., Herold, C. and Jaedicke, C. (2006). "Global landslide and avalanche hotspots". Landslides, Vol. 3, No. 2, pp. 159–174.

Nadim, F., Kvalstad, T.J. and Guttormsen, T. (2005). "Quantification of risks associated with seabed Instability at Ormen Lange". In Solheim et al. Ormen Lange – An Integrated Study for Safe Field Development in the Storegga Submarine Slide Area. Elsevier. pp. 311. 318.

NORSOK standard Z-013 (2001): "Risk and emergency preparedness analysis", rev. 2, www.standard.no.

NS 5814 (1991): "Requirements for risk analyses", Norwegian standard, www.standard.no.

Solheim, A. et al. (2005a). "International Centre for Geohazards (ICG) – Assessment, prevention and mitigation of geohazards". Norwegian Journal of Geology, 85, 1 & 2, pp. 45–62.

Solheim, A. et al. (2005b). "The Storegga Slide Complex: Repetitive large scale sliding with similar cause and development". Marine Petroleum and Geology, 22, pp. 97–107.

Stucky (2007). "Lake Sarez Risk Mitigation Project – Component A. Final Report to Ministry of Emergencies and Civil Defense of the Republic of Tajikistan". Renens, Switzerland, 20 January 2007.

World Disaster Report (2006). http://wwwredcross.ca.www.aknes-tafjord.no. Åknes/Tafjord project webpage.

Understanding to Predict

4

Luciano Picarelli

Abstract Today a significant effort is being spent in some advanced countries in the world to develop reliable methods for landslide prediction and risk mitigation. The solution of such a problem requires a great experience and a deep knowledge of soil behavior. In fact, only a clear understanding of the physical and mechanical processes which lead to slope failure and of the processes which govern following movement of soil or rock masses, can help in the setting up of effective actions for risk mitigation. Based on the analysis and interpretation of documented cases, the paper reports some examples of the strict relationship which exists between soil properties or pore pressure regime, and landslide mechanisms.

Keywords Soil behavior • Soil properties • Pore pressure regime • Landslide mechanisms • Landslide mechanics

4.1 Foreword

The Renaissance was a turning point in the human conception of science because of a radical change of the scientific approach in the analysis of physical natural and man-induced phenomena. The new revolutionary approach adopted turned around the role of experience as "mother of science". In fact, scientists started to think that only experience can provide a real input in the development of every theory. Previous conception of science essentially based on the discussion and comparison of abstract ideas was progressively abandoned and experiments replaced previous erudite philosophical disquisitions. The great scientists of that time and of subsequent centuries, Leonardo da Vinci, Galileo Galilei, Isac Newton and so on, provided extraordinary examples about the role that experience plays in the development of theory. In the *Leben des Galilei* (Galilei's Life), Bertoldt Brecht imagines a funny discussion between the great Italian scientist who tried to prove the validity of the Copernican theory (the Earth revolves round the Sun) and some professors of the Florence University who defended the old concept that is the Sun which revolves round the Earth, based on Aristotle's ideas about the Universe and Holy Writings. In spite of Galilei's comic efforts, there was no way of convincing them to watch the planets through his telescope which was under their nose, because they firmly claimed to rely more in their own ideas than in the tangible experience.

The experimental approach remains a milestone of the modern science, even though there are still researchers who, more or less as those Florentine professors, trust more in their abstract theories than in the richness of experience. Some of them do not

Luciano Picarelli (✉)
Seconda Universtà di Napoli, Italy

© Springer-Verlag Berlin Heidelberg 2009

care at all to check if their assumptions are validated by experience, or even refuse experimental results if these do not confirm their own theories!

Geotechnics is a branch of civil engineering which is firmly founded on experience. Theoretical concepts are developed and continuously improved through a continuous analysis and interpretation of experimental data; in turn, experiments are used to validate the new theoretical concepts. A clear example is the development of the Critical State Theory (Schofield and Wroth, 1968), which is based on evidence coming from laboratory testing on reconstituted saturated clay. Its extension to unsaturated soils (Alonso et al., 1990), has been developed based on laboratory experiments on unsaturated soil samples. Attempts for further extension to "structured" soils (Nova, 1992) are based on experimental remarks about the failures of theory in the interpretation of the behaviour of "structured" soils.

Similar considerations apply to the case of landslides. The understanding of the mechanics of landslides has been a progressive attainment based on site investigations and monitoring, and on laboratory testing and physical modelling interpreted in the light of theoretical considerations as well as of intuition based on experience.

These basic concepts inform the paper, which reports some examples, taken from personal files of the Writer, concerning the strict relationship which exists between soil properties, pore pressure regime and landslide mechanisms.

4.2 Organization of the Paper

Landslides represent one of the major natural hazards in several countries of the world. In Italy they involve very different geological and geomorphological contexts: the Alpine chain, where rock falls, rock slides and rock avalanches are spread; the Apennines chain, which is characterised by moderate to rapid first-time slides and mudslides and by slow active slides in highly fissured tectonized clay shales; volcanic areas, where extremely rapid flowslides and debris flows involving pyroclastic soils represent a permanent hazard (Picarelli et al., 2008a). Because of the highly density of population, of infrastructures, of industrial settlements as well as of ancient monuments and remnants, the risk is extremely high everywhere.

The paper reports some considerations about prominent aspects of the causes and mechanisms of landslides in Italy, with particular reference to events which involve stiff fissured clays and pyroclastic soils. Some points concerning soil behaviour, pore pressures and landslide mechanisms are discussed in order to demonstrate that only a clear understanding of experience can provide a correct assessment of slope behaviour and help in the establishment of criteria for risk mitigation.

4.3 The Role of Soil Properties and Behavior on Landslide Triggering

The measurement of soil properties is a fundamental phase of any geotechnical analysis, and especially of slope stability, because of the role of even small details of soil behavior. In particular, there are soils which present special features which require appropriate consideration in both testing and data interpretation. Some examples are reported below.

4.3.1 Shear Strength of Highly Fissured Clay

The Apennines chain is constituted by a sequence of thrust sheets including both flysch formations which present a significant highly OC fine-grained component (marly or clayey layers interbedded between layers of competent rock) and thick deposits of hard clays or clay shales. These deposits are highly fractured or completely disarranged because of tectonism (Picarelli et al., 2002). In particular, both the argillaceous component of flysch and clay shale deposits display an intensely fissured fabric provoked by shearing. In fact, the peculiar macrofabric of these material consists of shear lenses sizing between some millimeters to a few centimeters, bounded by smooth and shiny fissures (Fig. 4.1). For this reason, these materials are called *argille a scaglie* (scaly clay shales).

Picarelli et al. (1998) remark the peculiar behavior of scaly clay shales whose performance is

Fig. 4.1 Examples of highly fissured tectonized clay shales: (**a**) Red Flysch outcropping in the Brindisi di Montagna area; (**b**) specimen of the Bisaccia clay shale after rupture in a triaxial test: the red thread closely follows the slip surface

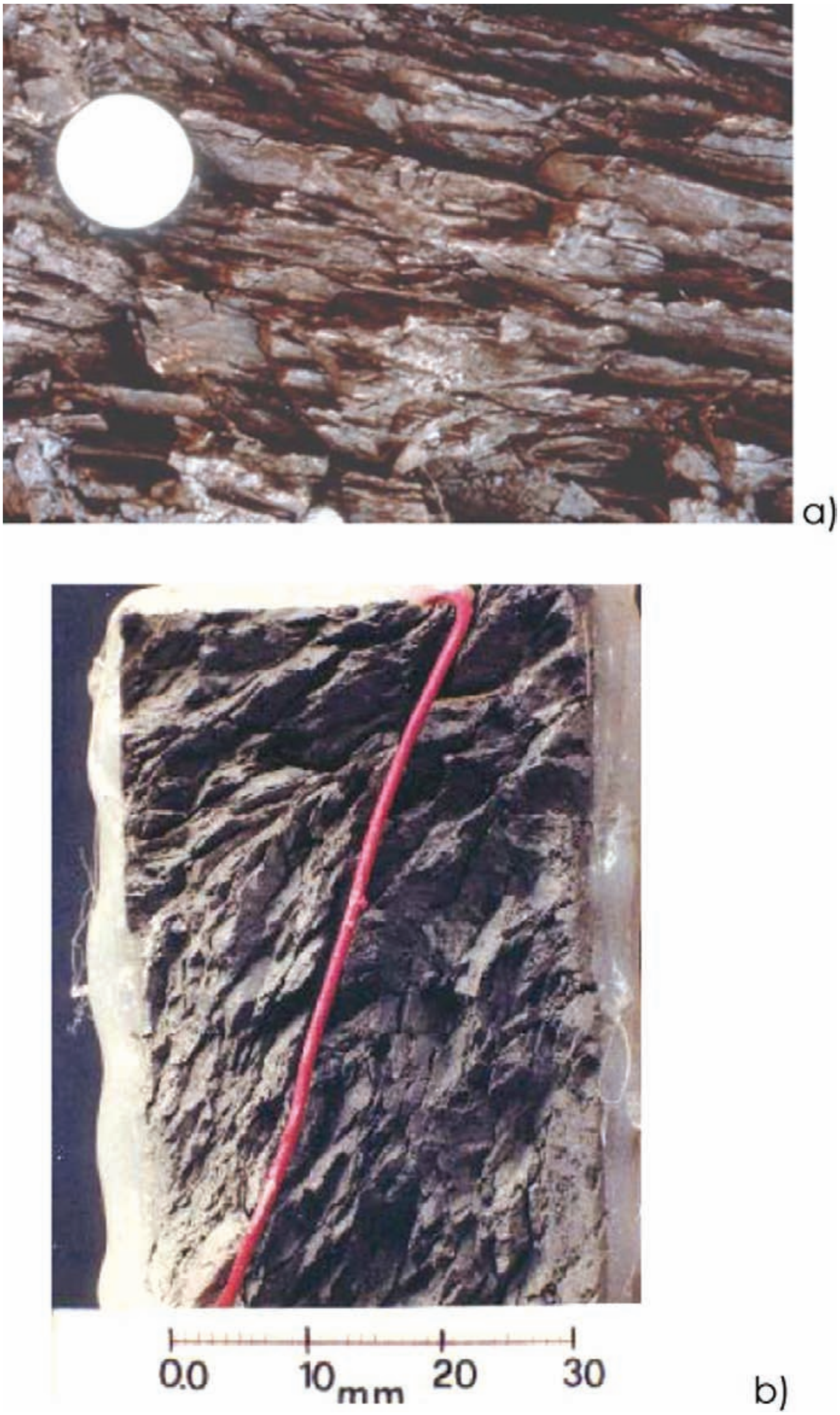

excellent when subjected to the weight of even large and heavy structures, but is very poor as a response to shallow or deep excavations. Also, slopes constituted by these materials are prone to landslides whose velocity is generally moderate to slow. In fact, broad sloping areas of the Apennines chain are highly unstable and can be exploited for civil construction only after complex and costly stabilization measures.

Figure 4.2, which reports the results of a undrained triaxial test on the Bisaccia clay shale, instrumented with local strain and pore pressure microtransducers, can synthetically explain both aspects of soil behavior. Figure 4.2a and b compare measured local strains to nominal values obtained through external measurements ("external strains"). For external strain less than 0.05%, i.e. for a stress level up to about 20%, the specimen displays a "stiff" response (Fig. 4.2c), and behaves quite uniformly, the local strain being less than the nominal one. For stress levels higher than 20%, local readings clearly show that a strain localization occurs in the middle part of the specimen. Also the excess pore pressure seems non uniform, as shown by the comparison of readings in the middle part of the specimen and at its base (Fig. 4.2e); this phenomenon seems to happen as the external axial strain reaches 0.8% (stress level higher than about 50%). Despite a high nominal OCR (Fig. 4.3), the soil behavior is ductile rather than brittle. The same occurs in drained tests, which show a slightly brittle behavior only for small confining stresses.

Figure 4.3 reports the failure envelope of the Bisaccia clay shale obtained by drained and undrained triaxial tests carried out on both reconstituted and undisturbed specimens. The natural soil presents a non linear envelope: for a mean effective stress less than 200 kPa its shear strength is only slightly higher than the critical strength measured on reconstituted specimens, while it is significantly less for a mean effective stress higher than 200 kPa. Such a result is in contrast with any theory, especially when accounting for the nominal OCR of the natural soil, shown in the figure. The only explanation for that can be found in the role played by the network of fissures.

Figures 4.1b and 4.2 can help to understand the mechanisms of failure. As far as the state of stress presents a small deviator component, the material behaves as a stiff intact OC clay (Fig. 4.2a, b and c). This is also shown by the results of isotropic and one dimensional oedometer tests not reported here (Picarelli et al., 1998). The soil response changes for higher deviator stresses, since the local shear strength is fully mobilized along fissures as shown by strain localization. Soil failure manifests itself by slipping along more or less aligned fissures bounding the shear lenses (see Fig. 4.1b). As for rock joints (Barton, 1976), the shear strength depends on a basic friction angle which is operative along fissures and is probably close to the residual value, and on a dilation angle which is a function of the "roughness" (the undulation) of the slip surface, i.e. of the arrangement of shear lenses at the onset of rupture. This explains the curved shear strength envelope. In fact, for high confining stresses the dilation angle decreases and the soil strength reduces to a value which is less than the critical strength obtained on reconstituted specimens, approaching the residual strength.

The low shear strength, which is governed by the distribution of fissures, can explain the high number of landslides in scaly clay shales, as well as problems encountered in tunneling (thickness of the plastic ring). In addition, the ductile (or slightly brittle) behavior of these materials can explain the fact that the velocity of first-time slope movements is generally rather slow or moderate (Leroueil et al., 1996).

The same results discussed above can explain the good performance of clay shales as foundation soils, at least for a state stress well below the failure envelope. In this case, in fact, the network of fissures is not necessarily mobilized and the soil displays a stiff response.

The same mechanisms govern the "ultimate" soil behavior. In fact, Picarelli (2005) remarks that the shape of the slip surface is not perfectly planar even though very smooth. Treating once again the slip surface as a discontinuity in rock, the residual friction angle should be equal to the basic friction angle, i.e. the friction angle along a planar and smooth surface, plus a "residual angle of roughness" which depends on the "ultimate" shape of the shear surface. Since the basic friction angle is often very low, even a small value of the "residual angle or roughness" can lead to relatively high values of the residual friction angle. Similar

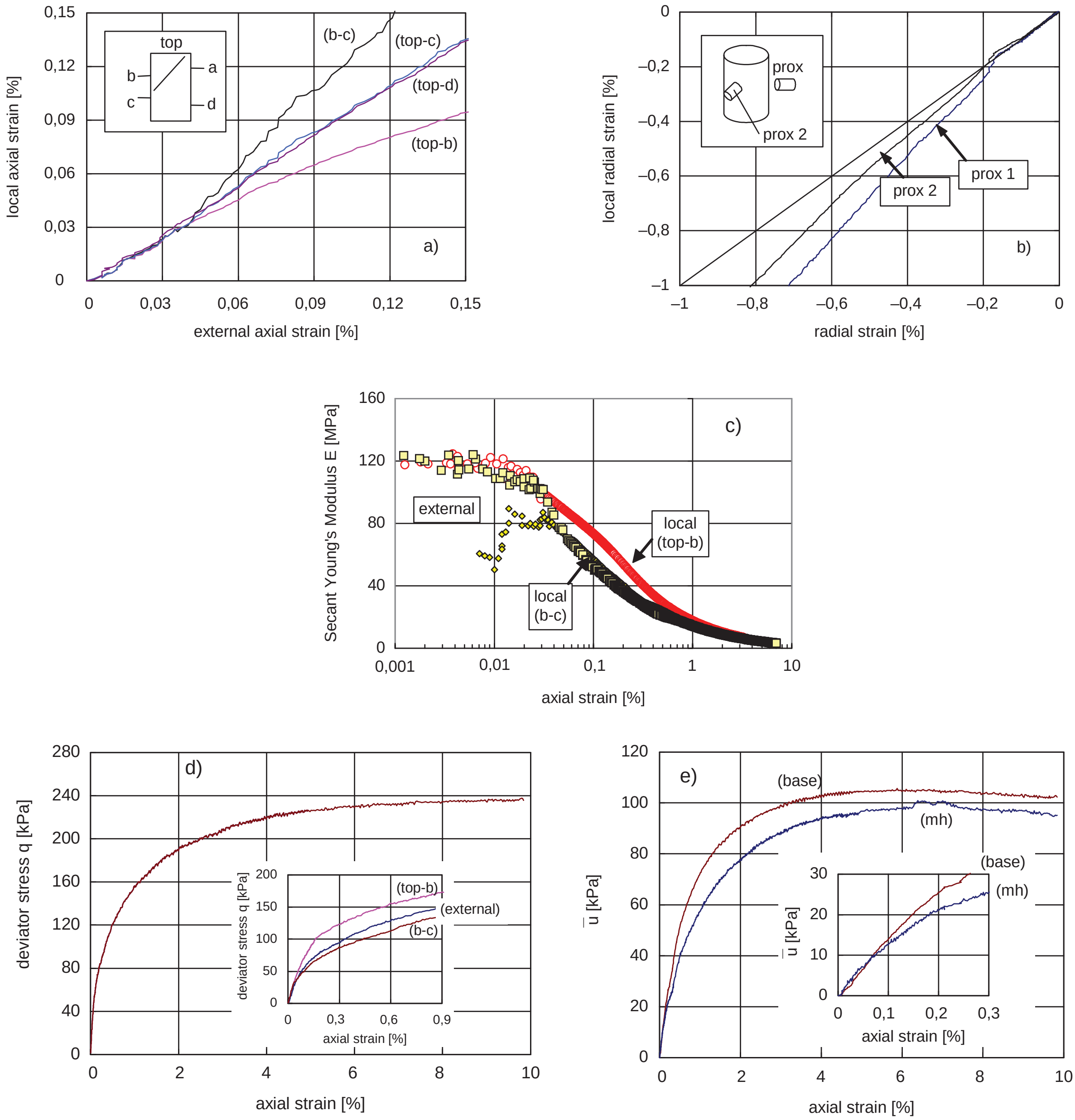

Fig. 4.2 Results of a undrained traxial test on the Bisaccia clay shale subjected to a confining stress of 400 kPa (Olivares, 1998): (**a**) local axial strains; (**b**) local radial strains; (**c**) secant Young modulus; (**d**) stress-strain curve; (**e**) local excess pore pressures

considerations are reported by Lo Presti and Frojo (2004) for soft rocks. This can explain why the residual friction angle measured on reconstituted specimens, whose surface of failure is probably much more regular and closer to a planar smooth surface, is often less than the one measured on undisturbed specimens (Picarelli, 1980).

The results of direct shear tests on undisturbed specimens of a highly fissured clay characterized by well aligned shear lenses can support these considerations. In fact, the residual strength, which is theoretically independent on soil fabric, is instead highly anisotropics as shown by the comparison of the results of tests on specimens prepared with shear

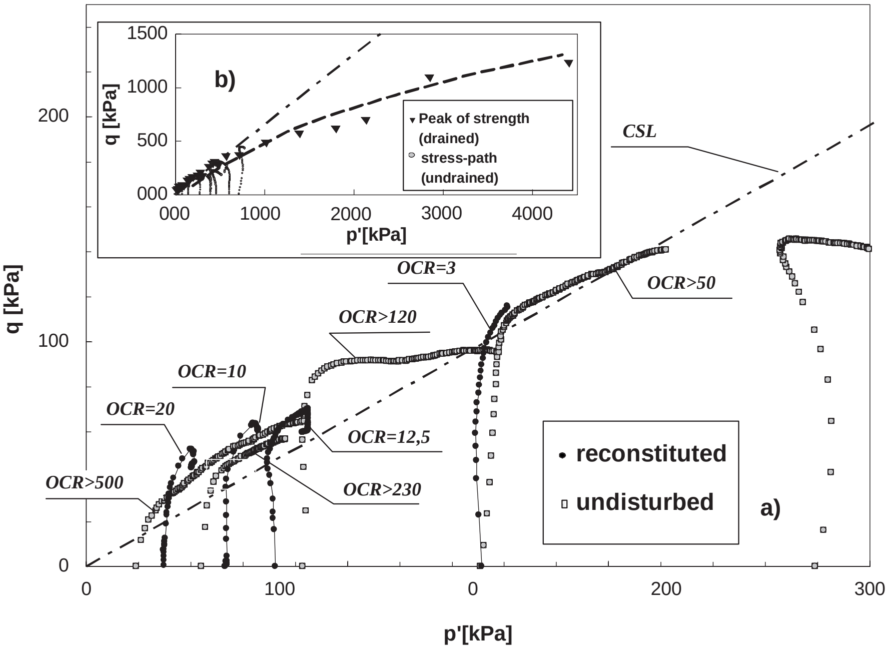

Fig. 4.3 Shear strength envelope of the Bisaccia clay shale (Olivares and Picarelli, 1999): (**a**) stress paths obtained in undrained tests for effective confining stresses less than 300 kPa; (**b**) complete shear strength envelopes obtained in drained and undrained tests

lenses oriented in the same direction as shear, and normally to it (Fig. 4.4). Since their basic friction angle is the same, depending only on the index properties and mineralogy, the anisotropy of the residual strength must necessarily reflect a different "residual angle of roughness", which is a function of the final arrangement of the shear lenses along the shear surface.

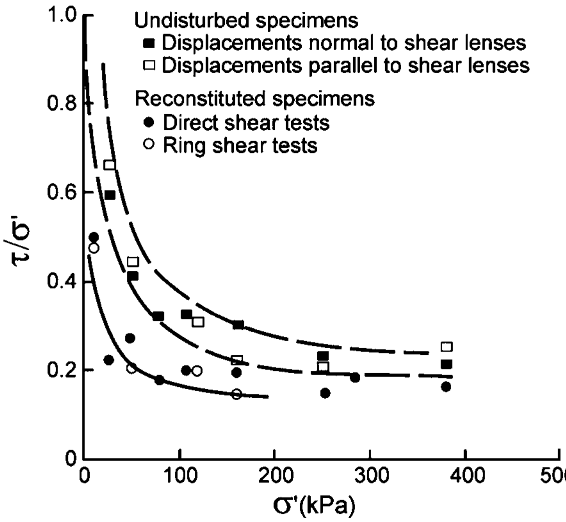

Fig. 4.4 Residual strength of the Laviano highly fissured clay shale (Picarelli, 1980)

4.3.2 Deterioration of Stiff Clays and Clay Shales

Experience suggests that slope failure, especially in hard clays and clay shales, can occur without an apparent cause. Since most of the landslides in clay occur during the wet season, the most obvious hypothesis about their trigger is the increase in pore pressure provoked by rainfall. However, this is not necessarily true.

As shown by Picarelli et al. (2004), in a given climatic period both the annual rainfall regime and pore pressures display recurrent features whose seasonal trend roughly replicates every year. In general, pore pressures fluctuate within the same interval bounded by two extreme values attained in the past, which usually are not reached in the present climatic phase (Fig. 4.5a). Therefore, in general the mean effective stresses, which follow a similar path, do not reach the failure envelope (solid line, in Fig. 4.5b). Therefore, the only mechanism which can explain slope failure is soil deterioration, i.e. a time-dependent decrease in strength (as by dotted lines in Fig. 4.5b), acting in conjunction with pore pressure increase. Often, deterioration is a long-lasting process; in many cases, it has already provoked a undetected damage somewhere in soil

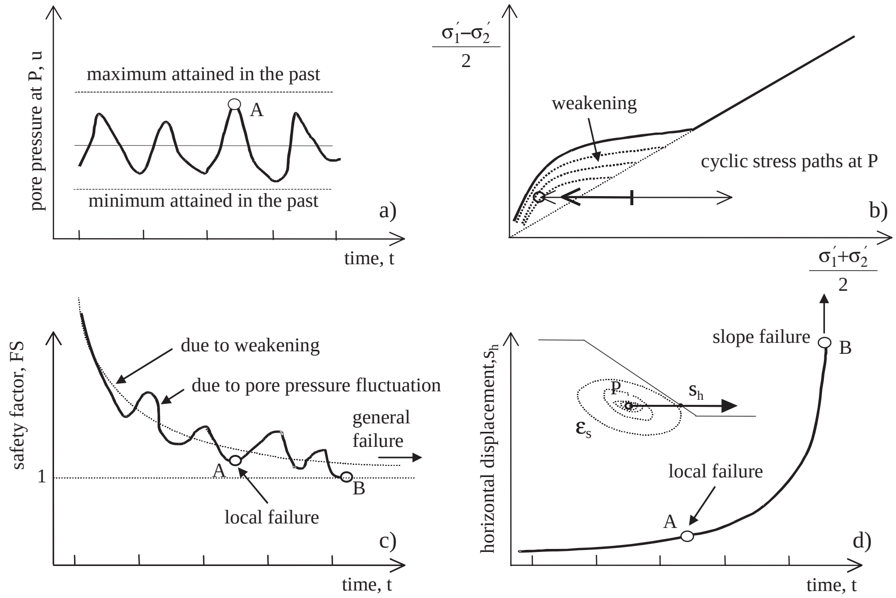

Fig. 4.5 (**a**) Seasonal changes of pore pressure in a representative point of a slope; (**b**) local stress paths; (**c**) decrease of the safety factor with time; **(d)** virtual horizontal displacement in a point of the slope (Picarelli et al., 2004)

structure (point A in Figs. 4.5c and 4.5d). Slope failure is hence the result of a combination of soil deterioration and pore pressure increase (Figs. 4.5b, c).

Deterioration is of little importance in granular soils, being a relevant phenomenon in stiff OC fine-grained soils which present some cohesion due to bonding (true cohesion) or to a curved failure envelope. The most important consequence of deterioration is a time-dependent loss of the extra-strength due to bonding or overconsolidation which turns brittle geomaterials into ductile soils.

Deterioration is induced by either mechanical or physical-mechanical processes. Mechanical processes are provoked by stress changes and associated volumetric or deviator plastic strains, and imply a change in soil fabric and structure caused by breaking of bonds and increase in the void ratio. Deterioration induced by the increase in the void ratio is generally called softening (Terzaghi, 1936); when provoked by shear strains, it is called strain-softening (Bjerrum, 1967). Strain softening first provokes the formation of short fissures (the minor shears), then the formation of a persistent slip surface.

According to Terzaghi, the fundamental factors which govern softening are: (**a**) a stress decrease; (**b**) the availability of free water; (**c**) a fissured soil fabric. In fact, softening typically involves cuttings and slopes in highly fissured clay subjected to erosion. Fissures can play a significant role since they make easier and faster the ingress of water upon unloading, enabling a rapid water content increase through swelling of intact clay adjacent to fissures.

Based on the results of 1D compression tests on high plastic clays (Fig. 4.6), Leroueil and Vaughan (1990) suggest that their high swelling is a result of destructuration, i.e. of breaking of bonds occurred during compression. Based on data on the London clay, they suggest that destructuration can occur also during swelling. A similar behaviour has been shown by other highly plastic clays outcropping in U.S. and in central America and by highly plastic clay shales in Italy (Bilotta et al., 1985), but is not necessarily provoked by destructuration by compression or swelling.

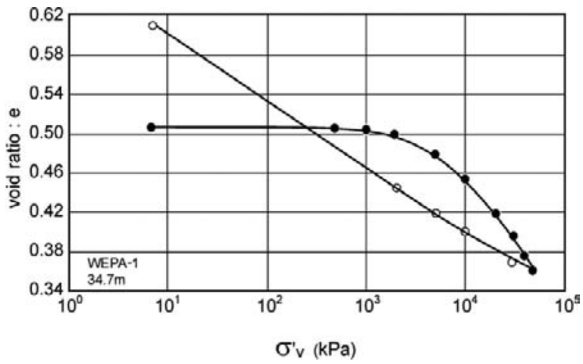

Fig. 4.6 Results of a one-dimensional compression test on the Culebra clay shale (Banks et al., 1975)

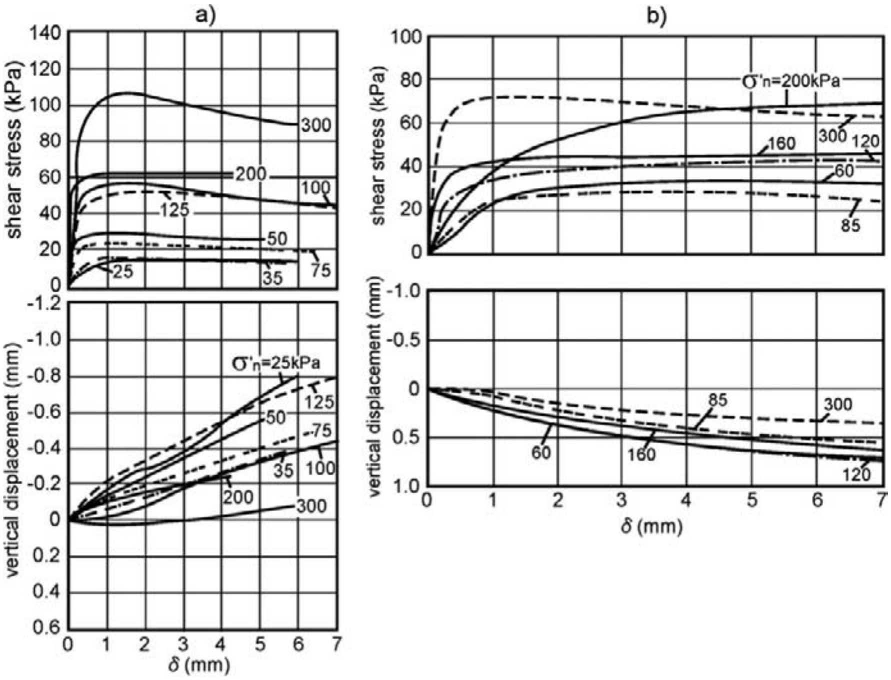

Fig. 4.7 Results of direct shear tests on the Bisaccia clay shale (from Cicolella and Picarelli, 1990): (**a**) conventional; (**b**) after a stage of swelling under a normal stress of 10 kPa

Figure 4.7a shows the results of conventional direct shear tests on highly plastic marine Bisaccia clay shale run, as usual, in a bath of distilled water under a normal stress less than the overconsolidation pressure. Figure 4.7b shows the results of further tests performed after a stage of swelling in the same shear box under a normal stress of 10 kPa, and a successive stage of consolidation under the established normal stress which falls in the same range of values adopted in previous case. A comparison between the two figures shows that pre-swelling determines a radical change of soil behaviour, that becomes contractive and ductile leading to a significant shear strength decrease.

Figure 4.8 shows the results of conventional tests conducted under a normal stress lower than the swelling pressure (around 0.6 MPa). While a part of the specimens were allowed to swell, as usual, for 48 h, others were sheared only after 10–100 days, during which they experienced a high volumetric strain. The difference in shear strength is very clear.

All data show that swelling in distilled water, as usual in the laboratory, is responsible for a radical change in soil behaviour. In addition, Fig. 4.8 shows that the effect of swelling is higher if secondary swelling is allowed.

Starting from works carried out by Di Maio (1996a, b), Picarelli et al. (1998) assume that such a peak strength decrease is caused by physical-chemical processes due to exposure to and absorption of distilled water, and consequent changes of interparticle forces due to the associated osmotic processes.

An impressive idea about the susceptibility of the marine Bisaccia clay shale to pore liquid is suggested by Fig. 4.9, which shows the dependence of the liquidity limit on the molarity of a NaCl solution used for testing. Such a solution is probably more similar than distilled water to the natural pore liquid. The liquidity limit obtained with distilled water is about two times the one obtained with NaCl solution, regardless its molarity.

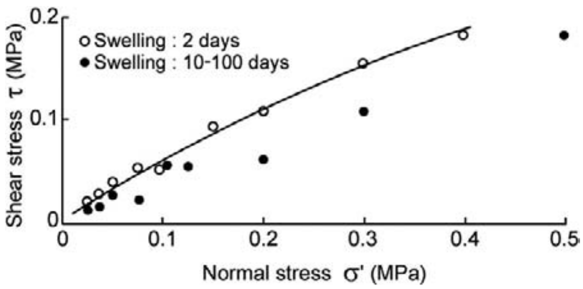

Fig. 4.8 Results of direct shear tests on the Bisaccia clay shale for normal stresses lower than the swelling pressure and after a different swelling time (Picarelli, 1986)

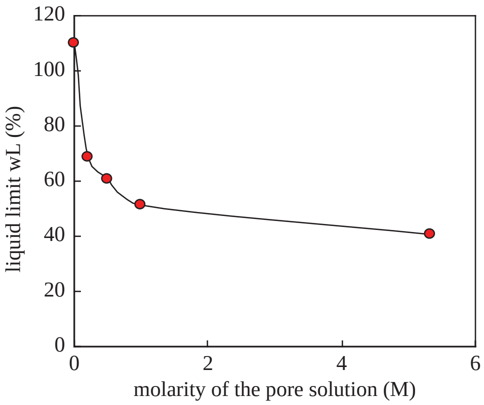

Fig. 4.9 Dependence of the liquidity limit of the Bisaccia clay shale on the nature of the pore liquid (from Picarelli et al., 1998)

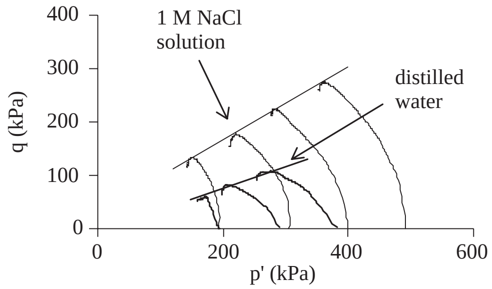

Fig. 4.10 Comparison of the failure envelopes of reconstituted Bisaccia clay mixed with distilled water and with a NaCl solution (from Di Maio and Onorati, 2000)

Figure 4.10 reports the results of triaxial tests executed by Di Maio and Onorati (2000) on reconstituted normally consolidated specimens obtained by mixing powdered clay with distilled water and with a 1 M NaCl solution. It suggests that the friction angle at constant volume (i.e. the critical friction angle) can strongly depend on the nature of the pore liquid. Similar data feature the residual friction angle (Di Maio, 1996b).

These data suggest that any variation of the natural environment can cause a change of the field soil behaviour. An example of the possible effects of infiltration of fresh water in a natural deposit subjected to swelling is shown in Fig. 4.11, which reports the results of oedometer tests carried out on two couples of undisturbed specimens of the Bisaccia clay shale taken respectively at a depth of 2.5 (C1) and of 21 m (C5bis). A specimen of each couple was tested in a bath of distilled water; the other one was tested in a 1 M NaCl solution. The influence of the nature of the bath does not appear significant in the stage of compression, when the pore water is expelled from the specimen, but becomes prominent in the following stage of swelling, when some liquid is absorbed from the bath: in fact, the specimens tested in distilled water (and especially the one taken at the greatest depth) display higher strains than

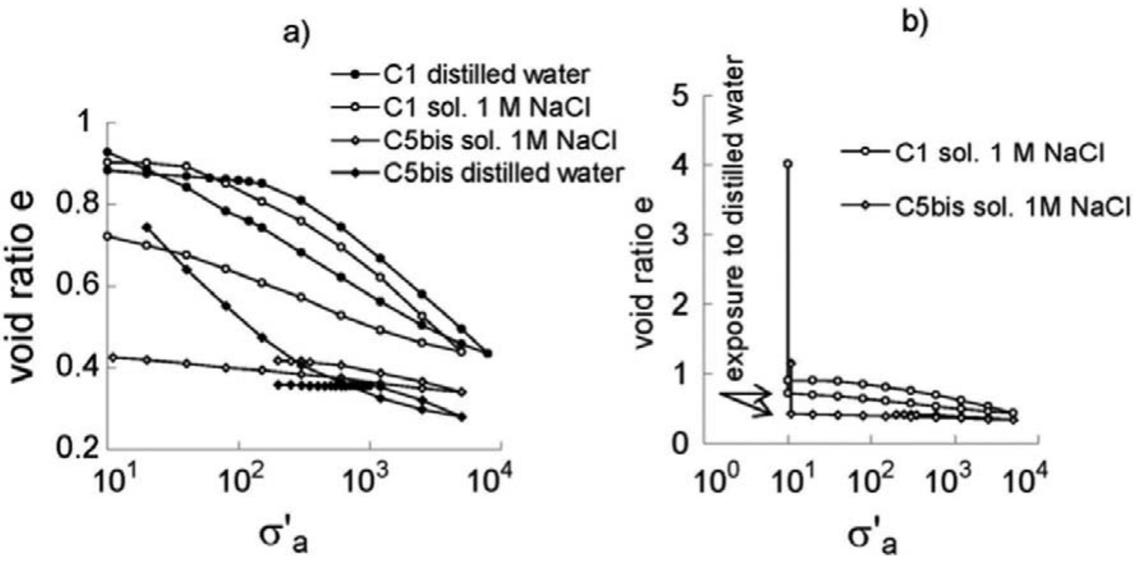

Fig. 4.11 Results of oedometer tests on undisturbed specimens exposed to different liquids (from Picarelli et al., 1998)

those tested in the solution. A the end of the tests performed in the NaCl solution, when the axial stress was 10 kPa, the solution was substituted with distilled water, giving immediately rise to further strong soil deformation.

These observations can justify the results of direct shear tests: primary and secondary swelling in distilled water provoke a chemical exchange between the distilled water and the natural pore liquid, an increase of the void ratio and a change of interparticle forces. As a consequence, also intrinsic soil properties, as the compressibility and swelling index or the critical and residual friction angle, change. In addition, also the general soil behaviour, that turns from dilative into contractive, seems to change (Fig. 4.8). Both effects contribute to a decrease of the shear strength. According to these results, the high swelling index exhibited by highly plastic clay shales whuich can be attributed to destructuration (Fig. 4.6) could be simply an effect of osmotic swelling.

Bearing on these results, it comes natural to assume that shallow layers of highly plastic marine OC clay subjected to swelling induced by erosion, may experience a time-depending shear strength decrease due to infiltration of fresh rain water which presents a very different composition than the natural pore liquid. This process can lead to long-term slope failures. An example is provided in Fig. 4.12 which shows some shallow landslides (either slides or flows) occurring on a gentle slope (Picarelli et al., 2006).

Fig. 4.12 Landslides occurring on gentle slopes in Bisaccia clay shale

To further investigate on the properties of the Bisaccia clay shale, a campaign of in situ tests was carried out (Picarelli et al., 1998). The upper part of the deposit is occupied by a slow active mudslide whose thickness ranges between 3 and 6 m. The tests were carried out through the mudslide body until the underlying parent stable formation. Fig. 4.13 shows the results of tests performed in two different points. In both cases, the tip resistance in the mudslide body is extremely small and does not show any clear trend with depth, revealing more resistant zones due to the presence of rock fragments or of lithorelicts of the parent formation embedded in the debris. However, since the cone penetrates into the cover of the stable parent formation, the tip strength starts to increase with depth. According to well known relationships between the tip resistance and the undrained cohesion, the minimum value of this last in the mudslide body can be assessed in the range between 10 and 20 kPa, while in the cover of the parent formation it reaches values of hundreds of kPa. The measurements made with the environmental cone show that the mudslide body is quite acid, having a pH less than 7, with minimum values of 4–5. However, differently from the tip resistance, the pH gradually increases with depth even in the mudslide body. In strong contrast with the features of the uppermost remoulded soils, the pH measured in the parent formation is always higher than 7. These results could be an indication of the effects of fresh water infiltration in the cover of the deposit.

Described phenomena of soil deterioration caused by osmotic phenomena appear more likely in highly plastic clay shales of marine origin than in other formations.

4.3.3 Shear Strength of Air-Fall Volcanic Ash

An extensive area around Naples is covered by pyroclastic soils produced by the activity of volcanic centers. These covers consist of volcanic ash, pumices and scoriae: volcanic ash prevails. Their grain size and fabric depend on the mechanisms of deposition, i.e. by pyroclastic flow, surge or air-fall (Picarelli et al., 2006). In spite of a significant fine-

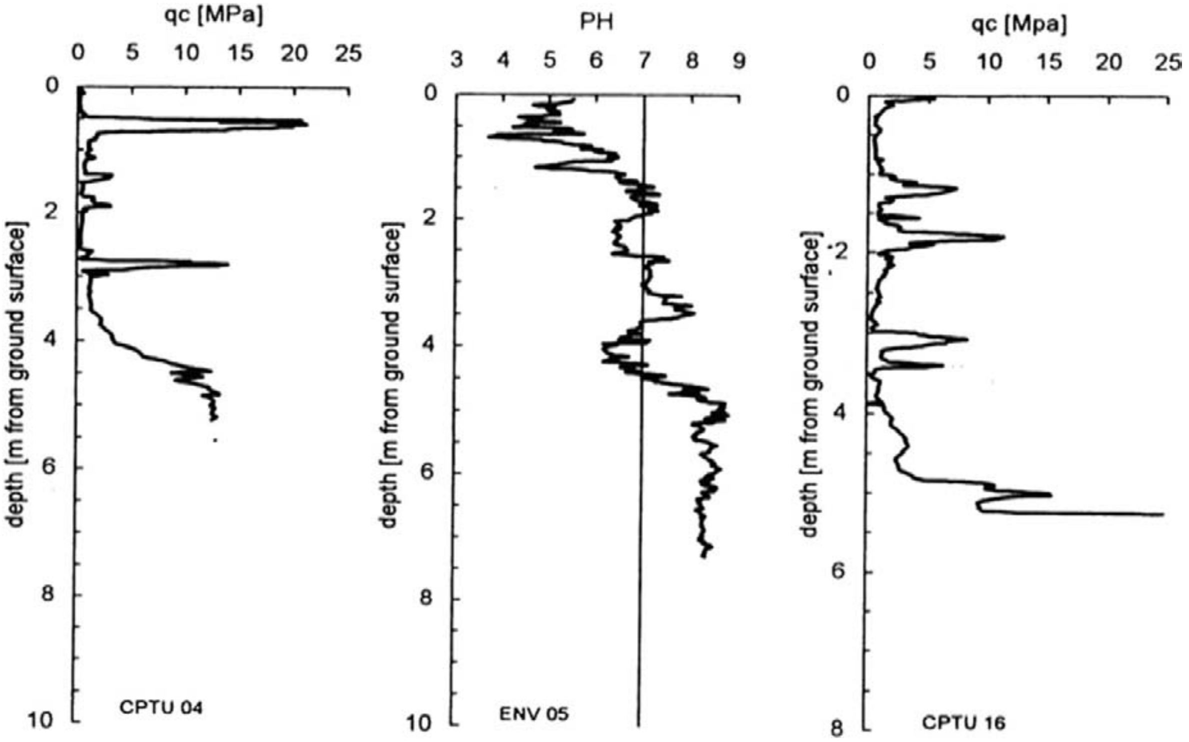

Fig. 4.13 Results of CPTU and environmental cone tests along two cross sections in a mudslide in the Bisaccia clay shale (Picarelli et al., 1998)

grained component (up to 30–40% of silt), non weathered volcanic ash is non-plastic because of the absence of active minerals.

The most catastrophic landslides (flowslides and debris flows) involve air-fall deposits which cover a large part of the region, even at large distances from the vents. These deposits are constituted by alternating layers of cohesionless volcanic ash and pumice. The void ratio of ash is very high, up to values close to 4. Because of its high void ratio, volcanic ash displays a ductile behavior in drained triaxial tests. For the same reason, the soil displays a small stiffness while the friction angle is quite high, falling in the range 33–39°.

The "drained" ductility of soil is not consistent to the mechanisms of landslides which are extremely fast, reaching velocities up to a few tens of meters per second. This suggests the occurrence of a drop of the resisting force just after failure. Hence, as in the case of landslides in highly fissured clay shales, data provided by field experience conflict with the virtual soil behavior based on usual laboratory tests. As a matter of fact, volcanic ash shows a radically different behavior in undrained tests. In fact, just after the peak, the material displays a drop of strength (brittle behavior) because of accumulation of positive excess pore pressures caused by the collapsible nature of soil associated with its open fabric. As a significant additional peculiar feature, the undrained peak strength of volcanic ash is generally mobilized before reaching the Steady State Line (Lade and Pradel, 1990). This is attained only after large strains, as a final stage of the post-peak phase, suggesting that the mobilized strength in undrained mechanisms of slope failure may be even lower than the theoretical one calculated through the Steady State Line. The envelopes of peak strength of a volcanic ash for different initial void ratios (Instability Lines) are shown in Fig. 4.14.

Therefore, differently from scaly clay shales which display a quasi-ductile behavior in spite of their very high overconsolidation ratio, very loose pyroclastic ashes, display a rather brittle behavior in spite of their very high void ratio. Therefore, while slope

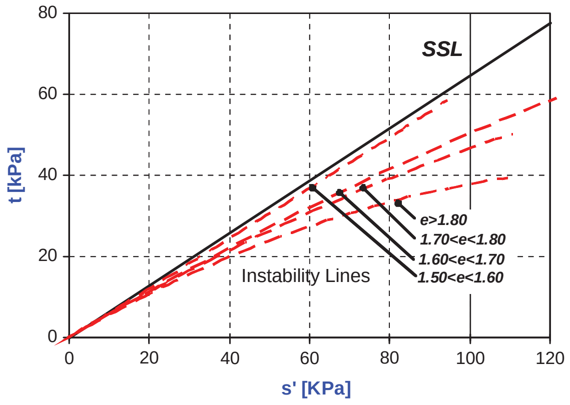

Fig. 4.14 Instability Lines of a loose volcanic ash (Lampitiello, 2004)

movements in scaly clay shales generally are rather slow slides, slope movements in loose volcanic ash may be fast flowslides or debris flows. This point will be resumed below, when the mechanics of flow-like landslides in volcanic ash will be discussed in greater detail.

4.4 The Role of Pore Pressure Regime on Landslide Behavior

Pore pressures play a prominent role on the stability of slopes: in unsaturated soils, any change in the water content affects suction and the associated apparent cohesion which has a great influence on the stability of shallow sloping layers; in saturated soils, any change in pore pressure affects the effective state of stress and the frictional component of strength. In both cases, small changes in the pore pressure regime can provoke significant slope deformation or even failure.

Pore pressure changes are caused by precipitations, by snow melting and by other special causes. The thickness of soil which is affected by such phenomena depends on its hydraulic conductivity (Kenney and Lau, 1984); open cracks can be responsible for significant effects even at high depth.

Experience shows the strict relationship existing between pore pressures and slope behavior, including the movement pattern of landslides. Some examples are reported below.

4.4.1 Pore Pressure Fluctuations and Influence on Movement Patterns of Translational Slides and Mudslides

A fundamental aspect of the mechanics of slow active translational slides in clay is the presence at their base of a continuous slip surface. During movement downslope, the landslide body generally experiences only small internal strains because most of the movement which is measured at the ground surface occurs along the slip surface. Since the shear stress–shear displacement relationship along a slip surface is ductile, no relevant acceleration is expected for usual pore pressure fluctuations. Only if a strong change of boundary conditions occurs due to surcharges, excavations, earthquakes or exceptional precipitation., a relevant acceleration can take place. As a matter of fact, active slides in clay are generally slow, presenting only small seasonal variations in the displacement rate. This justifies the idea that the displacement rate can be considered roughly constant and that only occasional measurements are necessary to monitor the slope behavior. However, the increasing use of automatic instruments today allows to monitor with continuity all the factors which affect the slope behavior and to assess the role of even minor factors.

The Miscano mudslide is an example of long-lasting slow active landslide in scaly clay shales (Picarelli et al., 1999). The mudslide is presumably in its late stage before a complete arrest: however, the inclinometer readings indicate that a relatively faster shallow mudslide is moving over the old landslide body (Fig. 4.15).

The local displacement rate ranges between about 0.01 and 2 mm/day. The relationship between the displacement rate measured at the ground surface by one of the inclinometers located in the accumulation zone and pore pressure, is reported in Fig. 4.16. In general, an increase in the displacement rate follows quite closely any increase in pore pressures, but the relationship is not so clear because the readings are not regular and continuous in time.

The mobilized residual strength varies with the season. In fact, the friction angle which justifies a safety factor equal to one assuming c’ = 0, depends on the pore pressure distribution. For the deepest

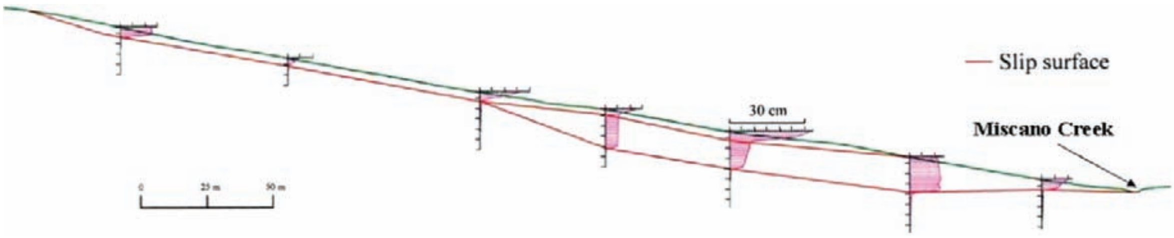

Fig. 4.15 The Miscano mudslide and representative displacement profiles in the period 1993–2001

landslide it is comprised between about 15° and 17°. It is worth to mention that a couple of direct shear tests carried out on reconstituted soil samples taken from the landslide body provided residual friction angles equal to 5° and 8°, which are well below the operative values. Picarelli (2000) mentions different possible explanations about the inconsistency which often characterizes measured residual friction angles with respect to operative values:

– natural inhomogeneities of soil along the slip surface;
– the curvature of the residual strength envelope at low stresses;
– the influence of initial soil structure on the residual strength (which is often measured on reconstituted specimens);
– the influence of distilled water used in the laboratory on the residual strength of reconstitute specimens (Di Maio, 1996b);
– the real mechanism of slope movement which can be affected by excess pore pressures induced during movement or by more complex phenomena.

However, in the assumption of rigid-plastic body which moves over a slip surface, Fig. 4.16 suggests that the residual strength is rate-dependent. The relationship between the mobilized friction angle and the average displacement rate along the slope is shown in Fig. 4.17: the increase of the coefficient of friction in the range of velocities comprised between 0.01 and 0.1 mm/day is around 4%, quite in a good agreement with data provided by Skempton (1985) based on laboratory tests. However, as discussed by Picarelli

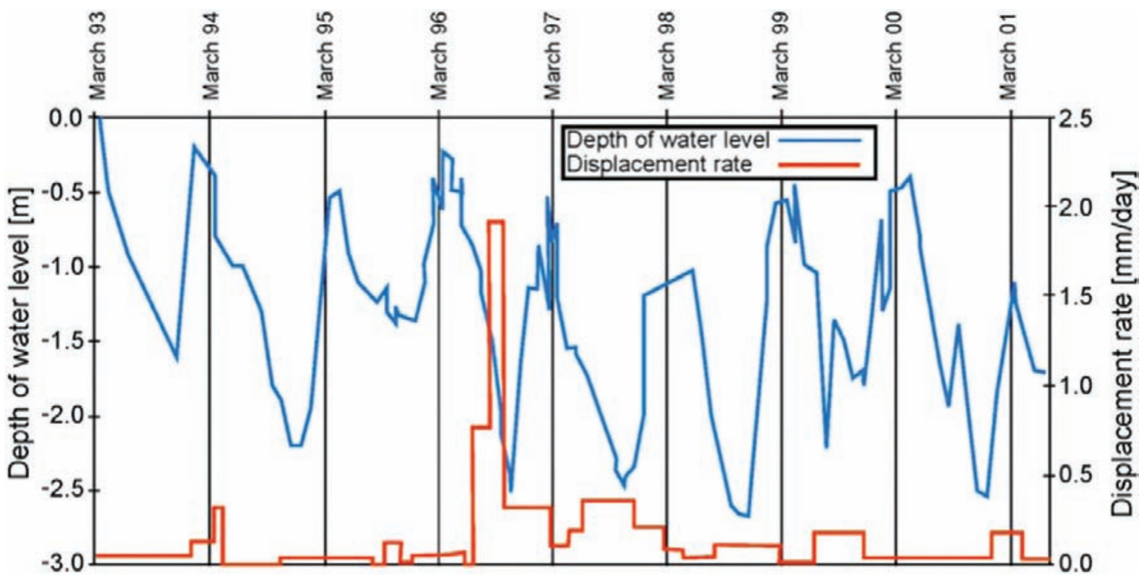

Fig. 4.16 Displacement rate–pore pressure relationship for the Miscano mudslide

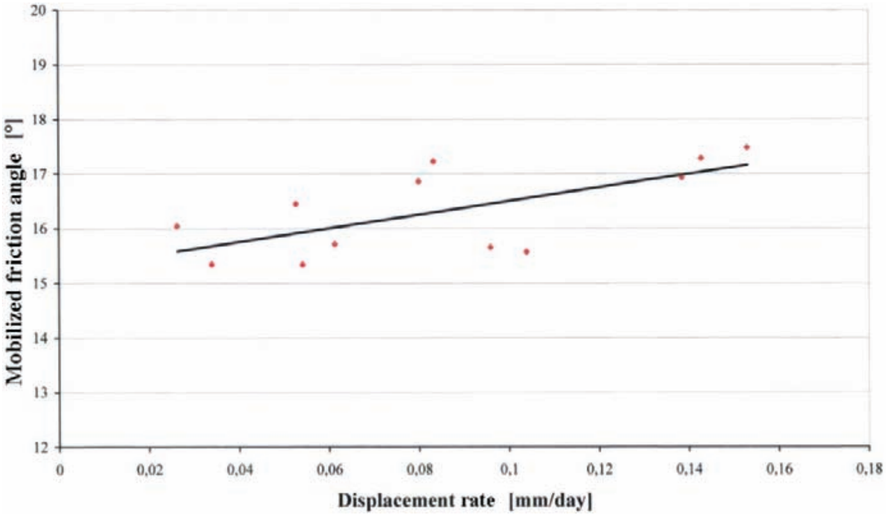

Fig. 4.17 Mobilised friction angle–displacement rate relationship for the Miscano mudslide

(2007), further elements besides viscosity, can explain such a result.

Continuous monitoring by automatic instruments can provide new and significant insights in the understanding of the mechanics of landslides.

Figure 4.18 shows the Vallcebre slide, Spain, a large translational landslide in stiff fissured clay, and Fig. 4.19 the evolution of pore pressures (which has been measured with standpipe piezometers). The figure shows that the pore pressure regime is quite uniform in time, but presents sudden and sharp increases. These cause an almost contemporaneous acceleration of the slide, even though the average displacement rate over much longer time spans remains relatively slow. Therefore, the real slope behavior is completely different from the one which is usually imagined, i.e. characterized by a relatively constant displacement rate, since the real mechanism

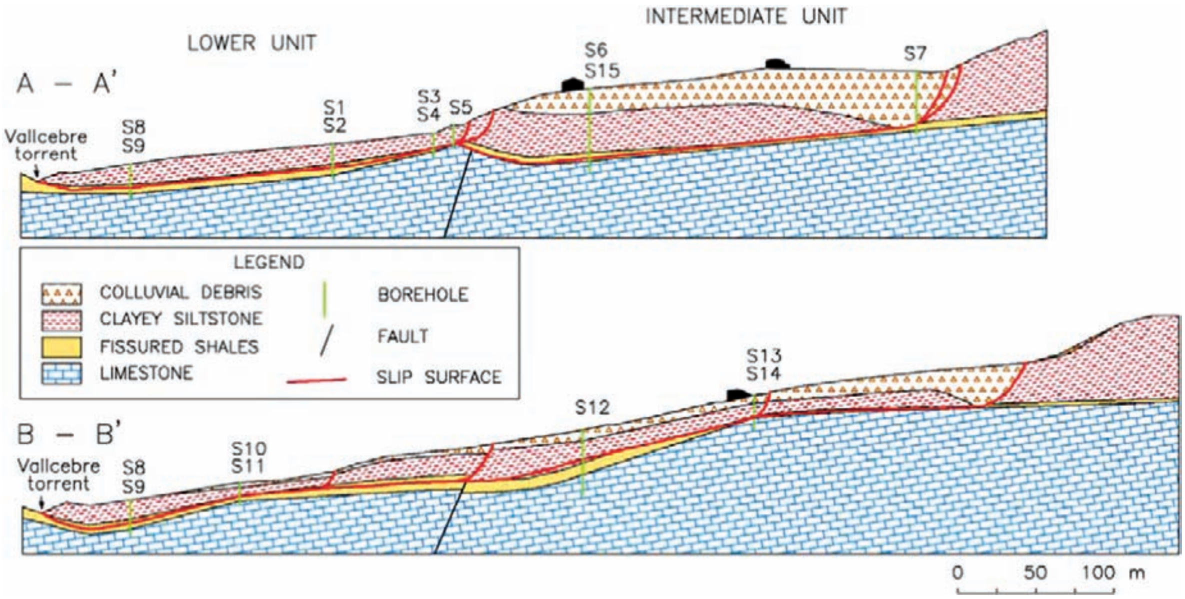

Fig. 4.18 The Vallcebre landslide (Corominas et al., 2005)

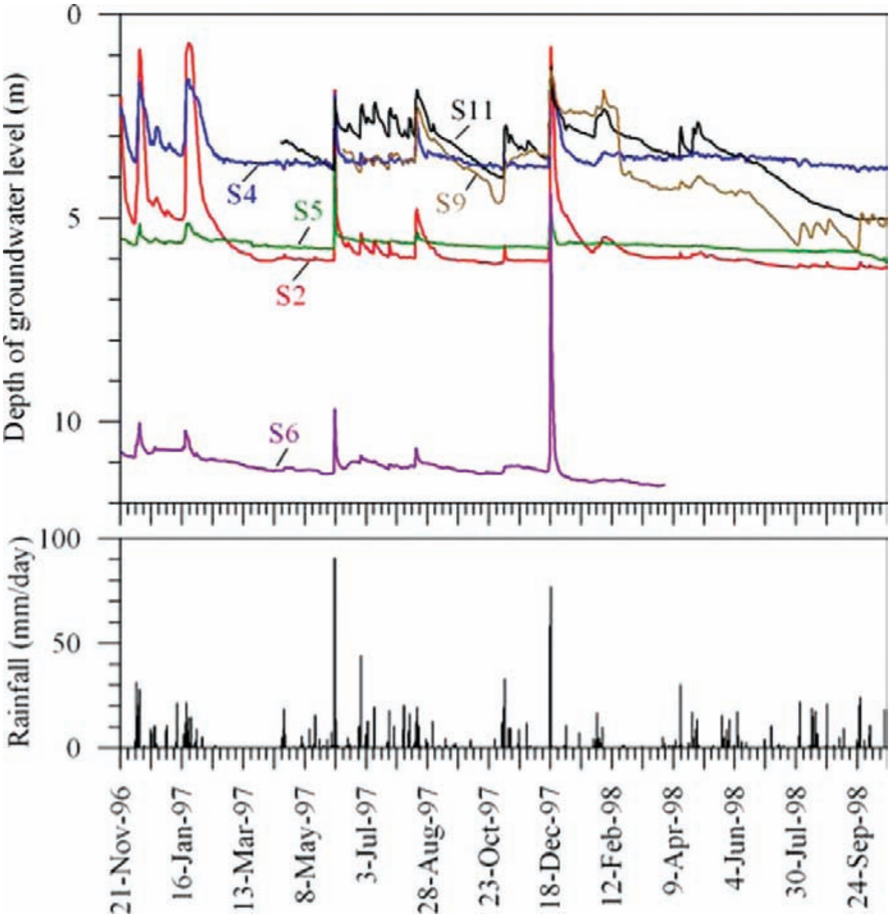

Fig. 4.19 Pore pressures in the Vallcebre landslide (Corominas et al., 2005)

is by intermittent stick-slip movement. Such a result is very likely due to the presence of cracks in the landslide body, which favor the rapid development and subsequent drop of cleft pressures.

In some cases similar hydraulic conditions can provoke a sudden slope failure. An example is provided by Picarelli and Viggiani (1988) who describe a translational slide (the Melfi landslide, November, 1980) provoked by the reactivation of a quiescent landslide body as a consequence of a 11 m high excavation. The slope consists of alternating layers of sandstone and marly clay, but its reactivated part presents a chaotic structure (a complex melange of sandstone elements and marly clay) as a consequence of previous local movements. A plan of the landslide, which covers 250 m in length with an average slope of 7°, is shown in Fig. 4.20. Accurate surveys carried out after the event, showed the presence on the ground surface of several transverse cracks, bounding single soil blocks having a length of a few tens of metres in the direction of the slope. Even though the cut was clearly the cause of the landslide, only the presence of a quiescent landslide body can explain the length of the mobilised soil body.

After the event, a campaign of geotechnical investigations including a number of boreholes and the installation of standpipe piezometers (the series of piezometers 1, 2, 3 … shown in the Fig. 4.20) was carried out.

According to the results of direct shear tests, the residual strength of marly clay is quite high, being characterised by a friction angle of 18–25°. Adopting such a value, the landslide, as a whole, can not be explained even assuming the water table at the ground surface (Picarelli and Viggiani, 1988). The only way to justify the long landslide shown in Fig. 4.20 is a failure mechanism as in Fig. 4.21, characterised by the retrogressive mobilisation of

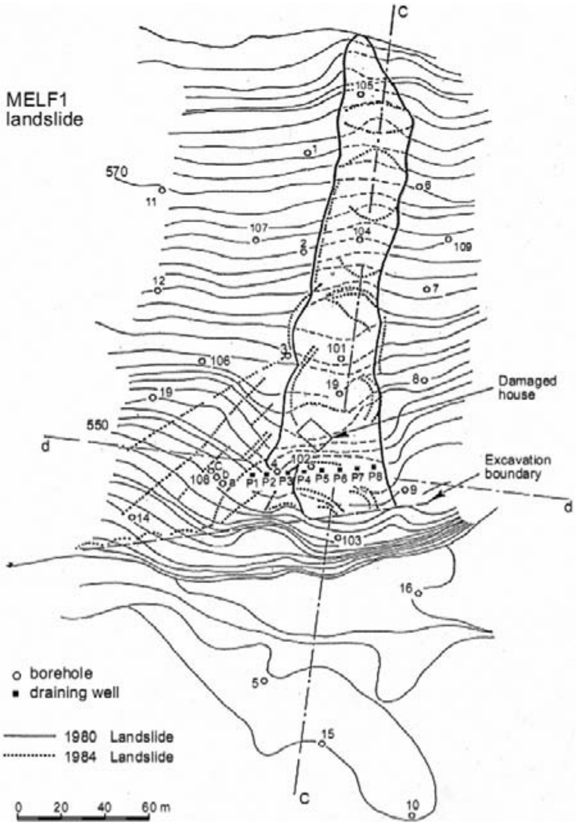

Fig. 4.20 The Melfi landslide and piezometers installed in the landslide area (Picarelli and Viggiani, 1988)

single blocks, having a length equal to the spacing between cracks, driven by cleft pressures (Henkel, 1967). A simple analysis performed in the assumption of cracks completely filled of water can validate such a model.

The high cut was eventually stabilised by a huge retaining structure constituted by large diameter piles having a continuous concrete beam on the top. Unfortunately no data about water levels were collected after the stabilization measures. In spite of such works, in February, 1984, during a very rainy winter, the landslide experienced a new full reactivation: in fact, fresh lateral shears replicated the ones recognised after previous event (Fig. 4.20), and once again, a series of cracks were observed on the ground surface; the retaining structure experienced a 1.5 m displacement and extensive tensile fissuring.

After the new reactivation, further investigations were carried out and a number of Casagrande piezometers were installed (the piezometers 101, 102, 103 ...., in Fig. 4.20). During the investigation drilling water was noted to raise to the ground surface at some distance from the holes, confirming the presence of open cracks in depth.

Figures 4.22 and 4.23 report some results of manual readings of the water level carried out on both series of piezometers as well as the rainfall heights cumulated over time intervals of ten days. Despite readings were not so frequent and regular, all data show that any heavy rainfall provokes a fast pore pressure increase followed by a rapid drop to a value very close to the one recorded prior to the rainfall: in addition, the peaks recorded by Casagrande cells appear sharper than those obtained by standpipes, with water levels attaining higher values. In two different dates (November, 1985, and March, 1986), in some Casagrande piezometers located in the middle part of the landslide, the water level reached the top of the pipe flowing outside (Fig. 4.23).

It is obvious that the difference in the response of the two series of piezometers is due to their different time-lag. In particular, both a relatively long time-lag (as in the case of standpipes) and a too long time interval between successive readings smooth the peaks of pore pressures which presumably acts in some parts of the slope. This suggests that piezometer heads significantly higher than the ground surface level could not have been recorded.

A double porosity model, accounting for interconnected fissures and cracks as a first set of

Fig. 4.21 Failure mechanism by retrogressive mobilisation of soil blocks driven by cleft pressures: the figure shows a block at the onset of failure due to water pressure in a vertical crack

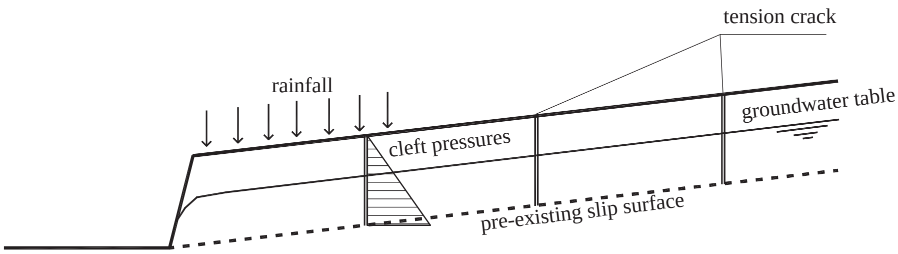

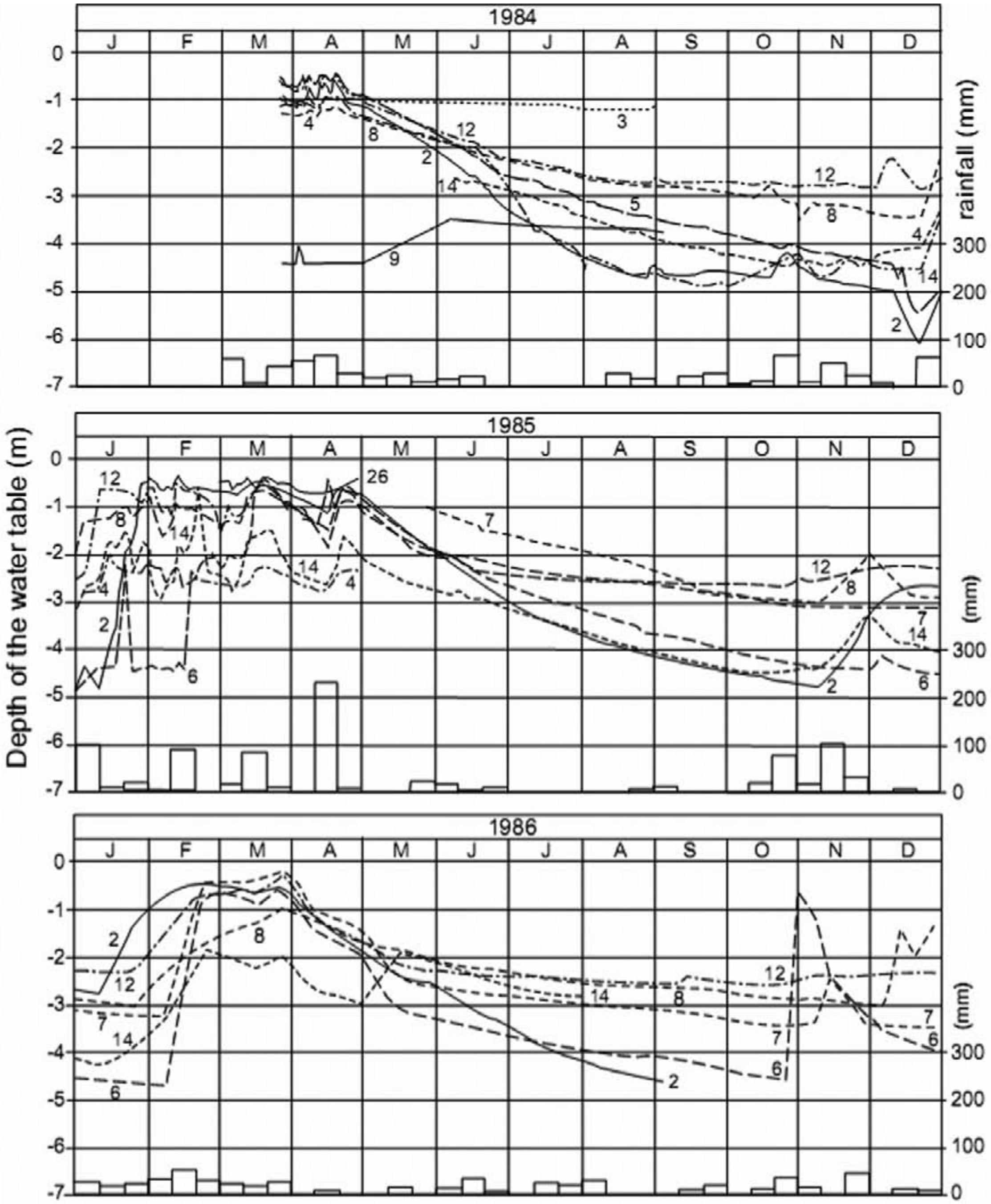

Fig. 4.22 Water level readings at standpipe piezometers (Picarelli and Viggiani, 1988)

"pores", and voids between particles or aggregates of particles as a second set, could reproduce the real hydraulic situation much better than the classic continuum porous model. In the double porosity model, the gross permeability of the subsoil depends on the first set of pores: in fact, through cracks, any change of hydraulic boundary conditions can rapidly propagate in the subsoil. The piezometer

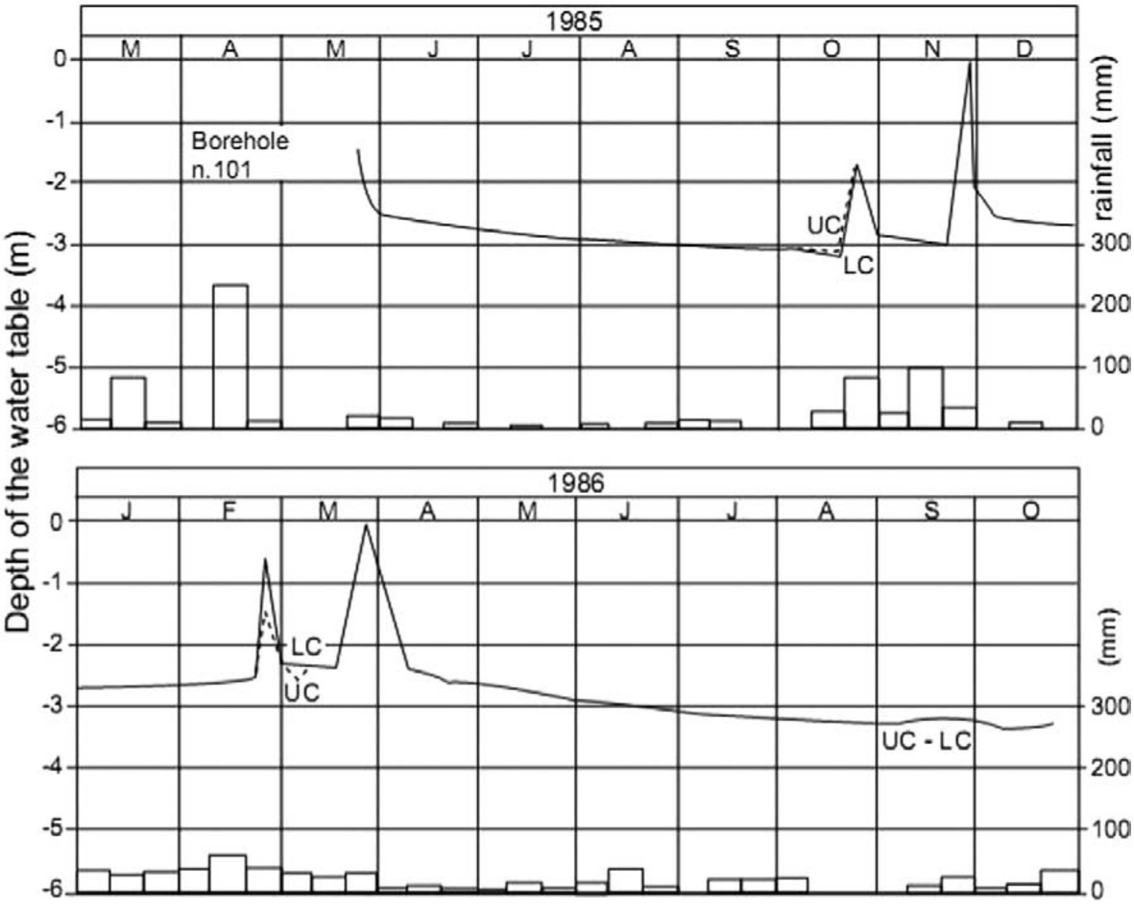

Fig. 4.23 Water level readings at the Casagrande piezometers no 101 (Picarelli and Viggiani, 1988)

heads which temporarily establish in the cracks represent a boundary hydraulic condition for the soil blocks. Because of the low permeability of these, which present only pores of the second set, the pore pressure equalization within the blocks is slower, and probably in some cases the internal hydraulic conditions cannot follow the continuous changes occurring at the boundaries. According to such an assumption, the fast peaks recorded by some piezometers should represent the pressure heads acting in the cracks, rarely those acting in the blocks.

The special role played by the hydraulic conditions can justify also the second event. Bearing on an accurate back analysis of the landslide accounting for the presence of the retaining structure, Picarelli and Viggiani (1988) argue that the presumed piezometer head at the time of the second reactivation (February, 1984) should have been about 3 m above the ground surface. Despite the absence of data regarding that period, this value can be justified based on a statistical analysis of all available data collected during subsequent monitoring, concerning the relationship between measured piezometer levels and cumulated rainfall heights over the last 90 days prior to the measurement. In fact, through such an analysis it can be demonstrated that the piezometer level in the middle part of the landslide area at the end of January, 1984, should have been more or less the one (3 m above the ground surface) which has been supposed to be responsible for the reactivation. As a matter of fact, the cumulated rainfall height in the time span comprised between November, 1983, and January, 1984, has been the second highest value recorded in the last sixty years.

Regarding the hydraulic conditions which allow the establishment of so high “artesian” pore pressures, a fundamental role is certainly played by the structure of the subsoil which favours seepage along pervious paths due to the presence of the open cracks as well as of sandy seams. Very likely, these paths are locally interrupted by fine-grained material (marly clay) because of the chaotic structure of the lowermost part of the slope due to previous landslide movement. Consequent changes in permeability along the flow paths can favour high local pore pressures.

A very different mechanism of sharp pore pressure generation has been discussed by Comegna et al. (2007) referring to some monitored mudslides in the Basento Valley, Italy. Figure 4.24 reports the water level measured in some Casagrande piezometers installed in the area of the Masseria Marino mudslide (Fig. 4.24a): the piezometer PA is located in the alimentation area; PVI is located in the accumulation area; PIV is outside the landslide. Figures 4.24d, and 4.24e and f report the pore pressures measured at PA, PIV and PVI showing quite regular pore water fluctuations depending on the rainfall regime (Fig. 4.24c). Such fluctuations can be reproduced using a simple infiltration model accounting for the real distribution of rainfall and a hydraulic soil conductivity consistent with the results of laboratory tests In contrast, the diagrams regarding the piezometers P6 and P4 located in the track (Figs. 4.25a and b) can not be directly associated with the precipitations, being characterised by irregular changes revealed by sharp peaks and sudden drops. In fact, the same model which has been satisfactorily adopted for the simulation of pore pressures can not reproduce the values measured upslope or outside the landslide area. Also, the figure shows a delay in the response of piezometer P4 with respect to piezometer P6.

Even if these results resemble those described for the Vallcebre and Melfi landslides, a different hypothesis has been proposed. In fact, measured pore pressures have been supposed to be a consequence of undrained (or partially undrained) conditions due to continuous stress changes within the landslide body caused by movement. The drops in pore pressure following the peak are hence the result of rapid excess pore pressure dissipation due to the strong piezometer gradients which exist in the landslide body. A simulation of such effects is reported by Comegna et al. (2007).

4.4.2 The Mechanics of Flow-Like Landslides in Saturated Soils

The generation of fast landslides is the result of the establishment of an unbalanced force which causes the acceleration of the soil mass (Leroueil et al., 1996). The unbalanced force may be the result of either a drop of the resisting force or of an increase of the driving force. The drop of strength may depend on the constitutive law of soil (cemented, dense or highly OC brittle soil) or may be provoked by a sudden pore pressure increase (undrained condition) which essentially affects the frictional resistance. Fast slope movements induced by excess pore pressures are some flow-like landslides, such as flowslides or mudslides.

According to several Authors, flowslides are slope movements induced by liquefaction of soil (Hungr et al., 2001). This is a well known phenomenon occurring in loose saturated granular soils, such as sands or non plastic silts, due to the generation of high positive excess pore pressures (Yamamuro and Lade, 1997). The requisite of full saturation implies that flowslides typically involve gentle submarine deposits or the slopes of tailing dams. In contrast, steep natural slopes constituted by sands or silts are generally unsaturated because of their high saturated permeability which does not allow the formation of an aquifer. In fact, the steepness of such slopes whose angle can be much higher than the friction angle, is due to the apparent cohesion associated with suction. Therefore, liquefaction should not to be a realistic triggering mechanism of flow-like movements on steep slopes, even though experience suggests that this is false. In fact, the generation of positive excess pore pressures has been certainly recognized as a trigger of flow-like landslides on steep slopes in Japan, China, Italy and other countries (Sladen et al., 1985; Sassa, 2000; Olivares and Picarelli, 2006).

The mechanism of liquefaction has been clearly described and proven through instrumented flume tests by Wang and Sassa (2001), Olivares and Damiano (2007) and other Authors. As a consequence of rainfall, the water content progressively increases and suction decreases until to slope failure. At failure, the soil can be either unsaturated or fully saturated. This depends on both slope angle and shear strength parameters: in the simple case

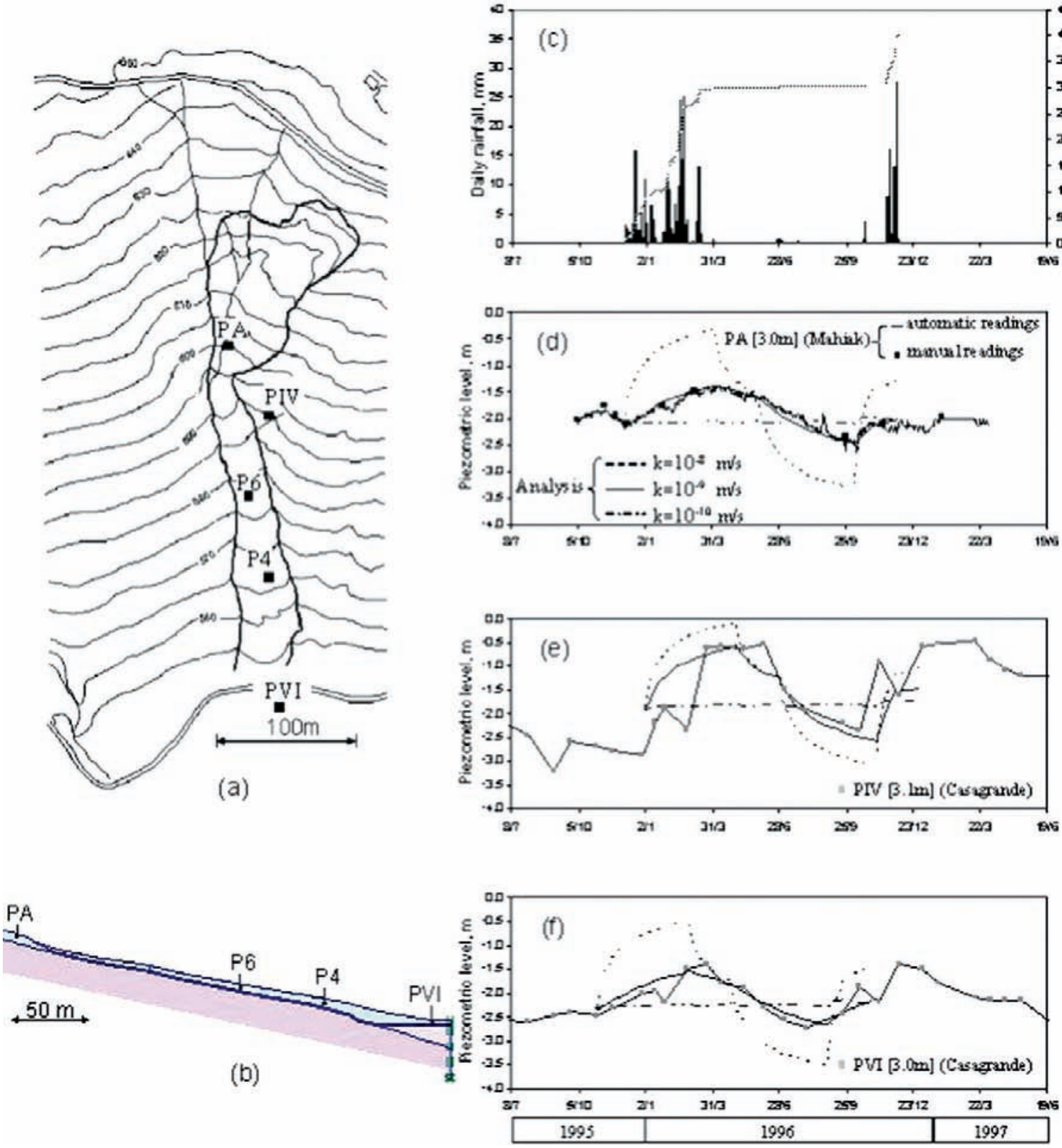

Fig. 4.24 Water levels measured in the Masseria Marino mudslide (Comegna et al., 2007): (**a**) plan of the landslide; (**b**) section; (**c**) rainfall regime; (**d**), (**e**), (**f**) measured and calculated water levels in the piezometers PA, PIV and PVI

of infinite slope in uniform cohesionelss soil (c' = 0), full saturation at rupture can establish only for slope angles less or equal to the friction angle (Olivares and Damiano, 2007). However, if the degree of saturation at failure is high enough, a build up of excess pore pressures can take place, provided that rupture or following movement is rapid enough.

These considerations enable to distinguish soil deposits which can liquefy or not, as a consequence of failure. In fact, if the slope is very steep, failure takes place well before a complete soil saturation and the landslide starts as a slide or a debris avalanche (Hungr et al., 2001), but not as a flowslide, i.e. the soil does not liquefy unless this mechanism is provoked by progressive failure in soil deposits located

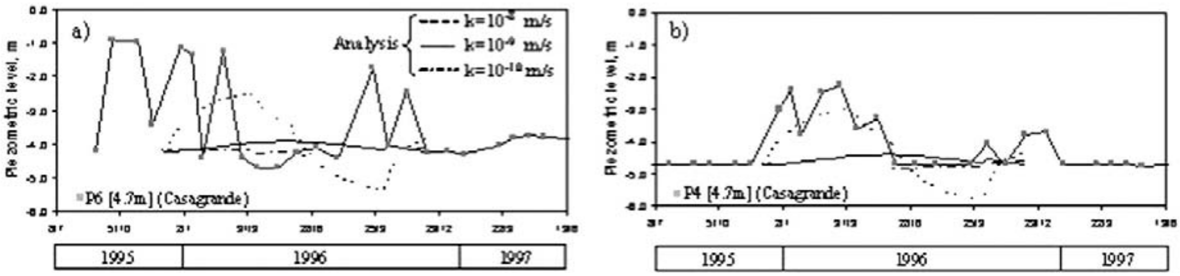

Fig. 4.25 Measured and calculated water levels in the piezometers P6 and P4 (Comegna et al., 2007)

downslope. This double hypothesis is visually demonstrated by Fig. 4.26 which shows two landslides in similar materials (volcanic ash). The Quindici event (Fig. 4.26a) was clearly a debris flow caused by liquefaction demonstrated by the spread of mud on the slope; the Monte Spina event was a debris avalanche which stopped at the toe, saving some buildings whose roofs are shown in the Fig. 4.26b. This naturally enables in the establishment of advanced criteria for mapping the potential sources of flowslides or of liquefied debris flow (Picarelli et al., 2008b).

Different mechanisms of excess pore pressure generation (undrained conditions) can be imagined, as by volumetric collapse due to suction decrease, by impacts (an example is provided by Cairo and Dente, 2003) or by progressive failure. In the first and second case, excess pore pressure building up is the cause of slope failure: if the slope of the Instability Line is less than that of the Critical State Line, a relatively low strength may be mobilized depending on the initial void ratio of soil (Fig. 4.14). Progressive failure is a typical process of slope rupture in brittle deposits subjected to an inhomogenous state of stress. Progressive failure has been described by Bjerrum (1967) thinking to drained loading conditions, but no reason exists for not being possible also in undrained conditions. It starts from the most stressed parts of the slopes and spreads in the slope because of the drop of strength due to induced plastic strains and consequent redistribution of the state of stress: therefore excess pore pressures can be a result, not a cause of soil failure. As a consequence of the drop of strength, the landslide takes the style of an avalanche involving the deposits encountered downslope along its travel. In some cases liquefaction has been supposed to trigger a mechanism of complete fluidization (Iverson, 1997; Musso and Olivares, 2004): this means that the mass can move downslope without any resistance at its base, attaining a velocity of tens of metres per second.

Some clues about the development of the undrained progressive failure can be found in the results of instrumented flume and full-scale field tests, which show a delayed development of excess pore pressures in different parts of the slope as the movement propagates (Olivares and Picarelli, 2006). This obviously means that the morphological features of the slope can play some role. For instance, in the case of concave slopes, which present a decreasing angle from the top to the toe, progressive failure could be a downslope process starting from the steepest part of the slope and triggering positive excess pore pressure in the soil mass encountered along its path, as the movement propagates. An inverse mechanisms (i.e. a retrogressive progressive failure) should provoke negative excess pore pressures. As a matter of fact, some flume tests reveal the triggering of either positive or negative excess pore pressures as a function of the mechanism of movement. An example is provided in Fig. 4.27 which shows the mechanism of progressive failure and the development of both positive and negative excess pore pressures in different parts of the same slope (Moriwaki et al., 2004).

Similar mechanisms as those discussed above seem to be the cause of flow-like landslides in fine-grained soils (Picarelli et al., 2008c), and justify their relatively high velocities (up to meters per hour). Differently from flowslides, which are characterized by a very fast dissipation of excess pore pressures which favors a rapid arrest, in the case of mudslides the consolidation process is very slow because of the low permeability of soil.

Fig. 4.26 The Quindici flowslide, 1998 (**a**) and the Monte Spina debris avalanche, 2004 (**b**)

Consequently, the landslide can last tens of years turning very slowly into a slide-like movement. The different mechanisms of movement in the very first phase of movement and in the last phase are sketched in Fig. 4.28. This can explain the different names given by American and English researchers to flow-like landslides in fine-grained soils: in fact, Americans call them earthflows because of the style displayed in the early phase, while English people call them mudslides, thinking to the last phase in which a slip surface develops at the base of the landslide body which roughly moves as a stiff body.

Mechanisms causing excess pore pressures and flow-like movements in fine-grained soils should include (Pellegrino et al., 2004): (i) rapid accumulation of debris discharged from the main or the secondary scarps: excess pore pressures can build up in the same debris under its own weight; (ii) stress increase induced by surges travelling over the landslide body; (iii) stress redistribution in the landslide body associated with any restraint met during movement, as narrowing of the main track or local variation of the slope of the sliding surface; (iv) seismic loading.

Figure 4.29 shows the pore pressures which have been measured in a part of the Masseria Marino mudslide during a phase of acceleration. Such values have been measured at a depth of 3 m. Since the piezometer head reaches an elevation of about 3 m above the ground surface, the pore pressure is certainly very close to the mean total stress, i.e. the effective stress is close to zero and a sort of liquefaction seems to take place. These considerations suggest that the mechanisms of flowslides and mudslides can be very close each other, even though the mobility of these landslides is rather different because of the different dissipation of energy which can take place in granular and in fine-grained materials.

4.4.3 Negative Pore Pressures as a Constraint for Slope Movement

If the soil is saturated and dilative, or experiences a reduction in the mean stress, negative excess pore pressures may be triggered (undrained conditions) inducing transient mean effective stresses higher than in the long-term conditions. This mechanism can delay the time of failure or act as a constraint for induced movement, causing an opposite effect with respect to the cases discussed above.

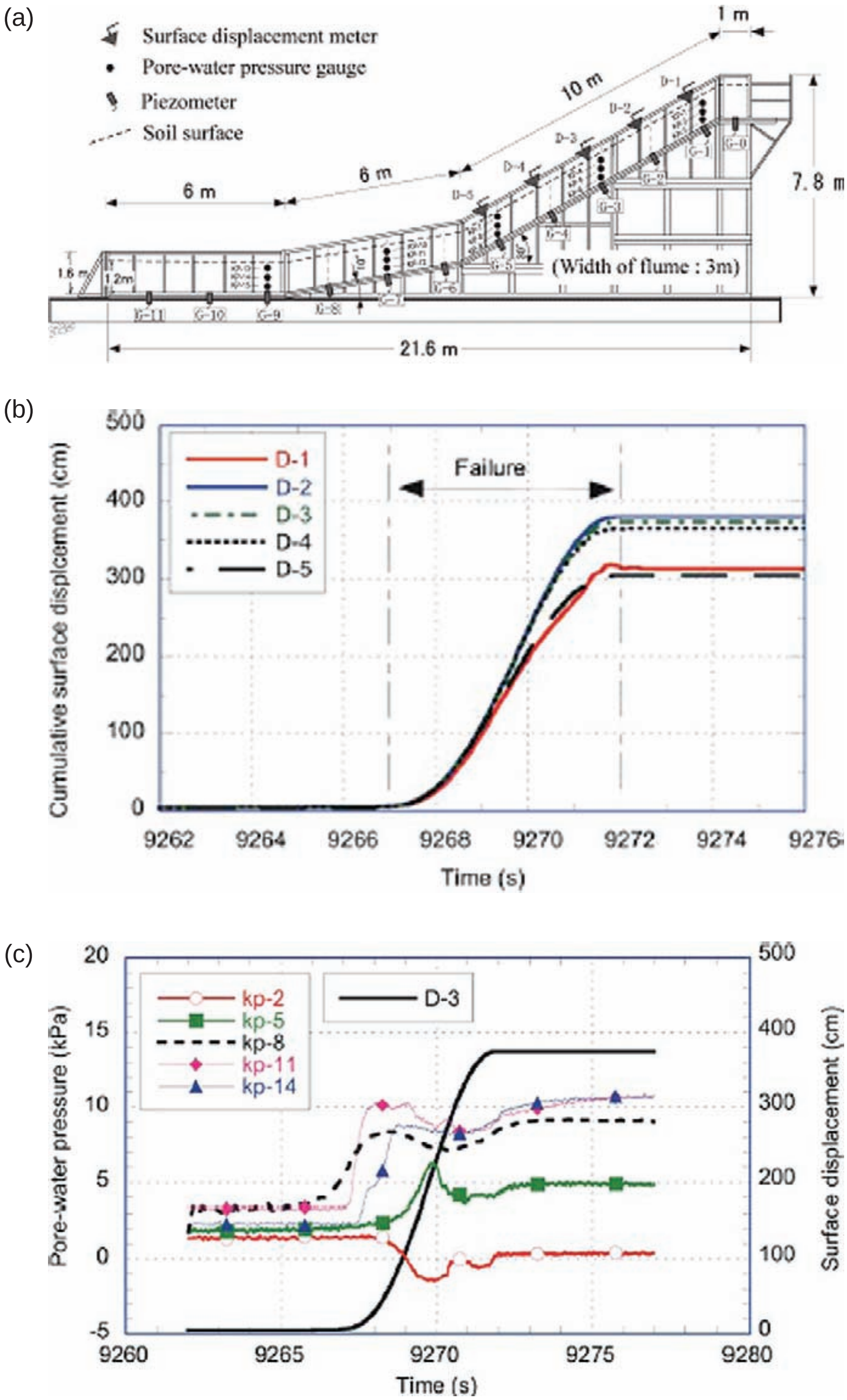

Fig. 4.27 Results of a full-scale instrumented flume test in decomposed granite (Moriwaki et al., 2004): (**a**) instrumented model slope; (**b**) displacements measured at the ground surface; (**c**) pore pressure measured within the soil mass along the slope

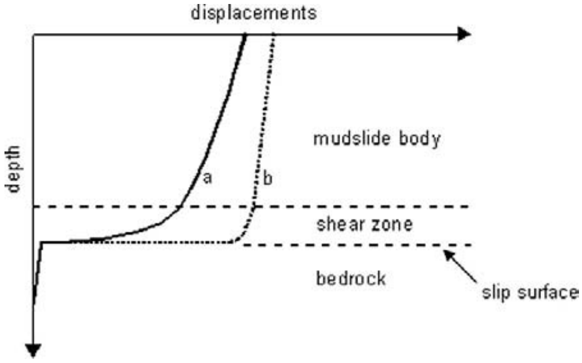

Fig. 4.28 Likely displacement profiles of a mudslide in the very early and in the late stage of movement (Comegna and Picarelli, 2005)

Literature is not rich of examples about such mechanisms, besides the classical case of failure of cuttings in clay (Skempton, 1977). However, considerations based on numerical modelling have been reported by Potts et al. (1997), showing that the progressive failure in OC clay can be delayed by negative excess pore pressures induced by failure.

A documented example about the role of negative excess pore pressures on slope movement is the lateral spread investigated by Picarelli and Urciuoli (1993) and Di Nocera et al. (1995) in a highly plastic thick deposits of clay subjected to intense erosion. As a consequence of continuous erosion, the deficient pore pressure regime may be practically permanent acting as a constraint to movement. Similar data about negative excess pore pressures induced by erosion in a site of the American mid West are reported by Neuzil (1993).

Finally, in previous section a clue as been shown about regarding negative excess pore pressures which can be induced in granular soils (Moriwacki et al., 2005). Further data suggesting the same mechanisms have been provided by Ochiai et al. (2004) regarding a full-scale model test in decomposed granites. Naturally, in granular soils the excess pore pressures rapidly equalize, and their very transient existence assume an academic more than a practical meaning.

4.5 Conclusions

Based on examples taken form experience, the paper shows the strict relationship which relates the soil properties and/or the pore pressure regime on the mechanisms of landslides. As a consequence, similar materials may display very different movement patterns and conversely, in similar hydraulic conditions, the soil properties can determine the establishment of very different landslide types. Naturally, this has a great engineering meaning since the effects of landslides on the environment, including man-made works, human activities and heritage (i.e. the risk), strongly depend on their size and movement patterns.

Acknowledgment The author would like to express his gratitude to dr. Furubayashi for his cooperation.

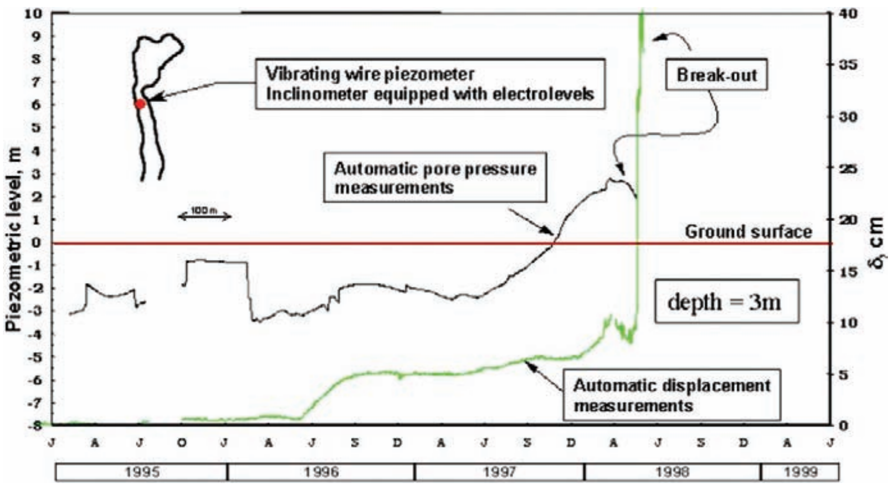

Fig. 4.29 Excess pore pressures and displacement rates measured in the Masseria Marino mudslide (Pellegrino et al., 2004)

References

Alonso EE, Gens A, Josa A (1990). A constitutive model for partially saturated soils. Géotechnique, 40(3): 405–430

Banks DC, Strohm WE, De Angulo M, Lutton RJ (1975). Study of clay-shale slopes along the Panama Canal. Rep. no 3, Engineering Analysis of Slides and Strength Properties of Clay Shales along the Gaillard Cut. TRechnical Rep. S-70-9, U.S. Army Engineering Waterways Experiment Station, Vicksburg Miss

Barton NR (1976). The shear strength of rock and rock joints. International Journal or Rock Mechanics and Mining Sciences & Geomechanics Abstracts, XIII: 205–279

Bilotta E, Pellegrino A, Picarelli L (1985). Geotechnical properties and slope stability in structurally complex clay soils. Geotechnical Engineering in Italy. An Overview, Cap. 3: Physical and Mechanical Properties, A.G.I., pp. 195–214

Bjerrum L (1967). Progressive failure of slopes of overconsolidated plastic clays. International Journal of Soil Mechanics and Engineering Division ASCE, SM5: 1–49

Cairo R, Dente G (2003). A flowslide in a pyroclastic soil fill. *In*: Picarelli L (ed), Patron, Proc. Int. Conf. on Fast Slope Movements – Prediction and Prevention for Risk Mitigation, Napoli, 1, pp. 53–61

Cicolella A, Picarelli L (1990). Decadimento meccanico di una tipica argilla a scaglie di elevata plasticità. Rivista Italiana di Geotecnica, XXIV(1): 5–23

Comegna L, Picarelli L (2005). The interplay between pore pressures and slope movements in fine-grained materials. *In*: Barla G and M Barla (eds.), Proc. 11th Int. Conference of the Int. Ass. of Computer Methods and Advances in Geomechanics (IACMAG), Turin, 3, pp. 497–504

Comegna L, Picarelli L, Urciuoli G (2007). The mechanics of mudslides as a cyclic undrained-drained process. Landslides, 4(3): 217–232

Corominas J, Moya J, Ledesma A, Lloret A, Gili JA (2005). Prediction of ground displacements and velocities from groundwater level changes at the Vallcebre landslide (Eastern Pyrenees, Spain). Landslides, 2(2): 83–96

Di Maio C (1996a). Exposure of bentonite to salt solution: osmotic and mechanical effects. Géotechnique, 46(4): 695–707

Di Maio C (1996b). The influence of pore fluid composition on the residual shear strength of some natural clayey soils. *In*: Senneset K (ed.), Balkema, Proc. 7th Int. Symp. on Landslides, Trondheim, 2, pp. 1189–1194

Di Maio C, Onorati R (2000). Influence of pore liquid composition on the shear strength of an active clay. *In*: Bromhead E, N. Dixon and M.L. Ibsen (eds.), Proc. 8th Int. Symp. on Landslides, Cardiff, 1: 463–468

Di Nocera S, Fenelli GB, Iaccarino G, Pellegrino A, Picarelli L, Urciuoli G (1995). An example of the geotechnical implications of geological history. Proc. 11th European Conf. on Soil Mechanics and Foundation Engineering, Copenhagen, 8, pp. 39–48

Henkel DJ (1967). Local geology and the stability of natural slopes. Journal of the Soil Mechnics and Engineering Division, ASCE, 437–450

Hungr O, Evans SG, Bovis MJ, Hutchinson JN (2001). A review of the classification of landslides of flow type. Environmental & Engineering Geoscience, 7(3): 1–18

Iverson RM (1997). The physics of debris flows. Review of Geophysics, 35(3): 245–296

Kenney TC, Lau KC (1984). Temporal changes of groundwater pressure in a natural slope of non fissured clay. Canadian Geotechnical Journal, 21: 138–146

Lade PV, Pradel V (1990). Instability and plastic flow of soils. Experimental observations. Journal of the Geotechnical Engineering Division, ASCE, 116(11): 2532–2550

Lampitiello S (2004). Resistenza non drenata e suscettività alla liquefazione di ceneri vulcaniche della Regione Campania. PhD Thesis, Seconda Università di Napoli

Leroueil S, Vaughan PR (1990). The congruent and general effects of structure of natural soils and weak rocks. Géotechnique, 40: 467–488

Leroueil S, Vaunat J, Picarelli L, Locat J, Homa L, Faure RM (1996). Geotechnical characterization of slope movements. *In*: Senneset K (ed.), Balkema, Proc. 7th Int. Symp. on Landslides, Trondheim, 1, pp. 53–74

Lo Presti D, Frojo F (2004). Resistenza al taglio residua di rocce tenere e terreni a grana fine. Rivista Italiana di Geotecnica, 38(3): 48–84

Moriwaki H, Inokuchi T, Hattanji T, Sassa K, Ochiai H, Wang G (2004). Failure processes in a full-scale landslide experiment using a rainfall simulator. Landslides, 1(4): 277–288

Musso A, Olivares L (2004). Post-failure evolution in flowslide: transition from static liquefaction to fluidization. *In*: Picarelli L (ed.), Patron, Proc. Int. Workshop on Occurrence and Mechanisms of Flow-Like Landslides in Natural Slopes and Earthfills, Sorrento, pp. 117–128

Neuzil CE (1993). Low fluid pressure within the Pierre shale: a transient response to erosion. Water Resources Research, 29(7): 2007–2020

Nova R (1992). Mathematical modelling of natural and engineered geomaterials. European Journal of Mechanical, A/Solids, 11(Special Issue), 1st ECSM, 135–154

Ochiai H, Okada Y, Furuya G, Okura Y, Matsui T, Sammori T, Terajima T, Sassa K (2004). A fluidized landslide on a natural slope by artificial rainfall. Landslides, 1(3): 211–220

Olivares L (1998). A stress-path controlled traxial apparatus equipped for local measurements of displacements and pore pressures. *In*: Evangelista A and L Picarelli (eds.), Balkema, Proc. Second Int. Symp. on The Geotechnics of Hard Soils-Soft Rocks. Napoli, 3, pp. 1435–1438

Olivares L and Damiano E (2007). Post-failure mechanics of landslides: laboratory investigation of flowslides in pyroclastic soils. Journal of Geotechnical and Geoenvironmental Engineering, ASCE, 133(19): 51–62

Olivares L, Picarelli L (1999). Discussion on "A laboratory study of the strength of four stiff clays" by JB BUrland, S Rampello, VN Georgiannou and G Calabresi, Géotechnique 46(3): 491–514

Olivares L, Picarelli L (2006).Modelling of flowslides behaviour for risk mitigation. Proc. Int. Conf. on Physical Modelling in Geotechnics, Hong Kong, 1, pp. 99–113

Pellegrino A, Picarelli L, Urciuoli G (2004). Experiences of mudslides in Italy. *In*: Picarelli L (ed.), Patron, Proc. Int. Workshop on Mechanisms and Occurrence of Flow-Like Landslides in Natural Slopes and Earthfills, Sorrento, pp. 191–206

Picarelli L (1980). Sulla resistenza residua di argille varicolori dell'Italia meridionale. Proc. 4th National Geotechnical Conf., Firenze, II, pp. 301–309

Picarelli L (1986). Caratterizzazione geotecnica dei terreni strutturalmente complessi nei problemi di stabilità dei pendii. Proc. 6th National Geotechnical Conf., Bologna, 3, pp. 155–169

Picarelli L (2000). Mechanisms and rates of slope movements in fine grained soils. Proc. GeoEng2000, Int. Conf. on Geotechnical and Geological Engineering, Melbourne, 1, pp. 1618–1670

Picarelli L (2005). Discussion on "Resistenza al taglio residua di rocce tenere e terreni a grana fine" by Lo Presti D and F. Frojo, Rivista Italiana di Geotecnica, 39(2): 63–67

Picarelli L (2007). Considerations about the mechanics of slow active landslides in clay. *In*: Sassa K, H. Fukuoka, F. Wang and G. Wang (eds.), Progress in Landslide Science, Springer Heidelberg, pp. 27–45

Picarelli L, Di Maio C, Olivares L, Urciuoli G (1998). Properties and behaviour of tectonised clay shales in Italy. *In*: Evangelista A and L Picarelli (eds.), Balkema, Proc. Second Int. Symp. on The Geotechnics of Hard Soils-Soft Rocks, Napoli, 3, pp. 1211–1241

Picarelli L, Evangelista A, Rolandi G, Paone A, Nicotera MV, Olivares L, Scotto di Santolo A, Lampitiello S, Rolandi M (2006). Mechanical properties of pyroclastic soils in Campania Region. *In*: Tan TS, KK Phoon, DW Hight, S Leroueil (eds.), Balkema, Proc. 2nd Int. Workshop on Characterisation and Engineering Properties of Natural Soils, Singapore, 4, pp. 2331–2384

Picarelli L, Olivares L, Avolio B (2008b). Zoning for flowslide and debris flow in pyroclastic soils of Campania Region based on 'infinite slope' analyis. Accepted for publication in Engineering Geology

Picarelli L, Olivares L, Comegna L, Damiano E (2008c). Mechanical aspects of flow-like movements in granular and fine-grained soils. Rock Mechanics and Rock Engineering, 41(1): 179–197

Picarelli L, Olivares L, Di Maio C, Silvestri F, Di Nocera S, Urciuoli G (2002). Structure, properties and mechanical behaviour of the highly plastic intensely fissured Bisaccia clay shale. *In*: Tan TS, KK Phoon, DW Hight, S Leroueil (eds.), Balkema, Proc. Int. Workshop on Characterisation and Engineering Properties of Natural Soils, Singapore, 2, pp. 947–982

Picarelli L, Russo C, Mandolini A (1999). Long-term movements on an earthflow in tectonised clay shales. *In*: Yagi N, T. Yamagami and JC Jiang (eds.), Balkema, Proc. Int. Symp. on Slope Stability Engineering, Matsuyama, 2, pp. 1151–1158

Picarelli L, Urciuoli G (1993). Effetti dell'erosione in argilliti di alta plasticità. Rivista Italiana di Geotecnica, 17: 29–47

Picarelli L, Urciuoli G, Mandolini A., Ramondini M. (2006). Softening and instability of natural slopes in highly fissured tectonized clay shales. Natural Hazards and Earth System Sciences, 6(4): 529–539

Picarelli L, Urciuoli G, Russo C (2004). The role of groundwater regime on behaviour of clayey slopes. Canadian Geotechnical Journal, 41: 467–484

Picarelli L, Versace P, de Riso R, Palmieri M (2008a). Landslide disaster management in Italy. Proc. 2007 Int. Forum on Landslide Disaster Management, Hong Kong, in press

Picarelli L, Viggiani C. (1988). A landslide in a structurally complex formation. *In*: Bonnard C (ed.), Proc. 5th Int. Symp. on Landslides, Lausanne, 1, pp. 289–297

Potts DM, Kovacevic N, Vaughan PR (1997). Delayed collapse of cut slopes in stiff clay. Géotechnique, 47: 953–982

Sassa K (2000). Mechanism of flows in granular soils. Proc. GeoEng2000, Int. Conf. on Geotechnical and Geological Engineering, Melbourne, 1, pp. 1671–1702

Schofield AN, Wroth CP (1968). Critical State Soil Mechanics. Mc-Graw-Hill Book Co., London

Skempton AW (1977). Slope stability of cuttings in brown London Clays. Proc. IX Int. Conf. on Soil Mechanics and Foundation Engineering, Tokyo, 3, pp. 261–270

Skempton AW (1985). Residual strength of clays in landslides, folded strata and the laboratory. Géotechnique, 35(1): 3–18

Sladen JA, D'Hollander RD, Krahn J, Mitchell DE (1985). Back-analysis of the Nerlerk berm liquefaction slides. Canadian Geotechnical Journal, 22: 564–578

Terzaghi K (1936). Stability of slopes in natural clay. Proc. 1st Int. Conf. Soil Mechanics, Harvard, pp. 161–165

Yamamuro JA, Lade PV (1997). Static liquefaction of very loose sands. Canadian Geotechnical Journal, 34: 905–917

Wang G, Sassa K (2001). Factors affecting rainfall-induced landslides in laboratory flume tests. Géotechnique 51(7): 587–600

5 Mechanics-Based Approach Toward the Mitigation of Debris Flow Disasters

Tamotsu Takahashi

Abstract This paper, at first, emphasizes the research on the mitigation of debris flow disasters is globally important and urgently needed by referring to Japanese statistics and other countries' recent cases. Then, introducing a chart describing the process of decision-making in coping with debris flow disasters, the discussion makes clear that debris flow mechanics play the core roll in decision-making. In this context, the problems how to identify the debris flow prone ravines and how to predict the onset of a debris flow in such a basin are discussed based on the mechanical considerations. The fluid mechanical methods to determine a standard design debris flow and to assess the hazards and the risks are outlined, in which debris flows are classified in reference to the grain concentrations and the predominant stresses in flows. The characteristics of debris flow are different depending on the types thus classified, and the resistance and the erosion or the deposition formulae applicable to each type debris flow are introduced. The estimations of debris flow hydrograph and the hazardous area are given by taking a particular debris flow case as an example. The performance design problems of the grid-type debris flow checking dam are also discussed.

Keywords Decision-making • Debris flow prone ravine • Prediction of debris flow • Hazard assessment • Debris flow classification • Grid-type dam

5.1 Introduction

A typical debris flow, although there are other types, is a mixture of water, mud and debris that suddenly pushes ahead with a vanguard of huge, jostling and roaring boulders. It has a quite fluidic character as if it were comprised of a kind of continuous fluid. The origin of debris flow is usually on a remote high mountain slope or in an ephemeral steep gully and once it initiates it surges down very fast sometimes swelling bigger and bigger by the entrainment of unstable gully bed material and/or plenty of woody debris on the way and other times deflating its peak discharge smaller and smaller by the detrainment of its composition onto bed. Because the source area is so distant and nevertheless the lead time from the onset to the flooding over the downstream fan area where people are living is so short, people can hardly notice the onset and even when they become aware of onset by chance they will be difficult to avoid the risk in a very short time. The prediction or the identification of debris flows is not an easy task, but an early warning and the evacuation in advance would be the effective measure to secure at least their lives provided there

Tamotsu Takahashi (✉)
Association for Disaster Prevention Research, Japan

K. Sassa, P. Canuti (eds.), *Landslides – Disaster Risk Reduction*,
© Springer-Verlag Berlin Heidelberg 2009

are no or only insufficient countermeasure structures in the basin. Therefore, research toward the mitigation of debris flow disasters should focus on the more reliable onset prediction in view of site and time and also on the definite and not costly methods to control the flow underway or to deflect before flooding takes place.

The importance of research on the mitigation of debris flow disasters can be understood by examining the Japanese statistics of casualties due to water related hazards as depicted in Fig. 5.1. This figure clearly shows the death toll has steadily decreased year by year. Namely, between 1946 and 1959 the total number of victims per annum often exceeded a thousand but recently it is less than a hundred. The long lasted war wasted the land, and making things worse, violent typhoons hit one after another and they caused severe flooding from the major rivers and extensive storm surges at bay areas. The improvement of major rivers and the afforestation of bare mountains and hill slopes have lessened large-scale flooding and they surely contributed to decrease in the number of casualties, but the improvement of minor rivers lags behind and the development of slope land as residential area makes the situation worse for the vulnerability to sediment hazards. As Fig. 5.1 shows, before 1964, among the victims due to total water related hazards, about 32% was due to sediment hazards but after 1965 this ratio has changed to about 50%. The term "sediment hazards" includes those due to cliff failure, debris flow and comparatively large deep-seated re-activated landslides. The Japanese statistics of casualties does not separate the cause of death into debris flow and deep-seated landslide. By such statistics, after 1967, about 50% of total casualties due to sediment hazards are due to debris flow and landslide.

The tendency that the majority of casualties are due to sediment hazards has become especially conspicuous recently. For example, in the case of "Nagasaki disaster" in 1982, 75% of the total 299 casualties and in the "San-in disaster" in 1983, 90% of the total 121 casualties were due to sediment hazards. More recently, almost all the remarkable disasters such as the "Gamaharazawa debris flow disaster" in 1996 (14 people were killed); the "Harihara River debris flow disaster" in 1997 (21 people were killed); the "Hiroshima disaster" in 1999 (24 people were killed); and the "Minamata debris flow disaster" in 2003 (19 people were killed) were sediment hazards.

The importance of sediment hazards is not limited to Japan. There are many countries exposed to even worse conditions. In China, more than a hundred prefectures and cities suffer from debris flow disasters every year, and more than a hundred people are killed and more than two billion yuan are lost. As an example, in the disaster of 2002, 1,795 people died due to water related hazards and among them 921 were due to sediment hazards like debris flows (Kuang 2003). In Colombia in 1985, more

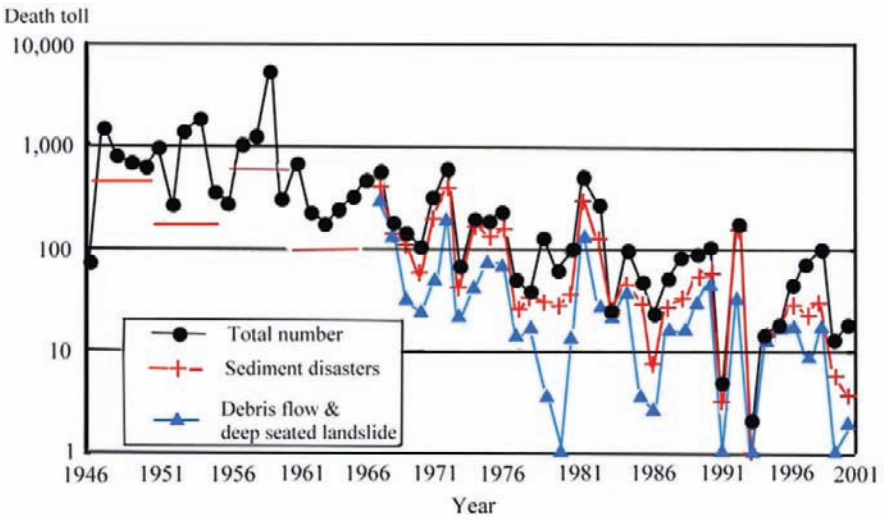

Fig. 5.1 Change in the casualties in Japan due to water-related hazards and a breakdown of causative phenomena. The death toll due to sediment disasters before 1967 is shown by the average numbers every five years

than twenty thousand people were killed by the lahars generated by the eruption of the Nevado del Ruiz volcano and Armero City disappeared. In Venezuela in 1999, the Caribbean cities were attacked by large-scale debris flows and more than twenty thousand people were killed. In Taiwan in 2001, a rainstorm associated with a typhoon generated many debris flows and killed 214 people. Many debris flow disasters also occur in other countries such as Nepal, Indonesia, the Philippines, Italy, Switzerland, France, among others.

Recent global warming could bring very severe debris flows due to the collapse of moraine dams caused by the retreat of glaciers to Himalayan and other high mountain range regions, and it could bring the increment of number and intensity of severe rainfalls; accordingly the frequency and the magnitude of the rainfall induced debris flows may increase.

Thus, the number of debris flow prone ravines and communities vulnerable to debris flow disasters are enormous distributing worldwide. The recent urbanization encroaches onto dangerous sloping lands and debris fans, and the tendency toward global warming are making the situation worse. Therefore, researches aiming at the mitigation of debris flow disasters are very important and in urgent need.

5.2 Decision-Making Against Debris Flow Disasters and the Significance of Research on Debris Flow Mechanics

The reactions to a risk generally consist of avoidance, mitigation, transference and toleration. Which of these reactions among others is selected would depend on the severity of disasters, the availability of controlling measures, cost and benefit balance, possibility for replacement, human emotions against disasters, etc. Majority of debris flow disasters are cruel to kill people and completely deprive of their properties but not overwhelming as to oblige people to tolerate. Therefore, one would think to avoid or mitigate the debris flow disasters.

Figure 5.2 outlines the possible process of decision-making against debris flow disasters. Given an objective area to think about, first the decision-makers must recognize the attributes of the area such as the items shown in the uppermost block. The social, economic or environmental importance of the area is the criterion to decide how much anti-hazard investment would be reasonable. The present state of land usage and the topographical condition of the space of human activity make the evaluation of risk's distribution possible. The geological, climatological, hydrological, morphological, vegetational and geotechnical conditions of the upstream river basin are the fundamental items in the estimation of debris flow that will attack the area, and the morphology of the river channel that penetrates the area is necessary information for the simulation of flooding and deposition within the area. Whether the alternate site that enables to relocate the things in the hazardous zone is available or not is also essential information in the decision-making.

Once the detailed attributes of the area as well as those in the upstream river basin are known, an objective debris flow to which magnitude the importance of the area is reflected can be determined; Importance of the area may be taken into consideration in the decision of the return period of rainfall that induces the design debris flow, namely, the more important the area is the longer return period will be adopted, so that the larger the magnitude of the objective debris flow becomes. The objective debris flow contains the information on the total volume, peak discharge, solids concentration and particle size distributions. Sometimes, several debris flows arising in a period would become the target.

Three kinds of alternative plan are listed up by the three blocks in Fig. 5.2 in a row. The left one does not work directly on debris flow itself. It is an issue concerning with statutes. The regulation of land usage and the relocation are the substantial measures to thoroughly avoid the hazards. Making buildings and infrastructures anti-hazard cannot be safe enough because a phenomenon larger than supposition may occur. To cope with severe debris flow only by insurance may be unrealistic because debris flow often risks on human life and in such a case the concerned government will be blamed if no other measures are implemented.

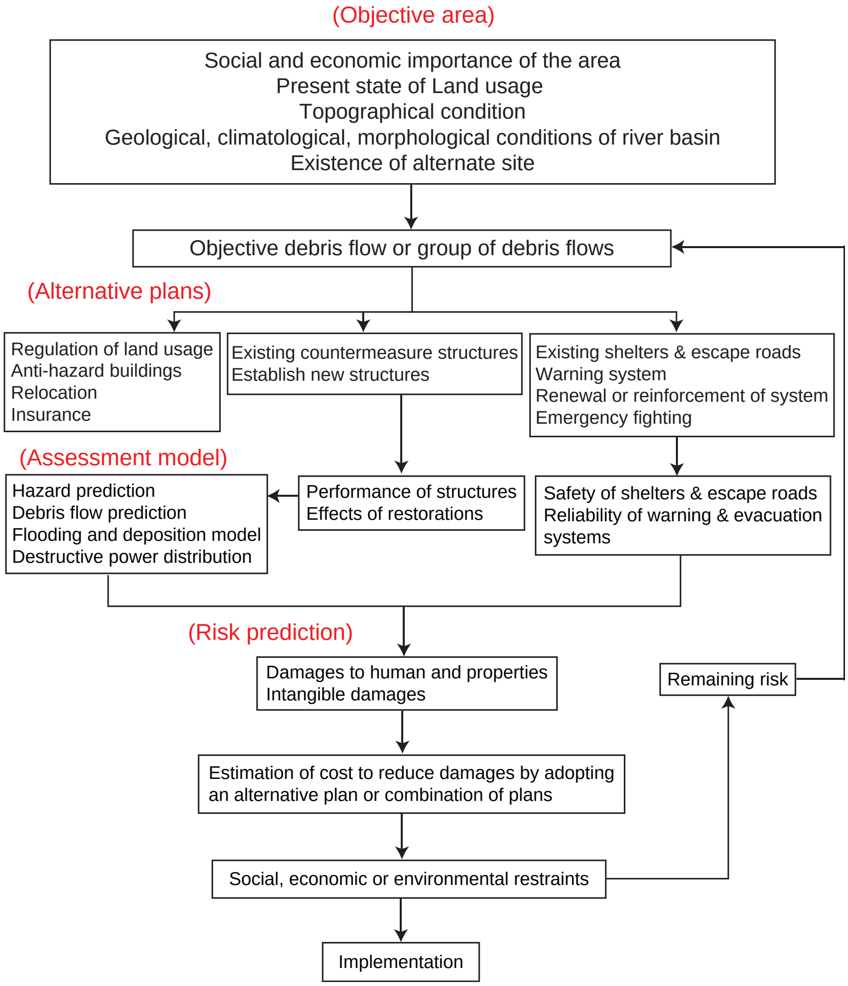

Fig. 5.2 The possible process of decision-making to reduce debris flow disasters

In Japan, the necessity of the regulation of land development in potentially hazardous area had been pointed out long before, but no laws to put the regulation into effect existed, so that it had been almost free to develop, although the designation of debris flow prone ravines and their potentially hazardous areas has commenced as early as 1977. The number of debris flow prone ravines in 1977 was 62,272, but it increased year by year: in 1986, 70,434; in 1993, 79,318; and in 2002, 89,518. This increment is partly due to the reassessment of the survey, but it is mainly due to the encroachment of inhabitants into potentially hazardous areas. Unfortunately, the mere designation of hazardous areas had not been influential. With the "Hiroshima disaster" as a turning point, the "sediment disaster prevention act" has been enforced since 2000. In the possible extremely hazardous areas designated by this act, all the organized housing land development is prohibited, and even a personal house building that do not have adequate strength to resist sediment hazards is prohibited. Local government can advise the inhabitants already inside that area to move to a safer area. This act designates the hazardous areas (not extremely hazardous) on the periphery of the extremely hazardous areas and in these areas local government is responsible to establish the reliable warning and evacuation systems.

In parallel with the implement of the sediment disaster prevention act, the designation of hazardous areas has been reassessed. Namely, areas designated so far are defined as category I, and the newly designated hazardous areas of categories II and III are added. The category I has been designated under the criterion that more than five families or some kind of public facilities such as school or administrative institution exist inside the area. Whereas, in the category II areas less than five houses exist, and in the category III areas no house exists at present, but if houses were constructed, they may well meet disasters. The total number of categories II and III ravines were 94,345 in 2002. These numbers of categories I to III ravines are of course too many to be adequately treated by the structural countermeasures (hard countermeasures), hence the nonstructural countermeasures (soft countermeasures) such as the regulation of development and the evacuation just before the onslaught of debris flow are important. This is the reason why the sediment disaster prevention act is enforced.

The second alternative plan shown in the middle block of the row in Fig. 5.2 is the execution of so called hard countermeasures in the upstream river basin and/or on the periphery of objective protection area. Generally, the aims of hard countermeasures can be categorized as (1) prevention from debris flow generation; (2) controlling it underway to the extent harmless to protection area; and (3) diverting it away from protection area. The methods fell into the category (1) may further be ramified to the reduction of material that produce debris flow and the reduction of causative water discharge. The former measures are comprised of the preventive measures from slope failure and land surface erosion such as planting trees on bare slopes, the stabilization of sediment accumulated on gully bed by such structures as groundsills and bed girdles, and the removal of landslide dams. The examples of latter measures are the drainage works such as the excavation of tunnel to drain the stored water upstream the landslide dam and the setting of channel works on the debris accumulation. The methods in the category (2) are the most popular ones like the construction of check dams and sand storage basin. Recently, the open-type dams are paid attention for its sustainable storage capacity and advantages in environmental point of view. The structures in the category (3) are such as channel works and training dykes. The aim of channel works is not only to pass through debris flow or flood flow safely but to prevent from the erosion of objective protection area by the action of channel widening and shifting.

The third alternative plan in Fig. 5.2 refers to the so-called soft countermeasures. Because the early warning and the evacuation to a safe refuge are essential to survive a cruel debris flow, the necessary lead time for evacuation should be secured and moreover the warning should have high reliability. The direct attack of debris flow has so strong power that emergency fight is unrealistic except for against the marginal flow after the main debris flow is deposited.

Next step in decision-making is the assessment of hazards. Under the situation of already existing and/or newly established hard countermeasures, a standard design debris flow that is more or less moderated within the upstream river basin by the effects of the hard countermeasures will attack the objective protection area and cause various hazards. Under the given topographical and land use conditions, the range of flooding and sediment deposition, and the distributions of deposit thicknesses and destructive powers must be obtained. The newly established hard measures should have the most effective performance under the smallest cost, so one must have a method that enables the quantitative performance design of structures such as the most appropriate type of structures and places to set them. The reliability of warning and evacuation system will be enhanced after repeated exercises. People will be motivated to evacuate only if they think the warning is reliable. In this context, hazard map should be correct and easy to understand.

Then, the process of decision-making proceeds to the step of risk prediction. Here, risk means the damages to human lives and properties such as houses, stores, factories, public institutions, infrastructures, farms, etc. It must not be forgotten that debris flow sometimes destroys invaluable thing that cannot be recovered.

To reduce damages one of alternative plan or combination of plans must be chosen. Each alternative plan needs cost, so the cost for a choice is estimated, and considering the financial and the other restraints, one priority plan is selected and put into implementation.

Thorough preventive plan is seldom executed in short period caused by various restraints, therefore, usually some risks remain even after some plans are implemented. The remaining risks should again be analyzed according to the procedure in Fig. 5.2, and under an appropriate annual execution program the safety level of objective area must be enhanced.

According to the discussion based on Fig. 5.2, it is now understandable that the knowledge of debris flow mechanics is indispensable, and what kind of research is necessary becomes clear. If the mechanism of debris flow initiation is unknown, one can hardly collect necessary and adequate attributes in the basin. The mere multiple regression analysis using unnecessarily many and irrelevant basin properties can have no universality and even leads to erroneous conclusions. Only a sound mechanical model, in which the necessary and the adequate attributable basin characters and rainfall characteristics are incorporated, can determine a standard designing debris flow whose hydrograph and other characteristics are quantitatively defined. Moreover, the time of occurrence that is necessary for decision-making can also be determined.

Thus, the objective debris flow or standard design debris flow for the countermeasure planning, which is brought about under the present state of basin due to the influence of a standard design rainfall, is obtained by applying a mechanical model. That objective debris flow will be moderated by some already existing hard countermeasures and/or by newly establishing them. Therefore, the performance of various optional structures including the effects of restoration of them must be assessed by a mechanical model. Thus, a debris flow deformed and moderated along the river channel will come out to the objective area. Then, the hazards on the area due to such a debris flow will be assessed by the application of two-dimensional flooding and deposition model. This hazard assessment enables the discussion on the performance of the planned soft-countermeasures; the delineation of the zone in which residents are necessary to evacuate, the location of shelters and their necessary capacity, the transmission system of evacuation advise/order. The real time simulation of human actions in evacuation coupled with debris flow flooding will be helpful to enhance the reliability of soft-countermeasure planning.

Hazard assessment model, especially that can assess the distributions of destructive power inside the objective area which may be most simply given as a function of flow velocity multiplied by flow depth, will be directly connected with the risk prediction model. For example, the destructive power distributions enable to assess the distributions of house destructions, and the number of destroyed houses would give the estimations of the loss of human lives and monetary loss. The reliable models necessitate very detailed simulation of flooding over complicated house and road distributions on complex topography.

The engineering designs of optional hard countermeasure structures; the comparisons of the performances between the alternative structures, the cost evaluations to construct them, and the design of anti-hazard buildings, are pure technical issue that is connected with the mechanical models of debris flow.

Although the state-of-the-art in view of debris flow mechanics is by no means complete, discussions on various problems are now possible based on mechanics, and by the refinement of this approach the mitigation of debris flow disaster will be accomplished.

5.3 Identification of Debris Flow Prone Ravines and Prediction of Debris Flow Onset Time

The mechanical causes of debris flow initiation can be classified into three types: (1) the debris on gully bed is eroded by the supply of water or landslide material that is already diluted as thin as a liquid, thereby the concentration of solids in the surface flow becomes as dense as it can be and is called debris flow; (2) the landslide block transforms into debris flow while in motion by the effects of stored water in the slid earth block or by the supply of water from outside; (3) the collapse of a debris dam. The debris flow initiation mechanism in category (2), although the earth block should already be water-saturated when landslide initiates, is the same as to the initiation of landslide. Therefore, the discussion in this category is handed over elsewhere (e.g. Takahashi 2007, Chigira 2007). From the mechanical point of view, the debris flow initiation process due to overtopping of a debris dam can be considered similar to the first category, and that due to collapse of the dam body is akin to the second category. Therefore, category (3) is also not discussed here because of limited space.

When it rains, some of the rain water will run off through as well as over the surface of the debris bed of a gully. If the bed slope is very steep, the debris bed will slide as the level of seepage flow rises, but it will not immediately turn into debris flow because the quantity of water would be insufficient. However, attention should be paid, even on such a steep slope bed, to that the surface water flow on unsaturated stable bed can pick up and entrain particles into flow and gradually develops to debris flow. If the bed slope gradient is intermediate, the debris bed will not slide before the seepage flow reaches the surface of the bed. With an increment of the runoff, the depth of the stream on the surface will increase and the operating shear stress to the downstream direction due to the static weights of surface water plus submerged debris bed will exceed the resistance in the debris layer near the surface. Accordingly, the upper part of that debris layer will come loose and start moving and entrained into flow as a so-called sediment gravity flow or immature debris flow. The flow is able to continue and develop to a (mature) debris flow in which grains are dispersed throughout the depth as long as the stream channel has an adequate slope gradient and plenty of sediment.

The mechanical consideration on the conditions for such kinds of phenomena results in the debris flow occurrence criteria as shown in Fig. 5.3. The curves in the figure are, respectively;

$$\tan\theta_2 = \frac{\Lambda\tan\phi + H_*(1+\Lambda^2\tan^2\phi - H_*^2)^{1/2}}{1-H_*^2} \quad (5.1)$$

$$\tan\theta = \frac{F_0}{F_2}\left\{1+\frac{c}{gaF_0}\frac{(1-c^2g^{-2}a^{-2}F_2^{-2}+F_0^2F_2^{-2})^{1/2}}{(1-c^2g^{-2}a^{-2}F_2^{-2})}\right\} \quad (5.2)$$

$$\tan\theta_1 = \frac{F_0}{F_1}\left\{\begin{array}{l}1+\frac{c}{\kappa g h_0 F_0}\\ \times\frac{(1-c^2g^{-2}\kappa^{-2}h_0^{-2}F_1^{-2}+F_0^2F_1^{-2})^{1/2}}{(1-c^2g^{-2}\kappa^{-2}h_0^{-2}F_1^{-2})}\end{array}\right\} \quad (5.3)$$

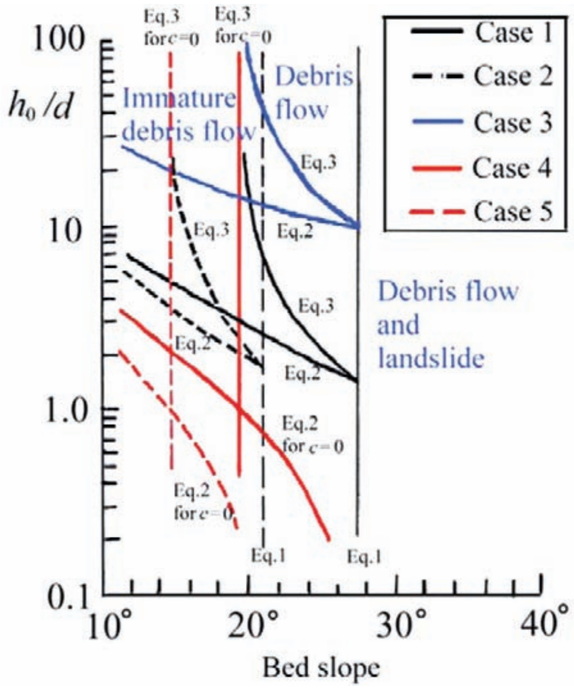

Fig. 5.3 The occurrence criteria of debris flows and immature debris flows

where:

$$\left.\begin{array}{l}\Lambda = \frac{C_*(\sigma-\rho)}{C_*(\sigma-\rho)+\rho}\ ,\ H_* = \frac{c}{gD\{C_*(\sigma-\rho)+\rho\}}\\ F_0 = C_*(\sigma-\rho)\tan\phi\\ F_1 = C_*(\sigma-\rho)+\rho(1+\kappa^{-1})\\ F_2 = C_*(\sigma-\rho)+\rho(1+h_0a^{-1})\end{array}\right\} \quad (5.4)$$

C_* is the grain concentration by volume in the static bed, ρ the density of fluid, σ the grain density, h_0 the depth of the surface flow, a the thickness of the layer that start moving, κ a numerical coefficient near unity, ϕ the internal friction angle, c the cohesive strength of the bed, and g is the acceleration due to gravity.

Equation (5.1) gives the steepest slope; θ_2, of a stable bed in which the surface level of seepage flow coincides with the bed surface. Equation (5.2) is the relationship between the slope angle and the thickness: a, which starts moving. The condition for the occurrence of a sediment gravity flow; i.e. the motion of particles is not due to the dynamic force of flow but due to the static weight of the water column, necessitates that a should be at least larger than the diameter of the representative particle of the bed; d. The curve in Fig. 5.3, which shows Eq. (5.2), is generated under the condition that $a = d$. The domain of the occurrence of a sediment gravity flow is, therefore, upper part of this curve. However, even a is larger than d, if a is considerably less than h_0, the particles in motion cannot disperse throughout the flow depth, but the layer of particle motion is covered by a less densely concentrated water flow; this type flow is called immature debris flow. Therefore, the condition for the occurrence of a debris flow should be $a \geq \kappa h_0$ ($\kappa \approx 1$). Because Eq. (5.3) is obtained by substituting $a = \kappa h_0$ into Eq. (5.2), the domain of debris flow occurrence in Fig. 5.3 corresponds with the right-hand side of the curve generated by Eq. (5.3). The slope θ_1 is the minimum slope angle necessary for an immediate occurrence of debris flow, and it is a constant when the bed is non-cohesive. The domain between the curves for Eqs. (5.2) and (5.3) is that for the occurrence of immature debris flow.

Figure 5.3 is depicted for the conditions: $c = 500$ Pa, $d = 7$ cm and $\phi = 45°$ (Case 1); $c = 500$ Pa, $d = 7$ cm and $\phi = 37°$(Case 2); $c = 500$ Pa, $d = 1$ cm and $\phi = 45°$ (Case 3); $c = 0$ Pa and $\phi = 45°$ (Case 4); and $c = 0$ Pa and $\phi = 37°$ (Case 5). For the cases $c = 0$ Pa, the curves are independent of particle diameter. The other parameters are: $C_* = 0.65$, $D = 300$ cm, $\sigma = 2.65$ g/cm^3, $\rho = 1.0$ g/cm^3, $\kappa = 1$. These values would be reasonable for many stony type debris flows. Then, if the debris bed which mainly consists of colluvium is thick, H_* is negligibly small.

The domain of debris flow occurrence in Fig. 5.3 tends to move towards a steeper slope as ϕ increases and to move towards a larger value of h_0/d as c increases. This means the larger the value of c and ϕ, the more difficult the generation of debris flow becomes. the surface flow depth exceeds the critical h_0/d value a debris flow occurs and the scale of flow becomes large in comparison with the case of small c value. Because c value is very sensitive to shift the debris flow arising domain, the estimation of c in the actual bed is important. Although the initiation of debris flow becomes difficult if c is large, once Figure 5.3 also shows that the smaller the representative particle diameter is, under a certain cohesive strength of the bed, the larger the relative depth of overland flow; h_0/d, should be to generate debris flow. The absolute depth of overland flow to generate debris flow is, however, not dependent on particle diameter; if particle diameter is 1/7, the critical relative depth to generate debris flow becomes almost 7 times under a constant flow depth.

It is clear from Fig. 5.3 that the flattest slope for debris flow initiation is about 15 degree and the minimum value of h_0/d at that critical slope is, if bed is non-cohesive, around 1. The h_0/d value is, however, not explicitly obtainable from rainfall condition. It is obtained knowing the water discharge on the bed and applying an appropriate flow resistance law. According to the experiments for the cases of h_0/d is nearly equal to 2 (Takahashi 1977), the following formula is approximately satisfied:

$$\left(\frac{h_0}{d}\right)^3 = (0.14 \sim 0.125)\frac{q_0^2}{gd^3} \tag{5.5}$$

where q_0 is the water discharge per unit width. We describe $q_0/(\sqrt{gd^3})$ as q_*. Therefore, we can conclude that a stony debris flow will occur on a gully bed steeper than about 15 degree when the surface water flow satisfying $q_* \geq 2$ or $h_0/d \geq 1$ appears.

Therefore, we can assess whether the objective basin is debris flow prone or not by examining whether the condition $q_* \geq 2$ is satisfied under the standard design rainfall within the sub-basins existing at upstream parts of the objective basin whose channel bed slope is steeper than 15 degree. This does not mean debris flow necessarily initiates from this assessment point. As shown by the red broken line representing Eq. (5.2) in Fig. 5.3, in the channel steeper than 15 degree, debris flow can be generated under smaller relative depth, so that debris flow may or may not occur upstream of the assessment point. The setting of assessment point at the flattest point to give rise to debris flow is mainly for the sake of simplicity, but larger basin area would have chance to have larger discharge. If there is no channel reach steeper than 15 degree, no debris flow except for immature debris flow can occur.

The debris flow routing coupled with flood runoff analysis explained in the next chapter does not use such a criterion but it will automatically obtain the debris flow, the immature debris flow or the flood flow hydrographs including these flow type transitions depending on the nature of the basin.

Therefore, this criterion will be useful to the primary selection of the debris flow prone ravines among many other ravines. The guidelines of Japanese Ministry of Land, Infrastructure and Transport suggest, without referring to rainfall, that a ravine having the area more than 5 ha at the assessing point of which channel gradient upstream is steeper than 15 degree, is debris flow prone. If herein introduced mechanics-based method is referred to, we can understand that this guideline is equivalent to consider that the debris flow prone ravine is the one whose representative bed particle diameter is 6.3 cm or less and it produces debris flow upstream the assessing point by the effective rainfall of 75 mm/h. This result seems reasonable in comparison with many actual data.

The occurrence time of debris flow is the time on which the critical condition to initiate debris flow; $q_* \geq 2$, is satisfied at the assessment point. This discharge under an arbitrary rainfall can be known by the application of an appropriate flood runoff analysis.

5.4 Debris Flow Routing in River Channel and Debris Flow Flooding on a Plane

5.4.1 The System of Governing Equations

The processes of debris flow deformation while in development or deposition can be quantitatively treated by the following well established system of equations (Takahashi et al. 1992):

The x- (down valley) and y-wise (lateral) horizontally two dimensional momentum conservation equations of flow are respectively:

$$\frac{\partial q_x}{\partial t} + \frac{\partial (uq_x)}{\partial x} + \frac{\partial (vq_x)}{\partial y} = gh\sin\theta_{bx0} - gh\cos\theta_{bx0}\frac{\partial (z_b + h)}{\partial x} - \frac{\tau_{bx}}{\rho_T} \tag{5.6}$$

$$\frac{\partial q_y}{\partial t} + \frac{\partial (uq_y)}{\partial x} + \frac{\partial (vq_y)}{\partial y} = gh\sin\theta_{by0} - gh\cos\theta_{by0}\frac{\partial (z_b + h)}{\partial y} - \frac{\tau_{by}}{\rho_T} \tag{5.7}$$

where $q_x = uh$ and $q_y = vh$ are the x- and y-components of the flow flux; u and v are x- and y-components of the depth-averaged velocity; θ_{bx0} and θ_{by0} are x- and y-components of the angle of inclination of the original bed surface; τ_{bx} and τ_{by} are x- and y-components of resistance to flow at the bottom, respectively; z_b the erosion or deposition thickness of the bed; ρ_T the apparent density of debris flow; t is time and h is the depth of flow.

The continuity equation of the total volume (water plus solids) is given by:

$$\frac{\partial h}{\partial t} + \frac{\partial q_x}{\partial x} + \frac{\partial q_y}{\partial y} = \begin{cases} i\{C_* + (1 - C_*)s_b\} + q_{in} & ;\ i \geq 0 \\ i & ;\ i < 0 \end{cases}. \tag{5.8}$$

where i is erosion (>0) or deposition (<0) velocity; s_b is the degree of saturation of the bed; and q_{in} is the water supply discharge from outside.

In the case of stony debris flow, the solids component in the flow is divided into two fractions; a coarse particle fraction whose particles are sustained in the flow by the effect of inter-particle collisions and a fine particle fraction whose particles are suspended by turbulence in the interstitial fluid. The continuity equations for coarse particle fraction and that for fine particle fraction are given by the following equations, respectively:

$$\frac{\partial (C_L h)}{\partial t} + \frac{\partial (C_L q_x)}{\partial x} + \frac{\partial (C_L q_y)}{\partial y} = \begin{cases} iC_{*L} & ;\ i \geq 0 \\ iC_{*DL} & ;\ i < 0 \end{cases}. \tag{5.9}$$

$$\frac{\partial (1 - C_L)h}{\partial t} + \frac{\partial (1 - C_L)q_x C_F}{\partial x} + \frac{\partial (1 - C_L)q_y C_F}{\partial y} = \begin{cases} iC_{*F} & ;\ i \geq 0 \\ i(i - C_{*DL})C_f & ;\ i < 0 \end{cases}. \tag{5.10}$$

where C_L is the volume concentration of coarse particle fraction in a pillar-shaped space in the flow having a height h and a bottom area of unity; C_F is the volume concentration of the fine fraction in the interstitial fluid; C_{*L} and C_{*F} are the coarse and fine particle fractions in a volume of static bed, respectively; and C_{*DL} is the volume concentration of the coarse particle fraction in a newly produced static bed when particles in flow are deposited.

In the case of turbulent muddy debris flow, all solid components are treated as one component, and the continuity equation for solids is given only by Eq. (5.9) in which C_L is replaced by C; the entire solids concentration in flow.

In the case of viscous debris flow, solid fraction cannot be separated from liquid fraction, and the continuity equation is only Eq. (5.8).

The equation for bed surface elevation change is

$$\frac{\partial z_b}{\partial t} + i = 0 \tag{5.11}$$

The fundamental system of equations to route debris flow is now prepared, but to carry out the analysis the laws of resistance to flow and the erosion and deposition velocity equations must be given appropriately. If flow is unidirectional like the one in a narrow gorge, the terms relating to y-direction should be neglected, so that the analysis is based on one-dimensional equations.

5.4.2 Laws of Resistance to Flow

The behaviors of debris flows are diversified depending on the properties of solid material, solids concentration, flow magnitude, river channel conditions, etc., and they often change their sediment transporting modes while in motion. The two-phase models that consider the debris flow is comprised of the mixture of two continuum media; fluid phase and solid phase, are able to classify debris flows and able to analyze the physics of respective flows.

If one considers the flow of a mixture of fluid (plain water or muddy water loading highly concentrated fine sediment) and coarse particles, one will easily speculate that coarse particles within the entire depth of flow move in enduring contact provided the concentration of those particles are higher than a threshold value but, if the concentration is less than the threshold, particles move detached each other dispersing in the entire depth or concentrated in a lower layer. The mechanism to sustain coarse particles in the entire depth for the enduring contact motion mode should be quasi-static pressure acting between contacting particles; the case of quasi-static debris flow regardless its velocity. For the dispersed flow mode, however, the mechanisms are not unique but they are possibly by frequent inter-particle collisions (stony debris flow), by strong turbulent mixing (turbulent muddy debris flow) and by the effect of the viscosity of interstitial fluid (viscous debris flow).

Takahashi (2007), after the consideration on predominant stresses in flow in each mode, gives the existence criteria of various motions of the mixture of solids and fluid as shown in Fig. 5.4. The vertical axis represents the mean coarse particle concentration in the flow. If coarse particles are not contained in flow (at the lowest point on the vertical axis), the flow is mere water or slurry flow. If, contrary,

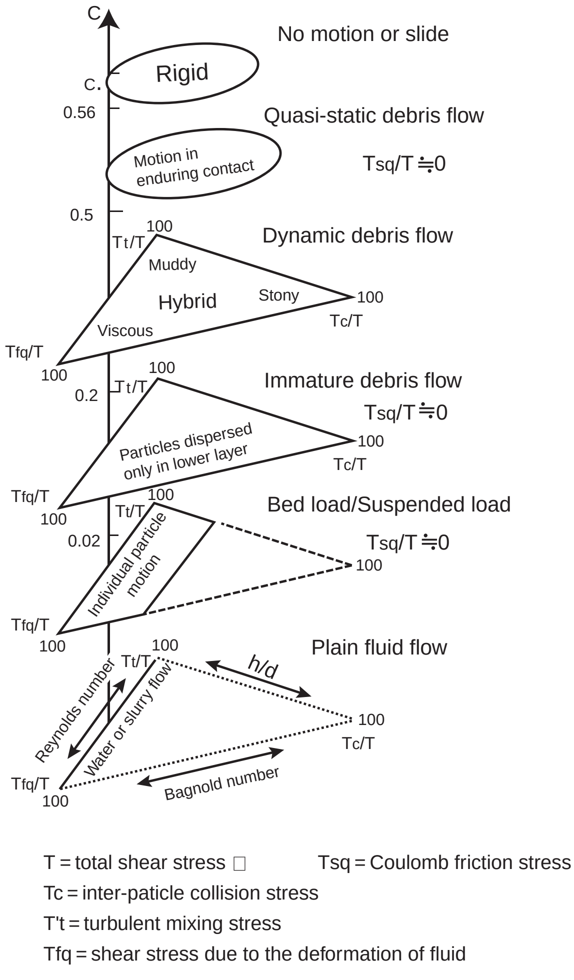

Fig. 5.4 The existence criteria of various motions of the mixture of solids and fluid

particle concentration is very large in a granular body, say larger than 0.56; according to Bagnold's examinations using a kind of natural beach sand (Bagnold 1966), particle's individual dislocation is impossible and so it must be a rigid body, so that if that body moves it should be sliding on the bed or only a part in the body adjacent to the bed is liquefied as to act as a lubricant: the liquefied part should have a particle concentration less than about 0.51 if the body is comprised of natural beach sand (Bagnold 1966), nevertheless the mean particle concentration of the whole body is larger than 0.56. Thus, the motions of the mixture as flow in mechanical sense exist between these extreme cases. Namely, they are individual particle transport (bed load and suspended load; $0 < C \leq 0.02$), immature debris flow ($0.02 < C \leq 0.2$), dynamic debris flow ($0.2 < C \leq 0.5$) and quasi-static debris flow ($0.5 < C \leq 0.6$). The boundary C values indicated are for the sake of reference only; they should depend on the properties of mixture such as cohesion, grain shape and the distribution of grain sizes.

Dynamic debris flow is a generic term for stony, turbulent muddy, viscous and intermediate hybrid debris flows and the territory of these constituents are given on a triangular horizontal plane attached perpendicularly to the vertical axis at a certain value between 0.5 and 0.2 in Fig. 5.4. The three apexes of that triangle represent that the inter-particle collision stress, the turbulent mixing stress and viscous stress, respectively, account for 100% of the total shearing stresses in flow. The three axes represent, as attached to the respective axes in the bottom triangle in Fig. 5.4, relative depth, Bagnold number and Reynolds number. Herein, Bagnold number is defined as the ratio of inertial grain stress T_c and viscous shear stress T_{fq}, and if Bagnold number is large, the inertial grain stress predominates in flow. Reynolds number represents, as is well known, the relative predominance of the turbulent mixing stress and viscous stress, and if Reynolds number is large, flow is turbulent. Therefore, the region of large Bagnold number and small relative depth is that for stony debris flow; the region of small Bagnold number and small Reynolds number is that for viscous debris flow; the region of large Reynolds number and large relative depth is that for turbulent muddy debris flow; and the other intermediate area is the region for hybrid debris flow.

Iverson and Denlinger (2001) and Pudasaini et al. (2005) developed the depth-averaged flow theories for quasi-static debris flow on a complex three-dimensional field. In these theories volume fraction of solid-phase among other input parameters has a given constant value and they cannot treat the sediment entrainment by bed erosion or sediment detrainment by deposition underway, nor explain how such a highly concentrated flow is produced. Herein, we do not discuss on the flow resistance law of quasi-static debris flow.

In the case of stony debris flow ($h/d_L < 20$, $C_L > 0.2$), the shear resistance at the bottom is well described by the equation of motion based on a Bagnold's type dilatant fluid concept (Takahashi 1978) as following:

$$\tau_{bx} = \left(\frac{\sigma}{8}\right)\left\{\left(\frac{C_{*L}}{C_L}\right)^{1/3} - 1\right\}^{-2}\left(\frac{d_L}{h}\right)^2 u\sqrt{u^2 + v^2} \tag{5.12}$$

$$\tau_{by} = \left(\frac{\sigma}{8}\right)\left\{\left(\frac{C_{*L}}{C_L}\right)^{1/3} - 1\right\}^{-2}\left(\frac{d_L}{h}\right)^2 v\sqrt{u^2 + v^2} \tag{5.13}$$

where d_L is the representative diameter of large particle fraction.

For an immature debris flow ($h/d_L < 20$, $C_L < 0.2$):

$$\tau_{bx} = \left(\frac{\rho_T}{0.49}\right)\left(\frac{d_L}{h}\right)^2 u\sqrt{u^2 + v^2} \tag{5.14}$$

$$\tau_{by} = \left(\frac{\rho_T}{0.49}\right)\left(\frac{d_L}{h}\right)^2 v\sqrt{u^2 + v^2} \tag{5.15}$$

For a bed load transport ($h/d_L < 20$, $C_L < 0.02$), we can apply the resistance law of plain water flow:

$$\tau_{bx} = \frac{\rho_T g n^2}{h^{1/3}} u\sqrt{u^2 + v^2} \tag{5.16}$$

$$\tau_{by} = \frac{\rho_T g n^2}{h^{1/3}} v\sqrt{u^2 + v^2} \tag{5.17}$$

where n is Manning roughness coefficient, and ρ_T in this case is equal to ρ; the density of plain water.

There is a generalized theory for the flow characteristics of all types of inertial debris flows; stony debris flow, turbulent muddy debris flow ($h/d_L > 30$) and hybrid debris flow ($30 > h/d_L > 20$) (Takahashi 2007) and that theory gives the particular resistance formulae to turbulent muddy debris flow, but herein for the sake of simplicity, for turbulent muddy flow, we use the resistance formulae same as those for bed load transport; (5.16) and (5.17). The ρ_T in this case is, however, the apparent density of the mixture of solids and fluid. If h/d_L is very large, say, h/d_L >500~1000, n has a nearly equal value to that for plain water flow, but if h/d_L is small (but larger than 30), it is far larger than that for plain water flow.

For the case of viscous debris flow, Newtonian fluid model is well applicable (Takahashi 2007) and the resistance law can be described as following:

$$\tau_{bx} = \frac{9\mu_a^2}{\rho_T g h^3 \sin\theta_{bx}} u\sqrt{u^2 + v^2} \tag{5.18}$$

$$\tau_{by} = \frac{9\mu_a^2}{\rho_T g h^3 \sin\theta_{by}} v\sqrt{u^2 + v^2} \tag{5.19}$$

where μ_a is the apparent viscosity of the mixture of solids and fluid.

5.4.3 Erosion and Deposition Velocities

The bed is assumed to be eroded by the dynamic action of the shear stress operating on the surface of bed assigned by the interstitial fluid of the overlying sediment-laden flow. This erosion process continues as long as the entrained-solids concentration in the flow is less than the equilibrium value. This conjecture leads to the empirical equation

$$i = K(\tau_{*f} - \tau_{*fc})\sqrt{\tau_f/\rho_m} \tag{5.20}$$

where K is a numerical constant (0.06 was found appropriate in a laboratory experiment for stony debris flow using non-cohesive material); τ_f is the shear stress on the bed produced by the interstitial fluid of the overlying sediment-laden flow; $\tau_{*f}\{=\tau_f/(\sigma\text{-}\rho_m)gd_L\}$ and τ_{*fc} are the non-dimensional shear stress and non-dimensional critical shear stress, respectively; and ρ_m is the density of interstitial fluid that contains fine particles. If τ_{*f} is smaller than τ_{*fc}, particles on the bed cannot be entrained into flow. The shear stress τ_f would be equal to the difference between the operating shear stress and the shear resistance on the bed, so that it is given as:

$$\begin{aligned}\tau_f = \{(\sigma - \rho_m)C_L + \rho_m\}gh\sin\theta \\ -(\sigma - \rho_m)ghC_L\cos\theta\tan\phi\end{aligned} \tag{5.21}$$

This equation means if C_L attains full growth as:

$$C_L = C_{L\infty} = \frac{\rho_m \tan\theta}{(\sigma - \rho_m)(\tan\phi - \tan\theta)} \tag{5.22}$$

τ_f becomes zero and particles can no longer be entrained. Substitution of Eq. (5.21) into Eq. (5.20) gives:

$$\begin{aligned}\frac{i}{\sqrt{gh}} = K\sin^{3/2}\theta\left\{1 - \frac{\sigma - \rho_m}{\rho_m}C_L\left(\frac{\tan\phi}{\tan\theta - 1}\right)\right\}^{1/2} \\ \times\left(\frac{\tan\phi}{\tan\theta - 1}\right)(C_{L\infty} - C_L)\frac{h}{d_L}\end{aligned} \tag{5.23}$$

Note that on the bed steeper than θ_2, the value of $C_{L\infty}$ obtained from Eq. (5.22) exceeds C_* and it even surpasses the maximum possible compaction value. But, experimental data reveal the maximum concentration attained by the erosion of bed is around $0.9C_*$, and the cross-sectional mean velocity can rather well be explained by the dilatant flow model even if the quasi-static flow model may seem appropriate. Therefore, on the bed steeper than θ_2, $C_{L\infty}$ and C_L in Eq. (5.23) must be replaced by $0.9C_*$ and consequently $i = 0$.

On the bed flatter than θ_1, even if the flow is fully developed, it is utmost immature debris flow, and in such a case $C_{L\infty}$ in Eq. (5.23) must be replaced by the equilibrium concentration for immature debris flow; $C_{s\infty}$, which is:

$$C_{s\infty} = 6.7C_{\infty}^2 \tag{5.24}$$

This equation is applicable only when $C_{s\infty}$ has a value less than $C_{L\infty}$ calculated by Eq. (5.22) (Takahashi 1991).

Equation (5.23) was derived under the assumption that the bed is not saturated with water. When the bed is saturated, the dynamic shear stress produced by the sediment-laden flow on the bed is transmitted deep into the bed, and an imbalance between the operating shear stress and resisting stress is produced within the bed. Thus, the surface layer of the bed becomes unstable due to excess operating stress and is easily entrained into flow. Thus, the erosion velocity in the saturated bed condition should be larger than in the unsaturated bed condition in which erosion takes place only on the surface in a manner like peeling off the surface cover. The erosion velocity equation under saturated bed condition was previously obtained (Takahashi 1991). However, it is rather difficult to know beforehand whether the bed is saturated or not. Therefore, if a modification of the K value in Eq. (5.23) is a good approximation, it would be convenient because Eq. (5.23) becomes only one necessary equation for bed erosion. Examination of previous experimental data reveals if $K = 2.3$ is used instead of 0.06, Eq. (5.23) becomes a good approximation of erosion velocity on saturated bed (Takahashi 2006). Moreover, it is pointed out that the actual gully bed rarely saturated up to the surface (Suwa and Sawada 1994). If coarse particles are surrounded by a matrix of cohesive fine material, K value would become smaller than non-cohesive case.

When the sediment-laden flow on the bed is turbulent muddy flow and small particles comprise the bed, the erosion velocity will be, similar to the case of stony debris flow, a function of the difference between the equilibrium concentration and the actual solids concentration in flow. But, the rate of particle entrainment would become large if upward turbulent velocity of fluid greatly exceeds the settling velocity of particles. Therefore, the erosion velocity is anticipated having the following form:

$$i = K_t \frac{C_{eq} - C}{C_*} |u_* - w_s| \tag{5.25}$$

where K_t is a numerical coefficient, C_{eq} is the equilibrium solids concentration, u_* is the shear velocity $(= \sqrt{gh \sin \theta})$, w_s is the settling velocity of particles. In the case of turbulent muddy debris flow, no separation into coarse and fine particle fraction is considered, and the equilibrium concentration is given theoretically, that is denser than that for stony debris flow (Takahashi 2007). The applicability of Eq. (5.25) and the appropriate value of K_t are not yet examined.

In the case of viscous debris flow, because flow is laminar, the entrainment of particles on the surface of bed, otherwise it is the fresh and very soft deposit of preceded debris flow surges, would be difficult. The viscous debris flow surges would possibly be produced by the initiation of motion of the soaked cohesive earth lumps or by the falling of soil mass from side banks onto debris flow, thereby, the debris flow surge should be full freighting once produced and it flows without bed erosion only to be deposited at the flattening area. Therefore, except for the erosion of fresh debris flow deposit, the consideration on erosion velocity formula would not be practical. According to the observation in the Jiangjia gully, China, the newly deposited bed produced by the preceding surge seems to be entirely reactivated and thoroughly removed and entrained with the arrival of a new surge. The equilibrium solids concentration in viscous debris flow can be obtained by the concept of laminar dispersion (Takahashi et al. 2000), in which heavy particles are dispersed in flow by the effects of squeezing flow within interstitial fluid.

Figure 5.5 puts together the equilibrium particle concentrations versus slope in stony, stony immature, turbulent muddy, and viscous type debris flows as well as sediment concentration in bed load transport.

Provided a steady unidirectional debris flow is flowing with neither erosion nor deposition, the flow is in equilibrium state. In such a case, writing the bed slope as θ_e, the bed shear stress is given from Eq. (5.6):

$$\tau_b = \rho_T g h \sin \theta_e \tag{5.26}$$

If the flow is stony type, from Eq. (5.12), the equilibrium mean velocity is given as:

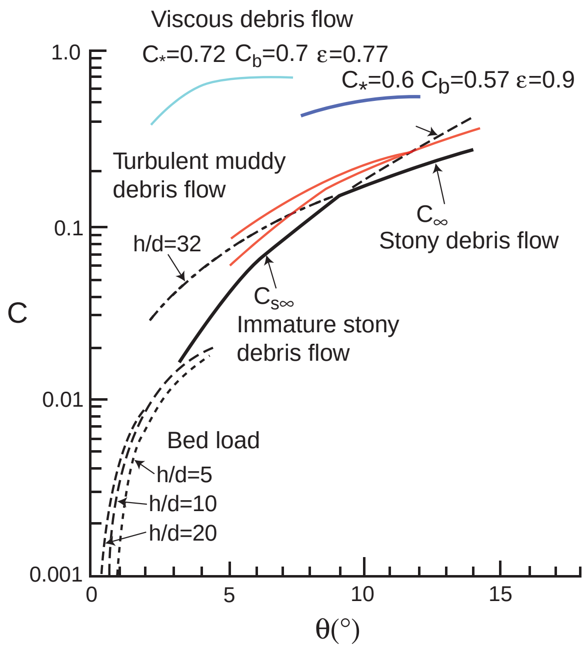

Fig. 5.5 Equilibrium particle concentrations versus slopes in the various kinds of debris flow

$$u_e = \frac{1}{d_L}\left(\frac{8\,g\rho_T \sin\theta_e}{\sigma}\right)^{1/2}\left\{\left(\frac{C_{*L}}{C_L}\right)^{1/3} - 1\right\}h^{3/2} \quad (5.27)$$

The equilibrium bed slope is given from Eq. (5.22) as:

$$\tan\theta_e = \frac{C_L(\sigma-\rho_m)\tan\phi}{C_L(\sigma-\rho_m)+\rho_m} \quad (5.28)$$

The discussion here means that the debris flow of depth h can disperse particles with the mean concentration of C_L if the mean velocity is larger than u_e. This, in turn, means that when a debris flow freighting particles with the concentration of C_L comes out to the downstream channel whose slope is flatter than θ_e, the debris flow will be deposited on the downstream channel. In fact, the debris flow will have some more inertial motion after it approaches the critical velocity to deposit and the deposition will begin after the velocity becomes $p_i u_e$ in which p_i is a coefficient less than 1.0.

The amount of excess coarse particles at a position in the flat channel reach is $h(C_L – C_{L\infty})$ per unit area. Describing the time necessary to deposit that amount as $(d_L/u)\delta_d$, the depositing velocity is given by:

$$i = \delta_d\left(1 - \frac{u}{p_i u_e}\right)\frac{C_{L\infty} - C_L}{C_{*DL}}\frac{q}{d_L} \quad (5.29)$$

Alternatively, if we describe the time necessary to deposit by $(h/u)\delta_d$, the term q/d_L in Eq. (5.29) changes to u. The value of δ_d in this case is, of course, different from that in the former case.

The two dimensional version of Eq. (5.29) is given by

$$i = \delta_d\left(1 - \frac{\sqrt{u^2+v^2}}{p_i u_e}\right)\frac{C_{L\infty} - C_L}{C_{*DL}}\frac{\sqrt{q_x^2+q_y^2}}{d_L} \quad (5.30)$$

Similarly, in the case of turbulent muddy debris flow, the depositing velocity would be proportional to the difference in concentrations between the equilibrium one at the referring position and the one in the coming out debris flow. But, herein, we consider the case where the debris flow comes out to a nearly horizontal place where almost all the particles contained in the debris flow become the excess constituents. Then, the particle deposition would be due to the gravitational particle settling, and if the dynamic effect of flow is ignored, the sediment volume that settles down onto the bed in a unit time would be described as Cw_s. Therefore, the parameter that determines the depositing velocity would be Cw_s/C_*. As long as the coming out debris flow still has sufficient velocity to be able to carry sediment with the concentration C, deposition will not occur. Hence, if we write the critical velocity of debris flow to commence deposition as u_c, by analogy to the stony debris flow case, the depositing velocity would be described as follows:

$$i = \begin{cases} -\left\{1 - \left(\frac{u}{u_c}\right)^m\right\}\frac{C}{C_*}w_s & ;\ u_* < u_{*c} \\ 0 & ;\ u_* \geq u_{*c} \end{cases}. \quad (5.31)$$

where u_{*c} is the shear velocity corresponding to u_c, and u_* and u_c can be obtained by the energy balance between energy production and dissipation (Takahashi 2007).

Although viscous debris flow can transport highly concentrated sediment, the flow that is fully developed on a very steep channel upstream must be overloaded when it comes down to a flatter reach, where the shearing velocity becomes too small to disperse coarse particles and the coarse particles unified with the interstitial fluid will stop. The volume change of material before and just after stoppage is negligibly small.

Writing the equilibrium coarse particle concentration for the depth h in the reach under consideration as C_e, and assuming a uniform solids concentration throughout the entire depth, the excess load per unit area that cannot be sustained by the particle dispersive pressure would be about $(\sigma - \rho_T)\,(C - C_e)\,gh\cos\theta$. This pressure causes the Coulomb friction force on the bed. This force contributes to decelerate the debris flow and to make gradual deposition from the lower to the upper layers in flow. If the depositing volume originally has the velocity $\alpha_p u\,(\alpha_p < 1)$ and it linearly approaches zero in the depositing process, the momentum conservation equation is given by

$$2\alpha_p u \rho_T \cdot i = (\sigma - \rho_T)(C - C_e)gh\cos\theta\tan\phi \quad (5.32)$$

The Newtonian fluid model for viscous debris flow gives the mean flow velocity as:

$$u = \frac{\rho_T g h^2 \sin\theta}{3\mu_a} \quad (5.33)$$

Substituting Eq. (5.33) into Eq. (5.32), we obtain

$$i = \frac{3\mu_a(\sigma - \rho_T)(C - C_e)\tan\phi}{2\alpha_p h \rho_T^2 \tan\theta} \quad (5.34)$$

The deposit thus formed by the stoppage of a viscous debris flow surge will again be activated and mixed up with the following surge, and the deposition and erosion processes are repeated.

5.4.4 Boundary Conditions

The upstream boundary condition for the debris flow routing along river channel can be given as a flood discharge hydrograph obtained after the application of a suitable flood runoff analysis if no landslide occurs.

The shallow landslide that often occurs synchronously with the severest rainfall intensity tends to contain sufficient water to be able to immediately transform into a debris flow. In such a case, a debris flow discharge hydrograph with given C_L, C_F and d_L values would be estimated via a deliberate consideration on the geological and the topographical conditions of the hollow at the upstream end of the basin that would produce landslide. Alternatively, the whole volume of landslide may instantly be melted down to a debris flow material and released from the original slope all at once.

Some large scale landslides do not melt down at once and gradually transform into debris flow while they are moving in the river channel. This process can also be analyzed (Takahashi 2007) but this is beyond the scope of this paper.

The debris flow hydrograph and its characteristics obtained after routing along the river channel becomes the upstream boundary conditions for the calculation of two-dimensional flooding process.

5.4.5 Application to the Horadani Debris Flow

A debris flow occurred in the basin of a small mountain ravine named Horadani in Tochio, Gifu Prefecture, Japan at about 7:50 a.m. on 22 August 1979. The topography of the basin of the Horadani Ravine is shown in Fig. 5.6. The altitude at the outlet is 800 m and that at the highest point is 2,185 m, the vertical drop of 1,400 m is connected by a very steep stem channel of 2,675 m long. The basin area is 2.3 km^2. The outlet of the ravine forms a debris flow fan of 500 m wide and its longitudinal gradient is about 9.5° on which Tochio is located. The upstream end of the channel works that penetrated Tochio was at the fan top, and upstream of the fan top it formed a wide torrent of 6–12° in longitudinal gradient for about 500 m long within which 11 check dams had been constructed and they were destroyed and washed away by the debris flow.

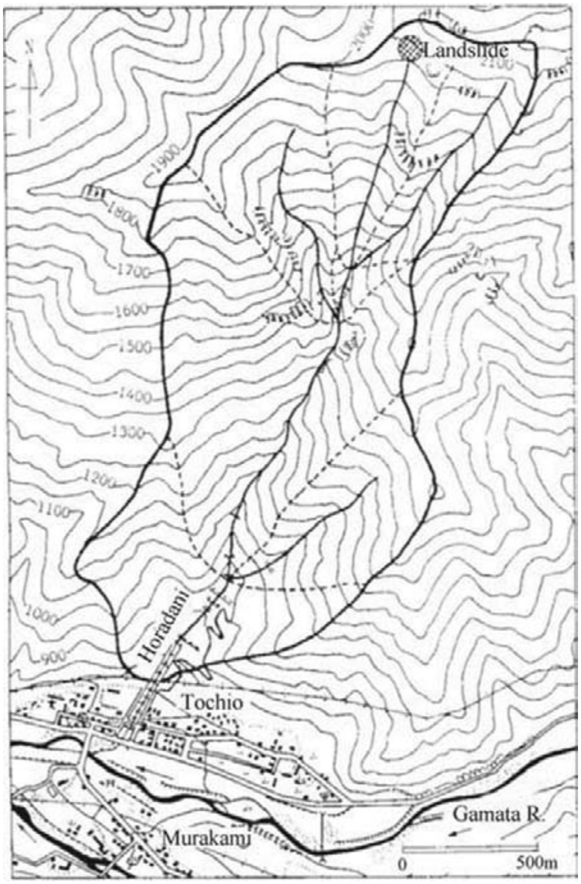

Fig. 5.6 Horadani basin in Tochio

The water supply discharge along the stem channel was calculated using the known “tank model”. The debris flow was triggered by a shallow landslide at the upstream end of the basin and it seemed to be transformed into debris flow before plunging into the channel bed. Therefore, as the boundary condition at the upstream end of the stem channel a debris flow of q_t = 40 m^2/s per unit width was supplied onto the channel bed for ten seconds from 7:50 a.m., in which $C_L = 0.5$ and $C_F = 0$ were assumed.

The one-dimensional debris flow routing along the channel was conducted under the conditions: d_L = 10 cm, $C_* = 0.65$, $C_{*F} = 0.2$, $C_{*L} = C_{*DL} = 0.56$, $\tan\phi = 0.75$, σ = 2.65 g/cm^3, $K = 0.05$, $\delta_e = 0.0007$, $\delta_d = 0.1$, $p_i = 0.33$, the width of channel is uniform 10 m and the thickness of deposit on the channel bed D = 4 m. The degree of saturation of the bed material is assumed to be 0.8 in the channel reach steeper than 21° and 1.0 in the reach flatter than 21°. In the reach of 500 m immediately upstream of the fan top in which check dams were installed the bed erosion is neglected (Takahashi and Nakagawa 1991).

The debris flow hydrograph at the fan top obtained by the routing of debris flow was used as the boundary condition for the calculation of the flooding and deposition in the fan area. Figure 5.7 shows the aerial photograph of the debris flow and the time-varying distributions of the surface stages (deposit thicknesses plus flow depths) on the fan. At ten minutes after the onset of the landslide (8:00 a.m.) the debris flow is just commencing to overflow from the channel works at the bend. At 8:05 a.m., the peak discharge has just passed through the channel and plenty of sediment has deposited around the channel bend from where sediment flooded mainly towards the left-hand side bank area. At 8:10 a.m., the deposition in the channel works develops further and the increase in the deposit thickness in the left-hand side bank area is evident. The deposition also proceeds in the right-hand side bank area especially along the roads which incline downward from the bank. By about 8:15 a.m. the debris flow discharge has decreased considerably and the enlargement of the debris flow deposition area has almost ceased. In general, the distributions of the calculated deposit thicknesses and the range of deposition correspond rather well to the actual situation. Therefore, we can conclude that this reproduction by the calculation is satisfactory. It is remarkable that the total substantial volume of deposit on the fan is about 50,000 m^3, whereas the total substantial volume of sediment supplied at the upstream end of the channel is only 2,000 m^3; the majority of sediment is produced by the erosion of channel bed in the upstream region. This result is proved by the field exploration. This fact implies that the estimation of the supplied debris flow volume or the volume of landslide may not have significant effects on the debris flow volume that runoff to the fan area if the erosion process in the upstream channel is important. To examine this conjecture, the debris flow discharge supplied at the upstream end was changed to 80 m^2/s; i.e. twice the former case, but the hydrograph of the debris flow at fan top was similar to the former case.

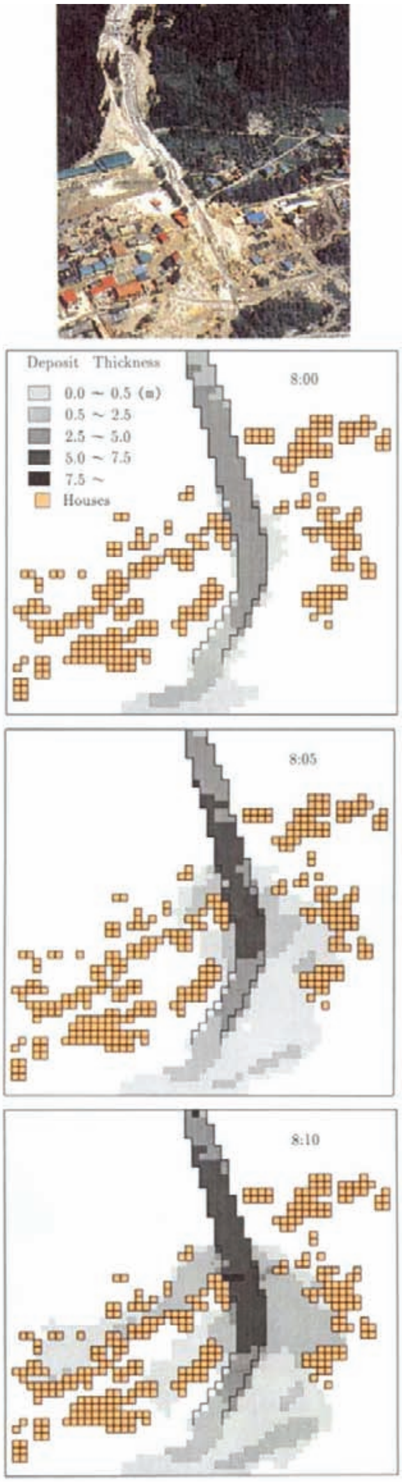

Fig. 5.7 Aerial photo of Tochio fan, and the calculated time-varying distributions of sediment deposit thicknesses

5.5 Debris Flow Control by a Grid-Type Dam

The low concrete-wall type check dam (closed-type sabo dam) has been a popular debris flow checking structure. But, it is easily filled up by sediment that is runoff by normal floods, and when a debris flow comes down, it often fails to check or control them; i.e. the closed-type sabo dam has a defect in the sustainability of its function. Furthermore, the stoppage of the sediment transport in the normal flood period by the closed-type sabo dam that is not yet filled up is said to be harmful to the ecosystem downstream due to the stabilization of the stream channels. Recent discussions of such defects have attached importance to the methods that can check the hazardous sediment but continually supply the safe and necessary sediment downstream. Sabo dams that have such functions are known as open-type sabo dams. These have large openings in the dam body through which the sediment runoff from the normal flood flow passes but when a debris flow occurs it works like a not yet filled up closed-type sabo dam.

There are two kinds of open-type sabo dam. One kind is the slit dam, or large conduit dam, which has large openings in the dam body, but the ratio of the total width of openings to the dam width is small so as to guarantee that the backwater effects are generated when a debris flow or large flood flow occur. Sediment is trapped behind (upstream) the dam due to large reduction in the flow velocity, so that this type dams may be suitable to check the turbulent muddy-type or the viscous-type debris flows because they are generally comprised of comparatively fine material. Another type is the grid-type sabo dam, where the individual open space between the pillars is normally less that the width of the opening of the slit dam but the ratio of the total open space to the dam width is large and virtually no backwater effect occurs even in the case of debris flow. For this type of dam, the sediment is checked by the clogging of the openings by the pinching stones. Therefore, this type dam is suitable to check the stony-type debris flow where the bore front is comprised of large boulders. Figure 5.8 shows this kind of dam installed in the Shiramizu-dani ravine that originates from the Yakedake volcano, and the lower photo shows from downstream

Fig. 5.8 An example of a grid-type sabo dam, and the clogging situation at front-row of the dam

the pinching stones that clog the space between the steel pipes.

The empirical design criterion for the suitable spacing between pipes is:

$$\left.\begin{aligned} l_s/d_{\max} &= 1.5 \sim 2.0 \\ l_s/d_b &> 2.0 \end{aligned}\right\} \quad (5.35)$$

where l_s is the spacing between the pipes; $d_{\max}$ is the diameter of the maximum size class particles accumulation in the front of the debris flow; and d_b is the diameter of the maximum size class particles transported as bed load by a normal scale flood flow.

5.5.1 Blocking Probability of Grid-Type Dam

According to the experiments, there are two types in the blocking processes of grid. One is due to the simultaneous arrival of two or more particles, and the other is due to the arrival of particles while the previously arrived one is rotationally moving around and touching with a column. The rotational motion of a particle around a column acts to narrow the free space between that particle and the other adjacent column and some occasions, depending on the position and number of rotating particles, the free space becomes too narrow to pass another particle that arrives a little later than the rotating ones. Thus, these already rotating and newly arrived particles make an arch bridge between the two adjacent columns to block the space. This explanation clearly shows the clogging proceeds stochastically.

If a particle collides with a column at an angle of θ_1 and begins the rotation around the column with an angular velocity of ω, the virtual diameter of the column D_c' at time t_1 after the collision is given by:

$$D'_c = (D_c + d)\sin(\theta_1 + \omega t_1) + d \quad (5.36)$$

where D_c is the diameter of the column and d is the particle diameter. The angular velocity is given by a modification of the angular momentum conservation equation as following (Takahashi et al. 2002):

$$\omega = 1.278(u_p/d)\sin\theta + 0.094 \quad (5.37)$$

where u_p is the velocity of particle just before the collision with the column.

Consider that i pieces of particles come down to the grid plane during the period T_L by random time intervals t_i at random lateral positions y_i. The velocity of the particle and their concentration are constants. When a particle collides with the column or with other particles rotating around the column, the new virtual column diameter D_c' is calculated, and then by comparing the length l_s and D_c'/2, we judge whether the space between two adjacent columns is clogged or not. Namely, i trials are done within the period T_L, and for each trial whether the spaces between columns are clogged is checked. Thus, we can obtain the clogging probability F_{cp} in the period T_L.

We need, however, in the computer simulation of debris flow blockage, the instantaneous blocking probability in a small time interval of Δt. If this probability; P_r, is assumed constant under constant u_p and C, the relationship between P_r and F_{cp} is given by:

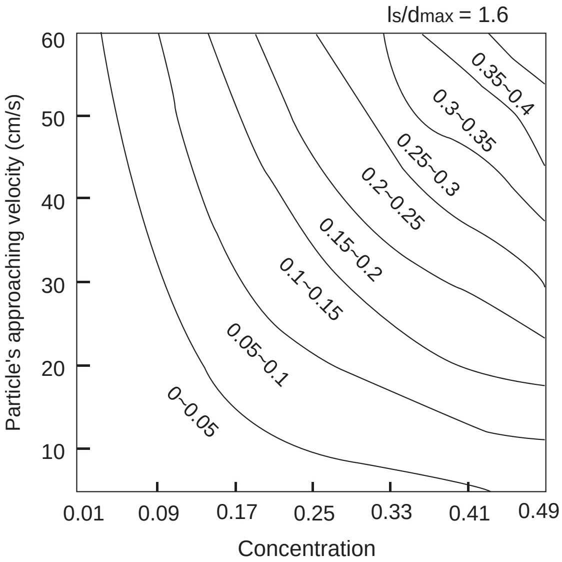

Fig. 5.9 Calculated instantaneous blocking probabilities

$$P_r = 1 - (1 - F_{cp})^{1/n} \tag{5.38}$$

where $n = T_L/\Delta t$

The calculated results of the instantaneous blocking probability P_r under the conditions $l_s/d_{\max} = 1.6$ is shown in Fig. 5.9. This figure evidently shows that P_r depends on both the particle concentration and the approaching velocity of particles. The similar calculations under different $l_s/d_{\max}$ values reveal that the larger the value of $l_s/d_{\max}$, the smaller the blocking probability becomes.

5.5.2 Numerical Simulation of Debris Flow Control by a Grid-Type Dam

We consider the case in which debris flow is generated by the occurrence of surface water flow or by the supply of an already liquefied surface landslide mass, and it bulks up downstream by the erosion of a steeply deposited debris bed in a gully. The assessment of the performance of the grid dam necessitates the integration of the debris flow routing model with the grid clogging model and the model of rebounding deposition behind the dam. Because the grid-type dam is installed expecting the blockage of grid by the arch action between the large boulders accumulating at the forefront of debris flow, the debris flow routing model must be the one that can predict the particle segregation processes during flowing down the channel.

Herein, Takahashi and other's debris flow routing method that considers the focusing of large particles toward the forefront is used. In this method, a single finite step in the numerical calculation is divided into two stages: In the first stage, similar to the example of application for the Horadani debris flow, a sediment bed composed of a well-graded mixture is eroded by surface water flow, thereby a debris flow is generated. In the second stage, larger particles in the debris flow move upward because of dispersive force produced by the collision of particles and are then transported forward faster than smaller particles, which remain in the lower part of the flow because the velocity is slower in the lower layer. The detailed explanation of the method can be found in Takahashi et al. (1992).

The debris flow depositing process behind a grid dam can be predicted by the application of the mentioned clogging probability. However, that clogging model did not consider the effect of the horizontal bar that would become crucial if the clearance between a horizontal bar and the surface of deposit just upstream of the dam becomes less than one particle diameter of the maximum size. To take this effect into account, when the clearance becomes smaller than the maximum diameter of debris flow material, this clearance value is considered as the effective grid spacing alternative to the previous effective spacing obtained by considering only the vertical posts. Thus, if the spacing is judged to be clogged in a time step, the bed level just upstream of the dam is raised with the height equal to the diameter of the largest particle and the riverbed variation upstream of the dam that is affected by the raised downstream bed height is then calculated.

The numerical simulations to reproduce the phenomena that appeared in the experiments are carried out (Takahashi et al. 2002). The experiments used a tilting flume 5 m long, 10 cm wide and 20 cm deep with a slope of 18°. The water saturated experimental material was laid in a stretch 1.5 m long and 10 cm deep within the upstream reach. The maximum and mean diameters of the material are 1 cm and 0.24 cm, respectively. At the downstream end of the flume a prescribed kind of open-type sabo dam was set. Then, a debris flow was generated by supplying water at a rate of 300 cm^3/s for 15 s. A part of the generated debris flow was checked by the dam but a rest flowed out the flume. The effective width of spacing between grids of dam was 1.6 cm.

The calculation was accomplished by setting $\Delta t = 0.02$ s and $\Delta x = 10$ cm. The particle sizes were classified into five groups, and in each time step the segregation of the particles were calculated together with the debris flow characteristics such as discharge, velocity, depth, and particle concentration, particularly the concentration of the largest class particles at the forefront. Then, the velocity and the concentration of the maximum diameter class particles were substituted into the clogging probability model and the instantaneous blocking probability was obtained under the condition $n = 1000$ and $\Delta t = 0.02$ s. If this probability was larger than an independently generated random number between 0 and 1, the grid was considered to be blocked. If the grid was judged blocked, the bed level just upstream of the dam was raised with the height equal to the diameter of the largest particle, and the riverbed variation upstream of the dam was calculated under the new bed level as the downstream boundary condition.

Figure 5.10 compares the longitudinal riverbed level changes at 3.8, 9.8 and 15.8 s after the first

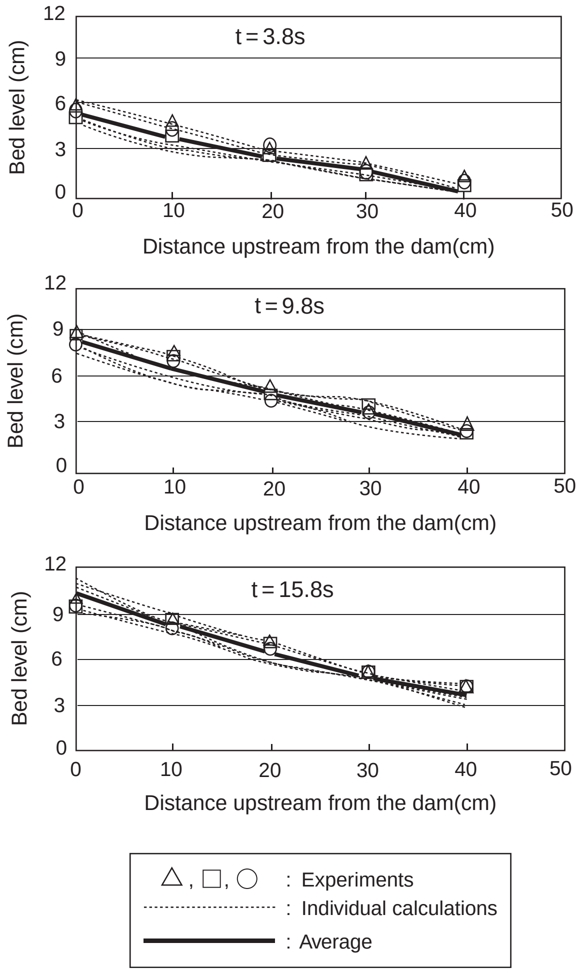

Fig. 5.10 Experimental and calculated bed levels behind the dam at different times

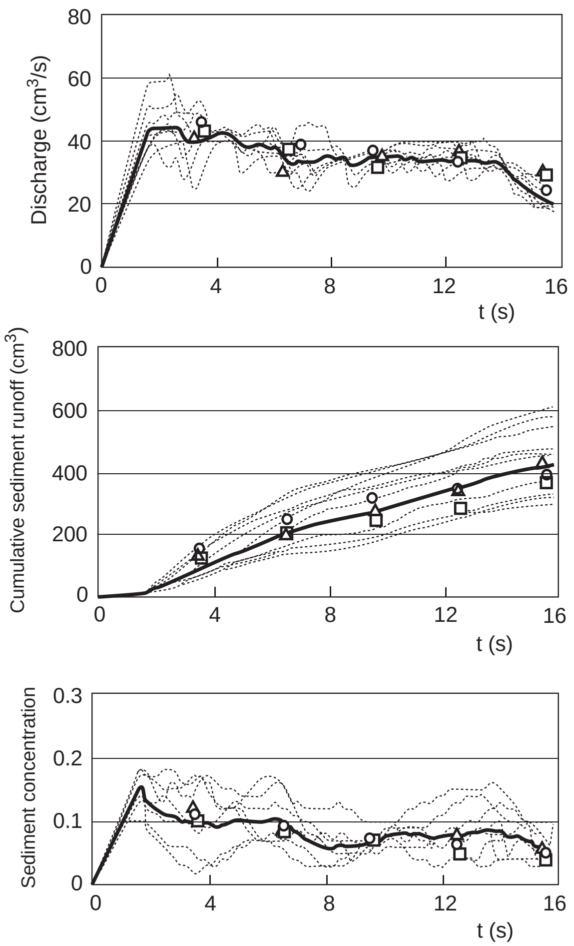

Fig. 5.11 Calculated and experimental hydrographs, cumulative sediment runoff and sediment concentrations just downstream of the dam

clogging of the dam. Because the value of the random number that gives the standard to judge whether the dam is clogged changes depending on the initially selected random number, the calculation was repeated ten times for each experimental case. The dotted line shows the respective ten results and the thick line is the average of these respective calculations. As is clear in the figure, the calculated results coincide well with the experiments.

Figure 5.11 compares the calculated debris flow hydrographs, cumulative sediment runoff volumes, and particle concentrations with the measured ones at the downstream end of the flume.

From the results shown in Figs. 5.10 and 5.11 it can be seen that blocking phenomena of a grid-type dam and its effects downstream can be well reproduced by the numerical simulations introduced herein.

5.5.3 Determination of the Optimum Grid Spacing of a Grid-Type Sabo Dam

Consider that a grid-type sabo dam will be constructed at the position indicated in Fig. 5.12. The dam will check debris flow if l_s/d_{max} is less than 1.5–2.0, the smaller that value the more surely the dam will check the debris flow. But, if the value of l_s/d_{max} is too small, then the dam framework will have more members than it needs, and this is a waste of money and materials. Moreover, the short spacing will check the large particles and drifting woods that runoff in a normal scale flood flow, which results in the consumption of storing capacity for the coming debris flow. If, on the other hand, the largest size particles that rarely exist in the basin are chosen to determine d_{max}, the concentration of these particles in the forefront of debris flow will be too small to clog the spacing and the debris flow containing large boulders, even though the size is less than predetermined d_{max}, may pass through the dam. Consequently, the difference in debris flow control efficiencies by setting d_{90} and d_{95} as d_{max} is experimented by the numerical simulations and from that we obtain a criterion to determine d_{max} in the design of a grid dam. Herein, d_{90} and d_{95} mean 90% and 95% of the particles are finer than the indicated values, respectively.

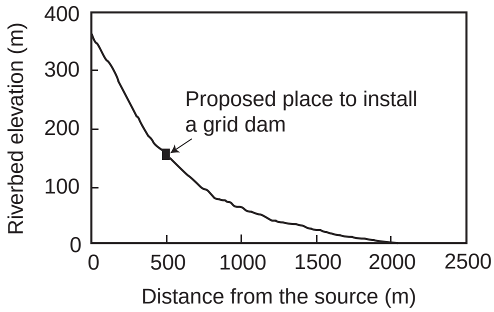

Fig. 5.12 The longitudinal profile of the river and the position at which a grid dam will be installed

We assume that the riverbed material has the size distributions as shown in Fig. 5.13. Particle size is classified into fifteen groups, the maximum size is 4 m and the minimum size is 100 μm. Only one particle size group is considered to be the fine fraction, i.e. 100 μm, and the existence ratio of the maximum size particles and the minimum size particles are 2% and 10%, respectively. The value of d_{90} is 0.5 m and the value of d_{95} is 1 m. The riverbed comprised of this material is assumed to be 5 m thick, however, in the reach having a steeper slope than the angle of repose of the material the bedrock is considered to crop out and no deposit exists. In the calculation, both l_s/d_{90} and l_s/d_{95} are set at 1.6; for Case 3 l_s is 0.8 m and for Case 2 l_s is 1.6 m.

The development of debris flow and the size segregation within flow along the river channel are calculated by the mentioned method, and for the sake of simplicity, water is supplied only from the upstream end by the hydrograph shown in Fig. 5.14. The river width upstream of the dam site is 10 m and that downstream of the dam site is 20 m, and the dam width is 8 m.

Figure 5.15 shows the debris flow hydrographs and sediment discharge graphs just downstream of

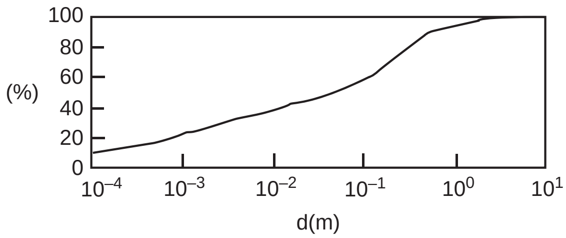

Fig. 5.13 Particle size distributions in the riverbed

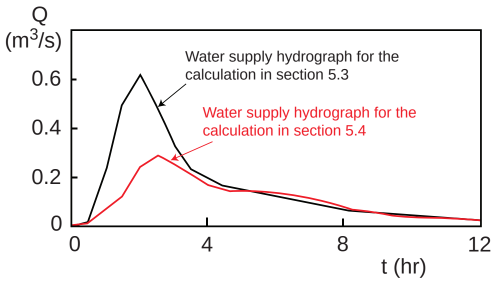

Fig. 5.14 Hydrographs supplied from the upstream end of the river channel

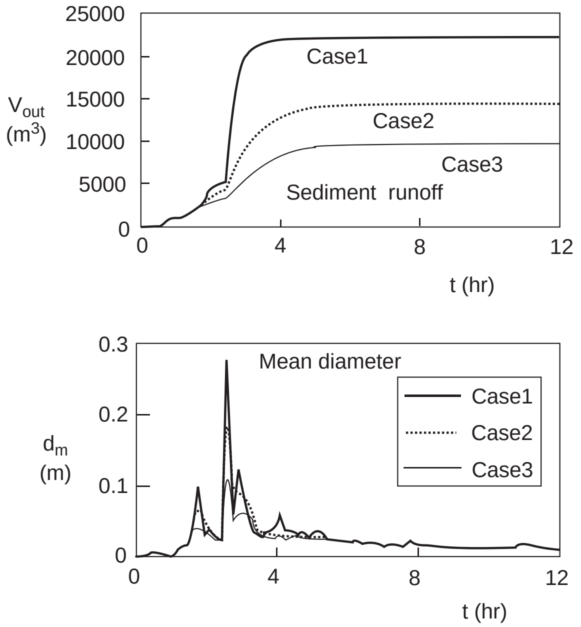

Fig. 5.16 Cumulative sediment runoffs and mean diameters just downstream of the dam site

the dam site in the cases of no dam (Case 1) and in Cases 2 and 3. When a grid dam is installed, either of Case 2 or Case 3, the peak discharge is cut to less than a half and the peak arising time delays. In the sediment discharge graphs, there remains a peak in Case 2 but no evident peak exists in Case 3. From these results, it can be seen that choosing the spacing corresponding to d_{90}; i.e. $l_s = 0.8$ m, will stop the peak sediment discharge.

Figure 5.16 shows the cumulative sediment runoffs and the mean diameters of runoff sediment just downstream of the dam site. In Case 2, 35% of the runoff sediment to the dam site was captured by the dam, whereas in Case 3, 60% was captured. In Case 3, because many large boulders were captured, the mean particle size that passed through the dam was smaller than that in Case 2.

These results clearly shows that if the position of a possible installation of a grid dam is decided beforehand, numerical simulations can give the optimum spacing between frames.

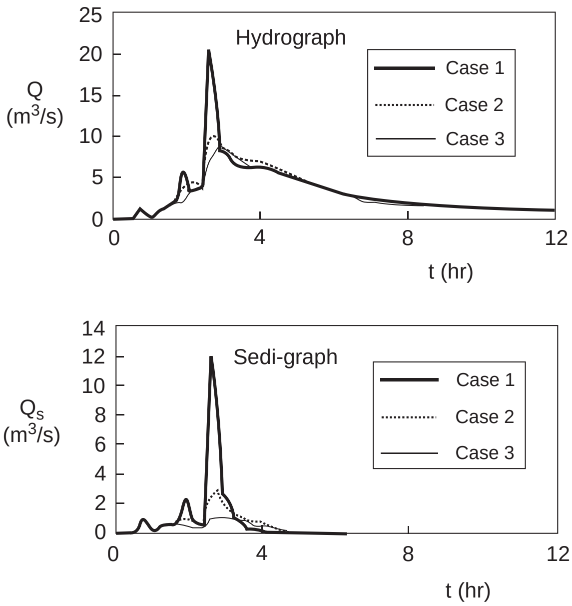

Fig. 5.15 Debris flow discharges and sediment discharges just downstream of the dam site

5.5.4 Determination of the Optimal Position to Install a Grid-Type Dam

Consider that the river channel has the longitudinal profile as shown in Fig. 5.17. The riverbed material is assumed to be the same as before and the spacing between the frames in this time is predetermined. Namely, the spacing is set to 0.8 m that is obtained as the optimum corresponding to d_{90}. The supplied water from the upstream end will entrain the riverbed sediment and a debris flow develops along the channel. Because the degree of convergence of large stones toward the forefront and the peak sediment discharge depend on the distance of travel, the efficiency of the dam to control debris flow will depend on its location.

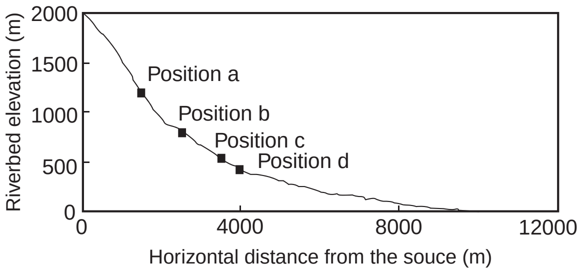

Fig. 5.17 Longitudinal profile of the river channel and the possible dam sites

The candidate sites for the installation of a grid dam are set at a, b, c, and d whose distances from the source are 1,500 m, 2,500 m, 3,500 m and 4,000 m, respectively. A preparative calculation which predicts the situations of debris flow at the respective positions is carried out. Figure 5.18 shows the results of the calculation in which the peak sediment discharges become larger toward the downstream direction, but at the positions c and d the peak values are almost the same. Namely, the debris flow has fully developed upstream of position c.

Hence, the numerical simulations for the case of no dam (Case 1), the cases of installation at positions c (Case 2), b (Case 3) and a (Case 4) are carried out and the dam functions in the respective cases are compared. The water discharge hydrograph supplied at the upstream end is shown in Fig. 5.14. The bed material is assumed to be laid 5 m thick. The river width is set to 10 m from the source to location d and that downstream is 20 m.

Figure 5.19 shows the hydrographs and sediment discharge graphs immediately downstream of position d in the respective cases. In comparison with the case without a dam (Case 1), the peak rate is reduced by a large amount. Case 2 has the biggest

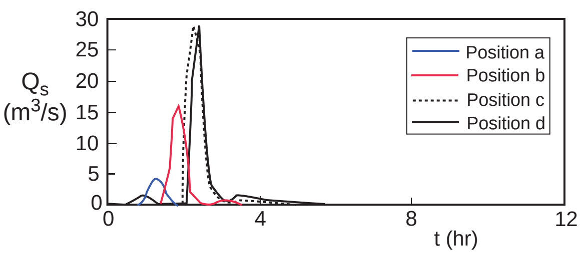

Fig. 5.18 Sediment discharge graphs at respective positions under the condition of no dam installation

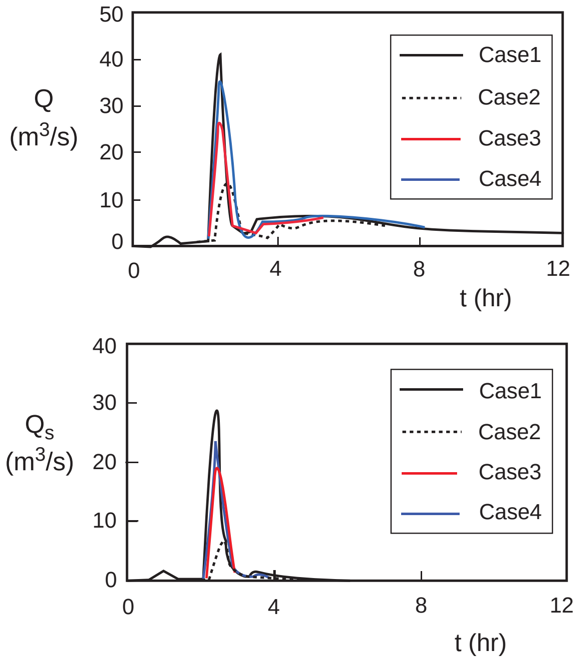

Fig. 5.19 Hydrographs and sediment graphs at the position d in the respective cases

reduction, then Case 3 and Case 4. In Case 2 the peak discharge is reduced about 66%, but in Case 4 it is only reduced by 12%. A similar tendency is found for the sediment discharge. The reason for such a tendency is as follows: At position a, the debris flow is still not sufficiently developed and the degree of accumulation of large particles in the forefront is low. Therefore, the dam is not easily clogged and plenty of sediment associated with water is passed through the dam. The flow thus passed through the dam continues to develop to a debris flow containing large boulders in front down to position d. Hence, the hydrograph and sediment discharge graph at position d in Case 4 are not much different from those in Case 1. Whereas, if a grid dam is set at position c, the debris flow has developed before it reaches that position and it is easily checked by the dam. Once the forefront is checked the succeeding debris flow will be deposited by the rebounding deposition. Therefore, the debris flow and the sediment discharges are greatly reduced at position d.

Figure 5.20 shows the cumulative sediment runoff and the mean particle diameters in the flow immediately downstream of position d. The functions described earlier are clearly shown in these figures.

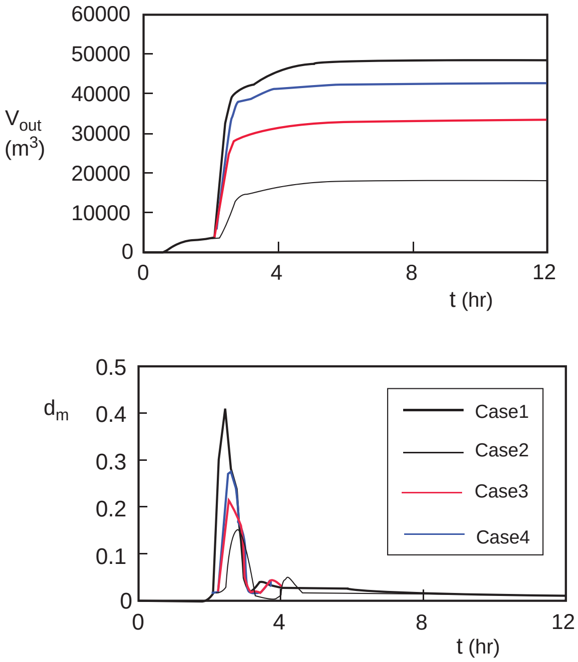

Fig. 5.20 Cumulative sediment runoffs and mean diameter of particles in flow immediately downstream of position d

The above numerical simulations reveal that the optimum position of grid dam installation is where debris flow attains its most developed stage. By the combination of these simulations for the selection of the optimum position and for the determination of the optimum spacing between frames, we can design the most efficient dam structure and the best place to install it.

5.6 Conclusions

In this paper, at first, Japanese statistics of casualties due to water related hazards and recent worldwide tendencies of major disasters were mentioned to commonly understand that the debris flow is one of the key factors in the disaster mitigation among other sediment hazards problems. Then, introducing and analyzing a flowchart of the processes of decision-making before the implementation of disaster mitigation plans, this paper emphasized that the mechanics-based approach is indispensable in almost all the aspects of debris flow disaster mitigation activities; i.e. assessment, understanding, prediction, control, and avoidance. As the typical examples of mechanics-based approach, the method to identify the debris flow prone ravines and the method to predict the time of debris flow initiation were discussed. Japanese authorized guidelines to identify the debris flow prone ravines, although they are simplified and take many empirical factors into considerations, adopted the results of mentioned mechanical considerations. Given the topographical and geotechnical conditions of the basin and the hyetograph of severe rainfall, the mentioned approach will be able to predict the onset of debris flow identifying the location in the basin and the time simultaneously.

The scale of debris flow that runoff from an arbitrary basin is predicted via the routing along the river channel by the application of fundamental system of mechanical equations: the momentum conservation equations, the mass conservation equations, the erosion and deposition velocity equations, and the equation for bed surface elevation change. The system of fundamental equations is the same for any type debris flows but the resistance to flow formulae, the erosion and deposition velocity formulae contained in the fundamental equations are different depending on the kinds of debris flows; the stony debris flow, the turbulent muddy type debris flow, and the viscous debris flow. The existence criteria of these kinds of debris flows, the resistance formulae, and the erosion and deposition formulae for the respective debris flows were given.

The debris flow developed or declined in the upstream river channel will runoff to the outlet of the ravine and flood over the residential area causing disasters. The two-dimensional flooding and depositing processes can also be analyzed by the same fundamental system of equations to the one-dimensional routing.

The Horadani debris flow was analyzed as an example of application of the mechanical method. The calculation revealed that if the bed material to be eroded and entrained into debris flow sufficiently exists, the erosion plays the major role to determine the magnitude of debris flow and the uncertainty in the estimation of debris flow triggering landslide volume does not affect much. The numerical simulation of debris flow flooding process using the proposed system of fundamental equations adequately reproduced the phenomena.

Thus, it is proved that the method is well applicable to delineate the hazardous area, and moreover, to assess the distributions of risks in an arbitrary basin under an arbitrary rainfall condition.

The performance of a grid-type sabo dam was taken up as a typical case in the design of the structural countermeasures in which the mechanics-based method becomes a strong means. The method to obtain the blocking probabilities of grid due to runoff debris flow was given. The debris flow routing along the river channel, in which particle segregations and the convergence of largest class stones toward the forefront are taken into account, was coupled with the grid blocking probabilities. This method made possible to assess the debris volume that is deposited behind the dam, the debris flow hydrograph, the sediment discharge graph, and the time varying mean diameters in flow that pass through the dam. How this method is effectively used was explained by taking the problems of the decision of grid spacing and the decision of the optimal location to install the dam as examples.

References

Bagnold RA. (1966). The shearing and dilatation of dry sand and 'singing' mechanism. Proc. Roy. Soc. London, A295: 219–232

Chigira M. (2007). Site characteristics of gigantic landslides. Kinmiraisha, Nagoya: 256p. (in Japanese)

Iverson RM and Denlinger RP. (2001). Flow of variably fluidized granular masses across three-dimensional terrain. J. Geophy. Res. 106 (B1): 537–552

Kuang S. (2003) Debris flow disasters and countermeasures in China, Symposium aiming to the mitigation of sediment hazards, Kyoto: 13p. (in Japanese)

Pudasaini SP, Wang Y and Hutter K. (2005). Modelling debris flows down general channels. Natural Haz. & Earth System Sciences, 5: 799–819

Suwa H and Sawada T. (1994). Comparison between the viscous debris flow and the stony one, Takahashi T (ed.), Japan-China Joint Research on the Prevention from Debris Flow Hazards: 56–67

Takahashi T. (1977). An occurrence mechanism of mud-debris flows, and their characteristics in motion. Annuals, DPRI, 23B2: 405–435 (in Japanese)

Takahashi T. (1978). Mechanical characteristics of debris flow. J. Hydraulics Div., ASCE, 104(8): 1153–1169

Takahashi T. (1991). Debris flow. Balkema, Rotterdam: 165p

Takahashi T. and Nakagawa H. (1991). Prediction of stony debris flow induced by severe rainfall. J. JSECE, 44(3): 12–19 (in Japanese)

Takahashi T, Nakagawa H, Harada T and Yamashiki Y. (1992). Routing debris flows with particle segregation. J. Hydraulic Eng., ASCE, 118(11): 1490–1507

Takahashi T., Nakagawa H. and Satofuka Y. (2000). Newtonian fluid model for viscous debris flow, Proc. 2nd Intern. Conf. on Debris-Flow Hazard Mitigation: 255–267

Takahashi T., Nakagawa H., Satofuka Y. and Wang H. (2002). Debris flow control by a grid-type sabo dam. Proc. Flood Defence, Science Press, New York

Takahashi T. (2006). The phenomena of sediment runoff and the countermeasures for sediment hazards, Kinmiraisha, Nagoya: 420p. (in Japanese)

Takahashi T. (2007). Debris flow; mechanics, prediction and countermeasures. Taylor & Francis, Leiden: 448p

Submarine Mass Movements and Their Consequences: An Overview

6

Jacques Locat and Homa Lee

Abstract Submarine mass movements pose a threat to coastal communities and infrastructures, both onshore and offshore. They can be found from the coastal zone down onto the abyssal plain and can take place on slope angles as low as 0.5°. They can move at velocities up to 50 km/h and reach distances over 1000 km. Their volume can be enormous, as illustrated by the 2.5 × 10^3 km^3 Storegga slide. Similar to their sub-aerial counterparts, submarine mass movements can consist of soil or rock and can take the form of slides, spreads, flows, topples or falls, but in addition they can develop into turbidity currents. Their main consequences are linked either to the direct loss of material at the site where the mass movement is initiated or along its path and to the generation of tsunamis.

Keywords Submarine mass movements • Hazard • Extent • Tsunamis • Flows • Mobility • Frequency • Magnitude

6.1 Introduction

Submarine mass movements and their consequences have been reported for many years, starting with the work of Heezen and Ewing in 1952 on the Grand Banks slide and tsunami. A recent overview by Lee et al. (2007a) describes the historical development of the field of submarine mass movements illustrating that this field has grown as a result of the search for resources, the development of communication networks and the need to better protect coastal communities against direct or indirect impacts of submarine mass movements, including tsunamis.

Jacques Locat (✉)
Laboratoire d'études sur les risques naturels (LERN), Université Laval, Quebec City, QC, Canada

Homa Lee
United States Geological Survey, Menlo Park, USA

Since 2000, a series of scientific meetings has been organized to promote exchanges on the topic of submarine mass movements and their consequences. As of today, a total of three international symposia has taken place: in 2003 in Nice (Locat and Mienert 2003), in 2005 in Solso (Solheim 2006) and in 2007 in Santorini (Lykous et al. 2007a). The next one will take place in Austin (Texas) in November, 2009 (http://www.geohazards.no/IGCP511/4th_international_symposium.htm). In addition, regular sessions were organized at annual meetings of the American Geolophysical Union, at the European Geophysical Union and at IGC congresses in 2004 in Florence, in 2008 in Oslo. This has been achieved via the IUGS and UNESCO funded IGCP-511 project on Submarine mass movements and their consequences, which, as of now, has about 150 active members worldwide.

K. Sassa, P. Canuti (eds.), *Landslides – Disaster Risk Reduction*,
© Springer-Verlag Berlin Heidelberg 2009

Therefore, since year 2000, the field of submarine mass movements and their consequences has grown substantially, thanks to major international projects like COSTA (Canals et al. 2004) and Euro-STRATAFORM and also to the knowledge developed as part of the Storegga project for which some of the major results have been published as a special volume of Marine and Petroleum Geology (Solheim et al. 2005).

In addition, the field of submarine mass movements is now integrated in books related to mass movements, e.g. for debris flows (Locat and Lee 2005), and for risk assessment (Nadim and Locat 2005). As a result of tsunamis generated by a submarine mass movement, which was triggered by an earthquake in Papua New Guinea (Tappin et al. 2001), a renewed interest has grown in a topic now called tsunamigenic landslides (Bardet et al. 2003).

This overview will present various images provided by swath bathymetry methods (often called multibeam sonar). Multibeam techniques use an acoustic signal emitted from a series of transmitters mounted on the hull of a vessel. The greater the number of transmitters and higher frequencies will provide more precise bathymetric information (Hughes Clarke et al. 1996; Locat et al. 1999). Reflection seismic surveys are often coupled with multibeam surveys. This method uses sound propagation in the water column and in the sediment which is reflected to the surface were it is recorded to generate a seismic profile made of the various reflectors. These reflectors may reflect either grain size or density changes and are then interpreted to generate a so-called seismo-stratigraphic profile. In most cases, boreholes are used in order to help validate the various interpretations. Seismic surveys can be carried out with a single geophone or a stream of geophones to generate 2D profiles or with geophone arrays to generate 3D profiles. The vertical resolution of the seismic method is directly controlled by the frequency which may range from les than 1 kHz to 12 kHz. An example of a 2D seismic profile is shown below in Fig. 6.12.

In the following, we presents an overview of recent developments in the field of submarine mass movements and their consequences by paying particular attention to: (1) extent and diversity of submarine mass movements including illustrations of consequences, (2) types and processes: the role of energy, and (3) risk assessment.

6.2 Extent and Diversity of Submarine Mass Movements and Tsunamis

As indicated by Lee et al. (2007a), submarine landslides are not distributed uniformly over the world's oceans, but instead they tend to occur commonly where there are thick bodies of soft sediment (Fig. 6.1), where the slopes are steep, and where the loads exerted by the environment are high. The more reddish tone in Fig. 6.1 represents either a zone of significant deltaic accumulation (e.g more than 10 000 m in the Gulf of Mexico) or thick glacial sequences (e.g. off the eastern coast of Canada). A compilation of landslide distribution for the North Atlantic has been given by Hünerbach and Masson (2004) and is shown in Fig. 6.2. It agrees with the above statement that submarine mass movements take place in all environmental settings, including along active or passive margins as shown below. One should consider this figure as a very partial map. For example, since the production of this map (Fig. 6.2) the St. Lawrence estuary was mapped and more than 30 slides were counted in this region alone (Campbell et al. 2008).

Without going into details here, the main triggering mechanisms are : seismic shaking, overloading, gas hydrate dissolution and excess pore pressure (coastal flow regime), wave loading, erosion and human activities (e.g. coastal construction).

Subaqueous mass movements of various types (Fig. 6.3) have now been found all around the World, either in lakes, fjords, estuaries, the coast, submarine canyons and along the continental slope. Most frequent types are slides, spreads, and flows and they can be all part of a single event! Turbidites, identified in Fig. 6.3, are only found in a subaqueous environment, but could be somewhat analogous to powder snow avalanches (Norem et al. 1990).

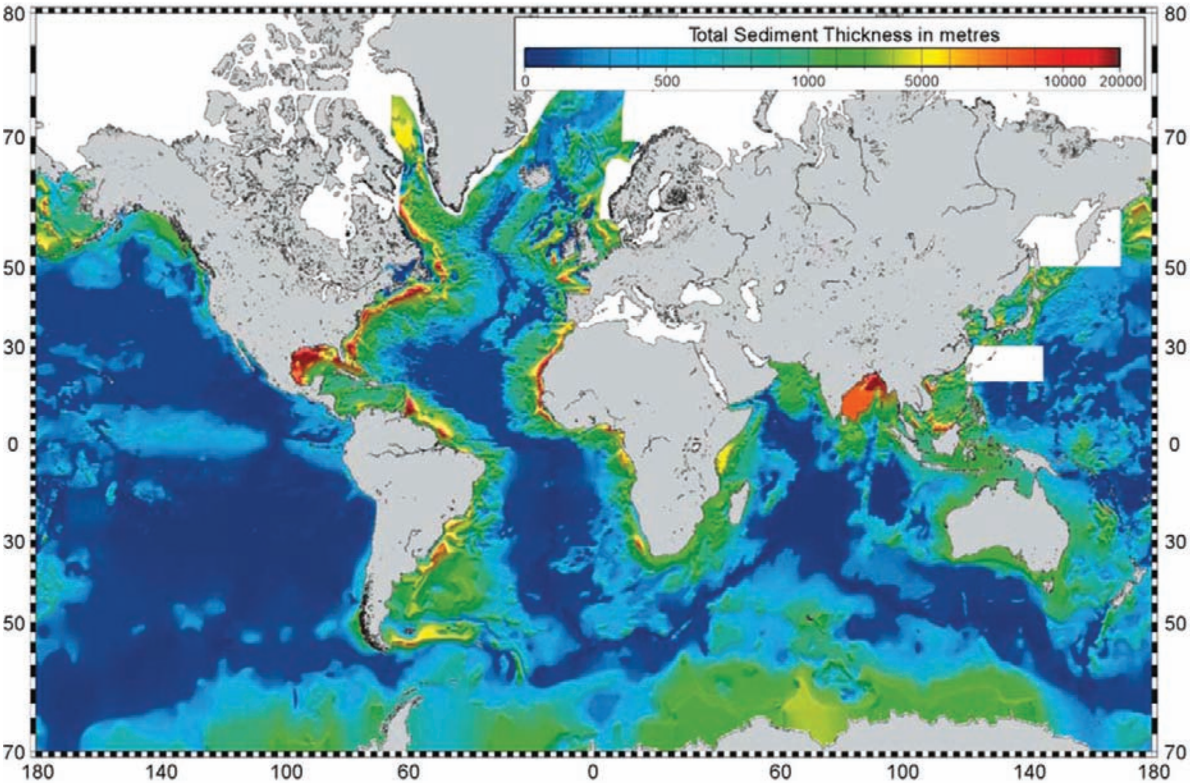

Fig. 6.1 Compilation of total sediment thickness for the main oceans (modified after Divins 2008)

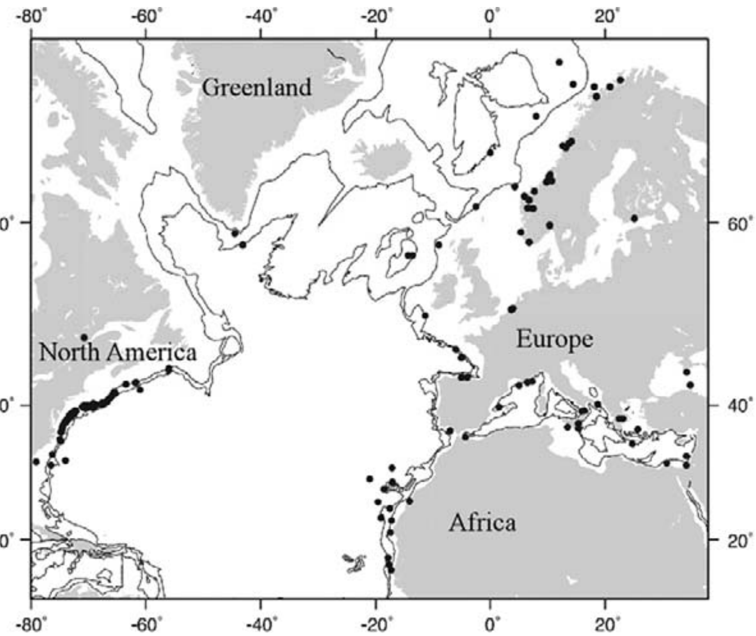

Fig. 6.2 Overview map of slope failures in the western and eastern North Atlantic including adjacent seas (Mediterranean, Black Sea, Baltic Seas), fjords of Norway and eastern Canada and failures in other limited/confined areas. Each point represents a single failure or slope failure complex either reported in literature or supplied through project partner data. In cases where a landslide extends over a larger area, the central position between headwall and toe of deposit is shown. Contour lines of 1000 and 3000 m are shown in grey. (source: Hünerbach and Masson 2004)

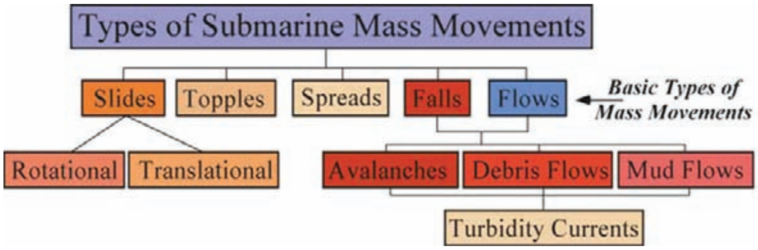

Fig. 6.3 Types and classification of submarine mass movements (Locat and Lee 2002)

6.2.1 Lakes

As recently shown by Mazzanti et al. (2007), Guyard et al. (2007) and Lajeunesse et al. (2008), the occurrence of subaqueous mass movements in lakes is quite common. In most cases, failures are triggered by earthquakes. Whenever the local morphological settings permits, the local sedimentary records of these events can be very well protected (Guyard et al. 2007).

At least in one case, failures were related to sediment loading produced by tailings accumulation in the lake. This is illustrated in Fig. 6.4 showing multibeam bathymetry images of the same part of the lake floor taken two years apart, i.e. in 2004 and 2006. Figure 6.4 is a nice example of how newly developed multibeam imagery techniques can be used for slope instability monitoring. This images show clearly that the few signs of instability along the esker slope rapidly evolved into significant mass wasting events leading to the transfer of tailings to the deeper part of the lake. It is interesting here to question the role of the esker (typically a stratified sand/gravel fluvio-glacial deposit) as it may act as a drain for the overlying aggrading delta thus discharging at the toe of the slope which results in some local instability along its flanks.

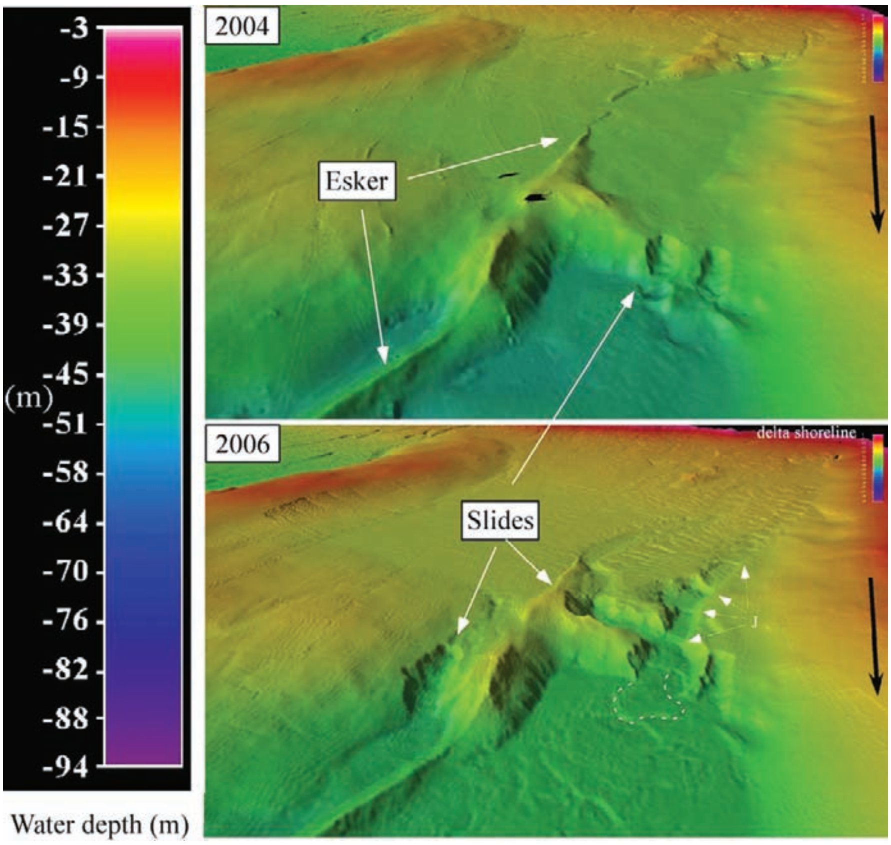

Fig. 6.4 Oblique view of portion of Wabush Lake (Labrador, Canada) floor showing the development between 2004 and 2006 of instability in the western side of the lake along the flank of an esker (snake-like feature). The average width of the field of view is about 500m. Small white arrows (J) represent position of step like features likely related to hydraulic jumps; black arrows give the overall sediment transport direction

6.2.2 Fjords

Fjords with high sediment accumulation rates are one of the environments most susceptible to failure, both in terms of the proportional aerial extent of deposits that can become involved in mass movement and also in terms of the recurrence interval of slope failures at a given location. Various sites have recently been reported such as the Saguenay Fjord (Levesque et al. 2006) where seismic shaking is the main trigger and the Finneidfjord in Norway where the triggering mechanism may be related to groundwater flow and/or free gas (Longva et al. 2003).

A striking example is shown in Fig. 6.5 where submarine failures caused by the magnitude 9.2 Alaska earthquake of 1964 generated tsunami waves with runup as great as 52 m (Lee et al. 2007b). Recent investigations have shown that a comparatively small fjord-head delta failure mobilized into a much larger debris flow that incorporated the full width of the fjord and progressed most of the fjord's length. Part of a subaqueous moraine also collapsed sending large (up to 40 m high) blocks across the fjord, generating the largest tsunami waves.

6.2.3 Inland Seas, Estuaries and Deltas

Many inland seas have been investigated for various types of mass movements and consequences. This is particularly true for the eastern Mediterranean and adjacent seas. In many cases, as with fjords, landslides will be triggered near deltas were sediments are rapidly deposited and also where layering may be more pronounced (i.e. potential planes of weakness). Typical examples were reported by Lykousis et al. (2007) for the Gulf of Corinth. In many cases, these mass movements are known to have generated tsunamis (see also Tinti et al. 2007)

In glaciated areas where the land has risen faster than sea level, large terraces were cut and are now exposed, e.g., along the St. Lawrence Estuary in eastern Canada. There, recent multibeam surveys have shown that numerous mass movement signatures could be found and that some of them could be linked to coastal instabilities (Cauchon-Voyer et al. 2008; Campbell et al. 2008). This is the case for the Betsiamites (Fig. 6.6) area where submarine mass movements have been clearly identified and dated (Cauchon-Voyer et al. 2008) and for which some may be associated with coastal events either recent (year 1663) or much older, i.e. about 7000 years old. The 1663 event is identify by the dashed line in Fig. 6.6. The now exposed part of the old (may be 7000 years old) slide is shown on land and the underwater part is more or less given by the two major channels perpendicular to the estuary which are separated by a more or less triangular apron.

Active river deltas are another likely site for slope instability. Rivers contribute large quantities of sediment to relatively localized areas on the continental margins. Depending upon a variety of environmental factors, including rate of sediment influx,

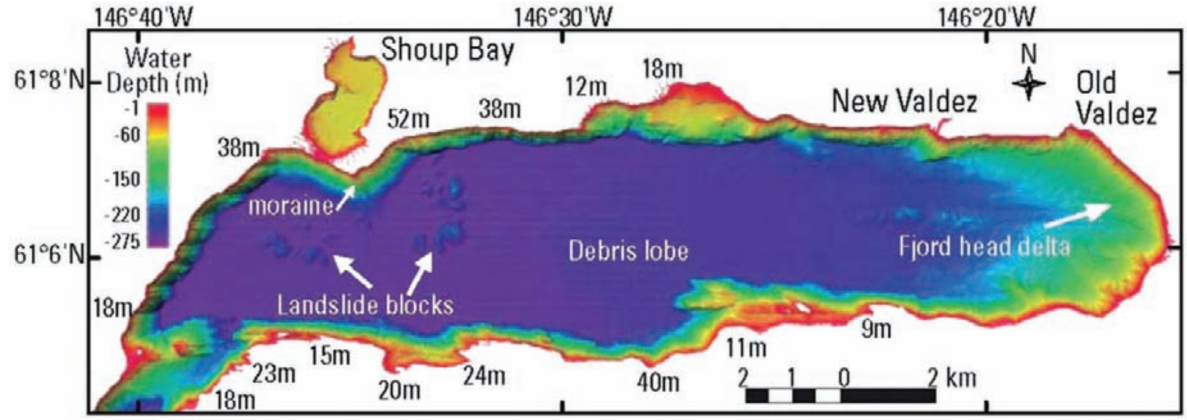

Fig. 6.5 Multibeam imagery of Port Valdez (Alaska, U.S.A.) showing landslide features discussed in the text. Labels around margin of the fjord show the estimated tsunami wave heights (runups) resulting from the 1964 earthquake (modified after Lee et al. 2007b). Mass movements originated mostly from the moraine, near the town of Shoup Bay, and fjord head delta

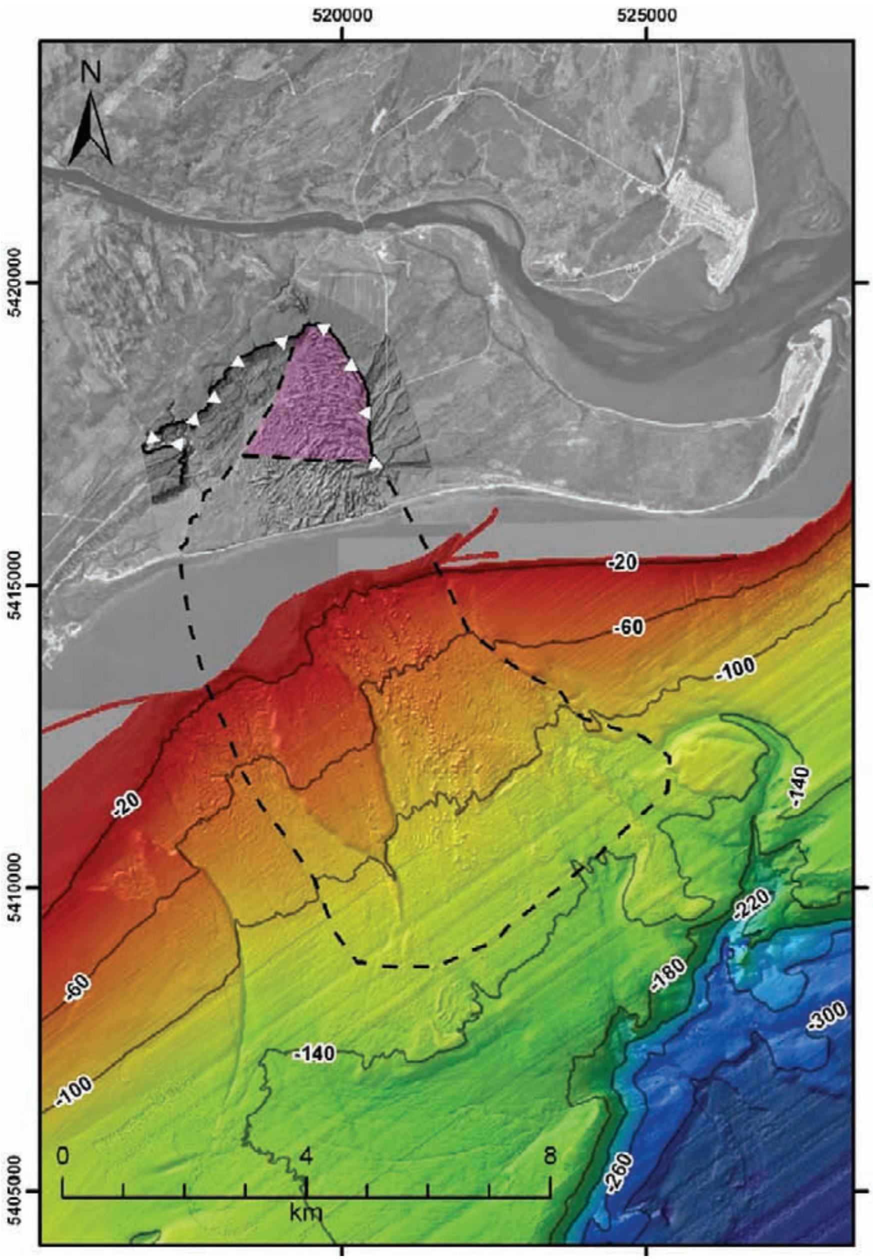

Fig. 6.6 The Colombier/Betsiamites slide complex involving both coastal and marine mass movements along the north shore of the St. Lawrence Estuary (Québec, Canada) (from Cauchon-Voyer et al. 2008 and Locat 2008)

wave and current activity, and the configuration of the continental shelf and coastline, thick deltaic deposits can accumulate fairly rapidly. These sediment wedges can become the locations of sediment instability and landsliding. To create large, deep-seated landslides, a thick deposit containing comparatively low-strength sediment or containing layers which can be weakened is needed. Most of the continental shelves were subaerially exposed during the last glacial cycle, so most sediment on the shelves from that time or before has been eroded, desiccated or otherwise diagenetically altered. Most sedimentation was diverted to the continental slope where it is potentially unstable. This appears to have been the case for the Nile delta, as reported by Garziglia et al. (2007) and by L'Heureux et al. (2007) for the Nidelv delta in Norway.

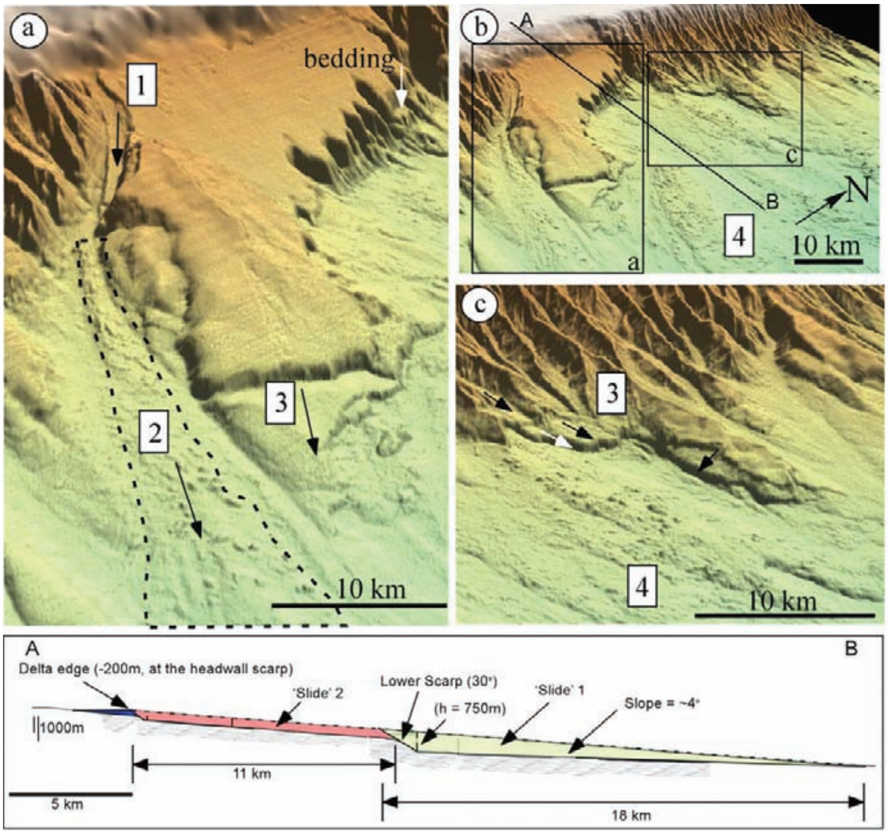

Fig. 6.7 The Currituck slide morphology (U.S. Atlantic coast) and 2D model. A general view is shown in (**b**) with enlargements in (**a**) and (**c**). The location of the cross section A-B is shown in (**b**). Note that the cross section is drawn without vertical exageration. 1: secondary debris flow path, 2: debris accumulation, 3: secondary failure surface, 4: debris along the main path of the flow. The lower panel represent a cross section along line A with the pink and green colors representing the two main phases of the slide (source: Locat et al. 2008, ten Brink et al., 2007)

A spectacular example is shown in Fig. 6.7 for the Currituck slide off the coast of South Carolina (USA, ten Brink et al. 2007). The slide likely took place at the time of low sea level (Prior et al. 1986). This slide removed a total volume of about 165 km^3 from this section of the continental slope. The departure zone still shows a very clean surface that dips at 4° and is only covered by a thin veneer of Holocene sediment. Multibeam bathymetric data suggest that this slide took place along three different failure surfaces. The morphology of the source area suggests that the sediments were already at least normally consolidated at the time of failure. The slide debris covers an area as much as 55 km wide that extends 180 km from the estimated toe of the original slope. A back analysis of slide initiation indicates that very high pore pressure, a strong earthquake, or both, had to be generated to trigger slides on such a low failure plane angle. The shape of the failure plane, the fact that the surface is almost clear of any debris, and a mobility analysis, all support the argument that the slides took place nearly simultaneously (ten Brink et al. 2007). Potential causes for the generation of high pore pressures could be seepage forces from coastal aquifers, delta construction and related pore pressure generation due to the local sediment loading, gas hydrates, and earthquakes.

With a position so close to the shoreline, the Currituck slide is believed to have generated a significant tsunami with wave amplitude up to 25 m in the starting zone 16.5 min after slide initiation. The damaging wave is shown to have reach the shoreline within about 90 min with run up values at a bout 5 m (Fig. 6.8, ten Brink et al. 2007). This image also presents the geometric control of the slide itself on the shape of the propagation front going towards the shoreline and also the fact that contrary to the wave going offshore, the onshore wave gets some amplification as it progresses into shallower waters.

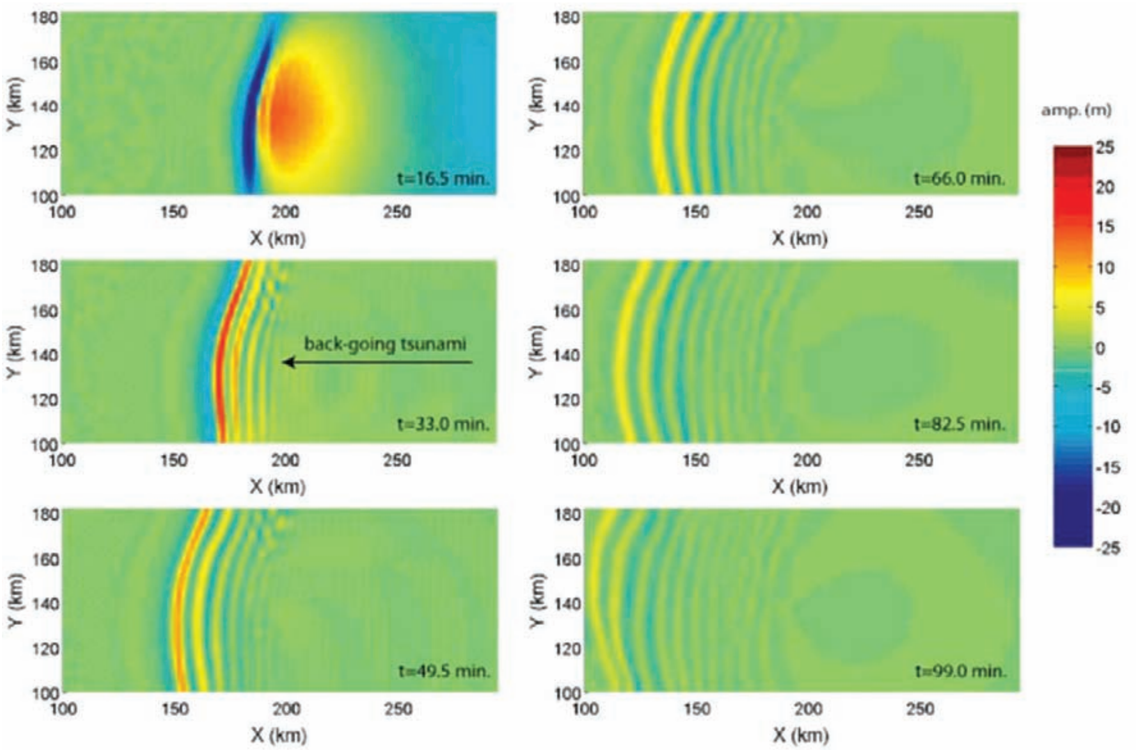

Fig. 6.8 Numerical simulation of the tsunami waves that could have been generated by the Currituck slide. (source: ten Brink et al. 2007)

6.2.4 Canyons

Submarine canyon-fan systems serve as conduits for passing large amounts of sediment from the continental shelf to the deep sea. The presence of extensive, thick sediment fans and abyssal plains off the coasts of many areas testifies to the importance of mass-movement mechanisms associated with these systems, which are capable of bringing sand-size and even coarser particles to locations hundreds of kilometres from shore. Landsliding appears to be an element that allows the formation of massive submarine fans. Landslides occur in submarine canyon heads because they are often sediment sinks that trap littoral drift and direct river-borne sediment. Such rapidly deposited sediment is commonly unstable leading to frequent failures (Sansoucy et al. 2007).

Also, sediment gravity flows in the floors of the canyons undercut the side banks leading to additional failures that may augment the original flows as has been observed along the Monterey Canyon, off Monterey in California (Fig. 6.9). This image appears very similar to a sub-aerial canyon with terraces cut into the slope, meanders, and secondary slides. This figure also reveals the presence of intra-canyon meanders suggesting the flow regime has decreased since its initial inception. Many canyons along the continental slopes have been formed at the time of low sea level which reached a maximum of −120 m about 21 000 years ago (Fleming et al. 1998; Locat et al. 2003b).

Some canyons were formed in fairly hard sedimentary rocks at the time of low sea level, e.g., the Port Phillip Bay entrance canyon (called the Heads), near Melbourne, Australia, which is a coral sanctuary and where disposal of rock resulting from dredging operations must be avoided (Edmunds et al. 2006). Notably, little is known about underwater rockfall apart from the very premilinary modeling of Beranger et al. (1998). Advances were recently made by the work of Turmel and Locat (2008) who have developed a numerical model that has been compared to the one of Beranger et al. (1998).

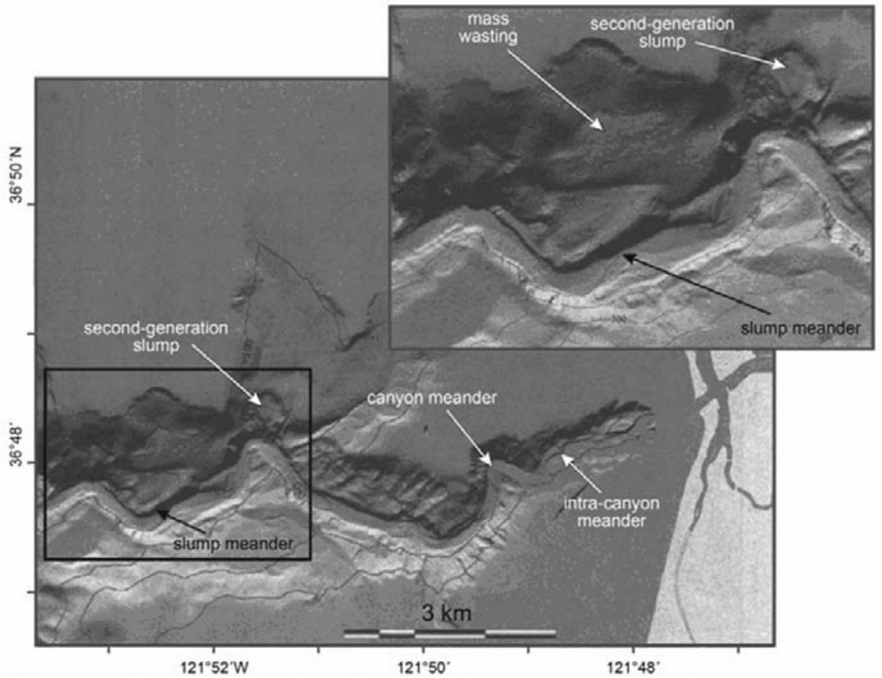

Fig. 6.9 Multibeam image of the headward part of Monterey marine Canyon (California, U.S.A.) showing canyon and intracanyon meanders slump (modified from Greene et al. 2002)

Turmel and Locat (2008) propose a finite volume approach to model the 2D rockfall behavior in a Newtonian fluid, such as water or air. Turbulent and incompressible flow around the moving rock is solved using a pressure-velocity iterative method on a dynamic 3D unstructured mesh of polyhedral cells. Pressure force, shear force, turbulent forces and gravity force are then applied to the moving rock. As shown in Fig. 6.10, the numerical results were also compared to what would be obtained in a sub-aerial case. Although Beranger and Turmel and Locat's modeling results are quite similar in the initial fall, they differ significantly after the first rebound. This is largely due to the hydrodynamic forces that are only taken into account in the Turmel and Locat model.

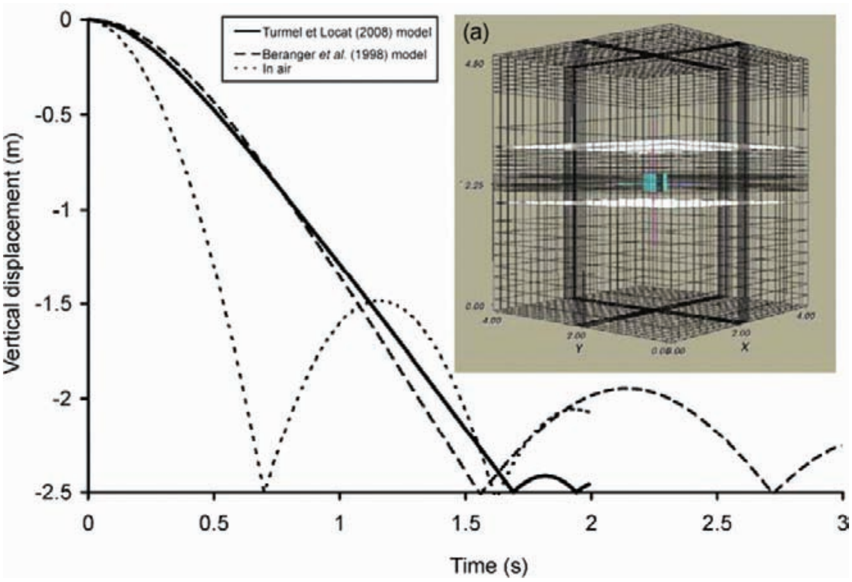

Fig. 6.10 Underwater rockfall simulation on a horizontal surface, for a block having a volume of 0.069 m^3, unit weight of 27 kN/m^3, drag coefficient of 2.0 and a coefficient of restitution of 0.8. In 'a' is shown the 3D grid used for the numerical modeling with the moving rock, in blue, at a given location during the fall. (adapted from Turmel and Locat 2008)

6.2.5 Continental Slope and Rise

Another common environment for undersea landsliding is the intercanyon area of the continental slope. Landslides have been reported all around the globe along continental slopes removed from submarine canyon-fan systems. Amongst the best examples is the giant Storregga slide complex which has received a major focus in relation to the Ormen Lange gas field development off Norway. A major compilation of the most significant contributions has been assembled in a 2005 special edition of Marine and Petroleum Geology (Solheim et al. 2005). Work related to this case history has resulted in a quantum increase in our ability to recognize submarine mass movements, date them, analyze the stability of slopes and their mobility, evaluate tsunami hazards and develop risk assessment procedures.

It is not easy to select a particular model to explain the Storegga slide (Fig. 6.11a). Amongst the many scenarios which have been proposed for the initiation of the Storegga slide, the role of gas hydrates has often been put forward. The result of back calculation of slope stability using gas hydrate dissociation as a triggering mechanism has been illustrated by Sultan et al. (2004) and some of the results are shown in Fig. 6.12 indicating how the process of gas hydrate dissociation with time has generated a relative increase in the pore pressure resulting in a decrease in the factor of safety (FOS) with time. They consider two of the most important changes during and since the last deglaciation (hydrostatic pressure due to the change of the sea level and the increase of the sea water temperature) in making their calculation. Their simulation results indicate that melting of gas hydrate due to a change in the gas solubility could be at the origin of a retrogressive failure initiated on the lower part of the Storegga slope. According to Sultan et al. (2004) this process would have occurred at the time of the Storegga slide, i.e. about 8100 years ago (Haflidason et al. 2005). An important unresolved question here regards the lateral extent and continuity of the failure and how the mechanism can also explain the slide's retrogression.

Another explanation has been proposed by Kvalstad et al. (2005) who suggest a retrogressive slide mechanism. Such an approach, shown in Fig. 6.11b and c, has the advantage of being able to reproduce the final stages observed in the morphological signature of the slide. On the other end, it still requires an initial failure in the lower part to initiate it. Overall, there seems to be agreement that many factors must be invoked in order to fully explain the overall extent and characteristics of the Storegga slide, including earthquakes and pore water seepage forces. According to Bryn et al. (2005), the destabilisation prior to the slide is related to rapid loading from glacial deposits with generation of excess pore pressure and reduction of the effective shear strength in the underlying clays.

The Storegga slide is also well known for the great tsunami that it generated, which left deposits in many areas in the North Atlantic (Bondavik et al. 2005). By compiling all the relevant data (Fig. 6.11a), Bondavik et al. (2005) have back calculated the propagation of the wave front as shown in Fig. 6.13. The figure clearly shows, and is supported by dated tsunami deposits on land, that a significant wave of 3 m reached a distance as far as the Faeroe Islands. This is another illustration of the great radius of influence that must be considered for risk assessment related to submarine mass movements.

Recently, multibeam data have been published on the Grand Banks slide (Mosher and Piper 2007; Mosher 2008, Fig. 6.14) which is one of the largest historical events (about 150 km^3). The slide took place on November 18, 1929, as a result of a $M = 7.2$ earthquake which occurred at the southern edge of the Grand Banks, 280 km south of Newfoundland.

The Grand Banks slide took place along the St. Pierre Slope in a context somewhat similar to the Storegga slide, i.e in an area of thick accumulation of sediments at the outlet of an ice-stream. However, the triggering here is clearly associated with an earthquake (Mosher and Piper 2007). Contrary to the Storegga slide, the Grand Banks slide area does not present high escarpments. In the starting zone, the depression left by the slide indicates that it was a shallow failure (5–100 m), extensive and that it coalesced rapidly downstream into the various channels to rapidly develop the turbidity current (see also a discussion by Locat et al. 1990, on the mobility of the debris). One of the main observations made by Mosher and Piper (2007), from the analysis of the Grand Banks slide morphology, is that the assessment of tsunami hazard

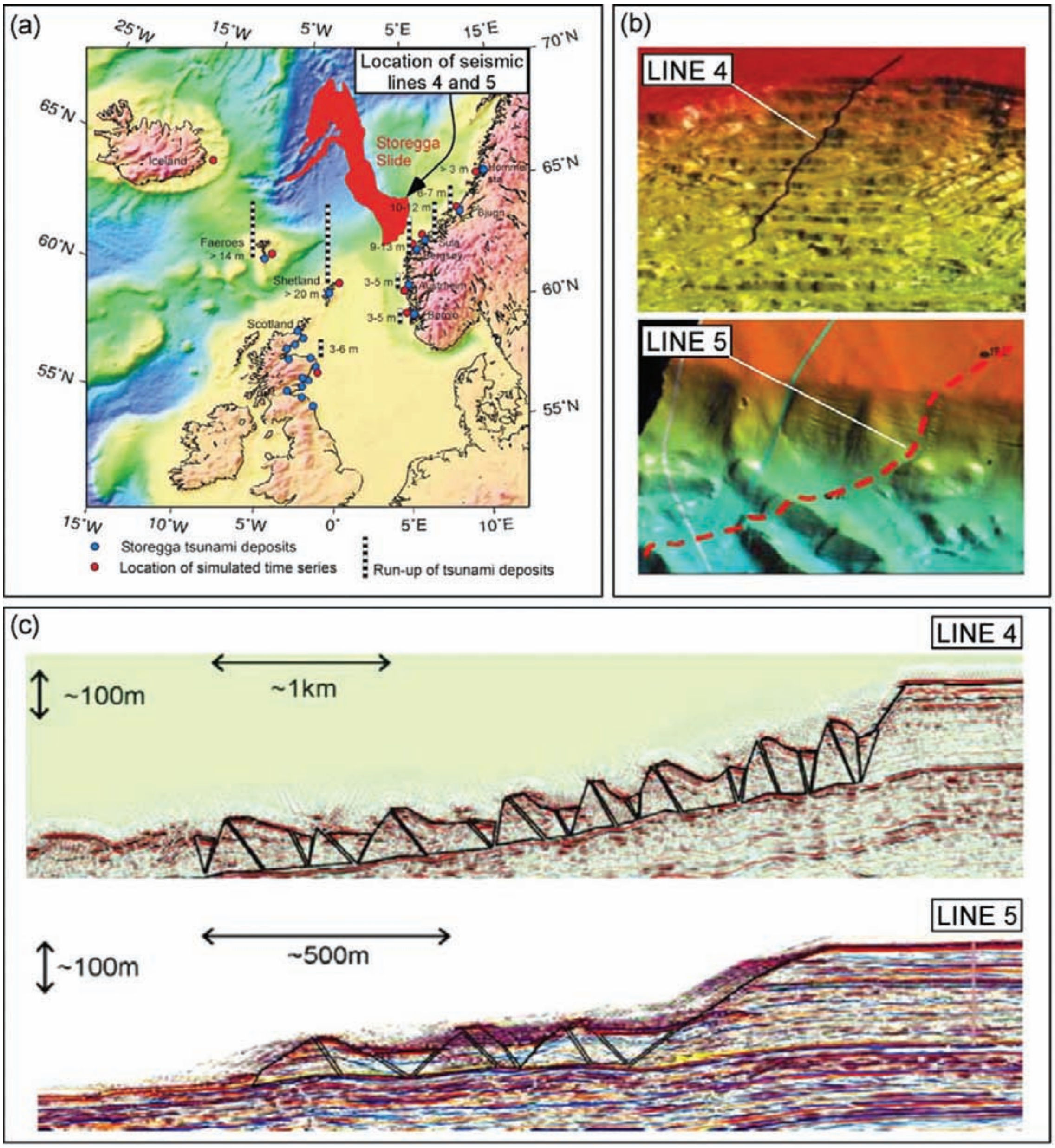

Fig. 6.11 The Storegga slide: (**a**) extent in red with run up of tsunami deposits (Bondavik et al. 2005), (**b**) position of seismic lines 4 and 5 shown in (**c**) obtained in the upper headwall area (see in (**a**)) showing the retrogressive nature of the slide in this area as shown by the interpreted slide/block morphology indicated by the black lines in (**c**) (modified after Kvalstad et al. (2005)

based on recognizable morphologic evidence alone may underestimate the landslide tsunami risk.

The Grand Banks slide tsunami has been recently modeled by Fine et al. (2005) and some of their preliminary results are shown in Fig. 6.15. Their simulation indicates that most of the tsunami wave propagation was completed within about 3 h after the event and traveled as far west as to Anticosti Island, Québec. At this point, the computed arrival times are in fairly good agreement with the observed ones. Although the Grand Banks slide is fairly well known as of now, there are still many aspects that

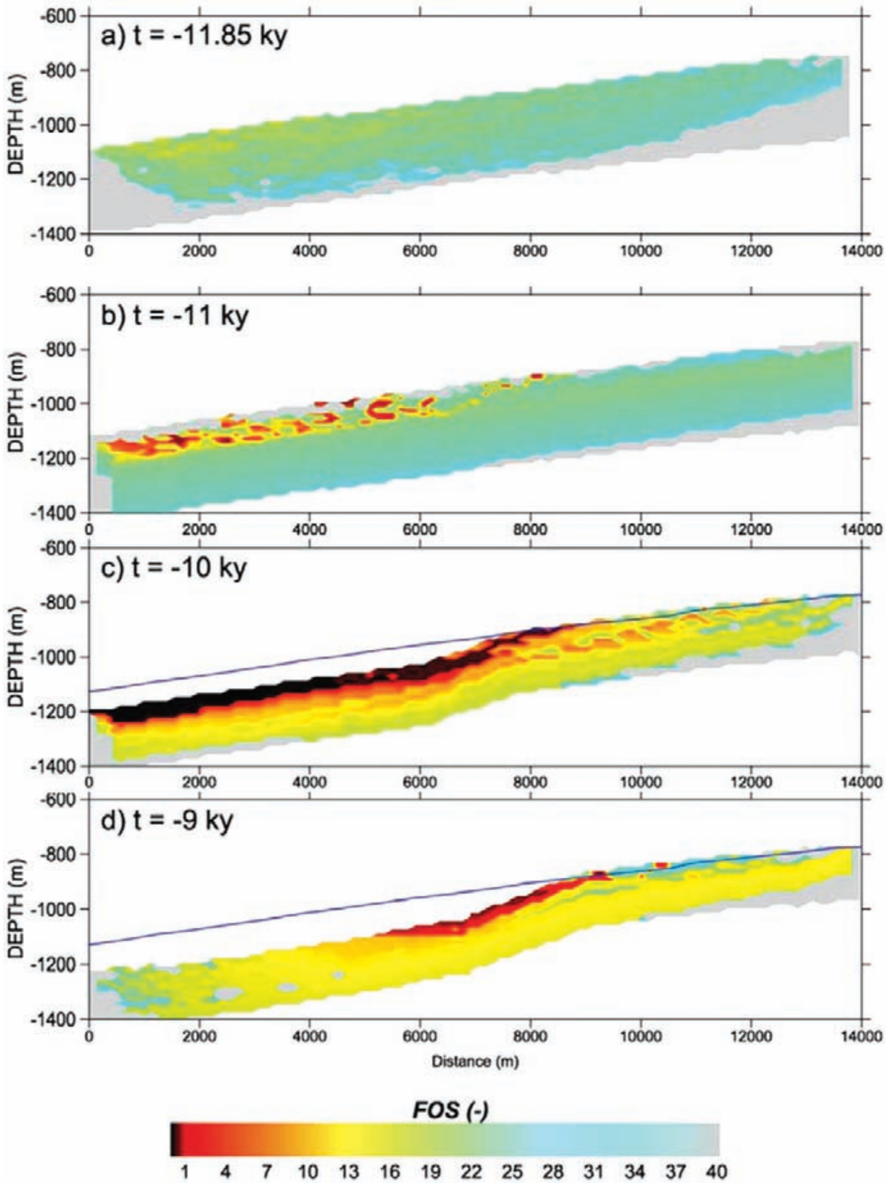

Fig. 6.12 Development of instability on the slope of Storegga as a result of gas hydrate dissociation (modified after Sultan et al. 2004). FOS: factor of safety; ky: 1000 years; (**a**)–(**d**) represent gas hydrate dissociation process with the related decrease in the FOS until sliding takes place and overall FOS increases

are not well covered and they include the detailed stratigraphic framework, and the geotechnical and rheological properties of the sediments involved. Moreover, the actual sliding mechanism appear quite complex and, as for the Storegga slide, it may not be easy to actually identify which phase of the slide can be directly related to the tsunami.

One of the most impressive submarine mass movements recently discovered is the Hinlopen slide (Fig. 6.16) which took place along a glaciated margin in the Arctic Ocean (Vanneste et al. 2006) and has involved a volume of about 1350 km^3 leaving a local scarp with a height of 1400 m with remaining slopes as high as 30° (see inserts in Fig. 6.16a). The Hinlopen slide developed catastrophically by dissipating sufficient energy to carry large rafter blocks (kilometer scale) over a distance of more than 60 km. Thess blocks are clearly seen in Fig. 6.16d and have been transported along with sub-parallel ridges of debris. It is believed by Vanneste et al. (2006) that the Hinlopen slide is pre-Holocene and may likely be related to climatic

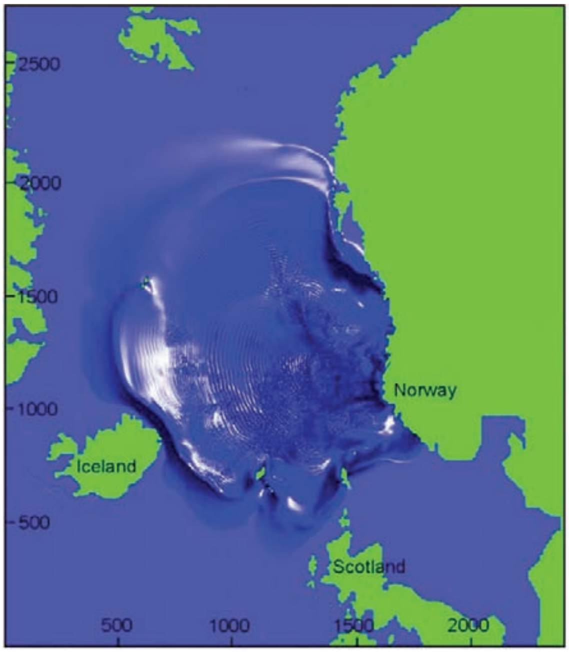

Fig. 6.13 Perspective view of sea-surface elevation 2 h after the release of the Storegga slide. The wave front, ca 3 m high has reached the Faeroe Islands and the Shetland Islands and approaches Greenland, Iceland and Scotland. The small ripples behind the wave front are caused by numerical noise. This noise does not affect the maximum surface elevations (modified after Bondevik et al. 2005)

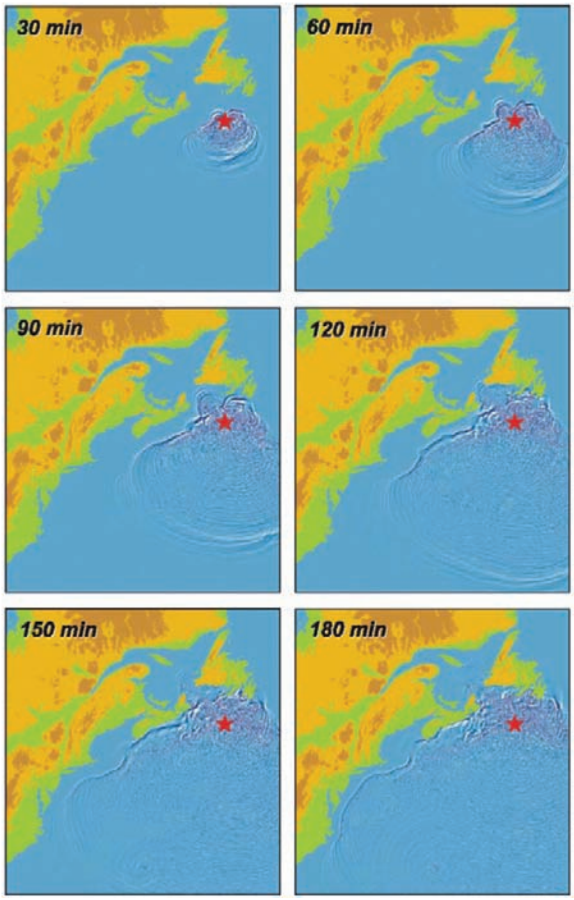

Fig. 6.15 Snapshots of simulated tsunami waves for 30, 60, 90, 120, 150, and 180 min after the 1929 Grand Banks slide failure. The star indicates the epicenter of the earthquake. (modified after Fine et al. 2005). The land part extends from Québec Labrador to the north, to New England to the South

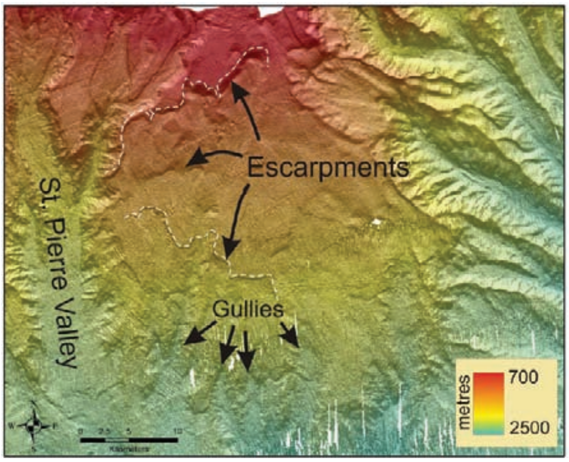

Fig. 6.14 Multibeam image over part of the St. Pierre Slope (off the coast of southern Newfoundland, Canada), main source area for the 1929 Grand Banks landslide, showing 80–100 m-high escarpments. (source: Mosher 2008; Mosher and Piper 2007)

changes. As for the Storegga slide, they believe that sliding surfaces were developed along contouritic clayey deposits during periods when the ice-related sedimentation was minimum. Then, as glaciers reoccupied the proximal margin, they dumped large quantities of glacial sediments or till over a potentially softer layer. As is believed to be the case for the Storegga slide (Bryn et al. 2005) and for the Grand Banks slide shown above, the failure may be related to various factors including softening of weak-prone layers and tectonic activity largely related to glacial rebound. According to Vanneste et al. (2006), a submarine landslide with these dimensions could have created a devastating tsunami, although its potential depends on sea ice

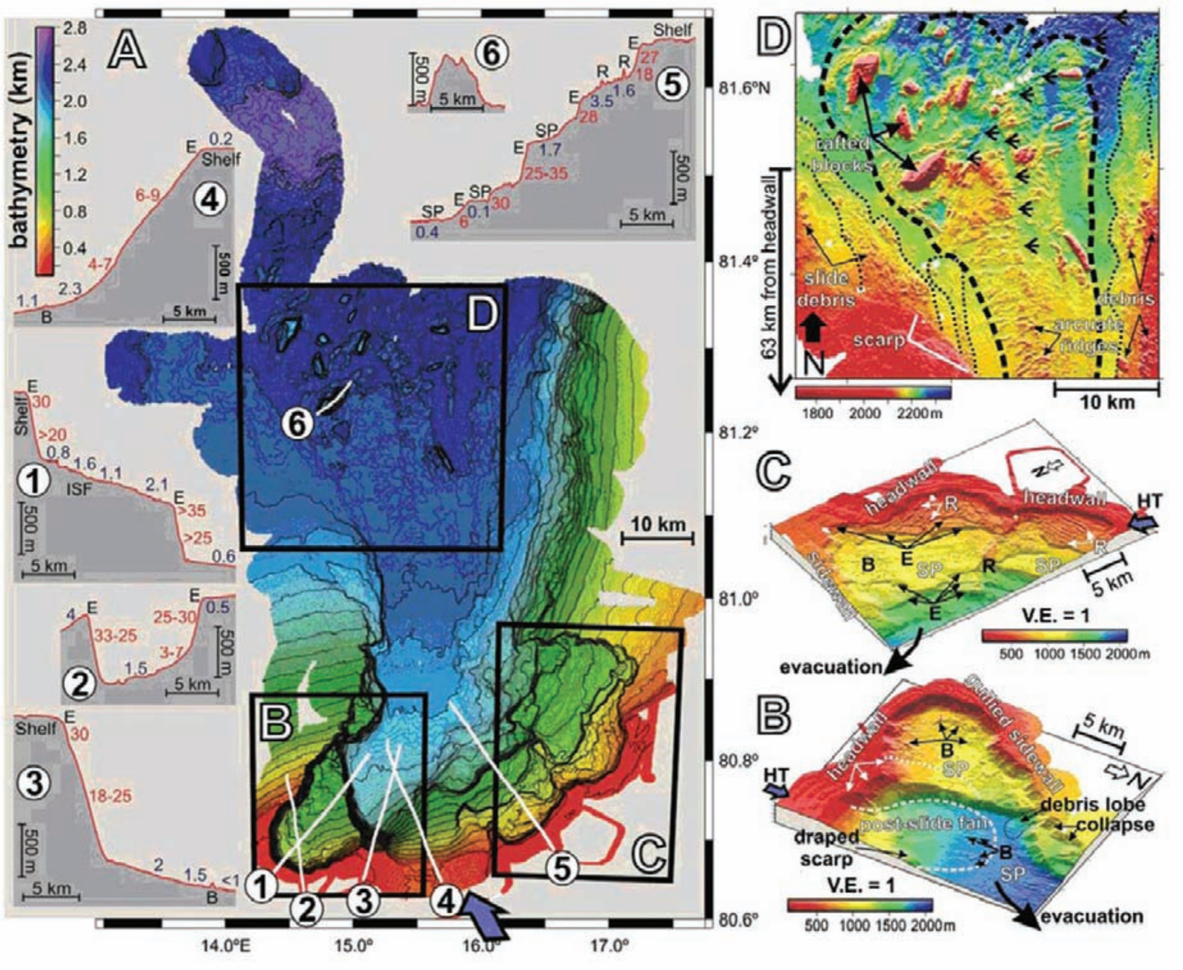

Fig. 6.16 (A) Swath bathymetry image (c. 4795 km2) of the Hinlopen Slide scar area on the northern Svalbard margin off the mouth of the Hinlopen Trough (HT). Contour interval is 10 m (thin) respectively 100 m (bold). The tracks, highlighted in the insets, nicely illustrate the different characteristics of the escarpments (e.g. slope and throw). Numbers along the tracks represent slope angles in degrees (red: maximum angles of escarpment, blue: mean dip of slip surface). The blue arrow south of the head scarp represents the sediment inflow from the Hinlopen Trough. The boxes mark the locations of the illuminated pseudo-3D views shown at the right (B–D). The western (B) and eastern (C) slide scar areas are displayed with a vertical exaggeration 1:1. The white dashed line (B) marks the outer limit of the post-slide sediment lobe derived from the Hinlopen Trough whereas the star represents the location of a sediment core containing ice-rafted debris. The black dashed curves (D) delineate blocky slide debris lobes, comprising both arcuate ridges and gigantic rafted blocks. Some glide tracks are indicated by black arrows (D). (Annotations: B = block, E = escarpment, ISF = irregular sea floor, R = detached sediment ridge, SP = slip plane) (modified after Vanneste et al. 2006)

conditions as well as the time lags of the multiphase, retrogressive movement.

When compared to their land counterparts, submarine mass movement signatures can sometimes be more easily described using various seismic methods. For example, 3D seismic methods, initially developed for the oil industry, are now more accessible to scientists and engineers searching for mass movement signatures. One spectacular example is the work reported by Huvenne et al. (2002) on the Porcupine area (Fig. 6.17) in a portion of the Atlantic sea floor just south of Ireland, which revealed the presence of a blocky mass movement deposit buried under about 100–200 m of sediments. Basically, the image shown in Fig. 6.17 is obtained by cutting the 3D bloc of seismic data at a certain

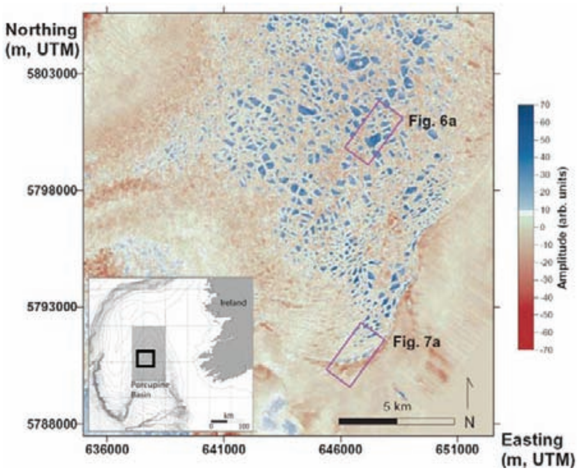

Fig. 6.17 Amplitude map of part of the mass movement horizon obtained by removing about 43 ms of seismic signal showing the detail toe and blocky part of the slope failure. Slide area is shown by the black box. The colour gradient shows the relative amplitude that reveals the blocky nature of the rock avalanche.The black square show the location of the landslide image in the Porcupine basin off south-western Ireland. UTM: Universe Transverse Mercator grid. Figures 6.6a and 6.7a shown noest to boxes in the figure refers to figures number in the paper by Huvenne et al. (2002) where more details can be found. (modified after Huvenne et al. 2002)

time interval, removing the data above and looking at the relative amplitude of the signal at this level and interpreting the intensity pattern which here reveals the blocky pattern of the rock avalanche deposit. Other examples of 3D seismics used to identify submarine mass movements are given by Martinez et al. (2005) and Gee et al. (2007).

Another interesting example of the use of 2D and 3D seismics has been integrated by Sultan et al. (2007b) to explain the development of submarine mass movements on a slope less than 2° likely caused by the underlying effect of an active compression zone (Fig. 6.18a) inducing basal stresses in the overlying sediments (Fig. 6.18b). This constitutes another triggering mechanism for submarine mass movements. Here the underlying basal stresses are modeled by cavity expansion theory generating added gravitational stresses under the overlying sediment mass. The stress intensity distribution is shown by the range in color seen in Fig. 6.18b. In order to identify the triggering mechanism of the observed landslide, Sultan et al. (2007) developed a three-dimensional slope stability model (SAMU-3D) based on the upper bound theorem of plasticity. Their results have shown that the gravity loading generated by the sediment weight alone is not sufficient to explain the observed submarine slide but that it could become unstable by considering the additional structural stress generated by the regional compressional gravity driven deformation.

6.2.6 Volcanic Islands

Major mass movements also occur along volcanic islands and the mass movements originating from these areas can sometimes develop into very far reaching debris flow and turbidity currents, e.g., the giant deposits off the western coast of Africa (Talling et al. 2007). Almost every volcanic island which has been studied until now presents signatures of very large mass movements intrinsically associated with the development and the collapse of volcanic edifices (e.g. Deplus et al. 2001; Le Bas et al. 2007).

On the 30th of December 2002, part of the western flank of the Stromboli volcano slid into the southern Tyrrhenian Sea, Italy (Fig. 6.19), in sequences that initiated two tsunamis that were generated only 7 min apart in Stromboli (Fig. 6.20, Tinti et al. 2006; Chiocci et al. 2008). Because of a previous multibeam survey in the area before the slide event, a unique opportunity existed to observe the morphological changes associated with the failure (both sub-aerial and submarine according to Chiocci et al. 2008), to better understand the collapse process of volcanic islands and the generation of tsunamis. According to Tinti et al. (2006), “the first tsunami was due to a submarine mass movement that started very close to the coastline and that involved about 20×10^{6} m^{3} of material. The second tsunami was engendered by a subaerial landslide that detached at about 500 m above sea level and that involved a volume estimated at 4–9×10^{6} m^{3}. The latter landslide can be seen as the retrogressive continuation of the first failure.”

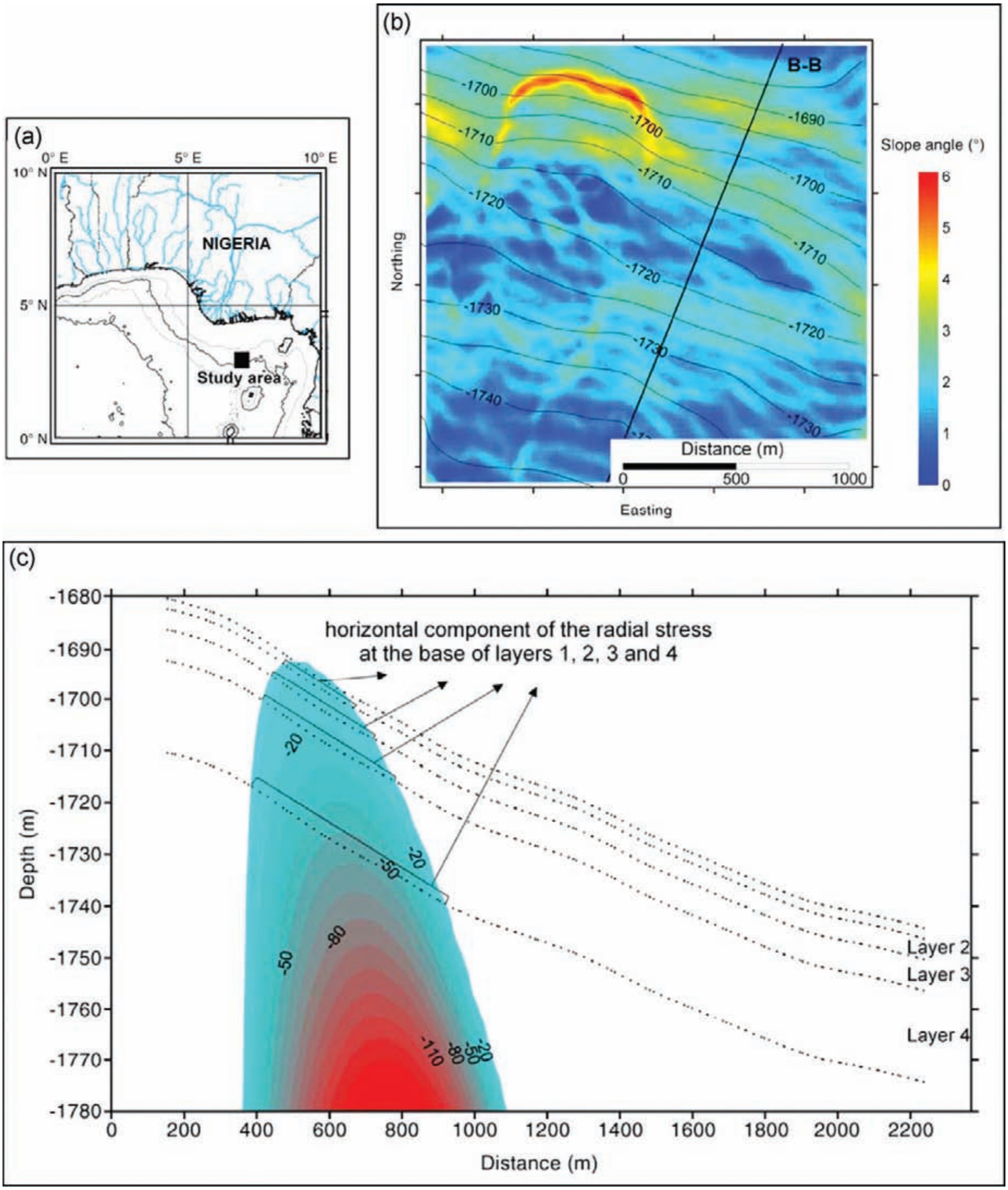

Fig. 6.18 Back analysis of deep submarine slide of the Nigeria coast. (**a**) site location, (**b**) slope angle of the study area. The maximum slope angle corresponds to 5° at the slope–scar level. Back calculations were carried out along the B–B cross-section which represents the morphology of the study area before sliding. (**c**): 4 different sedimentary layers identified using CPTU's data. A contour map of the radial compressive stress σ_r (kPa) generated by cylindrical cavity expansion is projected on the sedimentary layers. The colour grading in (**c**) reflect the intensity of the stress generated by the underlying faults using cavity expansion theory. (modified after Sultan et al. 2007b)

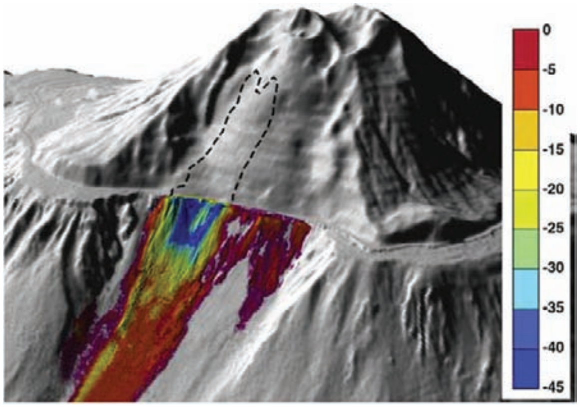

Fig. 6.19 Seafloor deepening due to the 30th December 2002 landslide (residual map between pre- and post-slide bathymetry), draped over a 3D view of the western flank of Stromboli Island. A maximum depression of more than 45 m is present at the center of the slide scar; each color cycle corresponds to some 10 m. The width of the base of the volcanoe, at sea level, a = is 4 to 5 km. (Chiocci et al. 2008)

6.3 Types of Processes: The Role of Energy

In the aquatic environment, all types of mass movements seen on land can be observed, in addition to turbidity currents (Fig. 6.3). Each type represents a different physics but also, if we consider slides, spreads and flows, represent different degrees of material transformation. To achieve it, one must provide sufficient energy to reach a given degree of remolding.

In a simple approach, one could consider that a given type of material (soil or rock) may need a certain amount of remolding energy to reach 100% of the value of the remolded undrained shear strength or fragmentation (E_{rN}, see also Locat et al. 2006). As a mass movement is taking place, and according to the type of failure (or a combination) some amount of remolding energy will become available (E_{rA}). This

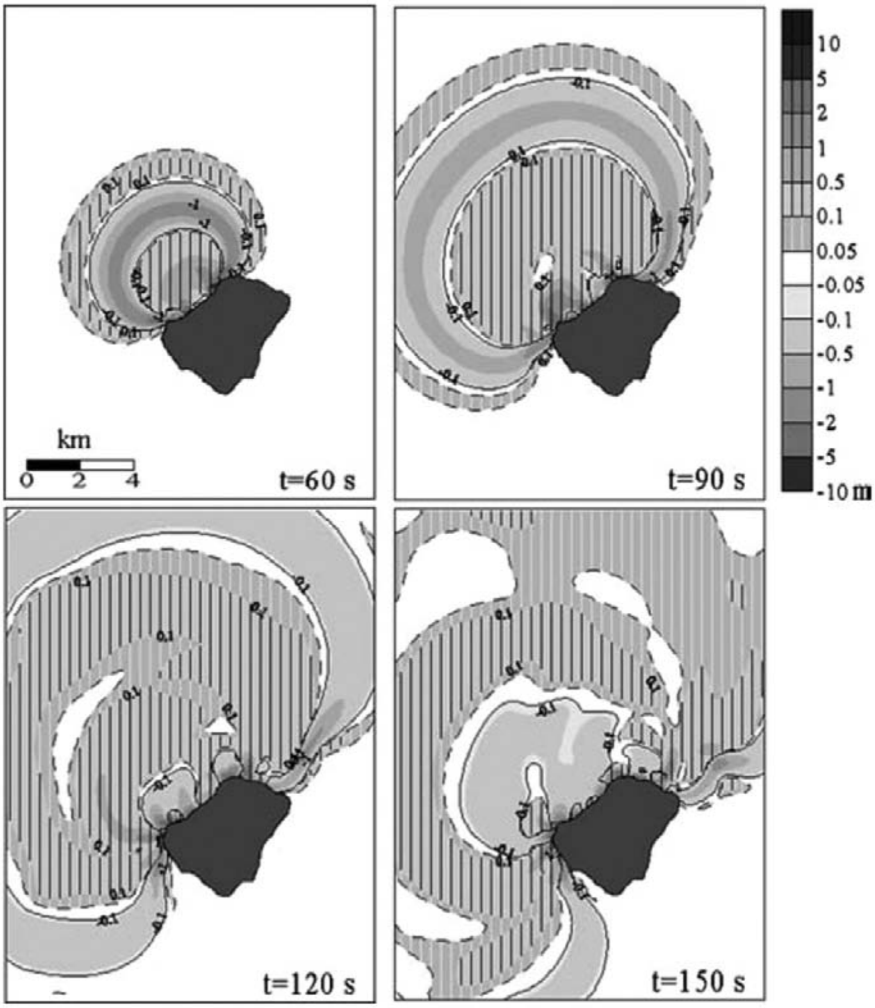

Fig. 6.20 Submarine-slide tsunami on Stromboli Island generated by the first slide. Snapshots of the water elevation fields computed on a grid. Contour labels are in meters. Palette goes from white to dark grey as magnitude increases. Positive elevations are striped, t: time in seconds after the slide (case 1B of Tinti et al. 2006)

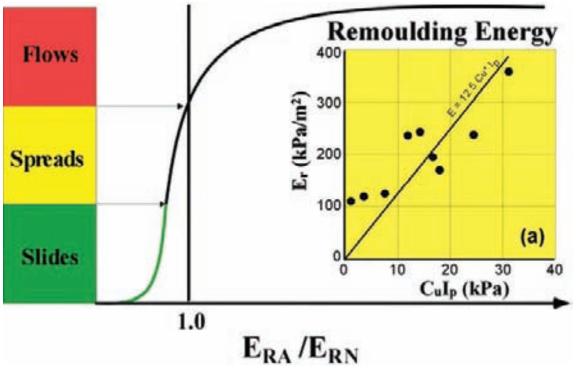

Fig. 6.21 Types of mass movements generated as a function of available remoulding energy. The insert (a) is from Leroueil et al. (1996)

concept is illustrated in Fig. 6.21 suggesting that for a flow failure to take place, 100% of the remolding energy must be available during failure and post-failure. This concept is analogous to the remolding index I_r, ($I_r = 14.9(E/c_uI_p{}^{0.69})$ of Vaunat and Leroueil (2002) and applied to sub-aerial quick clay slides in Québec by Locat et al. (2008) and by Locat et al. (2007) for a small submarine debris flow in the Saguenay Fjord.

Another aspect of post-failure transformation is the potential for an increase in the water content (Fig. 6.22) via the transformation of the moving mass (Jeong et al. 2004). This figure illustrates the transformation of a sediment (or soil) into a fluid-like material which can flow over large distances.

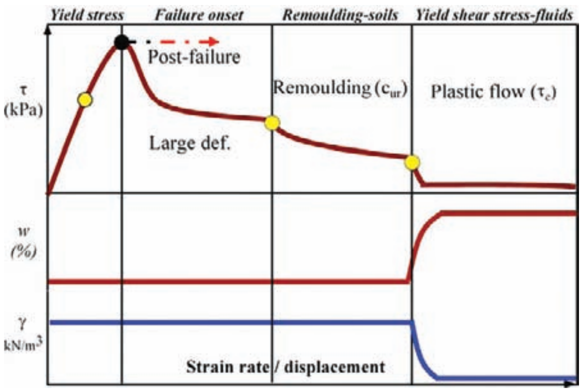

Fig. 6.22 Conceptual view of the effect of water entrainment during failure transforming a soil into a viscous fluid. In many underwater situations, such a concept must be invoked to achieve the required low strength of the flowing material. C_{ur}: undrained remolded shear strength; τ_c: yield strength (modified after Jeong et al. 2004)

Such a process has been by Schwab et al. (1996) to explain the great mobility of some Gulf of Mexico far reaching debris flows and the high water content of the debris flow deposit, compared to what could be estimated at the source area.

Another illustration of the concept of remolding energy is presented in Fig. 6.23 where a link is made between the depositional environments, sediment signature and properties in order to explain the development of slide, spread or flow failures. For sediments, one can see two types of deposits: homogeneous or layered, as underlined by their texture contrast. During formation and evolution of the sediment, various processes take place that change the physical and geotechnical properties and ultimately the intact and remolded undrained strength. Depending on the final morphological conditions of a given slide and the triggering mechanism (e.g. earthquake), energy will be used to transform the sediment package. Considering the effect of layering, one would be inclined to think that homogeneous sediments will tend to develop into slides whereas layered ones can evolve into spreads or flows. Kokusho and Kojima (2002) and Biscontin et al. (2004) have illustrated the strong effect of layering on the shearing resistance of the sediments and the degree to which it can totally transform the sediment into a flowing material. As suggested in Figs. 6.21 and 6.23, depending on the amount of available remolding energy and the needed energy for 100% remolding, either a spread or a flow can be generated.

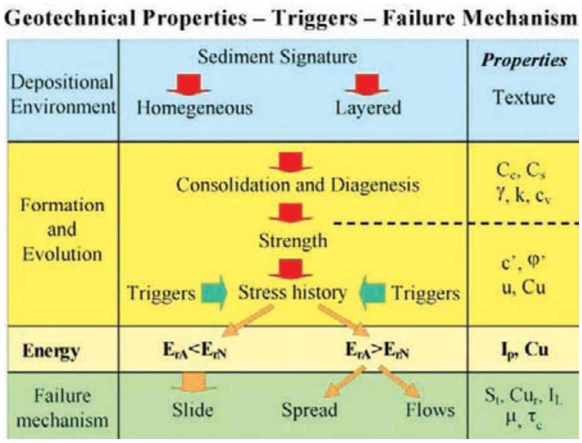

Fig. 6.23 Conceptual relationships between marine sediment geotechnical properties, submarine slide triggers, and sediment failure mechanisms (E_{rA}: remolding energy available, E_{rN}: remolding energy needed for 100% remolding)

Such a concept could be considered in the analysis of Talling et al. (2007) of the large and far reaching mass movements off the coast of the Canary Islands (Fig. 6.24). Their analysis indicates that as the sliding mass progresses down slope and as the gradient changes, the transported mass is partly disturbed and acquires a significant mobility but can also change from a turbidity current back to a debris flow when the flow velocity decreases. Even here, it is clear that a significant transformation of the initial sliding mass was necessary to develop an initial turbidity current.

An important observation originating from work on the Storegga slide was to clearly underline the scaling behavior of many type of debris flows (Fig. 6.25). Both the run-out and the ratio between fall height and run-out are best described as a power-law function (Issler et al. 2005).

According to Issler et al. (2005, p. 193), the data from the Storegga Slide complex points towards some mechanism that reduces the bottom shear strength, either progressively or above a certain threshold. Recent experiments revealed that lubrication through hydroplaning or progressive wetting of the shear layer is the key to explaining the high velocity and long run-out distances of subaqueous laboratory flows.

In closing this section, we can still ask a simple but interesting question to be raised here. By which process can a sediment that can sustain a 30° slope 400–1400 m high transform into a mobile material that will rest on a 1–2° slope as it is the case for the Storegga, Currituck and Hinlopen slides described above? We do not think that a complete answer exists yet, but there is clearly a need for an energy source provided by some mechanisms or combination of triggers.

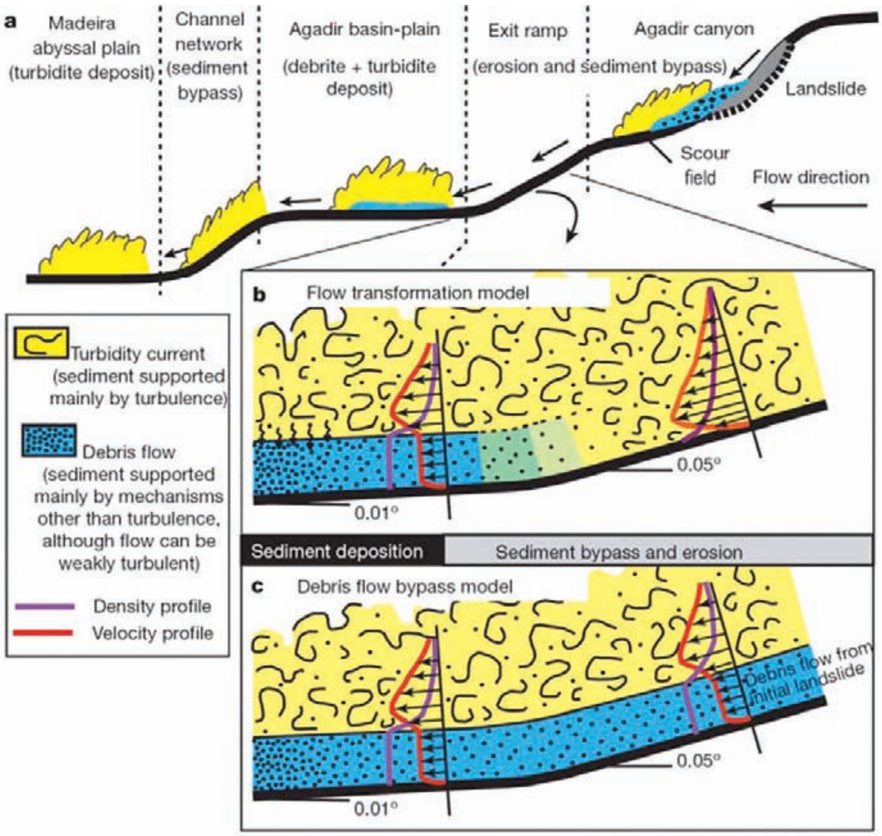

Fig. 6.24 Evolution of flow event that deposited bed 5 showing two alternative mechanisms for generating the debris flow. (**a**), Evolution of entire flow event from Agadir canyon to Madeira abyssal plain. (**b**), Debris flow forms owing to flow transformation from turbidity current beyond break in slope. The event comprises only a well mixed turbidity current in the lower Agadir canyon and exit ramp. (**c**), Debris flow forms by disintegration of initial landslide in upper canyon. The debris flow is present in the lower canyon and exit ramp but leaves no deposit (bypasses). We note that the turbidity current is actually much thicker than the debris flow in both models. Greenish shaded areas indicate gradual transition from turbidity current to debris flow. (modified after Talling et al. 2007)

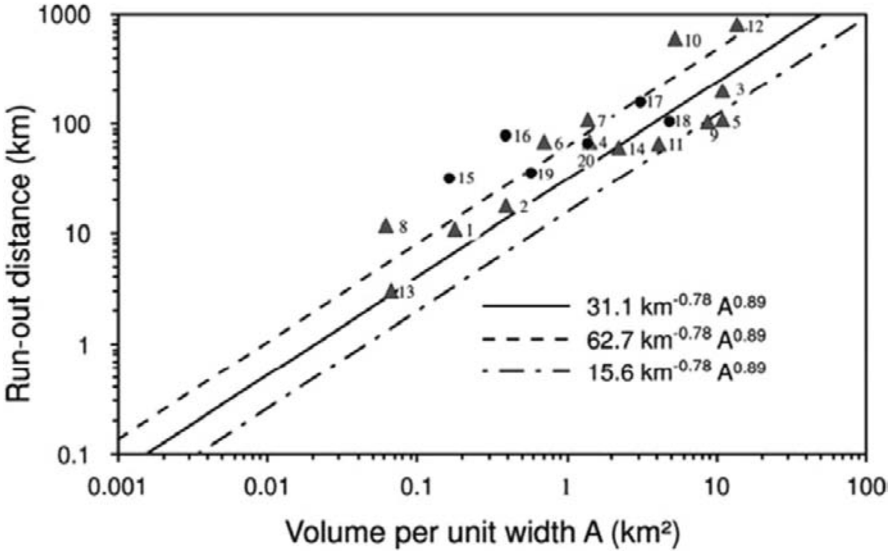

Fig. 6.25 Selected debris flows from world-wide database. 1, Kidnappers; 2, Kayak Trough; 3, Trænadjupet; 4, East Break East; 5, East Break West; 6, Sur; 7, BIG'95; 8, Afen Slide; 9, Icod; 10, Canary debris flow; 11, El Golfo; 12, Saharan debris flow; 13, New Jersey; 14, Gebra; 15, Isfjorden; 16, Storfjorden; 17, Bear Island; 18, North Sea; 19, Newfoundland f1; 20, Newfoundland f8. The lines indicate the regressions found in Storegga (adapted from Issler et al. 2005)

6.4 Risk Assessment

Amongst the submarine geohazards (Fig. 6.26), mass movements and their related phenomena pose a significant threat to coastal and seafloor structures, and coastal communities. Because of the great extent and types of submarine mass movements and their related capacity to reach very large distances, evaluating the risk associated with submarine mass movements requires an approach that is quite different from what is seen on land. One of the major differences is the very remote source which must be considered in the risk assessment procedure, i.e. for example, the very long run out of debris flows and turbidity currents can sometime reach distance more than 500 km, which is nothing comparable to sub-aerial situation regarding mass movements.

If one considers the example of the mouth of the Fraser River (Fig. 6.27), elements at risk near or at the shoreline are quite diversified not to mention the inhabited area not so far away from the beach. At this location, a major submarine slide generated by a strong earthquake could cause significant damages locally, but also at very large distances, depending on the seafloor configuration and water depth. This is one of the reasons why the VENUS project has selected this site to develop slope stability monitoring tools as part of larger ocean observatories (Lintern and Hill 2008).

Submarine mass movements, as they cover large areas, can have a significant impact on benthic ecosystems and fishing habitats. A good example of this was the impact of the Saguenay flood disaster on the Saguenay Fjord where the sediments which accumulated destroyed most of the benthic species who could recover within about 3 years of the event (see Locat et al. 2003 for more details on various components of this project).

As for the case of tsunamigenic landslides, from known cases of major submarine mass movements, the preliminary investigation may initially have to

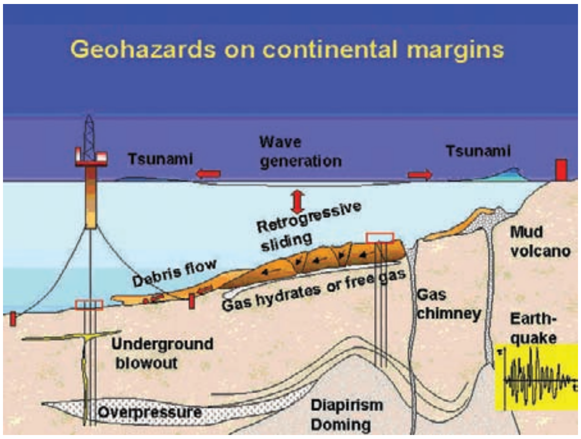

Fig. 6.26 Potential geohazards on deepwater margins (from Nadim and Locat 2005)

Fig. 6.27 The mouth of the Fraser delta and the infrastructures at risk: a VENUS location for monitoring submarine slope instability (adapted from Lintern and Hill 2008)

be conducted over a very large area, (e.g. in a radius of about 1000 km, Chaytor et al. 2007). These areas may be identified as a result of the initial inventory effort. Then a larger scale can be considered for detailed analysis to first establish the mass movement history, the remaining hazards and their potential to generate significant tsunamigenic landslides (Gonzalez et al. 2007).

In such a context, a global approach proposed by Locat (2001) for submarine risk assessment must take into account various hazards aspects related to geological setting, environmental forcing and hazard evaluation. The various elements can be used for understanding, predicting and mitigating various aspects of risk management decisions (Fig. 6.28). Many of these elements are also relevant for terrestrial hazards and risk assessment for landslides. For the sub-aqueous environment the geological model will sometime be determined with greater accuracy than on-land largely because of the use of 2D and 3D seismic data. On the other end, uncertainty will be higher than on-land for elements such as pore pressure and strength because out ability to monitor in situ pore pressure and strength is quite limited. Although cores can be obtained form the sea floor, if dissolved gas is

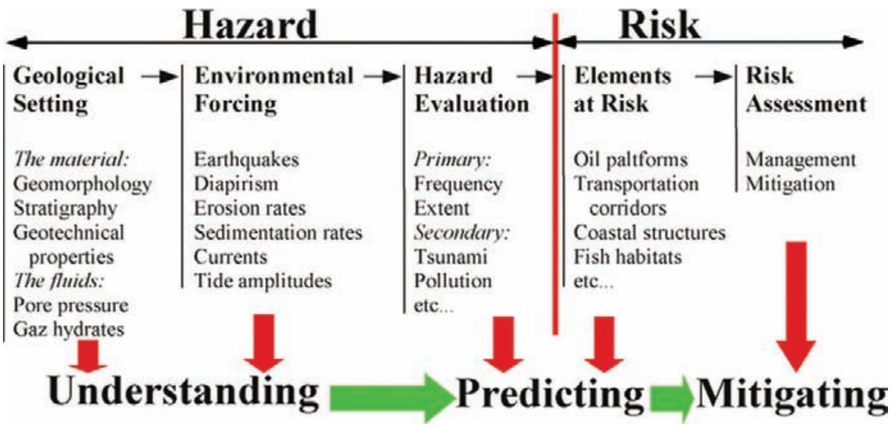

Fig. 6.28 Conceptual integration of hazard and risk components in response to understanding, predicting and mitigating impacts of submarine mass movements (modified after Locat 2001)

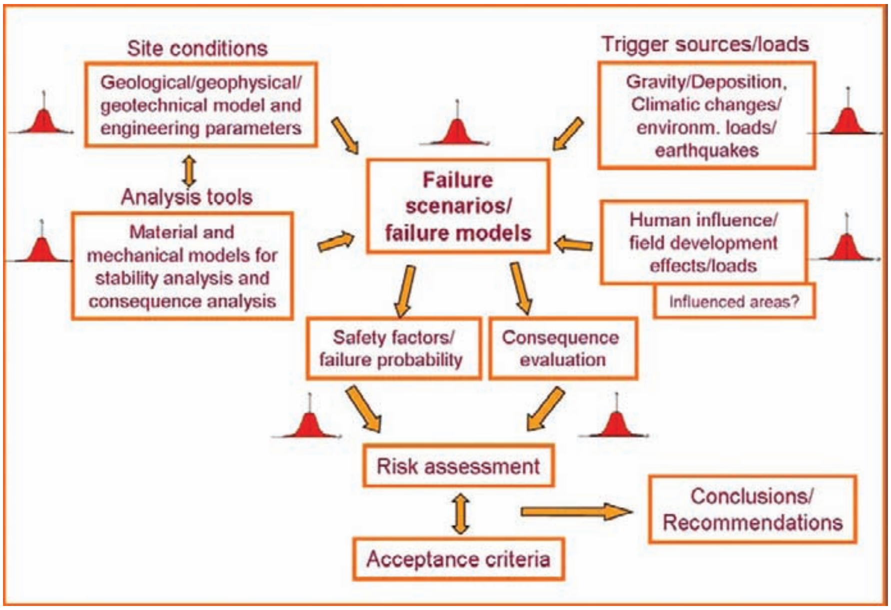

Fig. 6.29 General framework for risk assessment for submarine slides (from Nadim and Locat 2005)

present, sample disturbance will likely take place so that laboratory measurements of intact strength will often be unreliable.

From a more technical point of view, Nadim and Locat (2005) have proposed a general framework (Fig. 6.29) which has been largely validated through the Storegga project (Nadim et al. 2005) and is largely based on a statistical consideration and evaluation of uncertainty and reliability of the data or the computations.

6.5 Concluding Remarks

In the concluding remarks of the review paper on submarine landslides presented at the 8th ISL in Cardiff (Locat and Lee 2002), we underlined specific challenges on which we would like to comment below.

The integration of 3D slope stability analysis has been partly achieved by the work of IFREMER (Sultan et al. 2007a) in an attempt to understand the slope stability of the Var delta using pseudo-3D computations involving detailed bathymetry (Dan et al. 2007). At this time, the method does not use 3D seismic data for the analysis. This is still to be developed.

Recently, Tripsanas et al. (2008) have provided a synthesis of the various interpretations which can be made from core studies towards understanding and defining specific types of mass movements and their rheological characteristics.

The use of long cores to provide estimates of the frequency of catastrophic events in the aquatic environment is still needed and must be improved substantially in order to increase our capacity to evaluate the various types of submarine mass movement hazards. St-Onge et al. (2004, 2008) provides a good example of the great potential of long cores in the proximity of active instability zones. More development is expected as a result a greater interest in marine geohazards from the IODP program following the Indonisian tsunami of December 2004 (Camerlenghi et al. 2006). Good cores and in situ measurements are essential if one needs to get to the right mobilized strength. In addition, these IODP drilling proposals will offer the first opportunity, apart from the Storegga slide, to reduce the uncertainty about the geometry of the slides and their deposits so as to also improve our understanding of the characteristics of the failure surface or zone.

In situ measurement methods have also recently been developed, such as the PENFELD, which has been successfully used for in situ measurement of strength (Sultan et al. 2007a). Sultan et al. (2007b) have also illustrated the importance of in situ measurements using in situ vane and CPT in the Gulf of Lions to clearly show the impact of dissolved gas on the strength properties of sediments once they are taken on board. This is illustrated by Fig. 6.30 showing that below a depth of about 35 m, which corresponds more or less to the top of the gassy sediments, the strength results from laboratory tests start to deviate significantly from in situ results.

Identifying and understanding the physical processes involved in the transition from failure to post-failure is still a largely unresolved issue (Locat and Lee 2005). Significant contributions were made as part of understanding how the Storegga Slide disintegrated (Elverhøi et al. 2005). It is interesting here to note that the growing interest in tsunamigenic landslide research is pointing even more at the crucial role of transition processes from failure to post-failure since it has a direct influence on the acceleration and volume involved in the tsunami generation (e.g. Tinti et al. 2006, Bradshaw et al. 2007).

Monitoring the movement and observing the mobilization of actual landslides are still lacking but should improve with the development of ocean bottom and coastal observatories like the VENUS and NEPTUNE (Barnes et al. 2007) projects. Good candidates for this, in addition to the Fraser delta

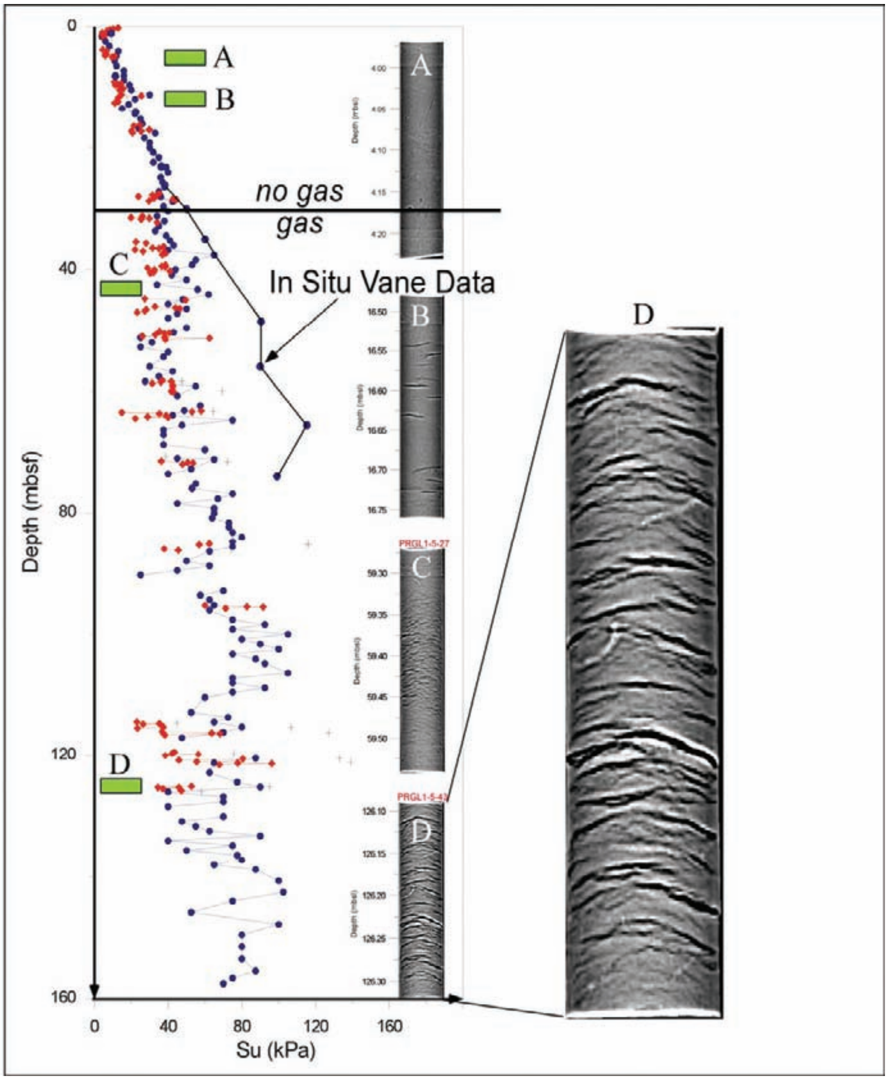

Fig. 6.30 PRGL1-5 CAT-Scan images and undrained shear strength profile for PRGL1-5: example of a strength profile obtained from in-situ testing and laboratory tests on samples from a Gulf of Lions site. (PRGL1: Borehole name in the Gulf of Lions). Green bars indicate position of samples used for CATSCAN analysis, mbsf: metes below sea floor

(Lintern and Hill 2008) are the Storegga escarpment and specific sites in the Gulf of Mexico.

Determining the role of subsurface water flow in initiating submarine landslides has been developed in recent years particularly by Dugan et al. (2007). This aspect of slope instability has not been developed here but is a crucial missing link in many cases, as it is often the case on land. For example, the study of the Finneidfjord slide (Longva et al. 2003) has shown that along fjord, the local and regional groundwater flow regime could play a significant role in both pore pressure distribution and likely the development of sensitive clays below sea level (i.e. freshwater seepage leaching the salt in a sediment that is still below the sea floor).

Integrating the role of gas hydrates in the analysis and prediction of submarine slope stability has been well developed by Sultan et al. (2004, see above) as part of the study of the Storegga slide whereas the actual geomechanical impact of gas hydrates dissociation of soil properties has been recently addressed by Gidley and Grozic (2008). Still how much (extent) gas and what rate of dissociation is needed to cause slope instability is not well known.

Evaluating the mechanics of giant submarine landslides and improving our understanding of the causes of their great runout distances still needs much additional study similar to what has been done by Vanneste et al. (2006) and Talling et al. (2007). Needed are answers on how such great mobility can be acquired and how can it take place in sediments or rocks with such high intact strength while transforming into such largely mobile debris flows.

Developing criteria to determine the cause of seafloor deposits that have been described as either landslides or migrating sediment waves has been partly achieved by the recent work of Lee et al. (2002) but for which some aspects are still being discussed (Cattaneo et al. 2004).

With respect to hazard, frequency, and extent of mass movements, significant advances have been made, as described above for risk assessment. Still, a lot of uncertainty remains because of the lack of well dated case histories. With the growing interest in coastal hazards potentially due to tsunamigenic landslides, more development is expected in the near future.

Acknowledgements The authors would like to thank K. Sassa for inviting us to contribute to the conference. We would also like to thank all of our national and international colleagues for their contributions along with various graduate students from Europe and North America who greatly contributed to the research efforts presented here. In particular we would like to thank our EuroSTRATAFORM colleagues, the U.S. Office of Naval Research, our COSTA colleagues and the related funding agencies from the United States Geological Survey and the National Science and Engineering Council of Canada. We would also like to underline the active contribution of the IGCP-511 executive including A Solheim, R. Urgeles, J. Mienert and V. Lykousis.

References

Bardet, J.-P., Synolakis, C.E., Davies, H.L., Imamura, F., and Okal, E.A., 2003. Landslide Tsunamis: Recent Findings and Research Directions. *Pure and Applied Geophysics* 160: 1793–1809.

Barnes, C.R., Bets, M.M.R., Bornhold, B.D., Juniper, S.K., Pierenne, B., Phibbs, and P. 2007. NEPTUNE Canada, University of Victoria The NEPTUNE Project – a cabled ocean observatory in the NE Pacific: Overview, challenges and scientific objectives for the installation and operation of Stage I in Canadian waters. *IEEE Explore*, pp. 308–313.

Beranger, C.E., Carpenato, R., Boote, D., and Zucarelli, F., 1998. Probabilistic assessment of rockfall impact on subsea pipelines. OMAE 1998: *Proceedings of the 17th International conference on Offshore mechanics and Arctic Engineering*, Portugal.

Biscontin, G., Pestana, J.M., and Nadim, F., 2004. Seismic triggering of submarine slides in soft cohesive soil deposits. *Marine Geology*, 203: 341–354.

Bondavik, S., Løvholt, F., Harbitzb, C., Mangerudc, J., Dawson, A., and Svendsen J.I., 2005. The Storegga Slide tsunami—comparing field observations with numerical simulations. *Marine Geology*, 22: 195–228.

Bradshaw, A.S., Baxter, C.F.P., Taylor, O.-D.S., and Grilli, S., 2007. Role of soil behavior ion the initial kinematics of tsunamigenic slides. In: V. Lykousis, D. Sakellariou and J. Locat (eds.), *Submarine Mass Movements and Their Consequences*, Springer, pp. 387–394.

Bryn, P., Berga, K., Forsberg, C.F., Solheim, A., and Kvalstad, T.J., 2005. Explaining the Storegga slide. *Marine and Petroleum Geology*, 22: 11–19.

Canals M, Lastras G, Urgeles R, Casamor JL, Mienert J, Cattaneo A, De Batist M, Haflidason H, Imbo Y, Laberg J.S., Locat J, Long D, Longva O, Masson DG, Sultan N, Trincardi F, Bryn P., 2004. Slope failure dynamics and impacts from seafloor and shallow subseafloor geophysical data: case studies from the COSTA project. *Marine Geology*, 213: 9–72.

Campbell, D.C., Duchesne, M., and Bolduc, A., 2008. Geomorphological and geophysical evidence of Holocene seafloor instability on the southern slope of the

St. Lawrence estuary, Québec. In: J. Locat, D. Perret, D. Turmel, D. Demers, and S. Leroueil (eds.), *Proceedings of the 4th Canadian Conference on Geohazards: from Causes to Management,* Presses de l'Université Laval, pp. 367–374.

Camerlenghi, A., Urgeles, R., and Ercilla, G., 2006. Scientific Ocean drilling behind the assessment of geo-hazards from submarine slides: an extended report to ECORD, IODP and the workshop participants. Magellan Workshop Series, Barcelona, 25–27 October 2006. http://www.geohazards.no/IGCP511/barcelona/ESF_Report_ECORD_IODP.pdf.

Cattaneo, A., Correggiaria, A., Marsset, T., Thomas, Y., Marsset, B., and Trincardi, F., 2004. Seafloor undulation pattern on the Adriatic shelf and comparison to deep-water sediment waves. *Marine Geology*, 213: 212–148.

Cauchon-Voyer, G., Locat, J., and St-Onge, G., 2008. Late-Quaternary morpho-sedimentology and submarine mass movements of the Betsiamites area, Lower St. Lawrence Estuary, Quebec, Canada. *Marine Geology*, 251: 233–252.

Chaytor, J.D., Twichell, D.C., ten Brink, U., Buczkowski, B.J., and Andrews, B.D., 2007. Revisiting submarine mass movements along the U.S. Atlantic continental margin: implicaiotns fro tsunami hazards. In: V. Lykousis, D. Sakellariou and J. Locat (eds.), *Submarine Mass Movements and Their Consequences*, Springer, pp. 395–403.

Chiocci, F., Romagnoli, C., and Bosman, A., 2008. Morphologic resilience and depositional processes due to the rapid evolution of the submerged Sciara del Fuoco (Stromboli Island) after the December 2002 submarine slide and tsunami. *Marine Geology*, in press.

Dan, D., Sultan, N., and Savoye, B., 2007. The 1979 Nice harbour catastrophe revisited: Trigger mechanism inferred from geotechnical measurements and numerical modeling. *Marine Geology*, 245: 40–64.

Deplus, A.C., Friant, A.L., Boudon, G., Komorowski, J.-C., Villemant, B., Harford, C., Ségoufin, J., and Cheminée, J., 2001. Submarine evidence for large–scale debris avalanches in the Lesser Antilles Arc. *Earth and Planetary Science Letters* 192: 145–157.

Divins, D.L., 2008. NGDC Total Sediment Thickness of the World's Oceans & Marginal Seas, Retrieved date goes here, http://www.ngdc.noaa.gov/mgg/sedthick/sedthick.html.

Dugan, B., Flemings, P.B., Uregles, R., Sawyer, D., Iturrino, G.J., Moore, J.C., Schneider, J., 2007. Physical Properties of Mass Transport Complexes in the Ursa Region, Northern Gulf of Mexico (IODP Expedition 308) Determined from Log, Core, and Seismic Data. *Proceedings Offshore Technology Conference*, Paper OTC 18704.

Edmunds, M., Bryant, C., Crozier, J. Gilmour, P., Pickett, P., Stewart, K., and Williams, J., 2006. Port Phillip Bay Channel Deepening Project. Trial Dredging Experiment: Deep Reef Impact Assessment. Report to Port of Melbourne Corporation. Australian Marine Ecology Report 334, Melbourne.

Elverhøi, A., Issler, D., De Blasio, F.V., Ilstad1, T., Harbitz, C.B., and Gauer, P., 2005. Emerging insights into the dynamics of submarine debris flows. *Natural Hazards and Earth System Sciences*, 5: 633–648.

Fine, I.V., Rabinovich, A.B., Bornhold, B.D., Thomson, R.E., and Kulikov, E.A., 2005. The Grand Banks landslide-generated tsunami of November 18, 1929: preliminary analysis and numerical modeling. *Marine Geology*, 215: 45–57.

Fleming, K., Johnston, P., Zwartz, D., Yokoyama, Y., Lambeck, K., Chappell, J., 1998. Refining the eustatic sea level curve since Last Glacial Maximum using far-intermediate field sites. *Earth and Planetary Science Letters*, 163: 327–342.

Gee, MJ.R., Uy, H.S., Warren, J., Morley, C.K., and Lambiase, J.J., 2007. The Brunei slide: a giant submarine landslide on the North West Borneo margin revealed by 3D seismic data. *Marine Geology*, 246: 9–23.

Greene, H.G., Maher, N.M. and Paull, C.K. 2002. Physiography of the Monterey Bay national Marine Sanctuary and implications about continental margin development. *Marine Geology*, 181, 55–82.

Gidley, I., and Grozic, J.L.H., 2008. Gas hydrates dissociation structures in subm,arine slopes. In: J. Locat, D. Perret, D. Turmel, D. Demers and S. Leroueil (eds.), *Proceedings of the 4th Canadian Conference on Geohazards: from Causes to Managements*, Presses de l'Université Laval, pp. 81–88.

Gonzalez, F.I., Bernard, E., Dunbar, P., Geist, E., Jaffe, B., Kanoglu, U., Locat, J., Mofjeld, H., Moore, A., Synolakis, C., Titov, V., and Weiss, R. (Science Review Working Group), 2007. Scientific and technical issues in tsunami hazard assessment of nuclear power plant sites. NOAA Technical Memorendum OAR PMEL-136, Pacific Marine Environmental Laboratory, Seattle, WA, 125pp. + appendices on CD.

Garziglia, S., Ioulalen, M., Migeon, S., Ducassou, E., Mascle, J., Sardou, O., and Brosolo, L., 2007. Triggering factors and tsunamigenic potential of a large submarine mass failure on the western Nile margin (Rosetta area, Egypt). In: V. Lykousis, D. Sakellariou and J. Locat (eds.), *Submarine Mass Movements and Their Consequences*, Springer, pp. 347–356.

Guyard, H., St-Onge, g., Chapron, E., Anselmetti, F.S., and Francus, P., 2007. The AD 1881 earthquake triggered sluimp and late Holocene flood-induced turbidites from proglacial lake Bramant, eastern French Alps. In: V. Lykousis, D. Sakellariou and J. Locat (eds.), *Submarine Mass Movements and Their Consequences*, Springer, pp. 279–286.

Haflidason, H., Lien R., Sejrup, H.P., Forsberg, C.F., and Bryn, P., 2005. The dating and morphometry of the Storegga slide. *Marine and Petroleum Geology*, 22: 123–136.

Heezen, B.C., and Ewing, M. 1952. Turbidity current and submarine slumps, and the 1929 Grand Banks earthquake. *American Journal of Science*, 250: 849–873.

Hughes Clarke, J.E., Mayer, L.A., and Wells, D.E. (1996). Shallow-water imaging multibeam sonars: A new tool for investigating seafloor processes in the coastal zone and on the continental shelf. *Marine Geophysical Research*, 18: 607–629.

Hünerbach, V., and Masson, D.G., 2004. Landslides in the North Atlantic and its adjacent seas: an analysis of their morphology, setting and behaviour. *Marine Geology*, 213: 343–362.

Huvenne, V.A.I., Croker, P.F., and Henriet, J.-P., 2002. A refreshing 3D view of an ancient sediment collapse and slope failure. *Terra Nova*, 14, 33–40.

Issler, D., De Blasio, F.V., Elverhøi, A., Bryn, P., and Lien, R., 2005. Scaling behaviour of clay-rich submarine debris flows. *Marine and Petroleum Geology*, 22: 187–194.

Jeong, S.W., Locat, J., and Leroueil, S., 2004. A preliminary analysis of the rheological transformation due to water infiltration as a mechanism for high mobility of submarine mass movements. *In: Proceedings of the 57th Canadian Geotechnical Conference*, Québec City, session 7G, pp. 15–22.

Kokusho, T., Kojima, T., 2002. Mechanism for postliquefaction water ¢lm generation in layered sand. *Journal of Geotechnique and Geoenvironmental Engineering*, 128: 129–137.

Kvalstad, T.J., Andresen, L., Forsberga, C.F., Berg, K., Bryn, P., and Wangen, M., 2005. The Storegga slide: evaluation of triggering sources and slide mechanics. *Marine and Petroleum Geology*, 22: 245–256.

Lajeunesse, P., St-Onge, G., Rendall, K., and Moreau-Labrecque, A., 2008. Mouvements de masse subaquatiques postglaciaires au lac Jacques-Cartier, Réserve faunique des Laurentides (Québec): résultats préliminaires. In: J. Locat, D. Perret, D. Turmel, D. Demers and S. Leroueil (eds.), *Proceedings of the 4th Canadian Conference on Geohazards: from Causes to Managements*, Presses de l'Université Laval, pp. 313–321.

Le Bas, T.P., Masson, D.G., eand Holtom, R.T., 2007. Slope failures of the flanks of the Southern Cape Verde islands. In: V. Lykousis, D. Sakellariou and J. Locat (eds.), *Submarine Mass Movements and Their Consequences*, pp. 337–345.

Lee, H.J., Locat, J., Desgagnés, P., Parson, J., McAdoo, B., Orange, D., Puig, P., Wong, F., Dartnell, P., and et Boulanger, É., 2007a. Submarine Mass Movements. In: C. Nittrouer et al. (eds.), *Continental-margin Sedimentation: Transport to Sequence*, Special publication No. 37 of the International Association of Sedimentologists, pp. 213–275.

Lee, H.J., Ryan, H., Haeussler, P.J., Kayen, R.E., Hampton, M.A., Locat, J., Suleimani, E., and Alexander, C., 2007b. Reassessment of seismically induced tsunamigenic submarine slope failures in Port Valdez, Alaska, USA. In: V. Lykousis, D. Sakellariou and J. Locat (eds.), *Submarine Mass Movements and Their Consequences*, Springer, pp. 357–365.

Lee, H., Syvitski, J.P.M., Parker, G., Orange, D., Locat, J., Hutton, E.W.H., Imran, J., 2002. Distinguishing sediment waves from slope failure deposits : field examples including the 'Humboldt slide', and modeling results. *Marine Geology*, 192: 79–104.

Levesque, C., Locat, J., et Leroueil, S., 2006. Dating submarine mass movements triggered by earthquakes in the Upper Saguenay Fjord, Quebec, Canada. *Norwegian Journal of Geology*. 86: 231–242.

L'Heureux, J.-S., Longva, O., Hansen, L., and Vingerhagen, G., 2007. The 1990 submarine slide outside the Nidlev river mouth, Trondheim, Norway. In: V. Lykousis, D. Sakellariou and J. Locat (eds.), *Submarine Mass Movements and Their Consequences*, Springer, pp. 259–268.

Lintern, D.G., and Hill, P.S., 2008. Using the VENUS underwater network to assess conditions leading to slope failures. In: J. Locat, D. Perret, D. Turmel, D. Demers and S. Leroueil (eds.), *Proceedings of the 4th Canadian Conference on Geohazards: from Causes to Managements*, Presses de l'Université Laval, pp. 189–193.

Locat, J., 2001. Instabilities along ocean margins: a geomorphological and geotechnical perspective. *Marine and Petroleum Geology*, 18: 503–512.

Locat, J., 2008. Localisation et magnitude du séisme du 5 février 1663 (Québec) revues à l'aide des mouvements de terrain. In: J. Locat, D. Perret, D. Turmel, D. Demers and S. Leroueil (eds.), *Proceedings of the 4th Canadian Conference on Geohazards: from Causes to Managements*, Presses de l'Université Laval, pp. 429–444.

Locat, J., Galvez-Cloutier, R., and R.C. Chaney 2003a. Contaminated Sediments: Characterization, Evaluation, Mitigation/Restoration, and Management Strategy Performance. *American society for Testing Materials (ASTM), Special Technical Publication (STP)* 1442, 343p.

Locat, J., and Lee, H., 2002. Submarine landslides : advances and challenges. *Canadian Geotechnical Journal*, 39: 193–212.

Locat, J., and Lee, J., 2005. Subaqueous Debris Flows. Chapter 9, In: Mathias et Hungr (eds.), *Debris-flows Hazards and Related Phenomena*, Springer, pp. 203–245.

Locat, J., Locat, P., Locat, A., et Leroueil, S., 2007. Linking geotechnical and rheological properties from failure to post-failure: the Pointe-du-Fort slide, Saguenay Fjord, Québec. In: V. Lykousis, D. Sakellariou and J. Locat (eds.), *Submarine Mass Movements and Their Consequences*, pp. 181–189.

Locat, J., Mayer, L., Gardner, J., Lee, H., Kamerrer, E., and Doucet, N., 1999. The use of multibeam surveys for submarine landslide investigations. *In: International Symposium on: Slope Stability Engineering: Geotechnical and Geoenvironmental Aspects*, Shikoku, pp. 127–134.

Locat, J., and Mienert, J., 2003. Submarine mass Movements and Their Consequences, *Kluwer series on Natural and Technological Hazards*, 542p.

Locat, J., Norem, H., and Schieldrup, N., 1990. Modélisation de la dynamique des glissements sous-marins. *In: Proceedings of the 6th Congress of the International Association of Engineering Geology*, Amsterdam, pp. 2849–2855.

Locat, J., Tanaka, H., Tan, T.S., Dasari, G.R., and Lee, H., 2003b. Natural soils: geotechnical behavior and geological knowledge. In: T.S. Tan et al. (ed.), *Characterisation and Engineering Properties of Natural Soils*, Balkema, vol. 1: 3–28.

Locat, P., Couture, R., Leroueil,. S., Locat, J., and Jaboyedoff, M., 2006. Fragmentation energy in rock avalanches. *Canadian Geotechnical Journal*, 43: 830–851.

Locat, P., Leroueil, S., and Locat, J., 2008. Remaniement et mopbilité des debris de glissements de terrain dans les argiles sensibles de l'est du Canada. In: J. Locat, D. Perret, D. Turmel, D. Demers and S. Leroueil (eds.), *Proceedings of the 4th Canadian Conference on Geohazards: from Causes to Managements*, Presses de l'Université Laval, pp. 97–106.

Longva, O., Janbu, N., Blikra, L.H., and Boe, R., 2003. The 1996 Finneidfjord slide; seafloor failure and slide dynamics. In: J. Locat and J. Mienert (eds.), Submarine Mass Movements and Their Consequences, Kluwer, pp. 531–538.

Lykousis, V., Sakellariou, D., and Locat, J. (eds.), 2007a. 3rd Symposium on Submarine Mass Movements and Their Consequences. *Advances in Natural and Technical Hazards Research,* Springer, vol. 27, 424p.

Lykousis, V., Sakellariou, D., Rousakis, G., Alexandri, S., Kaberi, H., Nomikou, P., Georgiou, P., and Balas, D. 2007b. Sediment failure processes in active grabens: the western gulf of Corinth (Greece). In: V. Lykousis, D. Sakellariou and J. Locat (eds.), *Submarine Mass Movements and Their Consequences*, Springer, pp. 297–305.

Martinez, J.F., Cartwright, J., and Hall, B., 2005. 3D seismic interpretation of slump complexes: examples from the continental margin of Israel. *Basin Research*, 17: 83–108.

Mazzanti, P., Bozzano, F., and Esposito, C., 2007. Submurged landslide morphologies in the Albano Lake (Rome, Italy). In: V. Lykousis, D. Sakellariou and J. Locat (eds.), *Submarine Mass Movements and Their Consequences*, pp. 243–250.

Mosher, D., C., 2008. Submarine mass movements in Canada: geohazards with far reaching implications. In: J. Locat, D. Perret, D. Turmel, D. Demers and S. Leroueil (eds.), *Proceedings of the 4th Canadian Conference on Geohazards: from Causes to Management,* Presses de l'Université Laval, pp. 55–62.

Mosher, D.C., and Piper, D.J.W., 2007. Analysis of multibeam seafloor imagery of the Laurentian Fan and the Grand Banks landslide area. In: V. Lykousis, D. Sakellariou and J. Locat (eds.), *Submarine Mass Movements and Their Consequences*, pp. 77–88.

Nadim, F., and Locat, J., 2005. Risk assessment for submarine slides. In: O. Hungr, R. Fell, R. Couture, and E. Eberhardt, Eds., *Landslide Risk Management*, Balkema, pp. 321–333.

Nadim, F., Kvalstada, T.J., and Guttormsen, T., 2005. Quantification of risks associated with seabed instability at Ormen Lange. *Marine and Petroleum Geology*, 22: 311–318.

Norem, H., Locat, J., and Scheldrup, B., 1990. A new approach to the study of the dynamics of submarine slides. *Marine Geotechnology*, 9: 93–112.

Prior, D.P., Doyle, E.H., and Neurauter, T., 1986, The Currituck Slide, Mid Atlantic continental slope-revisited. *Marine Geology*, 73: 25–45.

Sansoucy, M., Locat, J., and Lee, H., 2007. Geotechnical considerations of submarine canyon formation: the case of the Cap de Creus canyon. In: V. Lykousis, D. Sakellariou and J. Locat (eds.), *Submarine Mass Movements and Their Consequences*, Springer, pp. 221–230.

Schwab, W.C., Lee, H.J., Twichell, D.C., Locat, J., Nelson, H.C., McArthur, M., and Kenyon, N.H., 1996. Sediment mass-flow processes on a depositional lobe, outer Mississippi Fan. *Journal of Sedimentary Research*, 66: 916–927.

Solheim, A., 2006. Submarine mass movements and their consequences, 2nd international symposium: Summary. *Norwegian Journal of Geology*, 86(3): 151–154.

Solheim, A., Bryn, P., Sejrup, H.P., Mienert, J., and Berg, K., 2005. Ormen Lange—an integrated study for the safe development of a deep-water gas field within the Storegga Slide Complex, NE Atlantic continental margin; executive summary. *Marine and Petroleum Geology*, 22: 1–9.

St-Onge, G., Chapron, E., Guyard, H., Rochon, A., Lajeunesse, P., Locat, J., Scott, D., Stoner, J.S., and Hillaire-Marcel, C., 2008. High-resolution physical and magnetic properties of rapidly deposited layers associated with landslides, earthquakes, and floods. In: J. Locat, D. Perret, D. Turmel, D. Demers and S. Leroueil (eds.), *Proceedings of the 4th Canadian Conference on Geohazards: from Causes to Management,* Presses de l'Université Laval, pp. 219–228.

St-Onge, G., Mulder, T., Piper, D.J.W., Hillaire-Marcel, C., and Stoner, J.S., 2004. Earthquake and flood-induced turbidites in the Saguenay Fjord (Québec): a Holocene paleoseismicity record. *Quaternary Science Reviews*, 23: 283–294.

Sultan, N., Cochonat, P., Foucher, J.-P., and Mienert, J., 2004. Effect of gas hydrates melting on seafloor slope instability. *Marine Geology*, 211: 379–401.

Sultan, N., Gaudin, M., Berné, S., Canals, M., Urgeles, R., and Lafuerza, S., 2007a. Analysis of slope failures in submarine canyon heads: An example from the Gulf of Lions. *Journal of Geophysical Research*, 112: 1–61.

Sultan, N., Voisset, M., Marsset, B., Marsset, T.E., Cauquil, E., and Colliat, J.-L., 2007b. Potential role of compressional structures in generating submarine slope failures in the Niger Delta. *Marine Geology*, 237: 169–190.

Tappin, D.R., Watts, P., McMurtry, G.M., Lafoy, Y., and Matsumoto, T., 2001. The Sissano Papua New Guinea tsunami of July 1998, offshore evidence on the source mechanism. *Marine Geology*, 175: 1–23.

ten Brink, U., Twichell, D., Geist, E., Chaytor, J., Locat, J., Lee, H., Buczkowski, B., and Sansoucy, M., 2007. Report on the Current State of Knowledge Regarding Potential Tsunami Sources Affecting the U.S. Atlantic and Gulf Coasts: U.S. Geological Survey Administrative Report. 154p.

Tinti, S., Pagnoni1, G., and Zaniboni, F., 2006. The landslides and tsunamis of the 30th of December 2002 in Stromboli analysed through numerical simulations. *Bulletin of Volcanology*, 68: 462–479.

Tinti, S., Zaniboni, Z., Armigliato, A., Pagnoni, G., Gallazzi, S., Manucci, A., Brizuela Reyes, B., Bressan, L., and Tonini, R., 2007. Tsunamigenic landslides in the Western Corinth Gulf: numerical scenarios. In: V. Lykousis, D. Sakellariou and J. Locat (eds.), *Submarine Mass Movements and Their Consequences*, Springer, pp. 405–414.

Talling, P.J., Wynn, R.B., Masson, D.G., Frenz, M., Cronin, B.T., Schiebel, T., Akhmetzhanov, A.M., Dallmeier-Tiessen, S., Benetti, S., Weaver, P.P.E., Georgiopoulou, A., Zühlsdorff, C., and Amy, L.A., 2007. Onset of submarine debris flow deposition far from original giant landslide. *Nature*, 450: 541–544.

Tripsanas, E.K., Piper, D.j.W., Jenner K.A., and Bryant, W.r., 2008. Submarine mass-transport facies: new perspectives on flow processes from cores on the eastern North American margin. *Sedimentology*, 55: 97–136.

Turmel, D., and Locat, J., 2008. Numerical modeling of underwater rockfall. In: J. Locat, D. Perret, D. Turmel, D. Demers and S. Leroueil (eds.), *Proceedings of the 4th Canadian Conference on Geohazards: from Causes to Management,* Presses de l'Université Laval, pp. 245–252.

Vanneste, M., Mienert, J., and Bünz, S., 2006. The Hinlopen Slide: A giant, submarine slope failure on the northern Svalbard margin, Arctic Ocean. *Earth and Planetary Science Letters*, 245: 373–388.

Vaunat, J., and Leroueil, S., 2002. Analysis of post-failure slope movements within the framework of hazard and risk analysis. *Natural Hazards*, 26: 83–109.

Satellite Remote Sensing Applications for Landslide Detection and Monitoring

7

Vern Singhroy

Abstract This paper provides a brief overview of the application potential of EO images related to landslides mapping and monitoring. Our challenge is to recognize and interpret the detailed geomorphic characteristics of large and small landslides, and determine whether or not failure is likely to occur. It is clear from the examples provided that remote sensing images are increasingly being used because applications are becoming more convincing relative to traditional mapping and monitoring methods.

The examples shows that current high resolution stereo SAR and optical images are producing multi scale landslide inventory maps to improve mitigation. The availability of less than 3-m resolution stereo images from SAR and optical are providing, near air photo type geomorphic information on slopes, for more reliable landslide inventory maps.

Landslide prediction will remain complex and difficult even with ground monitoring techniques. Our examples have shown that InSAR results are complementary data sources relative to ground based observations, and are especially useful where other data sources are limited over large areas. Detail deformation maps produced from InSAR techniques are assisting in more accurate slope stability studies. When the acquisition and ground conditions are correct, SAR interferometry is a useful tool for detecting and monitoring mass movement and thus is able to contribute to the assessment and mitigation of landslide hazards.

Keywords InSAR • Landslide monitoring • Landslide inventory

7.1 Introduction

Landslides are among one of the serious geological hazards which threaten and influence the socioeconomic conditions of many countries. (Schuster, 1996). Large scale, stereo aerial photographs have been extensively applied in landslide investigations for several decades. They are very useful for the recognition, characterization and geomorphic analysis of landslides. Recently, there has been a considerable increase in satellite remote sensing images for slope stability investigations mainly because of the recent availability of high resolution radar and optical Earth Observation (EO) satellite systems and the development of advanced images processing tools such as InSAR monitoring techniques as shown by Singhroy 2005 and others.

Vern Singhroy (✉)
Canada Centre for Remote Sensing, Canada

K. Sassa, P. Canuti (eds.), *Landslides – Disaster Risk Reduction*,
© Springer-Verlag Berlin Heidelberg 2009

This paper provides examples of the uses of satellite images to detect and monitor landslide activity in different geologic environment. These examples should be used as a guide for the uses of remote sensing to map and monitor landslides.

7.2 Landslide Mapping

Stereo aerial photographs are used extensively to produce landslide inventory maps. They allow the identification of geomorphic, geologic and related land use features related to landslides as demonstrated from many studies such as Mollard and Janes, 1993, Guzzetti, 1990, Varnes (1974) and others (Fig. 7.1). Geological and geomorphological units related to landslide inventories can be interpreted on the basis of morphological, textural, and structural characteristics using stereo aerial photos and several types of remote sensing images. Landslide inventories using multi resolution remote sensing images to detect landslides and interpret their geomorphology and related geological units are usually mapped at

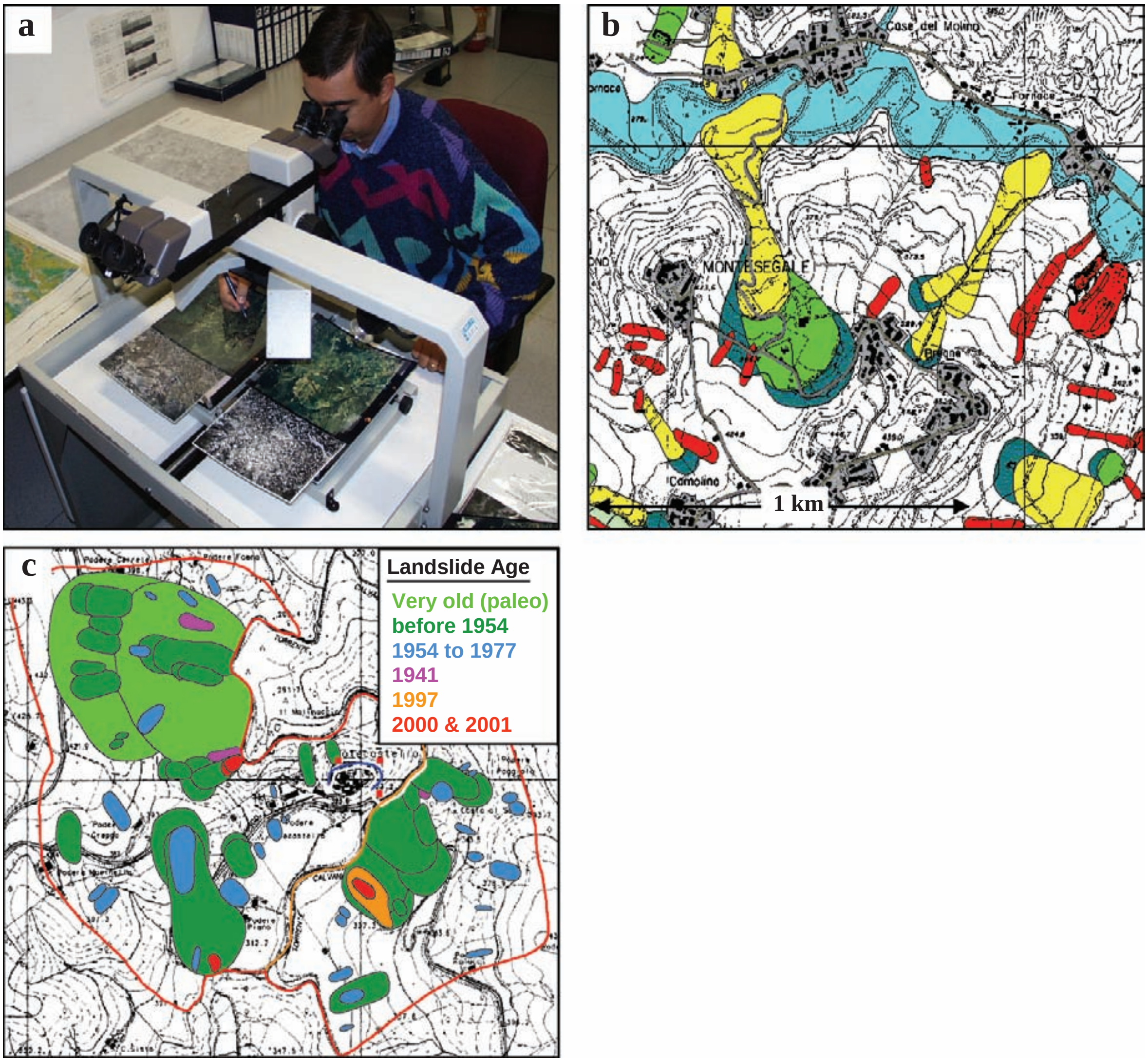

Fig. 7.1 Interpretation of stereo airphotos to produce 1: 100 000 scale landslide inventory maps of Italy (**a**). The various colour units refer to landslide types (**b**) and ages (**c**) (Guzzetti, 1990)

various scales, such as national (1;1000000), regional (1:100000), medium (1:25000–50000), and large scales (> 1:15000).

For instance, if the landslide inventory is being published at 1:15000, stereo aerial photos from 1:15000–1:25000 scale is the most useful. The amount of detail analytical information which helps the interpreter to make conclusions on type and causes of the landslide, will be very limited at scales smaller than 1:25000. Therefore, the suitability of remote sensing images for landslide inventory mapping is determined by the size of individual slope failures and the ground resolution cell of the image. Our experience has shown that 3-m stereo images are the most useful for detail landslide classification and interpretation for large scale inventories. Recent studies have shown that high resolution satellite images were cost effective compared to air photos for detailed landslide hazard assessment over large areas. The DEMs created from IKONOS stereo images are shown to be sensitive to micro terrain features than the maps created from digital contour data (Nichol et al. 2006). Table 7.1 show a selected list of the current high resolution radar satellites that are relevant for landslide inventory and related land use mapping. Many high resolution (less than 3 m) satellites images are available commercially. Recently, the combined use of both recent high resolution satellite images and existing air photos are increasingly being used for updating landslide inventory.

Bulmer (2002) used two distinct approaches to determine the characteristics of different landslides from remotely sensed data. With these approaches it is possible to derive qualitative and quantitative parameters on landslides that are necessary for improved understanding of landslide processes. The first approach is to determine the number, distribution, type, and geomorphology of landslides using remotely sensed data. The second approach measures the dimensions (length, width, thicknesses and local slope) along and across the landslides using imagery and topographic profiles. However when selecting and using remotely sensed data, Bulmer (2002) noted that the goal should be to determine: (1) the local lithology, (2) aerial extent of landslide deposits at each site, (3) local age relationships, (4) examine evidence for the cause and frequency of emplacement, (5) look for differences in landslide morphologies as keys to the magnitude and types of mass movement events, and (6) measure dimensions, slopes (local and regional), volumes, and material sizes.

Table 7.1 SAR system summary

	Design Life	Imaging frequency	Spatial resolution	Polarization	Look direction	Status
RADARSAT-2 	7 years	C-Band, 5.405 GHz	3 to 100 meters	Single (HH, VV, VH, HV) Dual (HH/ HV, VV/VH) Polarimetric	Left- and right-looking	Launch 2007 Dec
RADARSAT-1 	5 years	C-Band, 5.3 GHz	10 to 100 m	Single HH	Right-looking	In operation (Since 95)
Envisat ASAR 	5 years	C-Band, 5.331 GHz	30 to 1000 meters	Single (HH, VV) Alternating (VV/HH, VV/VH, HH/HV)	Right-looking	In operation (Since 02)
TerraSAR-X 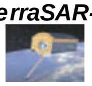	5 years	X-Band, 9.650 GHz	1 to 15 meters	Single (HH, VV) Dual (VV/HH, VV/VH, HH/HV)	Left-and right-looking	Launch 2007
ALOS PALSAR	5 years	L-Band, 1.27 GHz	10 to 100 meters	Single (HH, VV) Dual (HH/ HV, VV/VH) Polarimetric (exp.)	Right-looking	Launch 2005
COSMO-Skymed	5 years	X-Band, 9.6 GHz	1 to 100 meters	Single (HH, VV, VH, HV) Polarimetric	Left- and right-looking	2 Launch in 2007

There is a need to integrate both high and medium resolution images obtained airborne and spaceborne sensors to locate landslides for regional and national inventories Satellite images are generally lower spatial and temporal resolution, but they have the advantage of providing synoptic regional coverage and offer spatial continuity. The higher resolution airborne system is used to combine the advantage of spatial coverage offered by EO with both higher resolution, and better control on acquisition timing when sensing

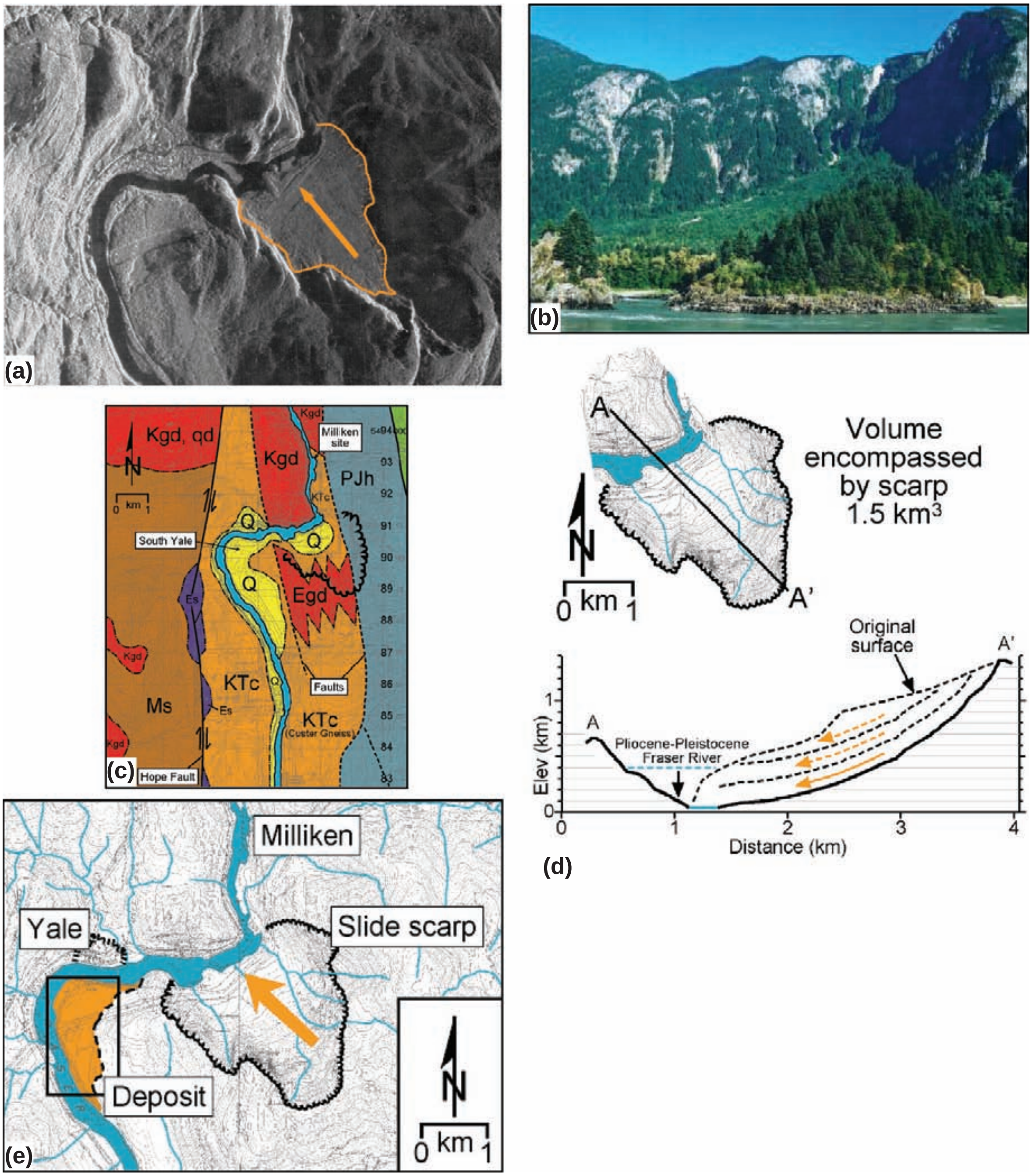

Fig. 7.2 South Yale Slide, Hope B.C. Canada, depicted in a high-resolution airborne radar image (**a**) and field photograph (**b**). Geological setting (**c**), slide transect (**d**), and inventory map (**e**)

a specific event. This was particularly true in the case of the recent may 2008 earthquake event in Shezwen Province, China where both high resolution airborne and lower resolution satellite images were combined to map the large amount of landslides triggered from the magnitude 8 earthquake.

Recent research has shown that high-resolution stereo SAR and optical images, combined with topographic and geological information have assisted in the production of landslide inventory maps (Singhroy et al., 1998; Singhroy and Mattar, 2000). The multi-incidence angle, stereo and high-resolution capabilities of the various radar satellites (Table 7.1) are particularly useful for landslide inventory maps Fig. 7.2 shows the uses of high resolution (3 m) airborne SAR is particularly useful to interpret and map deep seated landslide features and related geological units and structural features in the upper Fraser valley in British Colombia, Canada. Singhroy et al. (1998) has provided some simple guidelines for the selection of multi-incidence RADARSAT images to facilitate the mapping of geomorphic features of these large deep-seated slides. Image fusion and 3d visualization techniques combining optical and SAR images and DEM are particularly useful for regional landslide inventory mapping as shown in Fig. 7.3.

Other high-resolution optical systems such as IKONOS, IRS (Table 7.2) and the stereo capability of SPOT 4 are useful for landslide recognition and related land use mapping. Where possible, the highest resolution data that is available should be obtained and used to identify a range of geomorphic features and dimensional data on landslides of interest. Large landslides are easily recognized on 30 m Landsat TM images.

Disaster response comprises the rapid damage assessment, and relief operations, once the disaster

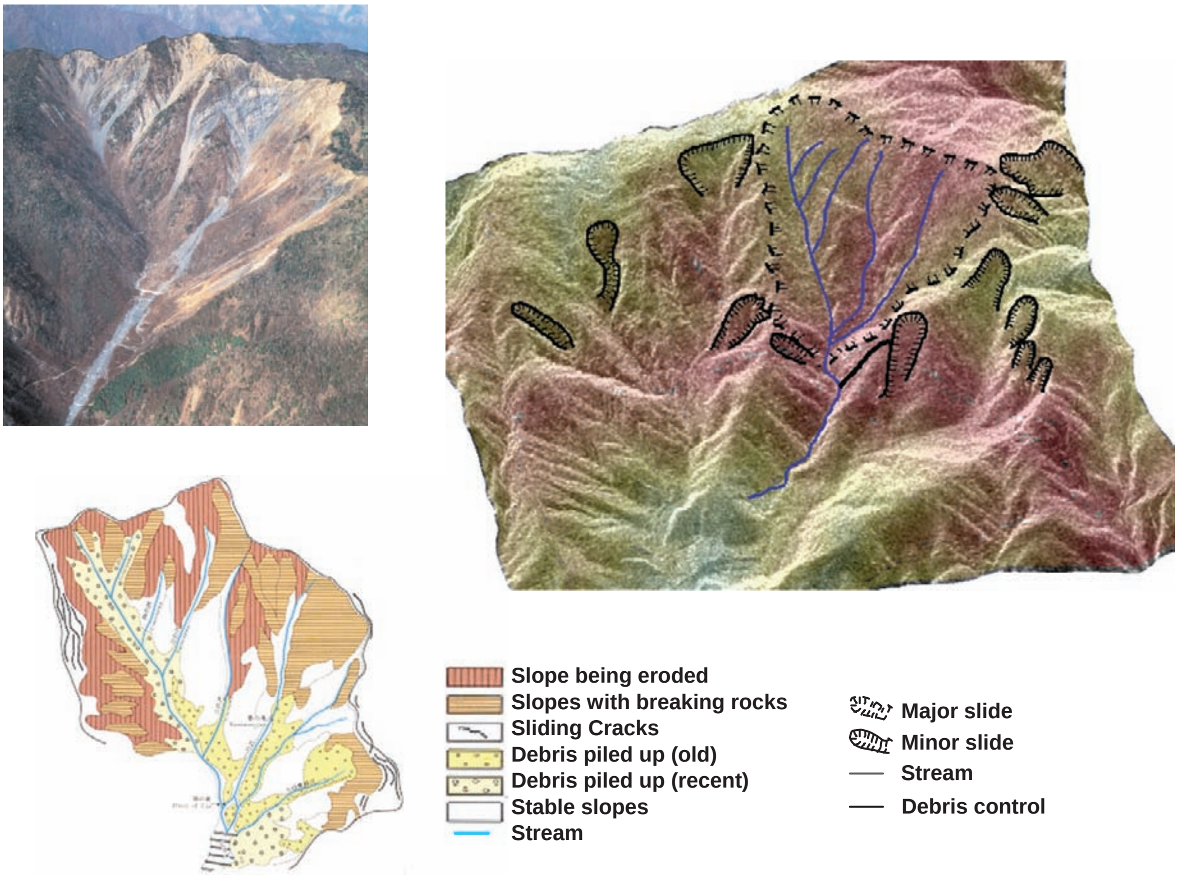

Fig. 7.3 Interpretation of RADARSAT image draped over DEM for landslide inventory in upper Oya Valley in Japan

Table 7.2 Landslides from satellite observations (modified from IGOS 2003)

Required Observations	Background monitoring/Assessment	Crisis Response
Characterize deformation with high accuracy and frequency (horizontal and vertical).	GPS network of stations continuously transmitting or reoccupied as necessary.	Additional GPS stations as needed to capture deformation. More frequent occupation (if data not continuously transmitted).
	Satellite, airborne and ground-based SAR interferometry at various wavelengths.	Request more frequent satellite tasking plus search archives for additional possible image pairs.
	Frequency depending on the type of ground instability (1 month to 1 year).	
	Other surveys e.g. leveling, laser scanning (terrestrial and airborne), aerial photography and high-resolution stereo satellite data, borehole inclinometers.	More frequent occupation of all ground-based instrumentation (if data not continuously recorded and transmitted).
	Frequency depending on the type of ground instability (1 month to 1 year).	
Map landslides, geomorphology, land-use, land cover, geology, structures, and drainage network.	Map existing landslides, depositional/ erosional processes, geologic structures, land-use and land cover using high-medium spatial resolution satellite and airborne imagery, aerial photography and geological and geophysical ground surveys.	Request over-flights to check extent and distribution of landslides.
Topography/Elevation (incl. Slope angle, slope length, slope position).	High quality DEM from LiDAR, photogrammetry or high-resolution satellites and InSAR techniques	Rapid local update needed of how the landscape has changed.
Soil strength parameters and physical properties (incl. clay mineralogy, weathering, soil moisture, water content).	Regular updated when necessary. Geotechnical in-situ and laboratory tests using inclinometers, penetrometers and piezometers. Tomographic subsurface surveys. Physical properties of soils, triaxial tests, odometers test as required by modeling process.	Request more frequent observations and If possible continuous recording of soil moisture.
Climate Trigger precipitation (rainfall, snow, magnitude, intensity, duration), temperature.	Meteorological data field measurements. Meteorological satellites data.	Continuous recording.
Seismic trigger Magnitude, intensity, duration, peak acceleration. Decay of shaking level with source distance (source, propagation shaking and site effects).	Accelerometer network monitoring. (Frequency: continuous or reoccupied as necessary) Model (Pseudo-static stability, Dynamic instability).	Continuous recording.

has occurred. Currently, damage assessment related to landslides and other disasters is done using aerial photography, videography and ground checks. In order to be able to use EO data for landslide damage assessment, two criteria should be met: High temporal and high spatial resolution (ca. 3–10 m stereo) is essential for landslide damage assessment and relief efforts. Images taken at the time of disaster or days after the event similar to other geohazards – earthquake and volcanoes – is a requirement to support relief efforts. Figure 7.4 (a, b, c, and e) shows the uses of high-resolution IKONOS (2.5 m)

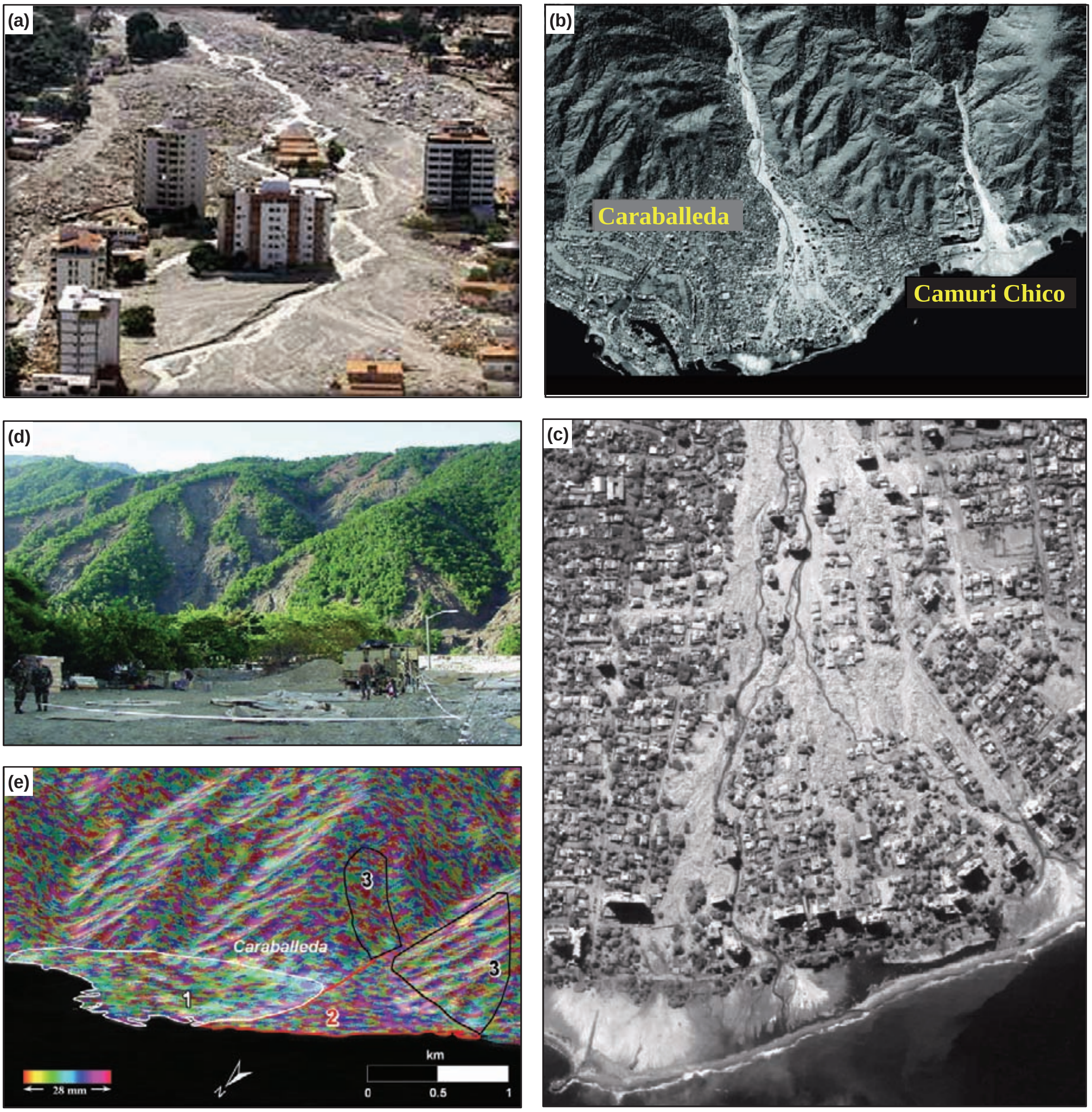

Fig. 7.4 **(a-e)** Landslides in Venezuela resulting from high-intensity rainfall and high-velocity water and debris flow which buried residential areas resulting in 50 000 deaths and 1.5 billion in damage on the north slope of Avila Mountain range (**a**). The photograph. (**b**) and (**c**) show high resolution Ikonos 2.5 m imagery. (**d**) shows the resulting landslide scars on the steep slopes. (**e**) shows an 8 m RADARSAT fine mode descending interferogram (Master: March 21st, 1998, Slave: January 22nd, 2000, Baseline of 740 m). Zone 1 is the relatively stable area of the city of Caraballeda, Zone 2 is the mud flow area, and Zone 3 indicates unstable slopes

and fine mode RADARSAT (8 m) images to assess damage and produce revised inventory maps related to high velocity mud flows resulting from rapid high intensity rainfall on the north slope of Avila mountain on coastal Venezuela. The landslide, which occurred on Dec 30th 1999, killed 50 000 people, and caused and $1.5 Billion (US) in property damage.

7.3 Landslide Monitoring Using InSAR

Remote sensing techniques are increasingly being used in slope stability assessment. (Murphy and Inkpen, 1996; Singhroy et al., 1998; Singhroy and Mattar, 2000; Singhroy, 2005). Recent research has shown that differential interferometric SAR techniques can be used to monitor landslide motion under specific conditions. (Vietmeier et al., 1999; Rott et al., 1999). Provided coherence is maintained over longer periods, as is possible e.g. in non-vegetated areas, to observe surface displacement of a few cm per year. Using data pairs with short perpendicular baselines, short time intervals between acquisitions, and correcting the effect of topography on the differential interferogram, reliable measurements of surface displacement can be achieved.

Interferometric Synthetic Aperture Radar (InSAR) techniques are being used to measure small mm displacement on slow moving landslides. An interferometric image represents the phase differences between the backscatter signals in two SAR images obtained from similar positions in space (Hanssen, 2001; Massonnet and Feigl, 1998; Rosen, 2000). In case of spaceborne SAR the images are acquired from repeat pass orbits. The phase differences between two repeat-pass images result from topography and from changes in the line-of-sight distance (range) to the radar due to displacement of the surface or change in the atmospheric propagation path length. For a non-moving target the phase differences can be converted into a digital elevation map if very precise satellite orbit data are available. Effects of noise due to changes of atmospheric propagation between various images can be strongly reduced by combined processing of several interferometric image pairs with different baselines (multi-baseline interferometry) (Ferretti et al., 1999). Therefore, small (less than 100 m between passes) orbital baseline, no precipitation at acquisition, vegetation free surfaces and high resolution topographic information to register SAR images are essential for reliable InSAR deformation maps. The current SAR satellites shown in Table 7.1 have repeat orbits varying from 11 days for Terra SAR X, 24 days for RADARSAT, 35 days for Envisat, 46 days for ALOS.

For motion mapping by means of InSAR it is necessary to separate the motion-related and the topographic phase contributions. This can be done by differential processing using two interferograms of different time periods calculated from two or three images if the motion was constant in time. If the motion is slow, the topographic phase can be taken directly from an interferogram of a short time span. With the advent of repeat-pass interferometry, it has become possible to detect subtle changes (at mm scales) in the landscape such as seismic displacement (e.g. Massonnet et al., 1996). However, landslides are difficult to study using radar interferometry (e.g. Fruneau et al., 1996) because they can experience ground deformations in excess of the phase gradient limit (Carnec et al., 1996) and which eliminate interferometric correlation (Massonnet and Feigl, 1998). Attempts are being made to better integrate radar interferograms, field measurements, and ancillary remote sensing of landslides to obtain "calibrated" interferograms which will provide useful geologic and geophysical information to the landslide monitoring community.

There are two important constraints for the application of InSAR to slope motion monitoring: (1) InSAR measures only displacements in slant range, the component of the velocity vector in flight direction cannot be measured. (2) InSAR can only map the motion at characteristic temporal and spatial scales (Massonnet and Feigl, 1998), related to the spatial resolution of the sensor and the repeat interval of imaging. Typical scales for SAR interferometry application to landslide movements are millimeters to centimeters per month (with 35 day repeat-pass images) down to millimeters to centimeters per year (with approximately annual time spans).

A precondition for the generation of an interferogram is coherence, which means that the phase of the reflected wave at the surface remains the same in the two SAR images. The loss of coherence (decorrelation) is the main problem for interferometric analysis over long time spans, as required for mapping of very slow movements. Whereas the signal of densely vegetated areas decorrelates rapidly, the phases of the radar beam reflected from surfaces, which are sparsely vegetated or unvegetated often remain stable over years. This has been utilized for mapping very slow slope movements in high Alpine terrain (Rott et al., 1999).

Motion analysis in vegetated areas uses stable objects such as installed corner reflectors or man-made constructions such as houses, roads and bridges etc. Using long temporal series of interferometric SAR images (typically about 30 or more repeat pass images over several years) objects with stable backscattering phase are determined by statistical analysis The analysis of the SAR time series with the Permanent Scatterer Technique PSInSAR^{TM} (Ferretti et al., 2000, 2001) enables the detection of very small movements of individual objects (e.g. single houses. With the Permanent Scatterer Technique the movement of small objects (down to about one square meter) can be monitored. A certain number density of stable objects (at least about 5 km^2) is needed to enable accurate correction of atmospheric phase contributions. This method has been applied to map subsidence and slow moving landslides as shown below. The examples described below is aimed at providing representative case studies of InSAR monitoring of landslides on different geologic environments.

The **Frank rock avalanche** case study is provided to demonstrate the capability of InSAR to monitor gradual motion on large rock avalanche in the Canadian Rockies. The Frank Slide, a $30 \times 106\ m^3$ rock avalanche of Paleozoic limestone, occurred in April 1903 on the east face of Turtle Mountain of southern Alberta, Canada. Seventy fatalities were recorded. This slide is still active. "Factors contributing to the slide have been identified as the geological structure of the mountain, subsidence from coal mining at the toe of the mountain, blast induced seismicity, above-average precipitation in years prior to the slide, and freeze-thaw cycles" (Cruden and Hungr, 1996). The Government of Alberta has installed GPS stations and several in-situ monitors to monitor post-slide activity at specific locations (Fig. 7.5a), and current InSAR monitoring are complementing the in-situ measurements. The fact that the rock covering the rock avalanche is bare and dry, leads to the high coherence and identification of more than 95% of the CTM targets for the Frank Slide area. Due to their great density and excellent coverage, the CTM measurements of this area are a reliable reflection of current deformation pattern. The most recent InSAR CTM results (Fig. 7.5b) have shown that during a period from April 2004 to October 2006, the foot of the eastern slope of Turtle Mountain, the ground surface above the Frank Mine was found to subside at an average rate of about 3.1 mm per year supporting the speculation that underground coal mining triggered the Frank landslide (Mei et al., 2006). Deformation on other areas of the debris avalanche is a result of gravitational mass movement. Our most recent results of the steep north slope scarp where in 2001, 6,000 tons of rock fell show, that this area is still unstable. The ALOS differential InSAR results for July 12-Aug 27/06 show deformation of 20 mm on the upper rocky and partly vegetated slopes (Fig. 7.5c). The ALOS PALSAR data show deformation not only on the exposed rocky surfaces but also on the vegetated South Peak. This is particularly useful since the South Peak is extensively monitored and does show similar gradual deformation.

The **Thunder River landslide in permafrost terrain** is within the Mackenzie Valley pipeline corridor, 200 km southeast of Inuvik in the Northwest Territories, Canada. The study area is characterized low relief sparse-to-open coniferous forest and shrub land. The Mackenzie Valley pipeline is a 1300 km, aimed at delivering natural gas to markets in Southern Canada and United States. The pipeline – when completed – is estimated to cost $ 7 billion. There are approximately 2,000 landslides along the proposed route The Mackenzie Valley will experience one of the highest rises in mean annual air temperature for any region in Canada, thereby triggering melting in the permafrost and landslide activity (Couture et al., 2006).

The Thunder River slide is an active layer detachment where excessive deep thaw encounters rich ground ice (Fig. 7.6). The deep thaw is caused by warm summers or the destruction of the insulating surface, mainly by forest fires. Our investigation has shown that differential InSAR using 8 m RADARSAT-1 fine mode provides a first step in monitoring regional permafrost activity and landslide motion at specific location within the Mackenzie Valley Pipeline corridor. Our results show that deformation on exposed slopes is 3 times more than on vegetated slopes from July to October 2006 (Alasset et al., 2007). As shown in Fig. 7.6, dark areas represent rapid motion (loss of coherence), and correspond to the landslide areas, and red areas show gradual motion in the low vegetated slopes. This result indicates that the exposed slopes are extremely active and will pose a serious treat to the pipeline safety.

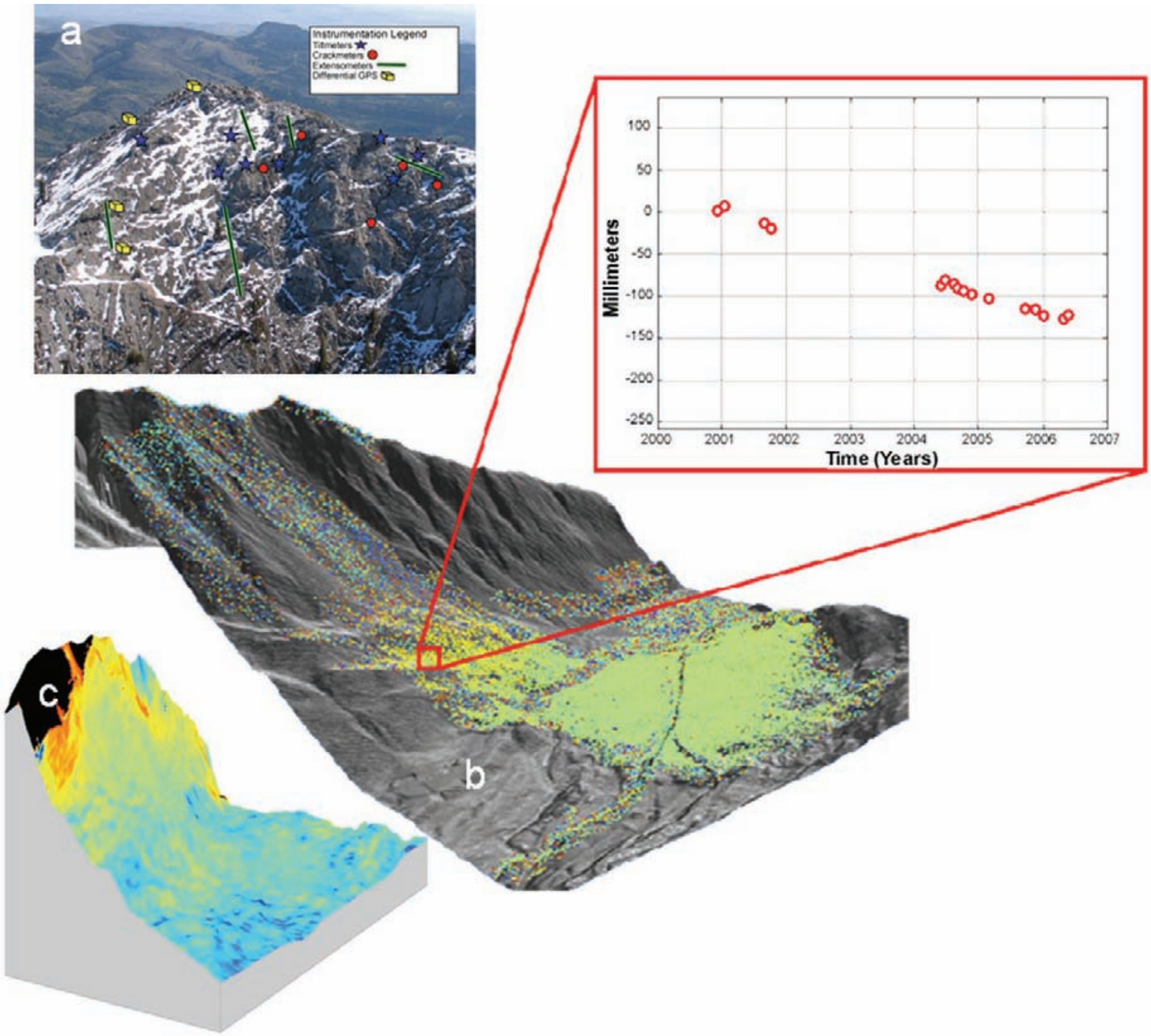

Fig. 7.5 InSAR montoring of Frank slide, Canada, modified from Mei et al., 2007

The **Little Smoky** deep seated retrogressive slide on glacial till that threatens Highway 49 Alberta, Canada. The little Smoky River occupies a broad pre glacial valley filled with interbedded tills. The glacial deposits continue to be downcut and undermined by the river resulting in oversteepening of the valley slopes which produce large scale land sliding (Froese et al., 2008). The estimated slip surface of the slide from slope inclinometer readings during 2002 indicated a rate of movement of 6–16 mm/year. Potential long term mitigative measures might consist of re-aligning the highway in a straight line from the bridge perpendicular to the valley slope with a deep cut to offload the upper part of the valley slope and placement of a toe berm at the base of the slope using material generated by the cut. Substantial erosion protection measures would also be required along the toe of the valley as recommended by Thurber Engineering 2002.

The valley slopes are heavily vegetated, and as such twenty three corner reflectors, designed for RADARSAT-C band, were installed to minimize temporal decorrelation caused by the vegetation. Figure 7.7 a and b shows the location of the corner reflectors and the profile and stratigraphy between A-A (Froese et al., 2008). The monitoring of the

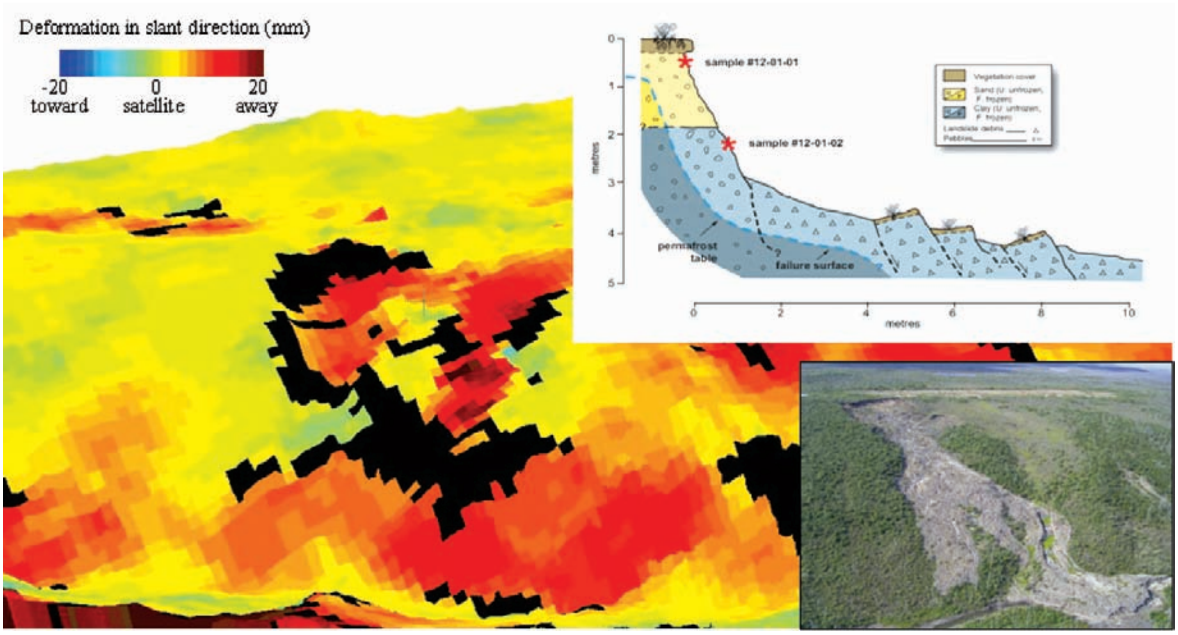

Fig. 7.6 InSAR monitoring of Thunder River landslide, Canada, modified from Alasset et al., 2007

corner reflectors were conducted using the Ascending F2N Radarsat-1 images line of site images. Fig. 7.7c shows an example of the InSAR results obtained for corner reflector #7 (CR7), located on the lowermost block of a rotational retrogressive slide, and a comparison with slope inclinometer deformation readings. CR7 shows a maximum of 50 mm from March to November 2007, compared to the inclinometer data which shows a movement of 12 mm over the same time. This difference is probably because the CR7 is located at the lower most rotational block and is likely moving faster. A more detailed review of these trends relation to relation to other corner reflectors and inclinometer measurements are currently on going by Froese et al. from the Alberta Geological Survey.

The **Castagnola landslide**is a deep seated gravitational movement on clayey terrains It is located in the northern Appenines, a few tens of kilometers to the East of Genoa. Covering a surface area of about 40 ha on the right bank of the Castagnola River, the landslide faces south west with an average slope inclination of 12°. The main scarp is at an elevation of 380 m with the toe approximately 80 m lower. A number of morphological features indicate recent movement with at least three slope ruptures being evident. The land surface, accordingly, has a terraced and hummocky appearance (Ferretti et al., 2005).

The landslide has a deep-seated gravitational movement with both translational and rotational components. It represents a serious socio-economic threat to a cluster of small villages, with many homes having been evacuated and/or abandoned. Furthermore, the slide is still active.

PSInSAR^{TM} was used to supplement information obtained from ten inclinometers, many of which had short lives owing to the significant amount of movement, typically 30–40 mm/year in the central part of the slide area. As is expected in rural areas, PS density is low but sufficient PS was obtained to corroborate the inclinometer data and geomorphology of the area. Despite the two data sets representing different time periods (1992–2001 for PS data and 2001–2002 for inclinometer data), a qualitative comparison showed good agreement in terms of direction of movement and deformation rates (Fig. 7.8 a, b, c, and d) (Ferretti et al., 2005).The analysis of this landslide was undertaken by the University of Florence and TRE on behalf of the Province of La Spezia, Italy.

Mount Padrio is large (30 km^2) deep-seated and rotational landslide in the Lombardy region of Italy's Central Alps. Figure 7.9 shows relatively a

b

c

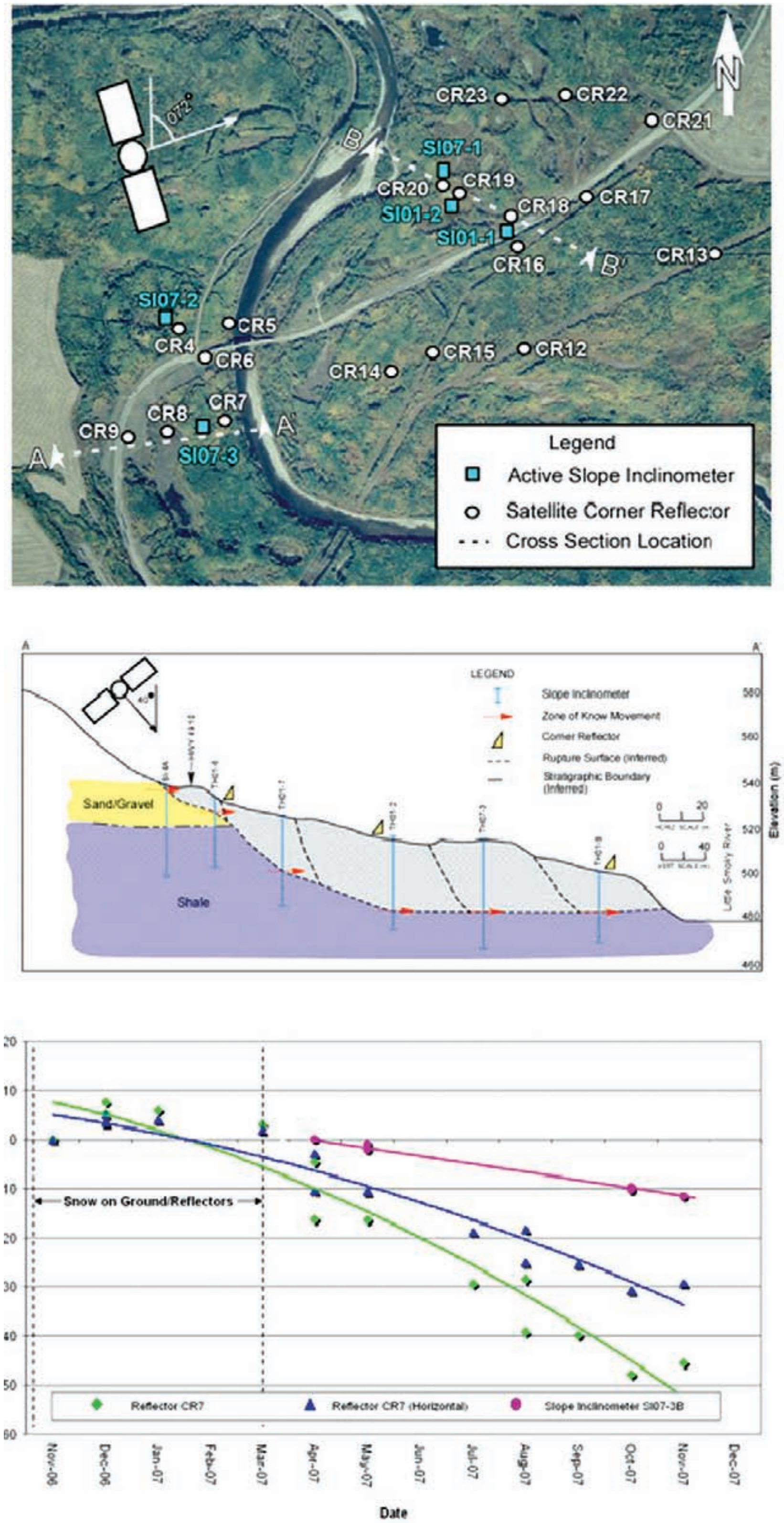

Fig. 7.7 InSAR montoring of Little Smoky landslide, Canada, modified from Froese et al., 2008

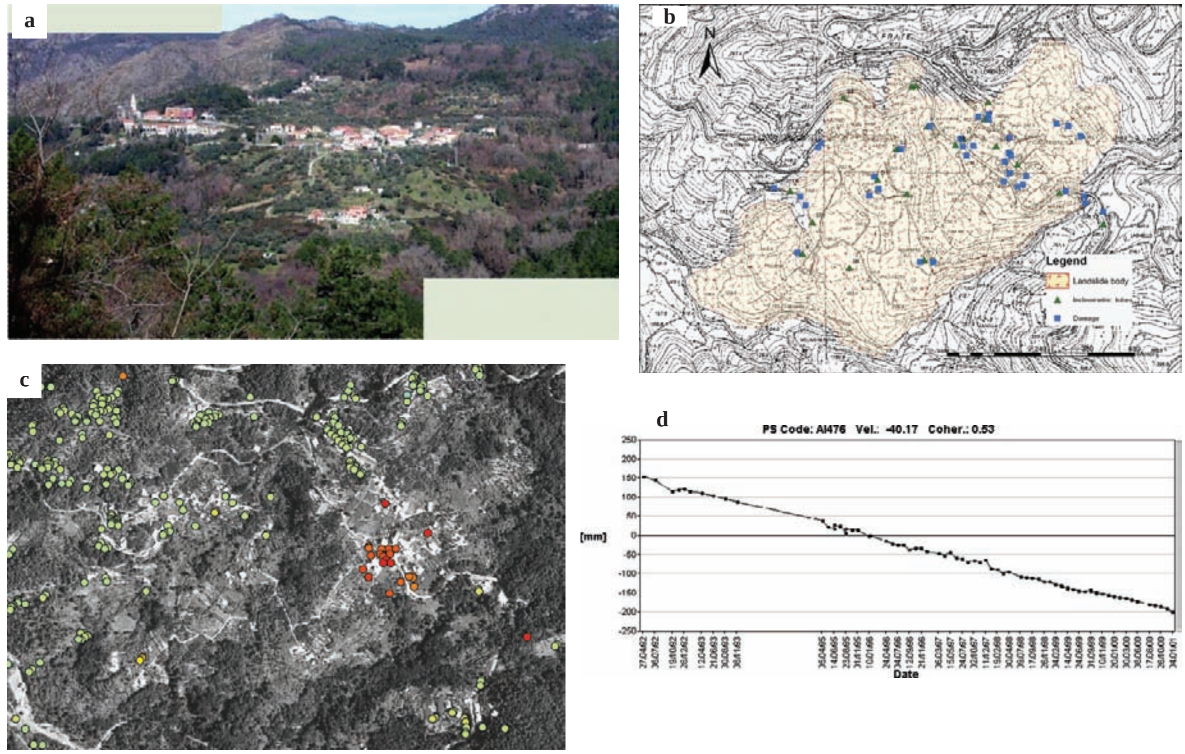

Fig. 7.8 (**a**) Photo of Landslide area (**b**) Boundary of Landslide area (**c**) Distribution of Permanent scatterers (PS). The colour the PS corresponds to their average yearly displacement Red-40 mm/year, green –no motion, blue + 40 mm/year – (**d**) Motion from 1992–2001 400 mm downslope. (Ferretti et al. 2005)

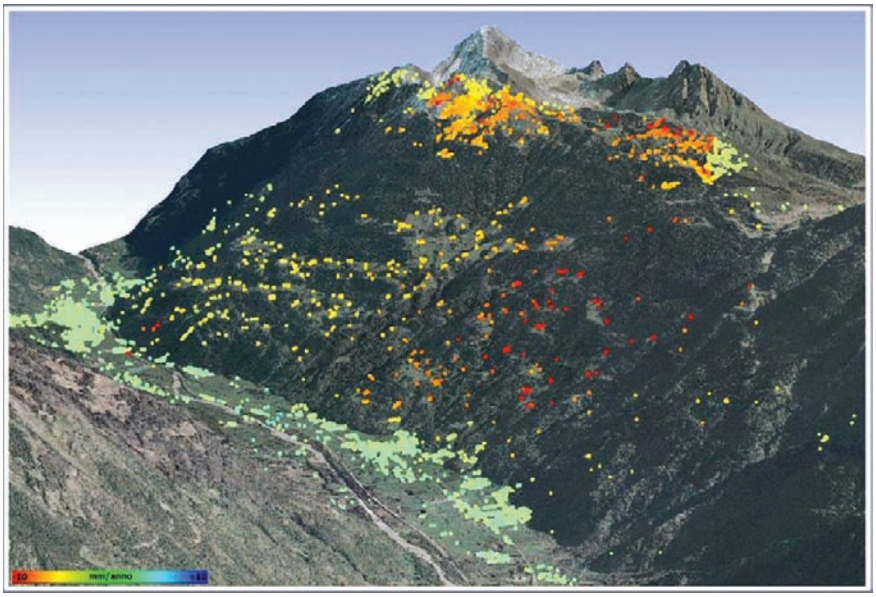

Fig. 7.9 PSInSAR monitoring of Mount Padrio (Ferretti et al. 2005)

high levels of motion at the scarp of the main slide (in the foreground), represented by red coloured PS. Progressing down the slope the displacement rate reduces until, close to the toe, there appears to be little motion evident. The PS data show good agreement with mapped landslides of the area. The site is structurally complex and failure mechanisms are challenging to comprehend in the toe areas owing to thick alluvial sediments filling the valley floor (Ferretti et al., 2005).

The PSInSAR^{TM} analysis identified more than 300 PS on the slopes representing both natural and artificial reflectors including bedrock outcrops, buildings and pylons. A power station and penstock, toward the upper end of the valley have been rendered dysfunctional as the result of slide activities on the mountain slopes. The PSInSAR^{TM} analysis was conducted by TRE for the Regional Government of Lombardy in partnership with the University of Milan Bicocca.

7.4 Conclusions and Future Research

Our investigation shows that current high resolution stereo SAR and optical images are producing multi scale landslide inventory maps to improve mitigation. The availability of less than 3-m resolution stereo images from SAR and optical are providing, near air photo type geomorphic information on slopes, for more reliable landslide inventory maps. Differential InSAR and PSInSAR^{TM}/CTM are providing a useful monitoring tool of various landslide processes under different slope, moisture and lithological conditions. Differential InSAR techniques provide a rapid and simple deformation activity of the geological process and therefore are easily understood. The CTM/ PSInSAR^{TM} technique are providing more detailed and accurate measurements because of a longer time series acquisition (average 30 images) that are useful for geotechnical investigations required for mitigation measures. The integration of CTM/ PSInSAR^{TM} and in-situ measurements will continue to be an on going process. Landslide prediction will continue to remain complex and difficult even with ground monitoring techniques. It is clear that both InSAR techniques (differential and CTM/ PSInSAR^{TM}) are making significant addition in monitoring seasonal slope activity at high risk sites.

Remote sensing images are only used in a limited way for landslide investigations, although its uses are increasing. There are several challenges that limit more uses, but these are gradually being address. These include

- satellite images interpretation for landslide inventory and monitoring requires is a high level of user knowledge of remote sensing systems and image processing techniques.
- InSAR deformation maps provide linear motion at the line of site. Although this is very useful, information, Landslide motion is very complex with nonlinear vectors. Therefore, InSAR techniques do not provide the complete 3d motion.
- There is need for more integration of InSAR results with ground measurements to improve reliability. This is in part due to the fact that most unstable slopes are generally not fully instrumented. Most high risk sites need an archive of acquisition (average 30 images) which does not exist in most cases.
- High resolution DEM is a requirement for producing accurate InSAR measurements and 3d visualization images. Low resolution images can cause phase unwrapping problems and inaccurate results. Currently, high resolution DEM does not exist on most sites. The increase high resolution satellite images do require high resolution DEM for InSAR processing and visualization techniques.
- There is need for more frequent high resolution revisits to monitor slope stability especially in wet periods. Current revisit time for existing SAR satellites is a serious gap to frequently monitor all geohazard process including landslides. Rapid 1-3 days revisits will not be available until the next 3–5 years with the planned launch of a series of SAR constellation such as Cosmo SkyMED, RADARSAT Constellation, and Sentinel.
- There is a need to standardize the InSAR processing software to produce accurate results using different satellite images. Commercial vendors of InSAR software claim that their specific brand is the best. Our tests have shown that InSAR results for most simple subsidence sites are reproducible. However, results for most slope stability are not reproducible using different software on

the same site. InSAR software developed at university and government laboratories are restrictive. This patchwork system is serious limiting the operational uses of InSAR techniques to produce reliable results.

- As noted in Table 7.1, many SAR satellites do have polarimetric capabilities mainly used to characteritize the morphological properties of targets. Polarimetric scatter can also be used to classify the textural properties of surficial materials. Wet landslide materials generally have poor coherence. There is therefore a need to investigate polarimetric InSAR techniques to improve motion measurements of wet slide materials.
- The uses of installed field corner reflectors are increasing on remote vegetated sites. These corner reflectors are custom made for a particular frequency and viewing geometry of a particular satellite (e.g. Radarsat). There is a need to design reflectors that are adaptable to various satellites and adapted to various foundations such as permafrost, rock, soft sediments.

Acknowledgment The author would like to thank Drs Froese, Alasset and Ferretti for providing examples for this compilation.

References

Alasset P-J, Poncos V, Singhroy V, (2007) InSAR monitoring of a landslide in a permafrost environment: constraints and results. Proceedings CIG/ISPRS Meeting, Toronto, Canada 11p.

Bulmer, MH. (2002) Studies of Landslides using Remote Sensing Data CEOS Landslide Hazard Team Report. 6p.

Carnec C, Massonnet D, King C. (1996). Two examples of the use of SAR interferometry on displacement fields of small extent. Geophys. Res. Letts., 23(24), 3579–3582.

Couture R, Riopel S, Hawkins R, Poncos V, Murnaghan K, Singhroy V. (2006) Coherent Targets for Interferometric SAR to Monitor Unstable Permafrost Slopes in the Mackenzie Valley, Northwest Territories. 34th annual Yellowknife Geosciences Forum, Yellowknife , Canada. 2p.

Cruden DM, Hungr O. (1996). The debris of Frank Slide and theories of rockslide-avalanche mobility, Can. J. Earth Sci., 23, 425–432, 1986.

Ferretti A, Prati C, Rocca F. (2001). Permanent scatterers in SAR interferometry. IEEE Trans. Geosc. Rem. Sens., 39, 8–20.

Ferretti A, Prati C, Rocca F. (2000). Nonlinear subsidence rate estimation using permanent scatterers in differential SAR interferometry. IEEE Trans. Geosc. Rem. Sens., 38, 2202–2212.

Ferretti A, Prati C, Rocca F. (1999). Multibaseline InSAR DEM reconstruction: The wavelet approach. IEEE Trans. Geosc. Rem. Sens., 37, 705–715.

Ferretti A, Prati C, Rocca F, Casagli N,. Farina P, Young B. (2005) Permanent Scatterers technology: A powerful state of the art tool for historic and future monitoring of landslides and other terrain instability phenomena Proc. Int. Conf. on Landslide Risk Management, Vancouver 9p.

Froese CR, Poncos V, Skirrow R, Mansour M, Martin D. (2008). Characterizing Complex Deep Seated Landslide Deformation using Corner Reflector InSAR : Little Smoky Landslide, Alberta. Proceedings 4th Canadian Conference on Geohazards. Quebec City pp. 287–293.

Fruneau B, Achache J, Delacourt C. (1996). Observations and modelling of the Saint-Etienne-de-Tinee landslide using SAR interferometry. Tectonophys. 265, 181–190.

Guzzetti F. (1990). Carta Inventario Dei Ovimenti Franosi Della Region Marche Ed Aree Limitarofe: Scala 1:100,000. CNR-IRPI, Purugia, Italy.

Hanssen RF. (2001)Radar Interferometry,. Kluwer Academic Publisher, Norwell, USA 308 pp.

Massonnet D, Feigl KL. (1998). Radar interferometry and its application to changes in the Earth's surface. Rev. of Geophys., 36(4), 441–500.

Massonnet, D., Vadon, H., and Rossi, M. 1996. Reduction in the need for phase unwrapping in the radar interferometry. IEEE Trans. Geosci. Rem. Sens., 34(2), 489–497.

Mei S, Poncos V, Froese C. (2007) InSAR Mapping of Millimetre-scale Ground Deformation over Frank Slide, Turtle Mountain, Alberta, Alberta Energy and Utilities Board, EUB/AGS Earth Science Report 2007, pp. 1–62.

Mollard JD, Janes JR. (1993). Airphoto Interpretation of the Canadian Landscape. Energy, Mines and Resources, Canada, Ottawa 415p.

Murphy W, Inkpen RJ. (1996). Identifying landslide activity using airborne remote sensing data, GSA Abstracts A-408, 28–31, Denver.

Nichol JE, Shaker A, Wong MS. (2006) Application of high-resolution stereo satellite images to detailed landslide hazard assessment. Geomorophology, 76, 68–75.

Rosen PA. (2000). Synthetic Aperture Radar Interferometry. Proc. of IEEE, 88(3), 333–385.

Rott H, Scheuchl B, Siegel A, Grasemann B. (1999) Monitoring very slow slope movements by means of SAR interferometry: a case study from a mass waste above a reservoir in the Ötztal Alps, Austria. Geophys. Res. Letters 26, 1629–1632.

Schuster RL. (1996). Socio- economic significance of Landslides. In: Turner, A.K, and Schuster, R.L (Eds.) Landslides: Investigation and Mitigation. Report 247, Transportation Research Board, NRC, National Academy Press, Washington DC, pp. 12–35.

Singhroy V. (2005). Remote Sensing for Landslide Assessment: Chapter 16, in Book on Landslides Hazard and Risk edited by Glade Anderson and Crozier. Wiley Press. pp. 469–492.

Singhroy V, Mattar K. (2000). SAR image techniques for mapping areas of landslides. ISPRS 2000. Proceedings. Amsterdam, pp. 1395–1402.

Singhroy V, Mattar, KE, Gray, AL. (1998). Landslide characteristics in Canada using interferometric SAR and combined SAR and TM images. Adv. Space Res., 3, 465–476.

Vietmeier J, Wagner W, Dikau R. (1999) Monitoring moderate slope movements (landslides) in the southern French Alps using differential SAR interferometry, Proceedings of Fringe '99,Liège, Belgium.

Varnes DJ. (1974). The logic of geologic maps, with reference to their interpretation for engineering purposes. U.S. Geol. Surv. Prof. P. 837.

Huge Landslides Caused by Massive Earthquakes and Long-Lasting Geotechnical Risks

8

Konagai Kazuo, Johansson Jorgen, Takatsu Shigeki and Ikeda Takaaki

Abstract A massive earthquake often causes long-lasting geological issues, and the May 12th 2008 Wenchuan Earthquake was no exception. To quickly cope with ongoing problems, archiving past case histories is certainly necessary. This paper provides case histories from the 2005 Kashmir Earthquake, Pakistan, and the 2004 Mid-Niigata Earthquake, Japan, in which tho ough monitoring of landforms has highlighted cause-and-effect sequence of events in the affected areas, and provides a basis for the recommendation of effective rehabilitation.

Keywords Risk evaluation • Prediction • Monitoring • Precursor stage of landslide

8.1 Introduction

The May 12th 2008 Wenchuan Earthquake and its aftershocks have sent huge amount of soil and rock sliding down mountain slopes into rivers, creating natural dams behind which lakes have been quickly formed. These lakes have posed immediate danger to people in lower reaches of these rivers. Even after the immediate crisis is solved through quick stabilization of the landslide masses and simultaneously by implementing alarm systems, there will remain huge amount of debris in mountains probably causing long lasting geotechnical issues.

Konagai Kazuo (✉)
Institute of Industrial Science, University of Tokyo, Japan

Johansson Jorgen
Institute of Industrial Science, University of Tokyo, Japan

Takatsu Shigeki
CTI Engineering Co. Ltd., Tokyo, Japan

Ikeda Takaaki
Research Institute of Technology, Tobishima Corporation, Chiba, Japan

Both, the 1999 ChiChi earthquake, Taiwan, and the 2005 Kashmir earthquake, Pakistan for example, formed a great number of debris deposits along their activated faults. Heavy rains in the monsoon of 2006 that followed the Kashmir earthquake were responsible for raising river beds. At Ghari Habibullah village, 4–5 km west of the northern segment of the Muzaffarabad fault, about 4–6 m of thick debris sediment was formed at the exit of a canyon onto a flat plain along the Kunhar river (Konagai et al., 2007). The ChiChi earthquake was followed by a number of typhoons in rapid succession. They included Toraji and Nari in 2001, Mindulle and Aere in 2004. About 3.9 typhoons on the average over the past ten years (1996–2005) have hit Taiwan, causing a three-fold increased risk of debris flows. As a result of these typhoons, increases of river bed elevations of about 4–8 m have been reported (W.F. Lee, 2007, personal communication).

To quickly cope with ongoing problems, archiving past case histories is certainly necessary. The following case histories are presented.

K. Sassa, P. Canuti (eds.), *Landslides – Disaster Risk Reduction*,
© Springer-Verlag Berlin Heidelberg 2009

8.2 The Kashmir Earthquake and Geotechnical Issues

A large devastating earthquake occurred in Kashmir on Oct. 8, 2005 at 8:50 (3:50UTC) local Pakistan time with its epicenter located at a latitude of 34°29′35″N and longitude of 73°37′44″E (Fig. 8.1). The depth of the earthquake was estimated to be about 10 km with a magnitude of 7.6. The earthquake killed more than 75000 people, most of which were on the Pakistani side of Kashmir. About 2000 people were killed on the Indian side of Kashmir.

Among many rehabilitation activities, Japan International Cooperation Agency (JICA) has prepared a rehabilitation and reconstruction plan for Muzaffarabad, the capital city of Azad-Kashmir, a self-governing state under Pakistani control. The JICA master plan recommended locating open spaces and expanding wider road networks to make the area more resistant to future disasters, by allowing easy and quick access to the area, and thus providing refugees with spaces for shelters and necessary goods. However, as described in the introduction, the urgent needs of Muzaffarabad will be more related to geotechnical/geological issues than the possible recurrence of a large earthquake.

8.2.1 Hattian Balla Landslide

The earthquake triggered a huge landslide far up in the Jehlum mountains. The huge landslide mass of about 80 million cubic meters in estimated volume, created a 137 m high natural dam blocking the water flow of two tributaries of the Jehlum river, Karli and Tang, and thus building up a large (Karli) and small (Tang) lakes behind the natural dam (Figs. 8.2 and 8.3). The full capacity of the smaller lake was quickly reached in February 15, 2005, while the full capacity of about 62 million m^3

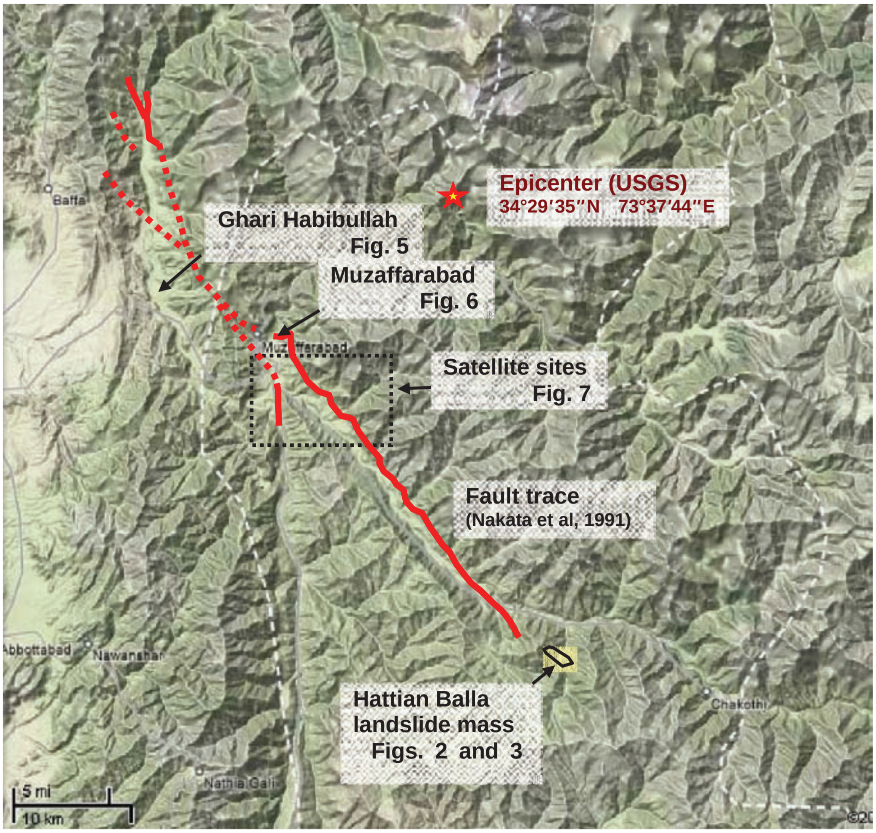

Fig. 8.1 Epicenter of the 2005 Kashmir Earthquake and fault traces (after Nakata et al., 1991)

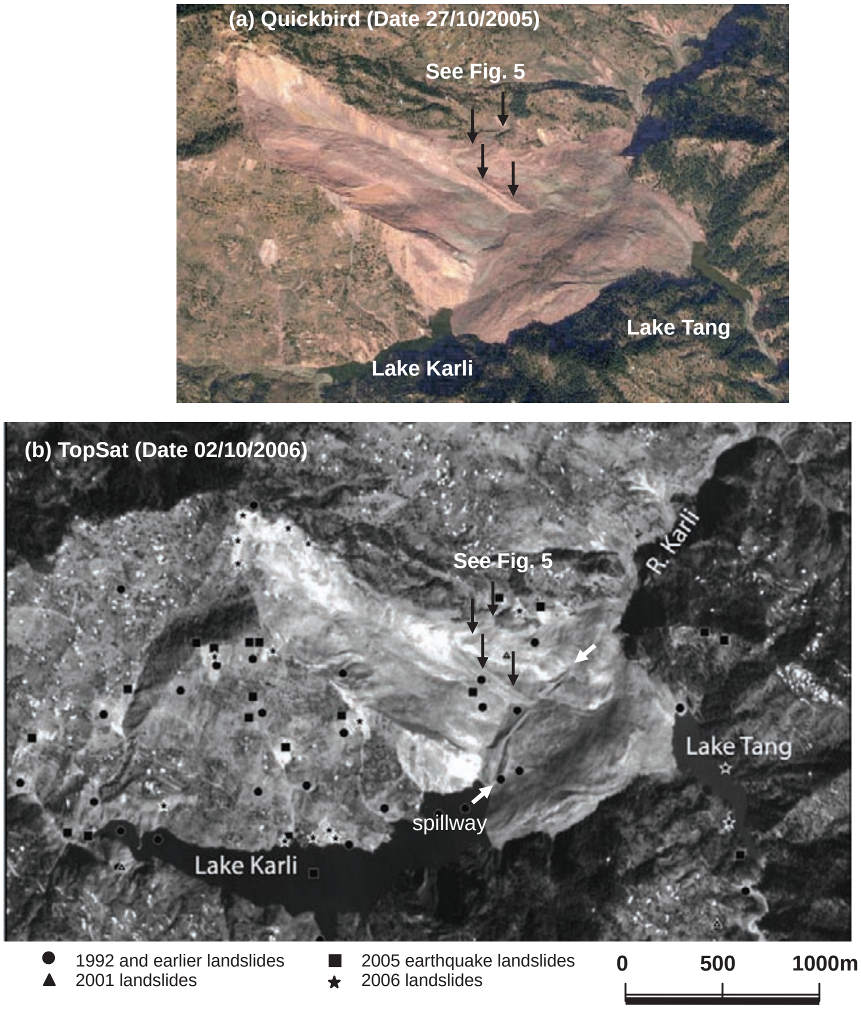

Fig. 8.2 Satellite imageries of Hattian Bala Landslide mass at different times: (**a**) Quickbird, 27/10/2005 and (**b**) TopSat, 02/10/2006. Marks in photo (**b**) show locations of landslides at different times (Dunning et al., 2007). *White arrows* show the spillway

for the larger lake had been reached in April, 2007. Over-spilled water flowing down the landslide mass is permeating the debris mass, disappearing in the middle of it, and again seeps out near its toe.

Ermini and Casagli (2003) proposed that the stability of a landslide mass can be evaluated with a dimensionless blockage index (DBI):

$$\mathrm{DBI} = \log_{10} A \times H/V \qquad (8.1)$$

where, A, H and V are the catchment area, dam height and landslide mass volume, respectively. Empirically landslide masses with DBI smaller than 2.75 hardly fail. DBI for the Hattian Bala landslide mass is about 1.85, given $A = 44.29$ million m^2, $H = 130$ m and $V = 80$ million m^3. Thus the landslide mass does not seem to be in imminent danger. However, some eye-witnesses report that the toe part is changing gradually in shape (Fig. 8.4), and the slow and steady change in the landslide mass is to be watched with vigilance.

The authors have surveyed the landslide mass at two different times in Nov. 2006 and Aug. 2007 to see any change in the landslide mass. Immediately after the first survey of 2006, the authors tried to estimate overall permeability, which is closely related to the porosity of the dam body, by making use of inflow, outflow, and lake elevation data from the report of the Water Power Development

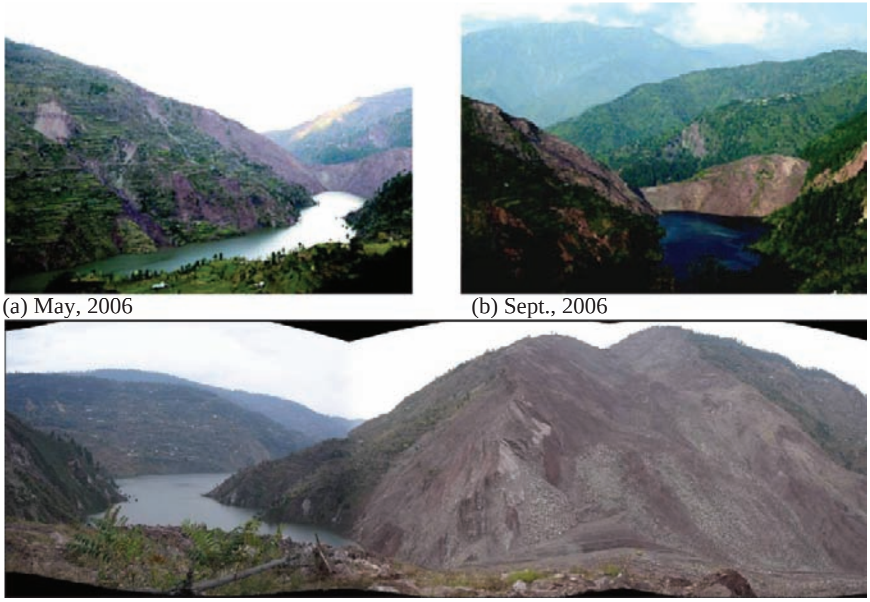

(a) May, 2006 (b) Sept., 2006

(c) November 15, 2006, view from opposite mountain side standing on debris that traveled from the scarp side. Upper lake is to the left in the photo.

Fig. 8.3 Larger reservoir (Lake Karli) behind Hattian landslide mass (photos (**a**) and (**b**) by Kodama Hiroyuki, Tobishima Corporation)

Authority (WPDA hereafter): "Study of Hattian Bala landslide", and also by the measurement of outflow, which the survey team members performed (Fig. 8.5). In this figure, a stone thrown onto a river surface induces a wave traveling in all directions with a velocity, v, which is approximately given as a function of water depth h and wave length λ by:

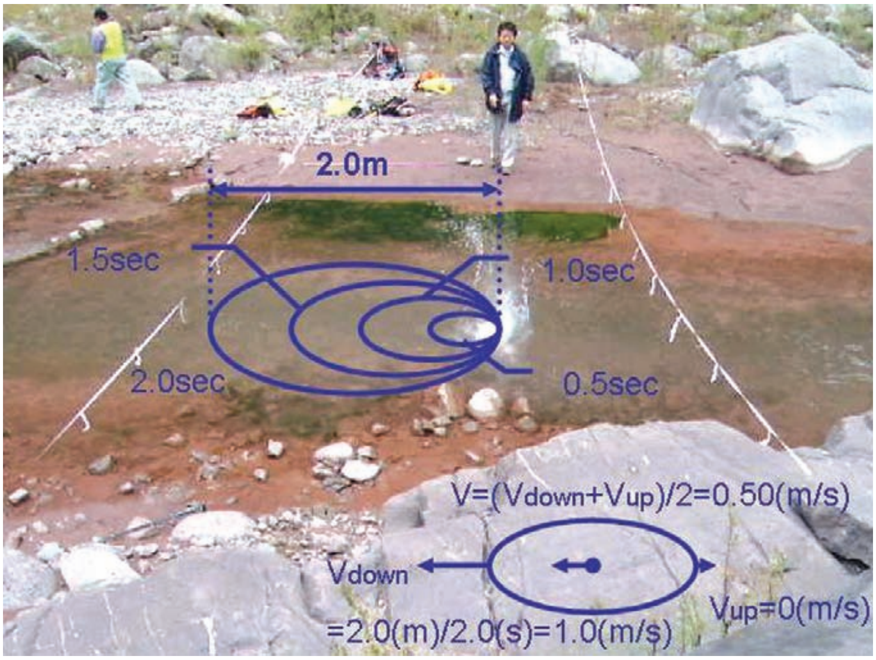

Fig. 8.4 Measurement of discharge seeping out from the toe of the avalanche mass

Fig. 8.5 Slight changes in landforms near the toe of the Hattian Bala landslide mass

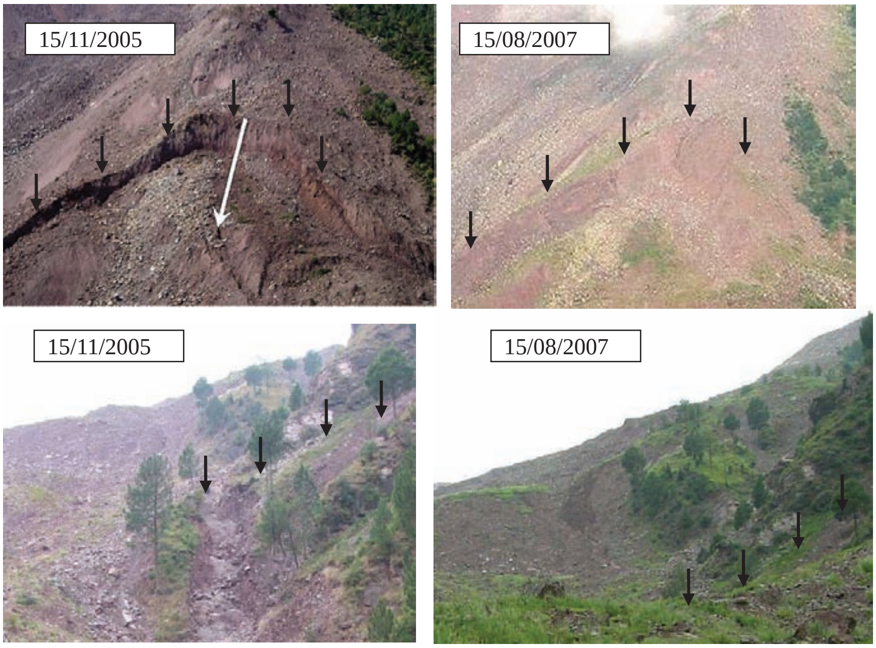

$$v = \sqrt{\frac{g\lambda}{2\pi}}\sqrt{\tanh\frac{2\pi h}{\lambda}} \text{ with } g = \text{gravitational acceleration.} \quad (8.2)$$

A steady water flow of laminar features, u, change its velocities in upstream and downstream directions respectively to be:

$$v_{up} = v - u \quad (8.3a)$$

and

$$v_{down} = v + u, \quad (8.3b)$$

Analyzing video images, λ, v_{up} and v_{down} were obtained for estimating water depths h and therefore the discharge Q.

Two extreme scenarios were reported in their provisional report. The first one assumed that the entire landslide mass had homogeneous features leading to both overestimation of the permeability for the greater part of the landslide mass with inclusion of finer grains and underestimation for the coarse toe part of the landslide mass. If the estimated porosity of the dam body is large, this can indicate that future dam body settlements are very likely; Settlements seldom occur evenly rather, they are differential, leading to crack development in the dam body and accompanying potential water infiltration/leakage. On the other hand, if the dam body is very impermeable the lake behind the reservoir can be filled up quickly causing the water to overspill and erode the landslide mass. Since the full capacity of the lake was eventually reached in April, 2007, it is now appropriate to take the second scenario that follows hereafter.

The second scenario was based on the WPDA report, which strongly suggested that the toe part has much larger permeability with larger boulders and rocks segregated there. Figures. 8.6 and 8.7 show time histories of inflows, outflow through the landslide mass, and lake elevations, respectively. Outflow through the landslide mass increased suddenly on Jan. 11, 2006. At that time, the water level for the larger lake was 1276 m, while the record for the smaller lake was not available. The measurement at the lower lake started on Jan. 23. Extrapolating the steadily increasing trend back to Jan 11, the water level of the lower lake on Jan. 11 was estimated to be at around 1212 m. Discharge through the landslide mass after Jan. 23 was seemingly coincident with the discharge flowing into

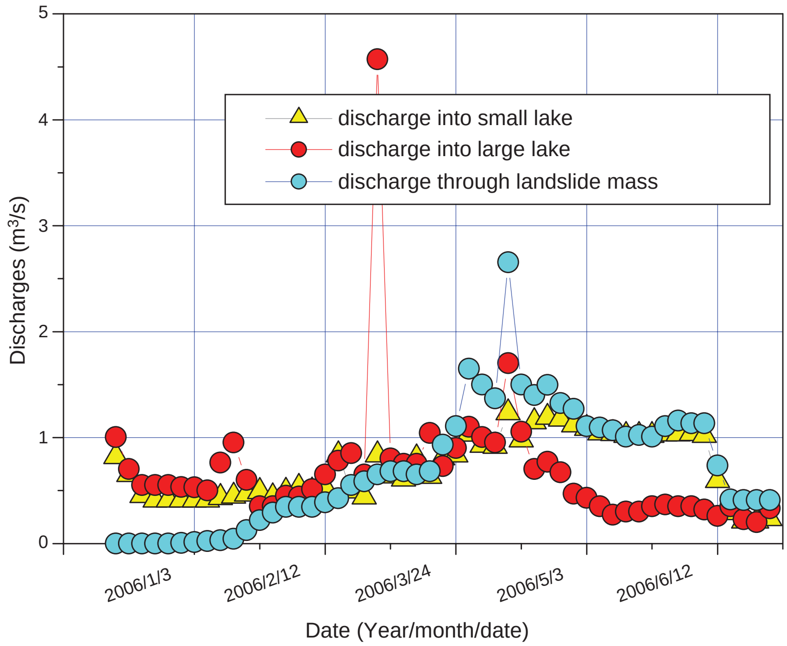

Fig. 8.6 Discharges flowing into small and large lakes and through landslide mass

either the larger or smaller lake. Due to segregation of rocks and boulders, it is often that the shallower part of a landslide mass has higher permeability than that for its deeper part. This suggests that the discharge through the landslide mass was directly from either the larger lake water above 1276 m elevation or the smaller lake water above 1212 m elevation. After April 13, the outgoing discharge was rather closer to that flowing into the smaller lake. However, the discharge through the soil mass was slightly larger than the inflow for the smaller lake after March 20, and it is noted the water level of the smaller lake had started to decrease steadily after April 21, though the inflow discharge was kept at around its maximum value of 1 m^3/s. This can be due to formation of water channels that proceed upstream through voids of course granular fabric, which have been originally filled up with finer substances. The landslide mass was seemingly changing its properties slowly but steadily.

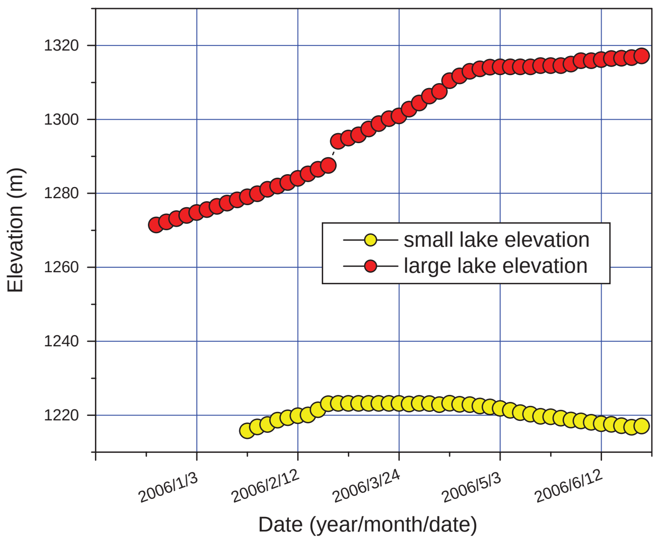

Fig. 8.7 Elevations of waters of large and small lakes dammed behind the landslide mass

Table 8.1 $\delta^{18}O$ ratios for the water samples from Hattian Balla landslide site

Location	$\delta^{18}O$ ratio (average)
Large lake	4.88
Spillway of large lake	5.09
Small lake	5.95
Spillway of small lake	6.39
Water from toe	5.70

Samples were taken on Aug. 23, 2007.

In the second survey of August 2007, samples of waters were taken from both lakes and the stream discharging out through the landslide mass in order to estimate discharges through the debris mass from large and small lakes. Table 8.1 shows $\delta^{18}O$ ratios for the water samples. The $\delta^{18}O$ ratio shows the percentage of stable isotopes of ^{18}O to ^{16}O in water, and often used as a measure of the temperature of precipitation, and as a measure of groundwater/mineral interactions. This variability arises due to the fact that when water evaporates, the lighter molecules of water—those with ^{16}O atoms instead of ^{18}O—tend to evaporate first, because of their lower mass. Though the two lakes are closely located, there is a clear difference in their $\delta^{18}O$ ratios. Assuming that the greater part of the discharges are near the surface part of waters stopped behind the landslide debris mass, $\delta^{18}O$ values from spillways may represents the greater part of the discharges. Based on this assumption, 53% and 47% of water discharges are estimated from the large and small lakes, respectively.

Though the landslide mass is seemingly stable for now, the above results suggest that change in the landslide mass is being accelerated slowly and steadily as the erosion goes on.

It is therefore strongly recommended that the following are monitored for the long term;

1) Total discharge through the landslide mass monitored at the toe.
2) Upper stream discharges flowing into small and large lakes, respectively,
3) Precipitations, and crack openings (if found to be potentially dangerous).

8.2.2 Geotechnical issues of Candidate areas for Satellite Towns

The Kashmir earthquake has formed a great number of debris deposits along the activated seismic faults. The flushed debris have caused some river beds to be raised several meters up, and were responsible for serious destruction of some built-up areas including Ghari Habibullah village, 4–5 km west of the northern segment of the Muzaffarabad fault (Fig. 8.8). Even within Muzaffarabad city, people living along valley on terraces are suffering adverse effects due to debris from mountains rising behind the activated Tanda fault, causing their dwellings to be half and/or entirely buried in debris (Fig. 8.9). People there are to be evacuated.

Among options for rehabilitating Muzaffarabad, one feasible idea will be to lay out satellite towns outside the municipal boundary as described in the JICA master plan. Staying away from unstable rims of terraces, terraces will be appropriate locations for developing satellite towns (Fig. 8.10).

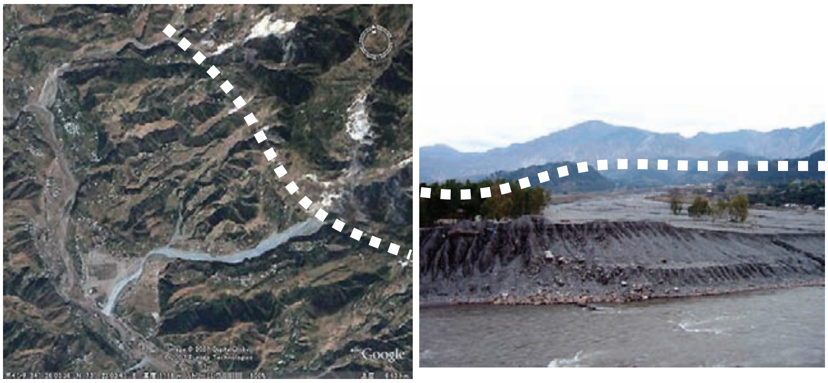

(a) Sattelite imagery (Google earth)

(b) Debris deposit

Fig. 8.8 Debris deposit from activated fault in Kashmir (Ghari Habibullah village): White broken lines show the activated fault in the Oct. 8, 2005, Kashmir Earthquake, Pakistan

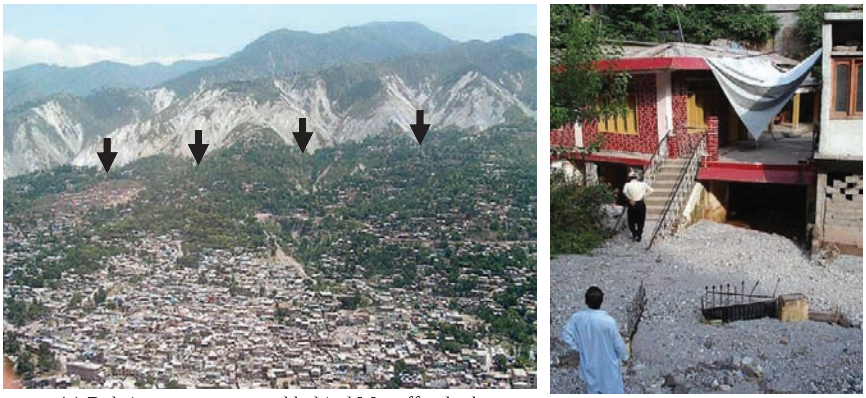

(a) Debris sources exposed behind Muzaffarabad (b) Houses half buried in debris

Fig. 8.9 Debris deposit from activated fault in Kashmir (Muzaffarabad): *Black arrows* show the activated fault in the Oct. 8, 2005, Kashmir Earthquake, Pakistan (photos provided by Geological Survey of Pakistan)

One difficulty will be the maintenance of roads, which will have to cross deep gorges. Earthquake-induced slope failures created debris deposits (which can become source material) beneath the mountains and during heavy rains further debris flows can occur. These flows will most likely follow the gorges, namely tributaries of the Jehlum and Nihlum rivers crossing roads and thus suspending traffic.

Here follows a brief description of geological and geo-technical features of some locations in these candidate areas for the Muzaffarabad satellite town.

8.2.2.1 Airport terrace

The Muzaffarabad airport is located at the southwest end of a river terrace with NW-SE trending mountains rising behind (34°20’21.02”N, 73°30’31.01”E). This terrace starts fanning out at the toe of the mountains, dipping slightly towards the Jehlum river. Along both sides of the terrace, there are two tributary rivers of the Jehlum down-cutting the terrace to the lower elevations. During the past heavy monsoon rains, a huge amount of debris has been carried along the south-eastern branch river (“Brora Nara” in Urdo) with large stones segregated up around its front. Figure 8.11 shows a remaining front of the massive debris flow (N34°20’37.8”, E73°30’57.6”). This latest debris mass is estimated to have been flushed in the 1992 monsoon rains and reached about 1 km away from the mountain toe. A pile of large stones of about 0.5–1 m in diameter is about 8–10 m high above the estimated original river bed. Though the source of information is not clear, there were remarkable debris flows in 1930, 1959 and 1992, roughly every 30 years at regular intervals. At

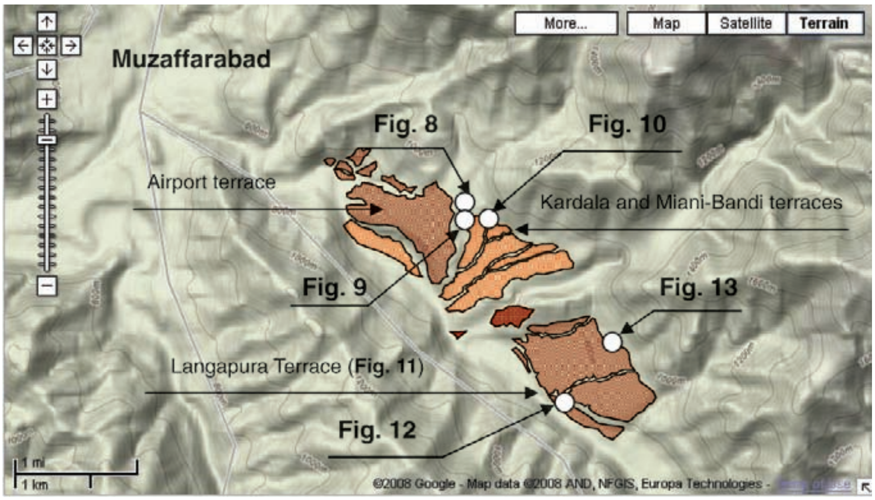

Fig. 8.10 Candidate relocation sites for Muzaffarabad (after JICA/ERRA, 2006)

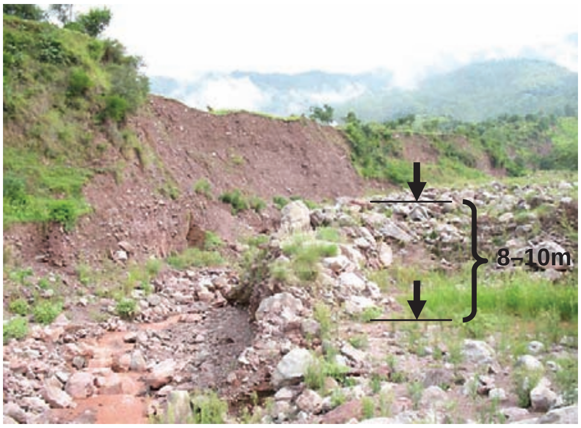

Fig. 8.11 Segregation of large boulders (N34°20' 37.8", E73°30' 57.6")

this point at the debris front, the river has been eroding the southern cliff of the terrace to the level lower than the estimated original river sediment surface, probably because this side was easy to down-cut. It is possible that terrace can be eroded deep inland where large boulders were gathered. People may have to set further back from the rim of the terrace at these particular points.

At this point of terrace-side erosion, boulders, stones and pebbles embedded in the purple-red colored soil matrix exposed there make up a loose granular fabric. Probably this soil matrix has less inclusion of dolomite making it less weakly cemented than those in Muzaffarabad city. During rains, waters flowing on the surface will erode its surface gradually leaving gullies on its surface, and some shallow stones embedded in the matrix will come off. Erosion of the toe part of the terrace cliff can trigger a cohesive slope failure as shown in Fig. 8.12(a). Once the soil mass has stopped the river, the water behind the soil mass will overflow the mass, and down-cutting will start to develop slowly but steadily up through the soil mass. After the entire deep gully is formed across the slipped soil mass, the slope failure will be reactivated. If necessary, stabilization of the slipped soil mass can be done by constructing a concrete spillway over the soil mass.

8.2.2.2 Kardala and Miani-Bandi Terraces

Figure 8.13 shows escarpments and cracks opened behind the Miani-Bandi terrace. The uppermost length crack extending across the mountains may suggest the presence of a deep slip surface (either hidden fault or deep landslide), while the others on the lower locations suggest shallower slides. As a whole, the middle part of the landslide mass is seemingly the thickest, immediately above the estimated original toe locations suggesting the landslide mass can move as a coherent body. A coherent soil mass can move much slower and smaller distance than those disrupted. However, continual movement of the mass may cause some difficulty for maintaining lifelines crossing the landslide mass. If it is unavoidable to construct link roads, water supply systems, etc. across this landslide mass, careful prior monitoring will be a must. Seepage points, which are often found around toe parts of landslide masses, are to be mapped, and extensometers are to be installed to monitor crack openings. Dwellings are to be set back from the toe part.

8.2.2.3 Langapura Terrace

Along the lowermost ridge of the northwestern part of the wide spread Langapura terrace near the

Fig. 8.12 Slope failure near the airport: The toe part of the soil mass is half cut down to lower elevation. When the scratch develops all through the soil mass, the slope failure can be reactivated. (a little downstream side of N34°20' 27.5", E73°30' 55.6")

(a) Slope failure near the airport

(b) Toe of the slipped soil mass half eroded

Fig. 8.13 Cracks and escarpments behind Miani-Bandi terrace (N34°20' 20.0", E73°31' 10.5")

Jehlum river, round boulders are making up granular fabric (conglomerate) embedded in soil matrix (Fig. 8.14). The presence of these round boulders suggest that the terrace materials (boulders and other suspended matters) have been carried by the Jehlum River and deposited tightly. Along the riverbed of a small river eroding shallow the terrace, sub-angular to angular boulders were rarely found suggesting that the amount of debris from mountains rising behind to the east, is only a small quantity. Therefore this area of the terrace is seemingly stable with a less serious threat of debris flows etc, and may be a possible location for developing a satellite town.

The thick surface material at the top, near the southern terrace rim, (Fig. 8.15(a)) includes a huge amount of angular stones and rocks. At some location, a thin silty layer of about 10 cm thickness was bedding within (Fig. 8.15(b)). All these suggest that the entire top surface mass at this part of the terrace was debris carried over centuries from the mountains behind, to the east. Some shallow surface

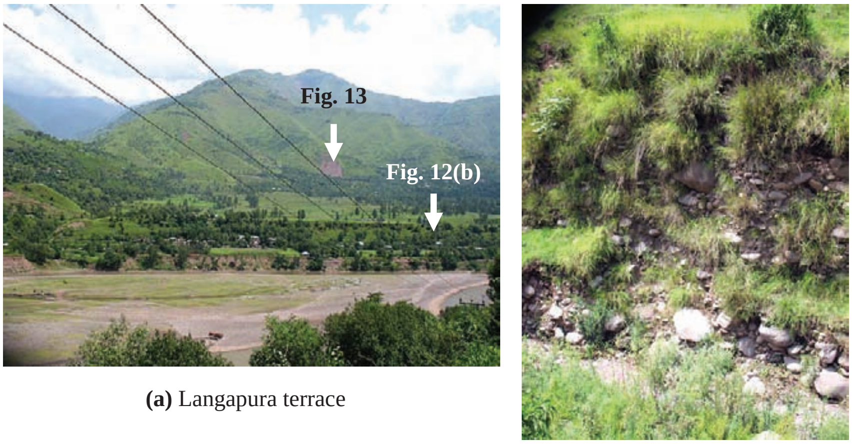

(a) Langapura terrace

(b) small scratch across the teraace rim

Fig. 8.14 Langapura terrace (N34.318993°, E73.530429°)

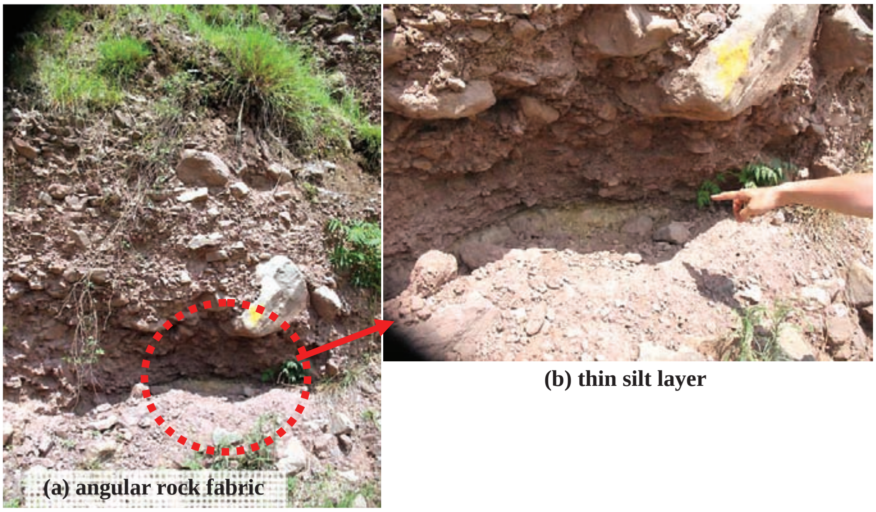

Fig. 8.15 Angular stone fabric (N34.316228°, E73.536258°)

failures along the terrace ridge suggest that the top surface material can be easily broken when it is soaked. Piles of fallen pieces of debris in repose line the toe of the terrace, and reach several tens of meters ahead over the lower terrace. This suggests that houses on the lower terrace should be set back at least this distance from the toe of the upper terrace.

There is a shallow-seated slope failure at a toe slope of mountains to the east behind the terrace (Fig. 8.16). There are some silty sand rocks with some signs of slaking. A soil mass of fine granular substances and pieces from these broken rocks can be sticky and paste-like when wet, and slump down towards the flatland of the terrace. Though catastrophic failure may not occur, construction of houses and/or lifelines on these soil masses are to be avoided.

8.3 Monitoring Landform Changes after the October 23rd Mid-Niigata Earthquake, Japan

An intense earthquake of magnitude 6.8 jolted central Japan at 17:56 JST on October 23, 2004. The hypocenter of the main shock was located at

Fig. 8.16 Shallow-seated slope failure at a toe slope of east mountains behind the terrace (N34.325555°, E73.539210°)

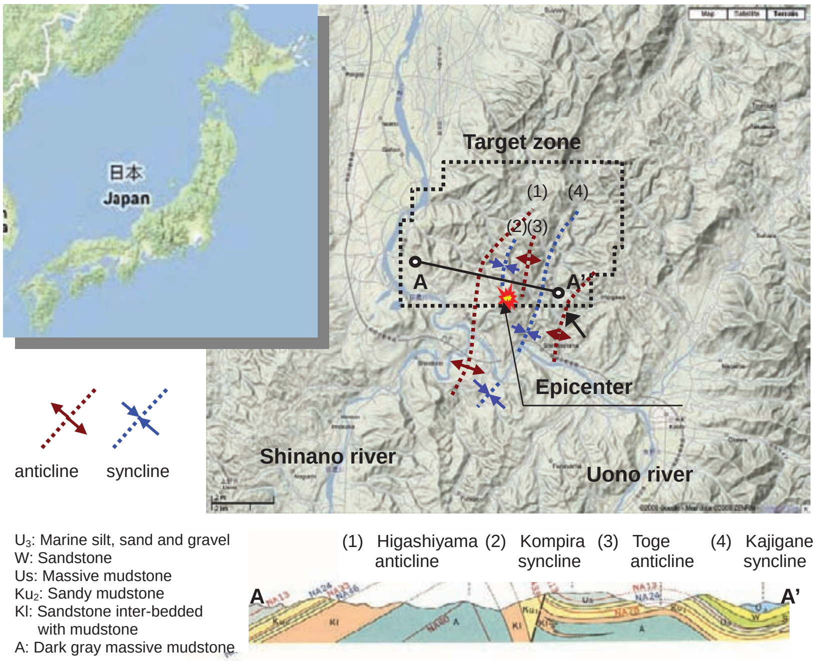

Fig. 8.17 Active folding zone jolted by the October 23rd 2004 Mid-Niigata Earthquake with its epicenter at a latitude 37°17′ 30′ N, and longitude at 138° 52′ 20″ E (after Konagai et al., 2008)

37°17’18”N; 138°52’12”E, in mid Niigata Prefecture, at a depth of 13 km (Fig. 8.17). The maximum acceleration of 1500 cm/s^2 was recorded at Ojiya K-net station which is about 10 km west of the epicenter (National Institute of Earth Science and Disaster Prevention, 2004). The main earthquake was followed by a series of strong aftershocks in rapid succession. These strong earthquakes had focal mechanisms of reverse fault type with the compression axes oriented NW/SE. The orientation is consistent with the historical information of large earthquakes in this area. The epicenters of the aftershocks were distributed along the NNE and SSW direction within a length of about 30 km immediately beneath the Higashiyama mountains zone. This continual tectonic movement has formed NNE-SSW-trending geological folds of sedimentary rocks in the source region. Since the up-folded rocks along anticlines have been expanded and cracked over centuries, anticlines frequently have their crests deeply eroded, with a number of debris deposits rimming the eroded hollows. Large-scale landslides are found even on gentle mountain sides dipping towards synclines because their toes are often deeply eroded by rivers. The region is thus one of the most landslide-prone zones in Japan.

Some past earthquakes have shown that earthquakes in such active folding zones can trigger long-lasting geotechnical rehabilitation issues. The May 8th, 1847 Zenkoji Earthquake jolted the active folding mountain terrain west of Nagano, central Japan. In 1884, 37 years after the earthquake, a crack near the southern summit of the Chausuyama twin peaks (Elevation 730 m, Location: 36°35’43”N, 138°06’32”E) began to open wide, which was an early sign of a long-lasting landslide. An 800 meter-long soil mass on the mountain-side began to gradually change its shape, causing a small village on its toe to rise up remarkably. After heavy rains in 1930, the entire soil mass began to creep down the slope exhibiting thick, wet and sticky features, and the maximum speed of 93 m/year was reached in 1932–1934. The slope was finally stabilized in the 1970 s with a tremendous amount of drainage works that were started in 1965 (Kato and Akabane, 1986). With all similar examples compiled in active folding zones, the quick stabilization of slopes in the Mid-Niigata mountainous terrain was considered to be a pressing need.

In addition to landslides, surface tectonic deformation is considered to have caused some problems for rehabilitating the affected areas. As will be discussed hereafter, the tectonic movements have seemingly caused the middle part of both the Shinano and Uono rives to be raised upward by about 0.5–1.5 m. Probably due to this tectonic deformation, the upper stream reach of the Uono River was flooded in the heavy rain of June, 2005, about eight months after the earthquake. Therefore the first and essential step for research to proceed and before any rational and scientific discussions on remedial measures take place, the procedure should be to separate soil deformations caused by the tectonic movement of the active folding zone from the overall soil deformations observed on the ground surface.

To study landform changes, the authors have gathered digital elevation models (DEM hereafter) at 6 different times; (1) 1975–1976, (2) Oct. 24, 2004, (3) Oct. 28, 2007, (4) May 2005, (5) May 2006, and (6) May 2007 (JSCE Active folding Project, 2008). Landform changes due to the earthquake are first assessed. Interferometric Synthetic Aperture Radar (InSAR) is one of the most advanced technologies that can measure elevation changes with high precision (United States Geological Survey 2005). However, thick vegetation and thousands of landslides have made fringe patterns too complicated for extracting pure elevation changes (Ozawa et al., 2005). Therefore, precise digital elevation models (DEMs, hereafter) before and after the earthquake were obtained using stereoscopy and Laser Imaging Detection and Ranging technology (LIDAR). The DEMs were then compared to detect elevation changes and translations of the topography. Lastly, all the changes of landforms due to landslides are excluded for detecting tectonic deformations of the ground surface, which can be useful in estimating the deformations of the internal soil deformations.

Figure 8.18 shows elevation changes for $11 \times 7\ \text{km}^2$ area of Higashi-yama mountains affected by the earthquake. Numerous amounts of dots with their elevations displayed with different colors are all arranged in 2 m by 2 m square. The result shows the elevation changes in Eularian coordinates, namely, changes observed from points fixed in space. Therefore they are not identical to displacements of soil particles (Lagrangian particles). Moreover, the elevation data from the 1970's are from aerial photographs, while the data for the post earthquake landforms are obtained through laser-profiling from aircrafts. In each method, careful data conditionings were made to minimize systematic errors (Konagai et al., 2008). The Lagrangian particle motions were obtained first and then the elevation changes were compared at several points of triangulations to verify the obtained result.

Figure 8.19(a) and (b) show respectively horizontal and vertical components of surface tectonic displacements extracted from the DEMs. The target zone may be slightly too small for discussing the entire tectonic deformation that spreads beyond the boundaries of the zone. It was, however, fortunate that Shinano River Office, Hokuriku Regional Bureau of the Ministry of Land, Infrastructure

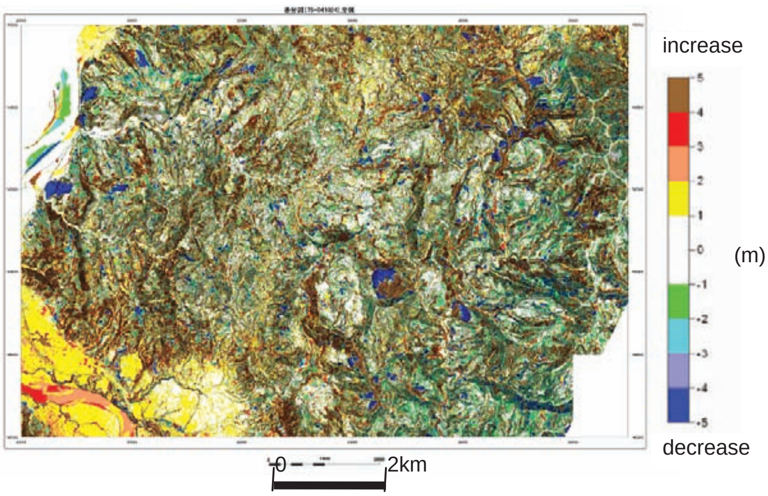

Fig. 8.18 Elevation changes between two digital elevation models at two different times, Oct. 24, 2004 and 1975–1976, respectively. Warm colors (*yellow, red* etc.) show increase in elevation while cool colors (*green, blue* etc.) indicate decrease in elevation. See legend

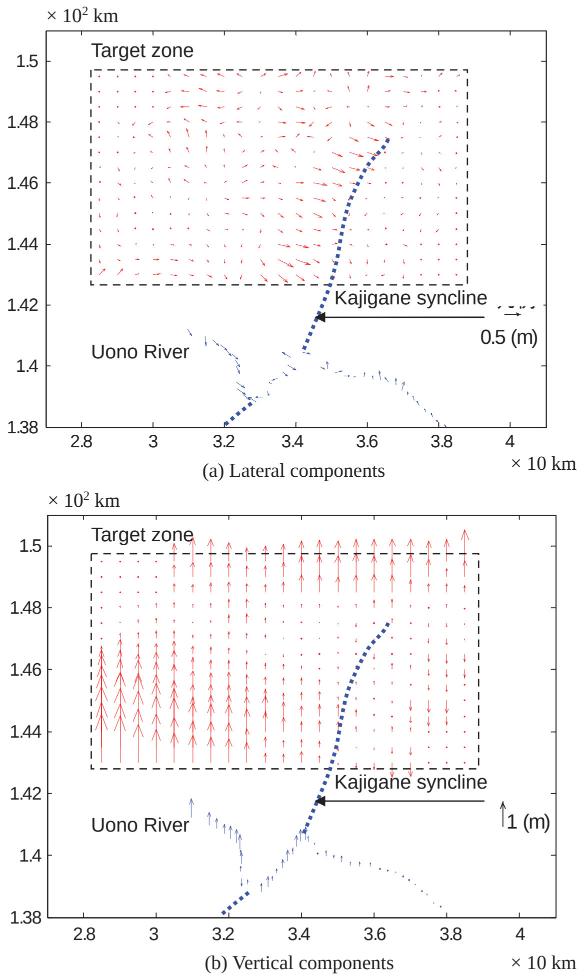

Fig. 8.19 Surface tectonic displacements (after Konagai et al., 2008): The surveyed area is included in Zone VIII of the Japanese National Grid System. NS and EW distances in the above figures have their origins at the south-west corner of Zone VIII located at 138°30'00"E, 36°00'00"N. Blue arrows are benchmark displacements along the Uono River measured by the Shinano River Office, Hokuriku Regional Bureau, MLIT

and Transport (MLIT), has been measuring exact locations of bench marks along both the Shinano and Uono rivers on regular basis. Lateral and vertical components of the bench marks' displacements due to the earthquake were also plotted on Figure 8.19(a) and (c), respectively. For the horizontal components, there is a NNE-SSW trending belt of large eastward movement to the west of and along the Kajigane syncline. For the vertical components, it is notable that there are two areas in the target zone, which have been pushed up by 0.5–1.5 m (Fig. 8.19(b)). The most remarkable hump spreads wide across the southwestern part of the target zone where the Uono river joins the Shinano River.

The Uono River, after flowing straight west through a flat wide spread valley of Horinouchi, meets the sedimentary silty sand rock ridge of Cenozoic Era. The river then abruptly changes its direction, from SE-NW to NE-SW, along this rock ridge, making a sharp down-folded bend. Then it forces its way through the narrow and lowest points among the mountains making a sharp up-folded bend. On the geological map of this area (Yanagisawa et al., 1986), the approximately 2 km-long stretch of the Uono River between these two bends continues straight to both the Kajigane and the Kodaka synclines at its north and south ends, respectively, suggesting that this 2 km-long stretch of the river is a part of the large Kajigane syncline.

Areas along the upper reach of this part of the Uono River were flooded due to heavy rainfall of June 27–28th, 2005, about 8 months after the earthquake (Fig. 8.20). Assuming that the same amount of water in the 2005 rain flowed down the Uono River as existed before the earthquake (ignoring the landform changes caused by the Chuetsu earthquake), possible water depths at all bench marks along the 57.5 km-long flooded zone (from BM No. 15 at 37°15'59"N, 138°51'44"E, to BM No. 72.5 at 37°15'33"N, 138°54'00"E) were estimated by using the Manning empirical equation. For this estimation, precise dimensions for the river cross-sections and inclinations at all benchmarks before and after the earthquake were provided by the Shinano River Office, Hokuriku Regional Bureau of the Ministry of Land, Infrastructure and Transport (MLIT).

Solid circles in Fig. 8.21 show the actual water levels at all bench marks reached in the 2005 flood, while open circles show virtual water levels calculated for the Uono River as it existed before the earthquake. At almost all points, the virtual water levels are lower than those reached in the 2005 real flood. Actual water levels were higher than the high water levels (HWL) at bench marks # 37.5, # 52.5 and # 62.5, while virtual water levels at these points do not reach the high water levels. This

Fig. 8.20 Flooding of Uono River on June 28, 2005 (Konagai et al., 2008)

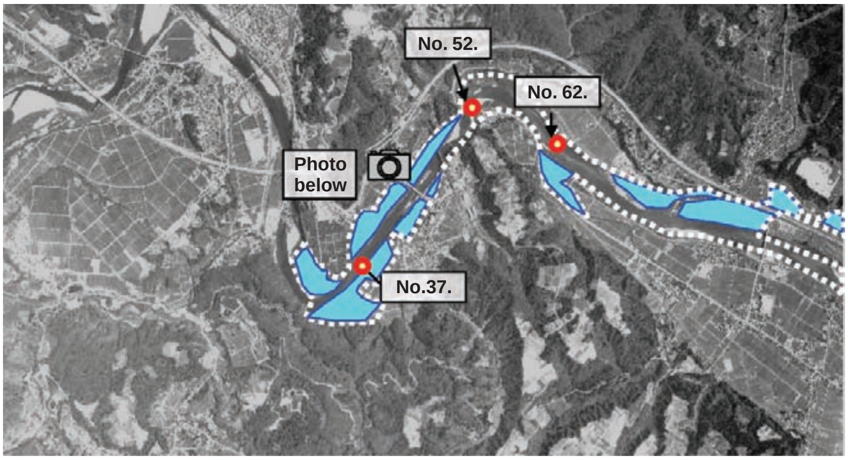

(a) Flooded farm lands (data provided by the Hokuriku Regional Agricultural Administration Office, Ministry of Agriculture, Forestry and Fisheries, and Uonuma City): Benchmark numbers correspond to those in **Fig 8. 22**

(b) Flooded area near Benchmark No. 42.5km (Photo by Kotajima, S.)

figure thus suggests that there was a cause-and-effect relation between the earthquake-induced tectonic deformation and the flooding of June, 2005.

The landforms in the target zone have changed largely due to the earthquake. However, the landforms excluding those due to rehabilitation works have shown little change since then. This was probably due to the fact that about 10 billion JPY was spent over 3 years to stabilize landslide masses on the front by means of constructing concrete-faced spillways. Post-earthquake DEMs at different times show the stabilization works were sequentially followed by reconstructions of road networks and then farm lands (Fig. 8.22).

8.4 Disclosing Digitally-Formatted Borehole Data

In addition to monitoring landform changes, it will merit the whole society to compile all available and reliable borehole data and disclose them. Though

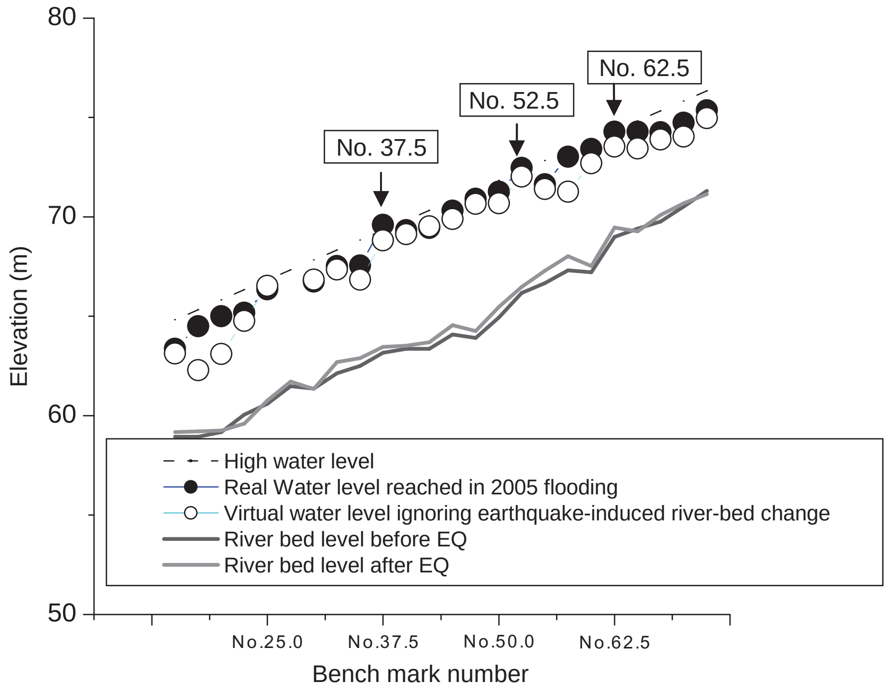

Fig. 8.21 Actual water levels at all bench marks reached in the 2005 flood, and the virtual water levels for the Uono River as it existed before the earthquake (Konagai et al., 2008)

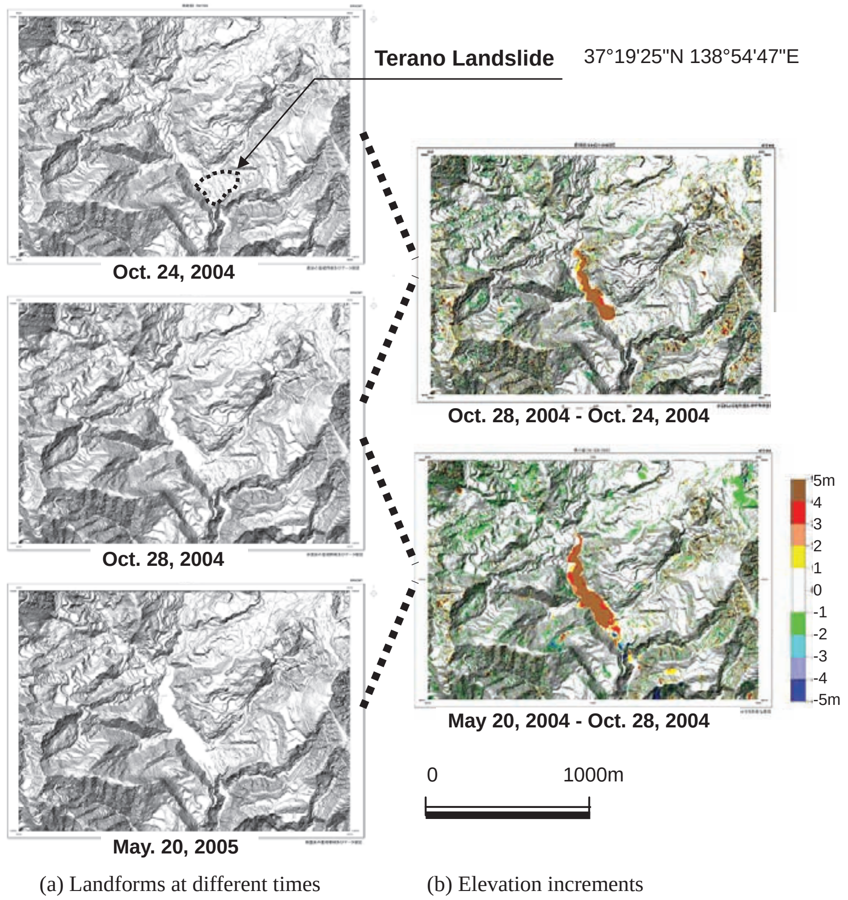

Fig. 8.22 Digital elevation models of the Terano landslide and its vicinity at different times: The area was devastated by the October 23rd 2004, Mid-Niigata Earthquake. Green colors on mountain slopes show that they are being eroded gradually, while the water that had carried soils and other suspended matters was stopped behind the landslide mass at Terano. The landslide mass was successfully stabilized by constructing a concrete-faced spillway over it. (JSCE Active folding Project, 2008)

some soil databases are available in some countries, they were mostly developed for mining industries. For disaster prevention, Taiwan became a pioneer for developing and disclosing soil data after the ChiChi earthquake of 1999. In Japan, Ministry of Land, Infrastructure and Transport (MLIT hereafter) is starting a project for disclosing digitally-formatted borehole data. An advisory committee (Chairman; Konagai K., IIS, University of Tokyo) has been organized for this objective. There are two major data sources that can be a platform for the system. They include:

(1) TRABIS (Technical Report and Boring Information System)

The original system dates back to the late 1980's. In 1986, it became a must for all trustees of the Ministry of Public Works (MPW, one of two predecessors of MLIT) projects to deliver borehole data written on prescribed sheets. The data delivered were then digitized and kept at the MPW computer center. The system was largely updated in 1994 in such a way that all trustees deliver their data on floppy disks following the prescribed format. The most updated format is available on the web. So far, information about 100,000 boreholes have been gathered.

(2) In 1984, Port and Harbor Research Institute of the Ministry of Transport (MT, another predecessor of MLIT) started to collect borehole data, in order to provide important pieces of information for constructing ports and harbors. Microsoft Access has been the platform for this database. A total of 28,300 boreholes are now available on the database.

8.5 Summary

Rehabilitation issues often attract less attention than issues that arise in the immediate aftermaths of earthquakes, and have never been given prominent coverage by news media. However, the Kashmir earthquake of 2005 has left a huge landslide mass in the upper stream reach of the Jhelum River, damming a total 62 million m^3 water behind it. The landslide mass is seemingly changing its permeability, which may cause slow and steady change in its rock/soil fabric. It is therefore mandatory to monitor any change in the landslide mass so that we should not miss any danger sign. The earthquake also formed a great number of debris deposits that may become future debris sources along the activated seismic faults. Heavy rains in the monsoon of 2006 that followed the earthquake of 2005 were responsible for raising river beds. Even within the city of Muzaffarabad, people living along valleys with gullies in the terraces are suffering from debris from mountains rising behind, with their dwellings being half and/or entirely buried in debris.

Among options for rehabilitating Muzaffarabad, one feasible idea will be to lay out satellite towns outside the municipal boundary as described in the JICA master plan. Staying a short distance away from unstable rims of terraces will allow terraces to be appropriate locations for developing satellite towns. One difficulty will be the maintenance of roads, which will have to cross deep gorges. During heavy rains further debris flows can occur. These flows will most likely follow the gorges that are tributaries of the Jehlum and Nihlum rivers crossing roads and suspending traffic. Clearing debris remaining on the roads would be just a stopgap. By means of connecting existing roads point-wise by constructing new bridges etc, a cost-effective bypass can be constructed allowing bi-directional traffic to be realized.

To map out a rational tactics for rehabilitations, it is of essence in order to have a clear perspective for dealing with long-lasting landform changes. For example the Zenkoji Earthquake, which occurred in the central part of Japan in 1847, indicates that an earthquake can cause extremely long-lasting geotechnical hazards. For this, monitoring landforms at different times is strongly recommended. In addition to monitoring landform changes, it will be beneficial if the whole society find ways to compile all available and reliable borehole data and disclose them.

Acknowledgments The authors are indebt to Dr. Allah Bakhsh Kauser, Director, Pakistan Geological Survey at Islamabad, and Mr. Zahid Ameen, Chairman, Development Authority Muzaffarabad, AJK Pakistan who have kindly taken all the trouble for our surveys in Muzaffarabad and Hattian Balla.

The latter part of this paper summarizes one of the outcomes of the Research and Development program for

Resolving Critical Issues, "Earthquake damage in active-folding areas: creation of a comprehensive data archive and suggestions for its application to remedial measures for civil-infrastructure systems," Special Coordination Funds for Promoting Science and Technology, Ministry of Education, Culture, Sports, Science and Technology. The authors would like to express their sincere thanks to all members of the project steering committee organized under the Japan Society for Civil Engineers as the core of the project.

References

Dunning S.A., Mitchell W.A., Rosser N.J. and Petley D.N. (2007), The Hattian Bala rock avalanche and associated landslides triggered by the Kashmir Earthquake of 8 October 2005, Engineering Geology, 93:130–144.

Ermini L., Casagli N. (2003), Prediction of the behaviour of landslide dams using a geomorphological dimensionless index. Earth Surface Processes and Landforms 28:31–47.

JSCE Active folding Project (2008), Earthquake Damage in Active-Folding Areas: Creation of a comprehensive data archive and suggestions for its application to remedial measures for civil-infrastructure systems (2005–2007), Research and Development Program for Resolving Critical Issues, Special Coordination Funds for Promoting Science and Technology, (Core research organization: JSCE, Leader: K. Konagai),.

JICA/ERRA Interim Report (2006), The urgent development study on rehabilitation and reconstruction in Muzaffarabad City in the Islamic Republic of Pakistan, Japan International Cooperation Agency (JICA), Earthquake Reconstruction and Rehabilitation Authority (ERRA).

Kato H. and Akabane H. (1986), Geology of Nagano District, with Geological Sheet Map at 1:50,000, Geological Survey of Japan, 120p.

Konagai K., Johansson J., Ikeda T., Numata A. and Takatsu S. (2007), Geotechnical problems for rational rehabilitations of areas affected by the Kashmir Earthquake of October 8, 2005, JICA/EWBJ Joint Seminar on Earthquake Natural Disaster Mitigation, Islamabad and Muzaffarabad, pp. 1–22.

Konagai K., Fujita T., Ikeda T. And Takatsu S. (2008), Tectonic deformation buildup in folded mountain terrains in the October 23, 2004, Mid-Niigata earthquake. Soil Dynamics and Earthquake Engineering, doi: 10.1016/j.soildyn.2008.01.013, in press.

Nakata, T., Tsutsumi, H., Kahn, S.H. and Lawrence, R.D. (1991), Active faults of Pakistan, map sheets and inventories. Special Publication no.21, Res. Center for Regional Geography, Hiroshima Univ., 141p.

National Institute of Earth Science and Disaster Prevention (2004). "2004 Mid Niigata Earthquake." http://www.hrr.mlit.go.jp/saigai/H161023/1023_top.html

Ozawa, T., Nishimura, S., Wada, Y., Okura, H. (2005), "Coseismic deformation of the Mid Niigata Prefecture Earthquake in 2004 detected by RADARSAT/InSAR." Earthquake Planets Space, 57. 423–428.

United States Geological Survey (2005). "What is InSAR?" Earthquake Hazard Program, Earthquake Research, http://quake.usgs.gov/research/deformation/modeling/InSAR/

Yanagisawa Y., Kobayashi I., Takeuchi K., Takeishi M., Chihara K. and Kato H. (1986), Geology of the Ojiya District, Quadrangle Series Scale 1:50,000, Niigata (7), No. 50, Geological Survey of Japan.

WPDA report (2006), Study of Hattian Bala landslide, Potential Hazards of landsliding and mitigation measures at Hattian Bala and other earthquake hit areas, National Engineering services Pakistan limited (NESPAK) and Geological Survey of Pakistan (GSP), Water and Power Development Authority, Government of Pakistan.

9 The Increasing Wildfire and Post-Fire Debris-Flow Threat in Western USA, and Implications for Consequences of Climate Change

Susan H. Cannon and Jerry DeGraff

Abstract In southern California and the intermountain west of the USA, debris flows generated from recently-burned basins pose significant hazards. Increases in the frequency and size of wildfires throughout the western USA can be attributed to increases in the number of fire ignitions, fire suppression practices, and climatic influences. Increased urbanization throughout the western USA, combined with the increased wildfire magnitude and frequency, carries with it the increased threat of subsequent debris-flow occurrence. Differences between rainfall thresholds and empirical debris-flow susceptibility models for southern California and the intermountain west indicate a strong influence of climatic and geologic settings on post-fire debris-flow potential. The linkages between wildfires, debris-flow occurrence, and global warming suggests that the experiences in the western United States are highly likely to be duplicated in many other parts of the world, and necessitate hazard assessment tools that are specific to local climates and physiographies.

Keywords Debris flow • Hazards • Risk • Climate change • Western USA • Southern California • Intermountain west USA

9.1 Introduction

An association between debris-flow occurrence and recent wildfire in mountain watersheds was recognized in southern California and northern Utah in the 1930 s and 1940s (Eaton, 1935; Bailey et al., 1947). Southern California (USA) is an area where this relationship between wildfires and debris flows is particularly well understood (Wells, 1987). There are several reasons for the commonly referred to "fire and flood cycle" in this area (Kotok and Kraebel, 1935). Southern California is within the Mediterranean climate chaparral biome. Consequently, it experiences wildfires nearly every year with most of them taking place immediately before the winter rainy season (Wells, 1987). Much of the burned area is on steep, brush-covered slopes drained by equally steep, short channels which facilitate debris flow occurrence.

The study of debris flows and wildfire received much of its continuing emphasis because of the dramatic increase in population and urbanization in southern California beginning during World War II and continuing to present. This placed many more

Susan H. Cannon (✉)
U.S. Geological Survey, Box 25046, DFC, MS 966,
Denver Co 80225, USA
e-mail: cannon@usgs.gov

Jerry DeGraff
U.S.D.A. Forest Service, Sierra National Forest,
1600 Tollhouse Road, Clovis, CA 93611
e-mail: jdegraff@fs.fed.us

© Springer-Verlag Berlin Heidelberg 2009

people and ever greater amounts of property and infrastructure at risk from both wildfires and any subsequent debris-flow activity. However, due to the combination of population growth and increased wildfire occurrence and size throughout the western USA, the concern for risk from both wildfires and subsequent debris flows is no longer limited to southern California.

The purpose of this paper is to examine the relations between population growth, increased wildfire magnitudes and frequencies, climatic variability and debris-flow generation, to describe some of the tools presently available to assess the associated debris-flow hazards, and to consider the potential implications of climate change on these relations. Population growth has placed many more people, property and infrastructure at risk throughout the western USA. Coincident with population growth, wildfire occurrence and size is increasing in the western United States. Although this may reflect an increased probability of anthropogenically-caused wildfire (e.g. arson, downed power lines, car fires, etc.), we also describe how, in some settings, past fire suppression policies that have lead to greater natural fuel availability. Climatic variation may also have a role in increasing forest vulnerability to more frequent and bigger wildfires. Regardless of the specific importance of these factors, greater wildfire frequencies result in increased likelihood of precipitation-induced debris-flow events in recently burned areas.

To reduce the risk to the public, it is crucial to more effectively identify where post-wildfire debris flows might occur and the rainfall conditions that may trigger these events. These predictions are necessary to effectively allocate limited financial resources for warning and protective measures over large potentially affected areas. Tools to predict when within a storm debris flows might occur, the probability that a given drainage basin will produce a debris flow, and the potential volume of the event in southern California and the intermountain west, USA, are described.

Recognition that climate oscillations on interannual and decadal time scales influence wildfire occurrence and size has implications for debris flow risk. Debris flows will be more likely during time when climatic variation promotes greater likelihood for large stand-replacing wildfires. This effect suggests that debris flow risk might also be influenced by global warming. Less clear is whether global warming will affect the number or strength of storms that carry the potential for triggering debris flows.

9.2 Wildfire and Debris Flow Coincident Hazards

Wildfire represents a distinct natural hazard with many immediate and disastrous consequences. By the 1920 s and 1930 s, it appears that the dual disaster of post-wildfire flooding was being recognized in southern California (Wells, 1987). Eaton (1935) was one of the earliest southern California researchers to correctly recognize that some of what being described as flooding was actually the occurrence of debris flows, as described in his account of the January 1, 1934 event that affected the Los Angeles Basin towns of Montrose and La Crescenta. Wells (1987) notes the failure by later researchers to correctly identify debris flows even while accurately describing that phenomenon. By the 1970 s, researchers began to more fully recognize the hazards associated with precipitation-induced debris flows from recently burned areas (Scott, 1971; Wells, 1981, 1987). As such, agencies and scientists involved in post-wildfire emergency response now incorporate methods for assessing debris-flow potential into their evaluations (DeGraff and Lewis, 1989; DeGraff et al., 2007).

The local population understandably feels the worst is over if a wildfire is prevented from burning over their homes and communities. This was especially true in southern California in October 2003. More than 4,220 homes were destroyed by wildfires that year, and nearly all of them were in southern California (Radeloff et al., 2005). However, that wasn't the end of the saga. Debris flows were triggered from many of the basins that had been burned by the Old and Grand Prix Fires in response to a late December 2003 storm event. Debris flows from two basins were responsible for the deaths of 16 people and costs for clean up and infrastructure repair were reported in the billions of US dollars (P. Mead personal communication, 2004). The often short time period between fire containment and storms that trigger debris flows adds a significant challenge to agencies and scientists responsible for protecting the public from these types of events. In addition to the lack of expectation, a second deceptive aspect of post-wildfire debris flows is that they can cause damage several kilometers from the actual fire boundary. While it is the effect of the wildfire on the vegetation and soil within the burned watershed that enables a debris flow to occur with the right triggering storm event, they can travel significant distances from their origin. A third characteristic that makes debris flows a significant concern is their speed in covering those distances. The debris flow impacting Camp St. Sophia, which was responsible for the greatest number of deaths, was estimated to be moving at about 4 m/s at the time of arrival (DeGraff et al., 2007) (Fig. 9.1).

A debris flow is composed of a slurry of finer-grained particles with large rock fragments including large boulders and woody debris entrained within it (Costa, 1984). Because debris flows are more viscous than flood waters, it maintains a relative coherent mass (Costa, 1984). The leading edge of the debris flow is typically a bouldery snout followed by a more viscous body that transitions to a very muddy water flow as it passed down a channel. Debris flow damage occurs by drag, buoyancy, lateral impact or burial (Campbell, 1985). Damage resulting from drag takes place as it passes by building foundations or bridge abutments. A frictional and differential pressure is exerted that can displace the structure. Buoyance damage results from the debris flow entraining an object like a vehicle or lifting a bridge off its foundation and rafting it to another location. Lateral impact primarily is damage inflicted by the large boulders or woody debris battering into structures or other obstructions within the debris flow path. Burial is common in low-gradient, wider reaches of the channel or in the runout area of the debris flow. Objects and structures within the runout area where the debris flow comes to rest may be partially or completely buried (Fig. 9.2). Levee deposits along the lateral margins of the debris-flow path more commonly cause partial burial.

While southern California may be widely recognized as a location where wildfires and debris flows commonly occur, many other parts of the western United States are subject to this combination of hazards. On September 1-2, 1994, debris flows were triggered in the recently burned watersheds on Storm King Mountain, Colorado in response to a torrential downpour (Cannon et al., 2001). Flows issued from fifteen channels onto or near Interstate Highway 70 trapping or engulfing thirty vehicles. Two people traveling with these vehicles were swept into the adjacent Colorado River

Fig. 9.1 Debris-flow damage at Camp St. Sophia in southern California. Fourteen people were killed at this site when the building they were taking shelter in (of which the rectangular concrete foundation in photo center remains) was swept away by the debris flow

Fig. 9.2 House damaged by debris flow generated from 2002 Missionary Ridge Fire in southwest Colorado (USA)

resulting in their sustaining serious injury. Between 2000 and 2004, twenty-six debris flows were generated from seven wildfire areas in northern Utah (Giraud and McDonald, 2007). Major damage to five houses and minor damage to 27 others inflicted losses amounting to $500,000. Many of the basins burned by the Missionary Ridge and Coal Seam Fires in 2002 in Colorado responded to a series of summer thunderstorms by generating damaging debris flows (Cannon et al., 2003) (Fig. 9.2). In the Sierra Nevada of California, burned watersheds upslope from El Portal, a gateway community to Yosemite National Park, generated several debris flows in March 1991. Major damage was avoided partly because debris flow protective measures had been installed (DeGraff, 1994).

9.3 Increasing Threats

9.3.1 Expanded Urbanization

Among the geographic regions of the United States, the Federal government controls a much higher proportion of land within the western United States. It includes land designated as national parks, national forest, set aside as military reserves and land managed by the Bureau of Land Management. For example, these Federally-managed lands represent just a little more than 67% of the State of Utah. Consequently, the booming population growth occurs on the border of these undeveloped or wildland areas. Within in the last decade the term *wildland-urban interface*, has been coined to describe this urban and suburban development in or near wildland vegetation (Fig. 9.3). It is recognized as a focal point for a number of environmental issues, including increasing property losses to wildfires (Radeloff et al., 2005).

In addition to southern California, other parts of the western United States experienced population growth for a number of diverse reasons ranging from a burgeoning elderly population attracted to the warm, sunny Southwest to a better quality of life that coupled wide open spaces with increased recreational and employment opportunities. Between 1900 and 1990, the population of the southwestern United States (California, Nevada, Utah, Arizona, New Mexico and Colorado) increased by about 1,500%, while during the same period, the population in the entire United States only grew by 225% (Chourre and Wright, 2005). This has resulted in development patterns similar to southern California arising along the Wasatch Front in Utah, around Reno and Las Vegas, Nevada, the Colorado Front Range and the

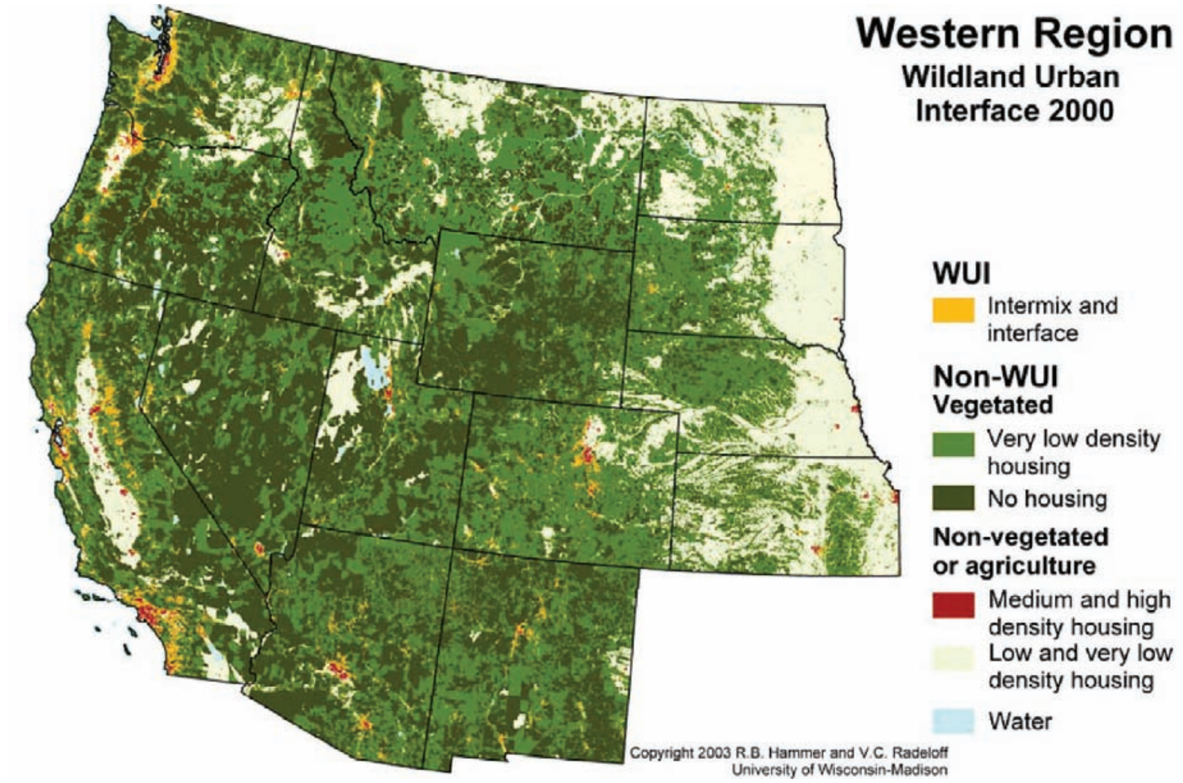

Fig. 9.3 Map of 2000 Wildland-Urban Interface in western U.S. (From Radeloff et al 2005)

Phoenix, Arizona and Albuquerque, New Mexico metropolitan areas (Fig. 9.4).

9.3.2 Increased Wildfire Frequency and Magnitude

The increase in wildfire occurrence is likely related to population. Radeloff et al. (2005) note human-caused fire ignitions are most common in the wildland-urban interface. As a recent example, they point out that human-caused ignitions were responsible for 43% of the fires during the record-setting 2000 wildfire season. There are many more opportunities for fire ignition with increased population during the dry, hot periods when vegetation is most vulnerable. Sparks from engines and activities such as welding, carelessness with fire from cigarettes to barbecues and fire setting by true arsonists to children experimenting with matches or fireworks are all more frequent occurrences with greater population. However, increased fire ignitions do not consistently account for the observed increase in number or size of destructive wildfires. For example, Keeley et al. (1999) contend that in the shrubland of southern California, any increase in fire starts has been largely offset by effective fire suppression.

The expansion of the wildland-urban interface and its attendant increase in population can affect the size of wildfires. Fighting wildfires tactically involves containing the fire to prevent it from growing larger and then controlling it until the wildfire is extinguished from a lack of fuel or application of retardant or water. Firelines are built by hand and machine to remove a swath of vegetation around the fire to deny it access to an additional fuels (Fig. 9.5). Fireline effectiveness during containment is increased by starting backfires to widen them. In a formerly rural area of scattered individual structures or small clusters of homes, it was possible to establish firelines across a broad front with little property loss. Urbanization limits the location of firelines and leaves far more property at risk. Keeley et al. (1999) note that the

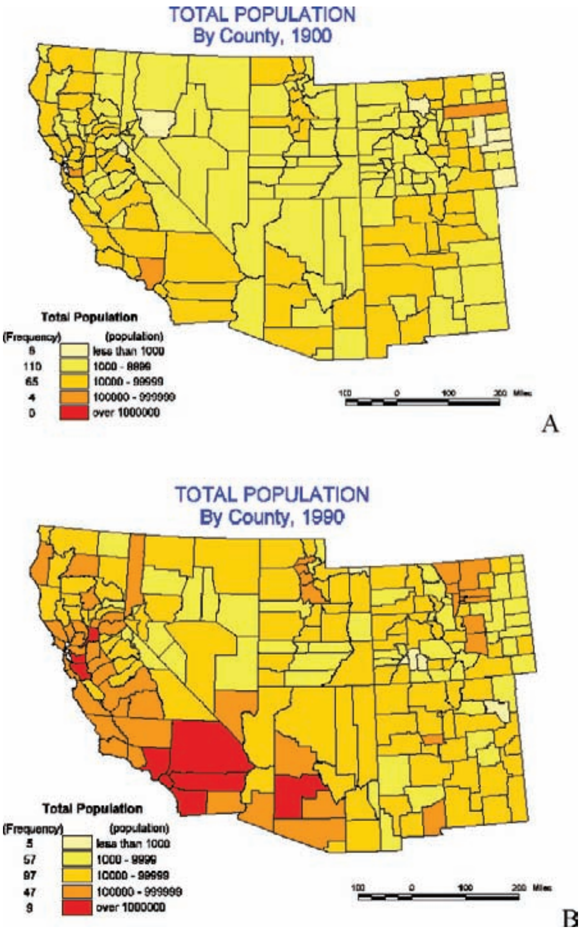

Fig. 9.4 Population change in the western USA between 1900 (**A**) and 1990 USA (**B**) (from Chourre and Wright, 2005)

Fig. 9.5 Fire line used for fire control of the 2007 Day Fire in the Topatopa Mountains of southern California. Dust rises from post-fire rehabilitation activity by large excavators

expansion of the urban-wildland interface makes it more and more difficult to put measures in place that would limit California shrubland wildfire from becoming larger and increasingly destructive.

Increased wildfire occurrence and size has another human component as well as a natural one. Over the last 80 years, suppression of wildfires was the common practice on national forests and other Western wildlands under both Federal and State control. This included fires triggered by both natural and human causes. The role of fire as a natural component of forest ecology was fully understood in only the last few decades. While efforts are being made to reintroduce fires as a frequent and natural aspect of these forest ecosystems, it is made difficult by the build up of fuels, (e.g. fallen woody material), resulting from previous suppression activities and grazing (Minnich, 1989; Allen et al., 1996; Grissino-Meyer et al., 2004). When fires occur in areas with heavy fuel loads, they are much more conducive to large and intense wildfires. This effect varies in importance among different wildland ecosystems within the western United States. While Grissino-Meyer et al. (2004) demonstrated that changes in forest species and density attributed to fire suppression result in increased fire frequencies and extents in southwestern Colorado, build up of high fuel loads, and long return intervals for large, intense fires, is expected in the Lodgepole Pine forests of northwestern Montana (Kauffman, 2004). Allen et al. (1996) found that the introduction of grazing animals in southwest USA Ponderosa Pine forests removed the fine fuels that carried frequent, low-intensity fires which served to prevent accumulations of significant fuel loads, and thus resulted in a changed the fire regime. However, Keeley and Fotheringham (2000) used historical records to demonstrate that the natural fire regime of southern California chaparral ecosystems in the past is little different from today. It remains dominated by wildfires driven by intense Santa Ana windstorms. Therefore, fuels treatments that might reduce fuel loads in northern Montana forests would be less likely to have the same beneficial results in southern California chaparral ecosystems.

The natural component responsible for periodically greater wildfire activity is climate. A number of studies have demonstrated how variations in climate resulting from atmosphere-ocean interactions influence fire occurrence and severity. In the southwestern

United States, large areas are burned after dry springs associated with the La Nĩna or high phase of the El Niño-Southern Oscillation (ENSO) phenomena in the Pacific Ocean. This association was evident from fire scar and tree growth chronologies covering the period of 1700–1905 and extended to 1985 by fire statistics (Swetnam and Betancourt, 1990). Their research showed large fires associated with deficient spring precipitation and reduced tree growth tied to the high phase of the ENSO. Fires over a large area were found to be synchronous in a manner which implies a greater control by seasonal climatic influence rather than just fire weather.

Similarly, the occurrence of large wildfires in northern California and Oregon reflect the influence of the ENSO and the Pacific Decadal Oscillation (PDO). Trouet et al. (2008) were able to link these synoptic-scale circulation patterns to interannual variations in specific fire weather indices. These indices are associated with fires becoming large or showing erratic behavior. Synoptic-scale circulation conditions that induce low atmospheric stability and humidity moisture levels produce high indices associated with widespread wildfires.

Westerling et al. (2006) see climate as the principle force behind wildfire risk at the interannual to decadal scales. Their conclusions are that climate variability at the interannual scale influences how flammable the forest fuels are when an ignition occurs. This would include both dead and live vegetation within the forest. These results are consistent with the findings of Trouet et al. (2008). Climate acting on a decadal scale alters the structure of vegetation communities (Westerling et al., 2006). Fuel continuity and drought tolerance of dominant species are identified as significant components affecting fire regime responses.

On these same interannual timescales affecting fire occurrence and severity, there is a connection to fire-related geomorphological events Pierce et al. (2004). Dating of fire-related sediment deposits on alluvial fans suggests that shifts in fire regimes also changed fire-related geomorphological events. In the western Ponderosa forests and subalpine forests of Yellowstone National Park, their data suggests that warmer periods experienced severe droughts, stand-replacing wildfires and large debris-flow events. Therefore, the increased threat of more and larger wildfires carries within it the increased threat of subsequent debris-flow occurrence.

The increased risk of wildfire-related debris flow highlights the need for methods to quantify the potential hazards posed by debris flows produced from burned watersheds. Science-based information on post wildfire debris-flow hazards is necessary to mitigate the impacts of fire on people and their property, and on natural resources. To reduce risk, it is crucial to more effectively identify the rainfall conditions that may trigger debris flows, where they might be generated, and how big they might be. Identification of potential debris-flow hazards from burned drainage basins is necessary to develop effective and appropriate mitigation strategies and decisions regarding emergency warnings, evacuation timing, and routes. Application of predictive models before the occurrence of wildfires can help identify potentially hazardous drainage basins and thus direct planning and use strategies for forests and areas slated for future development.

Tools for Assessing Debris-Flow Hazards from Recently Burned Areas

9.3.3 Rainfall Conditions and Intensity-Duration Thresholds

Debris flows generated during rain storms on recently burned areas have destroyed lives and property throughout the Western USA. Definition of the rainfall conditions that triggered these events, and of the rainfall intensity-duration threshold conditions for their occurrence, is a critical first step in a hazard assessment. Field evidence indicates that unlike landslide-triggered debris flows, these events have no identifiable initiation source and can occur with little or no antecedent moisture (Cannon et al., 2008). In addition, the great majority in the flows is derived from channel erosion and incision, rather than from an initial landslide event (Santi et al., 2008). Given these physical differences, rainfall and threshold conditions will be different from those that trigger landslide-triggered debris flows in a given location. Using rain gage and response data from five fires in Colorado and southern California, Cannon et al. (2008) documented the rainfall conditions that have triggered post-fire debris flows and developed empirical rainfall intensity-duration

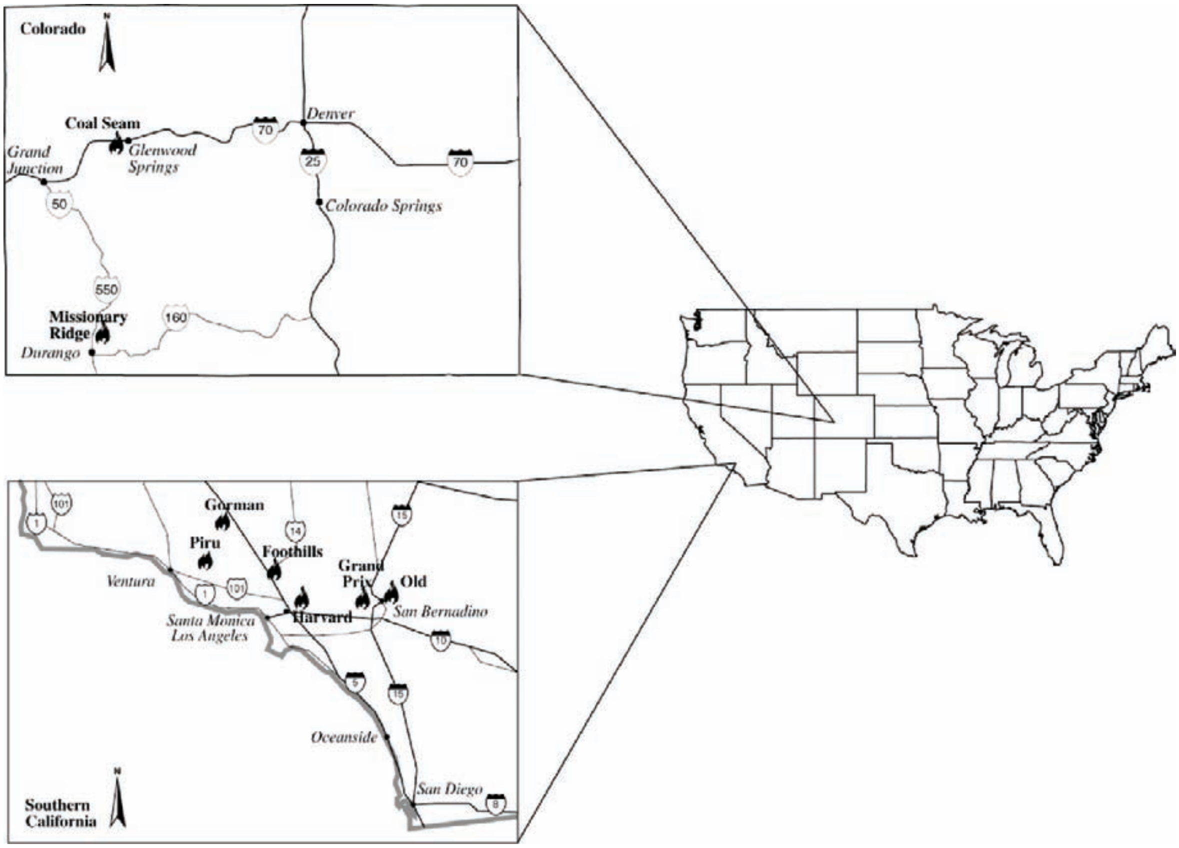

Fig. 9.6 Maps showing locations of fires in the study by Cannon et al. (2008)

thresholds for the occurrence of debris flows and floods following wildfires in these settings (Fig. 9.6).

Debris flows were produced from 25 recently burned basins in Colorado in response to 13 short-duration, high-intensity convective storms. Debris flows were reported after as little as six to 10 min of storm rainfall. About 80% of the storms that generated debris flows lasted less than three hours, with most of the rain falling in less than one hour. The debris-flow triggering storms ranged in average intensity between 1.0 and 32.0 mm/h, and had recurrence intervals of two years or less. Threshold rainfall conditions for floods and debris flows sufficiently large to pose threats to life and property from recently burned areas in south-central, and southwestern, Colorado are defined by:

$$I = 6.5D^{-0.7} \qquad (9.1)$$

and

$$I = 9.5D^{-0.7}, \qquad (9.2)$$

where I = rainfall intensity (in mm/hr) and D = duration (in hours). These thresholds define storm conditions with 2-year, or less, recurrence intervals. The threshold for southwestern Colorado is slightly higher than that for south-central, reflecting the larger and lower gradient drainage basins in the southwest.

Debris flows were generated from 68 recently burned areas in southern California in response to long-duration frontal storms (Cannon et al., 2008). The flows occurred after as little as two hours, and up to 16 h, of low intensity (2–10 mm/h) rainfall. The storms lasted between 5.5 and 33 h, with average intensities between 1.3 and 20.4 mm/h, and had recurrence intervals of two years or less. Threshold rainfall conditions for life- and property-threatening floods and debris flows during the first winter season following fires in Ventura County, and in the San

Bernardino, San Gabriel and San Jacinto Mountains of southern California represent recurrence intervals of less than or equal to two years and are defined by:

$$I = 12.5D^{-0.4}, \tag{9.3}$$

and

$$I = 7.2D^{-0.4}. \tag{9.4}$$

Threshold conditions change with vegetative recovery and sediment removal following a wildfire. A threshold defined for flood and debris-flow conditions following a year of recovery for the San Bernardino, San Gabriel and San Jacinto Mountains of:

$$I = 14.0D^{-0.5} \tag{9.5}$$

is approximately 25 mm/h higher than that developed for the first year following fires (Cannon et al., 2008).

The thresholds defined by Cannon et al. (2008) are significantly lower than most identified for unburned settings (Fig 9.7). This difference can be attributed to the differences between extremely rapid, runoff-dominated processes acting in burned areas and longer-term, infiltration-dominated processes on unburned hillslopes.

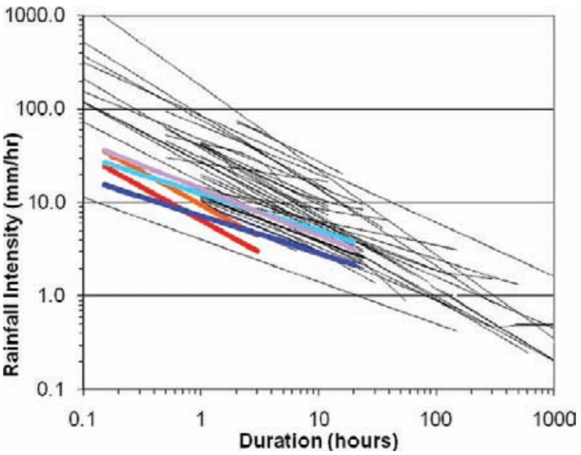

Fig. 9.7 Rainfall intensity-duration thresholds in Cannon et al. (2008) compared with a compilation of worldwide, regional, and local thresholds by Guzzietti et al. (in press); (http://rainfallthresholds.irpi.cnr.it/) – black lines. Old and Grand Prix Fire – *dark blue line*; Coal Seam Fire – *red line*; Missionary Ridge Fire – *orange line*; Piru Fire – *light blue line*; second winter following fire – *violet line*

This work illustrates three important points regarding the rainfall conditions that trigger debris flows for recently burned areas. Both convective thunderstorms and longer-duration synoptic storms can trigger debris flows from susceptible recently burned areas, and the conditions that result in debris flows are frequently occurring, or low-recurrence interval (<2 to 2 year) events. In addition, the conditions that trigger debris flows from recently burned areas vary considerably both within and between different climatic settings, indicating the necessity of separate thresholds for distinct geologic and climatic settings.

Based on the assumption that rainfall characteristics are the primary drivers of a post-wildfire runoff response, the thresholds presented here can provide guidance for rudimentary warning systems and planning for emergency response in similar settings. However, rainfall thresholds alone are not able to provide information on specific areas that are likely to experience post-fire debris flows or the size of potential events.

9.3.4 Debris-Flow Probability and Volume Models

A set of empirical models have recently been developed to estimate the probability of post-wildfire debris-flow activity and the volume of the response (Gartner et al., 2008) for both basins within the inter-mountain west and southern California.

A pair of models that calculate, for a given rainfall event, the probability of debris-flow production from individual drainage basins were developed using logistic regression analyses of a database from 388 basins that were burned by 15 recent fires located throughout the U.S. Intermountain West, and a separate database of information for 37 basins in 13 recent fires in southern California (unpublished data). The database used to develop the models consists of a set of potential explanatory variables that characterize runoff processes in burned basins (e.g. Moody et al., 2008; Beven, 2000). These variables include different measures of basin gradient, basin aspect, burn severity distribution within the basin, soil properties, and storm rainfall conditions in basins that were characterized either as having produced debris flows, sediment-laden floods, or having a negligible response. The statistical analysis consisted of building the model with the strongest predictive capability from the potential explanatory variables. The models describe debris-flow probability in the form

$$P = e^x / l + e^x, \tag{9.6}$$

Where P is the probability of debris flow. For the intermountain west,

$$x = -0.7 + 0.03(\%A_{30}) - 1.6(R) + 0.06(\%B_{H+M}) + 0.2(C) - 0.4(LL) + 0.07(I), \tag{9.7}$$

where $\%A_{30}$ is the percentage of the basin area with gradients greater or equal to 30%, R is basin ruggedness (calculated as the change in basin elevation divided by the square root of the basin area (Melton, 1965)), $\%B_{H+M}$ is the percentage of the basin area burned at a combination of high and moderate severity, C is the soil clay content (in percent), LL is the soil liquid limit, and I is average storm rainfall intensity (in mm/h). A model sensitivity (the percentage of basins known to have produced debris flows that are predicted by the model to have a probability of occurrence greater than 50%) of 44% was calculated for this model. Comparison of the p-values of the independent variables indicate that basin ruggedness and the percentage of the basin burned at high and moderate severity have the largest effect in the model.

For southern California,

$$x = -20.8 + 1.6(InE) + 0.1(S) - 0.7(InL) + 0.04(\%B_H) - 0.2(C) + 7.24(O) + 2.5(InI_3), \tag{9.8}$$

where E is the basin relief (in m), S is the average basin gradient (in percent), L is basin length (in m), $\%B_H$ is the percentage of the basin area burned at high severity, C is the soil clay content (in percent), O is the percent soil organic matter (by weight), and I_3 is the peak three hour rainfall intensity (in mm/hr). Model sensitivity is 76% and, in contrast with the intermountain west model, the peak three hour rainfall has the largest effect.

The differences between the controlling variables in the intermountain west and southern California models point to the effects of local climatic and physiographic setting on post-fire debris-flow susceptibility. To adequately characterize the hazards, it is necessary to develop models that are specific to each setting.

Models for estimating the volume of material that may issue from a basin mouth, for a given rainfall event, in the U.S. Intermountain west and southern California were developed by Gartner et al. (2008) using a series of multiple linear regression analyses on a database from 50 basins burned by eight fires located throughout the western U.S., and a separate database consisting of information from 25 basins burned by seven recent fires in southern California. In addition to measures of the volume of material either eroded from the channel network or deposited in a debris basin, the databases include the same independent variables as do the probability databases. The statistical analysis consisted of building the model with the strongest predictive capability from each of the two databases. The strongest models for both the western U.S. and southern California are virtually identical, and can be represented as:

$$In\ V = 7.0 + 0.6(InA_{30}) - 0.6(B_{H+M})^{1/2} + 0.2(T)^{1/2} + 0.3, \tag{9.9}$$

where V is debris flow volume (in m^3), A_{30} is the area of the basin with slopes greater than or equal to 30% (in km^2), B_{H+M} is the area of the basin burned at high and moderate severity (in km^2), T is the total storm rainfall (in mm), and 0.3 is a bias correction that changes the predicted estimate from a median to a mean value (Helsel and Hirsch, 2002). The R^2 and standard error of the residuals for this model are 0.83 and 0.90 (Gartner et al., 2008).

9.3.5 Application of Models for Hazard Assessments

These models can be quickly implemented on a GIS platform to generate debris-flow hazard maps either before, or immediately following, wildfires. Application

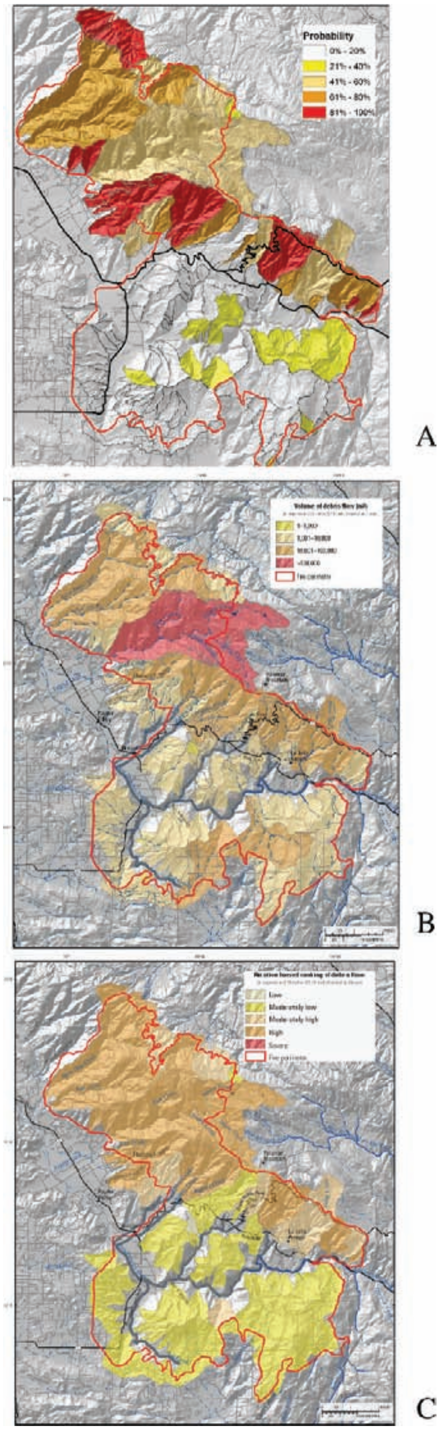

Fig. 9.8 Maps of debris flow (**A**) probability, (**B**) volume and (**C**) combined relative hazards for 2007 Poomacha Fire in southern California, USA in response to 57.15 mm of rainfall in 3 h

of the probability model for southern California and the volume model are illustrated using information from the 2008 Poomacha Fire in southern California. This fire burned nearly 50,000 acres in northern San Diego County in October of 2007. One hundred thirty eight homes and 78 outbuildings were lost in this fire.

Figure 9.8A shows a map of the probability of debris flow occurrence for the Poomacha Fire that was generated by calculating a probability for each basin based on the distribution of burn severity, gradient and soils within the basin and the probability model in response to 57.15 mm of rainfall in 3 h (a 10-year recurrence storm). Calculated values are then parsed into classes. Similar maps of the volume of material that can issue from basin outlets are generated using a similar procedure (Fig. 9.8B). The probability and volume rankings can be combined to give a relative measure of hazards for each basin (Fig. 9.8C). This combination serves to identify the spectrum of possible responses, from those basins that are most likely to produce the largest debris-flow events, to basins with a moderate probability of producing moderately-sized events, to basins with a low probability of producing small events. These maps provide information necessary to prioritize areas for pre-fire forest restoration efforts and post-fire erosion mitigation in southern California.

9.4 Implications in Response to Climate Change

Westerling et al. (2006) demonstrated that large wildfire activity during the period 1970–2003 in the western United States increased suddenly and markedly in the mid-1980s. While this effect is widespread, they found that the greatest increases of higher large-wildfire frequency, longer wildfire durations and longer wildfire seasons were in mid-elevation, northern Rocky Mountain forests. This is an important point because past land use practices, in general, and wildfire suppression efforts, in particular, have been advanced as the cause of increased wildfire occurrence and size. While Westerling et al. (2006) do not discount an effect from land use practices, they conclude that it is an overlay on the more significant control exerted by climate. Because the northern Rocky Mountains have experienced far less land use effect than other areas in the western United States, it makes clear the overall influence of climate on wildfire size and frequency.

Statistical associations between wildfire and hydroclimatology, particularly for northern Rocky Mountain forests, were found to be climate-driven by reduced winter precipitation and an early spring snowmelt (Westerling et al., 2006). Data from 1,166 large (defined as greater than 400 ha) forest wildfires between 1970 and 2003 permitted a detailed fire-climate analysis. A notable shift in the 1980s was found. Earlier wildfire observations defined a regime of a few large wildfires lasting about one week. This has altered to much more frequent large wildfires lasting about five weeks. This shift in the typical wildfire pattern coincides with a shift to unusually warm springs, longer summer dry seasons and drier vegetation. These conditions are linked to reduced winter precipitation and an earlier spring snowmelt during this same period (Westerling et al., 2006). Because the hydrology of the western United States is dependant on the winter snowpack, any reduction in accumulation and persistence into the spring means drier conditions earlier in the season for the forests (Running, 2006).

Whether this is a short-term trend or a long-term one has significant implications for both large wildfire and debris-flow occurrence. While the underlying mechanisms for this hydroclimatic shift associated with increased large wildfires in the 1980s can be argued, Westerling et al. (2006) point out that nearly every climate-model projects warmer springs and summers occurring over the region in upcoming

A

B

Fig. 9.9 Smoke plumes from extensive fires burning in southern California in the fall of 2007 (**A**), and Greece (**B**) in the late summer of 2007 illustrating potential application of the fire-flood-debris flow paradigm from USA to other settings throughout the world (images from NASA) decades. This means future conditions will favor the occurrence of large wildfires throughout the western United States.

Backlund et al. (2008) come to a similar conclusion. Fire-debris chronologies on alluvial fans and fire scars in tree rings record warmer and drier periods over the last million years being associated with more frequent and severe wildfires in the western United States. Based on modeling of global climate change, they suggest that large, stand-replacing wildfires will generally increase in frequency over the next few decades.

In addition to an increase in frequency and magnitude of fires, Wentz et al. (2007) found that increased warming can result in increased precipitation (on a global scale). Given that short-recurrence, garden-variety storms are generally sufficient to generate debris flows from burned areas, even small increases in precipitation will magnify the potential for debris flows from these areas.

The link between increased wildfires with their positive influence on debris-flow occurrence and global warming suggests that the experiences in the western United States are highly likely to be duplicated in many other parts of the world. Even if this were not the case, the continued population growth and urbanization within the Mediterranean climate chaparral biome around the world would still represent a significant increase in debris-flow risk to human populations. The multiple large fires in Greece in late summer of 2007 are only the latest in series of significant wildfires events within this extensive biome (Fig. 9.9).

9.5 Conclusions

In southern California and the intermountain west of the USA, debris flows generated from steep, short, recently-burned basins pose significant hazards. Increases in the frequency and size of wildfires throughout the western USA can be attributed increases in the number of fire ignitions, fire suppression, and climatic influences. Increased urbanization throughout the western USA, combined with the increased threat of more and larger wildfires, carries within it the increased risk from debris-flow occurrence. Preventing increased debris flow risk requires effective efforts to reduce the vulnerability of elements at risk (people, property, etc.). In the post-wildfire environment, time, money and physical constraints make imposition of mitigating measures at all possible locations an impossible task. Only by focusing these resources on the critical locations can effective risk reduction be achieved. This makes rapid identification of those critical locations a vital concern. Empirical models linked to a GIS environment are proving to be one of the best scientific means for this identification process.

Differences between rainfall thresholds and empirical debris-flow susceptibility models for southern California and the intermountain west indicate the strong influence of climatic setting on post-fire debris-flow potential. The link between increased wildfires with their positive influence on debris-flow occurrence and global warming suggests that the experiences in the western United States are highly likely to be duplicated in many other parts of the world, and the necessity of hazard assessment tools for additional climatic settings.

References

Allen CD, Touchan R, Swetnam TW (1996) Overview of fire history in the Jemez Mountains, New Mexico, In: Goff F, Kues BS, Rogers MA, McFadden LD, Gardner JN, (eds.), The Jemez Mountain region, New Mexico Geological Society, Forty-Seventh Annual Field Conference, September 25–28, 1996, 35–36.

Backlund P, Janetos A, Schimel D (2008) The effects of climate change on agriculture, land resources, water resources, and biodiversity in the United States. Final Report, Synthesis and Assessment Product 4.3, A Report by the U.S. Climate Change Science Program and the Subcommittee on Global Change Research, US Department of Agriculture, Washington, DC.

Bailey RW, Craddock GW, Croft AR (1947) Watershed management for summer flood control in Utah. U.S. Department of Agriculture, Forest Service, Miscellaneous Publication 639, 24p.

Beven KJ (2000) Rainfall-runoff modeling: the primer: John Wiley & Sons Ltd, Chichester, England, 360p.

Campbell RH (1985) Feasibility of a nationwide program for the identification and delineation of hazards from mud flows and other landslides: Chapter C, priority U.S. areas for the delineation of susceptibility to mud flows and other landslides. US Geological Survey Open-File Report 85-276-C, 1–6.

Cannon SH, Gartner JE, Holland-Sears A, Thurston BM, Gleason JA (2003) Debris-flow response of basins burned

by the 2002 Coal Seam and Missionary Ridge fires, Colorado. In: Boyer DD, Santi PM, Rogers WP (eds.), Engineering Geology in Colorado–Contributions, Trends, and Case Histories: AEG Special Publication 15, Colorado Geological Survey Special Publication 55, 31 pp.
Cannon SH, Gartner JE, Wilson RC, Laber JL (2008), Storm rainfall conditions for floods and debris flows from recently burned areas in southwestern Colorado and southern California. Geomorphology, 96, 250–269.
Cannon SH, Kirkham RM, Parise M (2001) Wildfire-related debris-flow initiation processes, Storm King Mountain, Colorado. Geomorphology, 39, 171–188.
Chourre M, Wright S (2005) Population growth of southwest United States 1900–1990. Impact of climate change and land use in the southwest United States, http://geochange.er.usgs.gov/sw/.
Costa JE (1984) Physical geomorphology of debris flows. In: Costa JE, Fleisher PJ (eds.), Developments and applications of Geomorphology. Springer-Verlag, Berlin, 268–317.
DeGraff, JV, Lewis DS (1989) Using past landslide activity to guide post-wildfire mitigation. In: Watters RJ (ed.) (1989) Proceedings of the 25th Symposium on Engineering Geology and Geotechnical Engineering, Reno, NV, pp. 65–75.
DeGraff JV (1994) The geomorphology of some debris flows in the southern Sierra Nevada, California. Geomorphology, 10, 231–252.
DeGraff JV, Cannon SH, Gallegos AJ (2007) Reducing post-wildfire debris flow risk through the burned area emergency response (BAER) process. In: Scaefer VR, Schuster RL, Turner AK (eds.), AEG Special Publication 23: 1440–1447.
Eaton EC (1935) Flood and erosion control problems and their solution. ASCE Transactions, 101, 1302–1330.
Gartner JE, Cannon SH, Santi PM, deWolf VG (2008) Empirical models to predict debris flow volumes generated from recently burned basins in the western U.S. Geomophology, 96, 339–354.
Giraud RE, McDonald GN (2007) The 2000–2004 fire-related debris flows in northern Utah. In: Schaefer VR, Schuster RL, Turner AK (eds.), AEG Special Publication 23, 1522–1531.
Grissino-Mayer HD, Romme WH, Floyd LM, Hanna DD (2004) Climatic and human influences on fire regiense of the souther western San Juan Mountains, Colorado, USA. Ecology, 85 (6), 1708–1724.
Helsel DR, Hirsch RM (2002) Statistical methods in water resources. U.S. Geological Survey Techniques of Water Resources Investigations, Book 4, Chapter A3, 510p. http://water.usgs.gov.pubs/twri/twri4a3/.
Kauffman JB (2004) Death rides the forest- perceptions of fire, land use and ecological restoration of western forests. Conservation Biology, 18 (4), 878–882.
Keeley JE, Fotheringham CJ, Morais M (1999) Reexamining fire suppression impacts on brushland fire regimes. Science, 284 (5421), 1829–1832.
Keeley JE, Fotheringham CJ (2000) Historic fire regime in southern California shrublands. Conservation Biology, 15 (6), 1536–1548.
Kotok EI, Kraebel CJ (1935) Discussion of “Flood and erosion control problems and their solution”. ASCE Transactions, 101, 1350–1355.
Melton MA (1965) The geomorphic and paleoclimatic significance of alluvial deposits in southern Arizona. Journal of Geology, 73, 1–38.
Minnich, RA (1989) Chaparral fire history in San Diego County and adjacent northern Baja California: An evaluation of natural fire regimes and the effects of suppression management. Keeley, SC (ed.), The California chaparral, Los Angeles Natural History Museum Series 34, 37–47.
Moody JA, Martin DA, Cannon SH (2008) Post-wildfire erosion response in two geologic terrains in the western USA. Geomorphology, 95, 103–118.
Pierce JL, Meyer GA, Timothy Jull, AJ (2004) Fire-induced erosion and millennial-scale climate change in northern ponderosa pine forests. Nature, 432, 87–90.
Radeloff VC, Hammer RB, Stewart, SI, Fried, JS, Holcomb, SS, McKeefryJF (2005). The Wildland Urban Interface in the United States. Ecological Applications, 15, 799–805.
Santi PM, deWolf VG, Higgins JE, Cannon SH, Gartner JE (2008) Sources of debris flow material in burned areas. Geomorphology, 96, 310–321.
Scott KM (1971) Origin and sedimentology of 1969 debris flows near Glendora, California. US Geological Survey Prof. Paper 750-C, C242–C247.
Running SW (2006) Is global warming causing more, larger wildfires? Science, 313, 927–928.
Swetnam TW, Betancourt JL (1990) Fire-Southern Oscillation relations in the southwestern United States. Science 249, 1017–1020.
Trouet V, Taylor AH, Carleton AM, Skinner CN (2008) Interannual variations in fire weather, fire extent, and synoptic-scale circulation patterns in northern California and Oregon. Theoretical and Applied Climatology, Online First, SpringerLink, DOI 10.1007/s00704-008-0012-x.
Wells WG II (1981) Some effects of brushfires on erosion processes in coastal Southern California. In: Erosion and Sediment Transport in Pacific Rim Steeplands, Christchurch, New Zealand, International Association of Hydrological Science, 132, 305–342.
Wells WG II (1987) The effects of fire on the generation of debris flows in southern California. Geological Society of America Reviews in Engineering Geology, 7, 105–114.
Wentz, FJ, Ricciardulli, L, Hilburn, K, Mills, C (2007) How much more rain will global warming bring? Science, 317, 233–235.
Westerling AL, Hildalgo HG, Cayan DR, Swetnam TW (2006) Warming and earlier spring increase western U.S. forest wildfire activity. Science, 313(5789), 940–943.

Recovery of the Buddha's Niches and Cliff in Bamiyan (Central Afghanistan) after the Taliban Destruction of 2001

10

Claudio Margottini

Abstract The historical site of Bamiyan is affected by geomorphological deformation processes which were enhanced during the talibans' bombing in March 2001, when the two standing Buddhas, dating back to VI C. a.D. were destroyed. Not only was invaluable cultural heritage irremediably lost but also the consequences of the explosions, as well as the collapse of the giant statues, added greatly to the geological instability of the area. Traces of rocks recently slid and fallen are relevant proofs of the deterioration of its stability conditions and most parts appear prone to collapse in the near future.

Under the coordination of the UNESCO, a global project to assess the feasibility conditions for the site's restoration was developed; field data were collected and a mechanism for the potential cliff and niches' evolution was provided. In the mean time some consolidation works were carried out in the most critical rock fall-prone areas to avoid any further collapse in the coming winter season, but also to enable archaeologists the safe cataloguing and recovering of the Buddha statues' remains, still laying on the floor of the niches. The Emergency activities started in October 2003 and included: the installation of a monitoring system, the realization of temporary supports for the unstable blocks, the stabilization of the upper-eastern and upper-western part of the small Buddha niche, the minimization of the environmental impact of the actions taken. Consolidation works were mainly implemented by professional climbers, directly operating on the cliff.

Keywords Rock fall • Mitigation works • Buddha Statues • Bamiyan – Northern Afghanistan

10.1 Introduction

In the great valley of Bamiyan, 200 km NW of Kabul, central Afghanistan, two big standing Buddha statues appear to visitors (Fig. 10.1), carved out of the sedimentary rock of the region, at 2500 m of altitude. Following the tradition, this remarkable work was done by some descendants of Greek artists who went to Afghanistan with Alexander the Great, probably around VI C. a.D..

Under the worldwide astonishment, the two statues were demolished on March 2001 by the Taliban, using mortars, dynamite, anti-aircraft weapons and

C. Margottini (✉)
APAT – Italian Agency for Environmental Protection and Technical Services – Via Curtatone 3 00185 Rome, Italy; UNESCO consultant, Norwich, UK

K. Sassa, P. Canuti (eds.), *Landslides – Disaster Risk Reduction*,
© Springer-Verlag Berlin Heidelberg 2009

Fig. 10.1 The Giant Buddha statues of Bamiyan in a depiction of Burnes, 1834

Fig. 10.2 The Eastern Giant Buddha before and after the destruction

rockets (Figs. 10.2 and 10.3). The Buddhists as well as the world community, UN and UNESCO failed to convince the Taliban to avoid the destruction of this unique cultural heritage. Nevertheless, since 2002 UNESCO is coordinating a large international effort for the protection of the World Heritage Site of Bamiyan and the future development of the area.

10.2 General Features of the Area

Extensive investigations were conducted on the site, even with the limitation of field investigation due to landmines. In detail the following activities were performed in the period 2002 until now. Most of collected information are reported in Margottini (2003b), Margottini (2004a), Margottini (2007) and Margottini et al. (2005), and developed according to the standars and procedure described in Hoek and Bray (1994) and Turner and Schuster (1996). Developed activities include:

1. the inventory of *geological* and *geomorphological* feature and existing mass movements;
2. the identification of predisposing factors to slope instability (*climatology, petrology, mineralogy, sedimentology, seismology, geophysical properties of rocks, mechanical behaviour of both rock masses (in situ and laboratory) and discontinuities, discontinuities distribution*);
3. the investigation of potential *triggering mechanisms of landslides*;
4. the *kinematic analysis* to identify potential failure mechanisms for cliff and niches;
5. the numerical *stability analysis of cliff and niches*, to identify the relationship between shear strength along the potential failure surface and conditions required to trigger the collapse;

Fig. 10.3 The Western Giant Buddha before, in the explosion and after the destruction

6. experiences in *previous restoration/consolidation works*.
7. a *manual crack gauge monitoring system* was also installed showing no movement in the period September 2003 – March 2007.
8. *Automatic crack gauge monitoring system* operating at the time of stabilisation works (November–December 2003 and April–May 2004)

The investigations performed in the Buddha niches and surrounding cliff in the Bamiyan valley (northern Afghanistan) highlight the following main features (Margottini, 2004a; Margottini, 2007; Margottini et al., 2005):

1. the area is located in mountainous central Afghanistan in a dry part of the world that experiences extremes of climate and weather. Winters are cold and snowy, and summers hot and dry. Mean annual precipitation in Bamiyan is about 163 mm and mean annual temperature, 7.4°C.
2. the area belong, geologically, to an intramountainous basin, subsequently filled with debris originating from the surrounding mountain ranges (Lang, 1968, 1972; Reineke, 2006). The neogenic, more or less horizontally bedded sediments can be distinguished into four strata, which are shown in Fig. 10.4. Starting with the Eocene Dokani-Formation (> 80 m sandy carbonates and anhydrite) and the Zohak-Formation (> 1000 m red conglomerates), the so called Buddha-Formation is deposited in the Oligocene and is built up by > 70 m yellow-brown pellites, sandstones, conglomerates and some volcanic material. On the top lies the miocenic Ghulghola Formation (> 200 m sandstone, clay and lacustrine carbonates) and the pliocenic Khwaja-Ghar Formation (approx. 200 m travertine, sandstone and conglomerate).
3. the rocks outcropping in the area are mainly conglomerate, with some strata of siltstone that largely slake when wet. The lower part of the cliff is predominantly siltstone, with two main set of discontinuities spaced every 20–40 cm. The central part of the cliff is mainly conglomerate, well cemented and with a limited number of vertical discontinuities mainly paralleling the profile of the slope.

The following Fig. 10.5 is reporting the general view of the site with main morphological features and the rupestrial settlements. In such a light, the Bamiyan areas is, likely, one of the magnificent world wide example of cultural landscape. Major geomorphological processes include water infiltration, gully erosion, progressive opening of discontinuities in the outer parts of the cliff, weathering and slaking of siltstone levels, toppling of large external portions as well isolated blocks along the cliff face, occurrence of mud flows probably when the siltstone is saturated, sliding of a large portion of the slope, accumulation of debris at the toe (Margottini, 2004a).

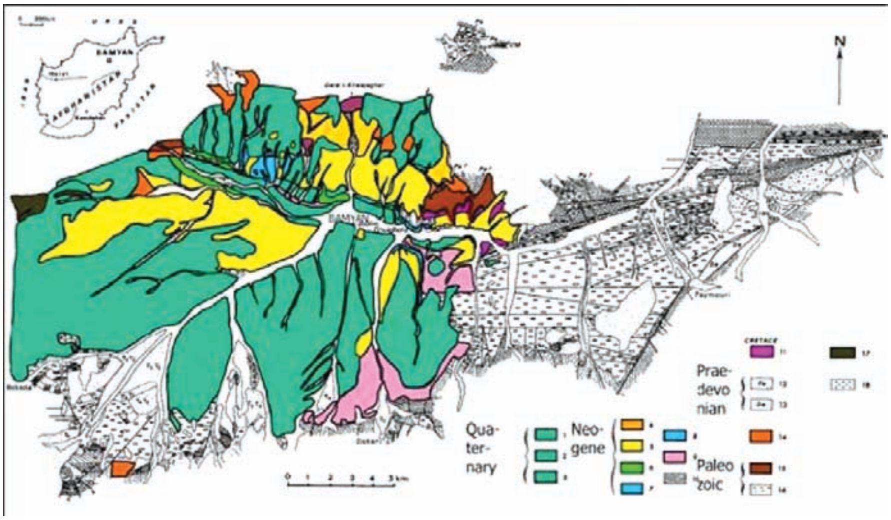

Fig. 10.4 Geological map of the Bamiyan region (Lang, 1968; redrawn in Reineke, 2006)

Fig. 10.5 The cliff with the Buddha's niches and the rupestrial settlement

Fig. 10.6 Rock slides affecting the caves inhabited since VI A.D

Large rock slide were detected in the lower part of the cliff, now stabilized, covered by large amount of debris; occurrence of such rock slide is kinematically conditioned by the presence of direct faults, not reaching the upper part of the cliff. Only two large rock slides it seems to affect the rupestrial caves and historical settlements.

10.3 Identification of Most Unstable Areas

The explosion of March 2001, as well as demolishing the statues, reduced the stability of the slope, mainly in the outer parts of the niches.

In the Eastern Giant Buddha niche, as well as the collapse of statue, there were three minor rock falls from the top of the niche. The blasting also degraded the upper-eastern part of the niche where a stairway is located inside the cliff, and the wall between the stairs and the niche is quite thin (about 30–50 cm). This part is presently the most critically unstable site. The western side, as consequence of an existing buttress, suffered less damage. Nevertheless, a rock fall occurred and some instabilities are now also evident only in the eastern part.

Major effects in the Western Giant Buddha niche were the collapse of the statue and the consequent instability of the rear of the niche. A small rock fall occurred from left side of the top of the niche. Probably, the strength of the greater thickness of wall between the stairway going up into the cliff and the niche (about 1 m), reduced the effects of blasting and resulted in less severe damage. Investigating the possible long term stability conditions of cliff were computed using the explicit-difference-finite code, FLAC (Itasca Consulting Group, 2000). Considering the Hoek and Brown (1980) shear strength criteria for conglomerate and siltstone, and with a major discontinuity ranging from the middle of cliff till the middle of the niche (only friction value for shear strength) the deformation of the cliff is relatively low and it seems to be now day in condition of stability. Since we consider the fracture in conglomerate reaching the lower sandstone formation and we decrease gradually the cohesion of siltstone due to fracturing/weathering, the cliff is become unstable when the cohesion is proxy to nil. In such situation maximum displacement and vector are at the base of the niche (Fig. 10.7).

In general, the niche and the cliff need holistic stabilisation work and not episodic and local intervention. Nevertheless, it must be recognised that one cannot propose a specific stabilisation plan at the moment because any intervention has to be specified for the local conditions. At the present stage, it is convenient to set up a general master plan, to be locally adapted according to further more specific investigations and data. The master plan includes mainly nails, anchors and grouting, that will have a low environmental impact on the site.

Finally, the field data (Colombini and Margottini, 2003a and b; Margottini, 2004a), kinematic analysis, mathematical modelling, caves and crack distribution and detail inspection of the effect of the explosion allow the realisation of Figs. 10.8 and 10.9 which report the most endangered sites for both niches. The explosions of March 2001, besides the demolition of the statues, reduced the stability of the shallower parts of the niches. In the East Giant Buddha niche, as well as the collapse of the

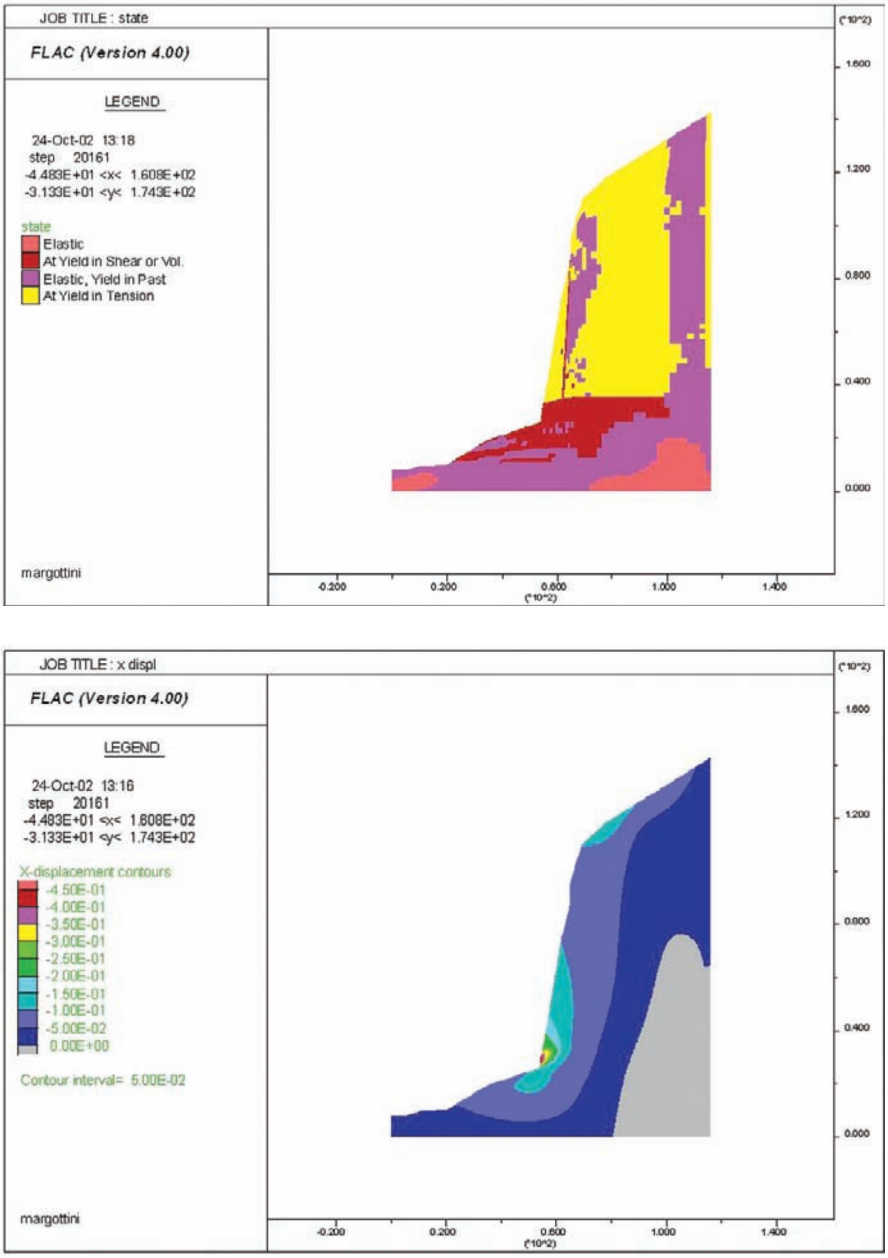

Fig. 10.7 State and displacement for the cliff of small Buddha in with fracturing reaching the lower part of the cliff and the lower siltsone exhibit no cohesion as consequence of internal fracturing or weathering

statue, three minor rock falls occurred from the top of the niche. Blasting also degraded the strength of the rear of the highest right part of the niche, where a stairway is located inside the cliff and the wall between the stairs and the niche is quite thin (about 30–50 cm). This part presently has the most critical instability (A3 in Fig. 10.8). As a consequence of an existing buttress, the left side did not suffer as much damage, although in the upper part a rock fall occurred and some instabilities are now evident.

In the West Giant Buddha niche, the major blast effects were the collapse of the statue and the consequent instability of the rear of the niche. A small rock fall occurred from the top of the niche (left side). Probably, the greater thickness of the wall between the stairway going up into the cliff and the

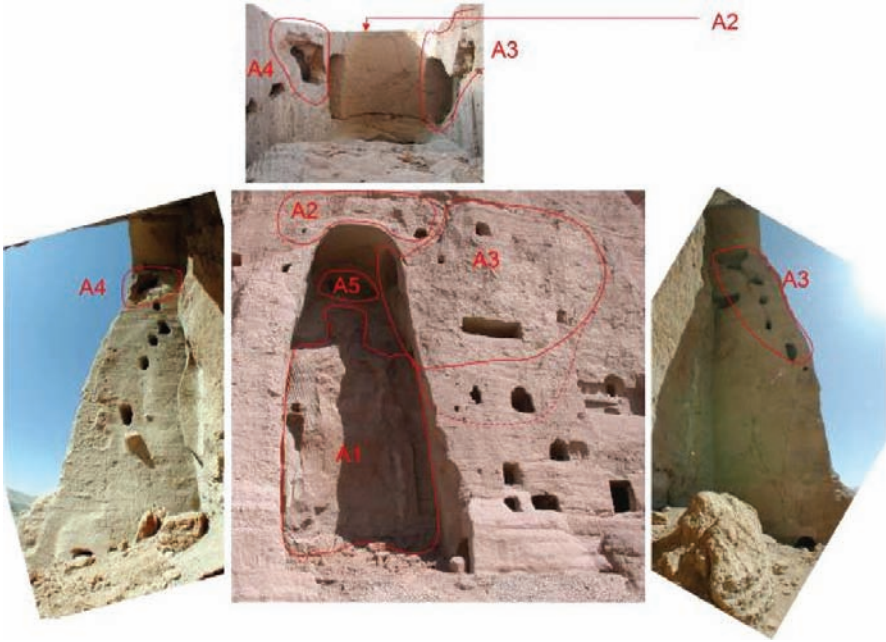

Fig. 10.8 Identification of most critical instability areas in the East Giant Buddha niche. The A3 block in the Eastern Giant Buddha niche, exhibit the most acute instability

niche (about 1 m), inhibited the propagation of the blasting effects, and resulted in less severe damage. A large crack, about 20–30 cm wide, is present in the corridor at the back of the head of the Statue. Figure 10.9 shows the most critical areas found in the field inspection and/or identified by analysing the different geological aspects investigated in this paper.

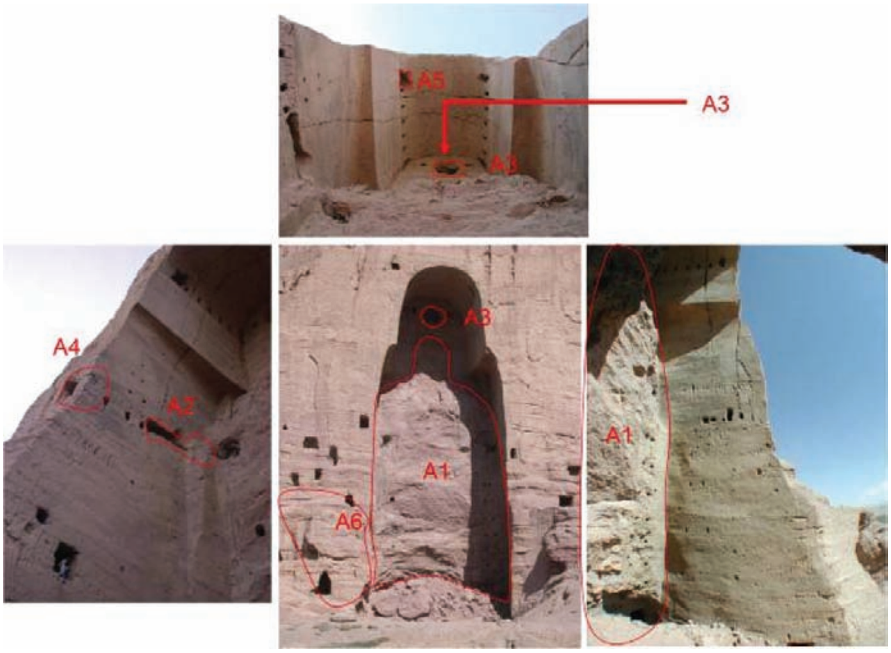

Fig. 10.9 Identification of most critical instability areas in the West Giant Buddha niche. The *arrow* points to a serious problem inside the niche. Other important areas to secure are A4 and the *top* of A6

10.4 Emergency Measures Taken in 2003–2006

10.4.1 Overall Strategy on the East Giant Buddha niche

After the general strategy for stabilisation, a follow up of activities was performed in September 2003, aimed at the identification of potential negative evolution of the cliff and niches during winter 2003–2004. The result of a field mission suggested an immediate response to the upper East side of Eastern Giant Buddha niche where the existing large fissures were widening and the risk of an immediate rock fall was estimated to be very high. This collapse could involve large part of the upper Eastern part of the cliff an than totally destroying the niche (Fig. 10.10).

Emergency consolidation works were immediately planned and carried out in this most critical rock fall-prone areas to avoid any further collapse in the coming winter season, but also to enable archaeologists the safe cataloguing and recovering of the Buddha statues' remains, still laying on the floor of the niches. The stabilisation activities started in October 2003 till the beginning of December 2003 (Eastern side). A second operational phase was implemented in the period April – June 2004 (Eastern side) and the final one in the period September – November 2006 (Western side and top). Figure 10.11 is reporting all the study area and the sites for intervention. Without considering the study phases, the practical activities included four different steps:

Fig. 10.11 Localisation of the three areas of interventions in the Eastern Giant Buddha niche

1. the installation of a *monitoring system*, to evaluate in real time any possible deformation of the cliff. Sensor were designed to monitor the entire working area, connected with an alarm system, to make workers in safe conditions;
2. the realisation of *temporary protection* includes steel ropes, and two iron beams suitable to avoid lateral deformation, inside the niche from an unstable cliff and blocks. Among the temporary work, a wire net was installed on the back side of both niches to allow archaeologists to work on the ground floor in safe conditions, just after the consolidation of the niche's wall;
3. the *final stabilisation* of the East side of the niche, west upper side and top. In these areas anchors, nails and grouting were executed, in order to reduce the risk of rock fall and collapse; particular care was addressed to the problem of grouting material since the very high slaking capability of siltstone. The anchors placed in 2003 were pre-grouted to avoid any oxidation and then percolation inside the niche. From 2004 it was decide

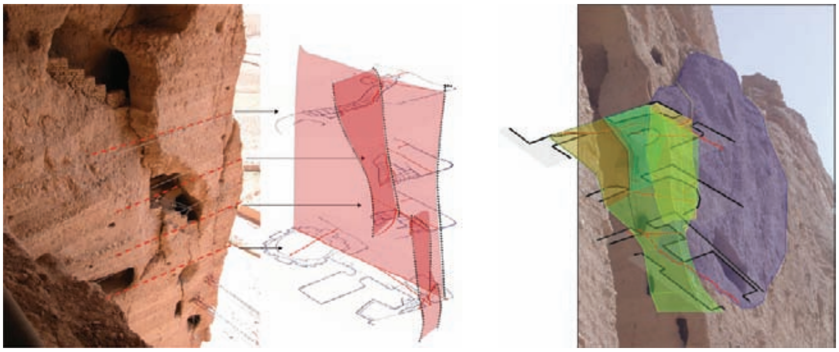

Fig. 10.10 Pattern of existing discontinuities at four different stories (*left*) and reconstructed unstable blocks in the upper East side of Eastern Giant Buddha niche (*right*)

to use only stainless steel materials, even if not pre-grouted.

4. *minimization of intervention* (anchor/nail head finishing) complete the execution of work. Anchor and nail heads were designed to be placed slightly inside the rock and then covered by a mortar allowing a total camouflage of the work. A number of tests on the better mixture, between cement, local clay/silt and water, to be used for covering the anchor/bolt heads, were also designed and developed in 2003, in cooperation with ICOMOS experts. The results highlight the better chromatic, stability and robustness of the mixture.

10.4.1.1 Implementation on the Eastern Wall

In the Eastern side of the niche a large external block was prone to collapse (Fig. 10.10), and many others in the in the inner part.

A real time monitoring network was planned and realised to monitor the most remarkable crack and discontinuities. 11 potentiometric crack gauges, 0–50 mm, 4–20 mA, fitted with couplings and connecting cable (tot. length 350 m) were supplied in the first phase 2003, with acquisition system (data logger) and data management software. An alarm system to detect any deformation (movement) possibly induced by the works on the main cracks present in this part of the cliff was also installed. The accuracy of the gauges was requested in 0.01 mm, to allow an accurate measurement of even small deformation. The position of sensors is reported in Fig. 10.12.

The temporary protection includes a network of 0.6” diameter steel ropes with a light pre-tensioning, to sustain the most unstable block from possible collapse; steel ropes were fixed to short nails, irregularly placed to avoid any stress concentration in a given line or area. Two temporary beams, located laterally, to support the cliff deformation were designed and executed. Each beam was calculated to offer a resistance of about 40 tons, similar to two designed long anchors. Figure 10.13 is showing the steel ropes and the two iron beams. The temporary protection elements were removed in 2006.

The consolidation was designed by means of passive anchors and nails, correctly grouted. Long anchors are having a spacing of about 4 m since they exhibit, in this configuration a factor of safety equal to 2, without considering the contribution of nails. Nails will not follow a precise configuration since they have to be designed on site to strength the shallower part of the block. Even anchors may have some not homogeneous distribution, function of internal cavities. Details on calculation are reported in the following Fig. 10.14. In these we have:

1. the geometrical distribution of load and the assumption for calculation, based on mechanic of rigid mass, and the related moment;
2. the assumption for moment calculation of anchors and the related factor of safety;

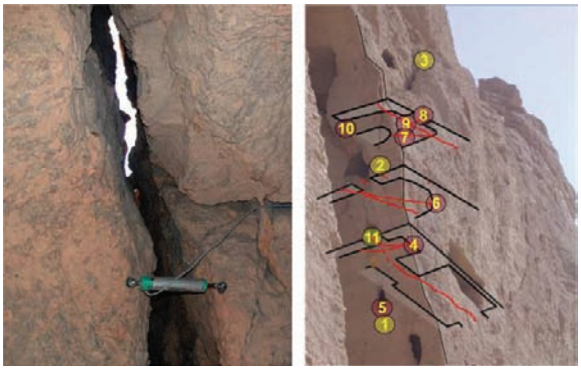

Fig. 10.12 Distribution of the 11 sensors monitoring the cracks underlining of the most unstable block. On the right a detail of such sensors

Fig. 10.13 The temporary beam (*left*) and steel rope (*right*) for the temporary support of upper Eastern part of small Buddha

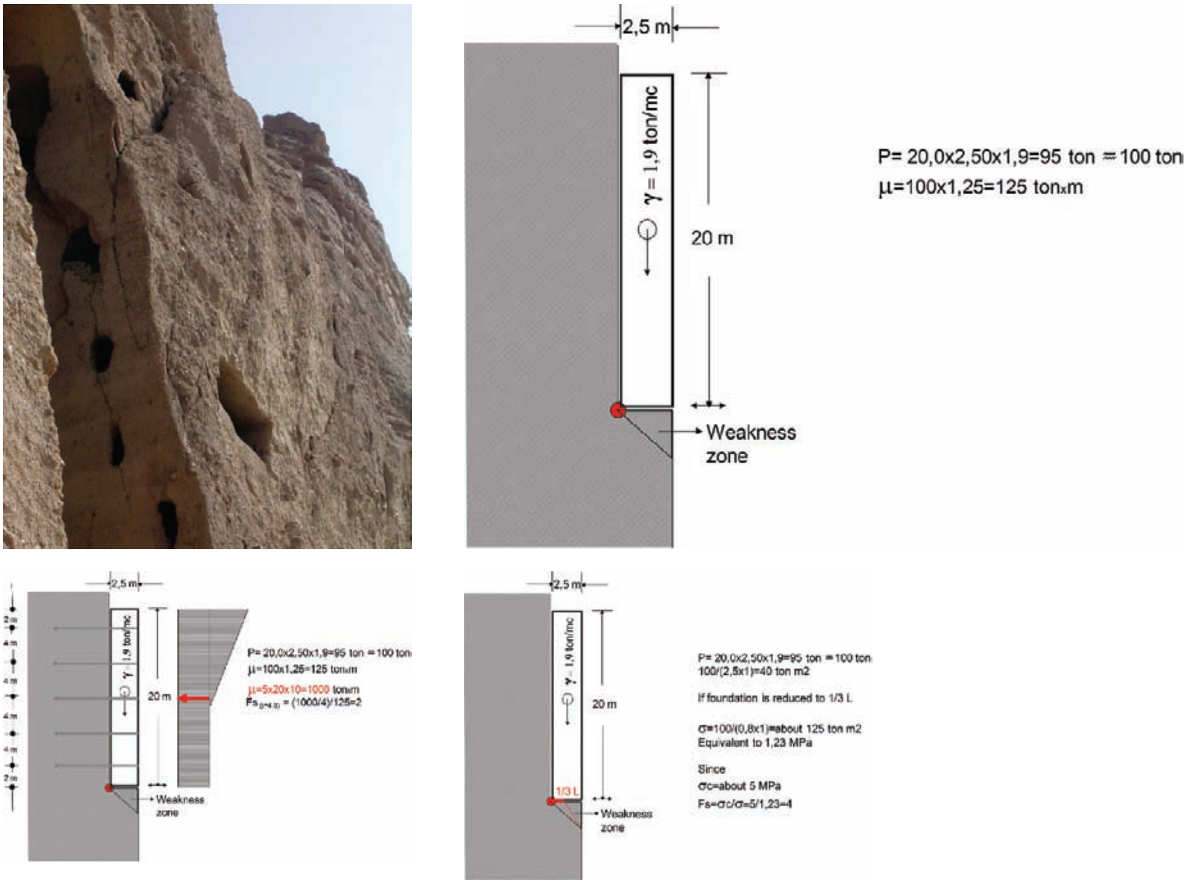

Fig. 10.14 The external block prone to collapse, the geometrical distribution of load and the assumption for calculation, moment calculation of anchors and the related factor of safety and an evaluation test about the possibility to generate toppling according to the static loads and the uniaxial compressive strength of material

3. a comparison test about the possibility to generate toppling according to the static loads and the uniaxial compressive strength of material;

A major concern, at the very beginning, was certainly the understanding of adherence between grouting material and siltstone, a very slaking material. For this reason the choice was addressed to low water release grouting. This can be achieved mixing water and cement with superplasticizer, a chemical additive suitable to maintain the water inside the mortar. The adopted composition was: W/C = 1/2.0 + superplasticizer

A comparison between the standard strength for anchors and the possible mobilised one was investigated. Since anchors are designed to provide 20 ton each, the borehole show a diameter of $\phi = 9$ cm and the active length was limited to only 5 m, we have:

$$2 \times \pi \times 4,5 \times 500 = 14131\text{cm}^2$$

Without direct tests, adherence between the mortar and the rock is generally calculated between 6 and 8 kg/cm^2; assuming 5 Kg/cm^2 we have about 70 tons. Then, assumed strength of anchor is 20 tons that divided by 70 give a result of about 28% of normal standards; alternatively, the real obtained adherence is about 1,41 kg/cm^2, that is much less than the design one of 5 kg/cm^2. The resulting factor of safety is about 5, suggesting a reasonable security with the designed loads. Anyway, due to the missing of information on detail geomechanical distribution of discontinuities on the deep, this feasibility assumptions were considered in favor of security.

The correctness of the adopted solution and also of the bounding capacity of grouting mortar is given from the anchor suitability tests, performed in 2004 to understand the bounding capacity of anchors in both siltstone and conglomerate. The design strength of passive anchors was assumed in 20 tons, for a bounded length, after the major discontinuity, at least of 5 m (about 4 tons per linear meter); the anchor suitability test was performed for 1 m length, till 40 tons, close to the yield capacity of steel. Up to this value no remarkable permanent elongation was detected, to demonstrate the correct bounding effect between siltstone and conglomerate and the anchors (Fig. 10.15). These data confirm, once more, the appropriate choice of superplasticizer as an additive suitable to avoid any slaking phenomena in the siltstone.

In detail, in the eastern part of the niche it has been placed:

1. 6 short passive anchors (Steel nails, dia 16 mm, FeB 44 K, threaded, with couplers anchor plates and nut – single bar length L = 2.5 m) with diameter = 36 mm and length about 5 m, placed on the internal side of the niche (diamond head rotary machine);
2. 29 stainless steel passive anchors with diameter = 26 mm and a length 5–10 m (in any case double then the last encountered fissure from surface), 20 on the internal side and 9 on the external;
3. 17 passive anchors, pre-grouted to avoid oxidation, with diameter = 90 mm and length 15 m., for a total length of 200 m, placed on the external part of the cliff (Anchor bars VSL, dia 26.5 mm, st 835/1030, pre-injected, with external corrugated sheathing, including plates and nuts).

Apart from the above technical aspects, the main difficulties in this project was not only the typology of intervention and the used materials but the way of how to execute the work, also in a country like Afghanistan with low availability of equipments. Certainly, the first idea was the construction of a scaffolding but, due to the very high probability of rock fall and then the possibility of destructing it, with additional risk for the workers staying below hanging rocks, the economic cost of scaffolding itself, and the approaching of winter season in 2003–2004, the need to find an alternative solution came up. After a careful investigation and evaluation of possible alternatives for implementing the job, the choice fall on the use of professional climbers.

Climbers, also supported by ground staff, were operating directly on the surface, hanged on top of the cliff, in a safe area, moving from top to down and then in safe condition with respect to any potential rock fall.

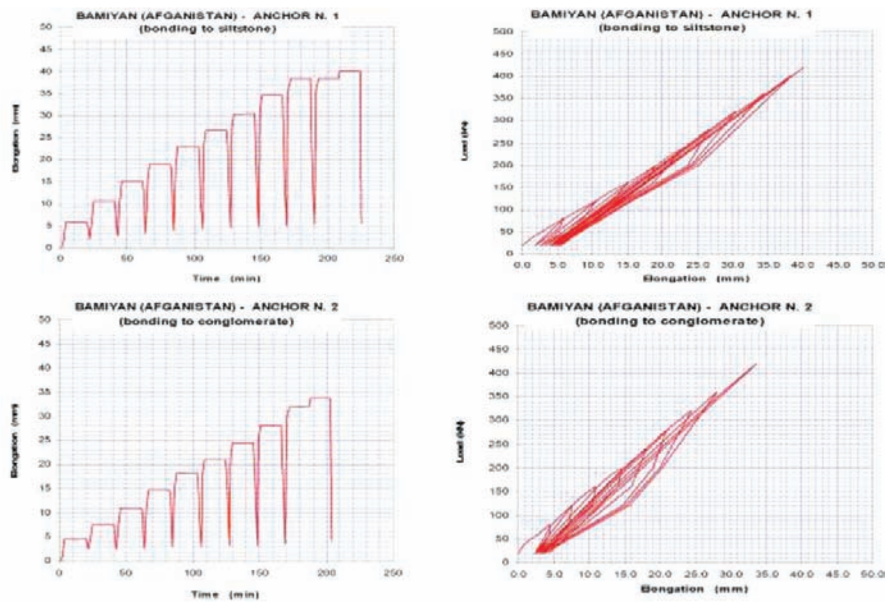

Fig. 10.15 Anchor suitability tests for siltstone and conglomerate, in 1 m. length anchor. The load (kN) and respective time (min) and elongation (mm) are reported showing, till 40 ton, the uphold of elastic domain and still the missing of any permanent deformation for the tested anchor

Also a major difficulty was the calibration of drillings with respect to the existing cavities. In fact, a large number of caves (around 800) and tunnels are located on the cliff constituting a unique example of rupestrial settlement. The selection of drilling was then requiring a detail investigation in their orientation and inclination to avoid with drilling and grouting into the archaeological caves.

As mentioned previously, high attention was posed to the methodology for consolidation. Short (16 mm) and medium (20 mm) length passive anchors (stainless steel) have been realised with rotary drilling machine, with diamond head, to avoid any possible vibration. Cooling fluid was facing the occurrence of slaking prone siltstone in presence of water: due to this, the usage of water was limited when drilling the conglomerate and a mix of compressed air and water was adopted when discontinuities were detected and when a possible level of siltstone was encountered. Pre-grouted long passive anchors, used only in the first phase 2003, (26 mm) have been realised with roto-percussion machine and use of air as flushing medium. From a temporal point of view they have been drilled only after the realisation of shorter ones and from the further part of the unstable blocks, towards the most critical one. The purpose of small anchors is to sew all together the unstable masses and fixing them the proxy stable geological background. The long anchors have to homogenise this part to the most internal and stable geological material. Direction and inclination of anchors have been defined on site but, in any case, direction of deformation and perpendicularity to discontinuities has been taken into consideration. Temporal execution considered the principle to start from the most stable place to the most unstable. This is to start consolidation from the part where disturbance can better be sustained. In particular, with respect to the internal side of the niche, the lowermost unstable block, has been approached from the bottom of it to the top. In fact, in the top of the niche there is an hanging block that cannot be touched without having stabilised the lower part. Grouting was made with cement added with superplasticizer to avoid any water release, capable to interfere with the slaking siltstone as well as to get the best possible adherence between bar and rock, namely composed as in Table 10.1.

Table 10.1 Composition of grouting materials for both anchoring and cracks filling

	Anchoring grout Kg/m^3	Cracks filling mortar Kg/m^3
Water	540	300
Cement	1360	610
Sand		1270
Additive Superplasticizer	7	7

In total, for grouting and filling in the Eastern wall of the niche, approx. 17 m^3 were injected, with 19.000 kg cement divided in:

1. short anchors grouting as 1.200 kg;
2. anchors grouting as 8.200 kg;
3. crack filling (from top) as 9.600 kg;

Minimisation of impact was implemented by covering with mortar of suitable colour all the anchor steel plates. In such a way it now very difficult to identify the place were anchors and nails were settled. The composition and color of mortar was established with the support of technicians from International Council of Monuments and Sites (ICOMS). A final arrangement should be provided by a conservator. The following figure is presenting the results of the executed activity.

The solution and the techniques adopted as well as the four steps improvement of activities proved quite satisfactory since the monitoring system did not record any remarkable deformation in the unstable blocks through the working period (Fig. 10.23).

Fig. 10.16 Installation of temporary struts. Note that, during the installation, the strut is fixed on top of the cliff, in the safe zone

Fig. 10.17 Final consolidation with the use of professional climbers and large rotary machine

Fig. 10.18 Execution of nails for the stabilisation of unstable blocks

Fig. 10.19 Execution of nails on the roof of the niche

Fig. 10.20 Execution of nails with rotary machine and diamond head, at the inner side of the niche

Fig. 10.21 Detail of execution of nails from inside the caves by means of small rotary machine and diamond head

Fig. 10.22 Covering of anchor heads with proper mortar (test site)

10.4.1.2 Implementation on the Western Wall

The western side of the niche is also suffering for the effect of explosion as well as for the sunk of existing buttress. The buttress was probably constructed to reduce the risk of collapse of this flank which was considered extremely unstable to justify a very massive intervention by French archaeological expedition in late '50, early '60, finally strengthened and mitigated in the impact by the Indian archaeological survey in '70. Since the buttress it seems to be connected with bolts to the cliff it is possible that the sunk of this structure may produce an horizontal stress, toward the external, inducing additional instability as testified by the intervention of Indians Archaeological Survey (Fig. 10.24, courtesy Prof. Maeda, Kyoto University). There are nowday some evidence (e.g. widening of small cracks) from which it is possible to hypothesise that the buttress is hanged to the cliff, more than sustaining it. This situation might increase the existing damage.

Effects of March 2001 explosion are mainly evident at the top of the niche, probably where there is a maximum concentration of stress in consequence of the morphology of the niche (arch and pillar, as described in Colombini and Margottini, 2003a). In particular (Margottini, 2004b; Margottini, 2006) there is a small pillar (Fig. 10.25) that needs

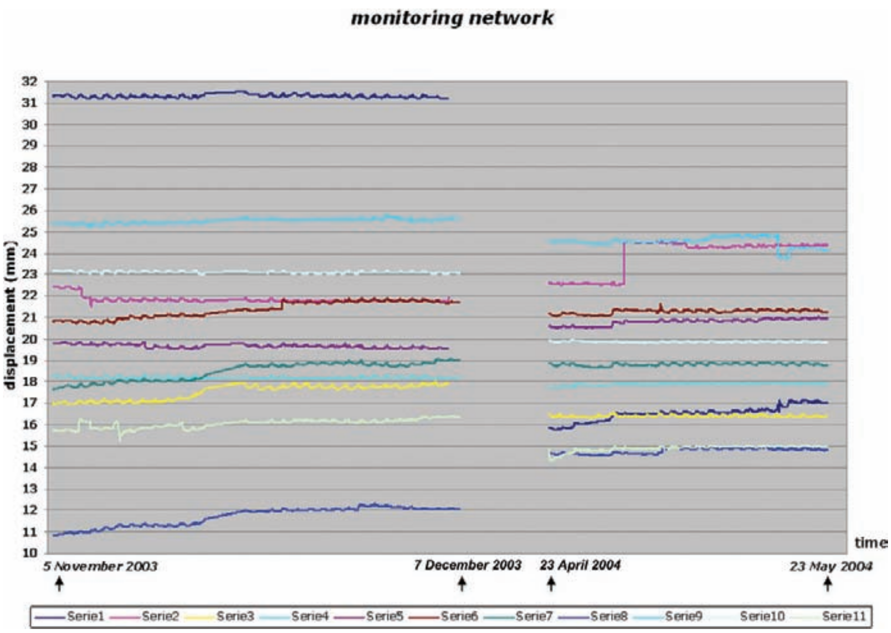

Fig. 10.23 Time evolution of the 11 extensometers operating in the period 5th November – 7th December 2003 and 23 April – 23 May 2004 in the Eastern wall of the niche, and showing no remarkable movements on the cliff. Some minor step have been caused by climbers, who hit the gauge placed on the cliff

Fig. 10.24 Consolidation works from the Archaeological Survey of India in 1969 (Courtesy of Prof. Maeda)

immediate emergency intervention before collapse, possibly inducing large deformation processes to the whole western part of the niche. This part was also completely restored by the Indian Archaeological Survey in late ’70. Apart from the planned minor emergency intervention, any large intervention in this area should include geotechnical investigation on present buttress foundation and, later on, the complete stabilisation of the niche. Likely, the manual monitoring system installed in 2003, does not exhibit presently any further deformation of most severe cracks. The present emergency intervention, planned in the upper part of niche, was designed in order not to fix any part of the buttress to the cliff, since it has not been investigated its possible evolution.

Fig. 10.25 The most unstable element (pillar) in the western side of Eastern Giant Buddha niche

Also in this situation the general strategy of an emergency intervention was developed in four steps:

1. a monitoring system on the most relevant discontinuities. No. 6 potentiometric crack gauges were newly installed and tested in the West wall of the niche of the Eastern Giant Buddha to monitor the cracks identified as most dangerous in the area of the drilling and grouting works. The scheme of installation is reported also in Fig. 10.26.
2. A temporary support (Fig. 10.27), by means of:
   a. the two existing long iron beams moved in the upper part of the niche, to provide some lateral support to the niche;
   b. two iron/wood beams capable to support any lateral deformation of the small pillar; The construction details of the beam has been finally adapted with the materials actually available in Afghanistan;
   c. steel ropes bounding completely the pillar and cliff; 13 no. temporary steel cables have also been installed on the Western side of the niche. 4 of them were fixed through steel bolts on the inner/outer wall of the niche whereas 9 cables were circular cables embracing horizontally

Fig. 10.26 The location or potentiometric crack gauges for discontinuity monitoring and alarm; in green are external sensors and red are internal to the cave

Fig. 10.27 The temporary support necessary for a secure execution of the work in the western wall: two long iron beam replaced in the upper part of the niche, the short iron/ wood struts for local support and the steel ropes

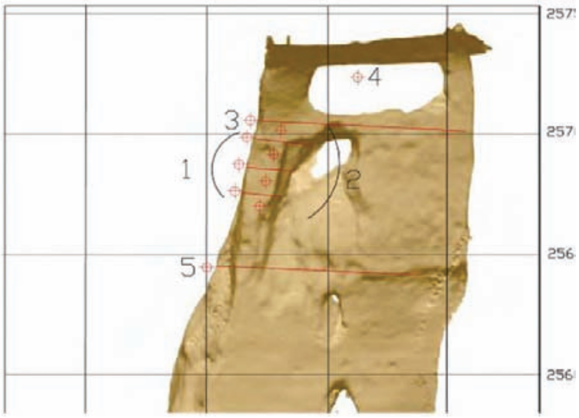

Fig. 10.28 Distribution of the anchors and chronological sequence of them

(6 no.), or vertically (3 no.), the rock pillar and the septum at elev. 2570.

3. Emergency intervention includes nails and grouting as follows:
   a. prior to starting the drilling works, the large cracks in the area of the pillar at the left wall of the Eastern Giant Buddha, were thoroughly filled in and grouted with cement grout. After the preliminary caulking, the main fissures were filled in using 0.96 m^3 of low water-release cement grout, with some 1,200 kg of cement. Grout composition utilized was, as usual, C:W = 0.5 with superplasticizer;
   b. For the drilling operations, a diamond rotary system, 50 mm dia.,has been adopted with the aim to limit as much as possible interferences, produced by vibratory effects, to the limited stability of the structure in this area. A total of no. 12 stainless steel passive anchors, dia 20.0 mm, have been installed, with a total drilled length for these 12 anchors of 52.4 m. In detail, nine of these nails connect internally the pillar, in both directions parallel to face and perpendicular to it to create a robust net; two short passive nails (located at below and above the critical pillar, with depth less then the back side plane where a large crack has been detected after the removal of fragments in the lower caves behind the feet of the Statue. One passive anchor parallel to surface aimed at stabilising the upper gallery where a large fissure is present;
   c. low water release grouting in the boreholes, maintaining the composition of water and cement successfully adopted in the eastern side which includes: W / C = 1 / 2.0 + superplasticizer. Approx. 2.0 m^3 were grouted for the nails installation with 2,400 kg of cement.
4. Minimisation of impact is following the same criteria established for the eastern side.

In the Western wall of the niche, the total grout for grouting and filling was estimated in approx. 3 m^3, with 3.600 kg cement (cracks and anchors). As mentioned before, the correctness of grouting was demonstrated by the suitability test for the anchors, that do not differentiate the anchor bounded to conglomerate from the one bounded to siltstone, in which slaking is highly possible.

Figure 10.28 is providing the distribution of the anchors as well as the chronological sequence of them. This last is quite important to avoid disturbance to the most critical part of the cliff without having stabilized the boundary conditions. In addition, it provides a further protection against water infiltration potentially slaking the siltstone as well as generating additional pore pressure.

10.4.1.3 Implementation on the Upper Part

In the upper part of the niche it was decided to install three permanent stainless steel passive

Fig. 10.29 Drilling for nails

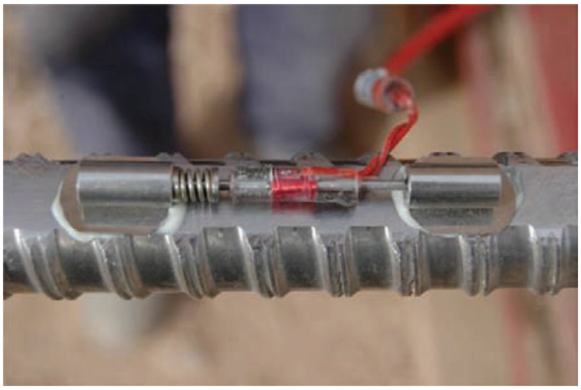

Fig. 10.31 Detail of a strain gauge

Table 10.2 Characteristics of the installed strain gauges

Transducer Type	Vibrating Wire
Standard range	3.500 microstrain
Sensitivity	1.0 microstrain
Accuracy	0.1% F.S.
Non linearity	Less than 0.5 % FS
Temperature Range	−30 °C to + 80 °C
Guage length	50.8 mm

anchors, 12.0 m long, sub-horizontal, with the following purposes:

1. to monitor the tensional state of the rock masses, by means of 10 strain gauges placed in two of the anchors;
2. to grout the medium part of the cliff to avoid water infiltration within the niche during snowmelt or prolonged rainfall.

The position of these long anchors is reported in the following Fig. 10.30.

Fig. 10.30 Position of anchors on the *top* of niche. The *yellow* ones are monitored with 10 strain gauges

540 l of cement mix were utilized for the grouting of the anchors (600 kg of cement). Open vertical fissures, reaching downwards the niche, were intercepted in the 3 boreholes at depths up to approximately 8 m (anchor no 39) and 9 m (Anchor 41) .

The anchors no. 39 and 41, were instrumented with the installation of a series of 5 spot weldable strain gauges (Fig. 10.31) in each anchor. The characteristics of these instruments are described below. The cables connecting the sensors have been conveyed into small grooves to suitable steel boxes located into the niche, were readings can be taken utilizing the portable datalogger with LCD display.

10.4.1.4 Location and Type of Anchors and Nails on the East Giant Buddha Niche

In conclusion, in the Eastern Giant Buddha niche n. 64 passive anchors and nails were installed, for a total length of 443.5 m. The total amount of grouting was established in 19,7 m^3 of cement grout with 24.000 kg of cement.

The following Fig. 10.32 are summarising all the long passive anchors and nail and the related location.

The following Table 10.3 is reporting type and length of each anchor and nail previously described.

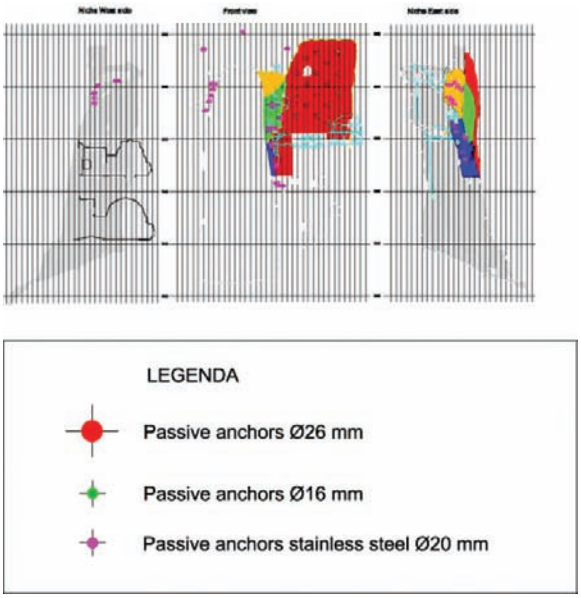

Fig. 10.32 Typology, position and length of executed anchors and nails (*red* is for passive anchors, pre-grouted, with diameter = 26 mm and length 15 m.; *violet* is for stainless steel passive anchors with diameter = 26 mm and a length 5–10 m.; *green* is for short passive anchors with diameter = 16 mm and length about 5 m, placed on the internal side of the niche) (topographic data from PASCO, 2003)

Table 10.3 Type and length of each installed anchor and nail (for numbers refer to Fig. 10.32)

anchor	"drill Ø 90 mm Dywidag Ø 26/50 mm"
n°	m
A	7.50
B	7.50
C	7.50
D	15.00
E	15.00
F	15.00
G	15.00
H	7.50
I	7.50
L	7.50
M	7.50
N	15.00
O	15.00
P	15.00
Q	7.50
R	7.50
S	7.50

anchor	"drill Ø 50 mm Gewi Ø 16 mm"
n°	m
1	4.20
2	5.15
3	5.20
4	5.30
5	4.85
6	4.50

anchor	"drill Ø 50 mm stainless steel Ø 20 mm"
n°	m
7	4.50
8	4.50
9	4.50
10	4.60
11	3.30
12	1.30(Gewi Ø 16 mm)
12 bis	5.00
13	5.00
14	7.00
15	7.50
16	7.50
17	7.50
18	7.50
19	7.50
20	7.50
21	3.00
21 bis	3.50
22	5.50
23	6.50
24	3.70
24 bis	5.00
25	4.50
26	2.50
26 bis	7.00
27	1.50
28	1.60
29	2.10
30	4.00
31	4.30
32	4.60
33	5.00
34	6.00
35	8.30
36	5.00
37	2.00
38	8.00
39	12.00
40	12.00
41	12.00

10.4.2 First Interventions in the Western Giant Buddha Niche

Despite of the destruction of the statue, the Western Giant Buddha niche did not suffer extensively as consequence of the explosion (Margottini, 2006). Emergency intervention includes (Fig. 10.33):

a. grouting of the large fissure placed in the corridor, back side of the niche.
b. Other minor sites to consolidate

The grouting of the large crack in the back side of the niche has been done from inside as well as from outside (top of the cliff). Initially, the fissure was grouted and closed in the internal part of the niche, in order to protect the niche from cement infiltration and leaching from the top. Small pipes were required inside the cement to avoid internal overpressure.

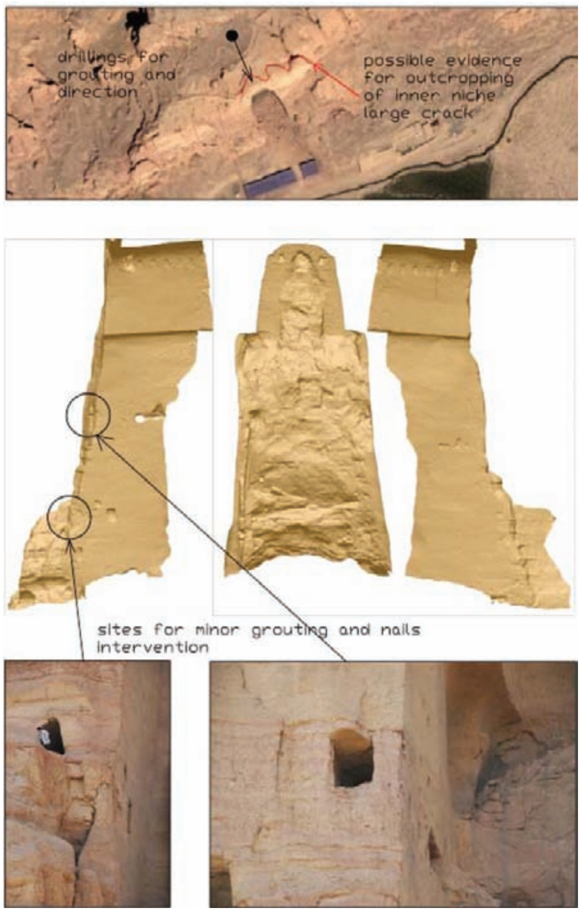

Fig. 10.33 Emergency intervention in the Western Giant Buddha niche (topographic data from PASCO, 2003)

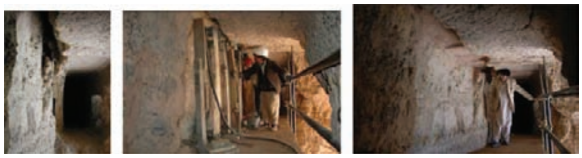

Fig. 10.34 The large crack in the corridor on the back side of the niche before, during and after the grouting

Fig. 10.35 Detail of the grouting from the top of cliff

From the top of the cliff, inclined drills were performed and, when the fissure was encountered in the perforation, it was grouted with the same mixture of cement and superplasticizer described in Margottini (2003a). A major attention was required for the execution of drillings on top of the cliff, due to the possible existence of land mines, even after a complete de-mining of the site as result of rainfall run off.

Other minor intervention were required in two small sites, as reported in the design of Fig. 10.36. The possible risk of collapse, even for small pieces of rock, was completely avoided.

Fig. 10.36 Drilling in the lower part of the niche

10.5 Conclusion

The present paper describe all the emergency intervention performed in Bamiyan (Central Afghanistan) for the consolidation of niches and unstable blocks resulting from the explosion, executed by Talibans in March 2001, aimed at destructing the VI c. A.D. giant statues of Buddha.

The effect of explosion was quite dramatic: the two statues totally collapsed but also some small part of the niches fall down and, mainly large part of the Eastern Giant Buddha Niche was close to the collapse. UNESCO was immediately prompt to undertake an emergency intervention for securing the remaining of such wonderful cultural heritages and, thanking to the generous Government of Japan financial support, the works started in November 2003.

The activities were developed according to the following general scheme:

1. engineering geological study of the site, including laboratory testing and filed work (the first were conducted in Europe in few samples and the latter conditioned in their execution from the presence of land mine);
2. installation of a high precision monitoring system;
3. realisation of temporary support infrastructure, to maintain stable the blocks at limit equilibrium, also during the execution of works;
4. execution of the consolidation work, with professional climbers to avoid any activities below the hanging and unstable blocks, with a system of small and long passive anchors and grouting;
5. minimisation of impact of anchor heads, with a mixture of special mortar, investigated in detail with the support of ICOMOS expert.

The result was quite satisfactory, in an area that is slowly coming out from decades of war, and in which it was necessary to adopt the maximum of professional judgment in identifying weak points and limits in knowledge and, in the mean time, to adopt technologies capable to solve the problems in very short time and in safe conditions.

After the investigations started in September 2002 and the practical intervention of October–December 2003, March 2004 and October–December 2006, the cliff and niche of the Eastern Giant Buddha (the most critical part) it is now more stable and the risk of collapse almost avoided. Also, the niche of Western Giant Buddha have been protected from water infiltration. Further work will be needed in the future, especially in back side of both niches but, at least, the major risk to have a collapse involving also the few remains not destroyed by Talibans it is now turned away.

References

Burnes A. (1834) Travel into Bokhara. London.

Colombini V., Margottini C. (2003a). Reducing the most critical rock fall-prone areas in the Buddhas niches in Bamiyan (Central Afghanistan). UNESCO Report, July 2003.

Colombini V., Margottini C. (2003b). Buddhas niches in Bamiyan valley: Emergency measures in autumn 2003, to permit future consolidation. UNESCO Report, September 2003.

Hoek E., Bray J.W., (1994) Rock slope engineering. Institution of Mining and Metallurgy, Third edition revise 1981, Reprinted.

Hoek E., Brown J.W., (1980). Empirical strength criterion for rock masses. Journal of Geotechnical Engineering Div. A.S.C.E., 106(GT9), 1013–1035.

ITASCA Consulting Group (2000). Fast lagrangian analysis of continua, vs. 4.0. Minneapolis, Minnesota, USA.

Lang, J. (1968). La serie neogene de Bamian (Afghanistan). C.R.Acad.Sci., 266, 26 S.2383–2384, Paris.

Lang, J. (1972) Bassins intramontagneux néogènes de l'Afghanistan Central- Rev. Geogr. Phys. Geol. Dynam., 14, 4(2), 415–427, Paris.

Margottini C. (2003a). The geomorphological instability of the Buddha niches and surrounding cliff in Bamiyan valley (Central Afghanistan). UNESCO Report, June 2003.

Margottini C. (2003b). The Buddha niches in the Bamiyan valley (Central Afghanistan): instability problems and restoration plans in the UNESCO intervention. Journal of the Japanese Landslide Society, 450(3), 246–249. (in Japanese).

Margottini C. (2004a). Instability and geotechnical problems of the Buddha niches and surrounding cliff in Bamiyan valley, Central Afghanistan. Landslides, n.1. January.

Margottini C. (2004b). Definition of 2004 activities for implementing the emergency consolidation of Eastern Giant Buddha and for beginning the preservation of Western Giant Buddha from geological hazards. UNESCO report March 2004.

Margottini C. (2006) Definition of 2006 activities for implementing the emergency consolidation of Large Eastern Buddha and for beginning the preservation of Large Western Buddha. UNESCO Report, August 2006.

Margottini C. (2007). Engineering geology and cultural heritages: the conservation of remaining Bamiyan Buddhas (Central Afghanistan). In Sassa K, Fukuoka H. Wang F. and Wang G. (eds.), Progress in Landslide Science. Springer-Verlag, Berlin Heidelberg.

Margottini C., Colombini V., Crippa C. Tonoli G. (2005) Emergency intervention for the Geo-Mechanical conservation of the Niches of Bamiyan Buddhas (Northern Afghanistan). In Sassa K, Fukoka H., Wang F. Wang G. (eds.), Landslides – Risk analysis and sustainable disaster management. Springer-Verlag, Berlin-Heidelberg.

Reineke T. (2006) Environmental Assessment of the Bamiyan Valley in the Central Highlands of Afganistan. In University of Aachen, Bamiyan Masterplan Campaign 2005. Aachen.

PASCO (2003) Buddhas laser scanner project.

Turner K, Schuster R. (1996) Landslides, investigation and mitigation. Special report, Transportation research board, National Research Council, 247, Washington.

Part III

Achievements of IPL Projects

Assessment of Global High-Risk Landslide Disaster Hotspots

11

Farrokh Nadim and Oddvar Kjekstad

Abstract Allocating resources for natural hazard risk management has high priority in development banks and international agencies working in developing countries. Global hazard and risk maps for landslides and avalanches were developed to identify the most exposed countries. Based on the global datasets of climate, lithology, earthquake activity, and topography, areas with the highest hazard, or "hotspots", were identified. The applied model was based on classed values of all input data. The model output is a landslide and avalanche hazard index, which is globally scaled into nine levels. The model results were calibrated and validated in selected areas where good data on slide events exist. The results from the landslide and avalanche hazard model together with global population data were then used as input for the risk assessment. Regions with the highest risk can be found in Colombia, Tajikistan, India, and Nepal where the estimated number of people killed per year per 100 km^2 was found to be greater than one. The model made a reasonable prediction of the landslide hazard in 240 of 249 countries. More and better input data could improve the model further.

11.1 Introduction

Information on hazards, vulnerabilities and risks at an appropriate scale is of fundamental importance for design and implementation policies and programs for mitigation of disaster risk. In order to be focused, relevant and effective, contingency planning, disaster preparedness and early warning systems require the knowledge of what kind of losses could be expected from what type of hazard. Lack of such data on a global scale led to the ProVention Consortium initiative to launch a collaborative project on "Identification of Global Natural Disaster Hotspots" – the "Hotspots Project", for short – in 2001.

The aim of the Hotspots Project was to perform a global assessment of the risk of mortality and economic losses for six major natural hazards: drought, floods, wind storms, earthquake, landslides and volcanoes. The overall study is published by the World Bank (The World Bank, 2006a and 2006b, and Dilley et al., 2005).

NGI's role in this collaborative project was to assess the global distribution of landslide hazard and risk. In many parts of the world landslides pose a major threat. They occur more frequently than other natural hazards. However, in terms of the number of fatalities from different hazards, landslides rank rather low compared to earthquakes, floods, wind storms and extreme temperatures. There is however, reason to believe that the number of causalities due to

Farrokh Nadim (✉)
International Centre for Geohazard/NGI, Oslo, Norway

Oddvar Kjekstad
International Centre for Geohazard/NGI, Oslo, Norway

K. Sassa, P. Canuti (eds.), *Landslides – Disaster Risk Reduction*,
© Springer-Verlag Berlin Heidelberg 2009

landslides derived from natural disaster databases is grossly underestimated. This is because the loss figures in the international databases are normally recorded by the primary triggering factor, and not by the hazard that causes the fatalities. For instance the 1999 Venezuela Disaster, with more than 20,000 deaths, is recorded as a flood, while most fatalities were caused by landslides in form of debris flows and mud flows.

11.2 Model Description

The general approach adopted in the study for the evaluation of global landslide hazard prone areas and risk hotspots is depicted on Fig. 11.1.

The study focused on slides with *rapid mass movement*, like rockslides, debris flows, snow avalanches, which pose a threat to human life. Slow moving slides have significant economic consequences for constructions and infrastructure, but rarely cause any fatalities.

11.2.1 Approach for Landslide Hazard Evaluation

Landslide hazard level depends on the combination of trigger and susceptibility (Fig. 11.1). In the first-pass estimate of landslide hazard, five parameters were used. These are described briefly below. More details are provided in Nadim et al. (2006).

11.2.1.1 Slope factor S_r

The slope factor represents the natural landscape ruggedness within a grid unit.

In February 2000, NASA collected elevation data for much of the world using a radar instrument aboard the Space Shuttle. The raw data collected on the mission were processed over three years. At the time of the study, NASA had released a global elevation dataset called SRTM30, referring to the name of the mission and the resolution of the data, which is 30 arc-sec, or approximately 1 km^2 per data sample near the equator. The SRTM30 data set covers the globe from 60° south latitude to 60° north latitude. Using the SRTM30 data set as the starting point and correcting the anomalies by using other datasets, Isciences (www.isciences.com) derived the grid of slope angles for this study. The slope data were reclassified on a geographical grid (WGS84) and the grid cells were categorized into 5 categories, from 0 to 4. The index S_r was set equal to zero for slope angles less than 1°, i.e. for flat or nearly flat areas, because the resulting landslide hazard is null even if the other factors are favourable.

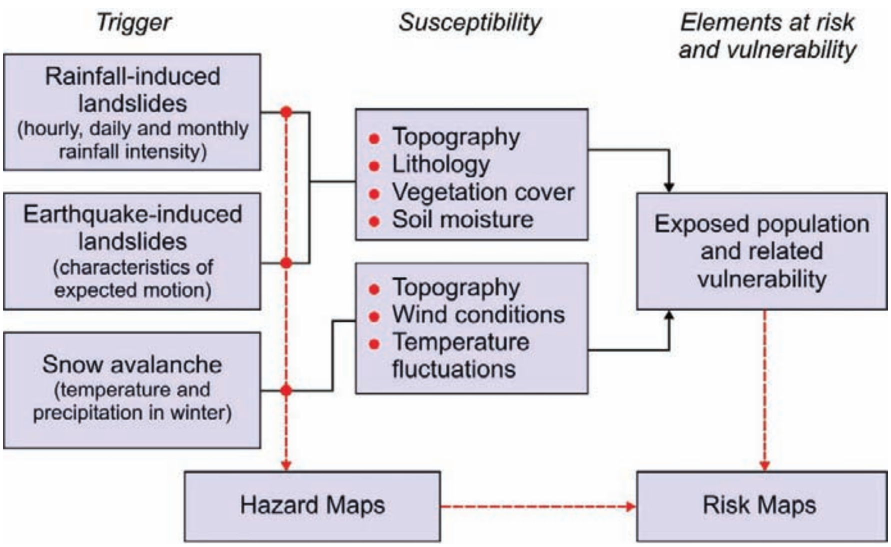

Fig. 11.1 General approach for landslide hazard and risk evaluation

11.2.1.2 Lithology factor S_l

This was the most difficult parameter to assess. Ideally, detailed geotechnical information should be used but, at the global scale, only a general geological description is available. Rock strength and fracturing are the most important factors to evaluate lithological characteristics, and these characteristics can vary greatly over short distances.

The dataset used in this study was the Geological map of the World at 1/25,000,000 scale published by the Commission of the Geological Map of the World and UNESCO (CGMW, 2000). The map is available on a CD-ROM. The grid Resolution is $2.5 \times 2.5°$ latitude/longitude. This map is the first geological dataset compiled at a global scale showing the geology of the whole planet, including continents and oceans. In the map, three main types of formation are identified: sedimentary rocks, extrusive volcanic rocks and endogenous rocks (plutonic or strongly metamorphosed). Usually old rocks are stronger than young rocks. Plutonic rocks will usually be strong and represent low risk. Strength of metamorphic rocks is variable, but these rocks often have planar structures such as foliation and therefore may represent higher risk than plutonic rocks. Lava rocks will usually be strong, but may be associated with tuff (weak material). Therefore, areas with recent volcanism are classified as high risk. Sedimentary rocks are often very weak, especially young ones. For the purpose of this study, five susceptibility classes were identified and the index S_l was assigned values from 1 to 5.

11.2.1.3 Soil Moisture Factor, S_h

S_h is a soil moisture index, which indicates the mean humidity throughout the year and gives an indication of the state of the soil prior to heavy rainfall and possible destabilization. The data for this study were extracted from Willmott and Feddema's Moisture Index Archive (Willmott and Feddema, 1992). The data cover the standard meteorological period 1961–1990. Resolution of the grid is $0.5 \times 0.5°$. Gridded mean monthly total potential evapotranspiration (Eo) and unadjusted (in respect to topography) total precipitation (P) are taken from:

- Terrestrial Water Balance Data Archive: regridded monthly climatology, and
- Terrestrial Air Temperature, monthly precipitation and annual climatology.

These data can be downloaded from the internet (Centre for Climatic research, University of Delaware). Estimates of the average-monthly moisture indices for Eo and P are only made for land-surface grid points (total of 85,794 points). The average monthly moisture indices are calculated according to Willmott and Feddema (1992) using the gridded average-monthly total Eo and P values, at the same resolution as the water-balance fields. For this study, five classes for soil moisture index were determined and the index S_h was assigned values from 1 to 5. The map of the global soil moisture index is shown on Fig. 11.2.

11.2.1.4 Precipitation Trigger Factor T_p

The categorization T_p was based on the estimate of the 100-year extreme monthly rainfall (i.e. extreme monthly rainfall with 100 years return period). The source of data was the monthly precipitation time series (1986–2003) from Global Precipitation Climatology Centre (GPCC) run by Germany's National Meteorological Service, DWD (Rudolf et al., 2005). The provided data are near real-time monitoring products based on the internationally exchanged meteorological data with gauge observations from 7,000 stations worldwide. The products contain precipitation totals, anomalies, number of gauges and systematic error correction factors. The grid resolution is $1.0 \times 1.0°$ latitude/ longitude. At the time of this study, the monthly values were available for 17 years, from 1986 to 2002. The maximum registered values per annum were used to calculate the expected 100-year monthly precipitation for every grid point assuming a Gumbel distribution. The results were divided into five susceptibility classes and the index T_p was assigned values from 1 to 5. The map of the estimated 100-year extreme monthly rainfall is shown on Fig. 11.2.

11.2.1.5 Seismic Trigger Factor T_s

The data set used for the classification of the seismic trigger factor was the expected Peak Ground

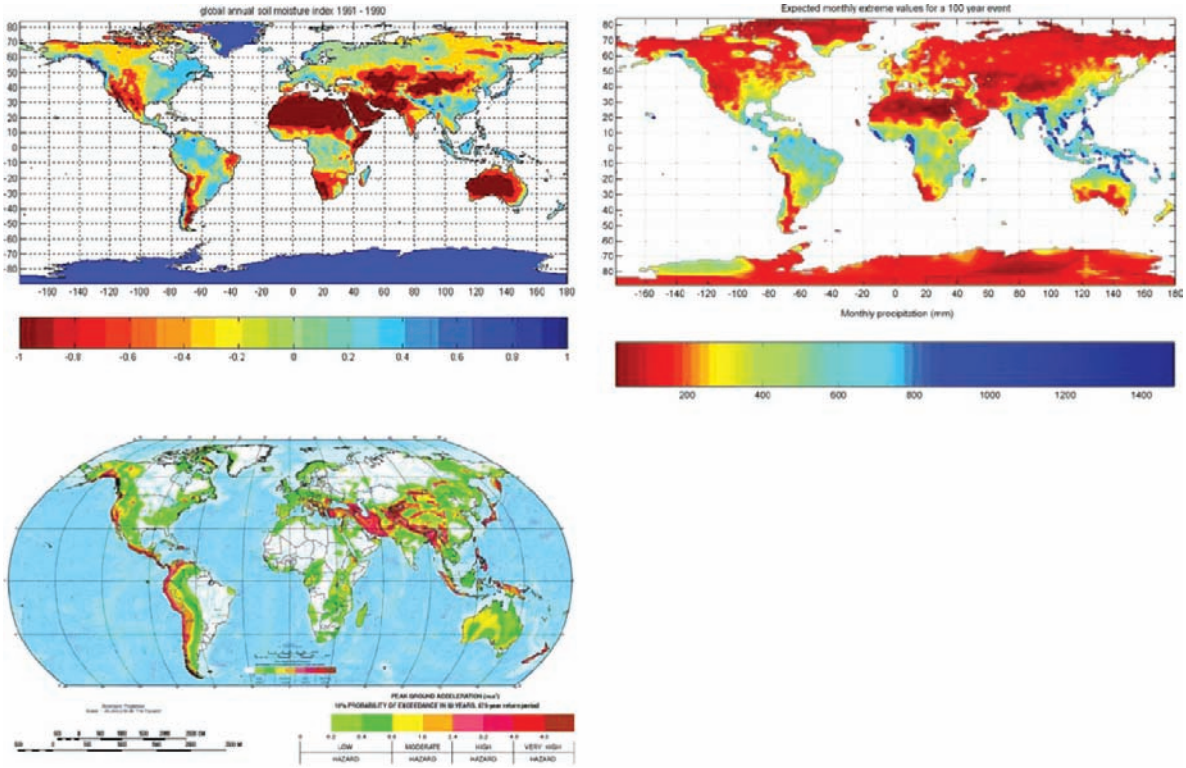

Fig. 11.2 Above, *left*: Global soil moisture index: 1961–1990 (Willmott and Feddema, 1992). Above, *right*: Expected monthly extreme precipitation values (mm) for a 100-year event (http://gpcc.dwd.de). *Left:* Expected PGA with a return period of 475 years. Scale varies from 0 m/s^2 (*white*) to 9 m/s^2 (*brown*)

Acceleration (PGA) with 475-year return period (10% probability of exceedance in 50 years) from the Global Seismic Hazard Program, GSHAP (Giardini et al., 2003; Fig. 11.2). The GSHAP PGA_{475} data were categorized into 10 classes and the index Ts was assigned values from 1 to 10.

11.3 Landslide Hazard Index $H_{landslide}$:

The relative landslide hazard level was estimated using a model similar to that suggested by Mora and Vahrson (1994) for regional analyses. For each factor, an index of influence was determined (range of values are given above) and the relative landslide hazard level $H_{landslide}$ was obtained by multiplying and summing the indices using the following equation:

$$H_{landslide} = (S_r \times S_l \times S_h) \times (T_s + T_p)$$

With the range of indices given above, the landslide hazard index varies between 0 and 1500. Based on the computed $H_{landslide}$, each basic grid cell in the global analysis (30 arc-sec $\times$ 30 arc-sec latitude/longitude) was classified as shown in Table 11.1. The annual frequency of serious landslides given on the last column was based on a crude calibration

Table 11.1 Classification landslide hazard based on the landslide hazard index

Value of $H_{landslide}$	Class	Classification of landslide hazard potential	Approximate annual frequency in 1 km^2 grid
< 14	1	Negligible	Virtually zero
15–50	2	Very low	Negligible
51–100	3	Low	Very small
101–168	4	Low to moderate	small
169–256	5	Moderate	0.0025–0.01%
257–360	6	Medium	0.0063–0.025%
360–512	7	Medium to high	0.0125–0.05%
513–720	8	High	0.025–0.1%
> 720	9	Very high	0.05–0.2%

in few areas (mainly in Europe) where the authors have access to reliable data. The overlapping ranges in the annual frequencies reflect the uncertainty in the estimates.

The snow avalanche hazard was evaluated using a similar model, but with only 3 parameters: slope factor within a selected grid (S_r), precipitation values for four winter months (T_p) and average temperature in winter months (T_t). Further details of the models are provided by Nadim et al. (2004) and by Nadim et al. (2006).

The estimation of expected losses was achieved by first combining the frequency of landslides and the exposed population in order to assess the physical exposure, and then performing a regression analysis using different sets of uncorrelated socio-economical parameters in order to identify the best indicators of human vulnerability for a selected hazard in a given country. The following formula for estimating the risk was used:

$$R = H \cdot Pop \cdot Vul$$

where:

R = risk proxy: number of expected human fatalities in landslides
H = annual hazard occurrence probability
Pop = population living in a given exposed area
Vul = vulnerability, depends on socio-politico-economical parameters

Defining physical exposure (*PhExp*) as the annual frequency of a hazard with specified severity multiplied by the number of persons exposed ($PhExp = H \cdot Pop$), the risk can be evaluated by logarithmic regression using the following formula:

$$ln(R) = ln(PhExp) + ln(Vul)$$

In the case of landslides, once the average physical exposure was estimated from the hazard model(s) described above and population density data, an estimate of risk was made using a proxy of vulnerability. This included a multivariate regression analysis to correlate the number of expected fatalities to socio-economic parameters following the approach outlined by Dao and Peduzzi (2004).

11.4 Results

The hotspots project included validation of predicted landslide hazard zones in a number of countries where data on geographical distribution of historical landslides were available. The countries where calibration was performed were Norway, Armenia, Georgia, Nepal, Sri Lanka and Jamaica (NGI, 2004). In general the prediction model was found to yield a good first-pass approximation.

The main regions of the world with moderate to very high landslide hazards (Fig. 11.3) were found to include: Central America, Northwestern South

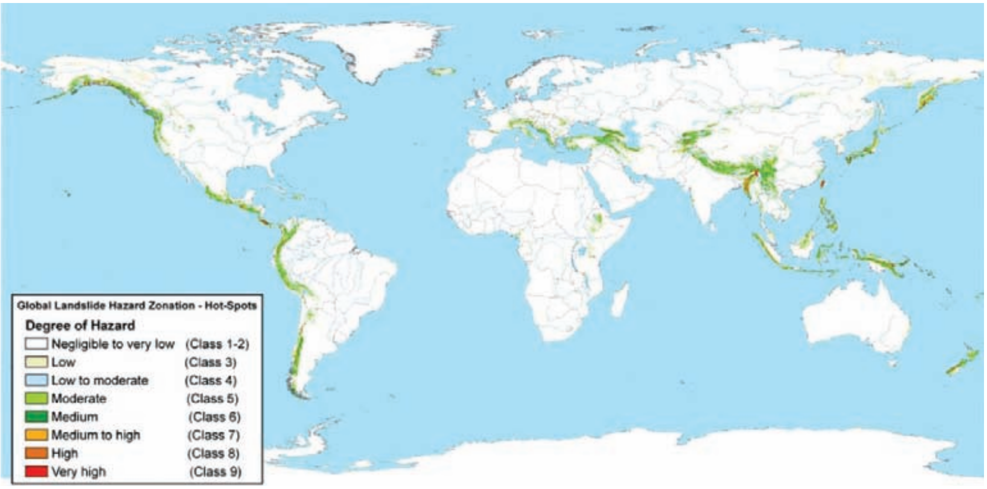

Fig. 11.3 Global landslide hazard hotspot zonation for the world

America, Northwestern USA and Canada, the Caucasus region, the Alborz and Zagros mountain ranges in Iran, Turkey, Tajikistan, Kyrgyzstan, the Himalayan belt, Taiwan, Philippines , Indonesia, New Guinea, New Zealand, Italy and Japan.

More detailed maps for Central Asia and Central America are shown on Fig. 11.4. Countries with medium to high, high, and very high landslide hazard in these regions include: Georgia, Armenia, Turkey, Iran, a small part of Southern Russia, Tajikistan, Kyrgyzstan, Afghanistan, Nepal, India and Southern China in Asia; and Guatemala, Mexico, El Salvador, Honduras, Nicaragua, Costa Rica, Panama, Columbia, Ecuador and Peru in Latin America.

In the predictions of landslide risk, the distribution of hazard, frequency of occurrence, population density, as well as loss figures from historical events, were the major input parameters. Some of the major findings of the landslide risk analyses were:

- The annual number of expected fatalities due to major landslides worldwide, as predicted by the model, was found to be in excess of 4300. This number is of the same order of magnitude as the reported average number of people killed per year (ca. 1700) in the past 30 years (EM-Dat, 2003).
- 98% of the recorded victims lived within areas predicted by the NGI model to fall in landslide hazard zones 5 and above.
- Localized areas of pixel size 1 km^2, with highest mortality risk, were found to be in Colombia, Tajikistan, India and Nepal where the predicted risk for number of people killed pr year pr 1 km^2 was found to be greater that 0.01.
- In countries like Guatemala, El Salvador, Honduras, Panama, Costa Rica, Mexico, Colombia, Afghanistan and Iran, the model predicted large areas with risk for number of people killed pr year pr 1 km^2 between 0.001 and 0.01.

The results showed strong correlation between high risk and physical exposure, and strong correlation between high risk and low Human Development Index (HDI) as determined by United Nation Development Program (UNDP). The analysis also showed high correlation between high risk and high percentage of forest cover, which is somewhat surprising. This might reflect the fact that the countries with highest forest coverage might also be the ones with the highest degree of deforestation. Deforestation is an important factor that needs to be addresses in more detail (Ref: World Disaster Report 2004), but the parameter is difficult to determine on the global basis with the existing data sets. The percentage "arable land" also showed a strong correlation with landslide risk, which indicates that rural population are more vulnerable to landslides than urban population.

The result of the regression analysis for landslide risk is shown on Fig. 11.5. It should be mentioned that out of the 249 countries that were included in the analysis, the model failed to explain landslide risk adequately in nine of the countries. This demonstrates the need for better data sets,

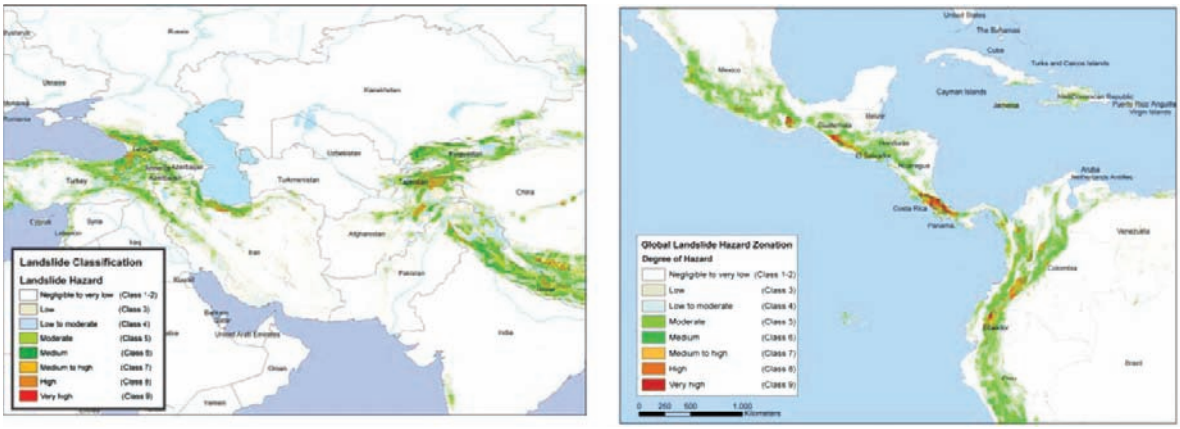

Fig. 11.4 Predicted landslide hazard hotspots areas in Central Asia (*left*) and Central America (*right*)

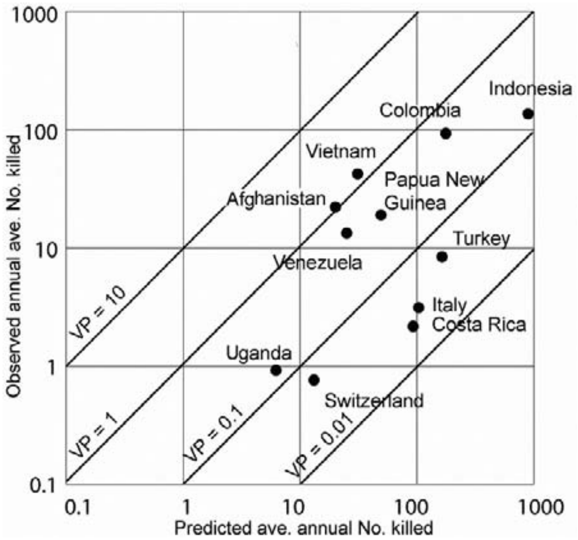

Fig. 11.5 Predicted killed versus observed landslide fatalities

especially on deforestation. Figure 11.6 shows the landslide risk hotpots in Central Asia and Latin America.

11.5 Suggestions for Model Improvement

As part of the Global Risk Update (GRU) project of ISDR, the global landslide hazard assessment model is being revised. In the new study, the landslide hazard due to earthquakes will be differentiated from the landslide hazard due to heavy precipitation, and effects of vegetation cover will be included in the model:

$$H_{\text{landslide, earthquake}} = (S_r \times S_l \times S_h \times S_v) \times T_s$$

$$H_{\text{landslide, rainfall}} = (S_r \times S_l \times S_h \times S_v) \times T_p$$

where S_v is a new index that describes the vegetation cover.

In GRU study, there will be more focus on the ratio of the extreme to average precipitation, rather than the absolute value of precipitation. Conceptually, this model would be a better representation of the physical processes that trigger landslides during heavy rainfall.

11.6 Conclusions

The probability of landslide and avalanche occurrence was estimated by modelling the physical processes and combining the results with statistics from past experience. The main input data used in the hazard assessment were topography and slope angles, extreme monthly precipitation, seismic activity, lithology, mean temperature in winter months (for snow avalanches) and hydrological conditions. Although the first-pass analyses were done with relatively simple models, they still

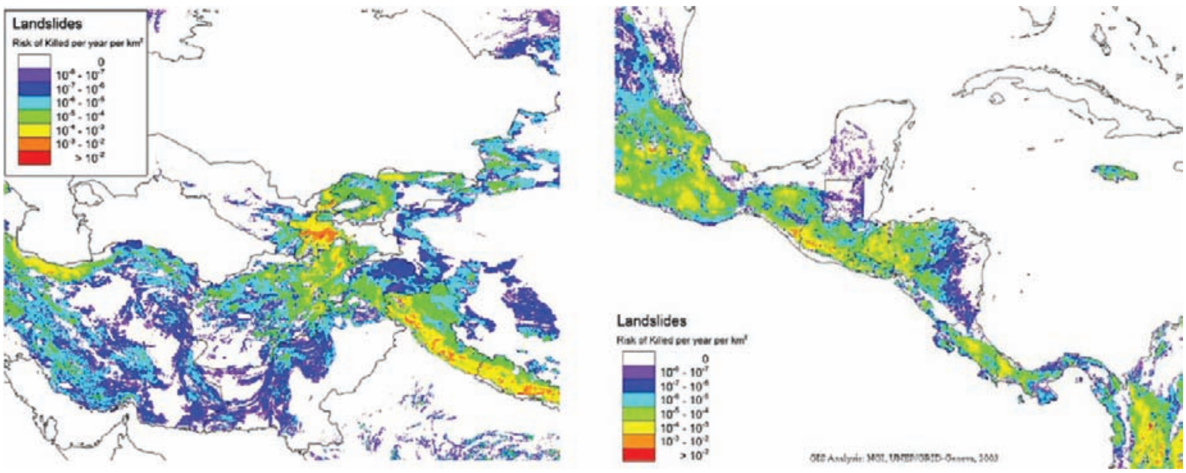

Fig. 11.6 Landslide risk hotspot zonation for Central Asia (*left*) and Central America (*right*)

provided a fairly good estimate of the landslide hazard. Validation of the global hazard prediction, which was carried out for Georgia, Armenia, Sri Lanka, Nepal, Jamaica and Norway, showed fair agreement between the boundaries of the known slide-prone areas and the hazard zones predicted by the global model. However, the analyses suffered from significant shortcomings in the quality and resolution of the available global data sets.

Working in a smaller area, it should be possible to refine the analyses using better resolution in the input data, as well as adding supplementary parameters such as land cover, deforestation and effects of long-term climatic change. With use of a more comprehensive set of site-specific data, it should also be possible to make a prediction of economic losses with the model, and not only fatalities, as was done in the present study.

The estimation of the risk associated with landslides was based on data on lives lost as recorded in various natural disaster impact databases. The estimation of expected number of lives lost was achieved by first combining the landslide frequency and the population exposed, and then doing a regression analysis using different sets of uncorrelated socio-economical parameters. The study identified the socio-economic parameters that seem to have the strongest correlation with expected fatality due to landslides. Improved data quality, adding new type of data sets to the model, and having loss data from the landslide-prone countries that are presently missing, are important for better understanding and identification of the most relevant socio-economic parameters that affect landslide risk.

The study clearly showed that the following countries and geographical areas are among the landslide hazard hotspots: Central America, North-western South America, the Caucasus region, the Himalayan belt, Taiwan, Philippines, Indonesia, Italy, and Japan.

The conclusions of this study were all based on a global model, which does have shortcomings when applied at a local level. Use or interpretation of the results for specific national conditions is not recommended without further detailed investigations. Several factors contribute to uncertainties in the predictions presented in the paper, the major one being the scarcity of high-quality, high-resolution data at a global scale. Additional factors that could lead to improved predictions are discussed and suggestions for revision of the model are given.

Acknowledgement The study was initiated by the World Bank's Hazard Management Unit (HMU), headed by Margaret Arnold, under the umbrella of the ProVention Consortium. The study was conducted as part of the ProVention activity on Natural Disaster Hotspots: A Global Risk Analysis. Major part of the funding was provided by United Kingdom's Department for International Development (DFID) and The Norwegian Ministry of Foreign Affairs. Margaret Arnold's support and encouragement throughout the work are gratefully appreciated. The authors acknowledge close cooperation with Columbia University, especially Robert Chen and Maxx Dilley. The landslide risk estimation model was developed by Pascal Peduzzi and Christian Herold of UNEP/GRID-Geneva. Their invaluable contribution is gratefully acknowledged. A number of NGI personnel participated actively in the project, among them Ulrik Domaas, Christian Jaedicke and Frode Sandersen. The authors are grateful to these individuals for their active participation and support.

References

CGMW (2000) Geological Map of the World, Commission for the Geological Map of the World. UNESCO Publishing.

Dao H, Peduzzi P (2004) Global evaluation of human risk and vulnerability to natural hazards. Enviro-info 2004, Sh@ring, Editions du Tricorne, Genève, isbn 282930275-3 (1): 435–446.

Dilley M, Chen RS, Deichmann U, Lerner-Lam AL, Arnold M, et al. (2005) Natural Disaster Hotspots – A Global Risk Analysis. Report International Bank for Reconstruction and Development/The World Bank and Columbia University: 132.

EM-DAT (2003) The OFDA/CRED International Disaster Database – www.em-dat.net – Université Catholique de Louvain – Brussels - Belgium.

Giardini D, Grünthal G, Shedlock K, Zhang P (2003) The GSHAP Global Seismic Hazard Map. In: Lee W, Kanamori H, Jennings P (eds.) International Handbook of Earthquake and Engineering Seismology. IASPEI.

Mora S, Vahrson W (1994) Macrozonation methodology for landslide hazard determination. Bulletin of the Association of Engineering Geologists, 31(1): 49–58.

Nadim F, Kjekstad O, Gregoire AS, Rodriguez C, Peduzzi P (2004) First-order identification of global slide and avalanche hotspots. NGI report 20021613-1, 31 March 2004. Norwegian Geotechnical Institute, Oslo, Norway.

Nadim F, Kjekstad O, Peduzzi P, Herold, C and Jaedicke, C (2006) Global landslide and avalanche hotspots. Landslides, 3(2): 159–174.

Rudolf B, Beck C, Grieser J, Schneider U (2005) Global Precipitation Analysis Products, Deutscher Wetterdienst, Offenbach a.M., Germany.

The World Bank (2006a) Natural Disaster Hotspots – A Global Risk Analysis. Disaster Risk Management Series No. 5.

The World Bank (2006b) Natural Disaster Hotspots – Case Studies. Disaster Risk Management Series No. 6.

Willmott CJ, Feddema JJ (1992) A More Rational Climatic Moisture Index. Professional Geographer, 44(1): 84–88.

World Disaster Report (2004) International Federation of Red Cross and Red Crescent Societies, IFRC, Geneva; http://ifrc.org.

International Summer School on Rockslides and Related Phenomena in the Kokomeren River Valley, Tien Shan, Kyrgyzstan

12

Alexander L. Strom and Kanatbek E. Abdrakhmatov

Abstract The annual field training course sponsored by ICL and IPL has been organized since 2006 in the Kokomeren River Valley in Kyrgysztan, Tien Shan. Students and young landslide researchers are visiting bedrock landslides of various types and learning different methods of their study. High emphasis is placed also on geological and neotectonic factors favorable for large-scale landslide formation. ICL Summer School on Rockslides and Related Phenomena promotes the capacity building in landslide hazard and risk assessment.

Keywords Rockslide • Rock avalanche • Landslide dam • Tien Shan • Capacity building

12.1 Introduction

Large-scale catastrophic bedrock slope failures belong to the most hazardous natural phenomena that endanger people living in mountainous regions. Unlike "common" landslides and rockfalls, which affect just collapsing slopes themselves and areas directly at their feet, simultaneous failure of millions and, sometimes, billions of cubic meters of rocks can devastate vast areas, extending up to 5–10 km and even more from their source zones. Moreover, they often have disastrous secondary effects like valley inundation due to river damming and subsequent outburst floods. It can be exemplified by the 1786 earthquake triggered Dadu rockslide in China that formed a dam, which subsequent failure killed about 100 000 people downstream, thus being the most disastrous rockslide catastrophe ever reported (Lee and Dai in press). In 1841 and 1858 catastrophic floods occurred due to failure of rockslide dams that had blocked the Indus River and its large tributary, the Hunza River, correspondingly (Hewitt 2002). In 1881 rock avalanche destroyed the Elm village and it was the first time when long runout event was described scientifically (Heim 1882; Hsü 1975).

In 1911 the Usoi rockslide dammed the Murgab River in Pamirs and formed the 500-m deep Sarez Lake that still poses a potential hazard for the large part of the Amu-Daria River basin (Gaziev 1984, Alford and Schuster 2000). In 1949 the Khait rock avalanche caused by strong M 7.4 earthquake – the most disastrous landslide event in Central Asia region – buried the Khait town with several thousands of its inhabitants (Leonov 1960). In 1963 breach of the Issyk Lake rockslide dam near Almaty City in Kazakhstan produced debris flow that devastated the entire valley and caused numerous casualties (Litovchenko 1964). Unfortunately this tragic list can be extended.

Alexander L. Strom (✉)
Institute of Geospheres Dynamics, Russian Academy of Sciences, Russia

Kanatbek E. Abdrakhmatov
Institute of Seismology, National Academy of Science, Kyrgyzstan

K. Sassa, P. Canuti (eds.), *Landslides – Disaster Risk Reduction*,
© Springer-Verlag Berlin Heidelberg 2009

To promote the capacity building in large-scale rockslides hazard and risk assessment the special field training course sponsored by ICL and IPL – the Summer School on Rockslides and Related Phenomena – have been organized in the Kokomeren River Valley in Kyrgysztan, Tien Shan since 2006. It's main objective is to acquaint students and young landslide researchers with various types of bedrock landslides and methods of their study. High emphasis is placed also on geological and neotectonic framework in which large rock massifs fail catastrophically, on surface ruptures in particular. The latter can be considered as traces of strong past earthquakes, which, as we assume, repeatedly shook the study region in the past and, therefore, can occur here in future, causing new large-scale bedrock slope failures.

12.2 The Study Area

The Tien Shan ("Sky Mountains") (Fig. 12.1) is one of the highest and most seismically active parts of the Central Asian Mountain belt. Numerous very large landslides are known here, yet only a small part of them have been described in publications (Fedorenko 1988; Zolotarev 1990; Strom 1998; Delvaux et al. 2001; Strom and Korup 2006; Abdrakhmatov and Strom 2006) and in unpublished technical reports.

The Kokomeren River basin was selected for the training course due to favorable combination of several factors:

- Presence of numerous rockslides and rock avalanched ranging from several millions to more than one billion cubic meters in volume within a limited area about 40 km from North to South and from East to West (Fig. 12.2) and variability of their types and morphologies. There are rockslides with compact bodies that form high natural dams and those transformed into long runout rock avalanches (Fig. 12.3); confined and unconfined events; rockslides deeply incised by erosion that provides excellent opportunity to study their internal structure (Fig. 12.4); evidences of river valley inundation.
- Expressive neotectonic structures, presence of numerous active faults and surface ruptures, which allow better understanding of geological and seismotectonic framework in which large rockslides have occurred.
- Arid climate, favorable to very good exposure of various morphological features and outcrops not masked by forestation.
- Accessibility of the study area located near the road at one-day trip distance from the Bishkek City – capital of Kyrgyzstan. Bishkek is connected by direct daily flights with Moscow, Istanbul and London. It is also possible to arrive via airport of the Almaty city – former capital of Kazakhstan.

12.3 The Completed and Future Activities

The idea to organize annual training course in the Kokomeren River arose during the NATO Advanced Research Workshop "Security of Natural and Artificial Rockslide Dams" that was held

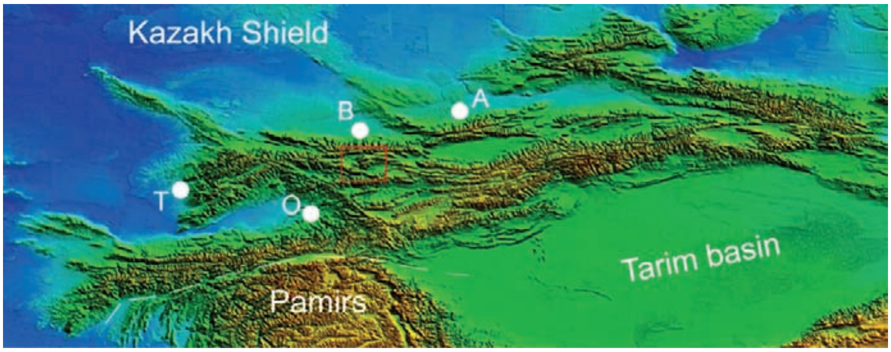

Fig. 12.1 Position of the Kokomeren River basin within the Tien Shan Mountain system

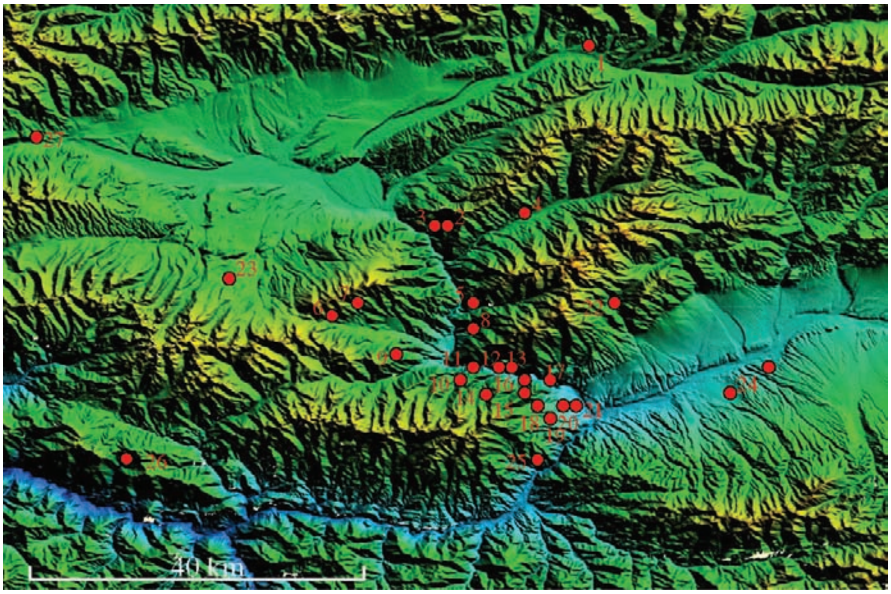

Fig. 12.2 Location of the large-scale slope failures in Kokomeren River basin between the Suusamyr and Djumgal intermontane depressions – the target area of the field training course. Fragment of the 3" SRTM DEM as the background. Three general types of slope failures are selected – landslides in unconsolodated N-Q sediments (LS), bedrock landslides with compact bodies – rockslides (RS), bedrock landslides transformed into long runout rock avalanches (RA). The Kyzylkiol caldera-like collapse is marked as well (site No 26). 1 – Snake-head RA; 2 – Seit RA; 3 – Pre-Seit RS; 4 – Oigaing RS; 5 – Burundu RS; 6 – Chongsu RA; 7 – Chongsu-2 RS; 8 – Sarysu RA; 9 – Toppling site; 10 – Kashkasu RS; 11 – Kashkasu mouth RS; 12 – Kokomeren RS; 13 – Kokomeren-satellite RS; 14 – Upper-Toruaigyr (left & right) RA; 15 – Displaced peneplain RS; 16 – Ancient RA; 17 – Mini-Köfels RS; 18 – Northern Kara-Kungey RA; 19 – Southern Kara-Kungey RA; 20 – Pre-Southern Kara-Kungey RA deposits; 21 – Western Djumgal LS; 22 – Mingteke RA; 23 –South-Suusamyr LS ; 24 – Chaek-1 and Chaek-2 LS; 25 – South-Aral RS; 27 – 1992 Chet-Kurumdu LS

in Bishkek in June 2004. The meeting convened 48 landslide experts from Austria, Belgium, Canada, China, Germany, Italy, Kyrgyzstan, Mexico, New Zealand, Russia, Switzerland, Tajikistan, UK, and the USA. Much of the preparatory work for the workshop and field trips was supported by IPL M-111 Project "Detail study of the internal structure of large rockslide dams in the Tien Shan and the International field mission – Internal structure of dissected rockslide dams in Kyrgyzstan". The 5-days field trip in the Kokomeren River valley after the workshop gave a stimulus to organize the annual Summer School in this particular region.

Its preparation started in 2005 and was supported by the IPL Projects M-111 and M-126 "Compilation of landslide/rockslide inventory of the Tien Shan Mountain System". The detailed 90-pages full-color Guidebook describing rockslides, large landslides and main neotectonic features of the region in question was prepared and was provided to the Summer School participants along with its electronic version on the CD. The PDF file with

Fig. 12.3 The Kashkasu rockslide dam (*left*) and the long runout Seit rock avalanche (*right*)

Fig. 12.4 The Kokomeren rockslide about 1.5 km^3 in volume, which body has been completely cut through by the river. Arrow marks the location of recent fault which motion could trigger slope failure

reduced figures' resolution can be downloaded from the ICL web site (http://www.iclhq.org).

In 2006 and 2007 young landslide researchers from Kyrgyzstan, Czech Republic, Italy and USA participated in the Summer School (Fig. 11.5). They worked on bedrock slope failures mapping, studied their internal structure, grain-size composition, geomorphic evidences of river damming. Several publications and presentations on the International scientific meetings were prepared based on these investigations (Korup et al. 2006; Strom et al. 2006; Hartvich et al. 2008; Strom and Štěpančíková 2008).

Since 2008 Rockslide Summer School will be supported also by the 6th Framework Programme EU-INCO Specific Support Action "International Working Group on Natural Hazards in the Tien Shan". Members of this Working Group will demonstrate geophysical and geotechnical methods of landslide field studies.

12.4 Perspectives of the International Co-Operation

Reliable and well-grounded landslide hazard and risk assessment in the Tien Shan region requires compilation of the complete and uniform inventory of such phenomena for the entire mountain system comparable to that of the European Alps (Heim 1932; Abele 1974). It can be exemplified by studies that were carried out in the Suusamyr basin and surrounding ranges in the Northern Tien Shan (Havenith et al. 2003) where several hundreds of landslides have been identified on satellite images, forming the database for slope stability analyses. One more promising field of future research is landslide dating that will provide additional input data for probabilistic hazard assessment. We believe that the ICL Summer School on Rockslides and Related Phenomena will promote wider International

Fig. 12.5 Participants of summer schools in the field

co-operation in these fields, as well as in the other landslide-related studies not only in Kyrgyzstan, but in other Tien Shan countries – Uzbekistan, Tajikistan, Kazakhstan and China as well.

References

Abele G (1974) Bergstürze in den Alpen. Wissenschaftliche Alpenvereinshefte 25:1–230

Abdrakhmatov K, Strom A (2006) Dissected rockslide and rock avalanche deposits: Tien Shan Kyrgyzstan. In: Evans SG; Scarascia Mugnozza G; Strom A; Hermanns RL (Eds.), Landslides from Massive Rock Slope Failure. NATO Science Series: IV: Earth and Environmental Sciences, Springer, 49:551–572

Alford D. and Schuster R (Eds.) (2000) Usoi Landslide Dam and Lake Sarez. An assessment of Hazard and Risk in the Pamir Mountains, Tajikistan.. UN Publication. Sales No. E.00.III.M.1.

Delvaux D Abdrakhmatov KE, Lemzin IN, Strom AL (2001) Landslides and surface breaks of the 1911, Ms 8.2 Kemin earthquake, Kyrgyzstan. Russian Geology and Geophysics 42:1583–1592

Fedorenko VS (1988) Landslides and rockfalls in mountains, and their forecasting. Moscow, Moscow University Press (in Russian)

Gaziev E (1984) Study of the Usoi Landslide in Pamir. Proc. 4th Int. Symp. on Landslides, Toronto, 1:511–514

Hartvich P, Mugnai F, Proietti C, Smolkova V, Strom A. (2008) A reconstruction of a former rockslide-dammed lake: the case of the Kokomeren River valley (Tien Shan, Kyrgyzstan). Geophysical Research Abstracts, 10, EGU2008-A-00000, 2008

Havenith H-B, Strom A, Jongmans D, Abdrakhmatov K, Delvaux D, Tréfois P (2003) Seismic triggering of landslides, Part A: Field evidence from the Northern Tien Shan. Natural Hazards and Earth System Sciences 3:135–149

Heim A (1882) Der Bergsturz von Elm. Deutsch. Geol. Gesell. Zeitschr. 34:74–115

Heim A (1932) Bergsturz und Menschenleben. Fretz and Wasmuth, Zürich

Hewitt K (2002) Styles of rock avalanche depositional complex in very rugged terrain, Karakoram Himalaya, Pakistan. In: Evans SG (Ed.), Catastrophic Landslides: effects, occurrence and mechanisms, Reviews in Engineering Geology. Geological Society of America, Boulder, Colorado, 345–378

Hsü KJ (1975) Catastrophic debris streams (sturzstroms) generated by rock falls. Geological Society of America, Bulletin 86:129–140

Korup O, Strom AL, and Weidinger JT (2006) Fluvial response to large rock-slope failures – examples from the Himalayas, the Tien Shan and the New Zealand Southern Alps. Geomorphology, 78:3–21

Lee CF and Dai FC (in press) The Dadu River Landslide Dam, Sichuan, China

Leonov NN (1960) Khait Earthquake of 1949 and the geological conditions of its occurrence (in Russian). Geology and Geophysics, Geophysical Series 3:48–56

Litovchenko AF (1964) Catastrophic debris flow along the Issyk River. Meteorology and Hydrology. No 4:39–42 (in Russian)

Strom AL (1998) Giant ancient rockslides and rock avalanches in the Tien Shan Mountains, Kyrgyzstan. Landslide News 11:20–23

Strom AL, Korup O (2006) Extremely Large Rockslides and Rock Avalanches in the Tien Shan, Kyrgyzstan. Landslides, 3:125–136

Strom AL, Djumabaeva AB, Dyikanalieva JK, Ormukov ChA (2006) Snake-head rock avalanche: rock slope failure caused by horizontal seismic acceleration. "Quantitative Geology from Multiple Sources" Proc. XIth International Congress for Mathematical Geology Liège, Belgium, September 3–8, 2006

Strom A, Štěpančíková P (2008) Seismic triggering of large prehistoric rockslides: pro and con case studies. In Proc. International Conference on Management of Landslide Hazard in the Asia-Pacific Region. In press

Zolotarev GS (1990) Methodology of Engineering-Geological investigations. Moscow State University Publishers: 384p

13 Landslide Investigation and Capacity Building in the Machu Picchu – Aguas Calientes Area (IPL C101-1)

Kyoji Sassa, Hiroshi Fukuoka and Raul Carreno

Abstract Cultural Heritages and other historical buildings constructed on stable grounds often stand for many years. Stable grounds are not always stable for ever in the face of weathering of rocks, toe erosion of the slope by rivers, climate change, earthquakes, and possible human activities. It is the frontier of research in Landslide Science to evaluate the risk of slopes which have been stable for more than 500–1000 years. It is very similar to earthquake risk evaluation and the preparedness for earthquakes along active faults such as the 2008 Sichuan (Wenchuan) earthquake in China. Such long-term risk evaluation addresses social and scientific research needs. This paper briefly introduces the successful lesson learnt for landslide risk evaluation and preparedness in the Tang Dynasty (618-907) Imperial Resort Palace in Xian, China for risk evaluation and preparedness of *Precursor Stage of Landslides* before failure, and then describes the landslide risk evaluation in Inca's World Heritage Machu Picchu, Cusco, Peru.

13.1 Introduction

IPL Project "Landslide Investigation in Machu Picchu World Heritage, Cusco, Peru" was proposed by K. Sassa and approved as IPL C101-1 at the First Session of the Board of Representative of ICL held at UNESCO in 2002. It has the following subprojects

C101-1-1: Low environmental impact technologies for slope monitoring by radar interferometry: application to Machu Picchu site (Italy)

C101-1-2: Expressions of risky geomorphologic processes as well as paleogeographical evolution of the area of Machu Picchu (Czech-Slovak)

C101-1-3: Shallow geophysics and terrain stability mapping techniques applied to the Urubamba Valley, Peru: Landslide hazard evaluation (Peru-Canada)

C101-1-4: A proposal for an integrated geophysical study of the Cuzco region (Italy)

C101-1-5: UNESCO-Italian-ESA Satellite monitoring of Machu Picchu (Italy)

All of these groups presented their research at the International Workshop on Landslides in Machu Picchu Machu, Peru which was jointly organized by the International Consortium on Landslides (ICL), Instituto Nacional de Cultura (INC), Peruvian Instituto Geológico Minero y Metalúrgico (INGEMMET) on 12-13 September 2005. The major investigation results reported at the workshop

Kyoji Sassa (✉)
(ICL), Kyoto University, Japan

Hiroshi Fukuoka
Kyoto University, Japan

Raul Carreno
Grudec Ayal, Cusco

K. Sassa, P. Canuti (eds.), *Landslides – Disaster Risk Reduction*,
© Springer-Verlag Berlin Heidelberg 2009

and updated information appear as Chaps. 13, 14, 15, 16 and 17 of this book. This chapter (IPL C101-1) describes the comparison with its subprojects at the end of chapter. ICL's application for to JICA (Japan International Cooperation Agency) to mitigate landslide disasters was accepted in 2007 under the title of "Technology transfer and capacity building project strengthening landslide risk reduction through the establishment of the community task force for disaster preparedness including landslide monitoring in the Peruvian mountainous region - Model case for Machu Picchu – Aguas Calientes town in Cusco". The major target is toward capacity building to reduce landslide and debris flow disasters. Subsequently, the project title was changed to "Landslide investigation and capacity building in Machu Picchu – Aguas Calientes Area" to reflect the content of this project in 2008.

This paper presents firstly the difficulty of risk evaluation for *Precursor Stage of Landslides* before the initiation of a large displacement by introducing a lesson from Xian, China, secondly the landslide risk evaluation at Machu Picchu at the present stage referring to the investigation results of subprojects, then the conclusions obtained from investigation and experiences is stated in the end.

13.2 Lesson Learned from Landslide Hazard Assessment in Cultural Heritage in Xian, China

13.2.1 Landslides at Cultural Heritage Sites

The return period of landslides varies considerably from annually to 1000 years or more. Landslide risk is easily understood and preparations are possible by residents and the local government where landslides may occur every year such as on slopes in active volcanoes where volcanic ash falls on the slope. In slopes where weathering rates are very high, landslides will occur every tens of years. Those areas are also easy to prepare for because residents and officers in the local government in charge of disaster reduction clearly remember the previous landslide hazard event. However, where the return period of landslides is very long, on the order of 1000 years, the issue is different. It is the same order of re-activation as with Active Faults causing earthquakes such as the Kobe (Hyogoken-Nambu) earthquake 2005 in Japan and the Sichuan (Wenchuan) earthquake 2008 in China. In the case of return period of the order of hundreds or thousands of years, areas may have been unihabited and hazard event lessons were not recorded or transferred to residents or governments.

Before the Kobe earthquake in Japan, it was commonly thought that it is of no use to prepare for events which may come on the order of 1000 years. It is NOT a matter to be tackled by us, but it is a matter of future generation. This thought was quite generally applied for landslides. Almost nobody examined the landslide risk of the order of hundred or thousand years. It was thought that the landslide risk evaluation technology did not reach the level any way.

In the case of cultural heritage which have stood over many years, they were likely constructed on a stable ground. If it were not stable, they should have already been destroyed and abandoned. The existing buildings and sites recognized as cultural heritage or historical building have stood over many hundreds to thousands of years. It is one of the reasons of designating these a heritage. However, *standing over a hundred or thousand years cannot guarantee the same safety in the future*. It was proved by the Kobe earthquake and the Sichuan earthquake. Difficulty of understanding the landslide risk of landslides in cultural heritage sites exists on this point.

Landslides can be classified into four types, (1) presently moving landslides, (2) reactivated types of landslides which move almost every year or every 10 years although their movements during one activation are often limited and not fast, (3) precursor stage of landslides, where the movement level is prior to failure, but a slight slope deformation is initiated, and (4) potential landslides, that are stable at present, but the slope may experience landslides when a trigger such as an earthquake, heavy rainfall or a further decrease of stability by natural or human toe cutting of slopes or progress of further weathering may occur. The factor of safety is marginal in the slope geometry, the underground structure, shear strength of soils and rocks and the ground water condition.

Once slope deformation starts, the shear strength in the shear zone decreases due to rock breakage or softening of over-consolidated soils and promotion of physical and chemical weathering with increased ground water flow through larger cracks. The slope deformation will be accelerated and reach the failure due to a decrease of shear strength in the shear zone.

Implementation of landslide risk investigation in the precursor stage of landslides or potential landslides depends on the significance of “Object” to be protected as well as the policy. It is usual to investigate potential landslides and precursor stage of landslides for the construction of nuclear power plants. It is necessary without doubt for the security and safety of society. What should be the philosophy for slopes of cultural heritage sites? Is it necessary or not necessary? If it were not the consideration of budgets, many people wish to avoid the destruction of cultural heritage.

13.2.2 Landslide Hazard Assessment Project for Imperial Resort Palace in Xian, China

An Imperial Resort Palace called Huaqing Palace or Lishan Palace is located in Xian, China. It was constructed in the Tang Dynasty (618–907) more than 1300 years ago. It attracts more than 3 million visitors per year from China and the rest of the world. The area is tectonically active. Large faults (Baouji-Sianyan-Tongguan fault system) are located in the area and great earthquakes including the Huaxain earthquake Mw 8 in 1556 is known (Geology and Mineral Resources of Shaanxi Province 1990, Xi’an Seismological Bureau. 1991). Fig. 13.1 (Top) shows the frontal view of the Lishan slope on the back side of Palace, and the photo (bottom) shows the view from the slope to the Palace and the central area of Lintong town in Xian. The slope of Lishan is a fault scarp, and the hot spring in this area is due to the ground water coming from deep layers through the fault. There is no volcano in this area. Therefore, this imperial resort palace was constructed by presumably selecting the site which could use the hot spring coming out through the fault, as well as enjoy the good scenery of the fault scarp (triangular facet) cutting the mountain ridge. The central pond in Fig. 13.1 is called as the Huaqing pond and buildings on the right side of the pond are hot spring baths for the Emperor and Lady Yang-Que-Fe and also officials working in the Palace.

Sassa and other 18 Japanese landslide researchers investigated the slope behind the Huaqing Palace together with 50 Chinese landslide researchers at the China-Japan Joint Field Workshop on Landslides in October 1987. Loess blocks on this slope already failed and other parts show phenomena of slope deformation at least on the surface. Opinions of researchers were diverse regarding the depth and the area of landslides (shallow and small soil creep to deep and large slides) and the present risk of this slope. The surface soil of this slope is mainly loess deposits; the bedrock is formed of Precambrian gneiss, which is seen outcropping. One individual believed that the hard Precambrian gneiss rock mass is very unlikely to be subjected to landslides, whereas another thought that this slope is the cliff of a large active fault and the rock mass should be sheared and fractured which may move on this steep slope of over 35 degrees. But the main opinions in both countries supported the former. The fact that this rock slope was stable since the Tang Dynasty (618–907), and although strong earthquakes repeatedly attacked this area (Lin 1997; Xi’an Seismological Bureau 1991) supported this opinion. However, participatns agreed with the existence of surface deformation and the necessity of further investigation. After some efforts, we obtained budgets for the Japan-China Joint Research on the Assessment of Landslide Hazards in Lishan, Xi’an since 1991 as a part of special project of the Ministry of Education, Sports, Culture, Science and Technology (MEXT) Japan contributing to the International Decade for Natural Disaster Reduction (IDNDR) and conducted for 8 years (3 years + 5 years).

13.2.3 Main Results of the Project

China and Japan investigated the slope by numerous drillings, two investigation tunnels for direct

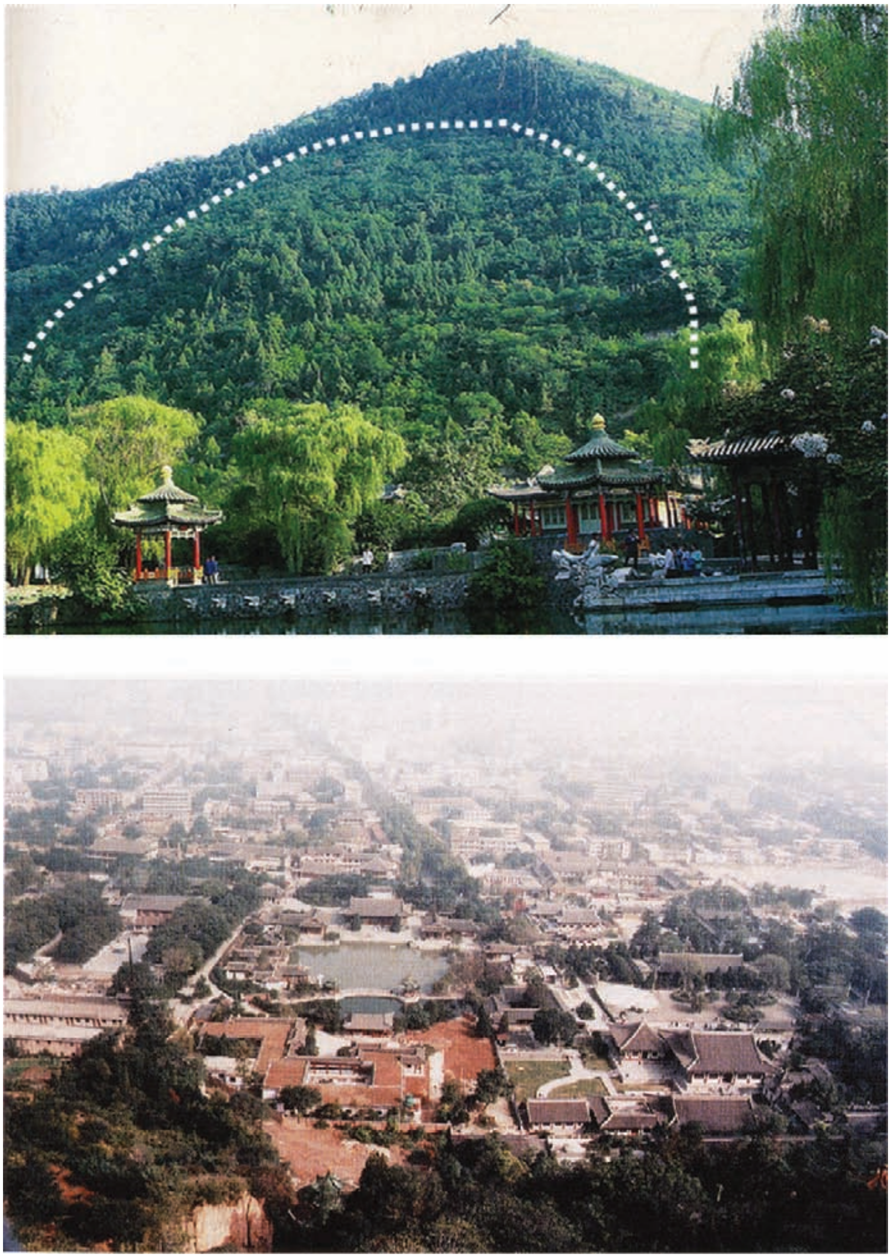

Fig. 13.1 View of Lishan slope (*Top*) and view from Lishan slope to the imperial resort palace "Huaqing Place" of Tang Dynasty and the centre of Lintong area in Xian, China

observation, GPS, Total Station, inclinometers, and geotechnical testing especially an undrained loading ring shear test, triaxial tests, estimation of travel distance, and others for 8 years. Initially most people and landslide experts believed that the slope must be stable because there is no trace of previous landslides since the Tang Dynasty in this slope and materials are Precambrian gneiss hard rock. Some people working in the Lishan Palace opposed the installation of monitoring equipment inside the Palace believing this may affect visitors. However, an understanding was soon obtained that preparedness is better than losing the entire Palace.

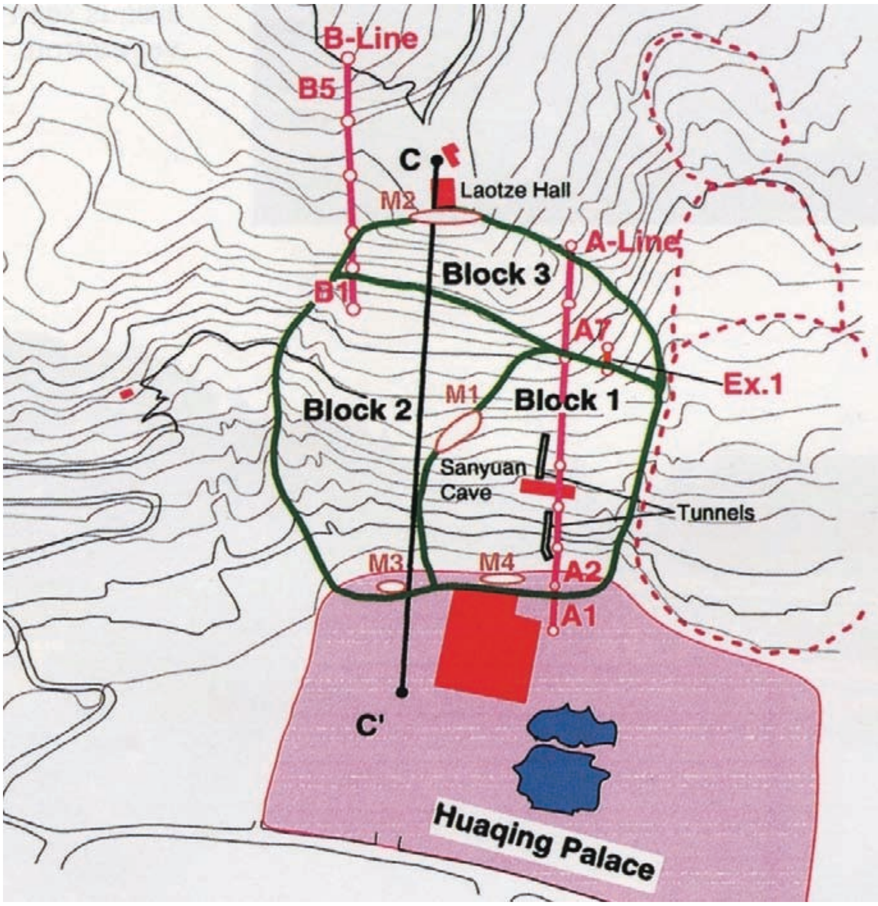

Fig. 13.2 Landslide zoning of the Lishan slope The *green line* shows the border of estimated precursor stage of landslide blocks Two *red lines* show a series of long-span extensometers (A1-A8) and (B1-B5)

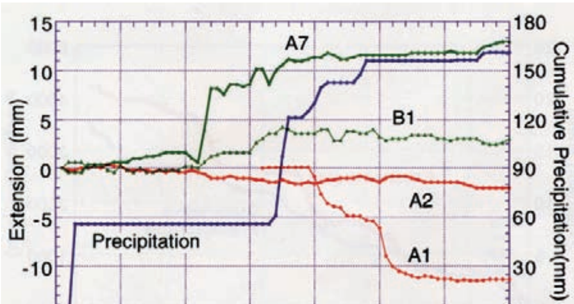

Fig. 13.3 The key record of landside movement as a block which was monitored in 1996 after the initiation of Japan-China Joint project in 1900 as a IDNDR (International Decade for Natural Disaster Reduction) special project. The record convinced the initiation of expensive landslide remedial measure by the Government of China, the Shaanxi Provincial Government and the Xian Municipal government

The key result that convinced the policy maker is shown in Figs. 13.2 and 13.3. Figure 13.2 is precursor stage of landslide blocks which were made based on careful field investigation and monitoring by K. Sassa (Sassa et al. 1997). Namely 3 blocks are suspected as precursor stages of landslides from careful investigation. To detect any of precursor stage of slope deformation, two long-span extensometer lines (A-line and B-line) were established. Figure 13.3 shows monitoring results in 1996 after 5 years of monitoring since the initiation of the investigation. Around 60 mm of precipitation was recorded, 3 weeks later A-7 extensometer recorded an extension of about 10 mm. Then another ∼100 mm rainfall fell on this area. The A-1 extensometer recorded about 10 mm of compression. We interpret this as evidence that Block No.1 moved firstly in the upper part of block, the landslide body was compressed for a short period, and during the second rainfall, the compression was released toward the Huaqing Palace. As a result, Block No.1 moved about 10 mm as a block within 2 months.

From the location of the 3 blocks, it is estimated that Block No. 2 may also move when Block No.1 moves by losing support along its border. Careful reading of the monitoring results of Fig. 13.3, extensometer B1 started to move at the almost same time, though the displacement is approximately 1/3 as much, namely 4 mm. This figure helps visualize the instability and marginal stability of this slope even in the order of a few to 12 mm of movement.

The movement is still in the precursor stage of slope deformation. However, the direct observation of potential sliding surface within the investigation tunnels provided the information on the shear zone development. The result was reported in the International Symposium on Landslide Hazard Assessment held in Xian on 13–16 July 1997 (Sassa et al. 1997), and later the study was published in 2001 (Sassa et al. 2001). The honorary chairperson was Mr. Qiyuan An, Secretary-General of the Communist Party of the Shaanxi Province understood the significance of the investigation and monitoring results (he is a seismologist), and took a key role in the initiation of landslide prevention works by investing three million U.S. dollars with funds from the municipal, provincial and national governments of China and started remedial works within one year. It is the first case in the world as far as we know of the initiation of extensive landslide remedial measures at a Cultural Heritage site for the mitigation of landslide risk during the *Precursor stage of a Landslide*.

This symposium and joint research result was well evaluated by participants from UNESCO and the IGCP (International Geoscience Programme) and others. The technology to mitigate precursor stage of landslide can be applied to other cultural heritage sites or other critically important sites in other countries. The IGCP-425 project "Landslide hazard assessment and mitigation for cultural heritage sites and other locations of high societal value" was initiated (Leaders: Sassa, Canuti and Carreno) in 1998. It acted as a base for the foundation of the International Consortium on Landslides.

13.3 Development of IPL Project on Machu Picchu

IGCP-425 project supported 31 subprojects. One of subprojects was No.15 "Protection of Inca Cultural Heritage on a Landslide Zone at Cusco, Peru" (leader: Raul Carreno). He introduced the problem of landslides at Machu Picchu. He investigated landslide activities in an area including the Hiram Bingham road. The landslides along the Hiram Bingham Road area (Block No.1 in Fig. 13.8 and 13.10) were reported earlier (Carreno and Bonnard 1997; Kalafatovich 1963).

The archaeological site (Inca's citadel area) was not included in the landslide area. But it is on an adjacent slope. Sassa wished to investigate the possibility to expand the landslide area to the citadel area. Subsequently, Sassa, Fukuoka, and Shuzui investigated the area with the support of the INC (Instituto Nacional de Cultura) of Peru in 2000. Then, they noticed that possibly Inca's citadel was constructed on the relatively flat area of the mountain ridge which had been formed a previous landslide. There was a possibility of another similar type of landslide occurring in the future. Namely, the slope may be either a precursor stage of a landslide in which case a slight slope deformation is already on-going, or there is a potential landslide which is completely stable but the safety factor is marginal. The investigation and initial monitoring of extensometers was conducted in 2001. Based on the monitoring results showing landslide movement there, IPL project C101-1 "Landslide Investigation in Machu Picchu World Heritage, Cusco, Peru (leader: K. Sassa) was proposed and approved at the First session of the ICL Board of Representatives held at UNESCO in 2002. Some colleagues applied subprojects by raising funds from their countries and also UNESCO. A total of 5 subprojects of C101-1 were approved. Within those subprojects, contents of 4 subprojects in addition to our activities are introduced in the following Chapts. of 14, 15, 16, and 17.

In 2004 a debris flow impacted the town of Aguas Calientes (also called Machu Picchu Pueblo) and 11 residents were killed. The Machu Picchu citadel is very important to the society of Peru and also in the rest of the world. Due to the limitation of the flat area at Machu Picchu, most people working for

Machu Picchu and visitors live or stay in the Aguas-Calientes area which is frequently affected by debris flows. Then, Sassa and Fukuoka proposed a project "Technology transfer and capacity building project strengthening landslide risk reduction through the establishment of the community task force for disaster preparedness including landslide monitoring in the Peruvian mountainous region – Model case for Machu Picchu – Aguas Calientes town in Cusco" to the Japan International Cooperation Agency (JICA) in 2005 and in 2006. The project proposal was accepted by JICA in 2007. As a result, the preliminary investigation team of JICA visited Peru and exchanged two agreements, one between the Instituto Nacional de Defensa Civil of the Government of Peru (INDECI, represented by its Chief, Mr. Luis F. Palomino) and the ICL, another between the Municipality of Machu Picchu (represented by its Mayer Mr. Edgar Miranda Quinones) and the ICL in order to implement this project for three years. This is now in preparation.

Figure 13.4 presents an air photo image of the targeted area including the Machu Picchu citadel, the access road (Hiram Bingham road) area, and Aguas Calientes town where two debris flow torrents pass through. Figure 13.5 shows the 2004 debris flow disaster. Another debris flow impacted this town in 2007, the debris flow height was fortunately just below the flood level and no person was killed.

13.4 Landslides in Machu Picchu

Figure 13.6 shows the general view of the Machu Picchu citadel. One can see the steep and rocky Huayna Picchu mountain peak showing the geological and geomorphologic circumstance of this area. In front of this mountain, a town is constructed; the central flat square called the *Plaza* and many buildings on both side of the mountain ridge. Machu Picchu was selected one of the New Seven Wonders of the World in 2007. One reason of the selection as one of New Seven Wonders might come from the creation of construction site of *Plaza and houses* on the mountain ridge. When Sassa et al visited there had a glance of panoramic view of them in 2000, it was a wonder for themselves.

However, interpreting the air photo (Fig. 13.7) and visual observation from chartered helicopters (Fig. 13.9) as well as the view from the opposite mountain Mt. Putukusi (Fig. 13.8), Sassa noticed that the relatively flat area on the top of mountain ridge was probably formed by previous landslides. Figure 13.7 photo shows that the citadel area (red

Fig. 13.4 The targeted area of Machu Pacchu Picchu project. *Left-Bottom*: Archaeological site (Machu Picchu citadel) *Center*: Reactivated landslide area on which the access switchback road is constructed. *Right-Top*: Aguas Calientes town which are threatened by two debris flow torrent

Fig. 13.5 A Debris flow along the *right side* torrent (Alcamayo) in Fig. 13.4 killed 11 residents in 2004. Railway was broken and President Toledo was blocked. Another debris flow along the left side torrent (Aguas Calientes) attacked the town again in 2007

circle) was scraped toward both sides of mountain ridge. It could be caused by river erosion onto the slopes in the part of curvature. Figure 13.8 presents a very flat plane (marked as Block No. 2) upon which the citadel was constructed. This plane may be a shear band (fault) which could be the sliding

Fig. 13.6 Location and view of Machu Picchu Inca citadel on the mountain ridge. The central square called as Plaza was possibly filled in cracks by Inca people to create a flat square. The Ground Penetration Radar visualized the profile (Chap. 7 Fig. 7.7 of this book)

Fig. 13.7 Airphoto of Machu Picchu (Geographical Institute, Peru) *Red circle* shows the location of Machu Picchu citadel. The Urubamba river is flowing in a Zigzag along faults/shear bands. The river erosion seemed to have attacked the toe of slopes and caused landslides (both sides of citadel)

surface because the inclination is almost parallel to the slope. The left side of Fig. 13.8 is Block No.1 of the Hiram Bingham Road which is already known as a reactivated type of landslide (Carreno and Bonnard 1997; Kalafatovich 1963). The difference is very clear in this photo. Block No. 1 was already

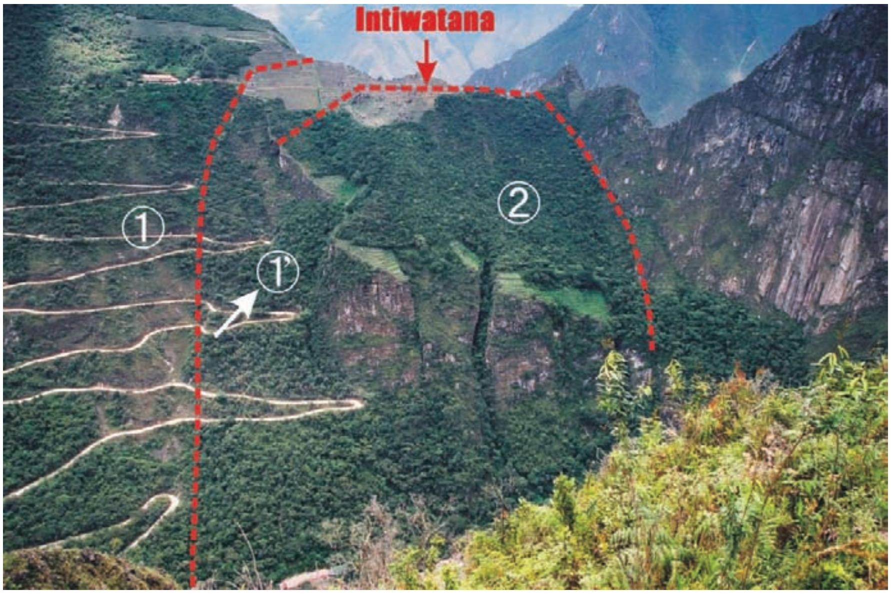

Fig. 13.8 Photo of Machu Picchu slope. Reactivated type of landslide (Block No.1) on which access road was constructed. A hard rock mass (Block No.2) which seemed to fail to the river and to the Block No.2. The flat ground surface was possibly a fault/shear band, the rock mass above this face slid in the past. Namely the present ground surface was likely the sliding surface of previous landslide.The vertical red dashed line is a border of Block 1 and the initial Block 2. The border of Block 2 probably failed to Block 1, then the Block 1 (reactivated landslide area) extended. The extended part of Block 1 is shown as **(1')** in the figure

affected by landslides, Block No.2 was not affected by landslides at present though smaller landslides seemed to fail from Block No. 2 onto Block No.1 and also down to the Urubamba river (to the front in this figure) along the border.

Figure 13.9 presents three photos taken from a helicopter (a) and from the ground (b and c). As indicated by the red line and arrow in (a), probably the previous landslide slid along the present ground surface. Usually such shear bands (faults) develop parallel as a system. Photo Fig. 13.9 (b) shows two parallel shear bands formed within the intact hard rock mass. Arrow “A” and Yellow dashed line in Fig. 13.9 (a) may be the shear band. Crushed rocks in this shear band enabled growth of vegetation because of soil and ground water as found in (b) and (c). Close-up photo of the point “A” indicates the rock mass was already sheared and displaced, namely the direction of previous landslide as show in red arrow in Fig. 13.9 (a). Integrating this information and consideration of available data, Fig. 13.10 was made which presents the landslide blocks in the north slope of Machu Picchu.

1) The Urubamba River flows from the left to right while undercutting the Machu Picchu slope. The river erosion was likely one of major causes of landslides on this slope.
2) Previously all slopes of Number 1–3 probably slid down. Block No. 1 is currently an active landslide as seen in Fig. 13.8, and it is one step lower compared to Block No. 2 and No. 3 (refer to cross sections in Figs. 13.11 and 13.12). Therefore, Block No. 2 slid for a second time. Because of the low elevation of Block 1, parts of Block 3 and Block 2 moved toward Block 1 which is shown as Block (1’). Currently small landslides (a), (b), (c) occurred along the border of Block No. 2. Deep landslide deposits exist as shown in Yellow zone along the river. (It is the same with Fig. 17.5 of Chap. 17, Casagli et al. 2008)
3) Green colored areas of Block No. 3 and Block No. 2 are those which are stable or almost stable zones at present.
4) Red colored areas of Block No. 1 are active areas, the brown colored part within Block No. 2 is an area which might be active.
5) Further examination and interpretation of landslide processes are given in the next section using two longitudinal sections and cross sections of A1-A2-A3, B1-B2-B3, and C1-C2-C3 shown in Fig. 13.10.

13.5 Possible Landslide Development Process in Machu Picchu

Figure 13.11 shows the interpretation of the landslide development process on the Maachu Picchu slope (Sassa et al. 2001, 2002 and 2005)

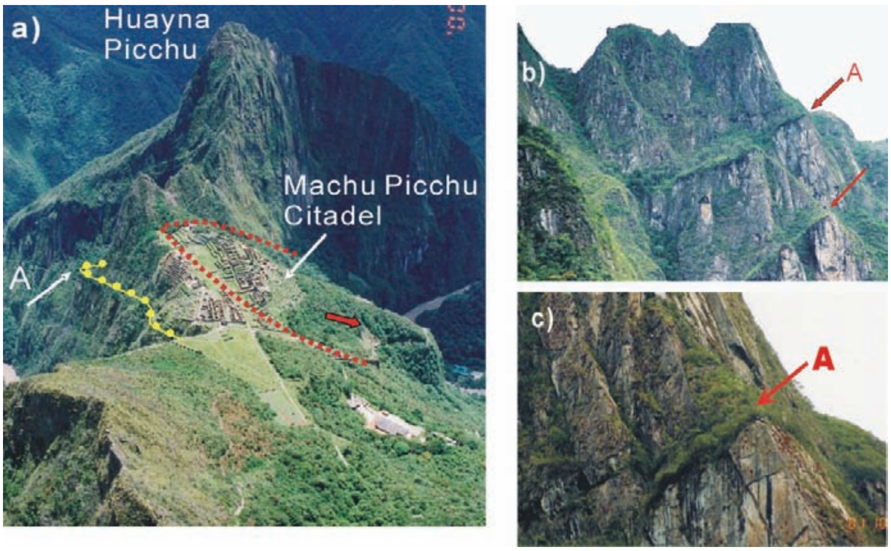

Fig. 13.9 Airphoto by chartered helicopter (Sassa 2000) and the view of Point A from the ground. The present ground surface was likely a shear band and the shear band shown as A is probably parallel to the ground surface

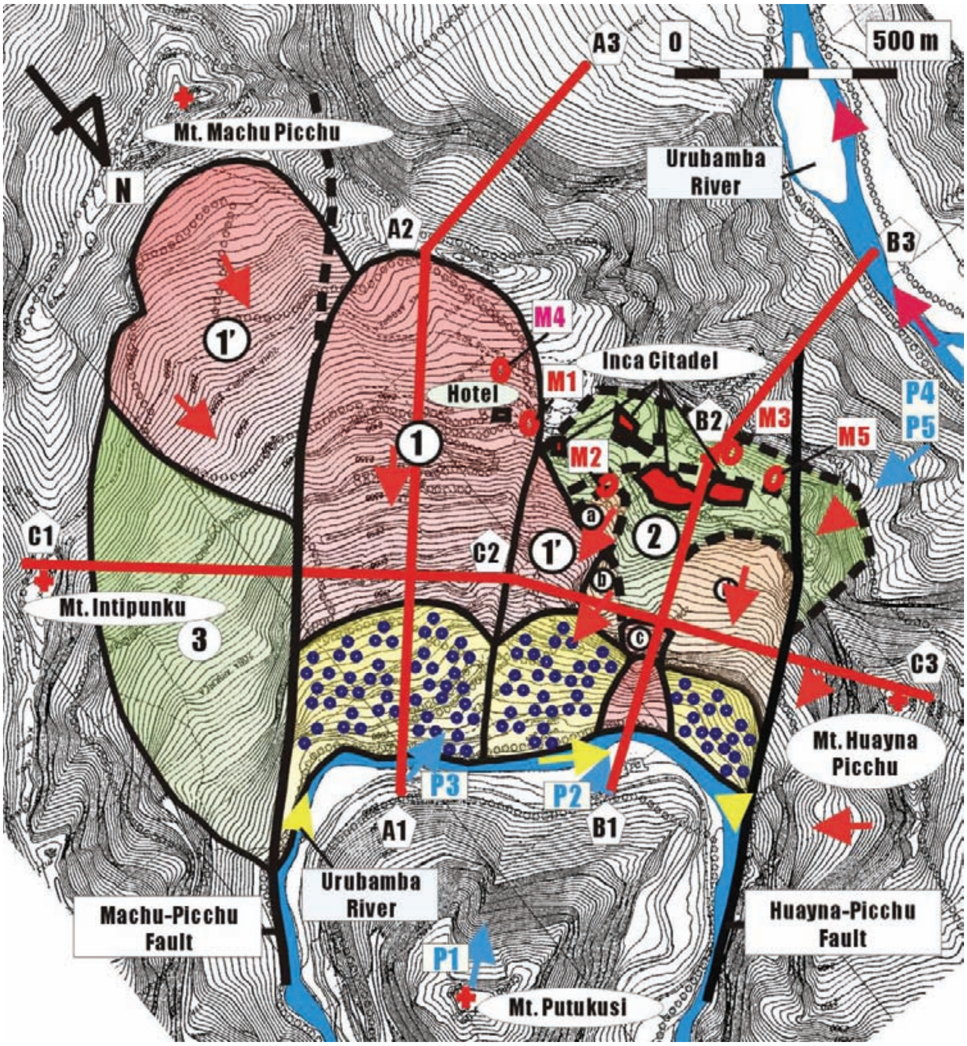

Fig. 13.10 Landslide Blocks of Machu Picchu slope (front side) The water flow of Urubamba river have attacked the Machu Picchu slope side because of its curved flow path. *Red color area* is reactivated landslides which are currently active. Block No.1 seemed to have pushed out the Urubamba river

The stages of landslide evolution were illustrated for Block 1 and Block 2 in a schematic form. A long time ago, it is probable that retrogressive landslides occurred on the front slope of Machu Picchu. After the whole landslide debris moved out to the Urubamba River, the downward erosion proceeded farther. The level of the Urubamba River shifted about one hundred meters downward almost to the present level. Three slopes of Block 1, 2, 3 showed the difference in the landslide evolution speed. The slope of Block 1 had been most heavily subjected to toe erosion of the Urubamba River as easily understood by the curved path of the river and flow direction in Fig. 13.10. Firstly, the slope started to slide as illustrated in the intermediate period (Stage 2) of Block 1. The initial landslide retrogressively expanded to the upper slope and toward the side slopes, then, the present situation of Stage 3, where active landslide debris covers the slope, was formed. One can see in Fig. 13.10 that the Urubamba River was pushed forward by the landslide

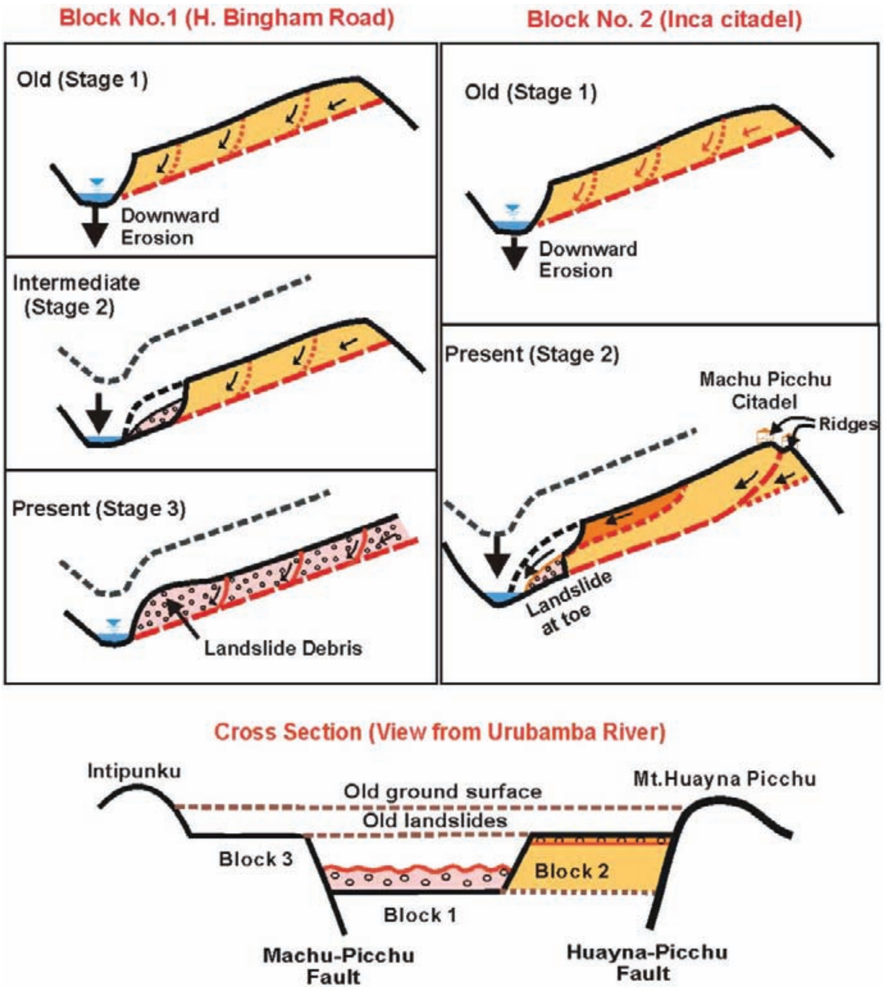

Fig. 13.11 Possible development process of landslides in Machu Picchu slope

debris provided by Block 1. So this landslide debris has probably worked for the protection of toe erosion of Block 2. Because of this protection, the evolution of Block 2 was much delayed and it is still in the Stage 2. The most delayed block in slope evolution is Block 3. After previous landslide debris moved out, no major landslides occurred because there is almost no river erosion as imagined from Fig. 13.10. The landslide evolution in the cross section is illustrated in the bottom of Fig. 13.11. Only Block 1 was subjected to major landslides at the present level of Urubamba River and located in the lower elevation which continues to the around present level of the river bed. And Block 2 is now following the process of Block 1. Figure 13.12 (Top) shows the longitudinal section along A1-A2-A3 in Block 1.The depth of landslides is not known, but the whole slope from the mountain ridge to the river is affected by active landslides and covered by landslide debris. Figure 13.12 (Middle) presents the longitudinal section along B1-B2-B3 in Block 2. The section B1-B2 shows the active landslide at the toe (c in Fig. 13.10), and others are still at the precursor stage. The potential sliding surface will be a shear band found in Fig. 13.9. If we consider that the potential sliding surface is located at the level as shown in Fig. 13.12 (Middle), the depth of landslide is around 100–150 m.

Figure 13.12 (Bottom) presents the cross section along C1-C2-C3. The potential sliding surface of Block 2 may be the extension of the present sliding surface of Block 1. In this figure, the sliding surfaces

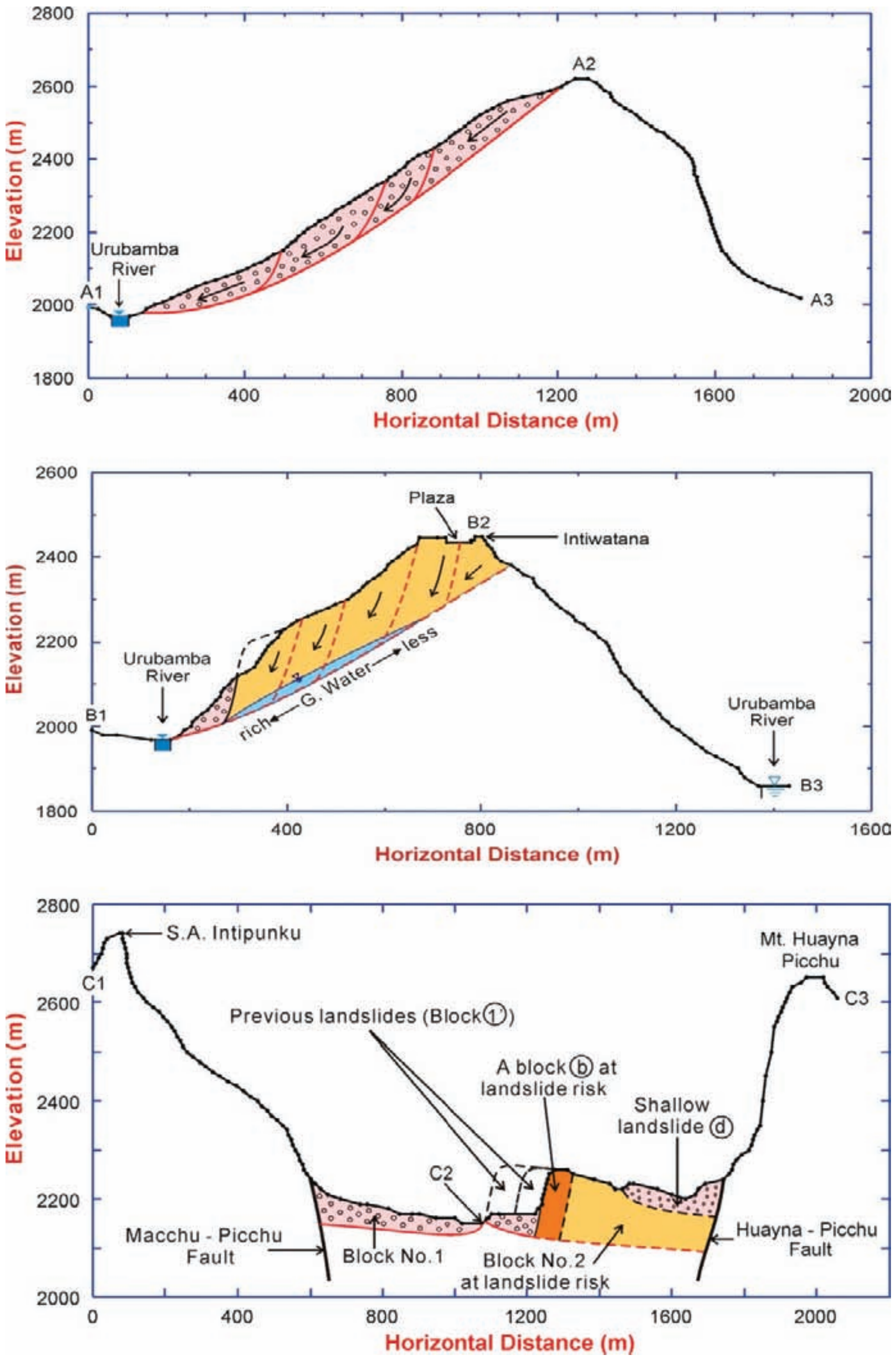

Fig. 13.12 Present state of landslides along Sections A1-A3 (*Top*), B1-B3 (*Middle*) and C1-C3

of real landslides are drawn by a solid line although the depth is not yet confirmed. The sliding surfaces of potential or precursor stage of landslides are drawn by a dot line.

There is a *Question* for the reason why the sliding surface goes up to the Plaza in Block 2 (Figs. 13.6, 13.9 and 13.12), which may split the Plaza of Inca Citadel. The reason is interpreted below from the data obtained up to now: The ground water will increase in the lower part of the slope collecting ground water from the upper slope because the shear band probably has a low permeability and dips parallel with the front slope. Ground water should increase in the lower slope because of rain fall infiltration has accumulated (illustrated in the middle figure of Fig. 13.12). Therefore, probably the ground water level and pore-water pressure is greater in the lower part of Block 2, and almost no ground water near the top of slope because of a very limited collection of rainwater. In this case, the top of Block 2 (area of Plaza and Intiwatana) is rather stable, so tensile stress should act between the lower instable part and the upper stable part. Accordingly tension cracks may be formed. The concavity in the Plaza likely corresponds to the tension crack, though the concavity was filled possibly by the Inca's to create flatter ground suitable for their living, which is not clearly visible on the ground surface at present. The cracks might have been filled by Inca's people and a flat square was formed. The underground structure detected by Ground Penetration Radar Survey (Fig. 16.6 of Chap. 16, Best et al. 2008) supports this estimate.

13.6 Landslide Monitoring in Machu Picchu

The Japanese team installed short span extensometers (2 sets of self-recording extensometers and 10 sets of manual reading extensometers) in 2000 and monitored them in 2000–2001. The monitoring results were reported in the UNESCO-IGCP Symposium "Landslide risk mitigation and protection of cultural and natural Heritage" held in January 2001 (Sassa et al. 2001). Some extensometer records showed about 5–15 mm movement during one month from 12 November to 17 December 2000. It was during the rainy season. It does not mean 10 cm/year, though some participants mentioned the possibility. Movements recorded in those extensometers did not mean the movement of the deep sheeted landslide in the citadel. The report was firstly introduced by *Yomiuri Newspaper* in Japan, then by "*New Scientists*" in UK, *Civil Engineering* by ASCE in USA and others. Articles in *Yomiuri Newspaper*and in *Civil Engineering* were published after the interview and review of the articles and correction of misunderstanding by Sassa. However, The New Scientist article was written only based on a telephone interview and was not reviewed by Sassa. The article by the "*New Scientists*" caused a sensation aournd the world. The number of visitors to Machu Picchu decreased very much, and the number of busses to the citadel was reduced. The number of guests to the President Toledo inaugural ceremony held in Machu Picchu citadel was also reduced. Therefore, UNESCO thought there was a necessity to inform a real state of investigation and published *"Rumbles at Machu Picchu"*article in "*World Heritage Review*," No. 20, May 2001 (Bandarin 2001) in consultation with Sassa. Because of the large social influence, the monitoring was stopped from the end of 2001 to 2005. Sassa was requested to summarize in an article on Machu Picchu published by the UNESCO Education Sector (Sassa 2005).

The Japanese team obtained permission to install long-span extensometers, GPS and the Total Station at Machu Picchu including Plaza area from the Government of Peru in 2004. Then, we installed 4 sets of long-span extensometers, 3 sets of static GPS receivers, and one total station with 3 prism mirror targets in September, November of 2004 and in March of 2005. Figure 13.13 is the plan map of the location of each instrument of extensometers, GPS, Total Station. Extensometer (04 E1) was installed from the front of the Cafeteria of the Machu Picchu Sanctuary hotel down slope. Top of Fig. 13.14 showed the upper pole of extensometer 04E1 (left) and the lower pole of extensometer (right) and close-up view of the top of the lower pole (left-middle). The super invar wire (1.0 mm in diameter) which has a metal of least temperature effect was connected between two poles. In this case, the upper pole fixed the super invar wire, the lower pole has a pulley on the top. The super invar wire pass through this pulley and goes down due to the weight. The extension occurs between two poles, the weight goes up, while the compression occurs between two poles, the weight goes down. This movement is recorded onto the recording paper by mechanically enlarged 5–10 times (option) and also electronically recorded in the extensometer installed in the protection box. GPS was also installed at the top of the pole. The monitored record from 1 April 2005 to 1 October 2006 is presented in Fig. 13.14 (Bottom). This location is inside the Landslide Block No.1.

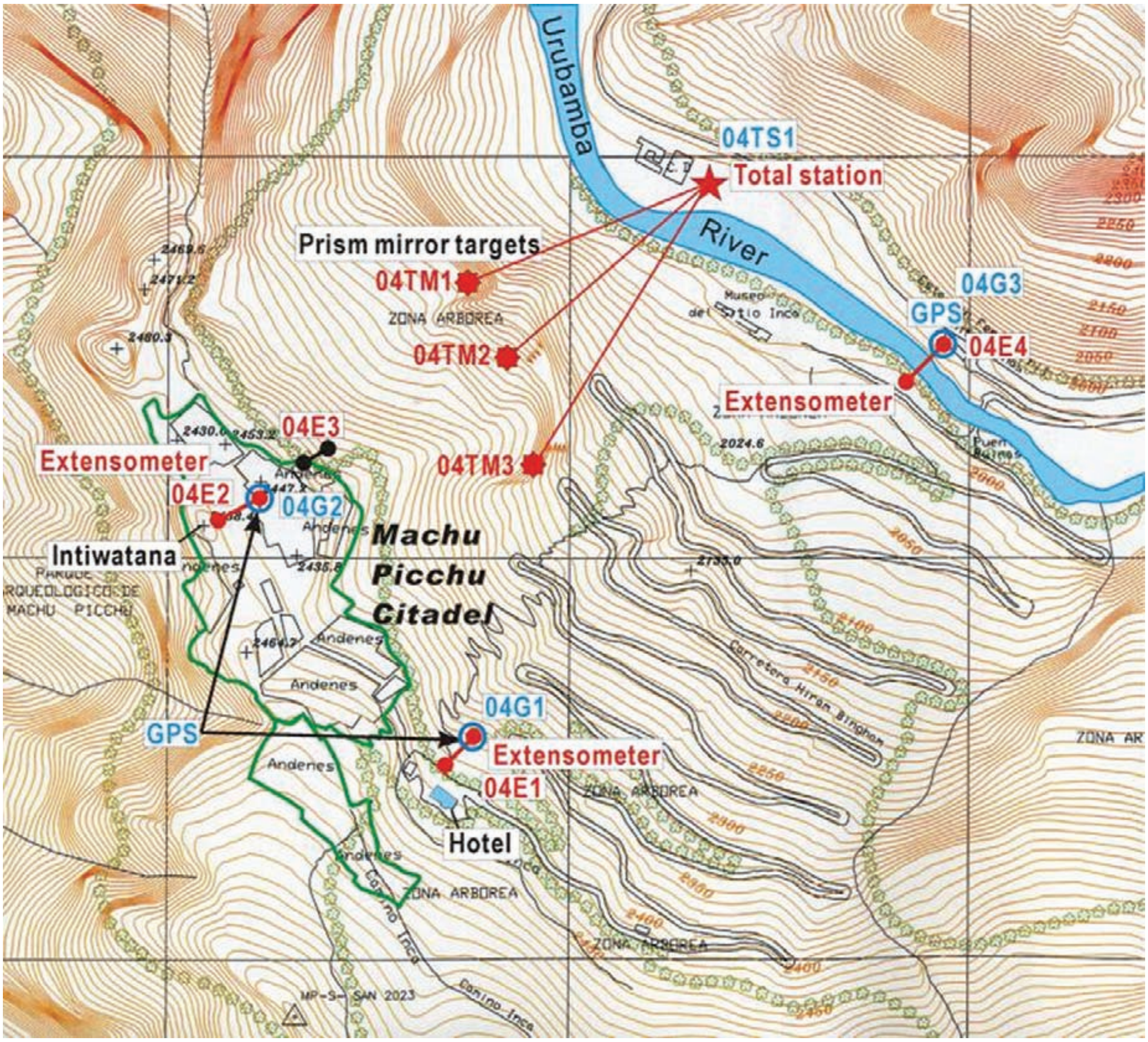

Fig. 13.13 Location of extensometers, GPS and Total Station

If the lower pole moves down while the upper pole is stable, an extension is recorded. When the upper pole moves downward while the lower pole is stable, compression is recorded. The recorded movement shows that extension of 11 mm occurred though a slight compression appeared in December 2005 and August 2006.

Extensometer 04E2 was installed crossing the Plaza from a big rock below Intiwatana to a stone wall of the Inca's citadel as shown in Fig. 13.15. Super-invar wire position of 04E2 is shown as a red line in Fig. 13.15 (Top), although the actual wire is very fine and not visible to tourists. The monitoring record from April 2005 to October 2006 is shown in Fig. 13.15 (Bottom). Compression appeared for the initial 4 months, thereafter almost no motion was recorded. The compression was interpreted as two possibilities: (1) the right end of extensometer is located possibly on the embankment (rock was not visible), and slope moved toward the Plaza. In this case compression should appear, (2) The span of extensometer is very long. A slight curvature of super invar wire might have occurred during installation. It could gradually be

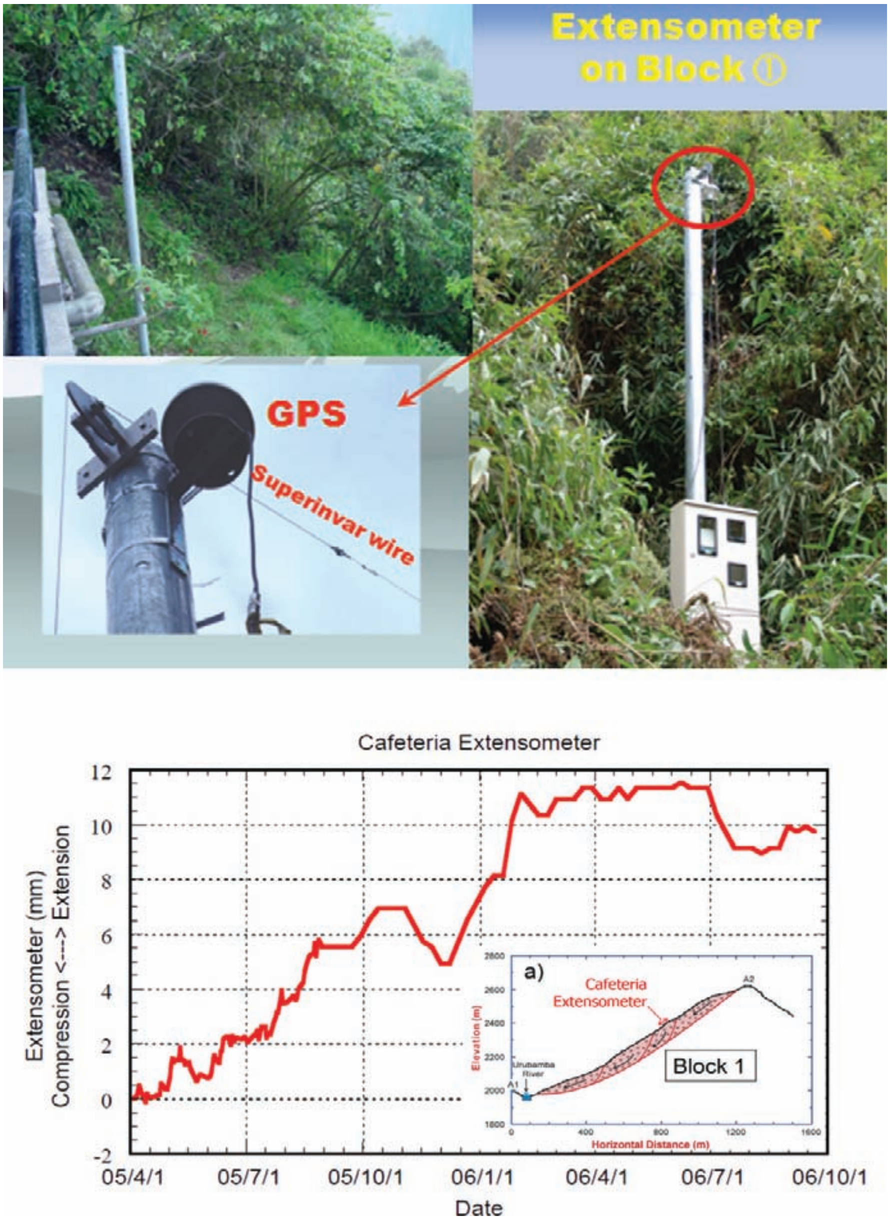

Fig. 13.14 Photo and the monitored record of extensomter (04E2) installed in front of the Cafeteria of Hotel. Super invar wire (1.0 mm diameter) is not visible, so the location is drawn in *dark-red*

extended for a few initial months. Monitoring period is too short to conclude. However, probably the possibility of (2) is high. If so, the distance between two poles crossing the *Plaza* did not change, it was stable for this one and half year period.

Extensometer 04E3 is located beneath the citadel in Block 2 (Fig. 13.13). The upper end of super invar wire was fixed to the outcropped rock in the lower end of citadel, and the lower pole was installed inside forests covering the slope. The monitoring record shown in Fig. 13.16 shows accumulated extension up to 13 mm. Namely the lower pole inside the forests was moving continually downward. Monitoring period for 1.5 years is short. Unfortunately we could not monitor after 1 October 2006. However, from the monitored records, the Block No.1 is active, and also the forest area below the citadel is active, whereas the Plaza area is not active for this monitored period.

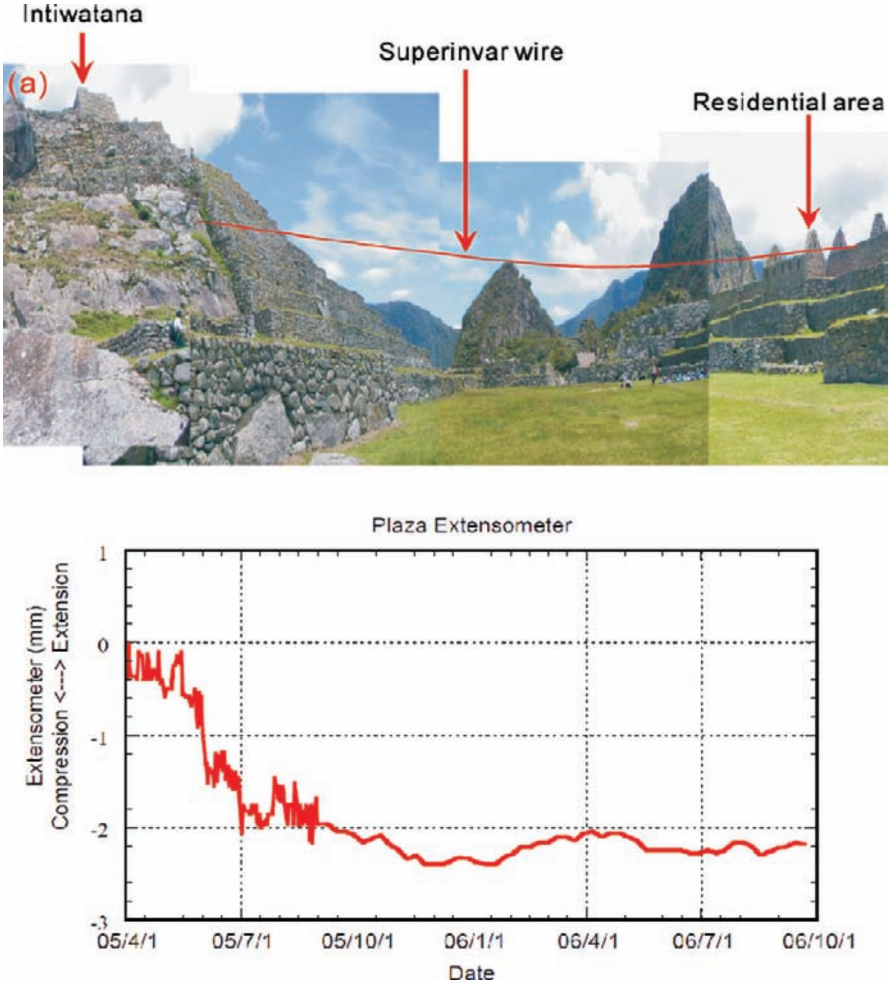

Fig. 13.15 Photo and the monitored record of extensomter (04E2) installed crossing the Plaza

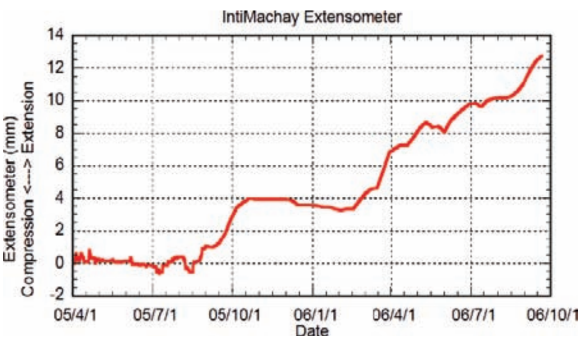

Fig. 13.16 Monitored record of extensometer (04E3) installed in IntiMachay below the Plaza

13.6.1 Comparison with Subprojects of C101-1

The following Chaps. 14, 15, 16 and 17 present the results of subprojects of C101-1, namely C101-1-1 (Chap. 14) , C101-1-2 (Chap. 15), C101-1-3 (Chap. 16), C101-1-5 (Chap. 17). The focus and the methodology was different for each team. C101-1-1 subproject team by Canuti, Margottini et al. monitored slope deformation by GPS, Interferometric Synthetic Aperture Radar (InSAR), and Ground based Radar monitoring. InSAR monitoring detected 5 cm relative movement for one year between the hotel and a point in the downward slope of Citadel in Block 2 (location is shown in Fig. 14.6 of Chap. 14, Canuti et al. 2008). But the reliability of the monitoring is not sufficient for a conclusion. GPS monitoring was for one year (not continual monitoring. Apparatus was brought for each monitoring period to Machu Picchu) detected 1.0 and 1.2 mm movement in two points in the downward slope of the citadel in Block No. 2 (location is shown in Fig. 14.7 of Chap. 14). No movement was monitored within the citadel area.

C101-1-2 Subprojects detected continual deformation of open fissures by 4–5 mm for 3 years in Temple at the citadel (Fig. 15.2 of Chap. 15, Vlimek et al. 2008). They also measured the distance crossing the Plaza using a portable extensometric type of tool. Though around 10 mm relative displacement is measured, it is not clear. C101-1-3 group conducted a geophysical survey in Block 1 and Block 2. Several ground water flow paths are defined and no subsurface failure planes were detected. The location of the greatest ground water path corresponds to the border of Block No. 1 and Block No. 2 (red line in Fig. 13.8). This group presented the underground structure of the *Plaza*. This result gave supports to the estimation that the flat surface of the central square was possibly constructed by filling debris into cracks as already mentioned. C101-1-5 group concentrated on investigating shallow landslides and debris flows using satellite Image and Field observation. They presented many images of debris flows, rock falls, and shallow landslides. The good aerial view of Block No.1 was presented in Fig. 17.4 of Chap. 17 (Casagli et al 2008). Head and side scarps of landslides and the Hiram Bingham road within the landslide mass is well visualized.

13.7 Conclusion

(1) Block No.1 (Hiram Bingham road area) is a reactivated landslide which is in the marginal state of stability. Usually this type of landslide does not move rapidly. However, the 2004 Niigata-ken Chuetsu earthquake induced landslide gave lessons that a rapid landslide occurred within reactivated landslide area (Sassa et al. 2005). The sliding surface was formed in the sand layer whereas the reactivated slow landslide was sliding in a silt layer. Drilling data from the ground of Block No. 1 are not available. Therefore, it is difficult to evaluate instability during an earthquake.

(2) Block No. 2 is possibly a precursor stage of a landslide or potential landslide. The border of Block 2 to Block No. 1 and to the Urubamba River is unstable due to its steepness. Movements were monitored in the forest area below the citadel (shown in Fig. 13.16). Some movements were detected by other monitoring methods by IPL C101-1-1 group in the forest area.

(3) The Citadel site was constructed on hard rock, and no clear movement was monitored by all teams for one or a few years. Because of this stable condition, the citadel has stood at present location since its construction over 500 years ago.

(4) Preparedness for disasters caused by earthquakes in active faults which are activated on the order of 1000 years is currently an important societal issue for many countries including Japan. The preparedness for landslides in the long return period would be necessary for very important asset for the society and human. The lesson learned from the Tang Dynasty Imperial Resort Palace in Xian, China is that the detailed field investigation and monitoring of landslides could provide a convincing evidence to justify the investment of very expensive remedial measures before the initiation of landslide movement, namely in the stage of precursor stage of landslides.

(5) Major causes of landslides in Machu Picchu are (1) rainfall penetration into the ground during the rainy season, (2) river erosion in the toe of the slope, (3) existence of shear zones (faults) parallel to slope within the rock mass where the sliding surface can be formed and the steepness of slopes as predisposed factors.

The existence of Block No. 1 gave objective evidence of potential instability in this area though drilling data are not available at present. However, apparently this is not enough to convince policy makers. It is a time that even “Stop Global Warming” is now on the political stage based on the extensive scientific research. If the landslide risk will be confirmed by scientific study spending considerable time and budgets, humans may prepare to reduce landslide causes in the area, namely to protect one of the Seven Wonders of the World and transfer it to the next generation. If no landslide risk will be confirmed for

Fig. 13.17 Photos at the ceremony exchanging the cooperation agreement with Mayor Machu Picchu and the welcome march by children in Machu Picchu in 16 August 2007

another 1000 years, we may leave it to our descendent.

(6) The IPL project on Machu Picchu presented considerable scientific information on this area from various aspects. However, drilling data are not available, no inclinometer and ground water monitoring using drill hole is available either, and no long-continual and wide-covered slope deformation monitoring is available.

The World Heritage Committee of UNESCO (2006) adopted the decision of 30COM 7B.35 - State of Conservation (Historic Sanctuary of Machu Picchu) introduced the International Workshop on Landslides organized in 2005 and stated as below.

> 7. Take note of the results of the International Workshop on Landslides at the Historical Sanctuary of Machu Picchu, in September 2005, which indicate reduced risk of landslides at the citadel, and requests that investigations continue and that training of local professionals be ensured in order to undertake systematic monitoring of the citadel as well as other vulnerable areas

(7) Fig. 13.17 shows the exchange ceremony between the Municipality of Machu Picchu and ICL for the cooperation of ICL-JICA Project in 2007. Many children in the city welcomed our agreement by marching in front of us. It will be the greatest pleasure if we can contribute something to create a safer community in this area.

Acknowledgments The Japanese investigation team was well received by the related agencies in Peru and obtained significant support and cooperation. We acknowledge the following persons and institutes for their cooperation to this investigation: Mr. Edwin Benavente, Mr. David Ugarte, Mr. Fernando Astete, Mr. Cleto Quispe, and other engineers of the Machu Picchu office of Instituto Nacional de Cultura (INC), Dr. Romulo Mucho, Dr.Victor Benavides, and colleagues of INGEMMET (Peruvian Instituto Geologico Minero y Metalurgico) for their cooperation and coordination of many of our Peruvian counterparts.

To prepare a new ICL-JICA project on Capacity building in Machu Picchu-Aguas Calientes, ICL exchanged agreement with Mr. Luis F. Palomino (Chief of Instituto Nacional de Defensa Civil of the Government of Peru (INDECI) and Mr. Edgar Miranda Quinones (Mayer of the Municipality of Machu Picchu). The preparation was much supported by Mr. Takao Omote (Director of JICA Lima office), Mr. Norio Naito (JICA Osaka office) and Dr Julio Kuroiwa (Disaster Reduction expert in Peru).

Prof. Mutsumi Ishitsuka, Instituto Geofisico del Peru (IGP) has cooperated from the beginning of this Machu Picchu investigation in all aspects. Many Japanese colleagues, Dr. Gonghui Wang, Dr. Fawu Wang, Dr. Haruo Shuzui, Mr. Minoru Hoshino, and others have cooperated with this investigation since March 2000.

All of them are deeply appreciated for their kind cooperation and contribution to implement field works and to analyze obtained results.

References

Bandarin F, Editorial Director. 2001. Rumbles at Machu Picchu. World Heritage Review, UNESCO, No. 29, p. 56.

Best M, Bobrowsky P, Duma M, Carlotto V. 2008. Geophysical survey at Machu Picchu, Peru: Results for landslide hazard investigation (IPL C101-1-3). In: Sassa K, Canuti P (eds.), Landslides: disaster risk reduction, Springer (this book).

Canuti P, Margittoni C, Casagli N, Delmonaco G, Falconi L, Ferrettti A, Lollino G, Puglici C, Spizzichino D, Tarchi D. 2008. Monitoring, geomorphological evolution and slope stability of Inca citadel of Machu Picchu : Results from Italian INTERFRAST project (IPL C101-1-1). In: Sassa K, Canuti P (eds.), Landslides: disaster risk reduction, Springer (this book).

Carreno R, Bonnard, C. 1997. Rock slide at Machupicchu, Peru. Landslide News, No.10, pp. 15–17, and also published in Landslides of the World. Kyoto University Press (Editor: Sassa, K. 1999. ISBN4-87698- 073-X C3051), pp. 311–316.

Casagli N, Fanti R, Reighini G. 2008. Integration of VHR Satellite image with field data for the analysis of debris sheet instability in the Machu Picchu area (IPL C101-1-5) In: Sassa K, Canuti P (eds.), Landslides: disaster risk reduction, Springer (this book).

Geology and Mineral Resources of Shaanxi Province. 1990. Evaluation and study of regional crustal stability and geological hazards of Xi'an area (in Chinese).

Kalafatovich C. 1963. Geologia del conjunto arquaolUgico de Machupicchu y sus alrededores. Revista universitaria UNSAAX, Vol. 121.

Lin Z. 1997. Lishan, Xi'an, Historic Cultural Heritage at Risk and Geological Setting. Proc. International Symposium on Landslide Hazard Assessment, pp. 25–30.

Sassa K. 2005. Precursory Stage of Landslides in the Inca World Heritage Site at Machu Picchu, Peru. Independent brochure for UNITWIN Programme, Education Sector of UNESCO, 4p.

Sassa K, Fukuoka H, Yang Q, Wang F. 1997. Landslide hazard assessment in cultural heritage, Lishan, Proc. International Symposium on Landslide Hazard Assessment, Xian. pp. 1–24.

Sassa K., Fukuoka H, Kamai T, Shuzui. H. 2001a. Landslide risk at Inca's World Heritage in Machu Picchu, Peru. Proc. UNESCO/IGCP Symposium on Landslide Risk Mitigation and Protection of Cultural and Natural Heritage, Tokyo, pp. 1–14.

Sassa K, Fukuoka H, Wang FW, Furuya G, Wang GH. 2001b. Pilot study of landslide hazard assessment in the Imperial Resort Palace (Lishan), Xi'an, China. Proc. UNESCO/IGCP Symposium on Landslide Risk Mitigation and Protection of Cultural and Natural Heritage, Tokyo, pp. 15–34.

Sassa K, Fukuoka H, Shuzui H, Hoshino M. 2002. Landslide Risk Evaluation in the Machu Picchu World Heritage, Cusco, Peru. Proc. UNESCO/Kyoto University International Symposium on Landslide Risk Mitigation and Protection of Cultural and Natural Heritage. Kyoto, pp. 469–488.

Sassa K, Fukuoka H, Wang FW, Wang G. 2005. Dynamic properties of earthquake-induced large-scale rapid landslides within past landslide masses. Landslides 2(2): 125–134.

UNESCO World Heritage Committee, 2006. 30 COM 7B.35 - State of Conservation (Historic Sanctuary of Machu Picchu), http://whc.unesco.org/en/decision/1121

Vlimek V, Kimes J, Zvelebil J, Astete F. 2008. Monitoring of slope movements at Machu Picchu (IPL C101-1-2). In: Sassa K, Canuti P (eds.), Landslides: disaster risk reduction, Springer (this book).

Xi'an Seismological Bureau. 1991. History of Earthquakes in Xi'an. 134p.

14 Monitoring, Geomorphological Evolution and Slope Stability of Inca Citadel of Machu Picchu: Results from Italian INTERFRASI project

P. Canuti, Claudio Margottini, N. Casagli, G. Delmonaco, L. Falconi, R. Fanti, A. Ferretti, G. Lollino, C. Puglisi, D. Spizzichino and D. Tarchi

Abstract The Geology of Machu Picchu area is characterised by granitoid bodies that had been emplaced in the axial zones of the main rift system. Deformation of the granite, caused by cooling and tectonic phases, originated 4 main joint sets, regularly spaced (few decimetres to metres). Several slope instability phenomena have been identified and classified according to mechanism, material involved and state of activity. They are mainly related to rock falls, debris flows, rock slides and debris slides. Origin of phenomena is kinematically controlled by the structural setting and relationship with slope face (rock falls, rock slide and debris slides); the accumulated materials is the source for debris flow. Geomorphological evidences of deeper deformations are currently under investigation.

A low environmental impact monitoring system has been established on the area having the purpose to minimize equipments usage and, in the mean time, to collect reilable data on surface deformations. The monitoring network comprise

P. Canuti (✉)
University of Firenze, Department of Earth Sciences, Via Giorgio La Pira 4, 50121, Firenze, Italy

C. Margottini
ENEA, Via Anguillarese, 301 – 00060 S. Maria di Galeria (Rome) Italy; ISPRA – Italian Institute for Environment Protection and Research – Via Curtatone 3, 00185, Rome, Italy

N. Casagli
University of Firenze, Department of Earth Sciences, Via Giorgio La Pira 4, 50121, Firenze, Italy

G. Delmonaco
ENEA, Via Anguillarese, 301 – 00060 S. Maria di Galeria (Rome) Italy; ISPRA – Italian Institute for Environment Protection and Research – Via Curtatone 3, 00185, Rome, Italy

L. Falconi
ENEA, Via Anguillarese, 301 – 00060 S. Maria di Galeria (Rome) Italy; Consorzio Civita, Via del Corso 300, 00186, Rome, Italy

R. Fanti
University of Firenze, Department of Earth Sciences, Via Giorgio La Pira 4, 50121, Firenze, Italy

A. Ferretti
Tele-Rilevamento Europa, T.R.E., Via Vittoria Colonna 7, 20149, Milano, Italy

G. Lollino
CNR-IRPI Torino, Strada delle Cacce 73, 10135, Torino, Italy

C. Puglisi
ENEA, 301 – 00060, Via Anguillarese, S. Maria di Galeria, Rome, Italy

D. Spizzichino
Consorzio Civita, Via del Corso 300, 00186 Rome (Italy); ISPRA – Italian Institute for Environment Protection and Research – Via Curtatone 3, 00185, Rome, Italy

D. Tarchi
European Commission, Joint Research Centre, SERAC Unit, Via E. Fermi, 1 – TP 723, 21020, Ispra (VA) Italy

K. Sassa, P. Canuti (eds.), *Landslides – Disaster Risk Reduction*,
© Springer-Verlag Berlin Heidelberg 2009

a GPS, multitemporal laser scanner survey, Ground based Radar interferometry (GB-SAR) and Satellite Interferometric Synthetic Aperture Radar (InSAR).

The preliminary results are partially confirming the field evidences of slope deformation but, in the mean time, they require a longer period of observations since the sliding processes are relatively slow.

Keywords Geomorphology • Slope instability • GPS • Radar • Monitoring • Machu Picchu

14.1 Geological Setting

The high Eastern Cordillera of Peru formed as a result of inversion of a Late Permian-Triassic rift system (e.g. Semper et al., 2002). The Geology of Machu Picchu area reflect the same pattern.

The area (Fig. 14.1) is characterised by granitoid bodies that had been emplaced in the axial zones of the main rift system that are now exposed at the highest altitudes, together with country rocks (Precambrian and Lower Paleozoic metamorphics) originally constituting the rift 'roots'. The Machu Picchu batholith is one of these Permo-Triassic granitoid bodies (a biotite Rb-Sr age of 246 ± 10 My by Priem et al. is reported for this intrusion in Lancelot et al., 1978).

The bedrock of the Inca citadel of Machu Picchu is mainly composed by granite and subordinately granodiorite. This is mainly located in the lower part of the slopes (magmatic layering at the top). Locally, dikes of serpentine and peridotite are outcropping in two main levels; the former is located along the Inca trail, near Cerro Machu Picchu (vertically dipping), the latter is located along the path toward "Templo de la Luna" in Huayna Picchu relief.

Superficially, the granite is jointed in blocks with variable dimensions, promoted by local structural setting. The dimension of single blocks is variable from 10^{-1} to about $3*10\ m^3$.

Soil cover, widely outcropping in the area, is mainly composed by individual blocks and subordinately by coarse materials originated by chemical and physical weathering of minerals.

Part of the slopes exhibit debris accumulation as result of landslide activity. Grain size distribution of landslide accumulation are closely related to movement types and evolution.

Talus and talus cones are composed by fine and coarse sediments, depending from local relief energy.

Alluvial deposits outcrop along the Urubamba river and its tributaries. They are composed by etherometric and polygenic sediments, that may be in lateral contact with the talus deposits.

Anthropic fill and *andenes*, on top of Citadel, reflect the work of Inca civilization in the area (Fig. 14.2).

Fig. 14.1 General view of Machu Picchu area

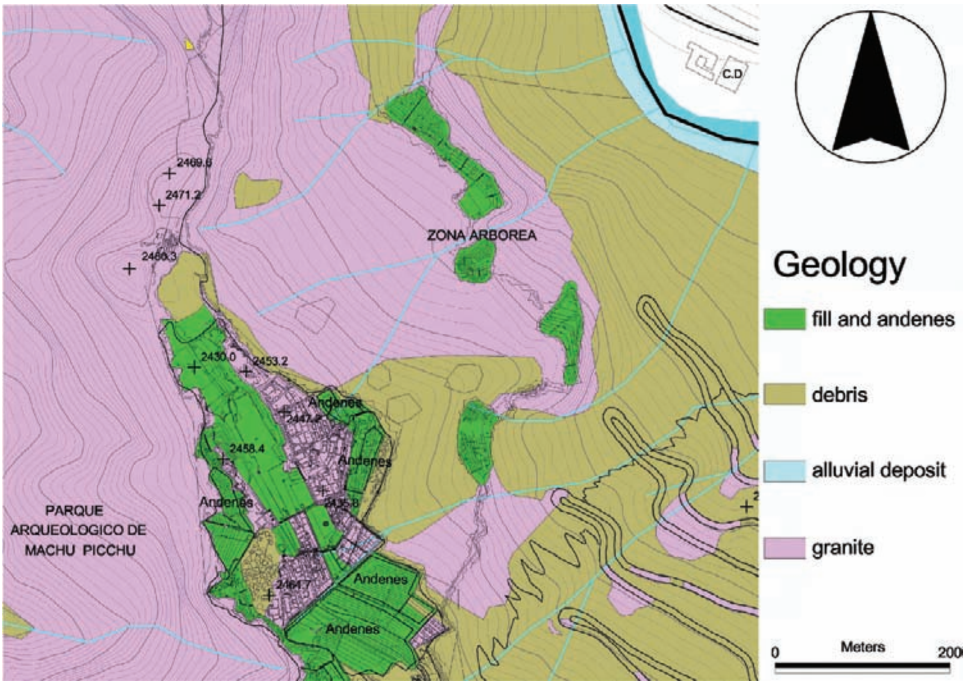

Fig. 14.2 Geological map of the Inca Citadel of Machu Picchu

Mechanical proprieties of local material are reported in the following Table 14.1.

14.2 Structural Setting

Deformation of the granite is highly localised into differently oriented sets of regularly spaced (few decimetres to metres) shear zones (Mazzoli et al., 2005). All of these shear zones show well-defined, sharp, fault-like discontinuities, characterised by slickenside surfaces and shear fibres. These indicate consistent reverse to oblique-slip (transpressional), to strike-slip kinematics, depending on fault set attitude. Most of these shear planes show limited measurable displacements (a few centimetres to decimetres being common) and essentially undeformed wall rock. However, in several instances ductile deformation of the granite has also occurred along the walls of fault-like discontinuities. These deformation zones range from a few centimetres- to decimetres-thick mylonite horizons, showing sharp contacts with surrounding undeformed granite, to more continuous shear zones displaying sigmoidally-shaped S foliations (progressively decreasing in intensity in wall rock granite) and S-C or composite S-C-shear band fabrics. Mylonite microstructures are characterised by extensive dynamic recrystallisation of quartz and grain-size reduction. Chlorite and white mica-dominated mineral assemblages point to lower greenschist-facies conditions for the deformation. Inversion of fault-slip data indicates that the latter occurred as a result

Table 14.1 Geotechnical parameters and proprieties

	Density (KN/m^3)	Ed (MPa)	Kn (MPa)	v	Sigmaf (MPa)	Tensile strength (MPa)	II(°)	c (kPa)
Granite	23–25	80,000–90,000	20–100	0.15	50–250	7–13	33.5–40.5	220–355
Granodiorite	23–25	100,000–150,000	20–100	0.15	60–250	7–13	35–42	270–355
Superficial cover	25	–	–	–	–	–	32	270
Talus	18–25	–	–	–	–	–	34–38	0

of mean N60°E oriented shortening, well compatible with regional data from the nearby Cusco area (Carlotto, 1998). Structural analysis clearly suggests that the analysed shear zones form part of a larger population of regularly spaced surfaces that most probably originated as early (cooling) joints in the igneous rock. Reactivation of differently oriented sets of precursor joints allowed the granite to deform effectively by relatively small displacements occurring on a very large number of shear zones, the strain being therefore localized at the m-scale, but distributed at the km-scale.

The structural settings of terrains is finally related to the main following dip orientations/dipping:

a) 30°/30° in the Machu Picchu hill ;
b) 30°/60°;
c) 225°/65;
d) 130°/90°.

Secondary systems (e.g. 130°/45°, 315°/30° and 310°45°) have been also surveyed in the area, with minor relevance.

14.3 Geomorphology and Slope Instability

During three joint missions in Machu Picchu in 2003 and 2004, the group performed a geomechanical and geomorphological survey of the entire area. Field observations were integrated with interpretation of stereoscopic aerial photos and of two optical very-high-resolution satellite images (*Quickbird*) dated 18 June 2002 and 18 May 2004, respectively.

The general morphological features of the area are mainly determined by the regional tectonic uplift and structural setting. As consequence, kinematic conditions for landslide type and evolution are closely depending on the above factors.

Several slope instability phenomena have been identified and classified according to mechanism, material involved and state of activity (Fig. 14.3). They are mainly related to the following: rock falls, debris flows, rock slides and debris slides. The area of the citadel has been interpreted as affected by a deep mass movement (Sassa et al., 2001, 2002) that, if confirmed by the present day monitoring systems, it could be referred to a deep-seated gravitational slope deformation (DSGSD), probably of the type of the compound bi-planar sagging (CB) described by Hutchinson (1988). A main trench with NW-SE trend, related to a graben-like structure, is located within the archaeological area and supports this hypothesis. Other trenches are elongated in the dip direction of the slope.

In the SW cliff the local morphological depends on the intersection between the systems 225°/65° and 130°/90° which bounds lateral evolution. This kinematic condition causes high angle rock slide which very often evolve in rock falls. These are also conditioned by 30°/30° and 30°/60° systems which originate overhanging blocks. The SW slope exhibit some morphological terraces, regularly spaced, the origin of which it is still under investigation (fluvial erosion, sagging, joint, etc).

The morphological evolution, in NE flank below the Inca Citadel, is constrained prevalently by the 30°/30° and 30°/60° systems and marginally the 225°/65° one; the intersection of the first two systems with slope face it is kinematically compatible with the occurrence of planar rock slides; the intersection of slope face with the 225°/65° is kinematically compatible with rock falls. Rock slides and rock falls may produce blocks with dimension variable from 10^{-1} to 10^{2} m^{3}.

Debris produced by rock slides and rock falls, as well as from weathering processes is periodically mobilised as debris slides and debris flow. The most recent phenomenon occurred in 1995 along the "carrettera" Bingham. Debris slides and debris flows are characterised by an indifferentiated structure varying from chaotic blocks immersed on coarse sand matrix. The grain size distribution is mainly depending on the distance from the source areas and slope angle.

Finally, it is interesting to notice, on the NE side, the presence of a large debris accumulation, just below the citadel, presently being eroded by all around dormant slides. The accumulation it is probably the result of an old geomorphological phenomena now stabilised, still not clear in its original feature. Anyway, the mass movements occurred certainly before the Inca settlement since some of their terraces (andenes), are founded over this accumulation area.

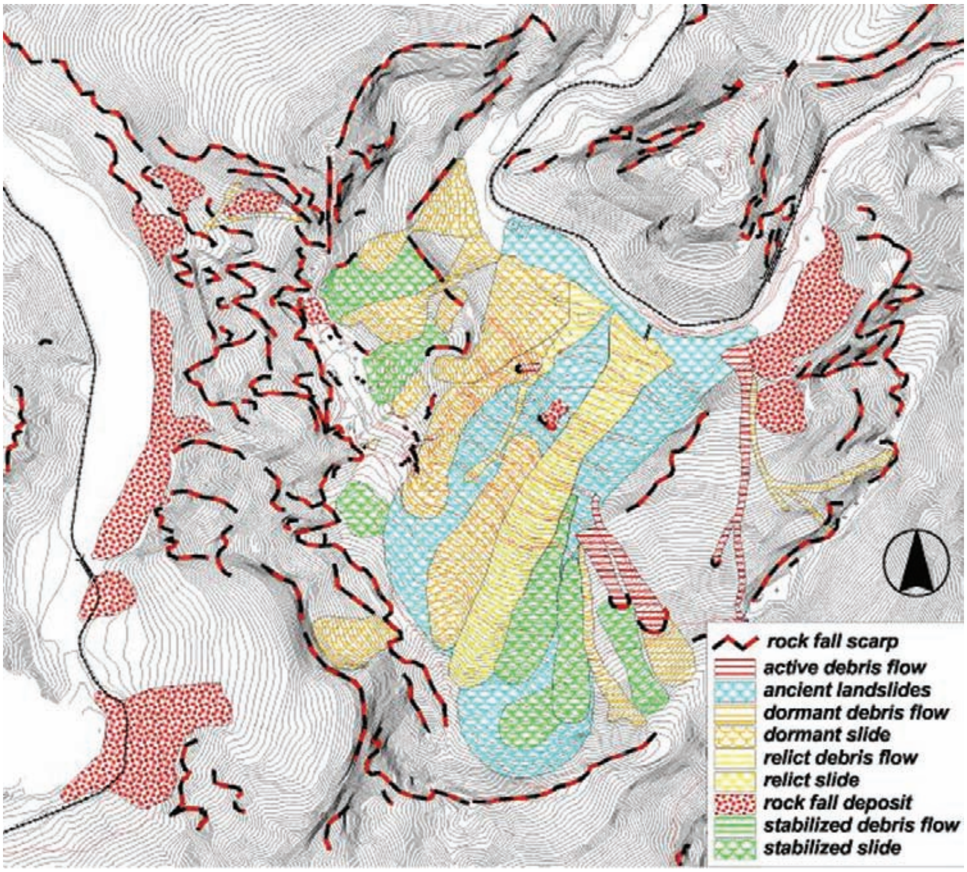

Fig. 14.3 Geomorphological map of the area

14.4 GPS Monitoring Network

A GPS network was installed in September 2003, in the Urubamba valley and Machu Picchu citadel. The GPS network is constituted by 3 control points (*a priori* FIXED) and 11 rover points installed inside the citadel's area.

A first survey was conducted in September 2004, after one year of monitoring. Displacement of rover points of the citadel was calculated using baselines generated from the adjusted geodetic coordinates of reference points. The results show that the points where a displacement was appreciated are (Table 14.2):

Table 14.2 Displacement detected along the three axis (N, E, h) for points 9 and 10. Red data are considered reliable (for location see Fig. 14.7)

	Delta N [m]	Delta E [m]	Delta h [m]
9	0.012	−0.002	0.002
10	0.010	−0.003	0.009

These results demonstrate how the major displacement vector runs along the North axis; while no significant displacement was detected along the Est and the ellipsoidical height direction.

14.5 Monitoring with JRC GB-SAR

On the 3rd October 2004 the LISA Radar system was installed in a small open area which is part of the old train station in Puente Ruinas, just at the beginning of the road going up to the archeological village (Fig. 14.4). From this site (Fig. 14.5) it is possible to see some buildings of the lower part of the "Ciudadela" entrance and to see the whole

Fig. 14.4 The LISA system

vegetated zone below, where it is expected to observe the possible sliding movement. With the data, that has been continuously acquired up until now, no significant displacements have been detected. Considering the very low displacement rate measured by other monitoring systems, we expect that at least a full year of measurement is needed to get reliable data in order to see every possible small displacement affecting the Inca site.

14.6 Interferometric Synthetic Aperture Radar (InSAR)

Recent advances in optical and radar imagery capabilities, e.g. high spatial resolution, stereoscopic acquisition and high temporal frequency acquisition, the development of new robust techniques based on the interferometric analysis of radar images, such as the Permanent Scatterers Technique (Ferretti et al., 2001), and the possibility of integrating these data within a Geographical Information

System (GIS) have dramatically increased the potential of remote sensing for landslide investigations (Hilley et al., 2004). The resolution is of the order of millimetre.

Due to the very rough topography, steep slopes and local weather conditions the Machu Pichu area is a very challenging test site for the application of satellite radar data. Apart from that, the lack of an historical data-set of ESA-ERS acquisitions prevented – at least in the first part of the

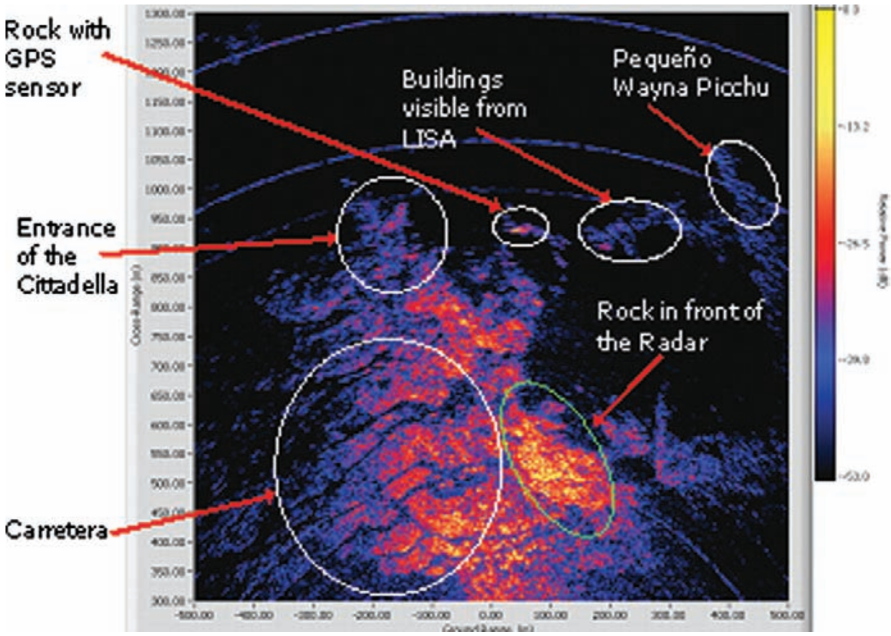

Fig. 14.5 Power image with reference points

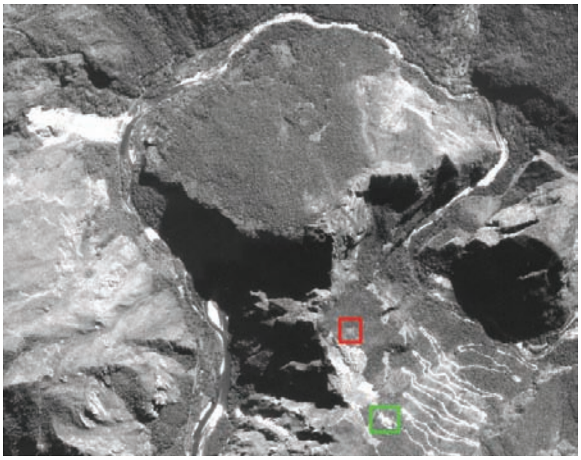

Fig. 14.6 Identification of the two reported PS: the *green* is considered stable and the detected movement is assigned to the *red* PS

project – the application of the POLIMI PS Technique. In fact, the identification of the measurement points and the estimation (and removal) of the atmospheric components can be usually carried out whenever at least 15–20 scenes are available. Unfortunately, just a few ERS scenes were acquired since 1991 for interferometric processing.

Nevertheless, in the framework of the INTERFRASI Project, all satellite radar data acquired by the ESA sensors ERS-1, ERS-2 and Envisat over the area of interest have been processed trying to identify coherent areas where displacement information could be recovered, by applying the conventional approach (DInSAR). However, the coherence level of the interferometric pairs turned out to be to low and no information could be recovered over the AOI.

Due to the lack of ESA-ERS scenes, more than 30 scenes gathered by the Canadian radar sensor RADARSAT in different acquisition modes have been planned and processed. The use of RADARSAT "Fine-Beam" data, characterized by higher spatial resolution with respect to ESA data, turned out to be very important in order to identify good radar targets. Moreover, the shorter repeat-cycle of RADARSAT (24-day rather than 35) allowed the creation of a time series of 16 radar data in two different acquisition modes in about 1 year. The increased resolution allowed the selection of a dozen of "PS Candidates" within the AOI, characterized by a sufficient level of signal-to-clutter ratio (SCR). An in depth analysis of the time series of RADARSAT data, however, highlighted severe decorrelation phenomena probably due to microclimatic conditions at the time of the acquisitions and strong phase artifacts due to tropospheric inhomogeneities. Preliminary results have shown evidence of differential motion between the radar targets of about 5 cm (Fig. 14.6), but the estimation, so far, it has to be considered not totally reliable using the data-set available. An independent confirmation with more PS is required.

14.7 Conclusion

The geological and geomorphological investigations conducted in the area of Machu Picchu highlight the presence on many slope instabilities, mainly with low depth. Several slope instability phenomena have been identified and classified according to mechanism, material involved and state of activity. They are mainly related to rock falls, debris flows, rock slides and debris slides. Origin of phenomena is kinematically controlled by structural asset and relationship with slope face (rock falls, rock slide and debris slides); the so accumulated materials is the source for debris flow.

In the area of the Carretera a precise mapping of debris deposits and past debris flows was carried out, leading to a zonation of processes within the limits of the ancient landslide detected by Sassa et al. (2001). The situation of the slope with the citadel is more complex due to the strong structural control of the master joints on the slope evolution. In this, planar rock slides are mainly affecting the NE flank while rock falls are predominant on SE cliff.

The analysis of monitoring data, integrated with field observations is suggesting (Fig. 14.7).

1. the stability of the upper part of the citadel were several GPS sensor do not exhibit any movements; also archaeological structures seem to be relatively undamaged;
2. the continues rock falls in the S-W side of the cliff and related citadel's border, were also archaeological structure have been damaged by progressive

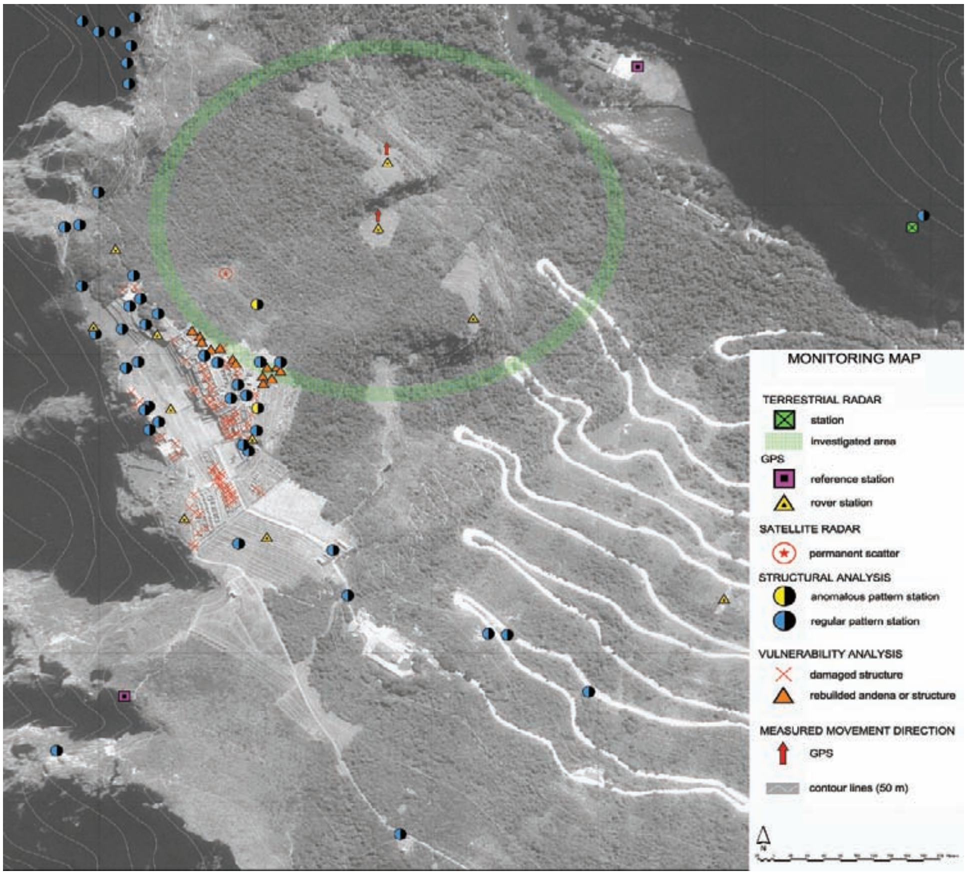

Fig. 14.7 Integrated map of surface deformation evidences and present monitoring data

lateral detensioning; this is probably the area with the highest short-term conservation problem.

3. the presence of a paleo-landslide in the North-East flank, with likely thickness of some tens meters, limited by a tension crack the discovering in 2004; in this area neither GPS nor PS nor JRC GBR-SAR detected any kind of deformation; in this area also structural geology detect some not regular pattern in the measurement.

Finally, the collected data are beginning to give a first picture of the slope evolution of the site. Nevertheless, the analysis of the monitoring data collected from the systems installed by Italian, Japanese and Czech-Slovak groups, together with data provided by Canadians and Peruvians, will allow a better evaluation of the mechanisms of slope processes and of landslides, leading to a complete harmonization amongst the observation of the different research groups involved.

As historical consideration, the data collected suggest the possibility that the site of Machu Picchu could have been selected by Incas also because of the availability of two large block deposits, useful for constructions: one on the so called “cantera” and the second in the paleo-landslide recently discovered.

Acknowledgements The present project has been found by the Italian Ministry of University and Scientific Research. Field activities greatly benefited fro the support of Istituto National de Cultural (INC) and INGMET.

References

Carlotto V. (1998). Evolution Andine et Raccourcissement au Niveau de Cusco (13–16°S) Perou. Mémoire H.S. 39, Université I de Grenoble, France, 203p.

Ferretti A., Prati C., Rocca F. (2001). Permanent Scatterers in SAR Interferometry, *IEEE Trans. on Geoscience and Remote Sensing*, 39(1), 8–20.

Hilley G.E., Bürgmann R., Ferretti A., Novali F., Rocca F. (2004). Dynamics of Slow-Moving Landslides from Permanent Scatterer Analysis, *Science*, 25 June 2004, 304(5679), 1952–1955.

Hutchinson J.N. (1988). General report: Morphological and geothecnical parameters of landslides in relation to geology and hydrogeology. Proc. 5th Int. Symp. on Landslides, July 1988, Lausanne. 1, 3–36.

Lancelot J.R., Laubacher G., Marocco R., Renaud U. (1978). *U/Pb radiochronology of two granitic plutons from the eastern Cordillera (Peru) — Extent of Permian magmatic activity and consequences*. Int. Journal of Earth Sciences, 67(1), 236–243.

Mazzoli S., Delmonaco G., Margottini C. (2005). Role of precursor joints in the contractional deformation of the granite pluton, Machu Picchu batholith, Eastern Cordillera, Peru. Rend. Soc. Geol. It., I (2005), Nuova Serie, 3 ff, in printing.

Sassa K., Fukuoka H., Kamai T., Shuzui H. (2001). Landslide risk at Inca's World Heritage in Machu Picchu, Peru. Proceedings UNESCO/IGCP Symposium on Landslide Risk Mitigation and Protection of Cultural and Natural Heritage, Tokyo, 1–14.

Sassa K., Fukuoka H., Shuzui H., Hoshino M. (2002). *Landslide Risk Evaluation in the Machu Picchu World Heritage, Cusco, Peru*. Proc. UNESCO/Kyoto University International Symposium on Landslide Risk Mitigation and Protection of Cultural and Natural Heritage. Kyoto, 469–488.

Sempere T., Carlier G., Soler P., Fornari M., Carlotto V., Jacay J., Arispe O., Neraudeau D., Cardenas J., Rosas S., Jimenez N. (2002). Late Permian-Middle Jurassic lithospheric thinning in Peru and Bolivia, and its bearing on Andean-age tectonics. Tectonophysics, 345(1–4), 153–181.

Dilatometric and Extensometric Monitoring of Rock Blocks Displacements Within Machu Picchu Archaeological Site, Peru

15

Vít Vilímek, Jan Klimeš, Jiří Zvelebil and Fernando V. Astete

Abstract The area of archaeological site of Machu Picchu was affected by large-scale slope movement in the past. This event in the paleogeomorphological evolution of the area, along with intensive fluvial erosion and tectonic disturbance of the rocks, has been significantly affecting the evolution of the landscape. Unknown triggering impulse for such huge slope deformation and presence of several younger generations of slope movements were reasons for complex geological – geomorphological investigation aimed to verify the potential recent activity of deep-slope movement. In order to understand the mechanism and recent activity of the mass movements the monitoring net of dilatometric and extensometric measurements was established during 2002, after preliminary field investigation in 2001 and aerial photo interpretations. The results of the monitoring supported by the field investigation suggest that large-scale slope movement is doubtful in close future. Nevertheless, continuation of monitoring will be useful and from point of view of the long-term landscape evolution the area is in unstable position. The recent detected movements can be explained by individual movements of rock blocks or several other mechanism including subsurface erosion and local sinking and deformation of archaeological structures.

Keywords Landslides • Monitoring • Machu Picchu • Peru

15.1 Introduction and Methodology

Various types of methods were used to study landslides at Machu Picchu historical site. To understand properly relation between morphological processes and resulting landforms during the time evolution we focussed mainly on geomorphological mapping, morphostructural analysis based on field studies as well as air-photo interpretation. We also applied hydrogeological and engineering-geological field investigation methods describing slope sediment and rock properties as well as evaluating stability conditions of the studied area. Beside these, monitoring net of dilatometric and extensometric measurements was established during 2001 (Vilímek and Zvelebil 2002).

To study the landscape evolution of Machu Picchu area is rather complex task and not only mass movements are involved. Neotectonics and

Vít Vilímek (✉)
Charles University, Prague, Czech Republic

Jan Klimeš
Academy of Sciences, Prague, Czech Republic

Jiří Zvelebil
Geological Survey of Czech Republic

Fernando V. Astete
Instituto National de Cultura, Cusco, Peru

K. Sassa, P. Canuti (eds.), *Landslides – Disaster Risk Reduction*,
© Springer-Verlag Berlin Heidelberg 2009

recent river erosion are significant forming processes as well. Both active and passive influences of neotectonics were documented (Vilímek et al. 2007). To get better understanding of the recent morphological processes and their dynamics within the Machu Picchu historical monument field research of its surroundings were carried out (e.g. Klimeš et al. 2007). They were focused namely on debris flows as important geomorphological process with high damaging potential to the man made constructions.

According to literature review (e.g. Carreño et al. 1996; Carreño and Bonnard 1997) and our preliminary field work results (Vilímek and Zvelebil 2002) it was apparent that the Machu Picchu archaeological site was built in the area highly affected by mass movements of various types and age. Nevertheless the main research question was the recent slope movements activity at the Machu Picchu. In order to get the proper data whether the Incaic buildings and terraces might be endangered by slope movements within short time period (in order of years or tens of years) we decided to install monitoring net measuring relative displacements across open fissures in rock outcrops. We chose localities where possible danger for important Incaic structures was clear or places where slope movements or neotectonic movement could appear. The preliminary field inspection in 2001 and 2002 showed that at some places signs of prehistoric slope deformation could be documented even inside the archaeological site.

Due to strict preservation rules of the archaeological site a permanent installation was not permitted and thus non-invasive technology of portable dilatometer and extensometer was chosen. For the dilatometric measurements, irreversible movements of order of 0,1 mm per year under fully favourable measuring conditions is possible to detect (Zvelebil and Stemberk 2000). The localities of ongoing dilatometric measurements are mark out on Figs. 15.1 and 15.2.

Two extensometric monitoring measurements profiles (see Fig. 15.3) were also established across the main square to verify the suggested ongoing potential activity of a large-scale slope deformation, with scarp area crossing the main square (e.g. Sassa et al. 2000). Fixed points for portable extensometric measurements were stretched between Intiwatana hill and rock outcrops at the border of the Lower City, they were fixed into the solid rocks avoiding the installation into fissures or largely dissected rock blocks.

From the geomorphological point of view the zone between Huayna Picchu Mt. (2 700 m a.s.l.) and Machu Picchu Mt. (3 051 m a.s.l) is possible to regard

Fig. 15.1 View on the archaeological site with show locations of dilatometric sites. Localities of dilatometric measurements are marked with arrows and letter (C = Cave, T = Principal Temple, I = Intiwatana, P = Plaza, W = Wayna Picchu, A = Acllawasi, M = Wairana o Mirador, R = Rodadero, Q = Qhata

Fig. 15.2 An example of dilatometric measurement – locality W (Wayna Picchu). Visitors are allowed to enter this area, thus the measurement is needed here

Fig. 15.3 Extensometer measurement sites show measurement points described by letters (ES1 = Plaza south 1, ES2 = Plaza south 2, EN 1 = Plaza north)

as double ridge with one peak represented by the Intiwatana hill and other by the Lower City in the Machu Picchu historical monument (Vilímek et al. 2007). The double ridge resulted from mountain ridge spreading described e.g. in Radbruch-Hall et al. (1977). This large slope deformation of prehistoric age was predisposed by tectonically highly disturbed rock mass – a zone between Huaynapicchu and Machupicchu faults. Arguing with Kalafatowich (1963) theory about graben-like structure between two above-mentioned faults, we supposed that the double ridge resulted from large slope deformation indicated by rather sub-horizontal striations found on Huaynapicchu fault and on other faults inside the archaeological area. The primary form of such spread is rather difficult to establish, for the fact that the central part of Machu Picchu had been anthropogenically intensively remodelled.

The quality of the measurement point installation is very important for acquisition of reliable data describing rock movements along monitored fractures. A portable extensometric tape was chosen with radius 25–35 m. The accuracy of this method is 0,5 mm per year (in minimally 3 year time series).

15.2 Results

The magnitudes of all the irreversible displacements indicated by dilatometric monitoring range from 0,5 to 4,75 mm during 2,5–3,7 years. The largest displacement was measured at the site T1 (see Fig. 15.4) showing high mobility within specific rock mass. Nevertheless, correlation of these measurements with nearby Intiwatana site (I1–I3) and Plaza (P) sites, which is located on the opposite side of the suggested extension zone of the Main Plaza, showed no coupling of the measured movements. Thus the detected irreversible movements may be attributed to local phenomena such as sinking of specific rock blocks due to the subsurface erosion and annual changes in water content of the soils, but they can not be explained by deep-seated rock slide activity.

Indications of irreversible movements within the block system at the edge of high nearly vertical rock wall near the summit of Mt. Huaynapicchu (Wayna Picchu) should be cautiously considered with regards to the safety of tourists and preservation of Inca ruins (Figs. 15.1 and 15.2). Their magnitudes (–2.75 mm during 2.75 years, and 1.2 mm during 1 year) are too large to be neglected with regards to the overall stability of this block system.

Other measurement sites can be divided into four main groups. The first include sites where constructions show high degree of damage (e.g. tower above highly fractured rock outcrop - site M1 - M4), nevertheless, measurements proved no significant movements there. Overall movements during 2 years are up to maximum of 0,5 mm. Other group consists of sites with uniform movement without large variations (e.g. cave on the steep slope of the

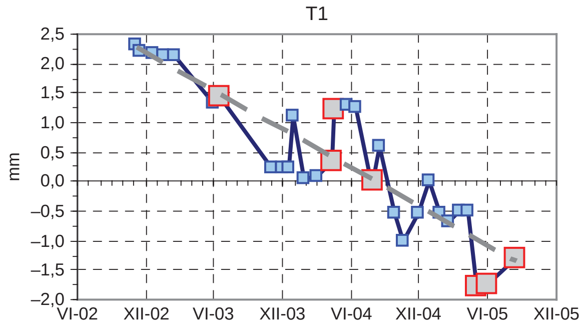

Fig. 15.4 The graph of dilatometric measurement at the locality T - Temple. The site T1 is on the east face of the block located. (Red points are our controle measurements, blue ones were measured by our Peruvian partners from INC)

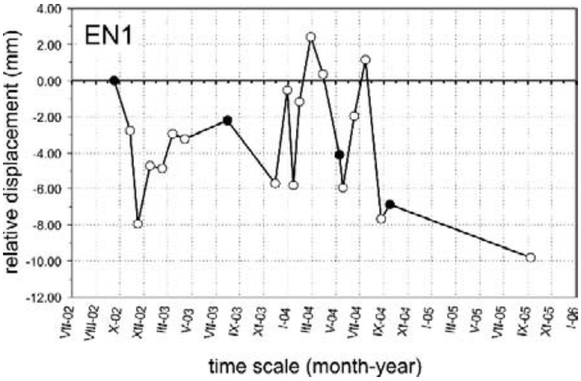

Fig. 15.5 The graph of extensometric measurement at the site EN1 – Plaza North. (Black points are our controle measurements, in white colour are presented measurements done by INC)

agricultural part of the archaeological site, measurement site C1) representing no danger within time span of years or tens of years. Last groups of measurements represent sites with very high movement variations without any trend. These movements are difficult to explain based on the available data.

The extensometric profile ES 1 and ES 2 (see Fig. 15.3) crossing the double ridge zone of the Main Plaza gave the medium indication of irreversible increase of the distance, whilst the northern EN 1 profile showed opposite trend – weak irreversible decrease of the distance. Nevertheless, correlation of these measurements shows no coupling of those movements, which should bear the evidence for single slope movement involving both sides of the double ridge zone. Therefore, the drift of rock blocks within the southern extensometric profile can be probably explained by individual, local block movements.

The observed trend in distance decrease at the EN1 (Fig. 15.5) profile is likely to be caused by a "back-toppling"-sliding activity within individual systems of blocks forming the upper rim of the slope. If the hypothetical landslide is deeper and larger, a higher degree of coupling should be shown by the recent measurements.

15.3 Conclusions

Recent activity of deep-seated slope movement was not confirmed by the installed monitoring network. None of the documented magnitudes and trends of irreversible deformations could be considered as an indicator of immediate danger of collapse of the rock objects and thus also the archeological structures in question. These conclusions was possible to make even though the irreversible displacements caused by slope movements are obscured by "noise" of reversible changes of volumes of rock blocks following circadial, seasonal, or even higher quasi-cycles of air temperature and ground water saturation changes.

If we compare our recent recorded magnitudes of surface measurements with other sites of large, deep-seated slope movements (e.g. Moser et al. 2002; Moser 2003), the magnitudes within Machu Picchu archaeological site are at least one-order smaller and do not confirm the existence of deep-seated slope movement at this site.

Detected recent movements and signs of previous movements inside the archaeological site (partly destroyed walls, see Fig. 15.6) might be caused by local gravitational movements of individual rock blocks or by several other factors. Among them subsurface erosion or annual changes in the water content of the soil is the most probable.

Possibly highly devastating impact of earthquakes on the Inca structures at the historical monument was proved by field measurements and modelling done by Cuadra et al. (2008). According to our field geomorphological investigations an

Fig. 15.6 Subsurface erosion along highly disturbed zone and followed sinking is probably reason for some damages in the original Incaic walls

earthquake might be the triggering factor for such huge block movement in the past, but dating was not possible up to now (Vilímek et al. 2007).

Acknowledgements The authors would like to thank various Peruvian instructions for their scientific and personal support, namely to INC (Instituto National de Cultura) in Cusco and at Machu Picchu. The research has been supported by the project MSM 00216 20831.

References

Carreño R., Lopéz R., Tupayachi L. (1996) Informe preliminary sobre el derrube de Machupicchu del 26.12.95 y situación del cerro Putucusi. Nota técnica, MS, PROEPTI, Cusco, Peru

Carreño R, Bonnard C. (1997) Rockslide at Machupicchu, Peru. Landslide News 10:15–17

Cuadra C., Karkee M.B., Tokeshi K. (2008) Advances in Engineering Software, 39(4):33–345

Kalafatovich C. (1957) La glaciación pleistocena en Urubamba. Revista Universitaria 46(112):235–252

Klimeš J., Vilímek V., Vlčko J. (2007) Debris Flows in the Vicinity of the Machu Picchu Village, Peru. In: Sassa K., Fukuoka H., Wang F., Wang G. (eds.). Progress in Landslide Science, pp. 313–318

Moser M., Meier H., Lotter M., Weidner S. (2002) Geotechnical aspects of deep-seated mass movements in Austria. In: Rybář J. et al. (eds.). Landslides – Proceedings of the 1st European Conference on Landslides, Prague, Czech Republic, June 24–26, 2002. – Swets & Zeitlinger, pp. 423–430. Lisse

Moser M. (2003) Geotechnical measurements for assessment of the kinematic and long-term behaviour of unstable mountainsides. In: Natau O., Fecker E., Pimentel E. (eds.). Geotechnical Measurements and Modelling. Proceedings of the International Symposium on Geotechnical Measurements and Modelling, 23–25 September 2003, Karlsruhe, Germany, A.A. Balkema, pp. 217–223

Radbruch-Hall D.H., Varnes D.J., Colton R.B. (1977) Gravitational spreading of steep-sided ridges ("sackung") in Colorado. Journal of Research of U.S. Geological Survey 5:359–363

Sassa K., Fukuoka H., Shuzui H. (2000) Field Investigation of the slope instability at Inca's World Heritage, in Machupicchu, Peru. Landslide News 13:37–41

Vilímek V., Zvelebil J. (2002) Slope instability at Machu Picchu: Ideas and Questions. Acta Montana 19:75–89

Vilímek V., Zvelebil J., Klimeš J., Patzelt Z., Astete F., Kachlík V., Hartvich F. (2007) Geomorphological research of large-scale slope instability at Machu Picchu, Peru. Geomorphology 89:241–257

Zvelebil J., Stemberk J. (2000) Slope monitoring applied to rock fall management in NW Bohemia. In: Bromhead, E. et al. (eds.), Landslides in Research, Theory and Practice, Proc. 8th Int. Symp. on Landslides, Vol. 3, Thomas Telford, London, pp. 1659–1664

16 Geophysical Surveys at Machu Picchu, Peru: Results for Landslide Hazard Investigations

Melvyn Best, Peter Bobrowsky, Marten Douma, Victor Carlotto and Walter Pari

Abstract Geophysical methods are being used more frequently to assess slopes for landslide hazard potential, especially in areas where traditional methods such as trenching and drilling are either difficult to employ or not allowed. This paper presents the results of DC resistivity, electromagnetic (EM) and ground penetrating radar (GPR) surveys to map fractures and zones of weakness in crystalline bedrock at Machu Picchu, Peru. DC resistivity surveys were carried out along the upper 8 switchbacks of the Hiram Bingham road leading to the sanctuary as well as across the sanctuary. EM surveys were carried out along the upper 3 switchbacks and across the sanctuary. EM surveys were carried out at several other locations within the sanctuary but the data were not sufficient to allow detailed interpretations. GPR surveys were carried out over the main and lower plaza areas. Inversion of the resistivity data located several lower resistivity zones along the switchbacks. These zones were associated with water seeping out of the rock in ditches. The water is confined to the upper switchbacks which was consistent with the disappearance of lower resistivity zones in the lower switchbacks. EM results along the switchbacks, although more subtle to recognize, located several coincident zones of lower resistivity. The GPR data provided information on the unconsolidated sediment above bedrock and the bedrock topography within the plazas. There is presently no evidence on whether any of the mapped fractures have been active in the recent past.

Keywords Geophysics • Landslides • Peru • Electromagnetic • Resistivity

16.1 Introduction

The UNESCO World Heritage Site of Machu Picchu, Peru, the royal estate of the Inca ruler Pachacuti in the 1400's, remained covered by vegetation and abandoned in the jungle for hundreds of years following the Spanish occupation of Peru (Wright and Zegarra 2000). Discovered early in the last century, the site is now host to some 1 million tourists per year. Recent shallow

Melvyn Best (✉)
Bemex Consulting International, Canada

Peter Bobrowsky
Geological Survey of Canada, Ottawa, Canada

Marten Douma
Geological Survey of Canada, Ottawa, Canada

Victor Carlotto
InstitutoGeologico Minero y Metalurgico de Peru

Walter Pari
Instituto Geologico Minero y Metalurgico de Peru,
Lima, Perú

K. Sassa, P. Canuti (eds.), *Landslides – Disaster Risk Reduction*,
© Springer-Verlag Berlin Heidelberg 2009

translational landslides, rock falls and debris torrents in the area have drawn international attention to the region surrounding the site and the neighboring town of Aguas Calientes (Klimes et al. 2007). The impact of the failures has ranged from significant including the loss of life (11 individuals in 2004) to economic concerns involving closure of the only road access between the site and the outside world (Hiram Bingham Road failure in 1996).

The additional potential threat for large-scale landslide events affecting the archaeological site itself prompted the Instituto Geologico Minero y Metalurgico de Peru (INGEMMET) to initiate a series of multi-national and multi-disciplinary studies to assess the slope instability conditions of the site. This included geomorphological studies (Vilimek et al. 2005), surface monitoring (Canuti et al. 2005), geotechnical evaluation (Sassa et al. 2005) as well as an evaluation of the sub-surface conditions in the area. This paper discusses the efforts and results of this latter geophysical work. INGEMMET in cooperation with the Geological Survey of Canada (GSC) and under the auspices of the Canadian International Development Agency (CIDA) began a multi-year, multi-parameter shallow geophysical assessment program at Machu Picchu in 2003. Geophysical and other remote sensing techniques are an essential component of this integrated study because standard trenching and drilling techniques are not permitted at the site. The data collected will be used to enhance other data collected by complementary studies conducted by collaborative international scientific and engineering teams.

The objectives of this study are to determine geological parameters such as bedrock faults and fractures, overburden lithology and thickness, etc. that are important for understanding potential landslide hazards in the area. The aim of this paper is, therefore, to present the results of the geophysical surveys in terms of these geological parameters. We focus on two of the surveys carried out where there were sufficient data to address the objectives - the switchbacks and the main plaza.

16.2 Geological and Geographical Setting

The Machu Picchu world heritage site is located approximately 100 km north of Cusco, Peru. The site is perched high in the Andes at an elevation of approximately 2500 m above sea level. The archaeological site straddles a ridge stretching between the peaks of Machu Picchu to the south and Huayna Picchu to the north. Access to the site from the town of Aguas Calientes located in the valley some 500 m below Machu Picchu is along a steep road consisting of multiple switchbacks. The slopes are covered with thin (1–2 m thick) overburden consisting mainly of rubble. The area has poorly developed soils, moist tropical conditions, and localized high annual precipitation. The high relief topography in the area is underlain by part of the Vilcabamba Batholith, a white grey colored granitic complex dated by Rb/Sr to be about ±246 Ma (Carlotto et al. 1999). The granitic complex is cut by several large faults and is characterized by extensive jointing. Landslides and debris flows are common occurrences throughout this region. Both faults and joints are thought to be primary contributors to rock slope instability in the area.

16.3 Geophysical Surveys

The specific objectives of the geophysical study were to determine thickness and type of overburden as well as to map fractures, faults, structure, slip planes and lithology within the bedrock. Additional archaeological objectives were to locate buried construction items, particularly large foundation blocks, voids and old walls within the sanctuary.

In order to achieve these objectives several geophysical methods were employed at the site (cf. Brooks and Pilon 1995). Geophysical methods have been used to map landslide-prone areas for many years. Recent examples include papers by Wang and Lu (2002), Lapenna et al. (2005), Pant et al. (1999), Sendlhofer et al. (1990), Hyde et al. (1997), and Godio and Bottino (2000). Most of these studies, however, use a single geophysical method to map the geological features. One of the best examples employing multi-parameter geophysical methods to study a single landslide is a paper by Bichler et al. (2004). These authors showed that an integrated approach using ground penetrating radar (GPR), DC resistivity, seismic reflection and seismic refraction surveys to map subsurface geology of the Quesnel Forks landslide in central British Columbia, Canada, provided significantly more information than any one of the systems used on their own.

The present study employed electromagnetic (EM), DC resistivity and ground penetrating radar (GPR) geophysical methods, although not all three methods were used at each location on the site. Additional geological results, slope stability implications and archaeological applications of this project appear elsewhere (Mamani et al. 2005; Carlotto et al. 2007)

16.3.1 Acquisition

Geonics EM-31 and EM-34 systems (Geonics 1991; McNeill 1980) operating in the horizontal coplanar (vertical dipole) mode were used to collect the EM data. EM-31 in-phase (ppt) and conductivity (mS/m) data were collected at a spacing of 3–5 m. EM-34 conductivity data (mS/m) were collected using 10 m and 20 m transmitter-receiver separations. The EM-34 station spacing was 10 m for the 10 m separation and 20 m for the 20 m separation. The plotting point for the EM-31 and EM-34 data was the mid-point between the transmitter and receiver.

A 48 electrode Iris Syscal DC resistivity system with a 5 m electrode separation was used to collect the DC resistivity data (Iris 2006). Apparent resistivity data were collected using a Wenner array with "a" values between 5 m and 75 m. Lines longer than the array length of 235 m (5 m × 47 electrode spacing) were acquired by continuously moving the back 24 electrodes to the front until the entire line was surveyed. The data were then concatenated to produce an apparent resistivity profile along the entire line.

A Sensors and Software PulseEkko 100 system using a 100 MHz antenna and a pulser voltage of 400 V was used to collect the GPR data (Sensors and Software 1999). The GPR system was operated with the antennae perpendicular to the line direction. No common midpoint (CMP) velocity analysis was carried out so a radar velocity was set at 0.1 m/ns. The transmitter-receiver separation was fixed at 1 m and the two antennae were moved together in steps of 25 cm. The measurement point is located at the midpoint between the transmitter and receiver antennae.

Figure 16.1 shows a photo of the switchbacks leading to the sanctuary at Machu Picchu as well as the location of the resistivity survey.

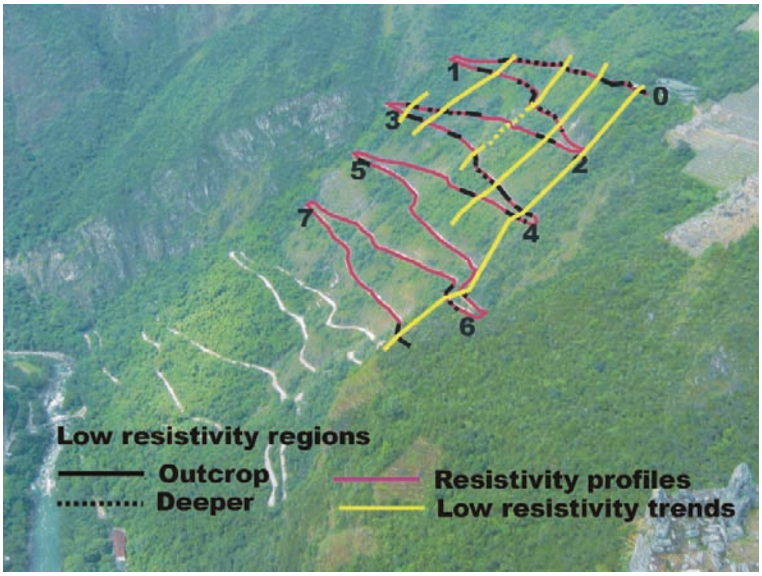

Fig. 16.1 Location of resistivity survey lines and the low resistivity areas along the switchbacks

16.3.2 Processing

The EM-31 and EM-34 data required little processing. The EM-31 data were plotted as conductivity (mS/m) and in-phase (ppt) profiles and the EM-34 data were plotted as conductivity (mS/m) profiles. The EM-31 conductivity data for the temple grid and main plaza grid were plotted as images.

The Syscal DC resistivity data were downloaded into Res2Dinv software for plotting and inversion (Loke and Barker 1996). The Res2Dinv program generates a 'best fit' resistivity model of the earth from the apparent resistivity profiles. Res2Dinv plots have the apparent resistivity profile of the field data at the top, the computed apparent resistivity profile from the best fit model in the middle and the best fit resistivity model at the bottom. When topography is included in the model only the best fit resistivity model is plotted.

The GPR data are stored on a PC during acquisition. These data files can be plotted as GPR sections which are plots of two way travel time (vertical axis) versus position of transmitter-receiver midpoint (horizontal axis). Depth (m) can be plotted on the vertical axis as well using the velocity of 0.1 m/ns. Processing of the GPR data was limited to trace averaging and filtering.

16.4 Results and Discussion

In this paper we concentrate on the switchback lines and main plaza area since they were two of the three areas surveyed in greatest detail. The final processed geophysical data discussed above provides the basis for the following discussion.

16.4.1 Switchbacks

The data collected along the switchbacks consisted of eight DC resistivity lines (lines 0–7) and EM-34 data (20 m transmitter-receiver separation) along lines 0, 1 and 2 (Fig. 16.1).

16.4.1.1 Resistivity Data

An apparent resistivity section is calculated from the inversion software and compared with the field apparent resistivity section. When the calculated and field apparent resistivity sections agree within a prescribed error then the model used to generate the calculated apparent resistivity section is called the best-fit resistivity model. Fig. 16.2 is a composite plot of all 8 lines showing the best-fit resistivity models with topography effects included. There are no significant differences between these plots and the best-fit model plots without topography since the topographical surface along each switchback, although steep and inclined, has no local relief and therefore is a simple plane surface.

The blue colours in Fig. 16.2 represent lower resistivity values. The average or background resistivity associated with these cross sections is around 4000 ohm-m which is consistent with granites. The lower resistivity values are only "relatively" low since the values vary between 700 and 1000 ohm-m, or 7–4 times lower than the background value. These low resistivity zones outcrop at some locations and occur at depth at other locations along the sections. The location of these low resistivity zones is shown in Fig. 16.1. The solid black lines are areas where the low zones outcrop and the dashed black lines are where the low zones are at depth. The yellow lines show the trends of the low resistivity values. It is interesting to note that all these zones only occur along the upper switchbacks, except for the continuous trend on the north side (right hand side) of the survey area that seems to follow a ridge that starts near the hotel (north end of line) on line 0.

The low resistivity zones are likely associated with water in minor fractures and/or shears within the granites. These fracture zones are not highly altered or they would have lower resistivity values. The water that percolates into these fractures at higher elevations apparently does not migrate all the way down the mountain which is one reason why the low resistivity zones are confined to the upper switchbacks. This is consistent with visual observations of where water was seeping out of the bedrock into the ditches along the road. The continuous trend on the north side may be associated with a larger fracture that allows water to further migrate. The ridge may structurally control this fracture.

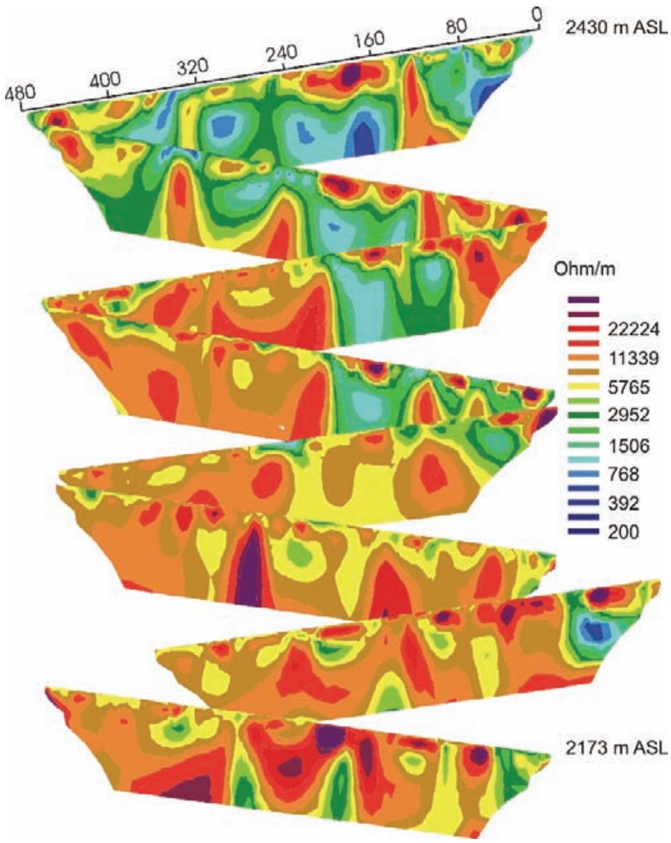

Fig. 16.2 Composite plot of topographically corrected best fit resistivity profiles along the switchbacks. Survey lines are show in Fig. 16.1

16.4.1.2 EM-34 Data

EM-34 data were collected along lines 0, 1 and 2 using a transmitter-receiver separation of 20 m. The apparent conductivity plot for line 2 is given in Fig. 16.3. The average background conductivity along these lines is around 0.75–1.0 mS/m or approximately 1400–1000 ohm-m which is lower than the resistivity computed from the resistivity inversions but still quite resistive. Although there are subtle variations in conductivity along these lines they are difficult to correlate to the geology. The EM-34 method had limited success in mapping fractures or shear zones on the switchbacks. Indeed both the EM-31 and EM-34 systems had limited success in the resistive environment of Machu Picchu. This is due to the high resistivity of the granite and the "relatively" high resistivity values associated with the fractures.

16.4.2 Main Plaza Area

We shall discuss the GPR data in this section since the EM-31 data did not provide any more information than that discussed previously. The data collected here consisted of 6 GPR lines in the main plaza and 3 GPR lines in the lower plaza. The lower plaza survey was related to archaeological studies and will not be discussed here.

16.4.2.1 GPR Data

Figure 16.4 shows the location of the GPR lines across the main and lower plazas. Figure 16.5 is a photo of the GPR equipment used at Machu Picchu. Figure 16.6 is a plot showing the GPR sections for the 5 lines across the main plaza. There are 3

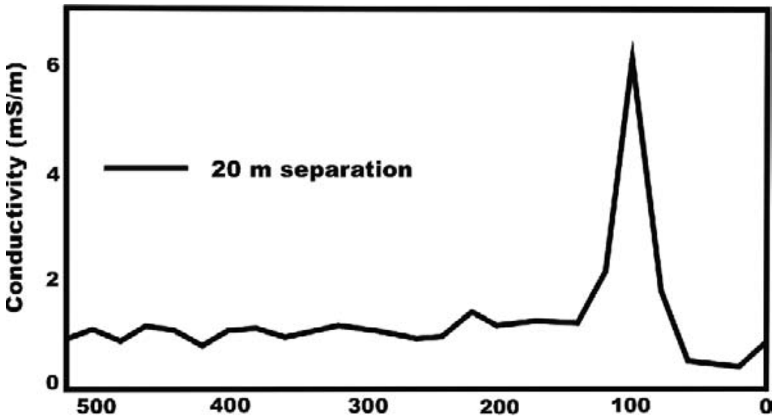

Fig. 16.3 Conductivity measured by EM-34 along Line 2

Fig. 16.4 Location of the GPR (Ground Penetration Radar) lines across the plazas

GPR facies indicated on these plots. The first (red) corresponds to the near surface soil and has a thickness between 0.5 and 1 m. Several weak reflectors can be seen that parallel the ground surface. The second facies lies beneath the soil and continues down to the bedrock. It consists mostly of broken reflectors, although there are several continuous reflectors within this facies. The disorganized nature of this facies is attributed to the rock debris and fill that was placed above bedrock during construction of the site. Trenching within the site confirmed the presence of such debris. The continuous reflectors are assumed to be locations where the workers placed clay and other soil to smooth out the debris-covered areas. The third facies represents the bedrock. There is considerable relief on the bedrock surface. There are broken reflectors within the bedrock and several steeply dipping events. These steep events are most likely associated with reflections from the lower walls of the terraces since they occur at the ends of the lines.

16.5 Conclusions

The granite bedrock underlying the archaeological site of Machu Picchu is very resistive with average values between 3000 and 4000 ohm-m and often with much higher resistivity values. Overburden, where it exists, is generally thin. The plazas have been filled with rock debris and covered with a layer of soil. Most likely the agricultural terraces on both east and west slopes of the sanctuary are similar in nature.

16.5.1 EM

Highly resistive bedrock with a thin overburden cover is a difficult environment for electromagnetic techniques. The EM-31 system provided limited information on overburden thickness and lithology and no information on bedrock fractures. Minor variations in the conductivity readings for the EM-31 do not appear to correlate with any geological features.

The subtle variations in the EM-34 conductivity values along the switchback lines correlate with the lows associated with the DC resistivity data. However, these subtle features may have been overlooked if the DC resistivity data were not available for comparison.

Fig. 16.5 Sensors, 200 MHz transmitter and receiving antenna assemblies of GPR in Machu Picchu

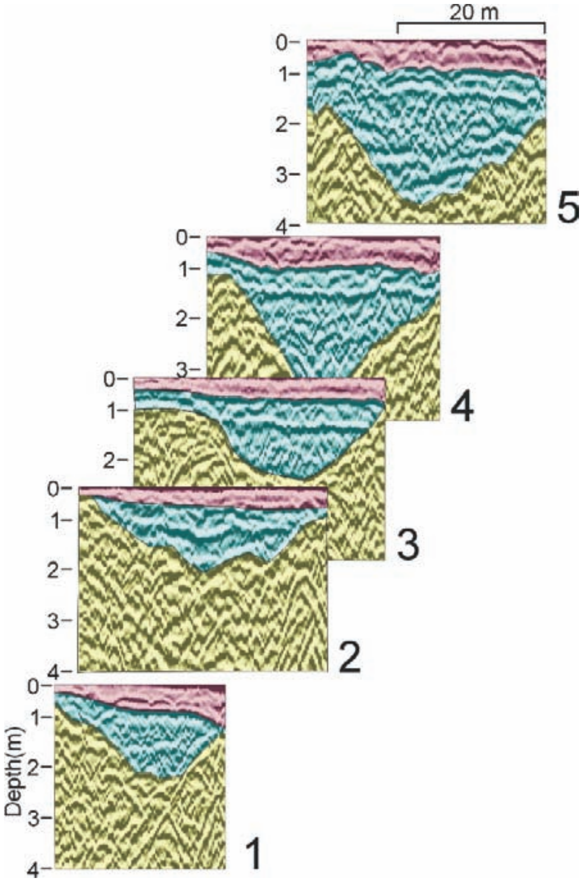

Fig. 16.6 Interpretation of the parallel radar profiles across the Planza in Machu Picchu

16.5.2 DC resistivity

The DC resistivity system provided useful information on potential locations of fractures/shear zones within the crystalline bedrock. Low resistivity zones associated with these fractures correlates line to line along the switchbacks. These low resistivity values are between 500 and 1000 ohm-m, indicating these zones are not very conductive. Significant clay alteration on the walls of the fractures is not likely since the resistivity values would be lower in that case. The low resistivity zones are most likely associated with relatively fresh water within the fractures. This is consistent with the fact that these zones are only observed on the upper switchbacks where visible surface water can be observed in the ditches.

16.5.3 GPR

The GPR data collected in the main and south plazas provided detailed information of the material beneath the surface to depths of 5 m or more. There is a thin veneer of soil (0.5–1 m thick) at the surface of these two plazas. Rock debris and rubble lie beneath the soil cover. The rubble and debris was used as fill to level out the bedrock topography in these areas. The fill can be as thick as 3.5 m in some sections of the main plaza. The more continuous reflectors seen within this debris facies are thought to be areas where clay/soil was placed to smooth out the debris, making it easier to move material within the plaza area. The reflectors within the bedrock are erratic and not very continuous but provide an indication that GPR may be able to locate fractures within the bedrock.

16.5.4 Landslide Potential

The geophysical evidence collected at this site provides a fairly good indication of the nature of the subsurface materials including both bedrock and overburden. Although isolated vertical fracturing was observed in the bedrock, there is no indication of a deep incipient or existing failure plane cutting through the granite. Similarly, although the site has been subjected to several shallow, surface failures in the past several years, there was no evidence in the overburden to indicate that the site is subject to extensive surficial failure. No parallel or subparallel to slope features were observed in the geophysical data. It is our belief that although the site and region are subject to debris flows and small slides, proper drainage and site management provides the best mitigative measures to reduce slope instability at this important site. Evidence for, and the likelihood of deep-seated catastrophic failure in the past or near future is lacking and such events are unlikely to occur.

There is presently no information on whether any of the fractures located during this study have been active in the recent past. Future investigations within the sanctuary will have to rely on long term monitoring of these and other known faults and fractures because trenching and drilling are forbidden. Monitoring at the site will require the use of GPS, strain gauges and remote sensing methods.

References

Bichler, A., Bobrowsky, P.T., Best, M.E., Douma, M., Hunter, J., Calvert, T. and Burns, R., 2004. Three-dimensional mapping of a landslide using a multi-geophysical approach. The Quesnel Forks landslide. Landslides, 1, 29–40.

Brooks, G.R. and Pilon, J.A., 1995. Ground penetrating radar survey of the Katz Slide, southwestern British Columbia; Cordillera and Pacific margin- Cordillere et marge du pacifique. Geological Survey of Canada, Report: 1995-A, 33–40.

Canuti, P., Margottini, C., Mucho, R., Casagli, N., Delmonaco, G., Ferretti, A., Pollino, G., Puglisi, C. and Tarchi, D., 2005. Preliminary remarks on monitoring, geomorphological evolution and slope stability of Inca Citadle of Machu Picchu (C101-1). In: K. Sassa, H. Fukuoka, F. Wang and G. Wang (eds.), Landslides: risk analysis and sustainable disaster management. Springer Verlag, Berlin, pp. 39–47.

Carlotto, V., Cardenas, J., Romero, D., Valdivia, W., and Tintaya, D., 1999. Geologia de los Cuadrangulos de Quillabamba y Machupicchu. Boletin No. 127, Serie A: Carat Geologica Nacional, INGEMMET, Instituto Geologico Minero y Metalurgico.

Carlotto, V., Bobrowsky, P., Best, M., and Douma, M., 2007. An assessment of geophysical methods for landslide studies. Proceedings of the international Symposium on Landslide Risk Analysis and Sustainable Disaster Management (IPL 2007), United Nations University, Tokyo, pp. 39–44.

Geonics, 1991. EM-31 Operating Manual: Geonics Limited, 1745 Meyerside Drive, Mississauga, Ontario, Canada.

Godio, A. and Bottino, G., 2000. Electrical and electromagnetic investigation for landslide charcterisation; monitoring, modelling and mapping of mass movements. Physics and Chemistry of the Earth, Part C: Solar-Terrestial and Planetary Science, 26(9), 705–710.

Hyde, C.S.B., Hunter, J.A., Lawrence, D.E. and Aylsworth, J.M., 1997. Correlating geophysical and geotechnical parameters of landslide-prone Champlain Sea sediments, Ottawa valley. *P*rogram with Abstracts – Geological Association of Canada; Mineralogical Association of Canada; Canadian Geophysical Union, Joint Annual Meeting, 22, 71.

Iris, 2006. Iris systems website: www.iris.instruments.com.

Klimes, J., Vilimek, V. and Vlcko, J., 2007. Debris flows in the vicinity of the Machu Picchu village, Peru. In: K. Sassa, H. Rukuoka, F. Wang and G. Wang (eds.), Progress in Landslide Science, Springer Verlag, Berlin pp. 313–318.

Lapenna, V., Lorenzo, P., Perrone, A., Piscitelli, S., Rizzo, E. and Sdao, F., 2005. 2D electrical resistivity imaging of some complex landslides in Lucanian Apennine Chain, southern Italy. Geophysics, 70(3), B11–B18.

Loke, M.H. and Barker, R.D., 1996. Rapid least-squares inversion of apparent resistivity pseudosections by a quasi-Newton method. Geophysical Prospecting, 44, 131–152.

Mamani, R.M., Caillaux, V.C., Pinto, W.P., Oviedo, M.J., Douma, M., Best, M. and Bobrowsky, P., 2005. The application of ground penetrating radar (GRP) at Machu Picchu, Peru (C101-1). In: K. Sassa, H. Fukuoka, F. Wang and G. Wang (eds.), Landslides: Risk Analysis and Sustainable Disaster Management, Springer Verlag, Berlin, pp. 55–59.

McNeill, J.D., 1980. Electromagnetic terrain conductivity measurement at low induction numbers. Technical Note TN-6, Geonics Limited, Ontario, Canada.

Pant, S.R., Li, T., Wagner, A., Fu W. and Jiaman, C., 1999. High resolution seismic refraction data interpretation; an example from Xiakou landslide, Sichuan, China. Journal of Nepal Geological Society, 19, 31–40.

Sassa, K., Fukuoka, H., Wang, G., Wang, F., Benavente, E., Ugarte, D. and Astete, F.V., 2005. Landslide investigation in Machu Picchu World Heritage, Cusco, Peru (C101-1). In: K. Sassa, H. Fukuoka, F. Wang and G. Wang (eds.), Landslides: risk analysis and sustainable disaster management, Springer Verlag, Berlin, pp. 25–38

Sendlhofer, G., Grummt, S. and Roth, T., 1999. Application of near-surface reflection seismic surveys in order to investigate landslides. BHM.Berg- und Huettenmaennische Monatshefte, 144(12), 476–482.

Sensors & Software, 1999. PulseEKKO 100 RUN, User's Guide version 1.2, Manual 25. Sensors & Software Inc., Mississauga, Ontario, 66p.

Vilimek, V., Zvelebil, J., Klimes, J., Vlcko, J. and Astete, F.V., 2005. Geomorphological investigations at Machu Picchu, Peru (C101-1). In: K. Sassa, H. Fukuoka, F. Wang and G. Wang (eds.), Landslides: risk analysis and sustainable disaster management. Springer Verlag, Berlin, pp. 49–54.

Wang, J. and Lu, J., 2002. The use of ground-penetrating radar in environmental geologic hazard surveys. Geology and Prospecting, 38(3), 70–73.

Wright K.R., and Valencia Zegarra, A., 2000. Machu Picchu: A Civil Engineering Marvel. ASCE Press, Reston, VA.

Integration of VHR Satellite Images with Field Data for the Analysis of Debris Sheet Instability in the Machu Picchu Area

17

Nicola Casagli, Riccardo Fanti and Gaia Righini

Abstract Since 1997 the Machu Picchu area has been in the spotlight for its slope instability. Firstly, Carreno and Bonnard (1997) described the general geological and geomorphological condition, then the studies of Sassa et al. (2001, 2002, 2005) contributed to define the interpretation of the structures, as the result of the detection of a deep-seated slow slide involving the archaeological area. However, the attention of these studies focused on the condition of the entire slope, with a minor consideration for the small and shallow landslides, even if debris flows often occur and cause damages and real catastrophes. Debris-flows occurred in 1995–1996, along the access road to the site, and in 2004, when the day after Easter a channelized debris flow produced 11 casualties in Aguas Calientes, the close tourist town. As part of the ICL Machu Picchu International Project, an integrated study of the instability condition of the debris was established: in this work the results deriving from both analyses of VHR satellite data and field surveys are shown.

Keywords Machu Picchu • Satellite remote sensing • Landslides • Slope instability

17.1 Introduction and Methods

The Citadel of Machu Picchu represents the most famous monument of the Inca civilization. It stands 2,430 m above sea-level in the middle of a tropical mountain forest in the eastern slopes of the Andes, overhanging the Urubamba river, which is a tributary of the Amazon river (Fig. 17.1). The archaeological remains were revealed to the modern world after the 1911 Hiram Bingham's expedition. The site was included in the UNESCO World Heritage List in 1983, for its natural and cultural relevance and has since become one of the main destinations for international tourism. The direct and indirect income deriving from tourism constitutes a significant component of the Peruvian economy, and the relationships between the cultural and natural heritage, land use and visitor pressure have become a major issue of concern for national and international authorities.

A symbol of this problem is the town of Aguas Calientes (also known as Machu Picchu Pueblo), located at the end of the railway from Cusco; the village is linked to the archaeological area via a 8 km road (Carretera Hiram Bingham) running on the

Nicola Casagli (✉)
Department of Earth Sciences, University of Firenze, Italy

Riccardo Fanti
Department of Earth Sciences, University of Firenze, Italy

Gaia Righini
Department of Earth Sciences, University of Firenze, Italy

© Springer-Verlag Berlin Heidelberg 2009

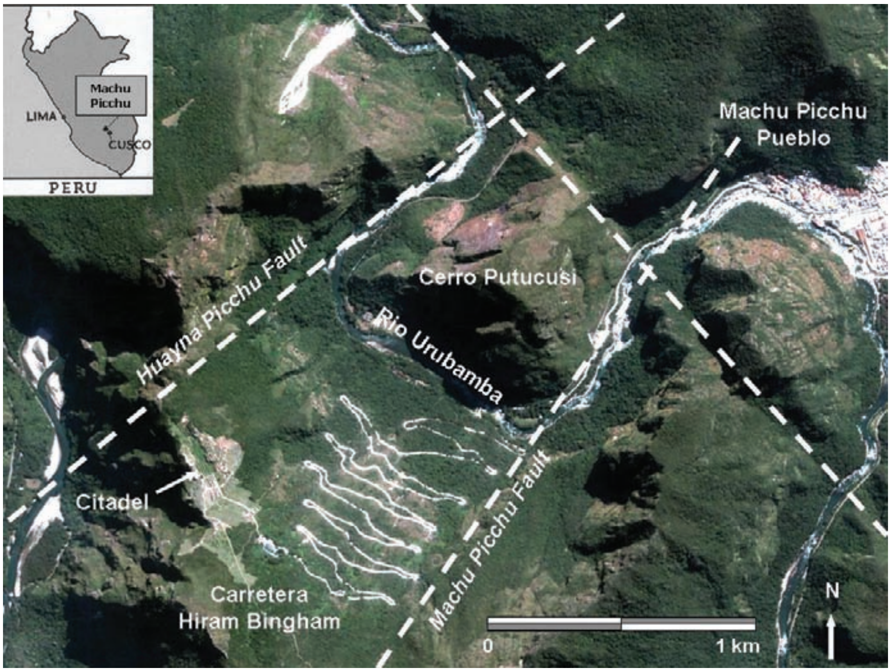

Fig. 17.1 The Machu Picchu area in a Quickbird satellite image (18 May 2004 – bands 3-2-1 in RGB colors)

left bank of the Urubamba river. The village was built without urban planning on a fan along the Urubamba river at the base of some granitic faces, in a site of very high risk in terms of flash flooding and rockfall hazard. On April, 10th 2004 a major debris flow, channelled in the Alcamayo stream, devastated the village, causing 11 fatalities and damaging the railway (Carreno and Kalafatovich, 2006; Vilimek et al., 2006).

The Citadel is also affected by slope instability processes, with extensive deep-seated slow deformations and frequent shallow debris flows. On December, 26th 1995 a rock fall-debris flow occurred on the Carretera Hiram Bingham interrupting the traffic from the railway station of Aguas Calientes (Carreno and Bonnard, 1997). Some recent studies, developed within the ICL International Project, were focused on the deep-seated, slow landslides affecting the citadel and the Carretera (in Sassa et al., 2005); whereas, this work focuses on the shallow debris instability, analyzed through the integration of results deriving from very high resolution (VHR) optical satellite data and field surveys.

Traditionally, optical satellite data represent a valuable tool for environmental monitoring due to the multi-spectral capability, the synoptic view, the high revisiting time and the medium spatial resolution. In new generation of sensors two of these characteristics have been substantially improved: (a) the concept of "multi-temporal resolution" has been modified by the possibility of programming the data acquisition, allowing information to be obtained shortly after an event, although acquisition still depends on the capability of the satellite and on the cloud cover; (b) with the introduction of the panchromatic band, the spatial resolution has increased to approximately 70 cm, decisively improving the possibility of deriving detailed ground observations of small-scale geomorphological processes.

In this paper VHR images have been used to produce a debris flow inventory. Quickbird (from DigitalGlobe) images were acquired in order to monitor frequent fast-moving, rock falls and debris flows triggered by intense rainfall, which have caused extensive damage in recent years. The Quickbird satellite, launched in October 2001, acquires panchromatic (black and white) images with a resolution of 70 cm in the range 0.45–0.9 μm of the electromagnetic spectrum, as well as multi-spectral images (4 bands) with a resolution of 2.44 m in the visible (bands 1, 2 and 3) and near infrared (band 4) covering a minimum surface area of 16.5 × 16.5 km.

The data deriving from satellite data analysis have been integrated with the information gathered during four field surveys, carried out in the years 2002–2005. The field works contemplated the inspection of the most recent debris flow events in the area and the data collection aimed at the reconstruction of geological and geomorphological features, with a special attention to the debris sheet. In particular, starting from the field data of the Carretera Hiram Bingham slope, two aspects have been handled: the interpretation of the distribution of debris thickness and the assessment of the effectiveness of the runoff drainage system. Both the topics and the potentiality of their integration were approached and the results constitute the first step for an exhaustive debris flow hazard assessment in this area, where the interactions between slope instability and land use can produce some very critical conditions.

The presence of the debris sheet is a direct consequence of the general geological conditions. In the area the Machu Picchu Batholith (also known as the Vilcabamba Batholith), a large intrusive body formed of white-grey granites and granodiorites, outcrops widely. Granite constitutes the highest relief, such as the Cerro Machu Picchu (3,066 m a.s.l.), the Huayna Picchu (2,678 m a.s.l.) and the Putucusi (2,560 m a.s.l.), which are the three peaks surrounding the archaeological site. The batholith has a complex structural history, due to the cooling processes and superimposed tectonic phases that have determined the present structure, with a NE-SW major joint system, including the Huayna Picchu and the Machu Picchu faults (Fig. 17.1). The intersection of this system with a regional NW-SW trend of master joints creates a regular network that controls the course of the Urubamba river. At a more local level, other joint sets become relevant and the most important dip toward NE, parallel to the slope below the citadel.

The rock mass is highly affected by chemical weathering as a consequence of the feldspar sericitization and, more frequently, of the limonitization. These chemical processes, added to the physical weathering, caused the local formation of variable thickness debris sheets, that represent the source material for shallow landslides.

17.2 Analyses of VHR Satellite Data

For the characterization of the 10 April 2004 debris flows, a multi-temporal analysis of Quickbird panchromatic and multi-spectral data was carried out: an archive image dated 18 June 2002 was available, while a new acquisition was scheduled for the middle of April 2004 with a good image being obtained on 18 May 2004.

Debris flow reconnaissance was the main purpose of the analysis and interpretation of the images. This involved aspects such as: the size of the features, their texture in the image, the variety of forms and the contrast in terms of the difference in spectral characteristics between the landslides and the surroundings.

Images were geocoded and orthorectified, and a radiometric enhancement was carried out on both panchromatic and multi-spectral images in order to develop the most suitable product for a visual interpretation. Afterwards, a field survey was conducted in the investigated area in order to validate the interpretation of the satellite images. Field observations were particularly focused in the areas of Aguas Calientes and of the Carretera Hiram Bingham, due to their high risk conditions.

Figure 17.2 (top & middle) shows the area of Alcamayo stream: the comparison of the satellite images of 2002 and 2004, using Bands 4-3-2 in RGB colours highlights the debris flow deposits related to the event of 10 April 2004. Their size and distribution can be detected with the panchromatic band data (Fig. 17.2 – bottom): six debris deposits were left in the channel of the Alcamayo after the event. Of these, the area labelled as number 4 attracts particular attention, since its position is just downstream of a confluence. In fact, this may have been the decisive factor concerning the damage in Aguas Calientes, as it may have produced an ephemeral dam that subsequently caused a flash flood after its sudden collapse, as supposed also by Vilimek et al. (2006). The area of the debris deposits measured on

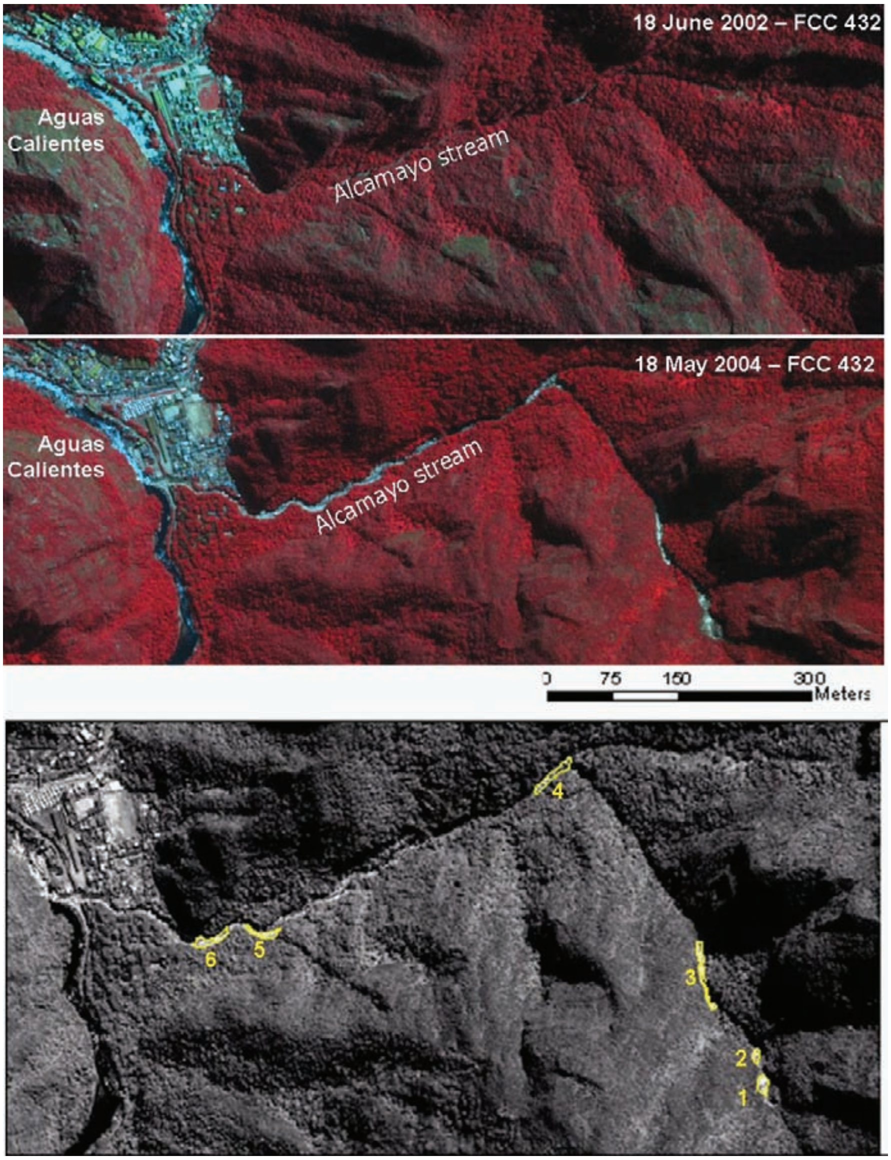

Fig. 17.2 Alcamayo stream and Aguas Calientes: comparison between the two Quickbird satellite images dated 18 June 2002 (*Top*) and 18 May 2004 (*Middle*), Bands 4-3-2 in RGB colours, and Panchromatic band with debris deposits (*Bottom*)

the Quickbird image is about 4,500 m^2 (Casagli et al., 2006) and it agrees with the evaluation of Carreno and Kalafatovich (2006) and Vilimek et al. (2006).

Figure 17.3 (top, left) shows the northern slope of the Huayna Picchu peak, where a major debris flow occurred within the period under investigation. The landslide is a large debris flow (length: 400 m; area: about 40,000 m^2): the event happened during the 2002–2003 austral summer, so it is not related to the rainfall which caused the Alcamayo flows and flood on April 2004. In fact, it appears in a picture taken in October, 2003 (Fig. 17.3 – top, right).

Figure 17.3 (bottom) shows a detail of the area mostly investigated during the field surveys, the northern slope of Cerro Machu Picchu and the Carretera Hiram Bingham: in the satellite image dated 18 May 2004 (panchromatic band) several small scars of rock falls and debris flows have been detected in correspondence with the road cuts.

Fig. 17.3 Debris flows and rock falls in the Northern slope of Huayna Picchu (*Top*, *left*: Quickbird satellite image 18 May 2004, Panchromatic band – *Top, right*: Picture taken on October, 1st 2003) and in the Carretera Hiram Bingham (*Bottom*: Quickbird satellite image dated 18 May 2004, Panchromatic band)

17.3 The Characteristics of Debris Sheets in the Area of the Carretera Hiram Bingham

The northern slope of Cerro Machu Picchu shows the evidences of several landslides: large and small rock avalanches, debris slides and debris flows (Canuti et al., 2005; Vilimek et al., 2007).

Among them, the debris flows deserve a special attention: their frequency determines a high risk for the public safety, due to the presence of the Carretera Hiram Bingham, where a lot of buses continuously shuttle for twelve hours a day. The 1995–1996 events are the more recent examples, but similar conditions are visible along the entire road track.

The main sources of debris flow hazard correspond to the sectors of the slope covered with thick debris deposits. For this reason, during the field surveys, the debris sheets were characterized with over 80 measurements (Fig. 17.4), aimed at assessing debris thickness, grain size and permeability.

The reconstruction of the debris thickness isopaches, shown in Fig. 17.5 (left), is an important outcome of the field survey. The existence of at least 250,000 m^3 of weathered debris on a 35° slope is demonstrated. In particular, the SE sector of the Carretera slope contains debris deposits up to 7 m thick and it is the area of highest hazard for new debris flow initiation.

The debris is composed by 30–60% sand matrix and 40–70% granitic blocks (size from some centimetres to 1 m) and its stability is controlled by its strength parameters: if the friction angle can be directly determined (about 38°), it is very difficult

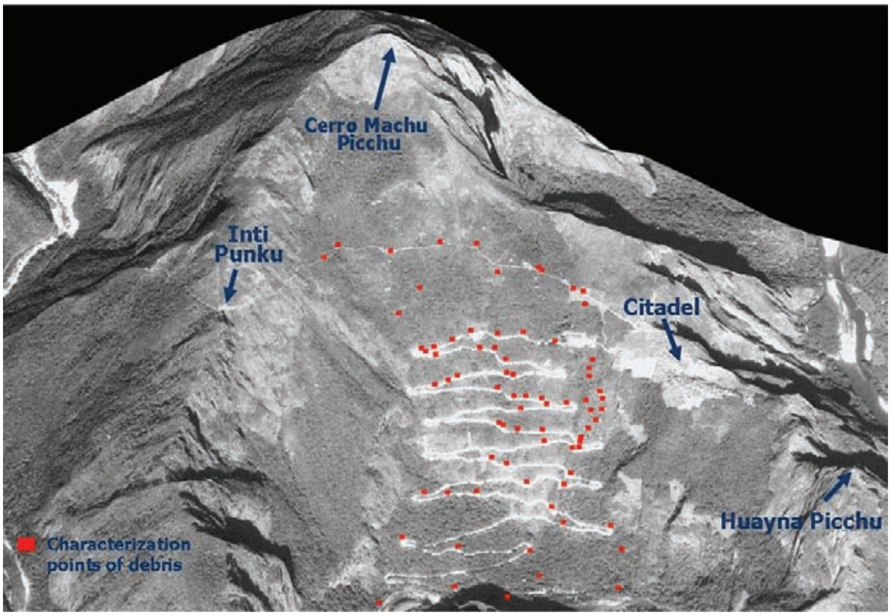

Fig. 17.4 Measure points of debris in the northern slope of Cerro Machu Picchu

to measure the in situ cohesion that guarantee the stability of the deposit also on very steep slopes.

In order to estimate the cohesion value, starting from the thickness and friction angle, a back-analysis with the Skempton and DeLory infinite slope model has been carried out. The debris reaches a significant factor of safety with c = 13 kPa (Fig. 17.5 – right).

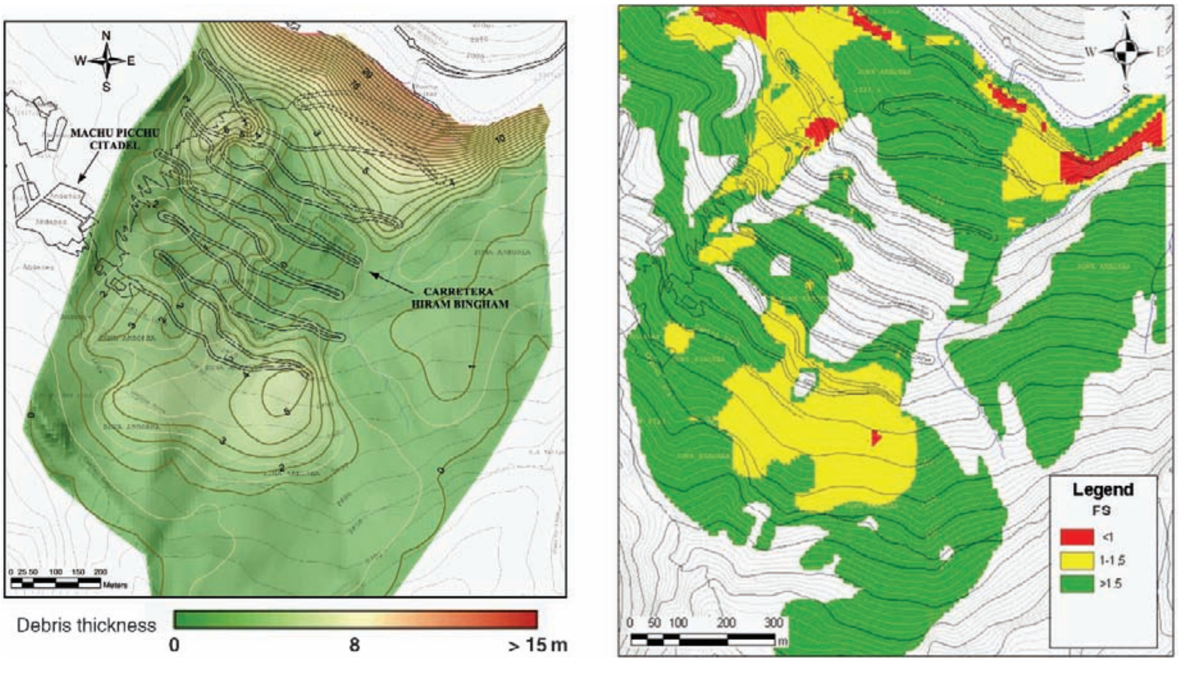

Fig. 17.5 Map of the debris thickness in the northern slope of Cerro Machu Picchu (*left*) and Factor of safety (FS) as result of the Skempton-DeLory back-analysis (strength parameters: Φ = 38° and c = 13 kPa). (*right*)

17.4 Conclusions

The results of this study confirm that the VHR satellite data is capable of detecting superficial landslides, even of small scale, and is very useful for supporting traditional field surveys. The comparison between the 2002 and 2004 Quickbird images allowed us to determine the main instability processes that occurred over this period, specifically within the Rio Alcamayo basin, on the northern slope of the Huayna Picchu and on the northern slope of Cerro Machu Picchu.

The integration of remote sensing data and field observations (debris thickness, geotechnical features, hydrological condition) was also employed to produce detailed maps of the debris cover and to qualitatively assess the instability potential of the future debris flow source areas.

References

Canuti P., Margottini C., Mucho R., Casagli N., Delmonaco G., Ferretti A., Lollino G., Puglisi C., Tarchi D. (2005) Preliminary remarks on monitoring, geomorphological evolution and slope stability of Inca Citadel of Machu Picchu. In: Sassa K., Fukuoka H. Wang F., Wang G. (Eds.), *Landslides. Risk Analysis and sustainable Disaster Management*. ICL-Springer, Berlin, 39–48.

Carreno R., Bonnard C. (1997) *Rockslide at Machu Picchu, Peru*. Landslide News, 10, 15–17.

Carreno R., Kalafatovich C. (2006) *The Alcamayo and Cedrobamba catastrophic debris flow (Juanuary, March and April 2004) in Machu Picchu area*. Landslides, 3, 79–83.

Casagli N., Fanti R., Nocentini M., Righini G. (2006) Assessing the capabilities of VHR satellite data for debris flow mapping in the Machu Picchu area. In: Sassa K., Fukuoka H. Wang F., Wang G. (Eds.), *Landslides. Risk Analysis and Sustainable Disaster Management*. ICL-Springer, Berlin, 61–70.

Sassa K., Fukuoka H., Kamai T., Shuzui H. (2001) *Landslide risk at Inca's World Heritage in Machu Picchu, Peru*. Proceedings UNESCO/IGCP Symposium on Landslide Risk Mitigation and Protection of Cultural and Natural Heritage, Tokyo, 1–14.

Sassa K, Fukuoka H, Shuzui H, Hoshino M (2002) *Landslide risk evaluation in Machu Picchu World Heritage, Cusco, Peru*. Proceedings UNESCO/IGCP Symposium on Landslide Risk Mitigation and Protection of Cultural and Natural Heritage, Kyoto, 1–20.

Sassa K., Fukuoka H., Wang F., Wang G. (Eds.) (2005) *Landslides. Risk Analysis and Sustainable Disaster Management*. ICL-Springer, Berlin, 385 pp.

Vilimek V., Klimes J., Vlcko J., Carreno R. (2006) *Catastrophic debris flows near Machu Picchu village (Aguas Calientes), Peru*. Envronmental Geology, 50, 1041–1052.

Vilimek V., Zvelebil J., Patzelt Z., Astete F., Kachlik V., Hartvich F. (2007) *Geomorphological research of large-scale slope instability at Machu Picchu, Peru*. Geomorphology, 89, 241–257.

Part IV

Parallel Sessions

Global Cooperation Field (1): Technological Development

A Look from Space

18

Nicola Casagli, Veronica Tofani and Robert F. Adler

Abstract Remote sensing can broadly be described as the detecting and measuring of electromagnetic energy emitted or reflected from distant objects. The measured electromagnetic energy which comes from different portions of the electromagnetic spectrum can be used to retrieve information on the properties of the earth surface. The purpose of this chapter is to present an overview of the current application of remote sensing to landslides detection (section 2), monitoring (section 3) and hazard analysis (section 4) and to illustrate how researchers around the world are currently using remote sensing techniques to map, monitor and manage landslides (section 5).

Keywords Remote sensing • Landslide mapping • Monitoring • Hazard assessment • SAR interferometry • Optical imagery

18.1 Introduction

The observation of the Earth from space has found many uses in the natural sciences but it is only in recent years that technological advances have extended the uses to landslides (Singhroy, 1995; Mantovani et al., 1996; Delacourt et al., 1998; Massonnet and Feigl, 1998; Ferretti et al., 2001; Canuti et al., 2004; Lee, 2005; Hong et al., 2007a).

Until now the low spatial resolution of the sensors, the unsuitable wavelengths of the measured electromagnetic energy and the lack of appropriate processing techniques and algorithms did not allow applications for landslides. Mantovani et al. (1996) argued that the use of remote sensing in the study of landslides was not fully exploited, with a limited number of researchers making a full use of multispectral images for evaluating landslide activity.

Even in the late 1990s stereoscopic air-photo interpretation continued to be the most frequent remote sensing tool applied in the mapping and monitoring of landslide characteristics (Metternicht et al., 2005).

Today, rapid advances are making Earth Observation (EO) techniques ever more effective for landslide monitoring, management and mitigation. Applications are originating from nearly all the types of sensors available today; the vey high spatial resolution obtained by optical systems, which are now in the order of tens of centimeters, the launching of SAR (Synthetic Aperture Radar) sensors purposely built for interferometric applications and with lower revisiting times are all leading to rapid developments that make the field extremely promising.

Nicola Casagli (✉)
Department of Earth Sciences, University of Firenze, Italy

Veronica Tofani
Department of Earth Sciences, University of Firenze, Italy

Robert F. Adler
NASA/Goddard Space Flight Center, Laboratory for Atmospheres, Greenbelt, U.S.A

K. Sassa, P. Canuti (eds.), *Landslides – Disaster Risk Reduction*,
© Springer-Verlag Berlin Heidelberg 2009

The types of applications generally depend on the characteristics of the sensors. Optical systems measure energy reflected in the visible, near infrared (NIR) and short wave infra-red (SWIR) portions of the electromagnetic spectrum. Another important aspect regards the distinction of passive and active systems. A passive sensor is one that records radiation emitted from an external source, such as the sun, and which is then reflected from the earth surface back to the sensor. It only acquire data during daylight hours; typical passive sensors are optical systems mounted on satellites. An active sensor instead emits its own radiation towards a target and then measures the return signal. Active sensors can operate day and night and are also considered all-weather systems as they can see through cloud cover. SAR systems are typical active sensors.

18.2 Landslide Detection and Mapping

Mantovani et al. (1996) argued that detection is a general term for mapping landslides within a remote sensing image. It includes two aspects: recognition (is it a landslide?) and classification (what type of landslide is it?).

Recognition of a landslide means whether it is possible to map a landslide, with varying forms and spectral characteristics, within a remote sensing image. Important aspects in the recognition of landslides are the size of the features, their contrast (the difference in spectral characteristics between the landslides and the surrounding areas) and their morphological expression (Mantovani et al., 1996)

Hereinafter the application of remote sensing tools according to their spectral band for the detection and mapping of landslides is described.

Earth observation optical systems are passive sensors, measuring reflectivity originating from a target on the earth surface and from the atmosphere, in a range of wavelengths varying between 0,4-1,1 μm (visible and NIR) and 1,1.-2,5 μm (SWIR). Environmental missions such as Landsat, TERRA-ASTER, SPOT and other environmental optical sensors have been not widely used for individual landslide mapping due to the insufficient spatial resolution. However, they are useful for indirect mapping methods, when the distribution of slope instability factors, such as geomorphology, lithology, land use, may be identified on these satellite images (Mantovani et al. 1996; Casagli et al., 2005). In this sense, medium resolution data have been used for mass movement detection (Scanvic and Girault, 1989; Nagarajan et al., 1998; Kaab, 2002; Liu et al., 2003). The most important characteristic of optical sensors is the spatial resolution, which represents the detail discernible in an image and refers to the size of the smallest possible picture element (pixel) that can be detected.

Most of previous studies aiming at the recognition of landslide features have used aerial photographs (scales varying from 1:50,000 to 1:10,000), in addition to satellite imagery of the Landsat TM and SPOT (Cheng et al., 2004; Lin et al., 2002; Zhou et al., 2002).

New generation very high resolution (VHR) satellite imagery (IKONOS, Quickbird) can provide a powerful tool for a quick reproduction of a regional map up to a scale of 1:2000, with a relatively low cost/benefit ratio due to the fact that these satellites have global coverage and the acquisition cycle is over a short-time period making the images readily available (Casagli et al., 2005; Moretti and Righini, 2004).

Some initial research has been conducted using the 5.8 m resolution IRS-1D (Gupta and Sasha, 2001) or simulated Ikonos data (Hervas et al., 2003; Nichol and Wong, 2008). In Casagli et al. (2005) an interpretation of the Quickbird images of the Machu Picchu area was carried out in order to identify the existence of particularly hazardous debris flows.

Paganini (2004) argues that in areas where conventional stereoscopic aerial photos are not available or updated, current and forthcoming high spatial resolution satellite data may allow large-scale mapping.

Application of the use of optical imagery for landslide detection can be found in Sects. 18.5.1 and 18.5.2.

One of the most promising research fields relative to the measurement of ground movements derives from the development of satellite radar interferometry. Rapid advances in both the remote sensing sensors and the data processing algorithms have allowed significant results to be achieved in recent years, underscored by the numerous applications shown in the following sections. The most common uses range from the mapping, monitoring and updating of regional landslides, ground subsidence monitoring and time series investigations of large landslides with important economic or social impact to regional landslide monitoring.

Landslide mapping at regional scale is certainly a field that benefits from this technique. Regional landslide inventories, traditionally based on aerial photo interpretation and field surveys, can be significantly improved by coupling with SAR interferometry.

Singhroy et al. (1998) analysed the capabilities of integrated SAR (Radarsat) and Landsat TM imagery, and interferometric SAR for landslide characterisation and inventory. Using examples from different physiographic regions of Canada they concluded that the synergistic use of microwave and optical/IR imagery and SAR interferometric techniques can supplement current airphoto interpretation techniques used to this end.

An interesting application of the use of SAR interferometry coupled with optical imagery is reported in Farina et al. (2006). In this study the Permament Scatterers (PS) technique (Ferretti et al., 2001), a multi-image interferometric approach, coupled with the interpretation of aerial-photos and optical satellite images, was applied at a regional scale as support for landslide inventory mapping. The use of optical images provided with spatial meaning to the pointwise information given by the PS, making easier to identify terrain features related to slope instability and the landslide boundaries.

Applications of SAR interferometry for landslide mapping are reported in Sects. 18.5.3, 18.5.4, 18.5.5, and 18.5.7.

In Table 18.1 is reported the present capability of the spaceborne SAR interferometry and the optical imagery for mapping slope movements over the standard spatial scale. It's worth noticing that while optical imagery is suitable to map landslides over every spatial scale, the DInSAR is not useful to detect and map at the continental scale.

Table 18.1 Capability of the spaceborne SAR interferometry and of the optical imagery to map slope movements over the standard spatial scales

Spatial scale	Dimension (km)	SAT DInSAR	Optical imagery
Patch	0–1	Yes	Yes
Landscape	1–10	Yes	Yes
Mesoscale	10–100	Yes	Yes
Regional	100–1000	Yes	Yes
Continental	1000–10000	No	Yes

18.3 Landslide Monitoring

Monitoring means the comparison of landslide conditions like areal extent, speed of movement, surface topography, soil humidity from different periods in order to assess landslide activity (Mantovani et al., 1996).

The measurement of superficial displacements induced by a slope movement often represents the most effective method for defining its behavior, allowing the observation of response to triggering factors and the assessment of effectiveness of corrective measures (Farina et al., 2006).

Different techniques are available for measurements of the ground displacements, starting from the traditional inclinometers, extensometers, topographic surveys, until more recent applications such as GPS, aerial photogrammetry, LIDAR measurements (Angeli et al., 2000; Gili et al., 2000; Kaab, 2000; Hervas et al., 2003; McKean and Roering, 2004).

Interferometric SAR, whether satellite- or ground-based (InSAR and DInSAR) are the techniques most researched during the last decade for slope motion monitoring (Metternicht et al., 2005).

In the following subsections an overview of the techniques that exploit the optical imagery and SAR imagery for measuring landslide activity is presented.

Hervas et al. (2003) in their work propose an image- processing method to map and monitor landslide activity using multitemporal optical imagery. Basically this approach proposes the use of very high resolution images (e.g., Ikonos or Quickbird type) acquired at different dates. The method consists on image orthorectification, relative radiometric normalisation, change detection using image difference, thresholding and spatial filtering to eliminate pixel clusters that could correspond to man-made land use changes.

Another application of this type is reported in Delacourt et al. (2004) which propose to use aerial photographs and Quickbird imagery to monitor landslide displacements. In particular in Delacourt et al. (2004) a very interesting technique based on optical correlation of aerial photographs (for time baselines that require imagery previous to the launch of the Quickbird satellite) and Quickbird imagery is presented.

In Yamaguchi et al. (2008) SPOT HRV imagery have been used to detect the rate of movement of an active landslide located in Itaya area in Northern Japan.

SAR (Synthetic Aperture Radar) interferometry (Zebker and Goldstein, 1986; Gabriel et al., 1989; Massonnet and Feigl, 1998) has proved an effective instrument to monitor slow ground deformations. A list of the SAR satellites and their main operational parameters is reported in Table 18.2.

SAR interferometry (InSAR) in its different configurations, implemented by using spaceborne, airborne or ground-based sensors, has demonstrated its potentiality in landslide monitoring. In general, InSAR is based on the quantitative comparison between paired and complex radar images of the same area, taken at different times, to produce interferograms representing, pixel by pixel, the phase difference between the two images. This phase difference depends on four main components (Canuti et al., 2004):

– topography, connected to the acquisition geometry, (generally the images are taken from a slightly different position);
– atmospheric effects;
– noise caused by the temporal decorrelation of the microwave signals connected to changes in the dielectric properties of the target area during the time interval between the acquisition of parameters, induced, for instance, by changes in soil moisture or surface roughness and vegetation growth;
– ground-displacements which have occurred in the time span between the two acquisitions, being the objective of landslide monitoring.

The data processing technique known as differential SAR interferometry (DInSAR), applied to satellite images, permits the removal of the topographic

Table 18.2 Operational parameters of the currently microwave satellites

SATELLITE	ERS 1	ERS 2	Radarsat 1	JERS	Envisat	Radarsat-2	Alos	TerraSAR-X	Cosmo/ SkyMed*
Space Agency	ESA	ESA	CSA/USA	NASDA	ESA	CSA/USA	NASDA	DLR/Infoterra GmbH	ASI
Launch date	1991	1995	1995	1992	2002	2007	2006	2006	2007
Lifetime	9 years	active	active	active	active	7 years	5 years	3 years	5 years
Band	C	C	C	L	C	C	X-L	L	X
Wavelength (cm)	5.7	5.7	5.7	23.5	5.7	5.7	3.0 Ğ 23.5	23.5	3
Polarization	VV	VV	HH	HH	HH/VV	All	All	HH/VV	HH/VV
Incidence angle (i)	23	23	20–50	39	15–45	10–50	ago–60	15–60	variable
Resolution range (m)	26	26	10–100	18	30	3–100	7–100	1–16	1–100
Resolution azimuth (m)	28	28	9–100	18	30	3–100	7–100	1–16	1–100
Scence width (km)	100	100	10–500	75	10	10–500	40–350	5–100	10–200 (up to 1300)
Passage rate (days)	3, 35, 176	35	24	44	35	24	2–46	2–11	5–16
Orbital elevation (km)	780	780	800	568	800	800	660	514	619

component. In those cases where the atmospheric and noise effects are negligible, the residual phase difference can therefore directly be related to the superficial displacements in the observed area along the line-of-sight of the satellite. DInSAR from satellite platforms allows the monitoring of slow ground movements which involve large portions of the land surface, such as subsidence phenomena, fault movements and along volcano displacements (Strozzi et al., 2001; Massonnet et al., 1993; Massonnet et al., 1995). The accuracy is a small fraction of the employed wavelength and it is usually centimetric or millimetric; the pixel resolution is usually within the order of tens of meters.

Rott (2004), Paganini (2004) and Singhroy (2002) summarise the potentials and opportunities of space-borne SAR sensors for monitoring slope instability as follows:

(a) detailed motion maps produced from C-band, whether using techniques such as PSI (Persistent Scatterers Interferometry), DInSAR or InSAR, can assist in more accurate slope stability studies. When the conditions are favourable (e.g., coherence, imaging geometry) C-band SAR interferometry is a useful tool for mapping and monitoring mass movements;
(b) if SAR time series are available, accurate analysis of displacement is possible using PSI technique. Successful mapping of continuos slow landslide movements has been achieved using multi-temporal DInSAR techniques. Movements of –5 to 5 mm/year have been detected;
(c) the access to archived SAR data (e.g., in excess of 10 years) is useful to study temporal variations of motion that enable assessing slope stability, complementary to other information;
(d) future SAR systems with higher spatial resolution (e.g., Radarsat-2, TerraSat-X, COSMO-SkyMed) will enable the mapping of smaller slides. With the PSI technique, the movement of small objects (e.g., down to about one square meter) can be monitored.

Though it looks promising as a technique for monitoring landslides, the characteristics of the currently operational satellites (Table 18.2) put strong constraints on the use of DInSAR as a monitoring instrument. In particular the spatial resolution of the SAR images, the time-interval between the successive passages of satellites and the wavelength of the radiation are unsuitable for a systematic monitoring of relatively rapid movements, concentrated in small areas and on steep slopes or narrow valleys (Rott et al., 2000; Refice et al., 2001). Quantitative information on landslide activity can be obtained in the case of extremely slow movements (velocity less than a few centimeters per month), affecting large areas with sparse vegetation (Fruneau et al., 1996; Rott and Siegel, 1999; Kimura and Yamaguchi, 2000; Rizzo and Tesauro, 2000) (Table 18.3).

The temporal scale is controlled by the time interval between the successive acquisitions. The passage rate of the present satellites over the same area range between 24 and 44 days, thus allowing a monitoring periodicity of one month (Canuti et al., 2004). Recently launched SAR missions such as s the Japanese ALOS, the German TerraSAR-X or the Italian COSMO-SkyMed program, seem to meet the operational requirements for an effective and systematic monitoring of slope movements as reported in the Sects. 18.5.1 and 18.5.6.

The technique of Permanent Scatterers (PS) developed by Ferretti et al. (2001) allows a significant reduction of atmospheric and noise effect as well as measurements close to one millimeter (Canuti et al., 2004; Colesanti et al., 2003). The pixel-by-pixel character of the PS analysis enables exploiting individual phase stable radar targets in low-coherence areas, making spaceborne interferometric measurements possible in vegetated

Table 18.3 Capability of the spaceborne SAR interferometry and of the optical imagery for monitoring slope movements at different temporal intervals

Temporal scale	SAT DlnSAR	Optical imagery
Second	No	No
Minute	No	No
Hour	No	No
Day	No	Yes
Week	No	Yes
Month	Yes	Yes
Year	Yes	Yes
Decade	Yes	Yes

Table 18.4 Velocity scale proposed by the IUGS/WGL (1995) and present capability of the spaceborne SAR interferometry and optical imagery to assess the indicated displacements rates

Class	Description	Speed	Speed (m/s)	SAT DlnSAR	Optical imagery
1	Extremely low	1.6 mm/year	$5\ 10^{-10}$	Yes	Partly
2	Very Low	1.6 m/year	$5\ 10^{-8}$	Partly	Yes
3	Slow	13 m/month	$5\ 10^{-6}$	No	Yes
4	Moderate	1.8 m/h	$5\ 10^{-4}$	No	No
5	Rapid	3 m/min	$5\ 10^{-2}$	No	No
6	Very rapid	5 m/s	5	No	No
7	Estremely rapid			No	No

areas (Metternicht et al., 2005). The technique requires sufficient spatial density of natural stable ground reflectors like individual isolated man made structures or exposed rock. Mapping of continuous slow landslide movements has been reported by Berardino et al. (2003), Colesanti et al. (2003) and Prati et al. (2004).

Applications of SAR interferometry and the PSI technique to landslide monitoring are reported in Sects. 18.5.3, 18.5.4, 18.5.5, 18.5.6 and 18.5.7.

In Table 18.3 is reported the capability of the spacerborne SAR interferometry and of the optical imagery for monitoring slope movements at different temporal intervals. Both the techniques are not suitable for monitoring at the second, minute and hour temporal scale while are useful for monitoring at the monthly, yearly and decade scale. At the daily and weekly scale is possible to monitor with the optical imagery but not with the radar imagery.

In Table 18.4 is reported the capabilities of the two techniques to assess the displacements rates as proposed in the velocity scale of IUGS/WGL (1995). The optical imagery is preferable for slow movements to the radar imagery. On the contrary the radar imagery is more suitable than the optical imagery to monitor extremely slow movements.

18.4 Hazard Analysis

Following the formal definition given by Varnes and IAEG (1984), hazard can be defined as the expected probability of a mass movement of a given intensity which takes place in a certain area within a given time span. This, essentially, means that landslide hazard assessment procedures must take into account both space and time prediction (Catani et al., 2005).

Predictions based solely on spatial probability of occurrence are, however, very common, due to the fact that they are relatively easier to carry out. In such cases the term "landslide susceptibility" should be considered more appropriate (Dai et al., 2002).

According to Dai et al. (2002) the factors which determine the probability of landsliding for a particular slope can be grouped into two categories: (1) preparatory variables which make the slope susceptible to failure without triggering it, such as geology, slope gradient and aspect, elevation, soil geotechnical properties, vegetation cover and long term drainage patterns and weathering; and (2) the triggering variables such as heavy rainfall, glacier outburst, earthquakes and man disturbance.

If triggering variables are not considered in the analysis the term susceptibility must be used to define the likelihood of occurrence of a landslide.

As stated by Metternicht et al. (2005) remote sensing has been used in the detection and identification of diagnostic features mostly related to the first category, and to a lesser extent, to the detection of potentially triggering factors as shown by studies of Kniveton et al. (2000), Buchroithner (2002), Huggel et al. (2002), Kaab et al. (2003).

Susceptibility analysis can be based on a number of techniques and data. According to Soeters and van Westen (1996), van Westen et al. (1997) and Aleotti and Chowdhury (1999), they can be divided into inventory, heuristic, deterministic and statistical approaches.

The most straightforward method to any study of landslide hazard is the compilation of a landslide inventory (Dai et al., 2002). The output of a landslide inventory provides the spatial distribution of mass movements, represented as polygons or points (Wieczorek, 1983) and for this reason it can be used as elementary form of hazard map, though they fail to identify areas that may be susceptible to landsliding unless landslides have already occurred (Dai et al., 2002).

In the heuristic approach expert opinions are used to estimate landslide potential from data on preparatory factors. These models are based on the assumption that the relationships between the landslide susceptibility and preparatory factors are known and specified in the models (Dai et al., 2002).

Deterministic methods, in which the relative probability of spatial occurrence of a mass movement is usually derived from the computation of the factor of safety, are probably the most objective means of hazard assessment (e.g. Wu and Sidle 1995; Montgomery and Dietrich, 1994). Unfortunately, due to the large spatial variability of the mechanical, hydrological and geometrical parameters involved in the equations (e.g. Burton et al., 1998), their application is very difficult at the basin scale while numerous are the application at the slope scale (Anderson and Lloyd, 1991; Crosta, 1998; Iverson, 2000; Crosta and Dal Negro, 2001, Tofani et al., 2006).

The uncertainties in the definition of strength parameters can be at least partially overcome by the application of probabilistic methods (for a more in-depth description of such techniques refer to Baecher and Christian, 2003).

Due to the described reasons, the most used methods for the assessment of relative hazard are those based on the weighting of landslide preparatory factors using statistical methods. The use of multivariate techniques, in which the natural and anthropogenic factors of hillslope instability are evaluated and weighted against each other in order to obtain the best estimation function, have long gained the approval of scientists and risk managers all over the world (Catani et al., 2005). Applications can be based on regressive methods (Bernknopf et al., 1988; Jade and Sarkar, 1993; Wieczorek et al., 1996), discriminant analysis (Carrara, 1983; Carrara et al., 1991; Chung et al., 1995; Baeza and Corominas, 1996) or neural networks (Bianchi and Catani, 2002; Lee et al., 2003; Lu and Rosenbaum, 2003; Ermini et al., 2005).

The methods mentioned so far do not result in real hazard maps as defined by Varnes (1984). Assessing the probability of occurrence at a certain location within a certain time period is able only when the temporal prediction is defined.

Canuti and Casagli (1996) propose three different approaches for hazard temporal prediction:

– Analysis of the time series of the landslide events
– Analysis of the time series of triggering factors
– Monitoring

The relationship between the occurrence of landslides and the frequency of triggering factors has been widely exploited.

Especially for rainfall-triggered landslides, various techniques have been developed which determine threshold values of “antecedent rainfall” (Caine, 1980; Crozier, 1986; Wieczorek, 1987; Crosta and Frattini, 2001; Montgomery and Dietrich, 1994; Terlien, 1998).

One of the most intriguing applications currently being investigated regarding the use of remote sensing is the prediction of shallow landslides at the worldwide scale. Drawing on recent advances of satellite remote sensing technology, experimental landslide prediction models are developed to identify the timing for landslides induced by heavy rainfall (Hong et al., 2006; Adler et al., 2000). Examples of these applications are reported in Sects. 18.5.8 and 18.5.9.

Another application of remote sensing to landslide hazard assessment is proposed in Catani et al. (2005). In this work a hazard analysis at the basin scale has been carried out by means of a statistical approach. The land cover map used in the model as one of the preparatory factors has been derived from the updating of Corine Land Cover Map using Landsat 7 ETM+ and ASTER. The hazard map has been realized using a coupled approach: a statistical method for the spatial prediction and the PS technique for the temporal prediction. In particular the former landslide inventory map has been updated with the PS technique in order to obtain information regarding the recurrence time of the mapped landslides.

Table 18.5 Contribution of optical, radar and meteo imagery to the spatial and temporal hazard assessment (0: non relevant, 1: minor contribution, 2: major contribution)

Hazard analysis							
	Space prediction				Time prediction		
	Inventory map	Heuristic approach	Statistical approach	Deterministic approach	Time series of the events	Time series of the triggering factors	Monitoring
Optical imagery	2	2	2	1	1	0	1
Radar imagery	2	1	1	1	2	0	2
Meteo imagery	0	0	0	0	0	2	1

In Table 18.5 is reported the contribution of the remote sensing to the spatial and temporal assessment of landslide hazard.

18.5 Applications of Remote Sensing to Landslide Analysis

This section is dedicated to illustrate how researchers around the world are currently using remote sensing techniques to map, monitor landslides and to assess landslide hazard.

18.5.1 *JAXA Activities on Space Utilization and Information Sharing for Disaster/Crisis Management*

by Takashi Moriyama (Japan Aerospace Exploration Agency (JAXA)

It is in Asia that the scale of damages caused by disasters has been tremendous. Asia occupies 60% of the total number of disasters in the world, 70% of the total economic losses and 90% of the total casualties. The reasons why Asia has been suffered from disasters include; (i) concentration of meteorological phenomena which cause natural disasters due to geographical factors, (ii) the circum-Pacific volcanic zone, or "Pacific Rim of Fire" and complicated plate-tectonics, and (iii) the vulnerable to natural disasters magnifying the impact thereof. In other words, such factors are derived from problems; (i) disaster warnings or information on evacuation are not properly delivered, (ii) knowledge and actions to avoid risks of disasters are not sufficiently shared among people, and (iii) disaster-tolerant and invulnerable social structures have not been prepared in the region.

At the second Earth Observation Summit held in April 2004, hosted by Prime Minister KOIZUMI Junichiro, delegates and participants of the Summit deliberated upon how science and technology can contribute to disaster reduction. Space technologies were focused on as a means of observing wider areas repeatedly. Thus, at the Summit, (i) that countries possessing artificial satellites should collaborate on construction of international collaborative schemes for disaster prevention/reduction was agreed upon, and (ii) that a system for monitoring disasters and environmental changes should be constructed within 10 years since then was decided upon.

In conjunction with such moves, JAXA announced a long-term space development vision for the next 20 years, "JAXA Vision – JAXA 2025 –," describing the JAXA decision that JAXA is determined to actively use aerospace technology to build a secure and prosperous society, through establishment of a priority system for natural disaster management.

JAXA will set up various frameworks to use the Advanced Land Observing Satellite (ALOS) "Daichi" (Fig. 18.1) for precise regional land coverage observation, launched in January 2006, and implement verification experiments utilizing thereof. "Daichi" has three high-performance sensors, including the Panchromatic Remote-sensing Instrument for Stereo Mapping (PRISM), which is comprised of three sets of optical systems to measure precise land elevation with 2.5-m spatial resolution and the Phased Array type L-band Synthetic

Fig. 18.1 ALOS characteristics. For large scale landslide detection, the PALSAR is the most useful sensor to detect landslide by change detection technique (comparison with 2 images) and SAR interferometory

Aperture Radar (PALSAR), which enables day-and-night and all-weather land observation. By combining data obtained from those sensors, JAXA can swiftly grasp real situations of disaster stricken areas.

With regard to the use of data acquired through “Daichi” observation, the following items are expected:

(i) Large-scale crustal deformations triggered by earthquakes
(ii) Collapse of or fire at a number of buildings

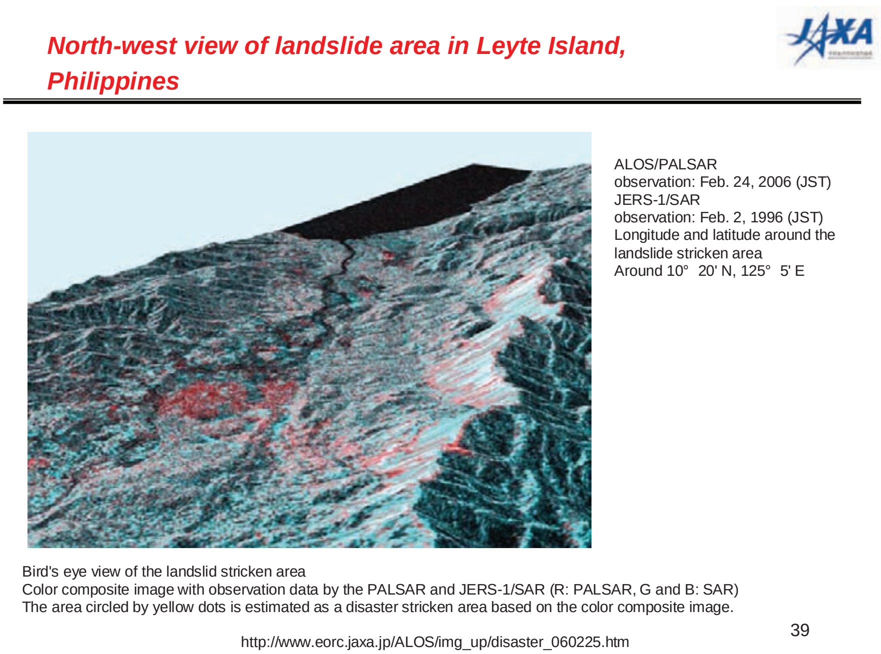

Fig. 18.2 Example of the successful detection of large scale landslide by comparison with JERS-1 and ALOS/PALSAR over Leyte island, Philippines

(iii) Detection of flooded areas
(iv) Changes in the shape of a mountain, pyroclastic flows, ash falls, or changes in volcanic craters through volcanic activities
(v) Large-scale landslides (Fig. 18.2)
(vi) Marine pollution, including oil drifts
(vii) Extractions of information on geographical, terrain and land surface changes for post-disaster restoration activities after disasters

The "Charter on Cooperation to Achieve the Coordinated Use of Space Facilities in the Event of Natural or Technological Disasters (in short, International Charter on Space and Major Disasters)" is a framework that (i) upon devastating disasters, organizations possessing earth observation satellites implement observation on a voluntary basis or upon request, and (ii) the organizations immediately provide disaster-stricken countries or relevant organizations with disaster information free of charge. Upon the huge landslide disaster on Leyte Island that occurred in February 2006, "Daichi" acquired images of the disaster, and the observation data as well as analysis information were provided to the International Charter Secretariat and ADRC.

18.5.2 Remote Sensing Based Investigation of Landslides in Himalaya Mountains

by Liqiang Tong, Chunling Liu (Aero Geophysical Survey Remote Sensing Center, Ministry of Land and Resources, China) Shengwen Qi (Institute of Geology and Geophysics, Chinese Academy of Sciences)

Investigation of landslides occurring in the Himalayas by remote sensing is one task of major investigation on land resources of "Investigation into great geological hazard in the Chinese Himalayas by remote sensing". Its overall target is to investigate great geological hazard by remote sensing, find out distribution of great geological hazards and hidden dangers, preliminarily discuss its stability and geologic environment, provide fundamentally geologic reference for Himalayas to reduce and prevent hazard, by use of satellite data.

Investigation work area of this project starts from Ali Area in the west to the large River Bend (Mt. Namjagbarwa) of Brahmaputra, to the Brahmaputra major fracture in the north, to the border between China and India, Nepal, Bhutan, Sikkim and some other countries in the south, and it is situated between 78° and 95°30' East Longitude and between 26° and 33° North Latitude. It is 1700 km long from east to west, and 60–250 km wide from south to north.

Himalayas region is situated in the south of Qinghai-Tibet Plateau, also is national boundary between China and Nepal, India, Bhutan, Sikkim, and some other countries. It extends 2450 km from east to west, and not only has Everest titled "first peak of the world", but also has notable grand Brahmaputra canyon with great drop in topography, great change in climate, and frequently geological hazards. In particular, along with further exacerbation of ecological environment in recent years, increase of local precipitation, rise of air temperature, and melting of glacier, geological hazards in the Himalayas region, such as landslide, mudflow, dilapidation, burst of ice lakes, etc., occur more frequently.

Working content of this project is to use satellite data to interpret scope, scale and structural features of landslides in the investigation area, and integrate geology, theory of the catastrophology and geographical spatial information techniques to analyze influencing factors and inducing factors of landslides and appraise hidden dangers, etc.

First of all, use data and image of American landsat ATM to carry out general investigation on regional landslide hazard; then use high-resolution images of French satellite SPOT-5 (see Fig. 18.3), Japanese ALOS (see Fig. 18.4) satellite and ASTER satellite to carry out detailed interpretation on landslides and typical sites which potential danger, according to outcome of general investigation. Interpretation of remote sensing is divided into somestages, i.e., (1) preliminary interpretation stage: comprehensively analyze the collected geological data and remote sensing images, comprehend tectonic framework, quaternary geology and formation lithology, give more emphasis on analyzing image characteristics of known geological hazards, and establish interpretation key of geological hazards in the work area; (2) particular

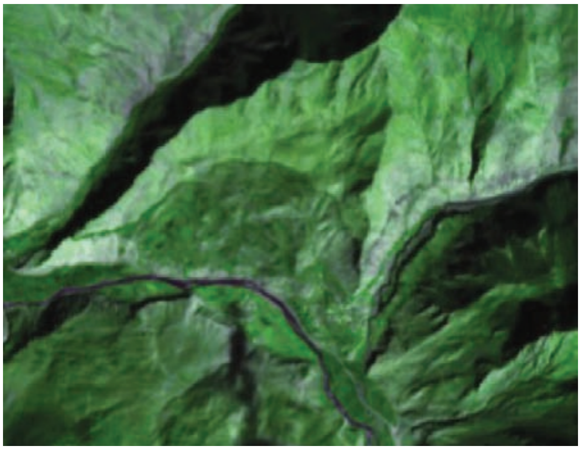

Fig. 18.3 Saiji landslide of Longzi County (Alos image)

interpretation stage: on the foundation of interpretation key of geological hazards established in the preliminary interpretation stage, interpret landslide body particularly; (3) field verification and synchronous interpretation stage: carry out field survey based on interpretation achievement, and carry out amendment and re-interpretation on landslide interpreting key; (4) reinterpret and check stage: after finishing field verification, amend the interpretation key overall, perfect interpretation results, interpret the amended achievement, and finish the investigation map of landslide hazard by remote sensing.

Remote sensing investigation shows that there are 151 large-scale (more than) landslides in the Chinese Himalayas region, which are principally located in the Lang County, Longzi, Cuomei, Zhada and some other counties. There are 10 concentrated distribution areas in the Chinese Himalayas region: Lang Town, Laduo Village and Jindong Village of Lang County; Liemai Village and Jiayu Village of Longzi County; neighborhood of Douyu Village of Longzi County; Bubula Mountain of Motuo County; north shore of Xubuqu in Cuomei Town of Cuomei County; Naixi Village of Cuomei County; Cuomulong Mountain-Kala Village of Zongga Town of Jilong County; south margin of Zhada Basin of Zhada County.

Fig. 18.4 Saiji landslide of Longzi County (Spot-5 image)

Average slope of landslides varies from 8.4° to 48.6°, and slope of most landslides varies from 10° to 30°. There are 6 landslides with slope more than 40°, 21 landslides with slope 30–40°, 63 landslides with slope 20– 30°, 54 landslides with slope 10– 20°, and 6 landslides with slope 8.4– 10°. It indicates by statistics that landslides with slope 10– 30° occur most easily, landslides with slope more than 40° or less than 10° occur infrequently.

Landslides of Himalayas are principally distributed in the river and lake facies half-consolidated varicoloured sandy conglomerate and clay rock of Zhada Group (N2-Qp1Z), grey silty sericite slate bearing grey thinly laminated metamorphic siltstone in the Jurassic Weimei Formation (J3w), grey to charcoal grey carbonaceous, silty and calcareous shale bearing siltstone and limestone in the Jurassic Menkadun Formation (J2-3 m), grey to charcoal grey limestone, sandy shale and sandstone in the Jurassic Nieniexiongla Group (J1-2 N), charcoal grey, taupe, celadon, amaranth silty sericite slate bearing grey thinly laminated metamorphic siltstone in the Jurassic Ridang Formation (J1r), varicolored shale, slate, metamorphic sandstone and quartz sandstone in the Triassic Xiukang Group (T3x), and gneiss, schist, slate and phyllite in the Precambrian.

Landslides in the Zhada Group, triassic Xiukang Group and Precambrian strata are pull-type landslides mostly, and their formation condition are principally controlled by regional geologic structure and intense cut of water system, where steep landform and highly fissured rock mass and loose sediments with thin surface layer are formed. Reasons inducing landslides have close relation with lateral erosion of bank slope by rivers.

Landslides in the Jurassic strata have characteristics of pull-type landslides and have characteristics of push-type landslides at the same time, and their formation condition are principally controlled by steep landform and stratigraphic structure with weak intercalation, and their inducing reasons have relation with groundwater and weak intercalation, or have relation with the erosive action of slope foot by rivers.

18.5.3 Exploitation of historical satellite SAR archives for mapping and monitoring landslides at regional and local scale

by Alessandro Ferretti (TRE-Tele-Rilevamento Europa)

Permanent Scatterer SAR Interferometry (PSInSAR^{TM}) is today one of the most advanced technologies for surface deformation monitoring capable of overcoming most of the limitations of conventional differential radar interferometry. It exploits long temporal series of satellite radar data, acquired over the same area of interest at different times, to identify "natural radar targets" (i.e. the so-called Permanent Scatterers) where very precise displacement information can be retrieved.

This approach has been developed by Politecnico di Milano (POLIMI) in the late nineties. Since then, the processing of thousands of SAR scenes acquired by ERS-1/2, ENVISAT and RADARSAT has demonstrated how multi-temporal SAR data-sets can be successfully exploited for surface deformation monitoring, integrating successfully continuous GPS and optical leveling data and allowing the analysis of large areas of interest.

One of the most promising application of this technology is related to the mapping of landslide distribution at regional scale. This task is traditionally based on geo-morphological analysis, both from aerial-photo interpretation and field surveys. However, whenever surface displacement rates are low (millimeters to centimeters per year), assessing the activity of a landslide is generally difficult or even impossible without the help of long-term monitoring tools. This is for example the case of Deep-seated Gravitational Slope Deformations (DGSD), characterized by large areal extent and surface displacements ranging from a few millimeters to tens of millimeters per year. Thanks to its capability to detect small displacements over long periods and large areas, PSInSAR^{TM} analysis can be considered complementary to conventional geological and geomorphological studies in performing landslides inventories at regional scale.

Lately, many regional governments in Italy have applied PSInSAR^{TM} to map and monitor slope instability phenomena using both ESA-ERS and RADARSAT images (Fig. 18.5). The availability of radar data in both ascending and descending satellite acquisition geometries enhances the PS coverage of the study area and allows the estimation of both vertical and horizontal (E-W) displacement fields.

The results achieved so far and, in particular, the activities carried out in agreement with the Italian Civil Protection authorities, confirm that the traditional geological-geomorphological and the innovative PSInSAR^{TM} approches are indeed complementary tools for accurate landslide mapping. In particular, the assessment of the degree of activity based on multi-year historical datasets can be invaluable.

The Italian Ministry of the Environment has recently awarded a contract for the processing of more then 12,000 SAR scenes acquired over Italy aimed at creating the first database of

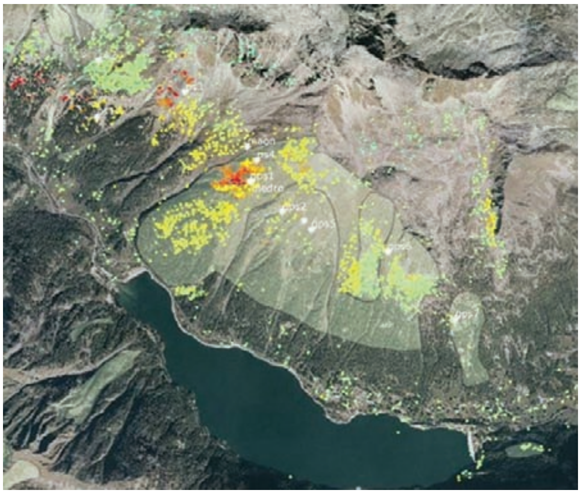

Fig. 18.5 Example of PSInSAR^{TM} data superimposed on an orthophoto. Colored dots correspond to "natural radar targets" (i.e. the so-called Permanent Scatterers). Color depends on the displacement rate in mm/yr of the measurement point. For each PS, a displacement time series is also available

interferometric information on a national level for mapping unstable areas. This is somewhat an evidence of the fact that, in less than ten years from its development, this technology has become a standard monitoring tool.

18.5.4 Spaceborne SAR Analysis for Landslides Mapping in the Framework of the PREVIEW Project

by G. Righini, N. Casagli, C. Del Ventisette, (Department of Earth Sciences, University of Firenze, Italy) M. Costantini, F. Malvarosa, F. Minati (Telespazio, Finmeccanica/Thales, Roma, Italy)

This work addresses the use of a multitemporal SAR interferometry technique for landslides mapping applications. The activities here described were carried out in the framework of an integrated project within the Sixth Framework Programme of the European Commission: Prevention, Information and Early Warning (PREVIEW). It proposes an end-to-end, integrated approach in close cooperation with all bodies involved in the risk chain in order to develop, on a European level, new or enhanced information services for risk management for the following types of hazards: Floods, Windstorms, Forest fires, Earthquake and Volcanoes, Landslides and Man-made hazards.

Deep seated, slow moving landslides on large areas were analyzed by spaceborne SAR interferometry: a test site in the Italian Alps of about 300 km^2 was selected for updating pre-existing landslide inventory maps based on the advanced processing technique of Persistent Scatterers Pairs - Differential SAR Interferometry (PSP-DIFSAR), developed by Telespazio .

The stakeholders most interested, and therefore involved, in these activities were the Italian National Department of Civil Protection and the Office of Prevention of the Civil Protection of Regione Lombardia, who are in charge of landslide risk management at national, regional and local levels.

The test site is located in Valfurva, east of Bormio, in the Rhaetian Alps of the Lombardia Region, where significant rock-slides and deep-seated gravitational slope deformations were recognised; in this area Sackung type deformations affect pre-Permian metapelites, metabasites and marbles, as well as Late Pleistocene and Holocene glacial and rock glacier deposits. The deformation started after the Late-Wurmian age (15,000 ± 11,000 years B.P.), and continued until few centuries ago, not excluding a present-day low-rate activity, Agliardi et al. (2001).

The evolution of fault systems, resulting in asymmetric trenches, led in some cases to the progressive failure of the slope during the last 10,000 years, as testified by large paleo landslide accumulations, and it is still in progress. Indeed, Lombardia Region is one of the most populated and urbanized region in Italy and it is also very prone to landsliding so the risk is high for human life and infrastructures. Local administrative authorities have a long experience in monitoring slope movements and recording historical data, measurements and investigations.One of the most hazardous phenomenon in the area is the 30 Mm^3 active “Ruinon” landslide, Crosta and Agliardi (2003). Such landslide is a typical rock slide with a slip surface depth of more than 90 m and characterized by a superficial debris flow almost 25 m thick.

The PSP-DIFSAR technique jointly exploits spatial and temporal properties of the data, in order to improve the density and the accuracy of the measurements, Costantini and Rosen (1999), Costantini et al. (2002).

SAR images from ERS-1/2 satellites in the period April 1995 – January 2000 and from Envisat satellite in the time range August 2002 – March 2008, have been used, allowing the deferred-time analysis of past movements and the record of recent slope movements. The landslide inventory map, coming from end-user, was thus updated with the information from PSP-DIFSAR processing on ERS and Envisat satellites data, with measurements of mean velocities and displacement temporal evolutions of sparse points on the ground. From ERS images 26345 coherent points (Fig. 18.6) were extracted (82.8 points/km^2) and the landslides characterized by the presence of points are 151 of the total 861 (27 km^2 of 62.75 km^2); instead, the coherent points extracted from Envisat images were 10624 (33.4 points/km^2).

The results were examined in Geographical Information System (GIS) environment and were

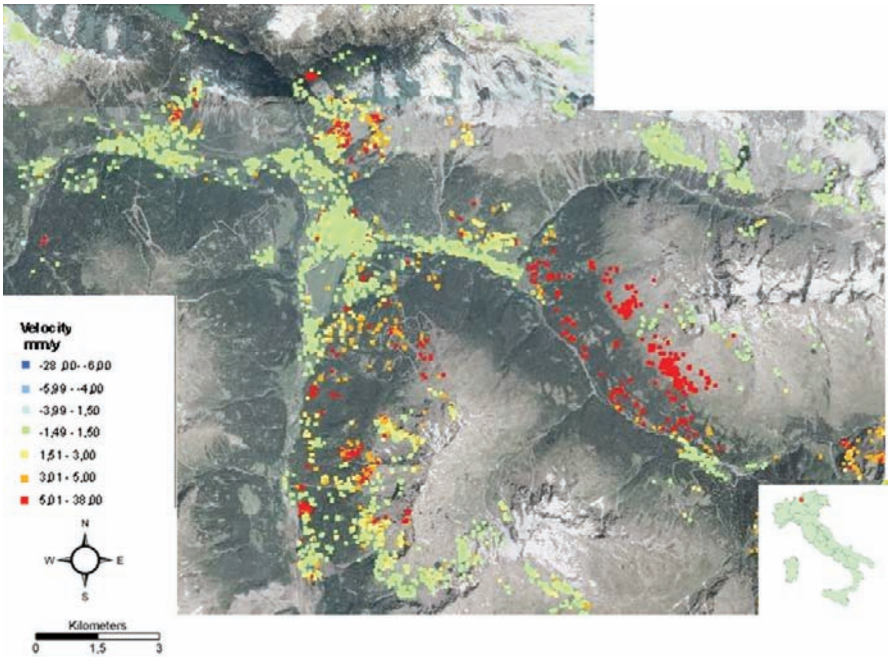

Fig. 18.6 Distribution of ERS1/2 points in the studied area

integrated with field surveys and in-situ measurements. The characteristics of the landslides were highlighted in the database: geometry, state of activity, typology, monitoring systems, interventions, source of information and the updating actions; furthermore, for each landslide area, the occurrence of points and the statistical description of their velocities were reported.

The main criteria used to define the state of activity were related to the mean velocities retrieved from the PSP-DIFSAR processing: e.g. if the velocity from Envisat data is above 2 mm per year then the land-

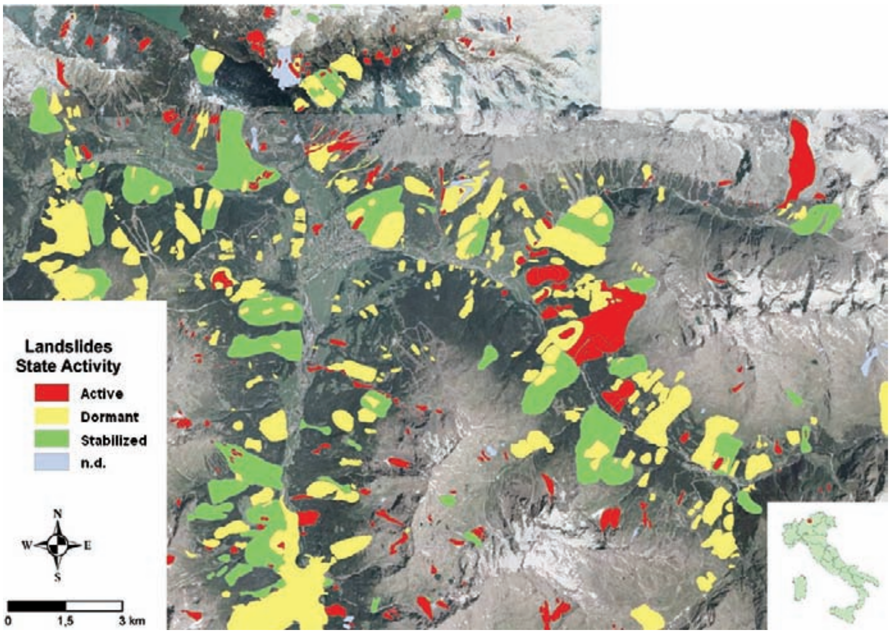

Fig. 18.7 Updated landslide inventory map

slide was classified as "active". Main changes on the landslides concerned the state of activity and geometry while in some cases new landslides have been pointed out. An updated landslide inventory map was thus developed (Fig. 18.7) in collaboration with end-users ; field surveys have been carried out concerning some critical situation and validation activities with in-situ instrumentation are still going on.

SAR images from ERS and ENVISAT satellites, with temporal range from 1995 to 2008, have been used for landslide inventory updating mainly concerning state of activity and geometry. PSP-DIFSAR technology has demonstrated its capabilities to map slow moving landslides for risk assessment and hazard zonation, even if the integration with traditional methods and field surveys is still necessary.

A system based on remote sensing techniques integrated in GIS with other traditional data can provide useful information to monitor the displacement of the land surface within landslide risk areas and can contribute to the mitigation of landslides hazards. both at national and local level.

Main limitations are due, of course, to the availability of radar satellite images and the processing of coherent points with good rate of reliability.

Acknowledgments We thank the entire Preview Project team and especially acknowledge the Office of Prevention of the Civil Protection of Regione Lombardia and the Italian National Department of Civil Protection both of which were involved in the activities described in this work.

18.5.5 Terrafirma Landslide Services for Europe Based on Space-Borne InSAR Data

by Valeria Pancioli, , Teresa Campolmi, Nicola Casagli (Department of Earth Sciences, University of Firenze, Italy), Hugo Raetzo (Swiss Federal Office for the Environment, Hazard Prevention, 3003, Switzerland)

Terrafirma is one of a number of services being run by the European Space Agency under the Service Element Program as part of the Global Monitoring for Environment and Security initiative (GMES) of the European Union. The project started in 2003 and will end in 2008 when it is planned that services will be adopted by the European Commission as part of their GMES strategy. Terrafirma is providing a Pan-European ground motion information service in each of the 25 member states of the EU to detect and monitor ground movements in relation to building stability, subsidence and ground heave, landslides, seismic activity and engineered excavations. The technology at the base of such a large-scale undertaking uses the data collected by European radar satellites, namely ERS1, ERS2 and ENVISAT processed through SAR interferometry (InSAR). By using state-of-the-art InSAR processing techniques, such as the Persistent Scatterers Interferometry (PSI) approach, thanks to the available archive of repeat satellite data, measurements of ground displacements with a millimetre scale accuracy can uniquely be provided back in time for the last 15 years.

The project is aimed at informing specialists, planners and the community at large about the new approach to the assessments of risks from ground movements across Europe and beyond. Terrafirma intends to achieve it through practical examples of how ESA satellites can create ground motion measurements that, when coupled with expert knowledge, geosciences and engineering information, provide insights into these problems at a detail level, sometimes technically not reachable through the use of conventional techniques. The services provided by Terrafirma are to be delivered to end-users, represented mainly by public or private organizations dealing with ground movements connected both to natural hazards and human activities, primarily by National Geological Surveys who, integrating pre-existing and possibly in situ data with InSAR results can offer them enhanced products providing causal and modelled information services.

The landslide services consists of two different products: Landslide Inventory (LSI) helps to update pre-existing inventory maps produced with conventional geomorphologic tools by integrating PSI ground displacement information with cartographic, optical and ancillary data used to identify possible diagnostic morphologies and terrain features related to landslide and to extend spatially the point wise PS information. Landslide Monitoring (LSM) usually related to a specific slope, in which PSI measurements are combined in a GIS environment with cartographic optical and ancillary data to obtain an accurate analysis of spatial distribution of the ground displacements.

The first two-year Stage 1 of the project (which ended in 2005) was focused on the consolidation of both service providers and users. In November 2005 Terrafirma entered Stage 2, aimed at rolling-out the service across all 25 Member States of the EC. During this stage, processing equally covering all of the EU25 Member States will be conducted along with the release of seven landslide products within Greece, Italy and Switzerland.

The present paper is focused on the description of the results obtained in Stage 2 for landslide mapping at regional scale in Graubuenden Canton (Switzerland) and landslide monitoring at local scale for the Gorgoglione landslide (Southern Italy).

The analysis, concerning the Canton Graubuenden (Switzerland), for supporting landslide investigation has been carried out through a combined approach based on the use of multi-interferometric analysis, and photo-interpretation. The technique employed is the Point Target Analysis (IPTA) developed by Gamma Remote sensing based on the extraction of natural benchmarks from the SAR scene, typically parts of buildings, metallic structure and rock outcrops, which are not affected by temporal and geometrical decorrelation, and on the analysis of a large dataset of SAR images (at least 25 scenes). This approach permits to obtain for every Persistent Scatterers the medium deformation rate with an accuracy of 0.1–1 mm/year (Werner et al., 2003).

For this purpose thematic layers, including landslide inventory, aerial photos, digital elevation model and topographic maps, were managed within a GIS environment.

Canton Graubuenden is located in the Swiss Alps between the Gotthard Cristalline Massive and Austrian-Italian border in the Penninic and Austroalpine nappes. This densely populated region is a landslide prone area. The Buendnerschiefer and the Flysch Formations of Eastalps are fine-grained rocks, which are affected by slope instability processes. The largest rock slide of the Holocene is located in Flims and concerns a total volume of 9 km^3 (Noverraz et al., 1998). There are also many installations for touristic purposes in the unstable slopes, sometimes they are located in the permafrost areas. Between St. Moritz, Chur and Disentis many other landslides are still active and there are high annually costs for the mitigation and the countermeasures. The damage concern inhabited areas, industrial zones and many roads in the lateral valleys. For the Canton a landslide inventory is not available, but several of the large landslides are known and the geological documents and field surveys have allowed an integration of InSAR technique for hazard assessment. The analysed area has an extension of about 3800 km^2. Radar datasets used are SAR images acquired by ERS1 and ERS2 satellite (spanning the temporal interval from 1992 to 2002) acquired both in ascending and descending geometry and SAR images from ENVISAT satellite (spanning the temporal interval from 2002 to 2008) acquired both in ascending and descending geometry processed through the IPTA analyses allowed us to investigate and confirm most of the large known landslide and to identify several new landslides, producing a final inventory of 112 landslides covering an extension of 270 km^2 that represent the 7% of the whole investigated area.

Landslide classification is based on the medium velocity computed for every landslides from ERS/Envisat IPTA data (Fig. 18.8).

The local case study is related to an earth landslide, in a silico-clastic turbidite formation (Boiano, 1997) in Gorgoglione locality, a small village located in Southern Italy (Basilicata region), affected by an ancient landslide, re-activated during the Irpinia earthquake in1980, as testified by its classification as area at moderate – to – very high risk (class R4) reported in the P.A.I. (Hydrogeological Asset Plan). Following an acceleration of the ground movements observed between late 2003 and the summer 2004, which induced the evacuation and the demolition of several buildings, field surveys, carried out by experts from GNDCI (National Group for Geo-hydrological Disaster Prevention of the Italian funded by the National Civil Protection Department), highlighted the presence of a general slope instability in the portion of the village located below the main square. After the 2003–2004 acceleration in situ instrumentation has been installed by the Gorgoglione municipality, but the causes of the slope movements are still under investigation.

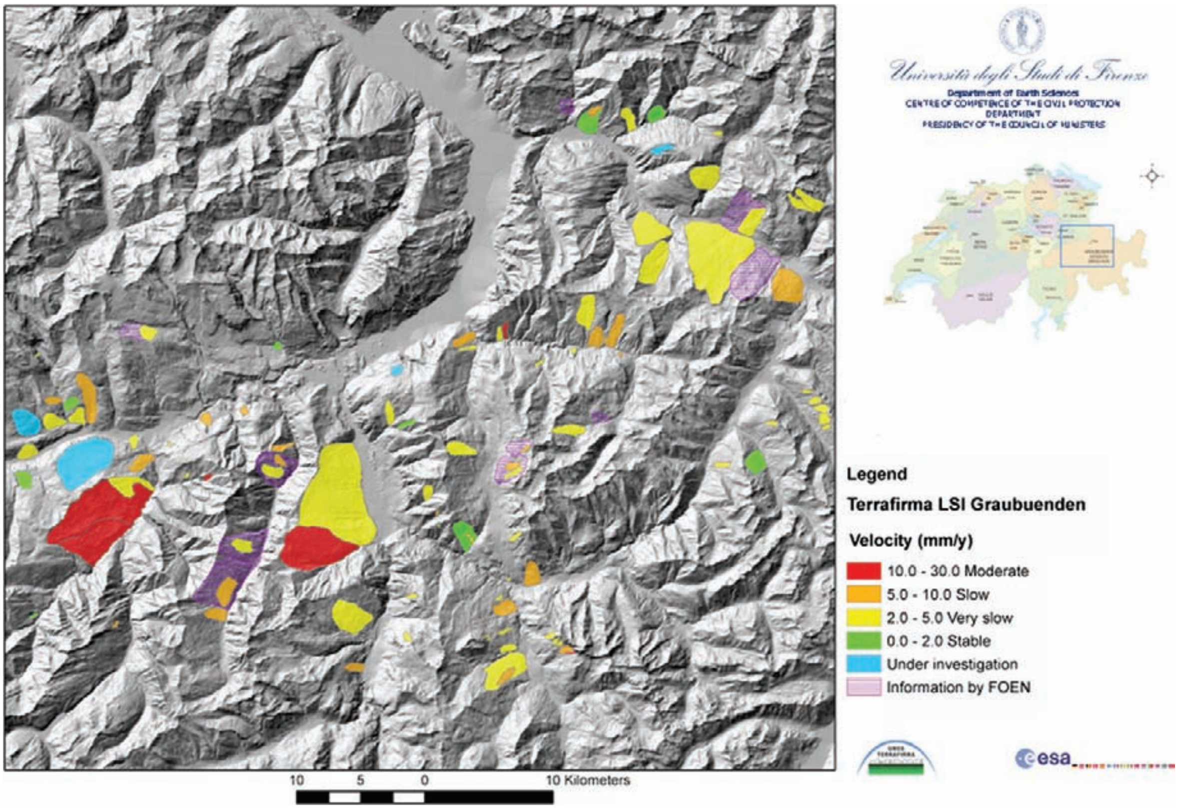

Fig. 18.8 Landslide inventory of the Graubuenden Canton carried out by means an integration of InSAR technique and conventional geomorphologic tools. The landslide intensity is classified on the basis of the velocity expressed in mm/yr

The Gorgoglione landslide is described as a compound landslide: an earth slide with rotational and translational components of the movement. A PSI analysis, through the Permanent Scatterers (PS) technique (Ferretti et al., 2001) developed at the Politecnico di Milano (POLIMI) in advanced mode (APSA), on historical ERS1/2 data and current ENVISAT data was performed. The PS spatial distribution and velocities highlighted the presence of movements in the southern portion of the village, mapped as area of high risk by the P.A.I., whereas the rest of the village is in a stable condition (Fig. 18.9).

The analysis has allowed us to redraw correctly the landslide boundaries, in particular to define better the landslide crown. Apart from the spatial distribution of movements, the APSA analysis provides information about the temporal evolution of displacement rates from a backscattering structure on the ground. For every acquisition used in the interferometric prosacessing it is possible to determine displacements values relative to a reference date. The whole observation period, spanning of 16 years, shows an overall movement of ca. 16 cm, resulting in a different displacement rate for the two time intervals, ca. 10 mm/y for historical dataset (1992–2002) and ca. 20 mm/y for current dataset (2002–2008). This difference is in agreement with the landslide acceleration occurred in the period from late 2003 and summer 2004. The PS analysis performed along the cross section, based on the velocity rate interpolation for every dataset, shows a good correspondence with the geomorphologic aspects; in particular the movement starts in correspondence to the disturbed flysch, with an initial increase of velocity that become constant along the slope. It is also evident, as highlighted before, that in correspondence of Piazza Zanardelli Envisat data show an increase of velocity with respect to ERS data (Fig. 18.10). The velocity rate pattern along the entire slope accounts for the high damage in the lower part of the village, where velocities of up 30 mm/y were measured.

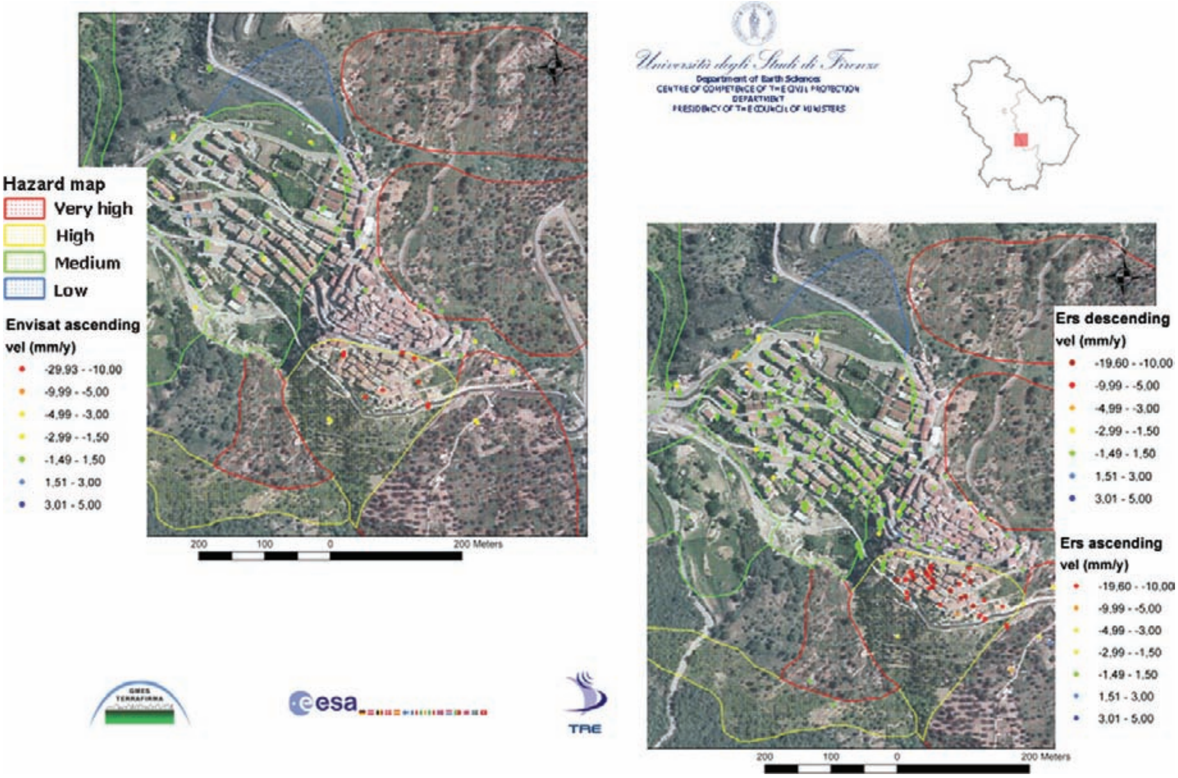

Fig. 18.9 Distribution of PS ERS and Envisat projected on aerial-photo and overlaid on the P.A.I. hazard map

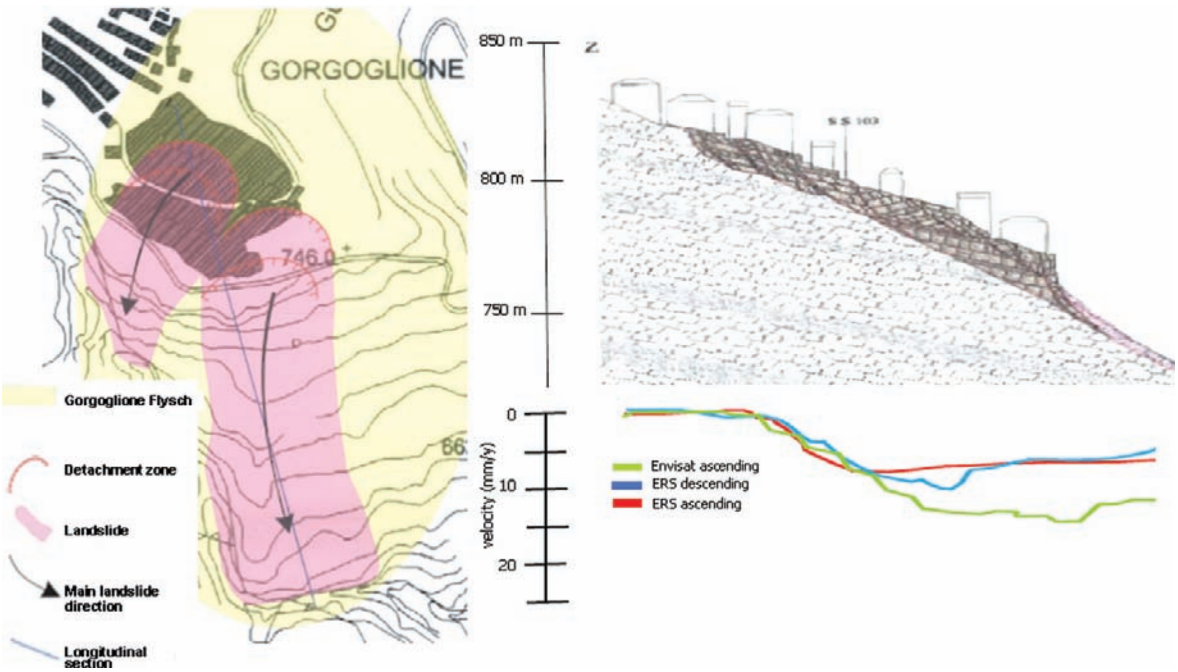

Fig. 18.10 Geomorphologic cross section along Gorgoglione landslide and PS velocity rate interpolation along the cross section

The upper part of the slope is characterized by the presence of a sharp boundary between PS with null velocity and PS with high velocity values. This suggests an advancing phenomenon without any retrogressive activity, this information is consistent with the geological cross section and with the slope instability behaviour since its reactivation in 1980.

The results confirm the capabilities of multi-interferometric InSAR data, integrated and coupled with conventional techniques, to support landslides investigation at regional scale.

Considering the high costs related to landslide damages and the difficulties in the assessment of the state of activity, especially over urban areas, the use of an InSAR approach can positively impact on the current hazard mitigation activities along national and local authorities. As a next step the monitoring of the actual movements using InSAR techniques could be implemented in the risk management procedures.

Acknowledgments This research is funded by the European Space Agency (ESA) within the Terrafirma project. The authors wish to acknowledge M. Doherty and P. Bally of the ESA for the support to the project along with Ren Capes, the Terrafirma project coordinator and his group of the NPA Satellite mapping. A. Corazza, P. Putrino of the National Civil Protection Department are acknowledged for the support in the collection of ancillary data and in the validation activities.

18.5.6 Exploiting Earth Observation Technology to Map, Monitor and Forecast Landslides: the ASI MORFEO Project

by Fausto Guzzetti, Roberto Carlà, Gianfranco Fornaro, Riccardo Lanari (Consiglio Nazionale delle Ricerche) Laura Candela (Agenzia Spaziale Italiana), Giovanna Ober (Carlo Gavazzi Space)

Advances in space borne, airborne and terrestrial remote sensing technologies have improved our ability to identify, map, and monitor ground deformations, including landslides. In 2001, the Italian Space Agency (ASI) launched a multifaceted call for technological and scientific applications of remote sensing technology to help identify, monitor, forecast, and mitigate natural and manmade hazards, including slope failures. In 2007, ASI lunched the MORFEO project, a coordinated research and development initiative aimed at the development and preliminary implementation of a prototype system to support the Italian National Civil Defence Department activities on landslide risk assessment and mitigation.

MORFEO, an Italian acronym for Monitoring Landslide Risk through Earth Observation technology, is a three-year project aimed at the exploitation of Earth observation (EO) data and technologies, consolidated and innovative ground-based monitoring tools, and existing and new thematic and environmental information, to improve the ability of the Italian National Civil Defence Department to promptly identify, map, monitor, and forecast landslides of different types, and in different physiographic environments. For the purpose, MORFEO implements five functionalities of interest for landslide civil defence:

(i) Identification and mapping of landslides (Ardizzone et al., 2007; Galli et al., 2008), at different geographical scales, through the exploitation of state-of-the-art EO data and technologies, including the dynamic 3-dimensional visualization of landslide areas captured by high and very high resolution satellite optical sensors.

(ii) Landslide monitoring, through the integration of state-of-the-art observation technologies (Ardizzone et al., 2007; Guzzetti et al., 2007b), including satellite and ground-based DInSAR and GPS, for monitoring known landslides, and for the rapid identification of new or incipient movements of natural and manmade slopes.

(iii) Landslide susceptibility, hazard, and risk modelling at different geographical scales and for different landslide types (Guzzetti et al., 2005, 2006a,b), through the use of original models that incorporate information derived from high and very high resolution satellite optical and radar images.

(iv) Forecasting of rainfall induced landslides, through models and thresholds and the exploitation of existing landslide information, quantitative rainfall forecasts, precipitation measurements obtained from networks of rain gauges and weather radars, and estimates of rainfall obtained from meteorological satellites (Guzzetti et al., 2007a, 2008).

(v) Landslide vulnerability and damage assessment (Galli and Guzzetti, 2007), through the design of event scenarios constructed exploiting existing high resolution landslide, topographic and thematic data, and high and very high resolution satellite optical and radar images.

Scientists and engineers working within the MORFEO project will be amongst the first to receive and test data acquired by the ASI COSMO-SkyMed constellation of satellites, equipped with radar sensors that can operate with very short revisiting times. Using this unique constellation of SAR sensors, state-of-the-art DInSAR techniques to monitor slope failures in urban areas and to evaluate the stability of large manmade slopes and embankments will be exploited.

The MORFEO team is headed by Carlo Gavazzi Space (CGS), a leading European company in space technology, and by IRPI, a research institute of the Italian National Research Council leader in landslide investigations. CGS and IRPI are assisted by a unique multi-disciplinary team comprising research institutes, university departments and Italian enterprises collectively experts in landslide identification and mapping, slope monitoring, landslide and environmental hazard and risk assessment and mitigation, and in the innovative exploitation of EO data and technologies. MORFEO is characterized by a significant research component, in terms of institutions involved and planned activities. Innovative research is a key aspect of the project because of the challenging task to successfully exploit multiple satellite, airborne, and ground based EO technologies for landslide risk assessment and mitigation.

Figure 18.11 and 18.12 show preliminary results obtained by partners of the MORFEO team. Figure 1, obtained by CNR IFAC, shows 3D-views of the Sarno area, Campania region, affected by multiple catastrophic debris flows on 5 May 1997. Figure 18.11a shows a high altitude, colour aerial photograph taken shortly after the event. Figure 18.11b shows a very high resolution satellite image acquired on July 1999. Analysis of the images indicates that combined state-of-the-art optical remote sensing and dynamic visualization technologies can be used to identify and map landslides effectively. Figure 18.12, prepared by CNR IREA and IRPI, shows surface deformation rate maps in an area of the Assisi Municipality, central Italy, affected by a deep-seated, slow moving landslide. The low resolution (left) and high resolution (right) maps cover the 9-year period from 1992 to 2000, and were obtained processing SAR data acquired by the European Remote Sensing (ERS-1 and ERS-2) satellites along descending orbits. Inspection of the maps reveals a good agreement between the measured surface deformation and the available information on the

(A) (B)

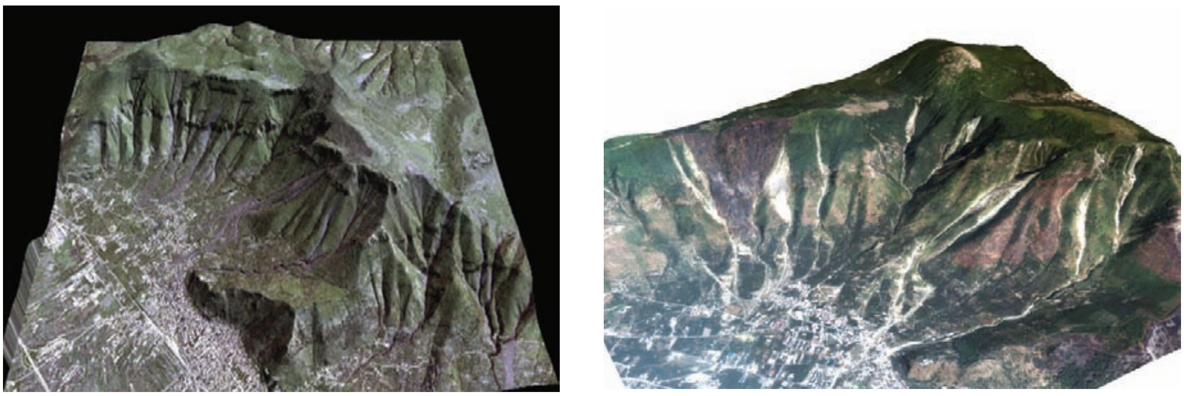

Fig. 18.11 3D-views of the Sarno area, Campania region, affected by multiple catastrophic debris flows on 5 May 1997. (**A**) high altitude colour aerial photograph. (**B**) very high resolution satellite image

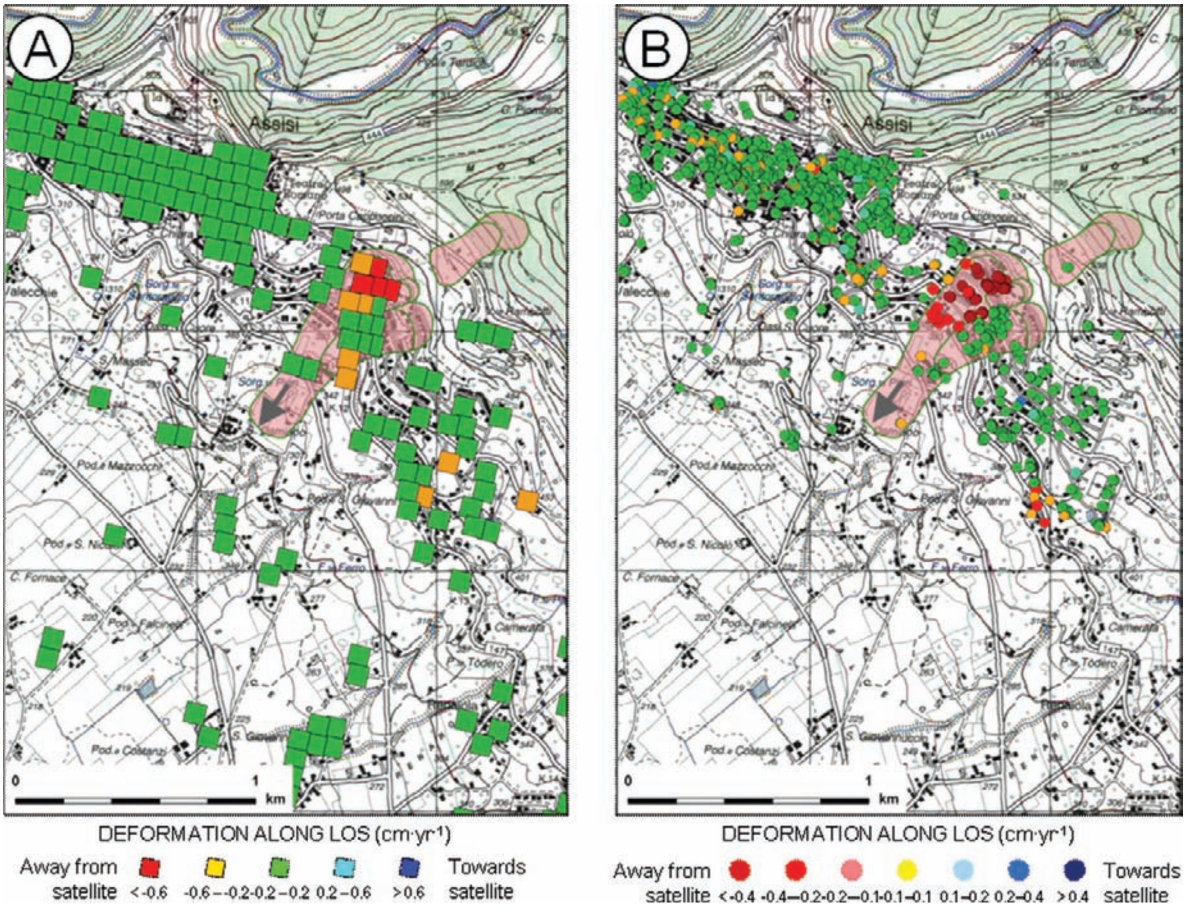

Fig. 18.12 Surface deformation rate maps for the Ivancich landslide area, Assisi Municipality, Italy, in the period from 1992 to 2000. (**A**) Low resolution deformation rate map. (**B**) High resolution deformation rate map. Pink areas show known landslides. Gray arrow shows landslide main direction of motion

location and extent of the landslide. This confirms the effectiveness of the space-borne DInSAR technology to investigate slow moving urbanized landslides in selected areas.

18.5.7 PSInSAR for the Investigating of Unstable Slopes and Landslides

by Wasowski J., Florio, Gigante G. (CNR-IRPI) Bovenga F. (CNR-ISSIA)

Recent years have witnessed an increasing number of initiatives focused on the exploitation of the space-borne synthetic aperture radar differential interferometry (DInSAR) techniques in geohazard investigations (IGOS Geohazards, 2004). These techniques are attractive because of their capability to provide wide-area coverage (thousands km2) and, under suitable conditions, spatially dense information on small ground surface deformations (e.g. Gabriel et al., 1989; Colesanti et al., 2003). Furthermore, the advanced multi-temporal DInSAR methods such as the Permanent/Persistent Scatterers Interferometry (PSInSAR; Ferretti et al., 2001) overcome the limitations of conventional DInSAR and extend the applicability of radar interferometry from regional to local-scale engineering geology investigations of landslides and ground instability in general (e.g. Colesanti and Wasowski, 2006; Ferretti et al., 2006; Farina et al., 2007; Wasowski et al., 2007). Also, thanks to the regular revisit schedule of radar satellites a long-term monitoring of small surface displacements is feasible.

Table 18.6 Advantages and limitations of the current SAR satellite systems and PSInSAR technique (modified after Wasowski et al., 2007)

Advantages	Limitations
Cost-effective for wide-area applications (hundreds and thousands of km^2)	Difficult to anticipate PS distribution without acquiring and processing radar data
High density of radar targets (from tens to hundreds per km^2 in urbanised zones)	The PS density can drop to zero in non-urbanised areas without rock outcrops
Use of "natural" radar targets (without deployment or maintenance costs)	A reliance on natural targets implies that their position cannot be chosen freely
High geo-coding accuracy of radar targets (positioning error within 5–10 m)	About 20 SAR images needed to identify PS (some areas have limited coverage)
High precision (mm) of measurements (comparable to or better than GPS)	Provides 1D deformation data (projection of 3D displacement) along sensor-target LOS
Possibility of retrospective studies exploiting imagery archives spanning over 10 years	A limited range of detectable displacement velocities (usually up to 10 cm/yr)
Regular satellite re-visiting time over the same areas	Satellite repeat-cycle (currently few weeks) suitable only for low displacement gradients
Possibility of continuous, long-term monitoring (several years)	Interferograms cannot be generated from SAR data acquired by different satellites

However, many landslides occur in environmental settings that are not well suited to the application of DInSAR (e.g. vegetated slopes, steep and rough topography). Also, with the exception of urbanised slopes, the density of radar targets usable for interferometric measurements in rural regions is typically low and this makes difficult PSInSAR analysis, as well as introduces considerable uncertainties in the assessments of true ground motions (e.g. Bovenga et al., 2006; Ferretti et al., 2006). Furthermore, the interpretation

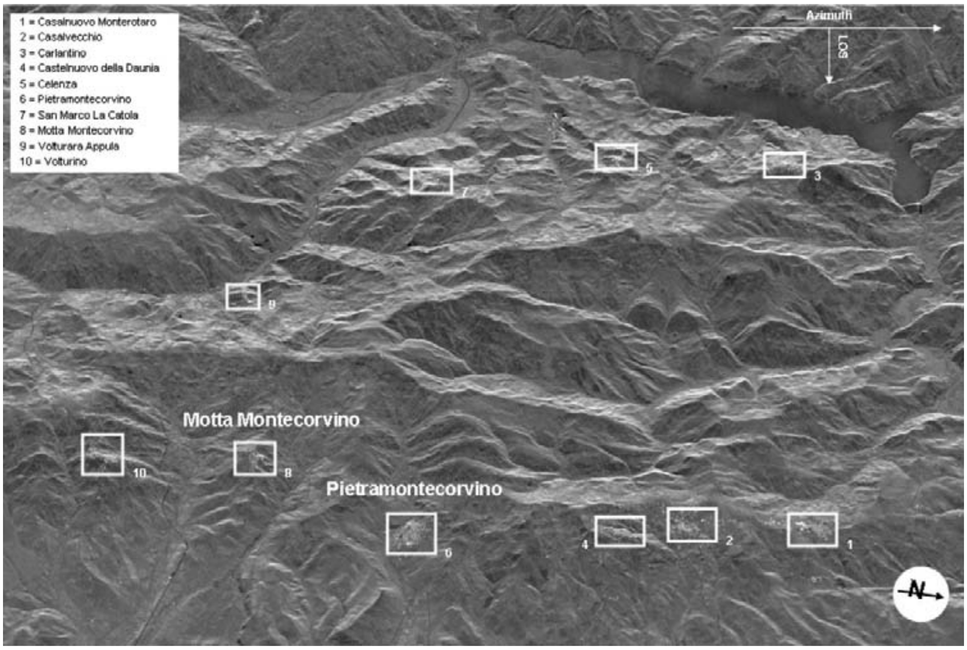

Fig. 18.13 Average SAR amplitude image of the Daunia study area (28 × 27 km): white-border rectangles enclose 10 town areas selected for the PS processing. The results for Motta Montecorvino and Pietramontecorvino areas are shown in Figs. 18.2 and 18.3. Note the prevailingly moderate relief hillslope topography. Radar dataset: European Space Agency (ESA) ERS 1/2 imagery 1992–1999

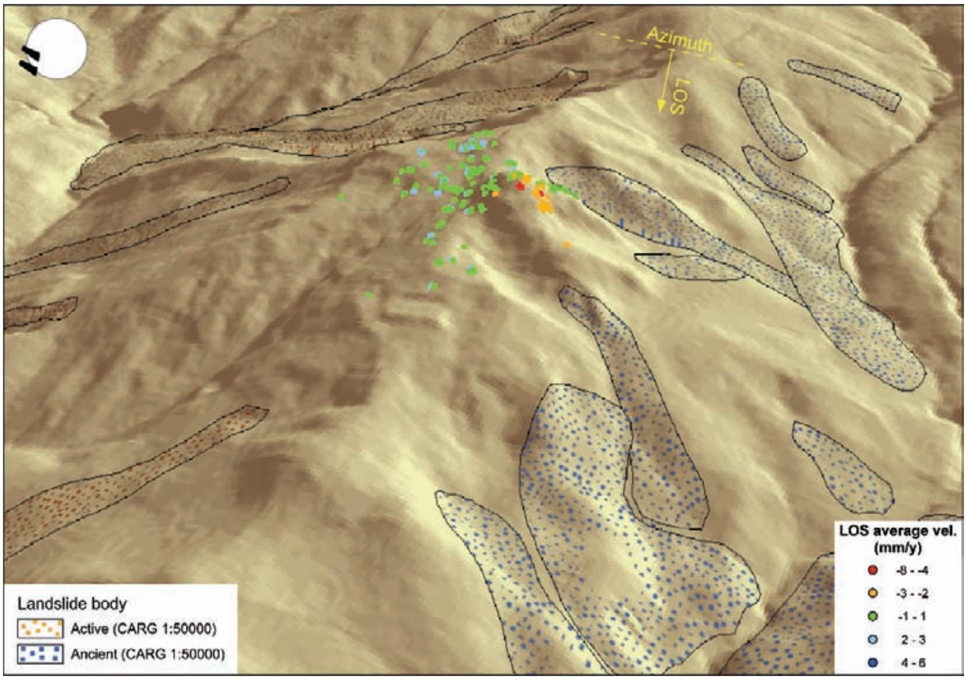

Fig. 18.14 Distribution and Line Of Sight (LOS) velocity of radar targets (PS - color dots) visualised on a high resolution DEM of the Motta Montecorvino area. Active and ancient landslides are from recent CARG maps (http://www.apat.gov.it). Moving PS are found at the northern periphery of this hilltop town, characterized by the presence of old landslide features

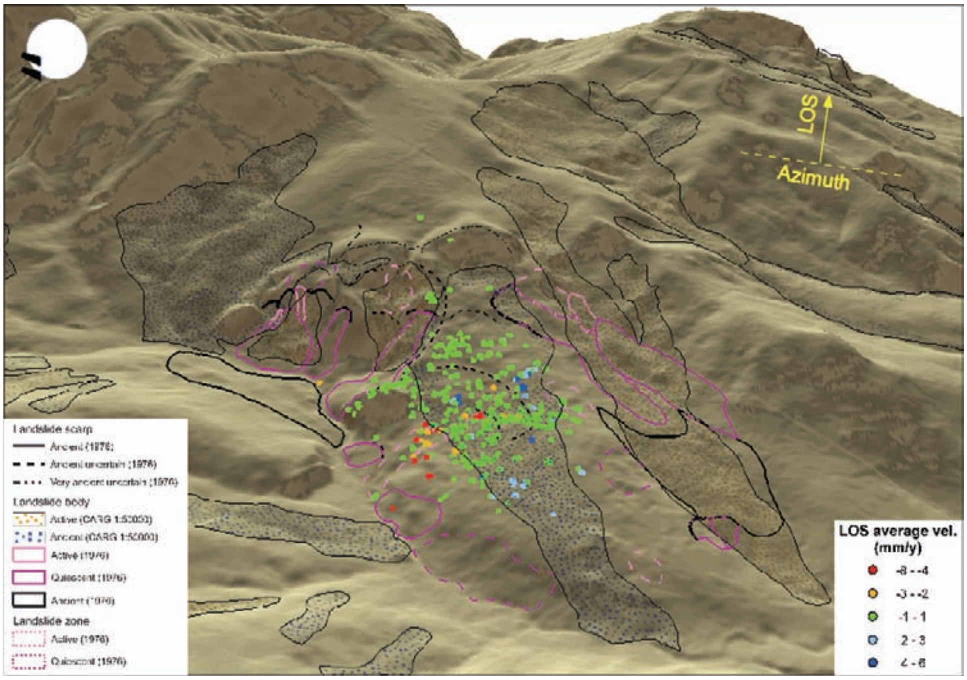

Fig. 18.15 Distribution and LOS velocity of radar targets (PS) visualised on a high resolution DEM of the Pietramontecorvino area. Landslide features including scarps, mappable bodies, as well as landslide zones are based on 1976 airphoto interpretation (after Zezza et al., 1994); active and ancient landslides are from most recent CARG maps (www.apat.gov.it). Complex relation between very slowly moving PS and landslide legacy of the area suggest that ground instabilities detected by radar likely reflect post-failure slope deformations and localized settlements

of the exact geological significance of millimetric to centimetric (per year) displacements currently detectable by PSInSAR can be very challenging, because (i) very slow ground surface deformations may arise from a wide variety of natural and anthropogenic causes and, (ii) most radar targets correspond to man-made objects (e.g. houses) and thus their structural behaviour (and ground-foundation interactions) should be taken into account.

Here, we first highlight the advantages and limitations of the PSInSAR technique (Table 18.6). Then we offer some examples of PSInSAR applications from landslide-prone towns located in the Daunia Apennine Mountains, Italy (Figs. 18.13, 18.14 and 18.15) to: i) illustrate the potential of the technique to provide, under suitable conditions, valuable reconnaissance and local scale complementary information with respect to what can be gained through direct and generally more costly in situ topographic/GPS measurements, ii) draw attention to the difficulties in interpreting the exact geological/geotechnical significance of small ground surface displacements; iii) provide some examples of how GIS tools can be used to visualise and assist in PSInSAR data interpretations.

Finally, we indicate that much progress can be expected in the near future thanks to the most recent (e.g. RADARSAT-2, TerraSAR-X, Cosmo-SkyMed) SAR dedicated missions with shorter repeat cycles and higher spatial resolution (meters) sensors. This and multidisciplinary approaches that integrate information obtained from space and from ground-based slope instability investigations will help to overcome some current limitations of the technique and difficulties in data interpretation.

18.5.8 Satellite Remote Sensing for Landslide Susceptibility Mapping and Landslide Occurrence Prediction on a Global Basis

by Yang Hong (School of Civil Engineering and Environmental Sciences, University of Oklahoma, NASA Goddard Space Flight Center, Laboratory for Atmospheres), Robert F. Adler (NASA Goddard Space Flight Center, Laboratory for Atmospheres), Dalia Kirschbaum (The Earth Institute, Columbia University), and George Huffman (NASA Goddard Space Flight Center, Laboratory for Atmospheres, Science Systems and Applications, Inc., Lanham)

Landslides rank among the most devastating natural disasters, causing billions of dollars in property damages and thousands of deaths in most years around the world. Landslide warning systems can save lives and reduce damages if properly implemented in populated areas of landslide-prone nations (Sidle and Ochiai, 2006). However, predicting landslide occurrences is very difficult and expensive in terms of time and money. Growing populations plus related environmental impacts such as deforestation, have put a growing number of people at risk from landslides. At the same time, the required data infrastructure and analysis capabilities required to minimize injuries and deaths due to landslides are not yet practical in most developing countries that need them the most. The challenge facing our science community is to better understand the surface and meteorological processes leading to landslides and determine how new technology and techniques might be applied to reduce the risk of landslides to people. Today, the possibility exists to take advantage of advances in satellite remote sensing and other global data sets in the development of: (1) a global landslide database; (2) global landslide susceptibility maps; and (3) high time resolution, multi-satellite precipitation analyses with sufficient accuracy and availability to be useful for detecting the heavy rainfall events that provoke landslides. This article discusses the use of information from satellite remote sensing in the study of rain-induced landslides on a global basis, with an eye toward developing a system to detect or forecast such events on a global basis.

Landslides pose a significant threat to populations worldwide, yet their occurrence and frequency are rarely assembled in a database on a global basis. In a recent study, Kirschbaum et al. (2008) compiled a global landslide inventory for rainfall-triggered events for several years, drawing upon news and scholarly articles, governmental and NGO reports, Relief organization information, and other landslide database sites. While this database is not able to capture all rainfall-triggered landslides that occurred in the evaluated years, it presents a lower boundary on the number of events globally and can provide insight into the statistical trends in landslide spatiotemporal distribution and impact. This inventory can serve as a valuable source for assessing patterns in hazard frequency and for use in validating models and susceptibility maps.

Recent advances in remote sensing techniques contribute to determining landslide susceptibility by providing information on land surface features and characteristics. This global view takes advantage of high resolution DEM data from the NASA Shuttle Radar Topographic Mission (SRTM). The 30-m SRTM data, used to derive topographic factors (slope, aspect etc), provide a major breakthrough in digital elevation mapping of the world. In addition, digital maps of soil characteristics prepared by the Food and Agriculture Organization and satellite-based land cover information (e.g., from NASA's Moderate Resolution Imaging Spectroradiometer [MODIS]) are combined with the information from the SRTM to estimate a static landslide susceptibility index for each point on the globe over land. The satellite precipitation information in this study includes the Tropical Rainfall Measuring Mission (TRMM) Multi-satellite Precipitation Analysis (TMPA; Huffman et al., 2007). As needed, the various land datasets are downscaled by linear interpolation to the SRTM full resolution grid to provide the susceptibility information at the finest resolution. A global landslide susceptibility map is then derived following Hong et al., (2007b) from these geospatial data based on each factor's relative significance to the sliding processes. Fig. 18.16 shows the resulting global Landslide Susceptibility Index (LSI) map with a descriptive scale ranging from "negligible" to "high". Excluding permanent snow/ice regions, Fig 18.1a shows that the low LSI areas cover about half of the land (52%), while the areas of high LSI (4%) are mostly located in tropical or sub-tropical regions: the Pacific Rim, the Himalayan belt, South Asia, the Maritime Continent, Central America, Northwestern USA and Canada, Rocky Mountains, the Appalachian Mountains, the Caucasus region, the Alps, and parts of the Middle East and Africa. The spatial distribution of major landslide occurrences, collected from news reports and other sources during the period of January 2004 through September 2006, generally confirms the regions identified by the derived LSI map.

The spatial distribution, duration, and intensity of precipitation play important roles in triggering landslides. Comprehensive modeling of the physical processes involved in landslides helps pinpoint causes of landmass movement (Keefer and Wilson, 1987; Iverson et al., 2000) in relation to rainfall. However, data requirements for implementation of such models can often be prohibitive, leading to simplification of the processes for practical use (Gritzner et al., 2001). In practice, landslide occurrence has been related empirically to rainfall intensity-duration statistics from rain gauge information for specific regions (Larsen and Simon, 1993; Godt et al., 2006) and on a quasi-global basis (Caine, 1980). The recent development of high time resolution, multi-satellite precipitation analyses has provided the potential of detecting heavy rain events associated with landslides in tropical and temperate latitudes without regard for the availability of rain gauges, an issue which frequently limits the application of the previous studies. By using the precipitation information from TMPA, Hong et al. (2006) derived the first satellite-based rainfall Intensity– Duration threshold curve from landslide cases in various climate and geological locations, in parallel to the previous rain-gauge-based studies (Fig. 18.17). Note that the TMPA-based threshold falls below Caine's threshold, likely because the TMPA is an area-average value, rather than a point accumulation.

Knowledge of landslide susceptibility (the "where" of the problem) and the ability to detect heavy rain events that meet threshold conditions (the "when" of the problem) provide the basis for exploring the potential and limitations for analyzing the occurrences of landslides, and even possibly forecasting them. A trial version of a simplified automated decision making procedure is operationally updated every 3-hour at NASA Goddard TRMM Website by integrating the landslide susceptibility zoning map and TRMM rainfall I-D information to locate the likelihood of landslide occurrence (http://trmm.gsfc.nasa.gov/). In order to perform the model validation, a landslide inventory was compiled for 2003 globally from multiple data sources: the International Landslide Centre and the University of Durham, International Consortium on Landslides, EM-DAT International Disaster Database (CRED).

Great strides are being made to integrate satellite remote sensing data into landslide hazard assessment. With fine tuning and regional evaluation,

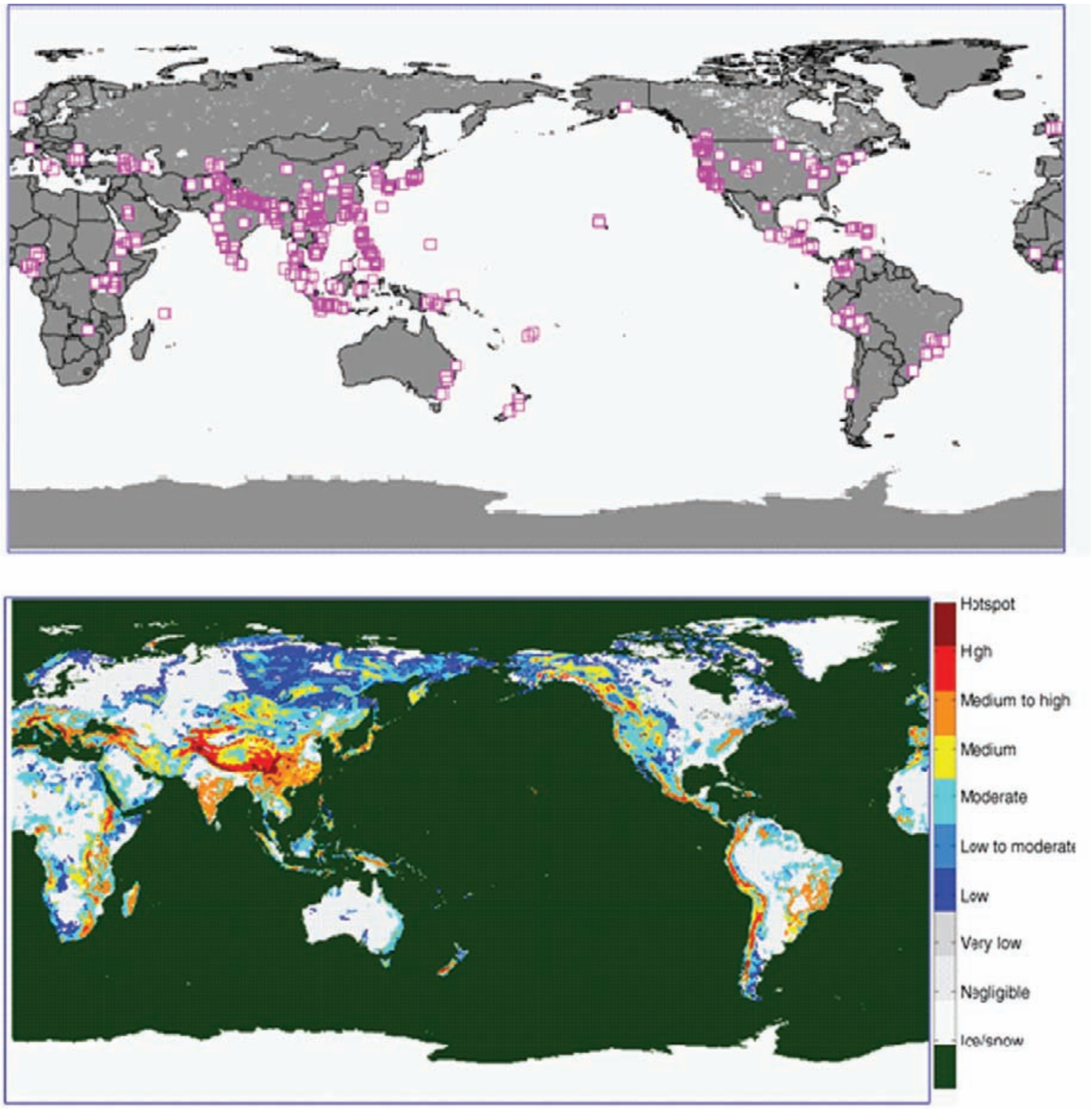

Fig. 18.16 (*upper*) landslide occurrences collected from news reports and other sources during period of January 2004 through September 2006 and (*lower*) Global Landslide Hazard Index and Hotspots

these early studies bear promise in approaching landslide hazard assessment globally and opening up the research community to addressing these issues in a broader context. However, it is important to realize the relative scale at which this type of analysis can be executed (Catani et al., 2005). It remains a matter of research to implement these concepts into a cost-effective method for capacity building in landslide risk management for developing countries.

In the future, increasing availability of improved, yet low-cost remote sensing products that can support locally-tuned landslide models will likely benefit disaster prevention for landslide-prone regions. In order to issue landslide warning forecasts, more accurate medium-range rainfall forecasts will be required to foresee the probability of a landslide occurring in high susceptibility regions at lead-times of several days. Prior to achieving that, the

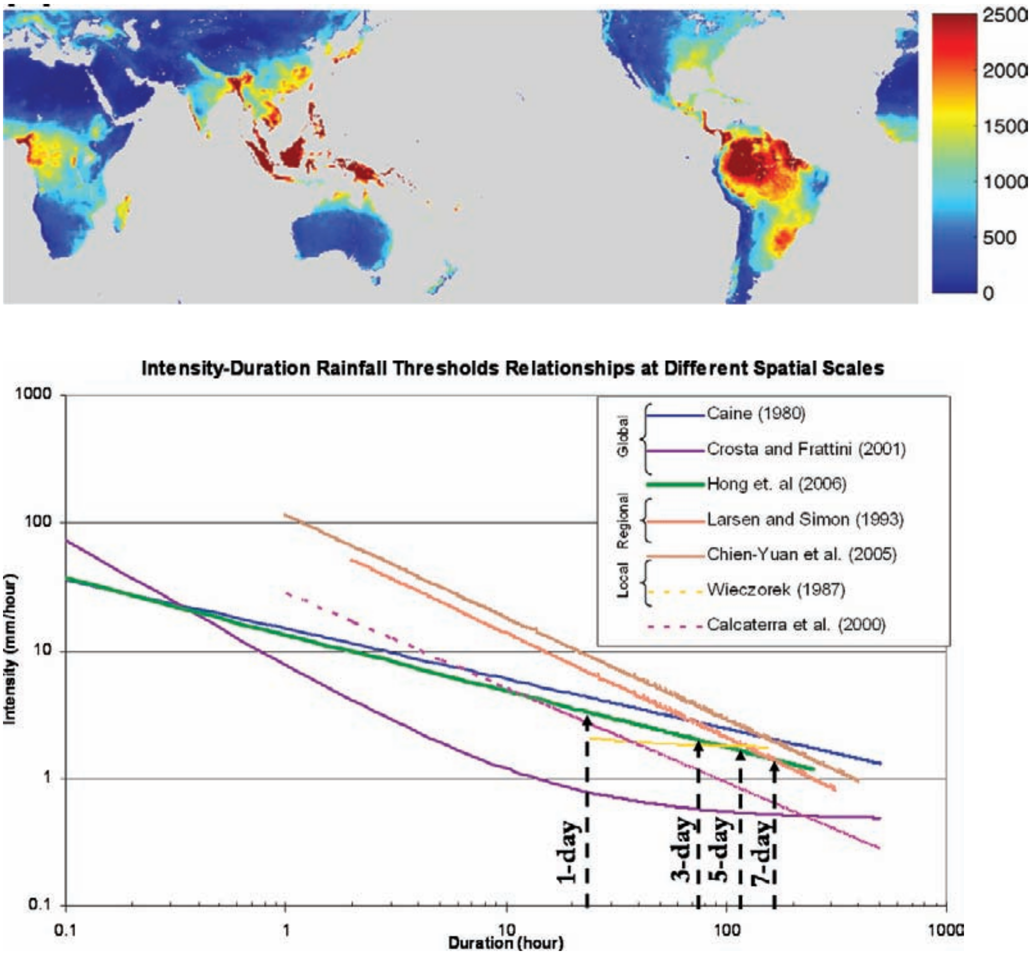

Fig. 18.17 (*upper*) Annual mean precipitation (mm/year) from TRMM-based Multi-satellite Precipitation Analysis data record of 1998–2007 and (*lower*) rainfall Intensity-Duration threshold at the global regional and local scales as derived from seven different studies. Note the satellite-based rainfall intensity-duration threshold curve (green; Intensity = 12.45 Duration-0.42) is adopted from Hong et al., 2006

challenge facing the research community is to continue to develop techniques to better understand landslide processes that translate into potential warning applications. Such efforts must be practical with respect to local expertise and facilities available. The development should also involve capacity building for the vulnerable countries so that they can take advantage of the technical advances. Wide interdisciplinary efforts and multi-agency collaboration is required for landslide disaster prediction, management, and mitigation activities around the globe.

This work is supported by NASA Applied Science and Precipitation Measuring Mission under Stephen Ambrose and Ramesh Kakar of NASA Headquarters.

18.5.9 Landslide Susceptibility Analysis Using ASTER Imagery and GIS

by Saro Lee, Hyun-Joo Oh (Geoscience Information Center, Korea Institute of Geoscience & Mineral Resources (KIGAM))

The aim of this study is to extract landslide-related factors from remote sensing data such as aerial

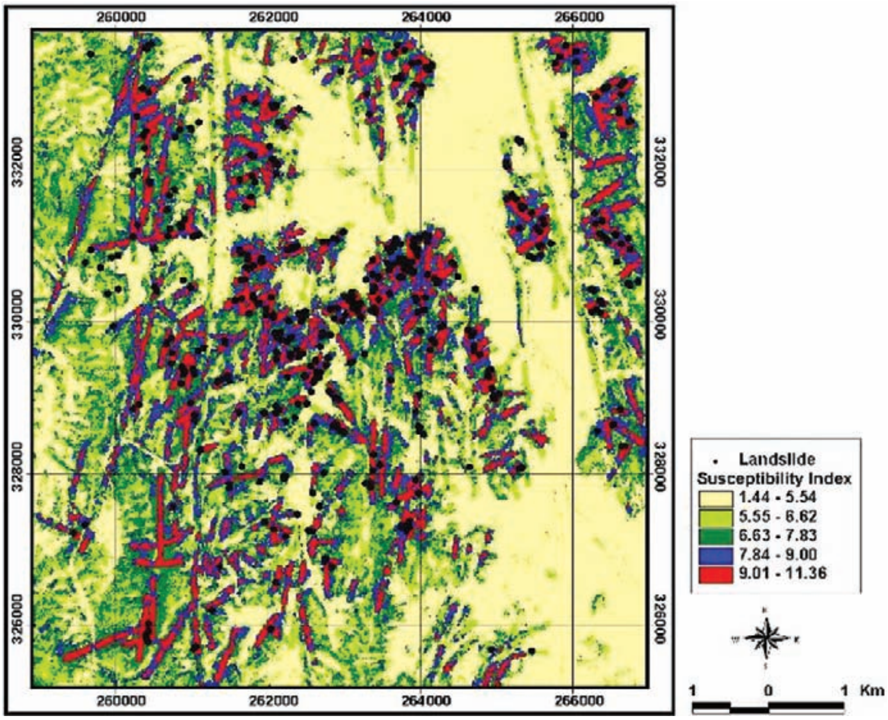

Fig. 18.18 Landslide Susceptibility map using frequency ratio model

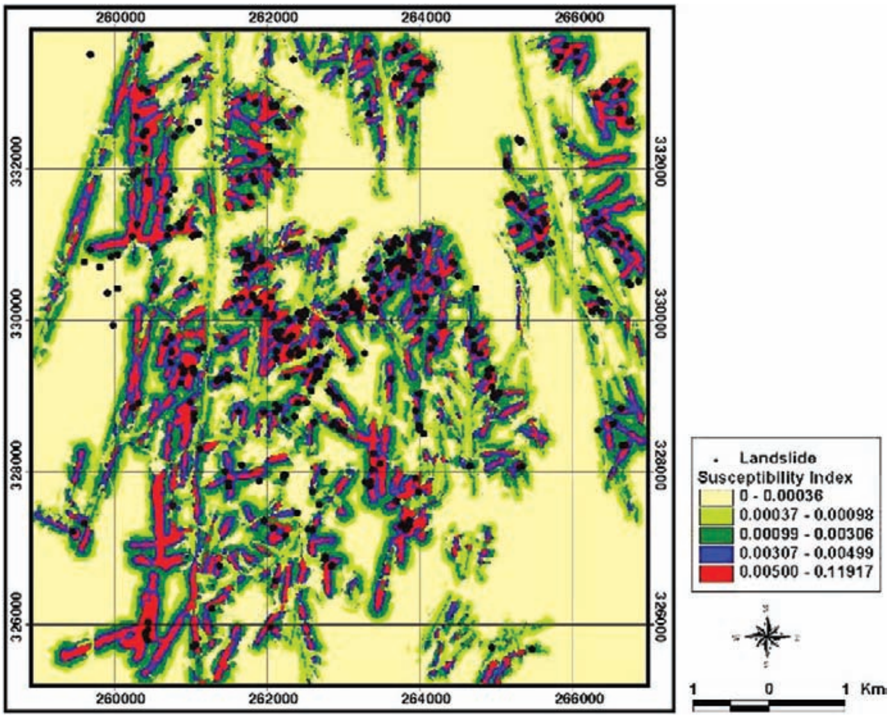

Fig. 18.19 Landslide Susceptibility map using logistic regression model

photographs and ASTER (Advanced Space borne Thermal Emission and Reflection Radiometer) satellite imagery, and to examine their application to the evaluation of the susceptibility to landslides near Boeun, Korea, using a Geographic Information System (GIS).

Landslide locations were identified from an interpretation of aerial photographs and field survey. Information about the factors that influence landslide occurrence was extracted from ASTER imagery. The slope, aspect and curvature of topography, were calculated from the Digital Elevation Model (DEM) that was made from ASTER imagery. Lineaments and land-cover layers were also extracted from the imagery. The difference herein is the manner of use of remote sensing data. ASTER imagery has many advantages for landslide susceptibility mapping. Where there are no topographic, soil, or vegetation maps, these can be quickly and easily extracted to give a susceptibility map from ASTER imagery. Thus, a DEM can be generated from bands 3 N (nadir-viewing) and 3B (backward-viewing) of ASTER imagery acquired by the VNIR sensor. A land-cover map can also be derived from ASTER imagery. There are some studies for landslides susceptibility mapping for the area using existing map data (Lee et al., 2003; Lee et al., 2004; Lee and Choi, 2004). But to our knowledge, the generation of such thematic maps from ASTER imagery has not been previously conducted for landslide susceptibility mapping in anywhere. This procedure was the focus of our work. Landslide-susceptible areas were analyzed and mapped using occurrence factors by a frequency ratio (Fig. 18.18) and logistic regression (Fig. 18.19) models.

The results of the analyses were verified using the landslide location data. In verification, the frequency ratio and logistic regression models showed 84.78% and 84.20% accuracies for each. This suggests a high accuracy in landslide susceptibility mapping. ASTER imagery can therefore be used in landslide susceptibility mapping. In particular, the method can be quickly and easily applied to areas with little map data, and at low cost. As a result remote sensing data are consequently useful in landslide susceptibility mapping. There are many high-resolution satellite images currently available, and these can be used to detect the locations of landslides. Although aerial photographs were used here for detecting landslide, the 15 m resolution ASTER images could be used for that, and considering the frequency of ASTER imagery, allows a comparison to be made before and after an event. An image resolution of 15 m can distinguish large-scale landslides, and this could be improved by the 1 m resolution images now commercially available.

References

Adler RF, Huffman GJ, Bolvin DT, Curtis S, Nelkin EJ (2000) Tropical Rainfall Distributions Determined Using TRMM Combined with Other Satellite and Rain Gauge Information, Journal of Applied Meteorology, 39(12), 2007–2223.

Agliardi F, Crosta GB, Zanchi A (2001) Structural constraints on deep-seated slope deformation kinematics. Engineering Geology 59: 83–102.

Aleotti P, Chowdhury R (1999) Landslide hazard assessment: summary review and new perspectives, Bulletin of Engineering Geology and the Environment, 58(1), 21–44.

Anderson MG, Lloyd DM (1991) Using a combined slope hydrology/stability model to develop cut slope design charts. Proceedings of the Institution Civil Engineers, 91(2), 705–718.

Angeli M, Pasuto A, Silvano S (2000) A critical review of landslide monitoring experiences. Engineering Geology 55, 133–147.

Ardizzone F, Cardinali M, Galli M, Guzzetti F, Reichenbach P. (2007) Identification and mapping of recent rainfall-induced landslides using elevation data collected by airborne Lidar. Natural Hazards and Earth System Sciences, 7, 637–650.

Baecher GB, Christian T (2003) Reliability and statistics in geotechnical engineering. Wiley, Cornwall, UK, 605pp.

Baeza C, Corominas J (1996) Assessment of shallow landslide susceptibility by means of statistical techniques. In: Proceedings of the Seventh International Symposium on Landslides, pp. 147–152.

Berardino P, Costantini M, Franceschetti G, Iodice A, Petranera L, Rizzo V (2003) Use of differential SAR interferometry in monitoring and modelling large slope instability at Maratea (Basilicata, Italy). Engineering Geology, 68, 31–51.

Bernknopf RL, Campbell RH, Brookshire DS, Shapiro CD (1988) A probabilistic approach to landslide hazard mapping in Cincinnati, Ohio, with applications for economic evaluation. IAEG Bull 24(1), 39–56.

Bianchi F, Catani F (2002) Landscape dynamics risk management in Northern Apennines (Italy). In: Brebbia CA, Zannetti P (eds.), Development and application of computer techniques to environmental studies, vol. 1. WIT, Southampton, UK, pp. 319–328.

Boiano U, (1997) Anatomy of a siliciclastic turbidite basin: the Gorgoglione Flysch, Upper Miocene, southern Italy: Physical stratigraphy, sedimentology and sequenze-stratigraphic framework. Sedimentary Geology, 1007(3), 231–262.

Bovenga F, Nutricato R, Refice A, Wasowski J (2006) Application of multi-temporal differential interferometry to slope instability detection in urban/peri-urban areas. Engineering Geology, 88(3–4), 218–239.

Buchroithner M (2002). Meteorological and earth observation remote sensing data for mass movement preparedness. Advances in Space Research, 29(1), 5–16.

Burton A, Arkell TJ, Bathurst JC (1998) Field variability of landslide model parameters. Environmental Geology 35(2–3), 100–114.

Caine N (1980), The rainfall intensity-duration control of shallow landslides and debris flows, Geografiska Annaler, 62A, 23–27.

Canuti P, Casagli N (1996) Considerazioni sulla valutazione del rischio di frana. Estratto da “Fenomeni franosi e centri abitati”, Atti del convegno di Bologna del 27 maggio 1994.

Canuti P, Casagli N, Ermini L, Fanti R, Farina P (2004) Landslide activity as a geoindicator in Italy: significance and new perspectives from remote sensing , Environmental Geology, 45, 907–919.

Carrara A (1983) Multivariate methods for landslide hazard evaluation. Mathematical Geology 15(3), 403–426.

Carrara A, Cardinali M, Detti R, Guzzetti F, Pasqui V, Reichenbach P (1991) GIS techniques and statistical models in evaluating landslide hazard. Earth Surface Processes and Landforms, 16, 427–445.

Catani F, Casagli N, Ermini L, Righini G, Menduni G (2005), Landslide hazard and risk mapping at catchment scale in the Arno River basin, Landslide, 2(4), pp. 329–342, DOI: 10.1007/s10346-005-0021-0.

Casagli N, Fanti R, Nocentini M, Righini G (2005) Assessing the capabilities of VHR satellite data for debris flow mapping in the Machu Picchu area. In: K. Sassa, H. Fukuoka, F. Wang, G. Wang (eds.), Landslides, Risk analysis and Sustainable Disaster Management, Proceeding of the First General Assembly of the International Consortium on Landslides.

Cheng K, Wei C, Chang S (2004) Locating landslides using multi- temporal satellite images. Advances in Space Research, 33, 296–301.

Chung CF, Fabbri AG, van Western CJ (1995) Multivariate regression analysis for landslide hazard zonation. In: Carrara A, Guzzetti F (eds.), Geographical information system in assessing natural hazards. Kluwer, Dordrecht, The Netherlands, pp. 107–142.

Colesanti C, Ferretti A, Prati C, Rocca F (2003) Monitoring landslides and tectonic motions with the Permanent Scatterers Technique. Engineering Geology, 68(1), 3–14.

Colesanti C, Wasowski J, (2006) Investigating landslides with satellite Synthetic Aperture Radar (SAR) interferometry. Engineering Geology, 88(3–4), 173–199.

Colesanti F, Ferretti A, Prati C, Rocca F (2003) Monitoring landslides and tectonic motions with the Permanent Scatterers Techni- que. Engineering Geology, 68, 3–14.

Costantini M, Malvarosa F, Minati F, Pietranera L, Milillo G (2002). A three-dimensional phase unwrapping algorithm for processing of multitemporal SAR interferometric measurements. In: Proceedings of the IEEE International Geoscience and Remote Sensing Symposium (IGARSS), Toronto (Canada), vol. 3, pp. 1741–1743.

Costantini M, Rosen PA (1999). A generalized phase unwrapping approach for sparse data. In: Proceedings of the International Geoscience and Remote Sensing Symposium (IGARSS), Hamburg (Germany) pp. 267–269.

Crosta G (1998) Regionalization of rainfall thresholds: an aid to landslide hazard evaluation. Environmental Geology, 35: 131–145.

Crosta G, Frattini P (2001) Rainfall thresholds for triggering soil slips and debris flow. Proc. of the 3rd Plinius Conference 2001.

Crosta GB, Agliardi F (2003) Failure forecast for large rock slides by surface displacement measurements. Canadian Geotechnical Journal, 40, 176–191.

Crosta GB, Dal Negro P (2003) Observations and modelling of soil slip-debris flow initiation processes in pyroclastic deposits: the Sarno 1998 event. Natural Hazards and Earth System Sciences, 3, 53–69.

Crozier MJ (1986) Landslides: Causes, Consequences and Envirorment. Croom Helm, London, p. 252.

Dai F, Lee C, Ngai Y (2002). Landslide risk assessment and management: An overview. Engineering Geology, 64, 65–87.

Delacourt C, Briole P, Achache J (1998) Tropospheric corrections of SAR interferograms with strong topography. Application to Etna, Geophysical Research Letters, 25(15), 2849–2852.

Delacourt C, Alleman P, Casson B, Vadon H (2004) Velocity field of the ’La Clapiere’ landslide measured by the correlation of aerial and QuickBird satellite images. Geophysical Research Letters, 31(15), 15619.

Ermini L, Catani F, Casagli N (2005) Artificial neural networks applied to landslide susceptibility assessment. Geomorphology, 66, 327–343.

Farina P, Colombo D, Fumagalli A, Marks F, Moretti S (2006) Permanent Scatterers for landslide investigations: outcomes from the ESA-SLAM project. Enginneering Geology, 88, 200–217.

Farina P, Casagli N, Ferretti A (2007) Radar-Interpretation of InSAR Measurements for Landslide Investigations in Civil Protection Practices. Proc. 1st North American Landslide Conference, Vail, Colorado, USA, 3–8 June 2007, pp. 272–283.

Ferretti A, Prati C, Rocca F (2001) Permanent Scatterers in SAR Interferometry. IEEE Trans. Geoscience And Remote Sensing, 39(1), 8–20.

Ferretti A, Prati C, Rocca F, Wasowski J (2006) Satellite interferometry for monitoring ground deformations in the urban environment. Proc. 10th IAEG Congress, Nottingham, UK (CD-ROM).

Fruneau B, Achache J, Delacourt C (1996). Observation and modelling of the Saint-Etienne-de-Tinee landslide using SAR interfer- ometry. Tectonophysics, 265, 181–190.

Gabriel AK, Goldstein RM, Zebker HA (1989) Mapping Small Elevation Changes over Large Areas: Differential Radar Interferometry. Journal Geophysics Research 94(B7), 9183–9191.

Galli M, Ardizzone F, Cardinali M, Guzzetti F, Reichenbach P (2008) Comparison of landslide inventory maps. Geomorphology, 94, 268–289.

Gili JA, Corominas J, Rius J (2000) Using Global Positioning System techniques in landslide monitoring. Engineering Geology 55, 95–113.

Galli M, Guzzetti F (2007) Vulnerability to landslides in Umbria, central Italy. Environmental Management, 40, 649–664.

Godt, JW, Baum RL, Chleborad AF (2006), Rainfall characteristics for shallow landsliding in Seattle, Washington, USA, Earth Surface Processes and Landforms, 31, pp. 97–110.

Gritzner ML, Marcus W, Aspinall R, Custer S (2001) Assessing landslide potential using GIS, soil wetness modeling and topographic attributes, Payette River, Idaho. Geomorphology, 37, 149–165.

Gupta R, Saha A (2001). Mapping debris flows in the Himalayas, natural resource management. GISdevelopment. net, p. 4.

Guzzetti F, Galli M, Reichenbach P, Ardizzone F, Cardinali M (2006a) Landslide hazard assessment in the Collazzone area, Umbria, central Italy. Natural Hazards and Earth System Sciences, 6, 115–131.

Guzzetti F, Peruccacci S, Rossi M, Stark CP (2007a) Rainfall thresholds for the initiation of landslides in central and southern Europe. Meteorology and Atmospheric Physics, 98, 239–267.

Guzzetti F, Peruccacci S, Rossi M, Stark CP (2008). The rainfall intensity-duration control of shallow landslides and debris flows: an update. Landslides, 5(1), 3–17.

Guzzetti F, Reichenbach P, Ardizzone, F, Cardinali M, Galli M, (2006b) Estimating the quality of landslide susceptibility models. Geomorphology, 81, 166–184.

Guzzetti F, Reichenbach P, Cardinali M, Galli M, Ardizzone F (2005) Probabilistic landslide hazard assessment at the basin scale. Geomorphology, 72, 272–299.

Guzzetti F, Manunta M, Ardizzone F, Pepe A, Cardinali M, Zeni G, Galli M, Lanari R, Reichenbach P (2007b) Analysis of ground deformation detected using the SBASS-DInSAR technique in Umbria, Central Italy. Submitted to: Pure and Applied Geophysics.

Hervas J, Barredo J, Rosin P, Pasuto A, Mantovani F, Silvano S (2003). Monitoring landslides from optical remotely sensed imagery: The case story of Tessina landslide, Italy. Geomorphology, 54, 63–75.

Hong Y, Adler R, Huffman G (2006), Evaluation of the Potential of NASA Multi-satellite Precipitation Analysis in Global Landslide Hazard Assessment, Geophysical Research Letter, 33, L22402, doi:10.1029/2006GL028010.

Hong Y, Adler R, Huffman G (2007a) Use of satellite remote sensing data in the mapping of global landslide susceptibility, Natural Hazards, 43(2).

Hong Y, Adler R, Huffman G (2007b) Use of Satellite Remote Sensing Data in mapping of global shallow landslides Susceptibility, Journal of Natural Hazards, DOI: 10.1007/s11069-006-9104-z.

Hong, Y, Adler R, Huffman G (2007c), An Experimental Global Monitoring System for Rainfall-triggered Landslides using Satellite Remote Sensing Information, IEEE TGRS, DOI: 10.1109/TGRS.2006.888436.

Huffman GJ, Adler RF, Bolvin DT, Gu G, Nelkin EJ, Bowman KP, Hong Y, Stocker EF, Wolff DB (2007d) The TRMM Multi-satellite Precipitation Analysis: Quasi-Global, Multi-Year, Combined-Sensor Precipitation Estimates at Fine Scale. Journal of Hydrometeor, 8(1), 38–55.

Huggel C, Kaab A, Haeberli W, Teysseire P, Paul F (2002) Remote sensing based assessment of hazards from glacier lake outbursts: A case study in the Swiss Alps. Canadian Geotechnical Journal, 39, 316–330.

IGOS GEOHAZARDS (2004) Geohazards Theme Report: For the monitoring of our Environment from Space and from Earth. European Space Agency publication, 55p.

IUGS/WGL—International Union of Geological Sciences Working Group on Landslides (1995) A suggested method for describing the rate of movement of a landslide.IAEGBull. 52, 75–78 Hamburg, pp. 1993–1939.

Iverson RM, Reid ME, Iverson NR, LaHusen RG, Logan M, Mann JE, Brien DL (2000) Acute sensitivity of landslide rates to initial soil porosity, Science, 290, 20.

Iverson RM (2000) Landslide triggering by rain infiltration. Water Resources Research, 36, 1897–1910.

Jade S, Sarkar S (1993) Statistical models for slope stability classication. Engineering Geology, 36, 91–98.

Kaab A (2000). Photogrammetry for early recognition of high mountain hazards: New techniques and applications. Physics and Chemistry of the Earth (B), 25(9), 765–770.

Kaab A (2002) Monitoring high-mountain terrain deformation from repeated air- and spaceborne optical data: examples using digital aerial imagery and ASTER data ISPRS, Journal of Photogrammetry and Remote Sensing, 57(1-2), 39–52.

Kaab A, Wessels R, Haeberli W, Huggel C, Kargel J, Khalsa S (2003). Rapid ASTER Imaging facilities timely hazard assessment of glacier hazards and disasters. EOS. Transactions American Geophysical Union, 84(13), 117–124.

Keefer DK, Wilson RC (1987) Real-time landslide warning during heavy rainfall: Science, 238(13), 921–925.

Kimura H, Yamaguchi Y (2000) Detection of landslide areas using radar interferometry. Photogrammetric Engineering Remote Sensing 66(3), 337–344.

Kirschbaum D, Hill S, Adler R, Hong Y (2008) Global landslide inventory database for hazard applications, Landslide (submitted).

Kniveton, D, de Graff P, Granicas K, Hardy R (2000). The development of a remote sensing based technique to predict debris flow triggering conditions in the French Alps. International Journal of Remote Sensing, 21(3), 419–434.

Larsen, MC, Simon A (1993) A rainfall intensity-duration threshold for landslides in a humid-tropical environment, Puerto Rico, Geografiska Annaler, 75, 13–23.

Lee S (2005) Application of logistic regression model and its validation for landslide susceptibility mapping using GIS and remote sensing data, International Journal of Remote Sensing, 26(7), 1477–1491.

Lee S, Choi J, Min K (2004) Probabilistic Landslide Hazard Mapping using GIS and Remote Sensing Data at Boeun,

Korea. International Journal of Remote Sensing, 25, 2037–2052.
Lee S, Choi J (2004) Application of a weight-of-evidence model to landslide susceptibility analysis, International Journal of Geographic Information Science, 18, 789–814.
Lee S, Ryu J, Lee M, Won J (2003) Landslide susceptibility analysis using artificial neural network at Boeun, Korea. Environmental Geology, 44, 820–833.
Lin S, Lin, J, Hung YHC, Yang, MD (2002) Assessing debris flow hazard in a watershed in Taiwan. Engineering Geology, 66, 295–313.
Liu JG, Mason PJ, Clerici N, Chen S, Davis AM, Miao F, Deng H, Lieng L (2003) Landslide Hazard Assessment in the Three Gorges Area of the Yangtze River using ASTER Imagery. Proceedings of IGARSS 2003 July 21–25, 2003.
Lu P, Rosenbaum MS (2003) Articial neural networks and grey systems for the prediction of slope stability. Nat Hazards, 30(3), 383–398.
Mantovani F, Soeters R, Van Westen CJ (1996) Remote sensing techniques for landslide studies and hazard zonation in Europe, Geomorphology, 15(3–4), 213–225.
Massonnet D, Rossi M, Carmona C, Adragna F, Peltzer G, Feigl K, Rabaute T (1993) The displacement field of the Landers earth- quake mapped by radar interferometry. Nature, 364, 138–142.
Massonnet D, Briole P, Arnaud A (1995) Deflation of Mount Etna monitored by space radar interferometry. Nature, 375, 567–570.
Massonnet D, Feigl KL (1998) Radar interferometry and its application to changes in the earth's surface. Review Geophysics, 36(4), 441–500.
Metternicht G, Hurni L, Gogu R (2005) Remote sensing of landslides: An analysis of the potential contribution to geo-spatial systems for hazard assessment in mountainous environments. Remote Sensing of Environment 98(2005), 284–303.
Montgomery DR, Dietrich WE (1994) A physically based model for the topographic control on shallow landsliding. Water resources research, 30(4), 1153–1171.
Moretti S, Righini G (2004) Dati ottici satellitari ad alta risoluzione per l'inventario dei movimenti di versante. Atti della 8° Conferenza Nazionale ASITA, Roma, 14–17 Dicembre 2004.
Nagarajan R, Mukherjee A, Roy A, Khire M (1998) Temporal remote sensing data and GIS application in landslide hazard zonation of part of Western Ghat, India. International Journal of Remote Sensing, 19(4), 573–585.
Nichol J, Wong MS (2008) Satellite remote sensing for detailed landslide inventories using change detection and image fusion. Internationa Journal of Remote Sensing, 26(6), 1913–1926.
Noverraz F, Bonnard C, Dupraz H, Huguenin L (1998) Grands glissements de versants et climat – VERSINCLIM – Comportement passé, présent et futur des grands versants instables subactifs en fonction de l'évolution climatique, et évolution en continu des mouvements en profondeur. Rapport final PNR 31, vdf Hochschulverlag AG an der ETH Zürich, 314pp.
Paganini M (2004). The use of space-borne sensors for the monitoring of slope instability: Present potentialities and future opportunities. In: J.R. Centre (ed.), Workshop on risk mitigation of slope instability. Ispra, Italy' Institute for the Protection and Security of the Citizen.
Prati C, Rocca F, Ferretti A (2004). Radar Interferometry using space- borne data: Potentials and operational capabilities. In J.R. Centre (ed.), Workshop on risk mitigation of slope instability. Ispra, Italy' JRC- Institute for the Protection and Security of the Citizen.
Refice A, Guerriero L, Bovenga F, Wasowski J, Atzori S, Ferrari R, Marsella M (2001) Detecting landslide activity by SAR interferometry. Proc ERS-ENVISAT Symposium, Goteborg.
Rizzo V, Tesauro M (2000) SAR interferometry and field data of Randazzo landslide (Eastern Sicily, Italy). Phys Chem Earth (B), 25(9), 771–780.
Rott H, Siegel A (1999) Analysis of mass movements in alpine terrain by means of SAR interferometry. Proceedings of IGARSS'99, Hamburg, pp. 1993–1939.
Rott H, Mayer C, Siegel A (2000) On the operational potential of SAR interferometry for monitoring mass movements in alpine areas. Proceedings of EUSAR 2000, Munchen, Germany, pp. 43–46.
Rott H (2004). Requirements and applications of satellite techniques for monitoring slope instability in Alpine areas. Workshop on risk mitigation of slope instability. Ispra, Italy' JRC-Institute for the Protection and Security of the Citizen.
Scanvic JY, Girault F (1989) Imagerie SPOT-1 et inventaire des mouvements de terrain: l'exemple de La Paz (Bolivie). Photointerpretation, 89-2(1), 1–20.
Sidle RC, Ochiai H (2006), Landslide Processes, Prediction, and Land use, American Geophysical Union Press, Washington DC.
Singhroy V (1995) Sar integrated techniques for geohazard assessment. Advances in Space Research, 15(11), 67–78.
Singhroy V (2002). Landslide hazards: CEOS, The use of earth observing satellites for hazard support: Assessments and scenarios. Final report of the CEOS Disaster Management Support Group, NOAA, p. 98.
Singhroy V, Mattar K, Gray A (1998). Landslide characterisation in Canada using interferometric SAR and combined SAR and TM images. Advances in Space Research, 21(3), 465–476.
Soeters R, Van Westen CJ (1996) Slope instability, recognition, analysis and zonation, Landslides: Investigation and Mitigation. Special Report 247. Transportation.
Strozzi T, Wegmuller U, Tosi L, Bitelli G, Spreckels V (2001) Land subsidence monitoring by differential SAR interferometry. Photogrammetric Engineering and Remote Sensing, 67, 1261.
Terlien MTJ (1998) The determination of statistical and deterministic hydrological landslide-triggering thresholds. Environmental Geology, 35(2–3), 124–130.
Tofani V, Dapporto S , Vannocci P, Casagli N (2006) Infiltration, seepage and slope instability mechanisms during the 20–21 November 2000 rainstorm in Tuscany, central Italy, Natural Hazards and earth System Sciences, 6, 1025–1033.
van Westen C, Rengers N, Terlien M, Soeters R (1997). Prediction of the occurrence of slope instability phenomena through GIS-based hazard zonation. Geologische Rundschau, 86, 404–414.

Varnes, D (1984). Landslide hazard zonation: A review of principles and practice. Paris' UNESCO, 63pp.

Wasowski J, Ferretti A, Colesanti C (2007) Space-borne SAR interferometry for long term monitoring of slope instability hazards. Proceedings of 1st North American Landslide Conference, Vail, Colorado, USA, 3–8 June 2007, pp. 234–243.

Werner CL, Wegmuller U, Wiesmann A, Strozzi T, (2003) Interferometric Point Target Analysis for Deformation Mapping. IGARSS Proceedings 2003, Toulouse.

Wieczorek G (1983). Preparing a detailed landslide-inventory map for hazard evaluation and reduction. Bulletin of the Association of Engineering Geologists, 21(3), 337–342.

Wieczorek GF (1987) Effect of rainfall intensity and duration on debris flows in central Santa Cruz Mountains, California. In: J.E. Costa, G.F. Wieczorek (eds.), Debris flows avalanches: processes, recognition and mitigation. Reviews in Engineering Geology, Gelogical Society of America, 7, 23–104.

Wieczorek GF, Gori PL, Jager S, Kappel WM, Negussy D (1996) Assessment and management of landslide hazards near Tully Valley landslide, Syracuse, New York, USA. In: Proceedings of the VII International Symposium on Landslides, Trondheim, June 1996, vol. 1. Balkema, Rotterdam, The Netherlands, pp. 411–416.

Wu W, Sidle RC (1995) A distributed slope stability model for steep forested basins. Water Resources Research, 31(8), 2097–2110.

Yamaguchi Y, Tanaka S, Odajima T, Kamai T, Tsuchida S (2008) Detection of a landslide movement as geometric misregistration in image matching of SPOT HRV data of two different dates. International Journal of Remote Sensing, 24(18), 3523–3534.

Zebker HA, Goldstein RM (1986) Topographic mapping from interferometer synthetic aperture radar observation. Journal of Geophysical Research, 91(B5), 4993–5000.

Zezza F, Merenda L, Bruno G, Crescenzi E, Iovine G (1994). Condizioni di instabilità franosa nei centri abitati dell'Appennino Dauno Pugliese. Geol. Appl. e Idrogeol., 29, 77–438.

Zhou C, Lee C, Li, J, Xu Z (2002). On the spatial relationship between landslides and causative factors on Lantau Island, Hong Kong. Geomorphology, 43, 197–207.

Mapping: Inventories, Susceptibility, Hazard and Risk

19

Javier Hervás and Peter Bobrowsky

Abstract Generation of landslide maps is of great significance for land use planning, engineering works design and civil protection and risk reduction programmes. Landslide maps may portray past and current landslide occurrence mainly in the form of inventories, zonation of the spatial probability of future landslide occurrence in the form of susceptibility maps, zonation of its spatio-temporal probability in the form of landslide hazard maps, and the expected damage or losses by landslides as risk maps.

This chapter introduces the interrelated concepts of mapping landslide inventories, susceptibility, hazard and risk. It further presents main landslide inventory methods, contents and tools. Then it discusses the differences between landslide susceptibility and hazard mapping and provides an overview of some of the most commonly used methods of susceptibility and hazard analysis, from qualitative (heuristic) approaches to quantitative (statistical and physically based) models. It also introduces the concept of landslide risk and discusses some qualitative and quantitative approaches to risk assessment and mapping. Finally, it provides case study examples of landslide mapping approaches and programmes.

Keywords Landslide mapping • Inventory • Susceptibility • Hazard • Risk • Zonation

19.1 Introduction

Mapping past and current landslide occurrence, delineating the areas where landslides may occur in the future, and evaluating the associated risk to population, infrastructure and property is of the utmost importance to land use planning, engineering works design and civil protection programmes which aim to minimize human and material losses due to landslides.

Javier Hervás (✉)
Joint Research Centre (JRC), Ispra, Italy

Peter Bobrowsky
Geological Survey of Canada, Ottawa, Canada

It is also widely recognized that without suitable landslide-related maps, disaster prevention and mitigation strategies cannot be appropriately implemented (Hervás 2003). Consequently, there is a need for extensive landslide mapping programmes at adequate scales as well as the application of cost-effective methods and models for reliable and comparable landslide susceptibility, hazard and risk assessment and mapping. All of these should be suited to the unique geological, physiographical, environmental and slope process settings under study.

Landslide inventory efforts and especially susceptibility, hazard and risk zonation mapping generally require extensive data collection and modelling work.

K. Sassa, P. Canuti (eds.), *Landslides – Disaster Risk Reduction*,
© Springer-Verlag Berlin Heidelberg 2009

Currently, a number of factors are contributing to the generation of more reliable, comprehensive and readily accessible landslide-related maps. These include the wide availability of remotely sensed satellite data at various spatial resolutions and spectral wavelengths, the ability to generate digital elevation models (DEM) from such data, off-the-shelf state-of-the-art GIS software tools and related database management systems (including also GIS-based models available in the public domain), and statistical software. Under such a "technologically dependent" scenario, the role of the expert earth scientist still stands out as critical to the success of the mapping endeavour.

On the other hand, issues such as the wide spectrum of terrain and environmental factors that condition and trigger landslide occurrence and the limited knowledge of their relative influence on causing landslides of different types, the frequent absence of information on landslide age, as well as the different methods and techniques applied to model the future spatial and temporal occurrence of landslides, collectively make landslide susceptibility, hazard and risk assessment a complex job (Bichler et al. 2004; van Westen et al. 2006). This is further exacerbated in efforts to harmonize the derived maps for comparative purposes. The latter is particularly important if maps are to be used in the legislation of land use and in risk prevention and mitigation (Hervás 2007; Günther et al. 2008 in this chapter).

This chapter provides a background and overview for thematic session on "landslide mapping: inventories, susceptibility, hazard and risk" within the First World Landslide Forum (November 2008) in Tokyo, Japan. The first part includes an overview of common types, approaches and models for landslide-related mapping, including landslide inventories and zonation of susceptibility, hazard and risk. The second part consists of selected extended abstracts submitted to the Forum, focused on recent landslide inventories/mapping and their application, new zonation approaches/models and programmes, and other case studies.

19.2 Landslide Inventories

Landslide inventories mainly show past and current landslide occurrence (Grignon et al. 2004). The generation of landslides inventories has evolved in time from the compilation of comprehensive paper datasheets and detailed geomorphological maps based mainly on field surveys, interpretation of aerial photographs and examination of historical archives (e.g. Carrara and Merenda 1976), to the additional processing and analysis of remotely sensed digital imagery and DEM (e.g. Fruneau et al. 1996; Hervás et al. 2003; McKean and Roering 2004; Metternicht et al. 2005; Farina et al. 2006) and the integration of the collected or derived information in digital databases. Ideally, the analysis of aerial or satellite imagery from different time periods is useful to produce multi-temporal landslide inventories, which can in turn be used for landslide hazard modelling in highly landslide-prone areas. Such databases usually include GIS-based maps and associated attribute tables, are often coupled with external database management tools and can be made readily available to a wide range of users (decision makers, practitioners, researchers and the general public) through web-based GIS applications (e.g. Grignon and Bobrowsky 2005; Trigila et al. 2007) (Fig. 19.1).

The main purpose of landslide inventory maps is to portray the location (spatial distribution), type and abundance of landslides in a region, to show the effects of major landslide triggering events, such as heavy rainfall, earthquakes, etc., to determine the frequency-area statistics of landslide areas and to provide reliable information to produce landslide susceptibility and hazard models (Galli et al. 2008) and, consequently, to assist in risk assessment models. Inventory maps are also useful to validate such models and the accuracy of the resulting landslide susceptibility and hazard maps.

The contents, symbology (map representation) and scales of available landslide inventories greatly differ. Symbology is largely dependent on the map scale (see RIC 1996a, b). For instance, in large and medium scale GIS-based landslide inventory maps (that is, those up to about 1:100,000) landslides can be represented as polygons, thus showing the deposit and scar boundaries for different types of landslides, or as linear features (polylines, e.g. for narrow debris flows) or as point features (for small landslides). Some inventory maps also depict landslide geomorphological features. However, neither landslide boundaries nor internal features can be shown in synoptic, small-scale landslide inventory maps, where landslides appear most often represented simply as point features.

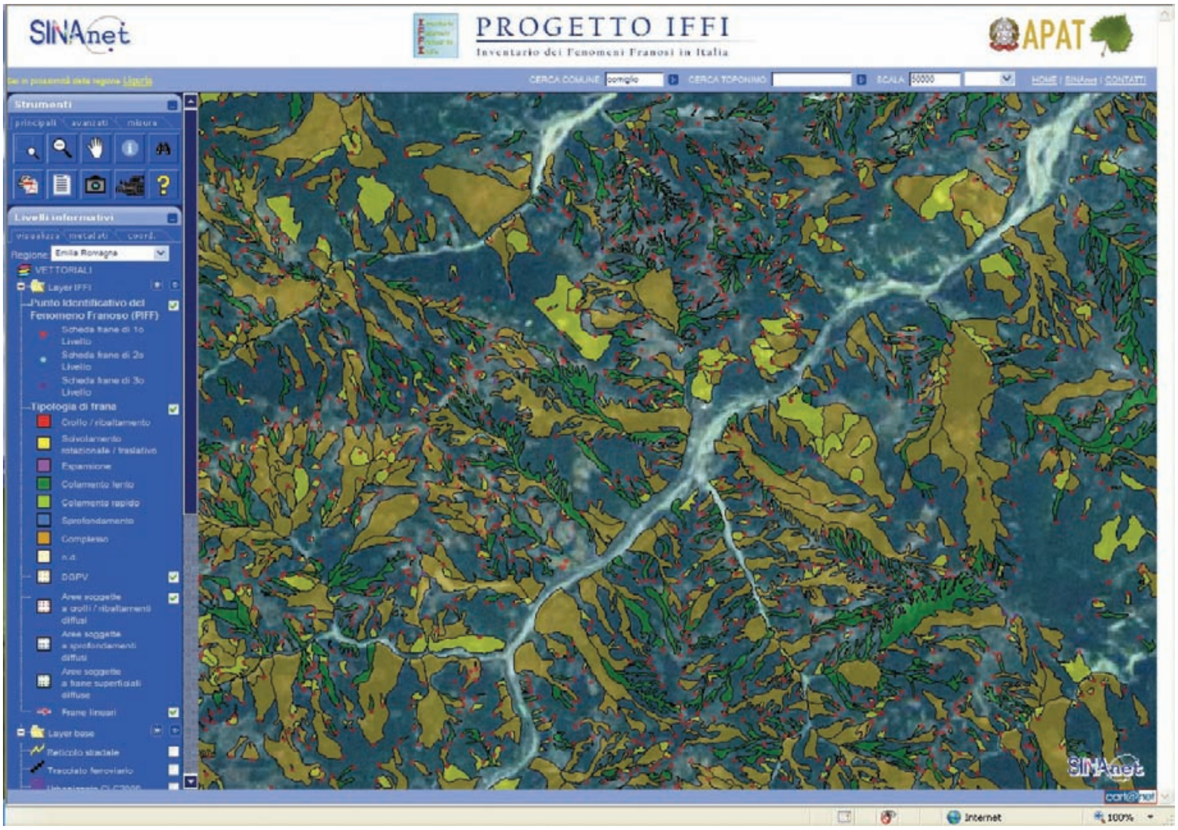

Fig. 19.1 WebGIS user interface of the IFFI Landslide Inventory of Italy over an area densely affected by landslides in Emilia-Romagna, Central Italy. Landslide boundaries together with their crown reference point (in *red*) are shown over a background Landsat image. Original display scale 1:50 000 (source: APAT, http://193.206.192.244/cartanetiffi/)

The basic rules and procedures for terrain data capture and representation according to scale of analysis are relatively straight forward (RIC 1996a), but are not always followed by practitioners. Similarly, the data collected specifically for slope stability mapping share many commonalities regardless of where on the globe the information is being collected (see for example RIC 1996b).

In GIS-based landslide inventories, map features are accompanied by attribute tables or external database management system datasheets (including also input masks), which contain relevant alphanumeric and where possible, graphical information on the features. Ideally, the information should minimally include a unique identification code, geographical and administrative location of the landslide concerned, landslide type, state of activity, occurrence or reactivation date(s), volume and/or surface extent, soil-bedrock type involved, slope angle, triggering mechanism and surveying date. Unfortunately and realistically, in many instances all this information may not be readily available (for instance, occurrence date, triggering mechanism and velocity), such that most inventories only contain a subset of the required data. Additional information on landslide consequences or damage incurred can be very useful (as it can help remediation measures), especially for input to landslide risk assessment models and in the production of risk maps.

19.3 Landslide Susceptibility and Hazard Mapping

Landslide susceptibility refers to the propensity of an area to landslide occurrence. In short, it is defined as the probability of occurrence of landslides of a particular type in a given location. Susceptibility thus refers to the spatial likelihood or probability (given in either qualitative or quantitative terms) for a landslide to occur in the future.

Landslide hazard refers to the probability of occurrence of landslides of a particular type and magnitude in a given location within a reference period of time. Here magnitude usually refers to size (volume) and velocity. Thus this concept of landslide hazard, based mainly on Guzzetti et al. (1999), which modifies that of Varnes and the IAEG Commission on Landslides and other Mass Movements on Slopes (1984), differs from that of susceptibility in that the former considers the magnitude of the event and, more importantly, it also considers the frequency (temporal occurrence or recurrence) of landslides. Unfortunately, the terms susceptibility and hazard are often erroneously used as synonyms, and therefore many so-called landslide hazard maps are actually susceptibility maps, as they do not consider the temporal dimension along with the spatial aspects in the evaluation of future landslide occurrence.

The proper assessment of landslide hazard requires good landslide records (historical archives, landslide catalogues, etc.), which are often not available, especially so for old and/or small landslides which have not resulted in casualties, not caused significant damage or occur in isolated unpopulated terrain. Additionally, historical archives (and other news information sources) may not be very precise with regard to the location of the landslide(s) in question; hence, the spatial allocation of the reported date becomes difficult, especially in areas with abundant and recurrent landslides (e.g. Blais-Stevens and Septer 2008). The frequent lack of landslide dating information is thus a major constraint to the generation of landslide hazard maps, and consequently of risk maps (van Westen et al. 2006). However, in areas with highly recurrent landslide events, the analysis of aerial photographs acquired at various time periods over the past 60 years or so has enabled many to make multi-temporal landslide inventories, which has then helped to produce hazard maps (Guzzetti 2005).

Most non-deterministic approaches to susceptibility and hazard mapping rely on the principle of precedence, that is, landslides will occur where the geo-environmental conditions that led to landsliding in the past will again occur in the future. Hence the association of past landslide occurrence (mainly from inventory maps) with the spatial (and, if possible, temporal) distribution of conditioning and triggering factors is usually a major driving element of the method or model employed. In some cases, however, the conditions that dominated in the past may have changed because of factors such as climate change, construction works, land use and also by landslide events themselves. This then changes the susceptibility of the terrain to future landslides, and reinforces the need to estimate the influence of all parameters when devising a landslide susceptibility or hazard evaluation scheme (Crozier and Glade 2005).

When modelling landslide susceptibility and hazard one usually considers conditioning (preparatory) factors, which make the slope susceptible to movement, and triggering (causative) mechanisms which initiate movement. Conditioning factors or parameters primarily include ground conditions regarding geological materials (soil/rock type, condition and discontinuities, etc.), geomorphological characterisation (slope angle, attitude, morphology, etc.) and processes, whereas triggering mechanisms include mainly physical processes (rainfall, rapid snowmelt, earthquakes, etc.) and anthropogenic processes (Popescu 1994). Some of these factors can be regarded as both conditioning and triggering elements. Approaches to landslide susceptibility and hazard evaluation may consider a large set of such factors, depending on the characteristics and extent of the area, the model used and the analyst's choice of parameters.

19.3.1 Approaches to Landslide Susceptibility and Hazard Mapping

Approaches to landslide susceptibility or hazard assessment depend on the objectives of the project, the scale and geographical coverage, the physical environment and landsliding processes, and the availability of input data to the possible models. Overviews of these approaches and principles (referring sometimes also to risk assessment) have been provided elsewhere, for example Hansen (1984), Varnes and the IAEG Commission on Landslides and other Mass Movements on Slopes (1984), van Westen (1993), Carrara et al. (1995), Soeters and van Westen (1996), Aleotti and Chowdhury (1999), Guzzetti et al. (1999), Dai et al. (2002), Crozier and Glade (2005), Guzzetti (2005), Huabin et al. (2005) and Chacón et al. (2006).

Many methods and models for landslide susceptibility and hazard assessment exist. They can be generally classified in the first instance as qualitative or quantitative. Qualitative approaches mainly include heuristic methods, whereas quantitative methods generally comprise numerical analysis of landslide inventories, statistical models and physically based models.

19.3.1.1 Qualitative, Heuristic Approaches

Qualitative approaches include mainly direct (geomorphological) and weighting (indexing) approaches (Soeters and van Westen 1996). In *direct, geomorphological mapping*, susceptibility is assessed by an expert directly in the field and with the aid of aerial photography and/or satellite image analysis and interpretation. Each mapping unit is thus directly assigned a susceptibility level.

The concept of mapping unit is central to the generation of landslide susceptibility, hazard and risk maps. Hansen (1984) refers to land mapping or sampling unit as that containing a set of ground conditions which differs from the adjacent units across definable boundaries. A mapping unit can be a terrain unit defined according to slope morphological properties, soil-bedrock association type or other unique terrain properties or conditions, as well as a raster/grid cell. The latter does not appropriately reflect terrain feature and soil-bedrock natural boundaries; however, it is very suitable to work with DEM, with information derived from remotely sensed digital imagery, and with raster-based GIS and external statistical packages. Further insight into possible types of mapping units can be found in RIC (1996a), Guzzetti et al. (1999) and Guzzetti (2005).

Direct susceptibility mapping heavily relies on the experience of the analyst and can therefore be considered highly subjective; the results obtained are thus difficult to compare with those by other experts in the same or in other areas (Barredo et al. 2000). This limitation, however, is not exclusive to heuristic approaches.

Nevertheless, this method can be fast and therefore cost-effective, for producing landslide susceptibility maps. Moreover, in the absence of a landslide inventory database, if applied by an expert aerial/satellite image analyst and field specialist, the quality of the resulting maps should not be undervalued. In this approach, GIS is mainly used for representation purposes, although it can also be used for integration of various types of imagery (including DEM-derived products) for additional interpretation purposes.

Weighting, indexing approaches combine maps of factors associated with landslide occurrence (e.g. soil/bedrock, slope angle, land use, etc.). Weights are then allocated to factor maps based on an estimate of their relative influence on landsliding. Such maps are in turn divided into classes (e.g. soil/bedrock types, slope angle ranges, land use types, etc.) to which weights are assigned using an expert's judgement. Finally, a susceptibility or hazard index is derived for each mapping unit.

The subjectivity inherent to these methods can partly be reduced, for instance, by applying a semi-quantitative model based on multi-criteria evaluation (Barredo et al. 2000), whereby the assigned weighting can be re-evaluated in order to achieve a good consistency ratio (Fig. 19.2). In these approaches, GIS is very useful to represent and combine factor map weights and therefore to derive landslide susceptibility or hazard indexes.

The landslide susceptibility index generated by weighting approaches and some quantitative methods below (ranging normally between 0 and 1 or 0 and 100) is usually reclassified into a few descriptive levels in order to produce maps that are easier to interpret by decision makers and practitioners (see Fig. 19.2)

Direct and index-based approaches can be suitable for mapping landslide susceptibility, and sometimes hazard as well, at various scales, especially at medium scales.

19.3.1.2 Quantitative Analysis of Landslide Inventories

Landslide abundance, derived from quantitative analysis of landslide inventories, is sometimes used

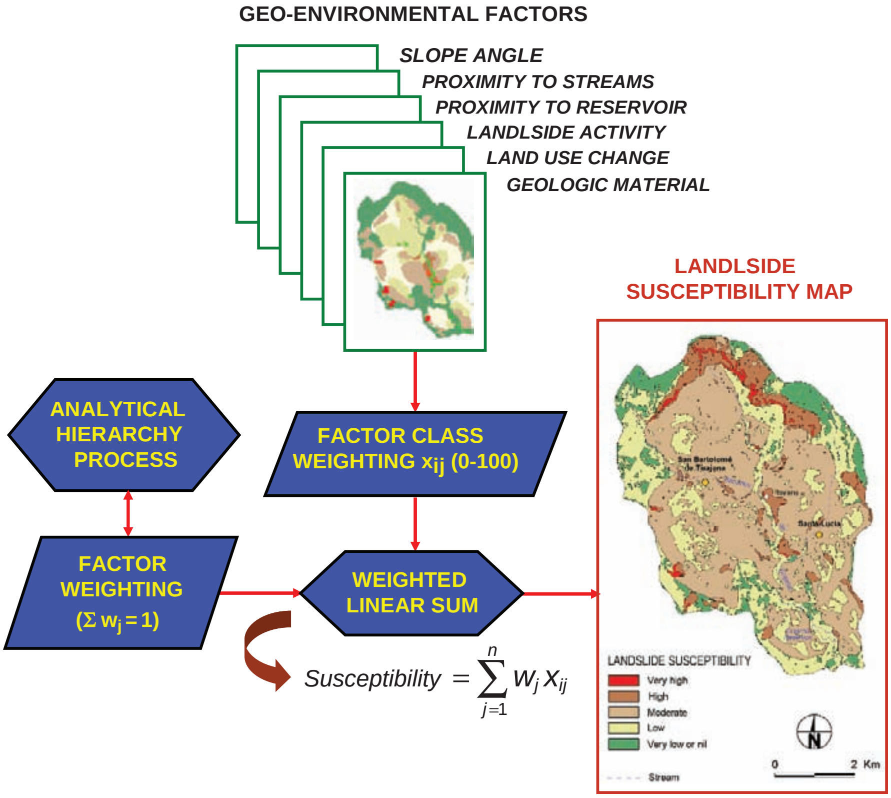

Fig. 19.2 GIS-based multicriteria evaluation model for assessing landslide susceptibility in the Barranco de Tirajana Basin, Gran Canaria Island (Barredo and Hervás, unpublished)

as a basic indicator of landslide susceptibility. This information is often expressed as landslide density maps, which are usually obtained by dividing the area occupied by landslides within a mapping unit by the total area of the unit. Alternatively, less significant landslide density maps can represent the number of landslides per mapping unit.

For small-scale landslide density maps and other susceptibility maps (e.g. over large regions or at nation-wide scales), the use of mapping units representing small administrative units (e.g. municipalities, districts or equivalent) can also be considered, because certain types of information and statistics are often available at administrative level.

19.3.1.3 Statistical Approaches

Statistical (probabilistic) analysis models enable to quantitatively correlate geo-environmental factors that may influence or cause slope instability with the distribution of past and current landslides, as revealed by landslide inventories. Statistical approaches generally require the collection of a large amount of data. The use of numerical models is now favoured given the availability of GIS and external statistical packages.

Statistical methods can be used to evaluate and map landslide susceptibility as well as hazard, provided that the necessary input data are available. They are particularly useful for medium-scale (regional) mapping. Such methods can generally be classified as either bivariate or multivariate.

Bivariate Analysis Models

In *bivariate statistical analysis* each factor map (e.g. lithology, slope angle, land use, etc.) is combined with the landslide distribution map, and weighting values based on densities are calculated for each factor class, for example, lithological unit, slope angle range class, land use type, etc. (Soeters and van Westen 1996).

A relatively simple method is the so-called *Information Value* (Yin and Yan 1988; Zêzere 2002). In this case, each instability factor is compared with the landslide distribution, and weighting values based on landslide densities for specific types of landslides are then calculated for each factor class using a logarithmic function. This finally results in a score of the relative susceptibility of each mapping unit to the occurrence of a particular type of landslide. Zêzere (2002) suggests, however, that a major constraint of such a method is that possible correlations amongst the other input variables (factors) are not addressed.

Another technique based on bivariate analysis is the so-called *Matrix-Assessment Approach* (DeGraff and Romesburg 1980; Fernández et al. 2003), whereby landslide susceptibility maps are created by constructing and analyzing cross tables between the different types of landslides and their conditioning factors.

A popular model is the so-called *Weights of Evidence* (Bonham-Carter et al. 1989; Thiery et al. 2007). It is based on a Bayesian probability model in a log-linear form to predict the spatial occurrence of a landslide event where well-known evidence (i.e. predictor variables influencing landsliding) are available. This model is freely available as an external extension to ESRI's ArcGIS™ and ArcView™ software.

Multivariate Analysis Models

In general, these models enable one to determine the relative contribution of each slope instability factor to the total susceptibility of a mapping unit (Carrara 1983). Multivariate analysis methods include, among others, discriminant analysis, logistic and multiple regression analysis and artificial neural networks. Amongst these, discriminant analysis and logistic regression are the most popular.

In *discriminant analysis*, a discriminant function is obtained by applying multivariate analysis to evaluate the relative weight of each conditioning factor of landsliding using a random sample of grid cells in the mapping area. Each cell of the sample will take a value according to the factors present within. After checking the validity of the results, the discriminant function is then applied to the entire mapping area (Santacana et al. 2003).

The goal of *logistic regression* in landslide susceptibility mapping is to find the best fitting function to describe the relationship between the presence or absence of landslides (dependent variable) and a set of independent parameters, such as lithology, slope angle, etc. Logistic regression generates the model statistics and coefficients of a formula useful to predict a logistic transformation of the probability that the dependent variable is 1 (probability of occurrence of a landslide event). Logistic regression, however, does not define susceptibility directly but this can be mapped using a predicted map of probability (Ayalew and Yamagishi 2005).

A joint conditional probability model combining some of the above mentioned models as well as the use of expert's knowledge has been proposed by Chung and Fabbri (1999) and Chung et al. (2002) for the prediction and mapping of landslide hazard.

Finally, other statistical approaches may include fuzzy logic and expert systems (see for example Guzzetti 2005).

19.3.1.4 Physically-Based Models

Physically-based models, also called geotechnical models, rely on physical laws influencing slope instability and are mainly based on slope stability analysis. These models are usually developed to study a particular type of landslide or to investigate the effect of a particular trigger (Guzzetti 2005). For rainfall-induced landslides they usually require input data, among others, on physical or geomechanical properties of the materials involved, chiefly cohesion, friction angle, unit weight of soil and of water, as well as on pore water pressure (given as a function of groundwater depth), geometry of the slope and depth and shape of the potential failure plane (Soeters and van Westen 1996; Dai et al. 2002). In seismic areas, peak ground acceleration data also need to be incorporated in the model.

In physically-based *deterministic models*, the susceptibility or hazard degree is expressed by the *factor of safety*. This is defined by Duncan (1996) as the ratio of the shear strength of soil divided by the shear stress required for equilibrium of the slope. For translational or nearly translational slides, the safety factor can be calculated using the simple, so-called *infinite slope model*.

An example of a coded physically-based stability model based on the infinite slope model is SINMAP (Pack et al. 1998). It computes and maps a stability index by modelling the spatial distribution of shallow translational landslides (e.g. slides and debris slides) controlled by shallow groundwater flow convergence. This model requires topographic data derived from DEM as well as data on soil and climate properties, and is available as a free extension to ESRI's ArcGIS^{TM} and ArcView^{TM} software.

Physically-based models can also be used for instance for rockfall hazard assessment and mapping based on 2-D and 3-D numerical modelling of rockfalls. The latter aims to define the fall path, the maximum runout distance, the envelope of trajectories and the veolocity and energy distribution along them (e.g. Crosta and Agliardi 2003).

Because of the association of the variation of some dynamic parameters (e.g. pore water pressure) with landslide triggers such as rainfall, physically-based models can be appropriate for evaluating and mapping landslide susceptibility as much as hazard in well surveyed and monitored areas. However, the collection of the input data to such models is costly, thus physically-based models are mainly suited to large scale susceptibility/hazard mapping (usually larger than 1:10,000) in small areas and for engineering site investigations.

19.4 Landslide Risk Mapping

Landslide risk refers to the expected damage or losses caused by landslides, including casualties, damage to property and infrastructure, and interruption of services and economic activities.

Landslide risk mapping is far less common than susceptibility or hazard mapping. Evaluating landslide risk (particularly in a quantitative manner) is still a complicated task, especially because the information needed to precisely estimate hazard and vulnerability may in many instances not be available (van Westen et al. 2006). In spite of this constraint, landslide risk assessment/mapping is becoming a fashionable topic of research. Recent treatises on the subject include, among others, Bonnard et al. (2004), Lee and Jones (2004), Glade et al. (2005) and Hungr et al. (2005). An expansion on the topic of landslide risk mapping centres on multi-hazard risk mapping, which is well reviewed by ARMONIA (2008).

Landslide risk maps are essential for land use and risk management regulations and for risk reduction plans, including also the setting up of risk mitigation measures (e.g. Bell and Glade 2004; Corominas et al. 2005; Reichenbach et al. 2005; AGS 2007; Hervás 2007).

Landslide risk can be expressed as the probability of a hazardous phenomenon causing damage or in monetary terms. Generally, the estimation of risk involves the assessment of hazard, elements at risk (also termed exposure) and their vulnerability. As noted earlier in the chapter, hazard refers to the probability of occurrence of landslide(s) of a given magnitude at a particular location within a reference period. The elements at risk are defined by Fell (1994) as the population, properties, and economic activities, including public services, etc., in the area potentially affected by the landslide(s). This concept is further developed by the Australian Geomechanics Society Landslide Zoning Working Group (AGS 2007) as the population, buildings and engineering works, economic activities, public services, utilities, infrastructure and environmental features in the area potentially affected by the landslide hazard. Vulnerability in turn refers to the degree of loss of an element or elements within the landslide-affected area, where element(s) is/are the structure(s) or person(s) within such an area (Fell 1994). Further principles and definitions regarding landslide risk can be found in Varnes and the IAEG Commission on Landslides and other Mass Movements on Slopes (1984), Fell (1994), Lee and Jones (2004), Guzzetti (2005) and AGS (2007). The latter additionally provides a framework for landslide risk management based on Fell et al. (2005), which can be used for landslide susceptibility, hazard and risk zonation.

19.4.1 Approaches to Landslide Risk Mapping

Approaches to landslide risk assessment and mapping can generally be classified as quantitative (probabilistic) or qualitative (heuristic). In short, the former establish quantitative levels of risk, whereas the latter determine risk in qualitative levels.

19.4.1.1 Quantitative Approaches

Quantitative landslide risk assessment uses numerical values and mathematical methods to usually estimate objective probabilities such as the probability of loss of life or of damage to structures or infrastructure due to landslides (Guzzetti 2005).

The quantitative level of risk is generally estimated based on the generic equation adopted by Varnes and the IAEG Commission on Landslides and other Mass Movements on Slopes (1984) for material losses, from definitions for hazardous natural events by United Nations' UNDRO and UNESCO offices, as follows.

$$\text{Risk} = \text{Hazard} \times \text{Elements at risk} \times \text{Vulnerability}$$

Generally, hazard is given in terms of probability, the elements at risk are expressed in terms of their amount and value, and the vulnerability (i.e. the elements degree of loss) is expressed on a scale from 0 (no damage) to 1 (total loss). The risk (total risk) is thus obtained by multiplying the hazard by the expected losses for all the elements at risk.

Landslide risk can be evaluated separately for life and property/structures. It can thus be defined for instance in terms of annual probability of loss of life of a specific individual, on the one hand, and of annual probability of loss of property value, on the other one (e.g. Dai et al. 2002; AGS 2007). This is expressed by Dai et al. (2002) as follows, where *R* stands for risk, *P* for probability, and *V* for vulnerability.

R (as annual *P* of loss of life to an individual) =
[Annual *P* of the landslide event] ×
[*P* of spatial impact given the event] ×
[*P* of temporal impact given the spatial impact] ×
[*V* of the individual (*P* of loss of life of the individual given impact)]

R (annual loss of property value) =
[Annual *P* of the landslide event] ×
[*P* of spatial impact (i.e. of the landslide impacting the property)] ×
[*V* of the property (proportion of property value lost)] ×
[Element at risk (e.g. the value of the property)].

Van Westen et al. (2006), in turn, represented total risk for expected material and human losses as follows:

$$\text{Risk} = \sum\left(H\sum(VA)\right)$$

where *H*, *V* and *A* are respectively hazard, physical vulnerability and amount or cost of the particular elements at risk.

Most of the studies on quantitative risk assessment and mapping published so far concern small areas or infrastructure site investigations. For instance, Bell and Glade (2004) generated risk maps portraying risk to people in buildings in a small town in Iceland, as probability of loss of life from debris flows and rockfalls separately. Corominas et al. (2005) developed a procedure to assess rockfall risk from a mountain slope to population and houses in a town in Andorra, before and after the implemention of rockfall barriers. This permitted to quantitatively evaluate risk reduction from protective works. Zêzere et al. (2008) evaluated and mapped landslide risk from shallow slides and translational and rotational slides triggered by rainfall, to roads and buildings in terms of direct economic losses, in a relatively small area in the neighbourhood of Lisbon, Portugal. In this work, values attributed to the road element were defined from reconstruction costs from past landslides and from average cost values for different road categories provided by authorities and insurance services. Vulnerability was defined with respect to the type of landslide and the element at risk. Similarly, monetary landslide risk to transport infrastructure, buildings and agricultural land was derived and mapped by Remondo et al. (2008) for shallow slides and flows, triggered mainly by rainfall, in a somewhat larger area in northern Spain. In this work, both monetary direct risk and indirect risk were calculated and mapped.

19.4.1.2 Qualitative Approaches

Qualitative risk assessment can be an alternative to quantitative assessment, especially over entire regions, when catalogues of historical events and their consequences may not be available, and when the magnitude, frequency and evolution of landslide processes in the area may be difficult to ascertain (Guzzetti 2005).

The IUGS Working Group on Landslides (1997) reports that in qualitative risk assessment knowledge of the hazard, the elements at risk and vulnerability is typically expressed as ranked attributes. The risk may then be ranked as a result of combination of these three parameters.

Simple qualitative estimates of risk can be performed in GIS by crossing an inventory map with different thematic layers depicting residential areas, public facilities, industrial installations, lifelines, etc.

A good example of qualitative risk mapping is provided by Reichenbach et al. (2005) for various areas in central Italy that are affected by slides, flows and rockfalls. They first established landslide hazard zonation by generating and analysing multi-temporal landslide inventories together with site-specific and historical information. The resulting landslide hazard classes were based on ranked, estimated landslide frequency and magnitude indexes. These authors then mapped and classified the elements at risk according to their typology, and estimated the vulnerability of each class on the basis of the magnitude and type of the expected landslide, thus resulting in qualitative levels of expected damage to the various classes of elements at risk. Vulnerability classes were then cross tabulated with hazard classes in order to ascertain the specific risk separately for each class of element at risk and each type of landslide. For each landslide hazard zone previously established, a value of total risk expressed in five classes was then assigned, based on the type and severity of the largest specific landslide risk previously attributed in the landslide hazard zone.

19.5 Conclusions

In this chapter we briefly introduce and review the interrelated concepts of mapping landslide inventories, susceptibility, hazard and risk. We emphasize the importance of extensive metadata in the characterization of landslides stressing the need for spatial information, type, abundance, age, triggering mechanism, failure parameters (slope angle, material, etc.) and volume data as basic properties of any proper inventory. Concomitantly we comment on the representation of these data in map form via scale and symbology.

We examine the differences between landslide susceptibility and hazard mapping, commenting on a few of the better known qualitative (heuristic) and quantitative (statistical and physically-based) methods of analysis. Added attention is given to a comparison between bivariate and multivariate statistical approaches.

Finally we refer to the important but difficult task of addressing landslide risk, implicating the inherent relationship of landslide hazard, exposure and vulnerability. Additionally, quantitative and qualitative approaches to risk assessment and mapping are briefly discussed.

Moreover, we highlight the need for more extensive hazard and risk mapping, as well as for the application of harmonized, comparable approaches to susceptibility, hazard and risk assessment where possible.

The first part of this chapter provides the prelude to a number of presentations which individually deal with topics already discussed. The extended abstracts that follow represent those presentations which can provide good case study examples of relevant issues in mapping landslide inventories, susceptibility, hazard and risk.

19.6 Extended Abstracts

19.6.1 Landslide Hazard Assessment, Vulnerability Estimation, and Risk Evaluation at the Basin Scale

Authors: Francesca Ardizzone, Mauro Cardinali, Fausto Guzzetti, Paola Reichenbach
CNR-IRPI, Perugia, Italy

The ultimate goal of many landslide studies is the determination of the risk posed by existing or future slope failures. To achieve this goal, information on landslide hazard (Guzzetti et al. 1999, 2005a, 2006) and vulnerability (Galli and Guzzetti 2007) to landslides is required. For the Collazzone area, central

Umbria, landslide hazard was ascertained, landslide vulnerability was determined, and landslide risk was evaluated, for different scenarios. To ascertain landslide hazard, a specific probabilistic model was adopted to predict where landslides will occur, how frequently they will occur, and how large they will be in a given area. A multi-temporal landslide inventory map was prepared through the interpretation of five sets of aerial photographs covering the period from 1941 to 1997, and field surveys in the period from 1997 to 2004. A 10 × 10 m digital representation of the topography (DEM) was used to partition the study area into 894 slope units. For each slope unit: (i) the probability of spatial landslide occurrence was obtained through discriminant analysis of a large set of thematic and environmental variables; (ii) the probability of experiencing one or more landslides in different periods was determined adopting a Poisson probability model for the temporal occurrence of landslides, and (iii) the probability of landslide size was obtained by analyzing the frequency-area statistics of landslides. Assuming independence of the three computed probabilities, landslide hazard was determined as the joint probability of landslide size, of landslide temporal occurrence, and of landslide spatial occurrence. The maps shown in Fig. 19.3 portray landslide hazard in the Collazzone area for four different periods and for landslides of two size classes.

Information on the vulnerability to landslides is lacking almost everywhere, hampering our ability to evaluate risk. For the Umbria region, landslide vulnerability curves were established exploiting information on landslide damage to buildings and roads caused by individual landslides of the slide type in the 24-year period between 1982 and 2005. Empirical observations revealed that, in Umbria, the proportion of direct damage caused to buildings

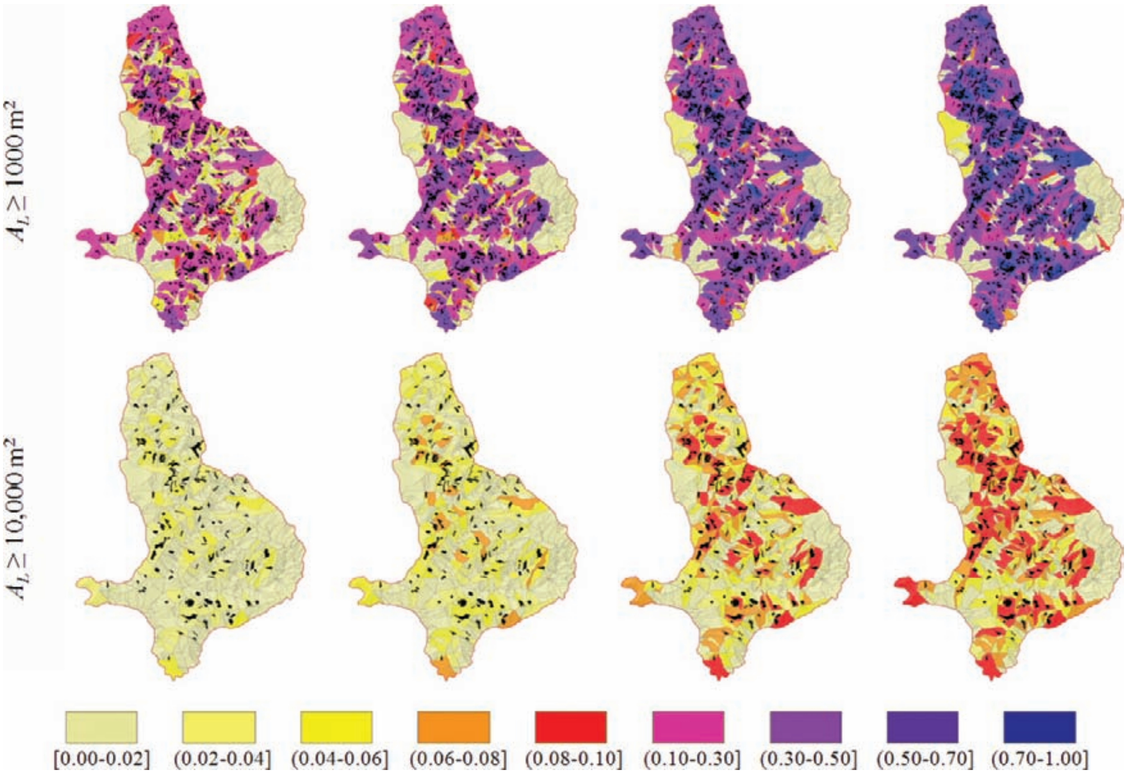

Fig. 19.3 Landslide hazard scenarios for four periods, from 5 to 50 years, and for two classes of landslide size, $A_L \geq 1000$ m^2 and $A_L \geq 10{,}000$ m^2. Colours show landslide hazard i.e., the joint probability of landslide size, of landslide temporal occurrence, and of landslide spatial occurrence

and roads by slides and slide-earth flows depends on the area of the damaging landslide. As a first approximation, the direct damage caused by a slope failure increases with the area of the hazardous landslide. However, the proportion of the damage does not scale linearly with the area, complicating the assessment of landslide vulnerability. Minimum and maximum vulnerability curves were established for roads in Umbria and were used to map the expected vulnerability of the road network to landslides in the Collazzone area.

Assuming independence of hazard and vulnerability, and exploiting (i) the multi-temporal landslide inventory map, (ii) the obtained landslide hazard assessment, and (iii) the available landslide vulnerability curves, landslide risk to the road network was evaluated in the Collazzone area, for different scenarios. Results indicate that landslide risk can be determined quantitatively over large areas, provided adequate forecasting models are adopted and reliable landslide and thematic information are available.

19.6.2 Forecasting Landslides and the Associated Risk to the Population of Italy

Authors: Francesca Ardizone[1], Mauro Cardinali[1], Angelo Corazza[2], Fausto Guzzetti[1], Francesco Leone[2], Silvia Peruccacci[1], Paola Reichenbach[1], Mauro Rossi[1], Paola Salvati[1], Gabriele Tonelli[3]
[1]CNR-IRPI, Perugia, Italy,[2]Dipartimento Nazionale della Protezione Civile,[3]Consultant

Italy has a long history of landslides and of landslide catastrophes. The impact of landslides is particularly severe on the population of Italy. Detailed investigations of slope failures with human consequences have shown that, in the period from 1400 to 2003, at least 1275 landslides have caused 11,564 deaths and 2295 injured people in 16.4% (1328) of the 8103 Italian municipalities. In the period from 1950 to 2002, landslides exhibited the largest mortality caused by natural hazards in Italy, larger than the mortality of earthquakes, floods, and volcanic eruptions. The chronic hazard imposed by landslides in Italy calls for innovative answers for the assessment and mitigation of landslide risk, with emphasis on the risk to the population (Fig. 19.4) (Guzzetti et al. 2005b, c; Salvati et al. 2003).

The Italian Department of Civil Protection (DPC), an Office of the Italian Prime Minister, has the responsibility to protect individuals, communities, and their properties, against natural hazards, including landslides, and to rescue people should a catastrophic event occur. To fulfill this challenging task, the DPC routinely conducts preventive actions, including the issuing of meteorological, hydrological, and landslide warnings based on numerical weather forecasts. The DPC is also eagerly involved in activities aimed at determining landslide hazards and risk at different geographical scales.

In 2007, the DPC asked IRPI, a research institute of the Italian National Research Council, to design and implement a prototype system for the quasi-real-time forecast of rainfall induced landslides in Italy. The system – currently under development – is based on two main components: (i) a set of national, regional and local rainfall thresholds for the possible occurrence of landslides, and (ii) a synoptic (small scale) assessment of landslide hazards and the associated risk in Italy.

To predict rainfall induced landslides, existing and new rainfall thresholds are used. The new rainfall thresholds, chiefly of the intensity-duration (ID) and normalized-ID types are established using innovative statistical techniques and a catalogue of rainfall events that have or have not resulted in landslides in Italy. To determine landslide hazards and risk, statistical models are prepared exploiting small scale thematic information and catalogues of historical landslides and historical landslides with human consequences in Italy, in the period from 1900 to 2005. The catalogues were compiled through a thorough literature and archive search. The two individual system components are then combined to form a national landslide warning system. The system will exploit rainfall measurements obtained from over 3000 rain gauges spread homogeneously in the twenty-one Italian Regions and autonomous Provinces that comprise Italy, rainfall estimates obtained from a network of ground-based weather radars installed or networked by the DPC, rainfall estimates obtained from meteorological satellites, and numerical weather forecasts.

Fig. 19.4 Maps showing Municipalities affected by landslides with direct human consequences in the 20 Italian Regions, for the period 1900–2007

19.6.3 Approaches for Delineating Areas Susceptible to Landslides in the Framework of the European Soil Thematic Strategy

Authors: Andreas Günther[1], Paola Reichenbach[2], Javier Hervás[3]

[1]BGR, Hannover, Germany, [2]CNR-IRPI, Perugia, Italy, [3]JRC, Ispra, Italy

The European Union's Thematic Strategy for Soil Protection, adopted in 2006, is a long-term political process that started with the formulation of a draft of a European framework directive devoted to the protection and sustainable use of soil in the European Union (Commission of the European Communities 2006a,b). Within this process, eight individual soil threats that are likely to hamper soil functions or lead to soil degradation within the European territory have been identified and are subjected to risk/priority area delineation procedures and the implementation of suitable risk mitigation strategies. Landslides are recognized as one of these soil threats.

The Soil Information Working Group (SIWG) of the European Soil Bureau Network (ESBN) developed a uniform framework for risk area assessments of the soil threats mentioned above in such that hierarchically ordered, nested geographical analysis schemes ("Tiers") are envisaged, leaving the issues of data quality, map resolution and costs open to the individual EU member states (Eckelmann et al. 2006). In this context, European-level continent-wide "Tier 1" risk area delineations for individual soil threats should be conducted with already available data, should render a relatively low spatial resolution (probably 1:1 Mill.), and should follow a qualitative zonation approach or a model approach combined with thresholds. "Tier 1" assessments are considered to serve for general risk/priority area identification and should be able to delineate zones where no further measures or spatial analysis have to be taken against those that are subjected to more detailed "Tier 2" assessments. "Tier 2" risk area delineations within areas identified by "Tier 1" should thus render higher spatial resolution, could be conducted by quantitative modelling approaches, and will most likely require data not yet available. For each soil threat, the European Commission is searching for a common methodology for risk area delineations that will enable each member state to conduct the analysis. A set of common criteria for spatial analysis procedures was elaborated by SIWG of ESBN and is already annexed in the current draft of the framework directive (Commission of the European Communities 2006b).

In contrast to the other soil threats, landslide risk cannot be simply reduced to risk on soil degradation because here the soil as part of mobilized slope material poses risk to other vulnerable objects exposed to a landslide threat. Therefore, we suggest that the impact of the landslide threat in the context of the Soil Thematic Strategy could be best evaluated with landslide susceptibility and hazard assessments. A wide range of assessment procedures exist, including empirically-based heuristic and statistical as well as physically-based evaluation techniques, each requiring different data and suitable to be implemented at different scales and for different types of landslides. Due to the complexity of landslide phenomena, the highly variable impact of the landslide threat in different European regions, and the differences in data availability, continent-wide "Tier 1" assessments can at the moment only be conducted using a reduced set of data. This should mainly consist of ground conditioning factors and optionally include the most important landslide triggering parameters like climatic and seismic factors. Since a systematic, harmonized coverage of landslide events does not yet exist throughout the European territory, a continent-wide "Tier 1" landslide susceptibility zonation is at the moment only feasible using heuristic, index-based analysis techniques (Günther et al. 2007).

Recent advances in harmonizing European geological and soil databases resulted in the availability of high-quality thematic data on ground conditioning parameters portraying hydrological, textural and structural properties of the weathered slope zone where most landslides originate. Additionally, continent-wide topographic, land-cover, climatic and seismic data are available at resolutions that can be combined with the ground conditioning factor data. The recommendation for preparing a European "Tier 1" landslide susceptibility model was formulated in such that a suitable weighting and scoring scheme will be elaborated to combine soil/parent material properties, slope angle and land cover to derive a landslide susceptibility index on a grid basis with a cell size fixed by the topographic raster data involved (Hervás et al. 2007). This speculative susceptibility model can be extended to a heuristic landslide hazard map in such that climatic (precipitation sums) and seismic (ground acceleration) data can be added. The grid cell-based susceptibility or hazard index values may be aggregated to suitable European administrative regions (e.g., EUROSTAT LAU units, especially municipalities) using simple zonal statistics in order to combine landslide susceptibility and hazard information with European census data. However, the preparation of a robust European heuristic landslide susceptibility or hazard model requires the calibration of suitable weighting and scoring schemes with representative landslide data (from available landslide inventories), and probably also local reclassifications of these to account for specific landslide phenomena in particular European regions. From these circumstances, it is clear that the preparation of a "Tier 1" landslide susceptibility map must be considered as a multiphase approach, requiring input of expert knowledge at each step of model improvement. In any case, even preliminary "Tier 1" assessments can be shown to perform much better than the European landslide hazard map produced by ESPON, which is solely based on expert opinion, suffers from data gaps and used extremely large mapping units (Schmidt-Thomé 2006).

Within the areas susceptible to landslides as delineated through the "Tier 1" model, quantitative, inventory-based statistical landslide susceptibility and hazard modelling can be performed through multivariate statistical analysis in "Tier 2" assessments (Reichenbach et al. 2007). In Italy, a country with a long tradition in landslide inventorying and spatial landslide hazard and risk assessment, it is shown that national-scale "Tier 2" evaluations can be performed and validated when appropriate mapping units are established and landslide inventory maps with associated databases are available in addition to high resolution ground material, topographic and landslide triggering thematic factor data. It is recommended that quantitative "Tier 2" analysis techniques should be conducted at scales in the order of 1:250,000, implying that mapping units smaller than the smallest EUROSTAT administrative units must be chosen. Even though administrative mapping units do mostly not reflect environmental or geomorphologic conditions, their use for a "Tier 2" assessment is favourable when considering the usability of the resulting maps for spatial planning and environmental protection measures. The concept of a common methodology for risk area delineations according to soil threats implies the provision of an assessment technique and guidelines on data needs, but does not explicitly account for data resolution and accuracy. It should be left open to individual European countries to use their national datasets when implementing "Tier 2" assessments on the landslide threat. The rational on methodological approaches presented here shows the limitations of "Tier 1" evaluations in countries where landslides are a widespread natural hazard and higher developed evaluations on a national scale exist (e.g., Italy). "Tier 1" must be considered to be important at the continental scale and for those countries where nation-wide landslide inventory data is not available or incomplete (e.g., Germany).

With respect to the fact that landslides are more localized and diverse phenomena than all the other soil threats, it is a matter of debate if higher resolution assessment schemes beyond "Tier 2" may be required in a common methodology to assess this particular soil threat. We thus recommend the application of physically-based landslide susceptibility and hazard models for different types of landslides and triggering factors within areas of high to very high landslide susceptibility as delineated by "Tier 2".

19.6.4 Hazard and Probability of Sea-Cliff Landslides on Variable Temporal Scales

Authors: Brian D. Collins[1], Robert Kayen[2]
[1]U.S. Geological Survey, Western Earth Surface Processes Team, [2]U.S. Geological Survey, Western Coastal and Marine Geology Team, Menlo Park, California, USA

Sea-cliff landslides from storm and wave impacts are a common occurrence along the west coast of the United States in areas of active tectonic margin uplift. Given the close proximity of homes and infrastructure to the cliff edge in many locations, we have performed hazard and vulnerability analyses to identify the likelihood of a cliff failure given both short- and long-term crest retreat rates. We use high frequency field visits and high resolution terrestrial lidar data of recorded failures over a recent 4 year time period (Collins and Sitar 2008) as an indication of landslide hazard for significant (>0.5 m) crest retreat to a 0.5 km length of sea-cliff in central California, USA (Fig. 19.5). We found average retreat rates from 1.2 to 2.6 m/yr, with average single failure events producing 0.9–1.2 meters of crest retreat. However, our observations also show that individual storms may cause several failure events within periods of only a few weeks and lead to between 4.6 and 9.4 m of total crest retreat in single areas.

We compare this data to long term measurements of crest retreat within this region between 1929 and 1998 (Hapke et al. 2007), based on analysis of historical maps and airborne lidar. The long term retreat rates averaged between 0.73 and 0.83 m/yr. Thus, the short term (recent) crest retreat rate is apparently 50% greater than the long term crest retreat rate.

We use total crest retreat distance as a proxy for vulnerability to provide a relative indication of risk for continued cliff failures along this developed stretch of coast. Three separate areas of structures and infrastructure (Fig. 19.5), each located behind the three areas of cliff studied; provide examples of how vulnerability plays into risk management. For locations where structures are closest to the cliff (BS1), the assessment leads to estimates of 8 and 15 years of remaining structural stability, corresponding to short- and long-term crest retreat rates, respectively (Table 19.1). For areas where structures and infrastructure are furthest from the crest (BN1), remaining stability is lost in 13 and 38 years for short- and long-term retreat rates, respectively. However, when values of maximum recorded crest retreat in a single season are used, the analysis indicates that only 1–3 especially large, winter seasons could result in complete retreat to the vulnerable limits of crest-top structures.

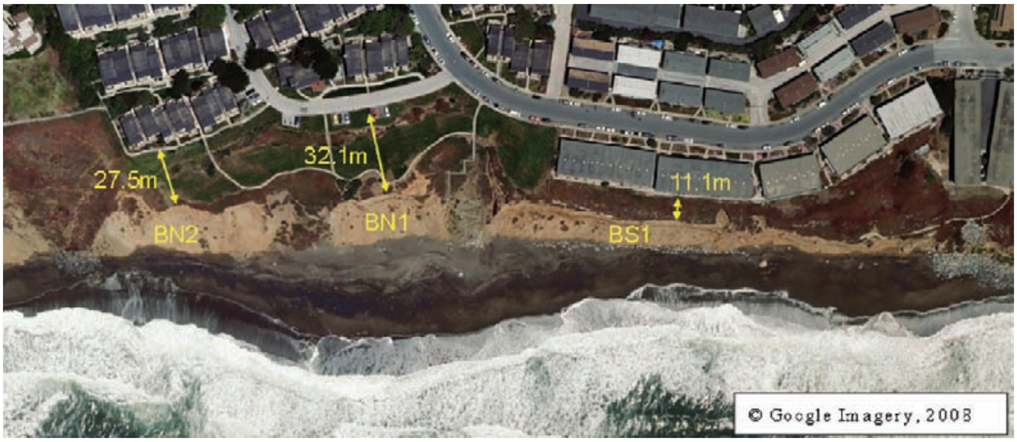

Fig. 19.5 Quaternary, weakly-lithified sand sea-cliffs in central California present both a geologic hazard, and an area of high risk due to built residences and infrastructure. Allowable distance for structural collapse (approximate vulnerability limits, AVL) are shown

Table 19.1 Hazard and vulnerability assessment for coastal cliff retreat

Location	BN2	BN1	BS1
Long term (69 yr) retreat (LTR) rate, (m/yr)	0.83	0.84	0.73
Long term (69 yr) retreat, (LTR) (m)	57.3	58.0	50.4
Short term (3 to 4 yr) retreat (STR) rate, (m/yr)	1.24	2.56	1.41
Short term (3 to 4 yr) retreat, STR (m)	4.6	9.6	4.2
Typical Single Event Size (m)	0.9	1.2	1.0
Maximum recorded retreat (MRR) in 1 year	4.6	9.4	7.5
Approximate vulnerability limit (AVL), (m)	27.5	32.1	11.1
Time required to reach AVL w/LTR rate (yr)	33	38	12
Time required to reach AVL w/STR rate (yr)	22	13	8
Time required to reach AVL w/ multiple MRR (yr)	6	3	2

Estimates of the frequency of these types of seasons are required to complete the risk assessment.

19.6.5 Landslide Susceptibility Study of Batu Feringgi and Paya Terubong Areas of Penang Island Malaysia Using Soil Characterization

Authors: Fauziah Ahmad[1], Ahmad Shukri Yahaya[1], Mohd Ahmadullah Farooqi[2], Habibah Abd Lateh[3]

[1]School of Civil Engineering, Universiti Sains Malyisa, Nibong Tebal, Penang, Malaysia, [2]USM and [3]School of Distance Education, USM

The predominantly hilly terrain of Penang Island combined with average maximum daily temperatures ranging between 27 and 35°C and rainfall as high as 325 cm makes the overall area vulnerable to landslips. Over the recent past, construction industry has shown a rapid growth mainly due to increase in the inflow of international tourists and such other economic reasons. Eventually, the magnitude of disaster associated with landslides has also increased and that is a cause of major concern for engineering geologists and geotechnical engineers. With this background, this paper attempts to characterize the largely granitic residual soils of two important areas of Penang Island, discussing the nature, structural features, mechanical behavior and field properties of soil samples extracted collectively from 12 data points on these areas. Although, there are other smaller geologic formations but, Penang Island is divided into two prime formations; namely, North Penang Pluton and South Penang Pluton. So, the two study areas are so chosen that each lie on different formations. The variation of index, strength and field properties of soils with depth are shown in Table 19.2. The correlation of compression index with liquid limit and initial void ratio is evaluated and found in agreement with the correlations found by other researchers (Poh 1985; Azzous et al. 1976). The following conclusions can be made:

Table 19.2 Summary of engineering properties

Property name	Location					
	Tantung bunge		Playa tiburon		Bata furring	
	Range	Mean	Range	Mean	Range	Mean
W_n (%)	9–38	23	15–30	23	11–41	24
LL (%)	32–75	51	65–90	73	32–44	37
PL (%)	24–43	32	17–34	25	22–33	28
G	2.66–3.0	2.68	2.56–3	2.63	2.65–3	2.71
PI (%)	12–42	24	30–53	38	6–14	10
Dry Density (KN/cum)	1.41–2.31	1.68	1.13–1.93	1.60	1.45–2.01	1.70
Bedrock Depth (m)	2.1–40	8.4	0.9–23.55	10.9	1.5–24	10.2
Gravel (%)	2–50	28	1–34	14	2–45	27
Sand (%)	15–76	38	32–85	55	22–55	40
Silt (%)	11–43	23	4–28	18	15–54	26
Clay (%)	0–33	12	0–42	13	0–22	7
c' (KN/m^2)	2.5–29	21	23–62	39	14–45	30
ϕ' (Deg.)	12–22	17.5	3.3–9.8	8.9	22–36	27
C_c	0.123–0.241	0.197	0.121–0.385	0.245	0.2–0.249	14

1. From the plasticity charts it is shown that soil at Batu Ferringhi area is silty type while at Paya Terubong and Tanjung Bungah area are clayey type.
2. From the plasticity charts it is shown that soil at Batu Ferringhi area is silty whereas at Paya Terubong and Tanjung Bungah area soils are clayey.
3. The value of effective cohesion shows a wide variation that is attributed to its unsaturated condition as the shear strength component due to matrix suction, gets included in cohesion intercept.
4. The value of effective cohesion shows a wide variation that is attributed to its unsaturated condition as the shear strength component due to matrix suction, gets included in the cohesion intercept.
5. The soil at the Playa Tiburon area shows such characteristics that it is highly susceptible to deep landslides. The soils at Tantung Bunge area, despite showing high liquid limit values, are only susceptible to shallow landslides.
6. The empirical relationships for coefficient of compression are found to show strong correlation with granites residual soils of Penang.

19.6.6 Landslide Detection Methods, Inventory Analysis and Susceptibility Mapping Applied to the Tien Shan, Kyrgyz Republic

Authors: Hans-Balder Havenith
University of Liege, Belgium

In the frame of the FP6 NATASHA project, a new inventory of landslides of the Tien Shan is being compiled for the Kyrgyz Republic. After completion of the project, the work is supposed to be extended to other Central Asian mountain regions in the Tajikistan, Uzbekistan, Kazakhstan and Western China.

This paper presents results of the last 5 years of landslide detection and landslide susceptibility mapping in the Central and Southern Tien Shan. First, landslide inventories have been compiled for areas of major interest in the Kyrgyz Republic: the Suusamyr region affected by a Ms = 7.3 earthquake in 1992 (Havenith et al. 2006a); the Mailuu-Suu valley, nuclear waste storage and former mining area (Havenith et al. 2006b); the Gulcha area (Fig. 19.6; Danneels et al. in press) affected by several loess-landslide disasters in 2002 and 2005. For the two first areas, landslides were mapped using KFA satellite images and aerial photographs. Recently, an automatic landslide detection method has been developed in order to map the loess-landslides in the third region of Gulcha. This method is based on a neural network scheme applied to detect particular slope failure features on the basis of satellite images. Mostly, multi-spectral ASTER images are used as inputs, but also other types of satellite images are being tested (e.g. SPOT, high-resolution images extracted from Google Earth). A series of characteristic features of landslide occurrence are taken into consideration, primarily spectral and secondarily simple morphological features (e.g.

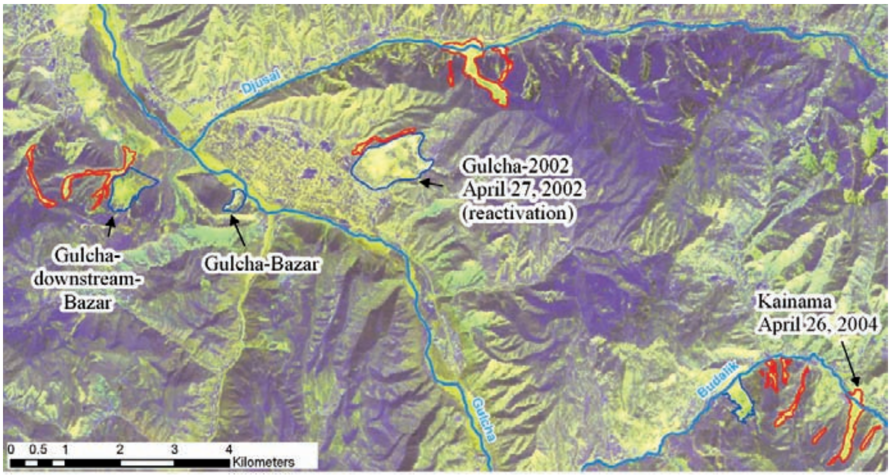

Fig. 19.6 ASTER image (VNIR bands, May 2004) covering the Gulcha study area with indication of earthflows (in *red*) and earthslides (in *blue*). Modified from Danneels et al., in press

vegetation index and slope angle). The combination of both allows for an accurate detection of slope failure occurrence in loess deposits. However, mapping of entire mass movements reveals to be unsatisfactory unless particular image analysis methods are implemented (this is the objective of ongoing research). The method is also tested for complex landslides (involving bedrock and loess deposits) and pure rockslides. For the two latter, the spectral characteristics seem to be less useful to detecting slope failure. First, most mass movements are not recent events and vegetation has partly covered the mass movements; secondly, simple rock faces and rockslide scarps may not be distinguished unless more complex morphological aspects (combined concavity in scarp and convexity in body area) are taken into account. Here, the limitation of the method is given by the resolution and accuracy of the digital elevation model (DEM). For the entire Tien Shan a 100 m SRTM DEM is available. However, the resolution of this DEM is by far insufficient to detect mass movements. Therefore, we produce for some target regions 15(30) m-resolution and 5m-resolution DEMs from ASTER and SPOT images as well aerial photographs. These DEMs are included in the analysis and locally show a clear improvement of the landslide detection.

Recently, we extended the application of the method to the detection of landslide/rockslide dams in high mountain regions. Actually, the risk connected with these dams is often larger than the one related to the mass movements themselves. Up- and downstream flooding as well as development of debris flows induced by formation and breakage of such dams caused extensive damage in many areas. At present, some dams endanger major engineering projects in the Tien Shan.

The inventory of mass movements (including rockslides, loess slides, natural dams, etc.) to be compiled for large areas within the Tien Shan will be used as input for landslide susceptibility and locally also hazard mapping with the aim to improve prevention of related risk. Landslide susceptibility mapping is carried out with statistical (e.g. neural networks and conditional analysis) and process-based (e.g. simplified Newmark) methods. Size-frequency analyses are applied to the whole inventory and sub-inventories. Such analyses may reveal incompleteness of the inventory (in the low-size domain) as well as regional (natural effects) and local (anthropogenic effects) differences – even though analyses published in literature suggest weak environmental influences on the size-frequency behavior of landslides.

To be able to perform reliable susceptibility and size-frequency analyses, these inventories need to be verified. At present, we perform local verification by manual mapping and control, but automatic verification methods are being developed. They will also allow us to determine the level of uncertainties. Ongoing research is focused on the propagation of uncertainties throughout the chain of processing.

19.6.7 Evaluation of a Satellite-Based Landslide Algorithm Using Global and Regional Landslide Inventories

Authors: Dalia Bach Kirschbaum[1], Robert Adler[2], Yang Hong[3]
[1]Columbia University, [2]NASA Goddard Space Flight Center, School of Civil Engineering and Environmental Sciences, [3]University of Oklahoma

Landslide hazard assessment research has predominately focused on site investigations, drawing on high resolution surface data as well as detailed landslide inventories and rainfall information to provide an estimate of static landslide hazard susceptibility. Given the mass of data required for such methodologies, research is generally limited to regions where such data is available, primarily in developed countries. To present a more dynamic representation of landslide hazard risk at larger spatial scales, Hong et al. (2006, 2007) has developed an algorithm which couples a landslide hazard susceptibility map with real-time satellite derived rainfall to forecast areas with high landslide potential.

This study evaluates the algorithm using a global landslide inventory database compiled for this purpose. The components of the algorithm are quantitatively evaluated for their relative skill both spatially and temporally. The results are then compared to the input data to identify the limitations and potential application of the algorithm. The goal of this analysis is to provide the information necessary to generate an improved version of this global landslide algorithm and to communicate its applicability to end-users.

The satellite based global landslide algorithm draws on a range of remote sensing data to develop a landslide susceptibility map and rainfall intensity-duration relationship. The susceptibility map is derived from six input datasets, including slope, soil type, soil texture, land cover, elevation, and drainage density. A detailed description of the susceptibility map and methodology is available in Hong et al. (2007). A satellite rainfall product is used to establish and evaluate the rainfall intensity-duration threshold conditions necessary for landslide initiation. The TRMM Multi-Satellite Precipitation Analysis (TMPA) product (Huffman et al. 2007) is available at 0.25°, 3-hourly resolution.

The landslide inventory database was compiled using information from journal articles, existing databases, online news media, and government and relief aid organization reports. The study considers all rapidly-occurring rainfall triggered landslide types in the database and focuses on the years 2003 and 2007 (Kirschbaum et al. 2008).

The landslide event locations in the database are compared to the susceptibility map and the satellite rainfall accumulation information. Approximately 70% of the landslide inventory events for the considered years are located in areas denoted as “high susceptibility.” High susceptibility areas are difficult to resolve in coastal regions and small islands due to the 0.25° base resolution of the susceptibility map as well as the way in which variables such as slope are calculated and weighted.

Satellite rainfall accumulation is extracted for the landslide events to determine if the existing intensity and duration information exceeds the threshold values at the 1, 3, and 7-day duration. Approximately 30% of the landslide events were located in areas where the rainfall exceeded the threshold at the designated temporal windows. A larger percentage of the landslides had rainfall accumulations that exceeded thresholds at the sub-daily level and were typically associated with high intensity-short duration rainfall events. A small subset of events did not resolve any significant rainfall for the landslide location, suggesting that the landslide events were improperly mapped.

The algorithm was run retrospectively for 2003 and 2007 to obtain a set of forecasts, which were then compared to the landslide events for the corresponding years. Results are plotted yearly both by month and latitude (Fig. 19.7). Figure 19.7 illustrates the comparable seasonal distributions for the algorithm forecasts and landslide events as well as a similar latitudinal trend for both datasets in the northern hemisphere. In the southern hemisphere, there are a substantially higher percentage of forecasts compared to the percent of reported landslide events. This is likely due to the under-reporting of landslides in South America and Africa.

Results indicate that the algorithm demonstrates some predictive skill over the Himalayan Arc region, portions of Southeast Asia, Central America, and Oceania (Fig. 19.8). There are severe over-reporting issues in the Indian peninsula, Eastern

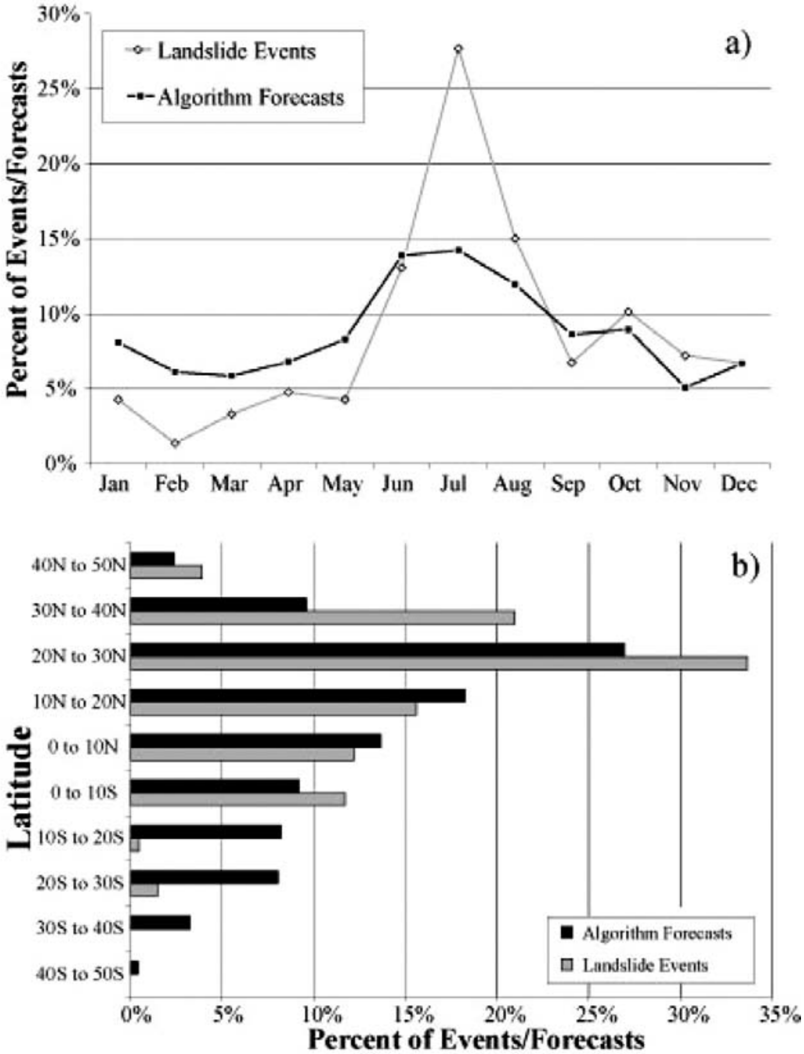

Fig. 19.7 (**a**) Temporal distribution of 2003 landslide events and algorithm forecasts, (**b**) distribution of landslide events and algorithm forecasts by latitude

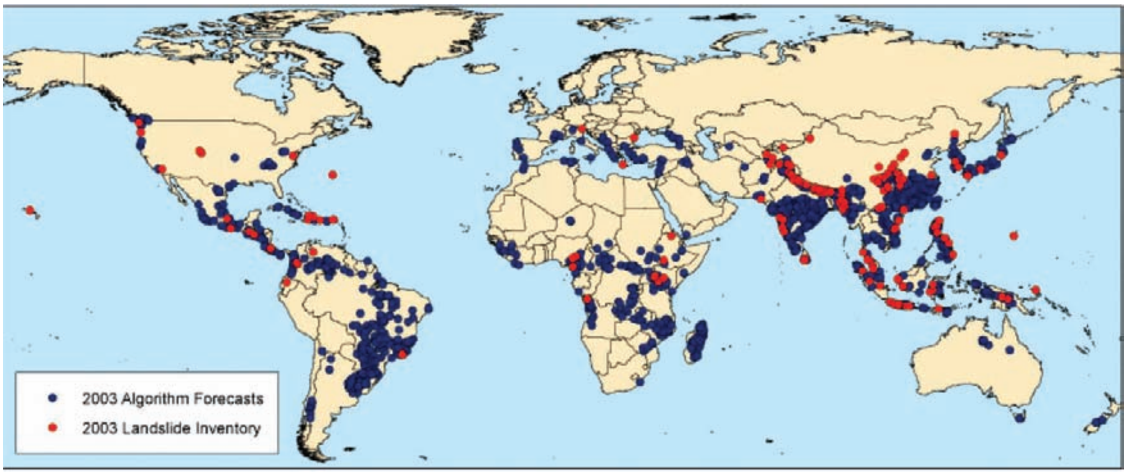

Fig. 19.8 Distribution of 2003 Landslide inventory events (*red*) and 2003 Algorithm Forecasts (*blue*)

Brazil, and portions of Africa. The high concentration these of Type I errors correlate regionally with an over-weighting of soil type and soil texture information in the susceptibility map. In contrast, the slope parameter is generally under-emphasized due to the way in which the values are calculated and the weighting of the variable. This is particularly true in areas with marginal but nonetheless critical slope gradients. These variables need adjustment to improve the susceptibility map and resulting algorithm skill.

This evaluation also considers algorithm performance at the regional scale, focusing on available landslide and surface data in Central America and the Caribbean. Extensive digital inventory data from landslides triggered by Hurricane Mitch provides a foray into the re-evaluation and calibration of susceptibility information at the regional and global scales.

The current algorithm represents a first version of this global evaluation effort. The algorithm demonstrates skill in forecasting areas of "high landslide potential" for specific regions; however, several improvements are necessary before the algorithm can become an operational forecasting and susceptibility evaluation tool:

1) Input variables to the susceptibility map must be recalculated and re-weighted according to global and regional sensitivity analyses.
2) Of the input variables, slope requires the most significant attention in better characterizing the physical threshold processes and understanding slope distribution at finer scales.
3) Integrating soil moisture information into the algorithm may provide a more representative realization of global susceptibility and introduce additional memory to the algorithm system.
4) The rainfall intensity-duration threshold curve should be considered against other global studies and possibly recalibrated using additional landslide information.
5) The resolution considered in this algorithm limits the ability to resolve features or processes with comparatively smaller spatial or temporal extents, including smaller topographic features, anthropogenically modified areas, high-intensity short duration rainfall events, and areas exposed to prolonged rainfall that saturates soils.

The results indicate that with the suggested improvements the global landslide algorithm has the potential to serve as a valuable tool for aid and governmental organizations as well as global landslide research in the future.

19.6.8 IFFI Project (Italian Landslide Inventory) and Risk Assessment

Authors: Alessandro Trigila, Carla Iadanza, Daniele Spizzichino
APAT – Agency for environmental protection and technical services/Geological Survey of Italy, Rome

Landslides represent one of the most relevant natural hazards in Italy. The main scope of the IFFI project is the identification and mapping of landslides over the entire Italian territory following rigorous and shared standardized criteria. Developed by APAT/Geological Survey of Italy and by the Regions and Autonomous Provinces, the project was financed in 1997 with 4.1 million Euro, by the Committee of Ministries for Land Protection. The IFFI inventory represents a useful tool for land use planning and management, landslide risk assessment and protection strategies.

The methodology applied to build up the national landslide inventory is based upon a collection of historical documents and archive data, aerial photo-interpretation, field surveys, the development of landslide data sheet and a detailed cartographic representation (Fig. 19.9).

The research of historical sources is fundamental in order to assess return period, magnitude and intensity of a landslide phenomenon through the reconstruction of past events.

The main information sources used to compile the IFFI database are: (a) National projects (AVI – Inventory of information on sites historically affected by landslides and floods in Italy for the period 1918/2000; SCAI – Special project for the study of unstable towns; CARG – Geological map of Italy, scale 1:50,000); (b) Landslide inventories by Regions, River Basin Authorities, research institutes and universities; (c) River Basin plans (PAI – L. 267/98); (d) Emergency Declarations (L. 225/92); (e) National and local public archives; (f) Scientific and technical papers and reports.

Aerial photo-interpretation has been a fast and efficient way to perform geomorphological surveys

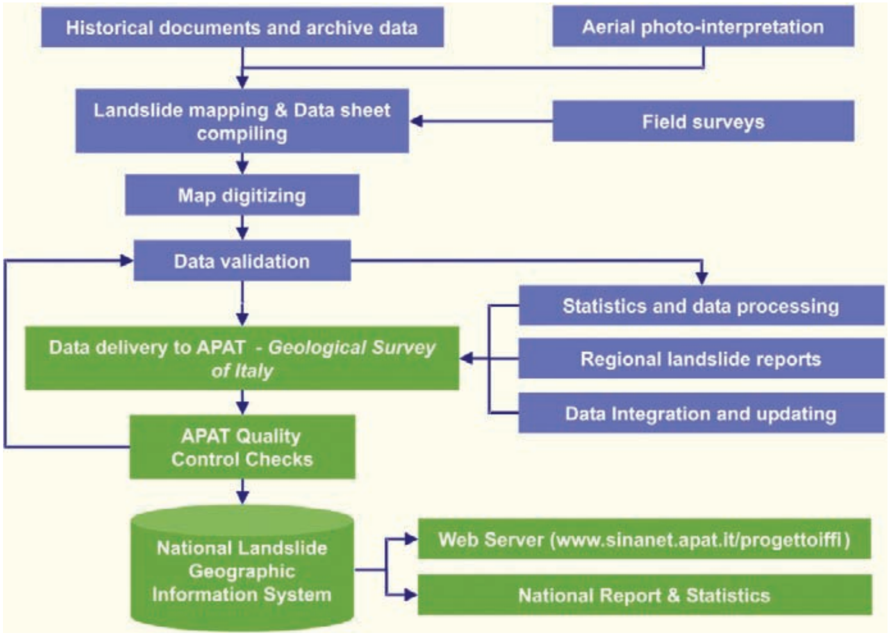

Fig. 19.9 IFFI Project work phases

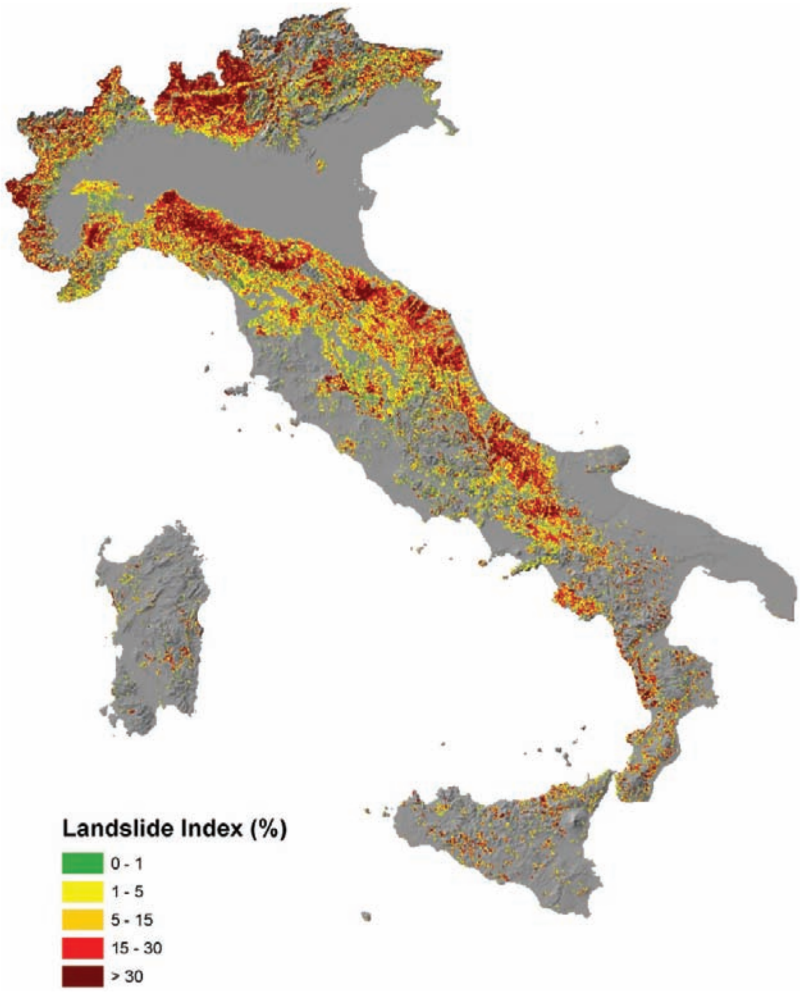

Fig. 19.10 Landslide Index (landslide area/total area × 100) calculated on a 1×1 km grid

over a large portion of territory. Field surveys have been used to verify and integrate the data collected in the aerial photo interpretation phase and to update the archive.

With the aim of homogenizing classification and glossary (i.e. type of movement, state of activity, intensity, velocity, distribution), the following international classification standards have been adopted: Cruden and Varnes (1996), Recommendations of the International Association of Engineering Geology (IAEG 1990), International Geotechnical Societies UNESCO Working Party on World Landslide Inventory (WP/WLI 1993a), Multilingual Landslide Glossary (WP/WLI 1993b), and International Union of Geological Sciences Working Group on Landslides (IUGS/WGL 1995).

The IFFI data sheet, organized in three different levels of increasing detail, has been compiled for every single mapped landslide. The 1st level contains basic data on landslide location, type of movement and state of activity and it is mandatory for each landslide; the 2nd level provides data on morphometry, geologic units, discontinuities, lithology, geotechnical properties, land use, causes and dates of activation; the 3rd level gives detailed information on damages, investigation processes and remedial measures for risk mitigation.

The 1:10,000 scale of representation has been adopted for the entire territory. A smaller scale has been adopted in uninhabited and high mountain areas.

Every single landslide is represented by: a georeferenced point located, as it is customary, at the highest point of the crown area; a polygon, if it is possible to map the landslide in respect to the scale of representation; and a line when the phenomena is too narrow to be appreciated (debris flows case).

The Landslide inventory database has been validated by performing spatial, relational and completeness quality control checks.

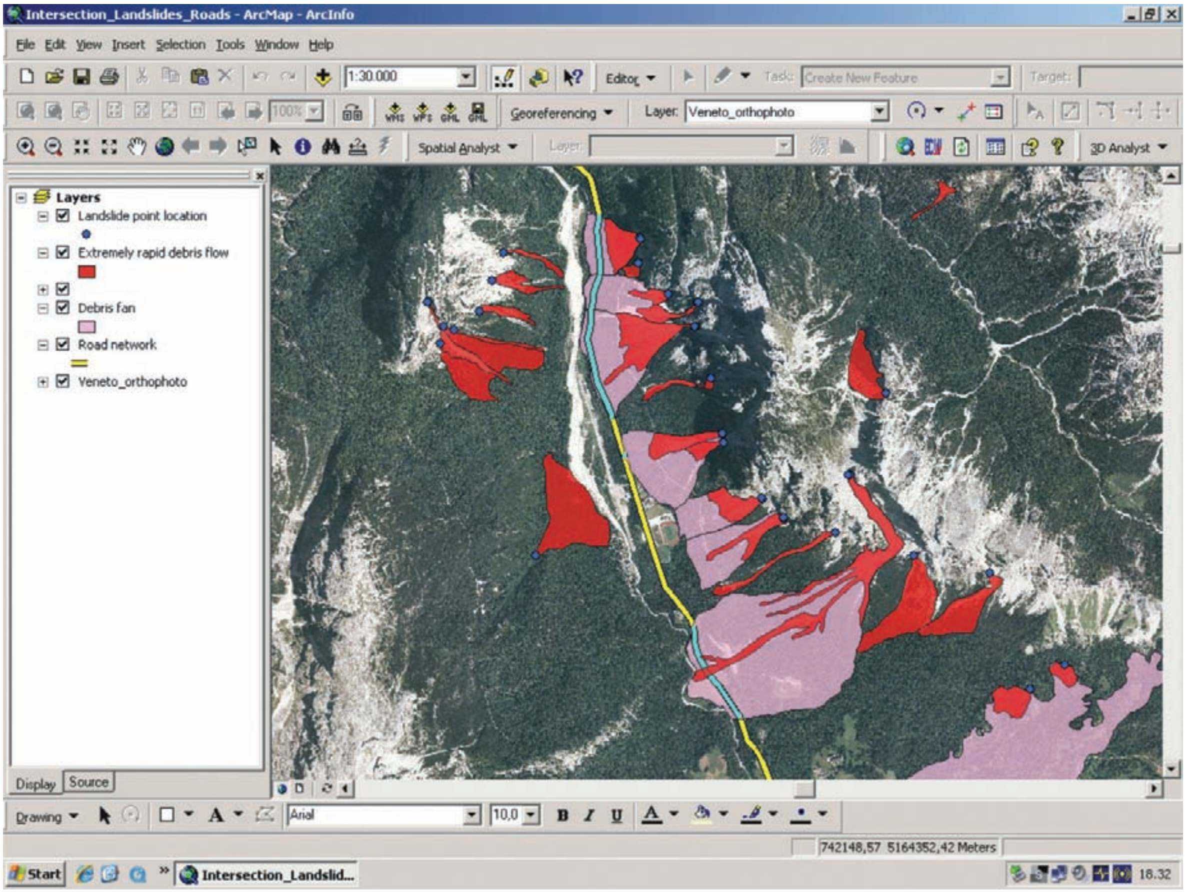

Fig. 19.11 GIS processing: transportation corridor segments exposed to landslide risk

Presently, the Italian Landslide Inventory holds about 470,000 landslides concerning an area of about 20,000 km^2 corresponding to 6.6% of the entire national territory. Italian municipalities involved in landslides are 5,596, equal to 69% of the total amount (Fig. 19.10).

With the aim of promoting the dissemination of landslide information, a WebGIS application (www.sinanet.apat.it/ progettoiffi) has been designed and developed. The IFFI website allows, through a simple and clear navigation, to visualize landslides, query the database, promote geographical investigation and consult documents, photos and videos. The WMS service guarantees interoperability and data sharing in compliance with the European Directive INSPIRE 2007/2/CE.

In the light of the wide distribution of landslides, the intense human activities on the national territory and the damages in terms of victims (2,552 during the last 50 years), the present work is aimed to give a preliminary landslide risk assessment at national level using IFFI inventory.

Through GIS processing techniques (vector intersection and spatial analysis) it has been possible to combine the landslide layer coming from IFFI inventory with the 2001 Population Census data (ISTAT -Italian National Institute of Statistics), the urban settlement data (Corine Land Cover 2000) and the main Italian infrastructure networks. The analysis estimates the interaction between landslides and urban areas. The population at risk and the critical points along highways, railways, road networks have been pointed out (Fig. 19.11).

This kind of analysis can address policy makers, professionals and stakeholders giving a DSS (Decision Support System) to establish priorities and planning actions in order to reduce the landslide risk.

19.6.9 Quantitative Landslide Risk Assessment at the River Basin Scale

Authors: Veronica Tofani, Nicola Casagli, Filippo Catani

Department of Earth Sciences, University of Florence, Italy

Landslides and mass movements in general are very common in Italy, especially along the main mountain chains such as Alps or the Apennines. The study area is no exception to this rule being strongly subjected to mass movements (Catani et al. 2005). The study area is the Arno river basin which is located in northern Apennines, Italy and has an extension of 9116 km^2. A new landslide inventory of the whole area was realized, using conventional (aerial-photo interpretation and field surveys) and non-conventional methods such as remote sensing techniques like DInSAR and PS-InSAR, (Farina et al. 2006). The great majority of the mapped mass movements are rotational slides (75%), solifluction and other shallow slow movements (17%) and flows (5%), while rapid flows and falls seem less frequent everywhere within the basin.

This research is aimed at assessing landslide hazard and risk at basin scale. The final goal is to create a dynamic tool, managed in GIS environment, useful for landslide risk pre-disaster planning and management.

The assessment of landslide hazard in terms of probability of occurrence in a given time, based for mapped landslides on direct and indirect observations of the state of activity and recurrence time, has been extended to landslide-free areas through the application of statistical methods implemented in an artificial neural network (ANN) (Ermini et al. 2005). On the basis of the more common landslides in the Arno river basin and the results of the univariate statistical analysis five preparatory factors were selected: slope angle, lithology, profile curvature, land cover and upslope contributing area.

Model validation confirms that prediction results are very good, with an average percentage of correctly recognized mass movements of about 90%. The analysis also revealed the existence of a large number of unmapped mass movements, thus contributing to the completeness of the final inventory. Temporal hazard was estimated via the translation of state of activity in recurrence time and hence probability of occurrence.

The definition of position, typology and characteristics of the elements at risk has been carried out with two different methodologies,:

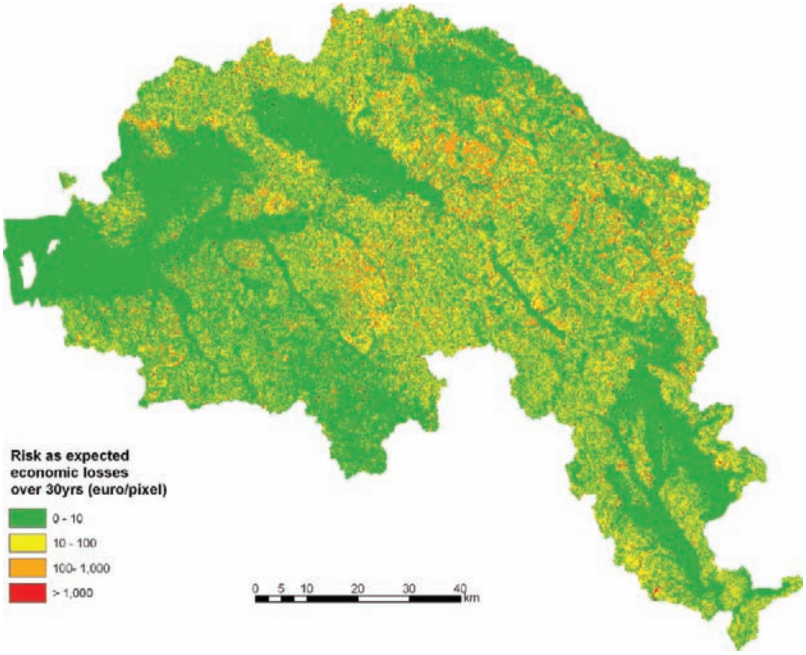

Fig. 19.12 Landslide risk map of the Arno river basin over a period of 30 yrs. The risk is expressed as economic losses due to landslides for each terrain unit (from Catani et al. 2005)

(i) buildings and infrastructures were directly extracted from digital terrain cartography at the 1:10,000 scale, whilst (ii) non-urban land use was identified and mapped based on an updated and improved CORINE land cover map at the 1:50,000 scale.

The definition of the exposure for each type of element at risk was based on their presumed asset and income values. Landslide vulnerability defined as the degree of lost of elements at risk due to a landslide of a settled intensity, usually expressed as a value ranging from 0 to 1, and was estimated on the basis of the typology and economic and social relevance of elements at risk.

Landslide intensity, usually defined as proportional to kinetic energy, was obtained considering landslide typology as a proxy for expected velocity. In the case of the Arno River Basin the definition of intensity is influenced by the fact that the large majority of mass movements are deep-seated reactivated slides evolving into flows. Two main cases were so considered: deep-seated rotational slides and shallow flows or planar slides with virtually constant depth. In the latter case, intensity as a function of volume was set proportional to the area of the mapped phenomenon. In the former case, a geometric model was used to compute the volumes. Four classes of intensity have been defined on the basis of the literature values (Fell 1994).

The landslide risk was assessed both in a qualitative and quantitative way. In the former case contingency matrices were used to intersect hazard classes with vulnerability and exposure classes, thereby classifying the territory of the Arno river basin in five classes of landslide risk (R0, R1, R2, R3, R4). The results display that 0.1% (about 9.17 km^2) of the whole territory shows the highest degree of risk (R4).

The quantitative assessment of risk was carried out through the application of the risk equation, therefore applying the product of the numerical values of hazard, vulnerability and exposure (Cruden and Fell 1997). The procedure lead to the definition of risk values expressed as economic losses for each terrain units and for different periods of time into the future (2, 5, 10, 20 and 30 years) (Fig. 19.12). In the next five years around 2.5 billions of euros should be expected as economic losses due to landslides. This value agrees with the data regarding the costs for landslide mitigation measures spent in the Arno river basin in the last five years.

References

AGS (Australian Geomechanics Society Landslide Zoning Working Group) (2007) Guideline for Landslide Susceptibility, Hazard and Risk Zoning for Land Use Planning. Australian Geomechanics 42(1), pp. 13–36

Aleotti P, Chowdhury R (1999) Landslide hazard assessment: summary review and new perspectives. Bulletin of Engineering Geology and the Environment 58:21–44

ARMONIA (2008) Assessing and Mapping Multiple Risks for Spatial Planning: approaches, methodologies and tools in Europe. EU Contract FP6-2003-Global-2-511208

Ayalew L, Yamagishi H (2005) The application of GIS-based logistic regression for landslide susceptibility mapping in the Kakuda-Yahiko Mountains, Central Japan. Geomorphology 65:15–31

Azzous AS, Krizek RK, Corotis RB (1976) Regression analysis of soil compressibility. Soils and Foundations 16:19–29

Barredo JI, Benavides A, Hervás J, van Westen CJ (2000) Comparing heuristic landslide hazard assessment techniques using GIS in the Tirajana basin, Gran Canaria Island, Spain. International Journal of Applied Earth Observation and Geoinformation 2:9–23

Bell R, Glade T (2004) Quantitative risk analysis for landslides – Examples from Bíldudalur, NW-Iceland. Natural Hazards and Earth System Sciences 4:117–131

Bichler A, VanDine D, Bobrowsky, P (2004) Landslide Hazard and Risk Mapping – a Review and Classification. Proceedings of the 57th Canadian Geotechnical Conference, 24–28th October, Quebec City, Canada, p. 12

Blais-Stevens A, Septer D (2008) Historical accounts of landslides and flooding events along the Sea to Sky Corridor, British Columbia, from 1855–2007. Geological Survey of Canada Open File 5741, p. 119

Bonham-Carter GF, Agterberg FP, Wright DF (1989) Weights of evidence modelling: a new approach to mapping mineral potential. In: Agterberg FP, Bonham-Carter GF (eds.), Statistical Applications in the Earth Sciences, Geological Survey of Canada Paper 89-9, Ottawa, pp. 171–183

Bonnard C, Forlati F, Scavia C (eds.) (2004) Identification and Mitigation of Large Landslide Risks in Europe: advances in risk assessment. A.A. Balkema, Netherlands, p. 317

Carrara A (1983) Multivariate models for landslide hazard evaluation. Mathematical Geology 15:403–426

Carrara A, Cardinali M, Guzzetti F, Reichenbach P (1995) GIS technology in mapping landslide hazard. In: Carrara A, Guzzetti F (eds.), Geographical Information Systems in Assessing Natural Hazards. Kluwer Academic Publishers, Dordrecht, The Netherlands, pp. 135–175

Carrara A, Merenda L (1976) Landslide inventory in northern Calabria, southern Italy. Geological Society of America Bulletin 87:1153–1162

Catani F, Casagli N, Ermini L, Righini G, Menduni G (2005) Landslide hazard and risk mapping at catchment scale in the Arno River basin. Landslides 2:329–342

Chacón J, Irigaray C, Fernández T, El Hamdouni R (2006) Engineering geology maps: landslides and geographical information systems. Bulletin of Engineering Geology and the Environment 65:341–411

Chung CJ, Fabbri AG (1999) Probabilistic prediction models for landslide hazard mapping. Photogrammetric Engineering and Remote Sensing 65:1389–1399

Chung CJ, Bobrowsky, PT, Guthrie R (2002) Quantitative prediction model for landslide hazard mapping, Tsitika and Schmidt Creek Watersheds, Northern Vancouver Island, British Columbia, Canada. In: Bobrowsky PT (ed.), Geoenvironmental Mapping: methods, theory and practice, Swets and Zeitlinger Publishing, The Netherlands, pp. 697–716

Collins BD, Sitar N (2008) Processes of Coastal Bluff Erosion in Weakly Lithified Sands, Pacifica, California, USA. Geomorphology 97:483–501

Commission of the European Communities (2006a) Thematic Strategy for Soil Protection. COM(2006)231 final, Brussels 22.9.2006, p. 12

Commission of the European Communities (2006b) Proposal for a Directive of the European Parliament and of the Council establishing a framework for the protection of soil and amending Directive 2004/35/EC. COM(2006)232 final, Brussels 22.9.2006, p. 30

Corominas J, Copons R, Moya J, Altimir J, Amigó J (2005) Quantitative assessment of the residual risk in a rockfall protected area. Landslides 2:343–357

Crosta GB, Agliardi F (2003) A methodology for physically based rockfall hazard assessment. Natural Hazards and Earth System Sciences 3:407–422

Crozier MJ, Glade T (2005) Landslide Hazard and Risk: Issues, Concepts and Approach. In: Glade T, Anderson M, Crozier MJ (eds.), Landslide Hazard and Risk. Wiley, Chichester, pp. 1–40

Cruden DM, Fell R (1997) Landslide risk assessment. In: Proceedings of the Workshop on Landslide Risk Assessment, Honolulu, Hawaii. Balkema, Rotterdam, The Netherlands and Brookfield, CT, p. 384

Cruden DM, Varnes DJ (1996) Landslide types and processes. In: Turner AK, Schuster RL (eds.), Landslides: Investigation and Mitigation. Transportation Research Board Special Report 247, National Academy Press, Washington DC, pp. 36–75

Dai FC, Lee CF, Ngai YY (2002) Landslide risk assessment and management: an overview. Engineering Geology 64:65–87

Danneels G, Bourdeau C, Torgoev I, Havenith HB (in press) Geophysical investigation and dynamic modeling of unstable slopes: case-study of Kainama (Kyrgyzstan). Geophysics Journal International

DeGraff JV, Romesburg HC (1980) Regional landslide-susceptibility assessment for wildland management: a matrix approach. In: Coates DR, Vitek JD (eds.), Thresholds in Geomorphology, Allen and Unwin, London, pp. 401–414

Duncan JM (1996) State of the art: limit equilibrium and finite-element analysis of slopes. Journal of Geotechnical Engineering 122:577–596

Eckelmann W, Baritz R, Bialousz S, Bielek P, Carre F, Houskova B, Jones RJA, Kibblewhite MG, Kozak J, Le Bas C, Toth G, Varallyay G, Yli Halla M, Zupan M (2006) Common criteria for risk area identification according to soil threats. European Soil Bureau Research Report No. 20, EUR 22185 EN, Office for Official Publication of the European Communities, Luxembourg, p. 94

Ermini L, Catani F, Casagli N (2005) Artificial neural networks applied to landslide susceptibility assessment. Geomorphology 66:327–343

Farina P, Colombo D, Fumagalli A, Marks F, Moretti S (2006) Permanent Scatterers for landslide investigations: outcomes from the ESA-SLAM project. Engineering Geology 88:200–217

Fell R (1994) Landslide risk assessment and acceptable risk. Canadian Geotechnical Journal 31:261–272

Fell R, Ho KKS, Lacasse S, Leroi E (2005) A framework for landslide risk assessment and management. In: Hungr O, Fell R, Couture R, Eberhardt E (eds.), Landslide Risk Management. Taylor and Francis, London, pp. 3–26

Fernández T, Irigaray C, El Hamdouni R, Chacón J (2003) Methodology for landslide susceptibility mapping by means of a GIS. Application to the Contraviesa area (Granada, Spain). Natural Hazards 30:297–308

Fruneau F, Achache J, Delacourt C (1996) Observation and modelling of the Sant-Etienne-de-Tinée landslide using SAR interferometry. Tectonophysics 265: 181–190

Galli M, Ardizzone F, Cardinali M, Guzzetti F, Reichenbach P (2008) Comparing landslide inventory maps. Geomorphology 94:268–289

Galli M, Guzzetti F (2007) Landslide vulnerability criteria: a case study from Umbria, Central Italy. Environmental Management 40:649–664

Glade T, Anderson M, Crozier MJ (2005) Landslide Hazard and Risk. Wiley, Chichester, p. 802

Grignon A, Bobrowsky P, Coultish T (2004) Landslide Database Management Philosophy in the Geological Survey of Canada. Proceedings of the 57th Canadian Geotechnical Conference, 24–28th October, Quebec City, Canada, p. 5

Grignon A, Bobrowsky P (2005) Empowering scientists, planners and the public to reduce landslide losses: a simplified web interface to access a national database in Canada. European Geosciences Union – General Assembly, April 24–29, 2005 Vienna, Austria. Digital Publication, Geophysical Research Abstracts, vol. 7, #EGU05-A-05511

Günther A, Reichenbach P, Guzzetti F, Richter A (2007) Criteria for the identification of landslide risk areas in Europe: the Tier 1 approach. In: Hervás J (eds.), Guidelines for Mapping Areas at Risk of Landslides in Europe. Proceedings of Experts Meeting, JRC Ispra, Italy, 23–24 October 2007. JRC Report EUR 23093 EN, Office for Official Publication of the European Communities, Luxembourg, (http://eusoils.jrc.it) pp. 37–39

Günther A, Reichenbach P, Hervás J (2008) Approaches for delineating areas susceptible to landslides in the framework of the European Soil Thematic Strategy (this volume)

Guzzetti F (2005) Landslide Hazard and Risk Assessment. PhD dissertation, Rheinischen Friedrich-Wilhelms-Univestität Bonn, Germany, p. 373

Guzzetti F, Carrara A, Cardinali M, Reichenbach P (1999) Landslide hazard evaluation: a review of current techniques and their application in a multi-scale study, Central Italy. Geomorphology 31:181–216

Guzzetti F, Reichenbach P, Ardizzone F, Cardinali M, Galli M (2006) Estimating the quality of landslide susceptibility models. Geomorphology 81:166–184

Guzzetti F, Reichenbach P, Cardinali M, Galli M, Ardizzone F (2005a) Probabilistic landslide hazard assessment at the basin scale. Geomorphology 72:272–299

Guzzetti F, Salvati P, Stark CP (2005b) Evaluation of risk to the population posed by natural hazards in Italy. In: Hungr O, Fell R, Couture R, Eberhardt E (eds.), Landslide Risk Management. Taylor and Francis, London, ISBN 041538043X, pp. 381–389

Guzzetti F, Stark CP, Salvati P (2005c) Evaluation of flood and landslide risk to the population of Italy. Environmental Management 36:15–36

Hansen A, (1984) Landslide hazard analysis. In: Brunsden D, Prior DB (eds.), Slope instability. Wiley, New York, pp. 523–602

Hapke CJ, Reid D, Borrelli M (2007) The National assessment of shoreline change: A GIS compilation of vector cliff edges and associated cliff erosion data for the California Coast: U.S. Geological Survey Open-file Report 2007–1112 (http://pubs.usgs.gov/of/2007/1112)

Havenith HB, Strom A, Cacerez F, Pirard E (2006a) Analysis of landslide susceptibility in the Suusamyr region, Tien Shan: statistical and geotechnical approach. Landslides 3:39–50

Havenith HB, Torgoev I, Meleshko A, Alioshin Y, Torgoev A, Danneels G (2006b) Landslides in the Mailuu-Suu valley, Kyrgyzstan: Hazards and Impacts. Landslides 3:137–147

Hervás J (ed.) (2003) Lessons Learnt from Landslide Disasters in Europe. JRC Report EUR 20558 EN. Office for Official Publications of the European Communities, Luxembourg, (http://eusoils.jrc.it), p. 91

Hervás J (ed.) (2007) Guidelines for Mapping Areas at Risk of Landslides in Europe. Proceedings of Experts Meeting, Ispra, Italy, 23–24 October 2007. JRC Report EUR 23093 EN, Office for Official Publications of the European Communities, Luxembourg, (http://eusoils.jrc.it), pp. 49

Hervás J, Barredo JI, Rosin PL, Pasuto A, Mantovani F, Silvano S (2003) Monitoring landslides from optical remotely sensed imagery: the case history of Tessina landslide, Italy. Geomorphology 54:63–75

Hervás J, Günther A, Reichenbach P, Chacón J, Pasuto A, Malet J-P, Trigila A, Hobbs P, Maquaire O, Tagliavini F, Poyiadji E, Guerrieri L, Montanarella L (2007) Recommendations on a common approach for mapping areas at risk of landslides in Europe. In: Hervás J (ed.), Guidelines for Mapping Areas at Risk of Landslides in Europe. Proceedings of Experts Meeting, JRC Ispra, Italy, 23–24 October 2007. JRC Report EUR 23093 EN, Office for Official Publication of the European Communities, Luxembourg, (http://eusoils.jrc.it) pp. 45–49

Hong Y, Adler R, Huffman G (2006) Evaluation of the potential of NASA multi-satellite precipitation analysis in global landslide hazard assessment. Geophysical Research Letters 33(L22402): doi:10.1029/2006 GL028010

Hong Y, Adler R, Huffman G (2007) Use of satellite remote sensing data in the mapping of global landslide susceptibility. Journal of Natural Hazards DOI: 10.1007/s11069-006-9104-z

Huabin W, Gangjun L, Weiya X, Gonghui W (2005) GIS-based landslide hazard assessment: an overview. Progress in Physical Geography 29:548–567

Huffman G, Adler R, Bolvin D, Gu G, Nelkin E, Bowman K, Hong Y, Stocker E, Wolff D (2007) The TRMM Multi-satellite Precipitation Analysis (TMPA): Quasi-Global, Multiyear, Combined-Sensor Precipitation Estimates at Fine Scales. Journal of Hydrometeorology 8:38–55

Hungr O, Fell R, Couture R, Eberhardt E (eds.) (2005) Landslide Risk Management. Proceedings of the International Conference on Landslide Risk Management, Vancouver, BC, Canada. A.A. Balkema, London, p. 764

IAEG–International Association Engineering Geology Commission on Landslides (1990) Suggested Nomenclature for Landslides. IAEG Bulletin 41:13–16

IUGS/WGL–International Union of Geological Sciences Working Group on Landslides (1995) A suggested method for describing the rate of movement of a landslide. IAEG Bulletin, 52:75–78

IUGS Working Group on Landslides – Committee on Risk Assessment (1997) Quantitative risk assessment for slopes and landslides – The state of the art. In: Cruden D, Fell R (eds.), Landslide Risk Assessment. Balkema, Rotterdam, pp. 3–12

Kirschbaum DB, Adler R, Hong Y (submitted) Global landslide inventory database for hazard applications. Landslides

Lee EM, Jones DKC (2004) Landslide Risk Assessment. Thomas Telford, London, p. 454

McKean J, Roering J (2004) Objective landslide detection and surface morphology mapping using high-resolution airborne laser altimetry. Geomorphology 57:331–351

Metternicht G, Hurni L, Radu Gogu R (2005) Remote sensing of landslides: An analysis of the potential contribution to geo-spatial systems for hazard assessment in mountainous environments. Remote Sensing of Environment 98:284–303

Pack RT, Tarboton DG, Goodwin CN (1998) The SINMAP approach to terrain stability mapping. 8th Congress of the International Association of Engineering Geology, Vancouver, BC, Canada, 21–25 September 1998, p. 8

Poh KB, Chuan NL, Tan SS (1985) Residual granitic soils of Singapore. In: 8th Southeast Asian Geotechnical Conference, Kuala Lumpur, pp. 31–39

Popescu ME (1994) A suggested method for reporting landslide causes. Bulletin of the International Association of Engineering Geology 50:71–74

Reichenbach P, Galli M, Cardinali M, Guzzetti F, Ardizzone F (2005) Geomorphological Mapping to Assess Landslide Risk: Concepts, Methods and Applications in the Umbria Region of Central Italy. In: Glade T, Anderson M, Crozier MG (eds.), Landslide Hazard and Risk. Wiley, Chichester, pp. 429–468

Reichenbach P, Günther A, Guzzetti F (2007) Criteria for the identification of landslide risk areas in Europe: the Tier 2 approach. In: Hervás J (eds.), Guidelines for Mapping Areas at Risk of Landslides in Europe. Proceedings of Experts Meeting, JRC Ispra, Italy, 23–24 October 2007. JRC Report EUR 23093 EN, Office for Official Publication of the European Communities, Luxembourg, (http://eusoils.jrc.it) pp. 41–44

Remondo J, Bonachea J, Cendrero A (2008) Quantitative landslide risk assessment and mapping on the basis of recent occurrences. Geomorphology 94:496–507

RIC (1996a) Guidelines and Standards to Terrain Mapping in British Columbia. Resources Inventory Committee, Government of British Columbia, p. 215

RIC (1996b) Terrain Stability Mapping in British Columbia: A review and suggested methods for landslide hazard and risk mapping. Resources Inventory Committee, Government of British Columbia

Salvati P, Guzzetti F, Reichenbach P, Cardinali M, Stark CP (2003) Map of landslides and floods with human consequences in Italy. Publication CNR GNDCI n. 2822, 1:1,200,000 scale

Santacana N, Baeza B, Corominas J, De Paz A, Marturiá J (2003) A GIS-based multivariate statistical analysis for shallow landslide susceptibility mapping in La Pobla de Lillet area (Eastern Pyrenees, Spain). Natural Hazards 30:281–295

Schmidt-Thomé P (eds.) (2006) The Spatial Effects and Management of Natural and Technological Hazards in Europe – ESPON 1.3.1 Executive Summary. Geological Survey of Finland, Espoo, p. 309

Soeters R, van Westen CJ (1996) Slope instability recognition, analysis and zonation. In: Turner AK, Schuster RL (eds.) Landslides: Investigation and Mitigation. Transportation Research Board Special Report 247, National Academy Press, Washington DC, pp. 129–177

Thiery Y, Malet J-P, Sterlacchini S, Puissant A, Maquaire O (2007) Landslide susceptibility assessment by bivariate methods at large scales: Application to a complex mountainous environment. Geomorphology 92:38–59

Trigila A, Iadanza C, Guerrieri L (2007) The IFFI Project (Italian Landslide Inventory): methodology and results. In: Hervás J (ed.), Guidelines for Mapping Areas at Risk of Landslides in Europe. Proceedings of Experts Meeting, JRC Ispra, Italy, 23–24 October 2007. JRC Report EUR 23093 EN, Office for Official Publication of the European Communities, Luxembourg, (http://eusoils.jrc.it) pp. 15–18

van Westen CJ (1993) Application of geographic information systems to landslide hazard zonation. ITC Publication 15, Enschede, The Netherlands, p. 245

van Westen CJ, van Asch TWJ, Soeters R (2006) Landslide hazard and risk zonation – why is it still so difficult? Bulletin of Engineering Geology and the Environment 65:167–184

Varnes DJ, IAEG Commission on Landslides and other Mass Movements on Slopes (1984) Landslide hazard zonation: a review of principles and practice. UNESCO, Paris, p. 63

WP/WLI-International Geotechnical Societies UNESCO Working Party on World Landslide Inventory (1993a) A suggested method for describing the activity of a landslide. IAEG Bulletin 47:53–57

WP/WLI-International Geotechnical Societies UNESCO Working Party on World Landslide Inventory (1993b) Multilingual Landslide Glossary, Bitech Publisher, Richmond, British Columbia, Canada, p. 59

Yin KJ, Yan TZ (1988) Statistical prediction model for slope instability of metamorphosed rocks. In: Bonnard C (ed.), Landslides. Proceedings of the 5th International Symposium on Landslides, Balkema, Rotterdam, pp. 1269–1272

Zêzere JL (2002) Landslide susceptibility assessment considering landslide typology. A case study in the area north of Lisbon (Portugal). Natural Hazards and Earth System Sciences 2:73–82

Zêzere JL, Garcia RAC, Oliveira SC, Reis E (2008) Probabilistic landslide risk analysis considering direct costs in the area north of Lisbon (Portugal). Geomorphology 94:467–495

Monitoring, Prediction and Early Warning 20

Kyoji Sassa, Luciano Picarelli and Yin Yueping

Abstract Landslide risk reduction is a societal pressing need in for counties and also areas along coasts, lakes, rivers in relatively flat countries. Engineering measures to stabilize dangerous slopes needs very high cost and not feasible for many cases. Monitoring, Prediction, Early Warning is the most economical landslide risk reduction measure which is applicable for both developed and developing countries. This chapter presents monitoring of triggering factors, slope deformation, other indicators in indoor experiments, field experiments as well as in natural condition. Methodology of prediction and early warning is examined based on these monitoring and topographical, geological and hydrological conditions.

Keywords Early warning • Time prediction • Real time monitoring • Real time warning system • Model experiment • International Programme on Landslides (IPL)

20.1 IPL C105 "Early Warning of Landslides"

Members of International Consortium on Landslides and other related landslide researchers together with representatives from United Nations organizations (UNESCO, WMO, FAO, UN/ISDR, UNEP, UNDP, UNU) and global NGO (World Federation of Engineering Organizations) etc gathered at the opportunity of Round Table Discussion for strengthening research and learning on landslide risk mitigation in Tokyo and promoting the International programme on Landslides in January 2006. Asian members discussed and decided to propose a project focusing currently important topics on landslides in Asian Country. Then, the International Consortium on Landslides applied a budget to the Ministry of Education, Sports, Culture, Science and Technology (MEXT), Japan within an Asian joint Research framework titled as "Asian Joint Project: Early Warning of Landslides" together with Korea, China, Indonesia, Thailand, Philippines and Japan. It was fortunately approved in 2007 as 3 years project (2007–2009).

Figure 20.1 presents the concept of proposed Asian joint project. "Early Warning of Landslides". The development of effective early warning technology needs various factors.

(1) The central flow from top to bottom is from the monitoring of triggering factors (rainfalls, snow

Kyoji Sassa (✉)
International Consortium on Landslides

Luciano Picarelli
Seconda Universtà di Napoli, Italy

Yin Yueping
China Geological Survey, China

© Springer-Verlag Berlin Heidelberg 2009

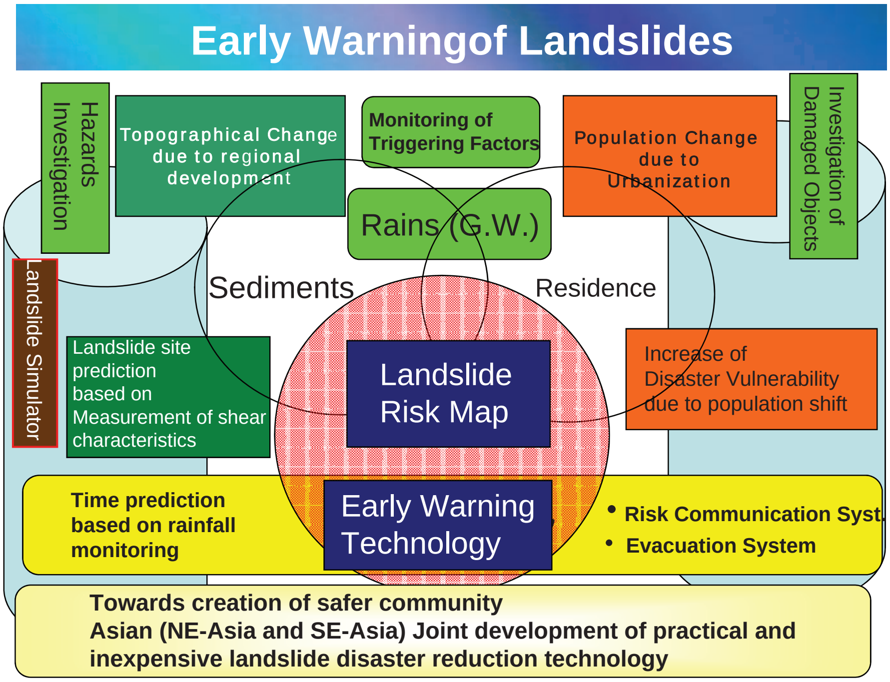

Fig. 20.1 Concept of IPL C105 early warning of landslides

melts, ground water levels) to development of landslide risk map and of early warning technology, then contributing to the creation of safer community.

(2) The left flow from top to bottom represents a aspect of technology for site and time prediction of landslides. Topographical change due to regional development has big impact on landslide risk. Landslide simulator (Dynamic loading undrained ring-shear apparatus (Sassa et al., 2004) to reproduce the formation of sliding surface and post-failure motion within an apparatus (Landslide simulator) is a strong tool for that.

(3) The right flow from top to bottom represents a social aspect. Population change due to urbanization has a great impact on landslide risk. The investigation of exposed objects is important for disaster assessment. Increase of disaster vulnerability due to population shift shall affect landslide risk map. Human or social aspect of Early Warning is risk communication system and evacuation system. Those developments will give great influence on effective early warning to reduce fatalities.

Figure 20.2 presents landslide types concerning landslide risk. Early warning is often issued without

Landslide Types affecting Risk

	Rapid Motion ⟺	Slow Motion
Deep Slides	(Rapid and Deep) Deep-sheeted rapid landslides	(Slow and Deep) Reactivated landslides
Shallow Slides	(Rapid and Shallow) Liquefied failures and debris flows.	(Slow and Shallow) Surface layer creep

- Landslide risk is affected by velocity and depth.
- Risk is different in areas (urban and rural)
- Landslide risk should be evaluated for each type of velocity, depth and area.

Fig. 20.2 Landslide susceptibility mapping and time prediction for early warning any mention of landslide type. However, Landside risk is quite different by landslide types. Landslides can be classified with regard to depth and speed from the aspect of risk. Deep and rapid landslides are most dangerous as single landslide. Shallow and rapid landslides are also dangerous especially when many landslides will occur during the same triggering event.

Slow landslides are relatively safe for people since they allow evacuation even during motion. However, often villages are constructed on reactivated landslides (previously landslide occurred and relatively flat areas are provided by past landslide events).The velocity is not so high, and travel distance is not great in this type of landslides. However, landslide movement can be enough to destroy houses, schools, and other buildings. The failure of houses and other structures may give damages to humans. Shallow and slow landslides are relatively not dangerous. Often early warning is not specified on these landslide types. Deep and shallow, rapid and slow movements have different mechanism, so the same criteria of early warning cannot be applied. We have to develop some criteria for different types. Risk is very different in urban environment or rural areas.

For reliable landslide risk mapping, the measurement of shear characteristics of soils is the most important. Shear characteristics mobilized during motion of landslides is available from the Landslide Ring-shear Simulator (undrained dynamic-loading ring-shear apparatus, Sassa et al., 2004). For triggering of landslides, pore-water pressure is the most important factor. Therefore, it is better to correlate the initiation of landslides with ground water level than rainfall itself. One possibility is to use a tank Model or leakage barrel model. Some application of tank model to simulate ground water level or volume of ground water for Zentoku landslides and landslide triggered by 2004 Niigata-ken Chuetsu earthquake are reported in Hong et al. (2004), Okada (2004). Some time prediction methods are presented by Picarelli, Versace, Jakob in this chapter.

The Asian joint project group proposed to organize a session on early warning of landslides in the First World Landslide Forum. The Italian group headed by Luciano Picarelli and others joined this initiative. The landslide research community has to cooperate to develop a new economical and effective based on mechanism of landslides, namely early warning technology. The followings are the basic consideration by Picarelli, and contribution from initial participants.

20.2 The Concept of Early Warning

Early warning is the whole of the actions to be taken before a catastrophic event, allowing individuals to take action in order to avoid or reduce the impeding risk (Gasparini et al., 2007). Lead time is the time interval comprised between the moment when the occurrence of the event is reasonably certain, and the moment of its actual occurrence.

In the last years, early warning systems have been employed for protection against some natural risks. In some cases, as for heavy meteorological events, volcanic eruptions and tsunami, they prove quite efficient, since the lead time available to take action, as evacuation or protection of some key structures and infrastructures, is long enough. In other cases (as for earthquakes, flash floods, rapid landslides), the lead time is so short that radical solutions for risk mitigation cannot be undertaken. In these cases, early warning can be adopted only for very limited goals or the signal must be launched well before the expected event, i.e. when its probability is high enough but it is not really certain. This last approach implies subjective decisions and can lead to false or missing alarms.

In case of rapid landslides, since the time elapsing between the onset of slope failure and its impact on exposed goods is typically in the order of tens of seconds, the problem is similar to the one posed by earthquakes, for which advanced procedures are being experienced (Gasparini et al., 2007), but even more complicated because often landslides may occur everywhere within wide areas which lack any type of instrument able to recognize the occurrence of the event. Research in this field is active, even though just beginning.

20.3 Landslide Prediction

The prediction of landslide triggering is a fundamental step in the setting up of early warning systems. In principle, prediction may be based on the analysis and elaboration of the precursors (rainfall), of indicators of impending rupture (pore pressure changes in the subsoil, ground displacements etc.) or of both.

Based on the collection of data regarding precipitation-induced landslides and triggering rainfall, thresholds have been established in some countries, as Hong Kong (Finlay et al., 1997), California (Wilson & Wieczorek, 1995), New Zealand (Glade et al., 2000) etc. Typically, such thresholds depend on a combination of rainfall intensity and duration; in particular, the critical intensity decreases as the rainfall duration increases. Because of the prominent role of slope morphology, stratigraphy and soil properties, these approaches can be employed only at a local scale. In fact, the relationship between landslide occurrence and rainfall features varies enormously from site to site.

Approaches based on the analysis of indicators of slope failure have been proposed for different types of slope movements. In particular, in the very last years, remote sensing methods are being strongly developed. Unfortunately, these methods can be used only for relatively slow landslides

In the case of rock falls, which occur suddenly, and shortly reach a high velocity, a timely prediction of failure is necessary. Generally, this is pursued through sensors measuring the progressive aperture of rock joints. The analysis of microseismic waves propagating from rock fractures subjected to pre-failure movement is quite a recent approach which is extensively tested in France (Senfaute et al., 2003).

A similar approach based on the analysis and interpretation of pre-failure movements is adopted in the case of creeping slopes (Saito, 1965) and could be used for special conditions, as for slopes subjected to a monotonic pore pressure increase (Picarelli et al., 2004). Failure can be predicted based on an equation fitting displacements recorded during the pre-failure stage, to be extrapolated up to general slope failure. The use of neural networks is another recommended procedure.

Other methods rely on the relationship between pore pressures and ground displacements. Several Authors show that movements of pre-existing slides in clay are activated since the pore pressure reaches a threshold. Through a statistical analysis of collected data regarding a slow mudslide, Mandolini and Urciuoli (1999) propose a relationship between the displacement rate and a combination of the rainfall heights which have been measured in different time spans preceding the present.

Today, a big effort involves researchers involved in the prediction of fast debris flows in unsaturated granular soils. Damiano et al. (2008) discuss a new method to interpret the data provided by TDR devices for a real-time investigation of the changes in the water content profile and consequent suction profile in pyroclastic soils subjected to infiltration. The method, which is being tested by flume tests appears promising, being able to provide reliable information: in fact, it can enable to perform timely analyses of the changes in the safety factor. The same experiences provide further useful data about the use of optical fibres to capture pre-failure soil movements caused by the volumetric collapse which is induced by saturation, and predict the consequent slope failure.

20.4 Implementation of Early Warning Systems

Early warning systems for rainfall-induced landslides are adopted in some regions of the world. In 1977 the Hong Kong Geotechnical Engineering Office established a warning system, which has been continuously updated and improved in the following years (Chan et al., 2003). Similar systems have been used to prevent the consequences of rainfall-induced debris-flows in the S. Francisco Bay (Keefer et al., 1987), in Nagasaki and in other parts of the world. D'Orsi et al. (1997) describe the Rio-Watch, an alert system based on a network of 30 telemetered rainfall gauges and weather radars which cover the city of Rio de Janeiro. Similar systems have been set up in the State of Oregon (Mills, 2002), in UK (Cole & Davis, 2002) and in the area between Seattle and Everett, Washington (Baum et al., 2005). In some countries, some organizations in charge of land protection provide continuous information through the WEB

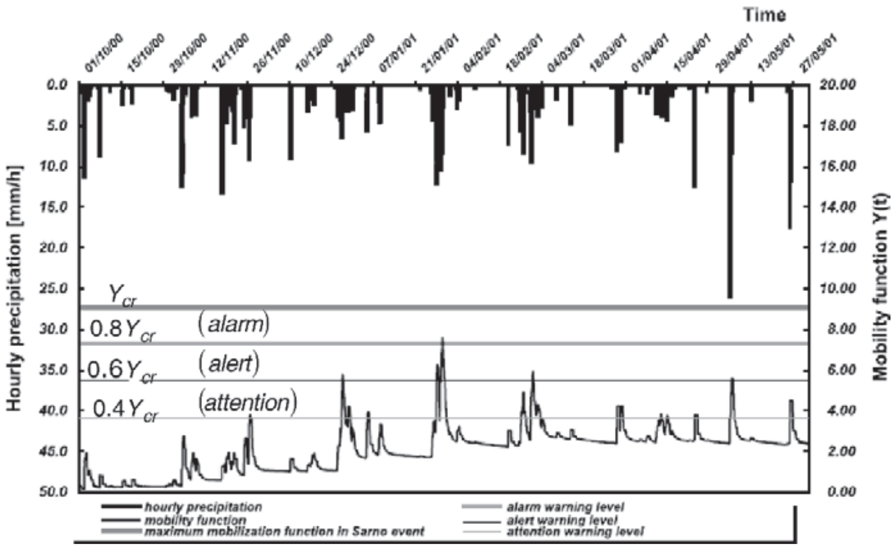

Fig. 20.3 Precipitations and warnings in Sarno area in the period October, 2000, May, 2001 (Picarelli et al., 2008)

about slope stability conditions in critical areas (Flentje et al., 2005).

After the catastrophic events occurred in 1998, an early warning systems has been established in the Sarno area, based on the so called FLAiR model (Forecasting of Landslides Induced by Rainfall), proposed in 1992 by Sirangelo and Versace (Picarelli et al., 2008).

FLaIR consists of two modules: RL (Rainfall-Landslide) and RF (Rainfall Forecasting). Through a calibration of available data collected in the past, the first module correlates precipitations and landslide occurrence in order to determine a mobility function Y(t) which, at any time, depends on the amount of infiltrated water and provides the probability, $P[E_t]$, of landslide occurrence at the time t. The second module provides a probabilistic prediction of impeding rainfall events through a stochastic rainfall or meteorological rainfall nowcasting, which is used to identify hazard conditions for landslide occurrence suitably in advance. Using both modules, the model enables a probabilistic evaluation of potential landslide occurrence.

The adopted strategy for risk mitigation is based on three warning levels: "attention", with instrumental real-time monitoring and real time simulation model running; "alert", involving civil protection agencies and field direct control; "alarm", involving population to be evacuated. A characteristic mobility ratio $\chi = Y/Y_{cr}$, is defined, Y_{cr} being the value of the mobility function associated with each warning level. The choice of the values of the index χ for each warning level must fit considering the necessity to have an adequate safety margin, which needs a low mobility ratio, and to avoid false alarms, which needs a high mobility ratio. Values of the mobility ratio presently used in Sarno are the following: $\chi = 0.40$, for the "attention" threshold, $\chi = 0.65$ for the "alert" threshold and $\chi = 0.85$ for the "alarm" threshold. The average time elapsing between the "alert" and "alarm" signal has been assessed to be in the range 4–5 h, which is considered long enough to assure evacuation.

In Fig. 20.3 are summarised the data on precipitations concerning the wet seasons 2000–2001. It is shown that in the period October, 2000 – June 2001, the attention level has been attained several times, the alert level has been reached three times, while the signal of warning has been launched only one time.

20.5 The Near Future

As shown, hydrological models can be very useful to predict rainfall-induced landslides in well known geomorphological contexts for which documented data are available. In some cases, as for failure in rock masses and in general everywhere a landslide is expected to occur suddenly and to develop rapidly, the analysis and use of indicators seems a useful criterion. However, rational and advanced approaches should be based on analyses having the goal to simulate the water infiltration and its consequences on the stability of slopes. In fact, numerical analysis could apply in areas occupied by uniform geomaterials whose properties have been adequately investigated in advance. This encourages the use of simplified codes, supported by GIS, as TRIGRS (Baum et al., 2002) which integrate data on rainfall with analysis of infiltration and slope stability over vast areas. A similar approach can be adopted at the scale of the single slope, using well known commercial or purposely develop codes. Today some research programs which follow a strategy based on a real-time use of short-term weather forecasting for slope stability analysis in large areas are active.

However, the still inadequate quality of rainfall forecasting at the scale of single slopes is a prominent problem. Presently, this does not yet allow a confident use of early warning procedures, due to the high probability of false or missing alarms. As a consequence, the numerical analysis should be supported by real-time monitoring of local rainfall and of fundamental indicators, as pore pressure or suction. Since accurate analysis is strongly affected by the difficulty in fixing reliable initial conditions, especially for unsaturated soil (suction), the main advantage of such an approach is that monitoring can provide local values of the pore pressure (or suction), i.e. of the initial conditions (Picarelli et al., 2008). As with FLaIR, the prediction can be carried out using as input a meteorological or stochastic forecasting or rainfall, or a Bayesian combination of both. Therefore, any numerical simulation can start from a correct initialisation of the governing factors. In addition, the continuous check of these factors can lead to a continuous real-time calibration and consequent adaptation of the model.

Just to summarise such considerations, the procedure to be adopted in instrumented sloping areas should require the following steps:

1. rainfall monitoring and forecasting;
2. start of analysis and models routing;
3. model calibration and adaptation;
4. iteration of analysis and prediction;
5. decision making.

In this framework, the basic situation corresponds to "normal" weather conditions, which are characterised by absence of rainfall or by "normal" rainfall. An advisory signal should be launched when weather forecasting anticipates the approaching of an abnormal rainstorm or when the rain gauge network reports unexpected severe rainfall. In case of further warning signals pre-established actions should be activated. A prominent action is strengthening of the monitoring in the instrumented sites and analysis of the likely effects of approaching rainfall (which can be roughly estimated through weather forecasting) accounting for monitored values of pore pressure (or suction): hence, numerical modelling starts to run. Data coming from monitoring should enable a continuous and timely check of the analysis by comparison of calculated and monitored values of pore pressure or suction during rainfall. In fact, the data provided by site monitoring of rainfall and suction can be used to update the initial and boundary conditions as well as other parameters which govern the slope behaviour: hence, the variation of the safety factor of the slope can be continuously adjusted. As a consequence, a framework about what can happen in next hours, i.e. of the presumed scenario of event, should be drawn in the assumption that rainfall will continue with the same intensity, or through stochastic forecasting of continuing rainfall. The process should be iterated until possible activation or deactivation of one of the established levels of warning. Decision making depends on the values of the thresholds which have been established. In this phase, any indicator of approaching failure is highly beneficial, supporting next decision.

The problem of early warning is crucial and delicate. In fact, false or missing alarms can compromise its reliability. However, it will certainly become a prominent tool for risk mitigation in the near future, especially in those densely inhabited areas where the hazard of landslides is critical and the social and economical cost of different procedures for risk mitigation too high for the involved communities.

20.6 Empirical Hydrological Models for Early Warning of Landslides Induced by Rainfall

Pasquale Versace (Università della Calabria, Italy)

The risk of landslide is extremely variable. In fact, slope movements have a wide range of velocity, size and run-out, thus their magnitude and impact on exposed goods can be either very low or very high, depending on site conditions, material involved and other factors. Velocity not only affects landslide destructiveness, but also the procedures to adopt for risk mitigation. Velocity can range between some tens of metres per second (as for rock falls and avalanches, debris flows and flowslides) and some millimetres per year (as for active slides in clay and some lateral spreads).

Early warning can be defined as the entirety of actions to be taken during the lead time, that is, the time interval elapsed between the moment of precursor occurrence and the moment of its actual occurrence. In more general terms, early warning is the provision of timely and effective information allowing individuals exposed to hazard to take action in order to avoid or reduce the damage and the loss of life.

From a general point of view, there are four crucial moments in landslide early warning, such as: precursor forecasting, precursor occurrence, event initiation and impact on people and goods (Picarelli et al., 2007).

Early warning systems prove quite efficient when the time between the detection of first reliable precursors and initiation of the event or between the initiation of the event and the impact on exposed goods is sufficiently long to take action such as evacuation or protection of structures and infrastructures.

When the time between the event and its impact is extremely short, adoption of early warning procedures must be based on precursor measurements. This is the case of rapid landslides, as the time elapsing between the onset of slope failure and its impact on exposed goods is typically in the order of tens of seconds.

When the time between precursor occurrence and event initiation is also short the forecasting of the precursor becomes indispensable. This is the case of shallow landslides when the time between the precursor and the event is in the order of tens of minutes.

Rainfall is largely adopted as a precursor for early warning of landslides, owing to the large prevalence of landslides induced by rainfalls.

The identification of the precursor is the most important issue in landslide forecasting, so the relationship between landslide triggering and intensity or duration of rainfall has been largely investigated to identify threshold values.

Based on the collection of data on landslides and related triggering rainfall, thresholds, often based on a combination of rainfall intensity and duration, have been obtained for several regions, as Hong Kong (Finlay et al., 1997), California (Campbell, 1975; Wilson & Wieczorek, 1995), New Zealand (Glade et al., 2000) etc.

In some of these countries, early warning systems have been conceived to prevent disasters. In fact, these thresholds, in combination with rainfall forecasting and real-time rainfall monitoring, can lead to operational landslide warning systems. As an example, in 1977, the Hong Kong Geotechnical Engineering Office established a Landslip Warning System, which has been continuously updated and improved over the years (Chan et al., 2003). Similar systems have been elaborated to prevent the consequences of rainfall-induced debris-flows in the S. Francisco Bay (Keefer et al., 1987) and in Nagasaki (Yano & Senoo, 1985). D'Orsi et al. (1997) report the Rio-Watch, an alert system based on a network of 30 telemetered rainfall gauges and weather radars covering the city of Rio de Janeiro, which issued 42 warnings between 1998 and 2003. Similar systems have been set up in the State of Oregon (Mills, 2002), in the UK (Cole & Davis, 2002) and in the area between Seattle and Everett, Washington (Baum et al., 2005). Even though a true early warning system has not been set up, in the landslide prone area around Wollongong, Australia, a monitoring system is active and provides continuous information through the WEB with regard to the slope stability conditions (Flentje et al., 2005).

Previous considerations show that today prediction of rainfall-induced landslides is mostly carried out through the so-called hydrological models (Fukuoka, 1980; Mitchue, 1985; Cascini & Versace, 1988), which are based on historical data regarding landslides and related triggering rainfall and do not require field instrumentations and measurements. *Hydrological* models are distinct from *physically-based* models, which attempt to reproduce the physical behaviour of the processes involved at hillslope scale. These models are complex and need many field investigations and surveys.

In Italy, Sirangelo and Versace (1992) proposed the general hydrological model FLaIR (*F*orecasting of *L*andslides *I*nduced by *R*ainfall), which has been recently extended to mudflows, in pyroclastic soils, occurred in Sarno area on May 1998 (Versace et al., 1998, 2003, 2007).

FLaIR consists of two modules: the *R-L module* (*R*ainfall–*L*andslide) correlates precipitation and landslide occurrence, in order to determine a *mobility function* $Y(t)$, which, at any time, depends on the amount of infiltrated water. This module enables model calibration and permits the reproduction of historical movements (Fig. 20.4).

The second module, *RF* (*R*ainfall *F*orecasting), provides a probabilistic evaluation of rainfall events through a stochastic modelling or meteorological nowcasting. It is used to identify hazard conditions for landslide occurrence suitably in advance.

Using both modules, the model enables a probabilistic evaluation of future landslide occurrence.

In the RL module the mobility function $Y(t)$ is associated with the probability $P[E_t]$ of landslide occurrence at the time t, by the relation:

$$P[E_t] = g[Y(t)] \tag{20.1}$$

where $0 \leq g(.) \leq 1$.

Among various relationships a simple threshold scheme can be assumed: the event is certain if the mobility function $Y(t)$ exceeds the threshold value Y_{cr} and impossible if this value is not exceeded. The mobility function can be linked to the antecedent rainfall $P(.)$ through the expression:

$$Y(t) = \int_0^t \psi(t-u)P(u)du \tag{20.2}$$

where $\psi(.)$ is a filter function which plays a critical role, because the choice of this function can model a wide range of situations.

The value $Y_\tau(t)$ that the mobility function will assume at time t, calculated at the time $\tau(\tau < t)$, may be written splitting the convolution integral (2) into two parts:

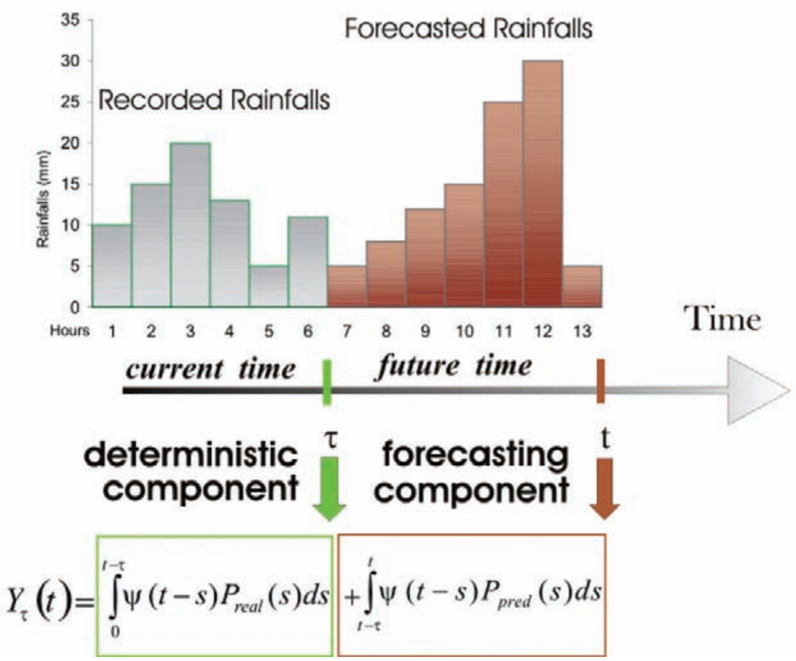

Fig. 20.4 Synthetic scheme of the mobility function components

$$Y_\tau(t) = \int_0^{t-\tau} \psi(t-u)P_{real}(u)du + \int_{t-\tau}^{t} \psi(t-u)P_{pred}(u)du \tag{20.3}$$

the first one, on the right-hand side, can be considered as the deterministic component and is calculated on the basis of observed rainfall P_{real} recorded rainfall up to time τ.

The second one is the stochastic component, associated to the predicted rainfalls P_{pred} which should fall in the interval $[\tau, t]$ and that can be estimated through rainfall forecasting models.

As a consequence, the model may be usefully employed to forecast the hazard of rapid landslides induced by rainfall, allowing the activation of the necessary procedures for civil protection.

The strategy of the civil protection agency with respect to landslide events is usually based on three warning levels: "attention" (or "advice"), with instrumental real-time monitoring and real time simulation model running; "alert" (or "watch"), involving civil protection agencies and field direct control; "alarm" (or "warning"), involving population to be evacuated. Using FLaIR, a characteristic mobility function ratio $\chi = Y/Y_{cr}$ can be associated with each warning level (Fig. 20.5).

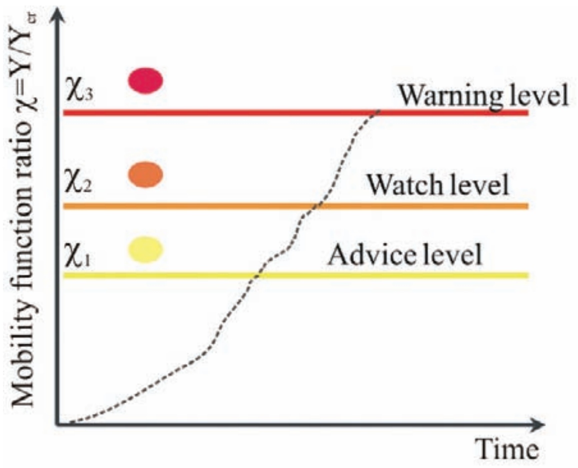

Fig. 20.5 Real time control of the mobility function ratio for evaluating the different critical situations

20.7 Landslide Monitoring, Prediction and Early Warning in Banjarnegara, Indonesia

Teuku Faisal Fathani, Dwikorita Karnawati (Gadjah Mada University, Indonesia), Kyoji Sassa (ICL), Hiroshi Fukuoka (Kyoto University, Japan), Kiyoshi Honda (Asian Institute of Technology, Thailand)

Abstract Landslide is one of most major disasters in Indonesia due to the susceptibility of the region and socio-economical conditions of the country. Since 2007, a community-based early warning system has been introduced in a pilot area at Banjarnegara, Indonesia. Simple extensometers and automatic raingauge have been installed for landslide monitoring and prediction with the participation of local community. Furthermore the Asian Joint Research Project for Early Warning of Landslides consisting of International Consortium of Landslide (ICL), Gadjah Mada University (GMU), Disaster Prevention Research Institute of Kyoto University (DPRI/KU) and Asian Institute of Technology (AIT) have conducted a preliminary investigation and established a real-time monitoring and early warning system at that pilot area. The outdoor unit of fieldserver gathers the data from multiple sensors (two long-span extensometers, raingauge, IP camera and water pressure sensor), whereas indoor processing unit will store data on the monitor, and send the data to AIT server through GPRS modem to be displayed in a webserver.

20.7.1 *Background of Landslide Early Warning in Indonesia*

As the dynamic volcanic-archipelagoes, more than 60% of Indonesian region are covered by the mountainous and hilly areas of weathered volcanic rocks, which are intersected by faults and rock joints. These geological conditions give rise to the high landslide susceptibility of the region. Moreover, the high rain precipitation which can exceed 2000–3000 mm per year, frequent earthquake vibrations as well as the extensive landuse changing and deforestation cause the occurrence of landslides frequently increase recently. Since the last 7 years, more than 36 landslide disasters occurred and result in 1226 people died or missing. Urgently, some efforts should be done to avoid or reduce the risk of landslides. Unfortunately, most landslide susceptible areas have very fertile soils and very good quality and quantity of water. This makes the susceptible areas are densely populated, and it create serious inducement to slope instability. Despite an effort to establish slope protection zone, which is restricted for any development and settlement, the relocation program is not easy to be carried out due to socio-economical constrains. Therefore, landslide monitoring, prediction and early warning system are urgently required to guarantee the safety of community living in such area.

20.7.2 Geological Condition of the Study Area

A pilot area for landslide monitoring, prediction and early warning program has been established in Banjarnegara Regency, Central Java Province, since year 2007. Based on the site investigation, it is clarified that not only the rain intensity but also the morphology and geological conditions of study area significantly control the occurrence of landslides. The unstable zone in the study area is situated at lower slope of mountains with the slope inclination of 20–60° (Fig. 20.6). The moving materials consist of colluvial deposits of silty clay overlying the inclined impermeable layer of clay, which is situated at the lower part of the andesitic breccias mountain. The clay layers are inclined at the same direction of the slope (i.e. 85°) and this becomes the sliding failure for the above colluvial soils. The moving zone is saturated at most of the rainy season due to the lower position of the zone comparing to the surrounding mountainous slopes. The existence of impermeable clay layer underneath the colluvial soils creates the saturation condition within colluvial soil gradually increased and maintained during the rainy season, until then the rise of pore water pressure within this soil induces the movement. Therefore, monitoring of the pore water pressure (groundwater table) in response to the rain infiltration should be the main concern in establishing early warning for the slope movement.

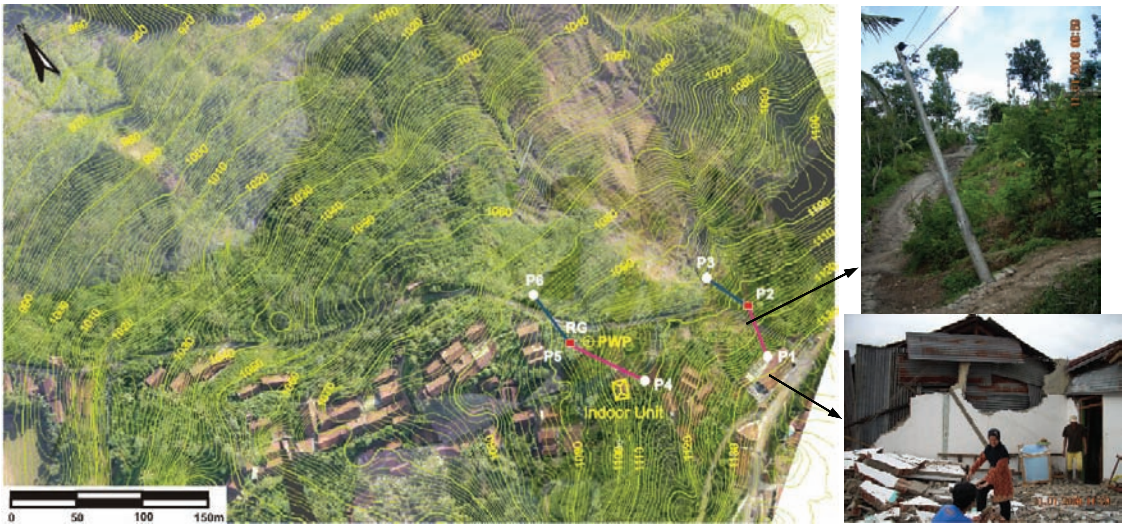

Fig. 20.6 Aerial photo, topography map and position of real-time monitoring equipment. Landslide fatalities are shown on the right

20.7.3 Community-Based Early Warning System

At the beginning of year 2007, Gadjah Mada University has developed simple and low-cost equipment for landslide monitoring and early warning, where the local community in remote areas can easily operate and maintain the equipment based on their own capability. As the initiation of quantitative investigation, two types of simple extensometers and automatic raingauge were installed at a pilot area in Banjarnegara. The first type of extensometer is a handmade manual reading extensometer. Another type is the automatic extensometer, where the relative movement between two points is mechanically enlarged by 5 times and recorded on a paper continually. Both types of extensometers are connected to the siren system in order to directly warn the local community for taking necessary actions in dealing with landslide disaster. Furthermore, a simple modified raingauge has also developed with hourly rainfall intensity recorded on a paper continually. This raingauge is also connected to the siren system to warn the community if the precipitation reaches a certain value. During the installment, five local operators have been trained on how to install and operate this simple equipment (Fathani & Karnawati, 2007).

20.7.4 Real-Time Monitoring and Early Warning System

In line with the installation of simple monitoring equipment, on September 2007, the Asian Joint Research Project for Early Warning of Landslides has conducted a field survey to support the installation of real-time landslide monitoring equipment. This system presents the results of real-time measurement by using long span extensometers, raingauge, pore pressure sensor, and monitoring scene by IP camera. The real-time monitoring equipment consists of outdoor unit and indoor unit. Outdoor unit is fixed on a center pole consists of fieldserver, two extensometers, raingauge, IP camera and water pressure sensor (Fig. 20.7). Fieldserver is a sensing device with real-time online data display system which gathers the data from multiple sensors and shows them in a webserver. The extensometer placed at two positions connected by a pulley and a super invar wire which can measure both extension (+) and compression (–). Indoor unit has two crucial components i.e. processing unit and GPRS modem. Indoor unit collects the data, then process and store data on the monitor, and send the data to AIT server every one hour. This unit also implements early warning that can be adjusted depending on the site condition.

Figure 20.6 shows the aerial photo and topography map of the landslide area mapped by the Balloon Photogrammetry System. This system combines the balloon aerial photography and digital photogrammetry for low-altitude aerial mapping. The balloon carries out a digital camera up to 400 m above the ground level and takes aerial photographs in appropriate viewing angle. The digital photogrammetry processes the photo-restitution to produce 3D model from the multi-view aerial photograph (Rokhmana, 2007).

The position of long-span extensometers poles (P1 to P6), raingauge, pore water pressure sensor and indoor unit are shown in Figs. 20.6 and 20.7. The installation of three poles (P1 to P3) were conducted on December 15th, 2007. The installation process had faced some problems since the slide occurring also on day of the system set up. As shown in Fig. 20.8, starting from December 23rd, 2007, the extensometer has been saturated (up to 660–920 mm of displacement), therefore it cannot measure the movement when the landslide occurred on December 30th, 2007, which destroyed the center pole (P2), buried the lowest pole (P3) and also attacked several existing houses, farm land and district road.

On January 19th, 2008, the monitoring system has been reinstalled at a new location about 150 m from the previous destroyed place (Fig. 20.6). Three new poles (P4 to P6) were erected with two long-span extensometers, raingauge and IP camera connected to center pole (P5). Pore water pressure sensor is placed inside a well near P5, whereas the indoor unit located in a house belongs to a volunteer resident near P4. The result of measurement of two extensometers, daily

Fig. 20.7 Outdoor unit of real-time monitoring equipment

rainfall and pore water pressure fluctuation are shown in Fig. 20.8 The accumulated movement of extensometer starting from January 19th until May 31st 2008 reaches of about 30 and 220 for Extensometer P4–P5 and P5–P6, respectively. Meanwhile the maximum rate of rainfall could reach 200–360 mm/day. It can be seen that the extensometer movements on March 7th and April 13th, 2008 were strongly related to the rainfall occurrence.

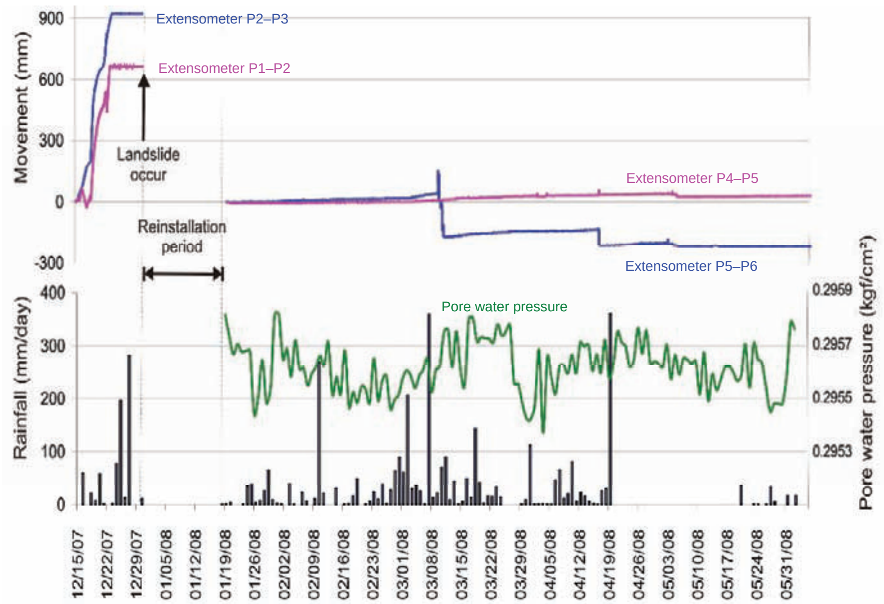

Fig. 20.8 The results of measurement by extensometers, raingauge and pore water pressure sensor

20.7.5 Conclusions

Some lesson learned can be derived from this program that the warning system should be based on a real-time telemetric system with the involvement of community participation. Therefore, both technical skill and communication skill are the main requirements to achieve the success of early warning system program. The system should include some technical aspect such as the geological surveys and site selection, development of equipment design which is simple (low cost) but effective, determination of early warning levels, installment and operation/maintenance at the field site, as well as include the social aspect such as social mapping and evaluation, public consultation and dissemination of program, community empowerment (including the technical training and evacuation drill) for landslide hazard preparedness and operational system of the early warning. Moreover, the communication with all stake-holders such as local, regional and national authorities, local leaders, local youth communities, and local non government organization should be established and maintained. The role of scientist or researcher is more like to be the motivator and facilitator, instead of the instructor or manager of program.

20.8 Early Warning of Landslides Based on Landslide Indoor Experiments

Katsumi Hattori, Hitomi Kohno, Yasunari Tojo (Graduate School of Science, Chiba University, Japan), Tomomi Terajima (Disaster Prevention Research Institute, Kyoto University, Japan), Hirotaka Ochiai (Forestry Agency of Japan)

Abstract An experiment to induce a fluidized landslide by artificial rainfall has been conducted on an indoor slope. The experimental slope is 10 m long, 1 m wide, and the slope gradients are 10° for the lower and 32° for the upper slope. A landslide initiated 65440 s (1h49m40 s) after the start of sprinkling at a precipitation intensity of 80 mm/h. During this experiment, pore pressure, self-potential, and soil displacement have been measured. The results suggest the relationship among motion of subsurface water, soil displacement, and electrical potential differences. Self-potential method seems to have capability for early warning system for landslides.

20.8.1 Introduction

Rainfall-induced landslides often cause catastrophic disasters. In order to mitigate the disasters, monitoring and forecasting of the landslides are important. There are hydraulic and geotechnical knowledge prior to a landslide based on the indoor and outdoor experiments (Ochiai et al., 2004). They are based on pore pressure and soil displacement using gaugemeters and CCD video cameras, respectively. The obtained facts are as follows; (1) development of the saturated area under the surface, (2) direction of the filtration of water changes from vertical to lateral to the slope, and (3) beginning of the apparent soil displacement about a few tens minutes before the catastrophic slide. On the other hand, the geophysical exploration method is one of powerful tools for subsurface monitoring such as electrical resistivity. The electrical resistivity tomography approach shows the slip surface very precisely and continuous measurements of resistivity could be helpful to identify the water condition under subsurface (Perrone et al., 2004) (Lapenna et al., 2005). Self-potential method is also applicable to monitor underground fluid motion based on the electro kinetic effect (Ishido & Mizutani, 1981). Laboratory experiments and geothermal application show the high capability to detect subsurface water motion (Rizzo et al., 2004), (Sasai, 2008), (Zlotnicki & Nishida, 2003). Self-potential method is passive measurement and simple in comparison with electrical resistivity tomography. In this paper, self-potential approach is conducted to develop an early warning system for landslides. The results of a laboratory experiment under precipitation control show the capability to monitor the underground water condition using self-potential method.

20.8.2 The Laboratory Experiment

The laboratory experiment of landslide under the precipitation control has been carried out to investigate electrical properties and understand the physical process associated with landslides. The background of this experiment is as follows. Based on the previous hydraulic knowledge, (1) the rain water penetrates vertically at the initial stage because of the unsaturated condition. (2) As a saturated area is developed, the water flow pattern turns to the lateral to the slope. (3) From geotechnical point of view, significant soil displacement starts about a few tens minutes before the main collapse. Then, a landslide takes place. The purpose of the experiment is to investigate whether electrical potential changes show those of hydraulic and geotechnical conditions.

The overview of the laboratory experiment system is shown in Fig. 20.9. The angle of an upper slope was 32° and that of a lower slope was 10°. The length and width of a slope are 9 m and 1 m, respectively. The soil density in the slope was almost uniform and the thickness was 70 cm. The soil is weathered granite and averaged grain radius is 0.39 mm. There is a sprinkler for an artificial precipitation. The intensity of the precipitation was controlled by 80 mm/h. 40 mm rain (with 80 mm/h) was precipitated two days before the experiment. It was found that water came out of from the slope very slowly. It means that groundwater system has been created before the experiment. It seems rather natural situation. A rubber sheet is used for insulation.

Pore pressure, self-potential, and soil displacement measurements have been performed. As for self-potential measurements, electrodes (Pb-$PbCl_2$), pasted the bentonite to reduce a contact resistivity, have been installed with intersensor distance of one meter in a depth of 20 cm and 50 cm and the reference electrode has been installed in the depth of 50 cm at the top of the slope. For pore pressure measurements, gauge meters have been set up in a depth 10 cm, 40 cm and 65 cm with one meter spacing. Here, electrodes and pore pressure meters were installed alternately. The electrodes and gauge meters have been connected to the 16 bit AD converter (National Instrument SCXI-1120) and fed to the data acquisition PC. The sampling rate is 100 Hz. Soil displacement has been recorded by CCD video cameras with motion of markers. The total amount of water flowed out from the slope has also been measured.

Fig. 20.9 Indoor experiment system of an artificial slope under precipitation control

The landslide occurred at the upper slope 65440 s (about 110 min) later from the beginning of the precipitation. Thus, the total amount of the rain fall was about 145 mm.

20.8.3 Observed Data

Figure 20.10(a,b) illustrate the 2D variation of hydraulic and electrical properties, respectively. The sequence of figure corresponds to the time progress after the precipitation start. The time stamp is given beside the panel. In Fig. 20.10(a), the color and contour indicate the pore pressure and hydraulic head. In Fig. 20.10(b), the color and contour show the potential differences the electric field. From Fig. 20.10(a), we found that filtration of precipitation water was vertical at the initial stage. Saturated area was developing and extending 50 min before the collapse. 20 min before the collapse, we can see the lateral flow of the underground water. 1 s before the collapse, the lateral flow is significant at the lower part of the upper slope. From Fig. 20.10(b), it is almost uniform at the beginning of experiment. The saturated area seems to be charged in negative. The most interest point is the appearance of a large electric field around the slip surface area a few tens minutes before the collapse.

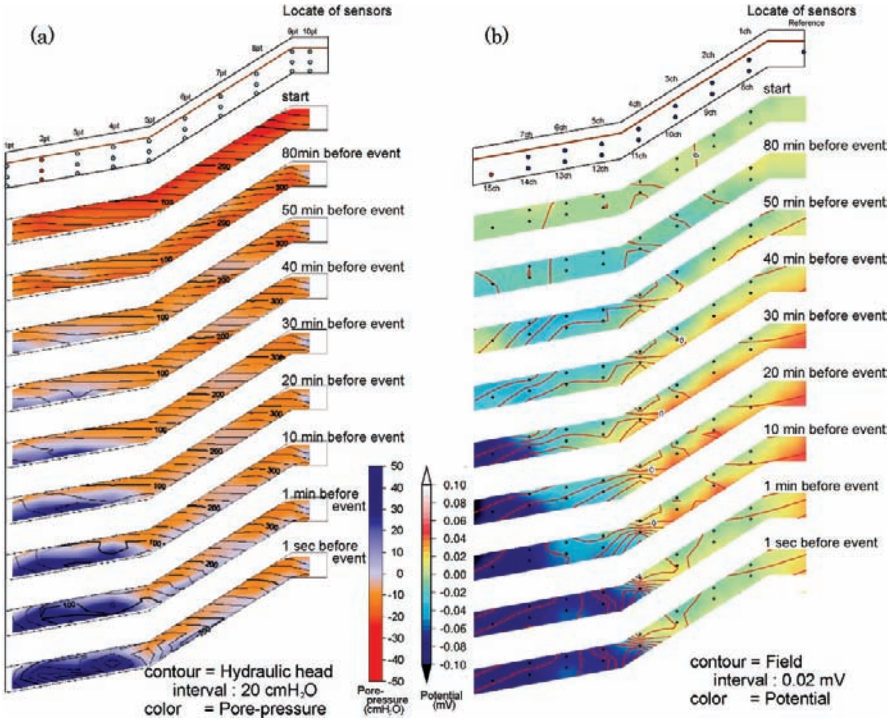

Fig. 20.10 2 dimensional maps of pore pressure and self-potential with time. (**a**) pore pressure and (**b**) electrical potential difference

A typical example of observed hydraulic and self-potential data is shown in Fig. 20.11. The position of the corresponding sensor is described at the top panel in the Fig. 20.10(a) (2 pt.) and (b) (15 ch). The curve of potential shows an interesting behavior. When the wetting front arrives at the position of electrode, the potential indicates the local minimum. While the area of the electrode turns to be saturated, the value shows the local maximum and a dramatic decrease. Furthermore, 30 min before the main slide, transient signals cam be seen only in self-potential changes. There is a remarkable step-like change around 90 min and rectangular changes around 105 min. These changes observed only below the upper boundary of the slipped body. The detected electric field is almost uniform. For the variation of pore pressure, transient signals such as impulsive and step-like changes are not described. The soil displacement data shows that the dislocation of the soil become apparent a few tens minutes before the collapse, so that there is a possibility that these transient signals are associated with dislocation of the soil.

20.8.4 Conclusion

Indoor laboratory experiment with simultaneous measurement of hydraulic, geotechnical, and electromagnetic approaches has been performed to investigate the rain-fall induced landslide process. It is found that self-potential variation seems to show the good relationship between hydrodynamics and electromagnetics and geotechnology and elecromagnetics. It means that there is a possibility to monitor the underground water condition or establish an early warning system of landslides with use of self-potential method.

Further analysis and experiments in both laboratory and in-situ field will be required to evaluate the electric phenomena with the hydrological and geotechnical changes. Such as pore pressure and the water flow out and geotechnical parameters such as the soil displacement.

Acknowledgment This work was partly supported by the JSPS Grants-in-Aid for Scientific Research #19403002, Research Foundation for the Electrotechnology of Chubu (REFEC), Chubu Electric Power Co. Inc., and NiCT R&D promotion scheme funding international joint research.

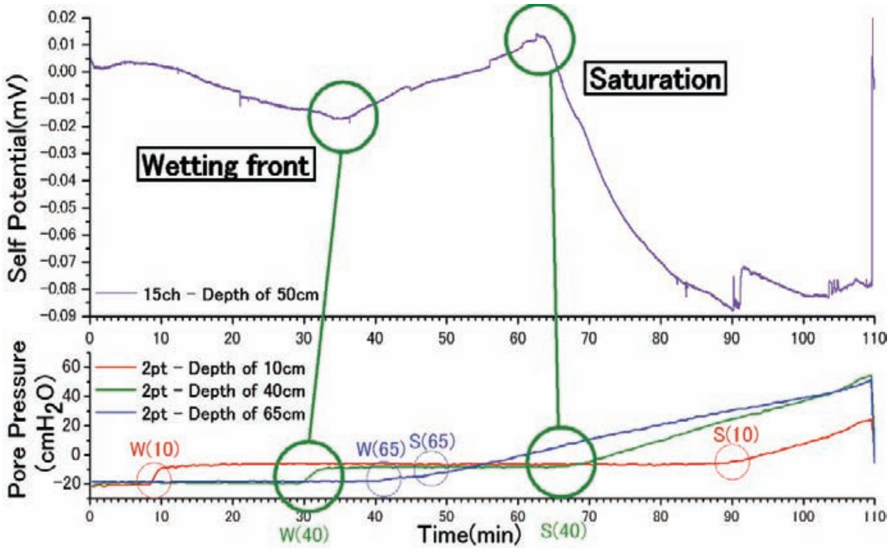

Fig. 20.11 A typical example of pore pressure and self-potential variation during artificial rainfall experiment. Time of the turning values of self-potential corresponds to the rise-times of pore pressure (wetting front and saturation)

20.9 A Real Time Debris Flow Warning System for the North Shore Mountains of Vancouver

Matthias Jakob, (BGC Engineering Inc., Canada)

Abstract The District of North Vancouver spans 160 km^2 at the foot of the North Shore Mountains that form the southernmost extension of the Coast Mountains. Numerous creeks draining the North Shore Mountains terminate as fans that have formed predominantly through debris flows. These fans have developed over the Holocene period, and those along the ocean inlets have become highly desirable properties due to low gradients, good drainage conditions and scenic locations. Between 1995 and 2003 a series of consultants reports have been released that quantified debris flow hazards and risk as well as propose engineering measures to reduce risk. Engineering measures on the highest priority creeks exceed the financial constraints of the District and thus a different risk reduction measure was chosen to compliment a long term risk reduction program in the form of a debris flow warning system. The Greater Vancouver Regional District has maintained records for some 15 years on the occurrence of landslides on the North Shore Mountains and some 32 storms were identified that had produced debris flows. An additional 32 storms that had not produced debris flows were selected based on rainfall amounts and intensity similar to those that had resulted in debris flows. A discriminant function analysis was conducted on all 64 storms for a large variety of rainfall antecedent and intensity variables to extract the significant discriminatory variables. The selected variables were the 4 week antecedent rainfall as well as the 2 day antecedent rainfall and the 48 h rainfall intensity. This function was able to correctly classify 80% of all cases. A high resolution calibrated weather forecast model designed and operated by the Geophysical Disaster Computational Fluid Dynamics Centre at the University of British Columbia is used to predict 48 h rainfall in one hour time steps, while the antecedent variables are calculated in real time for every approaching storm. The system is currently undergoing a testing phase and will be made operational in October of 2008.

20.9.1 Background

Debris flows are a common occurrence on the coastal mountains of British Columbia. They

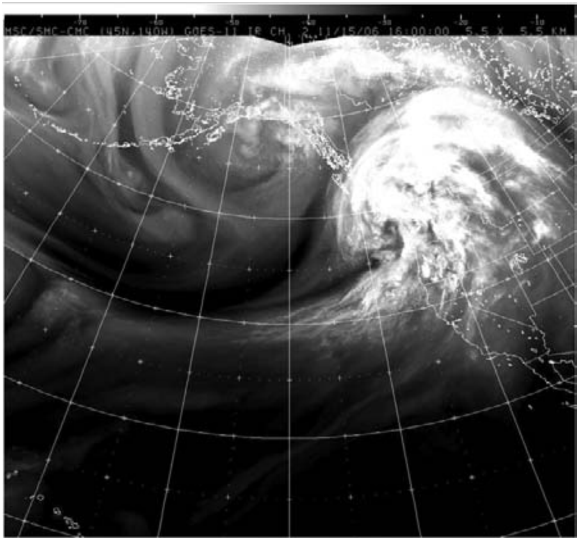

Fig. 20.12 Typical cyclone during late fall that can trigger debris flows along the North Shore Mountains (November 15, 2006)

occur primarily between October and January when numerous Pacific cyclones cross the coast with total rainfall amounts ranging between 40 and 150 mm and rainfall intensities up to 20 mm/h (Fig. 20.12). Debris flows are especially prevalent in areas logged over the past 15 years due to a pronounced loss in root strength and from poorly constructed logging roads. At the interface with urban development debris flows have impacted homes and other facilities. While the damages from debris flows on the North Shore Mountains pale in comparison with those in other countries, particularly the subtropical and tropical belts, the damage or potential damage affects a very affluent and increasingly risk adverse society. This fact has led to an active landslide risk management program with components of active engineering measures and warning systems.

20.9.2 Method

A large number of rainfall thresholds have been proposed for shallow landslides worldwide. These have recently been summarized by Guzzetti et al. (2008). Most are based on relations between rainfall intensity and duration and are plotted as envelopes below which shallow landsliding is unlikely and above which landsliding is possible. In the case of the North Shore Mountains, those thresholds are very low and application of an intensity-duration threshold for warning purposes would lead to tens of false warnings per year thus undermining the system's credibility (Fig. 20.13).

Previous work by Jakob and Weatherly (2003) has recognized that antecedent moisture conditions are crucial for explaining landslide occurrence and that the 4-week antecedent cumulative rainfall is the most significant variable in explaining the regional occurrence of shallow landsliding. Similarly to Jakob and Weatherly's study in 2003, antecedent and intensity data were gathered for all storms since 1990 that have caused shallow landslides in undisturbed (no logging or road building) terrain. An additional 32 storms were selected from the database over the same period with total rainfall amounts above 40 mm but for which no landslide records exist. Since the Greater Vancouver Regional District monitors the watersheds of the North Shore Mountains by helicopter after significant storms, it is believed that the assumption of no-landslides for those storms is reasonably correct. A forward stepwise discriminant function analysis was conducted on all 64 cases with the goal of (a) extracting the most significant variable to separate

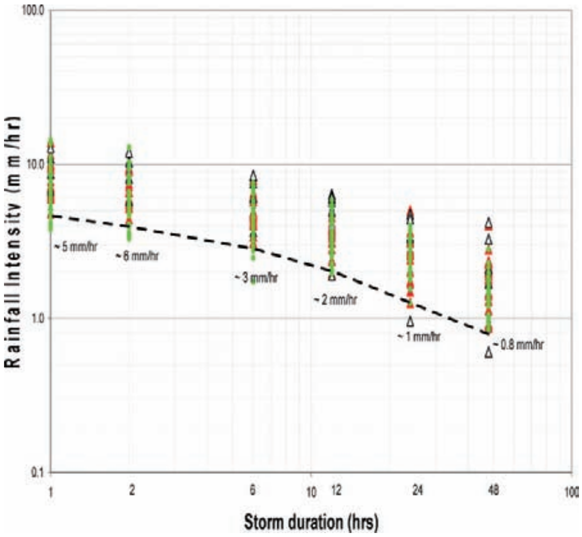

Fig. 20.13 Landslide Initiation Threshold for the North Shore Mountains

landslide from non-landslide initiating storms and (b) to create a discriminant function that allows calculation of the relative likelihood that a storm belongs to either group. The stepwise discriminant analysis identified three significant variables and the resulting function is shown in Eqs. (20.4) and (20.5).

$$\mathbf{LS} = -6.43 + 0.05A_{4\,W}; +0.28\mathrm{A}_{1\mathrm{d}} - 0.033\mathrm{A}_{5\mathrm{d}} \tag{20.4}$$

$$\mathbf{NLS} = -1.63 + 0.021A_{4\,W} + 0.104\mathrm{A}_{1\mathrm{d}} - 0.009\mathrm{A}_{5\mathrm{d}} \tag{20.5}$$

The results from the discriminant function analysis allow the real time calculation of a sliding time window of 4 week and 2 day antecedent rainfall based on rainfall records at the raingauge that was used for the original analysis. The 48-h rainfall intensity is being fed from a weather forecast model issued daily from the Geophysical Disaster Computational Fluid Dynamics Centre at the University of British Columbia. Using this statistic, a total of 75% of all landslide-triggering storms and 87.5% non-landslide triggering storms were correctly classified.

20.9.3 Debris Flow Warning Implementation

Section 20.3 summarized the development of a discriminant function model and classification functions for landslide and non-landslide initiating storms. Two of the variables (4 week and 2 day antecedent) will be measured via the DN25 rain gauge and be monitored real-time throughout the rainy season (between October 1 and April 30). The 48 h rainfall intensity will be produced from UBC's climate model.

Step 1: Backward computation of A_{4wk}, A_{2d}
Starting on October 1, every year, the four week and two day antecedent rainfall will be back-calculated from real-time data of the Berkeley rain gauge operated by BGC Engineering. The Berkeley gauge is not the calibration gauge, which is the DN25 gauge, but a regression analysis of monthly rainfall showed an almost perfect correlation ($r^2 = 0.99$) between the two gauges.

Step 2: Forward-looking prediction of the 48-h rainfall
Once a day, UBC's Geophysical Disaster Computational Fluid Dynamic Centre will forward their 48 h rainfall prediction for the North Shore Mountains. This data will arrive in the form of a meteogram, which will show the cumulative rainfall for pre-specified areas on the North Shore Mountains. At this point, predictions will be made for two rain gauge sites and forward looking calculations will be conducted simultaneously for these sites.

Step 3: Real-time calculation of the Classification Functions and ΔCS.
Both the A_{4wk}, A_{2d} variables and the Rainfall Intensity of 48-h will be entered into the classification functions. CS will be calculated as the difference between the LS and NSL function [$CS = F_{(LS)} - F_{(NLS)}$]. CS will then be plotted for the next 48 h. Implicit in these calculations is the recalculation of A_{4wk}, A_{2d} whenever a storm (as per definition in this report) is considered past. This re-calculation will occur on an hourly basis.

Step 4: Definition of Thresholds
The proposed real-time debris flow warning system will rely on the use of three separate thresholds, which are referred to as "Debris Flow Watch", and "Debris Flow Warning". These terms are defined as follows:

Debris Flow Watch
A debris flow watch will be issued when the CS line crosses negative one (-1) and more rainfall is being predicted in the next 48 h. The significance of a Watch is that hydroclimatic and hydrometeorological conditions are forming that provide conditions favourable for future debris flow occurrence. It is intended to provide information to those who need considerable lead time to prepare for a potential debris flow. It will include a qualitative statement of likelihood that the Advisory or Warning Levels will be exceeded. This qualitative statement will be: It is *likely* or *very likely* that the Warning Level will be reached. If it is unlikely that the

Warning level will be reached, no debris flow watch will be issued.

Debris Flow Warning
A debris flow Advisory will be issued with the CS line crosses the zero (0) line, and more rainfall is forecasted. In this instance, debris flow occurrence is *more likely than not* in the next 48 h and the predictions call for rainfall amounts in excess of 40 mm. This warning level is thus issued when hazardous weather conditions have developed, but the expected time of debris flow occurrence is still at least several hours in the future.

Step 5: Cancellation of Warning Levels
The cancellation of warning levels occurs in reverse order as described above. The debris flow warning is cancelled once the CS line drops below zero and forecasted rainfall for the next 48 h is below 40 mm. The debris flow watch is cancelled once the CS line drops below – 1 and forecasted rainfall for the next 48 h is below 40 mm.

20.9.4 Conclusions

This real time warning system will be the first regional operational debris flow warning system in Canada. It is expected that false warning will occur several times a year, which may eventually lead to some desensitizing of the population to warnings. However, for those individuals who live on creek fans created by debris flows, the debris flow watch and warning may provide sufficient time to leave their homes and stay in a safer place until the warnings have been cancelled. Over the long term, hazard avoidance or engineered mitigation measures are likely the preferred risk management option.

20.10 Study on Early Warning System for Debris Flow and Landslide in the Citarum River Basin, Indonesia

Kaoru Takara, Apip (Disaster Prevention Research Institute, Kyoto University, Japan), Agung Bagiawan (Water Resources Research Institute, Ministry of Public Works, Indonesia)

20.10.1 Introduction

This paper describes a distributed hydrological model of which advantage is to be able to calculate spatio-temporal patterns of rainfall-runoff and sediment transport dynamics in a catchment on a grid-cell basis. Since this model can quantitatively assess the possibility of the occurrence of debris flow and landslide in each grid-cell, it should be useful for early warning of sediment, debris flow and landslide disasters. The sediment runoff model are applied in the Lesti River which has small catchment located in the upper Brantas River basin, Indonesia as the case for study.

The objectives of this research are: (1) to verify the model performance by adding hillslope sediment transport algorithm and considering river channel routing processes to the model; (2) to illustrate how this model can be used for early warning; and (3) to develop a new method of lumping the distributed rainfall-runoff model to obtain a lumped-parameter model for larger river basins that require much computation time.

20.10.2 Physically-Based Distributed Model

The Cell Distributed Rainfall-Runoff Model Version 3 (CDRMV3) as a distributed hydrological model[1)] is used as a base of a distributed sediment transport model. The model includes a stage-discharge, *q*-*h*, relationship for both surface and subsurface flows[2)]:

$$q = \begin{cases} v_m d_m (h/d_m)^{\beta}, & 0 \le h \le d_m \\ v_m d_m + v_a(h - d_m), & d_m \le h \le d_a \\ v_m d_m + v_a(h - d_m) + \alpha(h - d_a)^m, & d_a \le h \\ v_m = k_m i, v_a = k_a i, k_m = k_a/\beta, & \\ \alpha = \sqrt{i}/n & \end{cases} \tag{20.6}$$

where q is discharge per unit width; h is water depth; i is the slope gradient; k_m is the saturated hydraulic conductivity of the capillary soil layer; k_a is the hydraulic conductivity of the non-capillary soil layer; d_m is the depth of the capillary soil layer; d_a is the depths of capillary and non-capillary soil layer; and n is the roughness coefficient based on the land cover classes. The continuity equation takes into account flow rate of each grid-cell or slope as:

$$\frac{\partial h}{\partial t} + \frac{\partial q}{\partial x} = r(t) \tag{20.7}$$

where t and x are time and distance along water flow, respectively; and r is the rainfall intensity.

The Lax-Wendroff finite difference scheme is used to solves the one-dimensional kinematic wave equation with the stage-discharge equation to simulate runoff generation and routing. The simulation area is divided into an orthogonal matrix of square grid-cells (250 m × 250 m).

20.10.3 Coupling of CDRMV3 and Sediment Transport Model

The concept of spatially distributed sediment runoff modeling is shown in Fig. 20.14. A sediment transport algorithm is newly added to the CDRMV3. Runoff generation, soil erosion and deposition are computed for each grid-cell and are routed between grid-cells following water flow direction. The sediment transport algorithm includes multiple sources of sediment transport, which are soil detachment by raindrop (DR) and hydraulic detachment or deposition driven by overland flow (DF). The basic assumption of this model is that the sediment is yielded when overland flow occurs. The eroded sediment is transported by overland flow to river channels.

Soil detachment and transport is handled with the continuity equation representing DR and DF as:

$$\frac{\partial (h_s c)}{\partial t} + \frac{\partial (q_s c)}{\partial x} = e(x,t) \qquad e(x,t) = DR + DF \tag{20.8}$$

where C is the sediment concentration in the overland flow (kg/m^3); h_s is the water depth of overland flow (m); q_s is the discharge of overland flow (m^3/s); and e is the net erosion (kg/m^2/h).

Soil detachment by raindrop is given by an empirical equation in which the rate is proportional to the kinetic energy of rainfall and decreases with increasing h_s. From the observation of rainfall characteristic in the study area[3)] and dampening soil detachment rate by h_s[4)], the empirical equation for DR for the ith grid-cell is expressed as:

$$DR_i = k\ KE e^{-b*h_{si}} = k\ 56.48\ r_i\ e^{-b*h_{si}} \tag{20.9}$$

where k is the soil detachability (kg/J); KE is the total kinetic energy of the net rainfall (J/m^2); and b is an exponent to be tuned.

Following the theoretical work of EUROSEM[4)], the concept of transport capacity is used to determine sediment transport rates in overland flow.

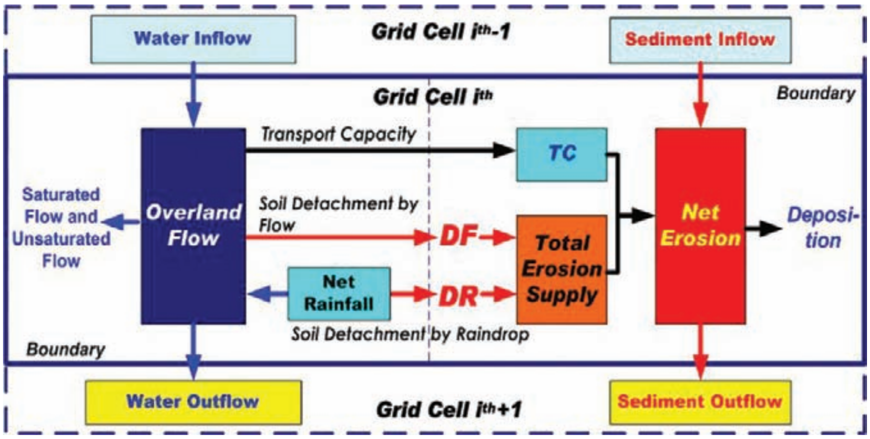

Fig. 20.14 Schematic diagram of the physically based rainfall-sediment-runoff model in the ith grid-cell scale

Sediment transport capacity of overland flow (*TC*) is defined as the maximum value of sediment concentration to transport, which is estimated for each grid-cell. Then for the *ith* grid-cell, *DF* is simulated as a result of overland flow and function of *TC* as follows:

$$DF_i = \alpha(TC_i/1000 - C_i)h_{si} \qquad (20.10)$$

where α is the detachment/deposition efficiency factor. Detachment or deposition by flow is assumed to be proportional to the *TC* deficit. Following the *TC* approach; if actual suspended sediment from upper grid-cells is lower than this capacity, detachment or erosion occurs, otherwise soil deposition excess.

The transportation capacity is calculated based on the Unit Stream Power (USP) theory. The USP theory contributing to *TC* is defined as a product of the overland flow velocity, *v,* and slope, *i,* in the *ith* grid-cell. A relationship between USP and the upper limit to the sediment concentration in the overland flow, C_t (ppm), can be derived[5)] (see Eq. (20.11)). *TC* is the product of C_t as follows:

$$TC = \log C_t = I + J\log((vi - v_{critical}i)/\omega) \qquad (20.11)$$

in which:

$$I = 5.435 - 0.386\log(\omega D_{50}/NU) - 0.457\log(U^*/\omega)$$

$$J = 1.799 - 0.409\log(\omega D_{50}/NU) - 0.314\log(U^*/\omega)$$

$$\omega = \sqrt{\frac{2}{3} + \frac{36}{(\frac{\rho_s}{\rho_w} - 1)g(\frac{D_{50}}{1000})^{2/NU}}} - \sqrt{\frac{36}{(\frac{\rho_s}{\rho_w} - 1)g(\frac{D_{50}}{1000})^{2/NU}}} \qquad (20.12)$$

where *vi* is the unit stream power, m/s (*v* is flow velocity in m/s and *i* is the slope gradient m/m); $v_{critical}i$ is the critical unit stream power ($v_{critical}$ is the critical flow velocity); ω is the sediment fall velocity (m/s) calculated by Rubey's equation; ρ_s is the sediment particle density (kg/m^3); ρ_w is the water density (kg/m^3); *g* is the specific gravity (m/s^2); D_{50} is the median of grain size (mm); and *NU* is the kinematic viscosity of the water (m/s^2). $U^*(= \sqrt{gih_s})$ is the average shear velocity (m/s).

This model does not explicitly separate rill and interrill erosion. Gullying, river bed erosion, river bank erosion and lateral inflow of sediment to river channel are not considered.

20.10.4 Simulation Result

The model parameters to be determined are *n* (m$^{-1/3}$s), k_a (m/s), d_a (m), d_m (m), β, D_{50}(mm), k_s (kg/J), α, *b,* and *F*1 (ratio of rainfall lossed by interception or evapotranspiration processes). The regional sensitivity results show that six parameter *F*1*,* K_a*,* d_m*,* d_a*,* α, and k_s are sensitive and identified as compared to *n, beta,* D_{50}, and *b*.

One of the simulated flood events in calibration time is shown in Fig. 20.15. The predicted runoff and sediment concentration were compared with the observed one. The model is generally successful in representing broad trends in water discharge and sediment concentration, but water discharge tends to overestimated along times of rising limb and falling limb of hydrograph, the range of modeled sediment concentration is somewhat lower and higher than observed. A summary of this flood runoff event is given by the model efficiencies are: 0.854 (R^2: the coefficient of determination) and 0.251 (*RRMSE*). We may be able to recognize that the

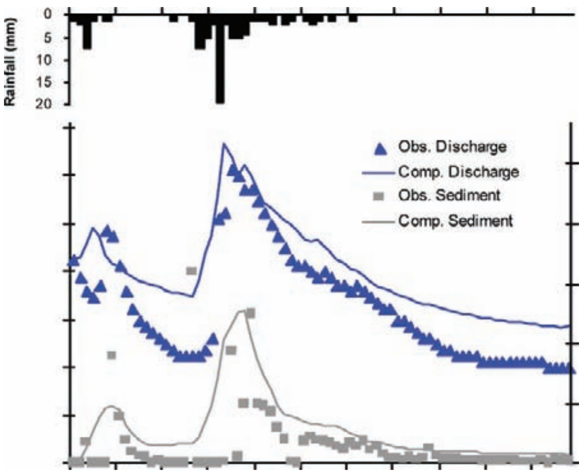

Fig. 20.15 Comparison of predicted sediment runoff with observed data for rainfall event 3–6 October, 2003

model prediction from an example is closer to the observed value.

An extensive sensitivity analysis utilized Monte Carlo simulation framework to produce an ensemble of sediment runoff simulation with respect to prescribed uncertainty in model parameters for each of the selected rainfall events was performed. To determine the uncertainty prediction at each time due to model parameters uncertainty, the predicted outputs were rangked to form a cumulative distribution function of the output variable based on the objective function selected, then the confidence intervals could be determined, which can be selected to represent the model uncertainty.

The calibrated model was applied to the discharge data sets for several rainfall events to test how well the calibrated parameters performed in reproducing an independent data set. These validation runs suggest that the hydrological condition is generally amenable to the hydrologically based on the distributed sediment runoff model under consideration.

20.10.5 Spatial Patterns of Erosion and Deposition

Figure 20.16 shows simulated erosion and deposition areas inside watershed for flood runoff event on 13–15 September 2004. A direct comparison with observed data is difficult since the threshold erosion rate above which these areas are mapped is not known. Figure 20.16 shows that the model was capable of locating the main sediment sources and sink within the Lesti River during this flood event. The model was also able to assign major erosion features. This three- dimensional representation shows that the simulated zones of soil detachment by flow are generally coupled with steep slopes and land use type, while the soil type assumed uniform over the catchment. Zones of deposition were simulated in valley bottoms and river banks.

The sediment transport algorithm for the distributed model includes multiple sources of sediment transport, which are soil detachment by raindrop and hydraulic detachment or deposition driven by overland flow. Estimations of the changes in total runoff and sediment yield with time and space in the catchment scale are required for solution of a number of problems. Design of dams and reservoirs, design of soil conservation, land-use planning, and water quality management are some of the examples. In addition, the processes controlling sediment runoff are complex and interactive. This complexity results in the term "erosion runoff processes" internal catchment area. The difficulty in the observation and measurement of the erosion and sediment transport processes during a runoff and erosion

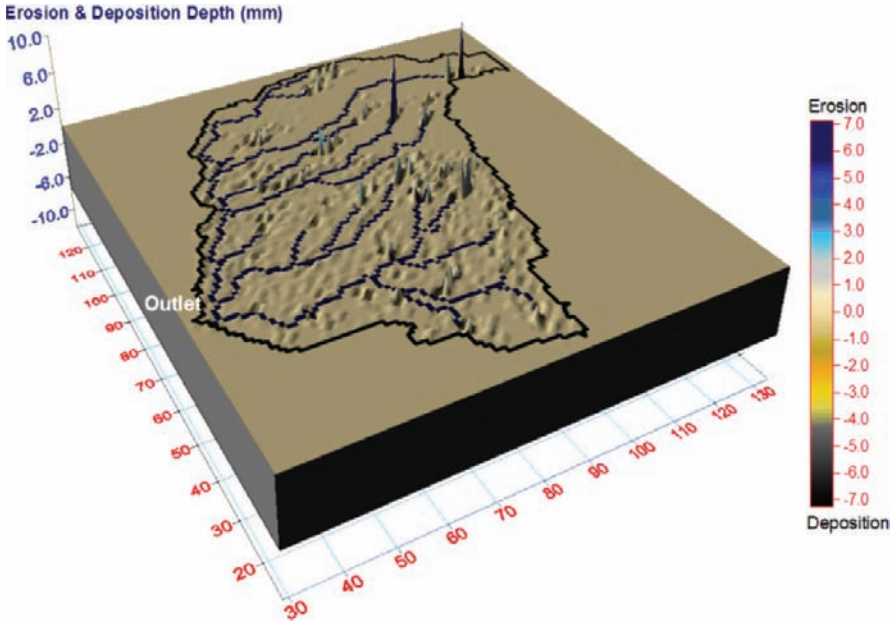

Fig. 20.16 Spatial distribution of erosion and deposition sources inside the catchment after rainfall event September 13–15, 2004

event due to small temporal and spatial scales makes necessary the use of a sediment runoff model for the spatio-temporal predictions of runoff, erosion, and deposition at the internal locations and catchment outlet. The recent developments of one dimensional model from this study are physically-based distributed sediment runoff model and its lumping which produced new lumped sediment runoff model version. Those models are used for the prediction of runoff and sediment transport processes at the catchment scale which facilitates the analysis of total sediment load in river channel and assists in the watershed and water resource management and planning. Application of this model to an Indonesian river basin is demonstrated.

20.11 Conclusion

As demonstrated here, the physically-based distributed rrainfall-runoff model can deal with overland flow, sediment yield, water content and some other elements relating to occurrence of debris flow and landslides at grid-cell scale on hillslopes. This has a potential ability for early warning of rainfall-induced sediment, debris flow and landslide disasters to be applied to small sized catchment, coupled with detail hydro-geo spatial information.

20.12 Other presentations

Development of a ubiquitous-based monitoring system for debris flows in Korea
Byung-Gon Chae (Korea Institute of Geoscience and Mineral Resources:KIGAM)

Development of Community-based Landslide Early Warning System in Indonesia
Dwikorita Karnawati (Department of Geological Engineering, Gadjah Mada University, Indonesia)

Distributed optical fiber sensors for precocious alerting of rainfall-induced flowslides
Luigi Zeni (Dept of Information Engineering, Second University of Naples)

Landslide geotechnical monitoring and mitigation measures in chosen location inside the SOPO Landslide Counteraction Framework Project, the Carpathian Mountains, Poland
Zbigniew Bednarczyk (Opencast Mining Institute, the Poltegor-Institute, Poland)

Preliminary Approach for a Nation-Wide Regional Landslide Early Warning System in South Korea
Dugkeun PARK*, Jeongrim OH*, Youngjin SON*, Minseok LEE (The National Emergency Management Agency (NEMA), Republic of Korea)

Rainfall height stochastic modelling as a support tool for landslides early warning
Roberto Greco (Seconda Università di Napoli, Italy)

Short-term weather forecasting for early warning
Pasquale Schiano, Paola Mercogliano, Gabriella Ceci (The Italian Aerospace Research Center (CIRA) and Euro-Mediterranean Centre for the Climate Change (C.M.C.C.)

Simple and low-cost wireless monitoring units for slope failure.
Taro Uchimura (University of Tokyo, Japan)

The warning criteria analysis of sediment runoff, debris flows, shallow landslides along the mountainous torrent
Tetsuya Kubota, Israel Cantu Silva, Hasnawir (Kyushu University)

References

Baum, R.L., Godt, J.W., Harp, E.L., McKenna, J.P. & McMullen, S.R. (2005). Early warning of landslides for rail traffic between Seattle and Everett, Washington, U.S. A. Proc. Int. Conf. on Landslide Risk Management, Vancouver, 731–740.

Baum, R.L., Savage, W.Z. & Godt, J.W. (2002). TRIGRS – a FORTRAN program for transient rainfall infiltration and grid-based regional slope stability analysis. US Geological Survey Open-File Report 02-0424.

Campbell, R.H. (1975). Soil slips, debris flows and rainstorms in the Santa Monica Mountains and vicinity, southern California. US Geological Survey Professional Paper 851.

Cascini L. & Versace, P. (1988). Relationship between rainfall and landslide in a gneissic cover. Proc. 5th Int Symp. on Landslides, Lausanne.

Chan, R.K.S., Pang, P.L.R. & Pun, W.K. (2003). Recent developments in the Landslip Warning System in Hong Kong. Proc. 14th Southeast Asian Geotechnical Conf.

Cole, K. & Davis, G.M. (2002). Landslide warning and emergency planning systems in West Dorset, England.

Instability: Planning and Management. London, Thomas Telford.

Damiano, E., Olivares, L., Minardo, A., Greco, R., Zeni, L., & Picarelli, L. (2008). Advanced monitoring criteria for precocious alerting of rainfall-induced flowslides. Proc. 10th Int. Symp. on Landslides, Xi'an, China, in press.

D'Orsi, R., d'Ávila, C., Ortigão, J.A.R., Dias, A., Moraes, L. & Santos, M.D. (1997). Rio-Watch: The Rio de Janeiro Landslide Watch System. Proc. 2nd Pan-American Symp. on Landslides, Rio de Janeiro, 1: 21–30.

Fathani, T.F. & Karnawati, D. (2007). Community-based early warning system at Central Java and East Java Province Indonesia, EWS Project – Final Report.

Finlay, P.G., Fell. R. & Maguire, P.K. (1997). The relationship between the probability of landslide occurrence and rainfall. Canadian Geotechnical Journal, 34: 811–824.

Flentje, P.N., Chowdhury, R.N., Tobin, P. & Brizga, V. (2005). Towards real-time landslide risk management in an urban area. Proc. Int. Conf. on Landslide Risk Management, Vancouver, 741–751.

Fukuoka, M. (1980) Landslides associated with rainfalls. Geotechnical Engineering, 11: 1–29.

Gasparini, P., Manfredi. G., & Zschau, J. (2007). Preface. Earthquake Early Warning Systems, Gasparini, P., Manfredi, G. & Zschau, J. eds., Springer, Berlin Heidelberg, V–XI.

Glade, T., Crozier, M. & Smith, P. (2000). Applying probability determination to refine landslide-triggering rainfall thresholds using an empirical Antecedent Daily Rainfall Model. Pure and Applied Geophysics, 157(6–8): 1059–1079.

Guzzetti, F., Peruccacci, S., Rossi, M. & Stark, C.P. (2008). The rainfall intensity-duration control of shallow landslides and debris flows: an update. Landslides 1(5): 3–18.

Hong, Y., Hiura, H., Shiona, K., Sassa, K., & Fukuoka, H. (2004). Quantitative assessment on the influence of heavy rainfall on the crystalline schist landslide by monitoring system – Case study on Zentoku landslide, Japan. Landslides 2(1): 31–41.

Ishido, T. & Mizutani, H. (1981). Experimental and theoretical basis of electrokinetic phenomena to rock-water systems and its applications to geophysics, Journal of Geophysical Research 86: 1763–1775.

Jakob, M. & Weatherly, H. (2003). A hydroclimatic threshold for landslide initiation on the North Shore Mountains of Vancouver, British Columbia. Geomorphology (54): 137–156.

Karnawati, D. & Fathani, T.F. (2008). Mechanism of earthquake induced landslides in Yogyakarta Province Indonesia, The Yogyakarta Earthquake, Star Publishing, California, 8-1–8-8.

Keefer, D.K., Wilson, R.C., Mark, R.K., Brabb, E.E., Brown, III W.M., Ellen, S.D., Harp, E.L., Wieczorek, G.F., Alger, C.S. & Zatkin, R.S. (1987). Real-time landslide warning during heavy rainfall. Science, 238: 921–926.

Lapenna, V., Lorenzo, P., Perrone, A., Piscitelli, S., Sdao, F. & Rizzo, E., (2005). Case history: 2D electrical resistivity imaging of some complex landslides in Lucanian Apennine (southern Italy), Geophysics, 70: B11–B18.

Mandolini, A. & Urciuoli, G. (1999). Previsione dell'evoluzione cinematica dei pendii mediante un procedimento di simulazione statistica. Rivista Italiana di Geotecnica, 33(1): 37–44.

Mills, K.A. (2002). Oregon's debris flow warning system. Geological Society of America Abstracts with Programs, 34(5).

Mitchue, M. (1985). A method for predicting slope failures on cliff and mountain due to heavy rain. Natural Disaster Science, 7(1): 1–12.

Ochiai, H., Okada, Y., Furuya, G., Okura, Y., Matsui, T., Sammori, T., Terajima, T. & Sassa, K. (2004). A fluidized landslid on a natural slope by artificial rainfall. Landslides, 3: 211–219.

Okada, K. (2004). Influence of rainfalls in prior to the earthquake. In: Sassa, K. Landslide disasters triggered by the 2004 Mid-Niigata Prefecture earthquake in Japan. Landslides 2(2): 135–142.

Perrone, A., Iannuzzi, A., Lapenna, V., Lorenzo, P., Piscitelli, S., Rizzo, E., & Sdao, F., (2004). High resolution electrical imaging of the Varco d7Izzo earthflow (southern Italy). **Journal** of **Applied Geophysics,** 56: 17–29.

Picarelli, L., Urciuoli, G. & Russo, C. (2004). The role of groundwater regime on behaviour of clayey slopes. Canadian Geotechnical Journal, 41: 467–484.

Picarelli, L., Versace, P., de Riso, R. & Palmieri, M. (2008). Landslide disaster management in Italy. Proc. 2007 Int. Forum on Landslide Disaster Management, Hong Kong, in press.

Picarelli, L., Versace, P., Olivares, L. & Damiano, E. (2007). Prediction of rainfall induced landslides in unsaturated granular soils for early waning setting up. Proc. 2007 Int. Forum on Landslide Disaster Management, Hong Kong.

Rizzo, E., Suski, B., & Revil, A., (2004). Self-potential signals associated with pumping tests experiments, Journal of Geophysical Research, 109: B10203, doi:10.1029/2004JB003049.

Rokhmana, C.A. (2007). The low cost monitoring system for landslide and volcano with digital photogrammetry, Proc. Joint Convention HAGI-IAGI-IATMI, Bali.

Saito, M. (1965). Forecasting the time of occurrence of slope failure. Proc. 6th Int. Conf. on Soil Mechanics and Foundation Engineering. Montreal, 2: 537–542.

Sasai, Y., (2008). Volcano-ElectroMagnetics in Japan: The 1986 Eruption of Izu-Oshima and the 2000 Caldera Formation of Miyake-jima Volcano, Electromagnetics in Seismic and Volcanic Area edited by Hattori and Telesca, Yubunsha Pub., 69–86.

Sassa, K., Fukuoka, H., Wang, G., Ishikawa, N. (2004). Undrained dynamic-loading ring-shear apparatus and application for landslide dynamics. Landslides 1(1): 7–19.

Senfaute, G., Merrien-Soukatchoff, V. & Morel, J. (2003). Microseismic monitoring applied to prediction of chalk cliffs collapses and contribution of numerical modelling. Proc. Int. Conf. on Fast Slope Movements. Prediction and Prevention for Rik Mitigation, L. Picarelli ed., Napoli, 1: 463–468.

Sirangelo, B. & Versace, P. (1992). Modelli stocastici di precipitazione e soglie pluviometriche di innesco dei movimenti franosi. Proc. XXIII Convegno Nazionale di Idraulica e Costruzioni Idrauliche, Florence, D361–D373.

Versace, P., Capparelli, G. & Picarelli, L. (2007). Landslide investigations and risk mitigation. The Sarno case. Proc. 2007 Int. Forum on Landslide Disaster Management, Hong Kong.

Versace, P., Sirangelo. B., & Capparelli, G. (2003). Forewarning model of landslides triggered by rainfall. Proc. 3rd Int. Conf. on Debris-Flow Hazards Mitigation: Mechanics, Prediction and Assessment, Davos.

Versace, P., Sirangelo, B. & Chirico, G.B. (1998). Analisi idrologica dell'innesco pluviometrico dell'evento di Sarno del 5 maggio 1998. C.N.R.-G.N.D.C.I., Publication n. 1925, Rome.

Wilson, R.C. & Wieczorek, G.F. (1995). Rainfall thresholds for the initiation of debris flows at La Honda, California. Environmental and Engineering Geoscience, 1(1): 11–27.

Zlotnicki, J. & Nisida, Y. (2003). Review of morphological insights of self-potential anomalies on volcano, Surveys in Geophysics., 24: 291–338.

Global Cooperation Field (2): Targeted Landslides: Mechanism and Impacts

Catastrophic Slides and Avalanches

21

Alexander L. Strom

Abstract Various manifestations of large-scale slope processes are described. Though many of them are prehistoric they exemplify the phenomena that have the highest potential to cause a humanitarian, economic or environmental catastrophe. They are described, based on the contributions of the 1st WLF participants.

Keywords Landslide • Rockslide • Rock avalanche • Catastrophe

21.1 Introduction

This chapter is focused on the most hazardous manifestations of the slope processes. Almost any landslide in populated area, especially those of them that move rapidly, could be considered as a catastrophic event. Nevertheless some of them have the highest potential to affect people causing victims, destroying property and infrastructure or changing the environment in such a way that it becomes inadmissible for the society – what is considered world-wide as a humanitarian, economic or environmental catastrophe.

The combination of three main parameters of landslide affects its potential to provide such a catastrophe – size of a landslide (its area or volume), the velocity of landslide motion, and the suddenness of its occurrence. Hereafter large-scale phenomena will be discussed with due regard that they do not exhaust all catastrophic landslide phenomena.

Alexander L. Strom (✉)
Institute of Geospheres Dynamics, Russia

The following topics will be described briefly:

- Megalandslides;
- Palaeo landslides, avalanches and their dating;
- Rockslide dams and their failures;
- Environmental and socio-economic impact of the above natural phenomena.

21.2 Megalandslides

One of the basic parameter that should be considered in the course of landslide hazard assessment is the size of event that characterize either the area affected or the volume of the material involved. Even slow moving, but very large landslide may have catastrophic economic consequences destroying property and infrastructure over a large area. Nothing to say how hazardous they could be when millions and billions tons of rock move downslope rapidly. That is why largest slope failures, dozens of million – billions cubic meters in volume, classified as 'megalandslides', should be considered as potentially most hazardous events.

Most of such large-scale landslides occur in high mountains playing an important role in mountain

K. Sassa, P. Canuti (eds.), *Landslides – Disaster Risk Reduction*,
© Springer-Verlag Berlin Heidelberg 2009

Fig. 21.1 The Kefels rockslide more than 2 km^3 in volume in the Tyrol Alps (Austria). *Red arrow* – direction of rockslide motion; *yellow arrow* – rockslide toe

relief evolution (Korup et al. 2007, Hewitt 2002, 2006, Hewitt et al. 2008). It will be discussed by K. Hewitt in his presentation, which abstract is presented in Sect. 21.7.1. However, several extraordinary exceptions are known when billions of cubic meters of rock slid along gently dipping surfaces in the lowland areas (Philip & Ritz 1999, Pánek et al. 2008). The latter case will be exemplified by landslides in Crimea Mountains described in the presentation of T. Pánek and his colleagues, which is presented in Sect. 21.7.2.

The extremely large landslides are known almost in all mountain regions of the world – in the Alps (Heim 1932, Abele 1974, Poschinger 2002, Brückl et al. 2001) (Figs. 21.1 and 21.2), in the Northern Caucasus (Strom 2004) (Fig. 21.3), in the Tien Shan (Strom & Korup 2006), in Iran (Watson & Wright

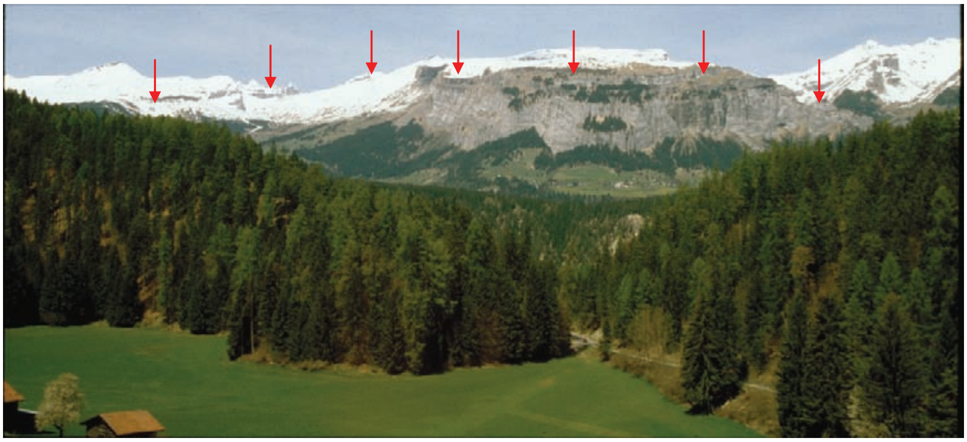

Fig. 21.2 Flimsenshtein – the headscarp of the Flims rockslide 7-12 km^3 in volume in the Hinterrhein River valley (Switzerland). Headscarp is marked by *red arrows*; forested hills at the foreground – rockslide body

Fig. 21.3 The Karivhoh rock avalanche about 2 km^3 in volume at the southern foot of the Rocky Range. The circus-shape rockslide scar is in the left background (marked by *red arrows*). Most of the hill in the foreground is the rock-avalanche deposit

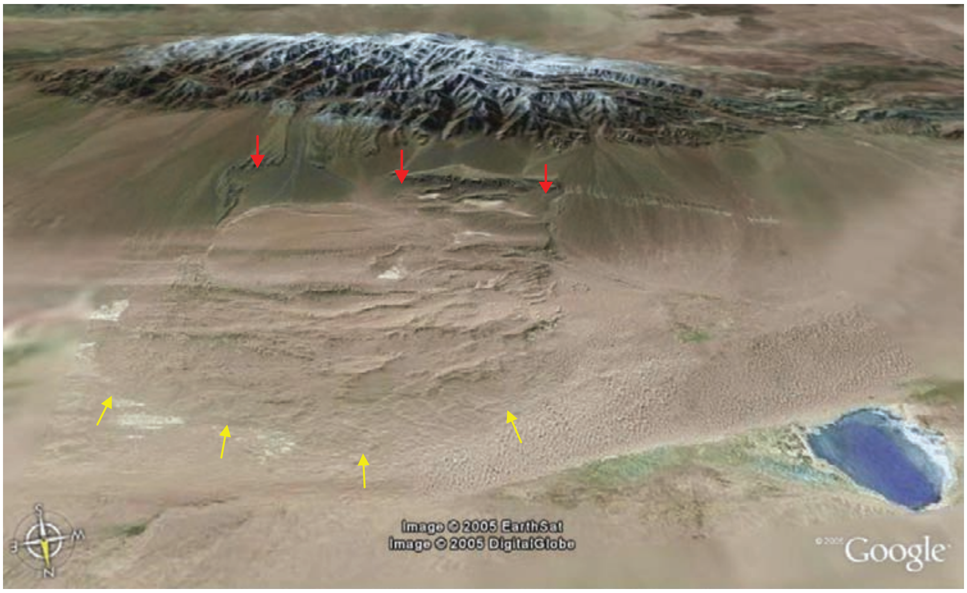

Fig. 21.4 The Google Earth view of the Bogdo landslide in Mongolia – the largest terrestrial landslide about 15 × 20 km in size. *Red arrows* – headscarp; *yellow arrows* – landslide toe

1969, Shoaei & Ghayoumian 1997), in the Mongolian and Gobi Altai (Philip & Ritz 1999, Strom 2006) (Figs. 21.4 and 21.5), in the Himalayas (Weidinger 2006, Korup et al. 2006, Mitchell et al. 2007) and Karakorum (Hewitt 2002, 2006), in the Southern (Hermanns et al. 2001, 2006) and Northern America (Eisbacher 1979), in the New Zealand (Whitehouse 1983, Korup 2002, 2004, McSaveney 2002).

Most of megalandslides are prehistoric, thus compilation of the complete and uniform inventories of landslides, rockslides and rock avalanches that have occurred in the millennia time-scale and their dating is one of the important steps of the comprehensive landslide hazard and risk assessment.

The largest historical non-volcanic megalandslides are the 2.2 km^3 1911 Usoi rockslide in the Pamirs (Scheko & Lekhatinov 1970, Gaziev 1984, Schuster 2002) (Fig. 21.6) and the ~1.5 km^3 1974 Mayunmarca rockslide in Peru (Kojan & Hutchinson 1978). Dozens of smaller but still very large events have occurred during the historical times causing significant loss in life and property.

Several cubic kilometer-order sectoral collapses occurred on the volcanic edifices, the most well known one – the 1980 rockslide on the St. Helens volcano (Voight et al. 1983). However, this specific

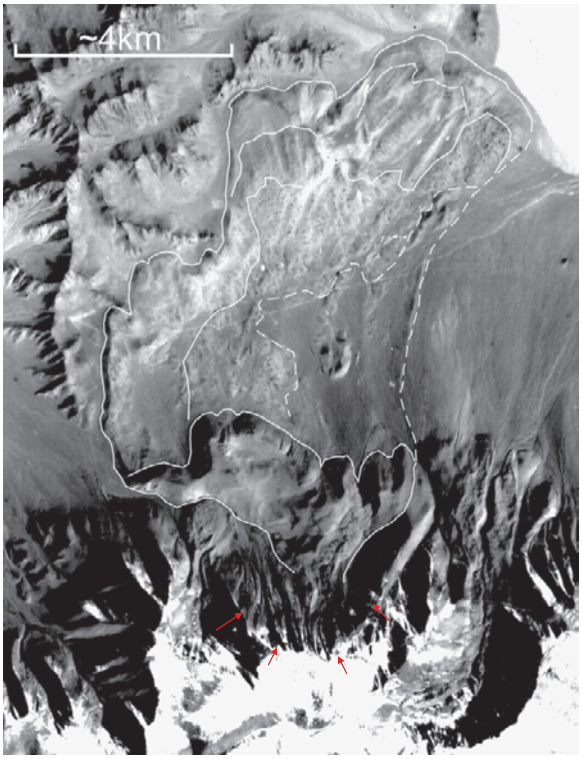

Fig. 21.5 Giant Bayan-Nur rock avalanche in Mongolian Altai. *Red arrows* – headscarp. The outer limit of debris and some internal boundaries are highlighted (after Strom 2006)

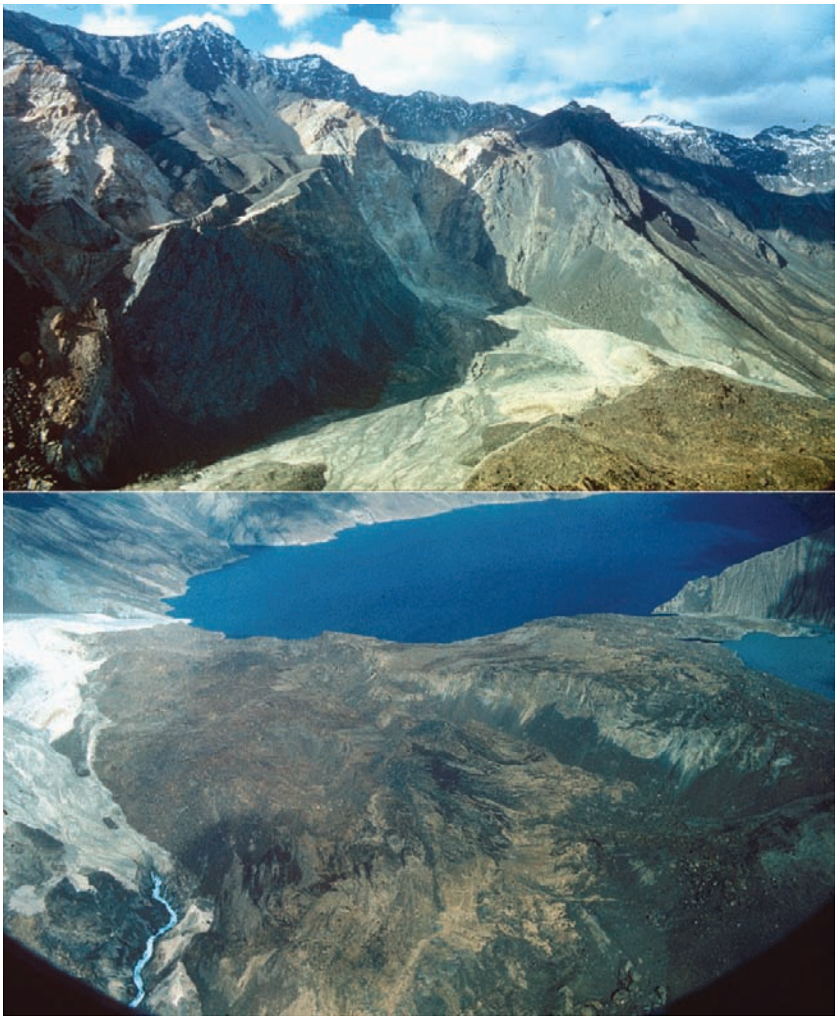

Fig. 21.6 Above - the gigantic, 700-m deep wedge-like scar of the Usoi rockslide; *bellow* – central part of the more than 600-m high blockage

type of large-scale landslides are described in other chapters.

Despite the ability of large-scale landslides to transform into long runout rock avalanches and to affect vast areas extending several kilometers from the foot of the collapsing slope (see Fig. 21.5), their secondary effects due to river valleys damming and dams breach are even most hazardous. Problems related to rockslide dams origin and stability and their failure are discussed hereafter briefly.

Excellent case studies of megalandslides and models of their origin and emplacement mechanisms have been studied and discussed in numerous scientific papers and several special monographs (Heim 1932, Abele 1974, Voight 1978, 1979, Eisbacher & Clague 1984, Evans & DeGrafff 2002, Hungr et al. 2005, Evans et al. 2006).

Considering the First World Landslide Forum as a global cross-cutting information and cooperation platform for both landslide researchers and representatives of the communities suffering from landslides, the impact of the catastrophic megalandslides on the environment and society is the last but not least topic that is discussed in this chapter.

21.3 Palaeo Landslides, Avalanches and Their Dating

The majority of the mountainous regions have a shortage of the written historical records on the hazardous natural phenomena. That is why even in those regions that have been inhabited for centuries and millennia, there is a limited number of large landslides, which origin, age and association with earthquakes and extreme climatic events can be determined based on the human testimonies provided by eyewitnesses. It highlights the importance of complex study of the past, prehistoric landslides, rockslides and rock avalanches, including their mapping, dating and reconstruction of the conditions that could cause or trigger large-scale slope failure.

It could be exemplified by the comprehensive, multidisciplinary study of past rockslides in the Andes region described in the material presented by R. Hermanns and his colleagues (their abstract could be found in Sect. 21.7.3). The extensive dating using various more traditional (^{14}C, lichenometry, dendrochronology) and novel (cosmogenic isotopes) technologies along with geological and geomorphic observations provided data allowing well-grounded estimate of rockslides' triggering by strong earthquakes and by climate change.

The importance of studying paleolandslides not only for landslide hazard and risk assessment but for seismic zoning and hazard assessment as well is highlighted by W. Mitchell, A, Petley and S. Dunning (see Sect. 21.7.4), being exemplified by the ~900 Mm^3 Keylong Serai rock avalanche in the High Himalayas in the North-Western India (Mitchell et al. 2007).

Study of the prehistoric events provides important additional data on the timing, recurrence and scale of slope failures even in the areas where the historical events have been well documented. Such investigations were performed in the Cordillera Blanka in Peru, affected by famous 1962 and 1970 catastrophic rock-ice avalanches (Plafker & Eriksen 1978). Recent findings of V. Vilimek and J. Kilmeš show that much larger events had occurred in the same source zone in the past. Results of these studies described briefly in Sect. 21.7.5 allow site-specific risk assessment for the densely populated area at the feet of the Huaskaran Mountain.

Large-scale past landslides could be identified not only in the tectonically and seismically active high mountains but in the tectonically stable regions as well. Most of them had occurred on the slopes of the large overdeepened valleys that originated in the periods of glaciation and the erosion basis lowering. Many of these landslides are inactive at present, being buried by thick Quaternary sediments. However, at some conditions they could be activated providing significant hazard for various structures. Case studies from the central part of the European Russia are described in the abstract presented by E. Samarin and O. Zerkal (Sect. 21.7.6)

It seems that the most disastrous landslides are those that occur in the coastal zones producing enormous tsunami that can affect ocean shores hundreds and thousands kilometers far from the landslide site, similar to the tsunami caused by strong earthquake. Slopes of active and dormant volcanic islands that rise hundreds meters and kilometers above the sea level and extend several kilometers more underwater are especially hazardous. Though such events are, fortunately, quite rare, study of the gigantic prehistoric phenomena associated with rapid collapse of dozens of cubic kilometers of rock provides data on what could happen if similar phenomenon would occur. This important brunch of catastrophic landslides investigations is demonstrated by P. Wassmer and his colleagues who describe effects caused by the giant prehistoric rockslide on the Tenerife island on the neighbouring Gran Canaria island in their presentation which abstract can be seen in Sect. 7.7).

One more example of the coastal mega-landslide of the Early Holocene age in Japan that could cause a gigantic tsunami is described by S. Hasegava (Sect. 7.8). Thy landslide, in turn, could be caused by a strong earthquake. Such a succession: earthquake – landslide – tsunami demonstrate the 'chain effect' when one catastrophic event (an earthquake) has even more catastrophic primary (a landslide) and even more catastrophic secondary (a tsunami) consequences.

21.4 Rockslide Dams and Their Failures

Landslide river damming, dammed lakes' impoundment (Fig. 21.7) and subsequent dams' breaching resulting in the catastrophic outburst floods seems to be the most disastrous effects of the large-scale slope instabilities (may be excluding the above mentioned gigantic subaerial-submarine landslides). It can be exemplified by the 1786 earthquake triggered Dadu rockslide in China that formed a dam, which subsequent failure killed about 100,000 people

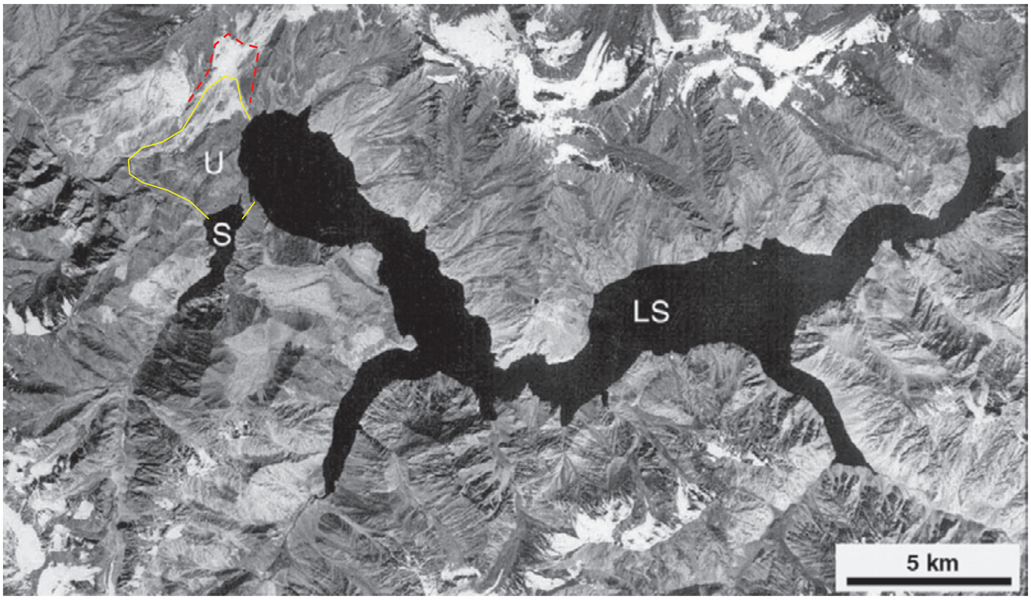

Fig. 21.7 The 1911 Usoi rockslide (U) damming the 500-m deep Sarez Lake (LS) that stores about 17 km^3 of water, and a small Shaddau Lake (S). *Red dashed line* – headscarp, *yellow line* – rockslide body

downstream, thus being the most disastrous rockslide catastrophe ever reported (Lee et al. 2004). In 1841 and 1858 similar catastrophic floods occurred due to failure of rockslide dams that had blocked the Indus River and its large tributary, the Hunza River, correspondingly (Hewitt 2002).

The case study of the Grijalva River (Mexico) damming by a modern landslide, circa, 50 Mm^3 in volume is described by I. Alcántara-Ayala and L Domingues-Morales (Sect. 21.7.9).

Interesting peculiarities of the landslide river damming by the postglacial Flims rockslide (see Fig. 21.2) are described in the presentaion of A. von Poschinger (Sect. 21.7.10). The importance of the precise age estimate of this European largest 9 km^3 river valley blockage is pointed out. The Flims rockslide, that was supposed initially to be a syn-glacial event, appeared to be post-glacial, according to the results of radiocarbon dating (Poschinger & Haas 1997). One more interesting phenomenon associated with this landslide is the alluvium mobilization and spreading upstream the Hinterrhein River valley. Besides the pure scientific interest (flow mechanism of these sediments is not understood until today) such phenomenon can almost double the area affected by landslide during its emplacement increasing its hazardows effects significantly.

The stability of the blockages and the longevity of the landslide-dammed lakes depend on many factors – geomorphic, geological and hydrological. Some of them could be quantified by the geomorphological dimensionless index proposed by Ermini & Casagli (2003). Landslide dams' evolution strongly depends also on the internal structure and grain-size composition of the landslide bodies, which, in turn, rely to the mechanism of their motion (Dunning et al. 2005, McSaveney & Davies 2006). Some novel methods of landslide dams modeling could be found in the presentation of by S. Dunning and W. Mitchell, which abstract is presented in Sect. 21.7.11.

21.5 Environmental and Socio-Economic Impact of the Above Natural Phenomena

Large-scale catastrophic landslides, rockslides and rock avalanches, along with debris flows and lahars, which represent more hydrological, rather then geological hazardous processes, have a significant effect both on the short-term and on a long-term river valleys evolution.

The comprehensive analysis of the evolution of mountain drainage system affected by large rock-slides led to elaboration of the 'disturbance regime' concept that was proposed recently by K. Hewitt (Hewitt 2006). Various aspects of the environmental impacts of such events are discussed in Sects. 21.7.1, 21.7.3, 21.7.10 and 21.7.11.

As it was pointed out above, size of landslide is not the only one factor leading to its catastrophic consequences. Other two important factors are the velocity of landslide motion and the predictability of its occurrence.

Landslide hazard in general is in direct proportion to the area affected and to impossibility to evacuate endangered people. It is evidently that simultaneous failure of billions tons of rocks has higher potential to cause a catastrophe. However, considering rather small probability of the largest landslides occurrence, attention is paid to medium-size events as well that occur unexpectedly, being caused by earthquakes or extreme climatic events. Their social and economic consequences could be quite catastrophic (Jibson 2006, Wang et al. 2006). Such events will be exemplified by N.E. Bongsiysi in his presentation (Sect. 7.12) who describes the 20th July 2003 landslide swarms in the Bambouto caldera in Cameroon. This event caused a significant loss of lives and property, being a real local catastrophe. In such cases, however, rapidness of landslide motion is a main factor causing catastrophic consequences, loss of lives at a first place. It can be illustrated by example of January 22, 1989 the M5.5 Gissar earthquake in Tajikistan. This event caused two large landslides in loess. One of them that moved so rapidly that people could not escape claimed 264 lives in the Sharora village (Fig. 21.8). In contrast, another, slowly moving landslide, though much bigger in volume, buried houses of the Oikuli-Poen village (Fig. 21.9), but their inhabitants survived.

One more landslide-related problem, quite important both from scientific and socio-economic

Fig. 21.8 The paled former Sharora village buried by a landslide with its inhabitants

Fig. 21.9 The former Oikuli-Poen village buried by relatively slow moving earthflow

points of view will be highlighted in the presentation of W.A. Mitchell and his colleagues from UK and Pakistan (Sect. 21.7.13). They describe fracture systems that originated in the vicinity of the fault trace ruptured during the 2005 M7.6 Kasmir earthquake and upslope of coseismically triggered landslides. Slope failures, including at least one large-scale rock avalanche were one of the most destructive consequences of this earthquake. Massive development of tension cracks above the present scars increases hazard of future slope failures significantly. It extends hazardous period in this severely affected region. However, at the same time it provides real opportunity to arrange some simple monitoring systems by controlling the behavior of these fractures that can serve as indicators of future slope movements.

Finally we would like to highlight one more aspect of socio-economic impact of large catastrophic landslides. These phenomena that we are unable to prevent and, often, unable even to predict, especially if slope failure is triggered by strong earthquake, could not be considered, nevertheless, as an 'utter evil'. Being an important factor of river valleys' evolution they often lead to formation of the geomorphic features favorable for settlements, agriculture and industry.

In some regions flattened benches on rockslide bodies, composed of shuttered debris are almost the only more or less planar surfaces, suitable for people settling in the extremely rugged terrain, typical of intact bedrock cliffs. It can be exemplified by the Ardon River valley in North Osetia, Caucasus, south from the Rocky Range (see Fig. 21.3). The most expressive example is from the Indus River Basin, where numerous rockslides had transformed the post-glacial river valleys into cascades of dams and reservoirs, partially breached and partially infilled by sediments (Hewitt 2002, 2006, Hewitt et al. 2008). Due to enormous dimensions of such blockages, supporting long-term river damming and, thus, lacustrine sedimentation, they produced significant flattened terrace-like surfaces wide enough both for housing and agriculture. Same phenomena took place in the Tien Shan, both in some small river valleys, completely infilled by lake sediments, and in the main streams like Naryn River that had been blocked in the central part of the basin by a gigantic Beshkiol rockslide for about 3000 years (Korup et al. 2006).

The existing rockslide blockages, being extremely dangerous due to possibility of outburst flooding (Costa & Schuster 1988, Schuster 2006) exemplify one more 'positive' effect of landslides, since they have large potential for power production. Here the Nature did the most expensive part of any hydraulic project – dam construction. Some of these dams are really outstanding 'structures' like the Usoi blockage in the Pamirs more than 500 m high that creates the Sarez Lake containing 17 cubic kilometers of water (see Fig. 21.7). There is a real possibility to convert this 'Damocles sword' hanging over the entire Pianj-Amu-Daria River valley into safe and effective structure producing light and power for people living in this remote area. One more interesting example is a rockslide in the Chinese Tien Shan (Fig. 21.10) that had blocked 2 joining river valleys by the nearly 300-m high dam creating 2 lakes which water levels differ for more than 200 m – an excellent place for the pumped storage power plant.

One more advantage of large catastrophic rockslides related to dam construction is their analogy with the blast-fill dams. Further development of this promising technology requires better knowledge of the internal structure and grain-size composition of large blockages created by artificial rockslides. Such data can be obtained either from large-scale natural experiments that are, however, too expensive, or from detail study of their natural analogues that are quite common and, moreover, had been often deeply eroded providing easy access to their internal parts (Strom & Pernik 2006).

The above examples demonstrate that mankind can not only suffer from landslides but can also benefit from this, generally unpleasant, neighborhood.

21.6 Conclusions

Large-scale catastrophic landslides, rockslides and rock avalanches are the inevitable companions of the mankind, especially of mountainous communities. Joint investigations of various aspects of these hazardous natural phenomena, both natural-science and social will support establishing better links between landslide researchers and the

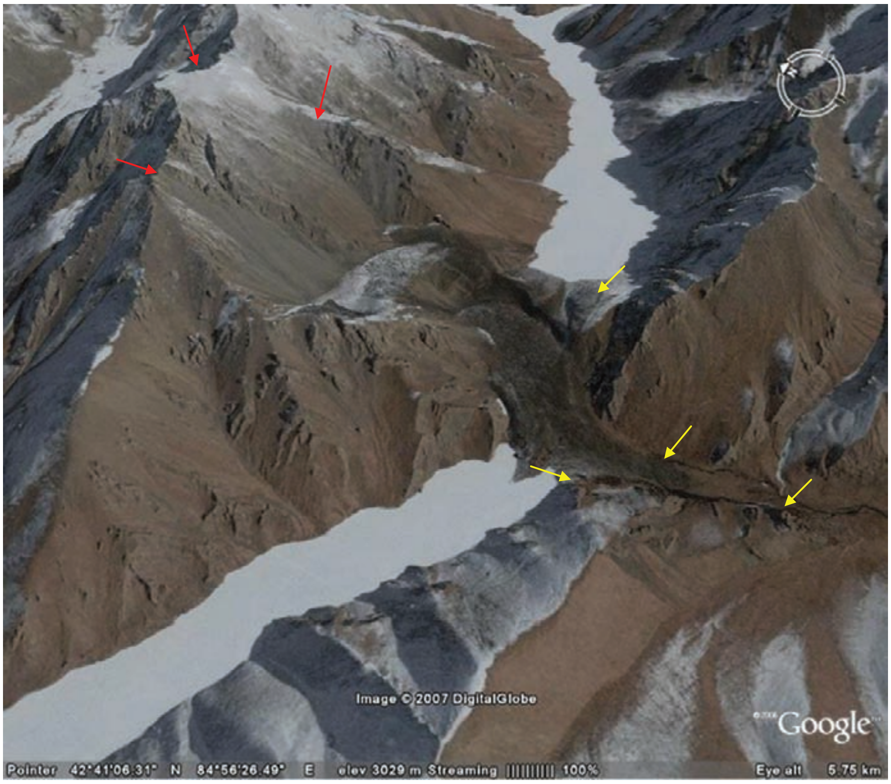

Fig. 21.10 The Google Earth view of the rockslide dam in the Chinese Tien Shan at 42°40‘58”N, 84°56’45”E. *Red arrows* – headscarp; *yellow arrows* – landslide toe

communities suffering from landslides, engineers designing landslide-affected structures and decision-makers.

Acknowledgments We want to acknowledge all colleagues who expressed their interest and submitted abstracts to the session of the 1st World Landslide Forum focused on the catastrophic slides and avalanches.

21.7 Invited Presentations

21.7.1 Catastrophic Landslides in Context and as Controls: Late Quaternary Developments in the Indus Gorges, Nanga Parbat-Haramosh Massif, Northern Pakistan

K Hewitt (Cold Regions Research Centre and Department of Geography and Environmental Studies, Wilfrid Laurier University, Waterloo, ON. Canada)

The paper concerns the role of landslides in the geomorphic evolution and hazards of mountain regions with large concentrations of catastrophic rock slope failures (CRSFs). Attention is focused on how the landslides act as controls in denudation, landscape evolution and the risk environment. Relations to the regional setting are emphasized. The discussion is based mainly on recent discoveries in the Nanga Parbat-Haramosh massif where, until 1989, only one CRSF was documented. Since then, more than 130 events have been identified within 100 km of the peaks Nanga Parbat (8,125 m) and Haramosh (7,397 m). The events of interest occurred in the late Quaternary and are post-glacial events. Most of those within the massif itself are reported here for the first time. Such discoveries pose new questions for the region, and shift the balance of concerns for landslide specialists.

The events discussed belong to a particular class of landslides: they are catastrophic (sudden, large magnitude, brief duration). They involve massive detachments of bedrock, descend at least 1,000 m, and generate a long-run out of crushed and

Fig. 21.11 The Lichar Landslide Complex on the west flank of Nanga Parbat where it blocked the Indus formerly mistaken for the 1841, earthquake-triggered event, which created a dam the failed catastrophically after 6 months. The main barrier shown is prehistoric. It was over 250 m high and lasted centuries at least, to impound vast quantities of sediment up-valley. This is in the most rapidly rising part of the orogen, close to the active Raikhot Fault and the Main Mantle Thrust. Yet, the landslide barrier has ensured there has been no net stream incision of the Indus here for most of the Holocene at least. Photographed by Ken Hewitt. *Red arrow* – direction of rockslide motion

pulverized debris commonly known as a rock avalanches. The magnitudes of the events range over five orders magnitudes, from at least 1 million m^3, to some 40 km^3 (Fig. 21.11). They display great diversity of detachment zone features and relations, styles of run out, morphology and composition of landslide debris, and post-landslide histories.

Looking at CRSFs in context reveals the influence of regional environments in statistical distributions of dimensions, spatial incidence and related variables. The Nanga Parbat-Haramosh massif (NPHM) has some of the greatest relief on Earth and highest measured rates of uplift, denudation, and river incision in bedrock. The great relief means that distributions and stability factors are complicated by extreme vertical gradients or zones with different (topo)climates, slope geometry, lithologies and geomorphic processes. Diversity of run out features and emplacement morphologies relate to interactions with rugged terrain, deformable or entrained substrates. The entire study area was glaciated and most rock slopes reflect former or on-going glacial activity. The role of rare, great earthquakes must be considered, especially in relation to the deep-seated megaslides.

Many studies have sought to understand how NPHM morphology relates to geotectonic evolution and glaciations. Formerly, however, many of the landslides were misinterpreted as due to glacial activity. Along the Indus, on the west flank of Nanga Parbat, a series of deposits and terraces up to 1,000 m above the river were regarded as Tertiary ‘molasse’ responding to tectonic uplift, or warped and folded glacial and fluvial materials. The new discoveries show most of the deposits to be emplacement forms of catastrophic landslides that crossed the valleys, climbed opposing slopes and disturbed the valley fill. Some comprise sediments backed up behind landslide barriers. The terraces are erosion-induced, as rivers have cut down through landslide barriers and sediments built up behind them. Extensive lacustrine deposits formerly attributed to glacier impoundments actually record landslide dams.

Cross-valley rock avalanche deposits blocked the gorges of the main Indus in 32 places in and around the NPHM. Many tributary streams were blocked by other landslides. Some dams lasted centuries, at least, and barrier remnants continue to affect stream behaviour after thousands of years. A few failed catastrophically to create large outburst floods. Again the conspicuous evidence of mega-floods along the Indus had been attributed largely to ice dam floods.

Over some 2,000 km of the Upper Indus streams surveyed, there is an average of one cross-valley rock avalanche barrier for every 12 km of river length. The density is even higher through the NPHM and its immediate surroundings. The unusual extent of rock bed channel where the Indus crosses the NPHM is evidently a response to higher rates of uplift and active faulting, as widely reported. However, it has not been recognised that multiple landslide impoundments have interrupted the apparent rates of incision, and sediment-starving by upstream impoundments must also have an effect. Immediately above where river enters the NPHM and where it leaves, there has been no net incision for the last 5,000 – 6,000 years at least. Up-valley of the NPHM the Indus flows almost entirely over or in extensive valley fill related to landslide barriers, and also where it exits the massif. Thus, relations between exceptional rates of uplift and stream incision are mediated and complicated by the extent of landslide interruptions.

The landslides affect denudation and morphology in all phases of their activity. As failures in bedrock, their contribution to primary erosion and denudation rates is huge, and to the unroofing of plutons and of the orogen as a whole. They help to control the geometry and evolution of interfluves. Conversely, the large masses of resistant landslide materials emplaced across valley floors have an opposite impact, interrupting sediment removal and slowing denudation rates. The widely accepted assumption that stream incision and thalwegs can be used as a proxy for rates of tectonic uplift needs to be revisited here. Likewise, rates of erosion based on present-day sediment yields must take account of the role of landslide interruptions. It is clear that the set of landslide-interruptions has been a decisive factor in intermontane sedimentation, on patterns of sediment release through the Holocene, and in present-day sediment transport.

By impounding, obstructing, and diverting the rivers, landslides disrupt stream continuity and responses to climate change, including deglaciation, as well as to tectonics. This applies especially to the assumed significance and relations among relief in excess of 7,000 m, rapid tectonic uplift, deglaciation, and stream incision in an active orogen. In general, features related to CRSFs have been misread or subordinated to interpretation through tectonic, climatic, glacial and river system dynamics. The latter are obviously of profound importance but the evidence used to identify their influence is compromised.

The findings introduce new geohazards concerns. They include the, as yet unresolved, questions of the age and timing of the landslides; the risk of further occurrences; what triggers them. Long runout events can be expected to interact with and modify other surface processes and generate secondary hazards including debris avalanches, debris flows, and landslide dams. There are hazards related to vast quantities of landslide and related impoundment materials still present in the valleys and their stability. These were formerly thought to be glacial and much older.

Apart from the new discoveries, there are new geohazard issues related to growing settlements, modern infrastructure, and rapidly changing activities. Many of the sites of frequent collapses and blockage of the mountain highways turn out to relate to prehistoric CRSFs. Meanwhile, nearly all the arable land, most village and town sites and modern infrastructure in the region lie on valley fill related by landslide activity. There are implications for almost 200 million people down-river and in the Indus Plains who depend upon water and power initiatives in the Upper Indus basin. Several major development projects in or close to the NPHM itself are of special concern.

The paper concludes by suggesting that similar discoveries in mountain ranges world-wide expand the questions and roles that landslide science can play. More than thirty mountain ranges are now known to have 50+ events and some, 100s. Like the area chosen for detailed study here, most involve relatively recent discoveries and changes in how Qauternary developments are viewed.

21.7.2 Giant Low-Gradient Landslides in the Northern Periphery of the Crimean Mountains: Predisposition, Structure, Chronology and Links to Adjacent Regions

T Pánek, J Hradecký, V Smolková, K Šilhán (Department of Physical Geography and Geoecology, Faculty of Science, University of Ostrava, Czech Republic)

The Crimean Mountains (CM) are among the regions with the highest concentration of slope deformations within the Europe. As a part of Caucasus – Crimean thrustbelt, mountains evolved as a consequence of several geodynamic stages involving Early Cretaceous orogenesis, Cretaceous-Eocene burial under thick sequence of sediments and subsequent post Eocene exhumation and uplift. Geomorphic analysis (field mapping, study of remote sensing products and GIS analysis) of the CM has detected extraordinary large landslides (5.4–18.9 km^2; ~0.2–1.2 km^3) in the northern periphery of mountains (valleys of Belbek, Kacha, Alma and Biyuk Karasu rivers) which is build by gently inclined Sarmatian limestones overlying weak, clay-rich Lower Neogene–Palaeogene substratum with a significant content of smectite.

The landslides are generally a spreading type, but the sliding mechanics were probably very complex, involving toppling, rotational slides, gravitational folding and translational block slides. All the studied landslides are located in the vicinity of regional faults and three of them have headscarps aligned along faults. A common feature is also location close (within several km) to the Mesozoic suture zone which is the most important tectonic feature in the northern periphery of the CM. Giant instabilities could be classified as fossil or almost stabilized features. Radiocarbon dating of deposits associated with the landslides has revealed at least two phases of increased landslide-activity during the Late Glacial chronozone and Holocene epoch. The main landslide phase presumably took place at some time between the Late Glacial and Atlantic chronozones (~11–6 ka BP). Minor reactivation of landslide toes occurred during the Subatlantic chronozone (1–2 ka BP) and some of them have been active up to recent times. We assume that first major landslide phase was possibly triggered by an earthquake, whereas late Holocene activity can be attributed both to seismic and hydroclimatic factors.

Ongoing investigation of fossil low-gradient megalandslides in the Southeastern Europe has revealed similar cluster of giant landslides in the peripheries of Carpathian Mountains (Romania), Stara Planina (Bulgaria) and northern foothills of the Caucasus Mountains (Russia) where individual landslides (or landslide complexes) reach even ~100 km^2 in area and ~10 km^3 by volume.

Described cases of extremely large low-gradient landslides serve as an useful indicators of major geodynamic events in regions, which recently reveal negligible or low intensive geomorphic processes.

21.7.3 Overview of Megalandslides in the Andes

RL Hermanns[1], L Fauque[2], L Fidel[3], D Welkner[4], A Folguera[5], A Cazas[6], H Nuñez[7] ([1]Norges geologiske undersøkelse, [2]Servicio Geologico Minero Argentino, [3]Instituto Geológico Minero y Metalúrgico del Perú, [4]Universidad de British Columbia, [5]Universidad de Buenos Aires, [6]Servicio Nacional de Geología y Técnico de Minas de Bolivia, [7]Direccion Nacional de Geología de Ecuador)

We have studied non volcanic rockslides involving a volume of several million cubicmeter (megalandslides) in various parts of the Andes in the last years. This paper is a review of our effort in the various Andean countries. Although several million cubicmeter large landslides have occurred at multiple places in the historic past, with the exception of the 1974 Mayunmarca landslide, Peru, in all regions, deposits of paleolandslides have been significant larger often exceeding the historic ones by one or more orders of magnitude. Our interest was to understand both limiting conditions of historic megalandslides and limiting conditions of the even larger prehistoric rockslides to assess if conditions for landslide generation have changed or if landslides of the magnitude of prehistoric events can also occur today.

An important step towards the understanding of conditions of prehistoric slides is dating of past events. Although our effort can only be restricted and regionally focused, we could date several prehistoric megalandslides using various cosmogenic nuclides for surface exposure dating, tephrochronology, and ^{14}C dating. Our data sets indicate that megalandslides along the east side of the Andes are several thousand to hundreds of thousand years old. In narrow valleys they cluster during periods characterized by more humid climate conditions and thus are interpreted as related to increased run off and scouring of mountain slopes. However, also age clusters of large megalandslides along active faults in northwestern Argentina and in northern Patagonia have been established. As both areas are characterized by fault offsets with apparent Holocene displacement these megalandslides are interpreted to be triggered by seismic events and conditioned by fracturing of intact rock mass by tectonic activity. Low frequency/high magnitude seismic events are the most plausible triggers. Megalandslides far away from trunk streams are in general older and have recurrence intervals in the tens of thousands and do not coincide with periods characterized by larger run off. However they were always found along tectonically active mountain fronts bordered by reverse faults suggesting tectonic oversteepening and fracturing as conditioning factor.

Along the glaciated water divide of the Andes multiple megalandslide have ages few to several thousand years post Last Glacial Maximum, hence suggesting glacial debutressing, unloading and changes in permafrost to be important conditioning mechanisms.

So far temporal data of megalandslides from the west slope of the Andes are less available. However, at several location megalandslides have been triggered in historical times during megathrustearthquakes although prehistoric events in the same regions are in general larger. Other megalandslides were found in regions where megathrustearthquake have occurred in the past; however they were not associated with megalanslides indicating that a strong trigger alone does not cause large slopes to collapse. We suspect that either multiple factors conditioned past megaslandslides including tectonic uplift and fast incision, climatic conditions different from today are responsible for the events or that crustal earthquakes within the South American plate which may result in stronger ground acceleration causes these larger prehistoric events. Anyhow this area is seen as a special focus area for future coupled neotectonic/landslide investigations as important urban centers concentrate along the west slope of the Andes.

Finally, within the Andes at the edge of the Altiplano plateau in Bolivia multiple megalandslides have occurred at the rim of La Paz valley in the past decade. Again in the same region much larger deposits of megalandslides have been found covering areas of up to 60 km^2. These surface area is larger than that of the city of La Paz itself and are of early Holocene age. First they have been interpreted to be realted to paleoseismic events along a fault system crossing the Altiplano plateau and the La Paz valley, however first paleoseismic investigations indicated that these faults have last been active several thousand years prior to landsliding. In any case further studies have to be carried out along other branches of the fault to finally exclude seismic triggering for the prehistoric megalandslides.

21.7.4 Co-Seismic Rock Avalanches in the Himalaya

WA Mitchell[1], DN Petley[1], SA Dunning[2] ([1]International Landslide Centre, Department of Geography, Durham University, UK. [2]Department of Geography, Northumbria University, Newcastle-upon-Tyne, UK)

Rock avalanches form the largest and most destructive type of slope failure within high mountains and are usually regarded as being triggered by either high magnitude rainfall events or by earthquakes which generate large numbers of slope failures of as a co-seismic response. For example, the 8th October 2005 M7.6 Kashmir earthquake killed an estimated 87,350 people, of which 25,500 can be attributed directly to seismically triggered landslides. Within these statistics 3.7% of landslide fatalities, some 1000 people were killed by the Hattian Bala rock avalanche, the largest slope failure associated with the earthquake.

Geomorphological evidence of former rock avalanche events has been reported from many parts of the Himalaya, particularly the Karakoram; however, to date, there has been no large scale attempt to produce a comprehensive map of their distribution across the orogen or determine the causes of their formation. In fact, there is a lack of evidence reported from a number of areas. Equally problematic is determining the trigger mechanism for such events that can be observed within mountain landscapes. However, it seems likely that rock avalanche debris may be a useful proxy record for past high magnitude seismic events. From studies in other mountain areas, it appears that the generation of rock avalanches requires earthquakes with a magnitude approaching M8. If a seismic trigger can be proposed with confidence, it suggests that examination of the distribution of rock avalanche debris in a tectonically active area may be a method in the deciphering the palaeoseismic record of large to great earthquakes where there is minimal other geological evidence.

This can now be achieved by new dating methods, particularly cosmogenic radionuclides. At present there are few dates for rock avalanches in the Himalaya; one particular example occurs in Zanskar north of the main divide of the High Himalaya. Cosmogenic ^{10}Be dates from quartz veins exposed on the surface of the rock avalanche give an error-weighted mean of 7510 ± 110 calendar years BP. It is suggested that this marks the occurrence of a major earthquake in this area at this time demonstrating Holocene activity on one of the fault strands associated with the Zanskar Shear Zone. Other rock avalanches have also been identified along the Karakoram Fault in Ladakh but these have not been dated; a similar situation exists for the >140 rock avalanches recognized within the Karakoram.

Using rock avalanche debris to determine the timing of large seismic events is a novel and radical means of developing a palaeoseismic catalogue for areas such as the Himalaya where the historical record is insufficient to allow the establishment of a recurrence interval for great earthquakes. Given the large populations of the Ganga basin and the continuing strain build-up in the Himalaya, developing the seismic record is a key issue in mitigating the inevitable disaster that will be associated the next great event.

21.7.5 Delimitation of a Prehistoric Rock Fall from Huascaran

V Vilímek, J Klimeš (Charles University, Faculty of Science, Prague, Czech Republic)

The area of rock and ice avalanches from Huascaran Mt. (Cordillera Blanca, Peru) was studied to compare the well known 1970 and 1962 events with a prehistoric one (or ones?) which is supposed to be much larger in the sense of both volume and reach. From the methodological point of view, we used aerial photo interpretation, geomorphological mapping and field research. We used the N type of Schmidt Hammer device for relative dating of mixed glacial and gravitational deposits originated through glacial and catastrophic gravitational processes (rock avalanches).

As the Rio Santa Valley (Calleyon de Huaylas) is densely populated and recently people have been even moving to the areas affected by the 1962 and 1970 Huascaran Rock and Ice avalanches, it is very important to outline in detail the hazardous areas and to describe local landforms and their respective forming processes. Catastrophic events from Huascaran Mt. are usually composed of several types of processes and consequently given different names. They are classified either as avalanches, because they started as a snow and ice avalanche, or as debris flows (also mud flows). Sometimes they are called landslides or rock slides. To understand the mechanism of origin and behaviour of a much larger prehistoric avalanche from the northern summit of Huascaran Mt. (6,655 m a.s.l.), it is important to study the known events and to compare them with selected large slope deformations known from other parts of the world.

The hugest avalanche from Huascaran Mt., which is historically documented, was triggered by the 1970 earthquake (M = 7.75). The avalanche route started under the northern summit of the mountain, then it followed the present river network and dragged downward a part of moraine material from the Huascaran slope. The major part of the material, which sedimented in the region of former villages Ranrahirca and Yungay, is not of river origin, although it passed through the river network. The transport of material from Huascaran was immense. In the accumulation region, there are many scattered huge blocks originating not from moraine sediments or from the debris mantle, but directly from the Huascaran rock wall. In the centre of the former Yungay village, the debris flow spread and its present surface is only slightly vaulted.

In the place, where the Ranrahirca River is mouthing into the Santa River, the direction of the main watercourse of this region (Santa River) it markedly turned under the slopes of the Cordillera Negra mountain range. Probably since a long time already, the Santa River has been 'pushed' away (by a huge amount of sediments) from Huascaran against its left riverbank. It has already affected the straight course of the Cordillera Negra foot. A pronounced depression is evident on the western slope of the Huascaran northern summit.

The highest variability of paleoavalanche boulders supports our hypothesis about the polygenetic origin of its sediments, which contain blocks of originally fresh rocks detached from rock slopes, moraine material and accumulations of previous events. The relative age (interpreted from the mean R-values) of the paleo-avalanche is closer to the moraine deposits than to the boulders of the 1970 avalanche.

The borders of the prehistoric avalanche from Huascaran Mt. were delimited both at the foothill of Huascaran and on the opposite slopes of the Cordillera Negra mountain range. The granodiorites from Huascaran Mt. were recently documented on the slopes of Cordillera Negra (composed mainly from volcanic material) even in a higher position than ever before.

21.7.6 Paleolandslides of the Central Part of the East European Plain, Russia

EN Samarin, OV Zerkal (Geological Faculty, Moscow State University, Moscow, Russian Federation)

There is a great number of urban agglomerations (such a Moscow, St. Petersburg, Nizhni Novgorod, Saratov, ect.) and many cascades of reservoirs at the East European plain, which occupies large part of the European Russia. Some of them are affected by landslides that require close attention to the landslide hazard assessment in this region.

East European plain is a part of Russian plate. Its relief represents a vast smoothed spaces 100–120 m to 200 m a.s.l. (rarely up to 300 m a.s.l.). The study of the landslide developed at East European plain started in the second half of XIX century due to intensive road construction. Generally modern landslide activity and landslide hazard within the limits of East European plain are estimated as low. However, these are several sections of river valleys where slope deformations are induced by lateral stream erosion. The bulk volumes of some landslides at these segments vary from few thousand cubic meters up to 300–400 thousand cubic meters and rarely more.

However, in the middle of XX century during Volga HPP construction landslides ranging from several millions to several tens millions cubic meters in volume were identified. Later abnormally large (for flatland area) landslides were recognized outside the Volga-river valley too. The study of geological condition of large landslide areas within the limits of East European plain showed that most of them are inherited from the previous geological epochs. In general, several periods of high landslide activity could be identifies – the Miocene, the Eopleistocene and the Holocene.

Formation and active development of large paleolandslides were caused, likely, by two major reasons. The first one was the change of base level of erosion accompanied by river valley Miocene overdeepening and block slide formation on the high (more that 300 m) valley slopes. The second one was the significant climate change during the deglaciation. It often led to the expanding of landslide-affected areas.

Most of Miocene and Eopleistocene landslides were completely (within the limits of glacier cover) or partially (at large river valleys outside of glacier cover) overlaid by Quaternary sediments. This post-glacial sediment cover masked paleolandslides. That is why hazard caused by paleolandslides evolution was underestimated at the initial stages of landslide hazard assessment.

21.7.7 The Güímar Flank Collapse on Tenerife Island and Evidences for Related Tsunami on the West Coast of Gran Canaria, (Canaria Islands, Spain)

P Wassmer[1], R Paris[2], FJ Pérez Torrado[3], JL Schneider[4] ([1]Laboratoire de Géographie Physique, Université Meudon, France, [2]GEOLAB-UMR, Clermont-Ferrand, France, [3]Dpto. Fisica-Geologia, Universidad de Las Palmas de Gran Canaria, Las Palmas, Spain, [4]Université de Bordeaux Talence, France)

Landsliding is a major process of morphological evolution on volcanic edifices. These mass movements are favored by structure dipping according to the slope and by superposition of material of various resistance. They can be triggered by local tectonic before (destabilization due to dome), during (phreato-magmatic interactions) and after the eruptive episode (Caldera collapse). In the Canaria Islands, not less than nine major flank collapses were identified.on the base of remaining scars and related large lobate deposits on the ocean floor. The Güímar collapse, that occured on the east flank of la Cañadas volcano on Tenerife is constrained between 840 and 780 ka. The movement involving a tremendous mass of material (45 km^3 for the subaerial scar 120 km^3 for the submarine debris avalanche deposit) is the only one that was not oriented to the open sea but was focused towards the channel between Tenerife and Gran Canaria. On the north western shore of Gran Canaria, the Agaete valley mouth, facing Tenerife Island, interrupts locally the sheer vertical high cliffs and fans out to the sea. On the walls of the valley, nine patches of enigmatic conglomerate are attached at altitudes ranging between 41 and 188 m a.s.l. Composed of heterometric angular to rounded volcanic clasts and fossils (rhodolites and marine shells) generally broken and never in life position, the deposits decrease in thickness with altitude from 5 to 0.1 m. Internally stratified, the material displays two main layers. The clast supported lower layer is characterized by poor sorting, reverse grading and shows sometimes more than one sequence. The basal contact with the substratum shows clear erosive features (rip-up clasts). The upper one is composed of less coarse material. Also clast supported and poorly sorted, it encloses numerous fossils and is only lightly reverse graded. The study of the clasts (size, morphology and nature) points out that the material is provided by two main sources. One can be related to the beach gravels and pebbles and the other to alluvial deposits along the valley. Measurements of clast imbrications within the conglomerate show that the direction of the palaeocurrent leading to the emplacement of the deposit was landward for the lower layer and seaward for the upper layer. All these sedimentological, stratigraphical and paleontolo-gical observations indicate that the assembly of outcrops along the Agaete valley seems to have a common origin. Some of them like clast imbrication oriented landward for the basal layer and seaward for the upper layer, or the presence of rip up clasts of substratum incorporated in the lower layer are determinant to allow linking these conglomerates to a common and single tsunami origin. Lower layers could reflect the runup of the wave in the valley mouth. The high energy of the wave front was responsible for the mobilisation of a huge amount of beach pebbles and alluvial material in the valley that lead to a kind of reverse debris flow with an erosive shearing at the base that leads to the reverse grading formation. The loss of energy with the distance to the sea explains the landward decreasing of the thickness of the deposits. Close to the turning over point, as the energy was close to zero the less coarse material emplaced abruptely. This part of the deposit was remobilized and the clasts were re-oriented seaward by the backwash. Local variations of the runup and backwash direction must be related to the role played by the topography on the uprush and backwash orientation.

The closest source possible for the Agaete tsunami deposits is the Güímar sector collapse on the east coast of Tenerife. Focused towards Gran Canaria Island, his age is compatible with the age of the deposits, poorly constrained between 35 and 1750 ka. The height reached by the water in the Agaete valley during the event (at least 188 m a.s.l.) doesn't correspond to the real height of the waves but to the runup level that could have been notably increased by the 'wave trap' shape of the Agaete valley mouth facing the source of the tsunamigenic sector collapse on Tenerife.

21.7.8 Matsushima Bay as an Early Holocene Coastal Mega-Landslide, Northeast Japan

S. Hasegawa (Faculty of Engineering, Kagawa University, Takamatsu Japan)

Matsushima, a group of island at the Matsushima Bay in Miyagi Prefecture is one of the three scenic spot in Japan. It is composed of more than 200 islands in the Matsushima Bay and the islands jut out in to the sea. Topographically the Matsushima Bay suddenly breaks the gently concaved coastline from Senadai Plain to the Ishinomaki Bay. Matsushima and the Matsushima Bay have been considered as a typical submerged coast, but they are inferred to have been formed by a coastal mega-landslide in Early Holocene age from geological and topographical evidences. Our conclusions are as follows:

1. The Matsushima Bay is the source area of a mega-landslide, about 10 km in length and 5 km in width.
2. The islands in the Matsushima Bay are hummocky hills formed by the mega-landslide and offshore reefs were formed by secondary landslides.
3. The islands and reefs are restored to the source area geologically and topographically. This restoration suggests that the part of Matsushima Hill have slid 5 km towards southeast as a mega-landslide and have broken up by secondary landslides.

4. About 20 m thick Holocene muddy sediments in Matsushima Bay directly cover the Miocene bedrocks. This indicates that the mega-landslide occurred in Early Holocene age. This estimated age corresponds to postgracial transgression and the sea-level at the slide was nearly that of present time.
5. This mega-landslide might have caused a mega-tsunami. A settlement and midden located on the hummocky hill about 40 m above sea-level have continued from early to middle Holocene.
6. One of the possible causes of mega-landslide was a big earthquake caused by an active fault named the Rifu-Nagamachi fault which runs through Matsushima Hill. The magnitude of earthquake from this active fault is estimated from 7.0 to 7.5 and the latest faulting is estimated from about 3,000–16,000 years ago.

21.7.9 The San Juan de Grijalva Catastrophic Landslide, Chiapas, Mexico: Lessons Learnt

I Alcántara-Ayala[1] and L Domínguez-Morales[2] ([1]Institute of Geography, National Autonomous University of Mexico, [2]National Centre for Disaster Prevention, Mexico)

Following a period of intense precipitations, on November 4, 2007, a catastrophic landslide took place in San Juan de Grijalva, a community located on the edge of the Grijalva river, near the Peñitas dam, in the south-eastern province of Chiapas, Mexico. The landslide involved a volume of circa 50 Mm3 that blocked the Grijalva river covering a run-out distance of 800 m length along the main channel, and including a meander zone between 200 and 280 width. Following the initial movement, a 50 m wave was produced causing considerable damages to several houses and a church. According to official information, the aftermath was 19 deaths and 6 people missing.

Above and beyond the direct and immediate effects of landsliding in the adjacent communities and landscape, further hazards associated to dam breaking were likely to occur as more than six weeks were needed to remove the huge volume of material filling the river. As a result of the presence of unstable hillslopes, and flooded areas, more than 3500 people were evacuated.

A discussion of the main processes of the Grijalva landslide, including geological, geomorphological and climatic settings, is presented in this paper, in addition to some reflections derived from the occurrence of this type of events in developing countries, and taking into account a hazard assessment perspective.

21.7.10 Chronology of the Flims Rock Slide

A von Poschinger (Bavarian Environment Agency, Germany)

In the last decade there was a new impetus in the investigation of the Flims rock slide. The Flims slide in eastern Switzerland concerns about 9 km^3 of rock mass and so it is known to be the largest in Europe and one of the biggest worldwide, at least not considering sub aquatic slides. The rock slide and its dimensions were known since about one century, but it due to till and erratic blocks on top of the slide mass it was supposed to have a syn-glacial age. The triggers of this new interest were the results of a radiocarbon dating, indicating a clear post-glacial age (Poschinger & Haas 1997). Even if only few new aspects about the slide event itself had been found, many new information about the main consequences of the rock slide could be shown up.

As a usual consequence for large rock slides several lakes were dammed. There extends and the lake level altitudes could be estimated. The longevity of the lakes can be determined by sediments and by morphological phenomena. Obviously, the main lake, called Lake Ilanz, drained soon after the filling of the basin in a catastrophic flash flood, but it drained only partly. A relict lake at lower level is supposed to have survived for a longer time. The flood event is assumed to have caused a sediment anomaly in Lake Constance, more than 100 km downstream.

Another consequence of the Flims event, less common to large rock slides, was the extent and the mechanisms of the displacement of the alluvium on the valley floor. Several hundreds of thousand cubic meters must have been squeezed out. They were forced to flow upstream the valley of the river Hinterrhein. The rather characteristic sediments can be found now at a distance of about 18 km from the tongue of the rock slide deposits. The flow mechanism of these sediments is not understood until today, but in any case the alluvial sediments must have reacted as a transport medium that was able to move large coherent components of loose rock with diameters of tens or even hundreds of metres on a distance of more than 10 km. By this, the radius of the catastrophic consequences of the rock slide was more than doubled.

21.7.11 Catastrophic Landslides – Quantifying the Link to Landscape Evolution

SA Dunning[1], WA Mitchell[2] ([1]Division of Geography, Northumbria University, Newcastle-upon-Tyne, UK, [2]International Landslide Centre, Department of Geography, Durham University, Science Site, Durham, UK)

Rock avalanches are considered a high magnitude, relatively low frequency event in the high mountains. Rock avalanches are triggered by a number of forcing factors, rainfall, seismic acceleration, and more debatably, through the longer term the action of glacial de-buttressing, and also long term creep (sackungen). Rock avalanches are an extremely efficient way of linking hillslopes to rivers and relieving the landscape of tectonic derived stress – notably the notion of achieving 'steady state landscapes'. It is becoming clear that rock avalanches are responsible for large proportions of mountain erosion and have significant effects on other landscape formational processes. During emplacement rock avalanches thoroughly fragment to leave a deposit composed of predominantly sand and gravel grades, material that should be readily transported by most major mountain river systems. A complication at this stage is added by the common formation of landslide dams by rock-avalanche debris, delaying for a period of several days to millennia the dispersal of this fragmented debris. The timing of the failure of such dams results in an interruption to the evolution of the mountain landscape and valley-fill over varied spatial and temporal scales, and a geomorphic imprint that may extend into the geological record and affect landscape evolution at regional scales. The geomorphic signature of this interruption and the subsequent dispersal of rock-avalanche debris is a key issue for both hillslope and river processes with as yet un quantified feedbacks and links to ongoing tectonics.

A newly commissioned analogue micro-scale modeling system using a river modeling table with uplift/subsidence options and rainfall simulation aims to begin to asses the spatial and temporal changes to hillslope and river processes at the reach scale. A modeling approach has been adopted as an alternative to current approaches utilizing the traditional geographic methods of substituting space for time i.e. site investigation of sites at varied stages of material dispersion and landscape evolution and attempting to draw a logical progression between them. Modeling has the advantage of simulating all stages of process disruption in the mountain landscape, including those that in the field may be destroyed by future processes. Tectonics (uplift) can be controlled; rates of hillslope / river coupling upstream and downstream of landslide dams can be assessed, as can the long-term development of river planform and long profile and valley fill. A key aspect of the model is the use of both silica sand and a weak, sand erodible 'bedrock' analogue allowing for the mixed bedrock-alluvial channels so common in mountain situations and so measurement of incision rate modifications. It is hoped that these simulations will provide invaluable information on the effect of catastrophic rock avalanches on the mountain landscape.

21.7.12 The 20th July 2003 Landslides Swarms Within the Bambouto Caldera and Their Effects

NE Bongsiysi (University of Buea, Cameroon)

The Bambouto caldera on July 20th 2003, witnessed a spontaneous swarm of more than 120 landslides that killed 23 people and resulted in the destruction of properties. It is located between longitudes 9°56'N and 10°06'N and latitudes 5°38'E and

5°45'E along the Cameroon volcanic Line (CVL) and is 16 km long in the east-west direction and 5–7 km wide in the north-south direction. The basal plutonic syenite complex occupies the central position of the caldera. The overlying volcanic complex, previously not well defined, is made up of successions of volcanic tephra and lava flows that alternate from more silicic varieties at the base to more basic rocks towards the top. Intensive weathering of the volcanic rocks resulted in an increase in Al_2O_3, Fe_2O_3, total water ($H_2O + LOI$) and SiO_2 and a decrease in the K_2O, Na_2O and MgO. This resulted in the formation of perched aquifers with gibbsitic or montmorillonite bands constituting the aquiclude base. The liquefaction of these perched aquifers resulted in numerous spontaneous slopes failure across the entire caldera.

The need to establish new fertile farms in order to improve on the yearly yield, attracted many families to settle, within the highly fertile caldera region. The development of the region resulted in deforestation, undercutting of slopes for structures (houses, roads and bridges), soil disintegration and increase in the rate of weathering. The 2003 landslides killed 23 people and produced large volumes of regolith charged with tree trunks, rock boulders, and objects (corrugated zinc sheets, broken furniture) derived from destroyed houses. The resultant sloth produced from the regolith caused floods in the streams which feed the River Meyi. The floods increased the rate of lateral erosion of the banks of the river at its lower courses, and together with the landslides destroyed 261 houses, 52 bridges, 86 culverts, 496 farms, 385 livestock killed, 229 families displaced and 1015 persons displaced. The caldera was completely cut off from the surrounding regions.

21.7.13 The Development of Tension Crack Arrays Associated with mw 7.6 Kashmir Earthquake, October 2005: Implications for Future Slope Stability

WA Mitchell[1], DN Petley[1], NJ Rosser[1], SA Dunning[2], AB Kausar[3] ([1]International Landslide Centre, Department of Geography, Durham University, Science Site, Durham, UK, [2]Department of Geography, Northumbria University, Newcastle-upon-Tyne, UK, [3]Geological Survey of Pakistan, Ministry of Petroleum and Natural Resources, Islamabad, Pakistan)

The M_w 7.6 earthquake which affected the middle Jhelum valley in Azar Jammu and Kashmir, Pakistan in October 2005 generated numerous coseismic landslides, ranging from small translational failures to extensive rock avalanches, concentrated along the Muzaffarabad-Tanda Fault. In this high mountainous area, many slopes did not fail but were seriously affected with the formation of complex arrays of tension cracks and small graben structures within bedrock and alluvium. These cracks can be found associated with two distinctive slope situations: (1) in the vicinity of the fault trace and (2) upslope of coseismically triggered landslides. Their presence is a clear expression of fracturing of the ground surface under tension due to perturbation of the dynamic stress field and reflects either direct tectonic processes related to seismo-tectonic fault rupture on the slopes or are associated with peak ground acceleration which has lead to seismo-gravitational fissure development on slopes that were originally under tension and close to failure. It is also clear that local geology and topography have had a major influence on the distribution of seismic stresses and the resultant fissure systems.

Both sets of tensional fissures indicate areas of future mass movement as slopes respond to changes in post-seismic stress and monsoon rains by increased infiltration and generation of high pore water pressures. On-going hazard in the area is associated with slopes at threshold stability coupled to the progressive and retrogressive failure of translational and deep seated failures. Disaggregation of hillslopes by the ground shaking has also increased the amount of sediment available for future transportation leading to increased debris flow generation associated with rainfall, spring snowmelt and summer monsoon events. Continuous monitoring of slopes which have been affected by tension crack arrays has been instigated at four sites to determine post-seismic slope response to slope stability in association with rainfall events. Three of these sites are located around Muzaffarabad with a further site up the Jhelum valley towards the hilltop village of Chikka which was severely damaged by the earthquake. Overall pattern of the monsoon rainfall data over the monitoring period shows that each slope is clearly reacting in a distinctive local way to on-going site specific strain conditions.

Extensive slope failures are therefore likely to take place in the near future as existing landslides continue to develop by retrogression of back and lateral scarps. The presence of tension crack arrays on many slopes that mirrors the configuration of the present scarps allows prediction of future slope failure pattern. Areas of hillslope that have not failed, but have a high density crack array, are also are likely to fail as a series of deep seated failures. Measurements of horizontal extension and vertical displacement will allow a better assessment of slope stability and potential landslide hazard in this disaster area where more than 2.5 million people are still displaced from their land.

References

Abele G (1974) Bergstürze in den Alpen, ihre Verbeitung, Morphologie und Folgeerscheinungen, Wissensch. Alpenverein 25: 230p

Brückl E, Brückl J, Heuberger H (2001) Present structure and prefailure topography of the giant rockslide of Kofels, Zeits. fur Gletscherkunde und Glazialgeol., 37: 49–79

Costa JE, Schuster RL (1988) The formation and failure of natural dams, GSA Bull. 100: 1054–1068

Dunning SA, Petley DN, Rosser NJ, Strom AL (2005) The morphologies and sedimentology of valley confined rock avalanche deposits and their effect on potential dam hazard. In: Hungr O, Fell R, Couture R, Eberhardt E (Eds.) Landslide Risk Management, Taylor & Francis, pp 691–704

Eisbacher GH (1979) Cliff collapse and rock avalanches (sturzstroms) in the Mackenzie Mountains, northwestern Canada. Canadian Geotechnical Journ. 16: 309–334

Eisbacher GH, Clague JJ (1984) Destructive mass movements in high mountains: hazard and management, Geological Survey of Canada Paper 84–16, 230 pp

Ermini L, Casagli N (2003) Prediction of the behaviour of landslide dams using a geomorphological dimensionless index, Earth Surface Processes and Landforms 28: 31–47

Evans SG, DeGrafff JV (Eds.) (2002) Catastrophic landslides: effects, occurrences and mechanisms. Geol. Soc. Am. Rev. in Eng. Geol. 15: 412

Evans SG, Scarascia Mugnozza G, Strom AL, Hermanns RL (Eds.) (2006) Landslides from Massive Rock Slope Failure. Proc. NATO Advanced Workshop, Celano, Italy, June 2002. Springer-Verlag, Dordrecht, 662p

Gaziev E (1984) Study of the Usoi Landslide in Pamir. Proc. 4th Int. Symp. on Landslides, Toronto, 1: 511–515

Heim A (1932) Bergsturz und Menschenleben. Zurich, Fretz and Wasmuth. 218p

Hermanns RL, Niedermann S, Garcia AV, Gomez JS, Strecker MR (2001) Neotectonics and catastrophic failure of mountain fronts in the southern intra-Andean Puna Plateau, Argentina. Geology 29: 619–623

Hermanns RL, Niedermann S, Villanueva Garcia A, Schellenberger A (2006) Rock avalanching in the NWArgentine Andes as a result of complex interactions of lithologic, structural and topographic boundary conditions, climate change and active tectonics. In: Evans SG, Scarascia Mugnozza G, Strom AL, Hermanns RL (Eds.) Landslides from Massive Rock Slope Failure. Proc. NATO Advanced Workshop, Celano, Italy, June 2002. Springer-Verlag, Dordrecht, pp 497–520

Hewitt K (2002) Styles of rock avalanche depositional complex in very rugged terrain, Karakoram Himalaya, Pakistan. In Evans SG (Ed.) Catastrophic Landslides : effects, occurrence and mechanisms, Reviews in Engineering Geology. Geological Society of America, Boulder, Colorado, pp 345–378

Hewitt K (2006) Disturbance regime landscapes: mountain drainage systems interrupted by large rockslides. Progr. Phys. Geogr 30: 365–393

Hewitt K, Clague JJ, Orwin JF (2008) Legacies of catastrophic rock slope failures in mountain landscapes. Earth-Science Reviews 87: 1–38

Hungr O, Fell R, Couture R, Eberhardt E (Eds.) (2005) Landslide Risk Management, Amsterdam, Taylor & Francis, 776p

Jibson RW (2006) The 2005 La Conchita, California, landslide. Landslides, 3: 73–78

Kojan KL, Hutchinson JN (1978) Mayunmarca rockslide and debris flow, Peru. In: Voight B (Ed.) Rockslides and avalanches 1, natural phenomena, Elsevier, Amsterdam, The Netherlands, pp 316–361

Korup O (2002) Recent research on landslide dams – a literature review with special attention to New Zealand. Progr. Phys. Geog. 26: 206–235

Korup O (2004) Landslide-induced river channel avulsions in mountain catchments of southwest New Zealand. Geomorphology 63: 57–80

Korup O, Strom A, Weidinger JT (2006) Fluvial response to large rock-slope failures: Examples from the Himalayas, the Tien Shan, and the Southern Alps in New Zealand. Geomorphology, 78: 3–21

Korup O, Clague JJ, Hermanns RL, Hewitt K, Strom AL, Weidinger JT (2007) Giant landslides, topography, and erosion. Earth Planet. Sci. Lett., 261: 578–589

Lee CF, Dai FC, Deng GH (2004) A study of the 1786 Dadu River Landslide Dam in Sichuan, Southwestern China. In: Abdrakhmatov K, Evans SG, Hermanns RL, Scarascia Mugnozza G, Strom A (Eds.) Security of Natural and Artificial Rockslide Dams. NATO ARW Extended abstracts volume. Bishkek, pp 125–126

McSaveney MJ (2002) Recent rockfalls and rock avalanches in Mount Cook National Park, New Zealand, In: Evans SG, DeGraff JV (Eds.) Catastrophic landslides: effects, occurrence, and mechanisms, Geol. Soc. Am. Rev. Eng. Geol., 15: 35–70

McSaveney MJ, Davies TRH (2006) Rapid rock-mass flow with dynamic fragmentation. In: Evans SG, Scarascia Mugnozza G, Strom A, Hermanns RL (Eds.) Landslides from Massive Rock Slope Failure. NATO Science Series: IV: Earth and Environmental Sciences, Springer, 49, pp 285–304

Mitchell WA, McSaveney MJ, Zondervan A, Kim K, Dunning SA, Taylor PJ (2007) The Keylong Serai rock avalanche, NW Indian Himalaya: geomorphology and palaeoseismic implications. Landslides 4: 245–254

Pánek T, Hradecký J, Smolková V, Šilhán K (2008) Gigantic low-gradient landslides in the northern periphery of the Crimean Mountains (Ukraine). Geomorphology 95: 449–473

Philip H, Ritz J-F (1999) Gigantic paleolandslide associated with active faulting along the Bogd fault (Gobi-Altai, Mongolia). Geology, 27: 211–214

Plafker G, Eriksen GE (1978) Nevados Huascarán avalanches, Peru. In: B. Voight (Ed.) Rockslides and Avalanches v. 1, Elsevier, Amsterdam, pp 277–314

Poschinger AV, Haas U (1997) Der Flimser Bergsturz, doch ein warmzeitliches Ereignis? Bull. angew. Geol., 2: 35–46

Poschinger A von (2002) Large rockslides in the Alps: A commentary on the contribution of G. Abele (1937–1994) and a review of some recent developments, In: Evans SG, DeGraff JV (Eds.) Catastrophic landslides: effects, occurrence, and mechanisms, Geol. Soc. Am. Rev. Eng. Geol., XV, pp 237–255

Schuster RL (2002) Usoi landslide dam, southeastern Tajikistan, in: Proc. Int. Symp. on Landslide Risk Mitigation and Protection of Cultural and Natural Heritage, Kyoto, pp 489–505

Schuster RL (2006) Impacts of Landslide Dams on Mountain Valley Morphology. In: Evans SG, Scarascia Mugnozza G, Strom AL, Hermanns RL (Eds.) Landslides from Massive Rock Slope Failure. Proc. NATO Advanced Workshop, Celano, Italy, June 2002. Springer-Verlag, Dordrecht, pp 591–616

Scheko AI, Lekhatinov AM (1970) Current state of the Usoi Blockage and tasks of future studies. In: Materials of Scientific-technical meeting on the problems of study and forecast of the mudflows, rockfalls and landslides, Dushanbe, pp 219–223 (in Russian)

Shoaei Z, Ghayoumian J (1997) Landslide Dam in Iran, Mechanism and History. In: Proc. International Symposium on Engineering Geology and the Environment, IAEG, Athens, Greece, 23–27 June, 1997, pp 1043–1047

Strom AL (2004) Rock avalanches of the Ardon River valley at the southern foot of the Rocky Range, Northern Caucasus, North Osetia. Landslides 1: 237–241

Strom AL (2006) Morphology and internal structure of rockslides and rock avalanches: grounds and constraints for their modeling. In: Evans SG, Scarascia Mugnozza G, Strom A, Hermanns RL (Eds.) Landslides from Massive Rock Slope Failure. NATO Science Series: IV: Earth and Environmental Sciences, Springer, 49, pp 305–328

Strom AL, Korup O (2006) Extremely Large Rockslides and Rock Avalanches in the Tien Shan, Kyrgyzstan. Landslides 3: 125–136

Strom AL, Pernik LM (2006) Utilization of the data on rockslide dams formation and structure for blast-fill dams design. Italian Journal of Engineering Geology and Environment. Special Issue on Security of natural and artificial rockslide dams NATO ARW, Bishkek (Kyrgyzstan), June 2004: 133–136

Voight B (Ed.) (1978) Rockslides and Avalanches 1: natural phenomena. Elsevier, Amsterdam, 833p

Voight B (Ed.) (1979) Rockslides and Avalanches 2: engineering sites. Elsevier, Amsterdam, 850p

Voight B, Janda RJ, Glicken H, Douglass PM (1983) Nature and mechanics of the Mount St. Helens rockslide-avalanche of 18 May, 1980, Géotechnique 33: 243–273

Wang HB, Sassa K, Xu WY (2006) Analysis of a spatial distribution of landslides triggered by the 2004 Chuetsu earthquakes of Niigata Prefecture, Japan. Natural Hazards, 41: 43–60

Watson RA, Wright JrHE (1969) The Saidmarreh Landslide, Iran. Geol. Soc. Am. Inc., Sp. Paper 123: 115–139

Weidinger JT (2006) Predesign, failure and displacement mechanisms of large rockslides in the Annapurna Himalayas, Nepal. Eng. Geol., 83: 201–216

Whitehouse IE (1983) Distribution of large rock avalanche deposits in the central Southern Alps, New Zealand, New Zealand Journ. Geol. Geophys., 26: 271–279

Cultural Heritage and Landslides: Research for Risk Prevention and Conservation

22

Paolo Canuti, Claudio Margottini, Riccardo Fanti and Edward N. Bromhead

Abstract The impact of natural hazards on our cultural heritage represents an important theme, involving a multi-disciplinary approach. In case of landsliding, engineering geologists can play a key role, through the identification of relationships between soil and structures. This chapter starts from the large perspective of UNESCO Convention (1972), as a bird's-eye view of the general problem of heritage conservation, arriving at the presentation of a series of case histories from different countries. This varied approaches to the problem of landslides and cultural heritage reflects the multitudes of interests associated with this topics.

Keywords Cultural heritage • Natural hazards • UNESCO • Risk prevention • Conservation

22.1 Introduction

Cultural heritage represents the legacy of human beings on the Planet Earth. The various artefacts are evidence of thousand of years of human activity adapting their living conditions to the changing environment.

The United Nations Educational, Scientific and Cultural Organization (UNESCO) seeks to encourage the identification, protection and preservation of cultural and natural heritage around the world that are considered to be of outstanding value to humanity. This is embodied in an international treaty called the Convention concerning the Protection of the World Cultural and Natural Heritage, adopted by UNESCO in 1972.

According to the Convention, the following shall be considered as "cultural heritage": monuments (i.e. architectural works, works of monumental sculpture and painting, elements or structures of an archaeological nature, inscriptions, cave dwellings and combinations of features, which are of outstanding universal value from the point of view of history, art or science); groups of buildings (i.e. groups of separate or connected buildings which, because of their architecture, their homogeneity or their place in the landscape, are of outstanding universal value from the point of view of history, art or science); sites (i.e. works of man or the combined works of nature and man, and areas including archaeological sites which are of outstanding universal value from the historical, aesthetic, ethnological or anthropological point of view). This broad definition can be put into a list of typologies, as in

Paolo Canuti (✉)
University of Firenze, Italy

Claudio Margottini
Agency for Environmental Protection and Technical Services (APAT) Rome, Italy

Riccardo Fanti
University of Firenze, Italy

Edward N. Bromhead
Kingston University, UK

K. Sassa, P. Canuti (eds.), *Landslides – Disaster Risk Reduction*,
© Springer-Verlag Berlin Heidelberg 2009

Table 22.1 Selected types of cultural heritage (modified after the World Bank, 1994)

Main categories	Sub-types	Examples
Sacred sites	Burial sites	Xian, China Tomb Fields, Bahrain
	Sites of religious significance	Mecca, Saudi Arabia Jerusalem, Israel
Archaeological sites	Pre-historic sites	Altamira, Spain Lascaux, France
	Historical sites	Historic roads, bridges, dams, fortifications, and walls.
	Engineering and industrial sites	Marib Dam, Yemen The Great Wall, China
	Submerged or marine sites	Alexandria, Egypt Mahabalipuram, India
	Sites within biologically diverse areas or protected reserves	Tikal, Guatemala Sacred groves, Ghana.
Monumental sculpture	Cave sculpture	Indian Buddhist cave sites Chinese cave sites
	Architectural sculpture	Thebes, Egypt Petra, Jordan.
Monumental painting	Cave or wall painting	Tombs in Luxor, Egypt Tassili, Algeria.
Architecture and town planning	Monumental architecture	Monte Alban, Mexico Copan, Honduras
	Indigenous or vernacular architecture	M'zab Valley, Algeria Chitral, India
	Historic settlements and town centers	Quito, Ecuador San Gimignano, Italy
Historic landscapes	Cultural landscapes	Cres, Croatia Land of the Dogon, Mali
	Historic parks and gardens	Sigiriya, Sri Lanka Shalimar Gardens, Pakistan
	Trade routes monuments and remains	The Silk Route Pan-African trade routes

Table 22.1 from the World Bank, 1994, where some selected types of cultural heritage are catalogued.

In order to pursue the aims of the Convention, UNESCO has been providing since 1978 a list of properties forming part of the cultural heritage and natural heritage which UNESCO considers as having outstanding universal value in terms of a set of ten criteria. After the 31st Session of the World Heritage Committee (2007), the UNESCO's List includes 851 sites forming part of the cultural and natural heritage which the "World Heritage Committee" considers as having outstanding universal value. These include 660 cultural, 166 natural and 25 mixed properties in 141 States Parties. In particular, 378 of them are in Europe, 193 in Asia, 149 in Africa, 110 in America and 21 in Oceania, and this distribution mirrors the world dissemination of human civilizations. Also the list of most represented countries reflects this aspect: Italy (41), Spain (39), China (35), Germany (32), France (31), United Kingdom (27), India (27), Mexico (27) are at the top of this inventory.

A significant number of the above sites and remains are not in equilibrium with the environment. They are continuously affected by several factors (both natural and human) with rapid and slow onset. Figure 22.1 describes the main disrupting factors affecting cultural heritage (modified after the courtesy of J. Hamie, written comm.).

Among rapid onset natural phenomena earthquakes, flooding and landslides are the main causes of disruption to sites of cultural heritage. It is difficult to say the percentage of loss caused by any one type of phenomena but, whilst earthquakes and flooding affect a very large area and a significant number of monuments at the same moment, landslides act more locally, at the scale of the site, thus making statistical analysis rather complicated.

As an example, it is possible to say that among the Italian UNESCO sites documented in the World Heritage List, 25% of them are affected by mass movements, 54% by flooding and 82% by earthquakes with an intensity higher than the damage level. It is also evident that many sites are suffering from multiple hazards. However, as stated above, a comprehensive listing of heritage in danger is a difficult to discern: among the International Organizations, UNESCO itself, its Advisory Body ICOMOS (International Council on Monuments and Sites) and the World Monuments Fund (WMF) attempts this task, but has different ways of looking at the problem.

WMF, a private organization founded in 1965, works with local partners and communities to

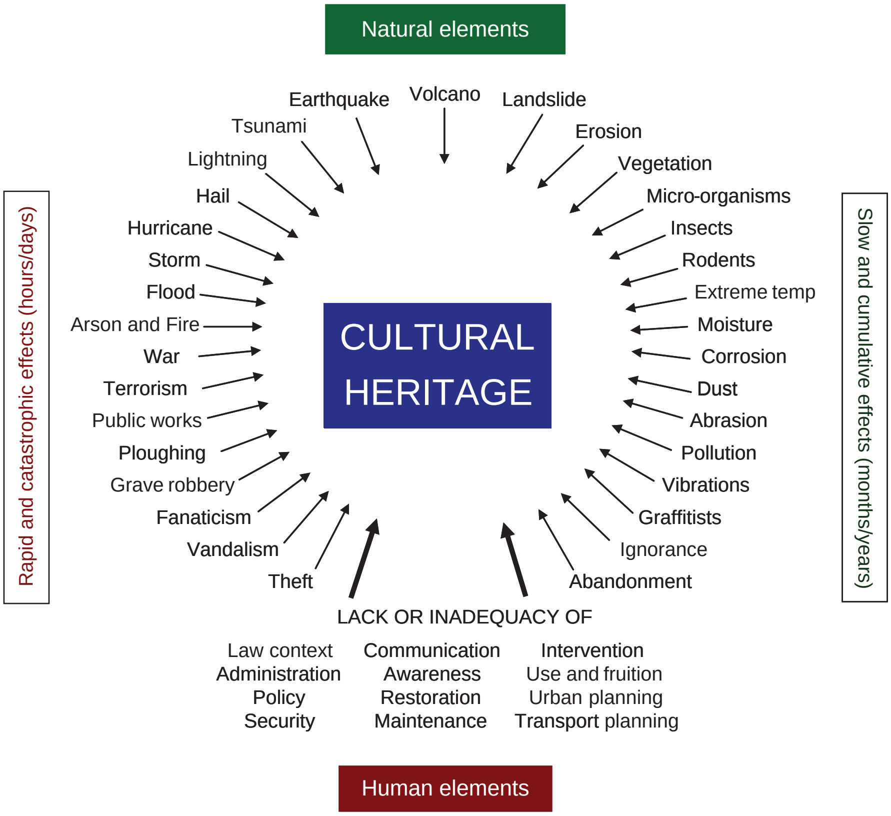

Fig. 22.1 Risk factors for Cultural Heritage (modified after Hamie)

identify and safeguard heritage through programs of project, planning, fieldwork, advocacy, grant-making, education, and on-site training. The main WMF initiative is the program World Monuments Watch and its biennial List of 100 Most Endangered Sites: since the Watch program was launched, 544 sites in 117 countries have been included on the List.

ICOMOS launched in 1999 the Heritage at Risk Program, which produced six reports between 2000 and 2007. The aim of these reports were to identify threatened heritage sites and monuments, to present typical case studies and trends, and to share suggestions for solving individual or global threats to cultural heritage. Each year an invitation is made to all ICOMOS National Committees, International Scientific Committees and ICOMOS' worldwide professional network, to provide short reports outlining risks in their country or area of expertise including case studies. Even if among the case histories there are some monuments and sites threatened by natural phenomena (earthquakes, flooding, landslides), the ICOMOS approach is mainly associated with restoration and conservation problems.

UNESCO's activity in this field has been derived directly from the World Heritage Convention. In fact, the Article 11 (4) states: "The Committee (of WHL) shall establish, keep up to date and publish, whenever circumstances shall so require, under the title of List of World Heritage in Danger, a list of the property appearing in the World Heritage List for the conservation of which major operations are necessary and for which assistance has been requested under this Convention. The list may include only such property forming part of the cultural and natural heritage as is threatened by serious and specific dangers, such as the threat of disappearance caused by accelerated deterioration, large- scale public or private projects or rapid urban or tourist development projects; destruction caused by changes in the use or ownership of the land; major alterations due to unknown causes; abandonment for any reason whatsoever; the outbreak or the threat of an armed conflict; calamities and cataclysms; serious fires, earthquakes, landslides; volcanic eruptions; changes in water level, floods and tidal waves".

Although the list of threats is very inclusive, UNESCO concentrates on particular cases: onslaught of urbanization policies and menaces to the wilderness conservation such as; wars and arson. The data of the List of World Heritage in Danger confirm this approach, especially if they are compared with the numbers of the World Heritage List. In the latter cultural properties dominate and Europe is the most represented region, whereas in the List of WH in Danger the distribution is reversed: African sites are at the top (Fig. 22.2) and natural sites form the greater part (Fig. 22.3). In addition, the List of WH in Danger is limited to 32 sites, considering the statement of Article 11.

These remarks on the UNESCO approach are confirmed by the comparison between the distribution of WHL sites and the global data on hydrogeological hazard (Fig. 22.4): Eurasian and South American sites represent the greater part of the World Heritage in Danger List, if landslides, avalanches and other natural hazards are considered as a matter of primary importance.

In the past UNESCO has highlighted some sensational cases, even though they did not enter the List of WH in Danger. For instance, 2002, when 10 World Heritage sites were threatened by massive floods sweeping across Central Europe: UNESCO activated a series of policy measures in order to prevent the risk of cultural heritage in Salzburg, Prague, Budapest and other cities. Also at a national level, the policies and the plans of conservation of

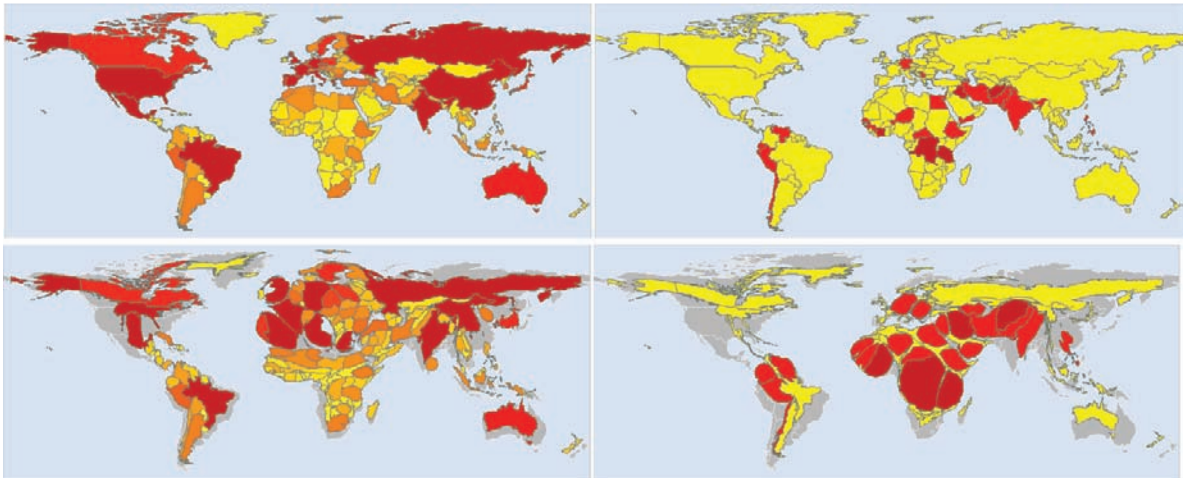

Fig. 22.2 Geographical distribution of the sites of UNESCO World Heritage List (*left*) and of UNESCO World Heritage in Danger List (*right*). Colour scales from *yellow* (*low*) to *red* (*high*). In the maps below, the data are represented by cartograms, highlighting the different weight of countries and areas. The cartograms have been realized with the MAPresso Prototype (Herzog, 2007), using the algorithms proposed by Gastner & Newman, 2004

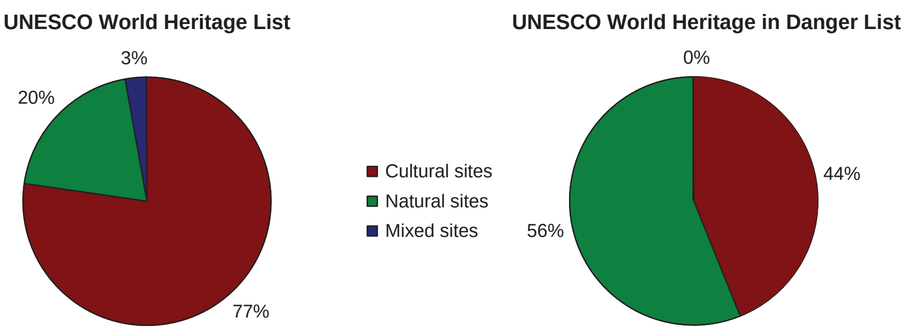

Fig. 22.3 Type distribution of properties documented in the UNESCO World Heritage List (*left*, 851 sites) and in the UNESCO World Heritage in Danger List (*right*, 32 sites) (data from UNESCO, 2008)

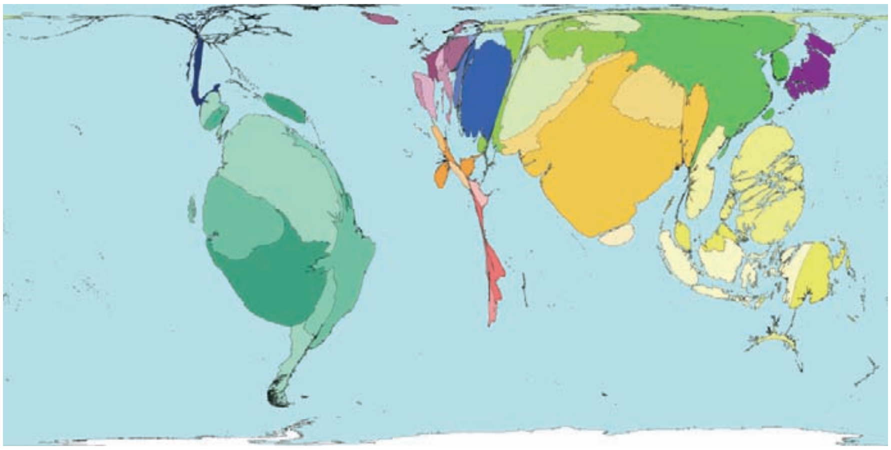

Fig. 22.4 Cartogram of number of fatalities from landslides and avalanches (1975–2000) (from Dorling et al., 2008 – see the Worldmapper website for details on this map and for other data and figures on natural disasters)

archaeological and architectural sites have been mainly oriented to reduce the impact of the human agents of deterioration, like urbanization, construction of public works, the use of the ground for agriculture or tourist management.

In general, the adopted measures to conserve cultural heritage from destruction via natural agents have been relegated to the background; even if natural processes, especially geological and geomorphological ones (sedimentation and erosional processes, debris and mud flows, inundations, landslides, fluvial dynamics), seriously affect the existence of the cultural heritage sites. In such cases emergency works are usually adopted. Nevertheless, the diagnosis of geological risk and the measures of conservation should be interrelated in order to recover cultural heritage sites and prolong their existence.

Within this framework, the conservation "in situ" is one of the main targets; for this reason the diagnosis of risk and the elaboration of measures of risk mitigation are the most important aims to preserve cultural heritage. From this point of view, landslides are a very interesting example: in fact, not only large and rapid movements can constitute a menace for heritage conservation, but also slow moving landslide activity or very small phenomena are able to destroy monuments or a site. Besides, it should be considered that some features are peculiar to landslides: in fact, they can present precursory phenomena or occur slowly, and this allows the planning of countermeasures. In these cases, the landslides can be considered as a predictable phenomenon and a remedy can be found: however, this requires a deep knowledge of landslide hazard and vulnerability of the elements at risk. This a multidisciplinary task that is not easy to achieve, but a very important one, in particular for cultural heritage.

Engineering geology contributes to this task, being the science devoted to the investigation, study and solution of the engineering and environmental problems which may arise as the result of the interaction between geology and the works and activities of human beings, as well as to the prediction of and the development of measures for prevention or remediation of geological hazards. From the above it is quite evident as engineering geology (in the widest sense of the term) is a major science for the protection of cultural heritage from environmental degradation and disruption.

This section introduces the case histories that constitute this chapter: they are examples of various problems from different countries, without the claiming to offer an exhaustive view on the topic. On the contrary, the presence of sites affected by small problems testifies the peculiarity of interactions between landslides and cultural heritage.

22.2 Landslide Process Activization on Sites of Cultural Heritage in Moscow, Russia

Valentina Svalova & German Postoev (IEG RAS Moscow, Russia)

In Moscow many cult and city constructions are located on coast of the river Moscow and, in particular, on the right high slope. The right coast of river Moscow on its significant extent is struck by deep block landslides with depth up to 90–100 m which formation occurred in preglacial time with basis of sliding in Callovian-Oxford clays of Jurassic system on 25–30 m below modern level of river Moscow. One of landslide sites is on Vorob'yovy mountains, on a high slope of the right coast of the river Moscow.

Within the limits of a considered site there is a historical monument of federal value “Andreevsky monastery”, based in 1648. It includes Resurrection cathedral (1689–1703), church of Saint Andrey Stratilat (1675), bell tower with church of Saint John Bogoslov (1748), being a monument of the Moscow baroque.

Also there the complex of buildings of Presidium of the Russian Academy of Sciences, constructed in 70– 80th years of 20-th century, bridge with station of underground “Vorob'evy mountain” and a sports complex are located. Landslide slope is in an active condition, and there are many attributes of activization of deep block landslide.

Another landslide site is in a southeast part of Moscow, occupying the right coast of river Moscow from museum – reserve “Kolomenskoye” up to station Moskvorech'e. The museum – reserve “Kolomenskoye” represents an imperial manor of XVI–XVII centuries, in which outstanding monuments of Russian architecture were kept (Figs. 22.5 and 22.6).

The greatest activity is shown with a slope in east part of a site, in area of an arrangement of city collectors. The slope in this place has height of 38–40 m. Motions of deep landslips have begun from 1960 in connection with construction of collectors. In 70th years of the last century there was a strong activization of a slope with formation of cracks by extent up to 500 m and displacement of a landslide in the plan over 1 m. Last serious activization of a landslide has taken place in 2002 with a motion on 53 cm.

Fig. 22.5 Museum – reserve “Kolomenskoye”

Fig. 22.6 The church of Beheading of the Honest Head of Iowan Predecessor near Kolomenskoye

Catastrophic activization of the deep blockglide landslide in the area of Khoroshevo in Moscow in 2006–2007, on the left-hand shore of the Moskva River, is threatening to the Holy Trinity Temple in Khoroshevo (monument of XVI century) and living houses (Fig. 22.7).

A crack of 330 m long appeared in the old sliding circus, along which a new 220 m long creeping block was separated from the plateau and began sinking with a displaced surface of the plateau reaching to 12 m. Such activization of the landslide process was not observed in Moscow since mid XIX century. The sliding area of Khoroshevo was stable during long time without manifestations of activity, though the height of the above-landslide scarp was critical, which indicated to its limit stability.

Fig. 22.7 Living houses in Khoroshevo

Landslide motions is extremely actual and difficult problem which decision is necessary for preservation of valuable historical monuments and modern city constructions. Mechanical models and system of monitoring of landslide processes are under elaboration.

22.3 Environmental Hazards: The Result of Engineering Geological Failures on Cultural Heritage

Jan Vlcko & Vladimir Greif (Comenius University Bratislava, Slovakia)

Outstanding cultural heritage, which is the evidence of our civilizations and the important source of memory, belongs to the mankind. Throughout the history, however, historical monuments have been suffering from natural and man-made disasters. The latter ones are closely connected with inadequate human interventions into geological environment. As a result a chain of slow long-lasting as well as abrupt and rapid, mostly negative environmental changes occurred in the rocks and soils, groundwater and the air.

The experience the authors gained during long-term investigations aimed at the preservation of historic town centers as well as historic sites of great value proved that the majority of damage to historic structures has been caused due to changes in the geological environment (foundation ground, subgrade) resulting from both the change of the stress distribution and the change of engineering properties of the soils and rocks triggered by:

– groundwater effects,
– natural geological hazards,
– dynamic effects,
– and static load effects.

As a result set of natural geological as well as man-induced geological hazards, posing a potential threat with either completely or almost identical consequences, was delineated. Between some of the hazards intricate interrelations may exist (e.g. landslides triggered by an earthquake, river erosion, and heavy rain or by undercutting the slope by a man). The mode of failure triggered by the non-catastrophic hazards can be attributed to differential settlement or to rotations accompanied with minor damage on historic monument (in complex structures such as medieval castles some parts may suffer from serious damage). Several examples can be found in Slovakia involving the UNESCO World Heritage sites as well (Vlcko, 1999).

22.3.1 Banska Stiavnica

The old medieval mining centre grew into a town with Renaissance palaces, 16th-century churches, elegant squares and castles. The urban centre blends into the surrounding landscape, which contains vital relics of the mining and metallurgical activities of the past.

The majority of historic buildings are founded on a soil consisting either of heterogeneous anthropogeneous sediments (fills, dumps, heaps) with unfavorable engineering geological properties, or of considerably altered pyroxene andesites with frequent discontinuities and fractured zones unfilled with mylonite or argillite.

The Holy Trinity Square, the most valuable architectural spot in Banska Stiavnica has a subterranean irregular network of old mine workings suffering from increased moisture and groundwater leakage from the water-bearing andesite rock mass despite the fact that restoration works on buildings located at the square had been carried out for several years. The most severe situation occurred at the Municipal Art Gallery (Fig. 22.8), where the

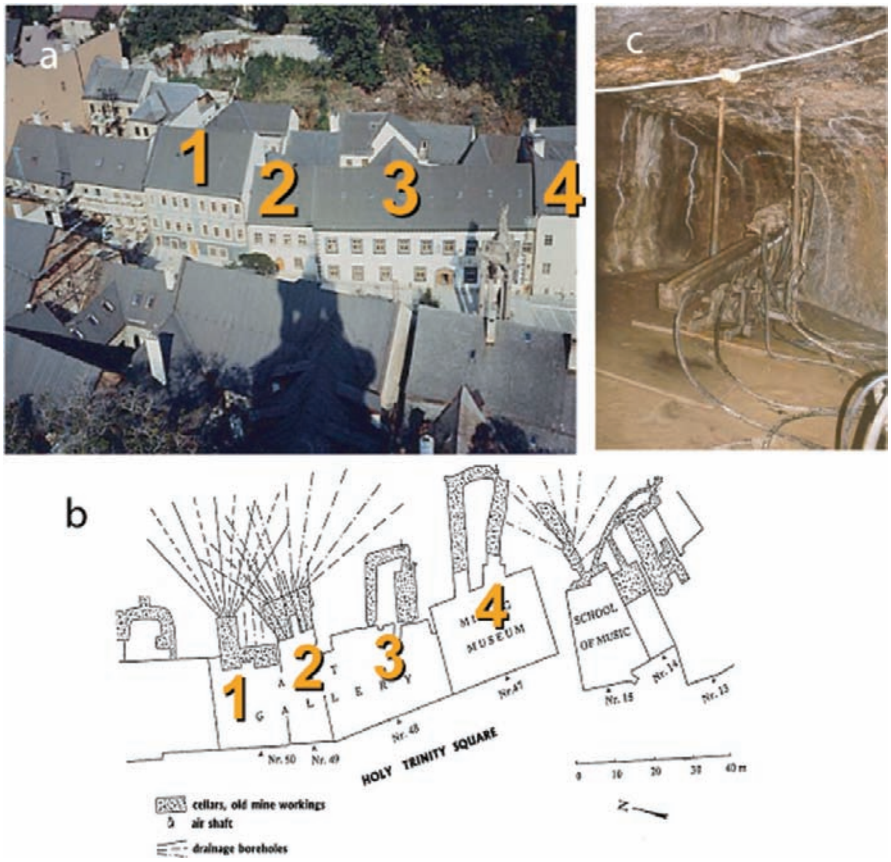

Fig. 22.8 Situation of the historic buildings endangered by ground water in Banska Stiavnica town (**a**), (**b**) and the drilling of the drainage boreholes in the basement of the Municipal gallery (**c**)

exhibition rooms and depositories strongly suffered by increased moisture. The intensity of leakage shows a direct dependence on precipitation. This process contributes to cellar walls damage, and it may bring about the deformation of the ground beneath the footings.

The study showed that the structural conditions of many buildings were rather poor with a need of extensive repair. In order to increase the strength of the foundation ground grouting was designed and implemented. This method on one hand secured the stability of the buildings; on the other hand in front of the buildings an impervious grout curtain was created, which had negatively affected the natural groundwater flow.

As a result several problems have arisen:

– drenching of the foundation ground through the rainwater percolation directly into the foundations,
– volume changes of foundation soils (particularly if they consist of cohesive soils such as argillites or clays),
– ultimate bearing capacity excess and differential settlement.

Considering the results of engineering geological investigation horizontal boreholes driven directly from old mine workings were recommended. To prevent the rain water percolation from the sloping back-door parts into cellars and old mine workings following works were proposed:

– Removal of the superficial soil from the sloping back-door parts.
– Filling in the discontinuities in the weathered and altered andesite bedrock with mortar and shotcrete.
– Usage of geosynthetics.
– Green design.

22.3.2 Spis Castle

Situated on a travertine rock 200 m above the surrounding land, at an elevation of 634 m, there is one of the most precious cultural monuments in Slovakia – the Spis Castle (Fig. 22.9).

Based on the results gained during the engineering geological investigation the destruction of the castle is affected by several geological and man-induced factors (Vlcko, 2004):

a) Lateral spreading caused by the subsidence of strong upper travertines into soft claystone strata fractured and separated the castle rock into several cliffs. At several places the wide, open discontinuities from the bedrock cross the castle walls and bring significant risk of failure and eventual collapse of the castle walls.

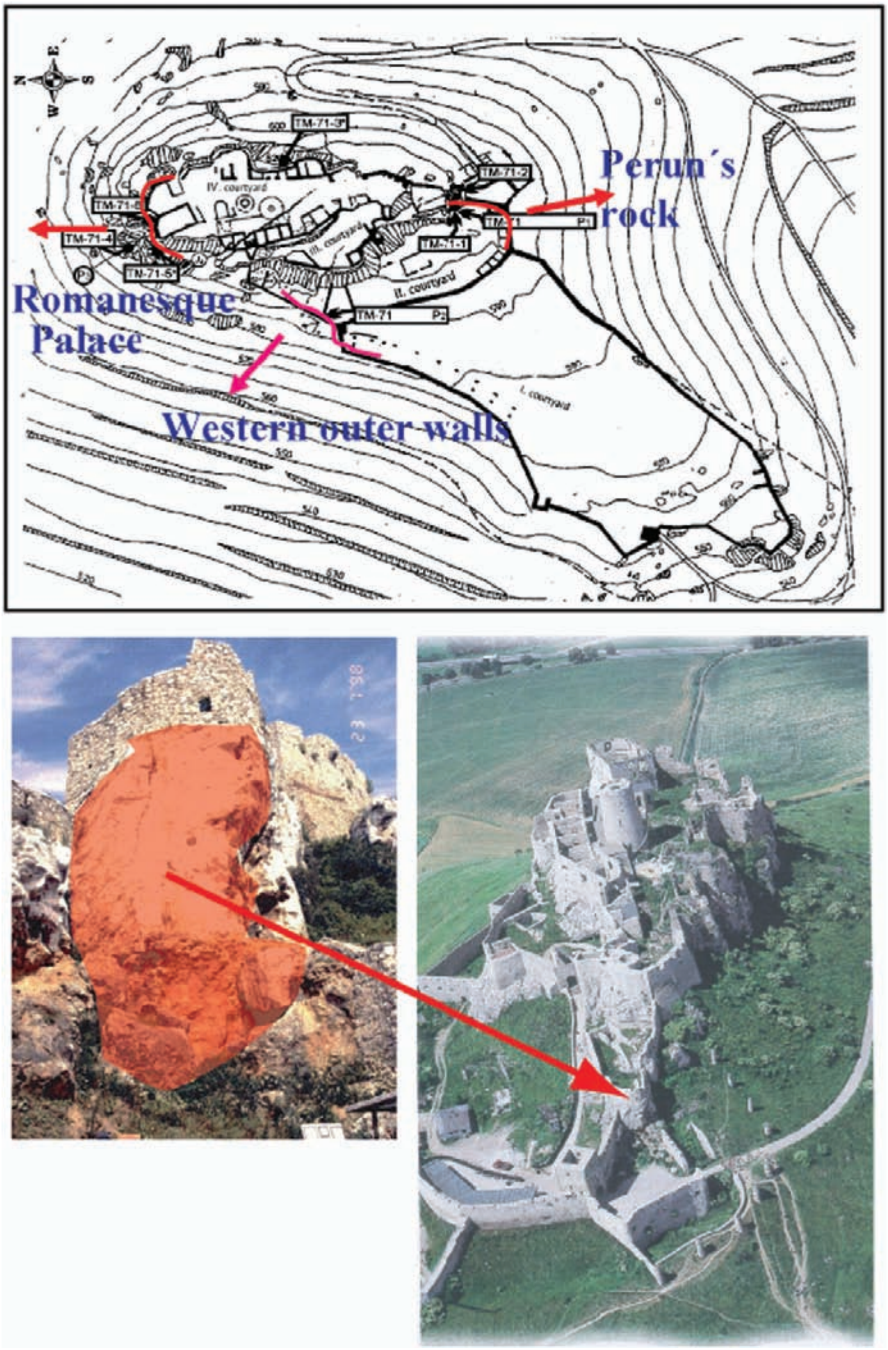

Fig. 22.9 Spis castle with the location of the Perun's rock exhibiting displacements due to the lateral spreading of the travertine rock mass

b) The results of the karst activity can be observed along lines of weakness such as fractures (joints, gravitational-tectonic lines) that are trigger points for the widening of open cracks (up to several decimeters) and further increasing permeability and softening of the bedrock to accelerate lateral spreading.

c) Weathering of the castle walls is a generally ongoing process that is affected by a number of factors. The original castle walls were constructed by mortaring travertine rubble. The mortar is not as resistant as the travertine to weathering and with time has experienced accelerated dissolution. The most intensive weathering of castle walls was observed at the contact between the stonework and the subgrade. At places along this contact the stonework has dripped off resulting in the development of overhangs.

d) The contribution of seismicity to the deterioration of the castle stonework cannot be discounted even though the area has been assigned to 6° MCS with the Slovak Standards Seismic Loading on Buildings. The presence of NS neotectonic faults between the Branisko Mountains and the

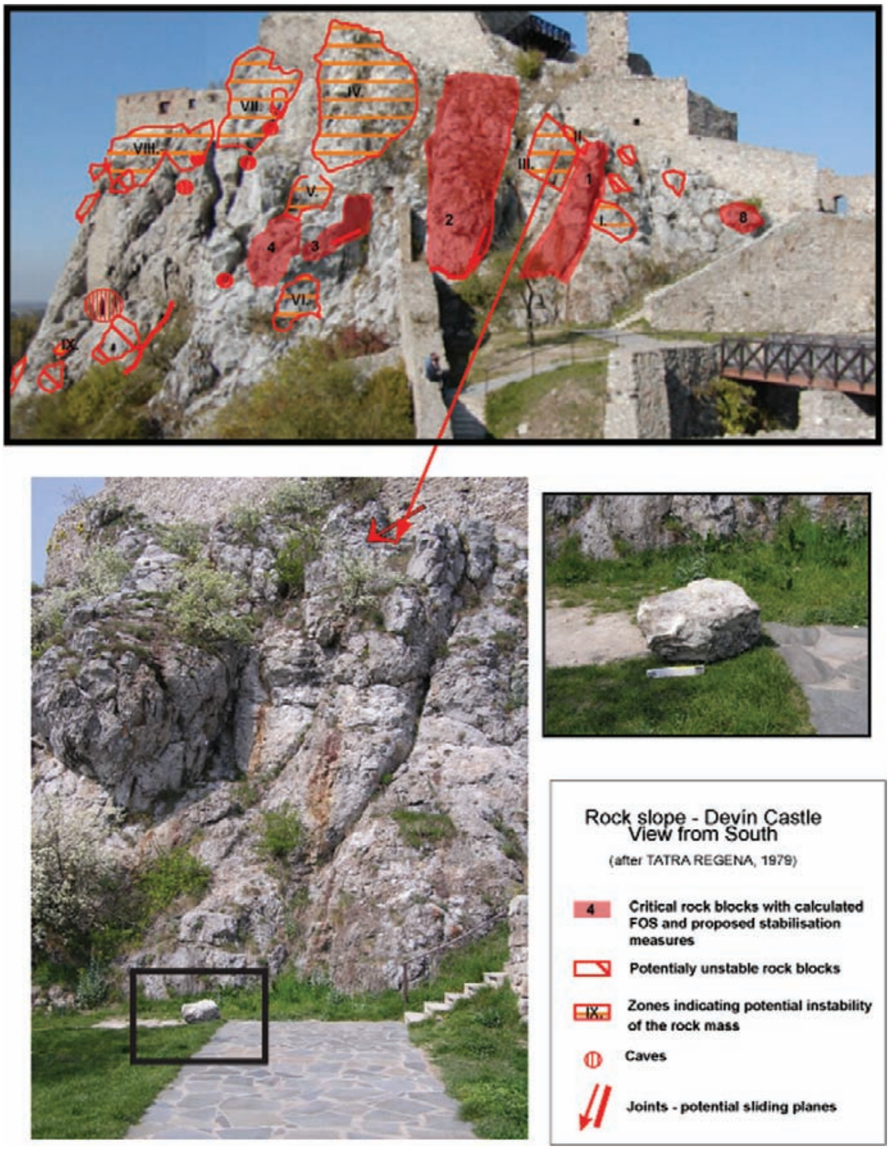

Fig. 22.10 Southern slope of the Devin castle with the marked unstable zones and critical blocks (*up*). A block fallen from the rock face in April 2007 (*down*)

Hornádska kotlina Basin further emphasizes the potential importance of seismicity but direct historical earthquake evidence is absent. Finally, lateral spreading and the rate of movement has likely been influenced since 1900 by travertine extraction at the nearby Drevenik quarry.

The results of the engineering geological investigation indicated that:

- The most intensive damage on castle walls occurred at the intersection of the main gravitational tectonic lines and in places where moving cliffs occur
- The weathering of the stonework and the underlying rocks as well as the widening of open cracks by karst processes are sources of potential instability
- Past earthquakes and other seismic effects (blasting) in a nearby quarry could promote creep movement
- The slope stability analysis gained by photogrammetric survey and joint set evaluation proved that attention has to be paid to travertines up to the depth of 4 m where they are strongly weathered and jointed.

22.3.3 Devín Castle

Devín Castle standing on a massive limestone – dolomite rock hill above the confluence of the Danube and Morava Rivers is an unusually impressive landmark. Due to several gravitational-tectonic lines the rock body is separated into huge blocks showing differential instability (Fig. 22.10). To detect early indications of catastrophic rock fall a real-time monitoring was adopted, slope stability calculations and geotechnical stabilization was recommended.

22.3.4 Conclusions

During the past decades UNESCO and many other international partners have been deeply involved in the restoration, preservation and maintenance of seriously damaged cultural property. This provides a unique opportunity to strengthen the cooperation between relatively diverse disciplines (human, technical and natural). The common goal of the disciplines involved in the process of safeguarding historic monuments is the identification of relevant factors causing damage to historic structures and the design of effective preservation and protection works which will perform their protective function throughout the lifetime of the historic structure.

This work was supported by the Slovak Research and Development Agency under the contract No. APVV-0158-06, Ministry of Education – Vega grants N. 1/0499/08 and N. 1/4045/07.

22.4 Effects of Landslides on Machu Picchu Cultural Heritage

Paolo Canuti (University of Firenze, Italy) & Claudio Margottini, Daniele Spizzichino (APAT, Italy)

22.4.1 Introduction

The scope of the present work is to provide a possible interpretation of the deformation patterns of archaeological structures and buildings from the geological and geomorphological perspective by highlighting the causal link between natural geomorphologic and anthropogenic processes (e.g. local subsidence, underground caves, structural deficit or deformation patterns due to past seismic activities). The main input to such interpretation was provided by the census activities of the whole structural conditions of the citadel, realized during the last three fields of survey (2003, 2004 and 2005).

A detailed vulnerability and damage data sheet for archaeological exposed elements has been built during the study. All the data collected have been analyzed through processing techniques (vectorial intersection and spatial analysis). The analysis of damage and vulnerability has been put in relation to exposed element positions versus potential landslides map. The main purpose of this work is to provide basic data and geological and geomorphologic evidence to support the above theory.

A damage/vulnerability map was developed through the following steps: i) synoptical reading of a multi layer project implemented on a GIS platform; and ii) provision of building typologies (exposure) including their tensional and deformation paths (vulnerability) and the morphological view of the area.

22.4.2 General Setting of the Archaeological Site of Machu Picchu

The monumental complex of Machu Picchu (Lat. 13° 09' South, Long. 72° 31' West), designated by UNESCO as World Heritage Site in 1983, was discovered on 24 July 1911 by Hiram Bingham, an American historian and professor of archaeology at Yale University. Although the citadel is only 80 km far from Cuzco in line of air, the whole site was never found during the Spanish conquest; the detail is important to understand the particular shape and geographical asperity of the area.

The archaeological site is indeed located on the crest of two mountains, 2430 m.a.s.l., with the Urubamba river at its foot in a very inaccessible zone of Andean forest.

All the theories provided so far are based on studies and archaeological discoveries but there are no historical sources which provide information as to what happened in the "Lost City". Actually, the site is affected by geological risk due to frequent landslide phenomena that threaten security and tourist exploitation. In the last years, the landslide scientific community has promoted a multi disciplinary joint programme for the monitoring and control of superficial deformation, with remote sensing techniques and field survey analysis to define the typology and magnitude of potential landslides. During the last geological field surveys it was possible to reconstruct in detail the geological model of the area.

22.4.3 Geological Setting

The area is characterized by granitoid bodies that had been emplaced in the axial zones of the main rift system that are now exposed at the highest altitudes, together with country rocks (Precambrian and Lower Paleozoic metamorphics) originally constituting the rift "roots" (Carlotto et al., 1999). The Machu Picchu batholith is one of these Permo -Triassic granitoid bodies. The bedrock of the Inca citadel of Machu Picchu is mainly composed by granite and subordinately granodiorite. This is mainly located in the lower part of the slopes (magmatic layering at the top). Superficially, the granite is jointed in blocks with variable dimensions, promoted by local structural setting (Mazzali et al., 2005).

The dimension of single blocks is variable from 10^{-1} to about 3×10 m^3. Soil cover, widely outcropping in the area, is mainly composed by individual blocks and subordinately by coarse materials originated by chemical and physical weathering of minerals. Part of the slopes exhibit debris accumulation as result of landslide activity. Grain size distributions of landslide accumulation are closely related to movement types and evolution.

Talus and talus cones are composed by fine and coarse sediments, depending from local relief energy. Alluvial deposits outcrop along the Urubamba River and its tributaries. They are composed by etherometric and polygenic sediments, that may be in lateral contact with the talus deposits. Anthropic fill and *andenes*, on top of Citadel, reflect the work of Inca activities in the area (Fig. 22.11).

22.4.4 Geomorphological Setting

The general morphological features of the area are mainly determined by the regional tectonic uplift and structural setting. As consequence, kinematic conditions for landslide type and evolution are closely depending on the above factors. Several slope instability phenomena have been identified and classified according to mechanism, material involved and state of activity. They are mainly related to the following: rock falls, debris flows, rock slides and debris slides.

The area of the citadel has been interpreted as affected by a deep mass movement (Sassa et al. 2001, 2002) that, if confirmed by the present day monitoring systems, it could be referred to a deep-seated gravitational slope deformation

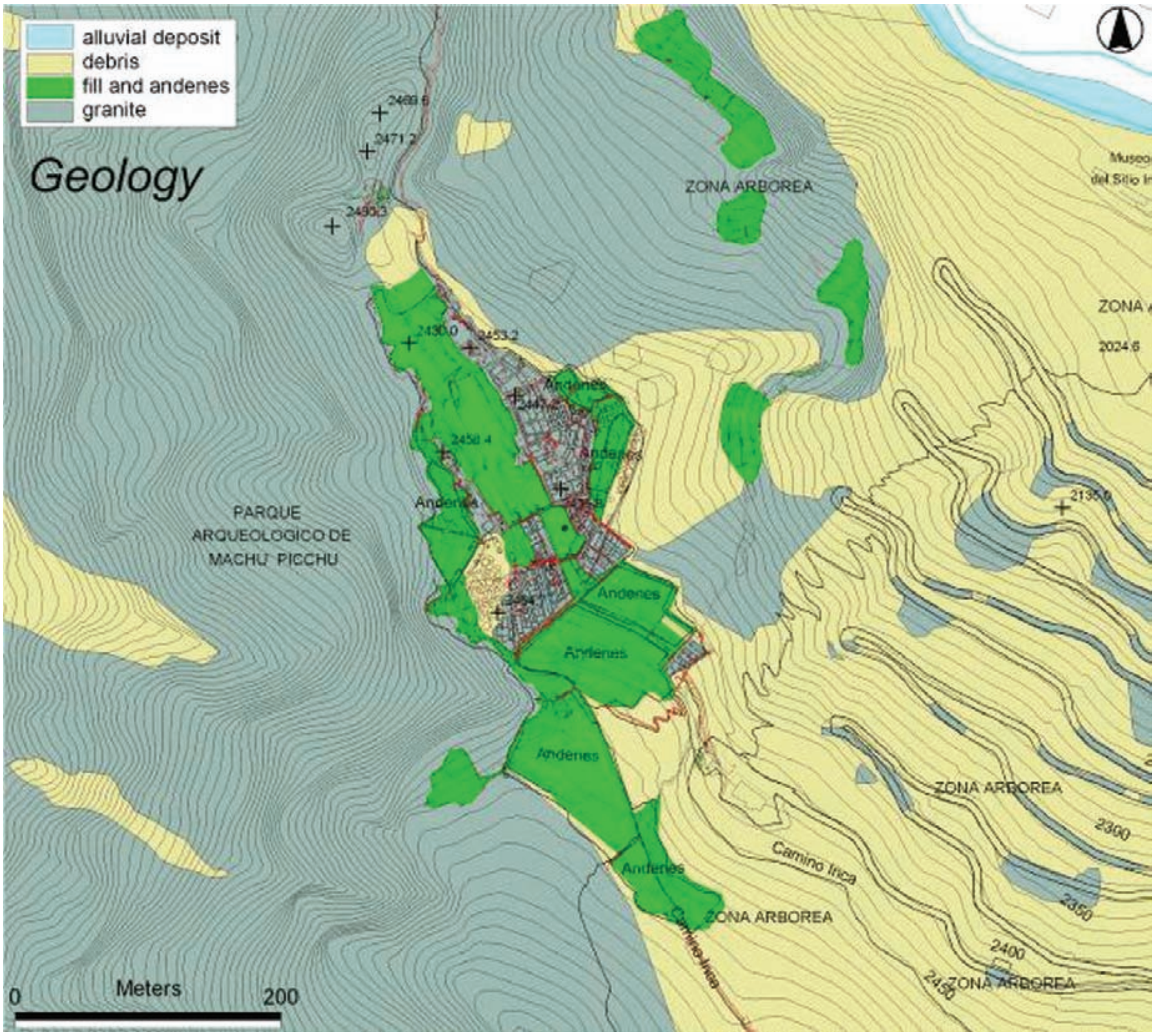

Fig. 22.11 Sketch of local geological map of the Inca citadel of Machu Picchu (by Canuti et al., 2005)

(DSGSD), probably of the type of the compound bi-planar sagging (CB) described by Hutchinson (1988).

A main trench with NW-SE trend, related to a graben-like structure, is located within the archaeological area and supports this hypothesis. Other trenches are elongated in the dip direction of the slope. Rock slides and rock falls may produce blocks with dimension variable from 10^{-1} to 10^{2} m^{3} (Carreño & Bonnard, 1997).

Debris produced by rock slides and rock falls, as well as from weathering processes is periodically mobilized as debris slides and debris flow. Debris slides and debris flows are characterized by an undifferentiated structure varying from chaotic blocks immersed on coarse sand matrix. The grain size distribution is mainly depending on the distance from the source areas and slope angle (Casagli et al., 2005).

Finally, it is interesting to notice, on the NE side, the presence of a large debris accumulation, just below the citadel, presently being eroded by all around dormant slides. The accumulation it is probably the result of an old geomorphological phenomena now stabilized, still not clear in its original feature. Anyway, the mass movements occurred certainly before the Inca settlement since some of their terraces ("*andenes*"), are founded over this accumulation area.

22.4.5 Exposure, Vulnerability and Damage of Cultural Heritage

The concept of value during exposure and damage analysis cannot be merely applied to Cultural Heritage (CH) due to their singularity, peculiarity and unrepeatability. In addition, the assessment of the damage severity based on money refund for restoration can be difficult to estimate due to the impossibility, in most of cases, to reproduce the original features of the damaged element (Delmonaco et al., 2004).

Vulnerability as usually defined as the degree of loss on an element or group of elements at risk, resulting from the occurrence of a natural hazard (landslide) of a given intensity (Varnes et al., 1984). Usually the vulnerability is expressed in a scale from 0 (no loss) to 1 (total loss) and is a function of the landslide intensity and of the typology of the element at risk $V = V(I;E)$.

In practical terms the vulnerability is expressed by the link between the intensity of the landslide and its possible consequences. Formally, the vulnerability may be expressed in terms of conditioned probability (Einstein, 1988): $V = P\ (damage \mid event)$; namely by the probability that the element at risk is prone to a certain degree of damage under the occurrence of a landslide of a given intensity. In the same time the vulnerability should consider also an assessment of the damage severity.

22.4.6 Methodological Analysis for Vulnerability Assessment

The vulnerability assessment of an exposed element may be performed through the analysis of damage of an element with same structural characteristics affected by a given landslide type with the same intensity. The methodological process should consider the following steps:

1. definition of the localisation of the element at risk; historical and/or direct analysis of damage of the element at risk, in correlation with different landslide typologies with different intensity;
2. intensity/damage analysis of classes of elements at risk characterised by the same building/structural typology;
3. implementation of a vulnerability function depending on each class of exposed elements with respect to minimum/maximum expected landslide intensity.

22.4.7 Methodology for the Analysis of Static-Structural Conditions of the Site

For each typology of element at risk a value of damage has been defined, after the stage of inventory and filing of a field survey catalogue (Fig. 22.12). The field catalogue for the survey of the static-structural conditions of CH exposed at landslide risk has been derived from similar experiences carried out for the assessment of seismic vulnerability/degree of damage. In particular, the following parameters have been adopted:

- geometric properties of the CH in terms of height and wall thickness, in order to correlate these data with e.g. the impact force of fast slope movements;
- presence of restoration works, useful to understand past damage and, as well, the present capability to resist to a landslide with a given intensity;
- presence or absence of coverage is a fundamental parameter to understand the impact of weathering on structures;
- presence of cracks in order to reconstruct damage derived from the interaction between structure and soil;
- analysis of active strain processes (i.e. sinking, swelling, tilting) and degradation (i.e. humidity, decreasing of resisting sections) sub-divided into vertical and horizontal elements;
- classification following the main building typologies and their static-structural characteristics.

22.4.8 Conclusion

The damage and vulnerability data collected for the citadel have been mapped with the use of GIS techniques and then connected by geomorphological dynamics and processes acting on the area (Fig. 22.13).

Fig. 22.12 Examples of cracks collected in the archaeological structures and buildings

A preliminary good relation between retrogressive phenomena on the NE portion of the citadel and deformation patterns along the archaeological builds has been achieved by mapping a first damage catalogue with evidence of tension cracks, patterns, caves and superficial deformations.

All the collected data and their interpretation should be helpful for the future development of the research activities so as to promote a landslide hazard and risk assessment, a stability model along a schematic profile (Fig. 22.14) and the design of low impact mitigation measures for the entire archaeological site.

Acknowledgments The investigation team was highly supported by the INC for the collection of exposure and vulnerability data. We are grateful to the INTERFRASI project team for their assistance in the filed survey and special thanks go to Dr. Luca Falcon and, Dr. Giuseppe Delmonaco for their helpful cooperation to the investigation and to Ilaria Basile and Chiara Gasponi for their work on the collection of data sheets and their analysis.

22.5 Risk Mitigation from Landslides for Cultural Heritage in Umbria Region: Some Applications

E. Martini, M. Cenci, L. Tortoioli, P. Tamburi (Regione Umbria, Italy) & D. Salciarini, P. Conversini (University of Perugia, Italy)

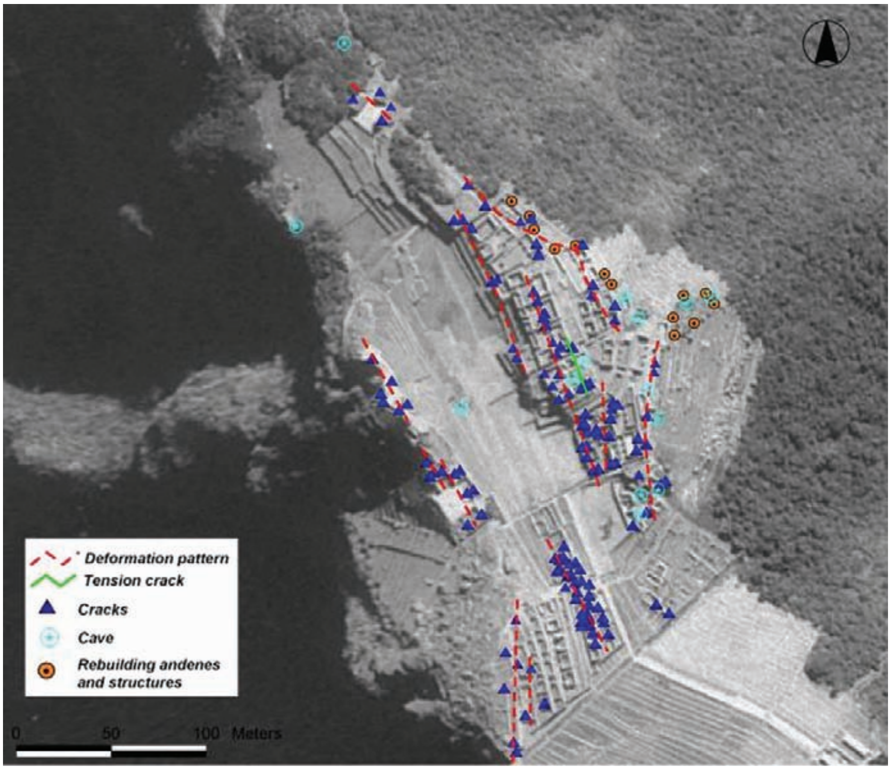

Fig. 22.13 Deformation patterns, tension crack, rebuilding *andenes* and structures and cave existing on the Machu Picchu Citadel

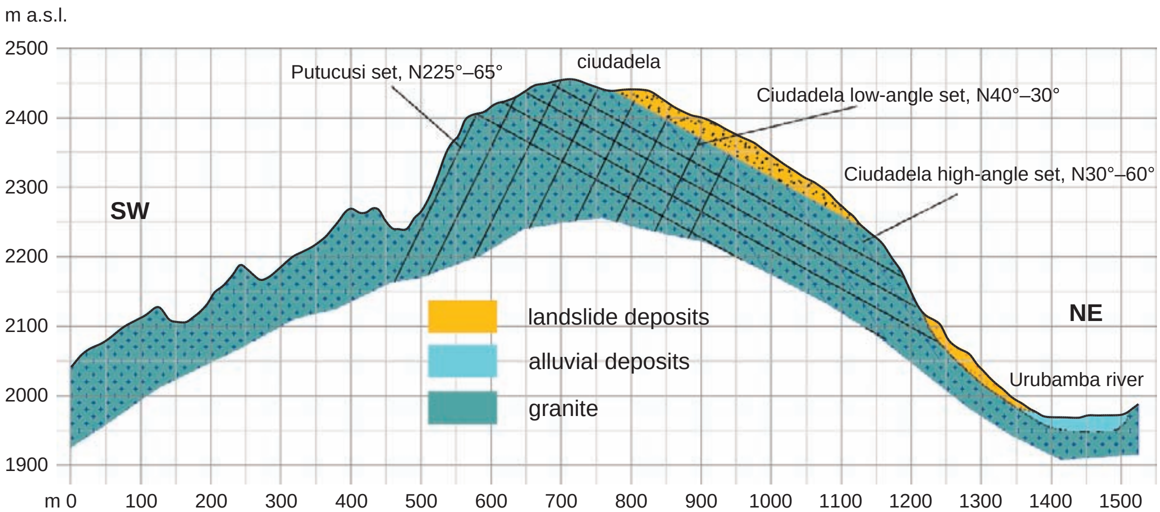

Fig. 22.14 Schematic profile for the implementation of stability model

22.5.1 Introduction

Umbria is the green heart of Italy and the wealth of natural and artistic wonders of this Region seems almost inexhaustible.

The risk related to landslides and hydrogeological instabilities is prevalently due to the historic development of the towns around castles, towers or medieval villages situated at the top of hills, as well as to the natural erosion increased by the land urbanization of the hillsides (Melelli and Venanti, 2007).

For this critical situation Region and Government were obligated to intervene for the private and public safety by approving 41 laws to consolidate unstable towns.

The *Hydro-geological assestement Plan* of Tevere River basin (PAI – *Piano per l'assetto idrogeologico*), in order to protect present and future residential and infrastructural activities from risk, identified 174 sites for landslides characterized by really high (R4) and high risk (R3).

This Plan represents the main tool for territorial planning and it is finalized to establish conditions that guarantee equilibrium and compatibility between hydro-geological dynamics and growing anthropogenic pressures on the land.

In this panorama, a lot of identified sites concerns sacred and archaeological sites, as well as historic settlement and town centers, among the others:

1. Orvieto, Pale and Rocca Ripesena (historic settlements and town centers);
2. S. Eutizio (sacred site);
3. Marmore Falls and Spoleto town (archaeological, historic settlements and town center).

22.5.2 Orvieto Town and Rocca Ripesena

"*Yesterday and today crucial moments [. . .] arrived at Orvieto, sited like Salzburg Castle, you ascend with the funicular from the station. City of solid stone, multi-coloured Duomo! Etruscan tombs, bought antique objects, enchanting view [. . .] Orvieto superb [. . .] Health very satisfying*". This is what Sigmund Freud wrote about Orvieto to his sister Martha on a postcard from Bolsena dated 9 September 1897.

Orvieto is situated on the borders between Umbria, to which it belongs, Tuscany and Latium. Built on the top of a steep cliff of tuff, it has always been a majestic and fascinating city (Fig. 22.15). Its strong points are, indeed, its central position and the fact that it is a small city of art on a human scale. It has been one of the most important Etruscan cities. The Middle Ages and the Renaissance have determined the city most salient characteristics.

Fig. 22.15 Orvieto, Cannicella landslide, 1977

Orvieto is sited at the top of an ellipsoidal tufaceous rock plateau, rising above the alluvial plain of the River Paglia in the Province of Terni. The geological formation of the hill is formed of a bottom layer of Pliocene marine clay covered by a series of fluvial-Iacustral rings made up of sandy, clay and volcanic sediments, topped by the tufa of the Orvieto cliff.

Orvieto town in the 1937 was included in Italian State Inventory of city needing consolidation works. From 1972 (Regione Constitution) Regione Umbria faced the Orvieto landslides through new and deepened studies, in collaboration with the National Research Council and University.

After a landslides in the *Gonfaloniera area* in 1972, near the hospital in 1977, and in the *Cannicella area* in 1979, the Umbrian regional authorities carried out a number of consolidation projects to prevent or reduce the risk of further landslides, relining the water and sewerage network, waterproofing and relaying roads, fixing and anchoring the tufa walls, re-facing and restoring the walls by the cliff, draining and readjusting the upper edge and the foot of the cliff, repairing the ditches that descend towards the valley, draining the landslides along the slopes and reinforcing all the unstable caves and grottoes (Fig. 22.16).

An "*Observatory*" has been set up to monitor and maintain these interventions and the reinforced areas. It uses a complex system of geotechnical instrumentation to monitor how the situation evolves and carry out any subsequent maintenance work required on the cliff and slopes.

The monitoring net is costitued by extensimeters, inclinometers, a geodetic net and piezometeres (Fig. 22.17).

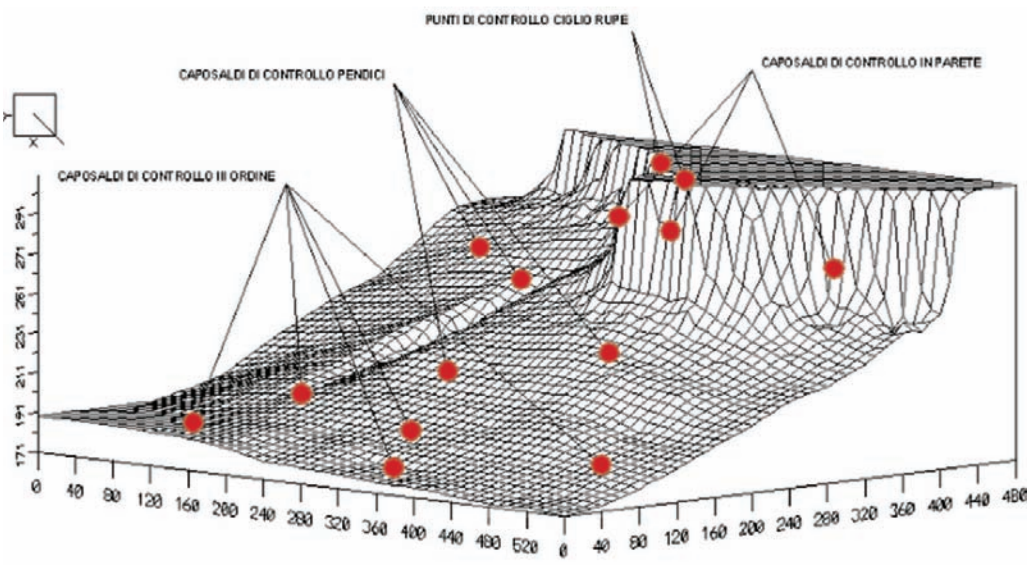

Fig. 22.16 Schemes of geothecnical monitoring net in Orvieto

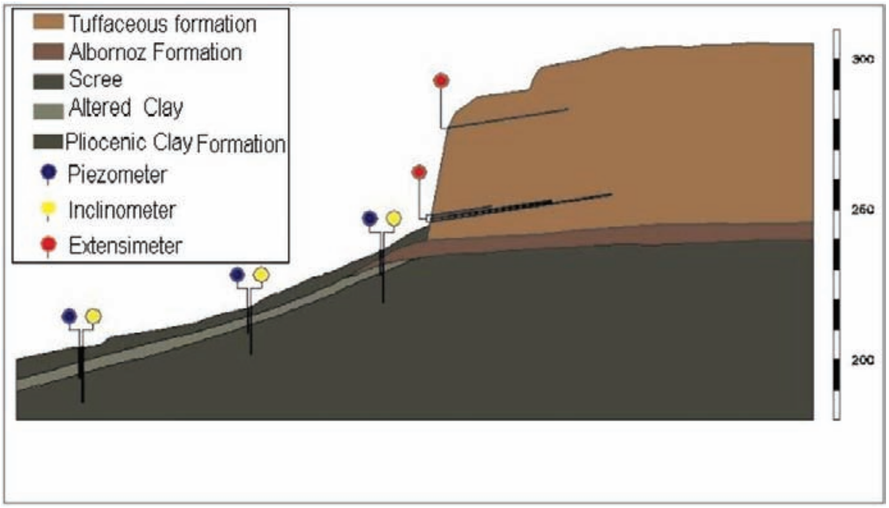

Fig. 22.17 Geology of Orvieto cliff and the monitoring net

22.5.3 Pale Village (Foligno, Perugia)

Pale is located on the right hand side of the Menotre River, at the foot of the calcareous mountain termed as Sasso di Pale.

During the XIV century, in this village growed up an important paper mill, thanks to the richness in water and so in energy. The first printed version of the Dante's Divina Comoedia was printed in Foligno (Perugia) on the paper coming from the Pale's industry.

After the heavy earthquake of 1997, many rock-fall processes occurred along the travertine cliff, on the west side of the village. Due to these events, all the houses situated in proximity of the edge of the cliff lied in a really high risk situation (Fig. 22.18).

The countermeasure works realized, related to the consolidation of the cliff, were:

– unstable rocks removing;
– anchoring of the cliff, by 5 m nails arranged in a grid of 1 m step;

Fig. 22.18 Pale: the house over the cliff

– deep anchoring of the cliff, with a grid of 4 m step;
– sub-horizontal drainage.

22.5.4 The St. Eutizio Abbey

The Saint Eutizio Abbey was founded in the 5th century by the syrian monks who were the spiritual father of San Benedict. Nearby there are the Hermits Caves with an enchanting trail that leads to Norcia. In this Abbey the Precian surgery school was founded, and it constitutes one of the first surgery school of the world.

The Abbey is built on the foot of a travertine formation.

After the 1997 earthquake, the incremented risk of rockfall needed prevention and protection designs for the risk reduction.

The countermeasure works realized were (Fig. 22.19):

– unstable rocks removing;
– anchoring of the cliff, by nails;
– digging of a well with a diameter of 3,4 m and 14 m depth;
– anchoring of the cliff to the well;
– hydraulic works.

22.5.5 The Marmore Falls

Marmore Falls, with its astonishing beauty, comes into view as a roaring water column divided into 3 falls, covering a drop of 165 m which wraps up the luxuriant vegetation into a cloud of white foam. The breath-taking scenery is the result of over two thousand years of work by the part of man who, from the beginning of the Roman period, tried to canalize the waters of the Velino river to them flow into the Nera river.

Its history began in 271 BC., when the Roman consul Manlius Curios Dentato did a land reclamation of the Reatina Plain creating a channel of over 2 km which ended at the edge of a cliff.

During the last twenty years of the XIX century, the Falls became, for the growing industry, a regulation instrument of the hydroelectric system for energy purposes, and the use of its waters for industrial purposes predominates on the naturalistic, intellectual and tourist conntations.

The Marmore Fall is included in the hydro-geological Plan of Tevere river basin, as one of the most dangerous areas. Due to the geological and geomorphological particular character of the area, it needs constant control activity, landslide reclamation and constant maintenance.

Regione Umbria decided to reinforce the mountain ridge by realization of 11 elliptic wells of 5 × 9 m, 30 m deep. On the wall of the wells were fit in some tie-beams made of "*Dywidag*" bar with iron plate, they are allocated in 9 series, each one made of a halo of 13 tie-beams.

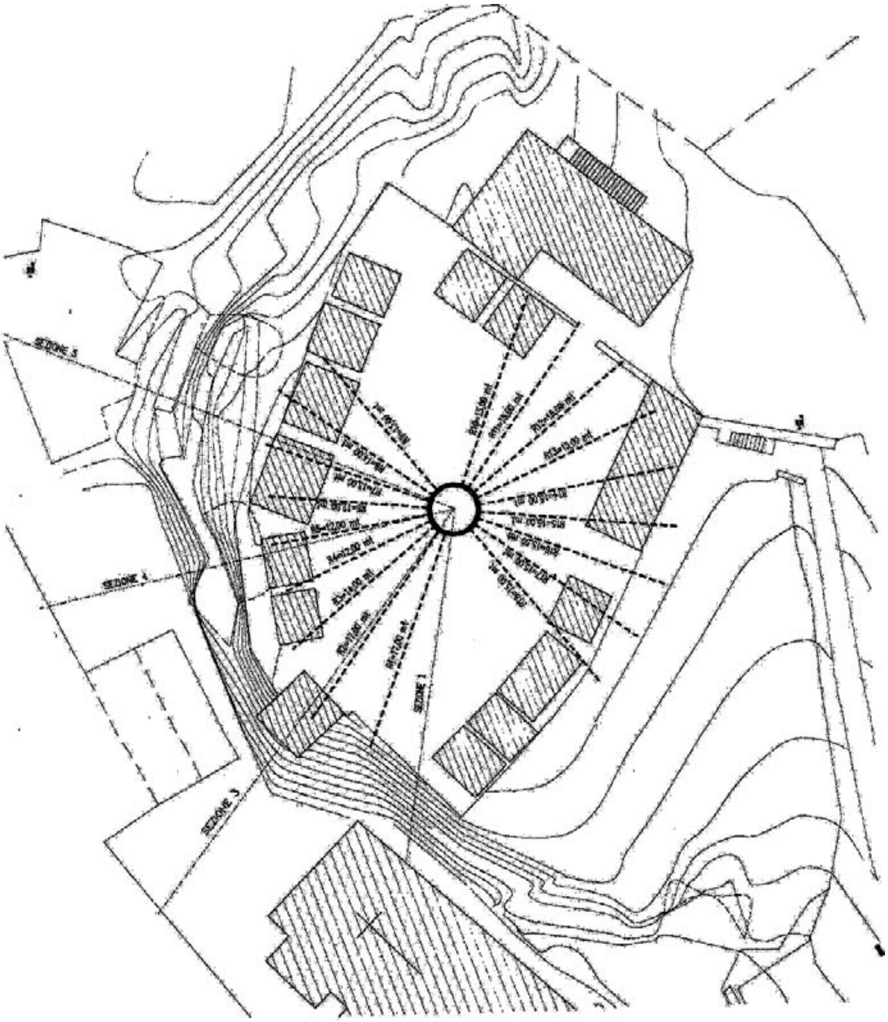

Fig. 22.19 Anchor well: project

At this moment, it has been realized 9 wells on the right part of the fall.

Moreover, on the left side of the river (*Campacci resort*) it has been realized works for consolidation, development of the public parks and was built a panoramic way. It was developed a real time monitoring system for verifying the safety condition.

22.5.6 The "Giro dei Condotti", Spoleto town

The *Giro dei Condotti* area is classified as SIC – *Site of European Community Importance*– and it lies in front of Spoleto Town, a typical mediaeval city, also known for the Festival dei Due Mondi. The area is connected to the town by the Tower Bridge (Ponte delle Torri), which wondered Goethe during his Italian Journey.

The Giro dei Condotti, a small footpath created for the water-pipeline maintenance works, is classified as really high risk site for rockfalls.

During 2003 some rockfalls caused the temporarily closing of the footpath, that was redeveloped after removing the blocks.

During 2004 a similar event occurred, consequently the planning for risk reduction started, involving 1,3 km of footpath between the bridge and the S. Leonardo Hermitage.

The site is characterized by a vertical 30 m high cliff 60 m over the footpath level.

Due to this characterizations, and to the artistic and natural conditions, it is complicated finding suitable risk mitigation works that minimize the perturbation of the high environmental and artistic characterization of the heritage.

22.6 Support of Poliphimos Cave in Maronia (Thrace, Greece)

B. Christaras, A. Dimitriou, N. Chatzigogos, Th. Chatzigogos, Th. Makedon, D. Vogiatzis, S. Filippidis, (University of Thessaloniki, Greece) & E. Moraiti (IGME, Greece)

22.6.1 Introduction

Poliphimos Cave is an under development site for touristic purposes. The cave is full of beautiful stalactites and stalagmites and it is of great palaeontological and touristic interest. In the present paper the stability conditions were studied regarding to wedge and planar failures. For this purpose, all the tectonic data were determined and recorded separately for each site in the cave and tectonic and stability diagrams were elaborated, in order to determine stability factors.

The main purpose, after determining any type of potential failure, was to propose the more appropriate stability methods. It is obvious that supporting methods have to be adapted to the safety of visitors and the monumental character of the cave.

The cave is located in a distance of 5 km from Maronia Town, near Komotini City, in Thrace – Eastern Greece. It is considered as an important natural monument which unfortunately has not already developed. According to the Greek mythology, Cyclope Poliphimos is considered that was living in the cave. According to the archaeological research, the cave was used as living and religious site, from the Neolithic until the Byzantine period. The cave is 2000 m long and covers an area of 10.000 m^2, according to Petrohilou (1984), who investigated the cave for first time. The present study was a part of a project, of touristic development of the cave, included in the *3rd EU Framework Program*. For this purpose, the stability conditions and the more appropriate protection measures of the cave were determined (Christaras et al., 2004).

22.6.2 Geological and Geotechnical Conditions

The area consists of compact coarse-grained karstic limestone which is traversed by faults of NNW-SSE to NW-SE and E-W directions. The cave is formed in low depth and for this reason, the stability is determined by discontinuities of the following directions: kl1 – 089/68; kl2 – 344/80; kl3 – 246/75; kl4 – 041/77, while the bedding is almost horizontal (Fig. 22.20).

The spacing between the discontinuities changes from 20 to 100 cm, their length appears to be more than 1 m and their dip is close to vertical. The majority of the discontinuities are opened and filled with calcite carbonate. The above mentioned geometrical features in conjunction to the practically horizontal bedding of the limestone form probably unstable blocks on the roof of the cave .

Wedge failures could also be created according to our observations. The RQD of the rock mass is estimated 75–90, the compressive strength 35–60 MPa and the RMR is 61–70, according to Bieniawski (1989).

The tectonic data were elaborated, using UNWEDGE software, in order to determine the unstable wedges or blocks. For this purpose, the

Fig. 22.20 Failure on the roof, along bedding

Table 22.2 Proposed support measures

Section	Potential wedges	Arrangement and length of rockbolts	Safety factors after bolting
152–151	kl1-kl3-ss2	2,0 × 2,5 m – L = 3 m	2,24
	kl1-kl2-ss2	2,0 × 2,5 m – L = 3 m	2,04
154–153	kl1-kl2-ss2	2,0 × 2,0 m – L = 3 m	3,32
	kl1-kl3-ss2	2,0 × 2,0 m – L = 3 m	2,00
156–155	kl1-kl3-ss2	2,0 × 2,0 m – L = 3 m	2,33
158–157	kl1-kl3-ss2	2,0 × 2,0 m – L = 5 m	2,21
	Kl2-kl3-ss2	2,0 × 2,0 m – L = 5 m	2,51
160–159	kl1-kl3-ss2	2,0 × 2,0 m – L = 5 m	2,31
	Kl1-kl2-ss2	2,0 × 2,0 m – L = 5 m	2,14
162–161	kl1-kl3-ss2	2,0 × 2,0 m – L = 5 m	1,97
151–150	kl1-kl3-ss2	2,0 × 2,5 m – L = 3 m	2,45

following pairs of values were used: (a) c = 10 t/m^2, φ = 30°; (b) c = 16 t/m^2, φ = 30°. The geometry of the blocks formed by the combination of the vertical discontinuities with the horizontal bedding creates potential unstable blocks, falling from the roof. The sides of the cave seem to be stable.

For the reinforcement support of the roof, an arrangement of stainless pre-tensioned self-drilling rockbolts is suggested (2 × 2 m and 2 × 2,5 m, length 3 m and 5 m [Table 22.2, Fig. 22.21]) as the optimum scenario of intervention, giving safety factors >2.

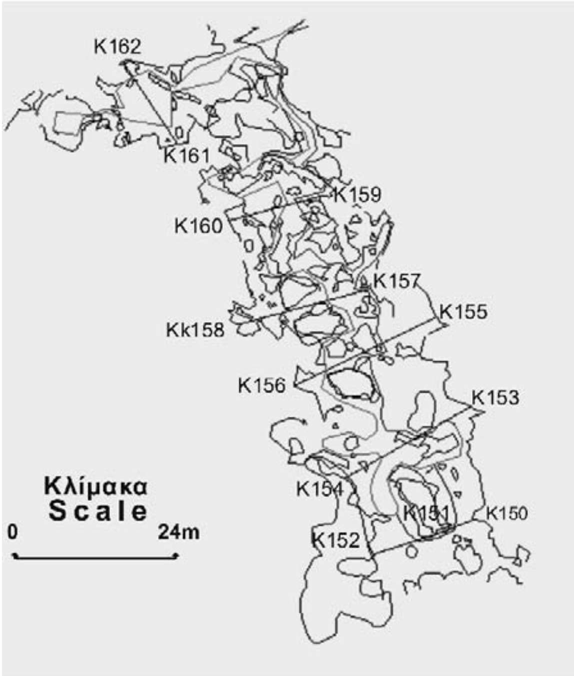

Fig. 22.21 The studded cross-sections

22.6.3 Conclusions

According to our investigation, we arrived to the following conclusions:

1. As the thickness of the overlying layers is small, the stability analysis was only based on the probable creation of unstable wedges due to the tectonic system and not to a stress pattern due to the load of the overlaying layers.
2. The probable unstable wedges are mainly observed at the roof of the cave, creating either falling or sliding blocks
3. The proposed support measures take into account the specific conditions and the monumental character of the cave.
4. The safety factors, after the application of the proposed support measures, are generally enough high (SF>2), having using relatively moderate admissions and mechanical characteristics for the rock mass.
5. For the reinforcement support of the roof, an arrangement of stainless pre-tensioned self-drilling rockbolts is suggested as the optimum scenario of intervention, giving safety factors >2.

Acknowledgement The present research was funded by the *3rd EU Framework Program* and the District of Eastern Macedonia and Thrace.

22.7 Rockfall Hazard and Risk for a High Promontory: Monemvasia Historical Site, Greece

Paul Marinos, George Tsiambaos, Haralambos Saroglou , Vassilios Marinos (NTUA, Greece)

Abstract The paper presents the kinematic rock instability of a high promontory, where Monemvasia historical site is situated in the Peloponnesian peninsula. The instability phenomena pose a significant threat on the site situated immediately down slope. Rock fall episodes occurred in the past, whereas, due to the relaxation of the high cliff, significant undermining of the castle frontiers has been observed at the slope crest.

The surveying and mapping of the high rock cliff was based on a new geodetic methodology (existing geodetic surveying method and its combination by the use of modern reflector- less total stations), which resulted in a three-dimensional Digital Terrestrial Model (DTM) of the ground surface.

The predominant types of kinematic instability are of planar failure and toppling of large blocks. In order to investigate the existing stability conditions and decide upon the stabilization measures, stability and rockfall analysis were carried out for numerous slope sections under different loading conditions.

A rock-fall hazard rating system was proposed, which was based on morphological, lithological and structural criteria. The rating system was applied for individual sections along the slope and a hazard map was produced, which depicted the areas having a high risk against rockfall occurrences.

Stabilization measures were designed based on the stability analysis as well as the hazard map. Moreover, an assessment of the residual risk after the stabilization was made by taking into account additional criteria.

22.7.1 Introduction

The impact of rockfalls on archaeological sites and historical monuments in the Greek territory is remarkable, since most of the landscapes are mountainous and the sites are usually founded near steep rock slopes. The geotechnical problems related to slope instability and the protection methodology of historical sites in Greece have been addressed by Marinos et al. (2002) and Marinos and Rondoyanni (2005). The hazard of rock falls increases in areas with intense seismic activity, due to fact that earthquakes are the principal triggering factor (Marinos and Tsiambaos, 2002).

The archaeological site of Monemvasia consists of an ancient city situated at the foot of a 100 m high limestone rock slope and an ancient city at the slope crest (Fig. 22.22). It is a typical example of a site with high impact of rockfalls. The mentioned area has inhabitants and attracts many visitors, thus the hazard is relatively high.

Rock falls existed long before the development of the city in the ancient time, as evidenced by the foundation of several ancient structures on large fallen blocks of rock as well as the abundance of rock fragments on the slope foot and in the scree material.

Fig. 22.22 Photo of a section of the high rock slope and the Monemvasia historical site

22.7.2 Engineering Geological Conditions – Rockfall Analysis

The geological formations encountered in the area consist of Jurassic bedded, dolomitic limestones and Cretaceous unstratified limestones. The rock slope overhanging the ancient city is formed on the Cretaceous limestone. Two major fault zones, with E-W and NE-SW strike, intersect the formation respectively, forming the high promontory.

The limestone rock mass is moderately fractured, intersected by numerous major vertical fractures, which have a parallel strike to the fault structures forming the rock face. The spacing of the discontinuities is relatively large (more than 1 m); hence the size of the rock blocks is large to very large. In places, the rockmass is very blocky and the size of the rock blocks is smaller, especially on the upper part and the crest of the slope, where the wall of the upper ancient city is founded. The limestone is karstified in places and karstic voids of large dimensions are formed, undermining the rock slope.

The stability conditions of the slope are mainly controlled by the following factors: (a) lack of persistency of the discontinuity planes, which results in instabilities in specific parts of the slope, (b) lack of weak zones, which would result in large scale failures, (c) the rock face is in a state of relaxation due to the high inclination.

The rock slope stability analyses were based on the prevailing mode of instability of each potential rock failure. The principal type of failure is rockfall due to toppling, but some planar or wedge failures also exist. The rock blocks were delineated and their geometry and mass was determined. Due to the inaccessible nature of the slope, the assessment of the above characteristics was based on the surveying of the rock cliff.

The height of the source of rockfalls is minimum 70 m above ground surface, while in some places it reaches 100 m. The rock block size ranges between 1.5 m^3 to about 30 m^3. Only two potentially unstable blocks have a size, which exceeds 300 m^3.

A parametric analysis was carried out for a range of rock block weights (between 0.5 and 10 tn) and for a range of rock fall source heights (between 70 and 100 m). The total kinetic energy, which is produced by the falling rock blocks, was calculated at different sections of the slope. The total energy was calculated at the locations where impact with ancient structures and human activity occurs, hence the dimensioning of the resisting rock fall barriers (up to 750 kJ).

The applied support measures can be divided in two categories: (a) those which apply an external force on the rock face, e.g. tensioned rock anchors, patterned rock bolts, and (b) those which offer protection once the rockfall will occur, mainly rock fall barriers and wire-mesh nets. Other support measures, such as grouting of rock joints, construction of buttresses in overhanging areas and removal of unstable blocks are necessary, but can be inapplicable or very difficult to construct in high rock cliffs. Since the slope is in a historical site, the measures have to comply with minimum alteration requirements of the existing slope face.

The scale of some potential failures is such, that no stabilization measures can minimize or withdraw the risk of a potential rock fall after the application of support measures. Consequently, a method of assessing the hazard (initial and residual after stabilization) of rockfalls at natural rock slopes was proposed.

22.7.3 Rockfall Hazard Assessment

In order to assess rockfall hazard, a number of rating systems have been developed. Pritchard et al. (2005) developed a rating methodology, which is applied to predict rockfall risk along railways. A similar system is the Rockfall Hazard Rating System (RHRS) (Pierson et al., 1990), which is most widely accepted. These systems give a reasonable assessment of the relative hazards due to rockfalls from cut slopes adjacent to highways and railways.

In the present study, a rockfall hazard rating system for natural rock slopes is proposed. It defines 19 rating parameters, grouped in 3 major categories, which have a different weight factor in the assessment of the total hazard. The categories are presented in Table 22.3.

The rating system was applied along the rock cliff, since the parameter rating differs for each slope segment. A hazard map (of the slope face) was produced, which depicted the areas having a high risk against rockfall occurrences and greatest impact on underlying structures.

Table 22.3 Rockfall rating system for natural rock slopes

Cat.	Parameters	Relation to	Weight (%)
A	Slope angle, Discontinuity condition, role of groundwater	Cause of a potential fall	55
B	Slope height, seeder height, rock block size, geometry of catchment area, slope accessibility, potential result of impact	Direct hazard of a potential fall	30
C	Number of potential blocks, possibility of occurrence, seismic activity	Indirect Hazard of a potential fall	15

22.7.4 Conclusions

The rock slope stability of the high vertical slope overhanging the archaeological site of Monemvasia promontory was studied, based on kinematic analysis of unstable blocks and calculation of their rockfall trajectories. It is evident that in some locations, even the installation of high capacity rockfall barriers cannot withdraw the hazard due to impact of falling rocks on structures, either because the size of the failure is extremely high or the catchment area is not sufficient for optimized protection. The application of active support measures (rock bolts) would be adequate if the height of the slope was not prohibitive.

To calculate the potential risk of the rockfalls, a rockfall hazard rating system for natural rock slopes is proposed and the locations with maximum residual risk after the stabilization are defined.

Acknowledgment The research is the result of a project of the National Technical University of Athens funded by the Ministry of Culture.

22.8 Geomorphology and Landslide Potential of the Bamiyan Valley (Afghanistan)

Giuseppe Delmonaco (APAT, Rome) & Claudio Margottini (APAT, Rome & University of Modena and Reggio Emilia, Italy)

Abstract The present work reports geomorphological and geotechnical investigations carried out in the UNESCO site of the Bamiyan valley (Central Afghanistan) in 2007 in order to reconstruct active deformation processes and geomorphological hazards affectings Cultural Heritage. The site is known worldwide for two standing giant statues of Buddha destroyed by Taliban in March 2001.

The geomorphological field survey has reconstructed the main active geomorphological processes along the cliff area mainly related to superficial waters (e.g. erosion, infiltration along joints, accumulation of mud/debris) and slope deformations (e.g. toppling, rock falls, rock slides, jointing). The geomorphological survey has been integrated with geotechnical, structural and kinematic analyses concentrated in 17 distinct sections of the cliff where geological processes were more prominent. This to detect and investigate potential failure modes of the jointed rock masses forming the Bamyian cliff. The kinematic analysis produced different results for the various slope failure modes analysed according to local structural and geomorphological characteristics of the cliff. A geomorphological map reporting the main processes surveyed in the area has been produced.

22.8.1 Geological Settings

The Bamiyan valley (Fig. 22.23) is an intramountainous basin, subsequently filled with debris material originating from the surrounding mountain ranges (Lang, 1971; Reineke, 2006). The Neogene near-horizontally bedded sediments can be distinguished into four strata. Starting with the Eocene Dokani Formation (>80 m sandy carbonate and anhydrite) and the Zohak Formation (>1000 m red conglomerate), the so called Buddha Formation is deposited in the Oligocene and built up by >70 m yellow-brown pelite, sandstone, conglomerate and some volcanic material. The top is composed by the Miocene Ghulgola Formation (>200 m sandstone, clay and lacustrine carbonate) and the Pliocene Khwaja-Ghar Formation (ca. 200 m travertine, sandstone and conglomerate. The Qal'acah Formation is almost contemporary to the Buddha Formation

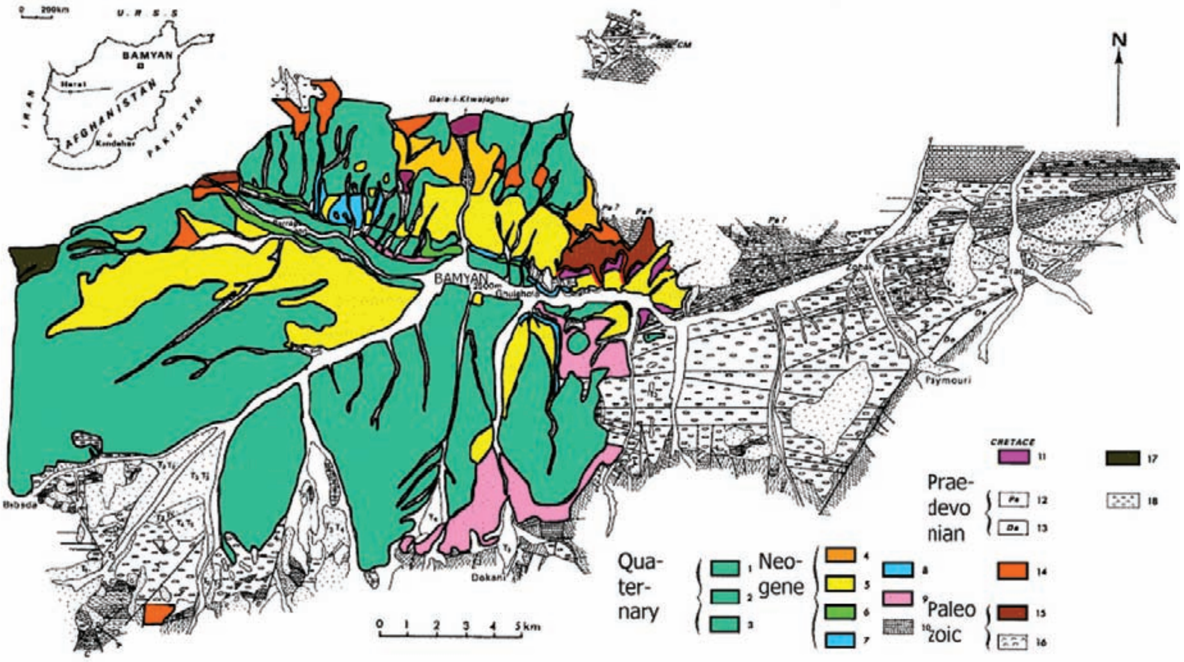

Fig. 22.23 Geological map of Bamiyan (Lang, 1971; redrawn from Reineke, 2006)

and reflects a detritic facies on the slope of a volcano (Lang, 1972).

At north and south of the fault lines of the tectonic graben, red clayey soils formed by metamorphic contact can be found. Along these fault lines, volcanic activity can be recognized. This may have modified (fritted) the surrounding sediments and changed their colour into red.

From the late Pliocene to the end of Pleistocene (Reineke, 2006) the Neogene sediments have been incised by fluvio-glacial erosion. Alternating warm and cold periods lead to changing conditions between accumulation and erosion, so that different Quaternary terraces developed.

The cliff and niches have been excavated into the so called Buddha Formation and are composed by alternance of conglomerate and siltstone (yellow at the bottom and red in the middle of the cliff) with some pelite, sandstone and volcanic material. The conglomerate is the predominant material in the cliff and presents a moderate cohesion The differentiated grain size distribution (from conglomerate to clay) is clearly demonstrating a not selective depositional environment, with high energy (flood plain). The siltstone exhibits an apparent moderate cohesion under dry conditions whereas, when saturated, the material tends to disaggregate completely. This is due, as demonstrated by mineralogical and petrographical analyses (Margottini, 2001), by the absence of cement in the matrix. All lithotypes forming the slope are variably jointed.

22.8.2 Geomorphological Analysis

Bamiyan is located at 2,540 m elevation on the N edge of the 600-km-long EW valley along the Herat fault, at the confluence of three different rivers. The flood valley is mainly formed by fluvial (alluvial and alluvial fans) and slope sediments (landslide and slope deposits). Its evolution is related with various factors such as lithological characteristics, tectonic activity, palaeoclimatic events, river and slope evolution in the cliff. The cliff where the Buddha statues are located presents a general E-W orientation an average slope inclination of ca. 85° and a total length of approx. 1,350 m. The cliff can be divided into two distinct sectors: the western side, where the West Giant Buddha statue is located, shows a N65°E orientation with a length of approx. 820 m, whereas the eastern portion, where the East Giant Buddha is placed, exhibits a N95°E orientation and a length of ca. 525 m. The two segments are separated by a large alluvial cone generated by two distinct torrents flowing into the Bamiyan river, still very active, that have diverted the river flow towards SSE. The change of orientation from EW to NNE-SSW occurs in correspondence of the torrent located at E. This configuration is likely due to tectonic activity regarding the Herat fault system and local faults oriented NE-SW.

The reconstruction of the geomorphological activity in the Bamiyan valley was developed with detailed field surveys integrated with a kinematic analysis on 18 distinct sectors of the cliff in order to define active and potential landslide types. In general terms, in the area the following active processes have been recognized:

- Water infiltration from the upper part of the cliff;
- Gully erosion in the upper catchment area and along the slope face;
- Accumulation of debris sediments at the toe;
- Mud flows;
- Toppling and rock-falls involving some isolated blocks;
- Rock-sliding along pre-existing joints;
- Active deformation processes with progressive opening of joints in the external part of the cliff.

Some processes, e.g. rock-falls and stress development along joints are affecting the niches of Buddha statues, accelerated also by the explosion of March 2001 that destroyed the statues. The Eastern Giant Buddha niche exhibits, at present, the most critical stability conditions. Recently, this area has been partly stabilized with urgent mitigation works. In the Western Giant Buddha site major effects were the collapse of the statue and the consequent instability of the back side of the niche.

Landslide deposits are diffusely outcropping along the slope toe, generated by rock falls and toppling of large conglomerate and siltstone blocks with modest run-out also evidenced by their typical sharp-edged shape. Block volumes vary from $<1\ m^3$ to $>10\ m^3$. Planar sliding deposits are diffusely outcropping at the base of the cliff and somewhat immersed and/or partially covered by the debris (Fig. 22.24).

The top of the cliff, as well as the outer walls, are largely affected by diffuse and intense erosion of conglomerate and siltstone, especially in the western side of the cliff. This produces gully erosion that is the typical landform that outcrops in the slope face and in the upper parts of the Buddha cliff. The concentration of gullies is very high in the very small basins located on the top of the cliff area, especially along the steep slopes of those tributaries creeks that form active debris cone when flowing into the Bamiyan valley. The easily erodible soils with a weak structure like those forming the Bamiyan cliff, the absence of vegetation as well as climatic conditions of the area are prominent factors in accelerating this type of phenomenon in the catchments located on the back of the cliff, with a typical retrogressive activity.

Fig. 22.24 Debris accumulation (*left*) and gully erosion on the slope face of the Bamiyan cliff

Recent and past landslide activity and soil erosion are the consequence of climate fluctuations that occurred in Central Asia from Late Pleistocene up to present (Esper et al., 2002; Kamp et al., 2004; Bush, 2005).

Considering the main geomorphological features briefly described above and the long-term evolution of the cliff vs. climate and tectonic activity, three main stages have been recognized (Delmonaco & Margottini, 2007) and briefly described.

Stage 1: At the end of the last maximum glacial (13,5 ky BP) the rock slope experienced development of vertical cracks and deep rock sliding phenomena due to the deepening of the valley. This resulted in straining of rocks and development of parallel cracks and joints with E-W orientation. The intersection of this system with the one linked to the tectonic stress, oriented at S (dip direction) generated deep rock sliding phenomena affecting conglomerate and siltstone layers at the base of the cliff. Old landslides, mostly in inactive or quiescent state of activity, occurred before the human exploitation of the slope as demonstrated by stable caves excavated in the landslide body. Nevertheless the presence of two caves with evidence of displacement reveals the occurrence of rock slides at least after the 5–6th century AD.

Stage 2: The sea level rise after the cold peak terminated in the Early Holocene promoted large deposition of debris and alluvial sediments. The reduction of the potential energy in the slope and a consequent decrease of stress conditions concentrated at the slope toe changed landslide kinematics in the Bamiyan cliff from deep landslides to toppling-sliding failure mode that are affecting the middle-high sectors of the slope.

Stage 3: The so-called Little Ice Age (15th–19th centuries AD), with more humid conditions than present, have promoted an increase of erosion and debris production from the upper catchments especially in the western sector of the cliff. In the middle of the slope, where the two segments of the cliff with different orientations converge, the most active areas of debris production outcrops, evidenced by the coalescent debris cones that have diverted the flowing of the Bamiyan river through SSE. At present, arid climate conditions with low annual rainfall amount and concentrated precipitation promote deep erosion of loose sediments (e.g. gullies), mud flows along the channels and water infiltration inside the slope materials causing decrease of cohesion along the joints and acceleration of toppling/falling processes.

22.8.3 Landslide Kinematic Analysis

Structural setting analysis and potential instability failure modes of the slope-forming rocks has been undertaken in June 2007 in order to provide a preliminary sketch on potential morphological evolution of the cliff.

The angle for most of the rock face is approximately 80–88°. The outcropping soft rocks present prominent discontinuity sets whose origin, especially the joint system parallel to the slope face, can be associated to the geomorphological evolution of the valley as well as to tectonic setting (Ambrasey and Bilham, 2003). This situation has caused apparent slope instability phenomena, somewhat aggravated by the explosions during the destruction of the Buddhist statues in 2001 around the niches areas. A total of 17 structural stations were selected by visual inspections in the areas of the cliff where historical structures (e.g. Buddha niches, external and underground caves) display prominent or potential instability conditions (Table 22.4).

Table 22.4 List of structural stations with orientation and global localisation

SITE ID	Dip Dir. (°)	Dip (°)	Location
Station 1	141	86	N34°49’44,1” E067°49’02.2”
Station 2	141	86	N34°49’47,3” E067°49’07.6”
Station 3	158	82	N34°49’47,4” E067°49’09.1”
Station 4	155	82	N34°49’47,5” E067°49’10.7”
Station 5	164	81	N34°49’47,7” E067°49’11.0”
Station 6	162	80	N34°49’49,1” E067°49’14.3”
Station 7	162	85	N34°49’51,0” E067°49’17.6”
Station 8	153	88	N34°49’51,4” E067°49’21.7”
Station 9	153	85	N34°49’51,8” E067°49’23.5”
Station 10	157	84	N34°49’54,8” E067°49’29.8”
Station 11	189	88	N34°49’54,5” E067°49’31.9”
Station 12	178	85	N34°49’54,1” E067°49’33.3”
Station 13	185	83	N34°49’53,3” E067°49’38.5”
Station 14	167	86	N34°49’52,9” E067°49’40.3”
Station 15	164	85	N34°49’53,3” E067°49’42.2”
Station 16	192	82	N34°49’53,2” E067°49’46.2”
Station 17	198	88	N34°49’52,9” E067°49’47.9”

The main joint orientation data in each observation point was represented with the Schmidt equal angle stereonet and rose diagrams. For the selected stations, kinematic analyses have been implemented to estimate the potential failure modes (toppling, plane and wedge sliding), that may develop along the slope. This was divided into two main sectors: W sector, where the Western Giant Buddha is located (stations 1–10) and the eastern side that includes the area of the Eastern Giant Buddha (stations 11–17). The two sectors displays different orientations, respectively 155/85° and 185/82°, due to tectonic effects (Figs. 22.25 and 22.26).

The toppling analysis has provided the following results (Fig. 22.27) considering a value of φ' = 30° along the joints in siltstone materials, as the weaker lithotypes where higher stress condition can develop.

In general, the toppling potential seems to be higher in the W part of the cliff, especially in potential remobilized volumes. In the E side a potential toppling failure mode exhibits minor potential volumes involved due to a higher density of fractures in the jointed mass that presents, as well, a higher number of joint sets.

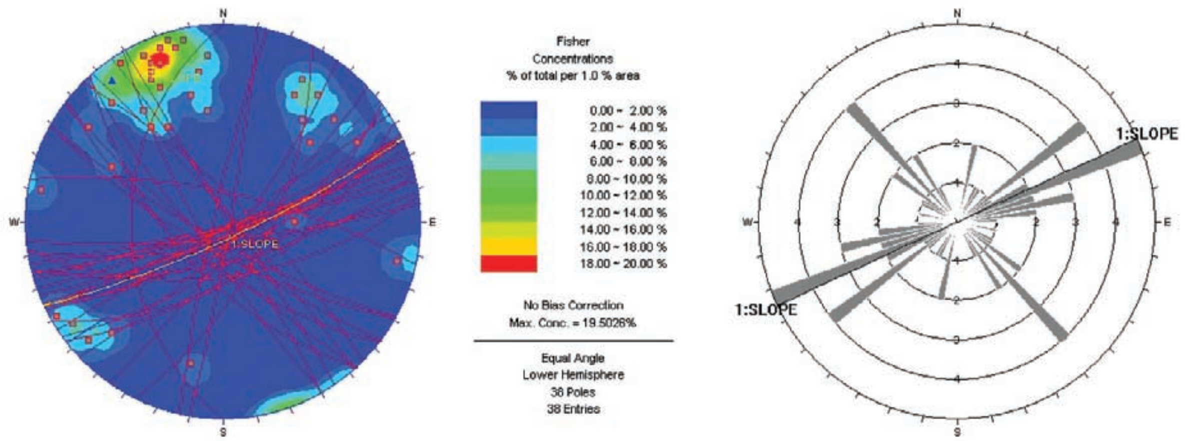

Fig. 22.25 Joints orientation sets of the W part of Bamiyan cliff (stations 1–10) represented through stereonet (*left*) and rose diagram (*right*)

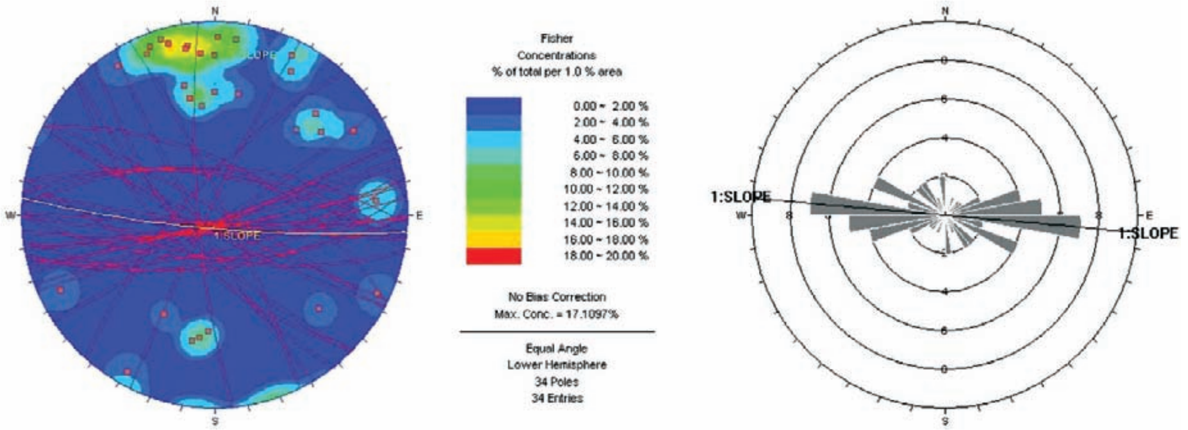

Fig. 22.26 Joints orientation sets of the E part of Bamiyan cliff (stations 11–17) represented through stereonet (*left*) and rose diagram (*right*)

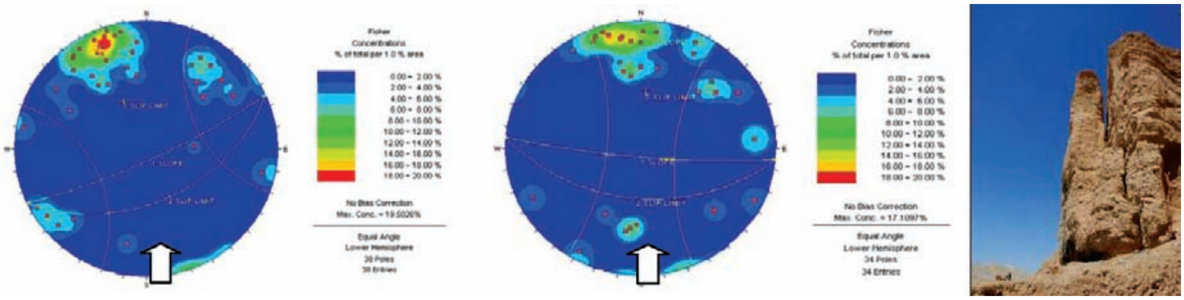

Fig. 22.27 Results of kinematic analysis for toppling for W side (*left*) and E side of the cliff (*middle*); the *arrows* show the region where toppling is possible (between slip limit and lower stereonet border). Toppling evolution in the cliff (*right*)

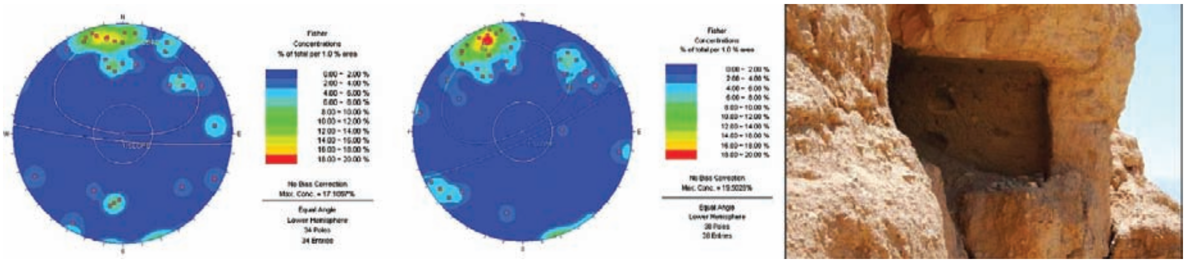

Fig. 22.28 Results of kinematic analysis for planar sliding for W side (*left*) and E side of the cliff (*middle*). Planar rockslide involving an ancient cavity (*right*)

The stereographic analysis for planar failure is shown in the Fig. 22.28.

Planar sliding is highly potential in both sides of the cliff, also as a secondary movement connected with toppling failure, that, factually, determines the sliding of vertical blocks previously deformed following a typical toppling evolution. This occurs especially when the "pivot" of the block is located inside a siltstone layer where the major stress is concentrated. In that case the evolution of failure is that typical of a sliding, sometimes with the development of circular-shaped rupture surface in cohesive materials (Mohr-Coulomb behaviour of weak siltstone).

Kinematic analysis for wedge failure is shown in Fig. 22.29.

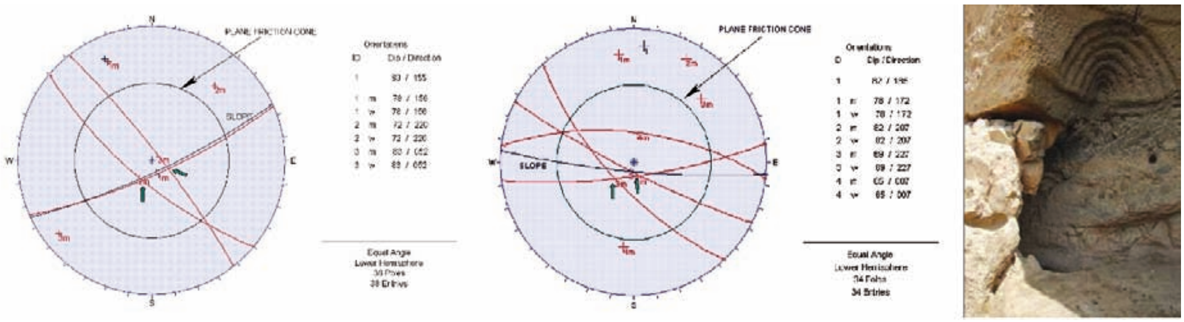

Fig. 22.29 Results of kinematic analysis for wedge failure for W side (*left*) and E side of the cliff (*middle*); the *arrows* show the intersections of planes that may cause sliding inside the potential area (crescent shaped region between slope limit and lower friction cone). Potential wedge sliding along the cliff (*right*)

Major planes have been selected with the Terzaghi weighted mean statistical technique.

In the W side, wedge failure is possible in rock blocks delimitated by joints 1-2 (oriented respectively 158°/76° and 220°/72°) and 1-3 (158°/76° and 052°/83°). In the E side wedge failure can be promoted by joints 1-2 (172°/78° and 207°/82° oriented) and joints 1-3 (172°/78° and 227°/69°). It can be affirmed that in the W portion, since the most important system is the discontinuity oriented parallel to the slope, this kind of failure mode is very difficult to occur, since this system primarily produces rock falls and toppling phenomena. As a matter of fact, no special evidence of wedge potential, although theoretically possible, has been surveyed in this area. On the contrary, the E side has shown wide sectors of the slope where wedge failure has been detected, especially in the lower parts of the slope where siltstone is prevalent, although this kind of failure mode can mobilize small volume of rocks due high frequency of discontinuities.

According to the main geomorphic processes reconstructed in the Bamiyan cliff, a geomorphological map has been produced (Fig. 22.30).

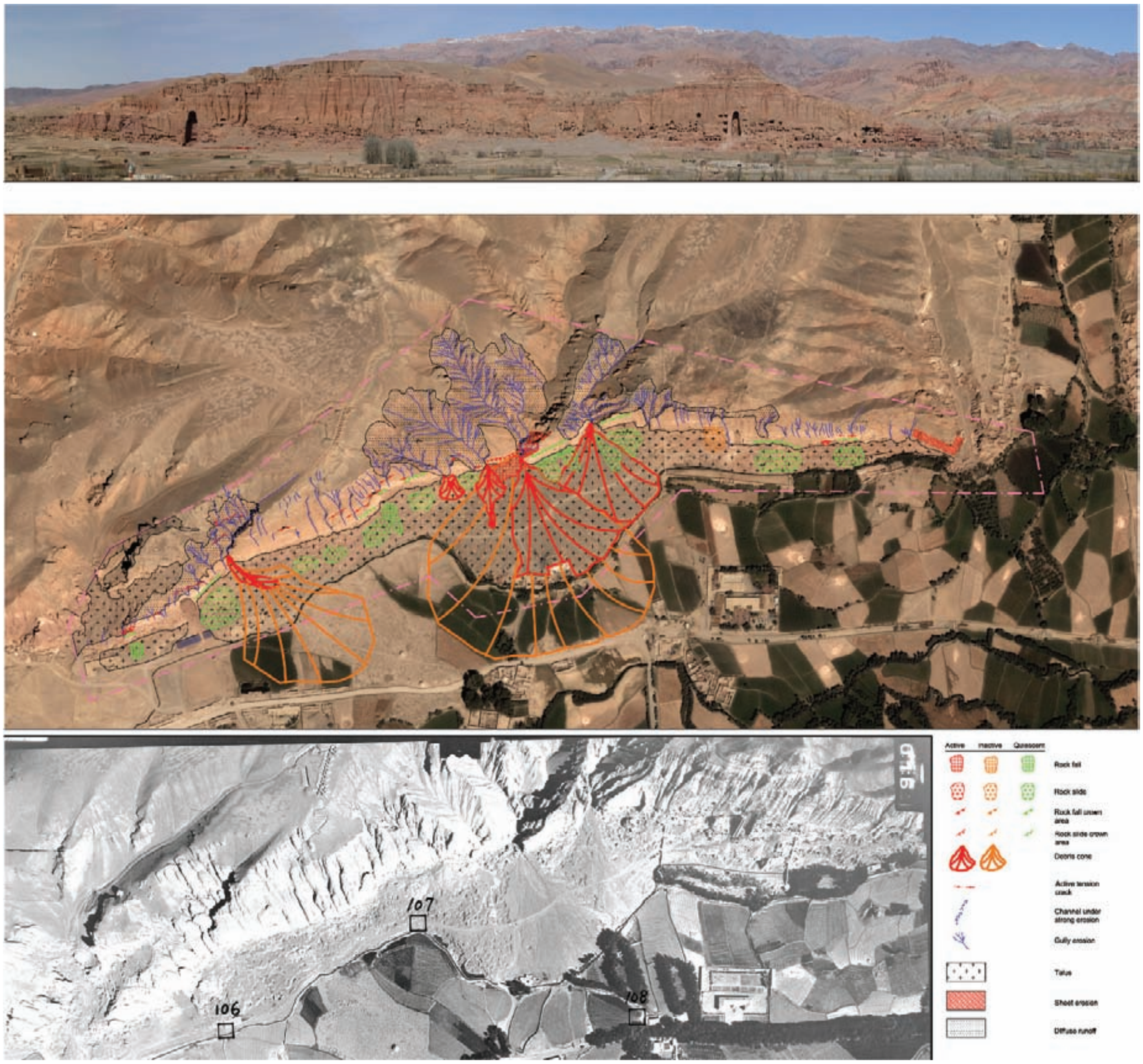

Fig. 22.30 View of the Bamiyan valley (*upper*) and geomorphological map of the cliff where the giant statues of Buddha are located. The distance between the niches is 790 m. The *lower* aerial photo is the first image of the Bamiyan valley (late '60)

22.8.4 Conclusions

The geomorphological investigation carried out in Bamiyan on the cliff where the giant statues of Buddha are located has evidenced that several active processes are affecting the area. Intense erosion is mainly affecting the upper part of the cliff and the slope face whereas landslide processes are involving different sectors of the slope. According to kinematic analysis undertaken in the structural stations detected along the cliff of Bamiyan, the slope may experienced, as in the past, toppling, planar sliding and wedge failure, although with distinct perspectives. Planar sliding is the most diffuse failure potential both sides of the cliff, although most of the movements have occurred in the past. This failure type can be considered as the secondary movement type after toppling evolution of unstable blocks, especially when the failure surface is located inside siltstone layers. Toppling of rock blocks is equally diffuse and may be considered the most hazardous landslide type for all the cliff, even if in the W side it can be expected a higher magnitude of events with respect to the E part of the cliff. Wedge sliding is potentially developing in both parts of the cliff. Nevertheless, the structural conditions suggest that this type of movement is more probable in the eastern sector, characterised by high potential frequency and low magnitude of events, as also surveyed during the field mission of June 2007.

Acknowledgments The authors are sincerely grateful to UNESCO that funded the research: a special gratitude to the functionaries of UNESCO Kabul for local support.

References

Ambrasey, N., Bilham, R. (2003). *Earthquakes in Afghanistan*. Seismological Research Letters, 74, 107–123.

Bieniawski, Z.T. (1989). *Engineering rock mass classification*. New York, Wiley.

Bush, A.B.G. (2005). *CO_2/H_2O and orbitally driven climate variability over central Asia through the Holocene*. Quaternary International, 136, 15–23.

Canuti, P., Margottini, C., Mucho, R., Casagli, N., Delmonaco, G., Ferretti, A., Lollino, G., Puglisi, C., Tarchi, D. (2005). *Preliminary remarks on monitoring, geomorphological evolution and slope stability of Inca Citadel of Machu Picchu (C101-1)*. Proceedings International Consortium on Landslides General Assembly, Washington DC, pp. 39–47.

Carlotto, V., Càrdenas, J., Romero, D., Valdivia, W., Tintaya, D. (1999). *Geologìa de los quadràngulos de Quillabamba y Machu Picchu*. Boletìn No. 127, serie A: Carta Geologica Nacional, Lima, 321 pp.

Carreño, R., Bonnard, C. (1997). *Rock slide at Machu Picchu*, Peru. Landslide News 10, 15–17.

Casagli, N., Fanti, R., Nocentini, M., Righini, G. (2005). *Assessing the capabilities of VHR satellite data for debris flow mapping in the Machu Picchu area (C101-1)*. Proceedings ICL General Assembly, Washington DC, pp. 61–70.

Christaras, B., Chatzigogos, Th., Dimitriou, An., Chatzigogos, N., Makedon, Th., Filippides, S. (2004). *Stability of Polifimos cave, in Maronia City of Thrace, N. Grrece*, Bull. Geol. Soc. Gr., vol. XXXVI/4, Thessaloniki, pp. 1892–1901.

Delmonaco, G., Falconi, L., Margottini, C., Puglisi, C., Spizzichino, D. (2004). *A novel procedure for exposure and vulnerability of cultural heritage at landslide risk: application to the historical Inca sanctuary of Machu Picchu*. 32nd IGC, Florence, Italy August 20–28, 2004.

Delmonaco, G., Margottini, C. (2007). *Geomorphological features of the Bamiyan valley*. Report on the UNESCO mission to Bamiyan (Afghanistan), 18–29 June 2007. UNESCO, Paris, 26pp.

Dorling, D., Newman, M.E.J., Barford, A., Wheeler, B., Protchard, J., Allsopp, G. (2008). *Worldmapper Project*. [Online] 11 April 2008. http://www.worldmapper.org/

Einstein, H.H. (1988) *Special lecture: landslide risk assessment procedure*. Proc. 5th Int. Symp. on Landslides, Lausanne, **2**, 1075–1090.

Esper, J., Schweingruber, F.H., Winiger, M. (2002). *1300 years of climatic history for Western Central Asia inferred from tree-rings*. The Holocene, 12(3), 267–277.

Gastner, M. T. & Newman, M. E. J. (2004). *Diffusion-based method for producing density equalizing maps*. Proc. Natl. Acad. Sci. USA 101, 7499–7504.

Herzog, A. (2007). *MAPresso, a free Java applet for unclassed choropleth maps and cartograms*. [Online] 11 April 2008. http://www.mapresso.com/index.html

Hutchinson, J.N. (1988). *General report: morphological and geotechnical parameters of landslides in relation to geology and hydrology*. Proc. 5th Int. Symp. on Landslides, Lausanne, **1**, 3–35.

ICOMOS, International Council on Monuments and Sites. *Heritage @ Risk. Report from 2000 to 2007*. [Online] 28 April 2008. http://www.international.icomos.org/risk/

Kamp, U. Jr., Haserod, K., Shroder, J.F. Jr. (2004). *Quaternary landscape evolution in the eastern Hindu Kush, Pakistan*. Geomorphology, 57(1–2), 1–27.

Lang, H.D. (1971). *Über das Jungtertiär und Quartär in Süd-Afghanistan*. Beih. Geol. Jb., 96, Hannover, pp.167–208.

Lang, J. (1972). *Bassins intramontagneux néogènes de l'Afghanistan Central*. Rev. Geogr. Phys. Geol. Dynam., Paris, 1972 (2), 14, 4, pp. 415–427.

Margottini, C. (2001). *Instability and geotechnical problems of the Buddha niches and surrounding cliff in Bamiyan Valley, central Afghanistan*. Landslides, 1(1), Springer Berlin/Heidelberg, pp. 41–51.

Marinos, P., Kavvadas, M., Tsiambaos, G., Saroglou, H. (2002). *Rock slope stabilization in Mythimna castle, Lesvos island, Greece*. Proc. of 1st European Conference on Landslides, Balkema, Prague, pp. 635–639.

Marinos, P., Rondoyanni, Th. (2005). *The archaeological site of Delphi, Greece: a site vulnerable to earthquakes, rockfalls and landslides*. Proc. of the 1st General Assembly of the International Consortium on Landslides: Springer, Kyoto, chap. 31, pp. 241–249.

Marinos, P., Tsiambaos, G. (2002). *Earthquake triggering rock falls affecting historic monuments and a traditional settlement in Skyros Island, Greece*. Proc. of the International Symposium: Landslide risk mitigation and protection of cultural and natural heritage, Kyoto, Japan, pp. 343–346.

Mazzoli, S., Delmonaco, G., Margottini, C. (2005). *Role of precursor joints in the contractional deformation of the granite pluton, Machu Picchu batholith, Eastern Cordillera, Peru*. Rend Soc Geol It, I, Nuova Serie, 3ff.

Melelli, A., Venanti, L.D. (Eds.) (2007). *Umbria underground. Archaeology and urban hydraulics*. 4 M Ed., Perugia, 229pp.

Petrohilou, A. (1984). *The caves of Greece*. Ekdotiki Athinon Ltd.

Pierson, L.A., Davis, S.A., Van Vickle, R. (1990). *Rockfall Hazard Rating System Implementation Manual*. Federal Highway Administration Report FHWA-OR—EG-90-01. FHWA, U.S. Department of Transportation.

Pritchard, M., Porter, M., Savigny, W., Bruce, I., Oboni, F., Keegan, T., Abbott, B. (2005). *CN rockfall hazard risk management system: Experience, enhancements, and future direction*. In: *Landslide Risk Management*, Proc. of the International Conference on Landslide Risk Management, Vancouver. A.A. Balkema.

Regione Umbria (1994). *Atlante Regionale – Studio dei Centri Abitati Instabili in Umbria*.

Reineke, T. (2006). *Environmental Assessment of the Bamiyan Valley in the Central Highlands of Afghanistan*. In: University of Aachen, Bamiyan Masterplan Campaign 2005. Aachen.

Sassa, K., Fukuoka, H., Kamai, T., Shuzui, H. (2001). *Landslide risk at Inca's World Heritage in Machu Picchu, Peru*. In: Proceedings UNESCO/IGCP Symposium on Landslide Risk Mitigation and Protection of Cultural and Natural Heritage, Tokyo, pp. 1–14.

Sassa, K., Fukuoka, H., Shuzui, H., Hoshino, M. (2002). *Landslide risk evaluation in Machu Picchu World Heritage, Cusco, Peru*. In: Proceedings UNESCO/IGCP Symposium on Landslide Risk Mitigation and Protection of Cultural and Natural Heritage, Kyoto, pp. 1–20.

Tevere River basin Authority (2006). *Hydro-geological assestement Plan of Tevere River basin* (*PAI*).

UNESCO, United Nations Educational, Scientific and Cultural Organization. *World Heritage Convention, 1972*. [Online] 21 April 2008. http://whc.unesco.org/en/

UNESCO, United Nations Educational, Scientific and Cultural Organization. *The 2005 Operational Guidelines for the Implementation of the World Heritage Convention*. [Online] 21 April 2008. http://whc.unesco.org/en/guidelines

UNESCO, United Nations Educational, Scientific and Cultural Organization. *World Heritage List*. [Online] 18 April 2008. http://whc.unesco.org/en/list

Varnes, D.J., IAEG Commission on Landslides (1984). *Landslides Hazard Zonation: a review of principles and practice*. UNESCO, Paris, 63 pp.

Vlcko, J. (1999). *Engineering geological failures on historic structures and historic sites*. Acta Geologica Universitatis Comeniane, Nr. 54.

Vlcko, J. (2004). *Extremely slow slope movements influencing the stability of Spis Castle, UNESCO site*. Landslides, 1(1), Springer Verlag.

World Bank (1994). *Cultural Heritage in Environmental Assessment. Environmental Assessment Sourcebook, Update, n. 8* (prepared by J. Taboroff). The World Bank, Environment Dept., 8 pp.

World Monuments Fund. *World Monuments Watch Program*. [Online] 18 April 2008. http://www.wmf.org

Landslides and Multi-Hazards

23

Hideaki Marui and Farrokh Nadim

Abstract Landslides occur frequently in connection with other types of hazardous phenomena such as earthquakes and volcanic activities. Strong earthquakes often cause a large number of landslides, including large-scale landslides, in mountainous areas. Volcanic activities could trigger giant landslides or debris avalanches on mountain slopes. It is not uncommon that such large-scale landslides cause river blockage and form natural dams, which are vulnerable to collapse by overtopping and breaching. The sudden collapse of a landslide dam can cause a catastrophic flood in the downstream area. Submarine landslides are also common phenomena. Large-scale submarine landslides cause catastrophic tsunamis. In assessing those catastrophic cases as a whole, it is necessary to pay special attention to extremely high threats to vulnerable settlements in hazardous areas. The risk assessment of such complicated combined landslide disasters around the world, particularly in developing countries, is a significant step for identifying the appropriate mitigation strategy against catastrophic damage. In recent decades we have experienced remarkable disasters induced by landslides. For example, a huge number of landslides were induced by the Chi-Chi earthquake in Taiwan (1999), by the Mid-Niigata Prefecture earthquake in Japan (2004) and the Northern Pakistan earthquake (2005). Most recently the Wenchuan earthquake occurred with magnitude 8.0 in central part of China on May 12, 2008. This gigantic earthquake caused a tremendous number of landslides, as seen in the satellite picture in Fig. 23.1. Large-scale landslides occurred in volcanic areas, such as at Stromboli Volcano in Italy (2002) (Fig. 23.2) and on Leyte Island in Philippines (2006) (Fig. 23.3). Whole such events manifest the significance of a thematic session within the First World Landslide Forum focussing on the issue of risk mitigation targeting "landslides and multi-hazards".

Keywords Earthquake • Volcanic activity • Landslide dam • Submarine landslide • Tsunami

23.1 Structure, Targets and Outputs of this Chapter

This chapter comprises the following subtopics:

(1) Earthquake-induced landslides.
(2) Landslides and volcanoes.
(3) Submarine landslides and tsunamis.

Hideaki Marui (✉)
Niigata University, Japan

Farrokh Nadim
ICG/NGI, International Centre for Geohazards/Norwegian Geotechnical Institute, Oslo, Norway,
e-mail: farraokh.nadim@ngi.no

© Springer-Verlag Berlin Heidelberg 2009

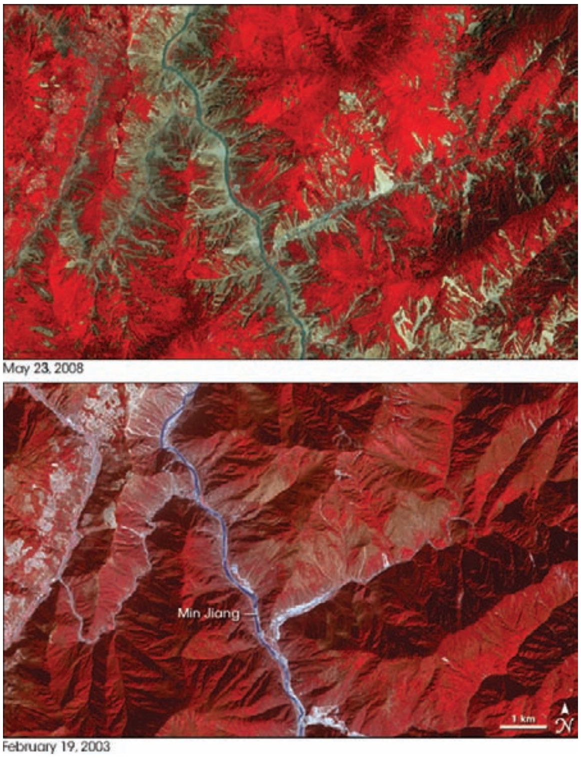

Fig. 23.1 Satellite photos showing extensive landsliding caused by Wenchuan earthquake of 12 May 2008 (http://earthobservatory.nasa.gov/Newsroom/NewImages/images.php3?img_id = 18042)

The session conveners will provide brief overview information of the session and introduce the speakers and individual titles of their presentations. Each speaker will provide a presentation on the related subtopic, followed by a short discussion. Concluding remarks will be provided at the end of the session.

Fig. 23.2 Large-scale landslide and subsequent debris flow on Leyte island in Philippines

Fig. 23.3 Large-scale landslide at Stromboli Volcano in Italy

The Session targets the audience with the following background:

- Experts on landslide hazard assessment, particularly in developing countries, who are working on issues related to "landslide and multi-hazards".
- Experts from the disaster management community who focus on recovery efforts following "landslides and multi-hazards" (UNDP, International Development Banks, Cooperation Agencies from Donor Nations (JICA, ADRD, GTZ, US-AID, CIDA, SIDA, etc.).
- Experts from Government agencies and ministries of public works who have to design policies and land-use planning guidelines for purposes of development (MLIT-Japan, EC, etc.).
- Experts from social, economic, and political sciences and risk management who are working on areas related to risk mitigation, which are related to "landslides and multi-hazards". (UNU, NGI, Universities).

The session should draw upon and systematize experiences and knowledge learned during the recovery processes after catastrophic disasters related to "landslides and multi-hazards" with respect to mitigating similar disasters in future in hazardous areas. The session should also highlight the appropriate methods and procedures of risk assessment on "landslides and multi-hazards" to mitigate future disasters. In addition, it should provide suggestions on how to plan, design and implement countermeasures to protect existing settlements and infrastructures which are confronted with the risk.

23.2 Earthquake-Induced Landslides

23.2.1 On the Legacy of Landslides in Earthquake Affected Zones

David Petley (Durham University, UK)

Introduction: It is well-established that earthquakes trigger very large numbers of landslides in upland environments. Using example from the 1999 Chi-Chi earthquake in Taiwan and the 2005 Kashmir earthquake in Pakistan, this paper reviews the impact of earthquake-induced landslides on both the short term recovery and the long term response phases of earthquakes. It is shown that in addition to inflicting quite large numbers of fatalities due to direct burial, landslides seriously disrupt recovery and relief operations by blocking transportation routes and diverting important strategic resources. Equally important though can be the impact upon long term recovery. Earthquakes often leave a legacy of unstable slopes that can continue for years or even decades afterwards. These landslides represent a direct threat in themselves but also block transportation infrastructure. A key factor that is often overlooked is the increase rate of sediment movement caused by the liberation of hillslope debris. In Taiwan this induced aggradation of some river beds by as much as 30 m, which proved to be devastating to local communities and to hydroelectric power systems. Finally, some suggestions are made for ways in which landslide hazards could be better managed in seismically-active areas.

23.2.1.1 Significance of Earthquake-Induced Landslides

It is well-established that landslides are a key secondary hazard associated with earthquakes in upland environments (Keefer, 1984), presenting a serious threat to communities in these regions. Indeed, in high mountain chains it is not uncommon for 20–25% of earthquake-induced fatalities to result from the effects of landslides (Petley et al., 2006). However, perhaps the most important impact of landslides occurs in the aftermath of the seismic event. In this phase, landslides can be a substantial constraint on both short term and long term activities. This paper seeks to explore the ways in which landslides associated with earthquakes continue to impact the affected area long after the initiating seismic event.

23.2.1.2 Extent of Earthquake-Induced Landslides

Keefer (1984) showed that the extent of earthquake-induced landsliding in mountainous areas can be large. For example, the $M_w = 7.6$ Chi-Chi earthquake in Taiwan in 1999 triggered an estimated 9270 large landslides Liao and Lee (2000), whilst the 2005 $M_w = 7.6$ Kashmir earthquake triggered at least 1300 large failures (Owen et al., 2008). The distribution of these landslides appears to differ according to a wide range of factors in ways that at present are not clear – in the case of the Chi-Chi earthquake the landslides are clustered around the epicenter, whilst in Kashmir they occurred mostly in the vicinity of the fault rupture, primarily on the hanging wall (north-east) block. Natural factors controlling the occurrence of landslides undoubtedly include the magnitude of the earthquake, the depth of the source area, the topography of the land, the geology of the slopes and the weather both before and at the time of the earthquake. The latter factor controls the amount of water that is present in the slopes, which is of course a key factor determining the stability of slopes. An additional key factor is the degree of human disturbance of the landscape. In particular, Petley et al. (2006), Sudmeier-Rieux et al. (2007) and Owen et al. (2008) have all argued that humans are a key factor in a substantial proportion of earthquake-induced landslides, primarily as a result of:

1. slope modification, often along transportation lines or to allow building construction;
2. land-use change; and
3. changes in the soil water conditions.

This increased occurrence of landslides in settled areas then has key implications in the aftermath of the earthquake.

23.2.1.3 Landslides in the Response Phase of an Earthquake Disaster

In the first part of the response phase to an earthquake, activities are focused on recovery and assistance of the victims. The occurrence of landslides can represent an important impediment to this process, preventing rescue and medical teams from travelling into the affected area. In the aftermath of the 2005 Kashmir earthquake this proved to be the case. Here, landslides damaged or in some cases destroyed many of the roads linking Kashmir to the rest of Pakistan, meaning that for the first few days there was a heavy reliance on aviation resources, and in particular on helicopters, to transport rescue and medical staff into the area and victims out of the region to hospital. Inevitably, the availability of helicopters was limited and their use was restricted to day time only, which meant that assistance was not provided with a desirable level of speed. Furthermore, considerable effort had to be expended during this response phase in order to reopen roads. If the occurrence of landslides had been less then this effort could have been focused instead upon direct assistance to the victims. Landslides occurred extensively along highways, especially on cut slopes, which meant that transportation was particularly badly affected. Roads to rural villages had in many cases been completely destroyed, meaning that provision of aid to these areas was effectively impossible without the use of helicopters.

A problem in the days after the earthquake was the continued occurrence of landslides along the road network. In part these landslides occurred as a result of aftershock activity, but in part they were probably the result of continued slope response to the main shock. Thus, in many cases roads that had been reopened were subsequently blocked once more, and the level of hazard for road users was high.

Finally, in some cases landslides may pose a threat to the population because they have caused damming of a watercourse. The key danger is that the dam can breach, releasing a high energy flood that inundates downstream reaches. In the case of the Chi-Chi earthquake a number of emergency efforts were required to ensure that catastrophic collapse of landslide dams did not occur. Fortunately, these efforts were successful. In Kashmir, at least two river blockages occurred. The largest of the two, at Hattian Bala east of Muzaffarabad, created a dam over 100 m high. Again, prompt action mitigated the short term hazard, although concerns remain about the stability of the structure.

23.2.1.4 Landslides in the Recovery Phase of an Earthquake Disaster

The occurrence of landslides in the recovery phase of an earthquake disaster is less well-documented, but in many cases may be more significant. Key impacts are as follows:

Increased Occurrence of Landslides During Heavy Rain

There is considerable evidence that in the aftermath of large earthquake events the occurrence of rainfall-induced landslides substantially increases. Lin et al. (2006) for example noted that more landslides occurred in the first typhoon after the Chi-Chi earthquake that had been triggered in the earthquake itself. It appears that the critical time is the first exceptional rainstorm event after the earthquake, even if this occurs some years later. In the case of Taiwan, this was Typhoon Bilis in 2000, although Typhoon Toraji in 2001 also had a very substantial impact. This pattern of post-earthquake landsliding appears to consist dominantly of shallow debris flows and debris slides, rather than deep-seated landslides. Unfortunately these shallow landslides are particularly hazardous to people, so the impacts are high. In the case of Kashmir, the rainfall events in the first two years after the earthquake were not exceptional, so it is likely that the biggest impacts in terms of post-event landslides have still to occur. Nonetheless, landsliding has been a substantial problem during rainy periods in the aftermath of the Kashmir earthquake, and over 200 earthquake-induced landslide deaths were recorded in Kashmir in 2006.

These post-event landslides are also often very problematic for reconstruction of infrastructure. In the case of Taiwan in the aftermath of the Chi-Chi earthquake, the strategically-important Central Cross Island Highway has been repeatedly reconstructed, only to be destroyed again by subsequent rainfall-triggered landslides (Chen & Petley, 2005). As a result, reconstruction has now been suspended and alternative alignments are being sought, even though the costs of the loss of this road have exceeded $200 million to date.

Increased Levels of Sediment Movement

A poorly appreciated problem in earthquake affected areas is that of increased levels of sediment movement within river channels. The occurrence of extensive landslides means that large amounts of sediment are released for transportation by rivers. In areas adjacent to the landslides themselves this can result in a high incidence of debris flow events, which may be particularly hazardous to communities and infrastructure on alluvial fans and in the vicinity of tributary channels. This sediment then reaches the river system, whereupon it can change the dynamics of the main channel system. In the case of the Chi-Chi earthquake, increased sediment production in the Techi River valley caused extensive aggredation of the river bed over tens of kilometres. In places the bed of the river has to date increased in elevation by as much as 30 m. This has had varying impacts, including:

- The loss of hydroelectric generation capability. In the case of the Techi River system the estimated costs in terms of loss of income and costs of reconstruction are about $800 million to date.
- Serious reductions in the quality of water caused by the increased level of turbidity;
- Damage to communities, roads and bridges. For example, large parts of the hot springs resort of Kukuan, located in the Techi river valley, including several hotels and the bridge joining the two main parts of the town, have been lost to increased levels of flooding caused by aggredation of the river.

It is not known how long this increased level of sediment movement last, but in Taiwan there is little sign that activity is reducing, even nine years after the earthquake.

23.2.1.5 Mitigation – Reducing the Impact of Landslides Caused by Earthquakes

Landsliding is a natural terrain response to the occurrence of an earthquake. Thus, it is unreasonable (and probably undesirable) to try to prevent the occurrence of landslides in earthquakes. However, some mitigation measures can be undertaken that can prove to be effective. These are detailed below. I should note that I believe that one measure that is often undertaken is probably not useful. This is the construction of landslide hazard maps using intricate but not physically-representative GIS-based algorithms. The triggering of earthquake-induced landslides is highly complex, to the degree that it cannot be captured at present using such techniques. Thus, maps derived from these approaches are at best misleading and at worst dangerous. Zonation can only be undertaken on either a site-by-site basis using a combination of stability analyses and geomorphological mapping, or in a crude way using for example slope angle or material as the key indicator. More complex techniques do not yield better results at present for earthquake-induced landslides, and time would be better spent on good quality geomorphological mapping.

Effective mitigation is possible using the following key techniques:

1. Good quality design needs to be applied to slopes along strategic transportation routes. In particular, there is a need to ensure that where slopes have been cut the stability of the slope is adaequately considered. Similarly, it is essential to ensure that embankments and bridge abutments are adequately designed for a seismic event;
2. In the event of a large earthquake, some slope instability is inevitable along even the best-designed roads. Adequate preparation is needed to ensure that these blockages can be cleared quickly and effectively;
3. In the event of an earthquake, programmes are needed to: a. identify slopes that are likely to be unstable in the next period of very heavy rain; b. mitigate any landslide dams that have formed; and c. control sediment production in key locations.
4. Studies are also required to look at the implications of extensive landslides upon disaster

response, and to ensure that the response plans are designed accordingly. For example, the earthquake threatened city of Kathmandu (2.5 million people live in the Kathmandu Valley, mostly in buildings that will perform very poorly in a large seismic event) is connected to the outside world by only three main roads, all of which traverse steep, landslide-prone terrain. In the event of a large earthquake, these roads are unlikely to be useable for some days at least. Therefore, plans for the delivery of aid cannot rely upon these roads.
5. Local people and the supporting agencies should be educated about the dangers posed by landslides and the techniques used to rescue buried victims.

23.2.1.6 Conclusions

Landslides are a substantial but often neglected aspect of large earthquakes in upland areas. In addition to killing people outright, they can also have an extremely serious impact in terms of hampering rescue operations and the delivery of assistance. In the long term, elevated levels of landslide activity can cause long term damage to communication and power networks, and the increased amount of sediment production and movement can also cause many problems. Whilst earthquake-induced landslides cannot be prevented, adequate consideration of the problem in advance can allow the impact of earthquake-induced landslides to be minimized.

23.2.2 Emergency Measures and Risk Management After Landslide Disasters Caused by the 2004 Mid-Niigata Prefecture Earthquake in Japan

Hideaki Marui (Niigata University)

Introduction: Various unforeseen phenomena have been observed and newly recognized as a result of the 2004 Mid-Niigata Prefecture Earthquake. This earthquake was the first catastrophic earthquake which occurred in the landslide prone area in Japan after the necessary management and preparation to apply modern research and investigation methods on landslide occurrence. Therefore, the Japan Landslide Society organized a research committee and carried out detailed and comprehensive field researches and investigations in the severely devastated areas, due to a huge number of landslides caused by this earthquake. As a result of the series of intensive geotechnical analyses successive to the preceding geomorphological and geological analyses, we have been convinced that it is absolutely necessary to develop a new theory on earthquake-induced landslides.

It was a remarkable aspect that a tremendous number of landslides were triggered by the 2004 Mid-Niigata Prefecture Earthquake. Because the epicenter was located at a depth of 13 km just in the landslide-prone area of the central part of the Niigata Prefecture, severe damage was caused by the earthquake-induced landslides. Furthermore, many landslide dams were formed mainly in the watershed of the Imogawa-River by the displaced soil mass of the earthquake-induced landslides. Some large landslide dams should pose a great threat of flood and debris flow in case of dam collapse to the settlement of the Ryuko-District in the downstream area of the watershed. It was urgently needed to arrange the emergency operations to avoid the destructive collapse of the major landslide dams. This contribution illustrates an overview of earthquake-induced landslides, river blockage by landslide dams and emergency operations against dam collapse and further of integral recovery works to inhibit future disasters.

23.2.2.1 The 2004 Mid-Niigata Prefecture Earthquake

On 23 October 2004, an earthquake with magnitude 6.8 occurred in central part of the Niigata Prefecture, namely 70 km south of Niigata City. As a consequence of the earthquake, 46 people were killed, about 4700 people were injured, and 2800 houses were completely and 10,000 houses were partially damaged by structural failures, landslides and so on. Furthermore important public infrastructures like railways and highways as well as other major roads were also heavily damaged. About 100,000 people were to be evacuated to 600 refuges soon after the earthquake. The total amount of the material damage was estimated to be about thirty billion dollars.

The hypocenter of the 2004 Mid-Niigata Prefecture Earthquake was located at shallow depth (13 km) in an active fault and fold system overlain by thick sediments of geologically young formations. An earthquake intensity of 7.0 (by Japan Meteorological Agency) was recorded in Kawaguchi Town close to the hypocenter for the first time since beginning of its recording using seismometers. The event was followed by strong aftershocks in rapid succession. The area suffered much successively from four major aftershocks with a magnitude of 6 or greater within 38 min after the main shock. The aftershocks were distributed 35 km along the NNE-SSW strike of the geological structure within a 20 km-wide zone between the Yukyuzan fault and the Shibata-Koide tectonic line. National Research Institute for Earth Science and Disaster Prevention has analyzed the distribution of asperities by using seismic waveform data observed by strong motion seismographs. The area with the highest asperity at eastern side of the epicenter corresponds to the watershed of the Imogawa-River, where especially many landslides occurred.

23.2.2.2 Characteristics of the Earthquake-Induced Landslides

The earthquake triggered about 3800 landslides in various types and dimensions, causing extensive damage to settlements, farmlands and infrastructures. It was generally thought in the past, that because of strong ground shaking during earthquakes a lot of slope failures occur on steep slopes with concave shape but only few reactivated landslides occur on relatively gentle slopes. However, this time there were also many reactivated landslides that occurred as a consequence of the Mid-Niigata Prefecture Earthquake in the neighborhood of the epicenters, and strong aftershocks occurred, especially on hillslopes in the Yamakoshi Village. Landslides occurred especially densely in the watershed of the Imogawa-River along the Kajigane-Syncline. The geology of the area consists of a thick sequence of Pliocene to lower Pleistocene sediments. Many landslides occurred along the dip direction of geological formations. Originally, heavily landslide-prone areas are widely distributed in the Tertiary mudstone areas in Niigata Prefecture. Usually reactivated landslides occur frequently in the northwestern part of the Yamakoshi Village which consists of mudstone. This time, however, most of landslides occurred in the southeastern part of the Yamakoshi Village which consists of sandstone and sandy siltstone.

Slope displacements induced by the earthquake can be classified mainly into the following categories: Shallow slope failures on steep slopes near ridges, Shallow slope failures on steep slopes along river channels, Reactivated landslides on relatively gentle hillslopes, Landslide dams formed by the displaced soils mass by the previous three categories of slope movements. For the mitigation of subsequent disasters, it was a matter of great urgency to implement emergency countermeasures against overtopping and successive failure of the landslide dams. Furthermore, abnormally heavy snowfall since 1986 years struck the area that was heavily damaged by the earthquake. It was also necessary to pay attention to the landslides caused by snowmelt.

23.2.2.3 River Blockages by Landslide Dam

More than 50 landslide dams were formed along the main channel of the Imogawa-River and its tributaries by the earthquake-induced landslides. Many of them were naturally overtopped soon after their formation without catastrophic collapse. However, there were two critical landslide dams among them because of their dimensions, namely Higashi-Takezawa landslide dam and Terano landslide dam. Figure 23.4 shows the main scarp of the Higashi-Takezawa landslide. Figure 23.5 shows the river blockage by the Higashi-Takezawa landslide. Both of them have a length of about 350 m and a volume of more than 1 million m^3. Generally, the stability of landslide dams against collapse should be evaluated for three mechanisms, – collapse by water pressure, by piping and by overtopping. In both cases of river

Fig. 23.4 Main scarp of the Higashi-Takezawa landslide

blockages, the length of the buried river channel is about ten times the maximum water depth of the reservoir. Therefore, the possibility of the destructive collapse of either dam by water pressure and/or piping was estimated to be low.

However, the water levels of the both reservoirs quickly rose soon after the blockage of the river channel by continuous rainfall. The settlement of the Kogomo-District in the upstream area was inundated and many houses were damaged by inundation with impounded water. There remained an apparent danger of overtopping and successive collapse of one or both of the dams, because the water level of the reservoir had significantly risen. Collapse of these landslides dams could cause outburst floods or debris flows which would endanger the downstream residential areas at Ryuko-District. Therefore, the inhabitants of the downstream areas had to evacuate.

Fig. 23.5 River blockage by the Higashi-Takezawa landslide and reservoir

It was urgently necessary to lower the water level of the reservoir. Emergency measures to prevent collapse of the landslide dams were carried out by the Ministry of Land, Infrastructure and Transportation. The reservoir at Higashi-Takezawa, which was formed by the largest landslide dam along the main channel of the Imogawa-River, has a critical significance. In order to reduce the danger of overtopping, the following emergency measures were undertaken. First, lowering the water level was tried using pumps and siphons. At the beginning, 6 pumps were used, and after that, additional 6 pumps were installed. It was not suitable to use drainage pumps for the long term; thus they should be used for only emergency purpose in the initial stages. Because of maintenance problems for the pumps, diversion pipelines were installed as an additional alternative measure to inhibit overtopping. These alternative diversion pipelines were quite effective. As a result, the water level was kept lower than the overflow elevation and lowered to a safer level. Finally, an open channel with a sufficient cross-sectional area for water discharge including that of snow melt during early spring was constructed.

It was absolutely necessary to retain the stability of the displaced soil mass by the earthquake-induced landslide against secondary landslide motion during construction of the open channel. Therefore, excavation of the upper part of the displaced soil mass was immediately carried out for security during the construction works. In addition, a successive slope failure with a volume of several 10,000 m^3 was caused by snowmelt at the main scarp of the Higashi-Takezawa landside at the last stage of spring. Although, this slope failure has no significant effect as to the safety factor of the displaced soil mass by the earthquake-induced landslides, an integral recovery works for this area with sufficient comprehensive permanent measures in due consideration of possible factors was carried out (Fig. 23.6).

1. The displaced soil mass was completely stabilized by three consolidation dams.
2. The old, steep landslide scarp behind the main scarp of the earthquake-induced landslide was reshaped into gentle gradient and covered by vegetation.

Fig. 23.6 An integral recovery works around the Higashi-Takezawa landslide area

23.2.2.4 Remarks for Mitigation of Future Disasters

In relation to hazard mitigation on successive landslides and slope failures it is urgently necessary to carry out field reconnaissance of slope deformations and assessment of slope instability immediately after the earthquake as a first step. Furthermore, it is again necessary to carry out the same reconnaissance of slope deformations and assessment of slope instability after snowmelt.

In recovery planning for heavily damaged roads by earthquake-induced landslides, it is necessary to consider the alteration of the original route plan in case the road is extremely heavily damaged at many places. In some cases stabilization of landslides is an essential prerequisite condition for reconstruction works of damaged roads.

Besides assessment of instability of individual slopes, it is also necessary to assess the danger degree of possible future disasters by transport of unstable debris materials along river channels in various torrent watersheds after the earthquake. The potential of the movement of unstable materials in torrent watersheds near to the epicenter should have been completely changed because of the strong effect of the earthquake.

Further, it is also an important task to develop appropriate methods of hazard zoning for prediction of landslides induced by future earthquakes.

23.3 Landslides and Volcanoes

23.3.1 Ground-Based InSAR Monitoring of an Active Volcano and Related Landslides

N. Casagli[1], F. Catani[1], C. Del Ventisette[1], L. Guerri[1], D. Tarchi[2], J. Fortuny[2], G. Antonello[2], D. Leva[3], C. Rivolta[3]
[1]Department of Earth Sciences, University of Firenze, V. la Pira 4, 50121 Firenze, Italy.
[2]Joint Research Centre, European Commission, V. E. Fermi 1, 21020 Ispra (VA), Italy.
[3]Ellegi-LiSALab s.r.l., V. XX Settembre, Legnano (MI), Italy.

Stromboli volcano (Italy) is characterized by a typical "Strombolian activity" which consists of very low energy explosions, every 10–15 min. In December 2002 an eruption caused a landslide on the NW slope of the volcano (Sciara del Fuoco slope, SdF) and produced a tsunami. Concerns over the possibility of further slope collapses of the SdF led to the set up of a permanent monitoring system of ground deformations. Figure 23.7 shows the 3D model of the Stromboli Island.

The ground-based radar interferometer (GB-InSAR) system installed on the Stromboli Island was designed by the Joint Research Centre of the

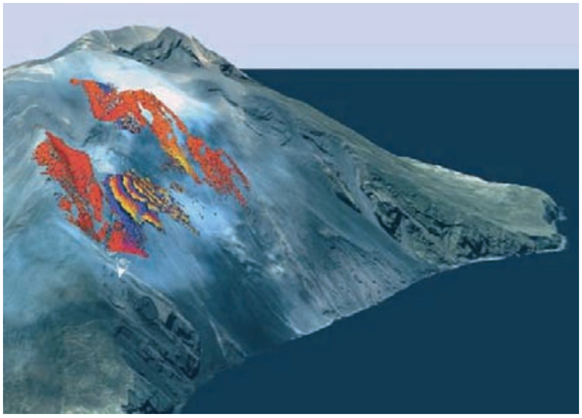

Fig. 23.7 3D model of the Stromboli Island (Sciara del Fuoco slope and NE crater) with an interferogram obtained from the GB-InSAR. The position of the radar is shown with the white symbol. The interferogram spans a time interval of 11 min (from 11.17 UT to 11.28 UT of 9 March 2007) showing a velocity greater than 300 mm/h

European Commission (Rudolf & Tarchi, 1999); it is continuously active since 20 February 2003 (Antonello et al., 2003; Casagli et al., 2004; Antonello et al., 2007) and produces, on average, 120 images per day of the area under investigation (NW flank of crater and the upper part of the SdF), characterized by a resolution of about 2 m × 2 m, with an accuracy of the measurement of less than 1 mm. Interferograms (obtained using pairs of averaged sequential images) contain the displacement vector along the line-of-sight (LoS) in the time interval between two acquisitions. Negative values of displacement indicate a movement toward the sensor (shortening along the LoS). On the crater area this direction of movement correspond to the inflation of the volcanic cone while, on the SdF, this is usually related to a local bulging or to the downslope sliding of the volcano-clastic material accumulated on the SdF slope. Conversely, a positive value of displacement identifies a movement backward with respect to the sensor (lengthening along the LoS) that on the crater area could be related to the deflation of the volcanic cone.

In January 2007, the GB-InSAR showed a progressive acceleration of deformation on the NE crater. The recorded velocity progressed from 0.04 mm/h to 0.7 mm/h toward the radar that suggest an inflation of the upper sector of the volcanic system. The increase in the deformation rate successively involves the portion the SdF (15 February 2007) in which the velocity increased from 0.02 mm/h to 0.25 mm/h, toward the sensor.

These events are related to the new eruption occurred at the end of February 2007. The effusive phase (from 27 February to 12 April) started with an explosion to the lower part of the crater (causing a landslide on the portion of the crater flank) and with the opening of the effusive vent at 600 m a.s.l. Velocities in the first hours of the eruption were so high that exceeded the capability of the GB-InSAR device.

After few hours from the effusion onset, the interferograms returned partly coherent and showed a complex deformation pattern characterized by:

1. a complete decorrelation on the crater flank due to the explosion and to morphological changes related to the crater collapse;
2. concentric interferometric fringes related to the bulging before the vent opening at 600 m a.s.l.;
3. parallel interferometric fringes related to landslide movements on the SdF.

During the entire effusive phase, velocity values, on the SdF slope, constantly decreased from 30 mm/h to 0.2 mm/h toward the sensor, with the only exception of two limited periods related to the opening of a new vent (8, 9 March) and to a major explosion (15 March).

In particular since 8 March the velocity recorded on the SdF increased again with movements toward the sensor. The interferogram highlighted a very high deformation rate (more than 300 mm/h, Fig. 23.1), which again exceeds the capability of the correct phase unwrapping. The arrangement of the interferometric fringes is related to the bulging due to the opening of a new vent, occurred at 14.30 UT of 9 March. Following the method proposed by Fukuzono (1985) and Voight (1988) it has been possible to predict in advance of one day the opening of the 9 March vent.

After 12 April, the eruption is to be considered concluded and the velocity recorded by GB-InSAR progressively decreased down to the values characteristic of the normal activity of the Stromboli volcano.

The GB-InSAR monitoring allowed us to highlight different deformation patterns, related to the eruption and to the associated landslides, suggesting different triggering mechanisms of the deformation process. Furthermore the GB-InSAR system has recorded changes in the deformation patterns, both on the crater area and on the SdF sector, in advance with respect to the onset of each one of the relevant events.

The absolute values of velocity recorded are plotted in Fig. 23.8: the red line represents movements toward the sensor (negative radar displacements), while the blue line represents movement backward with respect to the sensor (positive radar displacements). In the Fig. 23.8 the three different phases, above mentioned, are shown. The pre-effusive phase (from 10 January to 27 February) is represented in green area, characterized by very low, progressively increasing, deformation rates; the effusive phase (from 27 February to 12 April) in magenta area, characterized by very

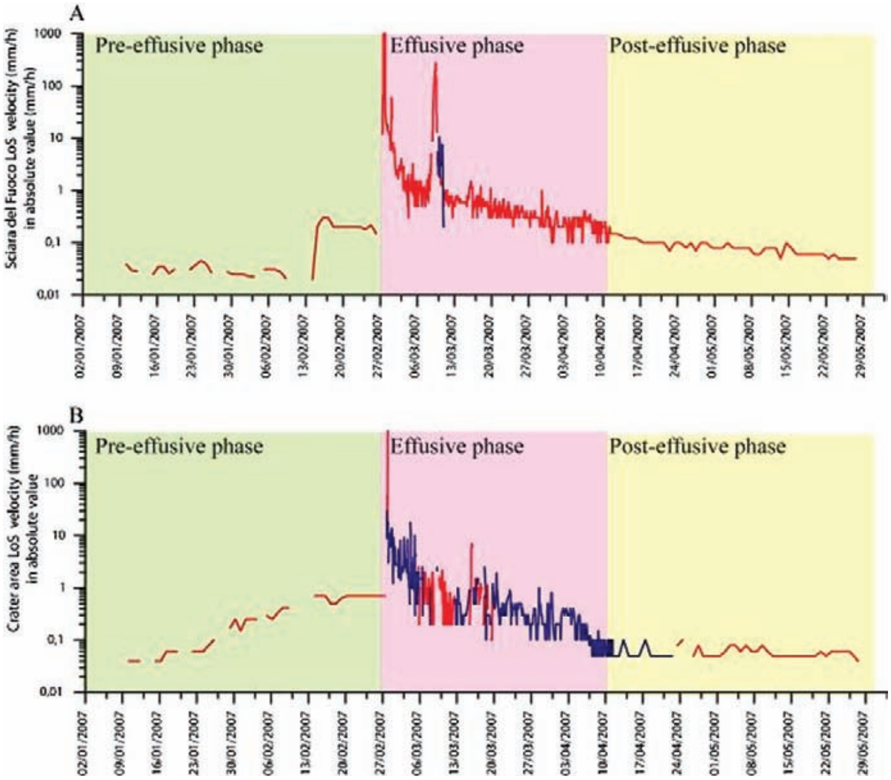

Fig. 23.8 GB-InSAR velocity plot during the 2007 Stromboli eruption measured on the Sciara del Fuoco (**A**) and on the crater (**B**). LoS velocity is in logarithmic scale to emphasize the low displacement rate in the first period of the pre-effusion phase and in the post-effusion phase. The *red line* represents a displacement toward the SAR sensor (negative radar displacement); the *blue line* represents the deformation backward with respect to the SAR sensor (positive radar displacement)

high velocity of deformation and the post-effusive phase (from 12 April; yellow area) in which the deformation rates decreased down to the pre-crisis values.

23.3.2 A Geotechnical Approach to Slope Stability Analysis at Active Volcanoes

P. Tommasi, L. Verrucci(CNR-IGAG, Italy), D. Boldini(DICMA, mbientali, Universita di Bologna, Italy), A. Graziani, T. Rotonda(DISG, Universita Sapienza, Italy)

Introduction: Factors affecting the stability of flanks of active volcano are first described with specific references to their influence on hazard evaluation. In particular, the importance of even relatively small landslides in determining risk is discussed with the aid of two case histories. Geotechnical analyses of instability phenomena affecting the volcanic islands of Stromboli and Vulcano are therefore presented providing major results concerning instability mechanisms and their rebound on hazard assessment.

Keywords Volcano stability • Geotechnical modelling • laboratory testing

23.3.2.1 General Aspects of Instability of Volcano Flanks

Flanks of active volcanoes are affected by a wide variety of instability phenomena ranging from rock slides or slumps in loose material displacing a few hundreds of m^3 up to lateral sector collapses involving hundreds of millions of m^3, even within the same volcanic edifice (McGuire, 2003). The largest collapses usually involve submerged volcanic edifices. Frequency of failure phenomena is usually inversely correlated to their dimension with the consequence that population often does not have an immediate perception of the hazard related to the largest events.

Also instability mechanisms are variable and largely influenced by volcanic activity in many respects (Voight & Elsworth, 1997). Therefore, for active volcanoes instability can depend on factors that are not considered or are less relevant for the stability analysis of slopes in other environments.

Most of the studies concerning the stability of active volcanoes deal with sector collapses, which due to the large amount of mobilized material are expected to propagate to large areas surrounding the volcano. Furthermore the collapse can determine stress changes and modifications to fluid pressures that can produce great changes in the physical system of the volcano, which can cause much more violent activity.

However, there are examples indicating that even failures of smaller extent may have significant impact on human lives and activities. In fact risk depends also on intensity of human activities, type of evolution of the failure phenomenon and physical environment in which the volcanic edifice is set.

For example, high risks may be expected when landslides:

– evolve into debris/rock avalanches/flows which (depending on the type of material, water content and slope morphology) that can reach tens of kilometers far from the source area at a speed of more than 300 km/h (Voight & Elsworth, 1997);
– produce tsunami waves having a high damage potential in relatively far-field conditions (i.e. on partially submerged volcanic edifices);

Furthermore, on the flank of active volcanic islands having a significant volcaniclastic or loose pyroclastic component, evolution of instability phenomena can be controlled by pore pressure development in the submerged portion of the slope.

In this paper a review of factors influencing stability of slopes on active volcanoes will be given first with a special regard to the geotechnical and engineering geology literature.

The contribution of geotechnical characterization and modelling to the evaluation of the hazard associated to landslides on active volcanoes will be discussed in succession, with the aid of two case histories concerning different types of instability phenomena on two volcanic islands of the Eolian archipelago, north of Sicily: the Stromboli volcano and La Fossa volcanic edifice on the Island of Vulcano.

23.3.2.2 Failures on the NW Flank of Sromboli Volcano

In December 2002 the NW flank of Stromboli volcano was involved in a sequence of landslide failures producing tsunami waves that reached the inhabited coast of the island. The sequence was initiated by a relatively shallow magma intrusion into the slope top, which induced large deformations in the upper part of the NE sector of the flank. Deformations progressively extended downhill involving also the submarine slope which successively failed. Eventually the already disturbed subaerial slope, deprived of support at its foot, slid into the sea.

Instability mechanisms acting in the different phases of the sequence varied according to the progressive change of stress/strain and hydraulic conditions that occurred as the evolution of the slope proceeded. In particular within the zone where shear displacement concentrated, significant modifications of the grain size of the volcaniclastic materials, and hence changes in strength and permeability, occurred. Similarly displacement rates and state of stress within the slope changed due to the progressive disruption of the slope itself.

Shear strength and stress-strain behaviour of the volcaniclastic materials (the weakest component of the deposit forming the NW flank of the island) were thereafter analyzed through laboratory investigations carried out on both dry and saturated material having different grain size and within different strain ranges. Experimental results contribute to explaining the evolution of instability processes towards failure in the submerged slope as well as the current evolution of the volcano flank.

In order to investigate the role of intruded magma in initiating instability phenomena, 3D numerical stress-strain analyses of the volcano flank were carried out, based on the geotechnical characterization. Results were compared to the observed deformations.

The relatively high shear strength of the dry material accounts for the overall stability of the slope in the ordinary state of stress and in the initial stages of deformation, when displacement rates are too low to determine drained conditions in the submarine slope.

Stress-strain analyses confirm that large deformations were confined to the upper part of the slope and vanish in the near-shore portion of the submarine slope according to the reconstruction presented by other authors.

The sudden failure necessary to generate the tsunami implies that in the submerged slope an abrupt decrease in shear strength had to occur. A failure mechanism characterized by this strength drop (i.e. static liquefaction) was observed in undrained and naturally drained laboratory tests (Boldini et al., 2005 and Tommasi et al., 2007).

23.3.2.3 Instability Phenomena of the La Fossa Volcanic Edifice in the Volcano Island

At La Fossa volcanic edifice the analysis of planar landslides along bedding planes in the pyroclastic cone and deep-seated gravitational deformations involving also the substratum is presented.

Instability phenomena and their relationships with volcanic activity were back-analyzed utilizing quantitative data from laboratory investigations, borehole core logging and in-situ surveys while the influence of the marine erosion along the sides of the NE sector on the state of stress and deformation of the volcanic edifice was evaluated by means of 3D modelling based on the geological and geotechnical investigations.

In particular, the alteration largely affects strength properties of both soil-like and rock materials thus representing a key-factor for the development of instability phenomena.

Deep-seated deformations inferred from morphological evidences and shear zones observed in a geotechnical borehole seem to have occurred under severe stress conditions that could act only during periods of particularly intense unrest, when fluid pressure in the edifice were much more intense.

Shallow slope instabilities are instead favoured by material alteration, and by the state stress induced by the erosional processes (largely submarine) acting on an edifice with a weak basement, as recognized also in other active volcanoes (Hürlimann et al., 1999).

23.4 Submarine Slides and Their Consequences

Farrokh Nadim (International Center for Geohazards/NGI)

Introduction: Submarine slides are common and very efficient mechanisms of sediment transfer from the shelf and upper slope to deep-sea basins. Typically such events last from less than an hour to several days and can severely damage fixed platforms, pipelines, submarine cables and other seafloor installations. Research on understanding the mechanisms behind and the risks posed by submarine slides has intensified in the past decade, mainly because of the increasing number of deep-water petroleum fields that have been discovered and in some cases developed. Production from offshore fields in areas with earlier sliding activity is ongoing in the Norwegian margin, Gulf of Mexico, offshore Brazil, the Caspian Sea and West Africa. Large submarine slides may generate tsunamis with the potential for severe damage along coastlines.

This paper reviews the recent advances in assessment and analysis of the risk associated with submarine slides and makes recommendations regarding the evaluation of triggering mechanisms and runout distance.

Keywords Submarine slide • Risk evaluation • Tsunami

Acknowledgments The author wishes to thank his many colleagues at NGI, ICG, and elsewhere, whose valuable contributions receive only a passing mention in the paper.

23.4.1 Background

Submarine landslides occur frequently on both passive and active continental margins, especially on the continental slopes. Despite the generally low slope angles, these are areas of sloping stratigraphy, often with more active and vigorous geological processes, including seismicity, than those found in the shallow, sub-horizontal continental shelf areas. The shelf edge and slope area contain the most recently deposited materials, and in areas with high deposition rate, underconsolidation/excess pore pressure may exist. During one single event enormous sediment volumes can be transported on very gentle slopes with inclinations in the range 0.5–3°, over distances exceeding hundreds of kilometers. The excess pore pressure often plays a major role in destabilization of submarine slopes. The expenses of finding and developing new fields in deep water are very high, and this greatly increases the economic consequence part of the risk aspect connected to submarine slides in the continental margin settings.

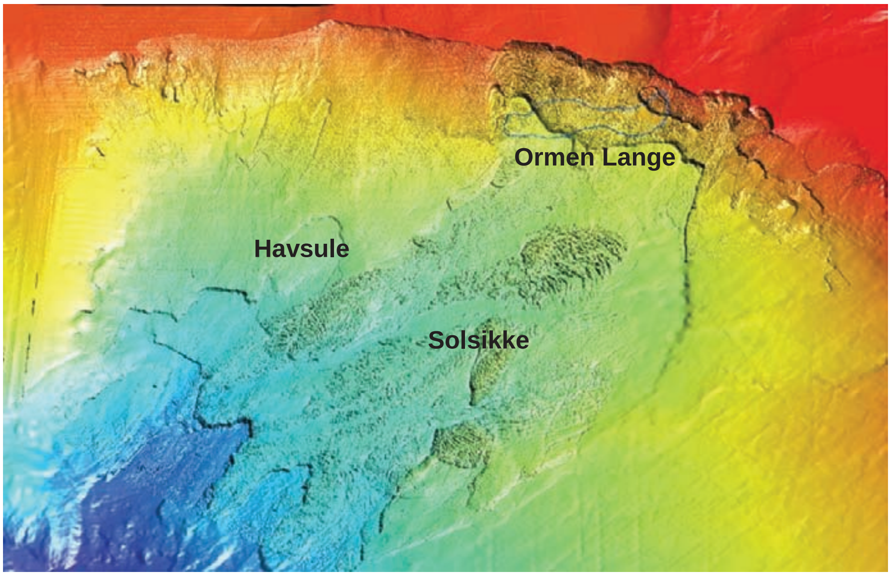

Fig. 23.9 Storegga slide and boundary of Ormen Lange gas field in the North Sea

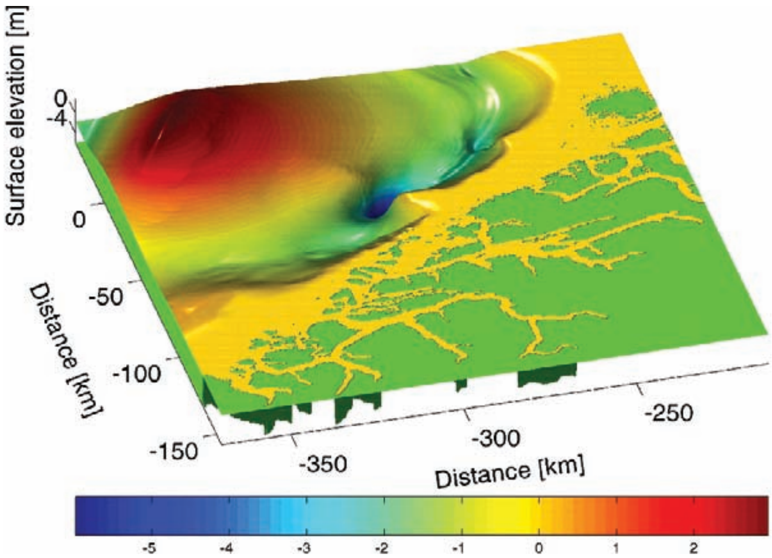

Fig. 23.10 Simulation of the tsunami triggered by the Storegga slide approaching the west coast of Norway

23.4.2 Tsunamis Triggered by Submarine Slides

The assessment of the risk associated with submarine mass movements is thus not just a matter related to commercial interests of oil companies. The societal and environmental consequences of such events could also be enormous for coastal communities. For instance, large submarine slides may generate tsunamis with potential for severe damage along the coastline. The tsunami generated by the earthquake-triggered Grand Banks slide in 1929 killed 27 people in Newfoundland. The 15 m-high tsunami that killed more than 2000 people in Papua New Guinea in 1998 was also a result of an earthquake-triggered submarine slide.

The ongoing development of the Ormen Lange field, which is the second largest gas field on the Norwegian Continental Shelf, has contributed greatly to the understanding of the offshore geohazards. The Ormen Lange gas field is located in the Norwegian Sea in water depths of about 800–1,100 m, approximately 120 km from the coastline, within the scar of the prehistoric Storegga slide (Fig. 23.9). The Storegga slide, which took place 8,200 years ago, is one of the world's largest known submarine slides with an estimated slide volume in excess of 3,000 km^3. Evidence of a major tsunami generated by the Storegga slide has been found along the coasts of Norway, Scotland and the Faeroe Islands (Fig. 23.10). Considering the enormity of the Storegga slide and the potentially catastrophic consequences of a similar event today, it was essential to clarify and quantify the risks associated with submarine slides in the area to obtain approval for field development from the authorities. A major effort was therefore undertaken to evaluate the stability situation of the slopes in the Ormen Lange area today, and quantify the potential risks associated with the field development in the future. The numerous studies carried out in the Ormen Lange offshore geohazards project were summarized in a special volume of Marine and Petroleum Geology journal in 2005. These studies represent the state-of-the-art in quantitative risk assessment for submarine slides.

23.4.3 Conclusions

Submarine slides are common and very efficient mechanisms of sediment transfer from the shelf and upper slope to deep-sea basins. They could occur on very gentle slopes and they have the potential for triggering a tsunami.

The increasing activity on the deepwater part of the continental slopes has set the focus on the need for a systematic treatment of the risk associated with submarine slides. Risk assessment requires quantitative description of geology and soil properties, identification of possible failure events, triggering sources and mechanisms and ability to judge the likelihood of occurrence and the damage potential.

References

Antonello, G., Casagli, N., Farina, P., Guerri, L., Leva, D., Nico, G., Tarchi, D. 2003. SAR interferometry monitoring of landslides on the Stromboli Volcano. Proceedings of FRINGE 2003 Workshop, 1–5 December 2003, ESA/ESRIN, Frascati, Italy.

Antonello, G., Casagli, N., Catani, F., Farina, P., Fortuny-Guasch, J. Guerri, L., Leva, D., Tarchi, D. 2007. Real-time monitoring of slope instability during the 2007 Stromboli eruption through SAR interferometry. Proceeding of 1st NACL, Veil (Colorado).

Boldini, D., Wang, F.W., Sassa, K., Tommasi, P. 2005. Mechanism of landslide causing the December 2002 tsunami at Stromboli volcano (Italy). In: Sassa, K., Fukuoka, H., Wang, F.W., Wang, G. (Eds.) Landslide: Risk Analysis and Sustainable Disaster Management, Springer, Berlin, pp. 173–180.

Casagli, N., Farina, P. Leva, D., Tarchi, D. 2004. Landslide monitoring on the Stromboli volcano through SAR interferometry. Proceedings of 9th International Symposium on Landslides, Rio de Janeiro, Brasil.

Chen, H., Petley, D.N. 2005. The impact of landslides and debris flows triggered by Typhoon Mindulle in Taiwan. *Quarterly Journal of Engineering Geology and Hydrogeology*, 38(3), 301–304.

Fukuzono, T. 1985. A new method for predicting the failure time of a slope failure. Proc. 4th Int. Conf. and Field Workshop on Landslides, Tokyo (Japan), pp. 145–150.

Hürlimann, M., Ledesma, A., Martí, J. 1999. Conditions favouring catastrophic landslides on Tenerife (Canary Islands). *Terra Nova*, 11, 106–111.

Jeanjean, P., Hill, A., Taylor, S. 2003. The challenges of confidently siting facilities along the Sigsbee Escarpment in the Southern Green Canyon area of the Gulf of Mexico – Framework for integrated studies. *OTC*

15156, Offshore Technology Conference´03, Houston, Texas, 5–8 May.

Keefer, D.K. 1984. Landslides caused by earthquakes. *Geological Society of America Bulletin*, 95, 406–421.

Kvalstad, T.J., Berg, K., Bryn, P., Wangen, M., Nadim, F., Forsberg, C.F., Gauer, P. 2005. The Storegga slide: Evaluation of triggering sources and slide mechanics. *Special issue of Marine and Petroleum Geology on Ormen Lange*.

Liao, H.-W., Lee, C.-T. 2000. Landslides triggered by the Chi-Chi earthquake. *GIS Development*: http://www.gisdevelopment.net/aars/acrs/2000/ts8/hami0007.asp.

Lin, J.-C., Petley, D.N., Jen, C.-H., Hsu, M.-L. 2006. Slope movements in a dynamic environment – A case study of Tachia river, Central Taiwan. *Quaternary International*, 147(1), 103–112.

Marui, H., et al. 2007. Landslide Dams Formed by the Mid-Niigata Prefecture Earthquake in Japan, Progress in Landslide Science, Springer, pp. 285–293.

McGuire, W.J. 2003. Volcano instability and lateral collapse. *Revista*, 1, 33–45.

Owen, L.A., Kamp, U., Khattak, G.A., Harp, E.L., Keefer, D.K., Bauer, M.A. 2008. Landslides triggered by the October 8, 2005, Kashmir earthquake. *Geomorphology*, 94, 1–9.

Petley, D.N., Dunning, S.A., Rosser, N.J. and Kausar, A.B. 2006. Incipient earthquakes in the Jhelum Valley, Pakistan following the 8th October 2005 earthquake. In: Marui, H. (Ed.) Disaster mitigation of debris flows, slope failures and landslides. *Frontiers of Science Series* 47, Universal Academy Press, Tokyo, Japan, pp. 47–56.

Rudolf, H., Tarchi, D. 1999. LISA: The Linear SAR Instrument. DG JRC, European Commission, Technical Note No. I.99.126. July 1999.

Sudmeier-Rieux, K., Qureshi, R.A., Peduzzi, P., Jaboyedoff, M.J., Breguet, A., Dubois, J., Jaubert, R., Cheema, M.A. 2007. An interdisciplinary approach to understanding landslides and risk management: a case study from earthquake-affected Kashmir. Mountain Forum, Mountain GIS e-Conference, January 14–25, 2008.

Tommasi, P., Boldini, D., Cignitti, F., Graziani, A., Lombardi, A. Rotonda, T. 2007. Geomechanical analysis of the instability phenomena at Stromboli. Volcano. I Canadian-U.S. Rock Mechanics Symposium, Vancouver, vol. 1, pp. 933–941, Taylor & Francis Group, London.

Voight, B. 1988. Material science law applies to time forecast of slope failure. *Landslide News*, 3, 8–11.

Voight, B., Elsworth, D. 1997. Failure of volcano slopes. *Geotechnique*, 47(1), 1–31.

Rainfall, Debris Flows and Wildfires

24

Jerome V. DeGraff and Hirotaka Ochiai

Abstract While rainfall is not the only triggering mechanism for debris flows, it is a significant one over a large part of the world. A better understanding of storm characteristics that commonly result in debris flows can improve preparedness and warning systems. Current research indicates that identifying regional variability in triggering storms events would advance risk reduction. Models that permit macro-scale analysis of debris flow initiation and mobilization enable researchers to better define the more vulnerable areas for future debris flow occurrence and the relative effectiveness of countermeasures. Similarly, a better understanding of debris flow occurrence within the broader continuum of erosion processes makes it possible to both understand their initiation and their impact on the fluvial environment. Large-scale human alteration of vegetation for forestry, agriculture or wildfire influences the probability that subsequent rainfall will induce debris flows. Understanding the interaction of vegetation, earth materials and rainfall provides a means for how these anthropogenic actions are influencing existing levels of debris flow hazard.

Keywords Rainfall-induced debris flows • Intensity-duration thresholds • Flume studies • Risk reduction • Debris flow mobilization • Wildfires • Rainforests

24.1 Introduction

Debris flows, due to their rapid movement and ability to travel significant distances from their points of origin, can pose a notable threat to people, property and infrastructure located within their paths. A spectacular example is the December 1999 storm event in northern Venezuela. This single storm triggered debris flows and flash floods that killed some 15,000 people representing approximately 5% of the local population (Larsen and Wieczorek, 2006). Extensive damage estimated at more than USD$2 billion was sustained by communities and infrastructure along a 50-km coastal strip (Fig. 24.1). It holds the unenviable record of being one of the worst natural disasters on records in the Americas (Larsen and Wieczorek, 2006).

In places as different as Japan, Slovenia and Dominica, W.I., rainfall-induced debris flows are responsible for people being injured or killed, property and infrastructure being damaged or destroyed and direct and indirect economic losses (Wang et al., 2005; Mikoš et al., 2006 and DeGraff et al., 1989). While the 1999 northern Venezuela event

Jerome V. DeGraff (✉)
USDA Forest Service, Sierra National Forest, Clovis, CA, USA
e-mail: jdegraff@fs.fed.us

Hirotaka Ochiai
Foresty and Forest Product Research Institute, Japan

K. Sassa, P. Canuti (eds.), *Landslides – Disaster Risk Reduction*,
© Springer-Verlag Berlin Heidelberg 2009

Fig. 24.1 Aerial view of debris-flow deposits up to 5 m in thickness and totaling about 1.8 million m3 on the fan of the Río San Julián at Caraballeda. Avulsion at the apex caused flow through center of fan to the *lower right* of photograph (Photograph by Lawson Smith, U.S. Army Corps of Engineers)

represents an extreme example, the cumulative effect of many smaller events happening in a locality every year or within a region over many years demonstrate the risk posed by the occurrence of this type of landslide (Schuster et al., 2002).

Risk from landslides as it applies to rainfall-induced debris flows is the combination of the hazard, i.e., debris flows, and the elements at risk. In an established formula, the specific risk from rainfall-induced debris flows would be (Varnes, 1984):

$$R_{df} = (E)(H_{df} \times V)$$

where: R_{df} – Risk (rainfall-induced debris flows)

E – Elements at Risk

H_{df} – Hazard (rainfall-induced debris flows)

V – Vulnerability

Rainfall-induced debris flow hazard is the probability of one happening during a particular period of time within a specific area. Obviously, rainfall-induced debris flows are linked to the probability of storm events capable of triggering their occurrence in a given area. Using the 1999 northern Venezuela example, the debris flows were induced by a low probability storm event. Calculating the specific probability of this storm was complicated by the length of the available record and distribution of recording rain gages. Different calculations placed its probability from >1,000-year to a 150 year recurrence (Larsen and Wieczorek, 2006). The storm event initiated many individual or coalescing debris flows from affected hill slopes. Consequently, the hazard was from multiple debris flows passing along channels in 24 watersheds (Larsen and Wieczorek, 2006).

Vulnerability modifies the hazard present in a given area. It is defined as ranging from complete destruction to none at all as reflected on a scale from 1 to 0. It is difficult to imagine how the passage of fast-moving viscous mass which usually has a bouldery snout and can entrain boulders and large woody debris would not cause nearly or complete destruction within its path. Debris flows cause damage by lateral impact, drag, burial and buoyancy (Campbell, 1985) (Fig. 24.2). However, it is possible due to the physical conditions at the points where debris flows intersect constructed features, and the character of the features themselves, that varying degrees of survivability will exist.

The elements at risk in a given area include the population, properties and economic activities, including public services, which may be impacted. At the time of the 1999 northern Venezuela event, the impacted area contained approximately 300,000

Fig. 24.2 Apartment building in Caraballeda extensively damaged by passage of debris-flow front at least 3.5 m in height, depositing boulders (>1 m long) on second floor of structure. Note apartment building in background similarly damaged by debris flow. (Photograph by Matthew C. Larsen, USGS)

people who either lived or worked there (Larsen and Wieczorek, 2006). Within this densely populated area, there were large numbers of homes, apartment buildings and commercial and government buildings. A significant network of roads, water lines, sewage and storm water collection systems as well as telephone and electrical infrastructure supported this developed area. Unquantified, except in terms of loss, are the economic activities present at the time of this event. With losses estimated at USD $2 billion, the pre-storm economic activities must have been substantial.

While not fully documented, it is suggested that debris flows and other shallow mass movements triggered by rainfall likely represent both the largest volume of mass wasting worldwide and the greatest number of slope movements (Sidle and Ochiai, 2006). It is therefore not a great leap to the realization that debris flows may be responsible for the greatest amount of environmental damage by landslides. Benda and Dunne (1997) point out that the sediment budget of many mountain drainage basins is dominated by landslides including debris flows. The delivery of large amounts of sediment to channels will have an impact to that localized area. It may also affect channels for distances up to tens of kilometers (Benda and Dunne, 1997). Sediment transmitted down channel may cause problems for a variety of water uses (Sidle and Ochiai, 2006). Communities and individuals that depend on diverted surface water for domestic supplies or local industries are forced to undertake additional treatment to ensure water quality. Diversions into agricultural conveyances such as ditches and canals are potentially impaired by sediment or need more frequent maintenance. Sediment may render bridges and other road drainage structures less effective by blocking or reducing their capacity to carry normal storm flows. Downstream aquaculture facilities, such as shrimp-growing ponds, may also be negatively impacted by a sudden influx of sediment (NOC, 1989)

The direct change to stream channels from debris flows can be drastic (Sidle and Ochiai, 2006). Long reaches may be scoured to bedrock in headwaters streams. Depending on changes in downstream gradient, some reaches will become narrowed due to the influx of sediment beyond the ability of normal flows or even change to a braded stream channel from a single channel. Debris-flow generated sediment can adversely affect the availability of spawning gravels, riparian vegetation and create temporary barriers to fish migration.

Where debris flows actually dam the stream, water will be come impounded behind the dam until it fails. This changes the channel by flooding upstream from where the dam forms and modifies downstream reaches by sudden release of water upon its later breaching. The channel where the dam formed is especially impacted for an extended period of time by the large amount of sediment deposited. These circumstances are dramatically demonstrated by two debris-flow dam forming events in Dominica, W.I. (DeGraff and Rogers, 2003).

Dominica is an island nation in the eastern Caribbean located north of Martinique and south of Guadalupe. Landslide dams affected its largest river, the Layou, in November 1997. The landslide dams formed in the Layou River at its junction with its tributary, the Matthieu. This location is approximately 8 km from where the Layou enters the Caribbean Sea.

The first landslide dam passed from the Matthieu into the Layou on November 12, 1997 nearly blocking the channel. The Layou became fully dammed 6 days later when another debris flow added to the deposit of the first. The impounded water rose quickly causing a breach of the dam and downstream flooding early on November 21st.

Four days later, a larger landslide blocked the mouth of the Matthieu. The leading part of this movement was a debris flow that entered the Layou River. The debris flow deposited on the remnants of the earlier landslide dam and formed the larger of the two blockages. On November 28, the second debris flow dam failed releasing the impounded water to again flood the lower reaches of the Layou River to the sea. The formation and failure of these natural dams significantly narrowed the Layou River at the landslide dam location and caused widespread aggradation throughout the lower reaches of the river (Figs. 24.3a and 24.3b).

Fig. 24.3a The Layou River eroding through the remnants of two breached debris flow dams re-establishing its channel on Dominica, W.I. The debris flows entered the river from the (now blocked) Matthieu River on the *left*. (Photograph by Jerome V. DeGraff, USDA Forest Service)

Fig. 24.3b The mouth of the Layou River near the community of Layou, Dominica, W.I. as it was seen 17 days after the last dam-breach flooding. Sediment-laden waters created a visible plume estimated to extend over a kilometer into the Caribbean. (Photograph by Jerome V. DeGraff, USDA Forest Service)

Not all debris flows are initiated by intense rainfall (Wieczorek, 1996). However, this triggering mechanism is a significant one across large parts of the world; especially in locations frequently subjected to cyclonic and monsoon storms (Sidle and Ochiai, 2006). Cyclonic storms such as typhoons and hurricanes are prevalent as sources for the intense rainfall leading to debris flow occurrence. Monsoons and strong frontal storms passing over coastal mountains ranges can also produce debris-flow inducing rainfall. Consequently, the areas globally where rainfall-induced debris flows would commonly occur include the coastal areas around the Pacific Rim, New Zealand and other large Pacific islands, Southeast Asia, the Caribbean region and parts of North and South America. Localized short-duration convective rainstorms also have the potential for producing rainfall intensities capable of inducing debris flows. This makes many mountains ranges in the world potential locations for this phenomenon.

Clearly, rainfall-induced debris flows represent a widespread hazard. It also represents a significant adverse impact on the environment. Rainfall-induced debris flows are a hazard that affects part of the world where large populations and their attendant property and economic activities are present. Those parts of the world are also where populations and social development are increasing. Consequently, the risk relationship would forecast an increased risk simply because more people, property and economic activities will be found where this phenomenon occurs.

To do nothing, predictably results in a greater toll in human lives and economic loss. Addressing the hazard component of the risk relationship through mitigation has the potential to mitigate future risk. This would permit future development, where rainfall-induced debris flows may occur, to be sustainable. Successful mitigation must be based on improved scientific understanding of how rainfall triggers debris flows, especially their initiation, and how vegetation or changes to vegetative cover influence this triggering mechanism.

24.2 Intensity-Duration Thresholds and Warning Systems

Triggering of debris flow is controlled by the nature of soil at or near the ground surface and the shallow groundwater response to the character of rainfall events. Campbell (1975) refined our understanding of this triggering mechanism. He defined the contributing conditions of water introduced into the slope-mantling soil that resulted in movement of a soil mass and its transformation down slope as a debris flow. His pioneering work found that once antecedent moisture requirements for the soil were satisfied, both the duration of a storm and the rainfall intensity occurring during the storm were controlling factors in initiating debris flows.

It is recognized that rainfall intensity-duration thresholds represent a surrogate for actual measurement of the infiltration and movement of water into the ground and its role in triggering debris flows. Caine (1980) first suggested that a rainfall intensity-duration relationship could be used to define when rainfall-induced debris flows would occur worldwide. The amount of water infiltrating during a storm is influenced by a number of physical factors that vary widely over short distances. Consequently, it is very difficult to measure rainfall infiltration or to represent it accurately over a large area. In contrast, rainfall is readily measured at recording stations and, while it is more variable in mountainous areas, it is amenable to extrapolation over large areas.

An update of the rainfall intensity-duration relationships globally was published by Guzzetti and others (2008). Like Caine's threshold, these new thresholds correspond to the *minimum* rainfall intensity-duration for the possible initiation of rainfall-induced debris flows as well as other shallow landslides. These thresholds represent an improvement by being based on a larger dataset and by maximizing the objectivity of inferring thresholds through statistical methods. However, the availability of data for such determinations is not consistent worldwide. Therefore, continued research of rainfall intensity-duration relationships is valuable to further refine global thresholds and better understand threshold differences among different climatic regimes. Continued regional-level studies will contribute greatly to this effort (Larsen and Simon, 1993; Godt et al., 2006).

One of the main reasons for the great interest in rainfall intensity-duration thresholds is their potential as a means to provide early warning of increased debris flow hazard. A real-time system for issuing warnings during major storms was successfully implemented in the San Francisco Bay area of California (Keefer et al., 1987). An intense storm event between January 3 and 5, 1982 impacted the San Francisco Bay area. The storm triggered numerous shallow landslides and debris flows resulting in the deaths of 25 people and damage exceeding USD $66 million (Ellen and Wieczorek, 1988). A regional intensity-duration relationship coupled with the widespread availability of recording rainfall stations in this region suggested that a warning system might prevent, reduce or eliminate the threat to life during a future storm event. The first use of this approach was during storms occurring between February 12 and 21, 1986. Using locally applicable thresholds, warnings of possible debris flow occurrence were issued by the National Weather Service (USA) through local radio and television outlets. Based on eyewitness reports, ten landslides triggered by the storms could be verified as coinciding with issued warnings (Keefer et al., 1987). It demonstrated the potential for reducing the loss of life through accurate warning of possible debris flow occurrence.

Scientifically defining the point at which debris flows might begin to occur during a storm will not be totally sufficient to prevent loss of life. An effective warning system also requires having a means for quickly communicating this information to vulnerable communities (Larsen, 2008). The best means will vary with locality (rural vs urban) and commonly available communication methods for a particular area. The San Francisco Bay area warning system depended on public communications through radio and television. While uniformly covering the area, it does assume that people are monitoring these communication devices and will continue to have electrical power during a storm event. As part of a warning system for debris flows and flash floods in Orange County (Southern California) during 2007–2008, a reverse 911 system was established. This permitted the sending of a recorded message to individual's mobile phones from the centralized emergency services communication center to issue timely warnings. This supplemented the radio and television warnings being issued.

Secondly, it requires that the population receiving the warning responds appropriately to the potential debris flow threat. To respond appropriately, people must understand the nature of the threat as it applies to their personal circumstances and have the means for taking the correct action. In some cases, evacuation to a safer location may put people at greater risk if the evacuation route would have more potential for being crossed by potential debris flow paths than the risk posed at their residence, school or work place. People will need pre-storm education and planning information to understand what is the best way for them to respond when warned of possible debris flow occurrence. Residents potentially at risk from debris flows and floods in Orange County during 2007–2008 were informed at public meetings and through media reports about planning that identified areas that should be evacuated when a warning was issued. Locations where community shelters would open were also provided.

Keefer et al. (1987) recognized that debris flows were the most life-threatening landslide type and focused their efforts on defining the intensity-duration relationship that identified threshold conditions that triggered these landslides during a storm event. Threshold accuracy is important for two reasons; one that is obvious and one that is less so. It is obvious warnings may not be issued in a timely manner if a threshold is inaccurate or too generalized for a particular area. People would be unable to act to protect themselves from the debris flow hazard. Less obvious is the problem when inaccurate thresholds cause repeated false alarms. This causes a warning "fatigue" that makes people less likely to act when future warnings are issued.

24.3 Debris Flow Initiation and Mobilization

Fully understanding the interactions from debris flow initiation to mobilization is not a simple task. The majority of debris flows begin as slope movements. When a debris flow is about to be initiated, it is an unmoving, saturated part of a slope. It is unlikely that an observer fortunate enough to be present would see any visible difference between this impending initiation site and slope surrounding it. However, initiation and mobilization would quickly transform this saturated soil block into a flowing sediment-water mixture. It would rapidly leave the initiation site and pass some distance down slope before returning to a static state as a deposit.

Field data are limited to what can be gleaned by examining the slope materials adjacent to the evacuated scar where the debris flow began and the resulting deposit. Any critical information on the role of water in initiation and mobilization is lost by the time it transformed into a flowing sediment-water mixture. Post-debris flow field evidence yields only the most general information about the role of water. Iverson (1997) accurately notes, "The capricious timing and magnitude of debris flows hamper collection of detailed data."

Reconstructing the likely pore water pressures at the time of debris flow initiation is difficult. Sidle and Ochiai (2006) identify four hydrological factors contributing to development of pore pressure within hillslope soil mantles. These are: precipitation, soil physical properties, infiltration and subsurface flow processes.

Precipitation data can potentially be developed from rainfall recording stations covering the area where a debris flow has occurred. Reconstructing the actual rainfall at the initiation site will be highly dependent on the type of recording devices and their placement. This is especially true for sites in mountainous locations where considerable variability can exist over relatively short distances (a few kilometers). It is unlikely in most instances that reconstruction of precipitation will be accurate enough to satisfy requirements for detailed modeling of infiltration and subsurface flow.

Soil physical properties can be reasonably determined by examination of exposed material within the scar at the debris flow initiation site. Instrumentation of nearby parts of the slope could provide information on infiltration. This would provide insight into the likely infiltration at the time the debris flow occurred. However, it may require a prolonged period of monitoring to obtain a data set that would be reliable in this reconstruction.

A reasonable substitute for field-derived data is to experimentally replicate the initiation and mobilization of debris flows through large-scale flume studies. One such facility was constructed by the U.S. Geological Survey in cooperation with the U.S. Forest Service at their H.J. Andrews Experimental Forest east of Eugene, Oregon (Iverson et al., 1992) (Fig. 24.4). Flume studies permit instrumentation to record transient information on pore-water pressures and other factors important to debris flow initiation and mobilization. For example, Reid et al. (2006) reported on flume experiments relating initiation style and timing to hydrologic triggers and soil density. Of particular value was identifying crucial transient pore pressure changes that would likely be undetected by conventional piezometers. Another advantage to these experimental methods is the ability to refine numerical simulations of shallow groundwater-soil interactions. Reid et al. (see following extended abstract) successfully used flume studies to examine the role of soil porosity in initiation behavior under different triggering conditions. Okada and Ochiai (seeing following extended abstract) combined flume simulation with initiation of a slide on a natural slope to better relate experimental results to field-based results.

Fig. 24.4 An completed debris flow experiment at the U.S. Geological Survey flume located in the H.J. Andrews Experimental Forest, Oregon (USA). The inset shows a debris flow moving down the flume. (Photograph from Logan and Iverson, 2007)

24.4 Debris Flows and Wildfires

In the mid-latitude Mediterranean climate chaparral biome, debris flow occurrence is a result of the wet-winter, dry-summer character of this zone and its propensity for wildfires. Since 2000, there have been large and destructive fires in many parts of this climate zone. Southern California experienced multiple large fires in 2003 and 2007 (Fig. 24.5). In Australia, 2001, 2003, 2005 and 2006 were years when large and destructive wildfires took place. The widespread wildfires in Greece in 2007 were only the latest affecting the Mediterranean coastal zones west to Spain.

When the fires are put out, the potential for disaster seems gone. It is really only a respite until

Fig. 24.5 Terra satellite image showing smoke plumes from multiple wildfires on October 25, 2003 in Southern California (USA). (National Aeronautics and Space Administration (NASA) photograph)

the winter rains come and debris flows occur on many of the fire denuded slopes. This tandem disaster of wildfire followed by flooding and debris flows was recognized in southern California in the 1930s. In some places, this recognition resulted in policies calling for rapid post-wildfire treatments to reduce the likelihood of debris flows. The recent increase in the size of these wildfires in the southwest United States has shown the need for better prediction of debris flow occurrence and volume (DeGraff et al., 2007). There is a need to make this determination rapidly to permit countermeasures to be in place before the first damage rain storm. There is also a need to understand how wildfire influences sediment generation and debris flow occurrence to ensure that countermeasures are effective.

While wildfires and subsequent debris flows were a problem more than 80 years ago, it is an even greater problem today with a larger population and far more property at risk. Following a wildfire in southern California, it is common to experience rapid creep on fire-affected slopes. This is locally referred to as “dry ravel” and produces granular accumulations behind obstacles, at the base of slopes and within channels (Fig. 24.6). This material consists of sand to small gravel-sized particles that can no longer remain on slopes due to the loss of plant root networks, anchoring stems and woody surficial cover.

During the winter following a wildfire, rain storms normally take place in this Mediterranean climatic zone. Storm runoff can rill the fire-bared slopes moving more granular material down slope toward stream channels. The effectiveness of particle transport by rilling is increased in areas where the fire has created or enhanced development of hydrophobic layers. These layers form within the soil within a few inches to a foot below the ground surface. During a fire, combustion of vegetation

Fig. 24.6 Dry ravel accumulating within days after the area was burned by the 2003 Cedar Wildfire near San Diego, California (USA). (Photograph by Jerome V. DeGraff, USDA Forest Service)

generates organic compound in the surrounding air. As fire passes over an area, these gases enter the pore spaces in the soil and cool to form a low to impermeable layer within the soil. This layer typically deteriorates over the first year following a wildfire thereby restoring the pre-wildfire permeability of the soil.

Sediment production from burned slopes is especially important because recent research shows that most, if not all, post-wildfire debris flows are initiated by runoff and erosion rather than from an initial slope movement. This is in contrast to the initiation of debris flows from an initial saturated mass on the slope that transforms into a flowing sediment-water mixture as described earlier. This difference in debris flow imitation has implications for applicability of duration-intensity thresholds. Therefore, the runoff accumulation mechanism is important for understanding occurrence of debris flows in the aftermath of wildfires.

This debris flow initiation mechanism helps to explain an unusual aspect of the real-time debris flow warning findings in the San Francisco Bay area (Keefer et al., 1987). The area where warnings were being issued based on rainfall duration-intensity thresholds included a 56 km^2 area burned by the Lexington wildfire. It was expected that the February 1986 storms would cause debris flows within the burned area. This expectation was based on studies of burned slopes near Los Angeles, California showing susceptibility to debris flows as well as the occurrence of small debris flows in Lexington wildfire area during the 1985–1986 rainy season. The few debris flows produced by the February 1986 storm were at odds with this expectation (Keefer et al., 1987). Among the possible conditions advanced to explain this variance (Keefer et al., 1987), the most probable based on current understanding is "...relatively little loose, surficial material was available for mobilization."

While runoff accumulation-initiated debris flows were initially recognized in southern California, they are widely found in the western United States (Cannon and DeGraff, keynote paper in this volume). Debris flows associated with the 1994 South Canyon wildfire on Storm King Mountain near Glenwood Springs, Colorado provides an example showing the wildfire-debris flow phenomenon as found in the interior western United States (Kirkham et al., 2000).

Lightning started the South Canyon Wildfire on July 2, 1994 which quickly grew to nearly 1,800 before being contained. It was notable not only for threatening the Glenwood Springs area but for the unfortunate loss of life of 14 wildland firefighters battling this fire.

Within days of the wildfire, dry ravel accumulation began building up as much as a 3-foot thickness of ash, silty sand and sand adjacent to most of the tributary drainages. Many slopes above the channels were mantled with aprons of similar loose material. Almost no rain fell on the burned area until a September 1, 1994 storm event. While a storm totally 17 mm over 24-h has a frequent recurrence for this area, it appear much of it fell during a 4 h period with intense downpours between 8 and 9 p.m. followed by another one about 10.30 p.m.

At about the time of the second intense downpour, debris flows initiated on the burned slopes of Storm King Mountain passing down channels leading to the Colorado River. The debris flows consisted of fine-grained material, rocks and burned woody debris that emptied onto or next to Interstate Highway 70 which parallel the Colorado River.

The debris flows reached the highway and engulfed, trapped, or overturned a total of thirty cares traveling on the highway. While some travelers sustained serious injuries; none were killed. Additional pulses of debris flow material were observed to issue from the canyons during the night of September 1 and early morning of September 2. Nearly 14 ha of low gradient areas along the Colorado River including where Interstate Highway 70 is located was inundated with approximately 69,800 m^3 of material.

Cannon (2001) analyzed the erosional response of 95 recently burned watersheds in Colorado, New Mexico and southern California to begin to identify the factors that best distinguished debris-flow producing drainages from those that only produced sediment-laden water flows. Further research helped to refine these factors and develop the relationships among them that were critical to predicting the probability range for debris flow occurrence and the likely volume (Cannon et al., 2001; Cannon et al., 2007; Gartner et al., 2008). A more in-depth description of the methodology is given in Cannon and DeGraff (this volume). This methodology may or may not be applicable in other parts of the

Fig. 24.7 View of a residential street near Devore, California several months after a December 25, 2003 frontal storm triggered a debris flow that passed down the street from the burned slopes above the community. (Photograph by Jerome V. DeGraff, USDA Forest Service)

Mediterranean climate chaparral biome. But the need will continue for this type of predictive capability because the wildfire trend favors future large wildfires and a large population remains at risk from both the wildfires and the subsequent debris flows.

Globally, the Mediterranean climate chaparral biome includes the coastal zones bordering the Mediterranean Sea; coastal Western Australia and south Australia; Chilean coast, southern California and Cape town region of South Africa. This is an extensive area which includes many densely populated areas. Parise and Cannon (see following extended abstract) compare the Mediterranean area to southern California to demonstrate a similar concern exists for wildfire-related debris flow occurrence in that region (Fig. 24.7).

24.5 Rainforests and Rainfall-induced Debris Flows

Sidle and Ochiai (2006) provide a review of how vegetation influences slope stability that notes many of the significant studies on this topic. It is woody rather than herbaceous vegetation that significantly augments the stability of soil on steep slopes. This augmentation is accomplished mainly in two ways. First, it reduces the moisture present in the soil through evapotranspiration. This can make a significant difference in how water will infiltrate and move through soil during a rainfall event. Second, woody vegetation increases the strength of the soil mantling the slope through the cohesion provided by their roots. The relative effectiveness of these factors depends on the vegetation present and the climatic regime.

Evapotranspiration losses due to vegetation limit debris flow potential. This takes place through two mechanisms. First, forest vegetation intercepts rainfall in the leafy crown and on the branches and main stem. Intercepted water evaporates before reaching the ground or arrives more slowly through stemflow. This has the effect of reducing the peak intensity of rainfall which is one of the factors in debris flow initiation. Greenway (1987) notes that this effect is not well studied and often included in other factors when modeling hydrologic processes. He notes that loss due to interception has been measured from 10% to 66%. In general, the importance of interception loss tends to diminish with greater storm duration and intensity.

The second component of evapotranspiration losses is through transpiration by the vegetation especially the trees present. Depletion of the moisture present in the soil will require greater infiltration to achieve saturation levels that would initiate debris flow occurrence. This would be significant in tropical rainforests because the transpiration rate is high all year long rather than being seasonal as in temperate forests (Greenway, 1987; Sidle et al., 2006). It is also important to note that deeper-rooted vegetation in tropical forests will affect soil moisture depletion through a greater thickness of the underlying soil where shallow landslides like debris flows would occur. Consequently, debris flow occurrence in the tropical moist climate rainforest is clearly strongly influenced by the interaction of rainforest vegetation with rainfall events.

On November 19–23, 1988, a major storm passed across the south of Thailand including Khao Luang, a principal mountain range. It caused a major flooding and debris flow disaster in the southern Thailand provinces of Surat Thani and Nakhon Si Thammarat (DeGraff, 1989; Rosenqvist and Shunji, 1990; Phien-Wej et al., 1993). Thousands of shallow landslides were triggered by the rainfall from this storm with the majority being debris flows. Villages within or adjacent to Khao Luang suffered the greatest impact. At least one major landslide dam formed and breached causing significant downstream flooding in the community of Ban Khiri Wong (DeGraff, 1990). Overall, a total of 373 lives were lost and property damage amounted to USD$ 280 million (Phien-Wej et al., 1993). A number of villages were totally swept away by debris flows or sediment-choked flood waters (Fig. 24.8).

The steep slopes of Khao Luang are mantled with deeply weathered granite regolith. It was unclear what the size of the 1988 storm represented in terms of recurrence; but available data suggested is was not highly unusual with at least six storms of similar size having occurred between 1953 and 1984. It was recognized that landslides were also triggered by these storm events (DeGraff, 1992). The 1988 storm event caused a notably greater number of debris flows and other landslides than those earlier storms. Given that the physical conditions such as slope steepness and soil character had not significantly changed, it appeared that some other factor had contributed to an enhanced response compared to past storm events. The significant change in the ten years prior to 1988 was a rapid reduction of natural forest cover to be replaced by tree crops such as rubber, coffee and fruit (DeGraff, 1989; Rosenqvist and Shunji, 1990). Nilaweera and Nutalaya (1999) examined the root strength of selected indigenous trees from this area. This was done in part to identify those species with slope stabilization potential. All the indigenous species common to the local rainforest proved to be suitable. However, it was found that the root morphology and strength of the rubber trees would not contribute to slope stability. What is still unknown is the hydrologic effect under cultivated tree plantations which have an open, single story canopy compared to under a natural rainforest which is a multi-story and more closed canopy.

Fig. 24.8 The storm affected area of southern Thailand as seen four month later. Debris flow scars are visible on nearest part of Khao Luang. Material mobilized by the debris flows coalesced into downstream deposits. Along the main channel of nearby Ban Kathun, deposition of sandy debris was up to 3 m thick. (Photograph by Jerome V. DeGraff, USDA Forest Service)

The influence of rainforest vegetation on the occurrence of debris flows was more clearly demonstrated in the eastern Caribbean. (DeGraff, 1992). Dominica, W.I. like many of its island neighbors retains a significant proportion of its original rainforest. Dominica is a 752-square kilometer island with a series of former volcanoes forming a highland the length of the country. The highest peak is Morne Diablotin at 1,447 m. The rise to these higher peaks from the sea over a few miles means valley slopes are generally steep. Mean annual rainfall ranges from about 1,015 mm to as high as 10,030 mm. During the period of June through October, it is often receives heavy rainfall from tropical storms and hurricanes.

Using black and white aerial photography and ground reconnaissance, 980 individual landslides were mapped in 1987. The average landslide size was 4 ha with the largest being 12.5 ha. Average landslide density is 1.2 landslides per square hectare. Debris flows are overwhelmingly the most common landslide type found on Dominica (DeGraff et al., 1989).

Additional landslide mapping in 1990 found 152 new landslides across the island. Many of these were triggered by Hurricanes Gilbert and Hugo as well as many tropical storms. There is a history of modification of the vegetative cover for various commercial purposes. There is also an equally strong commitment to maintaining the natural vegetation protected within their national parks.

Using the 152 new landslides triggered by a number of storm events over a three year period, it was possible to test whether a significant difference existed between areas with managed vegetation compared to natural vegetation (DeGraff, 1992) (Fig. 24.9).

Fig. 24.9 A view of Morne Micotrin, Dominica, W.I. All of the *upper* slopes are covered in protected rainforest. Areas of managed vegetation including grapefruit orchards, banana fields and slash and burn cultivation are seen in the foreground. (Photograph by Jerome V. DeGraff, USDA Forest Service)

To ensure that vegetation was the independent variable, the areas compared were limited to two predominant soil types on slopes between 11° and 40°. The statistical analysis addressed whether differences in landslide occurrence under different vegetation classes was proportional to the area of the vegetation class. In other words, was landslide occurrence independent of the vegetation cover type? CHITEST, a randomized test, (Romesburg and Marshall, 1985) was applied and the hypothesis of independence was rejected at a 95% confidence level. The frequency of landslide per hectare is nearly half for areas with natural rainforest compared to managed vegetation. To restate more simply, in areas with similar soil and slope, the factor that can ensure fewer landslides is to prevent natural rainforest from being converted to a managed vegetative cover.

The role of the tropical moist climate rainforests in limiting the occurrence of debris flows to natural rates provides another reason why preserving and carefully managing rainforests is important (DeGraff, 1992). It is not a small effect considering this climatic zone includes the Amazon Basin; Congo Basin of equatorial Africa and the East Indies, from Sumatra to New Guinea. Rainforests conservation has both ecological and natural hazard implications. Even conversion of rainforest cover to tree crop plantations may only reduce rather than avoid these potentially adverse natural hazard effects (Sidle et al., 2006). There can also be secondary impacts due to increased sediment delivery to stream systems and impacts to downstream resources.

24.6 The Case for Risk Reduction

As noted at the beginning of this paper, rainfall-induced debris flows can be extremely destructive events causing widespread damage and loss of life. This type of landslide also can have a significant adverse impact to streams with attendant environmental damage. Rainfall-induced debris flows are a potential hazard that exists over a large part of our planet where population concentrations are present. Many of these areas are also where population is increasing along with societal development.

Continuing current trends in population, social development and infrastructure increase the elements at risk and vulnerability components of the risk equation. Consequently, risk from rainfall-induced debris flows will increase. As Larsen (2008) points out, storms that trigger rainfall-induced debris flows will continue in the future. It is how human populations respond to this natural hazard that controls whether there are more or fewer natural disasters in the future. Implementation of proven landslide mitigation strategies and development of new ones can reduce risk. These measures could reduce vulnerability and limit the elements at risk.

There is clearly a better understanding of rainfall duration-intensity thresholds that could serve as a basis for warning systems. But to truly reduce the vulnerability of populations and their economic activities requires more than scientific understanding. Developing response plans to keep people safe once a warning is sounded will translate this scientific understanding into a real reduction in vulnerability. In some parts of the world, it will need additional scientific study for identifying applicable regional thresholds. It is likely that investment in rainfall reporting stations and communications will be needed for real-time monitoring of rainfall to contribute to this research and form the basis of a warning system.

Related to our understanding of critical storm thresholds that trigger debris flows is improving out understanding of how initiation takes place. Continued modeling and flume studies can clarify how infiltration of rainfall results in debris flow initiation and transferring that understanding to natural slopes are important research needs. From this information, it is possible to better understand how more intensive human development may be affecting natural slope response and thereby design in ways that do not contribute to debris flow initiation or, even, reduce this potential. Knowing more about the dynamics of debris flow initiation may prove a key to improved warning systems and hazard delineation.

Another area of research is related to dams formed by debris flows. There are two components that are important to this hazard aspect of rainfall-induced debris flows. One is our understanding of how debris flows forming and failing during a storm event may alter the expected downstream flooding. There is sufficient anecdotal evidence that this may exacerbate the flood effects normally predicted on the basis of past rainfall events and measured discharge. Secondly, more research is needed on predicting the time to failure for natural dams formed by debris flows. While there is general information suggesting days or weeks to failure (Costa and Schuster, 1988), improved assessment methods would contribute greatly to better evacuation planning and designing possible control of landslide dam-related flood events.

Human communities within the mid-latitude Mediterranean climate chaparral biome will benefit from all efforts to prevent or limit the size of wildfires. This is the most effective means for reducing the hazard from post-wildfire debris flows. Because it is unrealistic to think that no future wildfires will occur, it is also important to continue developing models that predict the most likely locations and size of these debris flows to ensure that countermeasures are in place before the next rainy season.

Vast areas of the world are located within tropical moist climate rainforests. These rainforest are a natural defense against rainfall-induced debris flows. Wholesale reduction increases the level of risk to local populations and their economic activities. This effect points out yet another reason for rainforest protection. It is also evident that agricultural practices should be modified to limit the impact where rainforest vegetation is converted to some form of cultivation. Adaptive management should be researched and implemented to this purpose. This could range from limiting the size or distribution of rainforest openings over time to large-scale re-establishment of rainforest vegetation where it has been removed.

Larsen (2008) points out that any landslide hazard mitigation strategy can only be sustainable if it is closely linked to local economic and social interest. Perhaps the most important of all is a concerted effort to educate people about the potential hazard. Education must be considered an ongoing part of any debris flow hazard reduction effort. While we often think of education as simply learning facts, it is actually changing behavior. Learning has occurred when people behave differently based on the information provided. If people are accepting of policies and requirements that avoid the most hazardous locations for critical infrastructure, support implementation landslide mitigation efforts and response appropriate when warnings are issued, then education will truly have taken place.

24.7 Deciphering Landslide Behavior Using Large-Scale Flume Experiments

Mark E. Reid (U.S. Geological Survey Menlo Park, CA), Richard M. Iverson(U.S. Geological Survey, Vancouver, WA), Neal R. Iverson (Department of Geological and Atmospheric Sciences, Iowa State University), Richard G. LaHusen (U.S. Geological Survey, Vancouver, WA), Dianne L. Brien (U.S. Geological Survey Menlo Park, CA) and Matthew Logan (U.S. Geological Survey, Vancouver, WA)

Some landslides accelerate catastrophically with potentially lethal consequences, whereas others creep intermittently downslope, perhaps causing property damage but rarely fatalities. Rainfall patterns that initiate slide motion vary as well. Some slides require prolonged rainfall to instigate motion, yet others occur following short, intense rain bursts. Such profound differences in behavior have fundamental implications for designing mitigation strategies, implementing effective warning systems, and reducing risk. However, precise evaluation of the causes of diverse landslide behavior in the field is difficult because controlling effects cannot be isolated; this limits our understanding of landslide dynamics as well as our prediction capabilities.

As an alternative to field investigations, we used the large-scale, USGS debris-flow flume in Oregon, USA to perform closely controlled landslide initiation experiments. These experiments focused on deciphering the influences of varying hydrologic triggers and differing soil porosities (or void ratios), relative to critical-state porosities, on failure style, timing, and landslide acceleration. In each of six experiments, we induced failure in a 0.65 m thick, 2 m wide, 6 m^3 prism of loamy sand placed behind a rigid retaining wall in the 31° flume bed. We systematically investigated triggering of sliding by groundwater injection, by prolonged moderate-intensity sprinkling, and by bursts of high intensity sprinkling. We used vibratory compaction to control soil porosity during placement and thereby investigated differences in failure behavior of dense and loose soils. About 50 sensors monitored at 20 Hz during each experiment included nests of tiltmeters and extensometers to measure soil deformation and define subsurface failure geometry, nests of tensiometers and pore-pressure sensors to record evolving pore-pressure fields, and nests of TDR probes to detect changes in soil moisture. We also extracted soil samples for laboratory measurements of porosity, shear strength, stress paths leading to failure, saturated hydraulic conductivity at differing porosities, unsaturated moisture retention characteristics, and compressibility.

All of our controlled landslide experiments used the same loamy sand soil. However, both precursory and failure behavior varied dramatically depending on the initial porosity of the soil relative to its critical-state value of about 0.44 (Fig. 24.10). With an initial porosity greater than the critical state (i.e., loose soil), sediment hydraulic conductivity was relatively high and the precursory wetting period prior to failure was relatively short. In these experiments, we were able to induce failure using three distinct water application methods: groundwater injection at the flume bed (as might be expected from bedrock exfiltration), prolonged moderate-intensity sprinkling, and initially wetted (but not saturated) by moderate-intensity sprinkling followed by a high-intensity burst of sprinkling. Each of these methods resulted in slightly different pore-pressure fields at failure and in different times to failure. For example, groundwater injection led to a water table that advanced upward, wetting over half the soil prism before pressures at the bed were sufficient to provoke collapse. With moderate-intensity surface sprinkling, an unsaturated wetting front propagated downward until reaching the bed, then a mostly saturated zone built upward, with the highest pressures at the bed at the time of failure. With the third trigger using a high-intensity sprinkling burst, failure occurred absent widespread positive pressures.

All of our experiments with loose soil resulted in nucleation of failure along the concrete flume bed with subsequent propagation of the failure surface upward through the soil prism to daylight near the retaining wall. The dynamic behavior during failure in the loose soil experiments was remarkably consistent and involved rapid soil contraction and nearly complete liquefaction within 2–3 s. As a consequence, all of the loose-soil experiments produced fast-moving debris flows that traveled far down the 100 m long flume.

In marked contrast, our experiments with dense soil produced slow-moving landslides exhibiting gradual and episodic downslope displacement. Controlled compaction of the soil resulted in lower hydraulic conductivities and greater shear strengths in comparison to the loose soils. We needed both sprinkling and groundwater injection to create destabilizing pore pressures in dense soils. In addition, the duration of precursory water-application required to induce failure was 4–5 times longer than for the loose-soil experiments. With dense soils, failure often nucleated within the soil prism and then propagated upslope and downslope through the soil, not along the bed (as it did with loose soils). Dynamic behavior during failure in the dense soil experiments consisted of repetitive cycles of slow (< 0.1 m/s) movement, each resulting in modest (< 0.3 m) displacement. Each movement cycle started with downslope displacement caused by elevated pore pressures. This displacement provoked soil dilation, a consequent decrease in pore

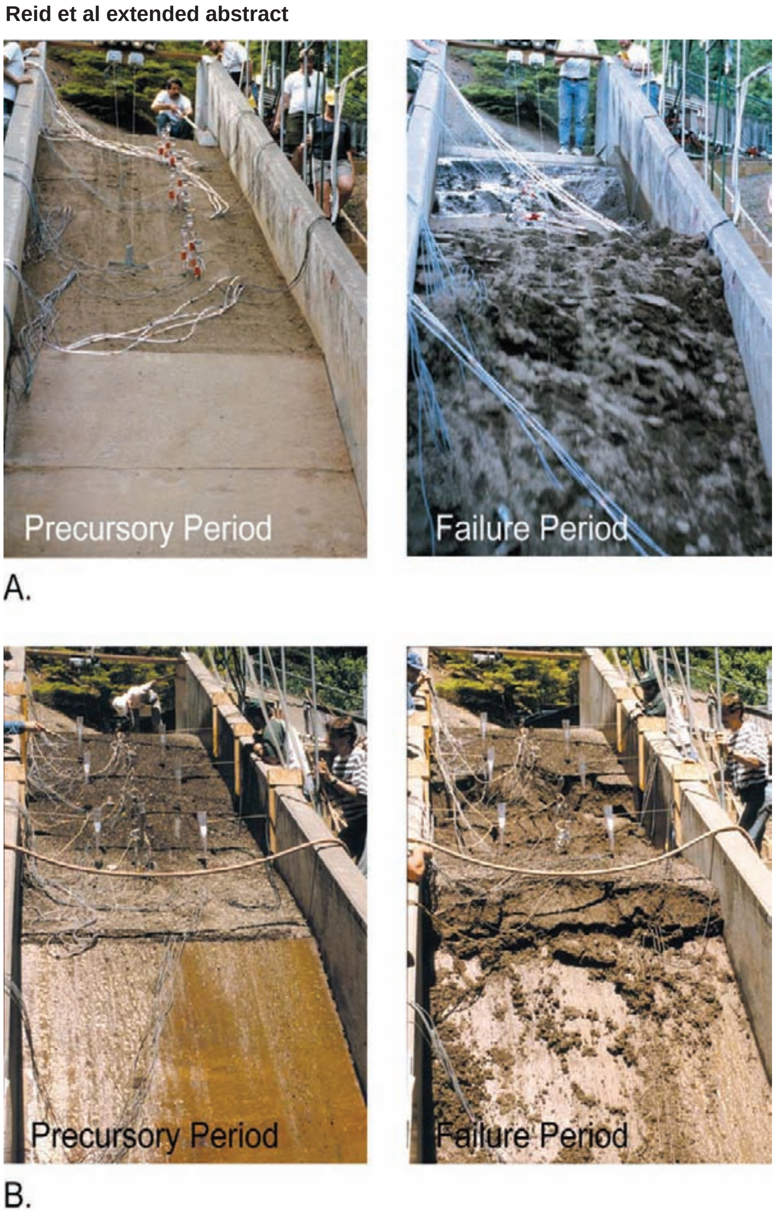

Fig. 24.10 Photographs illustrating dramatically different landslide behavior during two controlled experiments performed at the USGS debris-flow flume. (**A**) Behavior of loose soil (mean porosity = 0.52) prior to and during rapid, wholesale failure triggered by groundwater injection. (**B**) Behavior of dense soil (mean porosity = 0.41) prior to and during slow, episodic failure triggered by overhead sprinkling

pressures, and a temporary halt in slide movement. The cycle would then repeat, as pore pressures would slowly rebuild, triggering renewed slide displacement. Dilation of the dense soil during shear with concomitant pore pressure decline thereby regulated and retarded overall landslide motion.

Our experiments demonstrated that small variations in initial soil porosity can induce profound differences in landslide behavior, both in the hydrologic conditions required for the onset of failure and the dynamic response during failure. Loose soils respond quickly to hydrologic events, and mass failures in these soils create rapid, potentially life threatening, debris flows. Dense soils respond more slowly and produce slow-moving landslides that may exhibit episodic motion. Understanding these differences is crucial to better mitigation of landslide hazards.

24.8 Landslide and Debris Flow Experiments on Artificial and Natural Slopes

Yasuhiko Okada (Incorporated Administrative Agency Forestry and Forest Products Research Institute, Japan) Hirotaka Ochiai (Forestry Agency, Japan)

An experiment to induce a fluidised landslide by artificial rainfall was conducted on a natural slope at Mt. Kaba-san, Yamato village, Ibaraki prefecture, Japan. The experimental slope was 30 m long, 5 m wide, and the average slope gradient was 33°. A landslide initiated 24627.5 s (410 min 27.5 s) after the commencement of sprinkling at a rainfall intensity of 78 mm h^{-1}. The landslide mass was 14 m long and 1.3 m deep (at maximum). It first slid, then fluidised and changed into a debris flow. The travel distance was up to 50 m in 17 s. An equivalent friction angle of the fluidised landslide was 16.7°. Formation of sliding surface was detected by soil-strain probes. Motion of the surface of the failed landslide mass was determined by stereo photogrammetry.

Fluidised landslides, which travel long distances at high speed, are one of the most dangerous types of landslides (Sassa, 2000). Fluidised slope movement takes place both in artificial cut slopes and natural slopes and often results in extensive property damage and significant loss of life (Sassa, 1998). Many fluidised landslides have been observed in Japan, some of them have caused great disasters.

A debris flow that occurred in 1996 in Gamahara-zawa, Nagano prefecture, Japan, is an example of fluidised landslide. The debris flow was triggered by the collapse at around 1,300 m in altitude, moved approximately 39,000 m^3 of soil, of which 8,000 m^3 was deposited around the foot of the landslide and 31,000 m^3 travel down a slope 16.4° in mean inclination along a river for about 3 km. The debris flow eroded another 37,000 m^3 of soil, of which 15,000 m^3 was captured by a check dam. As a result, approximately 53,000 m^3 of soil reached the alluvial fan, which is 300 m in altitude, and 14 people were killed (Committee Investigation for Gamahara-zawa Debris Flow Damage on December 6, 1997). As the soil-volume balance shows, the debris flow expanded the volume while traveling down the slope by gathering up river-bed sediment, and almost doubled in the amount of soil. Sassa (1998) called this phenomenon a landslide-induced debris flow. The fludisation of the river-bed sediment was caused by the rapid loading of the landslide mass and expanded moving mass lead to the further fluidisation of the lower part which increased the volume.

In order to reproduce a fluidised landslide and to investigate its fluidisation mechanisms, the landslide experiment on a natural slope was conducted by sprinkling, in which natural slope has a complex and heterogeneous characteristics than the indoor models. A focus was placed on the sliding surface formation, hydrological characteristics, dynamic movements of the soil surface. The experimental slope was 30 m long and 5 m wide, and mainly covered by weathered disintegrated granite sand. Soil-surface movements were monitored by using stereo photogrammetry. Hence white-coloured targets were placed on the experimental slopes and the movements of these targets were traced by image analysis. To detect the formation of the sliding surface, soil-strain probes were inserted into the soil to 2 m depth at deepest. Tensiometers were used to measure changes in pore-water pressures within the soil.

A natural slope in the Koido National Forest at Mt. Kaba-san, Yamato village, 25 km north of Tsukuba city, Ibaraki prefecture, Japan was selected for the controlled experiment on landslide and possible fluidisation in cooperation with the Forestry Agency of Japan. The selected portion of hillslope (Fig. 24.11) was 30 m long, with an average slope gradient of 33° (maximum 35°) The soil was 1–3 m deep. A 5 m wide experimental slope was isolated from its surroundings by driving thin steel plates about 1 m deep into the soil. These plates prevented lateral diffusion of infiltrated rain water and cut the lateral tree root network that imparts resistance within the soil layer. The surface of the slope was covered by straw matting to prevent surface erosion and promote rainfall infiltration. Surface material on the slope consisted of fine weathered disintegrated granite sand, called "Masa" in Japan. Loamy soil blanketed the uppser portion of the regolith to a depth of about 1 m; this soil mainly originated from tephra of Mt. Fuji, Mt. Akagi, and other volcanoes west of Mt. Kaba-san. Artificial rain at the rate of 78 mm h^{-1} was applied to the slope

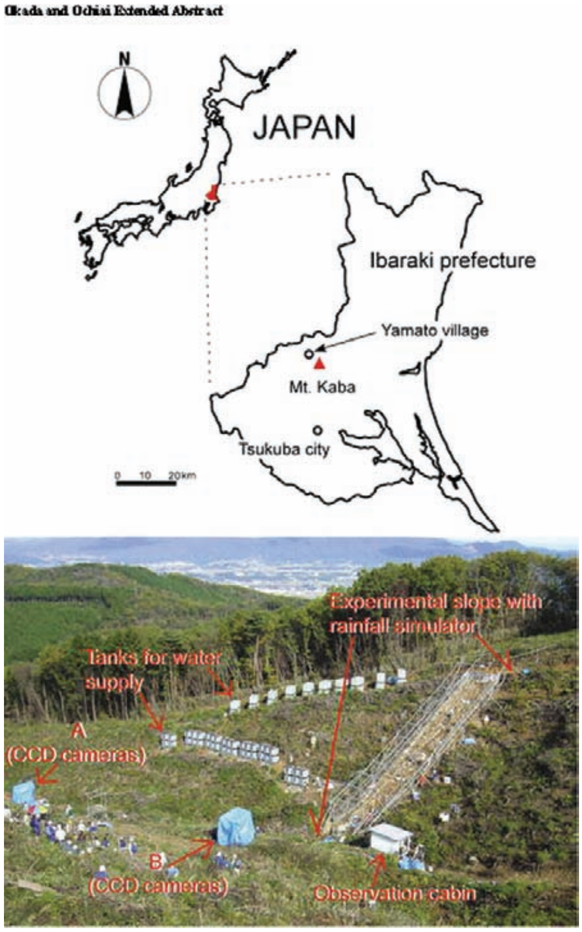

Fig. 24.11 View of experiment site at Mr. Kaba-san

segment during the experiment by way of a rainfall simulator. The simulator consisted of a framework of steel pipes with 24 sprinkling nozzles arranged 2 m above the soil surface. Soil-surface movement was measured by means of stereo photogrammetry. To obtain information on the formation of sliding surface, soil-strain probes were inserted into the soil. To measure saturation conditions within the soil, tensiometers with porous ceramic cups were set into the slope. Tensiometer can measure negative pore-water pressure in unsaturated soils and positive pore-water pressure in saturated conditions.

The experiment was conducted on 14 November 2003. Artificial rainfall was started from 9:13, the slope deformation was detected from around 15:00, then a clear movement was observed to start at 16:03. The initiated landslide was a type of an expected fluidised landslide, the landslide mass rapidly moved and traveled long. The cover of tensiometer started to incline downslope at 24,627.5 s (410 min 27.5 s) after sprinkling commenced. We interpret this as indicating that slope failure initiated at 24,627.5 s. As soil surface movement increased, a tension crack became visible at the head, and a compressive bulge resulting from downslope movement was observed 5 m above the base of the slope. The bulge enlarged before the main landslide mass began to undulate and rapidly enter the stream. The compressive bulge was observed only in the left part of the landslide. The failed landslide mass had entered the stream and was about to collide with the confronting slope. After collision, the fluidised landslide turned to the right, changed into a debris flow, and traveled downstream for 10 s on a less-than 10-degree gradient, as much as 30 m. It took about 17 s from the initiation of the landslide to the end of deposition.

Snapshots of the three-dimensional movements of the targets are shown in Fig. 24.12. Figure 24.12a is 0.5 s before failure (24627 s), Fig. 24.12b is two seconds after failure (24629.5 s), and Fig. 24.12c is 3.5 s after failure (24631 s). Targets 6 and 7, located just above the foot of the landslide, followed curved paths, which could not have been determined by conventional displacement measurement using extensometers. The landslide mass overrode the slope around targets 2 and 3 and then moved rapidly into the stream at the foot of the experimental slope.

When a sliding surface forms, soil above the sliding surface tends to move downslope, whereas soil below it remains stable. In this case, soil-strain gauge shows paired positive and negative values indicating sliding surface formation. At around the middle part of the landslide mass, the changes in strain gauges started to be observed around 1.15 m depth from about 300 min after the sprinkling. At around the lower part, the gradual changes in strain gauges were observed at 0.75 m depth from about 20 min. The changes in strain gauges were greatly accelerated from about 350 min after sprinkling began at both positions.

Pore-water pressure (0.5, 1.0, 1.5, 2.0, 2.5, and 2.9 m) at around the upper part of the landslide showed negative value at the start of the sprinkling, indicating that the soil at all depths were

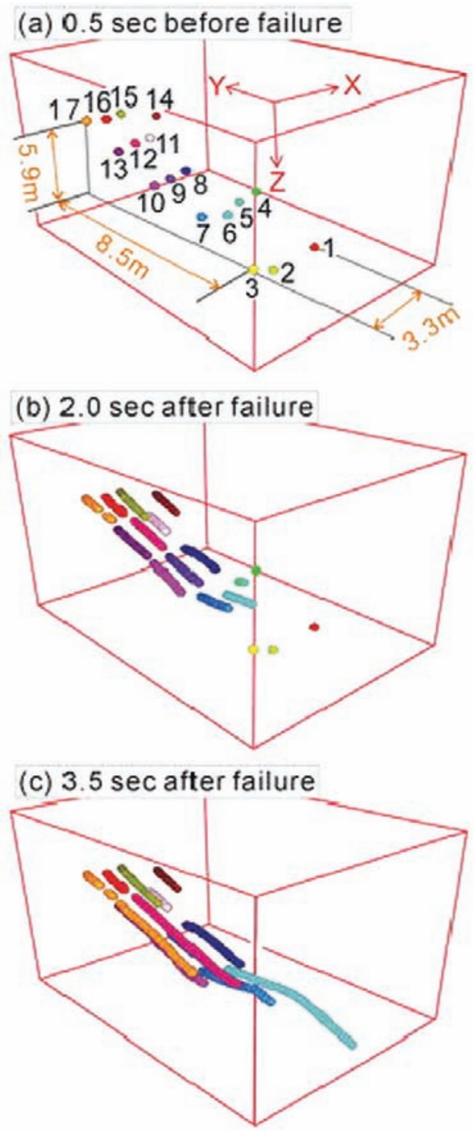

Fig. 24.12 Snapshots of the three-dimensional movements of the targets. (**a**) 0.5 second before failure (24 627 s), (**b**) 2 seconds after failure (24 929.5 s), and (**c**) 3.5 seconds after failure (24 631 s)

unsaturated or partly saturated. When the wetting front passed, the tensiometers showed increases in pore-water pressure in sequence of the depths. At 410 min, when the failure took place, all of the tensiometers showed positive pore-water pressures. The pore-water pressure of the deepest tensiometer (2.9 m) rapidly increased its values from about 290 min. This almost coincided with the time when the strain gauge at 1.1 m depth in the strain probe (middle part of the landslide) started to show strain. Hence, it can be deduced that general slope instability increased from 290 min, before final failure at 410 min.

Acknowledgments Landslide experiment on the natural slope was a part of project called APERIF (Areal Prediction of Earthquake and Rainfall Induced Rapid and Long-traveling Flow Phenomena), launched by the Special Coordinating Fund for Science and Technology of the Ministry of Education, Cultures, Sports, Science and Technology (MEXT) of Japan.

24.9 The Effects of Wildfires on Erosion and Debris Flows in Mediterranean Climatic Areas: A First Database

Mario Parise (National Research Council of Italy – IRPI, Bari, Italy) and Susan H. Cannon U.S. Geological Survey (Denver, CO, USA)

Wildfire can have profound effects on the hydrologic response of watersheds, and debris-flow activity is among the most destructive consequences of these effects (Fig. 24.13), often causing extensive damage to human infrastructure (Cannon and Gartner, 2005). The effects produced by wildfires on hillslopes in terms of development of erosional processes (Fig. 24.14) and occurrence of debris flows have been object of studies for several decades, and

Parise and Cannon Extended abstract

Fig. 24.13 Deposits left by December 25, 2003 debris flows from the area of the Old and Grand Prix Fires of in California

Fig. 24.14 Overall view of the Cucamonga Canyon hillslopes (California), affected by the Old and Grand Prix Fires of October 25, 2003

this research experienced a strong impulse in the last 15 years.

These studies vary in scale, intensity, and frequency in very different natural settings, from alpine territories, to Mediterranean ecosystems, to semi-arid lands. The continued high likelihood of catastrophic wildfires in Mediterranean climates (Fig. 24.15) has created the need to develop methods to identify and quantify potential erosion and debris-flow hazards from burned watersheds.

Following an analogous compilation of data related to the erosive response of recently burned basins in the Western United States by the United States Geological Survey (USGS; Gartner et al., 2005), we present here a first database dealing with the erosional effects of wildfires (Fig. 24.15) in the Mediterranean basin.

To date, scientific literature on the topic in Europe has not been catalogued, and is dispersed in a number of different journals and in conference proceedings. Even though most of the literature available on the Mediterranean countries deals with studies on experimental plots rather than analysis of post-wildfire landsliding and erosional events (as it is common, on the other hand, in the US literature), nevertheless the catalogue and analysis of these studies may provide preliminary information about the responses of recently burned watersheds in typically Mediterranean climates and environmental settings.

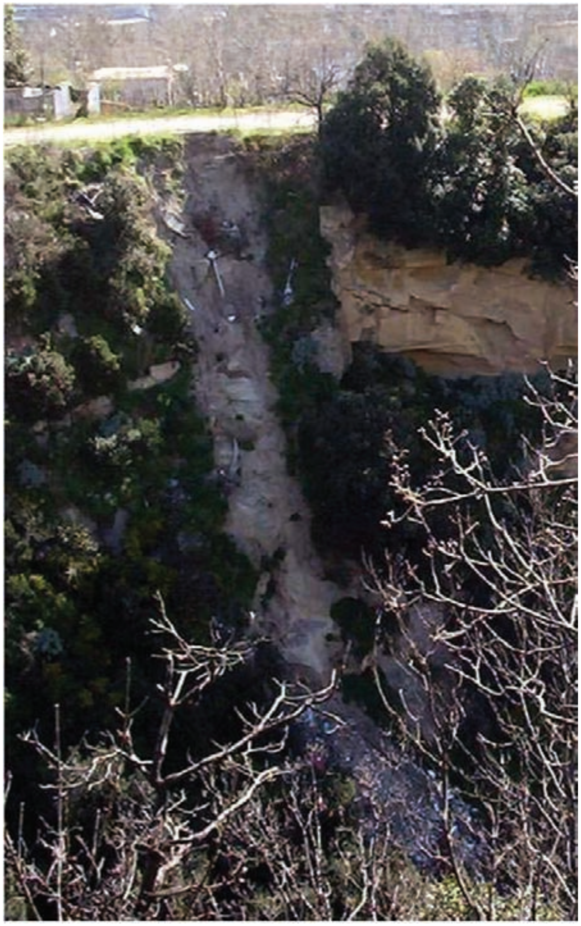

Fig. 24.15 Examples of shallow landslides and erosional features developed in areas affected by wildfires in Campania (southern Italy)

Aimed at providing a resource to researchers and land managers interested in the topic, we examined the available work and compiled a database which includes the primary morphometric characters of the affected watersheds, together with information about fire characteristics, rock type and soils, rainfall data, and the erosive response of the burned basins (characterized as debris flow, flood, or having no response). Besides illustrating the database, and performing the first statistical analysis on the data so far available, in the present contribution we will provide a preliminary comparison of the Mediterranean data with those deriving from studies in southern California.

References

Benda L, Dunne T (1997) Stochastic forcing of sediment supply to channel networks from landsliding and debris flow. Water Resources Research 33(12), 2849–2863.

Caine N (1980) Rainfall intensity-duration control of shallow landslides and debris flows. Geografiska Annaler 62A, 23–27.

Campbell RH (1975) Soil slips, debris flows, and rainstorms in the Santa Monica Mountains and vicinity, southern California. US Geological Survey Professional Paper 851.

Campbell RH (1985) Feasibility of a nationwide program for the identification and delineation of hazards from mud flows and other landslides: Chapter C, priority U.S. areas for the delineation of susceptibility to mud flows and other landslides. US Geological Survey Open-File Report 85-276-C, 1-6.

Cannon SH (2001) Debris-flow generation from recently burned watersheds. Environmental & Engineering Geoscience 7, 321–341.

Cannon SH, Gartner JE (2005) Wildfire-related debris flow from a hazards perspective. In: Jakob M, Hungr O (eds) Debris-flow hazards and related phenomena. Praxis, Springer Berlin, 363–385.

Cannon SH, Gartner, JE, Michael, JA (2007a) Methods for the Emergency Assessment of Debris-Flow Hazards from Basins Burned by the Fires of 2007, Southern California. US Geological Survey Open-File Report 2007-1384.

Cannon SH, Gartner JE, Wilson RC, Bowers JC, Laber, JL (2007b) Storm rainfall conditions for floods and debris flows from recently burned areas in southwestern Colorado and southern California. Geomorphology 96, 250–269.

Committee of investigation for Gamahara-zawa debris flow damage in Dec. 6 (1997) The research report of investigation for Gamahara-zawa debris flow damage in Dec. 6. The Japan **Society** of **Erosion Control Engineering** 50(3), 89–94 (in Japanese).

Costa JE, Schuster RL (1988) The formation and failure of natural dams. Geological Society of America Bulletin 100, 1054–1068.

DeGraff JV (1989) Landslide activity resulting from the November 1988 storm event in southern Thailand and associated recovery needs. In: Safeguarding the future, restoration and sustainable development in the south of Thailand. National Operations Center, National Economic and Social Development Board, US Agency for International Development, Bangkok, 43p.

DeGraff JV, Bryce R, Jibson RW, Mora S, Rogers CT (1989) Landslides: their extent and economic significance in the Caribbean. In: Brabb, EE, Harrod, BL (eds) Landslides: extent and economic significance, AA Balkema, Rotterdam, pp 51–80.

DeGraff JV (1990) Landslide dams from the November 1988 storm event in southern Thailand. Landslide News 4, 12–15.

DeGraff JV (1992) Increased debris flow activity due to vegetative change, In: Bell, DH (ed) Landslides, Proc., Sixth Intern. Symposium Landslides, Christchurch, N.Z., AA Balkema, Rotterdam, pp 1365-1373.

DeGraff JV, Rogers C T (2003) An unusual landslide-dam event in Dominica, West Indies. Landslide News 14/15, 8–11.

DeGraff JV, Cannon SH, Gallegos AJ (2007) Reducing post-wildfire debris flow risk through the Burned Area Emergency Response (BAER) process. In: Schaefer, VR, Schuster, RL, Turner, AK (eds) Conference Presentations, 1st North American Landslide Conference, Vail, CO, AEG Special Publication No. 23, pp 1440–1447.

Ellen SD, Wieczorek GF (eds) (1988) Landslides, floods, and marine effects of the storm of January 3–5, 1982, in the San Franciso Bay Region, California. US Geological Survey Professional Paper 1434.

Gartner JE, Cannon SH, Bigio ER, Davis NK, Parrett C, Pierce KL, Rupert MG, Thurston BL, Trebish MJ, Garcia SP, Rea AH (2005) Compilation of data relating to the erosive response of 606 recently burned basins in the western US. USGS Open-File Report 2005-1218.

Gartner JE, Cannon SH, Santi PM, deWolfe VG (2008) Empirical models to predict the volumes of debris flows generated by recently burned basins in the western U.S. Geomorphology 96, 339–354.

Godt JW, Baum RL, Chelborad AF (2006) Rainfall characteristics for shallow landsliding in Seattle, Washington, USA. Earth Surface Processes and Landforms 31, 97–110.

Greenway DR (1987) Vegetation and slope stability. In: Anderson MG, Richards KS (eds) Slope Stability, Geotechnical Engineering and Geomorphology, John Wiley & Sons, Chicester, UK.

Guzzetti F, Peruccacci S, Rossi M, Stark CP (2008) The rainfall intensity-duration control of shallow landslides and debris flows: an update. Landslides 5(1), 3–17.

Iverson RM, Costa JE, LaHusen RG (1992) Debris-Flow flume at H.J. Andrews Experimental Forest, Oregon. US Geological Survey Open-File Report 92-483.

Iverson RM (1997) The physics of debris flows. Reviews of geophysics 35(3), 245–296.

Keefer DK, Wilson RC, Mark RK, Brabb EE, Brown WM III, Ellen SD, Harp EL, Wieczorek GF, Alger CS, Ztkin RS (1987) Real-time landslide warning during heavy rainfall. Science 238, 921–925.

Kirkham RM, Parise M, Cannon SH (2000) Geology of the 1994 South Canyon fire area, and a geomorphic analysis of the September 1, 1994 debris flows, south flank of Storm King Mountain, Glenwood Springs, Colorado. Special Publication 46, Colorado Geological Survey, Denver.

Larsen MC, Simon A (1993) A rainfall intensity-duration threshold for landslides in a humid-tropical environment, Puerto Rico. Geografiska Annaler 75A, 13–23.

Larsen MC, Wieczorek GF (2006) Gromorphic effects of large debris flows and flash floods, northern Venezuela, 1999. Zeitschrift für Geromorphologie Supple 145, 147–175.

Larsen MC (2008) Rainfall-triggered landslides, anthropogenic hazards, and mitigation strategies. Advances in Geosciences 14, 147–153.

Logan M, Iverson RM (2007) Video documentation of experiments at the USGS debris-flow flume 1992–2006. US Geological Survey Open-File Report 2007-1315, version 1.0.

Mikoš M, Brilly, M, Fazarinc, R, Ribičič, M (2006) Strug landslide in W Slovenia: a complex multi-process phenomenon. Engineering Geology 83, 22–35.

Nilaweera NS, Nutalaya P (1999) Role of tree roots in slope stabilization. Bulletin Engineering Geology and Environment 57, 337–342.

NOC (1989) Safeguarding the future, restoration and sustainable development in the south of Thailand. National Operations Center, National Economic and Social Development Board, US Agency for International Development, Bangkok.

Phien-Wej N, Nutalaya P, Aung Z, Zhibin T (1993) Catastrophic landslides and debris flows in Thailand. Bulletin International Association of Engineering Geology 48, 93–100.

Reid ME, Iverson RM, Iverson NR, Brien DL, LaHusen RG, Logan M (2006) Hydrologic triggering of shallow landslides in a field-scale flume. Eos Trans. AGU 87, 52.

Romesburg HC, Marshall K (1985) CITEST: a Monte-Carlo computer program for contingency table tests. Computers & Geoscience 11, 69–78.

Rosenqvist A, Shunji M (1990) Flood damage analysis in southern Thailand. In: Proceedings, 23rd International Sumposium on Remote Sensing of Environment, Ann Arbor, Michigan 315–324.

Sassa K (1998) Mechanisms of landslide triggered debris flows. In: Proc. IUFRO Division 8 Conference, Kyoto, pp 499–518.

Sassa K (2000) Mechanism of flows in granular soils. In: Proc. International Conference of Geotechnical and Geological Engineering, GEOENG2000, Melbourne, pp 1671–1702.

Schuster RL, Salcedo DA, Valenzuela L (2002) Overview of catastrophic landslides of South America in the twentieth century. In: Evans SG, DeGraff JV (eds) Catastrophic landslides: effects, occurrence, and mechanisms, Reviews in Engineering Geology XV, Geological Society of America, Boulder, CO, pp 1–34.

Sidle RC, Ziegler AD, Negishi JN, Nik AR, Siew R, Turkelboom F (2006) Erosion processes in steep terrain truths, myths, and uncertainties related to forest management in Southeast Asia. Forest Ecology and Management 224(1–2), 199–225.

Sidle RC, Ochiai H (2006) Landslides processes, prediction, and land use. Water Resources Monograph 18, American Geophysical Union, Washington.

Varnes DJ (1984) Landslide hazard zonation: a review of principles and practice. Natural Hazards Series No. 3, UNESCO, Paris.

Wang F-W, Matsumoto T, Tanaka Y (2005) Two recent flowslides in Yamashina area, Kanazawa City, Japan. Landslides 2(3), 229–234.

Wieczorek GF (1996) Landslide triggering mechanisms. In: Turner AK, Schuster RL (eds) Landslides investigation and mitigation, Special Report 247, Transportation Research Board, National Research Council, Washington, 76–90.

Global Cooperation Field (3): Capacity Building

25 Case Studies and National Experiences

Srikantha Herath and Yi Wang

Abstract Landslides continue to be a major natural disaster causing loss of life, extensive human suffering and economic losses, despite advances in understanding of mechanisms, monitoring and mitigation technologies related to landslides. Sharing the globally accumulated expertise and implementing this knowledge effectively in different local contexts is the major challenge now facing landslide loss reduction efforts. Landslides characteristics differ according to climatic, geological and geographical conditions. They are also affected by different triggering mechanisms depending on the livelihood practices, infrastructure development and population density in each locality. Landslide risk reduction practices and institutional arrangements have evolved in different countries in response to varied landslide experiences brought about by these different geo-physical characteristics and drivers. An objective analysis of the practices adopted worldwide would provide invaluable guidance to develop pragmatic landslide risk reduction strategies and responsible institutions, especially in the developing countries where the impacts are greatest and the vulnerabilities are the highest, especially with increasing hazard potential due to climate change. This chapter describes national programs and methodologies adopted in landslide risk reduction in various countries as a contribution in this direction

Keywords Landslide risk reduction strategies • National programs • Institutional arrangements • Early warning • Loss assessment • Landslide monitoring • Hazard mapping • Risk evaluation • Landslide inventory • Remote sensing

25.1 Introduction

Landslides can occur in any part of the world either due to physical characteristics of the region or from one of the many triggering factors that destabilize landforms. However, major characteristics of landslides may differ from country to country due to specific characteristics of climate, geology as well as landuse practices. National landslide risk reduction practices generally evolve in response to major disasters, often catastrophic, and consequently are related to the region's physical characteristics and human interventions. The frequency of events, especially due to the triggering mechanisms such as rainfall and rapid development activities, may also have a strong influence on the evolution of landslide

Srikantha Herath (✉)
Environment and Sustainable Development Program,
United Nations University, Tokyo

Yi Wang
Environment and Sustainable Development Program,
United Nations University, Tokyo

K. Sassa, P. Canuti (eds.), *Landslides – Disaster Risk Reduction*,
© Springer-Verlag Berlin Heidelberg 2009

disaster mitigation practices of a country. These diverse experiences, in total, can provide the global community with a comprehensive overview of landslide mitigation practices and institutional arrangements that work for different conditions. This session is convened to provide a forum for such a compilation and provide directions to the implementation of Tokyo Action Plan of the International Program on Landslides.

The session discusses national landslide risk reduction practices, institutional mechanisms, risk assessment, and loss reduction methodologies that have been developed as a result of various landslide experiences. Papers are invited from different geographical and geological regions that would highlight specific characteristics of related to climate conditions, especially on rainfall, or geological conditions as well as land use practices. Specific sub topics of the session are

- Landslides in specific regions such as Central Asia, Latin America, Balkan, etc.
- Landslides in Loess, quick-clays, Volcanoes, mining or power plant sites, etc.
- Case studies highlighting national experiences in recovery, policy changes and mitigation needs
- Case studies on success stories of regional or national landslide risk reduction

25.2 Global Landslide Disaster Overview

Landslides continue to be a major hazard, and are the 7th largest killer among natural disasters after droughts, windstorms, floods, earthquakes, volcano and extreme temperature. According to CRED database, landslides have claimed 800–1000 lives in average during the last 20 years. Landslides also inflict heavy economic damage in many countries. For example, India, Italy and USA report about 1–3 billion US$ in annual losses, Japanese annual losses are reported to be between 4 and 6 billion US$. From the CRED database the total number of events, peopled killed per event, and economic losses per event from landslides from 1903 to 2004, it is seen that, Asia and Americas suffer the most from landslide disaster in terms of people affected, while economic losses are dominant in Europe and Americas as shown in Table 25.1 (em-dat).

Looking at recent trend, the same database (Table 25.2) shows that the majority of persons killed due to landslides are from the Asia and account for more than the rest of the world combined. It should however be noted that landslides occur mostly as secondary disasters together with earthquakes or floods and their impact statistics tend to be included in those primary disasters. Hence, the actual number of casualties and damage would be much higher than that reported as landslide losses.

The same data sources show that developing countries suffer most from natural disasters and this is true for landslides too. This arises from a number of factors. Often the local knowledge base required to identify landslide prone areas is either non-existent or fragmentary. Not enough research and investigations are carried out to understand the risks and identify hazard zones. Secondly risk reduction measures such as land use planning, appropriate building codes, safety regulations and

Table 25.1 Total number of people reported killed, by continent and by Avalanches and Landslides (1993–2002)

	No. of Events	Killed	Injured	Homeless	Affected	Total Affected
Africa	22	721	56	7,936	11,748	19,740
ave. per event		33	3	361	534	897
Americas	139	20,532	4,750	186,752	4,476,441	4,667,943
ave. per event		148	34	1,344	32,205	33,582
Asia	220	15,754	3,464	3,742,596	1,309,796	5,055,856
ave. per event		72	16	17,012	5,954	22,981
Europe	75	16,158	743	3,125	37,668	41,536
ave. per event		215	10	42	502	554
Oceania	15	528	52	8,000	2,963	11,015
ave. per event		35	4	533	198	734

Table 25.2 Landslide casualties during last 10 years

	Events	Killed	Affected
Africa	9	134	2715
America	27	862	156387
Asia	89	5031	1299822
Europe	5	33	2900
Ocenia	4	63	10795

response plans are not developed and applied. Appropriate financial mechanisms are not utilized and unfortunately expertise in landslide risk reduction is not covered in local institutes and universities.

While there are many factors that trigger landslides, and they can occur in any part of the world, some regions are more prone to landslides than others due to their geological characteristics and rainfall intensities. The Fig. 25.1 shows the geographical distribution of major landslides in the world. It is seen that the major component of the landslide risk area is defined by the tectonic region of the world as given in Fig. 25.2. Steep slopes as can be envisioned from the elevation map of Fig. 25.3, show that the landslide distribution is also common to the high elevation area of the world. The high landlside risk area is also a subset of the regions that receive intense rainfall identified in Fig. 25.4, which shows the maximum 24 hour rainfall. The high correlation between the landslide hazard distribution with the world tectonic region as well as the high intensity rains and elevation distribution shows the strong relation between the primary driving forces, defined by geology and elevation with the main triggering factor, the rainfall intensity, that cause landslides. This also suggests the possibility of using the experiences and methodologies developed in countries of similar driving forces in other countries if proper institutional framework and adequate support is established. In addition, the experiences of the countries with a high frequency of disasters in the development of risk management practices can be used in the countries where the disaster frequency is low, which making it difficult to get the necessary political and financial support in establishing response strategies.

25.3 Mitigating Landslide Losses

Strategies to be adopted to reduce landslide losses vary depending on the geo-physical characteristics, population distribution and the socio-economic conditions. For example, Hong Kong is a landslide prone territory with steep slopes that experience high intensity rainfall. However, given that it is primarily an industrial country with hardly any agricultural practice with a very high density of population and infrastructure, and confined to a small land area, it is possible to successfully apply structural measures centered strategy for landslide prevention and loss reduction.

On the other hand, in developing agricultural countries where population is distributed over a large area, characterized by steep slopes and high intensity rains, such as Nepal or Sri Lanka in South

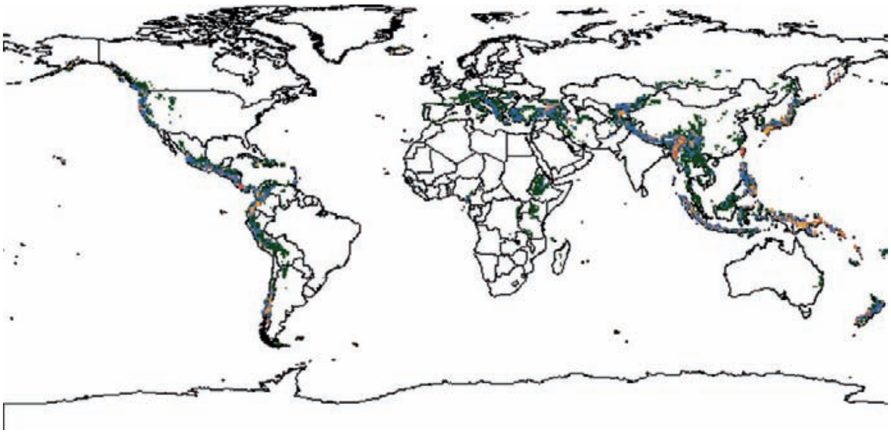

Fig. 25.1 Global distribution of landslides

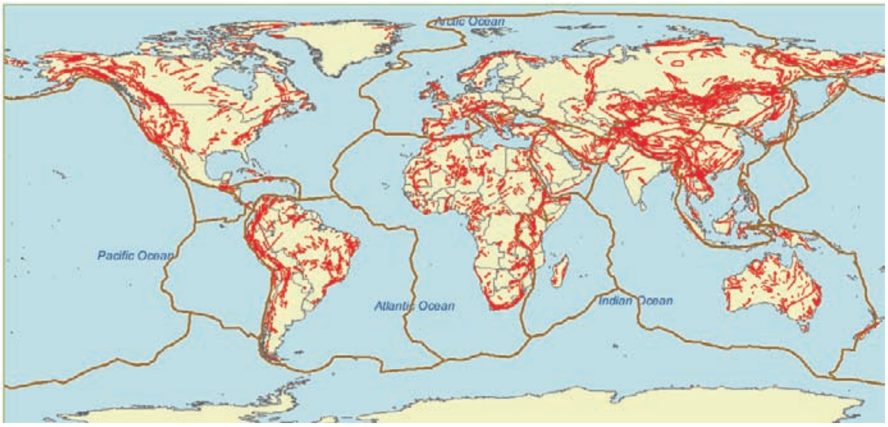

Fig. 25.2 World tectonic map

Asia or the countries in South Americas, it is not feasible to adopt an infrastructure driven strategy. In such cases, while adopting a certain degree of slope preservation in strategic areas such as those adjoining major roads, railways, etc., through appropriate drainage and retaining structures, main approach for loss reduction should be through soft measures. These soft measures should start with land slide hazard zonation followed with legislature for implementing land use planning and educating communities based on the derived hazard maps. Comprehensive landslide risk reduction strategies would include the following; (a) restriction of development in landslide-prone areas, (b) use of excavation, grading, landscaping, and construction codes, (c) use of physical measures (drainage, slope-geometry modification, and structures) to prevent or control landslides, and (d) development of warning systems (Slosson and Krohn, 1982; Schuster and Leighton, 1998; Schuster, 1996). Schuster and Leighton (1988) estimated that these methods could reduce landslide losses in California by more than 90%. Slosson and Krohn (1982) stated that enactment of these approaches had already reduced landslide losses in the City of Los Angeles by 92–97%. Furthermore, potential landslide area can be predicted by combing and analyzing the factors which are usually related the landslides, such as geology, soil type, land surface temperature, land cover, underground water level, slope aspect, slope inclination, elevation, etc. An improved understanding of rainfall characteristics, especially the intensity-duration-frequency relations can help in establishing landslide triggering thresholds for warning purposes.

In spite of improvements in hazard recognition, prediction, mitigation measures, and warning systems, worldwide landslide activity is increasing. This trend is expected to continue in the 21st century due to the following reasons:

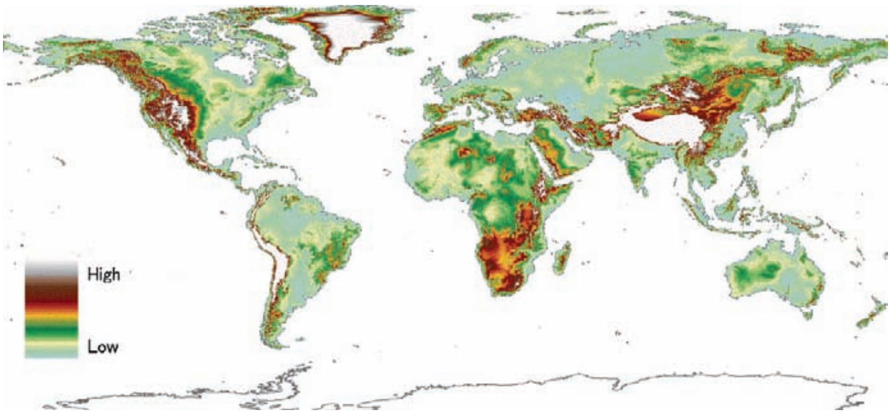

Fig. 25.3 Global Elevation Distribution

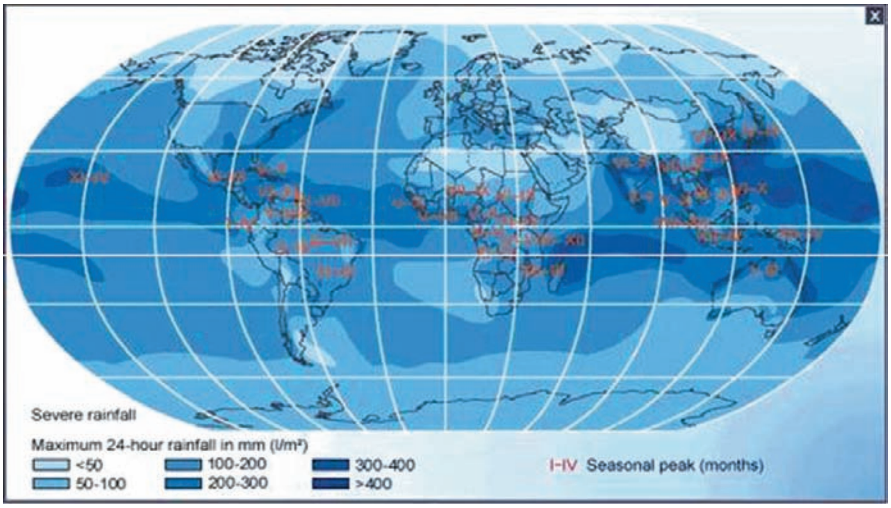

Fig. 25.4 Global Maximum 24 hour rainfall distribution (source: Munich Re)

- Increased urbanization and development in landslide-prone areas;
- Continued deforestation of landslide-prone areas;
- Increased regional precipitation caused by changing climatic patterns.

To address the landslide problem, governmental agencies of different countries need to develop a better understanding of landslide hazards and to make rational decisions on allocation of funds for management of landslide risk. Experiences of countries that have been successful in mitigating landslide risks through the development of necessary methodologies and establishment of appropriate institutions are invaluable in reducing the landslide risks globally, the target of the "International Program of Landslides" that is being coordinated by the International Consortium of Landslides.

25.4 National Experiences and Methodologies

This section briefly introduces the invited papers for the session 2 that describe different national experiences and methodologies developed and used in landslide disaster risk reduction.

25.4.1 Landslide Hazard Activities in the United States

Peter T. Lyttle (U.S. Geological Survey, 908 National Center, Reston, Virginia 20192, USA)

Abstract Landslides occur in all 50 states of the United States of America and cause on average 25–50 fatalities and damage of at least 3 billion U.S. dollars and an average of several dozen deaths annually. The indirect socioeconomic impacts are considerably greater, but are not satisfactorily documented. In 2003 the U.S. Geological Survey (USGS), in concert with its many partners in hazard mitigation efforts in the United States, published the National Landslide Hazards Mitigation Strategy – A Framework for Loss Reduction. This document briefly summarized current landslide research, mitigation activities, and defined the roles of various U.S. federal and state agencies, as well as groups within academia and the private sector. It recommended a long-term strategy that called for significantly increased funding, educational outreach, and development of partnerships to strengthen basic research into landslide processes, emergency preparedness, real-time monitoring, and training. Furthermore, the USGS has also entered into a long-term partnership with the National Weather Service (NWS) to develop a protocol for delivering debris flow warnings in several research areas in southern California. The USGS

information about debris flow rainfall thresholds is added to the well established NWS Flash Flood Watches and Warnings system. This has been a success and the USGS/NOAA partnership is exploring several other areas within the United States to expand landslide research and the debris flow warning system. . Recently several state geological surveys, and regional coalitions of counties, have achieved significant milestones in obtaining statewide or regional LiDAR coverages thus enabling these agencies to better inventory, delineate and study deep-seated landslides.

25.4.1.1 Introduction

This paper briefly describes the landslide activities of the U.S. Geological Survey (USGS) and its governmental partners at the federal and state levels in the United States. It does not attempt to discuss the excellent landslide research being carried out at many universities and colleges. The USGS leadership role in landslide hazards mitigation arises from the Disaster Relief Act of 1974 (Stafford Act), which delegates to the Director of the USGS the responsibility to issue disaster warnings for an earthquake, volcanic eruption, landslide, or other geologic catastrophe.

Annual losses directly attributable to landslides cost the United States a minimum of 3 billion U.S. dollars (USD) and an average of several dozen deaths (Schuster, 1996; Schuster and Highland, 2001). If indirect costs, such as disruptions to business and transportation, are included the loss estimates are clearly much larger. In the United States, the earthquake hazard scientific community is able to effectively influence national policy by having their national seismic hazard maps incorporated into national building codes, thus having a major life-saving impact. In the case of landslide hazards, most of the mitigation is accomplished at the local government level through zoning or permit regulations. Therefore it is important for the USGS and its partners to look for ways to educate and influence local citizens or community zoning officials. This paper will describe several examples of recent education campaigns.

Due to limited budgets and staff, the USGS and its state partners are able to issue warnings in a very limited number of locations throughout the United States, primarily only in those areas where considerable research has taken place, and where requisite information such as rainfall-intensity duration threshold values, detailed geologic maps, and accurate real-time precipitation information is available. This paper will briefly describe progress that the USGS and National Weather Service (an agency within the National Oceanic and Atmospheric Administration (NOAA) have made in implementing a pilot debris flow warning system in southern California.

While landslide inventories of specific areas or modestly-sized regions have been carried out within the United States, there has been no serious attempt to inventory all of the nation's landslides. This paper will refer to a few of the local examples, and will also describe an exploratory meeting of landslide scientists at the USGS and a number of state geological surveys that was recently held to explore ways to implement common protocols and standards for landslide inventories and databases, so that these worthwhile efforts may be more easily aggregated and used by others.

25.4.1.2 National Landslide Hazards Mitigation Strategy

In 2003 the USGS developed a comprehensive, multi-sector and multi-agency strategy to mitigate landslide hazards for the United States (Spiker and Gori, 2003). The strategy focused on nine major areas and suggested that $20 million USD would be needed annual to succeed. The nine areas include:

1. Research
2. Hazard mapping and assessments
3. Real-time monitoring
4. Loss assessment
5. Information collection, interpretation, and dissemination
6. Guidelines and training
7. Public awareness and education
8. Implementation of loss-reduction measures
9. Emergency preparedness, response, and recovery.

In 2007 the "Landslide Exchange Group" was formed, which consists of landslide scientists from the USGS, AASG and the Federal Highway Administration. The mission of this group is to develop common protocols for collecting landslide inventory information, and look for ways to better leverage and aggregate our information and make it available on the Internet. These cooperative projects in a few selected areas of the United States have been quite successful and show the types of excellent research that could be accomplished with the eventual creation of the cooperative grant programs.

25.4.1.3 Public Awareness and Education

The USGS is involved in several important education efforts to transfer landslide hazard research and mitigation techniques to the people who most need them. In an attempt to make planning officials more aware of how to use landslide hazard scientific information, the USGS has recently worked with the American Planning Association (APA) to produce a primer on landslide hazards, and to present a number of case studies of how specific communities have successfully incorporated landslide hazard information into their planning and zoning regulations (Schwab et al., 2005). The USGS is also working under the auspices of the International Consortium on Landslides and cooperatively with the Geological Survey of Canada to create a handbook on best practices for landslide hazard mitigation. This book is being created for the public in general, and will contain straight-forward definitions of landslides, illustrations and photographs to illustrate mitigation methods and tools, and will share some best practices to use around one's home or business.

25.4.1.4 Inventories and Hazard Mapping

The USGS has traditionally focused its landslide hazards research in specific geographic areas, such as the Pacific Northwest or southern California, and applied a broad spectrum of our scientific expertise to intensive studies. By taking this approach, and working with state and local partners, USGS is able to make significant advances in landslide process research, inventories of modern and ancient landslides, production of probabilistic hazard maps, and refinement of sophisticated landslide models.

Radbruch-Hall and others (1983) prepared a landslide overview map of the conterminous U.S. at a scale of 1;7,500,000. This map, which has recently been released in digital format (Godt, 1997) depicts areas where large number of landslides exist, and attempts to classify geologic units according to high, medium, or low landslide susceptibility. The USGS has compiled larger scale landslide inventory maps for many regions in the U.S. that document locations, types, and in some cases, relative ages of landslides. Some of these inventories document landslides triggered by single events such as a storm or earthquake (Coe and Godt, 2001). These products have proved particularly useful in understanding what geologic, topographic or hydrologic factors contribute to triggering the landslides, thus allowing better understanding of the landslide process.

Landslide susceptibility maps are another common product produced by the USGS in the last few decades (e.g., Brabb and Pampeyan, 1972; Pike et al., 2001; Pomeroy, 1977). These products provide local governments with more useful information on which to base land-use decisions even though they do not assess the temporal frequency or probability of landslides. In cooperation with the California Geological Survey, the USGS prepared maps showing relative susceptibility of slopes to rainfall-induced debris flows in southern California (Morton et al., 2003). These maps were produced by analyzing six sets of aerial photographs taken during rainy seasons that produced many debris flows, and using digital elevation models of the areas to define the spatial characteristics of the debris-flow initiation locations.

25.4.1.5 Warning Systems

Several important efforts to assess the likely frequency of landslides or probabilistic depiction of the likelihood of landslides have been carried out by the USGS (Bernknopf et al., 1988; Mark, 1992; Campbell et al., 1998; Jibson et al., 1998; Coe et al., 2000). By linking these products to real-time precipitation measurements and robust weather forecasts aided by new generations of radar, the USGS and its partner, the National Weather Service, has twice developed debris flow warning systems. A pilot area was chosen in southern California to test the concept and develop an intensive research study area. The USGS has committed to assess the potential for debris flow, to identify infrastructure that may be at risk, and summarize these results in a statement called an Outlook. The USGS also defines, and continually refines, the rainfall intensity-duration warning thresholds. NWS forecasters then analyze measured rainfall and forecast rainfall and issue combined flash-flood and debris-flow watches or warnings for the burned areas. Warnings are broadcast through the NWS Advanced Weather Interactive Processing System (AWIPS) to local emergency managers, flood control districts, and the media.

25.4.1.6 Conclusions

Much excellent landslide hazard research is being conducted in the United States, by the USGS, its partners in the state geological surveys, academia, and by others. Much of this work is being used to effectively educate community planning officials and the public in general. However, to successfully implement the national landslide hazards mitigation strategy envisioned by the USGS and its partners (Spiker and Gori, 2003), significant expansion of our current workforce will be necessary.

25.4.2 Landslide Mitigation Strategy and Implementation in China

(Yueping YIN, China Geological Survey, Beijing, 100011)

Abstract China has been implementing a nation-wide landslide investigation and mapping plan since 1999, which covers more than 1500 counties. The preliminary investigation has identified nearly 150,000 sites with potential risks. Detailed mapping projects are currently focused on the most hazardous areas. The outcomes of these investigations will include a series of maps on 1:50,000 scale as follows: landslide distributions and types; landslide susceptible zones; landslide risk zonation; contours of landslide triggering precipitations; estimation of property losses; landslide prevention plan and engineering measures. China has successfully carried out a number of large-scale landslide prevention projects since the early 1990s, with particular attention given to the Three-Gorges' reservoir area and the cities under rapid development in the western part of China. The weather-based landslide forecast system has been established that covers the landslide prone zone in the nation-wide. This paper also highlights China's state landslide prevention plan, predicting and preventing landslides by masses, i.e., by villagers in or near the landslide, the emergence plans and risk management systems.

25.4.2.1 Nation-Wide Landslide Investigation and Risk Zoning

China suffers from severe landslide hazards every year. Landslides threaten lives and properties in 30 provinces, resulting in an estimated 700–900 deaths and damages of properties exceeding $10 billion RMB (Chinese Dollar) annually. Since 1990, China has completed a geohazard mapping program at the scale of 1:500,000 that includes 55,000 landslides, 13,000 rockfalls and 17,000 mudflows, with descriptions of locations of these landslides, and the related geologic conditions. More special investigations and risk zoning of landslides have been ongoing since 1999, which covers landslide-prone areas in about 1500 counties. The key task of investigation is to identify the potential of landslides, to provide an emergency preparedness plan, and to establish warning systems for the existing villages. About 150,000 potential landslides have been identified, and 80,000 of them are monitored. This program, called "monitoring and preventing by masses", has proved to be very effective for landslide loss mitigation. The success rate of landslide prediction and warning is obviously rising since the mapping and risk zoning plan was conducted. Figure 25.2 presents the number of evacuations made possible by successful predictions during raining seasons from 1998 to 2005.

25.4.2.2 Detailed Mapping for High Risk Zones of Landslide Hazards

The occurrences of landslides are associated with very complex processes in China. Detailed surveying and mapping for high risk zones have been conducted on the basis of geologic conditions to clarify these. The relationships between the landslide susceptibility of different kinds of slopes and the landslide triggering factors, such as, rainfall, earthquake, and human activities, are comprehensively analyzed. This survey program is at the scale of 1:50,000, resulting in a detailed inventory and distribution maps that cover landslide susceptibility, geological and geo-environment conditions and the impacts of construction projects, such as dams and pipe lines, etc., in the high risk zones. These documents will be used for guidance for risk assessment for urban development and relocations. In China, the work on landslide hazard reduction is organized by government at central to local levels. Therefore, it is very important that geologists provide concise information for decision-makers. The four sets of maps described above are used extensively and through the maps, the government can easily understand the critical issues and make decisions.

25.4.2.3 Stabilization and Mitigation on Major Landslides

Since "International Decade of Natural Disaster Reduction" started in 1990, more than 200 major landslides that severely threatened the cities, main river courses, and other key public facilities have been stabilized. The Three Gorges Project is one of the largest water resources development programs in the world. The resettled population of the Three Gorges Reservoir area is about 1.2 million. During the first phase from 1993 to 1997, 82,000 people were resettled, and 550,000 populations were resettled in the second phase of the project from 1997 to 2003. By 2009, over 600,000 people will be resettled during the third phase of the project. The resettlement plan is a great challenge, since in the reservoir area it is difficult to find flat land that is suitable for construction. People have no alternative but to move to landslide-prone areas. A systematic landslide prevention project has been carried out at the Three Gorges Reservoir, which is aimed at protecting and stabilizing unstable slopes and rockfall deposits and solving the engineering problems encountered in the large-scale excavation and filling carried out in the resettlement construction plan since 2001.

25.4.2.4 Weather-Based Regional Landslide Hazard Warning

In 2003, the Ministry of Land Resources (MLR) and China Meteorological Administration (CMA) signed a cooperative agreement on operating a weather-based geohazard warning service during the raining seasons. CMA provides rainfall data, and MLR will make forecast for geohazard risks, and release warning notices through China Central Television (CCTV) at prime times after broadcasting daily weather forecast. In the same manner, the local cooperative agreements have also been signed in various provinces. The weather-based warning system is part of the landslide prevention program of "monitoring and prevention by masses". According to incomplete statistics in 2004, over 700 landslides were successfully predicted and warned, and 46,000 persons were evacuated from risky areas. On 24 August 2004, MRL and CMA jointly issued a warning of a class 4∼5 landslide hazard at the Zhejiang and Fujian Province coastal area in anticipation of the "Aily" Typhoon coming on 25–26 August. Two days later, the typhoon brought 400–600 mm rainfall, which triggered hundreds of landslides. No people were injured or died as tens of thousand of people were removed timely from the risky zones, although 260 empty houses were destroyed.

25.4.2.5 Geohazard Risk Assessment on Land-Use

The surge of infrastructure construction especially in the western mountain areas of China has created a serious concern about geohazards. According to statistics, about 80% of the landslide hazards are caused by inappropriate construction activities. In 1999, the Ministry of Land Resources issued an act that specified a compulsory geo-hazard risk assessment for various land-use purposes before the applications of these projects are approved. The assessment includes: (1) possible geohazards induced or intensified by the project, and (2) risks of geo-hazards induced by the construction project itself.

The largest project on landslide risk assessment in China is related to the natural gas pipeline project linking the Xinjiang Autonomous Region to Shanghai. The 4200 km long pipeline strides across various complicate geological and geomorphologic areas that pose significant constraints on the pipe alignment, construction and operation alternatives of the project. The detailed review of landslides and other geo-hazards for this project helped to avoid many major hazards that may threathen the project.

25.4.2.6 Education and Training for Geohazard Mitigation

In China, development standards in rural areas are behind those in the urban areas. The rural areas are much more hazard-prone due to the low input and poor knowledge regarding landslide prevention. The Ministry of Land Resources of China organized a series of training courses in 19 provinces in 2006. Three million people joined the course and learned some fundamental knowledge about safe housing and construction practices, simple means of observing and issuing warning of landslide occurrence during emergence situations, and evacuating and rescuing actions, etc. Tens of landslide disasters had been successfully warned and avoided in the raining season of 2007 as a result of the education plans.

25.4.2.7 Conclusions

This paper reviews the landslide hazards prevention plan carried out in China during the International Decade of Natural Disaster Reduction since 1990. With the rapid economic development in China, landslide hazards are increasing. This paper has briefly discussed various aspects related to this plan. They are the nation-wide landslide investigation and risk zoning; stabilization and mitigation of major landslides; weather-based regional landslide hazard warning; geo-hazard risk assessment on land-use and main actions on landslide hazard reduction. These measures have proved to be successful and will be even more rewarding in the future.

25.4.3 Landslide-Risk Reduction Strategies and Practices in the Philippines

Sandra G. Catane (National Institute of Geological Sciences, University of the Philippines, Diliman)
Mark Albert H. Zarco (Department of Engineering Sciences, University of the Philippines, Diliman)
Ricarido M. Saturay, Jr. (National Institute of Geological Sciences, University of the Philippines, Diliman)

Abstract The Philippines has been identified as one of the landslide hotspots in the world (Kjekstad, 2007). The frequency has dramatically increased during the last few decades due to rapid development, increasing demand for space and changing climate patterns. The two major landslide disasters in 2006 in Southern Leyte and Albay provinces placed the Philippines as the world's top climate victim in that year with more than 2,000 casualties and billions of pesos property damage. In the Philippines, compared with other geohazards the level of disaster-risk reduction lags behind for landslides. A shift in strategy from virtually responding only to disasters to improvement and institutionalization of disaster preparedness plans was a breakthrough in 2003. A comprehensive Geohazards Mapping Program was officially launched by the national government through the collaboration of various government agencies. A huge chunk of the national budget was infused into the Program while additional support was obtained from international funding agencies. As a result, 1:50,000 scale maps have been prepared for the entire country but still lack the accompanying booklet containing the

methodology. Empowerment of the local community is the strength of the recent READY project through the establishment of community-based warning systems in critical areas, public awareness campaign, and initiatives to mainstream landslide-hazard assessment. As a proven formula in other countries that have attained significant success in reducing landslide risk, the National Disaster Coordinating Council (NDCC) has yet to tap the academe and the private sector as partners in landslide-risk reduction efforts in order to accelerate work and elevate the level of landslide hazard and risk assessment.

25.4.3.1 Introduction

Confluence of geologic, geographic and climatic factors makes the Philippines prone to natural disasters, particularly from landslides. Many communities in landslide-prone areas continue to grow. In 2006, recent major landslide events in Southern Leyte and Albay provinces in 2006 claimed more than 2,000 lives and caused billions of pesos of property damage.

This paper outlines the development of landslide risk reduction efforts and strategies in the Philippines as part of institutional building. Risk-reduction practices and challenges to improve/enhance the current system are discussed.

25.4.3.2 Lanslide-Risk Reduction Strategies

National Government Programs

In 2003, the national government strengthened its disaster-mitigation program through the launching of the National Geohazards Mapping Program. The umbrella organization of the Program is the NDCC, which is chaired by the Secretary of National Defense and executed mainly by member agencies including the Mines and Geosciences Bureau (MGB), Philippine Institute of Volcanology and Seismology (PHIVOLCS) and the Philippine Atmospheric, Geophysical and Astronomical Services Administration (PAGASA). As part of the campaign, landslide susceptibility maps for the entire Philippines have been produced mainly for a scale of 1:50,000 for the entire Philippines (MGB, 2004), using slope as primary criterion. MGB and PHIVOLCS, both members of the (NDCC), agreed to split the responsibility on landslide hazard mapping and assessment on the basis of trigger mechanism, i.e. MGB and PHIVOLCS for rainfall-induced and earthquake-induced landslides, respectively.

The NDCC has recently launched a multi-agency project called Hazards Mapping for Effective Community-Based Disaster Risk Mitigation or the READY Project (NDCC, 2008). The project is being implemented by the Office of Civil Defence (OCD) in cooperation with NDCC member agencies including MGB, the National Mapping and Resource Information Authority (NAMRIA), PAGASA and PHIVOLCS. It is aimed at addressing the problem of disaster-risk management at the local level. The project has been implemented in 27 selected and high risk Philippine provinces. The project has three components: (1) multi-hazard and risk assessment, (2) community-based disaster risk mitigation using community-based early warning system (CBEWS) and information campaign, and (3) mainstreaming disaster risk reduction plan into the local development.

Formulated in 2000 in the aftermath of the Cherry Hills landslide, the Engineering Geological and Geohazard Assessment (EGGA) has been instituted and became one of the requirements for government and private developers prior to developing a site. It is also an additional requirement for larger development projects which require Environmental Impact Assessment (EIA), if deemed necessary.

The Academe

At least two universities have been independently conducting researches on landslides since the Cherry Hills landslide in 1999. These include the University of the Philippines (UP) and the Mapua Institute of Technology (MIT). The Cherry Hills landslide gained much publicity due the significant number of casualties (58) and its closeness to Metro Manila, the capital of the Philippines.

In 1999, the UP created a Geohazard Advisory Committee consisting of faculty scientists and engineers to address the landslide problems in its campuses all over the country. Later, some of the members of this committee continued to collaborate and expanded their researches. The group's activities include research and publication, giving lectures to other universities, providing advice to companies and communities, and in organizing training, workshop and conferences on landslides. Support from other countries such as Japan and Norway has recently started pour in through research collaboration.

Starting on June 2008, a Department of Science and Technology (DOST)-funded program will be implemented by the University of the Philippines as a collaborative research program of its units. The Program is aimed at developing low-cost sensors to monitor parameters in the field traditionally measured by commercially available but high-cost instruments (Marciano et al., 2008). The sensors are being designed to include features capable for real-time measurements, efficient connectivity, durability for deployment in steep and inaccessible terrains and more importantly, these will be cheap and affordable suitable for developing countries like the Philippines.

The MIT also shifted its gear by establishing a graduate program in engineering geology in cooperation with a foreign university. Equipment have been procured both for instructional and service.

Private Sector and NGOs

Ateneo de Manila's Manila Observatory has also conducted separate studies on landslides supporting collaboration with non-government organizations (NGOs). Other NGOs have their own projects and initiatives in landslide-risk reduction such as training communities on geohazards and providing assistance in rehabilitating affected areas. Private companies, whose infrastructures are affected or threatened by landslides and slope failures, either conduct their own in-house studies and mitigation measures or sub-contract other companies specialized in slope stabilization and ground improvement, often times involving consultants from the academe.

25.4.3.3 Practices and Challenges

Hazard Maps and Risk Assessment

The two national mapping programs of the government have been producing mainly 1:50,000 landslide susceptibility maps. These maps indicate the potential initiation sites for landslides but lack the time component which is present in landslide hazard maps. Confusion on how to interpret the existing landslide susceptibility maps and their acceptability have been major concerns for communities, land-use planners and other stakeholders because the map identifies large tracts of land as unsafe as the frequency and magnitude of landslide occurrence have yet to be incorporated in the assessment.

Landslide inventories in the Philippines are produced mostly by ground checks, and are very much likely to be incomplete especially for single, regional landsliding events. Topographic maps are only useful for identifying landslides which occurred before the mapping date (usually 1940s to 1950s) and which are larger than the map resolution. Limited capability and/or resources to conduct aerial surveys and limited access to satellite-based data make it difficult to efficiently produce landslide inventories, particularly for recent events.

Since most of the maps are 1:50,000, these cannot be directly used at the village level. Mapping with greater detail at the local level is still needed in the formulation and implementation of contingency plans.

Rain gauges have become the popular community-based monitoring instrument for the national program. These instruments, mostly manually operated, are intended to provide rough estimates of when landslides will occur or when evacuation is necessary. Rainfall threshold values have been established for lahar initiation in Mayon volcano (Rodolfo and Arguden, 1991) and Pinatubo volcano (Arboleda and Martinez, 1996; Tuñgol and Regalado, 1996), and for landslides in Leyte and Surigao (Garcia, 2006). However, since the relation between rainfall and landslide occurrence is empirically-determined and site-specific, threshold values established for an area could not be applied to other areas.

Slope Monitoring and Engineering Mitigation Measures

Despite the high frequency of landslides in the Philippines, slope protection is limited while instrumental monitoring of critical slopes is almost nonexistent (Zarco et al., 2007). In the few cases where distressed slopes are monitored, this is usually done visually due to high cost and the risk of pilferage of slope monitoring devices. Practically, slope monitoring can only be afforded by wealthy communities. In recent years, problematic slopes are most frequently stabilized by combining structural and bioengineering methods. However, improvement or installation of subsurface drainage is not frequently done despite water being a major destabilizing factor in most slopes.

Prior to the February 17, 2006 Guinsaugon disaster, landslides were limited mostly to relatively smaller and shallower slope failures of mainly soil materials. The Guinsaugon landslide challenged local scientists and engineers to better understand the mechanisms underlying slope failures in rock. It also highlighted the limited number of local experts in area of rock mechanics. Majority of the limited studies on the stability of rock slopes undertaken in the Philippines before February 17, 2006 were done as part of consultancy-based projects rather than being research driven. Furthermore, the volumes of data derived from these site-specific studies have yet to be systematically integrated into a form that is readily useful to geo-scientists and engineers.

25.4.3.4 Minimal Institutional Linkage Between the Government Agencies, Academe and Other Sectors

As the lead agency, the NDCC has been successful in bringing together government agencies to work on geohazard problems of the country. However, the Council did not recognize the need to involve the academe and private sectors. Turfing, proprietary data generated by private companies resulted to decentralization and limited access to relevant data. Delfin (2005) has pointed out that government agencies should make sure that critical data, as part of public domain, are accessible through their websites. Limited access to relevant data also resulted to difficulty in smooth and timely execution of disaster response and rehabilitation, limited peer review of methods and outputs, and uncoordinated efforts and conflicting statements/positions.

25.4.3.5 Limited Institutional Capabilities and Capacities

Very few geoscientists, who have the basic skills in geohazard mapping are involved in landslide-risk reduction. In the Philippines, only four universities offer geology courses resulting to very few graduates per year. Most geology graduates are immediately hired abroad due to attractive compensation. Locally, the uncompetitive compensation of a government geohazard specialist compared with those in the mining industry (due to the recent mining boom) makes government service much less attractive. Being traditionally a mining promotion and regulatory agency, MGB has yet to strengthen its capabilities as a geohazard research agency otherwise create a separate/sub-agency that will focus on geohazards only, similar to the USGS model as suggested by Delfin (2005). Furthermore, in spite the high number of civil engineers in the country they are not actively involved in the geohazard-risk reduction program. To maximize the existing manpower of the country, there is a need to further develop and enhance expertise in landslides by providing training, undergraduate and graduate scholarships, and by supporting research and publication.

25.4.3.6 Conclusions

Although landslide risk-reduction efforts has started to develop only recently in the Philippines, there is a need to improve the current practices and strategies. First generation landslide susceptibility maps were generated but these have yet to be peer reviewed and communicated properly to stakeholders. Construction of hazard maps that are larger scale than the current 1:50,000 maps and are more useful to communities should include time element. Hazard assessment which incorporates frequency, probabilities and takes into account the transport mechanism of landslides is desired.

Institutionalization of partnership between the government agencies and the academe and the private sector in the national landslide-risk reduction program is paramount. Likewise, the Commission on Higher Education and the academe should intensify its campaign in recruiting students to consider career in geohazards by opening new programs and courses in more universities throughout the country.

25.4.4 Towards Landslides Mitigation in Sri Lanka

N. Rupasinghe, A. Dias, (Central Engineering Consultancy, Bureau, Sri Lanka)

Abstract Landslides are the most recurrent and prominent disaster in Sri Lanka, well known for crippling impacts on transportation, especially in the mountainous areas subjected to high intensity rains. A compressive program on landslide hazard mapping has been carried out with the support of UN to support landslide risk reduction strategies including land use planning. However, holistic programs on landslide risk reduction only started to emerge recently, as national responses to catastrophic landslide and tsunami disasters in the recent past.

25.4.4.1 Overview of Landslide Risk Reduction Strategy Development in Sri Lanka

Sri Lanka is an island in the northern Indian Ocean just south of southernmost part of India and extends in latitude form approximately 060 N to 100 E and in longitude from approximately 800 N to 820 E with an extent of about 65,000 km^2.

Sri Lanka has been subjected to a number of extreme landslide disasters that produced great loss of life, material damage, and distress. The experiences indicate that destruction is inversely proportional to the state of preparedness. The direct impacts suffered in Sri Lanka are the loss of life due to drowning, destruction of houses, road damages, etc., and indirect losses such as hunger, shelter, looting, breakdown of the infrastructure facilities, etc., are experienced. The organizations related to disaster reduction are expected to respond immediately to disasters and reduce losses from direct impacts and reduce the indirect damages. While there is a remarkable sprit of solidarity and volunteerism in the aftermath of disasters, the potential is not adequately harnessed, trained, and directed.

Adams (1929) was the first to draw attention to the existences of three well-marked plains of erosion cut in the precambrian rocks of Sri Lanka. These “three terraces” present three successive stages of denudation brought about by successive uplift of Island as a whole. On morphological grounds Wadiya (1943) rejected this “erosion terrace theory” and postulated that the three peniplains are the result of successive bedrock uplifts. The recent detailed structural and tectonic mapping of central highlands indicates that in addition to the vertical epirogenic movements of the southerly drifting miniplate of Sri Lanka, there are horizontal thrust developed regionally and a series of strike slip faults along mega-lineaments (Vitanage, 1994). Some of the lineaments appear to be active and some of the older highly weathered lineaments are commonly associated with large destructive recurrent landslides. Since there are no simple mechanisms to foresee instabilities, monitoring is the most appropriate mechanism to understand their behavior.

Various occurrences of landslides investigated to date are known to be rain triggered. It has therefore been customary in Sri Lanka to interpret landslide event in terms of rainfall history, immediate preceding the any slide event. One exceptional series of rain triggered landslides took place in May 2003, an example shown in Fig. 25.5, when a tropical storm made its way across the Bay of Bengal. The storm first formed 700 km to the West of Sri Lanka on May 11 and then made its way North by about 500 km. It stalled for a week causing heavy rainfall 900 km away from the eye of the storm over the South-Western corner of Sri Lanka leading to an estimated 247 dead and over 200,000 and displacements. The May is the month when the heavy monsoon rains start and the South-West of Country is expected to become wet. Indeed, there has been heavy rainfall of order 600 mm in Sri Lanka in May during the period from 1920 to 1950 but not thereafter. According to the meteorological data this was the heaviest rain to hit the island since 1947.

Fig. 25.5 Fifty Seven (57) people were buried in this Landslide in Alapatha, Sri Lanka in May 2003

Landslide becoming a frequent disaster category, with frequent disruption to transport sector in the central mountain areas (as shown in Fig. 25.6) the government of Sri Lanka took serious note of the losses and initiated strategic plans for the reduction of landslide disaster during monsoon periods starting from year 1986. The report "Landslide Hazard in Sri Lanka" published by the National Building Research Organisation in 1986, brought up the strategic requirement of disaster mitigation against landslides as a national issue. Subsequently the above requirements were adopted in a cabinet paper submitted by the Ministry of Policy Planning and Implementation, which supported the development and use of scientific methodologies in landslides mitigation. The beginning of the International Decade for Natural Disaster Reduction in 1990 provided a conducive environment and the Landslide Hazard Mapping Project was implemented by the government of Sri Lanka, executed by the United Nations Center for Human Settlement(Habitat), Nairobi, funded by the United Nation Development Programme. Due to the multi-disciplinary nature of the impact studies involved in landslide disaster evaluation aspects, the National Building Research Organisation was selected as the executing agency for the Landslide Hazard Mapping Programme and subsequently institutional capacity was upgraded by establishing a separate division for the Landslide Studies & Services at the NBRO, 1992. After couple of years, the first national Symposium of Landslide in Sri Lanka was held in Colombo generating a wealth of information on Sri Lankan Landslides covering a diverse range of landslide types.

Fig. 25.6 Lanslieds along Kalawana – Rakwana Road in Sri Lanka

Landslide disaster risk reduction demands integration of a number of disciplines associated with the subject. Therefore, landslide disaster mitigation require collective and corporative efforts of all relevant R&D institutions lead by strong executing organizations of the country. One of the mechanisms that evolved during the disaster in May 2003 and implementation of Landslide Disaster Mitigation Works, was the establishment of a ad-hoc group named "Operation Professional Combine" established at Rathnapura, the most affected area. This was carried out in accordance with the action plan proposed by the Central Engineering Consultancy Bureau (CECB) at the council meeting at Disaster Management Committee held in Colombo, 28th May 2003. The "Operation Professional Combine" (OPC) consisted of hundreds of academics, professionals and volunteers from various backgrounds coming together for the first time in recent past. The objective of the exercise was to provide a comprehensive summary on destruction caused by landslides at Rathnapura district; propose recommendations to mitigate further losses and facilitate a basis for the next costly recovery phases in the disaster prone areas.

In addition to the above mentioned form of spontaneous developments, the Ministry of Disaster Relief Services was formed resulting from restructuring of the cabinet under the Gazette No.

1422/22, dated on 08th December 2005 in response to the 2004 Indian Ocean Tsunami Disaster and the national "Disaster Management Centre" was established under the National Council for Disaster Management in accordance with the Sri Lanka Disaster Management Act No. 13 of 2005 passed by the Parliament of Sri Lanka on 13th May 2005. The respective authorities cover the general subject of Disasters addressing Preparation, Response and Recovery. An "Emergency Operation" is proposed to be established at the Ministry providing efficient and immediate emergency services and coordinating activities, during the Post Disaster period.

The most recent development is the preparation of "Road Map for a Safer Sri Lanka" under the disaster Management Centre of the Ministry of Disaster Management and Human Rights. The proposals in this document adequately reflect the priority projects in the areas of natural as well as man-made disasters and human rights. The formulation of the Road Map represents a very significant achievement for the Disaster mitigation aspects of Sri Lanka since this clearly identifies the priority initiatives that need to be undertaken by various stakeholders-both the private sector and civil society- to lead to a Sri Lanka that can pro-actively carry out landslide disaster mitigation.

25.4.5 *Landslide Hazard Strategies in Slovakia*

Jan Vlcko (Comenius University, Bratislava, Slovakia) – Peter Wagner (State Geological Institute of Dionyz Stur, Bratislava, Slovakia)
Rudolf Ondrasik (Comenius University, Bratislava, Slovakia) – Libor Jansky (United Nations University, Bonn, Germany)

Abstract Mountainous landscape of Western Carpathians with variable geology cause potential instability in some parts of the territory. According to latest data almost 4% of the territory of Slovakia is covered by landslides. On the other hand, from relatively consolidated geological and existing climatic conditions results that the probability of unexpected and huge landslides with catastrophic consequences is relatively low. This idea was changed after catastrophic landslide which affected the mining town of Handlova in winter period 1960/61. The slide damaged a great part of city infrastructure and with its consequences on human property belongs to the biggest natural disasters in the country. For the first time landslide specialists, local and national authorities as well as the population recognised that even in relatively stable environmental conditions may occur the landslide having a character of a disaster with negative impact on the society. Since this event the systematic study of landslides and other slope movements has begun.

The paper deals with the stages of landslide studies in Slovakia and illustrates actual trends of landslides study and methods of investigation.

25.4.5.1 History of Landslide Studies in Slovakia

The Western Carpathians constitute a part of the European alpine orogenic system. Landslides are linked to the particular geomorphic and geologic units, primarily to the mountain ranges stretching towards the intra-mountain basins and tectonic depressions. The largest number of landslides has been found in the region of Flysch zone and along the foothills of Neogene volcanites.

Landslide study in Czechoslovakia (now Czech and Slovak Republics) is exclusively linked with the pioneering work and influence in engineering geology of Professor Quido Zaruba in the 1920s and 1930s, who started study of landslides in the West Carpathians in connection with the railway projects passing through the Outer Flysch belt and later on in connection with several dam projects.

The crucial point in landslide hazard study in Slovakia is strongly connected with Handlova catastrophic landslide. In response to landslide destruction a governmental program was established to record in a central archive all landslides of economic significance. The study was carried out in three time periods (in 1962 to 1964, 1974 to 1978 and 1981 to 1991) based on unified principles and methodology and the data were recorded in a landslide database archive. The archive began in 1962 with about 9000 landslide-prone areas, and had expanded to about 15,000 records 30 years later. In accordance with regional landslide study a theoretical background (e.g. famous and widely accepted landslide classification prepared by Nemčok, Pašek and Rybář 1974) and the knowledge about landslide distribution within individual lithological units in Slovakia were recognized. Later on the efforts of landslides inventory lead to the preparation of Slope Stability Atlas of Slovak Republic at the scale 1: 50,000 covering the whole state territory.

25.4.5.2 Actual Regional Studies of Landslides

A regional study was carried out when landslide susceptibility maps for selected regions in Slovakia since seventies of the last century were compiled. After adoption of unified principles in 1996 these maps were integrated into the set of maps of geofactors (1: 50,000) recently covering 70% of the territory. In accordance with latest trends in landslide research there were also several landslide susceptibility maps compiled adopting statistical methods, namely multi and bivariate techniques (Paudits, 2005; Jurko et al., 2005; Bednarik, 2007).

The requirements of engineering practice dealing with urban development in populated areas are at present formulated towards the landslide hazard and risk assessment and decision making. There are several examples varying from the estimation of landslide risk for urban-development plan from the wider area between the towns of Sered and Hlohovec at a scale 1:10 000 (Bednarik, 2007) or for the town Lubietova in detailed scale 1: 2 000 (Vlcko, 2002) where the landslide risk zones are delineated according to factor of safety calculated for particular slope in relation to designed type of foundations. These studies create a transition towards detailed slope analysis and design procedures.

25.4.5.3 Local Case Studies of Landslides

There are several case studies which rely upon quite good understanding of landslide by earth scientists. As an example we bring the final solution of the stability problems related to the mining town of Handlova. After disastrous landslide and after recognizing that both slopes of Handlovka River are unstable there was urgent need to make a final decision and to design measures to stabilize quite large part of territory (about 10 km^2). In order to

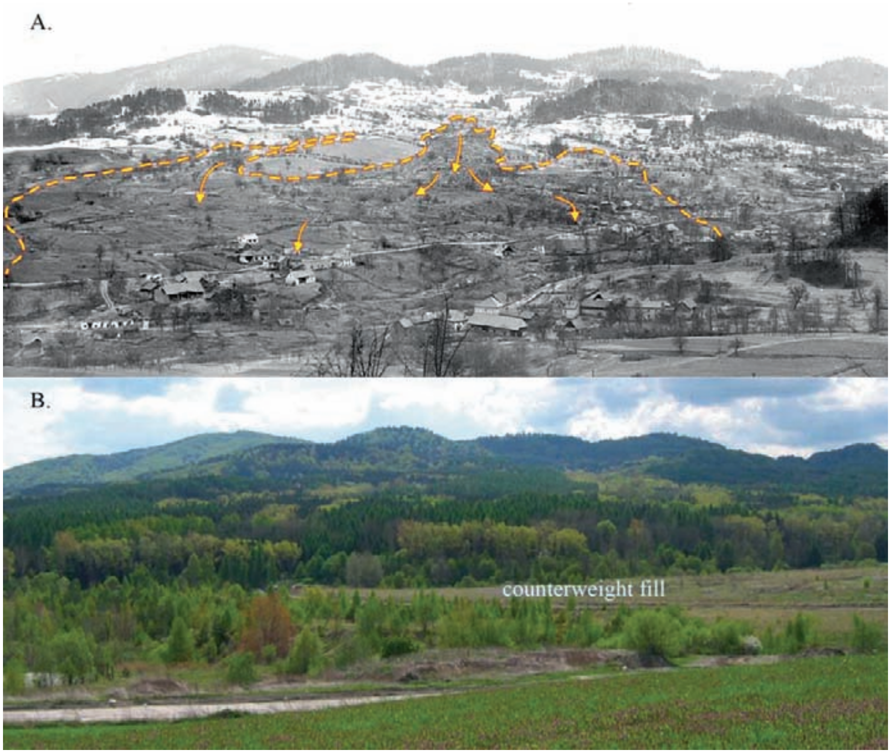

Fig. 25.7 A view at landslide area in Handlova. A – active slide in 1961 (photo by Nemcok and Malgot), B – present state of slope with counterweight fill at the toe (April 2008)

stabilize landside area various protective measures were applied: surface drainage, drainage wells and horizontal boreholes. Finally, the optimum economic and environmental problem solution was the construction of a counterweight fill from mine waste materials in the valley floor while the Handlovka River was canalized (Fig. 25.7). The fill is enough heavy to provide additional component of resistance near at the toe of both unstable slopes. From the environmental point of view the mine dumping in the surrounding area was strongly reduced and the waste material was used not only to the stabilization but also to the rehabilitation purposes.

25.4.5.4 Conclusions

The recent landslide studies in Slovakia are oriented towards probabilistic analysis, elaboration of warning systems, landslide hazard management etc. On this basis is elaborated a state programme supported by the Ministry of the environment of Slovak Republic entitled "Partial monitoring factors", in which over 30 unstable sites spread across the whole country are monitored, data gathered, processed and transferred through the internet to the responsible authorities as well as to the public (Klukanova and Liscak, 2004).

Slope movements along with the floods belong to the most dangerous natural hazards in Slovakia. The gained experience confirms the idea that attention must be paid primarily to more economic landslide precautions measures than to application of expensive stabilization measures. Moreover, the landslide problems must be under permanent control not only by the landslide specialists but also by the responsible bodies at both state and local level.

Acknowledgments This work was supported by the Slovak Research and Development Agency under the contract No. APVV-0158-06, Ministry of Education – Vega grants N. 1/0499/08 and grant N. 1/4045/07.

25.4.6 Case study on Local Landslide Risk Management During Crisis by Means of Remote Sensing Data

N. Casagli[1], D. Colombo[2], A. Ferretti[2], L. Guerri[1], G. Righini[1]

[1]Department of Earth Sciences, University of Firenze, Italy
[2]Tele-Rilevamento Europa - T.R.E. s.r.l. e-mail: nicola.casagli@unifi.it

Abstract A case study of rapid landslide mapping in Southern Italy is here presented. Remote sensing data were used due to their availability and capability for rapid landslide motion survey. Very high resolution optical images and data from radar satellites were processed and analysed; they were integrated with information from field survey and ancillary data. This procedure represented a valuable tool for civil protection activities during emergency planning and risk management.

25.4.6.1 Introduction

Following landslide movements in Cavallerizzo di Cerzeto (Italy), the Italian National Civil Protection Department (DPC) asked the Department of Earth Sciences, University of Firenze, to monitor the area using remote sensing data from both optical very high resolution (VHR) satellites and radar sensors by means of InSAR technique. Indeed, it is considered that new generation VHR images could provide a powerful tool for civil protection activities in risk assessment, emergencies and disaster management, since they are readily available due to the possibility of programming data acquisition: those images represent a valuable tool for change detection before and after an event and thus give quickly evidence of the phenomenon for emergency planning and risk management (Casagli et al., 2005; Voigt et al., 2007). InSAR processing, instead, can provide information on ground displacement and its temporal evolution with millimetric accuracy; in particular the Permanent Scatterers (PS) technique, developed by Telerilevamento Europa, has demostrated its capability in landslide motion survey (Colesanti et al., 2003; Farina et al., 2006).

25.4.6.2 Case Study of National Landslide Risk: Cavallerizzo di Cerzeto, Italy

The small village of Cavallerizzo di Cerzeto, located in Cosenza Province, Calabria region, Italy, was

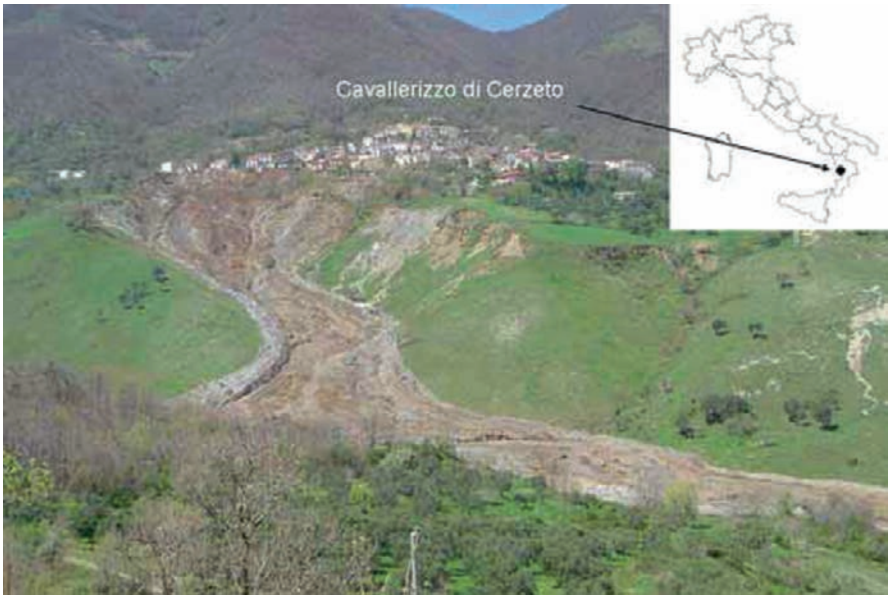

Fig. 25.8 Mud flow along the San Nicola stream just below Cavallerizzo di Cerzeto

affected and damaged a lot by a catastrophic landslide event on 7th of March 2005 triggered by heavy rainfalls. Subsequently, a huge mud flow evolved along the San Nicola stream (Fig. 25.8). The population was evacuated in time and nobody was injured.

The Italian National Civil Protection Department (DPC) was immediately activated and the Department of Earth Sciences, University of Firenze, competence centre of DPC for hydrogeological risk, was asked to monitor the area using remote sensing data from both radar processing and optical very high resolution(VHR) satellites images in order to obtain a rapid mapping of the event, damage assessment and residual risk analysis.

A good Quickbird archive image was acquired (dated on January 2003) while a new acquisition from the Ikonos satellite was programmed and resulted in a very good, clear image on 16th March 2005. These images were orthorectified and processed by means of radiometric and spectral enhancement; they were also rendered on a digital elevation model giving the 3D perspective views. These data were photo interpreted and change detection was carried out in order to identify the spatial extension of the landslide and main damages occurred: individual landslides and unstable areas around were recognised and mapped. Integration with information from PS analysis was then performed, using an ascending and descending radar images data sets collected by ESA ERS1/2 satellites over the nine year period 1992–2001 (Fig. 25.9) and 3 years (2003–2005) of RADARSAT images. The interpretation of Permanent Scatterers provided information n the deformation rate and gave evidence of older unstable areas, as well as those affected by recent movements. Moreover, ancillary data were collected such as orthophotos, thematic maps on geology, geomorphology, tectonics and topography. All these information were integrated in to the G.I.S. environment. Afterwards a field survey was carried out in order to validate and refine the results obtained from remote sensing data. All the data, information and results were reported to the Italian Civil Protection Department in charge of risk management: it was decided to permanently evacuate the village and relocate people to a new site.

The results demonstrate that a combined approach based on the use of multi-interferometric techniques and photo-interpretation represents a valuable tool for landslide rapid mapping and that, using this approach, it is possible to define the spatial extension and temporal evolution of landslides for the emergency management strategy.

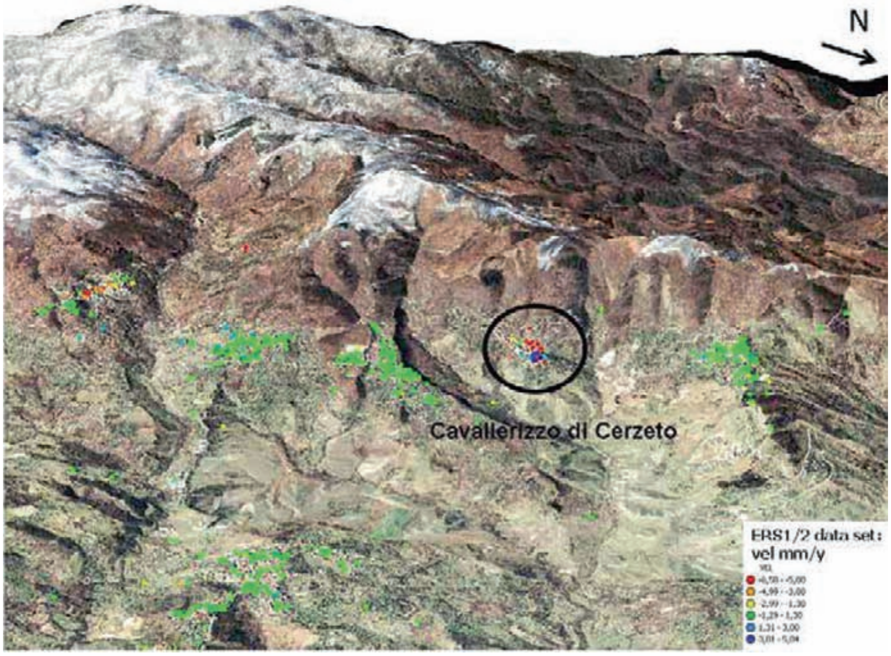

Fig. 25.9 3D view of Cavallerizzo di Cerzeto and surrounded area. IKONOS image rendered on DEM and PS from ERS1/2 dataset

25.4.7 The Development of Tension Crack Arrays Associated with Mw 7.6 Kashmir Earthquake, October 2005: Implications for Future Slope Stability

Dr Wishart Mitchell (International Landslide Centre, Department of Geography, Durham University)

The Mw 7.6 earthquake which affected the middle Jhelum valley in Azar Jammu and Kashmir, Pakistan in October 2005 generated numerous co seismic landslides, ranging from small translational failures to extensive rock avalanches, concentrated along the Muzaffarabad-Tanda Fault. In this high mountainous area, many slopes did not fail but were seriously affected with the formation of complex arrays of tension cracks and small graben structures within bedrock and alluvium. These cracks can be found associated with two distinctive slope situations: (1) in the vicinity of the fault trace and (2) upslope of co seismically triggered landslides. Their presence is a clear expression of fracturing of the ground surface under tension due to perturbation of the dynamic stress field and reflects either direct tectonic processes related to seismo-tectonic fault rupture on the slopes or are associated with peak ground acceleration which has lead to seismo-gravitational fissure development on slopes that were originally under tension and close to failure. It is also clear that local geology and topography have had a major influence on the distribution of seismic stresses and the resultant fissure systems. Both sets of tensional fissures indicate areas of future mass movement as slopes respond to changes in post-seismic stress and monsoon rains by increased infiltration and generation of high pore water pressures. On-going hazard in the area is associated with slopes at threshold stability coupled to the progressive and retrogressive failure of translational and deep seated failures. Disaggregation of hillslopes by the ground shaking has also increased the amount of sediment available for future transportation leading to increased debris flow generation associated with rainfall, spring snowmelt and summer monsoon events. Continuous monitoring of slopes which have been affected by tension crack arrays has been instigated at four sites to determine post-seismic slope response to slope stability in association with rainfall events. Three of these sites are located around Muzaffarabad with a further site up the

Jhelum valley towards the hilltop village of Chikka which was severely damaged by the earthquake. Overall pattern of the monsoon rainfall data over the monitoring period shows that each slope is clearly reacting in a distinctive local way to ongoing site specific strain conditions. Extensive slope failures are therefore likely to take place in the near future as existing landslides continue to develop by retrogression of back and lateral scarps. The presence of tension crack arrays on many slopes that mirrors the configuration of the present scarps allows prediction of future slope failure pattern. Areas of hillslope that have not failed, but have a high density crack array, are also are likely to fail as a series of deep seated failures. Measurements of horizontal extension and vertical displacement will allow a better assessment of slope stability and potential landslide hazard in this disaster area where more than 2.5 million people are still displaced from their land.

25.5 Conclusions

As introduced by sample of selected papers from the session, different countries have evolved their landslide risk reduction programs based on the unique landslide characteristics, needs of affected communities and the prevailing institutional arrangements. While it is recognized that the frequency of landslide type may lead to setting different priorities on different aspects of landslides, such as warning, response and evacuation, mitigation through structural measures, etc., all these components are important in building a holistic national landslide risk reduction strategy. This session will introduce many case studies and it is hoped that the policy session 3, "country dialogue" on landslide risk reduction will make use of these experiences to develop a comprehensive generic landslide risk reduction strategies and institutional support that would provide important lessons and directions to all countries.

References

Adams, F.D. (1929). "The geology of Ceylon". Canadian Journal of Research 11: 425–511.

Arboleda, R.A. and Martinez, M.L. (1996). 1992 lahars in the Pasig-Potrero River system. In: Newhall, C.G., Punongbayan, R.S. (Eds.) Fire and mud: eruptions and lahars of Mount Pinatubo. Philippine Institute of Volcanology and Seismology, Quezon City and University of Washington Press, Seattle, 1126 pp.

Bednarik, M. (2007). Landslide hazard risk evaluation in land use practice. PhD thesis, Bratislava, p. 130.

Bernknopf, R.L., Campbell, R.H., Brookshire, D.S., and Shapiro, C.D. (1988). A probabilistic approach to landslide hazard mapping in Cincinnati, Ohio, with applications for economic evaluation. Bulletin of the Association of Engineering Geologists, 25(1): 39–56.

Brabb, E.E. and Pampeyan, E.H. (1972). "Preliminary map of landslide deposits in San Mateo County, California." U.S. Geological Survey Miscellaneous Field Studies Map MF-344, scale 1:62,500.

Brabb, E.E., Pampeyan, E.H., and Bonilla, M.G. (1972). "Landslide susceptibility in San Mateo County, California." U.S. Geological Survey, Miscellaneous Field Studies Map MF-360.

Campbell, R.H., Bernknopf, R.L., and Soller, D.R. (1998). "Mapping time-dependent changes in soil-slip-debris-flow probability." U.S. Geological Survey, Geologic Investigation Series Map I-2586.

Casagli, N., Fanti, R., Nocentini, M., and Righini, G. (2005). "Assessing the Capabilities of VHR Satellite Data for Debris Flow Mapping in the Machu Picchu Area" In: Sassa, K., Fukuoka, H., Wang, F., Wang, G. (Eds.) 'Landslides –Risk analysis and sustainable disaster management'. Springer, Berlin Heidelberg Part II: 61–70.

Coe, J.A. and Godt, J.W. (2001). "Debris flows triggered by the El Niño rainstorm of February 2–3, 1998, Walpert Ridge and vicinity, Alameda County, California." U.S. Geological Survey Miscellaneous Field Studies Map 2384, http://pubs.usgs.gov/mf/2002/mf-2384/.

Coe, J.A., Michael, J.A., Crovelli, R.A., and Savage, W.Z. (2000). "Preliminary map showing landslide densities, mean recurrence intervals, and exceedance probabilities as determined from historic records, Seattle, Washington." *U.S. Geological Survey Open-File Report 00-303*, http://pubs.usgs.gov/of/2000/ofr-00-0303/.

Colesanti, C., Ferretti, A., Prati, C. and Rocca, F. (2003). Monitoring landslides and tectonic motions with Permanent Scatterers Technique. Engineering Geology, 68: 3–14.

Delfin, F.G. (2006). Guinsaugon tragedy: Issues and prescriptions. Opinion Section. Manila Times, 8 September 2008, p6. http://www.manilatimes.net/national/2006/sept/08/yehey/opinion/20060908opi6.html. Accessed 8 September 2006.

EM-DAT: The OFDA/CRED International Disaster Database, 2002, www.em-dat.net - Université Catholique de Louvain-Brussels-Belgium.

Farina, P., Colombo, D., Fumagalli, A., Marks, F., and Moretti, S. 2006 "Permanent Scatterers for landslide investigations: outcomes from ESA-SLAM project". Engineering Geology 88: 200–217.

Garcia, M.A.A. (2006). Landslides follow heavy, long rainy days. Science and Technology Post, January – March 2006. Department of Science and Technology, Republic of the Philippines. http://www.stii.dost.gov.ph/ sntpost/NewPOST/JanMar2006/landslides_follow_heavy_long_rainydays.html. Accessed 19 May 2008.

Godt, J.W. (1997). "Landslide Overview Map of the Conterminous United States – National Landslide Hazards Map." U.S. Geological Survey Open-File Report 97-289, http://landslides.usgs.gov/html_iles/landslides/nationalmap/national.html.

Jibson, R.W., Harp, E.L., and Michael, J.A. (1998). "A method for producing digital probabilistic seismic landslide hazard maps; An example from the Los Angeles, California, Area." U.S. Geological Survey Open-File Report 98-113.

Jurko, J., Paudits, P., and Vlcko, J. (2005). Landslide susceptibility zonation using GIS – statistical approach. In: Proc. International Symposium on Latest Natural Disasters – New Challenges for Engineering Geology, Sofia, pp. 1–7.

Kjekstad, O. (2007). The challenges of landslide hazard mitigation in developing countries. 1st North American Landslide Conference, Vail, Colorado, 3–8 June 2007.

Klukanova, A., and Liscak, P. (2004). National Environmental Monitoring of Slovak Republic – Part Geological Hazards. In: Engineering Geology for Infrastructure Planning in Europe, Springer Verlag Publishers, pp. 650–656.

Marciano, J.S., Saturay, R.M., and Talampas, M.C. (2008). Disaster risk management using sensors, networks and computing. In: the Proceedings of the International Conference-Workshop on the 17 February 2006 Guinsaugon landslide, Philippines, p. 26.

Mark, R.K. (1992). "Map of debris-flow probability, San Mateo County, California." U.S. Geological Survey Geologic Investigations Series Map I-1257-M, scale 1:62,500.

Mines and Geosciences Bureau. (2004). Accomplishment report for 2004. Mines and Geosciences Bureau, Philippines.

Morton, D.M., Alvarez, R.M., and Campbell, R.H. (2003). "Preliminary soil-slip susceptibility maps, Southwestern California." U.S. Geological Survey Open-File Report 03-17.

National Disaster Coordinating Council (NDCC). (2008). Hazards mapping for effective community-based disaster risk mitigation (READY) Project. In: the Proceedings of the International Conference-Workshop on the 17 February 2006 Guinsaugon landslide, Philippines, p. 27.

Nemčok, A., Pašek, J., and Rybář, J. (1974). Deleni svahovych pohybu. In: Sbornik geologickych ved, pp. 77–93, (In Czech)

Paudits, P. (2005). Landslide Susceptibility evaluation using statistical methods. PhD thesis, Comenius University, Bratislava, 149p.

Pike, R.J., Graymer, R.W., Roberts, S., Kalman, N.B., and Sobieszczyk, S. (2001). "Map and map database of susceptibility to slope failure by sliding and earthflow in the Oakland area, California." U.S. Geological Survey Miscellaneous Field Studies Map MF-2385, scale 1:50 000, http://geopubs.wr.usgs.gov/map-mf/mf2385/

Pomeroy, J.S. and Davies, W.E. (1975). "Map of susceptibility to landsliding, Allegheny County, Pennsylvania." U.S. Geological Survey Miscellaneous Field Studies Map MF-685B, scale 1:50 000.

Radbruch-Hall, D.H., Colton, R.B., Davies, W.E., Lucchitto, I., Skipp, B.A., and Varnes, D.J. (1983). "Landslide overview map of the Conterminous United States." U.S. Geological Survey Professional Paper 1183, scale 1:7 500 000. (Reproduced by Godt, J.A. (1997). USGS Open-File Report 97–289), http://landslides.usgs.gov/html_files/landslides/nationalmap/national.html

Rodolfo, K.S. and Arguden, A.T. (1991). Rain-lahar generation and sediment-delivery systems at Mayon Volcano, Philippines. In: Fisher, R.V., Smith, G.A. (Eds.) Sedimentation in volcanic settings. Society of Economic Paleontologists and Mineralogists, Special Publication 45, 71–88

Schuster, R.L. (1996). Socioeconomic significance of landslides. In: Turner, A.K., Schuster, R.L. (Eds.) Landslides: Investigation and Mitigation, Special Report 247, National Research Council. National Academy Press, Washington, DC, pp. 12–35.

Schuster, R.L. (Ed.) (1998). "Landslides: Investigation and Mitigation." Transportation Research Board, National Research Council, Special Report 247, National Academy Press, Washington, DC, pp. 12–35.

Schuster, R.L. and Highland, L.M. (2001). "Socioeconomic and environmental impacts of landslides in the Western Hemisphere." U.S. Geological Survey Open-File Report 01–0276, http://pubs.usgs.gov/of/2001/ofr-01-0276/

Schuster, R.L. and Leighton, R.W. (1988). Socioeconomic significance of landslides and mudflows. In: Kozlovskii, E.A. (Ed.) Landslides and Mudflows. UNESCO/UNDP, Moscow, pp. 131–141.

Schwab, J.C., Gori, P.L., and Jeer, S. (2005). "Landslide Hazards and Planning." American Planning Association Planning Advisory Service Report Number 533/534, 209p.

Slosson, J.E. and Krohn, J.P. (1982). Southern California Landslides of 1978 and 1980. Storms, Floods, and Debris Flow in Southern California and Arizona, 1978 and 1980. National Research Council, and Environmental Quality Laboratory, California Institute of Technology, 17–18 September 1980. National Academy Press, pp. 291–319.

Spiker, E.C. and Gori, P.L. (2003). "National landslide hazards mitigation strategy—A framework for loss reduction." U.S. Geological Survey Circular 1244, 56p.

Tuñgol, N.M. and Regalado, M.T.M. (1996). Rainfall, acoustic flow monitor records, and observed lahars of the Sacobia River in 1992. In: Newhall CG, Punongbayan RS, (Eds.) Fire and mud: eruptions and lahars of Mount Pinatubo. Philippine Institute of Volcanology and Seismology, Quezon City and University of Washington Press, Seattle, 1126 pp.

Vlcko, J: Landslide susceptibility map of Lubietova. Proc. Geologia a zivotne prostredie., p. 107–110, 2002 (In Slovak).

Vitanage, P.W. (1994). "Seismicity: Neglected Aspects of Sri Lankan Landslide Studies". Proceedings, National symposium of Landslide in Sri Lanka, 17-18, Colombo, Vol. 1.

Voigt, S., Kemper, T., Riedlinger, T., Kiefl, R., Scholte, K., and Mehl, H. (2007). "Satellite Image Analysis for

Disaster and Crisis-Management Support". Geoscience and Remote Sensing, IEEE Transactions on Vol. 45, Issue: 6, Part 1: 1520-1528.

Wadiya, D.N. (1943). "The three superposed peneplains in Ceylon". Records of the Geological Survey Department, Paper I: 25-38, Ceylon.

Zarco, M.A.H., Catane, S.G., and Gonzalez, R.M. (2007). State of the practice in slope mitigation measures: focus on the Philippines. 2nd Regional Training Course on Asian program for regional Capacity Enhancement for Landslide Impact Mitigation (RECLAIM Phase II), Phuket, Thailand.

26 Education, Capacity Building and Public Awareness for Disaster Reduction

Rajib Shaw, Yukiko Takeuchi and Badaoui Rouhban

Abstract Education is the key element for reducing disasters caused by natural hazards including landslides and achieving human security in the pursuit of sustainable development. The Hyogo Framework for Action 2005–2015 and "Words Into Action: A Guide for Implementing the Hyogo Framework" prepared by UN/ISDR emphasize the role of formal and non-formal education and awareness raising as a core component of risk reduction initiatives.

Past experience, projects, and programs have revealed enormously positive effects of education for vulnerability reduction and disaster risk management. Children and adults who know how to react in case of a disaster, community leaders who have learned to warn their people in time, and whole social layers who have been taught how to prepare themselves for natural hazards have contributed to better mitigation strategies and dissemination of information on the dangers of hazards. Education and knowledge have provided people with tools for vulnerability reduction and life-improving self-help strategies. Furthermore, more stable and disaster resilient education facilities, such as school buildings, provide a shelter in case of hazards and must be strengthened and improved through better engineering and technical knowledge.

Education also plays a substantial role in improving risk assessment procedures in nearby communities, in encouraging people to engage in building up resiliency and to generally reduce risk elements in communities. For education on risk reduction to have its desired impact on communities, it needs to reach out to the remotest development worker in the field. Such education needs to be made accessible and affordable for frontline practitioners who operate at community level and are often far removed from conventional knowledge centers such as universities.

Thus, while there is no argument that education is important, and it works, the challenge is how to effectively incorporate education for disaster reduction in the national and local government policy and programs, and how to reduce the gap between knowledge and practice through experiencing learning. A pro-active co-learning approach of linking school and formal education to community is the essential for the success of disaster education.

Rajib Shaw (✉)
Kyoto University, Kyoto, Japan

Yukiko Takeuchi
Kyoto University, Kyoto, Japan

Badaoui Rouhban
UNESCO, France

K. Sassa, P. Canuti (eds.), *Landslides – Disaster Risk Reduction*,
© Springer-Verlag Berlin Heidelberg 2009

Keywords Disaster education • Participatory • Community based • Co-learning • Experiencing learning

"Education, including formal education, public awareness and training, should be recognized as a process by which human beings and societies can reach their fullest potential. Education is critical for promoting sustainable development and improving the capacity of the people to address environment and development issues.

While basic education provides the underpinning for any environment and development education, the latter needs to be incorporated as an essential part of learning. Both formal and non-formal education is indispensable to changing people's attitudes so that they have the capacity to assess and address their sustainable development concerns".

Chapter 36 of AGENDA 21, on 'Education, Awareness and Training' (1992)

26.1 Introduction

The vision of education emphasizes a holistic, interdisciplinary approach to developing the knowledge and skills needed for a sustainable future, as well as the necessary changes in values, behaviors and lifestyles. However, education for sustainable development in not restricted to the transmission of knowledge and skills. It should be about learning how to obtain and synthesize the knowledge that equips us, individually and collectively, to forge a sustainable coexistence with our social and ecological environments (Shaw, 2008a). Disaster risk reduction education can be documented since the 1970s as scientists, engineers, technical experts, economic development workers and humanitarian aid responders began to produce guidance in the form of brochures, handbooks, and lesson plans for community outreach, public campaigns, and classrooms, on a relatively small scale (Petal, 2008).

During the International Decade of Natural Disaster Reduction (IDNDR) in the 1990 s significant public education efforts emerged in many nations, and "hazards education" took root in science classes in schools. The quality and quantity of publications expanded as desktop publishing made production more efficient. Since the turn of the millennium, especially as a result of communication and information-sharing opportunities facilitated by the Internet, disaster risk reduction champions have produced a plethora of educational materials for school children and the general public alike.

A major breakthrough in disaster education was observed in 2005 onward when the important of education was vividly recognized in the Hyogo Framework for Action (HFA: 2005–2015). One of the major pillars of HFA was education, training and capacity building. HFA identified selected issues of education, training and public awareness programs as follow:

– Providing easily understandable information on disaster risks and protection options, especially to citizens in high-risk areas, to encourage and enable people to take action to reduce risks and build resilience. The information should incorporate relevant traditional and indigenous knowledge and culture heritage and be tailored to different target audiences, taking into account cultural and social factors.
– Strengthening networks among disaster experts, managers and planners across sectors and between regions, and creating or strengthening procedures for using available expertise when agencies and other important actors develop local risk reduction plans.
– Promoting and improve dialogue and cooperation among scientific communities and practitioners working on disaster risk reduction, and encourage partnerships among stakeholders, including those working on the socioeconomic dimensions of disaster risk reduction.
– Promoting the use, application and affordability of recent information, communication and space-based technologies and related services, as well as earth observations, to support disaster risk reduction, particularly for training and for the sharing and dissemination of information among different categories of users.
– Promoting the inclusion of disaster risk reduction knowledge in relevant sections of school

curricula at all levels and the use of other formal and informal channels to reach youth and children with information;
- Develop training and learning programs in disaster risk reduction targeted at specific sectors (development planners, emergency managers, local government officials, etc.).
- Promoting community-based training initiatives, considering the role of volunteers, as appropriate, to enhance local capacities to mitigate and cope with disasters.
- Promote the engagement of the media in order to stimulate a culture of disaster resilience and strong community involvement in sustained public education campaigns and public consultations at all levels of society.

It can be said that school education is one of "disaster prevention in daily life". Everyone has chance equally to get school education. It leads to be a long-term countermeasure for disaster prevention for children to acquire knowledge and skill about it. Recently, some schools in Japan make disaster education using integrated learning period or collaborating with community. There are varieties of educational materials, such as "disaster education challenge plan (CP, 2005)" which shows good practice examples on the homepage. Some teachers say that they don't have confidence to teach disaster prevention even there are some educational materials. But it is not necessary for teachers or school itself to have all things about disaster prevention. There are some examples like Maiko High School, Otsu High School etc. that network with experts of disaster prevention such as municipality and university, and community support the education. It will be all right just to involve pupils, teachers or school system itself to network with those who teach what one doesn't know and organization or group to work with on disaster prevention. Town watching and disaster game which gather attention in these days are applicable to this.

In this chapter, different means of disaster education are discussed focusing on formal and nonformal education system. School and university education processes are described with reference to the formal education. School-community interaction is analyzed as a unique model of disaster education. For awareness raising and capacity building, community based disaster education and indigenous knowledge system are focused. Finally, a few suggested directions are provided for effective use of knowledge system in developing disaster education, capacity building and awareness raising programs.

26.2 UN Decade of Education for Sustainable Development

The United Nations General Assembly proclaimed the ten-year period from 2005 to 2014 as the United Nations Decade of Education for Sustainable Development (DESD). Governments around the world are invited to use the Decade to integrate education for sustainable development into their national educational strategies and action plans at all appropriate levels.

UNESCO is designated as the Lead Agency in the promotion of the Decade, and is required to consult with the United Nations and other relevant international organizations, governments, nongovernmental organizations and other stakeholders to develop a draft international implementation scheme for the Decade, bearing in mind the relationships between education for sustainable development and current international educational priorities.

The Rio Declaration from the World Conference on Environmental and Development 1992 began by stating: "*Human beings are at the centre of concerns for sustainable development. They are entitled to a healthy and productive life in harmony with nature*".

The Johannesburg Declaration at the World Summit on Sustainable Development in 2002 built on this aspiration and expressed the commitment of world leaders "*to build a humane, equitable and caring global society cognizant of the need for human dignity for all.*" Sustainable development is a dynamic and evolving concept with many dimensions and interpretations and reflects locally relevant and culturally appropriate visions for a world in which development "*meets the needs of the present without comprising the ability of future generations to meet their own needs*". The Millennium Development Goals provide targets for international actions to bring such visions into reality by: overcoming poverty; improving child, maternal and sexual health; expanding educational provision and redressing gender inequalities in education; and developing national strategies for sustainable development.

Then Secretary General of the United Nations, Mr Kofi Annan, argued that: "*Our biggest challenge in this new century is to take an idea that sounds abstract – sustainable development – and turn it into reality for all the world's people*".

Making the abstract real, and developing the capacities of individuals and societies to work for a sustainable future is, essentially, an educational enterprise. Indeed, the four principles for achieving sustainable human development enunciated at the World Summit for Sustainable Development in 2002 reflect the four pillars of education described in the Delors Report as in Table 1 (Delors, 2002):

Thus, education is the primary agent of transformation towards sustainable development, increasing people's capacities to transform their visions for society into reality. Education not only provides scientific and technical skills, it also provides the motivation, justification, and social support for pursuing and applying them. The international community now strongly believes that we need to foster - through education - the values, behavior and lifestyles required for a sustainable future. Education for sustainable development has come to be seen as a process of learning how to make decisions that consider the long-term future of the economy, ecology and equity of all communities. Building the capacity for such futures-oriented thinking is a key task of education.

Education for Sustainable Development has four major domains, reflecting diverse goals and audiences: promotion and improvement of: (1) *basic education*, 2) *reorienting existing education* at all levels to address sustainable development, (3) d*eveloping public understanding and awareness of sustainability*, and (4) *training*. Thus, the focus of DESD activities will be advocacy, communication and networking directed at facilitating all educators to include sustainable development concerns and goals in their own programs. These issues constitute the priorities for planning programs and activities that will support the objectives of DESD, and include: (1) Overcoming poverty, (2) Gender equality, (3) Health promotion, (4) Environmental conservation and protection, (5) rural transformation, (6) human rights, (7) intercultural understanding and peace, (8) sustainable production and consumption, (9) cultural diversity, and (10) information an communication technologies (ICTs). These many areas of overlap and common interest, both in approaches to education and in areas of substantive objectives, suggest that joint initiatives across DESD can add value to the common effort of each individually.

Table 26.1 Four pillars of education described in Delros Report

Achieving sustainable development requires:	Education provides the skills for:
Recognition of the challenge	*Learning to know*
Collective responsibility and constructive partnership	*Learning to live together*
Acting with determination	*Learning to do*
The indivisibility of human dignity	*Learning to be*

To achieve these goals and target these diverse issues, it is essential to promote the DESD through partnership. Partners in the DESD include all those organizations, networks, bodies and alliances that share the conviction that sustainable development depends to a large extent on broad-based awareness through educational and learning processes. It is required to mention one point that disaster risk education is not explicitly mentioned in the DESD scope and focus areas, however, there are several overlap areas of environment and sustainable development, which needs focus on risk reduction, and therefore needs disaster education.

26.3 Disaster Risk Education: Evolution and Challenges

Up until now, most of the educational efforts directed towards the public and children have neither been systematically conceived nor tested, nor has their impact been scientifically evaluated (Petal, 2008). Disaster risk reduction education is not yet an integral part of disaster risk management policy, planning and implementation. Often scientific and technical experts have taken the tasks of developing educational materials upon themselves with very little evidence of cross-disciplinary inputs from public health, communications, marketing and education professionals with experience in allied efforts. It is time now to begin to give substance to the terms “public awareness” and “disaster risk reduction education”, to lay out some of the “do’s and don’ts” that we have already identified, to identify the range of methods that are open to us, and to discuss how we might identify promising practices, evaluate our impacts, and scale-up to the level needed to achieve a tipping point in establishing a culture of safety. A new cadre of researchers and research-support will be needed to advance this goal.

Disaster risk education has different components and challenges. There are two specific types of risk education: one is to show the occurrence of hazards, which is more as the physical phenomena. Most parts of these are taught in schools as a part of geography curriculum. The other is to know the social environment, and to understand the impacts of disasters, which is more like a process based education.

Two major issues related to earthquake disaster pose the real challenge to the earthquake professionals. The first one is the nature of the event, which, unlike flood or typhoon, cannot be predicted in advance. The other issue is its occurrence, which, again unlike other events, occurs once in 10 or 50 or even 100 years. Thus, the priorities of preparing for the earthquake disaster in advance is relatively low in many countries. For the developing countries, while the post-disaster reconstruction exercise provides an opportunity for development, pre-disaster preparedness and mitigation measures are the only solution for earthquake risk reduction. However, the painful question is: how to motivate an individual and/or community to take pre-disaster risk reduction actions?

This question is not only critical for the developing countries, but also found to be relevant for the developed country like Japan, which has a high risk of earthquake, experiences of major earthquake disasters, and significant technical expertise and resources. Still the question arises: “Is Japan prepared for the next big one?” The same question will possibly be valid for other developed countries and obviously for the developing countries as well.

At the core of disaster risk reduction education is the axiom that disasters are not inevitable (Petal, 2008). We already know of and are continuously discovering a broad range of preventative actions that can be taken at every level to avert terrible losses of life, livelihood and community.

The mission of disaster risk reduction, both for children and for adults in all walks of life, is to convey an understanding of the natural and environmental conditions and the human actions and inactions that lead to disaster, to stimulate changes in individual and group behavior, and to motivate advocacy and raise expectations of social policy to reduce these threats. Since disaster risk reduction cannot be accomplished by any one sector or strata of society, it calls for the widest possible participation. The scope of disaster risk reduction education therefore includes every single stakeholder who may be affected by disaster in his or her lifetime, or their children or grandchildren’s lifetime, and everyone’s whose opinions and decisions affect others.

Each individual, family, organization, community, agency, department, jurisdiction, and policy-making body must come to recognize and embrace it’s own role in a large cooperative effort. Information must be sought and shared and each must feel that there are effective measures that they are able and responsible to undertake.

26.4 Components of Education and Public Awareness

Shiwaku K. (Earthquake Disaster Mitigation Research Institute, Japan), Shaw R. (Kyoto University, Japan)

Shaw et al. (2004) argued that knowledge, awareness and code of conduct are perceived in the sequence of: knowing, realizing, deepening, decision, and action, as the gradual change in behavior from knowing to code of conduct. Knowledge comes from two sources: experience and education. Experience here denotes not only experiences of damaging earthquakes, but general experience of earthquakes. Education has four parts: school, family, community and self education. School education is divided into two parts: education from teachers, and pro-active education with participation of teachers and students. Family education originates from parents, and other family members. Community education is related to education in the neighborhood, community organizations, NGO activities, research workers, and voluntary activities, etc. Self education is acquired from books, Internet, newspaper, TV and other sources through the student's own initiative. All these lead to "knowing" about earthquakes and its impacts (Shiwaku, 2008).

Thus, the components can be categorized as: Formal and Non-formal education. Formal education has a wider range, from the school to higher education in the university. Non-formal education, on other hand is extremely broad, having its components to community education, training, and capacity building. Following sections will show that even if there exists the broad category of formal and non-formal education, there are often overlap, especially the formal education needs to break its traditional boundary, and needs to be merged with the community education.

26.5 School Education

Fujita K., Takeuchi Y and Shaw R. (Kyoto University, Japan)

Speaking of disaster education in school, most people imagine the evacuation drill. It is almost uniform training, where students huddle under the table by alarm bell and evacuate to the school ground with teacher's instruction. In most schools, it is done on 1st Sept., "the Disaster Prevention Day". It is a memorial day based on the Great Kanto Earthquake happened in 1923. There are two problems of the Disaster Prevention Day; one is that students think of disaster only for one day in a year; and the Great Kanto Earthquake is rather difficult to imagine in local context (Yoshida, 2007).

While disaster education draws attention gradually and adopted in some schools, the number is not so large on a national basis. There is thought to remain some problems as follows.

(1) Lack of teachers' training

Awareness-raising of teachers will be the starting point of disaster education (Fukuwa, 2005). At first, teachers themselves should study and make a menu of disaster education. In Japan, there are about 24,000 elementary schools, 11,000 junior high schools, 5,500 high schools. Teachers are about 410,000, 280,000, 330,000 in the elementary schools, junior high schools and high schools respectively. They are professional of talking and education, and the best human resource for improvement of disaster-resistance both in quantity and quality. Understanding and realizing the urgency of earthquakes and crisis lead to their awareness raising and willingness increasing and be a starting point of serious study and education.

To conduct proper disaster education, it is necessary for teachers to have enough knowledge about disaster education (Takahashi et al., 2004). It is thought to be important to set up a forum regularly for teachers to study knowledge about earthquake and the way of effective disaster education. While disaster education is conducted through many opportunities, there is a problem of lack of human resource who stands on the side of teaching.

(2) Time pressure in school curriculum

While school education is under time pressure and by the introduction of five-day week system, class hours are cut, its role is more and more expected and it becomes impossible to spare much time especially for disaster prevention, in fact.

(3) Lack of involvements of parents and family

School education is related to motivate students and their parents or family to take countermeasures for disasters (Takahashi et al., 2004). To involve parents or family to school disaster education will lead to disaster resilient town development.

(4) Lack of linkage of scientific studies with social issues

According to the official curriculum guideline, 3rd and 4th grade elementary school students learn about disaster prevention of earthquake and volcano in social science. 6th grade students learn about natural phenomenon in unit of "earth and space" in science. Here, they can choose either "land change by eruption" or "land change by earthquake". There needs linkage between science and social science.

(5) In-school education

Though the importance of cooperation between school and community to conduct disaster education is recognized, there are not so many practical examples. One reason is considered that school, parents, community people respectively worry about the security and hesitate to collaborate.

(6) Events-oriented education

Typified by evacuation drill, events-oriented disaster education is common. Students may temporarily get knowledge or raise awareness for disaster prevention, but it gradually fades as time goes by. On the other hand, in process-oriented education, they study toward a goal which is given or they themselves set. Such kind of education becomes popular with introduction of integrated learning period.

Although the above factors are described in context to Japanese school education, author's experiences in the developing countries, especially in Nepal, Pakistan, India, Indonesia and Vietnam tells the same story. Thus, to have an effective school education, it is required to address the above mentioned problems.

But disaster education in school began to change in Japan, especially since the Great Hanshin-Awaji Earthquake (GHE) in 1995. This earthquake caused devastating damage, but brought us many lessons. Existing disaster education is positioned as one of safety education by Ministry of Education, Culture, Sports, Science and Technology (MEXT). There are conducted to acquire necessary skills to protect one's own life from disasters and to raise awareness for disaster prevention. In the area which experienced the GHE including Kobe, disaster education is practiced adding letting them consider one's lifestyle as human, which was not included in the area of existing disaster education defined by MEXT. That is, it aims to make use of many examples which can be education materials, such as mutual cooperation, spirit of volunteer, importance of life, reverence for nature, and so on, which was not assumed before the earthquake, and to nurture zest for living (Fujiwara and Ohnishi, 2002).

Introduction of integrated learning period, "Sogo Gakushu" in Japanese, was also an opportunity to find new way of disaster education. In 2002, integrated learning period starts from 3rd grade in elementary school to high school. According to the official curriculum guidelines for elementary school (MEXT, 2003), its aim is to nurture the abilities to find problems, learn and consider by pupils themselves, be proactive in judging and solving problems in a better way. Also, to acquire the way of learning and thinking like collecting information, research, summary, report, presentation and discussion, to nurture the attitude to address problem solving and searching activities creatively and actively, to deepen awareness of one's own lifestyle. As the examples, international understanding, information, environment, welfare and health are given. Disaster education is not listed, but it is considered to be suitable for the integrated learning period, as it cuts across information, environment and welfare (Umeda et al., 1999).

There is a good practice of disaster education using the integrated learning period. Otsu Elementary School in Kochi Prefecture conducted "Project of developing disaster resilient town in 2004 (Disaster Education Challenge Plan, 2006)". This is on scheme of "project learning (Suzuki, 2003)", using integrated learning period for 50 classes for 6th grade pupils. The contents are; to make evacuation route maps of the local area through DIG (Disaster Imagination Game), to implement "The 3rd Otsu Kids Disaster Prevention Drill" which pupils themselves plan and operate (for example, evacuation drill from affected room, proposal of disaster prevention idea products, and so on), to make and perform "puppet show of disaster prevention" for small children, activities for raising money and writing encouraging letters for victims by the Nigata-Chuetsu Earthquake, proposal of "disaster prevention cooking" and spreading to pupils and parents, to report their practices, propose and urge disaster prevention in the lecture for disaster prevention hosted by Kochi Prefecture, in which about 500 citizens participated.

26.6 Community Based School Education

Shaw R. (Kyoto University, Japan)

Shaw (2008b) has emphasized the need of community based school education. Among recent years, 2004 was the worst typhoon year, where more than 13 events hit the mainland Japan. Among these, Typhoon no 21 and 23 moved across Shikoku area. Because of this, in Saijo City of Ehime Prefecture, it recorded heavy rain, 75.5 ~ 150 mm rainfall per hour. Avalanche of rocks, earth and driftwood surged which seemed to be occurred by slope destruction of intermediate and mountainous area and forming destruction of natural dam. A lot of driftwood got stuck with bridge pier and water was held back and overflowed. As the water level rose suddenly, surrounding houses were flooded. In the flat part, each area was flooded above or below floor level. In the mountainous area, landslide disaster occurred frequently, roads were severed, many villages were isolated and house destruction and human suffering were caused. The casualty in Ehime prefecture by typhoon no.21 amounted to 14 people and this is the worst record in human suffering caused by typhoon.

Three emerging problems due to the typhoon were as follows.

(1) Ill-maintained forest and thinned wood in the mountains

Frequent small slope failure by the concentrated heavy rain of typhoon no.21 added to the damage. While "deep-seated landslide" which each ground slides is not related to the form of forest, "shallow landslide" which surface soil slides directly results from the extent of maintenance. In addition, in artificial forests which are not thinned for a long time, sunlight doesn't reach ground and bottom weed and young trees are difficult to grow. When it rains there, surface soil is hit directly by raindrops and clogged, and rain water which cannot soak through the ground runs on the surface. The "water road" caused by the erosion forms valley and finally draws mudslides involving surface soil and fallen trees. Abandoned thinned wood were also the problem. They flew into the river by the heavy rain, got stuck with bridge pier and water was overflowed downstream (Figs. 26.1 and 26.2).

(2) Concentration of elderly people in mountainous area

According to the rate of aging in each area of Saijo City, the first to forth areas are mountainous areas and it means there are many elderly people there. In the typhoons of 2004, especially mountainous area was seriously affected. Some areas were isolated because the roads were blocked. In such areas, young people's help is needed for elderly people to evacuate.

(3) Low awareness for disaster prevention

Referring to disaster history of Saijo City, there had been no such large typhoons in these days.

Fig. 26.1 Widespread landslide in Saijo covering the tunnel and national expressway

Fig. 26.2 Poorly maintained forest uprooted by strong wind (*top left*), transported land masses (*top right*), timber and other waste blocking the river flow (*bottom left*) and uprooted trees causing significant damages to buildings (*bottom right*)

These typhoons caused first dead since 1976 in old Saijo City. Fading memory of disasters leads declining awareness for disaster prevention. Also, judging with one's own experience is dangerous. According to the questionnaire survey in Ofuki area (OYO, 2005), many people didn't evacuate for the reason that they just thought it was not dangerous or judged from their long experience and thought it was not so dangerous to evacuate.

At the time of the typhoon no.21&23 in 2004, mountainous area of Saijo City was especially damaged. Land condition and concentrated heavy rain are major factors, but there are other reasons concerning so-called software. In the mountainous area, there live many elderly people and few young people. So some elderly people had difficulty to evacuate and needed help of young people. Low awareness for disaster prevention is also the problem. According to the research of OYO cooperation, not a few people didn't evacuate at the typhoon. The same problem is considered in the plain area.

Plain area is rather urban and there are many young people. So, it is necessary to make "disaster prevention network" between the plain area and the mountainous area, so as to help elderly people in the mountainous area in case of a disaster. As the driftwood stuck with bridge pier caused flood to the plain area, disaster in the mountainous area have relations with that in the plain area. Both residents have to know each other about the circumstances.

For these reasons, mountain watching is proposed to be implemented in Saijo City. Mountain watching is just like town watching and it is conducted in the mountainous area. Main target is children, and also residents in the mountain, teachers, municipal officials and forest workers are involved. The working field was upper area of a river along school. Participants watched the damaged site by the typhoon in 2004 and heard the story from victims.

At the same time, town watching was proposed to be implemented in plain area. The main target was students and teachers, parents, Jichikai and municipal officers are involved. They walk around the school zone and search for dangerous places, useful facilities in case of disasters and favorite places which they did not notice in daily life (Fig. 26.3).

Town watching was implemented in five elementary schools and mountain watching in three junior high schools as "disaster education program", which was an activity of 12-year-old education project.

Students were asked to describe what they knew about the typhoon in 2004. The answers were categorized to 4 groups; (a) impact on typhoon itself

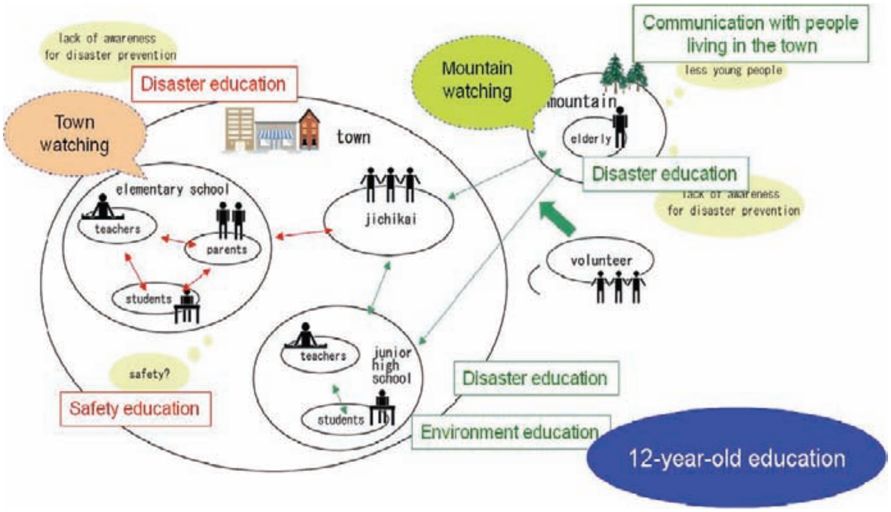

Fig. 26.3 Schematic diagram of collective community based education (town watching and mountain watching)

(e.g., it rained heavily, it caused great damage, etc.), (b) impact on land and infrastructure (e.g., the river was overflowed, there were lots of mudslide in mountains, etc.), (c) impact on houses and properties (e.g., the houses were flooded over the floor level, rice fields were flooded, etc.), (d) impact on human (e.g., people evacuated to the school gym, there were a few dead, etc.).

The results showed that the schools having more interaction with the local community, the impacts of the town and mountain watching was high. The importance of disaster education becomes well-recognized and the number of schools which adopt it increases. But there are some problems in current disaster education, for example, lack of teachers' training, time pressure in school curriculum, lack of involvements of parents and family, lack of linkage of scientific studies with social issues, in-school education and events-oriented education. Fujita et al. (2008) has pointed out similar approaches in Reihoku areas of Kochi prefecture.

26.7 Community Based Disaster Education

Takeuchi Y. (Kyoto University, Japan)
Prakash S. (National Institute of Disaster Management, India)

As more research on development has been conducted in various fields in recent years, the approach to disaster mitigation is becoming more and more community-based (Blaikie et al. (1994), Twigg and Bhatt (1998), Quarantelli (1989), Mileti (2001), Shaw and Okazaki (2003), and much more effort has been put into incorporating disaster management aspects into the holistic development of communities. Maskrey (1989) has rightly pointed out that, disaster management should not be treated as one single issue but should be incorporated into the socioeconomic activities of local people. The rationale for community involvement or community-based activities is now well rehearsed (Twigg, 1999). Because community-based activities (and community-based organizations) are deeply rooted in the society and culture of an area, they enable people to express their real needs and priorities, allowing problems to be defined correctly and responsive measures to be designed and implemented. Twigg (1999) also argued that the existence of community-based organizations allows people to respond to emergencies rapidly, efficiently and fairly, and therefore the resources will be used economically. Maskrey (1989) pointed out that "top-down" programs in which communities are not involved tend not to reach those worst affected by disaster, and may even make them more vulnerable. This is found to be similar in both developing and developed countries, as argued by Shaw and Goda (2004).

Community involvement is often faced the problem of sustainability (Shaw, 2004). Government, non-government and international organizations implement various programs before and after the disasters. Most of them are very successful during the project period, and gradually diminish as the years passed. There are many reasons for gradual decrease of people's involvement in a project. The most common elements are partnership, participation, empowerment and ownership of the local communities. Unless the disaster management efforts are sustainable at individual and community level, it is difficult to reduce the losses and tragedy. While people should own the problems, consequences and challenges of any mitigation and/or preparedness initiative, it is necessary to see people's involvement in a broader perspective, which is related to policy and strategy.

The first and most important issue of community based education is sharing of risk information to the local community (Takeuchi, 2008). Figure 26.4 shows the community hazard map, which shows potential of landslide risk in the community. This hazard map can be use together with the vulnerability map to develop community risk mapping. The key point here is share risk information, which is the first step of rick communication.

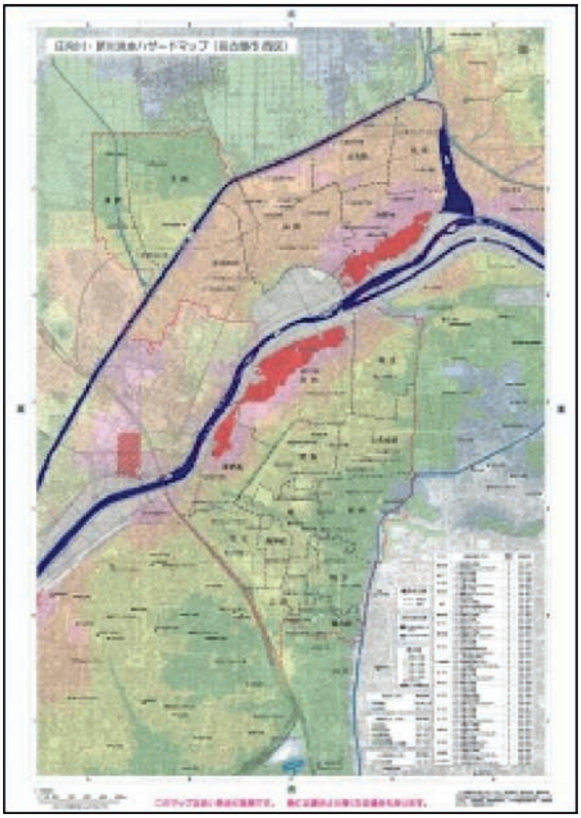

Fig. 26.4 Community Hazard Map for Risk Information Sharing

Figure 26.5 shows the display of risk information in the community. This is the second step of risk communication, where the risk elements are shown in the field. The display of the pillar identifies the risk areas, and thus, aware the local community to undertake appropriate pre-cautionary measures.

Disaster information or memories are often forgotten. It is important to display disaster memory and experiences in the field, which in turn raises awareness of the people and communities towards risk reduction, and urge to undertake pro-active stance to risk. Figure 26.6 shows the flood pole in Tokooka, which is often used by the local students and community members to discuss about the historical flooding of 2004.

A few issues which emerged from successful community based implementation are: leadership and local knowledge, teamwork and common voice, right information and appropriate ways of communication, institutionalization and participation, people's attitude and incentive, economic cycle and local contribution, local government and policy integration, and theory and application. Figure 26.5 shows the conceptual framework of community sustainability and up-scaling, incorporating the issues of flood impacts and interventions. In one hand, policy and institution are key factors for its sustainability at government level, while the incorporation of change agents and appropriate information make it

Fig. 26.5 Landslide-prone area (*left*), which is identified by the pillar on the *right* diagram

Fig. 26.6 Flood-pole in Toyooka-city to demonstrate the flood height in 2004 Typhoon 24

sustainable at grass-root level. A synergy of these two elements is required for long-term impact of community-based initiatives. In case of both Bangladesh and Vietnam, this synergy is ensured by working with local government. The institutional issues in both cases emphasize the need to strengthen the local institutions rather than creating new institutions. Capacity building of change agents is observed in both cases. Crucial information dissemination to different stakeholders was also found to be important.

Prakash (2008) has also pointed out the need of the community based disaster risk management and education in different parts of India.

26.8 Examples of Geo-Hazard Education in University

Karnawati D. (Gadjah Mada University, Indonesia)

Karnawati (2008) described the formal disaster education in higher education. Knowledge of geohazard mitigation has been introduced for undergraduate program in some universities in ASEAN countries, such as in Indonesia, Malaysia, the Philippine, and Thailand. However, such knowledge has not yet provided in a special subject. It is only provided as one topic of discussion which is integrated in any one of the subjects of Environmental Geology, Soil Mechanic, Geotechnics, Hydrology, Geohydrology, Volcanology and or Seismology. Discussion on Geohazard topic is focused on factors controlling the hazard occurrence, the mechanisms and processes leading to the hazard, how to predict, mitigate and control such hazard. Unfortunately, limited practical exercises and field works are provided for students due to the limited concerns on the importance of geohazard education. Similar to the undergraduate education, in the postgraduate program (master program) quite few universities in Indonesia and some other ASEAN countries provided special courses on Geohazard Management. Moreover, most of the existing geohazard education more emphasizes on the cognitive aspect of teaching for the enhancement of knowledge, but less effort to provide effective learning method which include sufficient field and laboratory works.

Despite some limitations in conducting geohazard education at the university level, students at the university are considered as the strategic target for human resource empowerment in geohazard prone area. Indeed, the students will be the future analysts and policy makers for geohazard management in their countries. Thus, they will be the seeds for agent of change to further trigger the development human resources on geohazard management in the countries. That is why mechanism and method of geohazard education in the universities need to be further enhanced through several stages as follows:

- Enhance the learning method on geohazard education.
- Provide more research opportunities on geohazard educations.
- Establish the education network on geohazard education.

- Establish the school on the move to support the enhancement of research and education on geohazard management.

Interactive learning method through student working groups by providing case studies needs to be done in order to enhance the existing learning method. More effective learning process can be stimulated by introducing real case problem supported by field work, working group discussion and seminars. This learning program should be a media for the students to learn to apply their knowledge as well their thinking skills critically and creatively to make sound decisions and to solve complex problems on geohazards. Even though, the case studies for the final year students to conduct their research works are also important. Supports from government agency also required as the internship program to provide facilities and opportunities for students to deal with the real problems in the field and communities. Since problems on geohazard management are complex, so interdisciplinary approach also need to be elaborated by inviting the related experts from other disciplines to be the external resources. Obviously, establishment of networks for geohazard educations at national and ASEAN levels are crucial to facilitate the effective learning and research program on geohazard education. Not only government agency, but also research institutes or research center, private companies, nongovernmental organization/agency, schools and universities are required to be actively participate collaborate in the network for geohazard education.

Establishment of collaborative research and education on geohazard management by integrating several disciplines such as Geology, Civil Engineering, Agriculture and Forest Science, as well as Social Science and Psychology are important to support the education program on geohazard management. This collaborative research and education could be facilitated through the networks. Since the year of 2003, ASEAN University Network/the South East ASEAN Engineering Education Network (AUN/SEED-Net) has also established the Field of Geological Engineering Networks consisting several universities from Member Institution Countries such as from Cambodia, Indonesia, Laos, Malaysia, Myanmar, Philippine, Singapore, Thailand and Vietnam as well as from Japan. In this network, education and research on geohazard has been carried out. Due to the leading experience to deal with geohazard problems, Gadjah Mada Universities in Indonesia has been assigned as the Host Institution for the network where students from other countries in the network are now conducting the learning and research on geohazard to obtain Master and Ph.D. Degree.

More active involvement of Geologist in disseminating their research outcomes, especially those related to geohazard management has been argued to be the key to raise public awareness. The disseminated materials should include information about mechanism of the geological process leading to geohazard, the symptoms of geohazards, and also practical knowledge on hazard preparedness and emergency responses.

26.9 Indigenous Knowledge and Public Awareness

Indigenous knowledge research aims to facilitate the targeting of development resources more effectively on the poor. The compatibility of local ideas with scientific ones is a central issue. It is absolutely necessary to facilitate communication between scientists and local people, on the assumption, fundamental to development interventions, that science may have something to offer them in tackling their problems. Furthermore, it is possible that if scientific and indigenous knowledge are comparable, and if scientists are able to access local knowledge, this might enhance new development of research practices (Takeuchi and Shaw, 2008). While, the perception of indigenous knowledge varies, following are some of selected popular definition of indigenous knowledge. Indigenous knowledge is defined as "... the unique, traditional, local knowledge existing within and developed around the specific conditions of women and men indigenous to a particular geographic area ..." (Grenier, 1998). One of the major issues of the IK is that, in many cases, it survived as part of process of the people and communities. Thus, IK is very much characterized by multi-disciplinary nature, and is based on food security, human and animal health, education, natural resource management, and various other community based activities. The other issue of IK is its dynamic evolution. IK is the result of a continuous process of experimentation, innovation, and adaptation. It has the capacity to blend with knowledge based on science and technology, and should therefore be considered complementary to scientific and technological efforts to solve problems in social and economic development.

In above-mentioned situation, in alluvial plain and delta area flood disaster happens every year. In the past, people have no control over the river, still, they guarded there life and assets by small scale technology, knowledge, wisdom, tradition and cooperation within community. For example, in the early 19th century (Edo period), flood fighting activities were mandated through the practice of "*goninggumi*", a unit of mutual assistance, cooperation and monitoring consisting of five families in a given community. There were several programs, including bamboo plating to prepare for and mitigate flooding (Settu city, 2007). Also, forest management in the flood plains is another such activity. During late 19th century (Meiji period), many flood control technologies implemented by engineers from Netherlands. People attained better safety of life and assets by these technological interventions like – concrete dikes, check dams, water gates and pump facilities and others.

In the present modern era, construction of large dike and dams by concrete is adopted as major technological solution. This policy aims at no-flooding from river. However, in earlier times, flooding from river was considered a natural phenomenon in which people never tried to block the flood rather developed some knowledge based tools to reduce the damage. Flood used to bring fresh coating of silt and mud helping soil regeneration and improved agricultural yield Looking at present threat posed by climate change, it is expected that mere technological options may not be sufficient to reduce disaster impacts. Moreover, some of these structures have failed in recent disasters and left people helpless. These experiences suggest that, in vulnerable area's, people should protect their life and asset by utilizing some historical indigenous knowledge and technology.

Although the application of traditional technology, knowledge and its application is gradually reduced in most parts of Japan, but there are several shortcoming to depend only on the modern disaster reduction technology. The traditional knowledge has been proven to be useful in the local cultural, socio-economic context, which may change from time to time, but the principles remain unchanged. Since most of these traditional knowledge and technologies are modified over a period of time, it has higher resilience and redundancy. Moreover, people and community's involvement is the key to the success of the indigenous knowledge. We have seen in recent days that too much dependency on the modern technology makes people dependent on the system. Thus, community's capacities get reduced and self-help concept often gets less importance. Many of the recent disasters have shown the failure of the system, and thereby making people helpless and causing larger damages. Thus, an ideal situation disaster reduction measure should incorporate balanced mixture of the modern technology and traditional knowledge.

26.10 Ways of Safety Culture

Tsunozaki E. (Asian Disaster Reduction Center)

The key factors of disaster risk management are risk perception, risk assessment and risk mitigation. Risk perception is very much linked to the education and awareness at different levels, starting from the community to the high-level decision makers. Risk assessment needs the intervention for both hazard and vulnerability. It is important to incorporate to risk perception and risk assessment in the development planning at different levels, including local, regional and national. Risk mitigation includes formulation of policy, strategy, and thereby enhancing decision-making. Thus, actions at local level should include capacity and institution building of local government, and confidence building of the community, while the actions at international level includes networking, training and dissemination of best practices. The key point of risk management is critical information. This information is generated by academic and research institutions, through scientific and technical innovations. However, there should be a direct link between the research and development and the policy making and decision making, since the end users of the research results will be the decision and policy makers. It is also important to turn the decision and policy into actions through the implementation process. Thus, the risk management can be seen as a dynamic process, where different stakeholders have its role and responsibilities. This is reflected in the disaster education program in other countries as well as for other types of hazards (Tsunozaki, 2008). It is argued that formal education plays an important role in developing the safety culture.

Risk communication is a two-way interactive tool for sharing risk information amongst government officials, researchers and local people. To reinforce the risk communication, government, researchers and local people must build upon each other knowledge. Government departments and researcher community usually possess much higher level of "risk information" compared to local communities. On the other hand, local communities are rich in terms of local knowledge. Available risk information needs to be complemented well with local wisdom to effectively reduce disaster risks of the communities. Even if there is a need to implement new technology for disaster reduction, local people must be involved to let understand the advantages as well as shortcomings of the technology (with specific details pertaining to new material used, investment required, time consumed and others). Government as well as academic disciplines needs to appreciate existing traditional practices and techniques to propose context based improvements most appropriate for a particular area.

The most affected people from disasters are the most vulnerable people in society. Elderly people, children, or handicapped people are regarded as vulnerable people, as example. They have many problems or troubles even in daily life and need support from family members or community people in order to live comfortably without any uneasiness or worry. In disaster situation, such problems or troubles emerge more obviously and they become more serious. Therefore, disaster education should contribute to building community which can help the most vulnerable people (Shiwaku, 2007). Here, this disaster education focuses on not only disaster situation but also daily life. Disaster education aims to that all people can live safely and comfortably. Such community can be resilience in disaster situation as results. Disasters make current problems on community more serious and visualize underlying risks or problems. Therefore, what is the most important is considering community in daily life.

School is a place where children, who are vulnerable people, spend much time next to their own houses. Students can acquire various kinds of knowledge during their infant stage to adolescence. It means that school contributes to character-building of people and that school should be emphasized for future generation. In addition to this, school has other roles. Community people come to schools for school events or their community activities. School is a cultural and spiritual center for community as well as education facility, and can be expected to build community linkage among community people including school children. Therefore, it is expected that the effects of disaster education can be transferred to community people as well as children if school become main place for implementation of disaster education.

Yamori (2006) states that it is necessary for disaster education in the future to focus on the process of restructuring "communities of practice" not on transfer of knowledge and skill between individuals. That is, it should be an important goal of education or learning to establish community in which educator and learner can "participate" together. For example in school, it will be all right just to involve pupils, teachers or school system itself to network with those who teach what one doesn't know and organization or group to work with on disaster prevention. Teachers or school itself don't need to have all things about disaster prevention.

The goal of education is to change people's behavior (Nathe, 2000). Awareness about risks and dangers needs to start in early education before abilities to address them can become part of growing civic and professional responsibilities as people mature (UN/ISDR, 2004). The responsibility of decision making from central government to local government varies at different levels. It can be said that only government cannot take all actions for prevention and mitigation. In the time of disaster, the most vulnerable people have the most serious effects. Now the importance of community based disaster management is recognized widely. The role of education should not be confined within the school itself, but should be promoted to family and community. The education should focus on students different items including importance of community and family, emphasizing to build a good relationship with community through its classes. The high awareness and actions in the students shows the success of the proactive co-learning process (Shiwaku and Shaw, 2008). It is thought that a pro-active co-learning education process which incorporates both school and community education can be the model type of disaster education in other schools.

Acknowledgments This paper is the collective work of several years in the field of disaster risk education. We are grateful to different academic, local governments and non-government organizations. The work is also benefitted with the collaboration from Saijo city government, and the research grant of JSPS/MEXT (Water Community) is highly acknowledged. The authors are also thankful to the contributors of the Session 7 of the World Landslide Forum, which form part of this chapter.

References

Blaikie, P., Cannon, T., Davis, I. and Wisner, B. (1994): *At Risk: Natural Hazards, People's Vulnerability, and Disaster*, Routledge, London

CP (2005): Challenge Plan, available at http://www.bosai-study.net/top.html, accessed on October 2007

Delors, J. (2002): UNESCO Task Force on Education for the 21st Century. Accessed from http://www.unesco.org/delors/, Accessed on 31st of January 2008

Disaster Education Challenge Plan (2006): Disaster Education Challenge Plan, available at: http://www.bosai-study.net/houkoku/plan08/index.html, accessed on October 2007

Fukuwa, N. (2005): "Disaster reduction starts from disaster education", Urban problem research, no.57-1, 2005

Fujita, K., Takeuchi, Y. and Shaw, R. (2008): Effective forest management to reduce landslide risk in Reihoku Area in Shikoku: A social perspective, Submitted to the **World Landslide Forum**

Fujiwara, S. and Ohnishi K. (2002): A study on disaster mitigation program for pupils in Hyogo-Prefecture and Kobe-City, Architectural Institute of Japan Research Report

IEDM (2007): Dealing with uncertainty: considering climate change risk in disaster management planning. IEDM preliminary report, 9 pages, Kyoto, Japan

Karnawati, R. (2008): Strategies for promoting education for natural disaster reduction in Indonesia and ASEAN regions. Submitted to the **World Landslide Forum**

Maskrey, A. (1989): *Disaster Mitigation: A Community-based Approach*. Oxfam, Oxford

MEXT (2003): Ministry of Education, Culture, Sports, Science and Technology Educational Guidelines, 2003

Mileti, D.S. (2001): *Disasters by Design*. Washington D.C: Joseph Henry Press.

Nathe, S.K. (2000): Public Education for Earthquake Hazards, Natural Hazards Review, November 2000, pp. 191–196

OYO (2005): Questionnaires and DIG conducted by OYO Corporation, Saijo City.

Petal, M. (2008): Disaster Risk Reduction Education, in Disaster Management. In: Shaw, R. and Krishnamurthy, R. (Eds.) *Global Challenges and Local Solutions*, University Press, Forthcoming

Prakash, S. (2008): A methodology for community based disaster risk management, Submitted to the **World Landslide Forum**

Quarantelli, E.L. (1989): Conceptualizing Disasters from a Sociological Perspective. *International Journal of Mass Emergencies and Disasters*, 7: 243–251

Settu City (2007): Settu city home page. http://www.city.settsu.osaka.jp/section/222_shougaigaku-sports/p106-107.pdf., Accessed on October 2007

Shaw, R. (2004): Community based disaster management: challenges of sustainability. In *Proceedings, Third Disaster Management Practitioners' workshop for Southeast Asia*, Bangkok, Thailand, pp. 113–117

Shaw, R. (2008a): Study on Sustainable Community Disaster Education through Town Watching in Saijo City and its effectiveness in landslide risk reduction. Submitted to the **World Landslide Forum**

Shaw, R. (2008b): Education for sustainable development: for proactive risk reduction initiative in urban areas. In: Shaw, R., Srinivas, H. and Sharma A., (Eds.) *Urban Risk: An Asian Perspective*. Springer Publication, Forthcoming

Shaw, R. and Goda, K. (2004): From disaster to sustainable civil society: the Kobe experience. *Disaster*, 28(19): 16–40

Shaw, R. and Okazaki, K. (2003): *Sustainability in grass-roots initiatives: focus on community based disaster management*. Kobe, UNCRD

Shaw, R., Shiwaku, K., Kobayashi, H. and Kobayashi, M. (2004): Linking experience, knowledge, perception and earthquake preparedness, *In Disaster Prevention and Management*, 13(1): 39–49

Shiwaku, K. (2007): Towards Innovation in School Disaster Education: Case Research in Kathmandu, Nepal, Unpublished Doctorate Thesis, Kyoto University

Shiwaku, K. (2008): Capacity building of local NGO as community leader in the affected areas of Pakistan earthquake of 2005. Submitted to the **World Landslide Forum**

Shiwaku, K. and Shaw, R. (2008): Proactive co-learning: A new paradigm in disaster education. *In Disaster Prevention and Management, An International Journal*, 17(2): 183–198

Suzuki, T. (2003): Project learning with portfolio: disaster education which connects community and school, Education and Business, Research Report. 3

Takahashi, J., Kojima, A. and Kodama A. (2004): "A study of the development of methods for educating children to cope with earthquakes", Ehime University Education Research Report, no. 22

Takeuchi, Y. (2008): The education of sediment disaster generation process including sediment transport to resident's action in Hiroshima City, Submitted to the **World Landslide Forum**

Takeuchi, Y. and Shaw, R. (2008): Japanese Experiences of Transferrable Indigenous Knowledge in Disaster reduction. In: Shaw, R. and Krishnamurthy, R. (Eds.) *Disaster Management: Global challenges and local solutions*. University Press, Forthcoming

Tsunozaki, E. (2008): Capacity building and awareness raising for disaster reduction through formal education. Submitted to the **World Landslide Forum**

Twigg, J. (1999): The Age of Accountability? Future Community Involvement in Disaster Reduction. *Australian Journal of Emergency Management*, 14(4): 51–58.

Twigg, J. and Bhatt, M. (1988): *Understanding Vulnerability: South Asian Perspectives*. London ITDG.

Umeda, Y., Sohma, T. and Kunugiza, K. (1999): The Great Hanshin Earthquake and school (4) The education of reducing disaster in "period for integrated study" of elementary school, Toyama University Education Research Report , no. 2, 59–77, 1999

UNISDR (2004): United Nations Inter-Agency Secretariat of the International Strategy for Disaster Reduction Living with Risk: A global review of disaster reduction initiatives, United Nations publication

Yamori, K. (2006): Frontier of disaster education. *Natural Disaster Science*, 24(4): 343–386

Yoshida, Y. (2007): Study on Effective and Sustainable Community Disaster Education through Town Watching in Saijo City, Unpublished Master Thesis, Kyoto University

International Cooperation Initiatives

27

Wolfgang Eder, Kaoru Takara and Fawu Wang

Abstract Numerous national and international organizations and initiatives – mainly under the umbrella of the UN "International Strategy for Disaster Reduction" (ISDR) – have engaged themselves in contributing to a "safer" world by promoting research projects on and preventive measurements against landslides. Other Organizations, undertakings or agencies like UNESCO, the World Bank-Global Facility for Disaster Reduction and Recovery (GFDRR), the United Nations University (UNU), the International Geoscience Programme (IGCP), the UN-International Year of Planet Earth (IYPE, 2008), the International Hydrological Programme (IHP), the International Flood Initiative (IFI), the International Sediment Initiative (ISI), the Disaster and Mitigation Programmes of World Meteorological Organization (WMO) and the International Science Council (ICSU), the Integrated Global Observing Strategy (IGOS) of the Global Earth Observation System of Systems (GEOSS), or the "Joint Technical Committee on Landslide and Engineered Slopes" of the International Society of Soil Mechanics and Geotechnical Engineering (ISSGME), the International Association of Engineering Geologists and the Environment (IAEG) and the International Society for Rock Mechanics (ISRM) are heavily involved in landslide risk mitigation measures.

Representatives of selected organizations, initiatives or undertakings are invited to present their recent activities and findings during a Round Table at the 1st World Landslide Forum.

Keywords Global disaster risk reduction • Capacity building • International undertakings and initiatives in landslide risk reduction

27.1 United Nations International Strategy for Disaster Reduction (ISDR)

Mission

The ISDR aims at building disaster resilient communities by promoting increased awareness of the importance of disaster reduction as an integral component of sustainable

Wolfgang Eder (✉)
ICL-Adviser, University Munich, Germany

Kaoru Takara
Kyoto University, Kyoto, Japan

Fawu Wang
Kyoto University, Kyoto, Japan

K. Sassa, P. Canuti (eds.), *Landslides – Disaster Risk Reduction*,
© Springer-Verlag Berlin Heidelberg 2009

development, with the goal of reducing human, social, economic and environmental losses due to natural hazards and related technological and environmental disasters.

Recognising that natural hazards can threaten any one of us, the ISDR builds on partnerships and takes a global approach to disaster reduction, seeking to involve every individual and every community towards the goals of reducing the loss of lives, the socio-economic setbacks and the environmental damages caused by natural hazards (Fig. 27.1). In order to achieve these goals, the ISDR promotes four objectives as tools towards reaching disaster reduction for all:

Increase public awareness to understand risk, vulnerability and disaster reduction globally The more people, regional organizations, governments, non-governmental organizations, United Nations entities, representatives of civil society and others know about risk, vulnerability and how to manage the impacts of natural hazards, the more disaster reduction measures will be implemented in all sectors of society. Prevention begins with information.

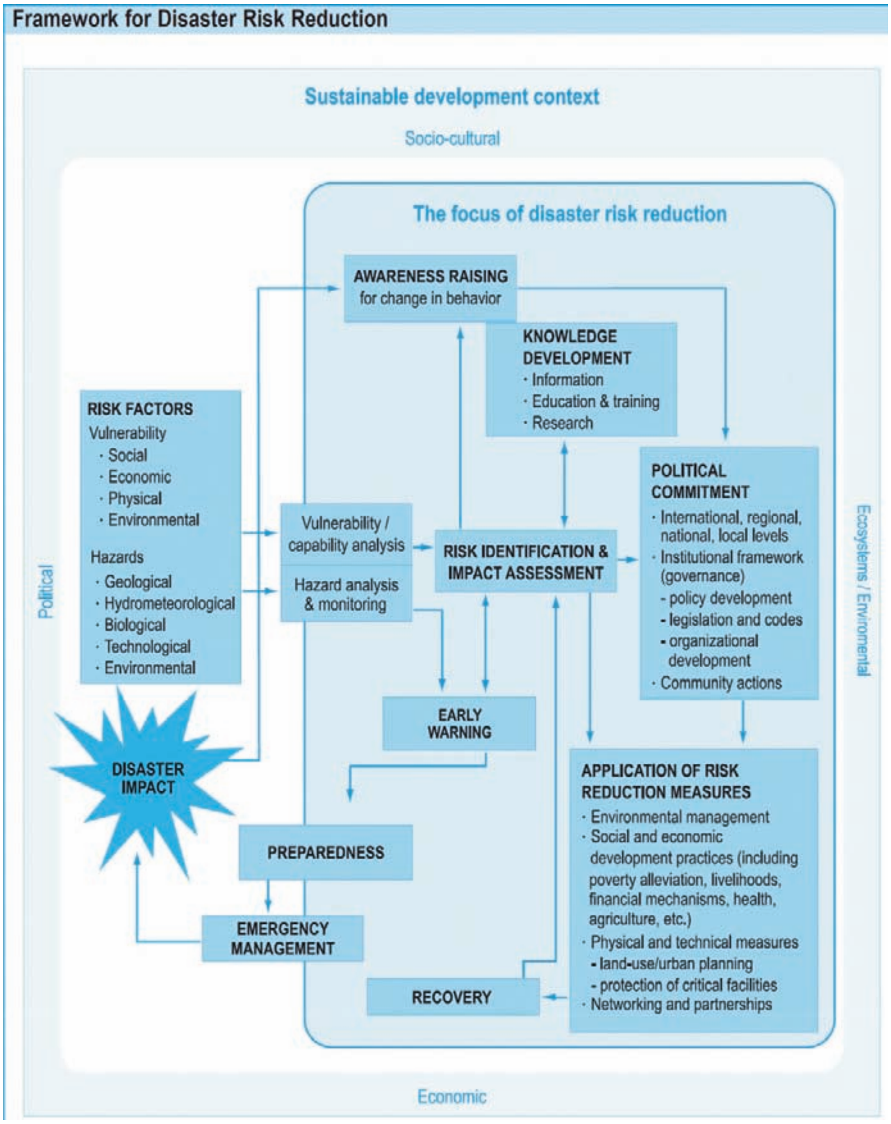

Fig. 27.1 The framework for disaster risk reduction in UN/ISDR

Obtain commitment from public authorities to implement disaster reduction policies and actions The more decision-makers at all levels commit themselves to disaster reduction policies and actions, the sooner communities vulnerable to natural disasters will benefit from applied disaster reduction policies and actions. This requires, in part, a grassroots approach whereby communities at risk are fully informed and participate in risk management initiatives.

Stimulate interdisciplinary and intersectoral partnerships, including the expansion of risk reduction networks The more entities active in disaster reduction share information on their research and practices, the more useful the global body of knowledge and experience will progress. By sharing a common purpose and through collaborative efforts we can ensure a world that is more resilient to the impact of natural hazards.

Improve scientific knowledge about disaster reduction The more we know about the causes and consequences of natural hazards and related technological and environmental disasters on societies, the more we are able to be better prepared to reduce risks. Bringing the scientific community and policy makers together allows them to contribute to and complement each other's work.

The ISDR combines the strengths of many key players through the **Inter-Agency Task Force on Disaster Reduction (IATF/DR)** and the **Inter-Agency Secretariat of the ISDR (UN/ISDR)**.

The **IATF/DR** is the principal body for the development of disaster reduction policy. It is headed by the UN Under-Secretary General for Humanitarian Affairs and consists of 25 UN, international, regional and civil society organizations. It meets twice a year in Geneva, Switzerland. Working Groups reporting to the IATF/DR bring together specialists and organisations to discuss issues of common and global relevance to disaster reduction such as climate variability, early warning, vulnerability and risk analysis, wildland fires and drought.

The **UN/ISDR** is the focal point in the UN System to promote links and synergies between, and the coordination of, disaster reduction activities in the socio-economic, humanitarian and development fields, as well as to support policy integration. It serves as an international information clearinghouse on disaster reduction, developing awareness campaigns and producing articles, journals, and other publications and promotional materials related to disaster reduction. The UN/ISDR headquarters is based at the Palais des Nations in Geneva. It conducts outreach programmes through its regional units in Costa Rica and Kenya.

27.2 Global Facility for Disaster Reduction and Recovery (GFDRR): Partnership for Disaster Reduction and Recovery

In June 2006, the World Bank's Board of Directors endorsed the establishment of the Global Facility for Disaster Reduction and Recovery (GFDRR), a longer term partnership under the ISDR system to reduce disaster losses by mainstreaming disaster risk reduction in development, particularly upstream country strategies and processes, towards fulfillment of principal goals of the Hyogo Framework of Action (HFA).

GFDRR helps developing countries fund development projects and programs that enhance local capacities for disaster prevention and emergency preparedness. GFDRR grants support disaster risk assessments, developing risk mitigation policies and strategies, preparation of disaster prevention projects and additional financing for recovery provided recipient governments demonstrate commitment to disaster prevention.

GFDRR pursues its objectives at global, regional and country levels and it addresses disasters both ex ante and ex post through its three tracks of financing. Australia, Canada, Denmark, Italy, Japan, Spain, Sweden, Switzerland, UK and World Bank are contributing in GFDRR. Track I supports annual work program of ISDR Sectt to enhance global and regional advocacy, partnerships, and knowledge management in disaster risk reduction. Track II of GFDRR is designed to provide ex ante support, primarily through a 3-year technical assistance program to enhance investments in risk reduction and risk transfer mechanisms. Track III is deployed to strengthen mobilization of international assistance for disaster recovery and supports primarily low-income countries to accelerate recovery operations.

GLOBAL FACILITY FOR DISASTER REDUCTION AND RECOVERY(GFDRR)

DONOR	FLAG	PLEDGED IN US DOLLARS($)	CONTRIBUTED IN US DOLLARS($)
		Year 2007 - 2010	
AUSTRALIA		5,081,000.00* *This includes contribution for Myanmar cyclone & China earthquake	5,081,000.00
CANADA		3,511,000.00	3,511,000.00
DENMARK		9,234,000.00* *This includes contribution for Bangladesh cyclone	9,234,000.00
European Commission		400,000.00	——
ITALY		5,000,000.00	5,000,000.00
JAPAN		6,000,000.00	6,000,000.00
Luxembourg		2,936,000.00	2,936,000.00
Norway		6,337,000.00	6,337,000.00
SPAIN		6,000,000.00	6,000,000.00
SWEDEN		8,753,000.00* *This includes contribution for Myanmar cyclone	8,753,000.00
SWITZERLAND		1,024,000.00	1,024,000.00
UNITED KINGDOM		8,761,000.00	8,761,000.00
THE WORLD BANK		15,000,000.00	15,000,000.00
	TOTAL	78,037,000.00	78,037,000.00

Fig. 27.2 GFDRR donor pledges and contributions until June 2008

With initial contribution of $ 5 million a year from World Bank's Development Grant Facility and additional $ 50 million from several donors, GFDRR is assisting several countries, regional and international organizations in identifying the disaster risks, developing risk mitigation and risk financing strategies, establishing institutional and legal systems for risk reduction, and strengthening regional cooperation in early warning, knowledge sharing and emergency preparedness (Fig. 27.2 for the 2008 situation).

27.3 United Nations University (UNU)

UNU is dedicated to the generation and transfer of knowledge, and the strengthening of individual and institutional capacities in furtherance of the purposes and principles of the Charter of the United Nations.

The mission of UNU is to contribute, through research and capacity building, to efforts to resolve the pressing global problems that are a concern of the United Nations, its Peoples and Member States.

In fulfilling this mission, UNU fosters intellectual cooperation among scholars, scientists, and practitioners worldwide — especially those in the developing world – and functions as (Fig. 27.3):

- an international community of scholars;
- a bridge between the United Nations and the international academic community;
- a think-tank for the United Nations system;
- a builder of capacity, particularly in developing countries; and
- a platform for dialogue and new and creative ideas.

But from the perspective of UNU's evolution, and its contributions "to efforts to resolve the pressing global problems that are the concern of the United Nations, its Peoples and Members States," the University's first three decades represent a significant period of achievement. Since its modest beginnings in September 1975, UNU has grown and matured into a decentralized, global network comprising UNU Centre in Tokyo, a worldwide network of 13 UNU Research and Training Centres/Programmes (UNU RTC/Ps), and liaison offices at United Nations headquarters (New York) and UNESCO headquarters (Paris).

To ensure that its work remains relevant and responsive to the rapid and profound changes of our modern world, UNU continues to evolve and expand. A new RTC/P, focusing on issues of global health, became operational in 2006.

UNU is one of the smaller United Nations organizations, and is reliant on voluntary contributions. Yet, the University has increasingly enhanced the nature and impact of its contributions to the UN system and to the international academic community.

Within its unique position as the only university in the United Nations system, UNU undertakes a wide range of knowledge generation, knowledge transfer, and knowledge application/management activities: basic and applied research, foresight and

Fig. 27.3 Some thematic focuses and activities of UNU

policy studies, capacity development, networking/collaboration with external partners, and dissemination and outreach.

27.4 UNESCO, IUGS, ICSU and other International Cooperation Initiatives

27.4.1 UNESCO's Role in Disaster Reduction

27.4.1.1 The Difference Between Natural Hazards and Natural Disasters

Natural hazards are naturally-occurring physical phenomena caused either by rapid or slow onset events having atmospheric, geologic and hydrologic origins on solar, global, regional, national and local scales. They include earthquakes, volcanic eruptions, landslides, tsunamis, floods and drought.

Natural disasters are the consequences or effects of natural hazards. They represent a serious breakdown in sustainability and disruption of economic and social progress.

But natural disasters are not entirely "natural", for people are agents of disasters. Severe floodings may be exacerbated by deforestation. Massive concentration of population in hazard-prone areas or in cities and settlements where houses or infrastructures are not safely constructed or built or where land-use is poorly planned lead to disastrous effects after an earthquake, even at a low scale.

The impact of natural hazards to man can be reduced through better understanding of the geodynamic processes of natural hazards, worldwide dissemination of scientific knowledge, adoption of appropriate public and management policies and increase of awareness programmes and information campaigns. The application of preventive and preparedness measures such as land-use restrictions, adequate building construction and wise environmental management aims to lessen the devastating effects of unavoidable natural occurring events, and

Fig. 27.4 Logo of UNESCO and the symbol for its 60th anniversary

is far cost-effective than recovery and short-term relief or reconstruction and rehabilitation. Figure 27.4 shows the logo of UNESCO and a symbol when celebrating its 60th anniversary in 2005.

27.4.1.2 Facts

Natural disasters are increasing in terms of frequency, complexity, scope and destructive capacity. During the past two decades, earthquakes, windstorms, tsunamis, floods, landslides, volcanic eruptions and wildfires have killed millions of people, adversely affected the life of at least one billion more people and resulted in enormous economic damages.

There is a basic relationship between development and disaster-proneness. No wonder, disasters are linked to poverty.

Poor and developing countries suffer the greatest damage in life losses, in social and economic terms because of their lack of resources, infrastructures and protective systems for disaster preparedness and prevention.

The risk of natural disasters is increasing as a result of population growth, urbanization, and alteration of the natural environment, substandard dwellings and public buildings, inadequate infrastructure maintenance as well as poverty exacerbation in numerous communities.

With further population growth, expanding public and private infrastructures, and continuing trends towards uncontrolled urbanization and industrialization, the risks of greater tragedies stemming from natural hazards are expected to increase in the next years and over the current new century. The toll from disasters will be particularly severe and tragic in poor countries.

There is a need for integrated approaches in development policies and planning, to take into account disaster reduction goals to the overall benefit of the socio-economic development process. Cost-benefit analyses support the rationale of disaster prevention-oriented actions.

27.4.1.3 Natural Hazards Must not Automatically Cause Disasters

Today, there is more scientific knowledge and technological know-how than ever before to anticipate the potential effects of a disaster before it strikes. Of all the global environmental issues, natural hazards present the most manageable of situations: the risks are the most readily identified, effective mitigation measures are available and the benefits of vulnerability reduction may greatly outweigh the costs.

Yet, while disaster relief captures the imagination of the public, disaster prevention often ranks relatively low on public agendas. Relief continues to be the primary form of disaster management. Decision makers tend to focus on relief to the exclusion of mitigation and preparedness that could help communities learn from disasters and reduce their vulnerability.

27.4.1.4 The role of Science and Technology

While we cannot prevent an earthquake or a hurricane from occurring, or a volcano from erupting, we can apply the scientific knowledge and technical know-how that we already have to increase the earthquake- and wind-resistance of houses and bridges, to issue early warnings on volcanoes and cyclones and organize proper community response to such warnings.

Over the last four decades, scientific knowledge of the intensity and distribution in time and space of natural hazards and the technological means of confronting them have expanded greatly. The dramatic advances in the understanding of the causes and parameters of natural phenomena and in the techniques for resisting their forces were presented, in the mid-80 s, by Dr Frank Press, a lead scientist, as the rationale which made propitious the launching of an international decade devoted to reduce significantly the consequences of natural hazards.

The Resolution of the United Nations General Assembly which proclaimed the International Decade for Natural Disaster Reduction called for a concerted worldwide effort to use the existing scientific and technical knowledge, adding new knowledge as needed, in order to underpin the adoption and implementation of public policy for disaster prevention. The International Strategy for Disaster Reduction is the successor of the Decade and provides a framework for each nation to fully utilize existing knowledge on the lithosphere, atmosphere, and biosphere and the know-how on disaster protection gained in prior years, and to build effectively and creatively upon past accomplishments so as to meet the projected needs for safer communities.

27.4.1.5 The Scientific and Technological Disciplines

Science and technology help us to understand the mechanism of natural hazards having atmospheric, geological, hydrological, and biological origins and to analyze the transformation of these hazards into disasters. Scientific knowledge of the violent forces of nature is made up of an orderly system of facts that have been learned from study, experiments, and observations of floods, severe storms, earthquakes, landslides, volcanic eruptions and tsunamis, and their impacts on humankind and his works.

The scientific and technological disciplines that are involved include basic and engineering sciences, natural, social and human sciences. They relate to the hazard environment (hydrology, geology, geophysics, seismology, volcanology, meteorology, and biology), the built environment (engineering, architecture, and materials), the policy environment (sociology, humanities, political sciences, and management science).

27.4.1.6 Prevention (the tools)

Although earthquake prediction is still not possible, a considerable ability exists today to make more accurate forecasts and to give warning of several impending hazard events. Warning of violent storms and of volcanic eruptions hours and days ahead saved many lives and prevented significant property losses. Modern technologies have been developed that reduce the exposure to natural hazard of the physical and built environment and other elements of socio-economic life.

Owing to progress in design and construction engineering, earthquake-resistant structures, including high-rise buildings, critical lifelines and industrial facilities are technically feasible and became a reality. One component of these breakthroughs in disaster reduction, in some instances, has been enhanced capacity to control or modify the disaster events themselves.

Scientific and technological solutions to the complex problems of disasters must be rooted in social realities, in the fullest sense of the term.

Science needs to be seen as only part of a continuum of action extending from the design of interdisciplinary research to the communication of results to diverse non-specialist user groups. In this vein, scientists will have to share with policy-makers and others, the responsibility for scientifically sound risk assessment and management.

Without science and technology, and their blending with other disciplines, there can be no world safer from natural disasters.

Thanks to science and technology, we already know much about natural hazards and about the ways and means to avoid or reduce many of their effects. Success in significantly reducing disasters is within our reach.

Now is the time to act within the International Strategy for Disaster Reduction

27.4.2 International Geoscience Programme (IGCP)

The IGCP is a joint operation by UNESCO and the International Union of Geological Sciences (IUGS), its logo in Fig. 27.5. It is the oldest and most successful example of scientific cooperation between a non-governmental organization (NGO) – the IUGS – and an international organization – UNESCO. The IGCP enjoys the highest reputation within the UN system as well as among the world's scientific organizations, and brings together junior and senior geoscientists from less and more developed nations. Over the past 36 years, tens of thousands of scientists have actively taken part in IGCP projects; for many of them the Programme has been the gateway to a successful personal career in and beyond geosciences. IGCP has been also responsible for some major geoscientific programmes of ground-breaking international standard – like the IGCP 425 "Landslide Hazard Assessment and Mitigation for Cultural Heritage Sites and Other Locations of high Societal Value" that developed to the "International Consortium on Landslides" and its "International Programme on Landslides".

Fig. 27.5 Logo of IGCP

The International Geoscience Programme fosters interdisciplinary geoscientific research among researchers internationally, through joint research work, meetings and workshops. Since its creation in 1972, IGCP has supported over 500 projects in about 150 countries.

IGCP's scientific objectives include:

– Increasing our understanding of the geoscientific factors affecting the global environment in order to improve human living conditions;
– Developing more effective methods to find and sustainably exploit natural resources of minerals, energy and groundwater;
– Increasing our understanding of geological processes and concepts of global importance, including an emphasis on socially relevant issues;
– Improving standards, methods and techniques of carrying out geological research, including the transfer of geological and geotechnological knowledge between industrialized and developing countries.

With reference to the above mentioned objectives, IGCP projects are focussing on the following "Themes": "The Global Change and Evolution of Life: evidence from the geological record", "Geohazards: reducing risks", "Earth Resources: sustaining society", "Geoscience of the Water Cycle", and "The Deep Earth: how it controls our environment"; in addition, IGCP may also provide support for fundamental "blue skies" research projects.

The IGCP Secretariat is based in UNESCO's Ecological and Earth Sciences Division, Paris, France (www.unesco.org/science/earth).

27.4.2.1 IGCP-Theme "Geohazards: Reducing Risks"

Geohazards, including landslides, can have drastic effect upon society, as demonstrated by the 2004 Indian Ocean Tsunami, hurricane Katrina (2005) or the recent (2008) cyclone in Birma or earthquake in China (Chengdu) – all accompanied by dramatic landslides. While more developed nations suffer mostly in financial terms, the human impact of geohazards is concentrated in the less developed world. As population increases, more and more people and businesses are exposed to geohazards.

Geoscience cannot eliminate geohazards, but it is increasingly able to reduce their impact and to mitigate associated risks. This has resulted in improved forecasting (where geohazards may occur, and how these may impact communities). The next challenge is to add spatial resolution and temporal precision.

Another challenge facing Earth scientists is how best to communicate information on risk reduction to governments and decision makers. Improved communication with stakeholders will assist in formulating policies on risk management.

27.4.3 International Year of Planet Earth

The "International Year of Planet Earth" (IYPE), a joint initiative of the International Union of Geological Sciences (IUGS) and UNESCO, runs from January 2007 to December 2009; the central year of the triennium (2008) having been proclaimed by the UN General Assembly as the UN Year (its logo in Fig. 27.6). The UN sees the Year as a contribution to their sustainable development targets as it promotes wise (sustainable) use of Earth materials and encourages better planning and management to reduce risks for the world's inhabitants.

The IYPE aims to ensure greater and more effective use by society of the knowledge accumulated by the world's 400,000 Earth scientists. The Year's ultimate goal of helping to build a safer, healthier and wealthier society around the globe is expressed in the Year's subtitle 'Earth sciences for Society'.

In addition to UNESCO and IUGS, twelve 'Founding Partners', 26 'Associate Partners' and a growing number of 'International Partner organisations' from all continents and representing all major geo-scientific communities in the world, have embarked on this initiative, The Year also enjoys the full political support of all 191 UN members. By March 2008, National Committees on the Year of Planet Earth had been established in 68 countries and regions around the world.

Fig. 27.6 Logo of IYPE

The main activities of the IYPE operate on an international as well national level through its SCIENCE and OUTREACH programmes and cover 10 broad, societal relevant and multidisciplinary themes, and are addressing disaster-related items such as minimizing natural hazard risk reduction, maximizing awareness or coping with disasters in an integrated approach.

The 10 themes are:

- Earth and Health (environmental, biological risks)
- Climate Change (global change mitigation)
- Groundwater (floods, pollution)
- Ocean (storms, tsunamis, sea level change)
- Soil (erosion, landslides)
- Deep Earth (earthquakes, volcanoes, tomography)
- Megacities (protection of infrastructures, disaster prevention)
- Hazards (risk analysis, disaster risk reduction)
- Resources (protection of energy, water and food)
- Earth and Life (bio-events in Earth's history, bio- and geo-diversity).

Questions, like

- How have humans altered the geo-, bio- and atmosphere and the landscapes, thereby "helping" to trigger geohazards (including landslides) and increasing societal vulnerability to them?
- What technologies and methodologies are required to assess the vulnerability of people

and places to geohazards - and how might these be used at a variety of spatial scales?

- How does our current ability to monitor, predict and mitigate vary from one geohazard to another? What methodologies and new technologies can improve such capabilities, and so help civil protection locally and globally?
- What are the barriers for each geohazard that prevent governments (and other entities) from using risk and vulnerability information to create policies and plans to reduce both?

may trigger the cooperation between IYPE, ISDR and ICL/IPL in order to find good answers to the common goal "to make the world a safer place" – respecting also the landslide risk prone areas of the world.

Additional information is available under www.yearofplanetearth.org.

27.4.4 The International Hydrological Programme (IHP)

IHP is UNESCO's international scientific cooperative programme in water research, water resources management, education and capacity-building, and the only broadly-based science programme of the UN system in this area (IHP logo in Fig. 27.7).

IHP's primary objectives are:

- to act as a vehicle through which Member States, cooperating professional and scientific organizations and individual experts can upgrade their knowledge of the water cycle, thereby increasing their capacity to better manage and develop their water resources
- to develop techniques, methodologies and approaches to better define hydrological phenomena
- to improve water management, locally and globally
- to act as a catalyst to stimulate cooperation and dialogue in water science and management
- to assess the sustainable development of vulnerable water resources
- to serve as a platform for increasing awareness of global water issues.

Fig. 27.7 IHP logo

The planning, definition of priorities, and supervision of the execution of IHP are ensured by the Intergovernmental Council. The Bureau of the Intergovernmental Council of the IHP co-ordinates the work of the Council between sessions.

27.4.5 International Flood Initiative (IFI) launched at World Conference on Disaster Reduction (2005, Kobe, Japan)

A new inter-agency* initiative aimed at minimizing loss of life and reducing damage caused by floods was launched at the 2005 World Conference on Disaster Reduction by UNESCO Director-General Koïchiro Matsuura. The headquarters for the new project will be based at a planned Centre for Water Hazard and Risk Management (CHARM) hosted by the Public Works Research Institute in Tsukuba, Japan. This new initiative is set to integrate the scientific, operational, educational and public awareness raising aspects of flood management, including the social response and communication dimensions of flooding and related disaster preparedness (IFI logo in Fig. 27.8).

The International Flood Initiative is a response to the increasing number of water related disasters, deaths and widespread damage to goods and assets. Since 1992, the yearly number of water-related disasters has risen from slightly over 50 to more than 150. They claim about 25,000 lives and affect over 500 million others annually, and cost the world economy more than $60 billion, (up from about $10 billion in 1950). And this does not

Fig. 27.8 IFI logo and image of flooding

include the cost of damage to cultural assets and natural resources.

Experts attribute the increase to rapid population growth, the concentration of population and property in urban areas and the higher value of assets. Climate change and global warming are exacerbating the situation, and, according to UNESCÒs International Hydrological Programme, are likely to further increase the frequency of water-related disasters.

At the same time, floods are naturally occurring phenomena, which contribute to the biodiversity and sustainability of ecosystems and to many human activities.

The International Flood Initiative will promote an integrated approach to flood management to maximize the long-term benefits of floods and to minimize the hardship, loss of life and damage to goods and assets that result from floods. To achieve this, it will focus on research, training, information networking, promoting good governance and providing technical assistance.

*UNESCO, World Meteorological Organization (WMO), the United Nations University (UNU), the United Nations Inter-Agency Secretariat of the International Strategy for Disaster Reduction (UN-ISDR), UN/ISDR Platform for the Promotion of Early Warning (PPEW), the International Association of Hydrological Sciences.

27.4.6 International Sediment Initiative (ISI)

The International Hydrological Programme (IHP) aims at the improvement of the scientific and technological basis for the development of methods for the rational management of water resources, including the protection of the environment (its logo in Fig. 27.9). The IHP Intergovernmental Council, at its 16th session (Paris, September 2004), approved the International Sediment Initiative (ISI) and endorsed the formation of a Steering Committee to plan and execute the proposed programme. Through the ISI, IHP encourages international cooperation in managing regional sediment problems and in finding local solutions.

ISI seeks to sustainably manage soil, sediment and water resources to improve the socioeconomic and ecological impacts of erosion and sedimentation. The Initiative also aims to provide better advice for policy development and implementation.

ISI's mission is: To organize and promote international information exchange and provide direct access to policy makers in Member States while activating scientific and professional communities

Fig. 27.9 ISI logo

in all regions and countries concerned. ISI will promote the elaboration and monitoring of sediment data to develop appropriate methods and procedures in sediment management.

ISI Main Activities and Projects:

– **Review of erosion and sediment-related research**

Information on ongoing research is an important contribution to the operation of the databases and information systems; however the inadequacy of knowledge about various aspects of erosion and sediment phenomena hinders progress in addressing key sedimentation problems.

– **Setting up a global erosion and sediment information system**

The online accessible system would be comprised of at least three main components:

- A Database to be generated from the Global Evaluation of Sediment Transport (GEST) and case studies.
- A Global Sediment Portal with links to other data sources such as ICOLD, GEMS/Water, USGS, EOLSS, ICID, SedNet, publications, etc.
- Documentation on information development, showing how to extract information out of scarce, scattered and unreliable data, and instructions on how to set up sediment databases for river basins in different parts of the world.

27.4.7 International Science Council (ICSU)

27.4.7.1 Natural and Human-Induced Hazards

"Natural and human-induced hazards" is one of the strategic priority areas for ICSU work over the next six years. A Planning Committee has been appointed to develop the details of a new international interdisciplinary programme in this area

1. The ICSU draft Strategic Plan 2006–2012 identifies natural and human-induced hazards as one of the major research-led issues for ICSU over the planning period. This grows out of long ICSU engagement in hazards initiatives, including the International Decade for Natural Disaster Reduction. The PAA on Environment and its relation to sustainable development (December 2003) saw hazards as a priority area for ICSU, and this was reiterated in the CSPR report on Foresight analysis (July 2004).
2. At its meeting in April 2005, the Executive Board gave the go-ahead for a scoping study on hazards, which was reported to the General Assembly in October 2005. A Planning Committee is being established to develop the details of the new programme and propose how it might be implemented.
3. The hazards programme runs much wider than tsunamis, but the 26 December 2004 Indian Ocean tsunami has clearly attracted worldwide attention and pushed the issue up the agenda. On 13 January 2005, ahead of the Kobe World Conference on Natural Disaster Reduction, the Executive Board issued a statement on the tsunami identifying both urgent and long-term needs and stressing the importance of bringing good science to bear effectively on policy-making (see ICSU Insight January 2005).

The planning and consultation process for this programme has been extended, in recognition of the need for the widest interaction and debate among potential partners and sponsors. It includes more consultation within and beyond the ICSU family and a one-day Consultation Forum, which was held on 29 October 2007. The Planning Group will submit its final report to the Committee for Science Planning and Review in April 2008. Figure 27.10 is the distribution of ICSU's 104 National members (January 2006).

Fig. 27.10 Distribution of ICSU's 104 National members (January 2006)

27.4.8 Integrated Global Observing Strategy (IGOS)

Today, our need for information on the current state of the Earth System and its processes is greater than ever before. Recognition of the effects of a growing population and increasing economic development has led to increased public and political awareness of the human and economic significance of the changes in the environment on Earth. Further research and long-term monitoring are required to improve the ability to detect, attribute and understand the various processes – including those involved in climate change – in order to reduce uncertainties, assess impacts, and predict change.

The Integrated Global Observing Strategy (IGOS) seeks to provide a comprehensive framework to harmonize the common interests of the major space-based and in-situ systems for global observation of the Earth. It is being developed as an overarching strategy for conducting observations relating to climate and atmosphere, oceans and coasts, the land surface and the Earth's interior. IGOS strives to build upon the strategies of existing international global observing programmes, and upon current achievements. It seeks to improve observing capacity and deliver observations in a cost-effective and timely fashion. Additional efforts will be directed to those areas where satisfactory international arrangements and structures do not currently exist.

IGOS is a strategic planning process, involving a number of partners, that links research, long-term monitoring and operational programmes, as well as data producers and users, in a structure that helps determine observation gaps and identify the resources to fill observation needs.

IGOS is a framework for decisions and resource allocation by individual funding agencies, providing governments with improved understanding of the need for global observations through the presentation of an overarching view of current system capabilities and limitations – thereby helping to reduce unnecessary duplication of observations.

IGOS focuses primarily on the observing aspects of the process of providing environmental information for decision-making.

IGOS is intended to cover all forms of data collection concerning the physical, chemical, biological and human environment including the associated impacts.

Fig. 27.11 Logo of IGOS-Geohazards

IGOS is based on the recognition that data collection must be user driven, leading to results which will increase scientific understanding and guide early warning, policy-setting and decision-making for sustainable development and environmental protection.

IGOS provides opportunities for capacity building and assisting countries to obtain maximum benefit from the total set of observations. Figure 27.11 is the logo of the IGOS for Geohazards.

27.4.9 Global Earth Observation System of Systems (GEOSS)

On February 16, 2005, member countries of the Group on Earth Observations agreed to a 10-year implementation plan for a Global Earth Observation System of Systems, known as GEOSS (Fig. 27.12 for its interoperability framework).

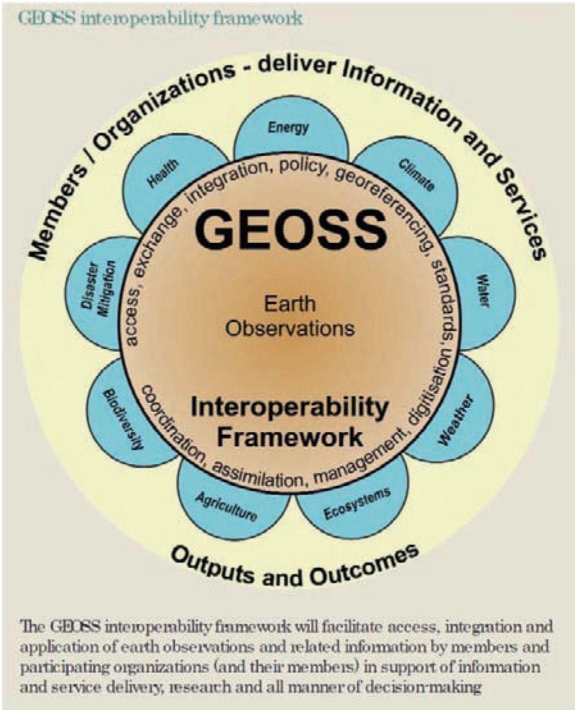

Fig. 27.12 GEOSS interoperability framework

The GEOSS project will help all nations involved produce and manage their information in a way that benefits the environment as well as humanity by taking a pulse of the planet. GEOSS is envisioned as a large national and international cooperative effort to bring together existing and new hardware and software, making it all compatible in order to supply data and information at no cost. The U.S. and developed nations have a unique role in developing and maintaining the system, collecting data, enhancing data distribution, and providing models to help all of the world's nations. EPA has a strong commitment to the GEOSS initiative.

27.5 Conclusions

Earth scientists are today's key players in managing and building a sustainable world, including issues on disaster and landslide risk reduction. As the world population continues to expand the impact of human activities on "System Earth" will increase – but, inevitably, also the vulnerability of humankind to natural hazards. Numerous national and international, governmental as well as non-governmental undertakings, including the UN-System, try to make society conscious of the importance of natural hazards risk reduction in order to mitigate or solve the problems to this end.

The "Round Table" presents an overview of international organizations and initiatives involved in landslide risk reduction.

Acknowledgments We appreciate very much the advice and support provided by Dr. Salvano Briceno (UN-ISDR), Dr. Badaoui Rouhban, Robert Missotten, Dr. Margarete Patzak (all UNESCO), as well as the fruitful cooperation with Prof. Kyoji Sassa and Prof. Hiroshi Fukuoka (ICL).

Policy and Institutional Framework for Landslide Mitigation and Risk Reduction

28

Gue, See-Sew, Karnawati, Dwikorita and Wong, Shiao-Yun

Abstract A global review on the current status of Institutional and Legislative Systems for landslide mitigation and risk reduction management has revealed that countries go through time-consuming processes to create and update policies, legislations and strategies. As such, the concept of a template for policy and institutional framework, as well as subsequent transformation to a National Slope Master Plan has been recommended. The template will serve as a blueprint to generate political commitment, which will enable the allocation of resources from the main stakeholders both in terms of manpower and budget. This will then facilitate the setting-up of a lead organisation or agency to ensure good governance to champion landslide mitigation and risk reduction. With a proper budget for the lead organisation, they can recruit the best candidates with attractive remuneration and sustainable career path for the efficient implementation of the National Slope Master Plan.

In addition, the template for this Master Plan will streamline the preparation of a local legal and regulatory framework, etc. to secure resources and provide best practices from lessons learned locally and internationally. The involvement and technical support of international agencies like ICL will expedite the development of reference knowledge kits and guidelines for adoption and adaptation. This will also assist other countries in need of support, especially those from developing and under-developed countries.

Keywords Policy • Institutional framework • Partnership • Guideline • Template • National slope master plan

28.1 Current Status of Global Disaster Reduction

A global review (UNDP, 2005) on the current status of Institutional and Legislative Systems for Disaster Risk Reduction Management has revealed that countries go through time-consuming processes to create and update policies, legislations and strategies for better management of Disaster Reduction. This review has discovered that the formation of a legal and regulatory framework is only a baby

Gue, See-Sew (✉)
WFEO and G&P Professionals, Malaysia

Karnawati, Dwikorita
University Gadjah Mada, Indonesia

Wong, Shiao-Yun
G&P Geotechnics, Malaysia

K. Sassa, P. Canuti (eds.), *Landslides – Disaster Risk Reduction*,
© Springer-Verlag Berlin Heidelberg 2009

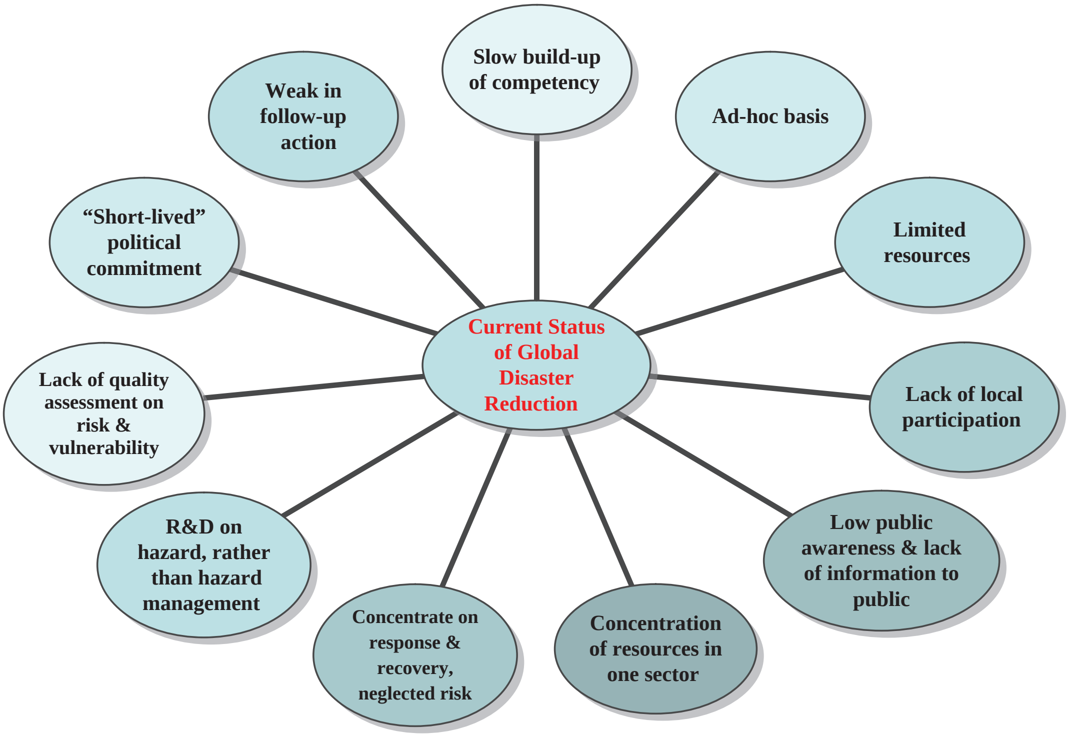

Fig. 28.1 Current status of Global Disaster Reduction (UNDP, 2005)

huddle in the entire process of Disaster Reduction Management and Implementation. Figure 28.1 has summarised the challenges in Disaster Reduction Management worldwide.

Political commitment is also the make or break factor in the effectiveness of disaster reduction. This phenomenon is particularly prominent in a developing country where "short-lived" political commitment is often encountered, partly due to constraint in resources and change in political priority. Such a situation often leads to the implementation of disaster reduction only on an ad-hoc basis and focuses more on emergency response and recovery during or after disaster, rather than on a systematic long-term risk mitigation and reduction. Low commitment and priority have also translated into limited allocation of resources, lack of local participation and weak follow-up action during policy implementation. Such a discouraging global scenario has resulted in low public awareness on the inherent risk of landslides as only restricted information is are made known to the public.

Poor institutional coordination on landslide mitigation and reduction, as well as the lack of capacity and capability have been identified as the key challenges faced. This is manifested in the slow build-up of competency at both national and local levels, the lack of capability in quality assessment on susceptibility, hazard, risk and vulnerability, the concentration of R&D on hazard assessment rather than risk management, etc. These are some of the challenges encountered during Landslide Risk Mitigation and Reduction Management.

The establishment of Disaster Management Legislation in Indonesia in 2007 is one example of strong Government Policy for mitigation and disasater risk management, despite the challenges for implementation (Pujiono, 2008). This national legislation has been further developed by establishing several National Regulations for multi-disaster management in Indonesia.

Meanwhile, Indonesia has also established a National Board for Disaster Management as the coordinator agency, and one of the national agenda of the agency in 2008 is to develop the National Guidelines for Multi-Disaster (including landslide) Risk Analysis. Risk analysis is the key to further developemnt of national and local master plans for landslide mitigation and risk reduction.

28.2 Aim of Policy and Institutional Framework Template

With the known shortcomings of disaster reduction management from a global perspective, an effective way of reducing loss of lives and properties during disasters is to formulate a general Policy and Institutional Framework leading to a template National Slope Master Plan, with contribution from international Centre-of-Excellences (COEs) like UNDP, International Strategy for Disaster Reduction (ISDR), and International Consortium on Landslides (ICL). A similar concept of a National Slope Master Plan (NSMP) on landslide management and risk reduction has been formulated in a number of countries, such as the United States of America by U.S. Geological Survey (USGS) (Spiker and Gori, 2003), Malaysia by Public Works Department (Public Works Department, 2008), Hong Kong by Geotechnical Engineering Office (GEO) (Chan, 2007).

The summary need statement for such a template is illustrated in Fig. 28.2. The "template" NSMP aims at establishing a sustainable landslide mitigation and risk reduction system which can be adopted or adapted to local conditions while serving as a blueprint to obtain political consensus, generating political commitment and elevating priority of landslide mitigation and disaster reduction. Such a template will be able to streamline the preparation of a local legal and regulatory framework, secure human and financial resources, and provide best practices and knowledge management, especially from lessons learned. In addition, the engagement and cooperation from international centres of excellence will expedite and facilitate the development of knowledge kits and guidelines for sharing knowledge and obtaining financial support for emergency rescue aid via organisations like IDA.

It is also common knowledge that landslides do not occur as one singular disaster, but may be induced by other disasters such as earthquakes and volcanic eruptions. Furthermore, landslides can also trigger other disasters such as flood, debris flood and tsunami. Therefore, mitigation of other

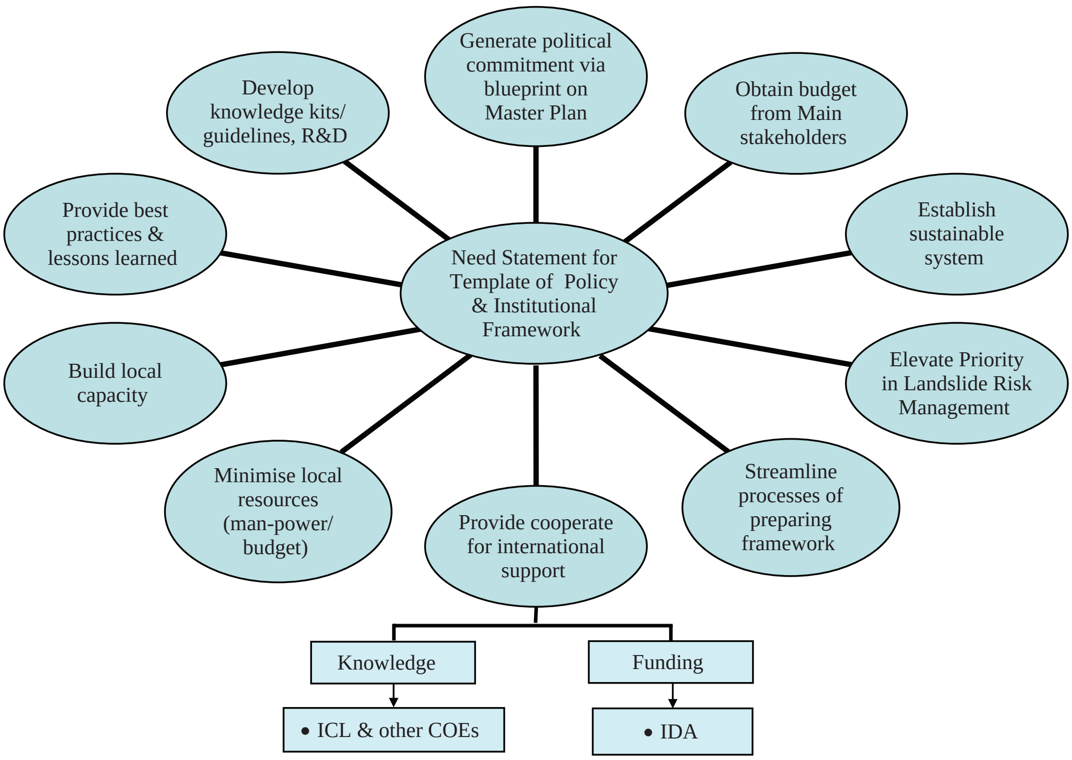

Fig. 28.2 The Need Statement for Template of Policy & Institutional Framework

disasters related to landslides should also be integrated in the template of the National Slope Master Plan.

28.3 Overview of Template Policy and Institutional Framework

The creation of a strong and resilient national landslide mitigation and disaster risk management framework has been identified as the key to a safer environment. Seven crucial factors to the success of good governance derived from international experience [Hong Kong (Chan, 2007), Malaysia (PWD, 2008), Italy (Casale and Margottini, 1999)] are illustrated in Fig. 28.3. Firstly, a specific yet flexible legal and regulatory framework should be established, including policies and legislation on landslide mitigation and risk reduction management, mechanisms and processes in ensuring legal accountability, mechanisms for effective implementation, enforcement etc. In the aspect of development planning, the relevant policy should cut-across development in both urban and rural areas for housing, infrastructure, agricultural, forestry, farming, mining, etc. Procedures and guidelines on planning implementation should incorporate an effective risk

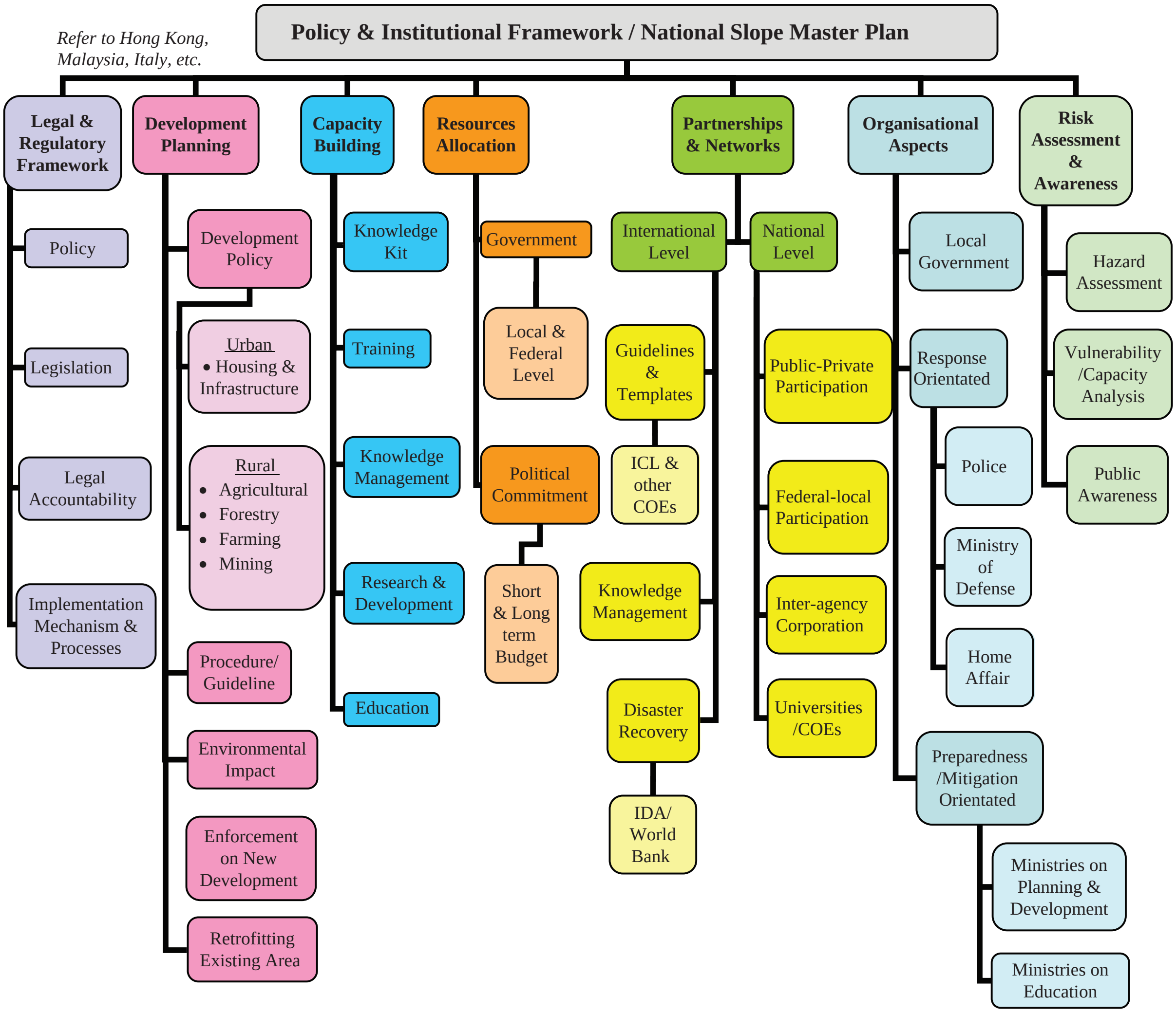

Fig. 28.3 Overview of Template Policy and Institutional Framework

assessment and mitigation system with attention to possible environmental impact and sustainability. Legal and regulatory framework and development planning used or proposed by Hong Kong (Chan, 2007), Malaysia (Public Works Department, 2008), Italy (Casale and Margottini, 1999), etc., could be utilized as a typical model.

The proposed policy and institutional framework leading to the template National Slope Master Plan form a blueprint to generate political commitment, hence attaining resources from main stakeholders and providing short and long term budgets for successful implementation. Such allocation of resources should consider the needs at both federal and local levels as landslide mitigation and risk reduction should be an inter-agency and inter-disciplinary affair.

The low competency level of mainstream stakeholders is a common constraint in the good governance of policy and institutional framework. Hence, the template NSMP will constitute a model for adoption or adaptation. It contains knowledge kits providing best practices and lesson learned, training schemes for stakeholders and practitioners, platforms for knowledge management and information sharing, etc. Furthermore, a mechanism for continuous capacity building should also be in-place through research and development activities by local universities or research institutions, as well as dissemination of knowledge in landslide mitigation and risk awareness to the primary and secondary educational system.

The governance of such a Master Plan should be undertaken by a main agency or a ministry responsible for local government. As landslide mitigation and risk reduction is a combined effort of many ministries, the lead agency should be under the Prime Minister's Office or a ministry that supports all the relevant agencies or stakeholders responsible across ministries and agencies that serve them best. This is to harmonise ministries and agencies involved and prevent rivalry for resources.

Under the lead agency or ministry, the operation of landslide mitigation and risk reduction may be divided into two major functional groups, one in response to landslide and the other in mitigation aspect. From the response perspective, it may be led by a response- oriented department like police, Ministry of Defence or Ministry of Home Affairs. Landslide mitigation should be under the leadership of preparedness and mitigation-orientated agencies in charge of planning, development, implementation, and enforcement as well as education. Therefore, depending on the local political interest and organisational structure, the template Master Plan may be adapted or adopted for different needs.

A summary of the possible contributing and triggering factors of landslides are shown in Figs. 28.4 and 28.5, respectively. Comprehensive strategies and action plans could then be implemented once the Master Plan is endorsed with commitment and budget.

Notwithstanding the above, the Master Plan will incorporate the elements of partnership and cooperation at both international and national levels, ensuring the involvement of relevant target groups. Support from expert organisations like ICL and other COEs should be called upon to expedite the development of the reference guidelines and methodology in knowledge management on landslide mitigation and risk reduction. Meanwhile, the mechanisms and processes on disaster response and recovery may be advocated by international rescue units and IDA. At the national level, participation from all sectors should be encouraged in order to ensure interaction between public and private sectors at federal and local levels. These should be further enhanced by contribution from universities and research institutions.

The entire implementation procedure should be entrenched with a "check and review" benchmarking system for continuous policy refinement. With that, the formulated template of a National Slope Master Plan may become a flagship programme, serving as a blueprint for a structured and systematic implementation plan.

28.4 Components of National Slope Master Plan

The followings are the components of the National Slope Master Plan. They are adapted from Malaysia (PWD, 2008) and USGS (2003):

1) Policy and Institutional Framework
2) Agricultural Development *(agricultural)*

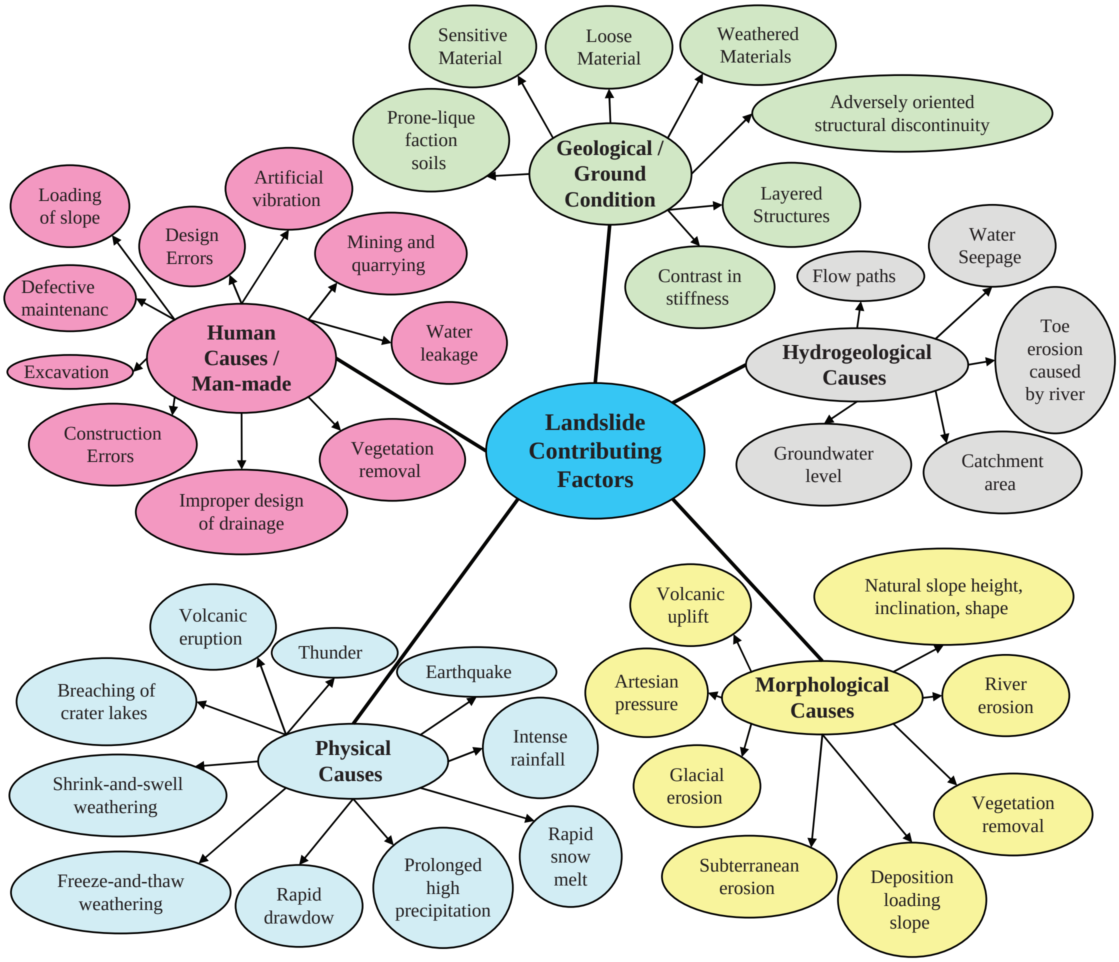

Fig. 28.4 Landslide Contributing Factors

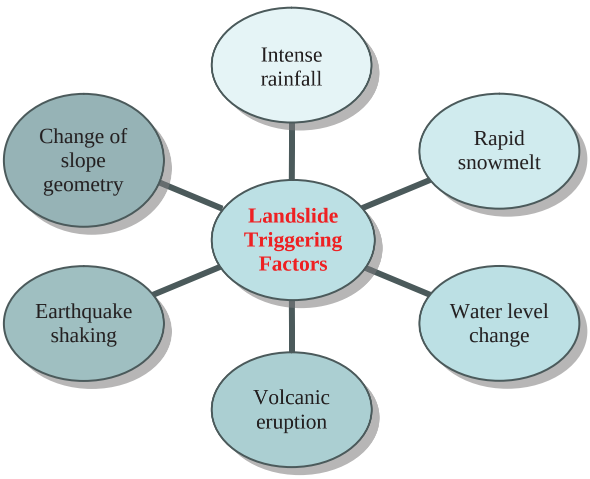

Fig. 28.5 Landslide Triggering Factors

3) Forestry Policy & Activity *(forestry)*
4) Hazard Mapping and Risk Assessments
5) Early Warning System and Real Time Monitoring
6) Loss Assessment
7) Information Collection, Interpretation, Dissemination and Archiving
8) Public Awareness and Education
9) Loss Reduction Measures
10) Training
11) Emergency Preparedness, Response and Recovery
12) Research and Development

The twelve components should be the functional groups under the lead agency. The lead agency should be the implementer of each component whereby the agency may take a coordination role or be involved in the actual operation. Such decision are dependent on the resources available for the agency and the intended organization structure within its agency.

28.5 Main Stakeholders

For successful implementation of a NSMP, personnel involved in two stages, namely the preparation stage (i.e. to develop Master Plan) and the implementation stage (i.e. to adopt/adapt such a framework as local landslide mitigation and risk reduction system). A detailed diagram on parties involved has been illustrated in Fig. 28.6. The main stakeholders contributing to the formation of a template Master Plan should be the local expert organisations and international organisations like ICL and COEs.

The remaining stakeholders are mostly common between the two stages, namely local government, governmental agencies, universities and research institutions, practitioner community, insurance institutions, emergency rescue units, public welfare agencies and the general public. Participation from relevant development planning agencies in various disciplines are vital to attain a shared and representative overview of the Master Plan for sectors like agricultural and forestry, housing and infrastructure, education, etc. In addition, media coverage may act as a catalyst to the implementation programme of landslide risk reduction as it highlights political commitment and promotes public awareness. Therefore, it has been included as one of the key parties involved in the implementation stage of the Master Plan.

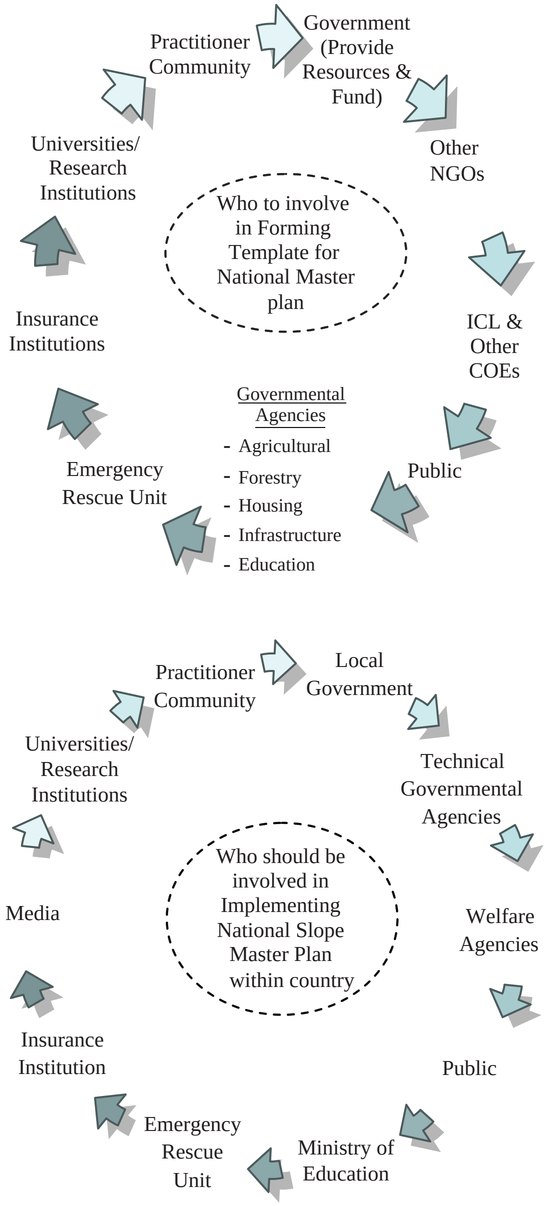

Fig. 28.6 Formation and Implementation of a National Slope Master Plan

28.6 The Stages of Master Plan Implementation

In order to achieve profound improvements in landslide mitigation and risk reduction, success at the implementation stage is vital. As such, four different stages of implementation are identified before, during and after a landslide event. A summary of the components involved at various stages is elaborated in Fig. 28.7. The four major stages are preparedness stage, mitigation stage, response stage and recovery stage.

In the preparedness stage, the Master Plan should be in-placed either by adopting it as a whole or by adapting it to local conditions. As such, the appropriate laws and regulations, implementation and enforcement policies and guidelines for development planning, training scheme for

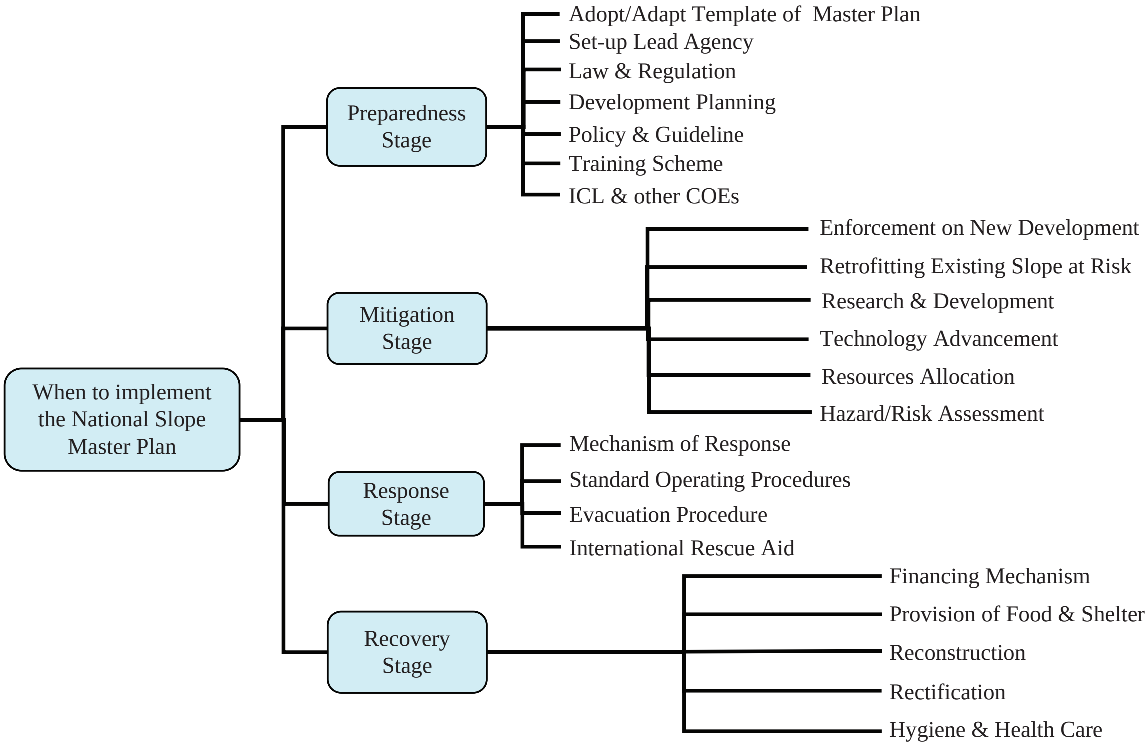

Fig. 28.7 Implementation Stages of National Slope Master Plan

stakeholders and promotion scheme for community awareness should be geared towards effective disaster reduction management.

In the mitigation stage, significant resource allocation from the main stakeholders is essential as it consist of planning and enforcement of good practices in new development, retrofitting of existing areas at risk, research and development and exploring advancement in technology and methodology. A similar approach has been adopted in Hong Kong where landslide mitigation and risk reduction have been incorporated into two (2) components, first in planning control of new development, and subsequently in retrofitting existing slopes at risk (Chan, 2007). Such policies have contributed significantly to landslide mitigation and risk reduction in Hong Kong with tremendous impact and benefits to Hong Kong residents. Hazard and risk assessment should also be included with the setting-up of an early warning system and landslide prediction model for slopes that are not feasible to improve and strengthen.

In the response and recovery stage, the National Slope Master Plan should facilitate efficient response mechanisms with the appropriate standard operating and evacuation procedures. During the disaster recovery stage in particular, mechanisms for financial allocation in terms of food and shelter, hygiene and health care, housing reconstruction, slope rectification, etc., shall be in-placed to minimize loss and impact to the community.

The stages of implementation shown in Fig. 28.8 summarises the implementation flow highlighting the elements to monitor, venues for publication, target groups for knowledge transfer and more importantly, feedback and review system for audit and improvement. Among the listed components, the core items for monitoring should be the status of political commitment (to ensure continuous resources allocation), building-up of competency among local stakeholders and practitioners, feedback on training schemes and quality of research and development by local COEs. International COEs can coordinate information from lessons learned by individual countries through their implementation processes, facilitating subsequent improvement in the configuration of template Master Plan.

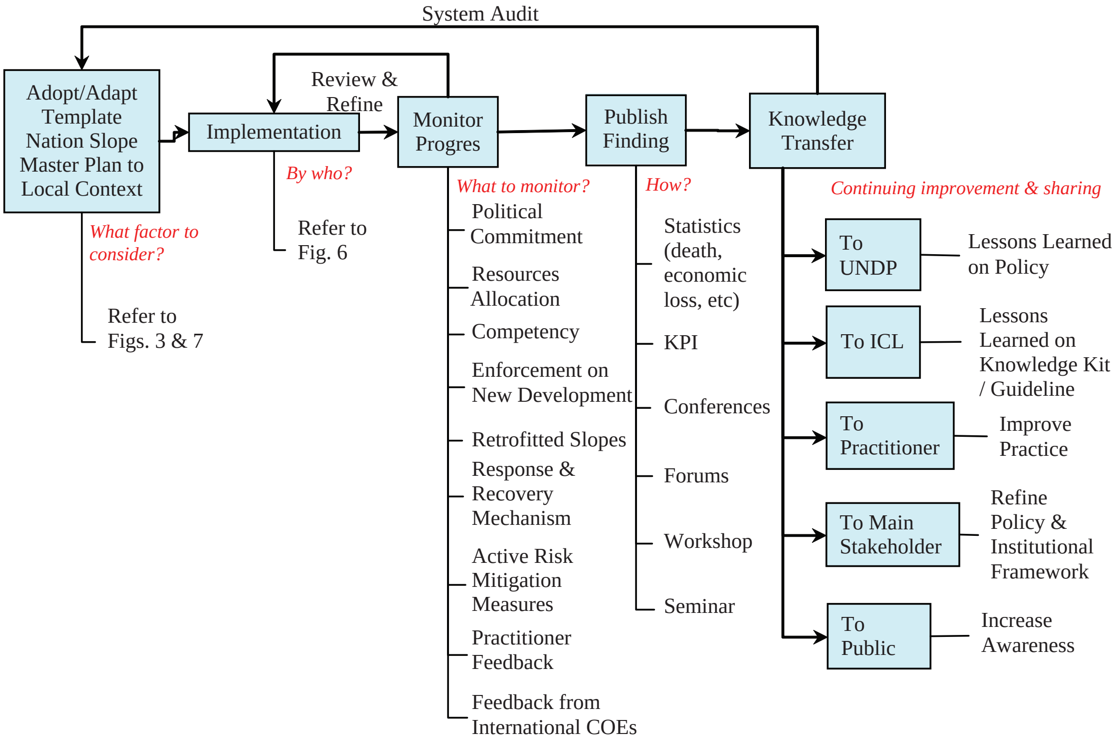

Fig. 28.8 Flow Chart of Implementation Process for a National Slope Master Plan

All progresses and best practices derived from the implementation of Master Plan should be shared through conferences, forums, seminars and workshops. Subsequently, distilled knowledge on best practices and lessons learned should be transferred to local COEs in the form of knowledge kits and guidelines.

28.7 Invited Presentations

28.7.1 Disaster Management Legislation in Indonesia: Challenges for Implementation

Pujiono, P. (Indonesian Society for Disaster Management, Indonesia)

Indonesia is one of the largest countries in the world with strategically situated and vast geographical spread with complex topo-geological features that constitute tremendous natural hazards. Socio economic make up and political complexity of the country, meanwhile, embodies the population's vulnerability to disasters. On the other hand, Indonesia's capacities to mitigate, respond and recover from disaster events leave so much room for improvement.

Impetus and driver of the Disaster Management Legislation could be traced to civil society movement in the field of disaster management all the way back in early 2003. The Indian Ocean tsunami propelled the tremendous momentum for proper political discourse towards legislating disaster management. After stalling, another major disaster, the Yogyakarta earthquake, provided the opportunity to recommence the debate and finally following another bout of procrastination the instrument was enacted into Legislation.

The disaster management legislation of Indonesia is one among the most progressive and comprehensive laws of disaster management. It calls for addressing multitude of hazards, to be implemented at all time, and involving all stakeholders. It directly links the country's constitutional mandate to the prevailing global disaster risk reduction regimes and the national institutional arrangements.

The law makers and government concurred to have the legislation implemented immediately following the ratification. Parties were designated to execute the legislation in accordance to an equally explicit timetable. Allegedly, however, the same features that make the legislation so outstanding are the very same factors that may have prevented its full implementation. Analysis on the determining factors could reveal the ideological and political environment, governance issues, as well as other pragmatic considerations that may have stall the implementation.

The legislation provides most of the required policy environment, institutional setup, and pragmatic provisions to address landslide risks in Indonesia. Therefore, a prospect of further delay on the implementation of the legislation may ultimately be detrimental to people's vulnerability to landslides. Conversely, there is now opportunity presents for the landslide discipline to formulate authoritative arguments towards the immediate and fuller implementation of the legislation.

28.7.2 Natural Hazard Legislation and Professional Landslide Guidelines in British Columbia, Canada

VanDine, D. F. (VanDine Geological Engineering Limited, Canada)

For more than 30 years in British Columbia (BC), Canada, for new residential development in areas with a potential landslide hazard, several provincial acts have required a Professional Engineer (PEng) or a Professional Geoscientist (PGeo) to write landslide assessment reports with the statement "the land is safe for the use intended". Those acts are the:

- BC Land Title Act (Sect. 86) – Subdivision Approvals
- BC Local Government Act (Sects. 919.1 and 920) – Development Approvals
- BC Local Government Act (Sect. 910) – Flood Plain Bylaw Variances or Exemptions
- BC Local Government Act (Sect. 692(d) Provincial Regulation M268) – Geotechnical Slope Stability (Seismic) Regulation, and
- BC Community Charter (Sect. 56) – Building Permits.

Other pieces of provincial legislation for proposed residential development exist in BC in which a PEng or PGeo may be involved, but there is no legislated requirement for the involvement of a PEng or PGeo.

Although landslide assessments are also frequently carried out for proposed non-residential development such as institutional, commercial, industrial and infrastructure, for emergency response, and for existing residential development, there is no associated provincial legislation.

Besides the fact that there is no provincial legislation for proposed non-residential development or for existing residential development, there are several other shortcomings of the pieces of legislation listed above. These shortcomings include:

- the perceived required use of the terms "certify" or "certified"
- the inconsistency as to which professional can carry out the work
- the various descriptions of experience required by the PEng and PGeo, and
- the undefined terms "safe", "safely" or "used safely for the use intended".

The Association of Professional Engineers and Geoscientists of British Columbia (APEGBC) is a licensing and regulatory body for PEngs and PGeos. It was constituted by provincial legislation in 1921 to protect the BC public from unqualified and non-licensed practitioners.

In 2006, the Association of Professional engineers and Geoscientists of British Columbia (APEGBC) published Guidelines for Legislated Landslide Assessments for Proposed Residential Development in British Columbia in an effort to address the aforementioned shortcomings, and to assist its members who carry out such work. These Guidelines outline what a PEng or PGeo should do when carrying out a landslide assessment with respect to proposed residential development associated with the above pieces of legislation. How to carry out such an assessment is left to the practitioner.

In April 2008, the Guidelines were revised to incorporate earthquake-induced landslides as required by changes to the 2005 National Building Code of Canada and the 2006 BC Building Code. This presentation reviews the relevant pieces of provincial legislation, further describes the shortcomings of the legislation and describes how the APEGBC Guidelines address the shortcomings.

28.7.3 Slope Safety System and Landslide Risk Management in Hong Kong

Chan, R. K. S. & Lau, T. M. F. (Geotechnical Engineering Office, Civil Engineering and Development Department, Hong Kong SAR, China)

The year 2007 marked the 30th anniversary of the implementation of the Slope Safety Management System by the Geotechnical Engineering Office (GEO) in Hong Kong. The GEO (formerly known as the Geotechnical Control Office) was established in 1977 by the Hong Kong Government to regulate geotechnical engineering and slope safety, in the aftermath of several serious landslides with multiple fatalities in the 1970s.

The unique slope safety problem in Hong Kong is largely the result of dense urban development on steep hilly terrain, the legacy of a large number of substandard man-made slopes mostly formed before the 1970s without adequate geotechnical input, and high seasonal rainfall. Over the last 30 years, the GEO has developed a comprehensive and holistic slope safety management regime to combat landslide disasters and reduce landslide risk to the community.

Under the comprehensive Slope Safety Management System, the Government has been taking a proactive approach to reduce the landslide risk through exercising geotechnical control of new works, systematically rectifying existing substandard man-made slopes under the Landslip Preventive Measures Programme, managing natural terrain landslide risk, maintaining all Government man-made slopes, setting safety standards for slope engineering practice, promoting public awareness and response in slope safety through public education, and providing landslide emergency services.

One of the principal duties of the GEO is to exercise geotechnical control on new works, through checking design submissions and auditing the adequacy of construction supervision of geotechnical works. The GEO was vested with the responsibility of checking private geotechnical submissions under the ambit of the Buildings Ordinance. Whereas the mandate for the geotechnical control of public works is derived from the administrative instruction issued by the policy bureau. Over the years, the GEO has initiated many legislative amendments and improvements to administrative instructions to enhance the slope safety management for the private and public sectors respectively.

Since 1976, the GEO has embarked on a long-term slope retrofitting programme, known as the Landslip Preventive Measures (LPM) Programme, to deal with the sizeable substandard government and private man-made slopes that were formed before the establishment of the GEO, in a risk-based priority ranking order. Under this Programme, all the high-risk substandard government slopes affecting developments and major roads will be upgraded to the required safety standard by 2010. In the last 30 years, significant improvements have been made on the output and robustness of the LPM works to meet the changing needs of the general public.

In order to facilitate the effective execution of geotechnical control and landslip preventive works functions, the GEO sets slope safety standards which are tailor-made to suit local geological and climatic settings of Hong Kong. Since 1979, the GEO has produced a number of technical guidance documents on slope engineering through research and development work. These publications provide recommended standards of good practice and are considered consensus documents of the geotechnical profession as the draft documents were circulated for comments widely throughout both the public and private sectors of the local profession, academic institutions and contractors, as well as overseas specialists in the respective fields. The systematic landslide investigation initiative, which was introduced in 1997 and became a part of the LPM Programme in 2000, has played a key role in advancing the state of knowledge on slope performance and better understanding of causes and mechanism of slope failures.

Since the early 1990s, the GEO has been carrying out systematic research and development work on natural terrain landslide hazards in Hong Kong. Studies of significant natural terrain landslides and the associated research have provided the basis for rationalizing the technical approach to deal with natural terrain hazards. In the last decade or so, significant progress has been made in the following areas: improved understanding of the mechanism and causes of natural terrain landslides through landslide studies, identification of natural terrain landslides and compilation of a historical landslide inventory, insights from landslide susceptibility analysis, improved understanding of rainfall-natural terrain landslide correlation, improved capability in debris mobility numerical modeling and promulgation of guidance on design of landslide debris-resisting barriers.

In recent years, notable advances have been made by the GEO in the novel application of digital technology and information technology to enhance the capability and efficiency on geotechnical development work. These include digital photogrammetry, Geographic Information System (GIS), Interferometric Synthetic Aperture Radar (InSAR) and Light Detection and Ranging (LiDAR). With the use of these technologies, the GEO was among the first in the world to apply quantitative risk assessment in geotechnical engineering for landslide risk management.

The efforts for continuous technical development and improved standards for landslide risk management are driven by the change culture instilled in the GEO through the setting up of the Steering Committee on Continuous Improvement (SCCI) in 1995, to steer and manage the change and continuous improvement programme. Strategic Plans, comprising 6 principal goals, were developed for implementation. These goals focused on staff development, improvement to the productivity and quality of the slope upgrading programme, technical advancement in landslide risk management, enhancement of geotechnical control and technical standards, and development of the GEO's Slope Information System.

When the current phase of the LPMP is completed in 2010, the overall landslide risk from man-made slopes will be substantially reduced to less than 25% of the 1977 level. To continue the efforts to manage the landslide risks in Hong Kong, a Landslip Prevention and Mitigation Programme (LPMitP) has been launched in late 2007 to dovetail with the LPMP which is due for completion in 2010 in order to deal with the remaining landslide risks. The LPMitP will be implemented on a rolling and risk management basis and it aims to tackle man-made slopes with moderate risk as well as vulnerable natural hillside catchments with known hazards.

This paper presents an overview of the Slope Safety Management System developed and managed by the GEO, the framework for continuous improvement in technical standards to enhance slope engineering practice, and legislation improvements in mitigating landslide hazards and risk reduction in Hong Kong. Some recent novel applications of digital technology to natural terrain risk management in the GEO and the newly launched LPMitP will be introduced.

28.7.4 A New Sustainable Landslide Risk Reduction Methodology for Communities in Lower Income Countries

Anderson, M. G. & Holcombe, L. (University of Bristol, United Kingdom)

Unplanned housing developments in vulnerable communities on steep tropical and sub-tropical hillslopes in many developing countries pose major problems for the residents themselves; for Governments, in terms of potential relocation costs; for engineers in determining the precise nature of the hazard and risk; and for donor agencies, such as the World Bank, in establishing the form of disaster mitigation policies that should be promoted. Some of these communities have, in the past, had to be relocated, at costs of millions of dollars, because of major slides triggered by tropical storm rainfall. Even so, evidence shows that: (1) risk reduction is a marginal activity; (2) there has been minimal uptake of hazard maps and vulnerability assessments and (3) there is little on-the-ground delivery of construction for risk reduction.

This paper directly addresses these issues by presenting a new low-cost, community-based approach to landslide risk reduction in such a context. It is founded on the vision that there is often sufficient capacity within Governments to address such landslide issues without needing to incur significant additional costs by employing non-Government specialist staff. Such expenditure adds to debt and only sub optimally builds within-country capacity.

The approach we present develops a cross-ministry Government management team, implements a community-based approach to landslide risk assessment, develops low-cost interventions and builds capacity through community knowledge transfer. We report on the successful pilot undertaken in St Lucia, West Indies and on the uptake of the methodology by regional organisations and international donors within the Caribbean region. Importantly, the implementation of this new methodology within communities, is demonstrated to reduce landslide risk, bring economic benefit to vulnerable communities and deliver some 90% of the total expenditure on-the-ground (i.e. management overheads of only 10%).

28.7.5 Malaysian Slope Master Plan

Abdullah, C. H., Mohamed, A. and Pandi, A. R. (Public Works Department, Malaysia)

Since 1993, Malaysia has experienced many landslides that have caused considerable numbers of death, destruction to properties and immense direct and indirect economic losses. The 1993 Highland Towers landslide incident near Kuala Lumpur is considered to be the landmark landslide that creates public awareness about the peril of landslides. In this incident, a tower block toppled over due to undermining of its foundation triggered by a landslide. No concrete actions were taken by the government or the private sector to address the landslide issues following the incident. In 2003, as a result of a massive rock slope failure that cut-off a toll highway that leads to Kuala Lumpur from the north for more than 6 months, the Malaysian Government decided to establish a branch within the Public Works Department of Malaysia to ensure that slopes in Malaysia are properly and systematically managed. The first major task assigned to the new branch is to produce a comprehensive National Slope Master Plan (NSMP) for Malaysia. The goal of the NSMP study is to provide a comprehensive and effective national policy, strategy and action plan for reducing loses from landslides nationwide. This paper highlights the key objectives, the scope, the methodology and the output of the NSMP study. The issues and problems faced by the study team to come up with a relevant Master Plan are also discussed.

The NSMP is divided into 10 components that cover all the topics pertaining to slope management. The components and their main objectives are as follows: (1) Policy and Institutional Framework – provide effective policy to minimize landslides in slopes nationwide; (2) Hazard Mapping and Assessments – develop a framework for establishing an inventory of hazard and risk maps for planning and decision making; (3) Early Warning System and Real Time Monitoring – establish a system for monitoring landslides that pose substantial risk; (4) Loss Assessment – compile and evaluate information on the social-economic impacts of landslide hazards; (5) Information Collection, Interpretation, Dissemination and Archiving - establish an effective system for landslide data collection and hazards information transfer; (6) Public Awareness and Education – develop awareness programs of landslide risk to general public, developers, engineers, decision makers and others; (7) Loss Reduction Measures - develop a plan for appropriate mitigation measures; (8) Training - develop programs for guidelines, training, and education for engineers, scientists, decision-makers; (9) Emergency Preparedness, Response and Recovery – improve the nation ability to respond and recover from landslide disaster; and (10) Research and Development – develop a predictive understanding of landslide processes, threshold and triggering mechanisms. The NSMP will provide an assessment of the status, needs and associated costs for a national landslide hazards mitigation strategic program for first, second and third phases. Each phase represent a period of 5 years. With these objectives in mind, the methodology adopted were literature review, study of works carried out by others for example

Geotechnical Engineering Office of Hong Kong, United States Geological Survey and Ministry of Land, Infrastructure and Transport.

The NSMP study encountered a number of problems during the course of the study especially on the database for landslides and the incurred cost of repairs. The reasons for this problem are poor record keeping, and even if the records are present; they are not in 'palatable' form which can be immediately digested and utilized. The information are also scattered among the government agencies, universities, contractors and consultants. Some of the documents are secret either due to their sensitive nature or due to the trade secrets employed by some of the companies. Other problems include the difficulty in getting feedbacks from stakeholders on questionnaires that were sent. On the matters pertaining to public awareness, Malaysia being a multiracial country with a diverse ethnicity, language and culture; a public awareness campaign and education will have to take these issues into consideration.

The NSMP will be tabled to the Malaysian Government for their endorsement, following which; it would then be implemented in phases. One of the major recommendations is to set up a dedicated engineering agency that would oversee all matters pertaining to slope management.

The success of the NSMP very much depends upon the political will of the Government, the setting up of the relevant agency, the fund provided and the collaboration among the stakeholders and the cooperation from the public.

28.7.6 Landslide Management in the UK – is it Working?

Gibson, A. D., Culshaw, M. G. and Foster, C. (British Geological Survey, England)

As a country with limited experience of significant natural disasters, the UK has not developed a sophisticated legal and regulatory framework for the mitigation of landslide hazards. The 1966 Aberfan disaster stimulated academic research into landslide mechanisms but even a number of high-profile events in the late 20th Century, and a series of 'near-misses' since then, have had short-lived impact upon social awareness, limiting political motivation to develop policy to manage landslide hazards.

In the UK, landslide events tend to be managed locally, with limited national coordination or communication of best practice. Government efforts in the 1980s and 1990s to make national assessments of geohazards (including landslides) and to provide generic guidance to land-use planning authorities had some success but, due to limited resources and political support, ultimately failed to develop into an effective, integrated, national response to landslides.

This paper examines how landslides are dealt with by UK government, partly through the devolved governments in Scotland, Wales and Northern Ireland. The existing system relies on a combination of planning guidance, which varies between the devolved governments, and building regulations. However, crucially, the system offers no framework for the legal or financial responsibilities for hazard management. As a result, landslide management in the UK has been influenced more by planning and political structure than actual risks to the population and, as a consequence, does not provide sufficient safeguard to the population. Examples are presented that show how this framework has affected the investigation and mitigation of different types of landslide. The paper will also show how exploitation of recent events in the UK and elsewhere, a greater awareness of climate change amongst the population and improved communication by the scientific community may lead to a long term change in policy and greater protection for the population.

28.7.7 Reducing Landslide Hazards through Federal, State, and Local Government Cooperation: The Seattle, Washington, Experience

Gori, P. L. (U.S. Geological Survey, USA) and Preuss, J. (PlanWest Partners, Inc, USA)

In the winters of 1995/1996 and 1996/1997, the Pacific Northwest in the United States experienced a series of devastating floods and landslides. After the winter storms of 1996/1997, the City of Seattle, Washington, initiated a major effort to reduce losses from landslides. By coincidence, at the time the storms occurred, the U.S. Geological Survey (USGS) was supporting a multi-hazards research project in the region. The USGS Landslide Hazards Program continued its scientific investigations in the region until 2006. The USGS research complemented and was coordinated with the City of Seattle's efforts. This paper documents the convergence of the City of Seattle, the State of Washington, and the USGS decisions to understand the landslide hazards facing the Seattle area and to implement policies that reduce damage from landslides.

This paper draws on a study by Planwest Partners, Inc and the U.S. Geological Survey (USGS) that evaluated the use by local government of recent USGS research on landslide hazards in Seattle. The methodology of the study includes a review of the research by USGS and the City of Seattle and its contractor concerning landslide hazards of the region, and it includes extensive interviews with Seattle public officials and others that are instrumental in landslide hazard reduction policy. In addition, two roundtable discussions, were organized, the first with the representatives of agencies involved with setting landslide hazard reduction policies and the second with USGS researchers. The initial interviews and roundtable discussion with city officials and agency representatives led to a review of Washington State and Seattle regulations and laws that encouraged passage and enforcement of landslide hazard reduction policies.

The United States relies on different levels of government to enact and enforce land-use decisions, which are the basis of numerous landslide hazard mitigation and reduction policies. Land-use and development decisions are for the most part made at the local level. They include density and type of land-use permitted, how buildings are sited, and the location of public improvements such as roads, parks, schools, and other public amenities. State governments enact general requirements that may facilitate the local policies. At the national level, federal government agencies such as the USGS have a minimal role in land-use planning and enforcement for the most part, but do provide information that may be of use to local governments as they implement land-use and hazard reduction policies.

Each level of government brought different capabilities to the task of reducing Seattle's exposure to future damage from landslides. When Seattle experienced the impact of two successive rain seasons of abnormally high rainfall, officials decided more stringent approaches to reduce the landslide hazard were needed. A key foundation of the new landslide hazard reduction approach was a scientific one – to understand the landslide hazards and to formulate remedial measures to combat it. Seattle commissioned the consulting firm of Shannon & Wilson to undertake an inventory and landslide characterization study.

Prior to the 1995/1996 and 1996/97 rainfall seasons, Seattle had among the most comprehensive, historical records of landslides in the U.S. The database representing 1,326 landslide events over 100 years was categorized and plotted using GIS. Shannon and Wilson's study characterized four key landslide types and their locations: (1) high bluff peeloff, (2) groundwater blowout, (3) deep-seated landslides, and (4) shallow colluvial (skin slides). The City of Seattle also commissioned the production of landslide hazard and seismic hazard maps from the USGS and the University of Washington. Seattle completed a comprehensive GIS application, adding the landslide inventory and the hazard maps to their existing municipal information.

The USGS contributed five key products that were used by Seattle to reduce its landslide damage and losses. These are: (1) Shallow Landslide Hazard Map of Seattle, Edwin L. Harp, John A. Michael, and William T. Laprade, Open File Report 2006-1139, (2) Report and Map showing Landslide Susceptibility Estimated from LIDAR Mapping and Historical Landslide Records, Seattle Washington, William Schulz, Open File report 2005-1405, (3) Preliminary map showing landslide densities, recurrence intervals and annual exceedance, probabilities as determined from historic records, Seattle, Washington by J.A. Coe, J.A. Mitchael, R.A. Crovelli, and W.Z. Savage. Open File Report 00-303. (4) Modeling 3-D Slope Stability of Coastal Bluffs Using 3-D Groundwater Flow, Southwestern Seattle, Washington, by Dianne L. Brien and Mark E. Reid, U.S. Geological Survey Scientific Investigations Report 2007-5092, (5) Rainfall Thresholds for Forecasting Landslides in the Seattle, Washington, Area–Exceedance and Probability by Alan F. Chleborard, Rex L. Baum, and Jonathan W. Godt Open File Report 2006-106. The scientific studies by USGS scientists were also made available to the general public in the form of non-technical fact sheets which included information about how the USGS prepared these products and how to use them.

Interviews conducted with representatives of the City of Seattle revealed that the products developed by the USGS Seattle Landslide Project were integrated into numerous venues for decision making and policy implementation. These uses include rigorous consideration of the potential landslide hazards in relation to decisions on siting and maintaining public facilities such as roads and schools, and implementation of the City's Drainage Plan and Critical Area Regulations. These maps and information are also used in conjunction with environmental review on public and private projects as well as strategic planning for response readiness.

The State of Washington contributed to the success of the adoption of landslide hazard reduction policies through the Growth Management Act (GMA) that requires all local jurisdictions, such as Seattle, to identify and regulate geologically hazardous areas. This statewide law establishes the "demand" for scientifically based products. The State of Washington monitors and enforces local compliance with GMA and has the authority to withhold state funds from communities that do not comply. The State also has ultimate authority to evaluate consequences and potential impacts of projects that go through the State Environmental Policy Act (SEPA) an act that mandates environmental review including identifying the consequences of new construction grading.

In the case of Seattle, three levels of government converged on the problem of landslide hazards. New information about the landslide hazards was made available by the USGS and Seattle and its contractor Shannon and Wilson. Existing State of Washington regulations that required loss reduction policies at the local level reinforced Seattle's desire to implement new land-use policies, new interagency coordination of emergency response, and new sources and methods of allocating funds for new public facilities. Also, the new funding mechanism that authorized the collection of drainage management fees gave Seattle a new revenue source to implement landslide hazard mitigation.

28.7.8 *Seismic Hazard Mapping Act of 1990 and Mapping of Landslides in California*

Anderson, R. L. and McCarthy, R. J. (Alfred E. Alquist Seismic Safety Commission, United States of America)

California's topography and geology is directly related to it's scenic beauty. Low hazard potential undeveloped land is at a premium in California as more and more development occurs. This tends to push development into areas that may be prone to a natural hazard such as flooding, naturally occurring asbestos, wildfires, fault rupture landslides, liquefaction, collapsing soils or tsunamis. In addition some development is purposely done in areas of known or potential hazards in order to take advantage of views from the properties. After World War II, residential development along and on hillsides began in earnest in Southern California. Landslide assessment and mitigation in California started in earnest after rain induced landslides occurred in 1952 and were followed later on with seismically induced landslides after the 1971 San Fernando and 1989 Loma Prieta earthquakes. Local laws and ordinances were used to require that landslide hazards be dealt with.

After the Loma Prieta earthquake of 1989 the State Legislature recognized that action needed to be taken to help citizens recognize seismically induced landslide hazards by providing a legal frame work requiring that the California Geological Survey conduct regional landslide mapping and requiring that development have a detailed landslide hazard assessment conducted. The law that required the mapping is known as the Seismic Hazards Mapping Act.

There are four basic types of landslide maps produced in California: (A) landslide inventory maps, (B) landslide hazard maps, (C) landslide risk maps, and (D) Landslide zone maps. The

Seismic Hazard Mapping Act requires that the California Geological Survey map seismic hazards of liquefaction and landslides. This paper focuses only on the landslide hazard (a modified version of the type B landslide map) element of the Seismic Hazard map. The seismic hazard zones map includes depicts areas that the California Geological Survey has identified that would require further investigation under the Seismic Hazard Mapping Act should they be developed. The seismic hazard zones map focuses only on areas susceptible to liquefaction or landslides or that have been observed to have either hazard occur in the past. The maps are produced at a scale of 1:24,000 and are registered to be used with United States Geological Survey 7.5 minute quadrangle topographic maps as a base map. The areas with the highest priority are those facing urbanization, redevelopment or areas that have high populations that may be subject to seismic hazards that would threaten public health and safety during an earthquake. These maps are incorporated into the safety elements to city and county general plans.

Prior to obtaining a permit in an area that has been identified by the State as an area requiring further investigation for a seismic hazard, the developer must conduct a site specific investigation to have a landslide or a liquefaction hazard assessment conducted in conjunction with a geotechnical report for the property to be permitted.

Should the site be prone to landslides, then a site specific mitigation scheme must be developed and approved by the lead reviewing agency. Once the landslide mitigation measure has been approved and all other appropriate issues from the development project have been addressed to the satisfaction of the lead agency then the project may be approved for development.

In order to help increase the quality and consistency of seismic hazard assessment the California Geological Survey developed the “Guidelines for Evaluating and Mitigating Seismic Hazards in California” and the “Recommended Criteria for Delineating Seismic Hazard Zones in California”. The “Guidelines for Evaluating and Mitigating Seismic Hazards in California” provides background information to the Seismic Hazards Mapping Act, as well as overviews for investigating seismic hazards including estimating strong ground motion, analyzing and mitigating landslides and reviewing site investigation reports. The “Recommended Criteria for Delineating Seismic Hazard Zones in California” assists California Geological Survey staff in mapping expected strong ground motion using a probabilistically based seismic hazard assessment approach and then uses the results in determines zones of liquefaction or earthquake induced landslide potential.

In addition to the guidelines, the American Society of Civil Engineers and the Association of Engineering Geologists along with the California Geological Survey and the Southern California Earthquake Center have provided training on the guidelines and the Seismic Hazards Mapping Act for practitioners as well as building officials.

28.7.9 Prevention Policies for the Protection Against Hydrogeological Disasters in Italy

Margottini, C. (Italian Ministry of Environment)

The Italian territory, for its morphological and geologic conformation, as well as for its geographical and climatic position, has always been affected by floods and landslide of high intensity and risk.

As an example it can be mentioned that in Between 1279 and 2002, the AVI catalogue (CNR-IRPI) filler 4521 events with damages, of which 2366 related to landslides (52.3%), 2070 to floodings (45.8%), and 85 to avalanches (1.9%). In the same period 13,8 victims for year in occasion of landslide phenomena and 49,6 for year for those alluvial have been reported. In last the 50 years victims to hydraulic phenomena are decreasing (31 victims year), but with an exponential increasing of the associated economic costs (APAT, 2007).

Surveying carried out from the River Basin Authorities has highlight the presence, in Italy, of approximately 13.000 individual areas ranging from high to very high risk for floods, landslides and avalanches (Fig. 28.9). These areas correspond to 29.517 Kmq and represent the 9,8% of the whole national territory (4.1% floods; 5,2% landslides; 0,5% avalanches), being involved 6,352 Italian municipalities (81,9% of the total), with city centers

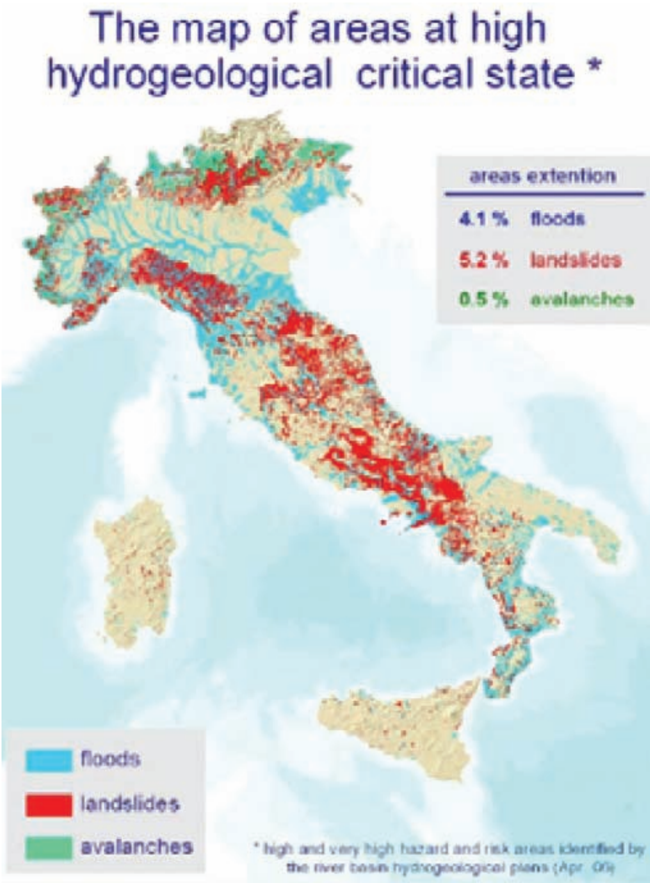

Fig. 28.9 The map of high and very high risk areas in Italy (Source Italian Ministry of Environment)

and important productive infrastructures and areas (Source Ministry of Environment).

The economic and social costs supported from the Italian State in order to supply the damages to the natural hazards are still little clear: in period 1968 to the 1992 they have been estimated in 75 Billions €, with medium value of a 3 Billions €/year (source Official Gazette of the Senate, 1992; costs brought up-to-date to 1992). Limitedly to the alluvial phenomena, the Yearbook of the Statistical Data of the APAT filler a total of 16 Billions € in period 1951–2005, with average value to 0,293 Billions €/year, that become 0,773 Billions €/year in period 1990–2005. Still less clear is the costs for the prevention: the distribution of the public works in Italy, period 2000–2005, evidences as the N04 Category (protection of the environment, hydrogeological disasters and water resources) shows public investments for € 9.338.928.387, 00, second category only after road construction (source Authority for the Vigilance on Contracts Publics). Limitedly to the relative laws of financing to works for the reorganization of idrogeologico dissesto (D.L. 180/98 and s.m.i and L. 179/02) and managed from the Ministry of the Atmosphere and Tutela of the Territory, is evidenced, in period 1998–2005, equal appropriations to € 1.491.538.585, 00 relative to 1959 participations (Source APAT, project RENDIS).

Without considering civil protection activities, the main prevention policies and related laws were generally promulgated as the answer of the State to occurred catastrophes. As an examples it can be mentioned the main law 183/89, creating the River Basin Authorities in Italy, developed after the Polesine flooding in Northern Italy of 1951 and the Florence flooding in 1966. This law remained largely not functioning until the Sarno mud slide of May 1998. After that, a new law was promulgated (law 267/98), aiming at implementing the knowledge of risk areas in Italy and posing financial resources on prevention policies. This legislation had a further implementation after the flash flood of Soverato (South Italy) in 2000, with additional prescriptions, mainly for protection from flooding and flash flood. In recent year some modification were introduced, adding complexity to the whole legislation.

At the state of the art, in the Italian Ministry of Environment, the hydrogeological protection, in its wider meaning, prefigure the overcoming of the separation between the single intervention on the territory and environment. This behind the knowledge of the complexity and the interdependences between natural processes, use of the territory, urban and territorial planning; this last also in presence of demographic dynamics that, in the general reduction of the anthropic pressure in Italy, tend to concentrate the population in few important centres; such interconnections are dramatically evident in occasion of the great catastrophic events. In fact, during the last few years, also as a result of the climatic variations and to the modifications of land use planning and management, the frequency and the gravity of the extreme events, flood and drought, it seems to increase from which it arises the necessity of new policies protect in more effective way the populations and the territory. Main milestones of this new policies are:

1. the restoration of fluvial environments, cliff and coasts, recovering, anywhere possible, their own characteristics of naturalness, by means of land use changing also at the level of river basin, the restructure of natural water flow, the recovery of sediment transportation to the coasts and the realization of intervention with low environmental impact;
2. the reduction of degree of exposure to risks, relocating the infrastructures and only applying passive defense works in case of real necessity;
3. the safeguard the water resources assuring the corrected destination and priorities, the correctness of effective requirements with respect to economic and environmental terms;
4. the establishment of short and medium term shared scale of priorities, concentrating on them the available financial resources;
5. the realization of an inter-institutional collaboration, activating, in the respect of roles and responsibilities, all the possible and valid synergies to the aims of a correct territorial occupancy.

The above items should receive adequate financial support in order to fulfill the requirement of security of population, e.g. prevention policy, before the occurrence of an extreme event and not as response and recovery after a disaster.

28.7.10 Landslide Mitigation and Risk Reduction Practice in Korea

Lee, S. G. (University of Seoul, Korea) and Hencher, S. (Halcrow China Ltd.; University of Leeds, UK)

Korea is a peninsula located in the middle part of eastern Asia and situated between China and Japan, covering an area of 221,000 km^2. In general, the peninsular is mountainous (about 70% of the total area) but rarely exceeding 1,200m in altitude. The climate of Korea has four distinct seasons. The mean annual temperature is 10°C with a maximum of 30°C in summer and minimum of -15°C in winter. The average annual rainfall is about 1,200 mm, 60% of which generally falls during the summer period from June to August. The geology of Korea if complex and includes a wide variety of rock types including igneous, metamorphic and sedimentary. Regardless of rock type, the depth of weathering is generally limited to a few metres.

Slope failures, including natural and man-made cut slopes failures are one of the major hazards encountered in Korea, resulting in an average annual loss of 60 lives and property valued at 60∼100 million U.S. dollars; the scale of damage has been rapidly growing with the booming of the construction industry. Most slope failures in Korea are triggered by rainstorms during the three month period from July to September.

Natural slope failures include debris flows and debris avalanches and these are typically initiated as shallow landslides along the boundary between thin saprolite and stronger rock on locally steep ground surfaces of between 35°∼44°. Landslides have been studied over recent decades by Korean government organizations such as the Korea Forest Research Institute (KFRI) and the Korea Institute of Geosciences and Mineral Resources (KIGAM), however these studies are at an early stage for developing a good understanding of landslide mechanisms in Korea such that the consequences may be properly mitigated.

Since 1998 road cut slopes have been investigated by government organizations under the auspices of the Ministry of Construction and Transportation (MOCT). In particular the Korea Expressway Corporation (KEC) has investigated 4,800 cut slopes along express ways and the Korea Infrastructure Safety and Technology Corporation (KISTC) together with the Korea Institute of Construction Technology (KICT) has investigated 12,650 cut slopes along other national roads. Finally 299 slope sites along railway routes have been investigated by the Korea Railroad Research Institute (KRRI).

These investigations were conducted generally to prioritize remedial works on the basis of perceived stability using simple data-sheets or tables but without geological face mapping. The data sheets, tables and methodologies deployed are distinct to each organization and as such, they are not interchangeable. Furthermore attention has been focused only on the stability of the cut-slopes themselves with little or no consideration given to the stability of the terrain above and adjacent to the cut-slopes.

It is estimated that there are more than 700,000 cut slopes along roads and in housing areas in the urban and rural regions of South Korea. The responsibility for the management and maintenance of these cut slopes belongs to local government and private entities but the system has not been properly controlled by the government, partly due to a lack of regulations with respect to the stability of cut slopes. The government does not currently have detailed information on the distribution and stability condition of cut slopes throughout the country.

Many cut slopes, both public and private, fail during and after construction with consequent injuries, loss of life and economic loss. It is important therefore that the main factors causing slope failure are investigated and measures taken to reduce the incidence of slope failure. There needs to be better consideration of cut slopes through from design to construction and to maintenance following construction.

In an attempt to reduce the casualties and loss from slope failures, the National Emergency Management Agency (NEMA), an organization under the Ministry of Government Administration and Home Affairs, commenced a 5-year Research and Development project in September 2006 entitled ’Technological Development in Estimation and Countermeasure of Slope Collapse’. It is intended to review methods for site investigation of slopes, soil and rock testing, determination of geotechnical parameters, design methods, landslide preventive measures, cut slope data basing, rating techniques and, finally, to develop a real-time streaming-based slope disaster information forecasting system.

In July 2007, the Korean government introduced a new “Steep-Slope Law”. It is a step towards allowing the Korean government to examine and control, systematically, the stability of cut slopes across the nation according to unified investigation techniques.

28.7.11 Institutional Frame Work for Community Empowerment towards Landslide Mitigation and Risk Reduction in Indonesia

Andyani, B., Karnawati, D. and Pramumijoyo, S. (Gadjah Mada University, Indonesia)

The author’s experiences as a volunteer in Aceh’s tsunami December 2004 and Yogyakarta earthquake May 2006 (Andayani and Koentjoro, 2008; in Karnawati et al., 2008) had taught some lessons which are necessary to be addressed in the National Plan for Disaster Risk Reduction. First, the need to improve community resilience against any potential disaster (such as landslide) has not yet been institutionally addressed in the existing disaster management effort. Second, the invlovement of social scientist or social disciplines needs to be further elaborated in the disaster mitigation and risk reduction. In fact, people’s psychological aspect had never been touched by disaster management system (Karnawati et al., 2008).

Admittedly, there have been quite intensive efforts to mitigate various natural disasters such as landslides, earthquake, tsunami and volcanic eruption. Most of the mitigation efforts covered hazard mapping, risk analysis, development of appropriate technology for landslide early warning and countermeasures, and those are usulally provided mainly based on the technical approach. Yet, there is still minimum consideration on soicio-cultural aspect. Accordingly, most of the hazard map, analysis, early warning system and technology, as well as the countermeasure facilities cannot be effectively implemented and operated by the community and the local authority, especially in the developing countries.

Therefore, it is suggested to establish more systematical approach and mechanism to include socio-cultural and economical considerations in the process of developing institutional frame work for disaster risk reduction. Indeed, research for social investigation and mapping needs to be formally established in parallel with the technical research for disaster mitigation and risk reduction.

One success story in incorporating the socio-cultural considerations in landslide mitigtion is the application of community-based landslide early warning system in Banjarnegara Regency, Central Java (Fathani and Karnawati, 2007). In early 2007, the Indonesian Ministry of Development for Disadvantage Region committed to improve the community resilience in landside prone area by providing a pilot program for community based landslide early warning system in one selected area in Banjarnegara, Central Java. This warning system was developed in coordination with the Local Government of Banjarnegara Regency and Gadjah Mada University. During the development process, community participation for landslide preparedness and the empowerement training for implementation of early warning system were intensively carried out. Stake holders consisting of schools, women organisation, village community, local red cross, local team of Search and Rescue, local police and NGO actively participated during the empowerment training and evacuation drill (Fig. 28.10). After installment of this early warning system, on November 7, 2007, the early warning alarm was on, and this alarm successfully made the local community living in the vulnerable site immediately leave the site and moved to the safer area. Then about 4 hours later, the landslide occurred without any victim. In fact, this become very good lesson learned which can save about 40 families living in the vulnerable site. The success of this community based early warning system encouraged the local government to further develope similar system to be applied in several other vulnerable sites in Banjarnegara Regency. This also stimulated the National Board for Disaster Management to develope further similar early warning in several different vulnerable Provinces in Indonesia.

The success of this community-based early warning system was due to an appropriate investigation on socio-cultural characteristics of the community. Therefore, in the next effort for landslide and seismic hazard mapping in Bantul Regency at Yogyakarta Province, similar investigation is also carried out in order to gurantee the effective

Fig. 28.10 Public education and evacuation drill in Kalitelaga Village, Banjarnegara Regency, Java, Indonesia (Fathani TF and Karnawati D, 2007)

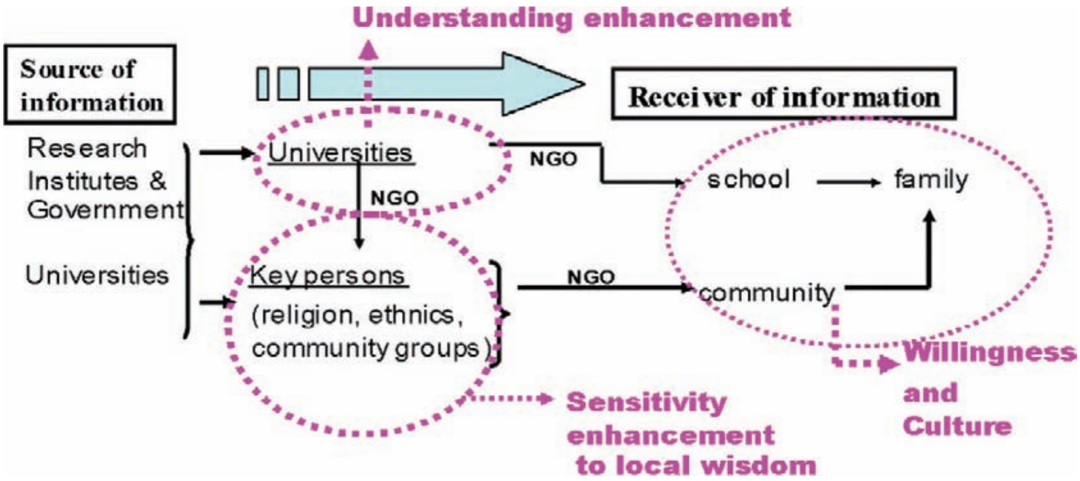

Fig. 28.11 Suggested institutional framework to support the development of community willingness and culture for landslide mitigation and risk reduction (Karnawati, et al 2005)

implementation of the produced hazard map. From the investigation and mapping on social characteristics, it was identified that the main obstacles in the implementation of hazard mapping is the poor knowledge and understanding on geohazard phenomena (including landslide), which then results in serious public anxiety and poor community's capability for disaster preparedness. In such situation, the introduction of any hazard map to the community accordingly will create more anxiety and socio-economical problems related to the land ownership and worse economical development and investment in the hazard prone area. To avoid such problems, in parallel with technical efforts for hazard mapping, continues public education is carried out thorugh the establishment of a motivation team in village or district level. This team consist of elements form school teachers, woman organisation, youth organisation, difable group and supported by the key persons in the village. The main mission of this team is to continuesly disseminate practical information about the cause of landslide hazard, how to prevent and how to prepare or to anticipate the hazard. Such information can be disseminate informally through the community radio, informal community meeting, traditional attractions, and other informal and popular media. Continues monitoring of activities and empowerment for the motivation team should be done under the responsibility of the local government and supported by the local university or NGO.

Learning from above case experiences, it is obvious that socio-cultural aspect should be appropriately considered to improve the community resilience with respect to disaster mitigation and risk reduction. The role of social and psychological disciplines is crucial to support the technical efforts in disaster mitigation. Cross-cutting coordination among research insitutions/ universities or technical departments (offices) as the source of information for disaster mitigation and the receiver organization/institutions which are responsible for community preparedness is proposed by Karnawati et al. (2005) as illustrated in Fig. 28.11. The main goal of this institutional frame work for community empowerment is to develop cultural willingness and preparedness for disaster (including landslide) mitigation and risk reduction.

28.8 Conclusions

The concept of a policy and institutional framework, as well as the subsequent transformation to a template National Slope Master Plan which includes many components to successfully implement Landslide Mitigation and Risk Reduction have been introduced in this chapter.

The main advantages of the formation of such template are summarised as follows.

28.9 National Level

1. To serve as a blueprint to generate political commitment, which will enable the allocation of resources from the main stakeholders both in terms of manpower and budget. This will facilitate the setting-up of a lead organisation or agency to ensure good governance and to champion landslide mitigation and risk reduction. With the Master Plan budget, the lead organisation could recruit the best candidates with attractive remuneration and sustainable career path for efficient implementation of the Master Plan.
2. To setup a lead agency for landslide mitigation and risk reduction at national level, ideally under the Prime Minister's Office or a Ministry that supports all the relevant agencies or stakeholders responsible across ministries and agencies that serve them best. This is to harmonise general directives and to prevent competition for resources.
3. To streamline the preparation of a local legal and regulatory framework, securing resources and providing best practices from lessons learned.
4. To implement landslide mitigation and risk reduction in two thrusts, first on planning control of new development, and second on retrofitting existing slopes. This is to ensure enforcement of good practices in new development, retrofitting of existing areas at risk, research and development and exploring advancement in technology and methodology.
5. To effectively set up institutional coordination for addressing the socio-cultural dimension in landslide mitigation and risk reduction.

28.10 International Level

1. To seek engagement and cooperation of stakeholders from international organisations such as ICL and its network of centres of excellence, to collate the experience and practices in the world on policies and legislations, etc. and develop a template on National Slope Master Plan, knowledge kits and guidelines as references for nations in need of help especially underdeveloped and developing countries. This will save cost and time in the development phase.
2. To provide financial support for emergency rescue aid via international aid organisations.

With these templates in place and continuous sharing of experience and resources, landslide mitigation and risk reduction can be more successful.

References

Andayani, B, and Koentjoro, (2008). Social and Psychological Management of Post Disaster Trauma, The Yogyakarta Earthquake of May 27, 2006, Star Publishing, California pp. 21-1–21-8.

Anderson, MG and Holcombe, EA (2006). "Sustainable landslide risk reduction in poorer countries". *Proc ICE Engineering Sustainability*, Vol. 159, pp. 23–30.

Anderson, MG, Holcombe, EA and Williams, D (2007). "Reducing landslide risk in poor housing areas of the Caribbean – developing a new Government-Community partnership model". *J International Development*. Vol. 19, No. 2, pp. 205–221.

Anderson, MG, Kemp, MJ and Lloyd, DM (1997). "Hydrological design manual for slope stability in the Tropics". Transport Research Laboratory, 58 pp.

APAT (Agency for the Protection of the Environment and for the Technical Services) (2007). Landslide Inventory of the Entire Italian Territory. By APAT Department for Soil Protection – Italian Geological Service. (www.mais.sinanet.apat.it/cartanetiffi/)

BC Community Charter (RSBC 2003, Chap. 26). [web]

BC Land Title Act (RSBC 1996, Chap. 250). [web]

BC Local Government Act (RSBC 1996, Chap. 323). [web]

BC Provincial Regulation M268 (2006). Geotechnical Slope Stability (Seismic) Regulation. Issued under the BC Local Government Act. [web]

California Geological Survey (1997). Guidelines for Evaluating and Mitigating Seismic Hazards inCalifornia, Special Publication No. 117, 73p.

Caribbean Development Bank (2004). Sourcebook on the integration of natural hazards into the Environmental Impact Assessment (EIA) Process, 207 pp.

Casale, R and Margottini, C (Eds.) (1999). Floods and Landslides: Integrated Risk Assessment *Springer*.

Chan, RKS (2007). Challenges in Slope Engineering in Hong Kong. *Thirty Years of slope Safety Practice in Hong Kong*.

Fathani, TF and Karnawati, D (2007). Community-based Landslide Early Warning System at Central Java and East Java Provinces, Indonesia. EWS Project – Final Report.

Hulme, D (2000). Impact assessment methodologies for microfinance: theory, experience, and better practice. *World Development* Vol. 28, No. 1, pp. 79–88.

Karnawati, D, Pramumijoyo, S and Koentjoro (2005). Public Education on Geoscience for sustainability of life in geohazard vulnerable area Indonesia. *Proceeding of the AGSO 2nd Annual Meeting*. Singapore, June 20–24, 2005.

Karnawati, D, Pramumijoyo, S, Anderson, R and Husein S. (2008). The Yogyakarta Earthquake of May 27, 2006, Star Publishing, California.

Mann, ME and Kerry, AE (2006). Atlantic Hurricane trends linked to climate change. *EOS* Vol. 87, No. 24, pp. 33–244.

Public Works Department (PWD) (2008). National Slope Master Plan of Malaysia.

Pujiono, P (2008), Disaster Management Legislation In Indonesia: Challenges For Implementation. World Landslide Forum (*under preparation*).

Spiker, EC and Gori, PL (2003). National Landslide Hazards Mitigation Strategy - A Framework for Loss Reduction. U.S. Geological Survey, Reston, Virginia.

UN-ISDR (2002). Natural disasters and sustainable development: understanding the links between development, environment and natural disasters. *Background Paper No. 5 of Department of Economic and Social Affairs – Commission on Sustainable Development*. www.unisdr.org (09.02.2003) [web].

UNDP (2005). A Global Review: UNDP Support To Institutional and Legislative Systems for Disaster Risk Management. [web].

USGS (2003). National Landslide Hazards Mitigation Strategy – A Framework for Loss Reduction, Circular 1244.

Wamsler, C (2006). Bridging the gaps: stakeholder-based strategies for risk reduction and financing for the urban poor. *Environment and Urbanization*, Vol. 19, No. 1, pp. 115–142.

Global Cooperation Field (4): Mitigation, Preparedness and Recovery

Climate Change and Slope Instability

29

John J. Clague

Abstract Pronounced step-wise atmospheric warming during the 20th century reduced ice cover in most of Earth's mountains by 25–50 percent. Net changes in temperatures responsible for this remarkable deglacierization are less than 2°C, a small fraction of the warming that occurred at the end of the Pleistocene. Yet the effects of warming of the past century have been profound. Alpine permafrost, which expanded during the Little Ice Age, is now thinning. Large areas at high elevations may become completely free of permafrost by the end of the 21st century. Loss of alpine permafrost and glacier downwasting appear to be partly responsible for accelerated mass wasting and catastrophic slope failures in high mountains in recent decades. New lakes appeared during the Little Ice Age when glaciers advanced across streams and rivers and blocked drainage. Most of these lakes drained one or more times during the past century, producing catastrophic floods orders of magnitude larger than normal nival or rainfall floods. In some instances, lakes have appeared upvalley of former, drained ones as glaciers have continued to retreat under a warming climate. Lakes also formed behind Little Ice Age end moraines when glaciers retreated in the early 20th century. Moraine dams are vulnerable to failure because they are steep-sided and consist of loose sediment. Outburst floods from lakes dammed by glaciers and moraines erode, transport, and deposit huge amounts of sediment over distances of tens of kilometers. They broaden floodplains, destroy pre-flood channels, and create a new braided planform. Outburst floods from glacier- and moraine-dammed lakes have claimed thousands of lives in the Andes and Himalayas and continue to be a hazard in these and other mountain ranges.

Keywords Landslides • Climate change • Permafrost thaw • Deglacieriztaion • Jökulhlaup • Moraine dam • Glacier dam

29.1 Introduction

Alpine glaciers in the Northern Hemisphere achieved their greatest extent of the past 10,000 glaciers during the "Little Ice Age" (AD 1200–1900; Holzhauser 1985; Grove 1988; Wiles et al. 1999; Luckman 2000; Luckman and Villalba

John J. Clague (✉)
Centre for Natural Hazard Research, Simon Fraser University, Canada

© Springer-Verlag Berlin Heidelberg 2009

2001). Although Earth's climate was variable during this period, alpine glaciers grew episodically, achieving progressively greater extents, until the Little Ice Age in the late 17th to mid-19th centuries.

Climate variability during the Little Ice Age (Moberg et al. 2005) probably was caused by several forcing mechanisms (Mann et al. 1998). Explosive volcanism has contributed to Northern Hemisphere temperature changes during the past 600 years (Bradley and Jones 1993; Briffa et al. 1998), and probably did so earlier during the Holocene. Some glacier advances coincided with intervals of elevated volcanic aerosols in the atmosphere (Porter 1986). Researchers have argued that solar activity influenced the climate of the past millennium (Lean et al. 1995; Crowley and Kim 1996; Crowley 2000); indeed, periods of late-Little Ice Age moraine formation generally coincide with solar minima (Lawrence, 1950; Wiles et al. 2004; Luckman and Wilson 2005). Ocean-atmosphere interactions influenced atmospheric circulation, and thus glacier behavior, during the past millennium (Hendy et al. 2002; Nesje and Dahl 2003; Lewis and Smith 2004; Mann et al. 2005). Finally, Ruddiman (2003) suggested that farm abandonment in Europe and Asia at the time of the Black Death plagues and attendant reforestation elevated levels of carbon dioxide and methane in the atmosphere and may explain the cool phases of the Little Ice Age. This assertion, however, remains to be proven.

The Little Ice Age ended about 100 years ago when climate around the world warmed. Glaciers in most mountain ranges in the Northern Hemisphere receded during the first two decades of the 20th century. Although some glaciers advanced in the 1920s, nearly all mountain glaciers underwent rapid and extensive recession over the next three decades. Most Northern Hemisphere alpine glaciers advanced small distances between the 1950s and early 1980s, but have retreated since then (Figs. 29.1 and 29.2). Most of these glaciers are 25–50 percent smaller today than at the end of the Little Ice Age.

The net change in average temperatures responsible for glacier and climate change following the Little Ice Age is less than 1°C (Mann et al. 1998). This change is a small fraction of the total warming that occurred during the demise of Northern Hemisphere ice sheets at the end of the Pleistocene. Corresponding changes in precipitation in most areas also are relatively small. Yet these changes have had significant effects on high mountain environments and on rivers flowing from these mountains. This paper summarizes and discusses these effects.

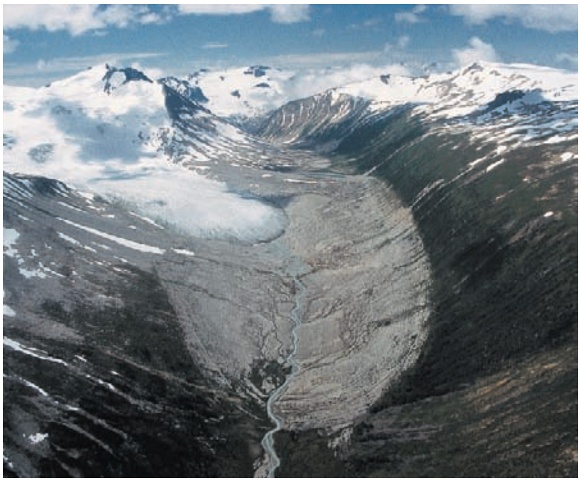

Fig. 29.1 Icemaker Glacier in the southern Coast Mountains of British Columbia. The conspicuous trimline delineates the much greater extent of the glacier in the late 1800s

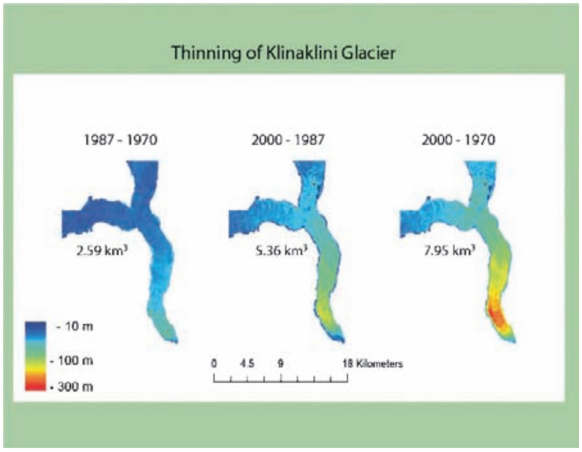

Fig. 29.2 Volumetric changes in Franklin Glacier, British Columbia, between 1979 and 2003 (data and image courtesy of Brian Menounos and Roger Wheate, University of Northern British Columbia). The glacier lost nearly 8 km^3 of its mass during this period

29.2 20th Century Permafrost Thaw and Deglacierization

Permafrost, which expanded in high mountains around the world during the Little Ice Age, now appears to be thinning and disappearing (Zhang et al. 2006). Twentieth-century warming and loss of permafrost have been implicated in the recent instability of slopes in mountain ranges in Europe and Asia (Watanabe et al. 2000; Gruber et al. 2004; Fischer et al. 2006; Gruber and Haeberli 2007); and an increase in large landslides in northern British Columbia during the 20th century (Geertsema et al. 2006) may be related, in part, to thaw of alpine permafrost. Sediments may mobilize as debris flows when their interstitial ice melts (e.g., Bovis and Jakob 2000), and masses of rock may fail, generating rock-slides and rock avalanches when ice within the fractures undergoes repeated thawing and freezing.

Alpine permafrost has a complex and patchy distribution that is controlled mainly by altitude, material properties, snow cover, and topography. A rough estimate can be made of changes in the extent of permafrost in high mountains of North America using independently determined temperature changes, bearing in mind that permafrost distribution is affected by more than just temperature. Using a range of mean annual temperature of 2°C on time-scales of decades and an adiabatic lapse rate of 4–6°C km^{-1}, the limit of permafrost shifted vertically 300–500 m during the Little Ice Age. The average rise in the limit of alpine permafrost in the 20th century, during which climate warmed 0.6–0.8°C, may have been 100–200 m. Even greater reductions in permafrost can be expected through the remainder of the 21st century. Further, permafrost warming alone, without thaw, may increase the likelihood that rock slopes will fail (Davies et al. 2001; Harris et al. 2001).

Glacier downwasting and retreat appear to be responsible for some catastrophic rock-slope failures in high mountains (Evans and Clague 1994, 1999; Holm et al. 2004). Many marginally stable slopes that were buttressed by glacier ice during the Little Ice Age failed after they became deglaciated in the 20th century (Fig. 29.3). An ancillary factor that may have contributed to such failures is steepening of rock slopes by cirque and valley glaciers during the Little Ice Age.

Fig. 29.3 Rock avalanche at Kendall Glacier, in the Cariboo Mountains of British Columbia. The landslide, which occurred in 1999, has a run-out length of 1200 m. The trigger may have been a severe storm, but loss of glacier ice on the lower part of the source slope may have contributed to failure. Photo courtesy of Carl Erickson, BC Forest Service

These effects are most pronounced in mountain ranges with the greatest ice cover (Himalaya, St. Elias Mountains, and Coast Mountains) because it is there that ice losses in the 20th century have been largest. An extreme example is Glacier Bay, Alaska, which until the end of the 18th century was completely occupied by glacier ice. Since then, the bay has become deglaciated, with the loss of over 1000 km^2 of ice. The ice loss is so great that the land is rising due to isostatic rebound (Larson et al. 2005).

29.3 Outburst Floods

New lakes formed in high mountains around the world when glaciers advanced across streams and blocked drainage during the Little Ice Age (Fig. 29.4). Many of these lakes drained one or more times in the 20th century, producing catastrophic floods (jökulhlaups) that were orders of magnitude larger than normal nival or rainfall floods (Fig. 29.5; Costa and Schuster 1988; Clague and Evans 1994; and references therein). The floods occurred due to progressive wastage of the glacier dams under a warming climate. In each case, a critical threshold of instability was reached, whence the dam failed. Sudden draining of these lakes typically happens due to rapid development of

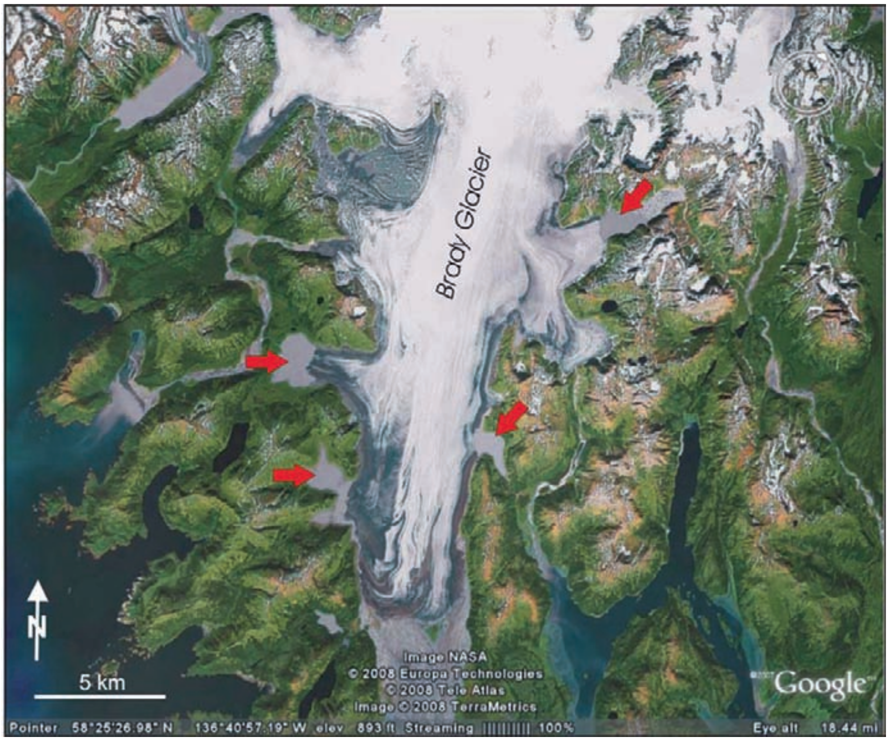

Fig. 29.4 Google Map image of lakes (*arrowed*) dammed by Brady Glacier in Glacier Bay National Park and Preserve in southeast Alaska. On occasion, the lakes partially or completely drain beneath the glacier

subglacial channels that serve as conduits for outflowing water. Glacier dams may also fail by collapse following rapid glacier advances ("surges") that block streams for only months.

New lakes also developed behind Little Ice Age end moraines as glaciers retreated in the late 19th and early 20th centuries (Costa and Schuster 1988; O'Connor and Costa 1993; Clague and Evans 1994, 2000). Many moraine dams are unstable and vulnerable to failure because they are steep-sided and consist of loose sediment. Irreversible rapid incision of the dam may be caused by a large overflow triggered by an ice avalanche or a rockfall. Other failure mechanisms include earthquakes, slow melt of buried ice, and removal ("piping") of fine sediment from the dam.

Fig. 29.5 Jökulhlaup caused by the sudden drainage of Summit Lake, north of Hyder, Alaska

Outburst floods from glacier- and moraine-dammed lakes display an exponential increase in discharge, followed by an abrupt decrease to background levels as the water supply is exhausted. Peak discharges are controlled by lake volume, dam height and width, the material properties of the dam, failure mechanism, and downstream topography and sediment availability. Floods from glacier-dammed lakes tend to have lower peak discharges than those from moraine-dammed lakes of similar size because enlargement of tunnels in ice is a slower process than overtopping and incision of sediment dams.

Floods resulting from failures of glacier and moraine dams may transform into debris flows as they travel down steep valleys. Such flows can only form and be sustained on slopes greater than 10–15° and only where there is an abundant supply of sediment in the valley below the dam (Clague and Evans 2000). Entrainment of sediment and woody plant debris by floodwaters may cause peak discharge to increase downvalley, which has important implications for hazard appraisal, because debris flows are more destructive that floods of the same size.

Outburst floods from lakes dammed by glaciers and moraines erode, transport, and deposit huge amounts of sediment over distances of tens of kilometers (Fig. 29.6). They commonly alter river floodplains tens of kilometers from the flood source. They broaden floodplains, destroy pre-flood channels, and create a new multi-channel, braided planform. The changes can persist for decades after the flood, although rivers quickly reestablish their pre-flood grades by incising the flood deposits.

A relation exists between climate and the stability of moraine and glacier dams. Most moraine-dammed lakes formed in the last century as glaciers retreated from bulky end moraines constructed during the Little Ice Age. The lakes soon began to fail as climate warmed. With continued warming and glacier retreat, the supply of moraine-dammed lakes susceptible to failure in most mountain ranges will decrease and the threat they pose will diminish (Clague and Evans 2000). The relation is different for glacier-dammed lakes. Typically, a glacier-dammed lake goes through a period of cyclic or sporadic outburst activity, lasting up to several decades. The cycle of outburst of floods from a lake ends when the glacier dam weakens to the extent that it can no longer trap water behind it. However, with continued glacier retreat, the locus of outburst activity may, in some cases, shift up-glacier to sites where new lakes develop, in areas that are becoming newly deglacierized (Geertsema and Clague 2005).

Fig. 29.6 Flood-devastated west fork of Nostetuko River valley, British Columbia. The photograph was taken in 2004, seven years after an outburst flood from moraine-dammed Queen Bess Lake

29.4 Changes to Streams

Changes in the delivery of water and sediment from a glacier can alter the stream and local base level in the valley below. During glacier advance, initial incision due to increased competence of meltwater streams is quickly followed by aggradation as sediment supply increases (Maizels 1979). Sediment stored within and beneath glaciers is delivered at an increasing rate to fluvial systems as glaciers advance (Karlén 1976; Maizels 1979; Leonard 1986, 1997; Karlén and Matthews 1992; Lamoureux 2000). Similarly, the area of subglacial erosion increases as a glacier advances, and meltwater may carry more sediment into river valleys than at times when glaciers are more restricted. Sediment pulses may propagate rapidly downstream in narrow mountain valleys when glaciers advance to maximum positions and, afterwards, when they begin to retreat. Glacier retreat typically exposes large areas of unstable, poorly vegetated sediment that is easily transferred to the fluvial system, causing valley-wide aggradation and complex changes in channel planform (Church 1983; Desloges and Church 1987; Gottesfeld and Johnson-Gottesfeld 1990; Brooks 1994; Ashmore and Church 2001; Clague et al. 2003; Wilkie 2006). This sedimentary response to deglaciation was termed "paraglacial sedimentation" by Church and Ryder (1972), although they formulated the concept based on larger-scale effects of continental ice-sheet deglaciation.

Climatically induced changes in discharge and sediment yield can cause rivers to aggrade their beds. Sediment delivery to streams in the Coast Mountains of British Columbia, for example, increased during the Little Ice Age, and the streams responded by aggrading their channels and braiding over distances up to tens of kilometers downvalley from glaciers in their headwaters (Church 1983; Gottesfeld and Johnson-Gottesfeld 1990; Wilkie

2006). Subsequently, during the 20th century, the streams incised their Little Ice Age deposits and reestablished single-thread channels characteristic of periods of lower sediment flux.

29.5 Conclusion

Climate warming during the 20th century and the first decade of the 21st century has changed the pace of some geomorphic processes in mountains. Rapid, large-scale deglacierization and thaw of alpine permafrost have increased the incidence of landslides and debris flows in mountains. Lakes that formed against retreating glaciers and end moraines have drained suddenly, catastrophically altering valley floors far downstream. Changes in sediment delivery to streams have altered local base level and channel planform in mountain valleys. If the model-based forecasts of continued warming are correct, loss of glacier ice and alpine permafrost will continue, and perhaps accelerate, through the remainder of this century.

29.6 Experience of Geophysical Study and Assessment of Dyke Breach Danger of Glacial Lakes of Tien-Shan

Yuri G. Aleshin (National Academy of Sciences, Kyrgyzstan)

Modern moraine-glacial lakes of Tien-Shan are the source of mudflows and outburst floods caused by the sudden breaching of natural dams. Scientists have identified hundreds of potentially dangerous lakes in Kyrgyzstan; dozens of them have a high likelihood of failure. Special attention must be paid to these lakes, including consideration of the possibility of evicting people from danger and construction of protective structures. Destructive hydro-geological processes operate in the moraine-glacial complexes. They are related to phase transformations in the "ice-water" system under the influence of climatic and anthropogenic factors. Moraine-glacier complexes include glaciers, bordering rock slopes, and terminal moraines. The most dangerous stage of terminal moraine degradation involves reduction in the strength of fragmental material as ice within the moraine thaws.

Moraine degradation may happen without obvious surface manifestations. At first, water moves through the moraine. Then subsurface cavities developed and collapse; depressions fill with water. The last stage is the sudden rapid development of a breach and draining of the lake. All stages in this evolutionary process may be determined through timely geophysical and geotechnical investigations. The main difficulty is to stabilize the moraine with geotechnical works where it is difficult or impossible to deliver appropriate equipment to the site.

The main methods of moraine dam investigation, where access is difficult, are geophysical in nature. These methods were tested during investigations of the moraine dam of Koltor Lake, which is located at 2730 m above sea level and impounds 2.5 million m^3 of water, and during those at the lake behind Glacier Petrov, which is located at 3740 m above sea level and contains 50 million m^3 of water.

Geophysical methods used to investigate moraine dams provide researchers with valuable information on stability. Terminal moraines with buried ice, debris fan deposits, buried ice, and subsurface water flow can be documented using these methods. Subsurface flow can cause piping, thus eroding the dam. It is possible to effectively control these destructive processes by identifying voids and moisture indexes using geophysical data.

29.7 Landslides as Proxies of Climate Change: Evidence from Past Activity Records in the Dolomites (Italy)

Lisa Borgatti (Bologna University, Italy) and Mauro Soldati (Modena and Reggio Emilia University, Italy)

Abstract This study concerns the relationships between climate changes and hillslope evolution

during the Late Quaternary, focusing on landslide processes. The research has been carried out in test areas located in the Dolomites (Italy), following the basic idea that modifications in landslide frequency may be interpreted as changes in the hydrological conditions of the slopes, which are in turn controlled by climate. By analysing a large data set, consisting of 75 radiocarbon dates, obtained with reference to 24 landslides, temporal clustering of dated mass movements in four periods of enhanced landsliding have been outlined. These four periods have been compared with different Late Glacial and Holocene paleoclimatic records, in order to check the correspondence between temporal concentrations of landslide events and climatic events. Besides the intrinsic difficulties in the correlation among these records, which are mainly due to different spatial scales, to dissimilar time-resolutions and dating constraints, some remarkable facts come forward. The period of enhanced slope instability in the Dolomites display a quite good correlation with cold and humid phases. At the same time, also periods of dry climate have a clear influence on landslide activity, resulting in gaps in the time series. The results suggest that landslide activity could have been climatically-driven and that, in particular, a positive moisture balance could have played a major role in conditioning slope instability at the hundred to thousand years time scale.

29.7.1 Introduction

Previous investigations have clearly shown that, from the Late Glacial to the present, climate has influenced slope evolution, either directly or indirectly, and that slope processes may be considered geomorphological indicators of climate changes (Goudie 1992). Temporal clustering of ancient landslide events has in fact been reported from different European regions such as Great Britain, Spain, Italy and Eastern Europe (see the review in Borgatti et al. 2001). Case studies from Africa (Thomas 1999; Busche 2001), from northern and southern America (Bovis and Jones 1992; Smith 2001; Trauth et al. 2003; Holm et al. 2004), and from Asia (Sidle et al. 2004) have also been recently presented. Research has been focused on the correlation between slope movements, climatic changes and land-use in prehistoric and historic times and on precipitation regime and seismicity as triggering factors of temporal and spatial concentrations of landslide events.

The results presented here concern the study of the relationships between climate and slope evolution from the Lateglacial to the present. The research has been carried out in study sites located in the Dolomites (Alps, northern Italy), to assess to what extent slope instability processes can be considered geomorphological indicators of climatic changes.

29.7.2 Study Area

Cortina d'Ampezzo (46°32'14.58"N, 12° 8'20.12"E) and Corvara in Badia (46°33'3.94"N, 11°51'35.10"E) are located in the eastern Italian Alps in the Dolomites (Fig. 29.7). The mountain groups, that rise from 1400 m a.s.l. in the valley bottom up to 3000 m a.s.l., are made up of dolomite rocks, with, in most cases, marls or limestones alternating with clayshales outcropping in the slopes underlying the dolomite peaks.

Active or inactive landslides are widespread: the dolomite cliffs are involved in lateral spreads, rock falls and topples, while rotational and translational slides and flows affect the slopes where clay-rich rocks outcrop. Specific investigations into the temporal occurrence of landslides have been carried out in the Dolomites since the '90 s (Panizza 1990). A large data set has been presented in Soldati et al. (2004), where the geological and geomorphological setting are thoroughly described.

29.7.3 Landslides Dating

In the study areas, the stratigraphy of landslide bodies has been reconstructed and many organic samples have been collected by means of coring or in natural or artificial scarps inside landslide accumulation zones. Direct or indirect dating of landslides has been carried out using and radiocarbon analyses by conventional or AMS methods. Conventional radiocarbon ages have been calibrated using Calib (Stuiver et al. 2004) and the intcal04

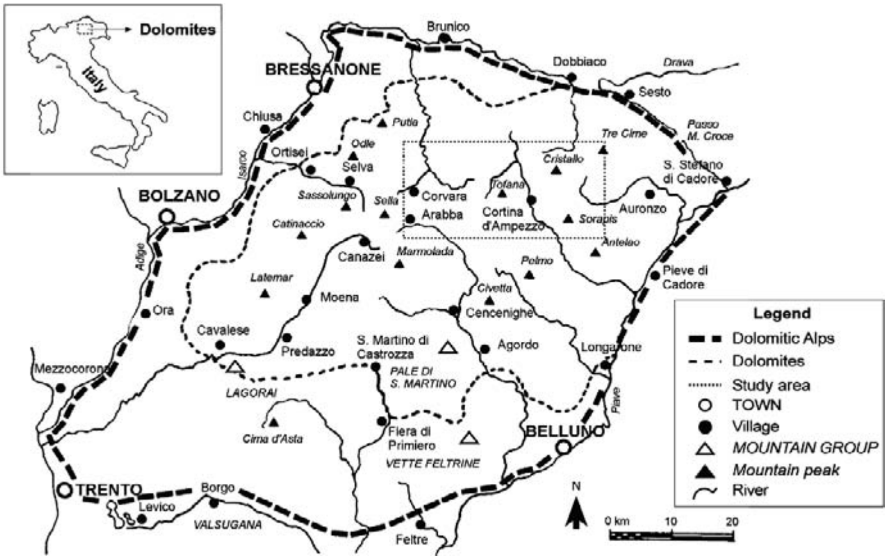

Fig. 29.7 Geographic setting of the Cortina d'Ampezzo and Alta Badia areas (Dolomites, Italy)

calibration data set (Reimer et al. 2004), with a 2 sigma error. In order to analyse the temporal occurrence of landslide events, the distributions of probability for each dating have been added together.

and the Preboreal; II. from 8200 to 6900 cal BP, during the older Atlantic; III. from 5800 to 4500 cal BP, between Atlantic and Subboreal; IV. from 4000 to 2100 cal BP, between Subboreal and Subatlantic.

29.7.4 Landslide Activity Records in the Dolomites

Starting from the synthesis of the set of data presented in Soldati et al. (2004) and from eleven new datings, the sequence of enhanced slope instability has been further developed, by analysing the statistical distribution of calibrated radiocarbon ages. The first outcome is a clear difference between the data sets of the two study sites. In the area of Cortina the ages are clearly older, with the oldest samples to be referred to more than 14 ka cal BP. This difference can be related to the timing of deglaciation and of the subsequent reforestation at different altitudes, together with the morphological setting, with respect to valley width and exposition. Moreover, in the area of Corvara the ages distribution shows a persistent landslide activity during the entire time span of the Holocene, whereas in Cortina the ages are more scattered. By analysing the complete data set (Fig. 29.8), four periods of enhanced landsliding can be outlined: I. from 10,700 to 8400 cal BP, between Younger Dryas

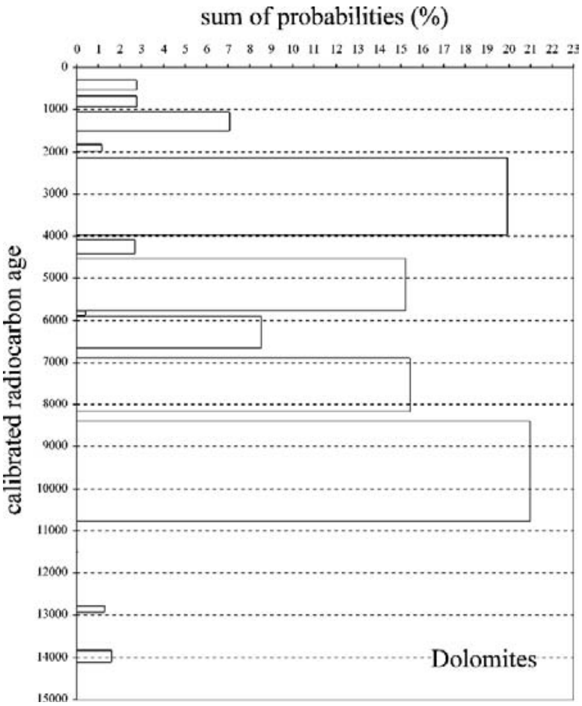

Fig. 29.8 Temporal distribution of dated slope instability events in the Dolomites

Many initial failures of large landslides occurred between 11,000 and 10,000 cal BP, i.e. during the Lateglacial - Holocene transition. The higher number of dated events in this time span could be a consequence of the amplified chance of finding buried plants debris. Otherwise, it could be related with slope release following permafrost melting and the subsequent increase of water availability at high altitudes. Period II could be related to the effects of the 8.2 ka event while the enhanced activity in the Upper Holocene follows cold and humid periods throughout the Subboreal and Subatlantic.

29.7.5 Conclusions

Landslides provide a record of climate variability at a range of temporal and spatial scales. Many factors may produce changes in frequency and magnitude of both first-time slope failures and reactivations of landslides. While a variety of triggers may account for the first–time failures of large landslides, reactivations are mainly due to changes in the hydrological regime, extending for long periods.

In this study, the effects of different environmental changes (temperature fluctuations, rainfall regime, vegetation disappearance), seismicity and human impact have been taken into account. The results show that clusters of landslide events and regional and global paleoclimatic framework are linked. This suggest that, in particular contexts, landslide can be considered as geomorphological indicators of climatic changes.

29.8 Impacts of Cryosphere Degradation on High Mountain Slope Instability: Recent Examples from the Italian Alps

Marta Chiarle (CNR-IRPI, Italy)

Slope instability has developed and accelerated in recent years in high altitude alpine areas due to permafrost thaw and loss of glacier ice. Hazards related to these processes affect mountaineers and hikers, as well as mountain huts, cableways, and other structures. Although rare, catastrophic events, such as rock-ice avalanches and outburst floods from glacier-dammed lakes, pose a risk to inhabitants and infrastructure in valleys, some of which are visited by large numbers of tourists.

Our research focuses on the characterization and interpretation of instability events in recent years in the Italian Alps that are thought to be related to climate warming. The most apparent and recurrent phenomena are rock falls from steep mountain walls. We have evaluated the potential role of permafrost thaw on recent rock wall failures by documenting the elevations, aspects, and thermal characteristics of source zones, including: the "Marco and Rosa Hut" rock fall at 3600 m a.s.l., Bernina, Central Italian Alps, August 2003; and the "Petites Murailles" rock fall at 3500 m a.s.l., Matterhorn, NW Italian Alps, August 2007. An unusually large number of small rock falls occurred on high elevation rock slopes (e.g. Mount Blanc and Matterhorn) in the warm summer of 2003, posing a significant hazard to climbers and attracting the attention of scientists and of the public. A few large events have also been reported in recent years, including the 2004 rock avalanche from Thurwieser Peak, Ortles-Cevedale, Central Italian Alps, and the April 2007 rock fall from the Monte Rosa east face, northwestern Alps, both areas visited by large numbers of tourists. Change of thermal conditions at glacier bed may have been responsible for the large (1.1 M m^3) ice avalanche on August 25, 2005, on the east face of Monte Rosa. This ice avalanche was one of the largest ever recorded in the Italian Alps.

Less frequently reported instability processes include debris flows and avalanches resulting from moraine collapse due to ground ice melting (e.g., Forni Glacier moraine, 2600 m a.s.l., Central Italian Alps) or to debuttressing caused by glacial thinning and retreat (e.g., Locce Glacier moraine, 2200 m a.s.l., Monte Rosa). Melting ice masses may serve as sliding surface for overlying scree (e.g., Val d'Arcia Glacier, 2150 m a.s.l., Dolomites).

Although a geomorphological response to climate change is becoming more evident in glacial and periglacial areas, with significant consequences for hazards and risk in high mountains, public authorities are paying little attention to the problem. Nevertheless, important scientific efforts are being made to improve knowledge of alpine permafrost distribution, cryosphere response to climate warming, and types, frequency, location and magnitude of ongoing instability processes related to climate warming, in order to provide hazard and risk scenarios for alpine areas under changing climate.

29.9 Natural Dams, Temporary Lakes, and Outburst Floods in Western Canada

Marten Geertsema (British Columbia Ministry of Forestry and Range, Canada) and John J. Clague (Centre for Natural Hazards Research, Canada)

Lakes are formed by a variety of natural dams in western Canada. The dams may be composed of snow and ice, soil, rock, or organic materials. The dams may last for minutes, or persist for millennia. Occasionally lakes drain catastrophically due to dam overtopping or failure.

29.9.1 Snow and Ice Dams

Ice jams and snow avalanches form short-lived natural dams in western Canada. Ice jams are dams formed by the accumulation of floating ice. They are particularly common in late winter on north-flowing rivers where the upstream areas melt before the lower reaches of the rivers. Examples are the Mackenzie and Liard rivers where ice jams back up water levels annually. Ice jams cause physical damage by scouring and by flooding. Ice jams are usually associated with spring thaw, but may occur at a variety of times during the winter (Brooks et al. 2001). They may persist for more than one month as in Prince George in the winter of 2007/08 (Fig. 29.9). There an ice jam which grew to more than 34 km long persisted for two months.

Snow avalanches may temporarily impound streams. The dams are typically short lived, but may cause outburst floods and debris flows (Butler 1989). In 1998 a snow avalanche dammed a mountain stream near Tete Jaune Cache, British Columbia. The outburst flood from the dam break caused a debris flow which closed a major highway.

Fig. 29.9 Ice jam on Nechako River, British Columbia (Photo City of Prince George)

Glacier dams may persist for decades. Some glacier dammed lakes fill and drain annually (or more often) because hydrostatic forces and plastic flow allow subglacial conduits to open and close. Alsek River in northwestern British Columbia has been dammed by glaciers in the past, with the most recent damming by Lowell Glacier circa 1850 (Clague and Evans 2000). Today Tweedsmuir Glacier (Fig. 29.10) is perilously close to damming Alsek River after surging more than 1200 m since 2006 (Chris Larsen: http://fairweather.gps.alaska.edu/chris/). At the time of writing (June 23 2007), the glacier terminous is within 100 m of the valley wall (Doug Makkonen, personal communication). Glacier dammed lakes may to go through general cycles of growth and decay, with flood volumes diminishing over time as glacier dams thin and retreat (Geertsema and Clague 2005). Both Salmon and Tulsequah glaciers dam lakes that display such cycles (Fig. 29.11).

29.9.2 Soil and Rock Dams

Soil dams in western Canada are formed by moraines, landslides and alluvial fans. Moraine dams form as glaciers retreat from their maximum positions. Moraine dam failures can result in catastrophic outburst flooding (Clague and Evans 2000). Once these dams fail, the lakes they impounded do not fill again.

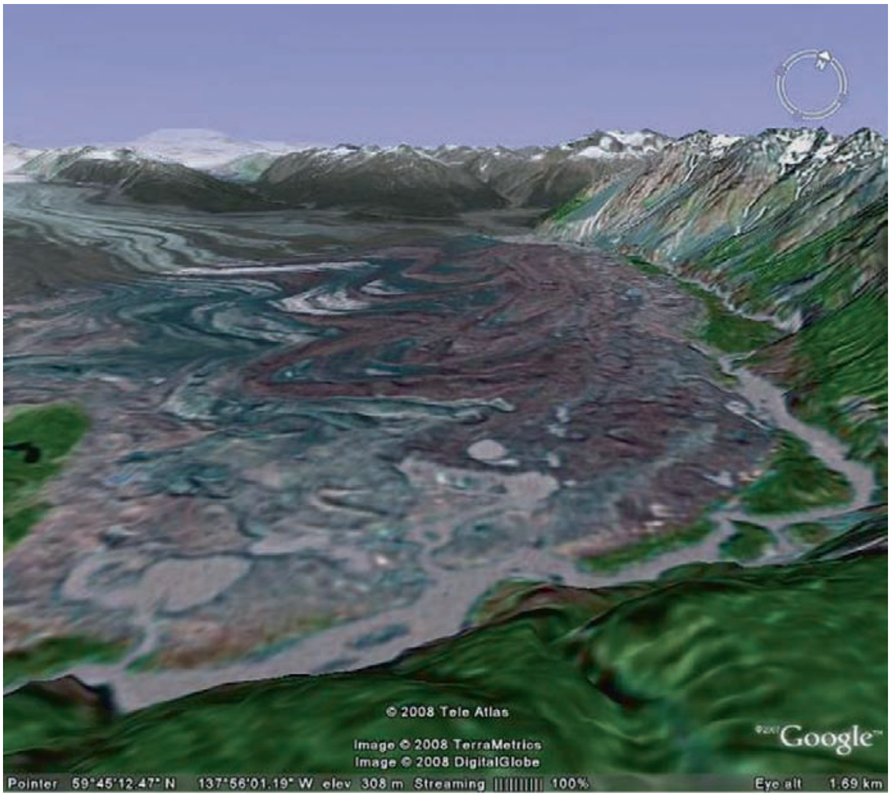

Fig. 29.10 Surging Tweedsmuir Glacier threatens to dam Alsek River in northwestern British Columbia

Landslide dams involving soil are especially common in northwestern Alberta and northeastern British Columbia (Cruden et al. 1993, 1997; Geertsema et al. 2006). Here deep-seated landslides in clayey glaciolacustrine deposits and tills commonly impound streams. On large rivers the dams rarely persist for more than a few hours, but on their smaller tributaries dams may persist for decades (Fig. 29.12).

Fig. 29.11 Lake No Lake, shown drained in 2001. Note the icebergs strewn over the lake floor. Tulsequah Glacier in background. The lake drains under the glacier one to two times annually

Rock debris dams originate from rock slides and occur in mountainous areas around the world (Costa and Schuster 1988). While rock slide dams may be porous, they are also among the longest-lived natural dams. Figure 29.13 shows an example of a rockslide in the Canadian Northwest Territories. The rock slide dammed Cathedral Creek and its tributary.

There are also other natural dams made entirely of rock. Lava flows have impounded rivers in northwestern British Columbia. In 1775 a lava flow in Nass Valley (Cathie Hickson, personal communication) created Lava Lake which persists to this day.

Catastrophic outbursts from landslide dams in western Canada are relatively rare. Usually dams are gradually incised. Flood volumes may be significant and can be traced on hydrographs. In exceptional cases dam bursts can be catastrophic. In notes from the Hudson Bay Journal John McLean (1849) wrote: "*I observed at one place a tremendous landslip, caused by the water undermining the soil. Trees*

Fig. 29.12 Contrasting landslide dams on Buckinghorse River (**a**) and a tributary of Buckinghorse River (**b**). The dam on the tributary has existed for more than a decade

were seen in an inverted position, the branches sunk in the ground and the roots uppermost; others with only the branches appearing above the ground; the earth rent and intersected by chasms extending in every direction; while piles of earth and stones intermixed with shattered limbs and trunks of trees, contributed to increase the dreadful confusion of the scene. The half of a huge hill had tumbled into the river, and dammed it across, so that no water escaped for some time. The people of Dunvegan, seeing the river suddenly dry up, were terrified by the phenomenon, but they had not much time to investigate the cause: the river as suddenly reappeared, presenting a front of nearly twenty feet in height, and foaming and rushing down with the noise of thunder." The landslide dam and outburst flood were thought to have happened sometime in the 1820s (Ted Binnema, personal communication).

Fig. 29.13 Rockslide dam impounding Cathedral Creek and its tributary in the Northwest Territories

29.9.3 Beaver Dams

Beaver (*Castor Canadensis*) dams are common in forested areas of western Canada. Beavers construct dams of sticks and mud. Breaches in the dams are continuously repaired by the beaver while local food supplies (the inner bark of deciduous trees) last, usually six to ten years. Dams are abandoned and prone to failure after the food supply is exhausted. Beaver dam failures may cause minor washouts that plague highways and railways. Occasionally, where beavers dam the outlet streams of lakes, failures can be catastrophic. Case et al. investigated a beaver dam failure near Prince George, BC, where the outlet stream of a 60 ha lake was raised 2.5 m. When the dam failed, 1.5 Mm^3 of lake water eroded and rerouted the outlet creek over a distance of 4 km. 80,000 m^3 of gravel was deposited at the mouth of the stream.

29.10 Causes and Timing of Landslide Distributions in Upland Northern England, UK

Wishart Mitchell (Durham University, England)

Mass movements are a natural component of the geomorphic system of upland areas. Bedrock conditions in northern England coupled with past climatic changes have provided ideal geotechnical conditions for slope failures at a variety of spatial and temporal scales. Attempts at providing a realistic inventory for northern England has shown that the number of landslides is seriously under-represented and that that they are much more widely distributed than previously envisaged. It is also apparent that many of the landslides are inactive having failed sometime in the past; however, there is a notable paucity of dates on landslides in this region. This paper reports present knowledge of the landslide distribution in the two main uplands of the Lake District and the Pennines examining the causes of such failures with particular reference to the timing of events. This may be of importance with respect to climate change which may lead to reactivation of currently stable slopes.

Landslide types within northern England range from extensive deep-seated bedrock failures to shallow translational failures within superficial deposits. The largest mass movements are recorded in the upland areas of the Lake District and the Pennines where there is sufficient relief to have promoted slope instability, reflecting geological conditions associated with variable lithology and bedrock discontinuities. This is particularly the case within the Pennines which are composed of Carboniferous sedimentary rocks associated with marine and deltaic sedimentation, exposing thick mudstone sequences overlain by coarse sandstones.

The cold climates of the Pleistocene affected the uplands of northern England in a number of ways. Although there is clear evidence across the region for the impact of ice sheets and valley glaciers, more important for slope development was the former presence of periglacial conditions particularly permafrost. This has led to the widespread redistribution of glacial and colluvial deposits that have failed as shallow translational and rotational landslides along many river valleys. Unlike the majority of larger deep-seated failures, many of these appear to be active as streams undercut slopes.

The rapid climatic ameliorations that marked the end of the cold stages would have been ideal conditions for slope failure and many of the larger deep seated landslides appear to relate to circumstances during deglaciation during the Late-glacial period associated with the disappearance of the last ice sheet and subsequently at the beginning of the Holocene following the Younger Dryas cold event. However, there is also evidence that many slope failures occurred during wetter and cooler phases of the Holocene demonstrating that evolution of the present landscape is complex and that smaller scale climate changes are important if determining slope stability in northern England. Improved dating of such events is therefore important in assessing the future impact of climate change.

29.11 Landslide tragedy of Bangladesh

Golam Sarwar (Committed to Earth Care, Bangladesh)

Landslide is a regular geologic hazard in Bangladesh, especially in Chittagong, the southeastern part of the country. Impacts of landslides on Bangladesh were studied using multidisciplinary approach taking the landslide of 11 June, 2007 as a reference. Landslides have caused the death to more than 300 people in Bangladesh since 2000, with a loss of hundreds of houses and millions of dollars of properties. A single event, the landslide of 11 June, 2007 caused the death of 135 people, including 59 children, and affected 1.5 million

Most of the landslides happened after heavy rainfall. However, the root cause of landslides of the area is the cutting of hills for urban development. Cutting hills in non-scientific way turn them unstable. In the City of Chittagong, 12 points are identified where hill cutting is done indiscriminately. More than sixty percent of the hills in the city have been converted into residential areas. Hills are also cut for the construction of brickfields and for the construction of roads. Infiltration of rainwater into the hills turned the soils heavy; the unstable hills could not support the weight and caused landslide in Chittagong. Heavy monsoon rainfall intensified by a strong storm from the Bay of Bengal caused abnormal precipitation in the area, which triggered the landslides. The combined effect of hill cutting and climatic change caused the 11 June tragedy.

A geophysical analysis is needed for a complete understanding of the landslides of Chittagong. People in the area are not aware of landslides and their potential for damage. People need to be aware of the potential risk of building house on hill slopes.

Detailed area planning for the urban area region and a comprehensive land-use planning are needed for Chittagong area to minimize landslide impacts. Influential people are involved in hill cutting in Bangladesh, violating existing rules and regulations. Legal instruments should be in place and the enforcement of existing rules should be ensured to avoid future landslide tragedies like that of 11 June.

References

Ashmore P, Church M (2001) The impact of climate change on rivers and river processes in Canada. Geological Survey of Canada Bulletin, 555

Borgatti L, Soldati M, Surian N (2001) Rapporti tra frane e variazioni climatiche: una bibliografia ragionata relativa al territorio europeo. Il Quaternario, 14: 137–166

Bovis MJ, Jones P (1992) Holocene history of earth flow mass movement in south–central British Columbia: the influence of hydroclimatic changes. Canadian Journal of Earth Sciences, 29: 1746–1755

Bovis MJ, Jakob M (2000) The July 29, 1998, debris flow and landslide dam at Capricorn Creek, Mount Meager volcanic complex, southern Coast Mountains, British Columbia. Canadian Journal of Earth Sciences, 37: 1321–1334

Bradley RS, Jones PD (1993) 'Little Ice Age' summer temperature variations: their nature and relevance to recent global warming trends. The Holocene, 3: 367–376

Briffa KR, Jones PD, Schweingruber FH, Osborn TJ (1998) Influence of volcanic eruptions on Northern Hemisphere summer temperature over the last 600 years. Nature, 393: 450–455

Brooks GR (1994) The fluvial reworking of late Pleistocene drift, Squamish River drainage basin, southwest British Columbia. Géographie physique et Quaternaire, 48: 51–68

Brooks GR, Evans SG, Clague JJ (2001) Flooding. In: Brooks, GR (ed), A synthesis of geological hazards in Canada. Geological Survey of Canada Bulletin 548, pp 101–143

Busche D (2001) Early Quaternary landslides of the Sahara and their significance for geomorphic and climatic history. Journal of Arid Environment, 49: 429–448

Butler D (1989) Snow avalanche dams and resultant hazards in Glacier National Park, Montana. Northwest Science, 63: 109–115

Church M (1983) Pattern of instability in a wandering gravel bed channel. In: Collinson JD, Lewin J (eds), Modern and ancient fluvial systems, Special Publication 6, International Association of Sedimentologists, pp 169–180

Church M, Ryder JM (1972) Paraglacial sedimentation: A consideration of fluvial processes conditioned by glaciation. Geological Society of America Bulletin, 83: 3059–3072

Clague JJ, Evans SG (1994) Formation and failure of natural dams in the Canadian Cordillera. Geological Survey of Canada Bulletin, 464

Clague JJ, Evans SG (2000) A review of catastrophic drainage of moraine-dammed lakes in British Columbia. Quaternary Science Reviews, 19: 1763–1783

Clague JJ, Turner RJW, Reyes A (2003) Record of recent river channel instability, Cheakamus Valley, British Columbia. Geomorphology, 53: 317–332

Costa JE, Schuster RL (1988) The formation and failure of natural dams. Geological Society of America Bulletin, 100: 1054–1068

Crowley TJ (2000) Causes of climate change over the past 1000 years. Science, 289: 270–277

Crowley TJ, Kim K-Y (1996) Comparison of proxy records of climate change and solar forcing. Geophysical Research Letters, 23: 359–362

Cruden DM, Keegan TR, Thomson S (1993) The landslide dam on the Saddle River near Rycroft, Alberta. Canadian Geotechnical Journal, 30: 1003–1015

Cruden DM, Lu Z-Y, Thomson S (1997) The 1939 Montagneuse River landslide, Alberta. Canadian Geotechnical Journal, 34: 799–810

Davies MCR, Hamza O, Harris C (2001) The effect of rise in mean annual temperature on the stability of rock slopes containing ice-filled discontinuities. Permafrost and Periglacial Processes, 12: 137–144

Desloges JR, Church M (1987) Channel and floodplain facies in a wandering gravel-bed river. In: Ethridge FG, Flores RM (eds), Recent developments in fluvial sedimentology, Special Publication 39, Society of Economic Paleontologists and Mineralogists, Tulsa, pp 99–109

Evans SG, Clague JJ (1994) Recent climatic change and catastrophic geomorphic processes in mountain environments. Geomorphology, 10: 107–128

Evans SG, Clague JJ (1999). Rock avalanches on glaciers in the Coast and St. Elias Mountains, British Columbia. In: Proceedings of the 13th annual Vancouver geotechnical conference, BiTech Publishers, Richmond, BC, pp 115–123

Fischer L, Kääb A, Huggel C, Noetzli, J (2006) Geology, glacier retreat and permafrost degradation as controlling factor of slope instabilities in a high-mountain rock wall: the Monte Rosa east face. Natural Hazards and Earth System Sciences, 6: 761–772

Geertsema M, Clague JJ (2005) Jökulhlaups at Tulsequah Glacier, northwestern British Columbia, Canada. The Holocene, 15: 310–316

Geertsema M, Clague JJ, Schwab JW, Evans SG (2006) An overview of recent large catastrophic landslides in northern British Columbia. Engineering Geology, 83: 120–143.

Gottesfeld AS, Johnson-Gottesfeld LM (1990) Floodplain dynamics of a wandering river, dendrochronology of the Morice River, British Columbia, Canada. Geomorphology, 3: 159–179

Goudie A (1992) Environmental change (3rd ed). Clarendon Press, Oxford

Grove JM (1988) The Little Ice Age. Methuen Press, London

Gruber S, Haeberli W (2007) Permafrost in steep bedrock slopes and its temperature-related destabilization following climate change. Journal of Geophysical Research, 112, F02S18, DOI: 10.1029/2006JF000547

Gruber S, Hoelzle M, Haeberli W (2004) Permafrost thaw and destabilization of alpine rock walls in the hot summer of 2003. Geophysical Research Letters, 31: 4pp

Harris C, Davies MCR, Etzelmuller B (2001) The assessment of potential geotechnical hazards associated with mountain permafrost in a warming global climate. Permafrost and Periglacial Processes, 12: 145–156

Hendy EJ, Gagan MK, Alibert CA., McCulloch MT, Lough JM, Isdale PJ (2002) Abrupt decrease in tropical Pacific sea surface salinity at the end of Little Ice Age. Science, 295: 1511–1514

Holm K, Bovis M, Jakob M (2004) The landslide response of alpine basins to post- Little Ice Age glacial thinning and retreat in southwestern British Columbia. Geomorphology, 57: 201–216

Holzhauser H (1985) Neue Ergebnisse zur Gletscher- und Klimageschichte des Spätmittelalters und der Neuzeit. Geographica Helvetica, 40: 168–185

Karlén W (1976) Lacustrine sediments and tree limit variations as evidence of Holocene climatic variations in Lappland, northern Sweden. Geografiska Annaler, 58: 1–34

Karlén W, Matthews JA (1992) Reconstructing Holocene glacier variations from glacial lake sediments: Studies from Nordvestlandet and Jostedalsbreen-Jotunheimen, southern Norway. Geografiska Annaler, 74: 327–348

Lamoureux S (2000) Five centuries of interannual sediment yield and rainfall-induced erosion in the Canadian High Arctic recorded in lacustrine varves. Water Resources Research, 36: 309–318

Larson CF, Motyka RJ, Freymueller JT, Echelmeyer KA, Ivins ER (2005) Rapid viscoelastic uplift in Southeast Alaska caused by post-Little Ice Age glacial retreat. Earth and Planetary Science Letters, 237: 548–560

Lawrence DB (1950) Glacier fluctuations for six centuries in southeastern Alaska and its relation to solar activity. Geographical Review, 40: 191–222

Lean J, Beer J, Bradley R (1995). Reconstruction of solar irradiance since 1610: implications for climate change. Geophysical Research Letters, 22: 3195–3198

Leonard EM (1986) Varve studies at Hector Lake, Alberta, Canada, and the relationship between glacial activity and sedimentation. Quaternary Research, 25: 199–214

Leonard EM (1997) The relationship between glacial activity and sediment production: Evidence from a 4450-year varve record of neoglacial sedimentation in Hector Lake, Alberta, Canada. Journal of Palaeolimnology, 17: 319–330

Lewis D, Smith D (2004) Dendrochronological mass balance reconstruction, Strathcona Provincial Park, Vancouver Island, British Columbia, Canada. Arctic, Antarctic, and Alpine Research, 36: 598–606

Luckman BH (2000) Little Ice Age in the Canadian Rockies. Geomorphology, 32: 357–384

Luckman BH, Villalba R (2001) Assessing the synchroneity of glacier fluctuations in the western Cordillera of the Americas during the last millennium. In: Markgraf V (ed), Interhemispheric climate linkages, Academic Press, New York, pp 119–140

Luckman BH, Wilson RJS (2005) Summer temperatures in the Canadian Rockies during the last millennium; a revised record. Climate Dynamics, 24: 131–144

Maizels JK (1979) Proglacial aggradation and changes in braided channel patterns during a period of glacier advance: An Alpine example. Geografiska Annaler, 61: 87–101

Mann ME., Bradley RS, Hughes MK (1998) Global-scale temperature patterns and climate forcing over the past six centuries. Nature, 392: 779–787

Mann ME, Cane MA, Zebiak SE, Clement A (2005) Volcanic and solar forcing of the tropical Pacific over the past 1000 years. Journal of Climate, 18: 447–456

McLean J (1849) Notes of a twenty-five years' service in the Hudson's Bay Territory. Richard Bentley, London, Vol. 1

Moberg A, Sonechkin DM, Holmgren K, Datsenko NM, Karlén W (2005) Highly variable Northern Hemisphere temperatures reconstructed from low- and high-resolution proxy data. Nature, 433: 613–617

Nesje A, Dahl SO (2003) The 'Little Ice Age' – Only temperature? The Holocene, 13: 139–145

O'Connor JE, Costa JE (1993) Geologic and hydrologic hazards in glacierized basins in North America resulting from 19th and 20th century global warming. Natural Hazards, 8: 121–140

Panizza M (1990) The landslides in Cortina d'Ampezzo (Dolomites, Italy). In: Cancelli A (ed), ALPS 90–6th ICFL, Switzerland – Austria – Italy, Conference Proceedings. Università degli Studi di Milano, pp 55–63

Porter SC (1986) Pattern and forcing of Northern Hemisphere glacier variations during the last millennium. Quaternary Research, 26: 27–48

Reimer PJ, Baillie MGL, Bard E, Bayliss A, Beck JW, Bertrand CJH, Blackwell PG, Buck CE, Burr GS, Cutler KB, Damon PE, Edwards RL, Fairbanks RG, Friedrich M, Guilderson TP, Hogg AG, Hughen KA, Kromer B, McCormac FG, Manning SW, Ramsey CB, Reimer RW, Remmele S, Southon JR, Stuiver M, Talamo S, Taylor FW, van der Plicht J, Weyhenmeyer CE (2004) IntCal04 Terrestrial radiocarbon age calibration, 26 – 0 ka BP. Radiocarbon, 46: 1029–1058

Ruddiman WF (2003) The anthropogenic greenhouse era began thousands of years ago. Climatic Change, 61: 261–293

Sidle RC, Taylor D, Lu XX, Adger WN, Lowe DJ, de Lange WP, Newnham RM, Dodson JR (2004) Interactions of natural hazards and society in Austral–Asia: evidence in past and recent records. Quaternary International, 118–119: 181–203

Smith LN (2001) Columbia Mountain landslide: late–glacial emplacement and indications of future failure, Northwestern Montana, USA. Geomorphology, 41: 309–322

Soldati M, Corsini A, Pasuto A (2004) Landslides and climate change in the Italian Dolomites since the Lateglacial. Catena, 55: 141–161

Stuiver M, Reimer PJ, Reimer R (2004) Calib radiocarbon calibration (5.0.2). http://calib.qub.ac.uk/calib/calib.html (November 2006)

Thomas MF (1999) Evidence for high energy landforming events of the central African plateau: eastern province, Zambia. Zeitschrift Geomorphologie N.F., 43: 273–297

Trauth MH, Bookhagen B, Marwan N, Strecker MR (2003) Multiple landslide clusters record Quaternary climate changes in the northwestern Argentine Andes. Palaeogeography, Palaeoclimatology, Palaeoecology, 194: 109–121.

Watanabe T, Nakamura N, Khanal NR (2000) Mountain hazards in the Kanchanjunga area, eastern Nepal; landslides developed on lateral moraines. Journal of Nepal Geological Society, 22: 525–532

Wiles GC, Barclay DJ, Calkin PE (1999) Tree-ring dated 'Little Ice Age' histories of maritime glaciers from western Prince William Sound, Alaska. The Holocene, 9: 163–173

Wiles GC, D'Arrigo RD, Villalba R, Calkin PE, Barclay DJ (2004) Century-scale solar variability and Alaskan temperature change over the past millennium. Geophysical Research Letters, 31: L15203

Wilkie KMK (2006) Fluvial response to late Holocene glacier fluctuations in the Nostetuko River valley, southern Coast Mountains, British Columbia. MSc thesis, Simon Fraser University, Burnaby, BC

Zhang Y, Chen W, Riseborough DW (2006) Temporal and spatial changes of permafrost in Canada since the end of the Little Ice Age. Journal of Geophysical Research, 111(D22): 14pp

Economic and Social Impacts of Landslides 30

Oddvar Kjekstad and Lynn Highland

Abstract The Session, Socioeconomic Impacts of Landslides, was organized to provide discussions on the socioeconomic impact of landslide events as well as best practice for mitigation of the risk associated with landslides. Social and economic losses, and their quantification, the consequences of landslides on infrastructure development, and land use policy, are critical aspects of socio-economic issues related to landslides. In addition the session will include case studies on recovery and resettlement, measures to reduce social vulnerability, investments for landslide risk mitigation and reduction, and insurance issues for landslide risk mitigation and reduction.

Keywords Landslide • Socio-economic losses • Fatalities • Direct costs • Indirect costs • Insurance • Vulnerability • Risk

30.1 Introduction and Scope

This report provides an overview of the myriad issues associated with socio-economic impacts of landslides around the world, together with examples of research that will be either presented or discussed at the World Landslide Forum, taking place in Tokyo, Japan, November, 2008. This report will not be exhaustive but will provide the basis for a discussion of landslide socio-economic impact information that is available either statistically, as case studies and/or based on investigations of targeted research locations. Much of the landslide information and data about world-wide landslide occurrence and effects is of an ad-hoc nature, presented in various languages, and landslide inventory collection and databases, for example, are not homogenous, or based on a universally-accepted methodology that cuts across nationalities. However, there is notable research which attempts to quantify the socio-economic effects of landslide hazard and there exist extensive activities and research on the mitigation of the hazard, both at the local level and nationally.

30.2 Background and Overview of Global Landslide Hazards

Reliable numbers for the socio-economic impact from landslides are difficult to obtain on a global scale, mainly because the landslide hazard assessment is often merged with other associated natural disasters such as earthquakes, flooding, meteorological events such as hurricanes or typhoons, and

Oddvar Kjekstad (✉)
International Centre for Geohazard – Norwegian Geotechnical Institute, Oslo, Norway

Lynn Highland
U.S. Geological Survey, Denver, CO 80225, USA

© Springer-Verlag Berlin Heidelberg 2009

wildfire, and not differentiated as a separate hazard. This often contributes to reducing the concern of individuals and authorities have about landslide risk. Examples of this multi-layered phenomenon of multiple hazards are addressed in this report.

It may seem that the frequency of landslide disasters is rising, but this perceived rise may be more a function of vulnerability (increased exposure of populations to hazard) than an actual increase in intensity or frequency. Because of this vulnerability, the thresholds for damage, property loss and fatalities can be reached with ever lower intensity of landslides. There is increased susceptibility of surface soil to instability as a result of more extensive human interaction of different kinds, increased vulnerability of exposed population and infrastructure as a result of growing urbanization, uncontrolled land-use and increased forest clearance and crop-growing practice (Kjekstad, 2007; Sidle and Ochiai, 2006). The effects of climate change must also be factored in at some level, as changing precipitation patterns, increased or decreased severe weather in an area, and changing migration and settlement based on favorable or unfavorable climate for farming occur. These changes may cause frequency, intensity and location of hazardous areas to change either rapidly, or long-term.

Landslides are one of the most widespread hazards on Earth and cause thousands of deaths and injuries and billions of dollars in damage worldwide each year. Statistics from The Centre for Research on the Epidemiology of Disasters (CRED, http://www.cred.be/) show that landslides contribute to about 17% of the fatalities due to natural hazards.

A World Bank report (Dilley et al., 2005) presents the following profile of world-wide exposure to landslide hazard issues:

- Land area of the globe exposed to landslides: 3.7 million km^2
- Population exposed: 300 million, or 5% of the world population
- Land area identified as high risk zones: 820,000 km^2
- Population living in high risk areas: 66 million people

When it comes to fatalities, the Americas (North, Central and South), and China, in general, have had the highest number. The economic losses from landslides are certainly underestimated (or not quoted at all), as landslides often occur as mentioned, as a consequence of other natural hazards such as earthquakes or floods.

Petley (2008) reports that in terms of the occurrence of landslide fatalities in the year 2007, by nation, the most seriously affected country was China with 695 landslide-induced deaths, followed by Indonesia (465), India (352), Nepal (168), Bangladesh (150) and Vietnam (130). In terms of trigger, 89.6% of worldwide fatalities were a result of landslides caused by intense and/or prolonged precipitation. Other triggering processes were construction (mostly undercutting of slopes) (3.4% of deaths), mining and quarrying (1.8% of deaths) and earthquakes (0.7% of deaths). No cause was identified for 3.4% of all landslides.

From a seasonal perspective, the dominant months for landslide occurrence in 2007, were June (12.7% of the fatalities), July (25.1% of the fatalities) and August (10.5% of the fatalities). No other month exceeded 10% of the total number of fatalities. This reflects the geographical distribution of the events, which is dominated by areas affected by the Asian summer monsoon. In 2007 the Southwest monsoon rainfall was particularly intense in Southern Asia in July and August, resulting in floods that affected millions and the extensive occurrence of fatalities from landslides. In contrast, tropical cyclones that resulted in landfall, especially in Central America and the Caribbean, which historically leads to large numbers of landslides, was much lower than the long-term average. The result of this appears to be an anomalously low landslide event rate in these areas. (It should be noted that any perceived rise in landslide occurrence, may be a function of increased exposure of population to the hazard as well as the fact that population is becoming more vulnerable). As with previous years, the number of recorded fatal landslides Africa remains very low (13 in 2007). It is likely that this indicates that a substantial number of fatal landslide events are not being reported, as the number of people exposed to hazards from landslides is high. In terms of economic impact, it is difficult to separate the losses from direct and indirect causes, as the losses are usually not well documented. Some figures from various sources are available:

- Annual landslide costs in Italy, Austria, Switzerland and France are estimated as USD 1–5 billion
- Munich Re numbers from the year 2000 alone show that storm surges, mudflows and landslides in the Swiss Alps during one season, September 2000 to March 2001, generated economic losses of about USD 8.5 billion. This data from 2000 will in itself modify the average annual losses for this region,
- Annual losses in the United States exceed USD 3.5 Billion (converted to Year 2007 US Dollars) (Schuster and Highland, 2001).
- Cruden et al. (1989) estimated that total annual landslide costs for Canada as USD 1 billion ($1.4 billion) per year, when converted to Year 2007 US dollars.

In the 20th century, the problem of deaths and injuries due to landslides was exacerbated by burgeoning populations in landslide-prone areas; undoubtedly, this trend will continue in the 21st century.

A recent effort to more accurately quantify the socio-economic impacts from landslides on a global basis, in a mapped GIS format, has been facilitated by a consortium of entities, including the World Bank. In the publication, Global Hot Spots for Landslide and Avalanche Hazard (Nadim et al., 2006), the probability of landslide and avalanche occurrence is estimated by the modeling of physical processes and combining the results with statistics from past experience. The main input data used in the hazard assessment are topography and slope angles, extreme monthly precipitation, seismic activity, lithology, mean temperature in winter months (for snow avalanches) and hydrological conditions. For the estimation of risk, the computations were based on human losses as recorded in various natural disaster impact databases. The estimation of expected losses was achieved by first combining the landslide frequency and the population exposed, in order to estimate the physical exposure, and then doing a regression using different sets of uncorrelated socio-economical parameters. The study identified the socio-economic parameters that seem to have the strongest correlation with expected fatality due to landslides.

This study clearly shows that the following countries and geographical areas identified as landslide hazard hotspots:

- Central America
- North-western South America
- The Caucasus region
- The Himalayan belt
- Taiwan
- Philippines
- Indonesia
- Italy
- Japan

The conclusions of this study are all based on a global model which does have some shortcomings when used at a local level. There will be future refinements of the model with new input parameters, new data, and modification and improvement of the methodology (Nadim et al., 2006).

30.3 Landslide Losses: Direct vs. Indirect Costs

Direct costs are the repair, replacement, or maintenance resulting from damage to property or installations within the boundaries of the responsible landslides or from landslide-caused flooding (Schuster, 1996). All other costs of landslides are indirect. Some examples of indirect landslide losses are:

1. Loss of industrial, agricultural, and forest productivity and tourist revenues as a result of damage to land or facilities or interruption of transportation systems (Fig. 30.1);
2. Reduced real estate values in areas threatened by landslides
3. Loss of tax revenues on properties devalued as the result of landslides;
4. Measures that are required to be taken, to prevent or mitigate additional landslide damage;
5. Adverse effects on water quality in streams and irrigation facilities outside the landslide;
6. Loss of human or animal productivity because of injury, death, or psychological trauma; and
7. Secondary physical effects, such as landslide-caused flooding, for which losses are both direct and indirect. (Table 30.1 shows estimated average annual costs in USD, of landslides in various nations, from a 2006 report by Sidle and Ochiai,

Fig. 30.1 Economic consequences of landslides on roads in Bhutan are substantial. The photo shows landslides challenges at Jumjha along the highway between the capital City of Thimpu to the Indian interior. This highway is frequently closed for several weeks during the monsoon due to blocking of the roads. This results in shortages of essential supplies (e.g. food & gasoline). Investigations are being performed to bypass this huge landslide by the use of a tunnel (Photo from Norwegian Geologic Institute (NGI))

which attempts to contrast direct costs with total costs.) Indirect costs may exceed direct costs; unfortunately, most indirect costs are difficult to evaluate and thus are often ignored or, when estimated, are too conservative.

One of the major problems of tracking landslide losses is that in many cases, landslides occur within the realm of a multi-hazard scenario, and losses that are actually landslide losses are attributed to the triggering event, and all losses become merged into one numerical figure. For example, one of the most damaging aspects of volcanic eruptions is the ensuing hazards from volcanic landslides. These volcanic landslides are characterized in some cases by edifice collapse, and also, rapidly melting snow, due to the intense heat from lava, and friction

Table 30.1 Estimated average annual costs (in USD) of landsides in various nations

Country	Average Annual Direct Costs	Average Annual Total costs	Comments
Canada		$70 milllion	A more recent estimate of total costs is up to $1.4 billion annually
Japan	$1.5 billion	$4 billion	
Korea	$60 million	–	Based on poor records
Italy	–	$2.6–5 billion	Rough Estimate
Sweden	$10–20 million		
Spain	$0.2 billion		
Former USSR	$0.5 billion		
China	$0.5 billion	–	Costs based on valuations in 1989
India	$1.3 billion		
Nepal	$19.6 million	–	Includes flood damage, but likely incomplete
New Zealand	–	26.3 million	90% of costs are sustained in rural areas

Source: Table modified from Sidle and Ochiai, 2006 generated by debris avalanches, which precipitates rapid-onset debris flows. Earthquakes that occur in volcanic areas also may increase the intensity of the hazard, causing weak volcanic rock to fail and become fast-moving debris avalanches (Fig. 30.2).

Lahars are often more impacting than the advance of lava, and can become fast-moving traps that populations living on volcano slopes and bases of these slopes cannot quickly evade in time. One example of the difficulty of separating losses by individual hazard, is the calculated monetary loss from the great Alaska earthquake of 1964. This earthquake caused unprecedented landslide occurrence, both in number and intensity, and in addition, a landslide-generated tsunami, which was so large that it not only damaged the area around Anchorage, Alaska but travelled as far as the northern coast of California, and caused fatalities and damage there. The high losses from this earthquake have traditionally been attributed to losses from earthquake shaking and faulting, even though the losses from landslides were much greater. Only intensive field work and other investigations revealed the true nature of the event, as a complex, multi-hazard phenomenon. The Northern Pakistan M = 7.6 earthquake of October 8, 2005 is another example of a primary hazard, a large earthquake, triggering at least one devastating debris avalanche (Fig. 30.3). The earthquake caused many smaller landslides and extensive cracking of the ground, on slopes. The major debris avalanche which buried a village, also created a landslide dam in a nearby river. The great volume of material precluded the landslide dam's removal and the blockage caused flooding upstream, and impeded the river flow, downstream (Harp and Crone, 2005). Eventually, a man-made channel was created over the landslide dam to facilitate a resumption of at least some of the former flow-rate of the river.

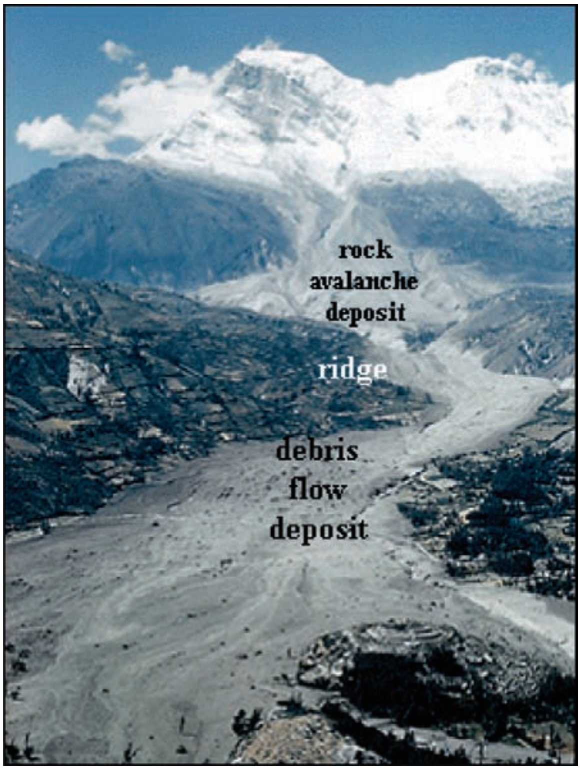

Fig. 30.2 A photograph of the after-effects of a multi-hazard event. It is an aerial view showing part of the Andes Mountains and Nevado Huascaran, the highest peak in Peru, South America. A massive avalanche of ice and rock debris, triggered by the May 31, 1970 earthquake, buried the towns of Yungay and Ranrahirca, killing more than 20,000 people. The avalanche started with a sliding mass of glacial ice and rock about 1,000 m wide and 1.6 km long that swept downslope for about 5.4 km to Yungay at an average speed of over 160 km per hour. The ice picked up morainal material of mud and rocks together with large quantities of water. (Photograph by Servicio Aerofotografico National, graphics by George Plafker, U.S. Geological Survey). Photograph and information from the Photographic Archives of The U.S. Geological Survey. http://libraryphoto.cr.usgs.gov/

Fig. 30.3 Photograph of the Hattian Bala, Pakistan debris avalanche, resulting from an earthquake (M = 7.6) in 2005. The view is the impounded lake, created by a landslide dam

Global climate change effects, are another example of how the landslide hazard is closely associated with another, primary event, and may not be revealed in landslide statistics. Glacial retreat, due to warming, in some cases, causes the lateral slopes which held the ice in place to become de-stabilized, resulting in slope failure, including glacial lake outburst (GLOF). With global climate change, this type of hazard is an increasing threat to human settlement and infrastructure in Nepal, and to some extent also in Bhutan and India (Fig. 30.4). In some cases insurance policies for new hydroelectric power plants in that region have become very expensive due to threats from GLOF. Other types of hazards occur due to glacial regret. For example, in Alaska for example, some glaciers are retreating, resulting in slope destabilization and failure, which in turn have caused major tsunamis when the slope failure occurs in bays, inlets, or other coastal areas where glaciers border these areas. Fishing, boating activities and water quality have been affected (Wieczorek et al., 2007).

Fig. 30.4 The Gangotri Glacier, India where the glacial retreat from the Indian sub-continent has been about 18 m per year. This study was carried out by The International Centre for Integrated Moutain Development (ICIMOD), Nepal, in 2007, to understand the impact of climate change on glacier retreats in the Himalaya Mountains (Photograph from ICIMOD)

30.4 Impacts of Landslides in Developing Nations

In absolute number, material damage from natural disasters in developed nations is the highest. However, as stated in Kjekstad (2007), a more realistic approach to ascertaining impact is to normalize the damage, in relation to a country's Gross National Product (GDP), using a comparative ratio. Some examples of these ratios are notable: 2% for the Kobe Earthquake 1995, 10% for the El Salvador Earthquake 2001, 5% for the Pakistan Earthquake 2005 (with landslides), and 4% for the tropical storm (with landslides) in Guatemala 2005. Clearly, it is in a nation's best interest to reduce these ratios, as to better use its remaining budget and wealth for economic growth. Kjekstad in the 2007 report notes three so-called pillars that embody logical steps and procedures for mitigating the hazard from landslides:

- Pillar 1: Hazard and Risk Assessment
- Pillar 2: Landslide Mitigation Measures
- Pillar 3: International Collaboration and Support

There is much that developing nations can learn from the foils, follies, and successes of the industrialized nations, and imparting such information by means of international meetings, sharing of databases and GIS information, and cross-cultural collaborations are essential to the collective knowledge regarding landslide hazard reduction, and indeed, for all types of shared goals for understanding and mitigation.

The hazard will most probably increase as population grows, weather and climate become more extreme and anthropogenic triggers increase. The social impact of landslides is frequently underevaluated. Critical consequences are loss of life, land and property, disruption of transportation, stranded communities with sometimes food, water and shelter shortage, damage to communication systems, loss of productivity and other revenues such as from tourism, psychological trauma, costs for mitigation etc. An example of social impact is the December 1999 slide disaster in Venezuela, where 33,000 people, 8 months after the disaster occurred, still lived in shelters or barracks in appalling conditions. Very often, the social impact is most severe for the poor population, as this less affluent population lives in the most hazardous locations and with poorest housing quality.

The devastating 2006 Guinsaugon, Leyte Island, Philippines, a rockslide-debri avalanche, occurred in a faulted, tectonically active area of weathered volcanic soils, in an area of high rainfall, which was heavily forested, with a high population density (Fig. 30.5). Agricultural development in the valley bottom had a major effect on the run-out of the rock avalanche. In terms of post-failure behavior, the run-out of the rockslide –debris avalanche was exacerbated by undrained loading of rice paddy fields on the valley floor beneath the debris sheet, leading to a spreading and thinning of the rockslide-debris avalanche debris. The extremely large numbers of fatalities and devastation of human habitat, including critically-needed farmland is thought to be the result of the intersection of geological/tectonic, climatic and cultural factors – a multi-faceted hazardous situation (Evans et al., 2007).

Landslide disaster risk can be reduced by mitigating the hazard and/or the vulnerability. Land use planning can prevent settlement in dangerous areas. Technology for identification of landslide hazard hotspots areas is available. Threats can be mitigated through engineered solutions. Disaster preparedness has proven to be very important, and if well planned, efficient. Pilot projects on disaster insurance in Latin America have proven to be successful and will certainly find a wider application in the years to come.

Fig. 30.5 A rockslide debris avalanche which buried the village of Guinsaugon, Southern Leyte, Philippines in February, 2006 (Photo by University of Tokyo Geotechnical Team)

30.5 Challenges of Slope Engineering and Social Concerns for Landslides in Developed Nations – Example of Hong Kong

The combination of extremely hilly terrain, deep weathered rock profiles, high seasonal rainfall and dense population developments resulted in some serious landslide problems in the past. Following a number of disastrous landslides in the early 1970s, the Government created a specialized organization, the Geotechnical Engineering Office (GEO), to regulate slopes safety. This makes Hong Kong an excellent example of the evolution of public policy by confronting the challenging and successfully mitigating landslide risks in an area that experiences a very large vulnerable population. Upon its establishment, the GEO implemented a comprehensive Slope Safety Management System that confronted the slope safety problems with the following measures:

- Imposing geotechnical control of new slopes
- Retrofitting substandard man-made slopes
- Setting standards
- Controlling land use in development planning
- Implementing a Landslide Warning and emergency services

The Slope Safety System has been evolved over the years to meet the ever-increasing public expectation on slope safety. New impetuses include providing greening and landscaping treatment to slopes and launching public education to partner with the citizens to properly maintaining man-made slopes.

The Government of Hong Kong has drawn up tasks that: (1) all the high-risk man-made slopes affecting major roads and developments will have been dealt with by 2010, thereby substantially reducing the overall landslide risk, and (2) The GEO will launch a Landslip Preventive Mitigation Programme (LPMitP) to dovetail with the Landslip Preventive Measures Programme (LPMP) which is due for completion in 2010, in order to deal with the remaining landslide risks (HKSARG, 2007). Figure 30.6 shows the gradual reduction of the fatality rate from landslides, in Hong Kong, tracked beginning in the 1990 s and falling drastically by 2005 (Chan, 2007).

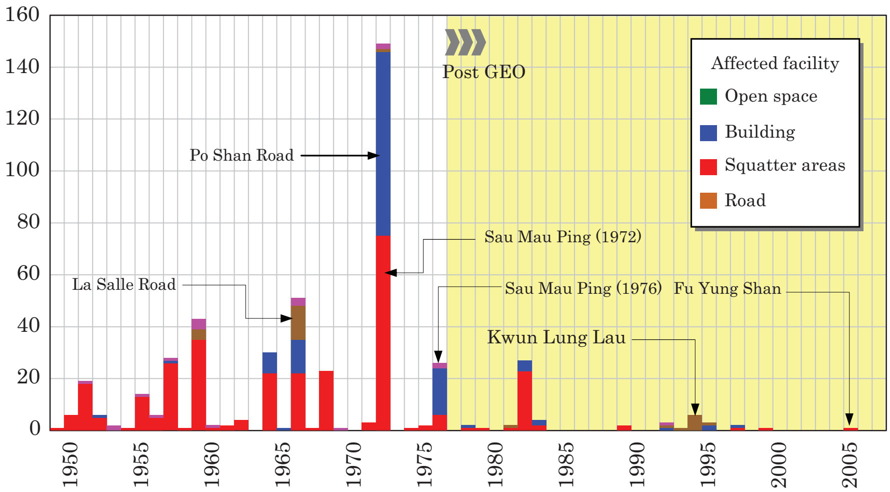

Fig. 30.6 Shows the gradual reduction of the fatality rate from landslides, in Hong Kong, tracked beginning in the 1950 s and falling drastically by 2005

Developed nations around the world have a varying approach to mitigating landslides but as economies develop, the price of mitigating destructive hazards becomes cost effective, based on the rising value of infrastructure and economic investment.

30.6 Human-caused Landslide Hazard

Landslides caused by human activity include those which result from construction of highways, logging roads, clearing land for crops, mining and quarrying, and any other activity that alters drainage patterns, changes in vegetation regimes, alters the grade of slopes, covers extensive areas through asphalt and concrete paving, and the excavation of large tracts of land, all of which change the morphology of the landscape.

Recent human settlements in the lower and middle Himalayas have also resulted in landslides causing damage to the lives and properties of the region. In the national highway between Sikkim and Tibet huge landslides have caused a disruption in the road communication route linking the capital city of Gangtok in Sikkim to the planar regions of India (Fig. 30.7).

Furthermore, landslides have also been caused by other types of man-made activities in the Himalayas. For example, Fig. 30.8 shows the approximately 700 m high Surabhi landslide that occurred after the building of a tourist resort in Northern India in 1998 (Vikram and Ahmed 2007). The landslide was presumably caused by lack of a drainage system beneath the resort and heavy rainfall.

One example of human-caused landslide hazard that has greatly impacted populations occurs in the Yangtze River, Three Gorges Dam area of central China. Millions of people live on the lower banks of the Yangtze River reservoir impoundment area, and many live on old landslide masses. The reservoir water level is being *slowly* raised, year by year, to allow for the orderly relocation of the millions of people living on the banks.

Fig. 30.7 Destruction of a commuter highway route to Sikkim Gangtok (Photograph from Bhasin et al., 2002)

Fig. 30.8 The approximately 700- m high Surabhi landslide that occurred after the building of a tourist resort in Northern India in 1998 (Vikram and Ahmed 2007). The landslide was presumably caused by lack of a drainage system beneath the resort and heavy rainfall

According to official statistics, 2,490 "slip masses" and 90 gullies created by mud-rock flows have been identified along the Yangtze River and its tributaries (Wu et al., 2001). Moreover, unlike many other large reservoirs around the world, which tend to be located in remote and sparsely populated areas, the Three Gorges reservoir area is so densely-populated that finding the space nearby to resettle people displaced by the reservoir has been difficult. Thus, even a moderate geological disaster in the reservoir area can entail enormous human and property losses (Fig. 30.9).

Experts are worried that filling the reservoir, and subsequent raising and lowering of the water level for annual flood seasons could activate the big landslide masses upstream of the Three Gorges Dam project.

China has made great advances in trying to reduce the fatalities from landslides through means of education, site monitoring, and early warning alert systems, and emergency response. Figure 30.10 shows the steady reduction in fatalities from 1998 to 2004. The goal is to reduce fatalities to 400 or less by 2010 (Zhang and Shan, 2005).

Fig. 30.9 Photo of the Quianjiangping landslide, located on a tributary of the Yangte River not far from the 3 Gorges Dam was re-activated one month after the filling of The Three Gorges Reservoir began, in 2003. 24 million cubic meters of landslide material slid into this tributary of the Yangtze, completely blocking the river. The landslide also created a 20-meter-high wave that capsized 22 boats. Within minutes, four factories, 300 homes and more than 1,000 mu (67 hectares) of farmland were destroyed. According to the official count, 14 people were killed and another 10 listed as missing. Low fatalities were due to the fact that people had been evacuated from the area when the landslide began cracking (Wang et al., 2004 – Photograph from Chinese National Geographic, no. 4, 2006, by Fan Xiao.)

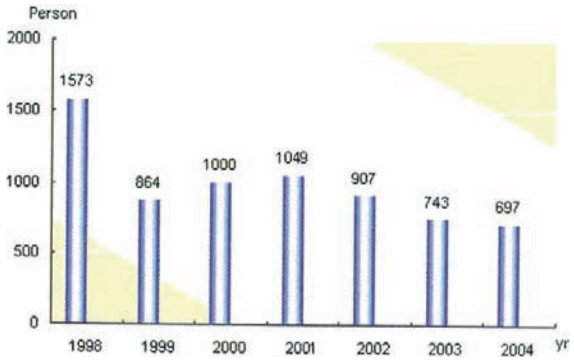

Fig. 30.10 Fatalities caused by geological hazards in 1998–2004. (Data from Ministry of Land and Resources of China. Graphic modified from Zhang and Shan 2005)

30.7 Socio-economic Impacts of Landslides in the Natural Environment

Many papers have been written on the socioeconomic impacts of landslides on the *built* environment. However, relatively few authors have discussed the effects of landslides on the *natural* environment, i.e., on (1) the morphology of both subaerial and submarine surfaces of the Earth, (2) the natural forests and grasslands that cover much of the Earth's surface, (3) quality of streams and other bodies of water, and (4) the habitats of native fauna, both on the Earth's surface and in its streams and oceans (Schuster, in press). Morphologic effects are part of a general tendency toward degradation of the Earth's surface by mass wasting and erosion. The effects on vegetation and wildlife are generally negative, in some cases disastrous (Schuster and Highland, 2006; 2007). Types of losses include, for example mass die-offs of fish, due to large amounts of landslide material contaminating bodies of water, directly impacting marine and riverine food sources which populations either consume or sell in local and/or national markets, destruction of forest access roads by ground failure which inhibits and/or disrupts commercial or locally-sustaining logging activity, and landslide dams which cause flooding of farmland, villages, and block the normal flow of downstream water, in turn, cutting off sources of water for drinking and irrigation.

Landslide activity triggered by wave action is the main process leading to the retreat of coastal cliffs. Cliff retreat has implications for a great deal of impact as a large percentage of people occupy steep coastal areas of the world. Commercial fishing, tourism, housing, and sediment loading are impacted by coastal retreat, and it is a landslide hazard that is not at the forefront of landslide research, at this time (Schuster and Highland, 2007).

Submarine, or what is known as sub aerial landslides occur in many areas of the world, particularly volcanic islands such as the Hawaiian Islands, Caribbean Islands and the Canary Islands. The hazard from this type of landslide has been studied in light of the potential for massive, damaging tsunamis that may occur after the rapid failure of steeply-situated, unconsolidated materials into oceans and inlets. Most areas that have experienced older or even ancient submarine landslides have the potential for massive failure of the same type in the future. Some sources have estimated that a massive failure of volcanic soils in the Canary Islands would have enough impact to generate a tsunami that could inundate the east coast of the United States and the Caribbean. Some researchers predict extreme consequences for the east coast of the U.S. and the Caribbean (Ward and Day, 2001). While others estimate quite moderate run-up heights (Løvholt et al., 2008). The probability of such an event seems however to be low and disputable.

30.8 World Landslide Forum Session on Socioeconomic Impacts of Landslides

The Session, Socioeconomic Impacts of Landslides, provides lectures illustrating the socioeconomic impact of landslide events as well as good practice for mitigation of the risk associated with landslides. Keywords for the Session are:

- Social and economic losses, and their quantification
- Consequences of landslides on infrastructure development
- Landslides and land use policy
- Case studies on recovery and resettlement
- Measures to reduce social vulnerability

- Investments for landslide risk mitigation and reduction
- Insurance issues for landslide risk mitigation and reduction

30.8.1 Consequences of Landslides on Infrastructure Development in China

By Zhang Yongshuang, ZHANG Chunshan, SHI Jusong, and Zhang, Jiagui

In recent 10 years, a series of large-scale linear engineering works have been planned and constructed in China including oil/gas pipeline, railway, express road, etc. During these engineering constructions, many geo-hazard problems occurred in mountainous area, and landslide is the most serious type among the various geo-hazards. The presentation will focus on two cases the "Yiwanshui landslide" of gas pipeline project and "102 landslide" on the highway from Sichuan to Tibet. Legislation related to geo-hazard management in China will also be covered.

The Yiwanshui landslide occurred in the gas pipeline from Zhong County to Wuhan city of Hubei province. The landslide is located in the northeastern side of Tiankeng valley, the slope is formed by ϵ_3 thick limestone. Both the rock formation and slope surface have the same dip direction. According to the original planning, the pipeline would pass through the Yiwanshui slope by tunnel. But when the tunnel was excavated to 165 m, the slope began to deform and existed obvious displacement. It is demonstrated later that the Yiwanshui landslide is an old landslide with sliding direction of NW. The landslide body is composed mainly by rock blocks mingled with soil, and its total volume capacity is $330\times10^4 m^3$. The formation of the old landslide was mainly controlled by lateral erosion of river water, as well as the bedding structural plane. In recent years before pipeline construction, the old landslide remained basic stability. The vibration of pipeline tunneling made the old landslide renew and occur obvious displacement, which led to considerable loss including damages of No. 318 national Road, high-voltage line, communication cable, and five family's houses. After utilizing such measures as backfilling the tunnel and tamping the surface fissures, the deformation of Yiwanshui landslide had been controlled. Consequently, the pipeline position had to be modified.

The 102 landslide is located in the right bank of Palongzangbu River near the No.102 maintaining station of the highway from Sichuan to Tibet of China. The landslide was first formatted in 1991, and mainly composed by Quaternary glacial deposits with a volume capacity of $510\times10^4 m^3$. At that time, the landslide debris accumulated in the Palongzangbu river valley and reached opposite bank, dammed the river for 40 minutes. The formation of 102 landslide was caused by both endogenic and exrogenic geological process. At the present time, the GPS-based monitoring system, as well as engineering works of slope protection, has been constructed, but it is still unstable especially in the rain season, impacting the traffic safety.

Considering the frequent occurrence of geo-hazards during engineering construction, China government has promulgated some management legislations about geo-hazard prevention and control. For example, it is mandatory required that geo-hazard risk assessment must be performed before project planning and construction. This requirement considerably decreased the loss caused by geo-hazard during engineering construction, showing obvious social and economic efficiency.

For purposes of the World Landslide Forum, there are a wide variety of landslide case studies presented that serve to well-represent the diversity and complexity of socio-economic impacts of landslides. The following are extended abstracts of authors and presenters for the WLF session on Socio-economic Impacts of Landslides

30.8.2 Effective Land Use Planning Solutions for Landslide Risk Management in Urban Areas in Asia

By N.M.S.I. Arambepola

Landsides and other mass movements are becoming one of the most frequent natural geological phenomena especially in the urban areas covered with mountainous terrain in many countries in Asia and the Pacific. It is not very clearly manifested by the number of loss of life but damages to property, lifelines and utilities are quite widespread and significant. This was seen in earthquake induced occurrences observed in Pakistan in 2005 October and also number of rain induced landslides reported recently in countries such as Nepal, Sri Lanka, India, Indonesia and Philippines. It also suggests that landslides can be one of the most significant outcomes of global climate change in future.

In many instances landslides occur without any prior warning and people do not understand well the nature of pre-event symptoms to take actions before the event occur. Hazard mapping can easily delineate the potential areas of high risk but very few countries have taken steps to implement national programs for hazard zonation mapping at any level. Therefore it is impossible to provide a lead-time to undertake precautionary measures in the potentially affected areas to prevent loss of life and property. This is the most important reason why landslides are becoming one of the most frequent of the natural calamities of geological nature.

Over the last decade, landslides have caused considerable socio-economic impacts in several Asia and Pacific region countries associated with mountain hill ranges including India, Indonesia, Philippines, Pakistan, Nepal, Sri Lanka, China, and Thailand etc. Their occurrence is due to intense rainfall occurrences or earthquake induced. Landslide vulnerability of communities is not uniform and there are large variations within Asia Pacific and largely associated with the socio-economic differences, political commitment, location of settlements, policies and practices.

Risk factors (physical, social and economic) that have not been addressed for a considerable time lead to landslide disaster events. Most of the landslides that have occurred in the past in Asia Pacific region had a mild impact on the urban areas, as their impact was concentrated towards the rural areas. However, recently reported events have proved the high vulnerability of the urban areas to landslides. Independent of the triggering mechanism, when landslides occur in the urban areas the human and economic damage is tremendous due to failure of many slopes simultaneously within a considerable area. It is resulted due to similarity in slope characteristics, land use practices, sub-surface formations etc and capable of affecting large population and heavily built infrastructure. In fact, the impact of the disaster event associated with such events is very closely related to the type of built environment (buildings and infrastructure) and other land use practices.

Escalation of events observed in the urban areas are accompanied by high level of inappropriate construction practices, uncontrolled development, reluctance of local planners and engineers for strict enforcement of land use controls and regulated practices in prone areas. This has created serious problems in landslide mitigation. Though the recent landslides that have affected the urban areas, have put some pressure for enforcement of the land use regulations by authorities, the better construction practices, appropriate policy guidelines for development of urban hill slopes as well as public awareness creation yet to feature in the agenda of urban local bodies. This paper summarizes some of the experiences of the Asian Disaster Preparedness Center (ADPC), Thailand in promoting the appropriate land use planning practices in urban areas prone to landslides in Asia in order to mitigate the landslide impacts.

30.8.3 Measures to Reduce Social Vulnerability in Squatter Settlements in San Miguelito, a Suburb of Panama City

By M.Sc. Eberto E. Anguizola M.

The suburban San Miguelito area outside the City of Panamá has a high concentration of inadequate housing. Many houses are constructed in landslide-prone hillsides, and man-made intervention has frequently destabilized the natural slopes, for instance by cutting into slopes to obtain a flat construction site, and secondly placing excavated material downslope. During rainfall, many of these cuts and fills have failed, in some cases with fatal result and loss of human lives. In addition, lack of drainage of surface water and waste water systems result in flooding during heavy rain as well as bad sanitary conditions.

The historical records from San Miguelito verify that landslides have been a continuous threat to the inhabitants. The ground in the area is heterogeneous, and primarily consists of volcanic soils of various origins (pumice tuff, conglomerates, andesitic material, etc.).

The population density in the area has grown rapidly since the 1960, and is now extremely high, 4850 persons per square kilometer, to be compared with an average of 226 persons per square kilometer for Panama City. The reasons for this development is connected to unemployment, restriction on living areas closer to the city centre, lack of regulations for urban development (before ca. 1980), and also political issues. Poverty and unsanitary conditions brings on a series of social problems.

The threat from landslides causes a constant burden on the life of the inhabitants in the San Miguelito area. A landslide mitigation demonstration project has therefore been launched in order to teach the community how to deal with the landslide hazard. The project i.a. includes hazard zoning of landslide exposed dwellings, installation of an automatic rainfall station with real time data transmission to the community centre, evaluation of construction practices and recommendation of improved construction methods and methods for surface water management that will reduce man-made landslides, evacuation and communication training etc.

30.8.4 Impact on Livelihoods of Landslide Affected Communities due to Resettlement Programmes

By Kishan Sugathapala

Landslides occur due to various reasons. Most of them are man-made causes. If the human settlements are located in the landslide prone areas the risk levels will be high. Further, if the locations that are susceptible to landslides are identified, introduction of mitigatary measures are inevitable. Therefore, in this kind of situation the communities with highest risk level, sometimes needs to be relocated. This is considered after careful investigation into variables such as; landslide hazard level, awareness, housing and structural condition, and livelihood. Affected communities are 'put into' two types of resettlement programmes after identification of risk level (high) and after a disaster event. In this connection, the resettlement becomes an inevitable solution instead of an option. Since in most cases the resettlement become necessary in type two mentioned above. One of the main concerns among others, in this kind of resettlement is the impact on the livelihood.

People with the location specific livelihoods are more vulnerable on this kind of resettlement programmes. Therefore, it is very relevant to identify the socio economic background including livelihood, occupation etc. in resettlement programmes.

When affected communities are categorised, it is also important to look into the issues, such as why they are settled in this particular location? In Sri Lanka one of the notable issues that we are considering is the background of affected communities that we earmarked for resettlement. The affected communities are surveyed for their socio economic background including their livelihoods and educational/skill level among other things. Main objective of this back study is to determine the socio cultural background which allow to determine inter and intra community linkages. Also, the location specificness of livelihood and the skills will determine the possibility of changes in type of livelihoods if resettlement is inevitable.

Further, this paper will discuss the issues related to landslide affected communities and the options available to reduce the impact with special reference to landslide/subsidence affected communities in Matale and Nuwara Eliya districts of Sri Lanka as per recent studies

1. Background of the session
   Oddvar Kjekstad,
   NGI, Norway
2. The Willingness of Society to Accept Landslide Risk *M. G. Winter and E. N. Bromhead*
3. Effective land use planning solutions for landslide risk management in urban areas of Asia
   NMSI, Arambepola, ADPC, AsianDisaster Preparedness Centre, Bangkok
4. Landslide risk reduction investments in Hong Kong
   Y.C Chan,
   Government of Hong Kong

5. Impacts on livelihoods of landslide affected communities due to resettlement programs
   Kisam Sighapala,
   Human Settlement Division, NBRO, National Building Research Organization, Colombo
6. Measures to reduce social vulnerability in squatter settlements in San Miguelito, a suburb of Panama City
   Eberto Angeziola,
   Instituto de Geosciencias, Panama City
7. Public Policies and Investments for Landslide Risk Reduction in Poor and Densely Populated Areas in Rio de Janeiro
   Francis Bogossian,
   Geomecanica, Rio de Janeiro
8. Hagerman Valley Landslides Triggered by Land-Use Change Endanger Lives and Destroy Natural and Cultural Resources
   Neal Farmer
   Idaho Department of Water Resources
9. Consequences of landslides on infrastructure development in China
   ZHANG Yongshuang
   Institute of Geomechanics, Chinese Academy of Geological Science
10. Disaster Insurance in Latin America
   Francis Ghiesquire, World Bank Global Facility for Disaster reduction and Recovery (GFDRR)

References

Bhasin, R., Grimsatd, E., Larsen, J.D., Dhawan, A.K., Singh, R. Verma, S.K., and Venkatachalam, K. (2002) Landslide hazards and mitigation measures at Gangtok, Sikkim Himalaya, Engineering Geology, vol. 64, 2002, pp. 351–368

Chan, R.K.S. (2007). Challenges in slope engineering in Hong Kong. Proceedings of the Sixteenth Southeast Asian Geotechnical Conference, Southeast Asian Geotechnical Society, Malaysia, pp. 137–151

Cruden, D.M., Thomson, S., Bomhold, B.D., Chagnon, J.-Y, Locat, J., Evans, S.G., Heginbottom, J.A., Moran, K., Piper, D.J.W., Powell, R., Prior, D. and Quigley, R.M. (1989) Landslides: extent and economic significance in Canada. In E.E. Brabb and B.L. Harrod, eds., Landslides: extent and economic significance, Proc., 28th Int'l. Geol. Congr., Symp. on Landslides, Washington, D.C., 17 July, pp. 1–23

Dilley, M., Chen, U., Deichmann, U., Lerner-Lam, A.L., Arnold, M., AGWE, J., Buys, P., Kjekstad, O., Lyon, B. , and Yetman, G. (2005) Natural Disaster Hotspots: A global risk analysis, International Bank for Reconstruction and Development/The World Bank and Columbia University, Washington, D.C

Evans, S.G., Guthrie, R.H., Roberts, N.J., and Bishop, N.F., (2007) The Disastrous 17 February, 2006 rokslide debris avalanche on Leyte Island, Philippines: a catstrophic landslide in tropical mountain terrain, Natural Hazards Earth System Sciences, Vol. 7, 2007, pp. 89–101,

Harp, Edwin L., and Anthony J. Crone (2005) Landslides Triggered by the October 8, 2005, Pakistan Earthquake and Associated Landslide-Dammed Reservoirs, U.S. Geological Survey Open-rile Report 2006–1054, 10p Online: http://pubs.usgs.gov/of/2006/1052/pdf/ofr-2006-1052.pdf

Highland, Lynn M. (2003) An account of preliminary landslide damage and losses resulting from the February 28, 2001, Nisqually, Washington, Earthquake, U.S. Geological Survey Open-File Report 03–211

HKSARG (2007) Administration's paper on post-2010 landslip prevention and mitigation programme (Legislative Council Brief), Panel on Development, Hong Kong Legislative Council, 11p

International Centre for Integrated Mountain Development (ICIMOD) (2007) Impact of climate change on Himalayan glaciers and glacial lakes, ICIMOD Report, June 2007

Kjekstad, Oddvar (2007) The challenges of landslide hazard mitigation in developing countries, Keynote Lecture, First North-American Landslide Conference, Vail, Colorado USA, 3–8 June, 2007.

Løvholt, F., Pedersen, G., and Gisler, G. (2008) Oceanic propagation of a potential tsunami from the La Palma Island, Journal of Geophysical Research, in press. doi: 10. 1029/2007JC004603, in press

Nadim, F., Kjekstad, O., Peduzzi, P., Herold, C., and Jaedicke, C. (2006) Global landslide and avalanche hotspots. Landslides, Vol. 3, No. 2, pp. 159–174

Petley, D.N. (2008) The global occurrence of fatal landslides in 2007 D.N. Petley Geophysical Research Abstracts, Vol. 10, EGU2008–A–10487, 2008, EGU General Assembly 2008

Schuster, R.L. (1996) Socioeconomic significance of landslides. In: A.K. Turner and R.L. Schuster, (eds.), Landslides – investigation and mitigation, National Res. Council, Washington, D.C., Trans. Res. Board Spec. Report 247, pp. 12–35

Schuster, Robert L., and Lynn M. Highland (2001) Socioeconomic and Environmental Impacts of Landslides in the Western Hemisphere. *In:* Castaneda Martinez, Jorge E., and Olarte Montero, Juan, eds., Proceedings of the Third Panamerican Symposium on Landslides, July 29 to August 3, 2001, Cartagena Colombia, 886p

Schuster, RobertL. and Lynn M.Highland (2006) The Third Hans CloosLecture, Urban Landslides: socioeconomic impacts and overview of mitigative strategies. Bulletin of **Engineering Geology and the Environment**, Vol. 66, No. 1, March 2006, pp. 1–27

Schuster, Robert L. and Lynn M.Highland (2007) Overview of the effects of mass wasting on the natural environment. Geological Society of America, Environmental & Engineering Geoscience, Vol. XIII, No. 1, February 2007, pp. 25–44

Sidle, Roy C. and Hirotaka, Ochiai (2006) Landslides: Processes, Prediction, and Land Use. Water Resources Monograph 18, American Geophysical Union, Washington, DC

Vikram, G. and Ahmed, I. (2007) Geotechnical characteristics of Surabbi resort landslide in Mussoorie Garhwal Himalaya India. Himalayan Geology, Vol. 28 No. 2, 2007, pp. 21–32, Printed in India

Wang, Fawu, Zhang, Ye-Ming, Huo, Zhi-Tao, Matsumoto, Tatsunori, and Huang, Bo-Lin (2004) The July 14, 2003, Quianjiangping landslide, Three Gorges Reservoir, China. Landslides, vol. 1, No. 2, July 2004, Springer, pp. 157–162

Ward, Steven N., and Simon Day (2001) Cumbre Vieja Volcano – Potential collapse and tsunami at La Palma, Canary Islands. **Geophysical Research Letters**, 28–17, pp. 3397–3400 Online: http://www.es.ucsc.edu/~ward/papers/La_Palma_grl.pdf

Wieczorek, Gerald F., Geist, Eric L., Motyka, Roman J., and Matthias, Jakob (2007) Hazard assessment of the tidal Inlet landslide and potential subsequent tsunami, Glacier Bay National Park, Alaska. Landslides, Vol. 4, No. 3, September 2007, pp. 205–215

Wu, Shuren, Shi, Ling, Wang, Reijiang, Tan, Chengzuan, Hu, Daogong, Mei, Yingtan, and Xu, Ruichun (2001) Zonation of the landslide hazards in the forereservoir region of the Three Gorges Project on the Yangtze River. Engineering Geology, Vol. 59, No. 1–2, January 2001, pp. 51–58

Zhang, L.. and Shan, W. (2005) Early warning and prevention of geo-hazards in China. In: Sassa, Kyoji, Fukuoka, Hiroshi, Wang, Fawu, and Wang, Gonghui, eds., Landslides: Risk analysis and sustainable disaster management, Proceedings of the First General Assembly of the International Consortium on Landslides, Washington, D.C., 2005, Springer, pp. 285–289

31 Environmental Impact of Landslides

Marten Geertsema, Lynn Highland and Laura Vaugeouis

Abstract Landslides affect the following elements of the environment: (1) the topography of the earth's surface; (2) the character and quality of rivers and streams and groundwater flow; (3) the forests that cover much of the earth's surface; and (4) the habitats of natural wildlife that exist on the earth's surface, including its rivers, lakes, and oceans. Large amounts of earth and organic materials enter streams as sediment as a result of this landslide and erosion activity, thus reducing the potability of the water and quality of habitat for fish and wildlife. Biotic destruction by landslides is also common; widespread stripping of forest cover by mass movements has been noted in many parts of the world. Removal of forest cover impacts wildlife habitat.

The ecological role that landslides play is often overlooked. Landslides contribute to aquatic and terrestrial biodiversity. Debris flows and other mass movement play an important role in supplying sediment and coarse woody debris to maintain pool/riffle habitat in streams. As disturbance agents landslides engender a mosaic of seral stages, soils, and sites (from ponds to dry ridges) to forested landscapes.

Keywords: Landslide • Environmental impact • Ecology • Biodiversity • Natural disturbance agent

31.1 Introduction and Scope

Landslides occur throughout the world, and especially in certain hotspots (Nadim et al., 2006). Much has been written about landslide impacts on human lives, and on infrastructure. Little attention, however, has been paid to landslide impacts on the natural environment (Schuster and Highland, 2007). Even less consideration has been given to the role that landslides play in disturbance ecology (Geertsema and Pojar, 2007).

Landslides are destructive agents. They change and modify the landscape – they disturb it. Destruction and disturbance is costly for the built

* We dedicate this chapter to Laura Vaugeois who was to be one of the conveners of this session. Laura was a landslide specialist with the Washington State Department of Natural Resources. She died on the 30th of April 2008 after a brief and sudden illness.

Marten Geertsema (✉)
British Columbia Forest Service, British Columbia, Canada
e-mail: marten.geertsema@gov.bc.ca

Lynn Highland
U.S. Geological Survey, Denver Federal Center, Denver, CO 80225, USA

Laura Vaugeouis
Washington State Department of Natural Resources, Olympia, WA 98504-7012, USA

© Springer-Verlag Berlin Heidelberg 2009

environment, it is costly for natural resources, and yet it is essential for ecosystem cycling in the natural environment.

The purpose of this paper is to provide a background and frame work for Session 8, on the environmental impact of landslides at the First World Landslide Forum in Tokyo Japan, November 2008. The paper is organized into two main parts, discussing: 1. the environmental costs of landslides; and 2. the ecological role of landslides.

31.2 A Brief Overview of Landslide Types

All solid materials on Earth are subject to deformation and failure. Landslide is a generic term for the mass movement of earth materials. Landslides occur in a variety of materials (earth, debris, rock, organics) move at varying rates (mm/year to tens of m/second), and can involve various styles of movements (topple, fall, flow, slide, spread). Landslides can have a variety of stages of activity ranging from relict to dormant to active. They can be retrogressive, progressive, advancing or enlarging, move along planar or curved surfaces, and be shallow or deep. In addition to this, they are often complex involving more than one type of material and style of movement.

Different types of landslides behave differently, have different associated hazards, and have different effects on the environment. Managing landslides and landslide-prone terrain necessitated their classification to enable intelligent and efficient communication. The main classifications used today are those of Cruden and Varnes (1996) and of Hungr et al. (2001).

31.3 Environmental Costs of Landslides

Landslides are destructive. They can have long-lasting effects on the environment. At the extreme range, topographic changes caused by some large rock slides can persist for many thousands of years. Landslides can overwhelm, and even pollute streams and waterbodies with excess sediment. In extreme cases they can dam streams and rivers, impacting both water quality and fish habitat. Landslides can wipe out large tracts of forest, destroy wildlife habitat, and remove productive soils from slopes. In some cases landslides cause tsunami, seiches, or outburst floods.

There is a continuum between the socioeconomic costs of landslides (session 6) and the environmental costs of landslides. This is because a healthy environment is important for sustaining human populations. Where a landslide causes a loss of resources by destroying farmland or forest, deposits sediment into a stream, or pollutes a drinking water source, the environmental impacts have attained a socioeconomic dimension.

31.3.1 Landslide Impacts on Forests

Forest destruction by landslides (Fig. 31.1) is common in many parts of the world, but particularly in tropical areas as a result of the combination of intense rainfall and earthquakes.

Schuster and Highland (2007) summarize a number of case studies. A large earthquake in Chile in 1960 triggered landslides that destroyed more than 250 km^2 of forest. After the 1976 Panama earthquakes (M6.7 and 7.0) 54 km^2 of tropical forest was wiped out by landslides (12% of the impacted area) (Garwood et al., 1979). Similarly, heavy rains and earthquakes removed 25% of the forest from the Reventador Volcano (Ecuador) in 1987, and

Fig. 31.1 Debris avalanches strip forests from the hillslope in coastal British Columbia

denuded 250 km^2 of forest and soil in Paez, Colombia in 1994 (Martinez et al., 1995).

Several studies have been made of coniferous forest damage due to landslides in southwestern Canada and the northwestern United States. Especially noteworthy have been studies of forest damage due to landslides on the Queen Charlotte Islands off the British Columbia coast. In a detailed study of revegetation patterns of landslide-destroyed forests in the Queen Charlotte Islands, Smith et al. (1986) found that forest cover returned to landslide areas more slowly than to logged areas; forest productivity of landslide areas was reduced by about 70 percent when compared to similarly-aged logged areas.

In the northwestern U.S.A., numerous studies of the effects of landslides on forest cover have been conducted by the U.S. Forest Service (e.g., Megahan et al., 1978); most of these studies have dealt with the effects of logging operations in causing destructive landslides.

In rare cases, forests have been destroyed by large water waves caused by high-velocity landslides. An outstanding example was the 1958 catastrophic destruction of virgin coniferous forest to an elevation of 530 m above the waters of Lituya Bay, southeastern Alaska, by a giant wave caused by a high-velocity rock slide (Miller, 1960).

31.3.2 Landslide Impacts on Streams

Schuster and Highland (2007) summarize a number of landslide impacts on streams. The main types of landslides that impact streams are debris flows, which may fill and/or erode the stream channel for great distances (occasionally 100 km or more). Debris flows provide important sediment transport links between hillslopes and alluvial channels (Butler, 2001), and thus are an important factor in drainage-basin sediment budgets. In addition, debris flows influence the spatial and temporal distributions of sediment in stream channels, either because they deposit sediment in the channels or because the deposits provide a source for accelerated transport of sediment farther downstream (Benda, 1990).

Landslide size and type play a role in impacts on streams. Obviously the size of the landslide in relation to the size of the stream is important. Earth flows along tributaries of Buckinghorse River in northeastern British Columbia overwhelm the sediment budget in streams, with dams persisting for decades (Geertsema et al., 2006). Dams from flows in the main river are extremely short-lived. Rockslide dams can persist for millennia (Costa and Schuster, 1988). Swanston (1991) noted variable impacts to streams by different types of landslides. Slumps and earth flows cause low-level, long-term contributions of sediment and large woody debris to channels; partial channel blockages; local channel constriction below the point of landslide entry; and shifts in channel configuration. In contrast, debris avalanches and debris flows cause large, short-term increases in sediment and large woody debris; channel scour; large-scale redistribution of bed-load gravels; damming and constriction of channels; accelerated channel erosion and bank undercutting; and alteration of channel shape by flow obstruction.

Landslide deposits, although important for stream morphology in the long term, can destroy fish habitat in the short term. Recovery rates depend on a wide range of factors.

An exceptional example of a recent lahar (volcanic debris flow) occurred as a result of the 1980 Mt. St. Helens, USA eruption (Schuster and Highland, 2007). A debris avalanche transformed into a 100 km long debris/mud flow (Fig. 31.2), filling and permanently modifying the channels of the Toutle and Cowlitz Rivers and continued into the

Fig. 31.2 Photo of a lahar, caused by the 1982 eruption of Mount St. Helens, Washington, USA (Photo by Tom Casadevall, U.S. Geological Survey)

much larger Columbia River, which was partially blocked by the sediment. Between June 1980 and May 1981, 45 million m^3 of sediment was dredged from the Cowlitz and lower Toutle Rivers to restore their original channels. The mud flow deposited more than 30 million m^3 of sediment in the Columbia River.

Today, nearly 30 years after the eruption of Mount St. Helens, the Toutle River still is receiving large amounts of sediment that is eroded from the debris avalanche and downstream debris flow. Sediment levels in the Toutle River range from 10 times to more than 100 times the amount before the eruption. Sediment levels will likey remain high for decades, increasing flood risks for downstream communities and threatening efforts to restore salmon and steelhead trout runs that were nearly wiped out by the original debris avalanche and debris flows.

31.3.3 Landslide Impacts on Drinking Water Quality and Environmental Health

Landslides can negatively impact drinking water sources by introducing suspended sediment and organic materials. In 2006 the Greater Vancouver Regional District introduced the longest water boiling advisory in its history. Poor water quality is thought to be linked to landslide activity in watersheds above drinking water reservoirs. In Washington State, USA, a bedrock landslide in the headwaters of Sumas River exposed natural asbestos. Elevated levels of nickel and chromium were found in sediments downstream of the landslide.

An unusual outbreak of coccidiomycosis occurred after the January 1994 Southern California earthquakev caused numerous landslides. The infection was caused by the fungus *Coccidioides immitis*, which is found in soil in certain semiarid areas of North and South America. The outbreak was associated with exposure to increased levels of airborne dust from exposed landslide surfaces in the aftermath of the earthquake.

31.3.4 Landslide Generated Tsunami

Landslide-generated tsunami occur in water bodies around the world (Locat and Lee, 2002). The 8000 year old Storegga submarine landslide off the coast of Norway is one of the most famous examples. Its tsunami inundated coastlines as far away as Greenland. Fan-delta collapse and translational sliding associated with the 1964 Alaska earthquake resulted in $\sim$ 75 M m^3 of shoreline in Valdez Harbour, Alaska (Schuster and Highland, 2007). The highest displacement wave in historic time, occurred from a rock slide generated tsunami in Lituya Bay, Alaska in 1958 (Pararas-Carayannis, 1999). The rock slide created a large crater on the floor of the inlet. The wave removed the forest from the mountainside up to a height of more than 500 m.

On December 4, 2007 a 3 M m^3 rock slide entered Chehalis Lake near Vancouver, Canada. The resultant tsunami removed trees from the shoreline to a maximum height of 18 m. In addition to trees growing on the hillslope, several ha of shoreline forest were destroyed (Fig. 31.3). Trees

Fig. 31.3 The 4 December 2007 Chehalis Lake rock slide and tsunami damage near Vancouver, Canada. Photos courtesy Frank Ullmann, BC Government

traveled beyond the lake and up to 14 km down a river (Tom Millard, BC Forest Service, personal communication).

31.3.5 Landslide Dams

Landslide dams can cause two main problems. (1) They flood valleys. (2) Sometimes the dams fail catastrophically resulting in outburst floods. The dams introduce a tremendous amount of new sediment load to streams. The dams themselves may either trap or deliver sediment.

Landslide dams may persist from several minutes to millennia (Costa and Schuster, 1988). Drowned forests may survive flooding if the dam is short-lived. Otherwise the submerged vegetation dies. In some instances additional landslides occur above the landslide dam, likely due to rapid drawdown, from falling water levels.

While most landslide dams do not fail catastrophically, enough do to warrant mention. The most devastating losses occur where human lives are lost, but there are also environmental consequences. Flood waves can destroy downstream forests and farmland. Sometimes the outburst floods trigger other landslides such as debris flows.

31.3.6 Landslides Impacts on Scenery in Parks

Landslides in parks can damage infrastructure, change topography, wipe out forests and add sediment to streams. But they can also become awe-inspiring testimonies to natural processes. Some major landslides have become tourist attractions. Both the 1903 Frank and 1983 Thistle landslides in Alberta, Canada, and Utah, USA, respectively, have highway pullouts with interpretative signs.

The most recent example of destruction in a major site occurred at a UNESCO world heritage site, the Valley of Geysers, Kamchatka, Russia. On 3 June, 2007 a massive landslide covered the geysers (Fig. 31.4). It certainly changed the valley. Yulia Kugaenko (see below) considers the Valley of Geysers a huge natural museum with both volcanic processes and landslides. She stresses the landslide was not a catastrophe, but a natural process on display.

31.4 The Ecological Role of Landslides

Natural disturbance is an important process of rejuvenation in ecology. There are many abiotic disturbance types including volcanic eruptions,

Fig. 31.4 Valley of Geysers before and after the 2007 landslide. Note the new lake formed by the landslide dam. Photos contributed by Yulia Kugaenko. Photo 1 by I.Shpilenok and V.Droznin. Photo 2 by Y. Muraviev

earthquakes, tsunami, wildfire, violent windstorms, floods, and landslides. These, in addition to biotic disturbances, such as insect outbreaks and tree diseases, contribute to natural cycling of both aquatic and terrestrial ecosystems. There is often a synergy between disturbance agents. For example, insect oubreaks or wildfire may predispose slopes to landslides (Fig. 31.5). Here we consider the ecological role of landslides as disturbance agents in the natural environment.

Episodic erosion and sedimentation events are essential to the long term structure, function and integrity of aquatic ecosystems (Keller and Swanson, 1979; Swanson, 1980; Swanson et al., 1982, 1988; Hogan, 1986; Naiman et al., 1992; Benda and Dunne, 1997; Nakamura et al., 2000; Montgomery et al., 2003).

The structure and function of fish-bearing streams depends in large part on the periodic input of sediment and woody debris. Much of this input comes from landslides. Log jams in particular are important for creating pool/riffle habitat.

Geertsema and Pojar (2007) argue that landslides contribute to biodiversity in three main ways: by changing site, soil, and vegetation (habitat). Landslides usually change the site conditions at a given location, for example, making conditions drier or wetter, or stonier or muddier, more pervious or less pervious, sunnier, more exposed, etc. Changes to site conditions then also lead to changes in soils developing on those sites. Changes to site and soil, and the resultant changes in vegetation, contribute to increased habitat diversity, which is expressed at the landscape scale. The following sections are derived largely from Geertsema and Pojar (2007).

Fig. 31.5 There is often an interplay between disturbance agents. Here, in the Northwest Territories, Canada, wildfire has likely contributed to retrogressive thaw flowing by reduction of an insulating moss layer, resulting in the thickening of the active layer, thawing permafrost

31.4.1 Site Diversity

Geertsema and Pojar (2007) define site as a segment of landscape that is relatively uniform in local climate, topography and soil. Landslides increase site diversity. One of the main ways that landslides impact site is by changing topography. Landslides create, at the same time, erosional and depositional landforms with zones of depletion and zones of accumulation (Cruden and Varnes, 1996). Within landslides a range of positive and negative microtopography is possible at various scales.

Examples of positive microtopography in landslides include hummocks and ridges that rise up from the main ground surface (Fig. 31.6). Hummocks and ridges are often drier and warmer than surrounding terrain. Rubble deposits resulting from rock slides tend to be very rapidly drained, often in extreme contrast to adjacent terrain. The complex microtopography in landslides contributes to a redistribution of sites, usually with a greater number of very wet and very dry microsites (Fig. 31.7).

Fig. 31.6 Dry ridges and wet depressions in a translational landslide near Fort St. John, Canada contribute to the biodiversity of the local landscape. Photo courtesy Ake Nauta

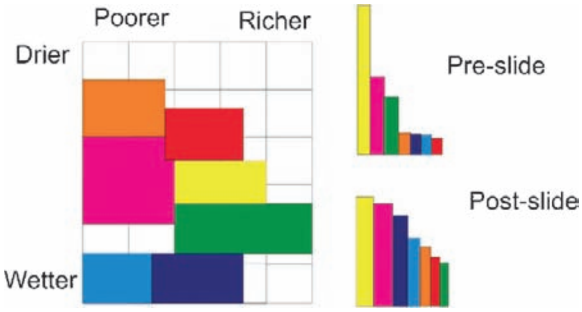

Fig. 31.7 Edatopic grid on right shows the distribution of site series (ecosystems) based on site moisture and richness. The distribution of various site series changes after a landslide has happened

Examples of negative microtopography include sag ponds below the main scarps of rotational landslides (Cruden et al., 1997). Other ponds result from variable topography in the zone of accumulation in earth flow deposits, or from the impoundment of streams (Cruden et al., 1993; Geertsema and Pojar, 2007).

Landslides also create open, at least temporarily exposed sites, often with more extreme microclimates than the surrounding landscape matrix—especially in forested terrain. Scarps created by landslides are steeper than the pre-slide slopes, and commonly form cliffs.

Repeated debris flows and slides tend to deepen channels in hillslopes, resulting in a gully-interfluve topography, often with deposits on terraces (Fig. 31.8) or in streams. This is especially the case in fine-textured tills and glaciolacustrine deposits and in soft, fine-grained bedrock.

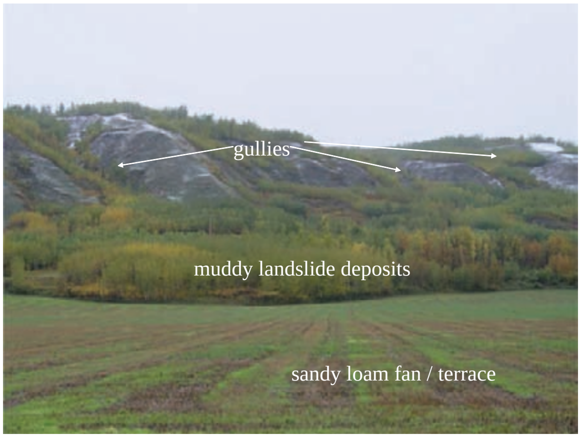

Fig. 31.8 Landslides play an important role in the formation of gullies and lobate deposits that are different from the terrace in the foreground. Modified from Geertsema and Pojar (2007)

31.4.2 Soil Diversity

Landslides change soil properties primarily by exposing parent material (the C horizon) by removing organic mats and A horizons. This can result in a mosaic of pedogenic stages in a landscape unit. At a given site, a Podzol (FAO Soil Classification) may be removed, exposing a Regosol, thus resetting the pedogenic clock to the initial stages of a Regosol Podzol sequence. Landslides that have translational movement typically raft intact mats of soil, and in the extreme case, large portions of forest may move as coherent units, maintaining both the forest and soil. The most thorough mixing occurs in flows.

If both site and soil change, soil changes may persist much longer and have greater ecological effects. For example, when a landslide exposes a phreatic surface, the site hydrology could change, and in the extreme case, lakes or wetlands can develop in the zone of depletion. Thus we could expect Gleysols, or perhaps Histosols to replace the original Podzol. At the other extreme, a landslide deposit may fill in a moist valley, replacing a wet Histosol with a soil that will develop on the new, drier site. In both instances, changes to site also bring about changes in soil.

An important influence of landslides on soil is the change in texture. Textural changes occur where landslides bring different material to, or remove material from, a given site. Material can be brought to the surface from below, as in mud volcanoes (Schwab et al., 2004) or sand blows resulting from liquefaction, but more commonly where landslide deposits cover a site. For example, both the mud of earth flows and the rubble of rock avalanches change the texure of surficial material on a gravelly terrace. Debris flows often impart a mixture of clasts and soil to a site with lateral sorting (e.g. Nakamura et al., 2000; Butler, 2001). In other cases landslides may remove sands and gravels or till, exposing fine-textured muds. Spreads that occur in marine clays overlain by sands, often result

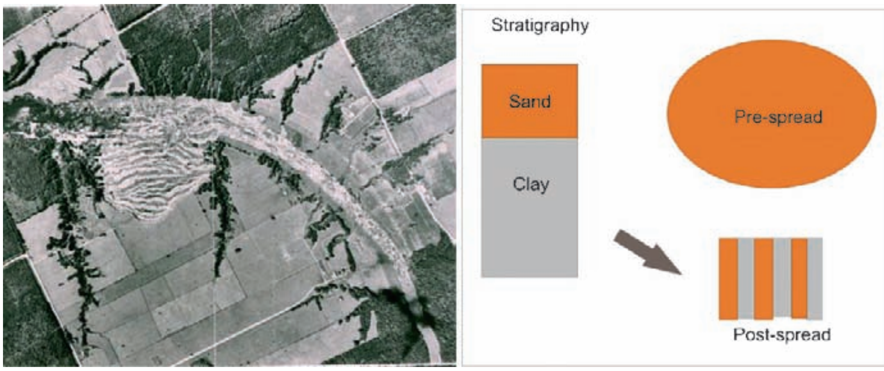

Fig. 31.9 Ribbons of sand and clay persist long after a spread has occurred in sensitive glaciomarine clays at the 1971 South Nation landslide, Ontario, Canada

in a thumbprint-like pattern of sand and clay ribbons 5–10 m wide (Eden et al., 1971; Mollard and Janes, 1984; Carson and Geertsema, 2002) (Fig. 31.9). Indeed, where various stratigraph units are involved in a landslide, textural sorting by the landslide process is common (Fig. 31.10). Post-landslide erosion also sorts surface deposits and thus changes soil texture. Landslides can also change local soil density and porosity.

Remoulding and liquefaction of clays and silts in earth flows, reduces structure and porosity, and increases soil density. In contrast, colluvial slopes in mountainous terrain generally have a looser structure and higher porosity than underlying tills. The mixing of wood with landslide debris can also increase the porosity of the soil. In general, landslide deposits occupy more volume than the original pre-movement source (Cruden and Varnes, 1996).

Landslides can also change soil chemistry at a site (Zarin and Johnson, 1995; Hugget, 1998). Deposition of foreign material can do this, but soil chemistry can also change due to the weathering of surficial materials and the exposure of material at depth. Geertsema and Schwab (1995) found that material exposed at depth in glaciomarine sediments had a pH of 8 and up to 5% carbonate as opposed to near-surface soil (pH <5) that had undergone leaching and acidic weathering in a coniferous temperate rainforest. Thus materials exposed in the surface of the landslide had soils highly variable in pH and soil chemistry, depending on whether surficial material or deeper material covered the ground surface. Smith et al. (1986) found that, on the Queen Charlotte Islands BC, pH of humus decreased with the age of landslides, and that organic carbon and total nitrogen increased with landslide age. Lambert (1972) found that the pH of tundra mudflow soils in the Northwest Territories ranged from 5.5 to 6.9 in comparison to 4.6 in the mineral soil of the surrounding climax vegetation. Burn and Friele (1989) also found that fresh to 43-year-old thaw slump soils near Mayo, Yukon had pH values of 7.3–7.4, compared to 6.2 in soils under mature spruce forest.

Fig. 31.10 Vertically stratified (preslide) units are often found adjacent to each other in landslide deposits

31.4.3 Habitat Diversity

Habitat diversity is a derivative of site and soil diversity, as expressed over landscapes (Geertsema and Pojar, 2007). Various combinations of micro-topography, substrate, soil, nutrient and moisture regime, and vegetation, result in a variety of habitats for different species.

A landscape typically consists of a mosaic of patches and corridors in a background matrix (Parminter, 1998). Habitat diversity of landscapes is strongly related to patterns of disturbance and recovery. Landslides alter both site and soil, and thus contribute to landscape evolution. Superimposed on the disturbed site and soil is the response of vegetation. Landslides result in a variety of habitats that differ from the surrounding matrix and provide substrates for both primary and secondary succession. In some landslides, rafts of vegetation and even stands of trees may simply move (translate) from one location to another, but in general deep unweathered parent material or rock is exposed, turning back the ecological clock to primary succession. The landslide, then, is one of the disturbance agents that contributes to habitat diversity by changing site, soil, and vegetation patterns.

In forested landscapes there is a distinct vegetative difference between landslides and the surrounding forest. For example in the Chisca River area of northern BC, a rock avalanche spread over black spruce muskeg; willow and birch shrubs have replaced the original forest. The larger, low gradient earth flows tend to create very complex micro-topographies, resulting in a wide range of moisture regimes. A corresponding spectrum of vegetation occupies the microhabitats in response to the variable site characteristics. Aquatic vegetation forms in ponds – often eventually passing on to peatland communities. Dry-site lichens may cover rubble and gravelly ridges in landslides. Such differences can persist for centuries, as on old landslides on the coast, where eventually coniferous forest takes over but remains different (species composition, productivity, soils) than the surrouding matrix forest.

Landslides of different age and type result in a mosaic of successional stages across landscapes. Globally landslide-ecological studies have been reported in Africa (Lundgren, 1978), in the Caribbean (Guariguata, 1990; Dalling, 1994; Walker et al., 1996; Myster et al., 1997; Myster and Walker, 1997), in Japan (Sakai and Oshawa, 1993; Yamamoto et al., 1995; Yajima et al., 1998; Nakamura et al., 2000), in New Zealand (Mark et al., 1964; Trustrum et al., 1984; Smale et al., 1997; Mark and Dickinson, 2001; Wells et al., 2001; Vittoz et al., 2001; Claessens, 2005), in the United States (Langenheim, 1956; Flaccus, 1958, 1959; Hull and Scott, 1982, Miles et al., 1984; Miles and Swanson, 1986; Shimokawa, 1984; Lewis, 1998; Butler, 2001; Francescato et al., 2001; Restrepo and Vitousek, 2001), with numerous publications on vegetation establishment on the landslides at Mount St. Helens (e.g., Dale and Adams, 2003), and in Canada (Lambert, 1972; Revel and Maze, 1972; Burn and Friele, 1989; Geertsema and Pojar, 2007).

In New Zealand, cohorts of trees result from earthquake induced landslides (Wells et al., 2001), generating habitat diversity across the landscape (Vittoz et al., 2001). Claessens found that kauri trees grew preferentially on recent landslide scars, and played an important role in stabilizing the landscape.

At Mount Tokachi in Japan, variable vegetation types covered a 1926 debris flow-generated landscape. Birch grew on sand at the outer margins of the debris flow deposits. Inward from the margins, on sandy-stony sediment, birch grew with a coniferous understory. The cobbly central areas of the debris flow were occupied by spruce (Yajima et al., 1998, Nakamura et al., 2000).

Lewis (1998) demonstrated that aspen stands occupied landslide deposits on the otherwise steppe-covered slopes of Kathul Mountain, Alaska. Mineral soil exposure and snow trapping on rough landslide deposits favoured the establishment of aspen. Aspen was unable to compete with steppe vegetation on the non-landslide terrain.

Lambert (1972) studied plant succession on tundra mudflows in the Canadian Northwest Territories. Two seres of plant succession occurred. Exposed silty soil was first colonized by a *Senecio* and cottongrasses, and later by grasses, horsetails, and the forb *Petasites*. Another community in the landslides included rafted islands of intact surface material and climax vegetation, including an assortment of lichens, mosses, grasses, sedges, forbs and shrubs. The mudflows then, set the successional clock back asynchronously to produce a mosaic of successional stages on the tundra.

Burn and Friele (1989) studied retrogressive thaw slumps in permafrost terrain near Mayo, Yukon. They distinguished seven vegetation units in the landslides, ranging from pioneer assemblages to 40-year old forest. Their work shows that episodic retrogression by thaw slumping produces a mosaic of vegetation communities.

In BC, Smith et al. (1986) studied revegetation patterns on debris slides and flows on the Queen Charlotte Islands. They distinguished 8 vegetation groups on 49 landslides. The differences were primarily attributed to age and position on the landslide. The deciduous red alder dominated the stands for about 5 decades, but then began to decline under as Sitka spruce became dominant. Rock-dominated slopes typically were not colonized by red alder – there western hemlock and Sitka spruce occupied the landslides.

Large earth flows or slides with hummocky or ridged microtopography often form ponds. Sometimes the microtopography predisposes sites to colonization by beaver. Thus landslides can both create ponds and facilitate the construction of beaver ponds – and support associated flora and fauna. In turn, at the landscape scale, beaver increase habitat diversity (Wright et al., 2002).

The pioneer vegetation established on many landslides provides important browse for ungulates – particularly in terrain dominated by conifer forests with moss-dominated understories. The floristic explosion on a landslide deposit also support other deciduous-dependent fauna.

Cliff collapse and large rotational landslides often create cliffs, usually with associated rubble fields. Soil cliffs provide habitat for cavity nesters such as bank swallows and kingfishers, and the rubble is excellent escape terrain for small rodents and contains den sites for a variety of mammals. Rock cliffs also provide safe escape terrain for mountain goats and mountain sheep.

Landslides may impound streams and drown upstream forests (Fig. 31.11). This can leave a legacy of standing dead trees (snags) and coarse woody debris providing habitat for many species (Swanson and Franklin, 1992). Snags are particularly important for cavity-nesters, and may be used as perch trees by raptors.

Fig. 31.11 This landslide on Wrigley Creek, Northwest Territories, Canada has increased the diversity of this landscape. The landslide created a hummocky microtopography, exposed cliffs, formed a lake, and drowned a floodplain forest

31.4.4 Influence of Landslides on Forest Productivity

Soil-stripping by landslides generally reduces the productivity of forests (e.g. Smith et al., 1986). In some environments however, the most productive forests grow on disturbed terrain. There are several examples of this. In the rainforests of coastal British Columbia thick mosses blanket stable slopes. Trees on these slopes have much slower growth rates than trees colonizing landslides (Banner et al., 2005). The same is often true for muskeg terrain in the boreal forest. Thick saturated moss slows tree growth. Landslides remove the surface cover, mix organic matter with mineral soil, allow soils to be warmer, and offer a more hospitable environment for trees.

31.5 Invited Presentations

31.5.1 The Spatial and Temporal Influence of Landslides on Stream Channels in Mountainous Terrain, British Columbia, Canada

Dan Hogan (BC Forest Service, Canada)

Landslides are an important geomorphic agent in British Columbia's steep, forested, coastal terrain.

They are episodically occurring, natural disturbance events that produce large quantities of clastic sediment and large woody material (LWM) that is delivered to adjacent streams. Because landslides leave a distinct footprint on the landscape, their historic date of occurrence can be determined and their temporal and spatial impact on the stream environment can be documented. The direct link between landslide occurrence and the evolution of stream channel morphology is established and presented here. The influence of forestry activities on landslide activity is also considered in the context of impaired fish habitats.

Dendrochronological studies indicate that four large landslide episodes occurred in coastal BC over the last 200 years; the landslides that occurred in 1891, 1917, 1934 and 1964 had a combined total volume of materials accounting for 85% of the total for the entire 200 years of record. The sediment and LWM delivered to the stream tends to cluster and initiate the formation of in-stream log jams. The formation of these jam structures alters the transport of water, sediment and LWM along the channel which in-turn leads to distinct morphological changes. Log jams that are large relative to the stream and tightly packed are effective sediment transport inhibitors. Upstream of these structures the stream is transformed from the morphologically diverse and complex pre-disturbance channel state to a greatly simplified form with shallow, in-filled pools, extensive riffles, less stable bars and increased frequency, extent and duration of a dry channel bed. Downstream the bed is typically much coarser textured and bedrock exposures are prevalent. Spatially, the channel can be influenced for lengths equal to or greater than 100 channel widths. This channel state persists for approximately one decade after which the integrity of the log structure is gradually reduced and fluvial transport slowly returns to more normal fluvial processes. As the jam deteriorates, upstream local gradients are gradually increased as sediment is moved downstream beyond the structure where the gradients are subsequentially reduced. Pools are deepened, riffles are scoured and the bed becomes coarser upstream and bars are re-built downstream. Back-channels are developed as the streamflows adjust laterally to bypass the jam. This morphological reversal typically continues between the second and fifth decade post landslide input. After approximately 50 years the log jams are sufficiently deteriorated to no longer interrupt sediment transport. The channel returns to the pre-disturbance state; the complex and diverse condition typical of coastal streams is a result of the long-term channel adjustment to earlier landslide impacts.

The morphological changes that occur upstream and downstream of the jams impact a range of fish habitats. These include spawning beds, egg incubation environments and rearing habitats. Forestry activities can alter the type, size and frequency of landslide occurrence. Because the severity of these impacts vary over time, depending on landslide timing and resultant jam structure, it is important that the natural landslide activity patterns are not altered. It must be the focus of forest management practices to mitigate increased extent of landslides to avoid increased duration of the early phases of landslide impacts while not altering the long term patterns that lead to complex habitats.

31.5.2 Landslides, Natural Protected Areas, and the Long-Term Management of Mountainscapes: Emerging Challenges from the Study of the El Triunfo Biosphere Reserve, Chiapas, Mexico

Carla Restrepo, Juan Carlos Castro Hernandez, Saul Hernandez Bezares , Miriam Janette Gonzalez Garcia (University of Puerto Rico-Rio Piedras)

In 1998 and 2004 two tropical storms triggered hundreds to thousands of landslides in the Sierra Madre de Chiapas of southwestern Mexico. A region that was particularly affected by these storms and associated landslides was the El Triunfo Biosphere Reserve (ETBR), an area of ~120,000 hectares that was set aside eighteen years ago to protect the elevated diversity of organisms and ecosystems of the Sierra Madre de Chiapas while promoting its sustainable development. Extensive landsliding in the ETBR raises numerous questions about the large-scale dynamics and conservation of these and other mountain ecosystems worldwide. Here we combine the classification of SPOT images with spatial analyses to examine the role of land cover/land use and reserve zonation on the distribution and extent of landsliding. We discuss the implications of our work for the management of the ETBR, including the role of protected areas in the conservation of landsliding as a key process driving the large-scale dynamics of mountainscapes.

31.5.3 Geoecological Imprint of Slope Deformations on Habitats – The Case Studies from the Czech Part of the Western Carpathians (Czech Republic)

Jan Hradecký (Department of Physical Geography and Geoecology, Faculty of Science, University of Ostrava)

Slope deformations represent one of the dominant morphogenetic processes in the Czech part of the Western Carpathians. Landslides significantly participate in the modification of landscape evolution processes. Entirely new, and in many cases, unique habitats evolve on the base of the differentiation of originally direct undisturbed slopes caused by landsliding. The study area contains slope deformations of various types, size dimensions and time of origin. The study brings knowledge of four different groups of slope deformations; within the deformations it analyses and interprets various reflections of landsliding disturbance, namely in partial landscape components. The slope deformations have created locations of palaeoenvironmental record which represents a valuable source of information (chronological, palynological, etc.) in terms of understanding geoecological aspects of not only the location itself but also a wider surrounding area. Within Miaší Mt and Černá hora Mt slope deformations the study focuses on the imprint of landsliding in soil variability. Evolution of specific geotopes in the extension zone of the Čertův Mlýn Mt deep-seated slope deformation is accompanied by the creation of a trench that was subsequently infilled with organogenic sediments. The occurrence of peat-bog biotopes in the Czech part of the Western Carpathians is often confined to landslides as in the case of the peat-bog on the southern slopes of Groníček Mt. High dynamics of changes of geotope features correlates with the occurrence of flow-like landslides (case study of debris flows in Smrk Mt massif). Habitat formation in areas affected by the catastrophic process of rock avalanche (Ropice Mt) is then considered to be an extreme case.

31.5.4 Mechanisms and Geoecological Consequences of Cryogenic Landslides in the Area of Marine Sedimentation – Russia

Marina Leibman (Earth Cryosphere Institute of Russian Academy of Sciences, Siberian Branch)

Maritime lowlands in the Arctic ocean margins are often composed of saline marine rocks, preserving their salinity due to perennially frozen state. Active surface processes such as landslides remove upper washed out soils, often of sandy-silty texture, to expose saline rather clayey deposits. Since the exposure, new geochemical properties and organic layer start to develop in a newly formed surface and active layer.

Depending on the triggers of a cryogenic landslide: thawing of the icy layer at the active layer base or melting of massive ground ice, different sliding mechanism may develop: either block movement of the sandy-silty rocks, or creep/flow of liquefied silty-clayey rocks. Observed is also cryogenic sliding of frozen blocks along the frozen shear surface due to gravimetric effect and wave action. Each mechanism causes different complex of consequences: geomorphologic, geochemical and geobotanical.

All types of cryogenic landslides are found on Yamal Peninsula, Russia. This region is known for widely distributed saline rocks of various sandy to clayey texture, massive ground ice rather close to the surface, complicated topography with the area of slopes exceeding that of flat surfaces, and thus vast area of slopes re-worked by landsliding. Yamal Peninsula is also studied in most detail due to natural gas production prospects. One more advantage of using this territory as a key for cryogenic landslide study is a remarkable landslide activation in

1989 and long term observations of shear surface recovery in terms of geochemistry and geobotany undertaken since then. Far less landslides appear after 1989, most of them are linked to re-exposed massive ground ice in 2005–2006 with unusually warm summers.

The main conclusions made through detailed study on the key site in Central Yamal are grouped into those concerning ionic composition of soils and ground water, succession of vegetation and related permafrost/active layer features, short-term and long-term evolution of landslide affected slopes, and impact of landsliding and its environmental consequences: biodiversity and reindeer pastures changes.

Geochemical processes on slopes exposed by landsliding cause a redistribution of ions within the active layer and upper permafrost. Due to suction, capillary processes, washing out by ground water, slopewash and other processes active layer loose salts which are in part accumulating beneath the permafrost table or on the ground surface from which they are washed away and reach the drainage network.

Bare surfaces are re-vegetating rather slowly with full recovery after decades, vegetative complexes differ from those removed, and only after several centuries shrub-moss cover possibly restore. Landslide affected slopes on Yamal underwent several cycles of landslide events after which they obtained a different from surrounding stable slopes appearance.

In terms of lithology active layer of landslide-affected slope is composed of clayey rather than sandy-silty deposits. In terms of geochemistry active layer soils and ground water contain much higher concentration of main ions, though reducing in time and acquiring a continental mode instead of marine one. In terms of geobotany, dwarf shrub moss-lichen tundra is replaced first by grass-lichen tundra and then by willow shrub grass-lichen tundra. Initial exposure of the surface and formation of a concave landform promoted snow accumulation, thermoerosion, water drainage and as a result, active layer deepening, then re-vegetation starts the inverse process.

Relief and environment changes due to landslides cause decrease of biodiversity but increase of biomass, especially in long-term effect, which improve the situation with reindeer pastures.

31.5.5 Details of the 2007 Landslide in the Valley of Geysers

V.A. Droznin, V.N. Dvigalo, E.I. Gordeev, Y.D. Muravyev (Institute of Volcanology and Seismology FEB RAS, Petropavlovsk-Kamchatsky, Russia)

The Kamchatka geysers are located in the 4 km long Canyon-shape valley of the Geysernaya River that drains the east border of the Uzon-Geysernaya volcano-tectonic depression. The spur (791 m height) collapse in the basin of the Vodopadny stream, the left feeder of the Geysernaya River resulted in the large 3 June, 2007 landslide. Its deposits blocked the Geysernaya River and resulted in formation of the dammed lake. The lake was flooded 4 days later and on the 7th of June the water started to overflow through the dam. After 4 h the river made a new bed in the dam and the water level lowered on 9 m and the maximum lake depth comprised 20 m (on echolocation date). Several large geysers were destroyed, several others occurred in the flood zone; small landslides went down the bluff shores of the lake, new short-life thermal springs were formed.

The landslide occurred as the result of two collapses. First, the spur (791 m height) in the form of so-called equal-plane (“body” 1) collapsed and formed main landslide deposits down the valley. Than, the adjoining southwest spurs (“body” 2) went down to the free from the main spur area. Table 31.1 gives the results of photogrammetric processing of aerial photographs on 1993 August, 23 and 2007 June, 12 for the territory suffered by the landslide.

31.5.5.1 Precursors

Neither precursors nor triggers were recorded prior to the event because recently scientists have not carried out any special observations in the Valley. We can just mention that the reserve ranger

Table 31.1 Quantitative characteristics of the 2007 June, 3 landslide

#1 body volume	12238000 м^3
#2 body volume	4762000 м^3
Deposit volume	20752000 м^3
dike volume	4159000 м^3
underwater part of the dike	**759000 м^3
Total volume of mudflows	
Area of deposits	994096 м^2
Lake surface on 2007 July, 7	76100 м^2

Zlotnikov V.A. reported he smelled hydrogen sulfide a day prior to the event when he was going down the valley of Vodopadniy stream in the landslide zone.

The diagram of relative 3D tidal deformation shows the time of the landslide that occurred in intra-month maximum.

The 1st body plane of rapture goes through the fissure tracing the volcano-tectonic fault in submeridional direction. Aerial photos revealed this fault in 1973.

31.5.5.2 Thermal Anomalies

The collapse in zone of the spur breakoff (791 m height) was accompanied by a large steam plume. The flow contained portions of heat rocks, they kept teaming long after they had stopped moving. The heat rocks were penetrated in the zone of the landslide formation. Now this zone shows the formation of a new thermal anomaly. The thermal anomaly is projrcted on the clift plane of the #1 body.

The rock redeposition caused by the landslide generated heat sufficient for keeping high temperature (to 60°C) in Vodopadny stream as long as one month after the event. A half-year later the water temperature decreased to 7,8°C.

31.5.5.3 Some Peculiarities of the Landslide

The collapsed rocks that form the landslide body are represented chiefly by Pleistocene lake sediments and loosely cemented tuff. The flow may be classified as a large-block, though scientists have not measured the fractal size. The large blocks are several meters in lateral dimension. The recent flow obstructed the way due to the water-bearing filling material of the flow. The eyewitnesses reported the flow had passed about 2 km for 2–2.5 min. but such a data are questionable. The data probably concern just the visible upper part of the Vodopadny stream watershed that is no longer that 1 km.

In spite of the doublet character of the landslide the single collapse amphitheater was formed in the area of its origin. The body 2 formed more than 0.22 km^2 allochthon. At least in side and front parts, the landslide moved along the snow cover, involving snow into the flow. Natural obstructions significantly influenced the landslide dynamics and its deposits profile. Extrusive formation "Triumphalnye vorota" blocked the flow on the Geysernaya River and significantly increased the dam height. The Vodopadny stream surface water discharge was not yet finished. We are demonstrates possible to the summer 2008 lakes distribution area on the flow deposits. The total water volume may comprise 400,000 m^3, 250000 of them in the largest. So, here is possible the same scenario as during the dam of the dammed lake washing out.

Geysernaya River carried out fragmental material into Shumnaya River. This material deposited in the lake and increased the volume of alluvial deposits, manifested in the form of the mobile spit. On 12 July its volume comprised 5000 m^3, on 10 September 2007 comprised 8000 m^3. Most material was carried out during cyclones and in spring, during snow melting. The time of the lake filling up is 70–100 years.

31.5.5.4 Conclusions

The largest geological catastrophe of the year 2007 on the territory of Russia occurred in the Valley of Geysers on the 3rd of June on Kamchatka. The spur (791 m height) collapse in the basin of one of the Geysernaya feeders resulted in the 20 million m^{3}rocks slide, the mudflow into the Shumnaya River valley and the dam and the dammed lake in the lower part of the river formation. Several large geysers were destroyed or flooded. We observed the alteration of the surface thermal regime in the Geysernaya hydrothermal system, small landslides along the lake banks resulted in thermal zones and hot springs migration. The paper discusses some results on the catastrophe consequences: possible reasons, current processes during and after the landslide.

Such landslides or even larger ones are typical for this region and explained by the caldera side, deeply opened by erosion. They are caused by: volcano-tectonic effects; lacustrine sediments thickness, depositing at an angle to the Geysernaya River valley, thermal waters circulation and so on. Today Geysernaya hydrothermal system is adapting to the altered hydrogeological conditions.

31.5.6 Landslide Adds to the Mystery and Natural Beauty of the Valley of Geysers

Yulia Kugaenko (Kamchatka Branch of Geophysical Survey of RAS)

Kamchatka is a huge natural museum of volcanology; its "exhibits" are active and extinct volcanoes as well as different associated formations: geysers, fumaroles, thermal springs etc. Dangerous slope processes (landfalls, landslides) are rather frequent phenomena for present-day hydrothermal fields of Kamchatka. Landfall and landslide forms of different scale and age were recognized here. Thus the big landslide on June 3, 2007 is not a unique phenomenon for the Valley of the Geysers. This natural catastrophe has strongly changed the Valley of the Geysers landscape: Geyizernaya River is dammed up by landslide deposits, as a result a new picturesque lake has been formed; a part of the geysers has been destroyed. Nevertheless the Valley of the Geysers still remains one of the main objects of ecologic tourism on Kamchatka. The photos taken in the Valley of the Geysers in different years before and after landside on June 3, 2007 are presented in this report. The characteristic of the Valley of the Geysers as an object of UNESCO World Natural Heritage is given. The main information on the landslide which occurred here on June 3, 2007 is briefly summarized.

The events in the Valley of the Geysers on June 3, 2007 should not be considered as ecological catastrophe. It is a natural process, an element of geological evolution of the territory. This process introduced certain additions to landscape originality of UNESCO World Natural Heritage Object "Volcanoes of Kamchatka". The unique landscape complex of the Valley of the Geysers did not become less interesting for the visitors. A picturesque lake has appeared here, on the caldera slope now there are nearly vertical parts of dislocation plane (wall length – 800 m, wall height – about 150 m), one can see some other results of catastrophic landslide. New lakes are observed on the avalanche flow surface.

The reorganization of surface hydrothermal system regime proceeds at present time in the Valley of the Geysers; abrupt alterations of the dam lake level activated further development of landslide processes on the Valley slopes. The Valley of the Geysers became even more interesting from the scientific point of view. The nature gives investigators a unique possibility to observe and study a wide spectrum of present-day geological processes caused by natural disaster on the geyser field.

31.5.7 Contribution of Topographically Bases Landslide Hazard Modeling to the Analysis of the Spatial Distribution and Ecology of Kauri (Agathis Australis)

Lieven Claessens (International Potato Centre, Kenya)

In this paper the use of topographical attributes for the analysis of the spatial distribution and ecological cycle of kauri (Agathis australis), a canopy emergent conifer tree from northern New Zealand, is studied. Several primary and secondary topographical attributes are derived from a Digital Elevation Model (DEM) for a study area in the Waitakere Ranges. The contribution of these variables in explaining presence or absence of mature kauri is assessed with logistic regression and Receiver Operating Characteristic (ROC) plots. A topographically based landslide hazard index, calculated by combining a steady state hydrologic model with the infinite slope stability equation, appears to be very useful in explaining the occurrence and ecological dynamics of kauri. It is shown that the combination of topographical -, soil physical – and hydrological parameters in the calculation of this single landslide hazard index, performs better in explaining presence of mature kauri than using topographical attributes calculated from the DEM alone. Moreover, this study demonstrates the possibilities of using terrain attributes for representing geomorphological processes and disturbance mechanisms, often indispensable in explaining a species' ecological cycle. The results of this analysis support the 'temporal stand replacement model', involving disturbance as a dominant ecological process in forest regeneration, as an interpretation of the community dynamics of kauri. Furthermore a threshold maturity stage, in which trees become able to stabilize landslide prone sites and postpone a possible disturbance, together with great longevity are seen as major factors making kauri a 'landscape engineer'.

31.5.8 Environmental Effects of Possible Landslide Catastrophes in the Areas of Radioactive Waste Warehousing in Kyrgyzstan (Central Asia)

Isakbek Torgoev (Scientific Engineering Center GEOPRIBOR of the National Academy of Sciences of Kyrgyz Republic)

The vast majority of natural and/or man-made catastrophes on the territory of Kyrgyzstan are triggered by earthquakes and mass gravitational movements on mountain slopes in the form of avalanches, landslides and mudflows. This happens due to the fact that mountain areas of Tien-Shan are forming the territory of the country bounds. About 90% of the whole territory is at a height of more than 1000 m, and more than 50% of the territory is at more than 2500 m above sea level.

The specific character of mountain areas of Kyrgyzstan, particularly the following: hillside topography in combination with tectonic deformations and frequent earthquakes; presence of areas with weakly stable soils (loess) and areas with a lot of atmospheric precipitation; intensive development of erosion; high mountain vulnerability to man-made influence - all this contributes to active development of landslide processes.

Presently the number of landslide sources in the country is more than 5000, from which 1000 landslides directly or indirectly threaten settlements, economic objects and infrastructure. About 15 thousand km^2 (or 7.5% of the country) are under potential landslide influence. The most number of landslides is registered in a comfortable for life activity mid-mountain area over 800–2000 m altitude ranges. The volumes of rocks and soils moving in the time of landslides run up to many millions of cubic meters.

Every year landslides in Kyrgyzstan cause very substantial economic, environmental and social damage. Within the 1993–2008 period more than 300 events of very large-scale landslides ($V \geq 10^5$ m^3) were registered as a result of which 240 people have been killed. Only the direct economic loss from landslides is on average $2 million annually.

In compliance with statistical data in Kyrgyzstan up to 70% of present landslides are related to human activity in mountain areas. These include mining of mineral resources, building and maintenance of transport communications, hydraulic structures and associated infrastructure in mountain areas. The distinctive features of "man-made" landslides are the following: considerably larger scale than the natural ones have; concentration of man-made landslides on the small-scale mining territories; long-term and continuous nature of their development, as well as higher hazards and geoecological risk due to their vast gravitational energy and accompanying multi-hazards. The greatest geoecological risk these landslides of man-made genesis represent in the warehousing areas of radioactive and toxic waste of mineral resource industry.

Under the conditions of complex mountain topography and deficit of balanced and available areas, the radioactive waste storehouses (tailing dumps and waste piles) were placed along riverbeds, in floodplains and over-floodplain terraces of mountain rivers, at the foot of slopes and/or on the slopes themselves including weakly stable ancient slope-sites. Taking into account that such a situation is highly subjected to landslide processes and events, as well as their frequent recurrence, landslides represent a source of a considerable environmental risk for a population of Kyrgyzstan.

The most hazardous are landslides, which are formed on the rims of river valleys since their development and especially the final stage - movement is often of synergetic nature (domino-effects). The synergetic nature of landslide movements in basins of river valleys is that a landslide event in narrow river valley generates a series of other hazardous events by the following scenario: landslide → rock fall-slide blockage of river bed or river valley → inundation upstream of the landslide dam → dam break → flood or mudflow downstream. Quite often these hazardous events triggered by landslides even exceed the initiating landslide event by their destructive force and causing damage.

The special hazard of development of such synergetic scenarios is that in the areas of landslide mass transit, in inundated zones or in outburst flood zones both dwellings, radioactive waste and dump sites may be at risk. In case of possible failure of these storehouses the distribution sphere of radioactive materials stored in them may be enlarged greatly due to their propagation through drainage network. Therefore, local landslide risk may be transformed into regional and/or transregional risk of radioactive contamination of surface waters of the area. In the present report were discussed the environmental risks related to direct and/or indirect landslide influence upon tailings of radioactive waste generated from mining and processing of uranium ore in two landslide hazardous areas of Kyrgyzstan, such as Mailuu-Suu and Min-Kush.

References

Banner, A., LePage, P., Moran, J., de Groot, A. 2005. The HyP^3 Project: pattern, process, and productivity in hypermaritime forests of coastal British Columbia – a synthesis of 7-year results. B.C. Min. For., Res. Br., Victoria, B.C. Spec. Rep. 10.

Costa, J.E., Schuster, R.L. 1988. The formation and failure of natural dams. Geological Society of America Bulletin 100, 1054–1068.

Benda, L. 1990. The influence of debris flows on channels and valley floors in the Oregon Coast Range, U.S.A.: Earth Surface Processes and Landforms 15, 457–466.

Benda, L., Dunne, T. 1997. Stochastic forcing of sediment supply to channel networks from landsliding and debris flow. Water Resources Research 33, 2849–2863.

Burn, C.R., Friele, P.A. 1989. Geomorphology, vegetation succession, soil characteristics and permafrost in retrogressive thaw slumps near Mayo, Yukon Territory. Arctic 42, 31–40.

Butler, D.R. 2001. Geomorphic process-disturbance corridors: a variation on a principle of landscape ecology. Progress in Physical Geography 25, 237–248.

Carson, M.A., Geertsema, M. 2002. Mapping in the interpretation and risk assessment of flowslides in sensitive Quaternary muddy sediments. In: Bobrowsky, P.T. (Ed.) Geoenvironmental Mapping, Methods, Theory and Practice. A.A. Balkema Publishers, The Netherlands, pp. 667–698.

Cruden, D.M., Keegan T.R., Thomson, S. 1993. The landslide dam on the Saddle River near Rycroft, Alberta. Canadian Geotechnical Journal 30, 1003–1015.

Cruden, D.M., Lu, Z.-Y., Thomson, S. 1997. The 1939 Montagneuse River landslide, Alberta. Canadian Geotechnical Journal 34, 799–810.

Cruden D.M., Varnes, D.J. 1996. Landslide types and processes. In: Turner, A.K., Shuster, R.L. (Eds.) Special Report 247: Landslides investigation and mitigation. TRB, National Research Council, Washington, DC, pp. 36–75.

Dale, V.H., Adams, W.M. 2003. Plant reestablishment 15 years after the debris avalanche at Mount St. Helens, Washington. The Science of the Total Environment 313, 101–113.

Dalling, J.W. 1994. Vegetation colonization of landslides in the Blue Mountains, Jamaica. Biotropica 26, 392–399.

Eden, W.J., Fletcher, E.B., Mitchell, R.J. 1971. South Nation River landslide, 16 May 1971. Canadian Geotechnical Journal 8, 446–451.

Flaccus, E. 1958. Landslides and their revegetation in the White Mountains of New Hampshire. Ph.D. dissertation, Duke University, Durham, N.H.

Flaccus, E. 1959. Revegetation of landslides in the White Mountains of New Hampshire. Ecology 40, 692–703.

Francescato, V., Scotton, M., Zarin, D.J., Innes, J.C., Bryant, D.M., 2001. Fifty years of natural revegetation on a landslide in Franconia Notch, New Hampshire, U.S.A. Canadian Journal of Botany 79, 1477–1485.

Garwood, N.C., Janos, D.P., Browkaw, N. 1979. Earthquake-induced landslides: A major disturbance to tropical soils. Science 205: 997–999.

Geertsema, M., Clague, J.J., Schwab, J.W., Evans, S.G. 2006. An overview of recent large catastrophic landslides in northern British Columbia, Canada. Engineering Geology.

Geertsema, M., Pojar, J.J. 2007. The influnce of landslides on biophysical diversity – a perspective from British Columbia. Geomorphology 89, 55–69.

Geertsema, M., Schwab, J.W. 1995. The Mink Creek Earthflow, Terrace, British Columbia. In: Proceedings of the

48th Canadian Geotechnical Conference, Vancouver B. C., pp. 625–634

Guariguata, M.R. 1990. Landslide disturbance and forest regeneration in the Upper Luquillo Mountains of Puerto Rico. Journal of Ecology 78, 814–832.

Hogan, D.L. 1986. Channel morphology of unlogged, logged, and debris torrented streams in the Queen Charlotte Islands. B.C. Minisry of Forests, Land Management Report 49, 94 pp.

Huggett, R.J. 1998. Soil chronosequences, soil development, and soil evolution: a critical review. Catena 32, 155–172.

Hull, J.C., Scott, R.C. 1982. Plant succession on debris avalanches of Nelson County, Virginia. Castanea 47, 158–176.

Hungr, O., Evans, S.G., Bovis, M., Hutchinson, J.N. 2001. Review of the classification of landslides of the flow type. Environmental and Engineering Geoscience 7, 221–238.

Keller, E.A., Swanson, F.J. 1979. Effects of large organic material on channel form and fluvial processes. Earth Surface Processes and Landforms 4, 361–380.

Lambert, J.D.H. 1972. Plant succession on tundra mudflows: preliminary observations. Arctic 25, 99–106.

Langenheim, J.H. 1956. Plant succession on a subalpine earthflow in Colorado. Ecology 37, 301–317.

Lewis, N.K. 1998. Landslide-driven distribution of aspen and steppe on Kathul Mountain, Alaska. Journal of Arid Environments 38, 421–435.

Locat, J., Lee, H.J. 2002. Submarine landslides: Advances and challenges: Canadian Geotechnical Journal 39, 193–212

Lundgren, L. 1978. Studies of soil and vegetation development on fresh landslide scars in the Mgeta valley, western Uluguru Mountains, Tanzania. Geografiska Annaler Series A- Physical Geography 60, 91–127.

Mark, A.F., Dickinson, K.J.M. 2001. Deschampsia cespitosa subalpine tussockland on the Green Lake landslide, Hunter Mountains, Fiord Ecological Region, New Zealand. New Zealand Journal of Botany 39, 577–585.

Mark, A.F., Scott, G.A.M., Sanderson, F.R., James, P.W. 1964. Forest succession on landslides above Lake Thomson, Fiordland. New Zealand Journal of Botany 2, 60–89.

Martinez, J., Avila, G., Agudelo, A., Schuster, R.L., Casadevall, T.J., Scott, K.M. 1995. Landslides and debris flows triggered by the 6 June 1994 Paez earthquake, southwestern Colombia: Landslide News, Japan Landslide Society, No. 9, pp. 13–15.

Megahan, W.F., Day, N.F., Bliss, T.M. 1978. Landslide occurrence in the western and central Northern Rocky Mountains Physiographic Province in Idaho. In Youngberg C.T. (Ed.) Forest Soils and Land Use: Proceedings of the 5th North American Forestry Soils Conference: Fort Collins, Colorado, August, pp. 116–139.

Miles, D.W.R., Swanson, F.J. 1986. Vegetation composition on recent landslides in the Cascade Mountains of western Oregon. Canadian Journal of Forest Resources 16, 739–744.

Miles, D.W.R., Swanson, F.J., Youngberg, C.T. 1984. Effects of landslide erosion on subsequent Douglas-fir growth and stocking levels in the western Cascades, Oregon. Soil Science Society of America Journal 48, 667–671.

Miller R,D.J. 1960. Giant Waves in Lituya Bay, Alaska: U.S. Geological Survey Professional Paper 354-C, pp. 51–86.

Miller, B.G.N., Cruden, D.M. 2002. The Eureka River landslide and dam, Peace River Lowlands, Alberta. Canadian Geotechnical Journal 39, 863–878.

Mollard, J.D., Janes, J.R. 1984. Airphoto Interpretation and the Canadian Landscape, Department of Energy, Mines and Resources, Canadian Government Publishing Centre, 415 pp.

Montgomery, D.R., Massong, T.M., Hawley, S.C.S. 2003. Influence of debris flows and log jams on the locations of pools and alluvial channel reaches, Oregon Coast Range. GSA Bulletin 115, 78–88.

Myster, R.W., Thomlinson, J.R., Larsen, C. 1997. Predicting landslide vegetation in patches on landscape gradients in Puerto Rico. Landscape Ecology 12, 299–307.

Myster, R.W., Walker, L.R. 1997. Plant successional pathways on Puerto Rican landslides. Journal of Tropical Ecology 13, 165–173.

Nadim, F., Kjekstad, O., Peduzzi, P., Herold, C., Jaedicke, C. 2006. Global landslide and avalanche hotspots. Landslides 3(2), 159–174.

Naiman, R.J., Beechie, T.J., Benda, L.E., Berg, D.R., Bisson, P.A., MacDonald, L.H., O'Connor, M.D., Steel, E.A. 1992. Fundamental elements of ecologically healthy watersheds in the Pacific Northwest Coastal Ecoregion. In: Naiman, R.J. (Ed.) Watershed management: Balancing sustainability and environmental change. Springer-Verlag. New York, pp. 127–188.

Nakamura, F., Swanson, F.J., Wondzell, S.M. 2000. Disturbance regimes of stream and riparian systems – a disturbance-cascade perspective. Hydrological Processes 14, 2849–2860.

Pararas-Carayannis, G. 1999. Analysis of mechanism of the giant tsunami generation in Lituya Bay on July 9, 1958. Tsunami Symposium, Honolulu, Hawaii, 11p.

Parminter, J. 1998. Natural disturbance ecology. In: Voller, J., Harrison, S. (Eds.) Conservation biology principles for forested landscapes. UBC Press, Vancouver, B.C., pp. 3–41.

Restrepo, C., Vitousek, P. 2001. Landslides, alien species, and the diversity of a Hawaiian montane mesic ecosystem. Biotropica 33, 409–420.

Revel, R.D., Maze, J.R. 1972. The central part of the Hope landslide: a botanical census. Syesis 5, 131–135.

Sakai, A. Oshawa, M. 1993. Vegetation pattern and microtopography on a landslide scar of Mt. Kiyosumi, central Japan. Ecological Research 8, 47–56.

Schuster, R.L., Highland, L.M. 2007. Overview of the effects of mass wasting on the natural environment, Geological Society of America, Environmental & Engineering Geoscience 8, 25–44.

Schwab, J.W., Geertsema, M., Blais-Stevens, A. 2004. The Khyex River landslide of November 28, 2003, Prince Rupert British Columbia, Canada. Landslides 1, 243–246.

Shimokawa, E. 1984. Natural recovery process of vegetation on landslide scars and landslide periodicity in forested drainage basins. In: O'Loughlin, C.L., Oierce, A.J. (Eds.) Symposium on the Effects of Forest Land Use on Erosion and Slope Stability, University of Hawaii, Honolulu.

Smale, M.C., McLeod, M., Smale, P.N. 1997. Vegetation and soil recovery on shallow landslide scars in tertiary hill country, East Cape region, New Zealand. New Zealand Journal of Ecology 21, 31–41.

Smith, R.B., Commandeur, P.R., Ryan, M.W. 1986. Soils, vegetation, and forest growth on landslides and surrounding logged and old-growth areas on the Queen Charlotte Islands. BC Ministry of Forests, Land Management Report 41, 95 pp.

Swanson, F.J. 1980. Geomorphology and ecosystems. In: Waring, R.W. (Ed.) Proceedings 40th Annual Biology Colloquium 1979. Forests: Fresh perspectives from ecosystem analysis. Oregon State University, pp. 159–170.

Swanson, F.J., Gregory, S.V., Sedell, J.R., Cambell, A.G. 1982. Land-water interactions: the riparian zone. In: Edmonds, R.L. (Ed.) Analysis of coniferous forest ecosystems in the western United States. USIBP Series 14, Hutchinson Ross, Strousberg, Pennsylvania, USA, pp. 267–291.

Swanson, F.J., Kratz, T.K., Caine, N., Woodmansee, R.G. 1988. Landform effects on ecosystem patterns and processes. BioScience 38, 92–98.

Swanson, F.J., Franklin, J.F. 1992. New forestry principles from ecosystem analysis of Pacific Northwest forests. Ecological Applications 2, 262–274.

Swanson, F.J., Kratz, T.K., Caine, N., Woodmansee, R.G. 1988. Landform effects on ecosystem patterns and processes. BioScience 38, 92–98.

Trustrum, N.A., Thomas, V.J., Lambert, M.G. 1984. Soil slip erosion as a constraint to hill country pasture production. Proceedings of the New Zealand Grassland Association 45, 66–76.

Vittoz, P., Stewart, G.H., Duncan, R.P. 2001. Earthquake impacts in old-growth Nothofagus forests in New Zealand. Journal of Vegetation Science 12, 417–426.

Walker, L.R., Zarin, D.J., Fetcher, N., Myster, R.W., Johnson, A.H. 1996. Ecosystem development and plant succession on landslides in the Caribbean. Biotropica 25, 566–576.

Wells, A., Duncan, R.P.,; Stewart, G.H. 2001. Forest dynamics in Westland, New Zealand: the importance of large, infrequent earthquake-induced disturbance. Journal of Ecology 89, 1006–1018.

Wondzell, S.M., King, J.G. 2003. Postfire erosional processes in the Pacific Northwest and Rocky Mountain Regions. Forest Ecology and Management 178, 75–87.

Wright, J.P., Jones, C.G., Flecker, A.S. 2002. An ecosystem engineer, the beaver, increases species richness at the landscape scale. Oecologia 132, 96–101.

Yajima, T., Nakamura, F., Shimizu, O., Shibuya, M. 1998. Forest recovery after disturbance by the 1926 mudflow at Mount Tokachi, Hokkaido, Japan. Research Bulletin of Experimental forestry Hokkaido University 55, 216–228.

Yamamoto, S., Nishimura, N., Matsui, K. 1995. Natural disturbance and tree species coexistence in an old-growth beech – dwarf bamboo forest, southwestern Japan. Journal of Vegetation Science 6, 875–886.

Zarin, D.J., Johnson, A.H. 1995. Base saturation, nutrient cation, and organic matter increases during early pedogenesis on landslide scars in the Luquillo Experimental Forest, Puerto Rico. Geoderma 65, 317–330.

32 Engineering Measures for Landslide Disaster Mitigation

Mihail E. Popescu and Katsuo Sasahara

Abstract Correction of an existing landslide or the prevention of a pending landslide is a function of a reduction in the driving forces or an increase in the available resisting forces. Any remedial measure used must involve one or both of the above parameters.

According to IUGS WG/L, landslide remedial measures are arranged in four practical groups, namely: modification of slope geometry, drainage, retaining structures and internal slope reinforcement. This chapter discusses the planning and designing aspects of the landslide remedial measures in each group and presents some illustrative examples. In addition, debris flow mitigation measures are discussed in some detail. Back analysis of failed slopes is an effective tool for reliable design of the remedial measures while advanced numerical methods are nowadays frequently used to design safe and cost effective landslide remedial measures.

Selection of an appropriate remedial measure depends on: (a) engineering feasibility, (b) economic feasibility, (c) legal/regulatory conformity, (d) social acceptability, and (e) environmental acceptability. There are a number of levels of effectiveness and levels of acceptability that may be applied in the use of these measures, for while one slide may require an immediate and absolute long-term correction, another may only require minimal control for a short period.

As many of the geological features, such as sheared discontinuities are not known in advance, it is more advantageous to put remedial measures in hand on a "design as you go basis". That is the design has to be flexible enough to accommodate changes during or subsequent to the construction of remedial works.

Keywords Landslide disaster mitigation • Engineering measures • Debris flows • Back analysis • Numerical methods • Effectiveness and acceptability of remedial measures

Mihail E. Popescu (✉)
Illinois Institute of Technology, USA

Katsuo Sasahara
Kochi University, Japan

K. Sassa, P. Canuti (eds.), *Landslides – Disaster Risk Reduction*,
© Springer-Verlag Berlin Heidelberg 2009

32.1 Introductory Remarks

Landslides and related slope instability phenomena plague many parts of the world. Japan leads other nations in landslide severity with projected combined direct and indirect losses of $4 billion annually (Schuster, 1996). United States, Italy, and India follow Japan, with an estimated annual cost ranging between $1 billion to $2 billion. Landslide disasters are also common in developing countries and economical losses sometimes equal or exceed their gross national products (Sassa et al., 2005).

The paramount importance of landslide hazard management and mitigation is by and large recognized. Herein lies the guiding principle of the current chapter; i.e., to describe engineering methods to mitigate the landslide hazard associated risks in an appropriate and effective way.

32.2 Landslide Disaster Mitigation Options

Risk mitigation is the final stage of the risk management process and provides the methodology of controlling the risk. At the end of the evaluation procedure, it is up to the client or policy makers to decide whether to accept the risk or not, or to decide that more detailed study is required. The landslide risk analyst can provide background data or normally acceptable limits as guidance to the decision maker but should not be making the decision. Part of the specialist's advice may be to identify the options and methods for treating the risk. Typical options would include (AGS, 2000):

- *Accept the risk* – this would usually require the risk to be considered to be within the acceptable or tolerable range.
- *Avoid the risk* – this would require abandonment of the project, seeking an alternative site or form of development such that the revised risk would be acceptable or tolerable.
- *Reduce the likelihood* – this would require stabilization measures to control the initiating circumstances, such as reprofiling the surface geometry, groundwater drainage, anchors, stabilizing structures or protective structures etc.
- *Reduce the consequences* – this would require provision of defensive stabilization measures, amelioration of the behavior of the hazard or relocation of the development to a more favorable location to achieve an acceptable or tolerable risk.
- *Monitoring and warning systems* – in some situations monitoring (such as by regular site visits, or by survey), and the establishment of warning systems may be used to manage the risk on an interim or permanent basis. Monitoring and warning systems may be regarded as another means of reducing the consequences.
- *Transfer the risk* – by requiring another authority to accept the risk or to compensate for the risk such as by insurance.
- *Postpone the decision* – if there is sufficient uncertainty, it may not be appropriate to make a decision on the data available. Further investigation or monitoring would be required to provide data for better evaluation of the risk

The relative costs and benefits of various options need to be considered so that the most cost effective solutions, consistent with the overall needs of the client, owner and regulator, can be identified. Combinations of options or alternatives may be appropriate, particularly where relatively large reductions in risk can be achieved for relatively small expenditure. Prioritization of alternative options is likely to assist with selection (Popescu and Zoghi, 2005).

32.3 Landslide Disaster Mitigation Engineering Measures

Correction of an existing landslide or the prevention of a pending landslide is a function of a reduction in the driving forces or an increase in the available resisting forces. Any remedial measure used must involve one or both of the above parameters.

IUGS WG/L (Popescu, 2001) has prepared a short list of landslide remedial measures arranged in four practical groups, namely: modification of slope geometry, drainage, retaining structures and internal slope reinforcement (Table 32.1). The flow diagram in Fig. 32.1 exhibits the sequence of various

Table 32.1 Short list for landslide remedial measures arranged in four practical groups: modification of slope geometry, drainage, retaining structures and internal slope reinforcement

1. MODIFICATION OF SLOPE GEOMETRY	
1.1.	Removing material from the area driving the landslide (with possible substitution by lightweight fill)
1.2.	Adding material to the area maintaining stability (counterweight berm or fill)
1.3.	Reducing general slope angle
2. DRAINAGE	
2.1.	Surface drains to divert water from flowing onto the slide area (collecting ditches and pipes)
2.2.	Shallow or deep trench drains filled with free-draining geomaterials (coarse granular fills and geosynthetics)
2.3.	Buttress counterforts of coarse-grained materials (hydrological effect)
2.4.	Vertical (small diameter) boreholes with pumping or self draining
2.5.	Vertical (large diameter) wells with gravity draining
2.6.	Subhorizontal or subvertical boreholes
2.7.	Drainage tunnels, galleries or adits
2.8.	Vacuum dewatering
2.9.	Drainage by siphoning
2.10.	Electroosmotic dewatering
2.11.	Vegetation planting (hydrological effect)
3. RETAINING STRUCTURES	
3.1.	Gravity retaining walls
3.2.	Crib-block walls
3.3.	Gabion walls
3.4.	Passive piles, piers and caissons
3.5.	Cast-in situ reinforced concrete walls
3.6.	Reinforced earth retaining structures with strip/ sheet - polymer/metallic reinforcement elements
3.7.	Buttress counterforts of coarse-grained material (mechanical effect)
3.8.	Retention nets for rock slope faces
3.9.	Rockfall attenuation or stopping systems (rocktrap ditches, benches,fences and walls)
3.10.	Protective rock/concrete blocks against erosion
4. INTERNAL SLOPE REINFORCEMENT	
4.1.	Rock bolts
4.2.	Micropiles
4.3.	Soil nailing
4.4.	Anchors (prestressed or not)
4.5.	Grouting
4.6.	Stone or lime/cement columns
4.7.	Heat treatment
4.8.	Freezing
4.9.	Electroosmotic anchors
4.10.	Vegetation planting (root strength mechanical effect)

phases involved in the planning, design, construction and monitoring of remedial works (Kelly and Martin, 1986).

Hutchinson (1977) has indicated that drainage is the principal measure used in the repair of landslides, with modification of slope geometry the second most used method. These are also generally the least costly of the four major categories, which is obviously why they are the most used. The experience shows that while one remedial measure may be dominant, most landslide repairs involve the use of a combination of two or more of the major categories. For example, while restraint may be the principal measure used to correct a particular landslide, drainage and modification of slope geometry, to some degree and by necessity, are also utilized.

Modification of slope geometry is a most efficient method particularly in deep seated landslides. However, the success of corrective slope regrading (fill or cut) is determined not merely by size or shape of the alteration, but also by position on the slope. Hutchinson (1977) provides details of the "neutral line" method to assist in finding the best location to place a stabilizing fill or cut. There are some situations where this approach is not simple to adopt. These include long translational landslides where there is no apparent toe or crest. Also, situations where the geometry is determined by engineering constraints; and where the unstable area is and thus a change in topography, which improves the stability of one area may reduce the stability of another.

Drainage is often a crucial remedial measure due to the important role played by pore-water pressure in reducing shear strength. Because of its high stabilization efficiency in relation to cost, drainage of surface water and groundwater is the most widely used, and generally the most successful stabilization method. As a long-term solution, however, it suffers greatly because the drains must be maintained if they are to continue to function (Bromhead, 1992).

Surface water is diverted from unstable slopes by ditches and pipes. Drainage of the shallow groundwater is usually achieved by networks of trench drains. Drainage of the failure surfaces, on the other hand, is achieved by counterfort or deep drains which are trenches sunk into the ground to intersect the shear surface and extending below it. In the case of deep landslides, often the most effective way of lowering groundwater is to drive drainage tunnels into the intact material beneath the landslide. From this position, a series of upward – directed drainage holes can be drilled through the roof of

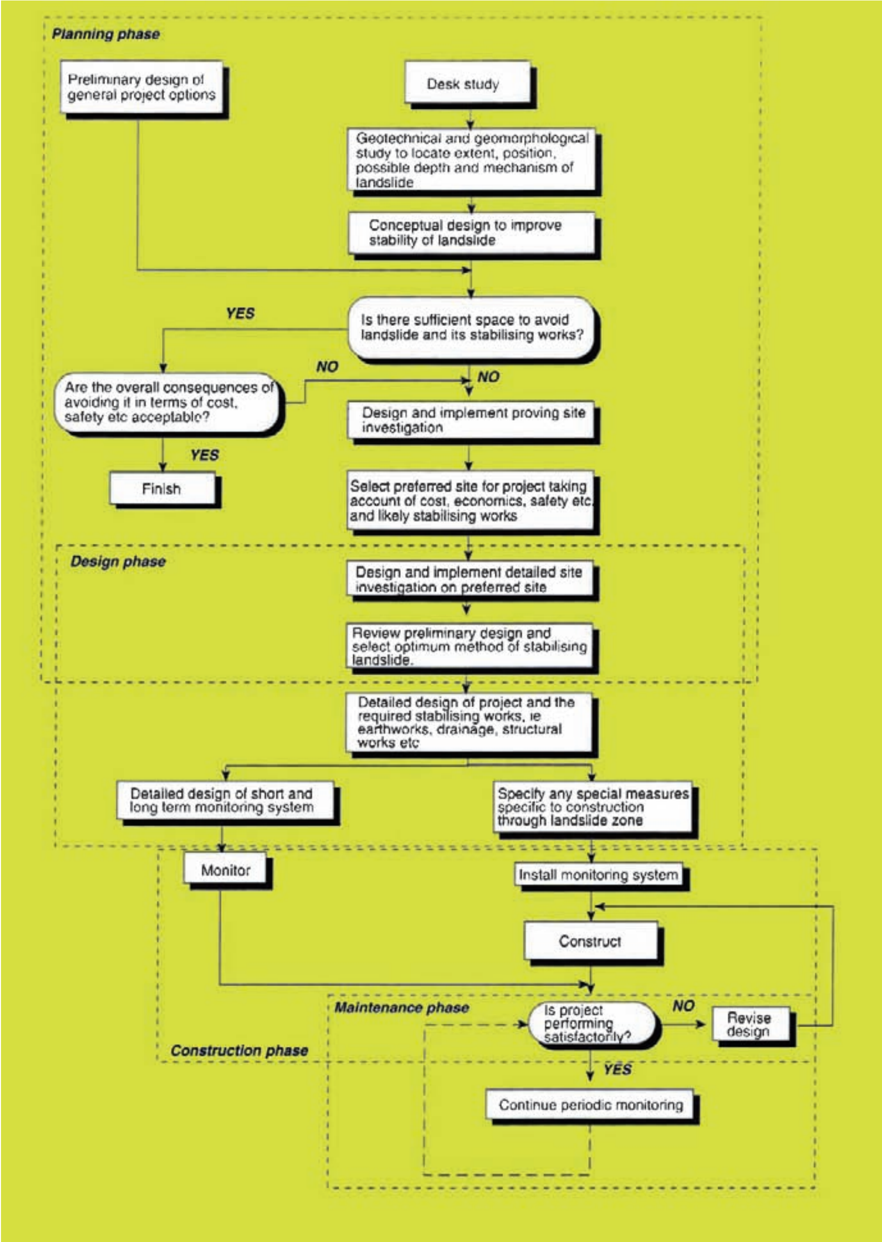

Fig. 32.1 Flow diagram showing the sequence of various phases involved in the planning, design, construction and monitoring of remedial measures

the tunnel to drain the sole of the landslide. Alternatively, the tunnels can connect up a series of vertical wells sunk down from the ground surface. In instances where the groundwater is too deep to be reached by ordinary trench drains and where the landslide is too small to justify, an expensive drainage tunnel or gallery, bored sub-horizontal drains can be used. Another approach is to use a combination of vertical drainage wells linked to a system of sub-horizontal borehole drains. Figure 32.2 presents pictures illustrating three of the most efficient drainage measures, namely sub-horizontal borehole drains, drainage wells and drainage tunnels (Japan Landslide Society, 2008).

Recent advances in the commonly used drainage systems include innovative means of drainage such as electro-osmotic dewatering, vacuum and siphon drains. In addition, buttress counterforts of course-grained materials placed at the toe of unstable slopes often are successful as a remedial measure.

Fig. 32.2 Comprehensive drainage measures: Sub-horizontal Drainage Boreholes (*upper*). Vertical Drainage Wells (*lower left*). Drainage Tunnels (*lower right*). Both drainage wells and drainage tunnels are associated with numerous sub-horizontal and sub-vertical boreholes for groundwater collection

They are listed in Table 32.1 both under “Drainage” when used mainly for their hydrological effect and “Retaining Structures” when used mainly for their mechanical effect.

During the early part of the post-war period, landslides were generally seen to be “engineering problems” requiring “engineering solutions” involving correction by the use of structural techniques. This structural approach initially focused on retaining walls but has subsequently been diversified to include a wide range of more sophisticated techniques including passive piles and piers, cast-in-situ reinforced concrete walls and reinforced earth retaining structures. A schematic view of the commonly used retaining and slope reinforcement measures is given in Fig. 32.3 along with pictures illustrating two of these measures, namely large diameter caissons and ground anchors (Japan Landslide Society, 2008).

When properly designed and constructed, these structural solutions can be extremely valuable, especially in areas with high loss potential or in restricted sites. However fixation with structural solutions has in some cases resulted in the adoption of over-expensive measures that have proven to be less appropriate than alternative approaches involving slope geometry modification or drainage (DOE, 1994).

Over the last several decades, there has been a notable shift towards “soft engineering,” non-structural solutions including classical methods such as drainage and modification of slope geometry but also some novel methods such as lime/cement stabilization, grouting or soil nailing (Popescu, 1996). The cost of non-structural remedial measures is considerably lower when compared with the cost of structural solutions. On the other hand, structural solutions such as retaining walls involve opening the slope during construction and often require steep temporary cuts. Both these operations increase the risk of failure during construction for over-steeping or increased infiltration from rainfall. In contrast, the use of soil nailing as a non-structural solution to strengthen the slope avoids the need to open or alter the slope from its current condition.

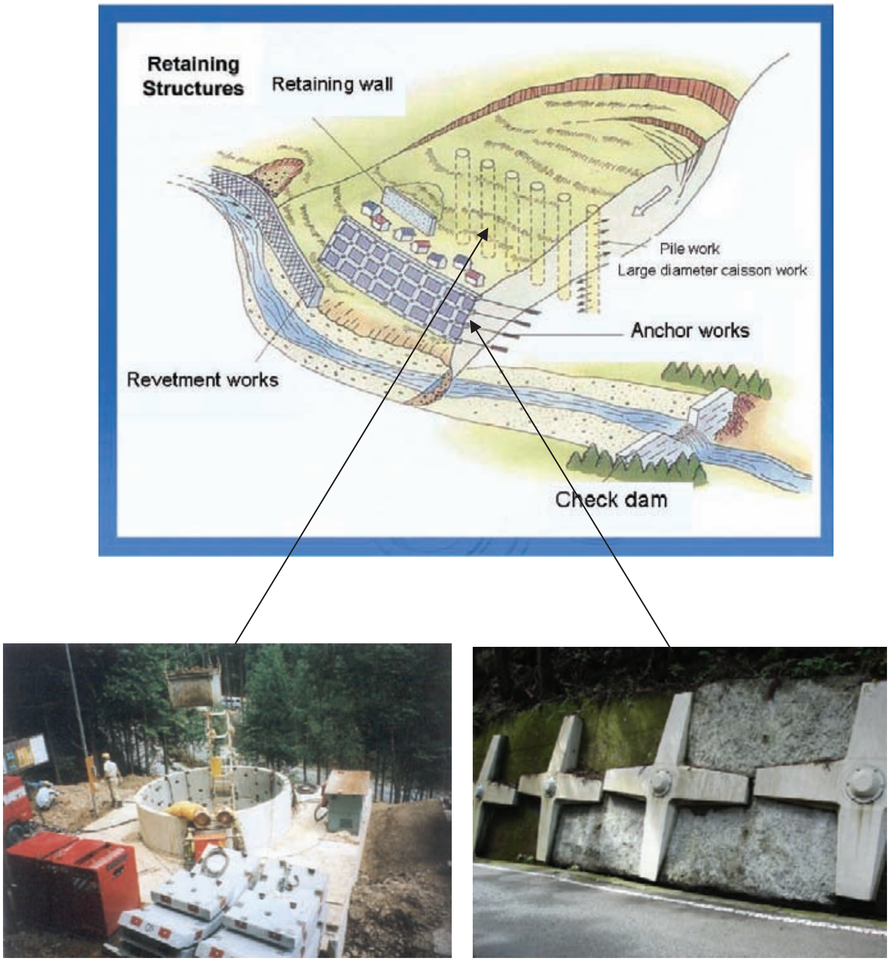

Fig. 32.3 Schematic view of the commonly used retaining and slope reinforcement measures (*upper*) along with pictures illustrating two of these measures: Large Diameter Caissons (*lower left*) and Ground Anchors (*lower right*)

Environmental considerations have increasingly become an important factor in the choice of suitable remedial measures, particularly issues such as visual intrusion in scenic areas or the impact on nature or geological conservation interests. An example of "soft engineering" solution, more compatible with the environment, is the stabilization of slopes by the combined use of vegetation and man-made structural elements working together in an integrated manner known as biotechnical slope stabilization (Fig. 32.4). The basic concepts of vegetative stabilization are not new; vegetation has a beneficial effect on slope stability by the processes of interception of rainfall, and transpiration of groundwater, thus maintaining drier soils and enabling some reduction in potential peak groundwater pressures. Except these hydrological effects, vegetation roots reinforce the soil, increasing soil shear strength while tree roots may anchor into firm strata, providing support to the upslope soil mantle through buttressing and arching. A small increase in soil cohesion induced by the roots has a major effect on shallow landslides. The mechanical effect of vegetation planting is not significant for deeper seated landslides, while the hydrological effect is beneficial for both shallow and deep landslides. However, vegetation may not always assist slope stability. Destabilizing forces may be generated by the weight of the vegetation acting as a surcharge and by wind forces on the vegetation exposed, though both these are very minor effects. Roots of vegetation may also act adversely by penetrating and dilating the joints of widely jointed rocks. The "Geotechnical Manual for Slopes" (Geotechnical Engineering Office of Hong Kong, 2000) includes useful information on the hydrological and mechanical effects of vegetation.

Fig. 32.4 Biotechnical slope stabilization: Combined use of vegetation and man-made structural elements working together in an integrated manner (*upper*). Vegetation planting combined with rock counterfort construction (*lower*). Vegetation has both hydrological and mechanical beneficial effects

The concept of biotechnical slope stabilization is generally cost effective as compared to the use of structural elements alone; it increases environmental compatibility, and allows the use of local natural materials. Interstices of the retaining structure are planted with vegetation whose roots bind together the soil within and behind the structure. The stability of all types of retaining structures with open gridwork or tiered facings benefits from such vegetation.

32.4 Debris Flow Mitigation Measures

Among debris flow mitigation measures, check dams are the most typical. Check dams in the stream capture debris flow directly and hold the sediment. Although check dams made of concrete are the most popular, some other types of check dams are also constructed for debris flow mitigation. Some relatively new types of check dams in Japan are presented in the following.

Concrete check dams (Fig. 32.5) are the most popular. They are constructed not only to capture the runoff sediment directly, but also to decrease the volume and discharge runoff sediment. The latter function represents the so called ‘sediment control function’.

The check dams filled with local sediment are used for construction cost reduction. This type of check dam is not made of concrete, but filled with sediments derived from the construction site and the inner sediment material is covered with steel walls. Steel walls are located in front of the dam and behind it (Fig. 32.5). The construction of this type of dam can avoid the transport stage of the sediment

Fig. 32.5 Concrete Check Dam (*upper*): concrete panels are pitched in the front of the dam body in order to harmonize with the surrounding landscape. Check Dam Filled with Local Sediment (*lower*): steel panels cover the dam body consisting of sediment

from outside of the jobsite. It saves much time and cost during the construction stage.

Check dams with pitching logs (Fig. 32.6) are sometimes used to harmonize the dam structure with the surrounding forest landscape. The dam body is made of concrete which provides enough strength against sediment and water discharge. Logs are used only for harmonizing with the landscape. This type of dam is generally constructed in a stream where the debris flow discharge is predicted to be very small and where a good looking landscape area like a national park is present. Logs derived by maintenance thinning of the forest are usually used for dam construction.

Check dams made of soil cement (Fig. 32.7) are sometimes constructed in a stream with much sediment yielding from a large landslide located upstream of the jobsite or on a pyroclastic fan at the foot of a volcanic mountain. They also utilize local sediment. Usually local sediment generated by the construction of the dam (e.g. digging of the riverbed or cutting the slope for the inserting wing of the dam) should be transported away from the jobsite unless it is utilized for the construction. The transport of the sediment needs much time and cost.

Fig. 32.6 Check Dam with Pitching Logs: pitching logs in front of the dam body harmonize with the surrounding forest landscape

But check dams with soil cement avoid such transport process and reduce the cement quantity for the construction of dam body. This very much contributes to the reduction of the overall construction cost of the check dam. In some cases, the construction cost is reduced up to 30% of the cost of the usual concrete dam in some volcanic areas of Japan. Soil cement is produced at the jobsite by agitating and mixing cement or cement milk with local sediment and other necessary materials at the jobsite. In Japan, two types of soil cement construction methods of check dams have been developed so far (Fig. 32.8). The first one is ISM method. In this method, local sediment without large gravel is

Fig. 32.7 Check Dam Made of Soil Cement: the wings are made of soil cement and the spillway is made of concrete

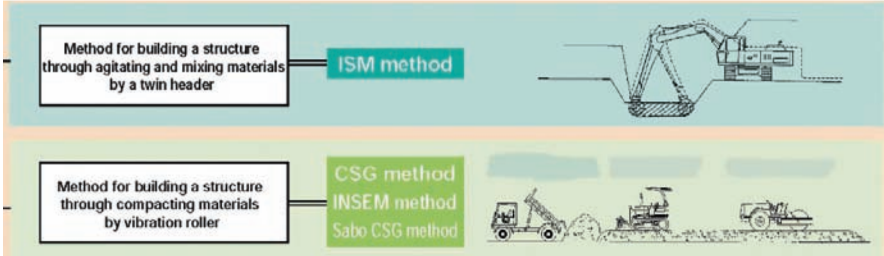

Fig. 32.8 Soil Cement Construction Methods. They are divided into two categories: the first one is the ISM method and the other includes CSG, INSEM and Sabo CSG method

mixed and agitated with cement milk at the pit. The other method is called Sabo CSG or INSEM method. The sediment generated at the jobsite is mixed directly with cement milk and compacted at the jobsite by a vibration roller. The construction of check dams with soil cement in volcanic areas of Japan is often combined with 'Unmanned Construction System', abbreviated UCS, also called "construction robot" (Fig. 32.9). In UCS, operation of the construction machine is conducted by remote control, so that the safety of workers is assured during the construction. At the foot of the active volcanic mountains, debris flow (lahar) often occurs even after a slight rainfall, so that it is difficult to keep safety of workers for the construction of check dams. But with UCS, workers have not always to work in the debris flow discharge area, so that the safety of the workers is very much improved. When UCS is adopted for the construction with soil cement, UCS machines are usually used for digging, transporting, mixing, agitating and filling sediment. In recent years, they are used even for the measurement of the dam body during construction in combination with GPS.

Open-type check dams (Fig. 32.10) are popular and have been constructed at many sites for debris

Fig. 32.9 Backhoe operated by Unmanned Construction System (UCS). Robot arm and surveying camera are set at the operating location. Operator remotely controls the machine by the robot arm and camera

Fig. 32.10 Open-type Check Dam: The Concrete Slit Dam (*upper*) is expected to have both sediment capture and retrieval functions as well as sediment discharge control function. The Steel Pipe Grid Dam is expected to catch the debris flow and discharge the captured sediment after the debris flow

flow mitigation. Concrete slit dams and steel pipe grid dams are typical in Japan. Open type check dams allow sediment discharge to down stream, usually through the slit or open space, and sediment capture at the large scale flood and debris flow. The captured sediment is discharged to downstream little by little at the small scale flood. Therefore it is expected that the sediment pocket behind the dam body can be retrieved after the large flood or debris flow. This represents the sediment capture and retrieval function of this type of dam. In recent years, sediment discharge control function has also received attention. When there is a large discharge of water flow into the slit or grid, water back filling occurs because the cross-sectional area of flow suddenly decreases. As the water is accumulating behind the dam body, flow velocity largely decreases, so that sediment deposition occurs behind the dam body and the sediment discharge to downstream decreases. Concrete slit dams are expected to have these functions. On the contrary, steel pipe grid dam are expected to capture debris flow sediment while the captured sediment is discharged to downstream little by little after the debris flow. These represent the debris flow capture function and the retrieval function of steel pipe grid dams.

32.5 Back Analysis of Failed Slopes to Design Remedial Measures

A slope failure can reasonably be considered as a full scale shear test capable to give a measure of the strength mobilized at failure along the slip surface. The back calculated shear strength parameters which are intended to be closely matched with the observed real-life performance of the slope, can then be used in further limit equilibrium analyses to design remedial works.

Shear strength parameters obtained by back analysis ensure more reliability than those obtained by laboratory or in-situ testing when used to design remedial measures.

In many cases, back analysis is an effective tool, and sometimes the only tool, for investigating the strength features of a soil deposit. However one has to be aware of the many pitfalls of the back analysis approach that involves a number of basic assumptions regarding soil homogeneity, slope and slip surface geometry and pore pressure conditions along the failure surface. A position of total confidence in all these assumptions is rarely if ever achieved.

Indeed, in some cases, because the large extension of a landslide, various soils with different properties are involved. In other cases the presence of cracks, joints, thin intercalations and anisotropies can control the geometry of the slip surface. Moreover progressive failure or softening resulting in strength reductions that are different from a point to the other, can render heterogeneous even deposits before homogeneous.

While the topographical profile can generally be determined with enough accuracy, the slip surface is almost always known in only few points and interpolations with a considerable degree of subjectivity are necessary. Errors in the position of the slip surface result in errors in back calculated shear strength parameters. If the slip surface used in back analysis is deeper than the actual one, c' is overestimated and ϕ' is underestimated and vice-versa.

The data concerning the pore pressure on the slip surface are generally few and imprecise. More exactly, the pore pressure at failure is almost always unknown. If the assumed pore pressures are higher than the actual ones, the shear strength is overestimated. As a consequence, a conservative assessment of the shear strength is obtainable only by underestimating the pore pressures.

Procedures to determine the magnitude of both shear strength parameters or the relationship between them by considering the position of the actual slip surface within a slope are discussed by Popescu and Yamagami (1994). The two unknowns – i.e. the shear strength parameters c' and ϕ' – can be simultaneously determined from the following two requirements (Fig. 32.11):

(a) F = 1 for the given failure surface. That means the back calculated strength parameters have to satisfy the c'-tan ϕ' limit equilibrium relationship;
(b) F = minimum for the given failure surface and the slope under consideration. That means the factors of safety for slip surfaces slightly inside and slightly outside the actual slip surface should be greater than one.

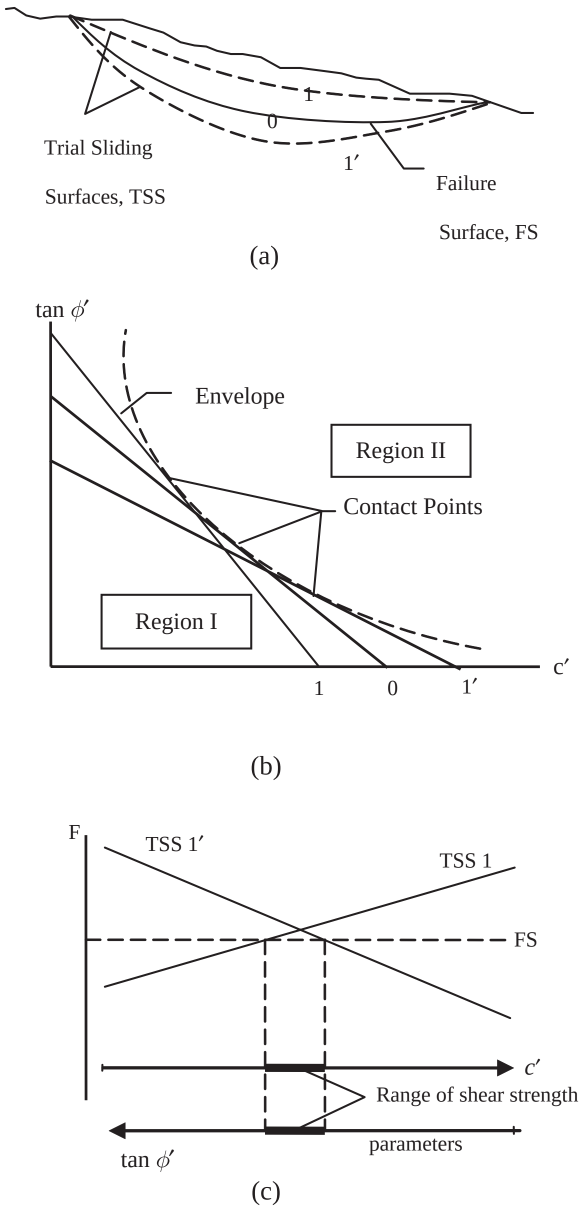

Fig. 32.11 Back Calculation of the Shear Strength Parameters from Slope Failures. The two unknowns (c' and φ') can be simultaneously determined from the following two equations involving the slope safety factor: F = 1 and F = minimum

The fundamental problem involved is always one of data quality and consequently the back analysis approach must be applied with care and the results interpreted with caution.

Back analysis is of use only if the soil conditions at failure are unaffected by the failure. For example back calculated parameters for a first-time slide in stiff, overconsolidated clays could not be used to predict subsequent stability of the sliding mass, since the shear strength parameters will have been reduced to their residual values by the failure.

It is also to be pointed out that if the three-dimensional geometrical effects are important for the failed slope under consideration and a two-dimensional back analysis is performed, the back calculated shear strength will be too high and thus unsafe.

Although the principle of the back analysis method discussed above is correct, Duncan and Stark (1992) have shown that in practice, as a result of progressive failure and the fact that the position of the rupture surface may be controlled by strong or weak layers within the slope, the shear strength parameters cannot be uniquely determined through back analysis.

The alternative is to assume one of the shear strength parameters and determine the other one that corresponds to a factor of safety equal to unity. Duncan and Stark (1992) proposed to assume the value of ϕ', using previous information and good judgment, and to calculate the value of c' that corresponds to F = 1. They recommended assume fully softened strength where no sliding has occurred previously, and residual strength where there has been sufficient relative shearing deformation along a pre-existing sliding surface.

Using the concept of limit equilibrium linear relationship c'-tan ϕ', the effect of any remedial measure (drainage, modification of slope geometry, restraining structures) can easily be evaluated by considering the intercepts of the c'-tan ϕ' lines for the failed slope (c_0', tan ϕ_0') and for the same slope after installing some remedial works (c'$_{nec}$, tan ϕ'$_{nec}$), respectively. The safety factor of the stabilized slope is:

$$F = \min\left(F_c = \frac{c'_0}{c'_{nec}}, F_\phi = \frac{\tan\phi'_0}{\tan\phi'_{nec}}\right)$$

Errors included in back calculation of a given slope failure will be offset by applying the same results, in the form of c' – tan ϕ' relationship, to the design of remedial measures.

The above outlined procedure was used to design piles to stabilize landslides (Popescu, 2006) taking into account both driving and resisting force. The principle of the proposed approach is illustrated in Fig. 32.12 which gives the driving and resisting force acting on each pile in a row as a function of the non-dimensional pile interval ratio B/D. The driving force, F_D, is the total horizontal force exerted by the sliding mass corresponding to a prescribed increase in the safety factor along the given failure surface. The resisting force, F_R, is the lateral force corresponding to soil yield, adjacent to piles, in the hatched area shown in Fig. 32.12. F_D increases with the pile interval while F_R decreases with the same interval. The intersection point of the two curves which represent the two forces gives the pile interval ratio satisfying the equality between driving and resisting force.

The accurate estimation of the lateral force on pile is an important parameter for the stability analysis because its effects on both the pile-and slope stability are conflicting. That is, safe assumptions for the stability of slope are unsafe assumptions for the pile stability, and vice-versa. Consequently in order to obtain an economic and safe design it is necessary to avoid excessive safety factors.

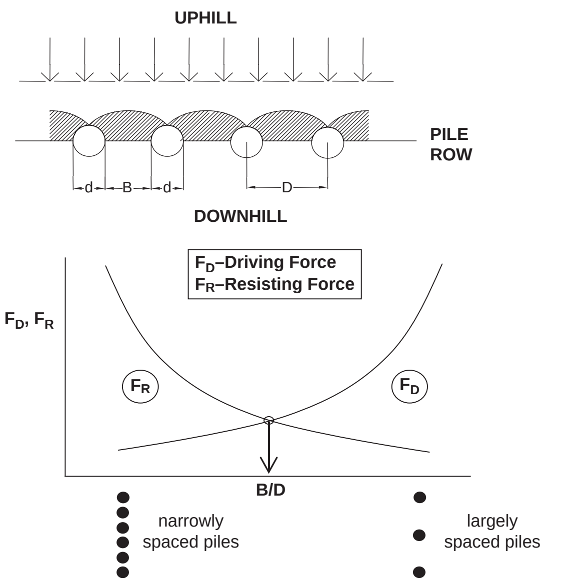

Fig. 32.12 Design of Piles to Stabilize Landslides. Both driving and resisting force acting on each pile in a row should be considered to derive the optimum non-dimensional pile interval ratio B/D

32.6 Optimum Planning and Design of Remedial Measures by Numerical Analysis

Nowadays the budget for landslide disaster mitigation works in many countries is continuously shrinking due to economical restrictions. Therefore cost effective landslide mitigation measures are hardly needed.

This goal can be achieved by the optimum planning and design of landslide mitigation measures taking into account the actual landslide characteristics, adopting new construction methods or cheaper materials and reconsidering the construction process options. The following presents some general concepts on the optimum planning and design of landslide mitigation measures.

Numerical methods are largely used in the planning and design of landslide remedial measures. These include 3-D seepage analysis for the planning of drainage works and 3-D limit equilibrium slope stability analysis or 3-D deformation analysis by Finite Element Method (FEM) for the design of restraint works such as stabilizing piles or ground anchors.

Formerly, when our calculation ability was limited by the computer availability and capability, simplified 2-D numerical methods have been used for both seepage analyses and slope stability evaluations in order to design remedial measures such as slope geometry modification, drainage works, retaining structures or internal slope reinforcement structures. While it is apparent that the landslide processes are always 3-D, the 2-D seepage and slope stability analysis methods only treat longitudinal unit width sections of the landslide mass neglecting 3-D topographical and geological effects and 3-D pattern of the groundwater movement within the landslide mass which is also 3-D.

In recent years more sophisticated and more reliable, computer based, numerical analysis methods have been developed and adopted for the planning and design of the landslide mitigation works. These methods greatly contribute to a safer and more cost effective design of landslide mitigation works.

As stated above, the groundwater movement within the landslide mass is affected by the 3-D shape and geological structure of the landslide mass. In order to take into account these 3-D factors in the design of the drainage works, reliable information on the 3-D topography and geology of the landslide area is needed. The 3-D seepage modeling requires information not only on the site 3-D topography and geology but also on the 3-D distribution and variability of soil hydraulic and physical properties which govern groundwater movement. This type of analysis can more accurately simulate the movement of groundwater and therefore can result in optimum planning and design of the drainage works. It is to be noted that more information on site topography and geology and more geotechnical investigations to better define the variability of soil parameters are needed for a 3-D seepage analysis as compared with a 2-D analysis. However the additional cost associated with the supplementary investigations is compensated by the more reliable and cost effective design of the drainage works.

The above statement is valid also for 3-D slope stability analysis methods or 3-D deformation FEM analysis approaches when used for the design of the restraint works. 2-D slope stability analysis methods such as Fellenius or Bishop method, for circular failure surfaces, and Janbu or Spencer method, for non-circular failure surfaces, can be easily incorporated in simple computer programs or even used in hand calculations. However they do not reflect the 3-D landslide topography and geology and the 3-D variability of soil mechanical and physical properties. Where the shape of landslide mass is like a whisky-barrel, with the cross-sectional width and depth maximum at the center longitudinal profile and becoming smaller towards the lateral boundaries of the mass, we should consider in the general equilibrium of the sliding mass not only the resistant force at the toe but also at the lateral boundary resistant forces. In such a case only a 3-D analysis can adequately reflect the effect of the resistant forces in the cross-sectional direction. In addition, 3-D analysis can consider the resistant force of the anchor works which have an oblique direction in respect to the longitudinal section of the landslide mass. A 2-D analysis can not model appropriately oblique forces in respect to the longitudinal direction. As far as stabilizing piles are concerned, the 2-D analysis methods assume that the pile row acts as a wall providing a resistant force in longitudinal section. However the actual situation is clearly 3-D and the 3-D location of stabilizing pile and their interval along the cross-sectional direction should be considered for an appropriate planning and design of the stabilizing structures. If the pile interval is too large, the soil between piles can move down slope and therefore the stabilizing piles do not play their role though they may have enough structural resistance. Interaction between the piles and soil along cross-sectional direction should be considered in addition to the forces acting along longitudinal direction. 3-D FEM deformation analysis can adequately incorporate this effect.

32.7 Levels of Effectiveness and Acceptability that may be Applied in the Use of Remedial Measures

Terzaghi (1950) stated that, “if a slope has started to move, the means for stopping movement must be adapted to the processes which started the slide”. For example, if erosion is a causal process of the slide, an efficient remediation technique would involve armoring the slope against erosion, or removing the source of erosion. An erosive spring can be made non-erosive by either blanketing with filter materials or drying up the spring with horizontal drains etc.

The greatest benefit in understanding landslide-producing processes and mechanisms lies in the use of the above understanding to anticipate and devise measures to minimize and prevent major landslides. The term major should be underscored here because it is neither possible nor feasible, nor even desirable, to prevent all landslides. There are many examples of landslides that can be handled more effectively and at less cost after they occur. Landslide avoidance through selective location is obviously desired – even required – in many cases, but the dwindling number of safe and desirable construction sites may force more and more the use of landslide – susceptible terrain.

Selection of an appropriate remedial measure depends on: (a) engineering feasibility, (b) economic feasibility, (c) legal/regulatory conformity, (d) social acceptability, and (e) environmental acceptability. A brief description of each method is presented herein:

a) Engineering feasibility involves analysis of geologic and hydrologic conditions at the site to ensure the physical effectiveness of the remedial measure. An often-overlooked aspect is making sure the design will not merely divert the problem elsewhere.
b) Economic feasibility takes into account the cost of the remedial action to the benefits it provides. These benefits include deferred maintenance, avoidance of damage including loss of life, and other tangible and intangible benefits.
c) Legal-regulatory conformity provides for the measure meeting local building codes, avoiding liability to other property owners, and related factors.
d) Social acceptability is the degree to which the remedial measure is acceptable to the community and neighbors. Some measures for a property owner may prevent further damage but be an unattractive eyesore to neighbors.
e) Environmental acceptability addresses the need for the remedial measure to not adversely affect the environment. De-watering a slope to the extent it no longer supports a unique plant community may not be environmentally acceptable solution.

Just as there are a number of available remedial measures, so are there a number of levels of effectiveness and levels of acceptability that may be applied in the use of these measures. We may have a landslide, for example, that we simply choose to live with; one that poses no significant hazard to the public, whereas it will require periodic maintenance for example, through removal, due to occasional encroachment onto the shoulder of a roadway.

Most landslides, however, must usually be dealt with sooner or later. How they are handled depends on the processes that prepared and precipitated the movement, the landslide type, the kinds of materials involved, the size and location of the landslide, the place or components affected by or the situation created as a result of the landslide, available resources, etc. The technical solution must be in harmony with the natural system, otherwise the remedial work will be either short lived or excessively expensive. In fact, landslides are so varied in type and size, and in most instances, so dependent upon special local circumstances, that for a given landslide problem there is more than one method of prevention or correction that can be successfully applied. The success of each measure depends, to a large extent, on the degree to which the specific soil and groundwater conditions are prudently recognized in an investigation and incorporated in design.

As many of the geological features, such as sheared discontinuities are not known in advance, it is more advantageous to put remedial measures in hand on a “design as you go basis”. That is the design has to be flexible enough to accommodate changes during or subsequent to the construction of remedial works.

32.8 Invited Presentations

32.8.1 The Forest City Landslide, South Dakota, USA (by Vernon R. Schaefer)

Following inundation of the Oahe Reservoir in the 1960 s in South Dakota, USA, numerous landslides developed along the reservoir rim. A particularly large landslide reactivated at the location where U.S Highway 212 crosses the reservoir. The landslide is locally known as the Forest City landslide, after the former village that occupied the location prior to reservoir impoundment. The U.S. Highway 212 Bridge was constructed prior to closure of the Oahe Dam, as a replacement to a bridge crossing the Missouri River some 10 km upstream. Unbeknownst to the bridge designers, the bridge was located at the toe of an ancient landslide. Rising reservoir levels caused reactivation of the landslide; however it took many years before this was recognized. Water levels began rising in the Oahe Reservoir in the early 1960 s and the first bridge distress was noted in 1962. By 1965 an expansion device at the bridge abutment had closed. The first recognition of geotechnical problems was in about 1968 and extensive monitoring of the landslide at the site began in 1972. Throughout the 1970 s and 1980 s intermittent monitoring and movements occurred, with occasional concerns for safety of the bridge. Hazard warning devices were installed at the bridge abutment in case of failure and loss of the traffic lanes. Continuing movements brought the need and realization for stabilization to the attention of political officials. Extensive remedial investigations began in 1988, with construction of several stabilization techniques during the 1990 s, including stone columns, unloading of the driving force and installation of shear pins in the toe of the slide.

The local importance of the Highway 212 bridge structure stems from the fact that it is the only reservoir crossing for some 140 km upstream and downstream of the bridge. The Forest City landslide measures approximately 1.7 km wide, 1.25 km long from head to toe, and 125 m high from head to toe. The depth of the sliding surface is from 60 to 120 m below ground surface. It has been estimated that the landslide involves on the order of 75 million cubic meters of soil and rock debris and covers over three square kilometers of land area.

The stratigraphy at the site consists of firm and weathered Pierre Shale overlain by glacial till materials consisting of a heterogeneous clay matrix with sand, silt and clay and numerous gravel beds, likely the result of erosion in geological time. Fill was placed at the toe of the slope to provide an abutment for the bridge. Extensive instrumentation was placed at the site to allow determination of the location of the failure plane and reasonable determination of water levels in the shale and overlying glacial till materials. The instrumentation showed that the movements were occurring at or just above the contact of the weathered shale and the firm shale. Water level measurements indicated a complex system between the shale, glacial till and reservoir levels. Laboratory testing of the Pierre Shale and back analyses of the failure indicated that the residual strength of the weathered shale was in the range of 6–8°.

The remedial measures (Fig. 32.13) were constructed in three phases. The first phase completed in 1993 consisted of drilling large diameter stone columns into the toe of the slide to stabilize local slides near the bridge abutment. The second phase completed in 1995 and 1996 consisted of excavating a deep corridor through the center of the overall sliding mass to unload the driving forces. The corridor was approximately 185 m wide, some 600 m in length and was made some 40 m into glacial till materials. Approximately 7 million cubic meters of material was removed from the cut. The third phase was completed in 1998 and consisted of the placement of 66 shear pins at the toe of the slide, to depths of 45 m below ground surface to intersect deep shear planes in the overall sliding mass. The shear pins were one meter by three meter rectangular reinforced concrete members. Figure 32.13 shows construction of the shear pins.

Fig. 32.13 Remedial Measures of the Deep Seated Forest City Landslide: Excavator used to construct the one meter by three meters shear pins (*left*). Reinforcing cage being lowered into the excavation (*right*)

Prior to the remedial measures the movements of the main slide and local slides ranged from 100 mm to 250 mm per year. The remedial measures have reduced the movements to less than 2 mm per year and have been performing well for nearly a decade.

32.8.2 Back Analysis of Landslides to Allow the Design of Cost-Effective Mitigation Measures (by S.R. Hencher, S.G. Lee, and A.W. Malone)

This paper concerns forensic studies of landslides and the improved understanding that can result from such studies, both for local mitigation and to allow more rational management of slopes. The true mechanism of a landslide is often difficult to unravel - there may be many contributing factors and the investigator needs to act as a detective, looking for evidence, developing theories and testing these through further observation, analysis and focused investigation. One of the key questions is often why a landslide has occurred at a particular location, at a particular time (especially where there is no immediate trigger) and with a particular geometry rather than elsewhere in the same slope or in adjacent slopes. It is noted that the very nature of landslides calls for experience in geomorphology, engineering geology, structural geology, hydrogeology and soil and rock mechanics in forensic investigation. Without such knowledge within the investigating team, landslides may well be misinterpreted with incorrect, simple explanations offered for what is fundamentally more complex. Reference is made to examples where different teams have given different explanations for the same landslide event and this is used to emphasis the need for a balanced investigation team.

In many cases, a fundamentally important aspect is adverse and often complex geology and hydrogeology and this is illustrated for several rock and deeply weathered slopes. The presentation is illustrated with reference to detailed investigations of landslides in Hong Kong, Korea, Malaysia and Europe. Cases include large scale rock failures and weathered rock examples from Hong Kong, the current massive landslide at Pos Selim in Malaysia (Fig. 32.14) and a fatal landslide in South Korea. Other examples are used to illustrate how landslides can be interpreted to gain a better understanding of mass shear strength, strain-controlled shear strength and hydrogeological controls.

Failures in engineered slopes are often particularly revealing in that they demonstrate flaws in thinking, investigation and analysis from which lessons can be learned. Examples include failed slopes that had been investigated using standard ground investigation and instrumentation techniques but where the true mechanism had been overlooked or missed.

It is acknowledged that whilst it is relatively easy to identify the key aspects of a landslide after the event, it is a much more difficult task to use that interpretation to make predictions regarding the hazard levels in other slopes. Examples are given of where such lessons have been used to reassess other slopes and to make decisions regarding the need for landslide mitigation works.

In terms of mitigation, it is very important that an ongoing, progressive landslide is properly understood to ensure that correct and cost effective mitigation measures are adopted. Monitoring is important for assessing an ongoing landslide risk but that monitoring must to be linked to models, identified through proper investigation and

Fig. 32.14 Pos Selim Landslide in Malaysia. Detailed investigations of the complex geology and hydrogeology conditions have been performed to define the landslide mechanisms

analysis that can then be tested through prediction and measurement.

32.8.3 Soft Engineering and Drainages for Slope Stabilization: Ground Water Control and Vegetative Bio Techniques (by G. Urciuoli and R. Papa)

Introduction: Soft engineering, also known as bioengineering, is a technique which uses native plant materials to stabilize eroding slopes and shallow landslides. This technique can give good results if it is jointed to other types of control works, as drainages of surface and subsurface water, constituting a more natural and less invasive method for soil stabilization, respect to “hard” engineering techniques (e.g. walls, piles).

Drainage: In saturated soils, drains are widely used as control works against slope instability, as they are less costly than other types of control works and are suitable for a large number of cases, even when the landslide is very deep and structural measures are inadequate. The mechanical role of drains inside slopes consists in a decrease in pore pressures in the subsoil and consequently of an increase in effective stresses and soil shear strength in the whole drained domain. In particular, increase in shear strength along the active or potential sliding surface, at the base of the landslide body, is responsible for slope stability improvement due to the work of drains. Therefore the first step in the design of a drainage system consists of determining a distribution of pore pressure changes, for which the factor of stability is increased up to the value chosen by the designer.

The next step consists of designing the geometric configuration of drains that determines the distribution of pore pressure previously calculated by means of slope analysis.

The effect of the drainage system is usually analyzed in steady-state condition, which is attained some time after drainage construction (in the long term). The analysis is carried out by considering continuously present, at the ground surface, a film of water, able to recharge the water table. In the literature, results of steady-state analysis are represented in non-dimensional design charts that technicians generally use to project drainage systems.

After drain excavation, a transient phenomenon of equalization of pore pressures occurs, provoking subsidence of the ground surface, whose intensity depends on: (i) compressibility of the soils concerned, (ii) thickness of the drained domain, (iii) lowering of the water table. Therefore problems related to excessive settlements are expected when the drained soil is very thick, as in the case of deep drains.

As regards the transient phase, two aspects have to be evaluated in the design:

- whether the delay until the complete efficiency of drains is compatible with the destination of the area,
- whether associated settlements can damage buildings and infrastructures at ground surface.

The water flow captured and discharged by drains depends strongly on the permeability of the drained soils. In steady-state condition the permeability does not affect the lowering of the pore pressures in the subsoil, which depends on the hydraulic conditions at the boundaries of the examined domain and the geometry of the drainage system. Thus the quantity of water discharged is not an indicator of the good working of drains, which must be investigated by means of piezometers, to measure the level of the water table as modified by drains. Indeed, pore pressure changes are the most direct and useful indicators of drains in good working order. Measurements of superficial and deep displacements are good indicators of overall slope stability and can be carried out to complete the framework of information obtained from piezometer surveys.

The role of vegetation: Also hydraulic interaction between the subsoil and the atmosphere and the role of vegetation on this phenomenon have been analysed, to predict soil water content and suction regime in the subsoil, as a function of meteoric and seasonal variations. Important differences in soil water content have been expected during dry seasons when evapo-transpiration is high (due to high temperature and direct sun radiation on soil surface) and there are leaves on the branches of trees.

During humid seasons suction in the subsoil decreases and assumes more or less the same values where there are trees and where vegetation is absent or has been cut.

32.8.4 Stabilization of Slopes: An Experience from Norway (by V Thakur, A Watn, S Christensen, E Øiseth, S Nordal, G Priol and K Senneset)

Over the last couple of decades the use of deep soil stabilization with dry mixing of lime-cement (Fig. 32.15) has increased in Norway. Especially lime-cement columns located in ribs for slope stabilization have been used on several occasions. The method has proved much cost competitive in comparison to traditional solutions. Unfortunately some failures of lime-cement stabilized slopes have occurred, putting focus on the relevance of the parameters for strength and deformation of both the undisturbed and the stabilized soil. Existing methods for in situ and laboratory testing are generally related to total strength parameters. A principle for design using effective strength parameters is believed to give a more realistic representation of the real strength of the lime-cement ribs and the interaction with the surrounding soil. The inhomogeneous nature of the stabilized soil thus requires a relatively large amount of data to establish relevant strength and deformation parameters. A real case of lime cement stabilization is presented in this paper. Also a numerical analysis based on effective strength parameters has been conducted and has given a more realistic representation of the real strength of the lime-cement ribs and the interaction with the surrounding soil. This modelling has been compared to a 3D FEM model using the Plaxis code in order to permit a better evaluation of the reinforcement produced by the ribs. This work constitutes the first step for the development of a new design principle for this kind of complex geotechnical structure. The background for this article is based on the experience of SINTEF and NTNU in projects connected to slope stabilization and embankments, and through involvement and guidance in academic theses at NTNU.

32.8.5 Modeling the Behavior of Rockfall Protection Fences (by Cantarelli G.C., Giani G.P., Gottardi G. & Govoni L.)

The paper presents an analytical model for a rock block impacting rockfall protection barrier metallic nets (Fig. 32.16). The model can be used to evaluate the net elongation and its braking time. The analytical model can also determine when an impact is exclusively elastic or when the barrier provides a plastic response.

The analytical procedure has been calibrated through a comparison between the computed prediction and the results of full scale impact tests carried out on several blocks of different size, following the instructions provided by the Guideline for European Technical Approval of Falling Rock Protection Kits (ETAG).

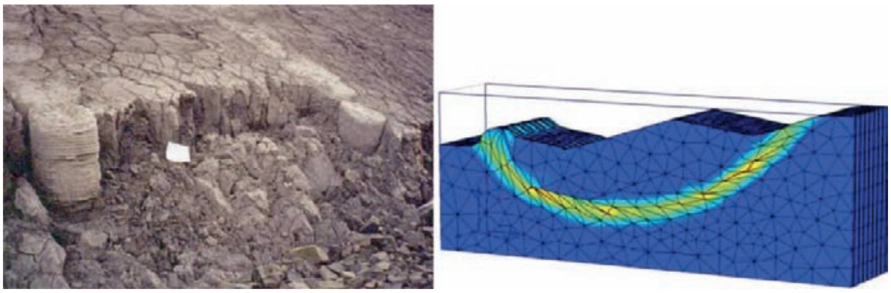

Fig. 32.15 Soil Stabilization Using Lime-Cement Piles (*left*); Three Dimensional Finite Element Modelling of the interaction between the reinforcing lime-cement ribs and surrounding soil (*right*)

Fig. 32.16 Full Scale Modeling of the Behavior of the Rockfall Protection Fences: Rock blocks of different sizes are dropped vertically onto the protection net to assess its deformation and breaking time

The results presented in the paper concern the experiments carried out on a vertical-drop test site, which is a structure able to accelerate a concrete block to an established speed and to impact it, in free-fall motion, onto a sample of rockfall protection barrier. The sample of the barrier is made of three functional modules (i.e. three fence segments) and is anchored orthogonally to a vertical slope. A crane is used to handle the testing block made out of polyhedron shaped concrete. During the impact test, the block trajectory is vertical and the block impacts into the centre of the middle functional module. No ground contacts occurs before the impact, ensuring that there is no energy loss except the air friction energy loss. Therefore the kinetic energy is a sole function of the mass and falling height of the block. As a result this kind of test is particularly suitable for the purposes of model calibration. The test site is also provided with high-definition video cameras for the direct measurement of the net maximum elongation and braking time in dynamic conditions. These measured values, when evaluated analytically, show a remarkably good agreement with the experimental results.

The metallic net behaviour is assumed elastic to describe the block arrest and the phenomenon is described by a non-homogeneous constant coefficient second order differential equation. The constant coefficients are determined by imposing the initial conditions. The motion equation in the post impact phase is obtained by integrating the net behaviour differential equation. Thus the net maximum elongation and the arrest time are determined.

The analytical model can be applied to other cases of blocks of different geometry impacting onto metallic nets. The results of these applications put into evidence how a barrier design based only on energetic criteria might not be suitable.

A final discussion shows how the analytical model proposed in this paper can also be used for debris flow or snow avalanche protection works.

32.8.6 An Evaluation Method of Landslide Prevention Works in Yuzurihara Landslide (by Nobuaki Kato, Ryosuke Tunaki, keiji Mukai, Kazuyuki Sato, Takumi Yoshizawa)

The presentation reports an evaluation method of landslide prevention works in Yuzurihara landslide.

Yuzurihara Landslide is located on about 20 km south from Takasaki City, Gunma prefecture, Japan (36°08'N; 139°02'E). It faces the southwest side of a mountain ridge and has the designated landslide prevention area of 600 m long 1700 m wide and 40–50 m deep (Fig. 32.17). There are about forty residences on the landslide area and the route 462 passes in the midst of the landslide. The basement rock of the landslide is crystalline shist belonging to the Sambagawa Belt.

The landslide became activated in 1910, 1938, and 1947. By 1969, ground water drainage works taken by Gunma prefectural government inactivated the landslide. In 1991, the landslide reactivated due to rainfall, which damaged the route 462 and residential structures. Afterwards, the landslide prevention works become large-scale, and it was replaced under the direct control of the Ministry of Construction in 1995.

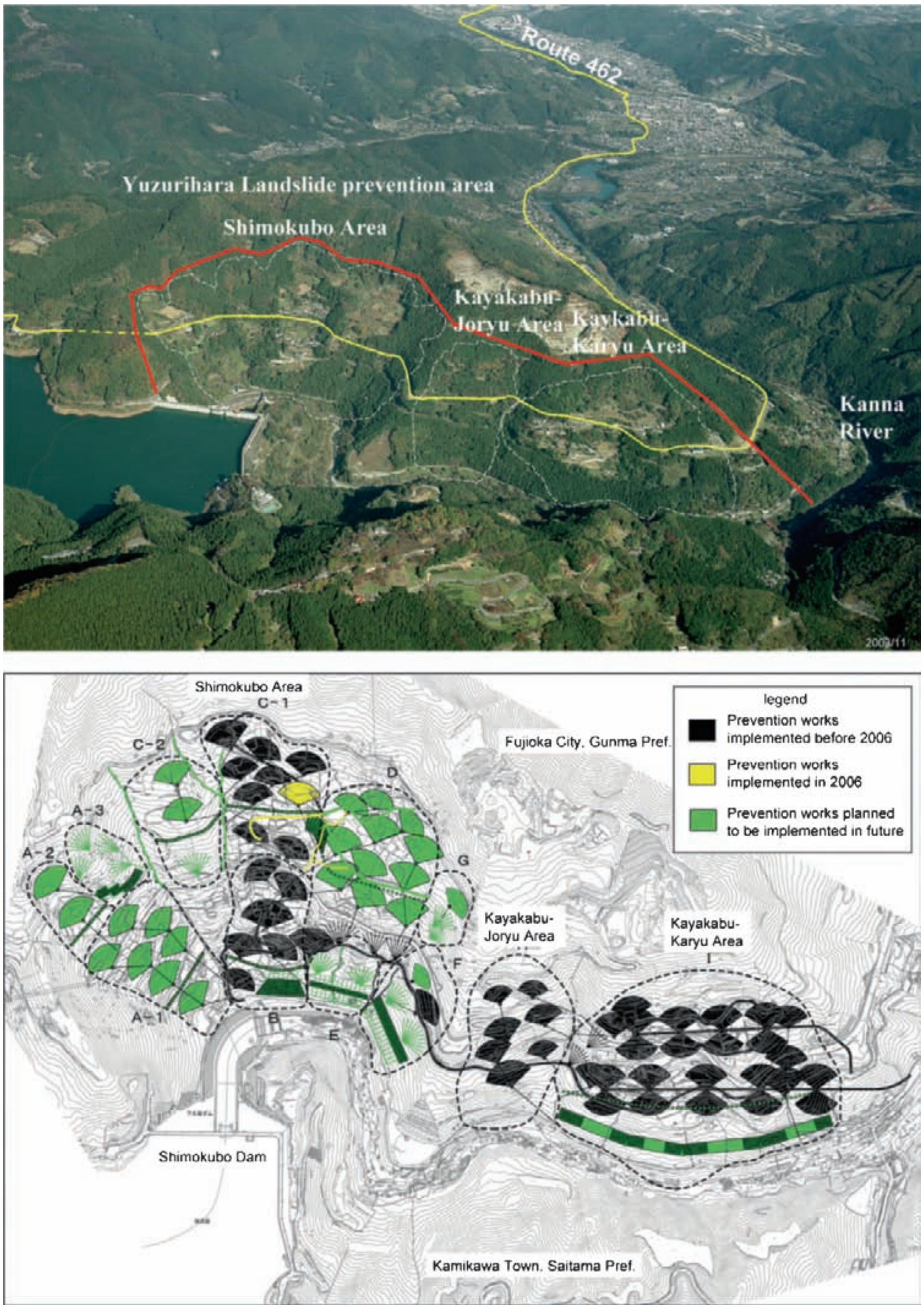

Fig. 32.17 Yuzurihara Landslide, Japan: Landslide area comprising several blocks (*upper*). Map of the mitigation works consisting mainly of large diameter vertical drainage wells and sub-horizontal drainage boreholes (*lower*)

The prevention area is divided into three areas, Kayakabu-Karyu, Kayakabu-Joryu and Shimokubo. In Kayakabu-Karyu area, nine units of drainage boring works and fourteen water catchment wells have been implemented by the prefectural government, and two units of drainage boring works, six water catchment wells and two drainage tunnels (683 m and 541 m long) have been implemented by the central government (Fig. 32.17). Control works have been completed in Kayakabu-Karyu area and Kayakabu-Joryu area. On the other hand, in Shimokubo area, the control works are now under construction.

In order to evaluate the effectiveness of the landslide prevention works, observations and stability analyses are executed in each year. Ground movement in the area is measured by GPS, extensometers, inclinometers and borehole type tilting meters, and ground water level is measured by groundwater level gauges.

Kayakabu-Karyu area is composed of a large block (Block I), and five small-scale blocks are located downward of the large block. The results of measurement show that the Block I and small-scale blocks have become non-active sinse the control works were carried out.

In Kayakabu-Karyu area, the safety factor of Block I is calculated by three dimensional analysis, and small-scale blocks are calculated by two dimensional analysis. The three dimensional stability analyses are executed under the conditions of two types of groundwater level, measured groundwater levels and simulated groundwater levels. To simulate the groundwater level at the return period of 100 years, a three dimensional saturated-unsaturated finite element groundwater seepage analysis model have been developed. The result of the stability analyses shows that the safety factor of Block I exceeds 1.10 at high water level of recent years, and was 1.03 at the return period of 100 years rainfall. On the other hand, at four small-scale blocks the safety factors fall below 1.00 at the return period of 100 years rainfall. The results of the stability analyses are consistent with the result of measurements which shows that the landslide in Kayakabu-Karyu area is generally non-active.

To optimize public investments, it is significant to carry out precise evaluation on effectiveness of landslide prevention work. In Japan, the budget for landslide preventions is decreasing and needs for accurate evaluating technique for landslide stability is growing. The authors are convinced that in Kayakabu-Karyu area, the three dimensional groundwater seepage analysis and stability analysis enabled to calculate accurate safety factor and to prevent over-investment on the landslide prevention works.

32.8.7 Optimum Design of Landslide Stabilizing Piles by Centrifugal Loading Experiments and FEM (by Yasuo Ishii, Kazunori Fujisawa, Yuichi UENO, Yuichi Nakashima, Keiichi Ito)

Pile works are one of the useful structural countermeasures against landslides, which are constructed to connect the movable landslide mass and the stable ground with steel pipe to restrain the movement.

In an effective plan of stabilizing piles, optimum pile design such as its position and intervals is desired in order to obtain high reliability and low construction cost of pile works.

In Japan, intervals of piles have been designed according to landslide depth under individual experience up to the present (Table 32.2).

Therefore the author estimates optimum design of landslide stabilizing piles by centrifugal loading experiments (Fig. 32.18) and their back analyses by FEM under changes of some geo-condition such as strength, ductility and so on.

This estimation shows that the intervals of piles can be changed due to geo-condition, moreover maximum intervals of piles can be less than eight (8) times of pile diameter.

According to these experiments and numerical analysis, optimum design of landslide stabilizing piles could be established. Moreover, the 3D slope stability analysis under reasonable pile works followed by the author, which resulted in moderation of landslides and reduction of the pile work costs.

Table 32.2 Japanese Practice for Determining Stabilizing Piles Interval Based on Landslide Depth.

Landslide Depth (m)	Standard Interval of Piles (m)
< 10	$\leqq 2.0$
$10 \sim 20$	$\leqq 3.0$
$20 \leqq$	$\leqq 4.0$

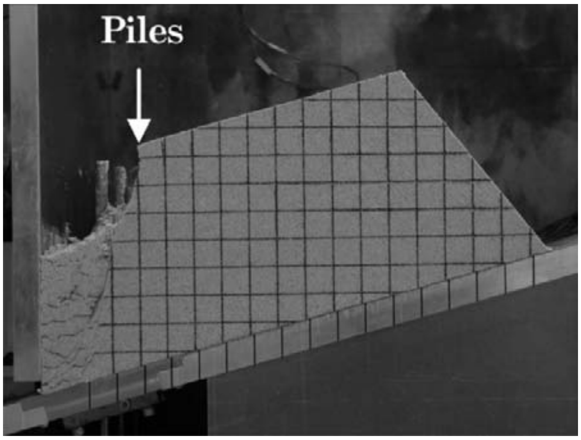

Fig. 32.18 Slope Condition after the Centrifugal Loading Experiment: Slope failure occurred around the piles inserted into the slope

32.8.8 Mitigation of Earthquake Triggered Landslide in Sri Lanka – A Myth or Reality? (by S.B.S. Abayakoon)

Sri Lanka is a pear shaped island located just below the southern tip of India within the rectangle bounded by 79.7E-81.8E and 5.9-9.8 N. General topography of the island can be described by three peneplanes cut into a rocky framework rising from the sea. The highest peneplane of elevation 1500–2500 m above Mean Sea Level (MSL) is completely surrounded by the middle peneplane of elevation over 900 m. The lowest coastal peneplane which is of average height less than 100 m is generally flat and sometimes gently undulating. The central highlands start from an elevation of about 270 m above MSL and comprise of nearly 22% of the total land area covered with hilly or mountainous terrain, embracing well over one million hectares, spread over seven districts.

The central region of Sri Lanka is hilly and mountainous with bedrock overlain by residual soils and colluvium. The occurrence of fresh landslides and reactivation of dormant landslides is a frequent phenomenon in this area during heavy rainy periods. These slides cause severe damage to life and property and therefore considered as the most significant natural hazard in Sri Lanka. It must be recorded that although there were about 40,000 casualties due to the Boxing Day Tsunami disaster of 2004, the possibility of reoccurrence of such disasters is quite remote. On the other hand, floods are quite common occurrences in Sri Lanka, but the damages to life and property due to floods are quite small compared to those due to landslides.

Policymakers and researchers have identified landslides as one of the major area that needs attention when one considers natural disasters of Sri Lanka. These have lead to development of landslide hazard maps and identification of traditional areas that are considered as vulnerable to future landslides. Recently, however, there has been an increase in the occurrence of landslides in areas away from those that are considered as landslide prone.

Traditionally, seismicity in Sri Lanka has not been considered important although it has been discussed by a few authors at various forums. However, the Boxing Day Tsunami disaster of 2004, that was a direct result of an earthquake occurred near the Island of Sumatra, a new awareness has been developed in this area of research. The said earthquake, measuring over 9.0 in Richter scale of Magnitude is supposed to have resulted in creating a new fault line within a few hundred kilometers of the southern coast of Sri Lanka.

Increase in the number of small scale landslides and the occurrence of new landslides in areas that have not been considered landslide prone, suggests that there may have been a connection between increased seismicity of the area, and landslide occurrences of the island. A study of the pattern of landslides before and after the Tsunami and ways and means of mitigating such occurrences in the future are now considered important and essential.

This paper describes some recent advances made in landslide research in Sri Lanka with special emphasis on effect of seismicity. As seismic events cannot be forecasted, mitigation against seismic vulnerability of landslides is not an easy task. However, some approaches that can be adopted are also discussed in detail. The paper also suggests possible directions in which the research can be advanced with modern day sophisticated analysis procedures.

32.9 Concluding Remarks

Much progress has been made in developing techniques to minimize the impact of landslides, although new, more efficient, quicker and cheaper methods could well emerge in the future. There are a number of levels of effectiveness and levels of acceptability that may be applied in the use of these measures, for while one slide may require an immediate and absolute long-term correction, another may only require minimal control for a short period.

Whatever the measure chosen, and whatever the level of effectiveness required, the geotechnical engineer and engineering geologist have to combine their talents and energies to solve the problem. Solving landslide related problems is changing from what has been predominantly an art to what may be termed an art-science. The continual collaboration and sharing of experience by engineers and geologists will no doubt move the field as a whole closer toward the science end of the art-science spectrum than it is at present.

References

AGS – Australian Geomechanics Society, Sub-Committee on Landslide Risk Management (2000). Landslide Risk Management Concepts and Guidelines, pp. 49–92

Bromhead, E.N. (1992). "The Stability of Slopes." *Blackie Academic & Professional*, London.

DOE: Department of the Environment (1994). "Landsliding in Great Britain", Jones, D.K.C. and Lee, E.M. (Eds.) *HMSO*, London.

Duncan, J.M., Stark, T.D. (1992). "Soil strength from back analysis of slope failures", Proc. ASCE Geotechnical Conf. on Slopes and Embankments, Berkeley, 890–904.

Geotechnical Control Office (2000). "Geotechnical Manual for Slopes." *Public Works Department*, Hong Kong.

Hutchinson, J.N. (1977). "The Assessment of The Effectiveness of Corrective Measures in Relation to Geological Conditions and types Of Slope Movement." *Bulletin IAEG*, 16: 131–155.

Japan Landslide Society (2008). "Landslides in Japan", http://www.tuat.ac.jp/~sabo/lj/

Kelly, J.M.H., and Martin, P.L. (1986). "Construction Works on or Near Landslides." *Proc. Symposium of Landslides in South Wales Coalfield*. Polytechnic of Wales, 85–103.

Popescu, M.E. (1996). "From Landslide Causes to Landslide Remediation, Special Lecture." *Proc. 7th Int. Symp. on Landslides*, Trondheim, 1: 75–96.

Popescu M.E. (2001). "A Suggested Method for Reporting Landslide Remedial Measures." *IAEG Bulletin*, 60, 1: 69–74

Popescu, M.E., Zoghi M. (2005). "Landslide Risk Assessment and Remediation", Chapter in Monograph on Natural, Accidental, and Deliberate Hazards, Craig Taylor and Erik VanMarke (Eds.) American Society of Civil Engineering, Council on Disaster Risk Management, Monograph No.1, Reston, VA, pp. 161–193.

Popescu, M.E. (2006). "Risk Assessment and Treatment in Slope Stability Forensic Engineering", *Proc. 4th ASCE Congress of Forensic Engineering*, Cleveland, pp. 141–153.

Popescu M.E., Yamagami T. (1994). "Back analysis of slope failures - a possibility or a challenge?", *Proc. 7th Congress Intern. Assoc. Engg. Geology*, Lisbon, (6), pp. 4737–4744.

Sassa, K., Fukuoka H., Wang, F.W., Wang, G. (Eds.) (2005). Landslides: Risk Analysis and Sustainable Disaster Management, *Springer*, New york.

Schuster, R.L.(1996). "Socioeconomic Significance of Landslides," Chapter 2 in Landslides – Investigation and Mitigation, Special Report 247, Transportation Research Board, National Research Council, Turner, A.K. and Schuster, R.L., (Eds.) *National Academy Press*, Washington, D.C.

Terzaghi, K. (1950). "Mechanisms of Landslides." *Geological Society of America*, Berkley, 83–123.

Watershed and Forest Management for Landslide Risk Reduction

33

Nicolas Dolidon, Thomas Hofer, Libor Jansky and Roy Sidle

Abstract Landslide hazard can be influenced by natural resource management and rural development related activities, such as forest management, road construction, agricultural practices and river management. Vegetation cover and its utilizations may play a role in mitigating the risk of landsliding. Moreover and above all, it does play a role in mitigating the processes leading to increased landslide hazard, such as gully erosion. Thus, forest management and development are of particular concern. But all people living in mountain areas rely on the soil stability for their livelihoods, and their livelihoods may influence this soil stability. Therefore all related activities have to be done on an appropriate way in order to promote soil and slope stability.

To identify best adapted practices in a particular area, to organize spatially the different land uses and to promote the implementation of the identified best practices, the ideal scale is the watershed. It allows addressing upstream-downstream linking issues, such as landslides, and provides a framework for sound land use planning. However, it is not always possible to implement actions exactly with the watershed boundaries.

From the lack of knowledge regarding the scientific evidence of the role of forests against landslides to the institutional challenge of implementing watershed scaled policies, many progresses have to be done regarding this issue. But the already existing scientific knowledge, the integrated projects which are already implemented and the results which are obtained are encouraging. Above all, they show that fundamental research, socio-economic levers and institutional development have to be carried out and developed in a sound way, towards a better understanding of all the natural and man-made processes and a better management of all natural resources, in particular water and soil of the mountain areas.

Keywords Landslides • Vegetation • Forest • Watersheds • Roads • Livelihoods

33.1 Aims and Structure of the Session

Following section will address the relationships between forest and watershed management and landslide risk mitigation. The idea is to show the

Nicolas Dolidon (✉)
e-mail: ndolidon@gmail.com

Thomas Hofer
Food and Agriculture Organization of the United Nations, Rome, Italy

Libor Jansky
United Nations University, Bonn, Germany

Roy Sidle
Kyoto University, Kyoto, Japan

K. Sassa, P. Canuti (eds.), *Landslides – Disaster Risk Reduction*,
© Springer-Verlag Berlin Heidelberg 2009

influence of forests and their management on landslide mitigation and to explain the importance of other land uses in both ensuring sustainable livelihoods and protecting the soils from landslides and other kinds of degradation. The papers presented in this session will consider landslides from a broad perspective, ideally at the watershed scale, integrating them in natural and human ecosystems.

A first part aims at explaining the framework and the main issues related to watershed and forest management for landslide risk reduction. The second part presents abstracts from several papers dealing with these topics. Their order allows going gradually from natural processes to related human activities. The papers in this session include:

1. Zieaoddin Shoaei: The role of forests and trees in landslide risk mitigation
2. Dr. David J. Wilford and Matthew E. Sakals: Effects of forest management activities on landslide risk
3. Lee H. MacDonald C. Ramos-Scharron, D.B.R. Coe, A. Korte, M. Welsh, and E. Brown: Effects of Roads on Landslides, Sediment Production, and Downstream Resources
4. Ian Cherrett: Honduras: people's participation brings food security
5. Benjamin Kiersch: Potential of payment for ecosystem services schemes for landslide risk reductio
6. Frédéric Berger, Jérôme Lopez, Freddy Rey and Luke Dorren: An example of a policy for managing a forested watershed to mitigate landslide risk: the French Risk Plan Prevention

33.2 The Framework of Watershed and Forest Management for Landslide Risk Reduction

33.2.1 *What is a Risk?*

In order to understand the interrelated roles of watershed and forest management in landslide risk reduction and their links to each other, one first needs to define and understand clearly the number of key-concepts. The first step is to define risk. Analysis of risk depends on a number of factors, including, hazard, the elements at risk, and their vulnerability. Varnes (1984) says "natural hazard is the probability of occurrence within a specific period of time and within a given area of a potentially damaging phenomenon". The Canadian Standards Association (CSA, 1997) defines a hazard as a source of potential harm or a situation with a potential for causing harm, in terms of human injury; damage to property, the environment and other things of value; or some combination of these. The United Nations International Strategy for Disaster Reduction (UN-ISDR) proposes following definition for a hazard: "a potentially damaging physical event, phenomenon or human activity that may cause the loss of life or injury, property damage, social and economic disruption or environmental degradation" (UN-ISDR, 2004).

In the case of landslide management, the landslide is the "source of potential harm", the "potentially damaging phenomenon". These definitions imply that a potential landslide, to be considered as a hazard, has to constitute a threat to something of value such as human lives, property, or the environment for example. Under such a perspective, landslides which have no harmful potential would not be considered hazards (Wise, Moore and VanDine, 2004). This is not a view shared by everyone. Some other definitions consider that the probability of the phenomenon itself, characterized by the susceptibility of the terrain, the frequency of landslides and their magnitude, is always a hazard, even if it does not threaten anything of value (Lee and Jones, 2004, quoted from Fourniadis, Liu and Mason, 2007). It is proposed, for the purposes of this session, to adopt the following definition: a landslide hazard is the existence of a probable landslide of a given magnitude in a specific area within a given period of time. The hazard is assessed by its probability of occurrence. Of course landslides are natural and normal processes and if they don't threaten anything of value it does not make any sense to mitigate them.

This leads to the second component of a risk i.e. the elements at risk. The British Columbia Ministry of Forests and Range (2002) lists potential elements at risk as human life and bodily harm, public and private property (including building, structure, land, resources, recreational site, and cultural heritage feature), transportation system/corridor, domestic water supply, fish habitat, wild life (non-fish) habitat and migration, visual resource and timber. The nature of the element at risk is as important as the hazard to define and characterize the risk. Indeed, the impact of a given hazard depends on the vulnerability of the element at risk. UN-ISDR suggests that a risk is "the probability of harmful consequences, or expected losses (deaths, injuries, property, livelihoods, economic activity disrupted or environment damaged) resulting from interactions between natural or human-induced hazards and vulnerable conditions."

Einstein (1988), cited by Deoja (2001), says that risk is the "probability of an event multiplied by the consequences if it occurs". This is the mostsimple definition on which everybody agrees.

Varnes (1984) defines the total risk (R_s) for a given element at risk as the product of the hazard (H) and the vulnerability of the element at risk (V).

$$\mathbf{R_s = H\ x\ V}$$

He defines vulnerability as "the degree of loss to a given element or a set of elements at risk resulting from the occurrence of a natural phenomenon of a given magnitude". For example, a thick wall may be less vulnerable to a small landslide than a wooden house. The total risk (R_t) is then defined as "the number of lives that could be lost, persons injured, damage to property, or disruption of economic activity due to a particular natural phenomenon". It is the product of specific risk (R_s) and the element at risk (E).

$$\mathbf{R_t = R_s\ x\ E}$$

The introduction of the factor E corresponds to the total value given to the element(s). For instance a forest road has not as much value as human lives, and one sawmill has less value than a whole settlement or several industries. According to this description of risk, there are three factors that can be influenced to reduce it: the hazard itself (H), the presence of the element(s) at risk (E) and its (their) vulnerability (V).

Figure 33.1 shows a massive landslide in Peru. The process of landsliding is clear and corresponds to the hazard. However looking at this picture it is not possible to say whether there is a risk, except for the environment, because one can not see potential elements at risk, nor assess their vulnerability.

Fig. 33.1 Landslides are natural processes and their mitigation is not always possible or cost effective. Here an example from Peru (picture B. Kiersch)

33.2.2 What are the Main Possible Risk Reduction Strategies?

The first thing to be addressed in risk mitigation is the possibility of reducing the probability of occurrence of the hazard. A variety of different methods may be adopted to mitigate risk depending on the type of hazard and the local conditions. With regard to mitigating the risk of landslides, some methods relevant to watershed and forest management will be addressed in this session.

In a naturally dangerous zone, even if all efforts are undertaken, there is no guarantee of a zero probability of hazards. Hence, it is important to work on hazard reduction. But the first option to be considered is to move vulnerable elements away from the zone at risk, avoiding the building for instance of new dwellings, industries, or infrastructures there. It must not be forgotten that the safest way to reduce the risk is to minimize exposure to hazards. Current research efforts aiming at understanding landslides involve the mapping of hazard probability in a given region (Sassa et al., 2005, 2007). These maps are necessary tools to reduce risk, enabling the sound spatial development of human activities. This should be an integral part of watershed management.

Another response to risk is to reduce vulnerability to the hazard. This is mainly possible through construction methods. When talking about watershed and forest management, a key issue is road building, their stability and dangers of road induced landslides.

Fig. 33.2 In some cases, forests do not reduce the probability of occurrence of landslides. For example, this deep-rooted landslide, triggered by the earthquake in Pakistan in November 2005 (picture T. Hofer, FAO)

33.2.3 What are the Respective Roles of Watershed and Forest Management in Landslide Risk Reduction?

Risk can be reduced by influencing either (1) the hazard, (2) the vulnerability of given elements or (3) their location; as well as by a combination of these three. This session explores how forest management, watershed management and combination of these may be utilized as a means for risk mitigation.

33.2.3.1 About Forest Management

Forest management covers a wide range of activities and issues ranging from silviculture and forest management planning, as well as their consequences such as tree species, age repartition, stand density, stand health and stability. Silvicultural and harvesting interventions, as well as the forest development, especially road construction, are also encapsulated within this term.

Vegetation cover, and particularly forests, sometimes has a role to play in landslide hazard reduction (topic 1). It seems, however, they have only minimal influence on deep-rooted landslides. Figure 33.2 is an example of deep-rooted landslide which has been triggered by an earthquake in Pakistan in 2005. The forest cover did not play any mitigating role for such a deep and massive mass movement. However, in some cases the effect of forests in reducing the likelihood of shallow landslides has been considered significant (Alcantára-Ayala, Esteban-Chávez and Parrot, 2006).

The condition of the forest may also play a role. A healthy and stable stand, with few gaps and site-adapted tree species can have a better protection role than a stand damaged by, for example, insects or a storm. Silviculture and the way forests are managed is thus important for slope stabilisation (Rickli, Zimmerli and Böll, 2001). Figure 33.3

Fig. 33.3 In some other cases, forests stabilize the soil and limit the occurrence of shallow landslides up to certain slope steepness, like in Switzerland in August 1997 where landslides have been triggered by heavy rainfall. (picture Oberforstamt Obwalden)

shows a case where even though forest did not avoid all landslides, it limited their number up to a given slope after heavy rainfall in Switzerland.

Forest development is also of high concern. Harvesting operations and road construction in particular can increase the probability of occurrence of landslides. These interventions highlight the role of forests: once the system is disturbed, the hazard probability increases.

33.2.3.2 Watershed Management

Forests, cropland, grassland, roads or buildings have different impacts on the probability of occurrence of a landslide. Risk reduction and especially hazard mitigation can be affected by soil type in the failure zone, and sometimes even above this zone. Different land use practices may also have an impact on soil stability (see for example the papers of Wilford and Sakals, MacDonald et al., and Cherrett). This means that the security of some people, human activities and natural habitats, generally located downstream of the potential failure zone, may be affected by upstream land owners and above all land users, who are carrying out activities on the unstable zone or sometimes even upslope from it. Some activities carried out downslope from an unstable zone, like road building or river management interventions, may also increase the probability of landslides. In order to preserve the security of the exposed people, land users have to know how to manage their land in the best possible way, so as not to increase the probability of occurrence of a landslide. Figure 33.4 illustrates an example of the possible consequences of a wrong watershed management practice: a drainage dug in a sensible soil grew to become a gully of which one side evolved in a landslide. Around 10,000 m^3 soil have been lost on this 0.3 ha big area within 30 years, and the main cause is a small drainage meant at protecting the downstream located area from excess run-off.

However, land users have to be motivated to implement the best practices. In fact, factors such as lack of land tenure security or market prices may create a motivation to implement inappropriate management schemes (Stocking and Murnaghan, 2001). These may be modified where incentives including compensation and other driving factors

Fig. 33.4 An example of man-made landslide process. Starting form a badly located drainage channel which has been eroded to form a gully, recurrent landsliding from the sides of the gully led to 10,000 m^3 soil losses within 30 years on a 0.3 ha big area of this hill of the Kathmandu valley, Nepal (picture N. Dolidon, FAO)

motivate the land user to adapt his/her methods in light of the responsibility he/she has for the security of other people. A proposal for a system of incentives is set out in a study in this session on Payment for Ecosystem Services Schemes (Kiersch, Sect. 33.3.5).

Risk depends also on the distribution of all human activities, infrastructures, settlements, industries, which could be possible elements at risk. So it is of high importance to organize the spatial distribution of these elements in a sound way. This involves risk mapping and the adoption and enforcement of corresponding law and policy to guide the development of different human activities.

It is necessary to assess and map landslide hazards distribution in order to determine suitable zones for the development of human activities. This includes assessment of the zones where specific land uses and management practices play a protection role. There is also a need to provide land managers with landslide assessment guidelines and encourage them to implement the corresponding action (Berger and Rey, 2004). But why at the watershed scale?

The watershed scale approach seems to be useful for landslide risk reduction for several reasons. The percentage of forest cover at the catchment's scale has an influence on hydrology and thus may be a driving factor for landslides (Cemagref, ONF and CRPF, 2006).

Moreover, landslides are an example of a phenomenon linking upslope management and downslope effects, as well as downstream effects. In fact, the occurrence of a landslide may have a direct destructive effect, and may also lead to an increased erosion rate, which is a problem often well-addressed by watershed management policies.

If a landslide occurs in one given watershed, it will have hardly any influence on the neighbouring one, but it may impact the whole watershed ecosystem concerned and its population through water quality modifications, soil loss, destruction of infrastructure and ecosystems. Similarly measures taken for landslide risk reduction in one given watershed will have limited influence on risks in neighbouring watersheds. This is why not only the watershed scale matters, but also the adoption of an ecosystem approach to watershed management.

From a practical point of view, as explained by FAO (2006), a watershed approach permits people to link together who otherwise may not have met. It is very important in landslide management that all stakeholders understand each other's position, needs and constraints. Therefore, gathering all stakeholders in one given watershed enables more informed decision making on landslide risk mitigation. It also allows for implementation of the best adapted and accepted legal, financial, technical and political actions.

33.2.4 Why Watershed and Forest Management Together?

Watershed management deals with several land use types, policy issues, involvement of all stakeholders of natural resources and is thus much broader than forest management. So why should we address them together if the scale of approach is not the same?

Forests represent the most important land cover of mountain areas worldwide. In the Millennium Ecosystem Assessment, the authors of Chap. 24 on Mountains (Körner and Masahiko coordinating leading authors 2005) present five studies according to which forests are variously gauged to occupy between 25% and 48% of mountainous areas. Because of climatic conditions, forests are not located in the highest mountainous areas but in valleys and middle altitude slopes, where the population density may not be as high as in plains, but is still rather high. This means that the proportion of forest cover in densely populated mountain areas is higher than the mean proportion of forest cover in the mountains in general. That is to say, that in the main populated mountainous areas, the mean forest cover might be higher than 50%. Consequently, all issues that deal with mountains and people, such as landslides, have to take into account this strong forest component.

Almost 1 billion of the world's poor rely directly on forests for their livelihoods (World Bank, 2002). Forests play a role both in food security and in income earning. They are the home of many indigenous peoples and constitute an important pool of biodiversity and many different specific natural habitats. They may play a role in climate change mitigation through their carbon sequestration function and provide several other environmental services. Forests are also subject to industrial commercial exploitation by the timber industry as well as a source of many non-wood products. The recreational role of forests is often understated but is now becoming of increasing relevance for development of sound management strategies. Because the activities linked with forests are relevant to and concern many different stakeholders, it is important to address all forest related issues in a coherent way which both links people together and comprises all related ecosystems. Watershed management provides this framework.

Since forests are often very extensive ecosystems, management plans have to be made on as large scale when possible. A sound forest road network for example, should be planned at a large scale, and the watershed level happens to be a good one. Therefore, it is of interest to embed certain issues of forest development and management plans in broader watershed development plans.

33.3 Subtopics Relevant to Forest and Watershed Management for Landslide Risk Reduction

The following section deals with the topics which have been presented during the First World Landslide Forum in Tokyo. After a global introduction explaining the choice of topics, each one is presented by the abstract provided by the speaker.

The topics are organised to address in turn physical and natural phenomena, the impact of human activities on them, and finally propose ways to organise and influence these activities in order to reduce landslide risk. The first presentation will deal with an example from Iran showing the effect of vegetation and forest cover on hazard probability reduction. The second and the third one illustrate the impact of specific examples of forest management and development activities, focusing respectively on British Columbia (Canada) and California (USA). The aim of the fourth topic is to address the issue of livelihood production and slope stability through a successful example from Honduras, and the fifth topic deals with experiences from Latin America and Asia with schemes for payment for ecosystem services which are often used to link upstream service providers and downstream beneficiaries. Finally, risk mapping and the following watershed management issues will be addressed through a presentation about the French experience.

33.3.1 The Role of Forests and Trees in Landslide Risk Mitigation

As previously explained, several studies show a possible role for forest and vegetation cover in landslide hazard probability reduction. There are still gaps in understanding all the processes related to this issue, and there is need for further research. But a logical reasoning can lead to some hypothesis on how trees and forest cover could modify landslide hazard probability. The main potential effects are the reduction of the water yield through increased evapotranspiration; increased soil strength due to the effect of root system; preservation of good soil structure thanks to the protection against splash erosion and maintenance of good biological activity in the soil. The steepness of the slope, the intensity of triggering rainfall events and the quality of the stand may all place limits on these beneficial effects. Figure 33.5 shows how a bare soil can easily be degraded through small shallow landslides.

The example below presents a study carried out in Iran which explains how these factors have influenced and reduced the probability of landsliding.

Zieaoddin Shoaei
Agricultural Research and Education Organization (AREO) - Iran

Considerable number of landslides and debris flow events has originated from Alborz Ranges at the southern parts of Caspian Sea basin with west to east orientation. Due to the expansion human activities towards both higher marginal lands and forest areas and also land use changes, the number of landslide events has increased rapidly during recent decades. The landslides mass movement poses high risk on both the lives and properties of inhabitant at the lower part of the basins. Some of these events are disastrously fast-moving with highly destructive debris flows that mainly occur some years after

Fig. 33.5 In addition to a potentially threatening event for downstream located elements, landslides, in particular shallow landslides, must be considered as a major erosion process. Poor vegetation cover often leads to increased shallow landsliding, like here in Navarra, Spain. (picture N. Dolidon, FAO)

deforestation triggered by high intensity rainfalls. Landslide and debris flow events which have occurred over longer time periods are accompanied by root decay and loss of soil strength.

According to the Iran's Forest and Rangeland Organization, 15% of the northern forest area has been cleared either partly or completely during the last 20 years for activities such as wood industry and cultivation. This is due to both inadequate management of forests and lack of proper legislation for forest protection.

The effects of forest management on slope stability are investigated through some research programs performed in Watershed Management Institute of the Ministry of Agriculture. The results have been used for clarifying the mechanisms of both the deforestation-induced landslides and debris flows in order to plan for the extension and education of the issues to the local authorities and residents. This paper is aimed to present a summary of research works:

- The main effective factors in the deforestation-induced landslides are reduction in soil strength due to the tree roots decay and consequently decreasing in soil strength.
- The deforestation-induced landslides and debris flows are particularly hazardous due to their occurrence with little warning.
- The reinforcement of soil on slopes by tree root is due to the type of trees. Investigation showed that more than 90% of shallow landslides occurred in tea planting farms is due to the changes of previously deep root trees with the current shallow root tea trees. An example in shown in Fig. 33.6 that indicated the initiation of landslides on newly planned tea orchard development.
- Tree roots may increase the shear strength of soil from 37% to 66% depending on both root depth and density. An example of some research work is shown in Fig. 33.7 that is the effect of root area on soil shear strength increment. These researches have been implemented for different types of trees in different climate of the country
- The small and shallow mass movements will impede drainage and will result in further large scale landslide and debris flow events.
- The loss of shear strength caused by roots decay may take place between 10 and 15 years after tree cutting in highlands.

Fig. 33.6 Initiation of landslides due to the changes of dense forest cover to tea trees orchard, north of Iran, (Along Alborz Ranges, Southern parts of Caspian Sea basin. Average elevation: 1800 m (photo by J. Ghayoumian and Z. Shoaei 1997)

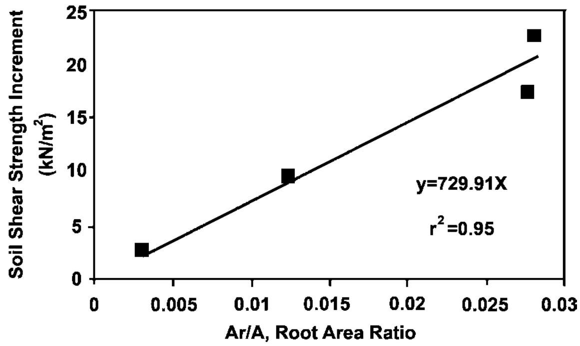

Fig. 33.7 The effect of tree roots area on the increment shear strength of soil (source: Shafaei Bajestsn M. and Salimi Golsheikhi, M. 2002)

- The result confirms the high sensitivity of slopes with dips between 25° and 35°. Thus any changes in vegetation cover in this zone should be prohibited. In inevitable conditions the original vegetations to be restored.
- Development of rules and regulations for forest management and land use changes has the highest priority for landslide risk mitigation in the country.

33.3.2 Effects of Forest Management Activities on Landslide Risk

After these explanations and raised concerns about the effects of vegetation on slope stability and some of the effects of human activities, the present section goes one step further towards forest management. Through the example of the forests located on alluvial fans, it shows how forest management and development activities have to be adapted to sensible contexts.

The definition of a fan is given by Wilford, Sakals and Innes (2005), quoting Bull (1977). They say that "a fan is a cone-shaped deposit of sediment formed where a stream emerges from the confines of a mountain" (Bull, 1977).

Dr. David J. Wilford and Matthew E. Sakals
British Columbia Ministry of Forests and Range – PO Box 9529 stn prov govt – Victoria BC V8W 9C3 – Canada

In mountainous terrain, alluvial fans are conspicuous locations for infrastructure and residential development, and are excellent locations for growing trees, but these landforms can present significant risks because they are frequently the runout zones for landslides. It is possible for forest harvesting on fans in the watersheds of fans to occur without unduly increasing landslide hazards, but if undertaken inappropriately, forestry activities can elevate the natural levels of landslides and the runout distances of those landslides. This effect can have significant consequences for natural and anthropogenic features on alluvial fans. This paper presents research results, management strategies, and forest legislation aimed at reducing landslide risks to safety, infrastructure, and environmental values on fans in British Columbia, Canada.

Forest legislation in British Columbia (BC) specifies that forest management must be conducted in a manner that will not cause landslides, destabilize alluvial fans, impact fish habitat, nor degrade the productive capability of forest soils. There are a series of key management tools to achieve these objectives: terrain stability assessments, research and publications regarding forest land management, and a recently developed 5-step method of analyzing risks on fans.

Terrain stability assessments identify landslide initiation zones (landslide prone terrain). The methods have been developed over the past 30 years to identify naturally unstable terrain (Class V) and terrain that is subject to landslides following conventional forestry practices (Class IV and to a lesser degree Classes III and II). Class V terrain units are generally withdrawn from the "productive forest land base" and are treated as forested reserves. Detailed terrain field analyses and prescriptions are done in Class IV and V units prior to forestry development (road construction or forest harvesting).

A considerable body of research in BC has identified that conventional forestry practices within, upslope of, and downslope of landslide prone terrain can result in a significant increase in the frequency and/or severity of landslides. This has led to the use of special road construction practices and also a greater use of helicopters for harvesting forests. Interest is increasing in maintaining the hydrologic and geomorphic influence of forests in the Class V forested reserves through Protection Forest management, but such actions are still in the research and planning stages. Research on landslides in coastal BC has identified rainfall thresholds for the initiation of landslides. This research has formed the scientific basis for operational forestry shut-down guidelines that are implemented to reduce safety risks to forest workers on potentially unstable slopes and on areas below potentially unstable slopes, including alluvial fans. Forests on alluvial fans have been identified as playing a protective role – maintaining the location of stream channels, storing sediment from landslides, and limiting the lateral spread of landslides across the fan surface. A Land Management Handbook describes key features to identify where forests are playing this protective role and presents appropriate forest management strategies for "hydrogeomorphic riparian forests" that reduce the risk of landslide impacts. This and other documents (Land Management Handbooks) published by the BC Ministry of Forests and Range are used by forest practitioners to identify and manage landslide prone terrain, identify and manage for hydrogeomorphic hazards on fans, and to undertake landslide risk analysis.

Currently, researchers are developing a 5-step method of identifying risks to alluvial fans from landslides issuing from their watersheds. Step 1 involves identifying fans and delineating their topographic watersheds. Step 2 involves identifying the elements at risk on fans, such as houses, bridges, and other infrastructure, as well as fish habitat and forest sites. Step 3 involves a detailed investigation of the fan to determine the type and frequency of hydrogeomorphic processes (both natural and human related), and to describe modifications to the fan surface due to land use activities (e.g., removal of the hydrogeomorphic riparian zone, diking, road construction). Step 4 involves a description of the watershed, including landslides and changes to forest cover – both natural (e.g., wildfires and forest health issues) and human related. Step 5 is the application of a framework to determine present and future risk, including potential mitigative strategies. The methodology provides a framework for local governments to assess risks on alluvial fans due to landslides associated with natural factors such as wildfires and insect epidemics. The methodology also draws a clear link between forestry activities in remote areas of watersheds and the landslide risks to values on downstream alluvial fans – this link was historically overlooked due to the site-level focus on landslide initiation zones, however several court decisions have identified the critical need for foresters to take a watershed-level perspective.

Forest and watershed management research, legislation, and practices in British Columbia over the past three decades have significantly reduced the risks of landslides to values on alluvial fans. Future application of Protection Forest management strategies to current forested reserves on landslide prone terrain should lead to even further risk reduction.

33.3.3 Effects of Forest/Mountain Roads on the Occurrence of Landslides and Land Degradation

Forest roads are one of the most important triggers for landslides and lead to increased erosion rates. Hence, it is necessary to develop roads with care and to adopt appropriate construction methods. This section seeks to demonstrate the links between these issues and of current thinking related to them in the light of climate change.

L.H. MacDonald, C. Ramos-Scharron, D.B.R. Coe, A. Korte, M. Welsh, and E. Brown
Watershed Science Program – Colorado State University – Fort Collins, CO 80523 – USA

Unpaved roads are often considered to be the predominant sediment source in forested catchments. In steep, wet climates roads can cause a 10- to 300-fold increase in the landslide erosion rate, and this increase is due to the effects of roads on hillslope flow paths and the structural integrity of hillslopes. The hydrologic changes leading to slope failures include the generation of infiltration-excess (Horton) overland flow, the interception of subsurface stormflow by road cuts, and increase in pore pressures resulting from the concentrated delivery of this overland flow to hillslopes or convergent hollows. The decrease in structural integrity is due to the oversteepening and loss of support as a result of road cuts as well as the downslope oversteepening resulting from the placement of road fills. The proportion of sediment that is delivered to the stream will generally be very high for road-induced failures in hollows and inner gorge landforms, and much lower for planar hillslope failures. The pulsed input of sediment from road-induced landsliding can greatly alter stream channel habitat and morphology.

Roads also can increase sediment production rates by more than an order of magnitude as a result of road surface erosion, and this increase has been documented for more stable geologic terranes as well as steep, humid areas. The high surface erosion rate stems from the generation of surface runoff from the highly compacted road travelway, the availability of fine sediment due to traffic and road maintenance procedures such as grading, and the high overland flow velocities resulting from the lack of vegetative cover. Empirical and physically-based models have been developed to predict the amount of road surface erosion from the amount and type of precipitation, road surface area, steepness of the road segment, soil type, and traffic level. The proportion of this sediment that is delivered to the stream network depends primarily on mean annual precipitation ($R2 = 0.9$), but increases by about 40% in the absence of any engineered drainage structures. The chronic input of the fine sediment from roads has been linked to adverse changes in stream habitat and the health of coral reefs.

Climate change can greatly increase road-induced landslides and road surface erosion by increasing the magnitude of large storm events and increasing the amount of rain relative to snow. Our multi-year studies in California's Sierra Nevada show that road surface erosion increases by 3–10 times as the proportion of rain increases, despite an associated decrease in total precipitation. Extensive field surveys also show that relatively few road segments typically generate most of the road-related increases in sediment yields. With our present understanding the road surface erosion and the risk of road-induced landslides can be greatly decreased by improved road designs and maintenance practices. Hence the greatest needs are to develop and provide land managers with the tools for identifying high-risk segments, and then to make the necessary investments in road reconstruction and restoration. Fortunately the biggest benefits can be achieved relatively easily.

33.3.4 Agricultural Practices to Ensure Sustainable Livelihoods and Slope Stability

This entire section addresses natural resources management and its relationship to human activities within watershed ecosystems. Forests and related activities are of high importance. But the sustainable livelihoods of mountain people are as important as forests and different management practices may have an impact on landslide hazard. Agroforestry practices may sometimes be a very good way to ensure food security without increasing the landslide risk. In such cases, they are consequently more sustainable than other non-adapted practices. Following is an example of successful agricultural practices which limited landslides and soil degradation even in particularly severe conditions in Honduras. It shows also the importance of people's participation in rural development.

Ian Cherrett
Food and Agriculture Organization of the United Nations – Regional Office for Latin America end the Caribbean – Santiago de Chile – CHILE

The potential for replacing slash and burn agriculture with more sustainable systems, especially agroforestry systems on tropical hillsides, has not yet been adequately recognised. Starting in Honduras in the late 80 s and now being more extensively adopted in meso America the benefits of these changes include a reduction in vulnerability to landslides in regions increasingly subject to climate instability with rapid oscillations between drought and heavy rains in degraded landscapes, those most vulnerable to landslide risk. This topic looks at the process involved, its impact and the lessons generated.

In 1988 a drought (el niño) hit the Pacific coast of Honduras leading to a large scale food aid program for the hillside farmers affected. The farmers of Lempira Honduras were some of the worst affected, they were typical meso American hillside subsistence farmers producers of maize and beans on steep slopes in a degraded deforested landscape in which productivity, even with fertilizers, was declining and malnutrition chronic. In 1998, ten years later when Hurricane Mitch hit the country, the same farmers provided tons of emergency food aid to their fellow citizens in other parts of the country. One of the reasons was that their new farming system had reduced vulnerability to climate extremes, both drought and excessive rainfall, and therefore had reduced dramatically their vulnerability to landslides.

The department of Lempira, with a population of 100,000, is one of the poorest and most isolated regions of Honduras, located in hilly terrain close to the border with El Salvador. In 1990, when the Lempira Sur project was begun, 72 percent of the people lived below the poverty line, and malnutrition was chronic. The soil was poor, yields were low, and erosion and drought were common due to the prevailing slash-and-burn farming and extensive cattle ranching systems. This is the dry forest ecosystem of the Pacific with a distinct 6 months dry season and an average of 600–1200 mms of rainfall a year, a rain fall that can be erratic and very heavy in short periods.

The Lempira Sur project was initiated by FAO at the request of the Honduran Government with funding from the Dutch Government. Its main goal was to ensure food security by changing the predominant land use systems in a region of rapidly degrading tropical hillsides. Initially twelve hundred small-scale farmers and their families in 84 villages were the direct beneficiaries, but as the project has expanded the lives of many more people have improved because of it and the landscape of Lempira has changed.

The project staff were aware from the beginning that the problem was not technical but social, they had come from projects that had developed hillside technologies but failed in getting farmers to adapt them. So from the beginning the decision was made to make the project demand driven based on participatory driven processes. During this stage of problem analysis with farmers certain local practices were identified including the retention of certain species of tree in the areas cleared for maize. This plus the fact that water management was the issue for farmers not soil erosion lead to the development of a change strategy based on the "innately innovative and experimental sector of the farming population". Slash-and-burn farming, which had been used for generations, was recognised as part of the problem but alternatives had not shown themselves to be sufficiently viable as a result, crop yields had fallen dramatically and population pressures had reduced the possibility of leaving the land fallow for any length of time.

The farmers together with the extension workers and agronomists of the project worked together to build an alternative agroforestry system starting from existing farmer experiments and adding the technical knowledge of the project staff but always the changes were made on the fields by the farmers who validated what did and did not work, a variant of farmer to farmer or farmer field schools but very much farmer driven as the aim was to change a system not a specific practice. By the mid-1990s an agroforestry system was being adopted based on maximising soil coverage (a hillside zero tillage system emphasising the use of mulch from the grains and leguminous bushes of the fields) with three plant levels, crops, bushes and trees. Following the name of the region where it has been developed, it has been called Quesungual farming technique.

The focus on maximising water retention enabled the maize in particular, resist intermittent dry periods and leading farmers were able to double yields while the average was a 50% increase after three years and with reduced external inputs. Despite the good results, many farmers were sceptical. The big breakthrough came in 1997 when an El Niño-associated drought hit the area. The crops on the farms using the new method withstood the drought, (20% loss, traditional system 80% loss). The others did not. In 1988 adoption was widespread and the capacity of the new system to resist the floods of hurricane MITCH convinced any laggard and put Lempira on the national map, the most backward region of the country sent food to the refugees from the hurricane of the developed region of the country. With extra food available, people can look beyond simple survival.

The needs of the households in Lempira Sur have changed, and therefore, so has the focus of the project. An increase in production does not necessarily improve nutrition and consumption within the families. Therefore, following these first accomplished steps, new initiatives have been started that support the families inside their homes, with house improvements starting with improved stoves, and backyard gardens. Especially the women are involved in these new activities as a more stable basic grain system that reduced costs and liberated labour time enabled the families to diversify their economies, including crop and animal diversification, post harvest, commercial activities, local finance systems and cooperative etc.

Hurricane Mitch in 1998 impacted severely the degraded hillsides of Honduras. Landslides were counted in the tens of thousand and thousands of people died, where as the covered soils of the Lempira hills remained almost untouched except for the recent roads and the harvest was affected only up to 10%. The economic development of the department of Lempira Sur had really started.

And this region, which 10 years earlier could barely feed its own people, was able to provide food aid for other parts of the country. Every municipality in the south of Lempira sent approximately two tons of food aid to the more developed regions of the country after Mitch, it was very impressive to see the level of organization and solidarity.

The Quesungual farming system, illustrated by Fig. 33.8, is an agroforestry system in which crops are grown interspersed with trees and there is zero tillage with a maximum of mulch. This allows for the natural reconstruction of the soil (it requires two crop cycles for the changes to impact on crop yields) and above all the retention of water from reduced erosion through the mulch and more extensive root coverage increases soil coherence and stability and therefore reduces erosion. In addition the tree and crop diversity reduces the impact of the rain drops as well as helps improve soil structure, and so the landscape enters a virtuous cycle. Recent research of the system by the International Centre for Tropical Agriculture (CIAT) shows that soil erosion from this system is marginal, less than the original forest cover (dry pacific forest).

Fig. 33.8 Quesungual farming system: Farmers control soil erosion through growing crops interspersed with trees. (picture G. Bizzarri, FAO)

FAO with CIAT has extensively studied the system that has evolved and there is physical data on water retention rates, soil erosion levels, changes in crop yields and production costs. The World Bank has measured the impact of the project on the forest cover, it is the only region of Honduras where the forest cover is growing. The abuse of chemicals, fertilizers, herbicides etc. has reduced and the fauna and flora is recovering and above all the population has entered a process of economic growth. When the tropical storm STAN hit the region in 2005 the rainfall in Lempira was the same as the Pacific region of Guatemala (400–500 mms), the impact was totally different. The watersheds of Guatemala collapsed, the innumerable landslides destroyed whole communities while in Lempira the few landslides were associated with road construction. Since then FAO has been working closely with the Guatemalan government on a national watershed strategy where the lessons of Lempira are being adapted.

This example shows that specific agricultural methods, at the beginning designed to ensure food security and mainly driven by factors like overpopulation and soil erosion, can also increase soil stability even during the most extreme events. The effect on landslides may have been indirect, but it has been real. Ensuring both sustainable livelihoods and slope stability is possible and an issue in many other regions of the world. The example of the Lempira Sur project and its associated Quesungual farming system maintains the hope to fix these kinds of problems where they still exist.

The other lesson is that slope stability comes from maximising soil coverage based on a strategy of water management. It is not forest coverage per se as has been pointed out in various studies it is soil coverage and a system that maximises soil coverage from organic materials covering the soils to deep penetrating roots eases the impact of heavy rains, ensures water absorption greatly reducing run off (increasing soil humidity by 22 days a year in Lempira critical for grain production). It has shown to be able to resist landslides with rain falls of 400 mms in 24 hours which the current deforested hillsides of meso America can not, something that occurs with increasing frequency every 4–5 years. What would happen if 1500 mms fell in two days as happened in Nicaragua during MITCH is another question.

33.3.5 Potential of Payment for Ecosystem Services Schemes for Landslide Risk Reduction

Motivating land users to implement the most appropriate adapted management strategies is important to mitigate landslide hazard. There is an ever growing use of systems involving payment for ecosystem services which takes into account the downstream positive effects of upstream activities. It is interesting to consider the possibility of implementing such schemes for landslide hazard reduction.

Benjamin Kiersch
Independent Consultant – Cochabamba – BOLIVIA

The concept of Payments for Environmental Services (PES) has received much attention in recent years as an innovative concept to finance environmentally sound management of natural resources, particularly in Latin America and Asia. PES are particularly important in the watershed context, where upstream and downstream people are linked by the hydrological system. As explained on Fig. 33.9. In a typical payment scheme, one or more upstream service providers provide a well defined water-related environmental service to downstream beneficiaries, who compensate the providers for the

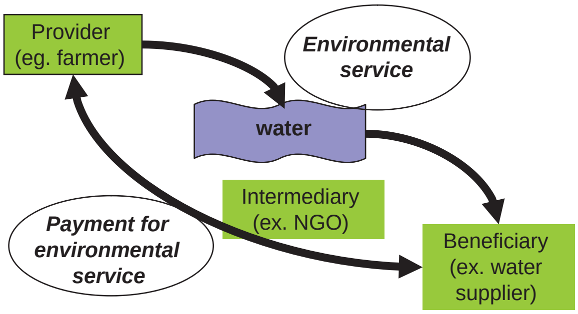

Fig. 33.9 Classical Payment for Ecosystem Services Scheme (author: B. Kiersch). In the framework of the landslide risk reduction, the water (quality, quantity) would be replaced by "soil stabilization" or equivalent

service provision through the payment scheme. Environmental services of interest in watersheds can be divided in services regarding water quality, such as low sediment concentration, and services regarding streamflow, such as the maintenance of a minimum flow by maintaining or improving the infiltration capacity.

The reduction of risk from landslides is a potential environmental service to be included in payment schemes for environmental services. Since direct assessment of water-related environmental services is technically difficult and costly, compensations are usually based on the area covered by land uses assumed to provide the desired service, and calculated on a per-hectare basis. The land uses which are considered under the scheme vary according to the services provided, but typically include forest conservation, reforestation, conservation of natural grassland, and soil and water conserving agricultural practices.

The presentation analyzes six water-related PES schemes in mountainous areas from Latin America (Costa Rica, Ecuador and Peru) and Asia (Philippines, Indonesia) in different stages of implementation as to their potential to reduce the risk of landslides in the watershed. Many schemes specifically target forest conservation on steep slopes and close to water courses, which are considered priority zones to achieve the desired environmental services. Thus, PES schemes in practice today may reduce the risk of landslides, even if landslide risk reduction is not specifically included as an objective to be achieved by the scheme.

33.3.6 An Example of a Policy for Managing a Forested Watershed to Mitigate Landslide Risk: The French Risk Plan Prevention

Complete watershed management processes aimed at reducing landslide risk should start with a hazard and risk assessment. This allows risk mapping, identification of safe areas and of the most dangerous ones. The following step is the identification of areas in which the presence of forests limits the probability of occurrence of a landslide. This is necessary in order to adapt management guidelines for these areas and encourage land managers to follow them. Political and legal actions can then aim at orienting human activities in the safest zones and promoting the best management practices for protection forests.

Fllowing part, explains how this process has been carried out in France at the level of the municipality. It considers its strengths and the needs for improvement in order to better take into account watershed scale issues and inter-municipality relationships.

Frédéric Berger, Jérôme Lopez, Freddy Rey and Luke Dorren
Agricultural and environmental engineering Research CEMAGREF – 2, rue de la papeterie –BP 76 – 38402 Saint Martin d'Hères – France

Forests mitigate partially or totally a number of natural hazards in mountain watersheds, such as erosion, floods, landslides, rockfalls and snow avalanches. This protective role changes as a function of the hazard considered, but also as function of the position of the forest vis-à-vis the area considered by the hazard as well as the spatial scale considered (tree, slope, catchment, or watershed). For avalanches, landslide, floods or erosion, active protection, which refers to the prevention or reduction of the hazard occurrence, is possible in the departure or source zone. In the transition and deposit zones, the forest offers passive protection, which refers to the reduction of the magnitude of the hazard, mainly against erosion and rockfall. However, against avalanches and landslides, forests cannot offer passive protection.

A forest reacts differently to hazards according to varying species and vegetation layers. In addition, the protective role varies through time. For example, if regeneration is absent or insufficient, then an old forest is less stable through time and therefore its protective role decreases. To increase their stability of such forests, management of mountain forests with a protective role against natural hazards is often essential. Moreover, "optimal management" must be considered, due to the financial restrictions affecting this management. In this case, the term "optimal" means, according to the economic situation, the minimum silvicultural actions that must be carried out to maintain or increase the role of mountain forests in hazard control.

Up to now it has been admitted that a silviculture, that is based on the natural cycles of forests guarantees best the stability of protection forests. All the foresters of European alpine countries agree in saying that guidelines are necessary, giving aid in field observations and recommendations for intervention planning. Therefore, these countries are working on a common guide as a tool for decision-making concerning the management of mountain protection forests, using the following principles: the use of natural processes favouring forest stability and intervention only when necessary. Since September 2006, France has published a minimal tending guideline specifically dedicated to mountain forests with a protective function. This guideline is an efficient helping tool for making silvicultural decisions, but it does not suffice for land management if no risk and protection forest mapping has been done before.

Taking into account natural hazards in land management based on risk mapping and prohibiting building in risk zones seems to be the oldest and the most efficient method of risk prevention. Increasing housing pressure has often led to violation of those prohibitions and consequently to disasters. As a result, hazard prevention measures are being revised and this, logically, also outside areas where the disasters occurred. The protective role of forests is hardly considered in those procedures. Although the elements at risk are mainly located in the valleys bottoms, the origins of the hazards are located in natural lands upslope, where there is little and increasingly less land management (abandonment of agricultural, forested or pastoral activities because of shifting economies).

Prevention against landslides in this context can be done by implementing two complementary policies: assuring passive protection, close to the elements at risk, downslope of the hazard source zones and active protection upslope by adapted management of natural lands. Passive protection, referring to technical engineering, now predominates in many countries. However, the high cost of installing and maintaining these works forces managers to consider measures for prevention such as the use and management of protection forests. In this context, Austria, Switzerland and France have developed similar methodologies for zoning protection forests. The main goal of these methods is to identify and map the forested zones with a protective function, and to disseminate this information to the public.

In France, Risk Prevention Plans (RPP) are standard documents that determine risk areas and building authorizations. Traditionally, the RPP defines 3 different administrative zones on a map: the red zones which are "no building" zones, blue zones, which are "building zones under certain conditions" and white zones, which are "building" zones. Before 2001, the protective role of forests had not been taken into account in the existing RPP. It was then decided to create "green zones" in these documents, corresponding to forest zones with a protective function against natural hazards. For these zones, obligations, prohibitions and recommendations for forest management are explained (harvesting restrictions, conditions for road building, etc.), which are based on the French protection forest guideline. The proposed management rules are not only applied to the public but also to private forests. A RPP can be established for a single commune, but for landslides and flooding, a multi communal RPP, covering a complete catchment or watershed, exists.

This paper presents a critical analysis of the "green zone" in the French RPP, in the context of managing a forested watershed to mitigate landslide risks in a sustainable way.

33.4 Conclusion

Watershed and forest management are of high relevance when it comes to addressing landslide risk reduction. Although knowledge of the role of forests in landslide hazard mitigation has still to be improved, it is obvious that some specific practices can have a significant effect. This is also the case for agricultural goods production. But these activities have to be considered within the whole watershed natural and human ecosystem in order to better take into account all influencing factors. This is why they have to be guided by a sound watershed management policy and adapted guidelines.

The main problem while assessing the influence of forests is that one does not see the landslides which do not occur thanks to the forest cover. The only landslides studied are the ones which took place despite the forest cover. Comparative experiences in exactly similar conditions with changing vegetation cover should be carried out to better understand the role of forests.

Appropriate risk and hazard assessment and mapping, adapted watershed management practices, as well as forest and agricultural management and development techniques, may all contribute significantly in reducing landslide risk. Another important issue to be considered regarding watershed management and landslides is the resilience of mountain people to natural disaster. Adapted techniques, such as diversifying vegetation cover types and crop species and mixing different land uses, may improve the way natural resources and corresponding livelihoods can be rehabilitated after landslide events.

References

Alcantára-Ayala, I., Esteban-Chávez, O. & Parrot, J.F. 2006. Landsliding related to land-cover change: A diachronic analysis of hillslope instability distribution in the Sierra Norte, Puebla, Mexico. *Catena* 65(2): 152–165.

Berger, F., & Rey, F. 2004. Mountain Protection Forests against Natural Hazards and Risks: New French Developments by Integrating Forests in Risk Zoning. *Natural Hazards* 33: 395–404.

Bull, W.B. 1977. The alluvial-fan environment. *Progress in Physical Geography* 1:222–270.

Canadian Standards Association (CSA). 1997. Risk management: Guideline for decision-makers; Etobicoke, Ont. CAN/CSA - Q850-97.

Cemagref, O.N.F. & CRPF. 2006. *Guide des Sylvicultures de Montagne – Alpes du Nord francaises*. French Agricultural and environmental engineering research institute (Cemagref), French National Forest Office (ONF) and Regional Centre for Forest Property (CRPF).Meylan, France.

Deoja, B.B. 2001. Hazards and risks to and from linear infrastructures in mountainous regions. *In* Li, T., Suresh C.R., Bishal N.U. (eds.) *Landslide Risk Mitigation in the Hindu Kush-Himalaya*, pp. 189–201. Kathmandu, International Centre for Integrated Mountain Development.

Einstein, H. H. 1988. Special lecture: Landslide risk assessment procedure. Proceedings 5th International Symposium on Landslides, Lausanne, 2, 1075–1090.

Food and Agriculture Organisation of the United Nations. (FAO) 2006. *The new generation of watershed management projects and programmes*. FAO forestry paper No. 150. Rome.

Fourniadis, I.G., Liu, J.G. & Mason, P.J. 2007. Regional assessment of landslide impact in the Three Gorges area, China, using ASTER data: Wushan-Zigui. *Landslides* 4(3): 267–278.

Ghayoumian, J. & Shoaei, Z. 1997. *Landslide Distribution and the Controlling Factor in Iran*, International Symposium on Engineering Geology and the Environment, Athens, Greece June 23–27, 1997.

Körner, C. & Masahiko, O., coordinating leading authors. 2005. Mountain Ecosystems. *In* Hassan, R., Scholes, R., Ash, N. (eds.) *Ecosystems and human well-being: current state and trends: findings of the Condition and Trends Working Group*, pp. 681–716. Millenium Ecosystem Assessment.

Lee, E.M., & Jones, D.K.C. 2004. *Landslide risk assessment*. Thomas Telford, London.

Rickli, C., Zimmerli, P. & Böll, A. 2001. Effects of vegetation on shallow landslides: an analysis of the events of August 1997 in Sachseln, Switzerland. Kühne, M. (ed.) Proc. Int. Conf. on Landslides 2001, Davos: 575–584.

Sassa, K., Fukuoka, H., Wang, F. & Wang, G. (eds.) 2005. *Landslides. Risk Analysis and Sustainable Disaster Management*. Berlin Heidelberg, Springer-Verlag

Sassa, K., Fukuoka, H., Wang, F. & Wang, G. (eds.) 2007. *Progress in Landslide Science*. Berlin Heidelberg, Springer-Verlag

Shafaei Bajestsn M. & Salimi Golsheikhi M. 2002. Study on the effect of root of different types of trees on soil strength along Karoon Riverbank. *Journal of Agricultural and Natural Science and Technology*, Vol. 6 No. 4, Winter 2002 (in Persian)

Stocking, M., Murnaghan, N. 2001. *Handbook for the field assessment of land degradation*. London, Earthscan publications Ltd.

United Nations – International Strategy for Disaster Reduction. 2004. *Living with risk: A global overview of disaster risk reduction initiatives*. United Nations ISDR, Geneva. Annex1. Also available at: http://www.unisdr.org/eng/about_isdr/basic_docs/LwR2004/Annex_1_Terminology.pdf

Varnes, D.J. 1984. Landslide hazard zonation: a review of principles and practice. *Natural hazards,* 3. Paris, UNESCO.

Wilford, D.J., Sakals, M.E. & Innes, J.L. 2005. *Forest management on fans: hydrogeomorphic hazards and general prescriptions*. Land Management Handbook No 56. Victoria, British Columbia, Canada, B.C. Min.For., Res. Br. Also available at: <http://www.for.gov.bc.ca/hfd/pubs/Docs/Lmh/Lmh57.htm>

Wise, M., Moore, G.D. & VanDine, D.F., eds. 2004. *Landslide risk case studies in Forest Development Planning and Operations*. Land Management Handbook No 56. Victoria, British Columbia, Canada, B.C. Min.For., Res. Br. Also available at: <http://www.for.gov.bc.ca/hfd/pubs/Docs/Lmh/Lmh56.htm>

World Bank. 2002. *Sustaining forests: a development strategy*. Washington, The International Bank for Reconstruction and Development/The World Bank. Also available on the Internet: http://siteresources.worldbank.org/INTFORESTS/Resources/SustainingForests.pdf